



UNIVERSITAT ROVIRA I VIRGILI

## VISIBLE LIGHT PHOTOREDOX PROMOTED TRANSFORMATIONS OF INERT CHEMICAL BONDS

Yangyang Shen

**ADVERTIMENT.** L'accés als continguts d'aquesta tesi doctoral i la seva utilització ha de respectar els drets de la persona autora. Pot ser utilitzada per a consulta o estudi personal, així com en activitats o materials d'investigació i docència en els termes establerts a l'art. 32 del Text Refós de la Llei de Propietat Intel·lectual (RDL 1/1996). Per altres utilitzacions es requereix l'autorització prèvia i expressa de la persona autora. En qualsevol cas, en la utilització dels seus continguts caldrà indicar de forma clara el nom i cognoms de la persona autora i el títol de la tesi doctoral. No s'autoritza la seva reproducció o altres formes d'explotació efectuades amb finalitats de lucre ni la seva comunicació pública des d'un lloc aliè al servei TDX. Tampoc s'autoritza la presentació del seu contingut en una finestra o marc aliè a TDX (framing). Aquesta reserva de drets afecta tant als continguts de la tesi com als seus resums i índexs.

**ADVERTENCIA.** El acceso a los contenidos de esta tesis doctoral y su utilización debe respetar los derechos de la persona autora. Puede ser utilizada para consulta o estudio personal, así como en actividades o materiales de investigación y docencia en los términos establecidos en el art. 32 del Texto Refundido de la Ley de Propiedad Intelectual (RDL 1/1996). Para otros usos se requiere la autorización previa y expresa de la persona autora. En cualquier caso, en la utilización de sus contenidos se deberá indicar de forma clara el nombre y apellidos de la persona autora y el título de la tesis doctoral. No se autoriza su reproducción u otras formas de explotación efectuadas con fines lucrativos ni su comunicación pública desde un sitio ajeno al servicio TDR. Tampoco se autoriza la presentación de su contenido en una ventana o marco ajeno a TDR (framing). Esta reserva de derechos afecta tanto al contenido de la tesis como a sus resúmenes e índices.

**WARNING.** Access to the contents of this doctoral thesis and its use must respect the rights of the author. It can be used for reference or private study, as well as research and learning activities or materials in the terms established by the 32nd article of the Spanish Consolidated Copyright Act (RDL 1/1996). Express and previous authorization of the author is required for any other uses. In any case, when using its content, full name of the author and title of the thesis must be clearly indicated. Reproduction or other forms of for profit use or public communication from outside TDX service is not allowed. Presentation of its content in a window or frame external to TDX (framing) is not authorized either. These rights affect both the content of the thesis and its abstracts and indexes.

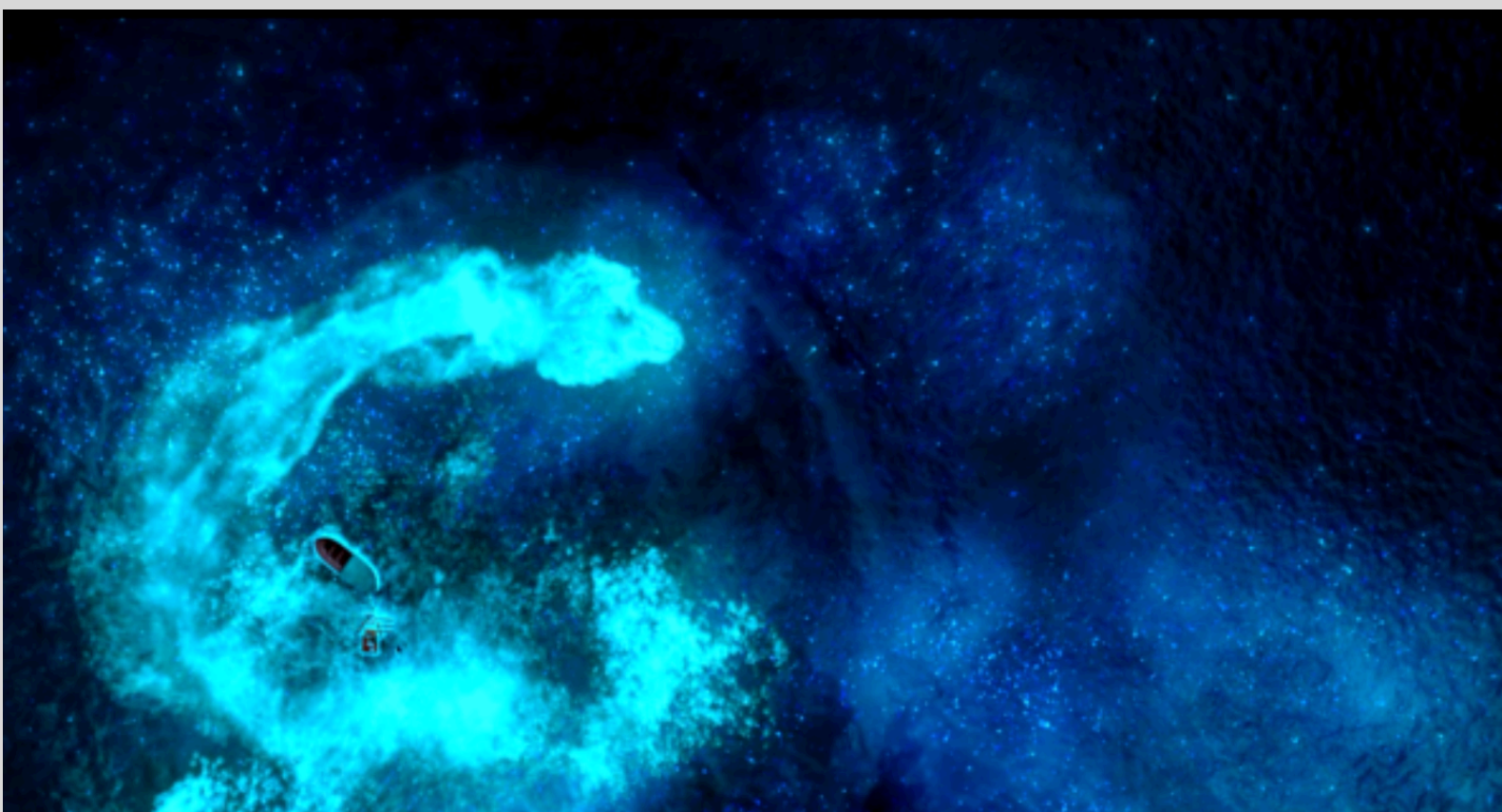


UNIVERSITAT  
ROVIRA i VIRGILI

# Visible Light Photoredox Promoted Transformations of Inert Chemical Bonds

---

Yangyang Shen



DOCTORAL THESIS  
2018

# Visible Light Photoredox Promoted Transformations of Inert Chemical Bonds

**Yangyang Shen**

Doctoral Thesis

**Supervised by Prof. Rubén Martín Romo**

Institut Català d'Investigació Química (ICIQ)

Universitat Rovira i Virgili (URV)

Department of Analytical Chemistry & Organic Chemistry



UNIVERSITAT  
ROVIRA i VIRGILI



Tarragona 2018



Prof. Rubén Martín Romo, Group Leader at the Institute of Chemical Research of Catalonia (ICIQ) and Research Professor of the Catalan Institution for Research and Advanced Studies (ICREA),

STATES that the present study, entitled “Visible Light Photoredox Promoted Transformations of Inert Chemical Bonds”, presented by Yangyang Shen for the award of the degree of Doctor, has been carried out under my supervision at the Institute of Chemical Research of Catalonia (ICIQ).

Tarragona, October 2018

Doctoral Thesis Supervisor

*Ruben Martin*

Prof. Rubén Martín Romo



Prof. Rubén Martín Romo, Group Leader at the Institute of Chemical Research of Catalonia (ICIQ) and Research Professor of the Catalan Institution for Research and Advanced Studies (ICREA),

STATES that the present study, entitled “Visible Light Photoredox Promoted Transformations of Inert Chemical Bonds”, presented by Yangyang Shen for the award of the degree of Doctor, has been carried out under my supervision at the Institute of Chemical Research of Catalonia (ICIQ).

Tarragona, October 2018

Doctoral Thesis Supervisor



*Ruben Martin*

Prof. Rubén Martín Romo

## **List of Publications**

At the time of printing, the results reported herein have been published in the following journals:

1. Yangyang Shen, Josep Cornella, Francisco Juliá-Hernández\*, Ruben, Martin\*  
“Visible-Light-Promoted Atom Transfer Radical Cyclization of Unactivated Alkyl Iodides”  
*ACS Catal.* **2017**, *7*, 409-412.
2. Veera Reddy Yatham, Yangyang Shen, Ruben Martin\*  
“Catalytic Intermolecular Dicarbofunctionalization of Styrenes with CO<sub>2</sub> and Radical Precursors”  
*Angew. Chem. Int. Ed.* **2017**, *56*, 10915-10919.
3. Yangyang Shen, Yiting Gu, Ruben, Martin\*  
“*sp*<sup>3</sup> C–H Arylation and Alkylation Enabled by the Synergy of Triplet Excited Ketones and Nickel Catalysts”  
*J. Am. Chem. Soc.* **2018**, *140*, 12200-12209.

## **Table of Contents**

<b>Acknowledgement</b> .....	I
<b>Preface</b> .....	IV
<b>Abbreviations &amp; Acronyms</b> .....	VI
<b>Abstract of This Doctoral Thesis</b> .....	VII
<b>Chapter 1. General Introduction</b> .....	1
1.1. General Background.....	2
1.2. Photophysical and Redox Properties of Visible-Light Photocatalysts.....	3
1.3. Catalytic Functions of Visible-Light Photocatalysts.....	5
1.4. The Renaissance of Visible Light Photoredox Catalysis.....	7
1.4.1. Merging Organocatalysis with Visible Light Photoredox.....	7
1.4.2. Visible Light Photoredox Promoted Cycloaddition.....	9
1.4.3. Visible Light Photoredox Promoted Dehalogenation and Atom Transfer Radical Addition.....	10
1.4.4. Photochemical Transformations Enabled by Triplet Energy Transfer.....	12
1.4.5. Photochemical Transformations Enabled by Non-Metal Based Visible Light Photoredox.....	13
1.5. Merging Photoredox with Transition Metal Catalysis: the Metallaphoredox Catalysis.....	12
1.5.1. The Initiation: Palladium Metallaphotocatalysis.....	18
1.5.2. Copper Metallaphotocatalysis.....	20
1.5.3. Gold metallaphotocatalysis.....	21
1.6. Summary.....	22
1.7. General Objective of this Doctoral Thesis.....	23
1.8. Bibliography.....	24
<b>Chapter 2. Visible-Light-Promoted Atom Transfer Radical Cyclization of Unactivated Alkyl Iodides</b> .....	28
2.1. Introduction: Atom Transfer Radical Addition/Cyclization.....	29
2.1.1. Traditional Methods to Promote ATRA/ATRC.....	29
2.1.2. Visible Light Photoredox Promoted ATRA/ATRC with Activated Halides.....	33
2.2. Visible Light Photoredox Promoted Unactivated Halide Reduction.....	36
2.3. General Aim of the Project.....	37
2.4. Visible Light-Photoredox Promoted ATRC of Unactivated Alkyl Iodides.....	37
2.4.1. Optimization of the Reaction Conditions.....	38
2.4.2. Preparative Substrate Scope.....	45
2.5. Mechanistic Considerations.....	48
2.5.1. Determination of Redox Potentials by Cyclic Voltammetry.....	48
2.5.2. Mechanistic Considerations: ON/OFF experiment.....	49
2.5.3. Mechanistic Considerations: Luminescence Quenching Experiments.....	49
2.5.4. Mechanistic Considerations: the excimer of amine and photoexcited alkyl halide.....	51
2.5.5. Mechanistic Considerations: Catalytic Cycle and Discussions.....	52
2.6. Visible Light Photoredox ATRC: The Conclusion.....	53
2.7. Bibliography.....	52

2.8. Experimental Section.....	36
2.8.1. General Considerations.....	56
2.8.2. Luminescence Quenching Experiments.....	56
2.8.3. Quantum Yield Determination.....	57
2.8.4. Emission Spectra of Different Light Sources.....	58
2.8.5. Synthesis of Starting Materials.....	58
2.8.6. Preparative Scope for Iodine Transfer Radical Cyclization.....	66
2.8.7. X-Ray Crystallographic Data.....	73
2.8.8. Bibliography of Known Compounds.....	78
2.8.9. <sup>1</sup> H and <sup>13</sup> C NMR Spectra.....	79
<b>Chapter 3. Catalytic Intermolecular Dicarbofunctionalization of Styrenes with CO<sub>2</sub> and Radical Precursors.....</b>	<b>133</b>
3.1. Introduction: CO <sub>2</sub> Fixation <i>en route</i> to Phenyl Acetic Acid.....	134
3.1.1. The Global Crisis: Carbon Dioxide Concerning.....	134
3.1.2. Catalytic CO <sub>2</sub> fixation of Organic Matter <i>en route</i> to Carboxylic Acids.....	135
3.1.3. Photochemical Carboxylation with CO <sub>2</sub> .....	142
3.2. General Aim of the Project.....	143
3.3. Catalytic Intermolecular Dicarbofunctionalization of Styrenes with CO <sub>2</sub> and Radical Precursors.....	144
3.3.1. Mechanistic Rationale.....	144
3.3.2. Optimization of the Reaction Conditions.....	144
3.3.3. Substrate Scope with Langlois Reagent.....	146
3.3.4. Substrate Scope with Other Radical Entity.....	149
3.4. Mechanistic Considerations.....	150
3.4.1. 'ON/OFF' Experiment.....	150
3.4.2. Luminescence Quenching Experiments.....	150
3.4.3. The Competitive Off-Cycle via Decarboxylation.....	151
3.5. Conclusions.....	152
3.6. Bibliography.....	154
3.7. Experimental Section.....	157
3.7.1. General Considerations.....	157
3.7.2. Synthesis of starting materials.....	157
3.7.3. Intermolecular Dicarbofunctionalization of Styrenes with CO <sub>2</sub> .....	158
3.7.4. Fluorescence Quenching Experiments.....	168
3.7.5. X-ray Crystallography.....	169
3.7.6. Bibliography of Known Compounds.....	178
3.7.7. <sup>1</sup> H and <sup>13</sup> C NMR Spectra.....	179
<b>Chapter 4. <i>sp</i><sup>3</sup> C–H Arylation and Alkylation Enabled by the Synergy of Triplet Excited Ketones and Nickel Catalysts.....</b>	<b>222</b>
4.1. The Merger of Nickel Catalysis and Photoredox.....	223
4.1.1. Fundamental Aspects of Ni Catalysis in Cross-Coupling Reactions.....	223
4.1.2. The Macroscopic Revolution of Ni Catalysis.....	224



4.2. Multifunctional Visible Light Photocatalysts.....	228
4.2.1. Chiral-at-metal Complex as Multifunctional Photocatalyst.....	228
4.2.2. Diaryl Ketone with Hydrogen Bonding as Multifunctional Photocatalyst.....	230
4.2.3. Diaryl Ketone Possessing Chiral Ligands.....	231
4.3. Benzophenones: Multifunctional Photocatalysts for Synthetic Applications.....	232
4.4. $sp^3$ C-H Functionalization via HAT Enabled by Photoredox Catalysis.....	234
4.4.1. Photoredox generated Alkoxy Radical enabled Remote C-H Functionalization.....	235
4.4.2. Photoredox generated Amidyl Radical enabled Remote C-H Functionalization.....	236
4.4.3. Photoredox, HAT and Ni-Catalyzed $sp^3$ C-H Arylation.....	238
4.5. General Aim of the Project.....	240
4.6. Metallatriplet Catalysis: The Synergy of Triplet Excited Ketones and Nickel Catalysts.....	240
4.6.1. Metallatriplet Catalysis: Mechanistic Hypothesis.....	241
4.6.2. Metallatriplet Catalysis: Optimization of the Reaction Conditions.....	242
4.6.3. Metallatriplet Catalysis: Scope of $sp^3$ C-H Arylation.....	250
4.6.4. Metallatriplet Catalysis: Scope of $sp^3$ C-H Alkylation.....	257
4.6.5. Metallatriplet Catalysis: Mechanistic studies.....	262
4.7. Metallatriplet Catalysis: The Conclusion.....	268
4.8. Bibliography.....	269
4.9. Experimental Section.....	274
4.9.1. General Considerations.....	274
4.9.2. Synthesis of triplet catalyst A1 and starting materials.....	274
4.9.2.1. Scalable synthesis of the diary ketone catalyst.....	274
4.9.2.2. Synthesis of the starting materials.....	275
4.9.3. Preparative Scope for Metallatriplet Catalysis.....	277
4.9.3.1. $sp^3$ C-H Arylations.....	277
4.9.3.2. Scalable Synthesis of <b>3</b> , <b>21</b> , <b>37</b> and <b>57</b> .....	293
4.9.3.3. Enantioselective $sp^3$ C-H Arylation.....	294
4.9.3.4. $sp^3$ C-H Alkylations.....	295
4.9.4. Bibliography of Known Compounds.....	302
4.9.5. X-ray Diffraction of <b>Ni-1</b> .....	303
4.9.6. $^1\text{H}$ and $^{13}\text{C}$ NMR Spectra.....	310
<b>Chapter 5. General Conclusions.....</b>	<b>401</b>

## Acknowledgements

First and foremost, I would like to offer my sincerest gratitude to my PhD advisor, **Rubén Martín**, for giving me the opportunity to pursue my PhD studies in his group. Over the past four years, his persistent support and motivation, profound insight and discussion, and incredible stock of knowledge and patience help me to evolve into a better researcher. Ruben likes sharing with us his experience, but at the same time, his curiosity drives us to think more independently and critically, leading us to an advanced level of analyzing and understanding chemistry. Additionally, I am very grateful for the freedom and trust he gave to me over these years. I also appreciate him for all the ways that we've been through together in which he prepared me for my future career.

Secondly, I would like to thank the members of the jury, **Prof. Julia Pérez Prieto**, **Prof. Marcos García Suero** and **Prof. Xile Hu** for accepting to be part of my examination committee. **Prof. Josep Cornella**, **Prof. Xueqiang Wang** and **Prof. Arkaitz Correa Navarro** are also warmly thanked for taking time to evaluate this thesis as external reviewers.

I have to offer my special thanks to **Ingrid** for all her administrative support and work through all these years. **Miriam** and **Sope**, thank you for the help to make the group run more efficiently. It's my honor to have you around.

I would like to thank the current and past members of the Martin group, especially the members that shared lab 2.12 with me. I really enjoyed working together with you guys.

**Álvaro**, the column boy full of 'unusual' jokes! Thank you for helping me with the apartment at the beginning, for driving me home so many times, for teaching me lots of 'interesting' Spanish, for being an example of leveraging working, learning and playing, for your contagious courage when facing problems. And also, thank you for showing me another side of PhD life by shooting me with your dirty gloves. 'Four years! Lifer!', the voice coming from your mouth contained desperation and hope while the microphone was playing our favorite song 'Blank Space'. Now, it's my turn to 'print and staple' this wonderful torture. Thank you for everything you did for me and to me! I will miss you! As much as I will miss you, **Caye**! I still remember the first party in your apartment. It was a 'cultural shock' to see a crowd of scientific worker dancing in madness with rock and roll. Your lovely smile had the power to disperse the unhappiness. I hope you have forgotten the sorrows dealing with the '**Boring and Silly**' projects. As your lab neighboring, I couldn't remember how many times you 'stole' my Hamiltons. I missed the time you made me 'suffering' with your questions. Thank you and hope to see you soon, **Caye**! **Elo**, the girls in lab 2.12 always have many questions to ask! Thank

you for lots of help with the sophisticated renewal of NIE card, for explaining so many rules and chemical names at the beginning, for helping me with the very first reaction, for reminding us the lab duties, for being an excellent model of how to present research, and a big thank you for proofreading this manuscript. I hope you enjoy everything in Germany.

**Paco**, an incredible postdoc I have ever met! A big thank you for initiating photochemistry with Josep Cornella in the group. Only with your help and encouragement could I successfully finish my PhD study. Thank you for numerous discussions on chemistry, for always being critical with my progress, for always telling Ruben good things about me, for all the constructive advice with the papers. A deepest appreciation goes for your being a great benchmark as a researcher! I got to learn so much from you! Your experience, altitude, enthusiasm, execution, persistence is being gold mine to me. You will be an outstanding chemist in the future. I hope you and your family enjoy life in Stockholm.

**Pep** (Prof. Cornella), Thank you for your preliminary photochemistry project with Paco! You have both sharp eyes and fat ass! It was a big fun to work with you. How I wish I could had overlapped with you a longer period. **Manuel** (Prof. van Gemmeren), it was awesome to meet you, your spicy sauce impressed me a lot. **Dani**, thank you for your useful experience and knowledge on complex synthesis and mechanistic study. **Reddy**, it has been great to work with you on photochemistry; thank you for your Indian food. **Shang-Zheng**, very clever and hardworking, it has been great pleasure to share lab and apartment with you; I wish you all the best with your thesis. **Bradley**, looks like the ‘Young MacMillan’, so brave to do the challenge chemistry; good luck with your projects. **Hongfei** and **Basu**, two brilliant postdocs, very nice to meet you and I am sure you will do a great job.

For the fellows in lab 2.7, most of the reason I went there was for chemicals. I wish to get to know more about you guys. **Xueqiang** (Prof. Wang), a sincerest gratitude for you. Thank you for your impressive words to Ruben, for making me confident to pursue PhD in Spain, for all your help with the accommodation, for sharing your precious experience about the group. **Toni & Morgane**, you were always the first one to ask questions in group seminar. Your helpful ideas and advice were very valuable to me. Thank you for being very nice lab mates. **Rubén** (Manzano), thank you for the help with my apartment at the very beginning and best wishes to your research group. **Javier**, **Masaki** and **Yasu**, it was a pleasure to meet and work with you. **Alicia**, it was nice to work with you, I hope you enjoy the new job in ICIQ. **Marino**, **Andreu** and **Raúl**, it was so nice to have you guys in the group. Thank you for all the helpful discussions and advice. I wish all the best for your PhD. **Rosie**, a big thank you for proofreading of our papers and thesis. I will remember our discussion about chemistry

and life. I hope you enjoy your stay in US. **Georgios**, good luck in Switzerland and you will have a great PhD life; **Daniel**, a knowledgeable postdoc, always giving constructive opinions, I wish you all the best with your independent career. **Antonio**, I hope I have more time to know you, but I am sure you will do a great work. **Yaya** and **Fei**, I am glad to meet you two and I hope all the best to your projects.

I want to mention those people who did short stay in our group. **José-Manuel**, thank you for working on the asymmetric project. You did an excellent work here. I hope all the best for your future study. Best wishes for **Irene**, **Naoko**, **Thomas**, **Lilly**, **Ryu**, **Yomoyuki** and **Riccardo**, I hope you enjoyed the time in our group.

I also would like to express my deep appreciations to many friends in ICIQ for sharing their experience and giving me supports all the time. It is a long journey and my PhD study enriched by all of your companions.

Special thanks to the ICIQ supporting units. Your efficient work enabled quick and solid publications of our projects.

By far the best thing for my PhD was meeting **Yiting**. (Thanks again to **Rubén** for enrolling her). Thank you so much for all the precious support, help, companion, understanding over the last three years.

Last, but not at least, this thesis certainly would not have been possible without the love, support and understanding of my family, especially my dear grandma and wife Yiting. Thank you very much for all the encouragement and support through my hard times, and all the trust on every step and decision I made.

## Preface

The whole work presented in this dissertation has been carried out at the Institute of Chemical Researcher of Catalonia (ICIQ), during the period of November 2014 to September 2018 under the guidance of Professor Rubén Martín. The thesis contains five chapters: a general introduction, three research chapters, and a last chapter with a general conclusion of all the research work. Each of the research chapter includes an introduction and an aim of the presenting project, followed by a discussion of experimental results, mechanistic analysis, conclusions, and experimental sections.

The first Chapter deals with the historical background and modern development of visible light photoredox catalysis. A brief overview of photophysical properties and redox potentials of selected visible light photocatalysts are presented, followed by the discussion of general catalytic manners of commonly used visible light photocatalysts.

The second Chapter, “Visible-Light-Promoted Atom Transfer Radical Cyclization of Unactivated Alkyl Iodides”, describes the synthesis of exo-cyclic trisubstituted vinyl iodides via visible light photoredox promoted atom transfer radical cyclization of unactivated alkyl iodides. Preliminary mechanistic studies and control experiments have indicated an activation mode challenging the canonical photoredox catalytic cycle. The results in this chapter have been published in *ACS Catal.* **2017**, *7*, 409-412 in collaboration with Dr. Josep Cornella and Dr. Francisco Juliá-Hernández.

The third Chapter, “Catalytic Intermolecular Dicarbofunctionalization of Styrenes with CO<sub>2</sub> and Radical Precursors”, describes the synthesis of substituted phenylacetic acid with styrenes, radical precursors and CO<sub>2</sub> via visible light photoredox catalysis. With the present work, many valuable phenylacetic acids that are not easily accessible with traditional method can be efficiently synthesized under mild conditions. Preliminary mechanistic studies and control experiments have indicated a reductive quenching pathway. The results in this chapter have been published in *Angew. Chem. Int. Ed.* **2017**, *56*, 10915-10919 in collaboration with Dr. Veera Reddy Yatham.

The last research Chapter, “*sp*<sup>3</sup> C–H Arylation and Alkylation Enabled by the Synergy of Triplet Excited Ketones and Nickel Catalysts”, presents our efforts toward the indirect *sp*<sup>3</sup> C–H functionalizations with cheap diaryl ketone and nickel salt as catalytic combination. The successful arylation and alkylation of hydrocarbons with our system holds promise for a more prolific use of diaryl ketone as visible light photocatalyst in the context of metallaphotoredox arena. Preliminary mechanistic studies and control experiments have suggested the ketone functions as HAT & SET

catalyst. The results in this chapter have been published in *J. Am. Chem. Soc.* **2018**, *140*, 12200-12209 in collaboration with Yiting Gu.

## **Abbreviations & Acronyms**

acac = acetylacetonate

ATRA = atom transfer radical addition

ATRC = atom transfer radical cyclization

BDE = bond dissociation energy

Cy = cyclohexyl

equiv = equivalent

ET = energy transfer

h = hour(s)

HAT = hydrogen atom transfer

Int = intermediate

LED = light emitting diode

*o* = ortho

*p* = para

Piv = pivalate

PMP = *para*-methoxyphenyl

rt = room temperature

SET = single electron transfer

*t* = tert

THF = tetrahydrofuran

Ts = tosyl

TBDPS = tert-butyldiphenylsilyl

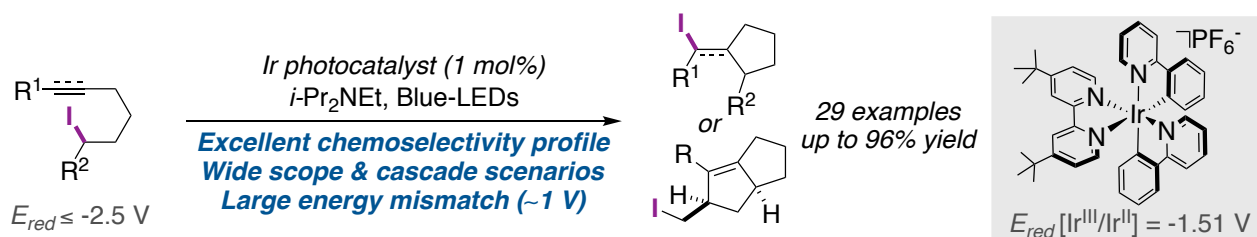
TBS = tert-butyldimethylsilyl

## Abstract of This Doctoral Thesis

In recent years, visible light photoredox catalysis has become a powerful alternative to existing methodologies for generating transient radical species via outer-sphere mechanisms. Consequently, numerous well-known chemistry could be interwoven with visible light photoredox catalysis, thus unlocking novel enabling techniques for both C-C and C-X bond formation under exceptionally mild conditions with broad substrate scope and functional group tolerance.

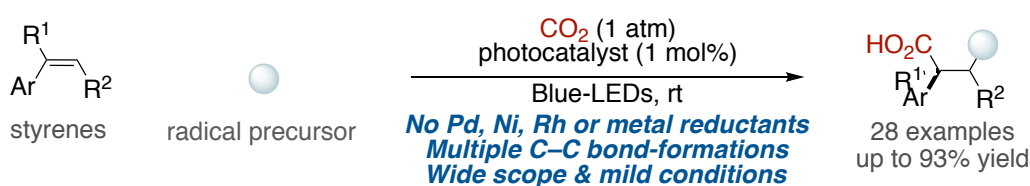
In line with the research interest in Martín's group of activating inert bonds or molecules, such as unactivated halides, carbon dioxide or  $sp^3$  C-H bonds, among others, this Doctoral Thesis focuses on the development of novel techniques to make use of these functionalities via visible light photoredox catalysis. The transformations realized herein contribute to the understanding of more prolific use of inert chemical bonds to the synthesis value added compounds.

### Visible light-mediated atom transfer cyclization of unactivated alkyl iodides



### Scheme 1. Visible light-mediated atom transfer radical cyclization of unactivated alkyl iodide

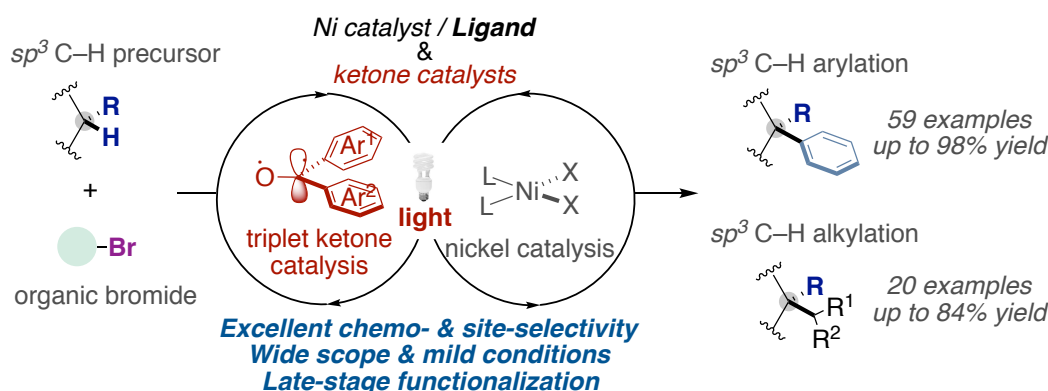
Our very first effort in visible light photoredox catalysis aimed at developing a visible light-mediated atom transfer radical cyclization of unactivated alkyl iodide. Due to the large mismatch in reduction potential, unactivated alkyl iodide are challenging substrates to directly reduce with visible light photocatalysts. The successful development of this transformation and preliminary mechanistic studies challenge the perception that a canonical photoredox catalytic cycle is being operative. The careful control experiments revealed that a rather elusive exciplex between tertiary amine and alkyl iodide might come into play to facilitate the interaction of the substrate and photocatalyst via electron transfer or energy transfer. This protocol operated under mild conditions and exhibits excellent chemoselectivity profile while avoiding parasitic hydrogen atom transfer pathways.





## Scheme 2. Photoredox catalyzed dicarbofunctionalization of styrenes with CO<sub>2</sub> and radical precursors

In 2017, we described a redox-neutral intermolecular dicarbofunctionalization of styrenes with inert CO<sub>2</sub> at atmospheric pressure and carbon-centered radicals. At the outset of this work, the synthesis of valuable phenylacetic acids with CO<sub>2</sub> remained confined to single bond formation with relatively simple backbones. Our protocol took advantage of photoredox catalysis to generate open-shell species that add across the double bond, setting the stage for generating a benzyl anion via single-electron transfer prior CO<sub>2</sub> insertion. In this manner, this protocol offers the opportunity of triggering a double C–C bond-formation with concomitant CO<sub>2</sub> insertion, and in the absence of any Ni catalyst or sophisticated ligand backbone, thus exploiting a previously unrecognized opportunity that complements existing catalytic carboxylations.



## Scheme 3. *sp*<sup>3</sup> C–H functionalization enabled by the synergy of diaryl ketone and nickel catalyst

Our last venture into photoredox catalysis focused on the functionalization of native *sp*<sup>3</sup> C–H bonds. At the outset of our study, the vast majority of visible light photocatalysts function as either electron or energy transfer catalysts. Driven by the observation that diaryl ketones are capable of abstracting a hydrogen atom from a hydrocarbon feedstock at the triplet excited state, we wondered whether we could utilize simple ketones as photocatalysts within the context of *sp*<sup>3</sup> C–H functionalization under visible light irradiation. Although the radical-type character of triplet excited states of diaryl ketones suggests the viability for triggering hydrogen-atom transfer (HAT) and single-electron transfer (SET) processes, among others, their use as multifaceted catalysts in C–C bond-formation via *sp*<sup>3</sup> C–H functionalization of alkane feedstocks still remains rather unexplored. In this PhD thesis, we have unlocked a modular photochemical platform for forging C(*sp*<sup>3</sup>)–C(*sp*<sup>2</sup>) and C(*sp*<sup>3</sup>)–C(*sp*<sup>3</sup>) linkages from abundant alkane *sp*<sup>3</sup> C–H bonds as functional handles using the synergy between nickel catalysts and simple, cheap and modular diaryl ketones. This method is distinguished by its wide scope that

is obtained from cheap catalysts and starting precursors, thus complementing existing inner-sphere C–H functionalization protocols or recent photoredox scenarios based on iridium polypyridyl complexes. Additionally, such a platform provides a new strategy for streamlining the synthesis of complex molecules with high levels of predictable site-selectivity and preparative utility. Mechanistic experiments suggest that  $sp^3$  C–H abstraction occurs via HAT from the ketone triplet excited state, thus offering a new technique for bond-forming reactions within the metallaphotoredox arena.

In conclusion, we have developed new methods for the functionalization of inert chemical bonds or molecules via photoredox catalysis under exceptionally mild conditions and with an excellent chemoselectivity profile. We also carried out preliminary mechanistic studies to understand how and why these reactions proceeded.

# **Chapter 1.**

## **General Introduction**

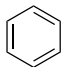
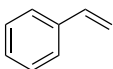
## 1.1. General Background

“... And if in a distant future the supply of coal becomes completely exhausted, civilization will not be checked by that, for life and civilization will continue as long as the sun shines! If our black and nervous civilization, based on coal, shall be followed by a quieter civilization based on the utilization of solar energy, that will not be harmful to progress and to human happiness.

The photochemistry of the future should not however be postponed to such distant times; I believe that industry will do well in using from this very day all the energies that nature puts at its disposal. So far, human civilization has made use almost exclusively of fossil solar energy. Would it not be advantageous to make better use of radiant energy?”

---Giacomo Ciamician (1912)

One century ago, the Italian photochemist Giacomo Ciamician had the vision of transforming solar energy into valuable compounds in a way similar to photosynthesis that nature does.<sup>1</sup> Taking into consideration that photochemistry deals with chemical changes promoted by just the absorption of a photon, it is reasonable to assume that the use of light as an abundant, clean and inexpensive natural source for building up molecular complexity holds promise to revolutionize approaches in organic synthesis, particularly if light can be used to change our dependence on fossil fuels.<sup>1</sup>

	$\lambda$ (nm)	E (kcal/mol)	Group	$\lambda$ (nm)	BDE (kcal/mol)
UV	200	143	C=C	180	C-C 83
	300	95	C=C-C=C	220	O-O 35
Vis	400	72		260	C-H 99
	500	57		282	O-H 111
	600	48			C-N 73
	700	41			C-O 86
IR	1,000	29			
	5000	6	C=O	280	C=C 146
	10000	3	C=C-C=O	350	C=O 180

**Scheme 1.1. The absorption and bond dissociation energy of common organic scaffolds**

Taking a close look at the literature data, there are certainly a wide variety of photochemical reactions that proceed under UV irradiation, inevitably requiring a specialized photochemical device.<sup>2</sup> However, the use of high energy UV-light can be rather problematic due to the ability of a wide range of functional groups to absorb in the UV region, which may lead to deleterious side reactions arising

from photoexcitation of the substrate itself.<sup>2</sup> Not surprisingly, chemists have been challenged to utilize visible light energy in lieu of UV-light for C–C and C–heteroatom bond-forming reactions. To such end, chromophores capable of collecting photons from visible light and transferring such inherent energy to organic substrates have attracted considerable attention within the context of organic synthesis.<sup>3</sup> As shown in Scheme 1.1, visible light has less energy than UV-light, thus preventing decomposition pathways derived from the excitation of the substrate upon irradiation. Conceptuality aside, the utilization of simple, and cheap visible-light emitting device such as compact fluorescence light bulbs represents an important step-forward for improving the practicality and generality of light-induced reactions, suggesting that these techniques might find immediate application in various disciplines, including organic synthesis, material science or drug discovery, among others.<sup>3</sup>

The utilization of chromophores for enabling visible light photocatalytic reactions can be traced back to the work of Burstall when preparing tris(bipyridine)ruthenium(II) chloride  $[\text{Ru}(\text{bpy})_3\text{Cl}_2]$ .<sup>4</sup> While this field remained relatively dormant for a period of time, with notable exceptions by Kellogg, Pac, Deronzier, Willner, Kern and Sauvage, Tanaka, Fukuzumi, Oda and Okada,<sup>12-22</sup> the recent years have witnessed an exponential growth in the area of visible light photocatalysis.<sup>5-7</sup> Indeed, this field of expertise has undoubtedly entered into a new era of continuous development that have found application in water splitting, energy storage, phototherapy or photovoltaic devices, among others.<sup>8-</sup>

11

## 1.2. Photophysical and Redox Properties of Visible-Light Photocatalysts

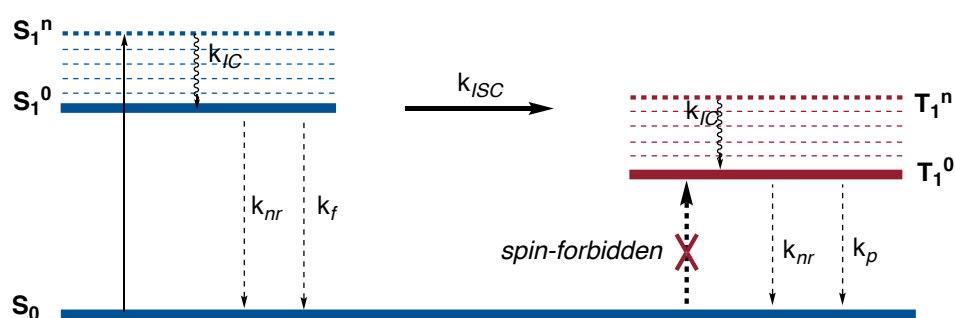


**Figure 1.1. Generalized Jablonski diagram for photocatalyst**

The optical and redox properties of visible light photocatalysts allow them to be employed in single-electron transfer (SET) or energy transfer (ET) processes. The photophysical changes during the irradiation could be summarized by the Jablonski diagram which is also applicable to other related photocatalysts (Figure 1.1).<sup>23</sup> The photochemical process is initiated by the absorption of a photon by the singlet ground state  $\text{PC}(S_0)$ , allowing the electron to occupy a higher energetic singlet excited

state  $\mathbf{PC}(*S_1^n)$ , which then typically relaxes to the lowest vibrational levels of singlet excited state  $\mathbf{PC}(*S_1^0)$  via internal conversion ( $k_{ic}$ ). The  $\mathbf{PC}(*S_1^0)$  state can return back to the singlet ground state via radiative (fluorescence,  $k_f$ ) or non-radiative ( $k_{nr}$ ) pathway. However, the  $\mathbf{PC}(*S_1^0)$  state can also undergo an efficient intersystem crossing (ISC,  $k_{isc}$ ) with high quantum yield to the triplet state  $\mathbf{PC}(*T_1^n)$  followed by internal conversion to produce the lowest triplet excited state  $\mathbf{PC}(*T_1^0)$ . Such excited stage is reasonably long-lived (*e.g.*  $\tau = 1100$  ns for **Ru-1**) due to the spin forbidden transition of the triplet state ( $\mathbf{PC}(S_0) - \mathbf{PC}(*T_1^0)$ ). As for  $\mathbf{PC}(*S_1^0)$ , the  $\mathbf{PC}(*T_1^0)$  slow deactivation through the radiative (phosphorescence,  $k_p$ ) or non-radiative ( $k_{nr}$ ) pathway might lead to the  $\mathbf{PC}(S_0)$ . From a chemical standpoint, the long-lived triplet excited state  $\mathbf{PC}(*T_1^0)$  serves both as a better single-electron reductant or oxidant than the corresponding  $\mathbf{PC}(S_0)$  ground state. While the enhanced reducing ability is explained by shifting one electron from the HOMO into a higher energetic state, the oxidizing feature derives from the singly occupied ‘HOMO’ in the ground state which is available to meet an extra electron. In addition, it is worth noting that the long-lived triplet excited state can participate in bimolecular quenching through triplet energy transfer sequences.

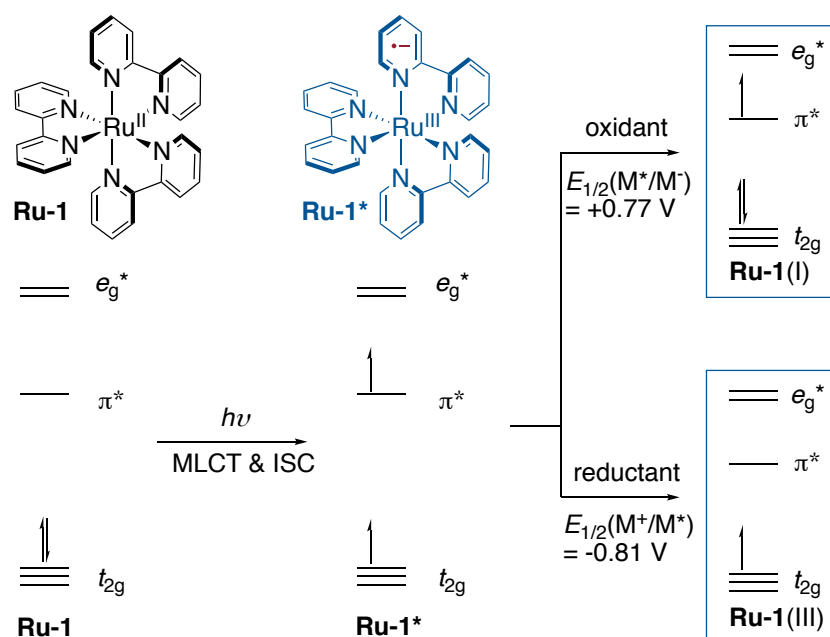


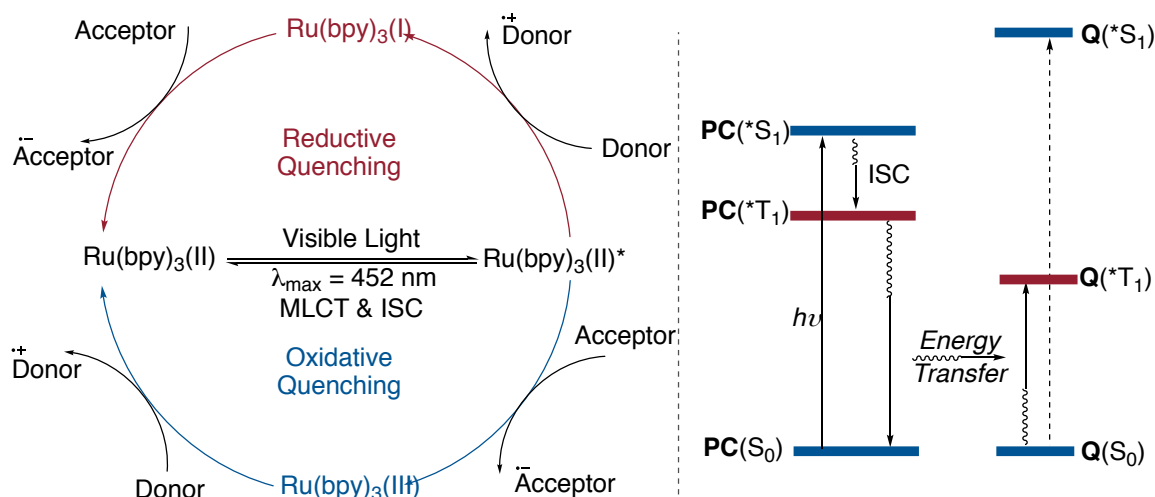
**Figure 1.2. Simplified molecular orbital and electron shift of photoexcited Ru-1**

Taking **Ru-1** as a model, visible light photoexcitation facilitates that an electron from a metal-centered  $t_{2g}$  orbitals shifts to a ligand-centered  $\pi^*$  orbital. This process is better described as a metal to ligand charge transfer (MLCT), generating a transient species in which the metal has formally been oxidized to a higher oxidation state whereas the ligand backbone has been reduced to a radical anion (Figure 1.2).<sup>23</sup> As the photocatalyst has a fully coordinated metal center, a subsequent single-electron transfer takes place via an outer sphere-type mechanism. Regardless of whether a single-electron

reduction or oxidation event occurs, the presence of a singly occupied orbital suggests that the original configuration will be recovered by a subsequent SET process.

### 1.3. Catalytic Functions of Visible-Light Photocatalysts

Upon photoexcitation,  $\text{Ru}(\text{bpy})_3^*$  typically facilitates a single electron transfer (SET) with organic molecules. Depending on the reaction conditions and on the nature of the substrate, the SET of  $\text{Ru}(\text{bpy})_3^*$  proceeds via either reductive quenching or oxidative quenching (Scheme 1.2, *left*).<sup>23</sup> In a reductive quenching,  $\text{Ru}(\text{II})^*$  serves as an oxidant by accepting an electron from an electron donor, thus affording the reduced species  $\text{Ru}(\text{I})$  species (Scheme 1.2, *left*). With such higher reducing ability, the  $\text{Ru}(\text{I})$  is particularly prone to regenerate the ground state  $\text{Ru}(\text{II})$  in the presence of an appropriate electron acceptor. Such reductive quenching scenario is typically facilitated by tertiary amines, serving as effective quenchers for  $\text{Ru}(\text{II})^*$ . If an oxidative quenching operates, however,  $\text{Ru}(\text{II})^*$  functions as a reductant by donating one electron to an electron acceptor, thus delivering  $\text{Ru}(\text{III})$  that is particularly predisposed to a SET from an electron-rich donor to recover back the ground state  $\text{Ru}(\text{II})$ . Common oxidative quenchers that accept electron from  $\text{Ru}(\text{II})^*$  are viologens, polyhalomethanes, polynitroarenes and persulfate. As the redox quenching depends on the redox potentials of the photocatalyst, this can be modulated by a subtle change in the electronic parameters of the latter; specifically, the presence of electron-donating substituents increases the reducing ability of the photocatalyst whereas the inclusion of electron-withdrawing substituents improves its oxidizing character.<sup>23</sup> While SET processes effectively quench the triplet excited state of the photocatalyst, energy transfer (ET) can be used for similar purposes (Scheme 1.2, *right*). The long-lived triplet excited state can effectively be quenched with appropriate substances possessing a lower triplet energy than the triplet energy of photocatalyst. In this manner, the triplet energy of the photocatalyst is transferred to the quencher, thus recovering back its ground state while delivering a triplet state at the quencher. Such energetic triplet excited state may be used to participate in a myriad of organic transformations, ranging from cycloaddition, to ring-opening or isomerization events, among others.<sup>23</sup>



**Scheme 1.2. Single electron transfer and energy transfer**

In order to identify whether quenching occurs or not, Stern-Volmer luminescence is typically employed. In the absence of a quencher, the photoexcited catalyst emits a stable emission, while in the presence of increased concentration of the quencher, the emission is attenuated.

$$I/I_0 = 1 + k_q\tau_0[Q]$$

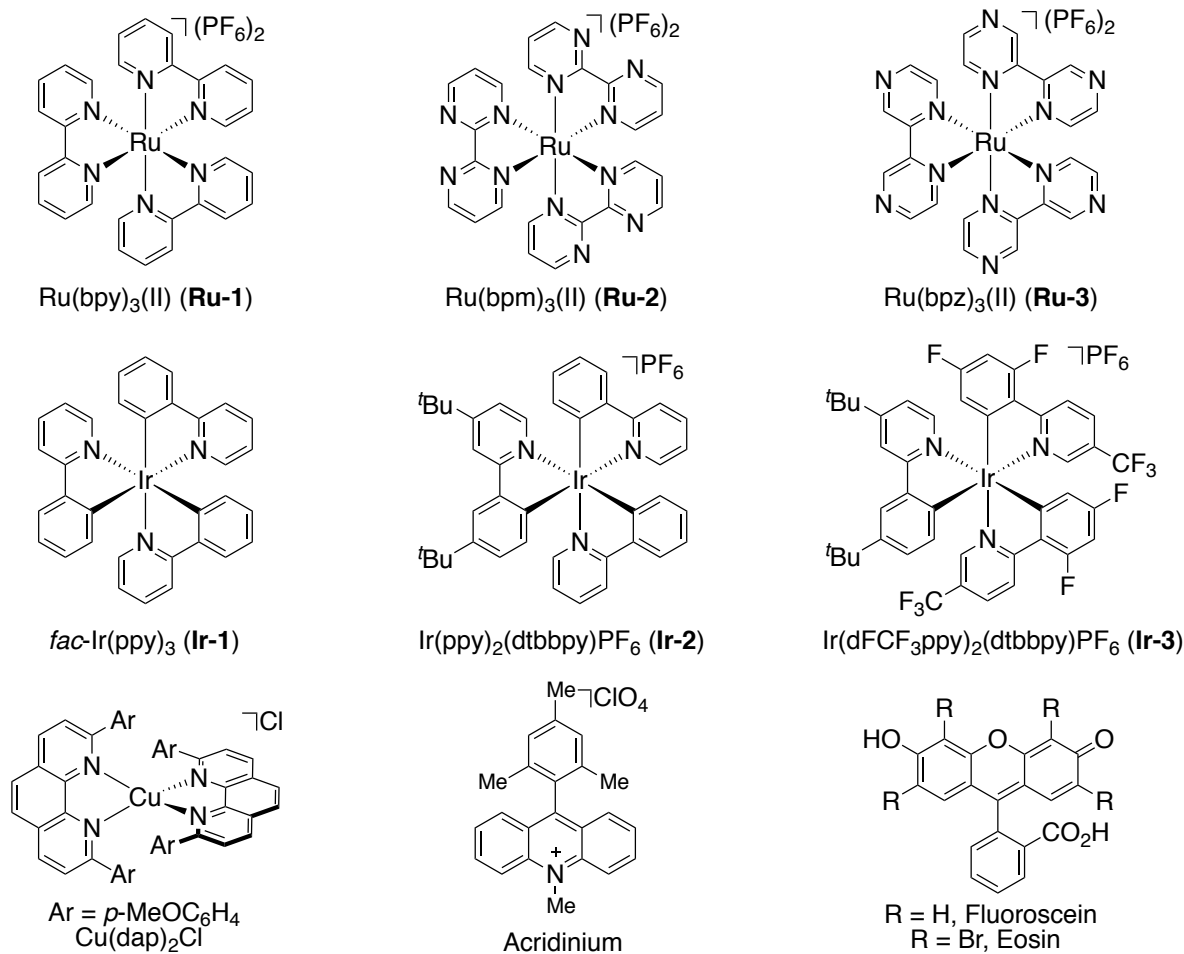
The formula that describes this phenomenon is the Stern-Volmer equation, in which  $I_0$  stands for the luminescence intensity of the photocatalyst without quencher,  $I$  represents the intensity of luminescence in the presence of the quencher, and  $\tau_0$  is the lifetime of photocatalyst. Plotting the ratio of  $I/I_0$  against the quencher concentration would give a straight line in an ideal scenario. The observation of this relationship between emission intensity of photocatalyst and concentration of a quencher provides evidence that the quencher involves in single electron transfer with the photocatalyst.

A number of commonly employed photocatalysts with selected redox potentials and photophysical properties are listed in Table 1.1 and Scheme 1.3.<sup>23</sup>

Photocatalyst	$E_{1/2}$ (V) (M <sup>+</sup> /M <sup>*</sup> )	$E_{1/2}$ (V) (M <sup>*</sup> /M <sup>-</sup> )	$E_{1/2}$ (V) (M <sup>+</sup> /M)	$E_{1/2}$ (V) (M/M <sup>-</sup> )	Excitation $\lambda_{\text{max}}$ (nm)	Emission $\lambda_{\text{max}}$ (nm)	Excited state lifetime $\tau$ (ns)
Ru(bpy) <sub>3</sub> <sup>2+</sup>	-0.81	+0.77	+1.29	-1.33	452	615	1100
Ru(bpm) <sub>3</sub> <sup>2+</sup>	-0.21	+0.99	+1.69	-0.91	454	639	131
Ru(bpz) <sub>3</sub> <sup>2+</sup>	-0.26	+1.45	+1.86	-0.80	443	591	740
<i>fac</i> -Ir(ppy) <sub>3</sub>	-1.73	+0.31	+0.77	-2.19	375	494	1900
Ir(ppy) <sub>2</sub> (dtbbpy) <sup>+</sup>	-0.96	+0.66	+1.21	-1.51	---	581	557
Ir(dFCF <sub>3</sub> ppy) <sub>2</sub> (dtbbpy) <sup>+</sup>	-0.89	+1.21	+1.69	-1.37	380	470	2300
Cu(dap) <sub>2</sub> <sup>+</sup>	-1.43	---	+0.62	---	---	670	270
Acridium <sup>+</sup>	---	+2.06	---	-0.57	430	---	---
Eosin Y	-1.11	-0.83	+0.78	-1.06	539	---	2400



**Table 1.1. Redox potential and selected photophysical properties**

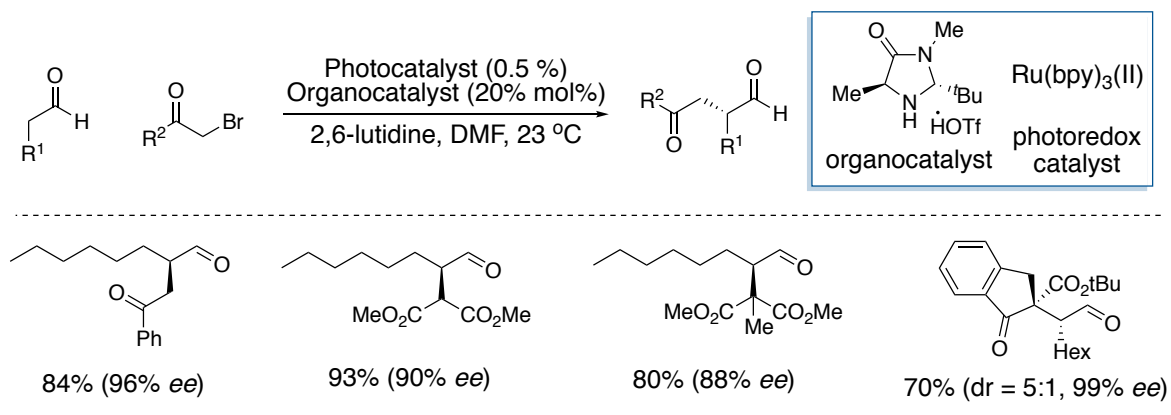


**Scheme 1.3. Commonly utilized visible light photocatalysts**

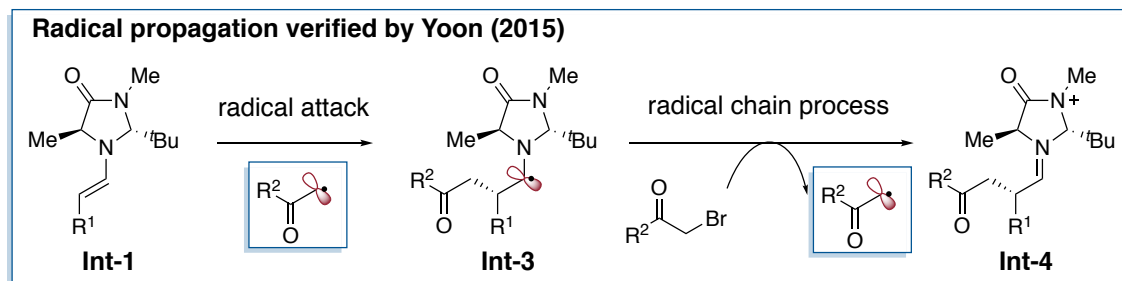
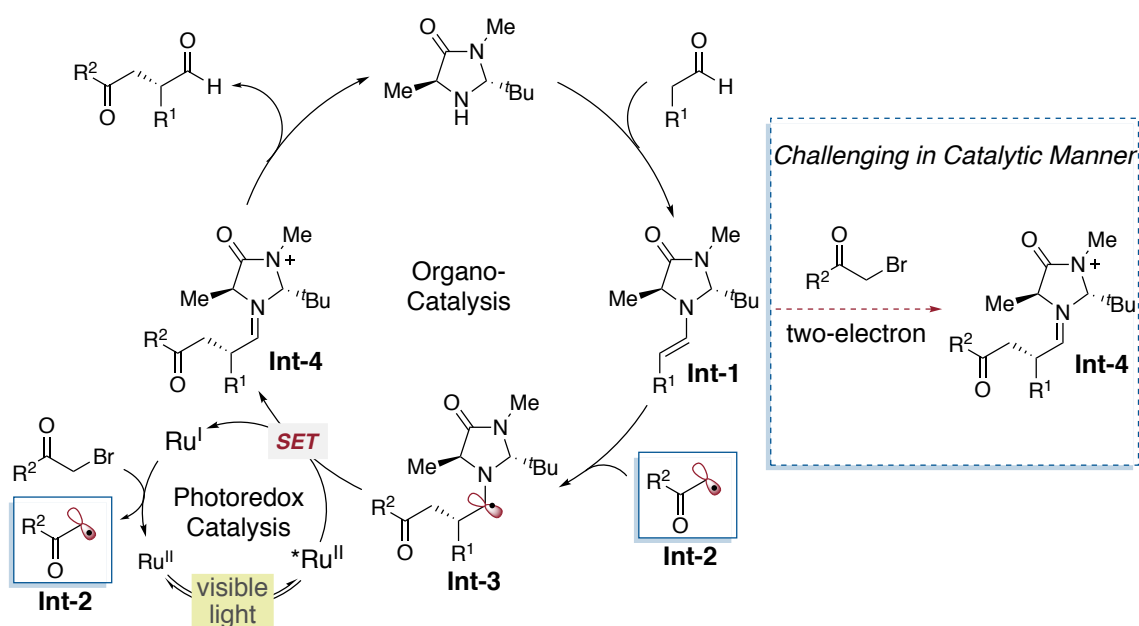
#### 1.4. The Renaissance of Homogeneous Visible Light Photoredox Catalysis

As judged by the wealth of literature data, it is evident that visible light photoredox catalysis has witnessed a renaissance. This is largely due to the seminal work of MacMillan<sup>24</sup> and Yoon,<sup>25a</sup> inevitably contributing to the adoption of visible light photocatalysis as a new tool to build up molecular complexity under exceptionally mild reaction conditions.<sup>25b</sup> It is worth noting that there is a vast literature data on heterogeneous photoredox catalysis that have showed to be a powerful, yet practical, alternative to the conventional homogeneous photoredox scenarios.<sup>26a,26b</sup> However, this area of expertise will not be treated here, as this PhD thesis is focused on the development of homogeneous photoredox scenarios.

### 1.4.1 Merging Organocatalysis with Visible Light Photoredox



**Scheme 1.4. The Synergy of organocatalysis and Photoredox**



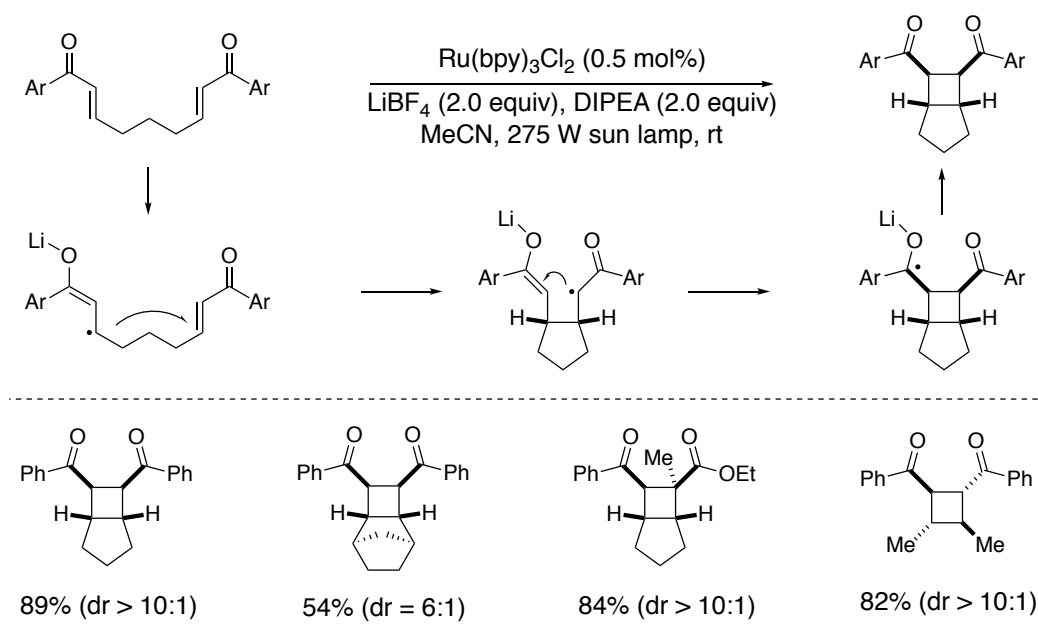
**Scheme 1.5. The mechanism of the synergy of organocatalysis and photoredox**

MacMillan and Nicewicz made use of  $\text{Ru}(\text{bpy})_3(\text{II})$  as visible light photoredox catalysts to meet the long-standing challenge of an asymmetric alkylation of aldehydes that was particularly difficult via

classical 2-electron pathways (Scheme 1.4).<sup>24</sup> The reaction proceeded via generation of an electron-deficient radical **Int-2** that might react efficiently with an electron-rich chiral enamine **Int-1**. The resulting  $\alpha$ -amino radical **Int-3** can then be oxidized by photoexcited Ru(II)\* via SET to produce ground state photocatalyst and an iminium ion **Int-4** that ultimately deliver the alkylated aldehyde by hydrolysis. The transformation proceeded in excellent yields and enantiomeric excesses (*ee*) for a range of alkyl aldehydes and  $\alpha$ -carbonyl bromides. While a canonical oxidative quenching was claimed by MacMillan, the Yoon group demonstrated later on that this assumption was better described as a chain-propagation event by measuring the quantum yield of these reactions (Scheme 1.5, *bottom*).<sup>47</sup>

### 1.4.2. Visible Light Photoredox Promoted Cycloaddition

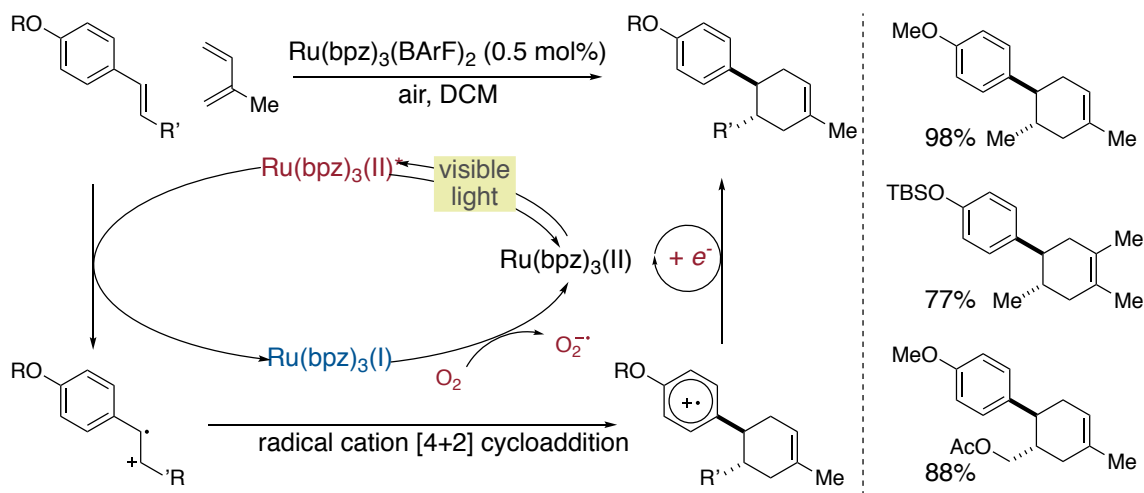
Concurrently with MacMillan's work, Yoon and co-workers demonstrated the ability of Ru(bpy)<sub>3</sub>(II) photocatalysts to trigger intramolecular [2+2]-cycloadditions under visible light irradiation instead of conventional UV-light (Scheme 1.6).<sup>25</sup> The reaction was initiated by reductive quenching, with the lithium salt proposed to facilitate the SET reduction of the enone to the radical anion, followed by radical addition to furnish the desired product with excellent diastereoselectivities (*dr*).



**Scheme 1.6. Photoredox catalyzed [2+2] cycloaddition**

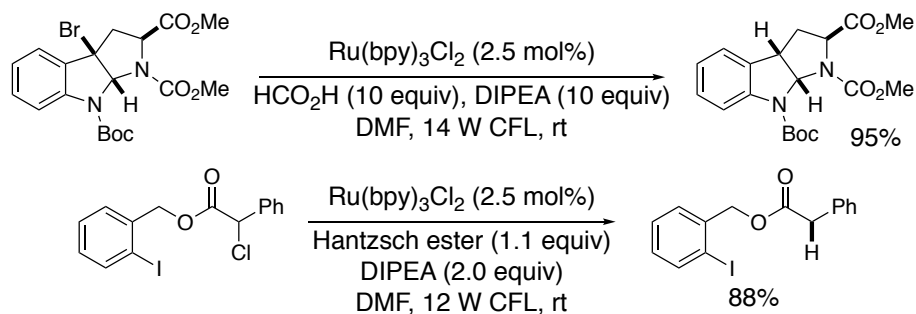
In addition to the intramolecular [2+2] cycloaddition, Yoon and co-workers reported another system using a more oxidizing photocatalyst Ru(bpz)<sub>3</sub>(II) to promote intermolecular radical cation Diels-Alder cycloaddition.<sup>48</sup> Specifically, the excited Ru(bpz)<sub>3</sub>(II)\* ( $E_{1/2}^{\text{II}*/\text{I}} = +1.45$  V vs SCE) was able to directly oxidize the *trans*-anethole ( $E_{1/2}^{\text{red}} = +1.2$  V vs SCE) (Scheme 1.7). The corresponding radical

cation was found to couple isoprene, giving rise to a radical cation adduct that subsequently ends up in the neutral species by a final single-electron transfer from either oxygen or Ru(bpz)<sub>3</sub> (I). Interestingly, higher yields were obtained under air, presumably because the turnover of the ruthenium catalyst could be improved by oxygen. Importantly, the radical ionic Diels-Alder-type reaction was found to be orthogonal with conventional thermal [2+4] cycloaddition, as the coupling reaction efficiently delivers the targeted product with two electron-rich partners.<sup>49</sup>



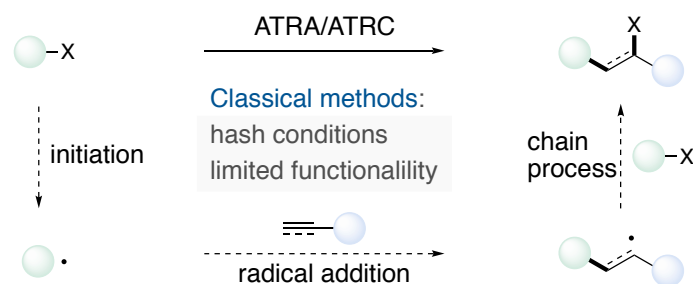
**Scheme 1.7. Radical cation Diels-Alder cycloaddition**

### 1.4.3. Visible Light Photoredox Promoted Dehalogenation and Atom Transfer Radical Addition



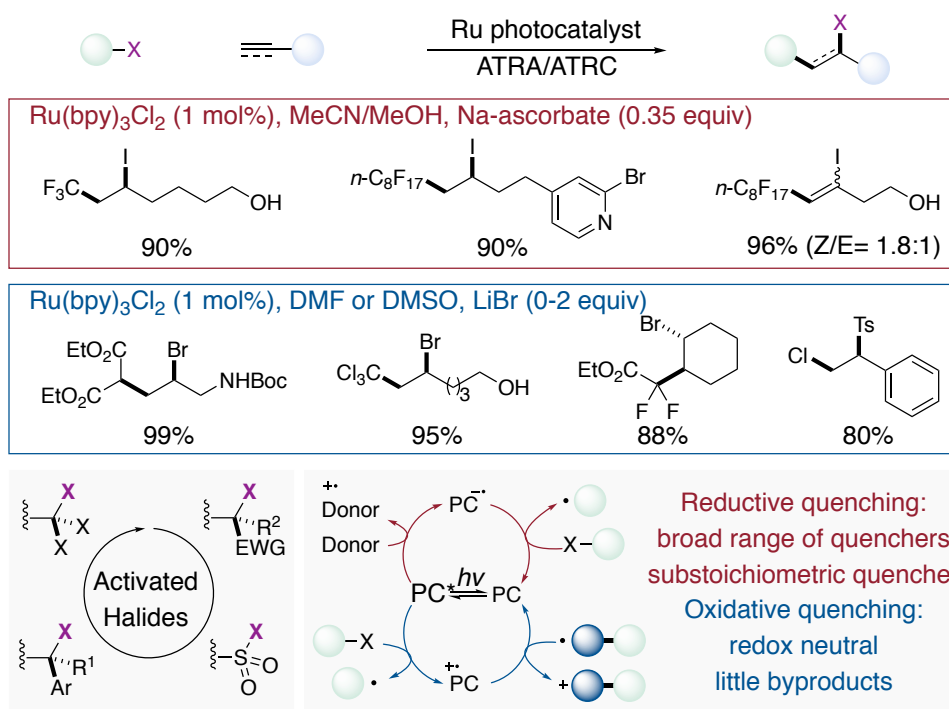
**Scheme 1.8. Visible light photoredox catalyzed photodehalogenation**

Independently from MacMillan and Yoon's reports, Stephenson described a photodehalogenation of activated halides under tin-free conditions,<sup>50</sup> representing a complementary approach to the studies reported by Kellogg,<sup>13</sup> Fukuzumi-Tanaka,<sup>19,21</sup> and Kern-Sauvage (Scheme 1.8).<sup>20</sup>



**Scheme 1.9. Classical Atom Transfer Radical Addition Procedure**

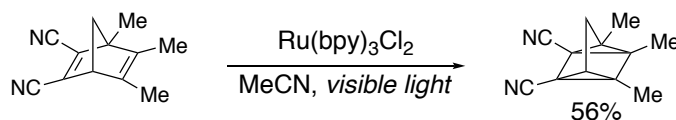
Atom transfer radical addition (ATRA) reactions rank among one of the most fundamental reactions within the organic synthesis toolbox, and is characterized by the formal addition of halogenated compounds across a  $\pi$ -component such as alkenes or alkynes.<sup>51,52</sup> The synthetic interest of this transformation relies on its high efficiency and atom-economy, in which two new C–C and C–halogen bonds are simultaneously formed, thus constituting a rather powerful technique for preparing complex halogenated species that can be used for further functionalization (Scheme 1.7). Historically pioneered by Kharasch,<sup>53,54</sup> this field has been extensively developed by the elegant contributions from Curran<sup>55-61</sup>, Oshima<sup>62-64</sup> or Renaud,<sup>65-67</sup> among others.<sup>68,69</sup> Generally, ATRA reactions proceed through a radical chain process, typically requiring stoichiometric amounts of toxic and hazardous initiators such as peroxides, organotin reagents or triethylboron. While other initiators have been employed for similar purposes,<sup>70-77</sup> the moderate functional group tolerance has hampered the application profile of ATRA reactions.



### Scheme 1.10. Photoredox promoted ATRA/ATRC with activated halides

Prompted by its interest in photoredox catalysis, the Stephenson group disclosed an efficient atom transfer radical addition or cyclization (ATRA/ATRC) enabled by visible light photoredox catalysis. The reactions can be performed with either reductive quenching pathway or oxidative quenching pathway with activated halides (Scheme 1.8).<sup>78,79</sup> These transformations are distinguished by the mild condition, broad functional group tolerance and excellent substrate scope, allowing to prepare a wide range of fluorinated compounds. In a formal sense, this study showcased the potential of photoredox catalysis for ATRA-type transformations, suggesting that the implementation of more complex scenarios would a priori be within reach.<sup>52,81</sup>

#### 1.4.4. Photochemical Transformations Enabled by Triplet Energy Transfer

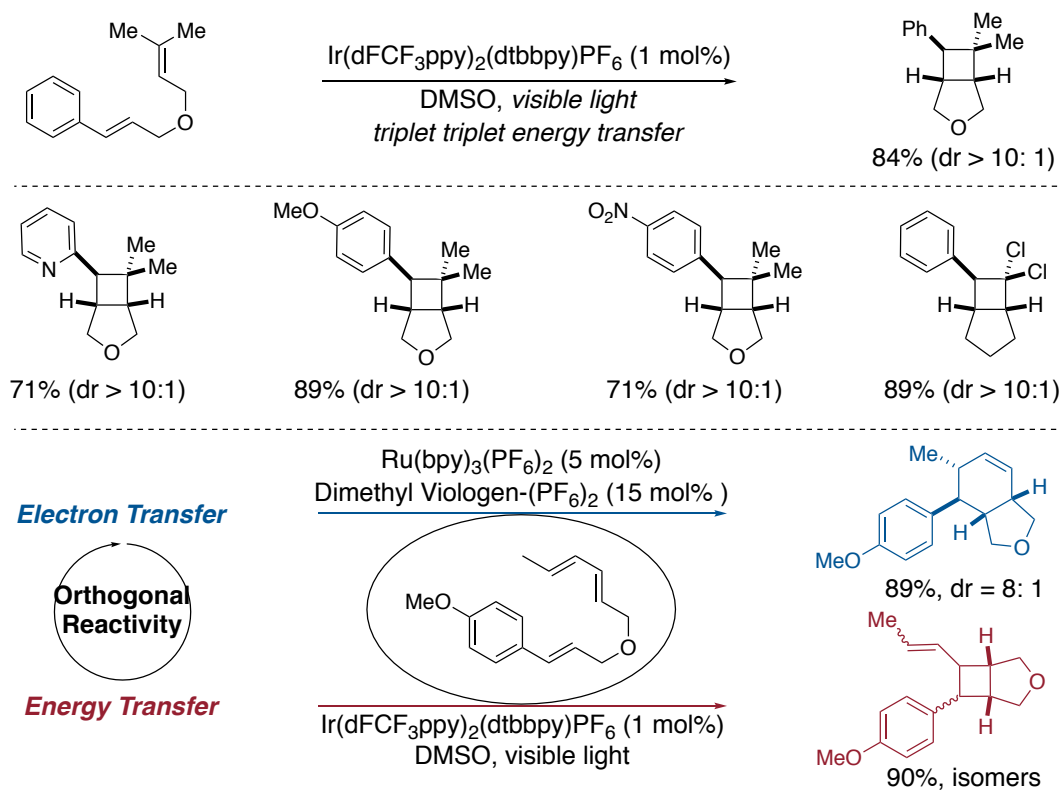


### Scheme 1.11. An Early Example of [2+2] Cycloaddition via Energy Transfer

Despite the advances realized in photoredox catalysis, it is somewhat surprising that a rather limited number of organic transformations are driven by triplet energy transfer. In 1986, it was shown that  $\text{Ru}(\text{bpy})_3$  promoted the intermolecular [2+2] cycloaddition of substituted norbornadiene under visible light irradiation via triplet-triplet energy transfer (Scheme 1.9).<sup>82</sup> The dramatic mismatch of redox potential between the 1,3-diene ( $E_{1/2}^{0/-1} = -1.39 \text{ V}$ ,  $E_{1/2}^{+/0} = +1.82 \text{ V}$ , vs SCE) and  $\text{Ru}(\text{bpy})_3^*$  ( $E_{1/2}^{\text{II}*/\text{I}} = -0.81 \text{ V}$ ,  $E_{1/2}^{\text{III}/\text{II}^*} = +0.77 \text{ V}$ , vs SCE) indicated a disfavored electron transfer pathway. Further evidence about triplet energy transfer pathway was gained under UV light irradiation, enabling the transformation in a rather efficient manner.

Yoon and co-workers demonstrated that the success of previously reported cycloaddition reactions (Scheme 1.6 and Scheme 1.7) highly relied on the redox potential of the substrates and photocatalysts. Specifically, only electron-deficient alkenes that can be easily reduced or olefins that are particularly prone to oxidation could be utilized. Driven by these observations, Yoon disclosed a [2+2] cycloaddition via energy transfer (Scheme 1.12, *top*), in which electron-rich, neutral and deficient alkenes efficiently underwent the targeted cyclization.<sup>83</sup> Taking into consideration the redox potentials of the styrene ( $E_{1/2}^{\text{red}} = +1.42 \text{ V}$  vs SCE) and the oxidation potential of **Ir-3\*** ( $E_{1/2}^{\text{III}*/\text{II}} = +1.21 \text{ V}$  vs SCE), a pathway consisting of an electron transfer process was highly unlikely. A close look at the triplet energies, however, indicated that a triplet-triplet energy transfer was more likely ( $E_{\text{T}}$  (styrene) = 60 kcal/mol vs  $E_{\text{T}}$  (**Ir-3\***) = 61 kcal/mol). This interpretation gained credence by the

observation that the more strongly oxidizing **Ru-3** ( $E_{1/2}^{\text{III}*/\text{II}} = +1.45 \text{ V vs SCE}$ ) possessing a lower triplet energy ( $E_T = 47.4 \text{ kcal/mol}$ ) did not catalyze the cycloaddition reaction. These observations suggested that orthogonal cycloadditions could be implemented by either electron transfer or energy transfer; as shown in Scheme 1.12 (*bottom*), this turned out to be the case, obtaining different products depending on the photocatalyst utilized.



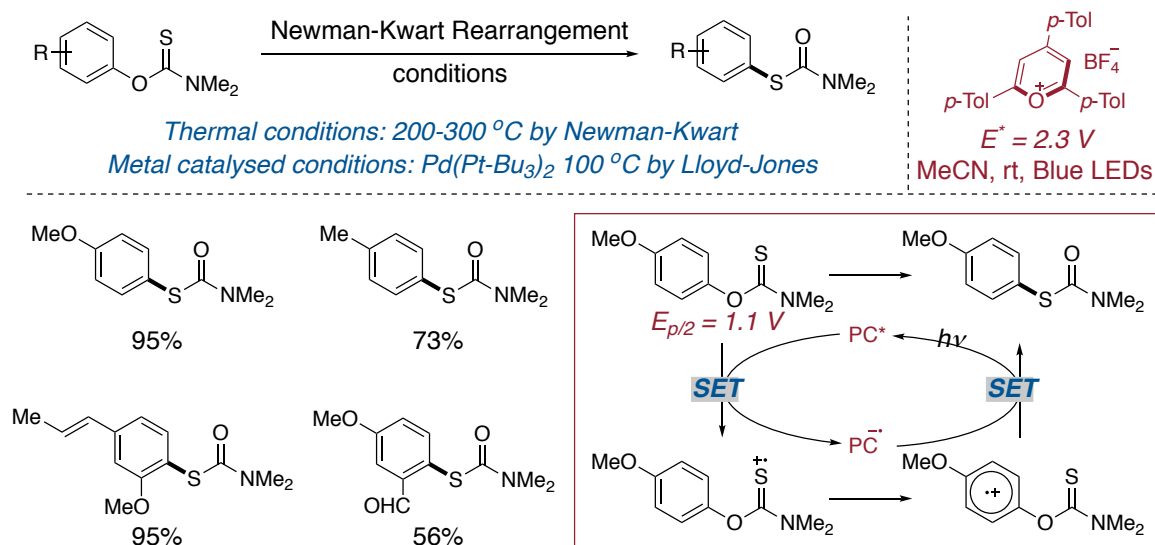
**Scheme 1.12. Orthogonal Cycloaddition Enabled by Energy Transfer**

## 1.4.5. Photochemical Transformations Enabled by Non-Metal Based Visible Light Photoredox

### 1.4.5.1. Non-Metal Based Visible Light Photocatalyst Enabled Photochemical Reactions

Despite the versatility of Ru(II) and Ir(III) photocatalysts in a wide number of chemical transformations under visible light irradiation, the high price and limited supply of these noble metals reinforce a change in strategy. Although some efforts have been made with earth-abundant Fe or Cu

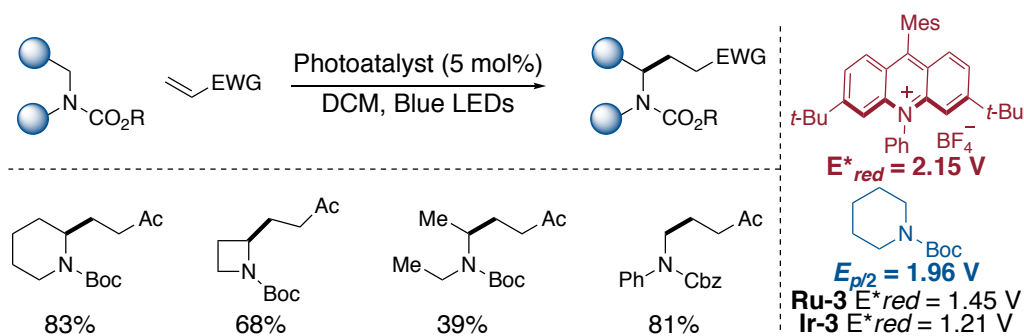
photocatalysts, chemists have recently been challenged to come up with non-metal-based alternatives with improved practicality and generality.<sup>84a</sup>



### Scheme 1.13. Visible light photoredox promoted Newman-Kwart rearrangement

Driven by the observation that Newman-Kwart rearrangements<sup>84b</sup> – undoubtedly one of the most important methods to prepare thiophenols – typically require harsh conditions (200-300 °C) and exclusion of air and moisture, a number of alternative methods have been proposed to trigger these reactions. Although Lloyd-Jones described a rather powerful protocol for effecting Newman-Kwart rearrangements based on Pd(0) catalysts, high temperatures and a rather limited substrate scope was found.<sup>84c</sup> Indeed, electron-rich substrates were not particularly prone for C–S bond-formation, thus remaining an elusive goal in these endeavors. Aiming at providing a solution for these challenges, Nicewicz demonstrated that a photoredox strategy based on pyrylium photocatalysts might provide a conceptually new approach for Newman-Kwart rearrangements.<sup>84d</sup> Specifically, it was found that electron-rich substrates were particularly efficient for such transformation, an argument that goes in line with the ease for triggering a SET-oxidation (Scheme 1.13). The resulting radical cation facilitates an intramolecular attack at the *ipso* position, thus representing a complementary approach to classical Newman–Kwart Rearrangements based on either electron-neutral or electron-poor arenes.<sup>84e</sup>





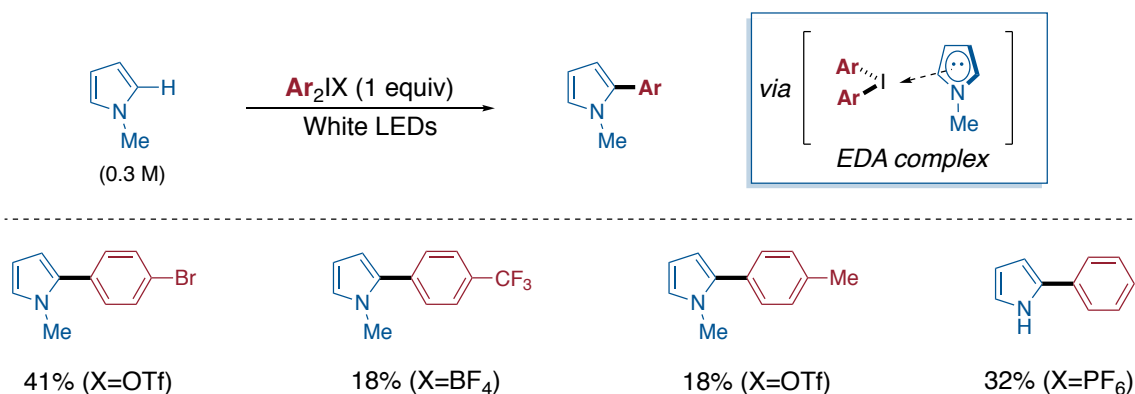
**Scheme 1.14. Alkylation of amide enabled by selective oxidation potential**

The versatility of organic photocatalysts capable of triggering a rather uphill SET oxidation was further demonstrated by Nicewicz in the  $\alpha$ -alkylation of amide backbones (Scheme 1.14).<sup>84f</sup> Indeed, *N*-Boc amines typically require about 1.96 V to be oxidized to the corresponding  $\alpha$ -amido radical, an unrealistic scenario with classical Ir or Ru complexes; however, the utilization of acridinium salts as photocatalysts enable the  $\alpha$ -alkylation of *N*-Boc amines with a wide range of  $\alpha,\beta$ -unsaturated carbonyls, thus serving as a testament to the possibilities that organic photocatalysts might offer in organic chemistry.

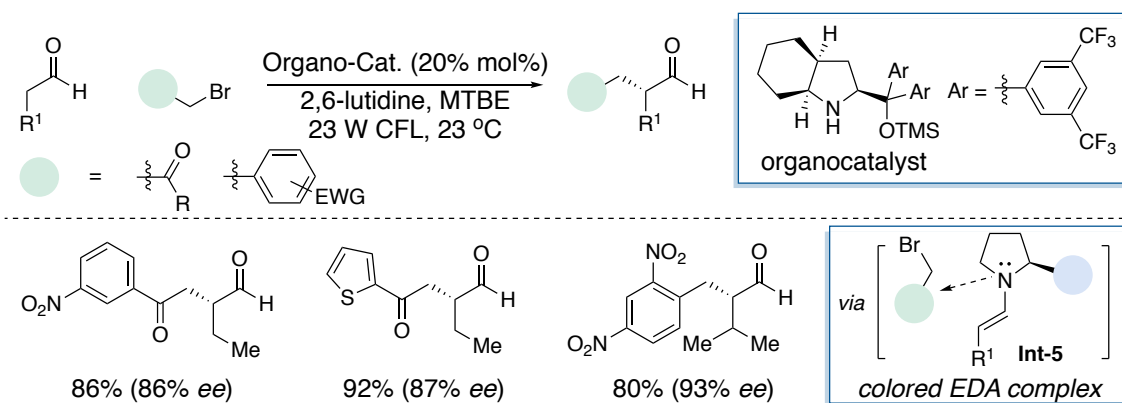
Inspired by the ability of biological photosynthesis to promote the oxidation of water via multiple photon excitation, König described that consecutive photoinduced electron transfer could be used in organic synthesis.<sup>84g</sup> Specifically, it was found that the in situ generated radical anion of perylene bisimide (PDI) is colored and reasonably stable in the ground state, thus being readily available for an additional excitation by visible light, thus yielding a more reducing species (Scheme 1.15, *bottom left*). Such ability to be engaged in successive photon excitations was turned into a strategic advantage to promote the rather uphill reduction of aryl bromides, including the always-elusive aryl chlorides via the formation of aryl radical species (Scheme 1.15, *top*).



Prompted by the inherent synthetic potential of EDA complexes to trigger SET, it comes as no surprise that these transformations recently attracted considerable interest at the Community.

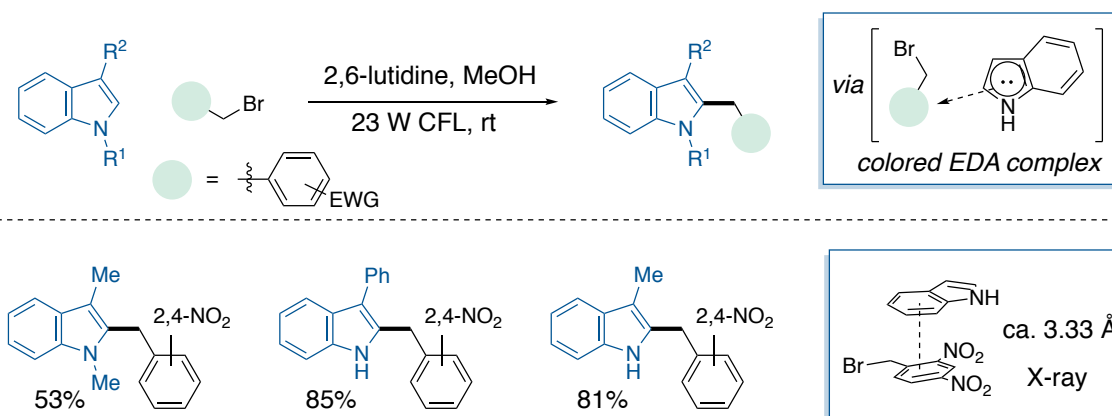


An early example on the potential of EDA complexes was discovered by Chatani and co-workers in 2013 (Scheme 1.17).<sup>84k</sup> Specifically, it was found that a photochemical arylation of pyrroles could be effected with diaryl iodonium salts in the absence of an external photocatalyst under white LED irradiation, suggesting the involvement of a colored EDA complex between the electron-rich pyrrole and the electron-deficient diaryl iodonium salt.



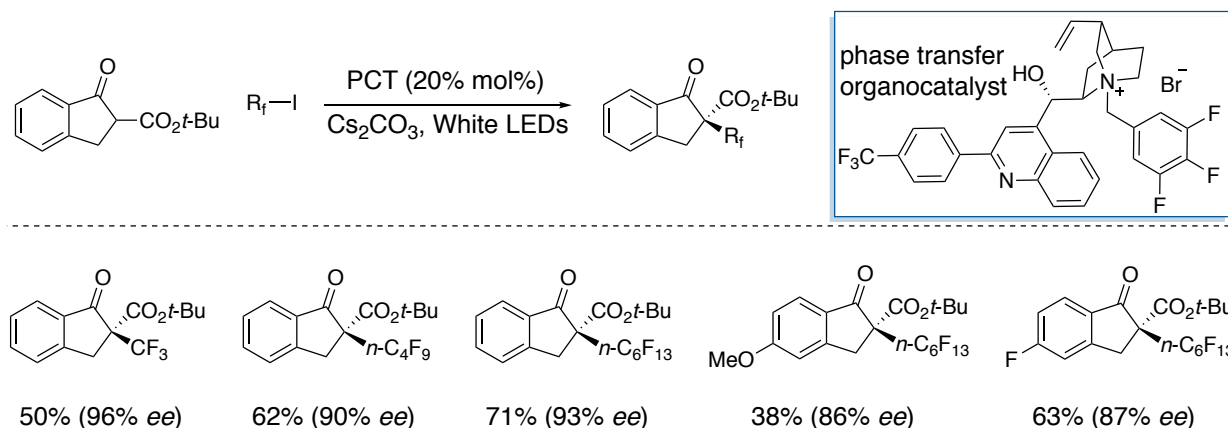
In the same year, Melchiorre and co-workers uncovered complementary radical pathways by irradiating in situ generated organic intermediates in the absence of photoredox catalysis, resulting in a highly enantioselective  $\alpha$ -alkylation of aldehydes with activated alkyl bromides and Hayashi-Jørgensen type organic catalyst (Scheme 1.18).<sup>84l</sup> Control experiments indicated that none of the starting precursors absorbed light in visible region; however, a ground-state colored substance was obtained upon mixing both precursors, revealing a new absorption band in the visible range. Such colored entity ended up being an EDA complex that resulted from the combination of electron-rich

enamine and the electron-deficient alkyl bromide, leading to a single-electron transfer process via inner-sphere mechanisms. The corresponding radical intermediate followed a similar reaction outcome to that of Scheme 1.4 via either an organocatalytic cycle or a chain-propagation process. While a significant step-forward, the catalytic  $\alpha$ -alkylation of aldehydes with unactivated alkyl electrophiles is still beyond reach.<sup>24,84l</sup>



**Scheme 1.19. EDA complex enabled alkylation of indole**

In 2015, Melchiorre's group reported the alkylation of indole following an otherwise identical mechanistic rationale (Scheme 1.19).<sup>84m</sup> In this case, however, the authors managed to isolate and fully characterize the EDA complex by X-ray crystallographic analysis. The measured distance between two aromatic rings was ca. 3.33 Å, which is significantly shorter than the usual van der Waals radii between two aromatic molecules (3.40 Å).

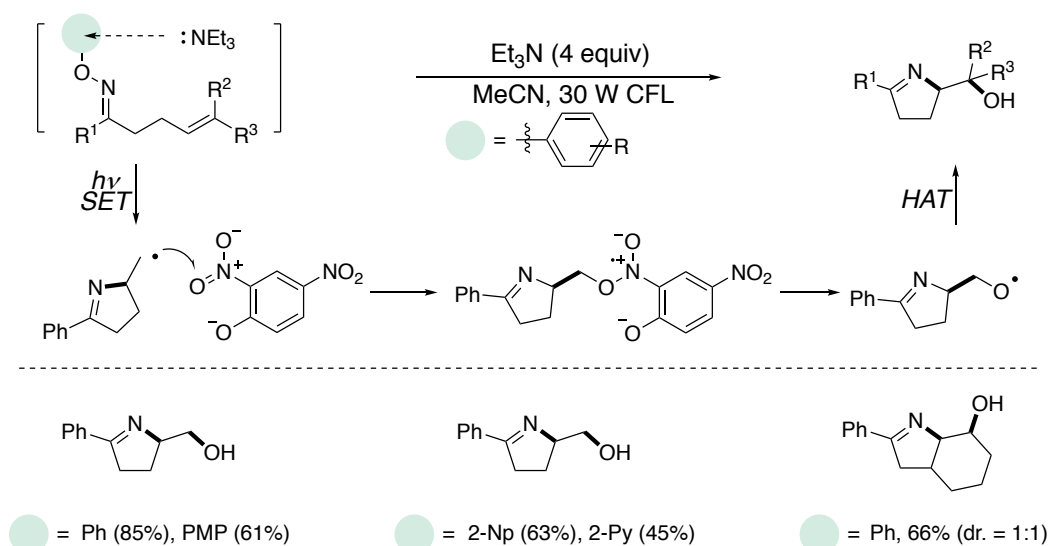


**Scheme 1.20. EDA complex enabled perfluoroalkylation of  $\beta$ -ketoester**

Concurrently, the Melchiorre group described that the formation of EDA complexes was not limited to the utilization of nitrogen-containing nucleophiles. Indeed, it was demonstrated that the  $\alpha$ -

alkylation of  $\beta$ -ketoesters with a wide range of perfluoroalkyl iodides could be affected in the presence of phase transfer catalysis under visible light irradiation.<sup>84n</sup>

Simple tertiary amines could also form the EDA complex in the presence of an appropriate electron acceptor. In 2015, the Leonori group (Scheme 1.21) disclosed an intramolecular iminohydroxylation of alkene via cyclization of *N*-centered radical initiated by the formation of an EDA complex between triethylamine ( $E_{\text{red}}^{1/2} = -0.76\text{V}$  vs SCE in MeCN) and aryl hydroxylamine (Ar = 2,4-NO<sub>2</sub>C<sub>6</sub>H<sub>4</sub>,  $E_{\text{red}}^{1/2} = -0.55\text{V}$  vs SCE in MeCN).<sup>84o</sup> In the absence of hydrogen donor, the nitro group in phenoxy anion leaving group served as oxidant to convert the carbon radical into a hydroxyl group. Interestingly, a wide range of aryl oximes bearing either electron-rich or electron-deficient substituents could all successfully afford the desired product.



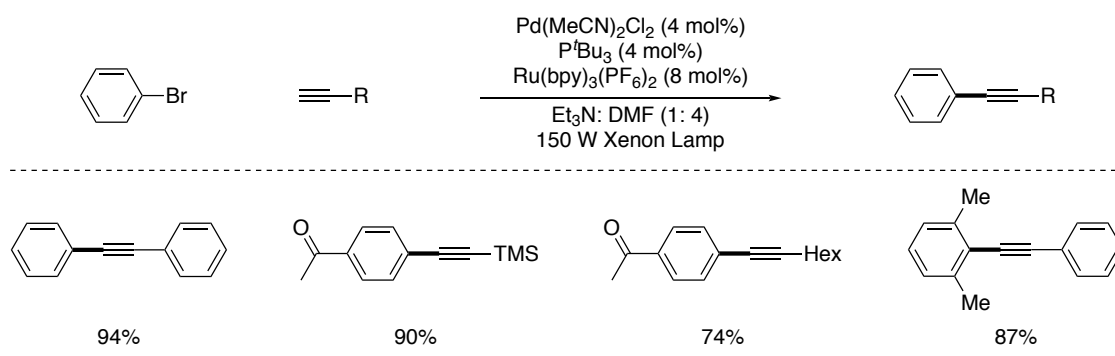
**Scheme 1.21. EDA complex enabled intramolecular iminohydroxylation of alkene**

## 1.5. Merging Photoredox with Transition Metal Catalysis: Metallaphoredox Catalysis

### 1.5.1. The Initiation: Palladium Metallaphotocatalysis

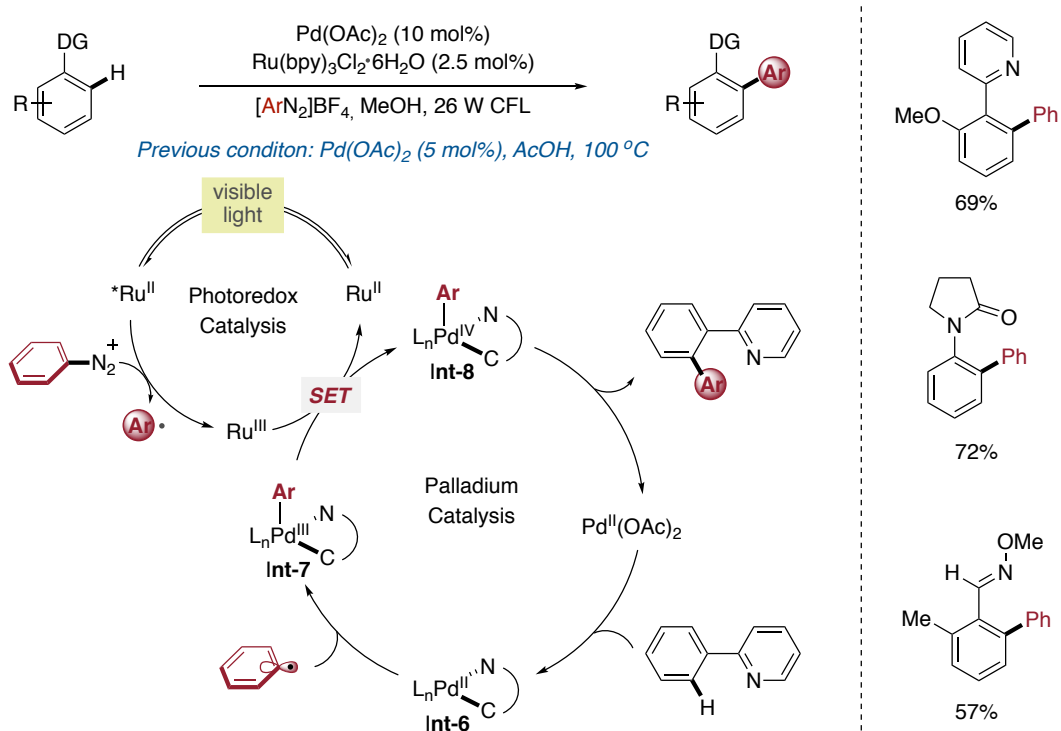
The prospective potential of combining visible light photoredox catalysis with transition metal catalysis was first recognized in 2007 by Osawa, who successfully developed a protocol containing both Pd(II) and Ru(II) catalysts for promoting a Sonogashira coupling of aryl bromides and terminal alkynes (Scheme 1.22).<sup>85</sup> This seminal contribution demonstrated that the inclusion of a photocatalyst and high-energy irradiation dramatically enhanced the efficiency of the Sonogashira coupling in the absence of conventional Cu catalysts, allowing to couple even sterically hindered substrate combinations. Although no mechanistic investigations were conducted, the authors claimed that the

photoexcited  $\text{Ru}(\text{bpy})_3^*$  catalyst had an effect on the oxidative addition of the aryl bromide to  $\text{Pd}(0)\text{L}_n$ .



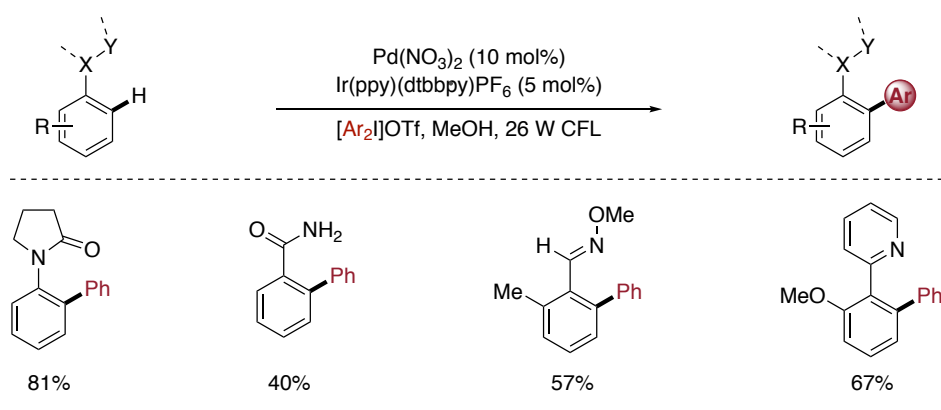
**Scheme 1.22. Dual photoredox/Pd-catalyzed Cu-free Sonogashira coupling**

Inspired by Osawa's seminal work,<sup>85</sup> Sanford designed a dual catalytic Pd/photoredox catalysis for a directed  $sp^2$  C–H arylation with aryl diazonium salts, affording *o*-substituted biaryl compounds under mild reaction conditions (Scheme 1.23).<sup>86</sup> Unlike classical two-electron oxidation techniques requiring elevated temperatures and acidic media,<sup>87</sup> the presence of  $\text{Ru}(\text{bpy})_3\text{Cl}_2$  in MeOH under visible light irradiation provided the desired C–H arylation at room temperature with high chemoselectivity profile. Based on the work of Deronzier,<sup>16</sup> Sanford suggested that the aryl radical generated from the aryldiazonium salt via oxidative quenching could be recombined with **Int-6**, giving rise to **Int-7** that could be further oxidized to Pd(IV) **Int-8** by Ru(III) via SET. Finally, a fast reductive elimination from **Int-8** delivers the desired product. Theoretical calculations suggested that an alternative mechanism involving reductive elimination from Pd(III) **Int-7** and subsequent oxidation of the Pd(I) species to Pd(II) catalyst by the oxidized photocatalyst could not be ruled out.<sup>88</sup>



**Scheme 1.23. Dual photoredox/Pd-catalyzed *ortho*-directed C-H arylation with diazonium salt**

Subsequently, Sanford described a follow-up protocol employing air and moisture stable diaryliodonium salts in the presence of a stronger reducing photocatalyst  $\text{Ir}(\text{ppy})_2(\text{dtbbpy})(\text{PF}_6)$  (5 mol%) and  $\text{Pd}(\text{NO}_3)_2$  (10 mol%) as precatalyst (Scheme 1.24).<sup>89</sup> Beyond any reasonable doubt, the seminal studies highlighted above provided the fundamental blueprint for inspiring the development of metallaphotoredox reactions to build up molecular complexity.<sup>90-97</sup>

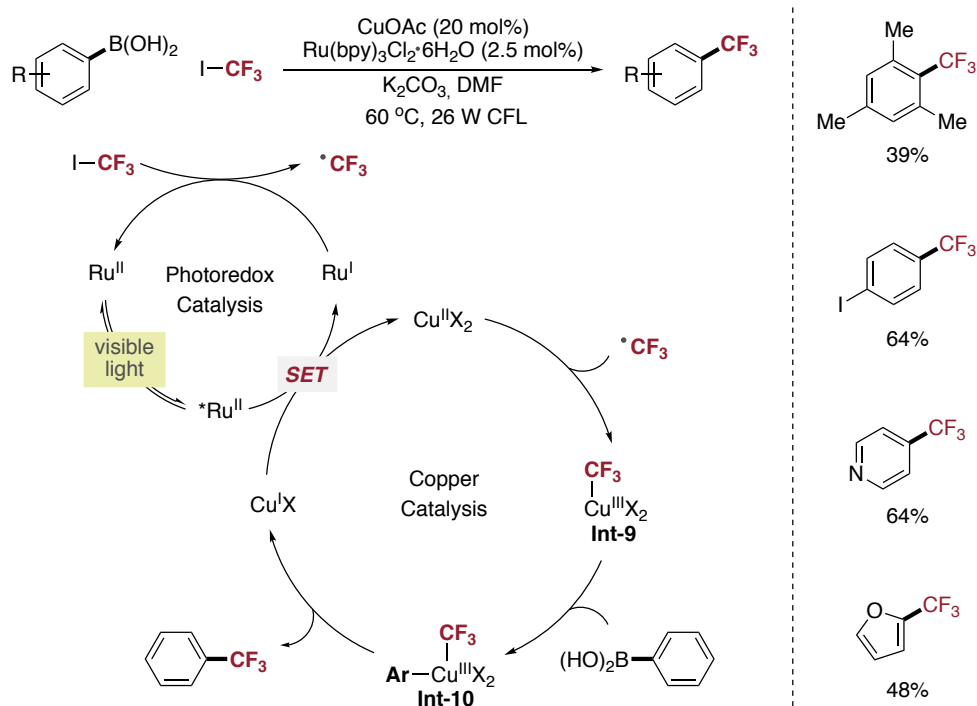


**Scheme 1.24. Dual photoredox/Pd-catalyzed *ortho*-directed C-H arylation with iodonium salt**

### 1.5.2. Copper Metallaphotocatalysis

Prompted by the utmost significant relevance of trifluoromethyl arenes for enhancing metabolic stability, Sanford designed a Cu-catalyzed trifluoromethylation enabled by  $\text{Ru}(\text{bpy})_3\text{Cl}_2$  species

(Scheme 1.25).<sup>99</sup> The reaction was believed to proceed via a reductive quenching pathway, thus generating a Cu(II) intermediate and Ru(I) species upon visible light irradiation. A trifluoromethyl radical is then generated via reduction of CF<sub>3</sub>I by the Ru(I) complex, leading to the regeneration of Ru(II). Subsequently, the CF<sub>3</sub> radical is captured by the Cu(II) intermediate to afford a Cu(III) **Int-9** complex, setting the scene for a transmetalation with the aryl boronic acid under basic conditions to give **Int-10** followed by reductive elimination.<sup>100,101</sup>



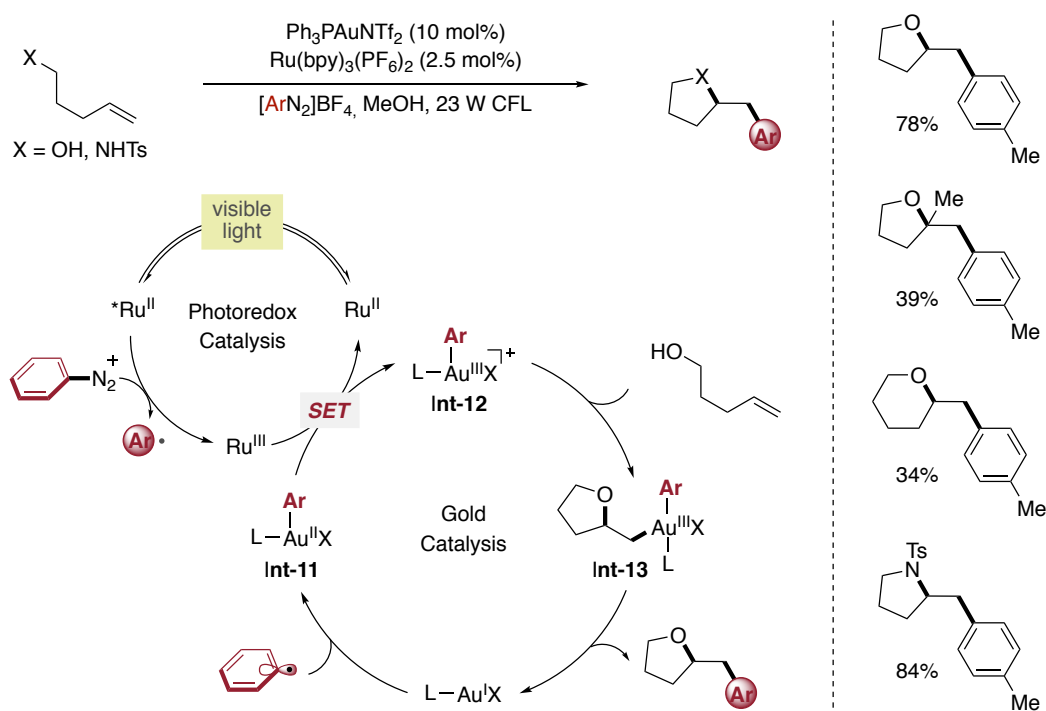
**Scheme 1.25. Dual photoredox/Cu-catalyzed trifluoromethylation of aryl boronic acids**

### 1.5.3. Gold metallaphotocatalysis

The merger of photoredox and gold catalysis was first recognized by Glorius and co-workers in 2013 (Scheme 2.26).<sup>102</sup> Specifically, it was demonstrated that a dual catalytic system enabled the oxyarylation/aminoarylation of unactivated  $\gamma$ -hydroxyalkenes,  $\gamma$ -aminoalkenes or  $\delta$ -hydroxyalkenes with aryldiazonium salts to give access to benzylated heterocyclic tetrahydrofurans, pyrrolidines and tetrahydropyrans. In contrast to previous reports on oxidative gold-catalyzed heteroarylations of alkenes,<sup>103,104</sup> this method avoided the use of strong external oxidizing agents such as Selectfluor, hypervalent iodine reagents or tBuOOH, which limited the substrate scope of previously-reported processes. Notably, high diastereoselectivities were observed when internal alkenes were used, an observation that is consistent with a trans-selective oxyauration and a stereoretentive reductive elimination from the Au(III) complex **Int-13**. In addition, the concept could be further expanded to accomplish intermolecular, three-component couplings of alkenes, methanol and aryldiazonium (or



diaryliodonium) salts.<sup>105</sup> In their original report, aryl radical capture was initially proposed to occur after Au(I)-mediated 5/6 exo-trig cyclization; however, subsequent computational and stoichiometric studies<sup>105-107</sup> suggested that the aryl radical was trapped by Au(I) prior to cyclization, resulting in a Au(II) complex that was oxidized to Au(III) by the Ru(III) photocatalyst. A rapid oxyl/amino cyclization followed by reductive elimination from **Int-13** led to the targeted product while recovering back the Au(I) complex. The ability to access Au(III) by means of photoredox catalysis was particularly important, allowing to apply this technology in multiple endeavors.<sup>109-117</sup>



**Scheme 1.26. Gold metallaphotoredox catalyzed intramolecular oxyl/amino arylation**

## 1.6. Summary

This chapter describes the evolution of homogeneous photoredox catalysis from its inception, including the general description of the photophysical and electrochemical properties of the corresponding photocatalysts, showing the prospective potential that these technologies at the Community. In a relatively short period of time, these methods have not showed only the ability to improve existing non-photoredox transformations, but also offered a conceptually new manifold to build up molecular complexity via SET or ET processes, holding promise to revolutionize approaches in organic synthesis. While this field has gained considerable momentum, several aspects need to take into consideration: (1) the high cost and limited supply of noble iridium photocatalysts that are commonly employed in photoredox transformations; (2) the implementation of scale-up processes

necessarily require engineering such as flow chemistry techniques; (3) a cheap and convenient standardized photochemical device remains to be invented for bench studies; (4) the pioneering vision from Ciamician back in 1912 about the use of solar energy still remains to be fully implemented in the photoredox arena.

### 1.7. General Objective of this Doctoral Thesis

The last decade has witnessed the dramatic development of visible light photoredox catalysis, enabling the implementation of a wide number of previously inaccessible transformations that occur via either SET or ET processes under exceptionally mild conditions. Despite the numerous advances realized, the functionalization of particularly inert chemical bonds still remains rather underexplored. Prompted by the inherent interest of the Martin group for designing new methods for activating a priori unreactive chemical bonds, the following thesis is aimed at providing new photoredox techniques capable of enabling a series of C–C bond-forming reactions that otherwise would be beyond reach using classical metal-catalyzed manifolds. To such end, the following objectives will be taken into consideration:

- To expand the visible light promoted ATRA/ATRC to accommodate the use of *unactivated alkyl halides*, a current limitation not yet explored within the photoredox arena.
- To develop a dicarbofunctionalization of olefins with *carbon dioxide* as coupling partner under photoredox conditions, allowing to meet an elusive goal in conventional metal-catalyzed carboxylation technologies.
- To unlock new concept for functionalizing *native  $sp^3$  C-H bonds* by the synergy of non-noble metal-based photocatalysts and nickel catalysts.

## 1.8. Bibliography

1. Ciamician, G. The Photochemistry Of The Future. *Science* **1912**, *36*, 385.
2. Fagnoni, M., Dondi, D., Ravelli, D., Albini, A. Photocatalysis For The Formation Of The C–C Bond. *Chem. Rev.* **2007**, *107*, 2725.
3. Schultz, D. M., Yoon, T.P. Solar Synthesis: Prospects In Visible Light Photocatalysis. *Science* **2014**, *343*, 1239176.
4. Burstall, F. H. Optical Activity Dependent On Coordinated Bivalent Ruthenium. *J. Chem. Soc.* **1936**, 173.
5. Tucker, J. W., Stephenson, C. R. J. Shining Light On Photoredox Catalysis: Theory And Synthetic Applications. *J. Org. Chem.* **2012**, *77*, 1617.
6. Juris, A., Balzani, V., Barigelletti, F., Campagna, S., Belser, P., Von Zelewsky, A. Ru(II) Polypyridine Complexes: Photophysics, Photochemistry, Electrochemistry, And Chemiluminescence *Coord. Chem. Rev.* **1988**, *84*, 85-277.
7. Campagna S., Puntoriero F., Nastasi F., Bergamini G., Balzani V. Photochemistry And Photophysics Of Coordination Compounds: Ruthenium. *Top. Curr. Chem.* **2007**, *280*, 117.
8. Kalyanasundaram, K. Photophysics, Photochemistry And Solar Energy Conversion With Tris(Bipyridyl)Ruthenium(II) And It's Analogues. *Coord. Chem. Rev.* **1982**, *46*, 159.
9. Ayele, D.W., Su, W.-N., Rick, J., Chen, H.-M., Pan, C.-J., Akalework, N.G., Hwang, B.-J. Advances In Organometallic Chemistry And Catalysis *Wiley, NY*, **2013**, 501.
10. Navarro Yerga, R. M., Álvarez Galván, M. C., Del Valle, F., Villoria De La Mano, J. A., Fierro, J. L. G. *Chemsuschem* **2009**, *2*, 471.
11. Kudo, A., Miseki, Y. Heterogeneous Photocatalyst Material For Water Splitting. *Chem. Soc. Rev.* **2009**, *38*, 253.
12. Hedstrand, D. M., Kruizinga, W. H., Kellogg, R. M. Light Induced And Dye Accelerated Reductions Of Phenacyl Onium Salts By 1,4-Dihydropyridines. *Tetrahedron Lett.* **1978**, *19*, 1255.
13. Van Bergen, T. J., Hedstrand, D. M., Kruizinga, W. H., Kellogg, R. M. Chemistry Of Dihydropyridines. 9. Hydride Transfer From 1,4-Dihydropyridines To  $Sp^3$ -Hybridized Carbon In Sulfonium Salts And Activated Halides. Studies With NAD(P)H Models. *J. Org. Chem.* **1979**, *44*, 4953.
14. Pac, C., Ihama, M., Yasuda, M., Miyauchi, Y., Sakurai, H. Tris(2,2'-Bipyridine)Ruthenium(2<sup>+</sup>)-Mediated Photoreduction Of Olefin With 1-Benzyl-1,4-Dihydropyridine: A Mechanistic Probe For Electron Transfer Reaction Of NAD(P)H-Model Compounds. *J. Am. Chem. Soc.* **1981**, *103*, 6495.
15. Cano-Yelo, H., Deronzier, A. Photo-Oxidation Of Some Carbinols By Ru(II) Polypyridyl Complex-Aryl Diazonium Salt System. *Tetrahedron Lett.* **1984**, *25*, 5517.
16. Cano-Yelo, H., Deronzier, A. Photocatalysis Of The Pschorr Reaction By Tris-(2,2'-Bipyridyl)Ruthenium(II) In The Phenanthrene Series. *J. Chem. Soc. Perkin Trans.* **1984**, *2*, 1093.
17. Goren, Z., Willner, I. Photochemical And Chemical Reduction Of Vicinal Dibromide Via Phase Transfer Of 4,4'-Bipyridinium Radical: The Role Of Radical Disproportionation. *J. Am. Chem. Soc.* **1983**, *105*, 7764.
18. Maidan, R., Goren, Z., Becker, J. Y., Willner, I. Application Of Multielectron Charge Relays In Chemical And Photochemical Debromination Processes. The Role Of Induced Disproportionation Of N,N'-Dioctyl-4,4'-Bipyridium Radical Cation In Two-Phase Systems. *J. Am. Chem. Soc.* **1984**, *106*, 6217.
19. Hironaka, K., Fukuzumi, S., Tanaka, T. Tris(Bipyridyl)Ruthenium(II)-Photosensitized Reaction Of 1-Benzyl-1,4-Dihydropyridine With Benzyl Bromide. *J. Chem. Soc. Perkin Trans.* **1984**, *2*, 1705.
20. Kern, J.-M., Sauvage, J.-P. Photoassisted C-C Coupling Via Electron Transfer To Benzylic Halides By Bis(Di-Imine) Copper(I) Complex. *J. Chem. Soc. Chem. Commun.* **1987**, 546.
21. Fukuzumi, S., Mochizuki, S., Tanaka, T. J. Photocatalytic Reduction Of Phenacyl Halides By 9,10-Dihydro-10-Methylacridine: Control Between The Reduction And Oxidative Quenching Pathways Of Tris(Bipyridine)Ruthenium Complex Utilizing An Acid Catalysis. *Phys. Chem.* **1990**, *94*, 722.
22. Okada, K., Okamoto, K., Morita, N., Okubo, K., Oda, M. Photosensitized Decarboxylative Michael Addition Through N-(Acyloxy)Phthalimide Via An Electron-Transfer Mechanism. *J. Am. Chem. Soc.* **1991**, *113*, 9401.
23. Prier, C. K., Rankic, D. A., Macmillan, D. W. C. Visible Light Photoredox Catalysis With Transition Metal Complexes: Applications In Organic Synthesis. *Chem. Rev.* **2013**, *113*, 5322.
24. Nicewicz, D. A., Macmillan, D. W. C. Merging Photoredox Catalysis With Organocatalysis: The Direct Asymmetric Alkylation Of Aldehydes. *Science* **2008**, *322*, 77.
25. (a) Ischay, M. A., Anzovino, M. E., Du, J., Yoon, T. P. Efficient Visible Light Photocatalysis Of (2+2) Enone Cycloadditions. *J. Am. Chem. Soc.* **2008**, *130*, 12886; (b) Yoon, T. P. Photochemical Stereocontrol Using Tandem Photoredox-Chiral Lewis Acid Catalysis. *Acc. Chem. Res.* **2016**, *49*, 2307.
26. (a) Hodgson, G. K., Scaiano, J. C. Heterogeneous Dual Photoredox-Lewis Acid Catalysis Using A Single Bifunctional Nanomaterial. *ACS Catal.*, **2018**, *8*, 2914; (b) Savateev, A., Antonietti, M. Heterogeneous Organocatalysis For Photoredox Chemistry. *ACS Catal.*, **2018**, *8*, 9790.
27. Hopkinson, M. N., Tlahuext-Aca, A., Glorius, F. Merging Visible Light Photoredox And Gold Catalysis. *Acc. Chem. Res.* **2016**, *49*, 2261.
28. Arora, A., Weaver, J. D. Visible Light Photocatalysis For The Generation And Use Of Reactive Azolyl And Polyfluoroaryl Intermediates *Acc. Chem. Res.* **2016**, *49*, 2273.
29. Chatterjee, T., Iqbal, N., You, Y., Cho, E. J. Controlled Fluoroalkylation Reactions By Visible-Light Photoredox Catalysis. *Acc. Chem. Res.* **2016**, *49*, 2284.
30. Staveness, D., Bosque, I., Stephenson, C. R. J. Free Radical Chemistry Enabled By Visible Light-Induced Electron Transfer. *Acc. Chem. Res.* **2016**, *49*, 2295.
31. Majek, M., Von Wangelin, A. J. Mechanistic Perspectives On Organic Photoredox Catalysis For Aromatic Substitutions. *Acc. Chem. Res.* **2016**, *49*, 2316.

32. Koike, T., Akita, M. Fine Design Of Photoredox Systems For Catalytic Fluoromethylation Of Carbon–Carbon Multiple Bonds. *Acc. Chem. Res.* **2016**, *49*, 1937.
33. Goddard, J.-P., Ollivier, C., Fensterbank, L. Photoredox Catalysis For The Generation Of Carbon Centered Radicals. *Acc. Chem. Res.* **2016**, *49*, 1924.
34. Dumur, F., Gignes, D., Fouassier, J.-P., Lalevée, J. Organic Electronics: An El Dorado In The Quest Of New Photocatalysts For Polymerization Reactions. *Acc. Chem. Res.* **2016**, *49*, 1980.
35. Margrey, K. A., Nicewicz, D. A. A General Approach To Catalytic Alkene Anti-Markovnikov Hydrofunctionalization Reactions Via Acridinium Photoredox Catalysis. *Acc. Chem. Res.* **2016**, *49*, 1997.
36. Nakajima, K., Miyake, Y., Nishibayashi, Y. Synthetic Utilization Of  $\alpha$ -Aminoalkyl Radicals And Related Species In Visible Light Photoredox Catalysis. *Acc. Chem. Res.* **2016**, *49*, 1946.
37. Reiser, O. Shining Light On Copper: Unique Opportunities For Visible-Light-Catalyzed Atom Transfer Radical Addition Reactions And Related Processes. *Acc. Chem. Res.* **2016**, *49*, 1990.
38. Fabry, D. C., Rueping, M. Merging Visible Light Photoredox Catalysis With Metal Catalyzed C–H Activations: On The Role Of Oxygen And Superoxide Ions As Oxidants. *Acc. Chem. Res.* **2016**, *49*, 1969.
39. Chen, J.-R., Hu, X.-Q., Lu, L.-Q., Xiao, W.-J. Exploration Of Visible-Light Photocatalysis In Heterocycle Synthesis And Functionalization: Reaction Design And Beyond. *Acc. Chem. Res.* **2016**, *49*, 1911.
40. Morris, S. A., Wang, J., Zheng, N. The Prowess Of Photogenerated Amine Radical Cations In Cascade Reactions: From Carbocycles To Heterocycles. *Acc. Chem. Res.* **2016**, *49*, 1957.
41. Jamison, C. R., Overman, L. E. Fragment Coupling With Tertiary Radicals Generated By Visible-Light Photocatalysis. *Acc. Chem. Res.* **2016**, *49*, 1578.
42. Ghosh, I., Marzo, L., Das, A., Shaikh, R., König, B. Visible Light Mediated Photoredox Catalytic Arylation Reactions. *Acc. Chem. Res.* **2016**, *49*, 1566.
43. Gentry, E. C., Knowles, R. R. Synthetic Applications Of Proton-Coupled Electron Transfer. *Acc. Chem. Res.* **2016**, *49*, 1546.
44. Hernandez-Perez, A. C., Collins, S. K. Heteroleptic Cu-Based Sensitizers In Photoredox Catalysis. *Acc. Chem. Res.* **2016**, *49*, 1557.
45. Pitre, S. P., Mctiernan, C. D., Scaiano, J. C. Understanding The Kinetics And Spectroscopy Of Photoredox Catalysis And Transition-Metal-Free Alternatives. *Acc. Chem. Res.* **2016**, *49*, 1320.
46. Tellis, J. C., Kelly, C. B., Primer, D. N., Jouffroy, M., Patel, N. R., Molander, G. A. Single-Electron Transmetalation Via Photoredox/Nickel Dual Catalysis: Unlocking A New Paradigm For  $sp^3$ – $sp^2$  Cross-Coupling. *Acc. Chem. Res.* **2016**, *49*, 1429.
47. Cismesia, M. A., Yoon, T. P. Characterizing Chain Processes In Visible Light Photoredox Catalysis. *Chem. Sci.* **2015**, *6*, 5426.
48. Lin, S., Ischay, M. A., Fry, C. G., Yoon, T. P. Radical Cation Diels-Alder Cycloadditions By Visible Light Photocatalysis. *J. Am. Chem. Soc.* **2011**, *133*, 19350.
49. Martin, J. G., Hill, R. K. Stereochemistry Of The Diels-Alder Reaction. *Chem. Rev.* **1961**, *61*, 537.
50. Narayanam, J. M. R., Tucker, J. W., Stephenson, C. R. J. Electron-Transfer Photoredox Catalysis: Development Of A Tin-Free Reductive Dehalogenation Reaction. *J. Am. Chem. Soc.*, **2009**, *131*, 8756.
51. Kamigaito, M., Ando, T., Sawamoto, M. Metal-Catalyzed Living Radical Polymerization. *Chem. Rev.* **2001**, *101*, 3689.
52. Courant, T., Masson, G. Recent Progress In Visible-Light Photoredox-Catalyzed Intermolecular 1,2-Difunctionalization Of Double Bonds Via An ATRA-Type Mechanism. *J. Org. Chem.*, **2016**, *81*, 6945.
53. Kharasch, M. S., Skell, P. S., Fischer, P. Reaction Of Atom And Free Radical In Solution. XII. The Addition Of Bromo Esters To Olefins. *J. Am. Chem. Soc.* **1948**, *70*, 1055.
54. Kharasch, M. S., Jensen, E. V., Urry, W. H. Addition Of Carbon Tetrachloride And Chloroform To Olefins. *Science* **1945**, *102*, 128.
55. Curran, D. P., Chen, M.-H., Spletzer, E., Seong, C. M., Chang, C.-T. Atom-Transfer Addition And Annulation Reactions Of Iodomalonates. *J. Am. Chem. Soc.* **1989**, *111*, 8872.
56. Curran, D. P., Bosch, E., Kaplan, J., Newcomb, M. Rate Constants For Halogen Atom Transfer From Representative  $\alpha$ -Halo Carbonyl Compounds To Primary Alkyl Radicals. *J. Org. Chem.* **1989**, *54*, 1826.
57. Curran, D. P., Chang, C.-T. Atom Transfer Cyclization Reactions Of  $\alpha$ -Iodo Ester, Ketones, And Malonates: Examples Of Selective 5-Exo, 6-Endo, And 7-Endo Ring Closures. *J. Org. Chem.* **1989**, *54*, 3140.
58. Curran, D. P., Seong, C. M. Atom-Transfer Addition, Annulation, And Macrocyclization Reactions Of Iodomalononitriles. *J. Am. Chem. Soc.* **1990**, *112*, 9401.
59. Curran, D. P., Tamine, J. Effect Of Temperature On Atom Transfer Cyclization Reactions Of Allylic  $\alpha$ -Iodo Ester And Amides. *J. Org. Chem.* **1991**, *56*, 2746.
60. Curran, D. P., Kim, D. Iodine Atom Transfer Addition Reactions With Alkynes. Part 1: Alkyl Iodides. *Tetrahedron* **1991**, *47*, 6171.
61. Curran, D. P., Kim, D., Ziegler, C. Iodine Atom Transfer Addition Reaction With Alkynes. Part 2;  $\alpha$ -Iodocarbonyls. *Tetrahedron* **1991**, *47*, 6189.
62. Yorimitsu, H., Nakamura, T., Shinokubo, H., Oshima, K. Triethylborane-Mediated Atom Transfer Radical Cyclization Reaction In Water. *J. Org. Chem.* **1998**, *63*, 8604.
63. Yorimitsu, H., Nakamura, T., Shinokubo, H., Oshima, K., Omoto, K., Fujimoto, H. Powerful Solvent Effect Of Water In Radical Reaction: Triethylborane Induced Atom-Transfer Radical Cyclization In Water. *J. Am. Chem. Soc.* **2000**, *122*, 11041.
64. Yorimitsu, H., Shinokubo, H., Matsubara, S., Oshima, K., Omoto, K., Fujimoto, H. Triethylborane-Induced Bromine Atom-Transfer Radical Addition In Aqueous Media: Study Of The Solvent Effect On Radical Addition Reactions. *J. Org. Chem.* **2001**, *66*, 7776.
65. Weidner, K., Giroult, A., Panchaud, P., Renaud, P. Efficient Carboazidation Of Alkenes Using A Radical Desfonylative Azide Transfer Process. *J. Am. Chem. Soc.* **2010**, *132*, 17511.
66. Renaud, P., Ollivier, C., Panchaud, P. Radical Carboazidation Of Alkenes: An Efficient Tool For Preparation Of Pyrrolidinone Derivatives. *Angew. Chem. Int. Ed.* **2002**, *41*, 3460.

67. Panchaud, P., Ollivier, C., Renaud, P., Zigmantas, S. Radical Carboazidation: Expedient Assembly Of The Core Structure Of Various Alkaloid Families. *J. Org. Chem.* **2004**, *69*, 2755.
68. Liu, H., Qiao, Z., Jiang, X. Palladium-Catalyzed Atom Transfer Radical Cyclization Of Unactivated Alkyl Iodide. *Org. Biomol. Chem.* **2012**, *10*, 7274.
69. Bergeot, O., Corsi, C., Quiclet-Sire, B., Zard, S. Z. Radical Instability In Aid Of Efficiency: A Powerful Route To Highly Functional MIDA Boronates. *J. Am. Chem. Soc.* **2015**, *137*, 6762.
70. Yang, Z.-Y., Burton, D. J. A New Approach To  $\alpha$ ,  $\alpha$ -Difluoro-Functionalized Esters. *J. Org. Chem.* **1991**, *56*, 5125.
71. Metzger, J. O., Mahler, R. Radical Addition Of Activated Haloalkanes To Alkenes Initiated By Electron Transfer From Copper In Solvent-Free Systems. *Angew. Chem., Int. Ed.* **1995**, *34*, 902.
72. Forti, L., Ghelfi, F., Libertini, E., Pagnoni, U. M., Soragni, E. Halogen Atom Transfer Radical Addition Of  $\alpha$ -Polychroester To Olefins Promoted By Fe<sup>0</sup> Fillings. *Tetrahedron* **1997**, *53*, 17761.
73. Monks, B. M., Cook, S. P. Palladium-Catalyzed Intramolecular Iodine-Transfer Reaction In The Presence Of  $\beta$ -Hydrogen Atoms. *Angew. Chem. Int. Ed.* **2013**, *52*, 14214.
74. Quebatte, L., Scopelliti, R., Severin, K. Combinatorial Catalysis With Bimetallic Complexes: Robust And Efficient Catalysts For Atom Transfer Radical Addition. *Angew. Chem., Int. Ed.* **2004**, *43*, 1520.
75. Lübbers, T., Schäfer, H. J. Iodo-Atom-Transfer Cyclization Of  $\Delta^{6,7}$ -Unsaturated 2-Iodo Esters With Chromium(II) Acetate. *Synlett* **1991**, 861.
76. Gilbert, B. C., Kalz, W., Lindsay, C. I., Mcgrail, P. T., Parsons, A. F., Whittaker, D. T. E. Initiation Of Radical Cyclisation Reaction Using Dimaganese Decarbonyl. A Flexible Approach To Preparing 5-Membered Rings. *J. Chem. Soc., Perkin Trans. 1*, **2000**, 1187.
77. Cao, L., Li, C. *P*-Meoc<sub>6</sub>h<sub>4</sub>m<sub>2</sub><sup>+</sup>BF<sub>4</sub><sup>-</sup>/TiCl<sub>3</sub>: A Novel Initiator For Halogen Atom Transfer Radical Reaction In Aqueous Media. *Tetrahedron Lett.* **2008**, *49*, 7380.
78. Nguyen, J. D., Tucker, J. W., Konieczynska, M. D., Stephenson, C. R. J. Intermolecular Atom Transfer Radical Addition To Olefins Mediated By Oxidative Quenching Of Photoredox Catalysts. *J. Am. Chem. Soc.* **2011**, *133*, 4160.
79. Wallentin, C., Nguyen, J. D., Finkbeiner, P., Stephenson, C. R. J. Visible Light-Mediated Atom Transfer Radical Addition Via Oxidative Reductive Quenching Of Photocatalysts. *J. Am. Chem. Soc.* **2012**, *134*, 8875.
80. Studer, A., Curran, D. P. Catalysis Of Radical Reactions: A Radical Chemistry Perspective. *Angew. Chem. Int. Ed.* **2016**, *55*, 58.
81. Sun, J., Li, P., Guo, L., Yu, F., He, Y.-P., Chu, L. Catalytic, Metal-Free Sulfonylcyanation Of Alkenes Via Visible Light Organophotoredox Catalysis. *Chem. Commun.*, **2018**, *54*, 3162.
82. Ikezawa, H., Kutal, C., Yasufuku, K., Yamazaki, H. Direct And Sensitized Valence Photoisomerization Of A Substituted Norbornadiene. Examination Of The Disparity Between Singlet- And Triplet-State Reactivities. *J. Am. Chem. Soc.* **1986**, *108*, 1589.
83. Lu, Z., Yoon, T. P. Visible Light Photocatalysis Of (2+2) Styrene Cycloaddition Via Energy Transfer. *Angew. Chem., Int. Ed.* **2012**, *51*, 10329.
84. (a) Wenger, O. S. Photoactive Complexes With Earth-Abundant Metals. *J. Am. Chem. Soc.*, DOI: 10.1021/Jacs.8b08822; (b) Zonta, C.; De Lucchi, O.; Volpicelli, R.; Cotarca, L. (2007). *Thione–Thiol Rearrangement: Miyazaki–Newman–Kwart Rearrangement And Others*. Topics In Current Chemistry. (c) N. Harvey, J. N., Lloyd-Jones, G., C. The Newman–Kwart Rearrangement Of *O* - Aryl Thiocarbamates: Substantial Reduction In Reaction Temperatures Through Palladium Catalysis. *Angew. Chem. Int. Ed.* **2009**, *48*, 7612; (d) Perkowski, A. J., Cruz, C. L., Nicewicz, D. A. Ambient-Temperature Newman–Kwart Rearrangement Mediated By Organic Photoredox Catalysis. *J. Am. Chem. Soc.* **2015**, *137*, 15684; (e) Zonta, C., Cotarca, L. (2007). *Thione–Thiol Rearrangement: Miyazaki–Newman–Kwart Rearrangement And Others*. Topics In Current Chemistry; (f) Mcmanus, J. B., Nicewicz, D. A. Generation And Alkylation Of *A* - Carbamyl Radicals Via Organic Photoredox Catalysis. *J. Am. Chem. Soc.* **2018**, *140*, 9056; (g) Ghosh, I., König, B. Reduction Of Aryl Halides By Consecutive Visible Light-Induced Electron Transfer Processes. *Science* **2014**, *346*, 725; (h) Lima, C. G. S., Lima, T., Duarte, M., Jurberg, I. D., Paixão, M. W. Organic Synthesis Enabled By Light-Irradiation Of EDA Complexes: Theoretical Background And Synthetic Applications. *ACS Catal.*, **2016**, *6*, 1389; (i) Kosower, E. M. *J. Am. Chem. Soc.* 1956, *78*, 5700; Nagakura, S. *J. Am. Chem. Soc.* **1958**, *80*, 520; (j) Fox, M. A.; Younathan, J.; Fryxell, G. E. *J. Org. Chem.* 1983, *48*, 3109; Sankararaman, S.; Haney, W. A.; Kochi, J. K. *J. Am. Chem. Soc.* **1987**, *109*, 7824; (k) Tobisu, M.; Furukawa, T.; Chatani, N. Visible Light-Mediated Direct Arylation Of Arenes And Heteroarenes Using Diaryliodonium Salts In The Presence And Absence Of A Photocatalyst. *Chem. Lett.* **2013**, *42*, 1203-1205; (l) Arceo, E., Jurberg, I. D., Álvarez-Fernández, A., Melchiorre, P. Photochemical Activity Of A Key Donor–Acceptor Complex Can Drive Stereoselective Catalytic *A*-Alkylation Of Aldehydes. *Nat. Chem.* **2013**, *5*, 750; (m) S. R. Kandukuri, A. Bahamonde, I. Chatterjee, I. D. Jurberg, E. C. Escudero-Adán, P. Melchiorre. X-Ray Characterization Of An Electron Donor-Acceptor Complex That Drives The Photochemical Alkylation Of Indoles. *Angew. Chem. Int. Ed.* **2015**, *54*, 1485-1489; (n) Woźniak, Ł.; Murphy, J. J.; Melchiorre, P. Photo-Organocatalytic Enantioselective Perfluoroalkylation Of *B*-Ketoesters. *J. Am. Chem. Soc.* **2015**, *137*, 5678; (o) Davies, J.; Booth, S. G.; Essafi, S.; Dryfe, R. A. W.; Leonori, D. Visible-Light-Mediated Generation Of Nitrogen-Centered Radicals: Metal-Free Hydroamination And Iminohydroxylation Cyclization Reactions. *Angew. Chem. Int. Ed.* **2015**, *54*, 14017.
85. Osawa, M., Nagai, H., Akita, M. Photo - Activation Of Pd - Catalyzed Sonogashira Coupling Using A Ru/Bipyridine Complex As Energy Transfer Agent. *Dalton Trans.* **2007**, *8*, 827.
86. Kalyani, D., McMurtrey, K. B., Neufeldt, S. R., Sanford, M. S. Room - Temperature C–H Arylation: Merger Of Pd - Catalyzed C–H Functionalization And Visible - Light Photocatalysis. *J. Am. Chem. Soc.* **2011**, *133*, 18566.
87. Kalyani, D., Deprez, N. R., Desai, L. V., Sanford, M. S. Oxidative C–H Activation/C–C Bond Forming Reactions: Synthetic Scope And Mechanistic Insights. *J. Am. Chem. Soc.* **2005**, *127*, 7330.
88. Maestri, G., Malacria, M., Derat, E. Radical Pd(III)/ Pd(I) Reductive Elimination In Palladium Sequences. *Chem. Commun.* **2013**, *49*, 10424.
89. Neufeldt, S. R., Sanford, M. S. Combining Transition Metal Catalysis With Radical Chemistry: Dramatic Acceleration Of Palladium-Catalyzed C-H Arylation With Diaryliodonium Salts. *Adv. Synth. Catal.* **2012**, *354*, 3517.

90. Chow, P. - K., Cheng, G., Tong, G. S. M., Ma, C., Kwok, W.-M., Ang, W.-H., Chung, C. Y.-S., Yang, C., Wang, F., Che, C.-M. Highly Luminescent Palladium(II) Complexes With Sub - Millisecond Blue To Green Phosphorescent Excited States. Photocatalysis And Highly Efficient PSF - Oleds. *Chem. Sci.* **2016**, *7*, 6083.
91. Zoller, J., Fabry, D. C., Ronge, M. A., Rueping, M. Synthesis Of Indoles Using Visible Light: Photoredox Catalysis For Palladium - Catalyzed C-H Activation. *Angew. Chem. Int. Ed.* **2014**, *53*, 13264.
92. Zhou, C., Li, P., Zhu, X., Wang, L. Merging Photoredox With Palladium Catalysis: Decarboxylative Ortho - Acylation Of Acetanilides With A - Oxocarboxylic Acids Under Mild Reaction Conditions. *Org. Lett.* **2015**, *17*, 6198.
93. Xu, N., Li, P., Xie, Z., Wang, L. Merging Visible - Light Photocatalysis With Palladium Catalysis For C-H Acylation Of Azo - And Azoxybenzenes With A - Keto Acids. *Chem. Eur. J.* **2016**, *22*, 2236.
94. Cheng, W. - M., Shang, R., Yu, H. - Z., Fu, Y. Room - Temperature Decarboxylative Couplings Of A - Oxocarboxylates With Aryl Halides By Merging Photoredox With Palladium Catalysis. *Chem. Eur. J.* **2015**, *21*, 13191.
95. Lang, S. B., O'Nele, K. M., Tunge, J. A. Decarboxylative Allylation Of Amino Alkanoic Acids And Esters Via Dual Catalysis. *J. Am. Chem. Soc.* **2014**, *136*, 13606.
96. Xuan, J., Zeng, T.-T., Feng, Z.-J., Deng, Q.-H., Chen, J.-R., Lu, L.-Q., Xiao, W.-J., Alper, H. Redox - Neutral A - Allylation Of Amines By Combining Palladium Catalysis And Visible - Light Photoredox Catalysis. *Angew. Chem. Int. Ed.* **2015**, *54*, 1625.
97. Twilton, J., Le, C., Zhang, P., Shaw, M. H., Evans, R. W., Macmillan, D. W. C. The Merger Of Transition Metal And Photocatalysis. *Nat. Rev. Chem.* **2017**, *1*, 0052.
98. Ye, Y., Sanford, M. S. Merging Visible - Light Photocatalysis And Transition - Metal Catalysis In The Copper - Catalyzed Trifluoromethylation Of Boronic Acids With CF<sub>3</sub>I. *J. Am. Chem. Soc.* **2012**, *134*, 9034.
99. Alonso, C., Martínez De Marigorta, E., Rubiales, G., Palacios, F. Carbon Trifluoromethylation Reactions Of Hydrocarbon Derivatives And Heteroarenes. *Chem. Rev.*, **2015**, *115*, 1847.
100. Rueping, M., Koenigs, R. M., Poscharny, K., Fabry, D. C., Leonori, D., Vila, C. Dual Catalysis: Combination Of Photocatalytic Aerobic Oxidation And Metal Catalyzed Alkynylation Reactions: C-C Bond Formation Using Visible Light. *Chem. Eur. J.* **2012**, *18*, 5170.
101. Yoo, W. - J., Tsukamoto, T., Kobayashi, S. Visible - Light - Mediated Chan-Lam Coupling Reactions Of Aryl Boronic Acids And Aniline Derivatives. *Angew. Chem. Int. Ed.* **2015**, *54*, 6587.
102. Sahoo, B., Hopkinson, M. N., Glorius, F. Combining Gold And Photoredox Catalysis: Visible Light - Mediated Oxy - And Aminoarylation Of Alkenes. *J. Am. Chem. Soc.* **2013**, *135*, 5505.
103. Zhang, G., L. Cui, L., Wang, Y., Zhang, L. Homogeneous Gold-Catalyzed Oxidative Carboheterofunctionalization Of Alkenes. *J. Am. Chem. Soc.* **2010**, *132*, 1474.
104. Brenzovich, W. E., Benitez, D., Lackner, A. D., Shunatona, H. P., Tkatchouk, E., Goddard, W. A., Toste, F. D. Gold-Catalyzed Intramolecular Aminoarylation Of Alkenes: C-C Bond Formation Through Bimolecular Reductive Elimination. *Angew. Chem. Int. Ed.* **2010**, *49*, 5519.
105. Hopkinson, M. N., Sahoo, B., Glorius, F. Dual Photoredox And Gold Catalysis: Intermolecular Multicomponent Oxyarylation Of Alkenes. *Adv. Synth. Catal.* **2014**, *356*, 2794.
106. Hopkinson, M. N., Tlahuext - Aca, A., Glorius, F. Merging Visible Light Photoredox And Gold Catalysis. *Acc. Chem. Res.* **2016**, *49*, 2261.
107. Tlahuext - Aca, A., Hopkinson, M. N., Daniliuc, C. G., Glorius, F. Oxidative Addition To Gold(I) By Photoredox Catalysis: Straightforward Access To Diverse (C,N)-Cyclometalated Gold(III) Complexes. *Chem. Eur. J.* **2016**, *22*, 11587.
108. Zhang, Q., Zhang, Z. - Q., Fu, Y., Yu, H. - Z. Mechanism Of The Visible Light - Mediated Gold - Catalyzed Oxyarylation Reaction Of Alkenes. *ACS Catal.* **2016**, *6*, 798.
109. Shu, X. - Z., Zhang, M., He, Y., Frei, H., Toste, F. D. Dual Visible Light Photoredox And Gold - Catalyzed Arylative Ring Expansion. *J. Am. Chem. Soc.* **2014**, *136*, 5844.
110. Patil, D. V., Yun, H., Shin, S. Catalytic Cross - Coupling Of Vinyl Golds With Diazonium Salts Under Photoredox And Thermal Conditions. *Adv. Synth. Catal.* **2015**, *357*, 2622.
111. Um, J., Yun, H., Shin, S. Cross - Coupling Of Meyer-Schuster Intermediates Under Dual Gold - Photoredox Catalysis. *Org. Lett.* **2016**, *18*, 484.
112. Alcaide, B., Almendros, P., Busto, E., Luna, A. Domino Meyer-Schuster/Arylation Reaction Of Alkynols Or Alkynyl Hydroperoxides With Diazonium Salts Promoted By Visible Light Under Dual Gold And Ruthenium Catalysis. *Adv. Synth. Catal.* **2016**, *358*, 1526.
113. Tlahuext - Aca, A., Hopkinson, M. N., Garza - Sanchez, R. A., Glorius, F. Alkyne Difunctionalization By Dual Gold/Photoredox Catalysis. *Chem. Eur. J.* **2016**, *22*, 5909.
114. Kim, S., Rojas - Martin, J., Toste, F. D. Visible Light - Mediated Gold - Catalyzed Carbon(sp<sup>2</sup>)-Carbon(sp) Coupling. *Chem. Sci.* **2016**, *7*, 85.
115. Cornilleau, T., Hermange, P., Fouquet, E. Gold - Catalyzed Cross - Coupling Between Aryldiazonium Salts And Arylboronic Acids: Probing The Usefulness Of Photoredox Conditions. *Chem. Commun.* **2016**, *52*, 10040.
116. Gauchot, V., Lee, A. - L. Dual Gold Photoredox C(sp<sup>2</sup>)-C(sp<sup>2</sup>) Cross Couplings-Development And Mechanistic Studies. *Chem. Commun.* **2016**, *52*, 10163.
117. He, Y., Wu, H., Toste, F. D. A Dual Catalytic Strategy For Carbon-Phosphorous Cross - Coupling Via Gold And Photoredox Catalysis. *Chem. Sci.* **2015**, *6*, 1194.

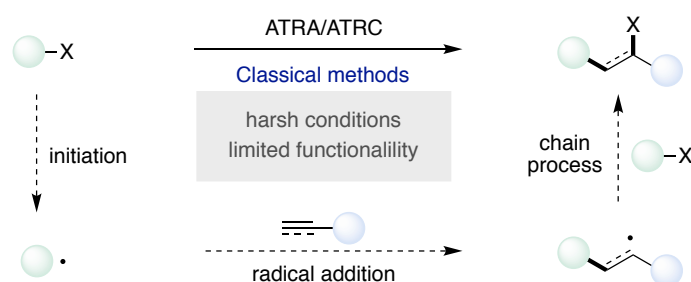
## **Chapter 2.**

### **Visible Light-Promoted Atom Transfer Radical Cyclization of Unactivated Alkyl Iodides**

## 2.1. Introduction: Atom Transfer Radical Addition/Cyclization

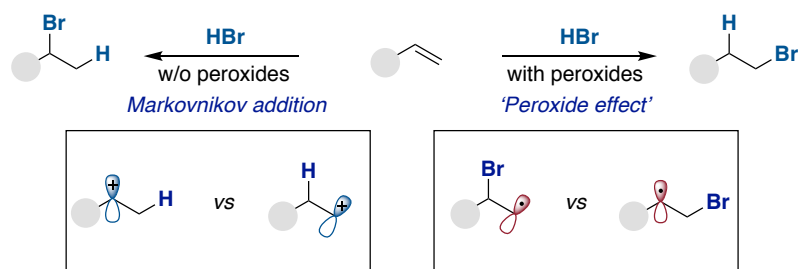
### 2.1.1. Traditional Methods to Promote ATRA/ATRC

Atom transfer radical addition or cyclization reactions (ATRA/ATRC) of halogenated compounds with  $\pi$ -components rank among the most fundamental transformations within our chemical portfolio. Such interest arises from the high efficiency and atom-economy of these processes, enabling the simultaneous generation of two new C–C and C–halogen bonds via the cleavage of a single covalent C–halogen bond, and allowing to access more complex organic halides that might be amenable for further functionalization.<sup>1,2</sup>



**Scheme 2.1. Classical atom transfer radical addition**

The development of ATRA reactions was pioneered by Kharasch when studying the addition of HBr to alkenes. Specifically, Markovnikov selectivity<sup>3</sup> was expected for a classical mechanism consisting of the intermediacy of carbocations by addition of a proton across the alkene. However, the addition of peroxides resulted in a rather intriguing *anti*-Markovnikov scenario, contributing to the perception that a “peroxide effect” came into play (Scheme 2.2).<sup>4</sup> Such a regioselectivity switch could be explained by the generation of bromine radicals via hydrogen atom abstraction (HAT) that were added across the double bond to generate an alkyl radical, thus setting the stage for a chain-propagation via subsequent HAT to HBr.

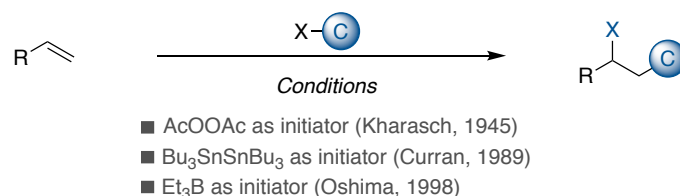


**Scheme 2.2. Markovnikov addition and the peroxide effect**

Prompted by the seminal studies from Kharasch with peroxide as initiators of chain-radical processes, this field has been extensively developed by elegant contributions of Curran, Oshima or

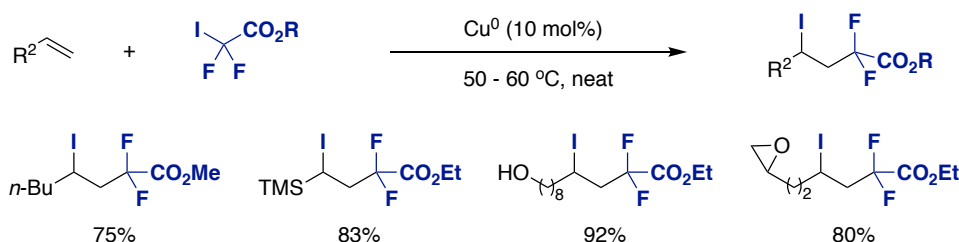


Renaud, among others (Scheme 2.3).<sup>5-19</sup> Despite the inherent synthetic interest in ATRA reactions, these technologies typically need stoichiometric amounts of toxic or hazardous radical initiators such as peroxides, organotin reagents or triethylboron, among others (Scheme 2.3.). These drawbacks have partially been alleviated by the implementation of metal-catalyzed ATRA reactions.<sup>20-27</sup>



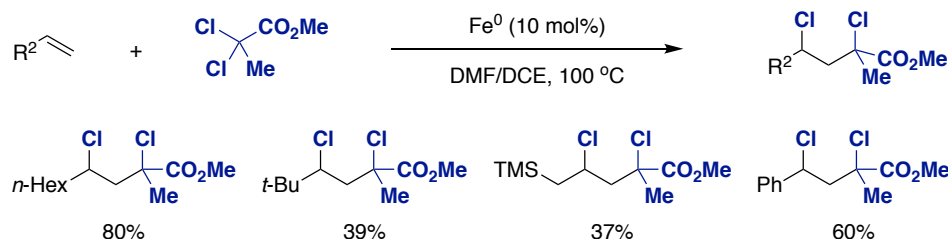
### Scheme 2.3. Classical ATRA conditions

Among various scenarios, particularly attractive was the method developed by Burton in 1991, describing a new approach en route to  $\alpha,\alpha$ -difluoro-functionalized ester with cheap Cu powder under solvent-free and mild conditions (Scheme 2.4).<sup>20</sup> This transformation was particularly noteworthy taking into consideration that these compounds were typically obtained from a prefunctionalized  $\beta$ -hydroxy derivative via Reformatsky reaction. Under these conditions, a wide variety of sensitive functional groups, such as alcohol and terminal epoxides could all be well accommodated. Although Cu was utilized as the catalyst, the reaction was proposed to operate via a radical chain mechanism.



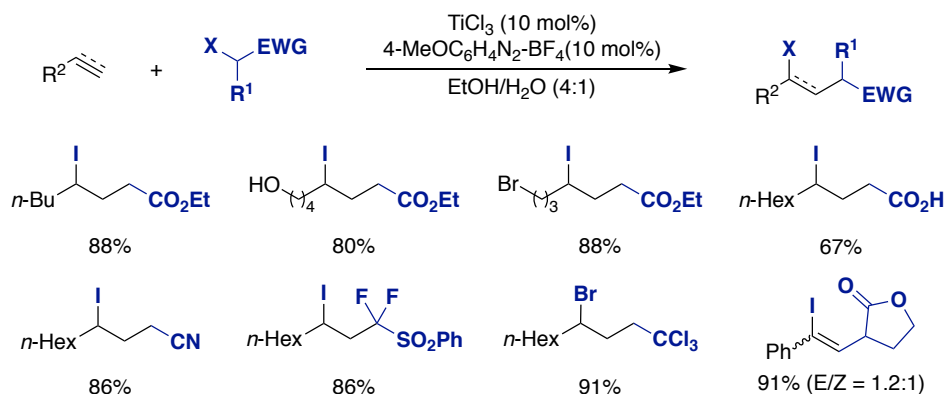
### Scheme 2.4. Cu(0) promoted ATRA reactions with activated alkyl iodides

Another example make use of cheap Fe(0) to catalyze an otherwise similar transformation. In this case, however, gentle heating was required to facilitate the SET from Fe(0) to the less activated alkyl chlorides.<sup>22</sup>



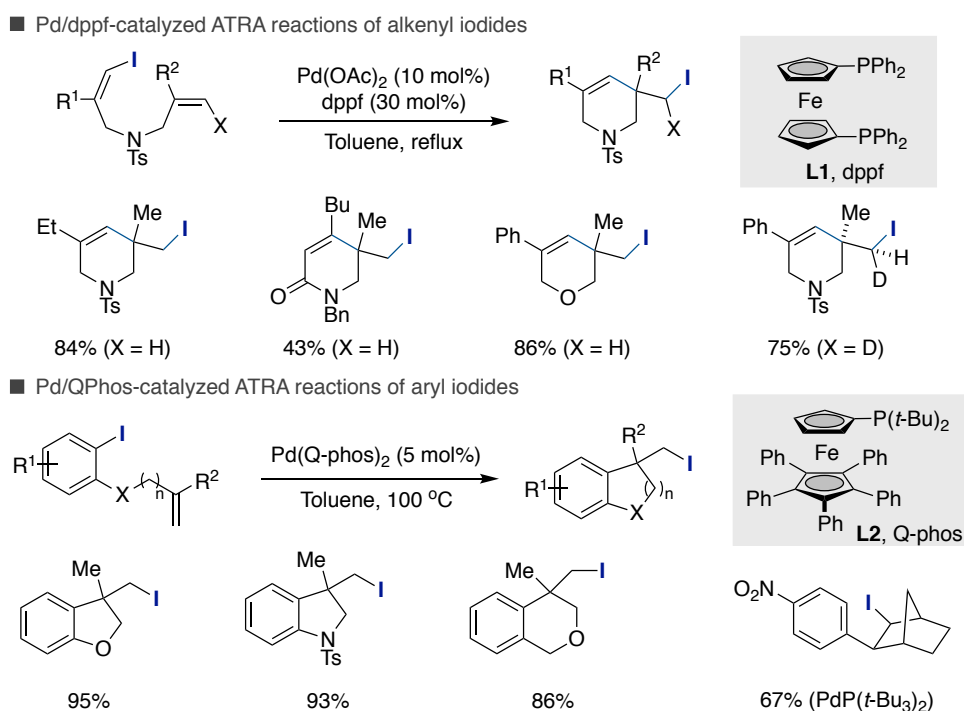
### Scheme 2.5. Fe(0) promoted ATRA reactions with activated alkyl chlorides

In 2008, Li and co-workers developed a novel system to mediate ATRA transformations with a series of activated organic halides.<sup>27</sup> Specifically, it was found that diazonium salts and  $\text{TiCl}_3$  as catalysts can promote a wide range of ATRA reactions with broad scope and excellent functional group tolerance in EtOH/ $\text{H}_2\text{O}$  (Scheme 2.6).<sup>26</sup> Even terminal alkynes can give rise to the desired product in excellent regioselectivities, albeit with *E/Z* mixtures. The initiation relies on the generation of aryl radical from an aryl diazonium salt and  $\text{TiCl}_3$  followed by a chain-propagation process.



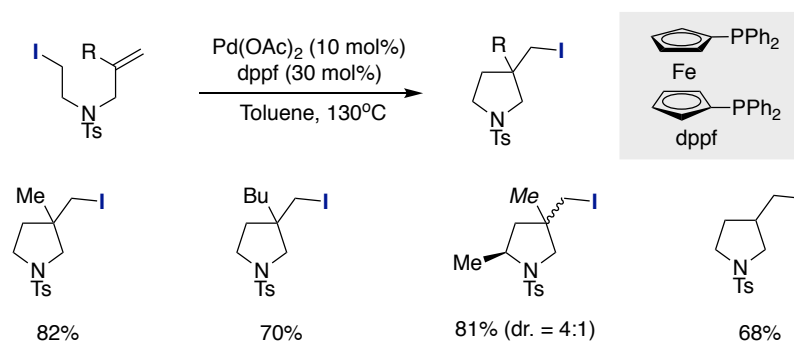
**Scheme 2.6.  $\text{TiCl}_3$  and diazonium salt promoted ATRA with activated alkyl halides**

Alternatively, bimetallic Rh–Ru complexes,  $\text{Cr}(\text{OAc})_2$  or  $\text{Mn}_2(\text{CO})_{10}$  can be employed as catalysts for initiating ATRA reactions.<sup>20–26</sup> Still, however, ATRA reactions are typically restricted to relatively activated substrates, thus lowering down the application profile of these transformations, particularly within the context of late-stage functionalization.



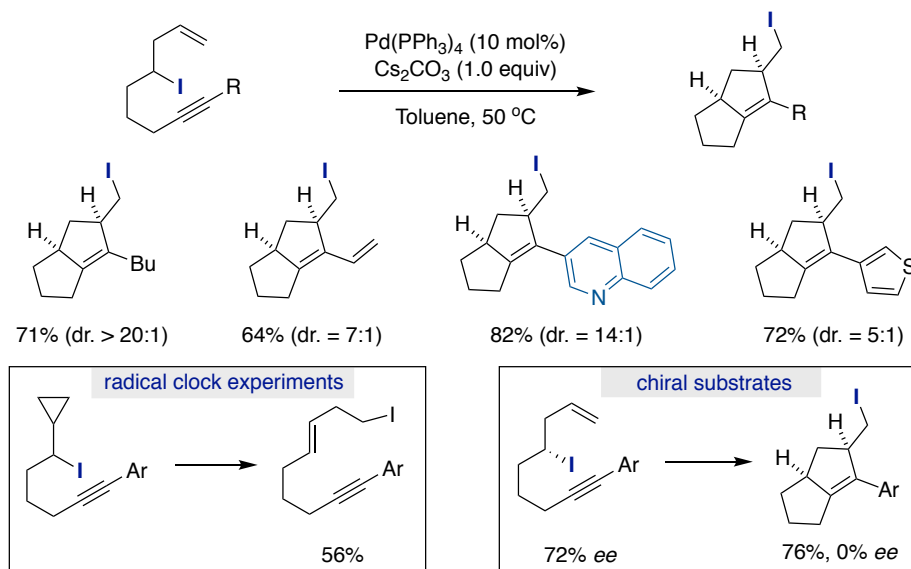
**Scheme 2.7. Pd-catalyzed iodine atom transfer cyclizations**

In 2011, Tong and Lautens independently reported a remarkable Pd-catalyzed iodine transfer reaction from aryl or vinyl iodides (Scheme 2.7).<sup>27a,27b</sup> These reports are genuinely Pd-catalyzed reactions, as shown by the stereochemical course of a deuterated analogue (Scheme 2.7, *top right*)<sup>27a</sup> and in the presence of a norbornene backbone, suggesting a scenario consisting of a reductive elimination from Pd(II) to form the targeted C(*sp*<sup>3</sup>)-I bond (Scheme 2.7, *top*).<sup>27b</sup> No  $\beta$ -hydrogen elimination takes place in the latter, probably due to the inability of adopting the necessary *cis*-agostic interaction with the  $\beta$ -hydrogen.



Scheme 2.8. Pd(0)-catalyzed intramolecular iodine transfer

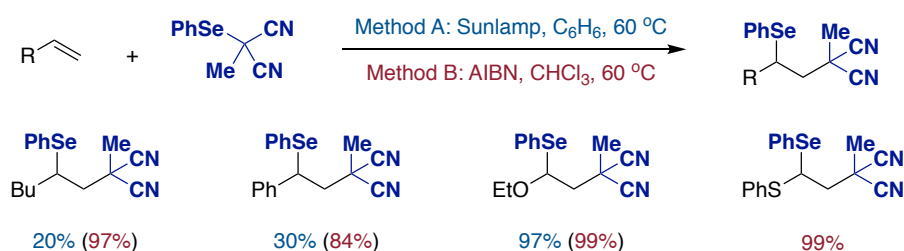
Interestingly, ATRC reactions could be extended to unactivated alkyl iodides under similar reaction conditions to those reported by Tong in which a tether was required for the reaction to occur, most likely due to a Thorpe-Ingold effect (Scheme 2.8).<sup>27c</sup>



Scheme 2.9. Pd(0)-catalyzed iodine transfer with double cyclization

In 2013, Cook and co-workers described a ATRA-type reaction via multiple C–C bond-formations with unactivated alkyl iodides and Pd(0) catalysts in the presence of Cs<sub>2</sub>CO<sub>3</sub> (Scheme 2.9).<sup>23</sup> In

virtually all cases analyzed, the transformation gave rise to the corresponding double cyclization event in excellent diastereoselectivities. The authors provided evidence of a radical pathway in the presence of radical clocks as well as by the observation that racemic products were obtained with chiral precursors (Scheme 2.X, *bottom*). While Pd-catalyzed reactions showed complementary reactivity to that of classical ATRA triggered by other radical initiators, it is worth noting that these procedures typically proceed with high catalyst loadings. Additionally, substrates susceptible to oxidative addition such as aryl sulfides or aryl halides were not be tolerated, thus leaving ample room to develop more applicable ATRA and ATRC-type reactions.



**Scheme 2.10. Selenium group transfer radical addition**

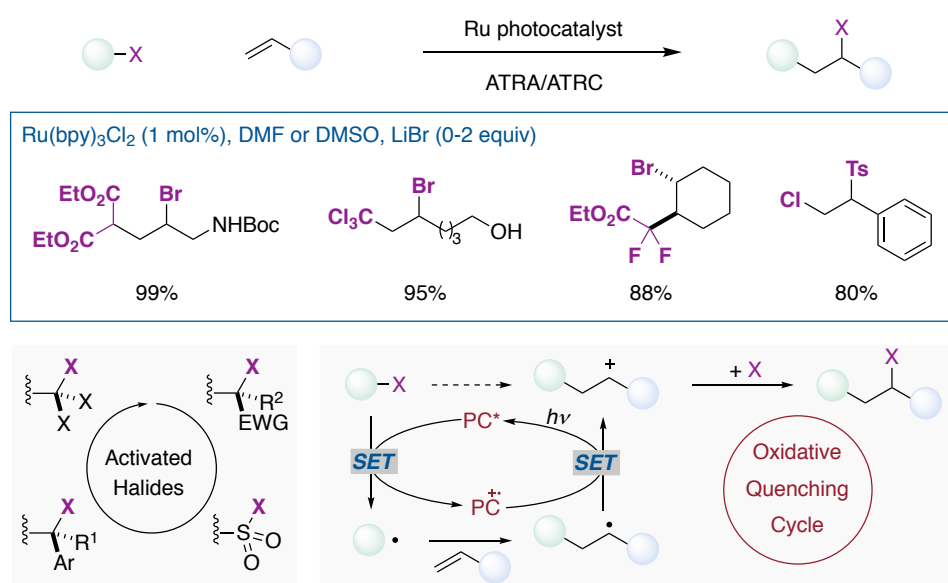
From a mechanistic standpoint, ATRA reactions should by no means limited to halogen atom transfer. Indeed, this concept has been expanded to other translocation scenarios. For example, Curran reported that a selenium group can be utilized in ATRA reactions in high yields for a wide number of substrates. Key for success was the utilization of methyl(phenylseleno)malonitrile, allowing to significantly expand the scope of olefin partners, enabling the addition to electron-rich olefins which are problematic in traditional ATRA reactions, such enol ethers and thioethers.<sup>27c</sup>

### 2.1.2. Visible Light Photoredox Promoted ATRA/ATRC with Activated Halides

In the past decade, visible light photocatalysis has gained considerable attention as a method for generating carbon-centered radical intermediates via single-electron transfer (SET) processes.<sup>28</sup> Unlike classical SET protocols based on radical initiators or metal-catalyzed protocols initiated by a chemical activation mode and inner-sphere mechanisms,<sup>29</sup> photoredox catalysis is capable of employing energy of visible light to promote otherwise analogous processes via outer-sphere mechanisms under exceptionally mild conditions, holding promise for a more practical synthetic benefit by using visible light.<sup>28</sup>

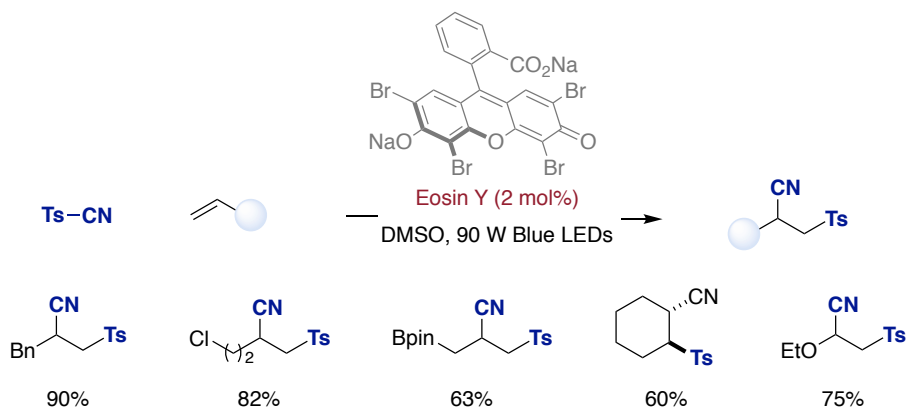
Among all the transformations enabled by photoredox catalysis, particularly illustrative is the implementation of *redox-neutral* ATRA/ATRC, which might lead to elegant bond-disconnections for rapidly advancing molecular complexity in both atom- and step-economical fashion. The conventional methods to promote ATRA make use of toxic initiators, high energy UV light irradiation,

high catalyst loadings of transition metals and/or elevated temperatures. As a consequence, these reactions normally suffer from a wider application profile, and have found limited use within the context of late-stage functionalization of complex molecules. Aimed at providing a solution to this challenge, and prompted by the ability of visible light photoredox catalysis to trigger SET processes, Stephenson and co-workers found that ATRA reactions could be realized at ambient temperature with low catalyst loading, high chemical yielding and broad scope (Scheme 2.11).<sup>30</sup> In this case, a rather different mechanism to that of conventional ATRA reactions was proposed. Specifically, the transformation occurred via oxidative quenching and a subsequent anionic halide recombination to give rise the corresponding alkyl halides.



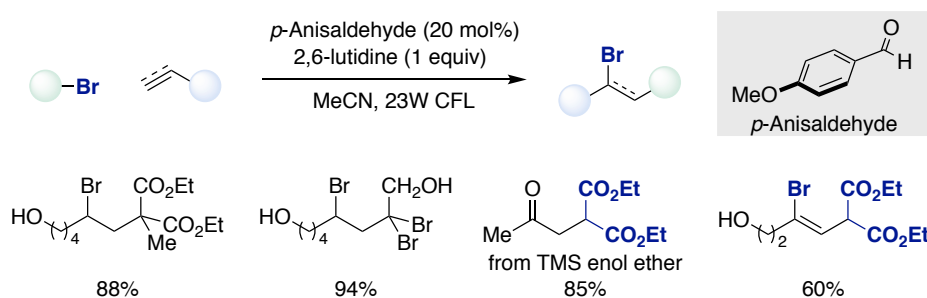
**Scheme 2.11. Photoredox promote ATRA via oxidative quenching**

Chu and co-workers employed organic photocatalyst Eosin Y ( $E_{\text{red}}^{1/2} = -1.15$  V vs SCE In MeCN) to functionalize  $\alpha$ -olefins with tosyl cyanide (TsCN,  $E_{\text{red}}^{1/2} = -0.78$  V vs SCE in MeCN). The mechanism followed by the same oxidative quenching and ionic recombination proposed by Stephenson, an assumption that was later on confirmed by quenching studies and the low quantum yields observed in these processes (Scheme 2.12).<sup>31a</sup>



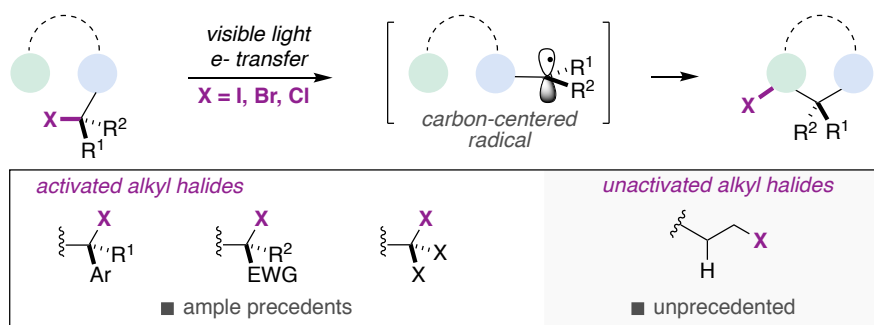
**Scheme 2.12. Sulfonylcyanation of alkenes enabled by organic photoredox catalysis**

Apart from the conventional use of radical initiators and single electron transfer processes, there is evidence that triplet energy transfer could also be used for triggering ATRA reactions. In 2014, Melchiorre and co-workers described an ATRA reaction that operated via energy transfer mechanisms by using an aromatic aldehyde as the formal catalyst (Scheme 2.13). They found that a wide range of energy transfer agents (*eg.* benzophenone, carbazole) could promote the reaction with moderate yield under CFL irradiation.<sup>31b</sup>



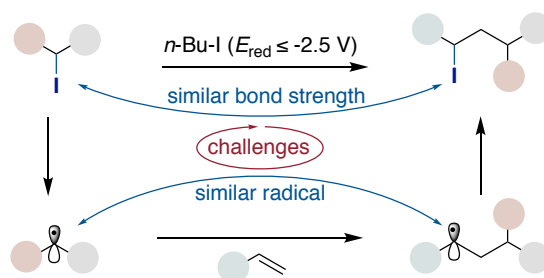
**Scheme 2.13. Intermolecular ATRA enabled by energy transfer**

Taken together, the current portfolio of photoredox ATRA/ATRC reactions remains confined to activated organic halides possessing weak C(sp<sup>3</sup>)-X bonds adjacent to  $\pi$ -systems, electron-withdrawing groups or heteroatoms, thus rapidly triggering a thermodynamically favoured SET processes (Scheme 2.14).<sup>30-33</sup>



### Scheme 2.14. Visible light photoredox ATRA/ATRC of activated halides

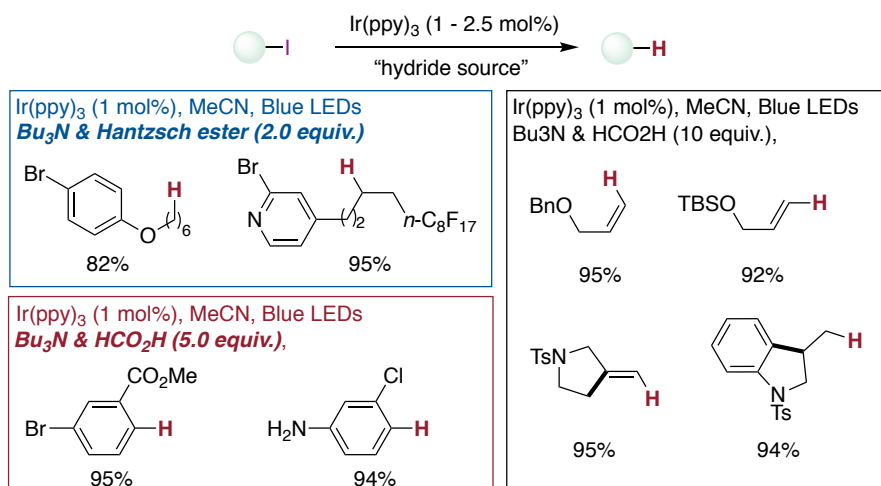
In line of these precedents, one might easily argue that unactivated alkyl halides might not be within reach in photoredox ATRA reactions due to the rather uphill SET process required to generate an open-shell intermediate ( $n\text{-BuI}$ :  $E_{\text{red}} \leq -2.5\text{V}$ ) that will subsequently trigger the addition across the  $\pi$ -component. Although the use of a strongly reducing photocatalyst may be employed to drive the reaction forward, the inherent similarities between the initial and the final C-halide bond or between the initial and final alkyl radical leaves a reasonable doubt on whether this reaction could ever be effected within the context of photoredox catalysis (Scheme 2.15).



Scheme 2.15. The challenges involved in photoredox ATRA with unactivated alkyl halide

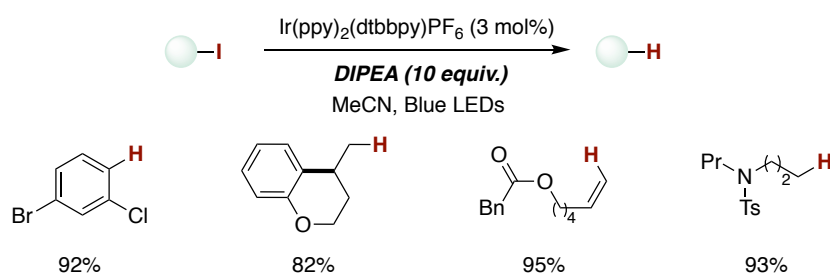
## 2.2. Visible Light Photoredox Promoted Unactivated Halide Reduction

Photoredox catalysis has nicely shown the capability of reducing molecules by a downhill redox SET process. However, there are not a wide number of photocatalysts capable of overcoming the redox potentials required to effect the reduction of unactivated alkyl halides ( $n\text{-BuI}$ :  $E_{\text{red}} \leq -2.5\text{V}$ ). Stephenson's group reported a seminal discovery by employing a strongly reducing photocatalyst  $fac\text{-Ir(ppy)}_3$  ( $E_{1/2}^{\text{Ir(II)/Ir(III)}} = -2.19\text{ V vs SCE in MeCN}$ ) together with excess amounts of different reductants combination (Scheme 2.16).<sup>33a</sup> Under these conditions, a series of unactivated alkyl, vinyl and aryl iodides were smoothly reduced at ambient temperature. These results are particularly interesting when considering that conventional methods aimed at the same goal make use of toxic tin reagents. As expected, the presence of aryl bromides and chlorides were tolerated, probably due to the rather uphill SET process required to generate transient radical intermediates from these entities.



**Scheme 2.16. Photoreduction of unactivated iodides with Ir(ppy)<sub>3</sub>**

Concurrently with Stephenson's report, Lee and co-workers showed a rather similar transformations and substrate scope (Scheme 2.17).<sup>33b</sup> Although the redox potential of Ir(ppy)<sub>2</sub>(dtbbpy)<sup>+</sup> ( $E_{1/2}^{\text{Ir(II)/Ir(III)}} = -1.51 \text{ V vs SCE in MeCN}$ ) suggest that a SET might occur with aryl iodides ( $E_{1/2} = -1.71 \text{ to } -1.55$ ), such a pathway was highly unlikely with unactivated alkyl iodides ( $E_{1/2} \leq -2.1 \text{ V}$ ). However, Lee observed that unactivated alkyl iodides could be utilized as substrates, albeit longer reaction times were required; intriguingly, no mechanistic explanation was provided. The SET to C(*sp*<sup>3</sup>)-I bond is likely occurring at the  $\sigma^*$  (C-I) orbital prior C-I scission, whereas the reaction of C(*sp*<sup>2</sup>)-I bond may involve a localized radical anion intermediate followed by orbital rotation to favor the subsequent heterolytic cleavage of the C-I bond. Regardless of the mode of action, the seminal work of Lee paved the way for designing ATRA reactions with unactivated alkyl iodides.



**Scheme 2.16. Photoreduction of unactivated iodides with Ir(ppy)<sub>2</sub>(dtbbpy)PF<sub>6</sub>**

### 2.3. General Aim of the Project

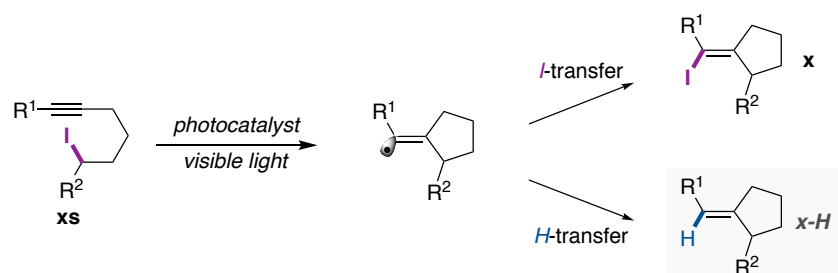
At the outset of this PhD thesis, the development of photoredox-mediated ATRA reactions remained restricted to the utilization of activated alkyl halides. Driven by this observation, we aimed at providing a solution to this challenge, hoping that such a pathway might open up new perspectives for the utilization of unactivated alkyl halides within the photoredox arena beyond



photodehalogenation processes. In line with other metal-mediated ATRA reactions (see for example, Scheme 2.9), we anticipated that we could tackle this challenge by incorporating a  $\pi$ -component within the alkyl side-chain, thus enabling an ATRC process.

## 2.4. Visible Light-Photoredox Promoted ATRC of Unactivated Alkyl Iodides

As indicated above, Stephenson and Lee's independently work paved the way for the utilization of unactivated alkyl halides in photochemical transformations under visible light irradiation,<sup>33</sup> suggesting that the implementation of ATRC reactions might be within reach under appropriate reaction conditions. However, we anticipated that this could not be particularly straightforward, as the in situ generated alkyl radical might trigger a HAT process prior to intramolecular cyclization, leading to otherwise similar products to those described by Stephenson and Lee. Additionally, we should take into consideration that the product should be stable under the reaction conditions, preventing a subsequent C–I homolysis, and that the overall transformation should be kinetically and thermodynamically downhill. With all these considerations in mind, we decided to start our investigations with unactivated alkyl iodides decorated with triple-bond on the side-chain as radical acceptors. In principle, a 5-*exo-dig* radical cyclization should trap effectively the in situ generated alkyl radical, thus changing the hybridization of the C–I bond ( $sp^3$  to  $sp^2$ ), making the reaction thermodynamically and kinetically downhill. However, it was unclear whether the lower bond-dissociation energy of the final  $sp^2$  C–I bond would ultimately lead to a parasitic HAT process.



**Scheme 2.17. Challenges associated to the ATRC reaction with unactivated alkyl halides**

## 2.4.1 Optimization of the Reaction Conditions

entry	photocatalyst	amine	conversion	yield of <b>1</b>
1	<i>fac</i> -Ir(ppy) <sub>3</sub>	DIPEA (0.5 equiv)	68%	39%
2	<i>fac</i> -Ir(ppy) <sub>3</sub>	DIPEA (1.0 equiv)	78%	41%
3	<i>fac</i> -Ir(ppy) <sub>3</sub>	Cy <sub>2</sub> NMe (0.5 equiv)	82%	34%
4	<i>fac</i> -Ir(ppy) <sub>3</sub>	Cy <sub>2</sub> NMe (1.0 equiv)	96%	15%
5	Ir(ppy) <sub>2</sub> (dtbbpy)PF <sub>6</sub>	DIPEA (0.5 equiv)	78%	45%
6	Ir(ppy) <sub>2</sub> (dtbbpy)PF <sub>6</sub>	DIPEA (1.0 equiv)	100%	28%
7	Ir(ppy) <sub>2</sub> (dtbbpy)PF <sub>6</sub>	Cy <sub>2</sub> NMe (0.5 equiv)	100%	20%
8	Ir(ppy) <sub>2</sub> (dtbbpy)PF <sub>6</sub>	Cy <sub>2</sub> NMe (1.0 equiv)	83%	39%

Conversion, yield and ratio were calculated with GC-FID with decane as internal standard.

**Table 2.1. Photoredox ATRC of unactivated alkyl iodides**

Driven by our ongoing interest in cross-coupling reactions of unactivated alkyl halides,<sup>34</sup> and encouraged by Stephenson and Lee's contributions,<sup>33</sup> we initiated our study with (6-iodohex-1-yn-1-yl)benzene as model substrate under Ir(III) photocatalyst conditions with an appropriate tertiary amine. As expected, the unactivated C(*sp*<sup>3</sup>)-I bond can be photocleaved to give reduced product **1-H** with the formation of the targeted ATRC product (**1**) after three days reaction time (Table 2.1). Intriguingly, the use of 50 mol% of amine showed high reactivity, albeit in low chemoselectivity (entry 1, 3, 5 and 7), as stoichiometric quencher was often required in a typical reductive quenching scenario.

entry	solvent (0.1 M)	conversion	yield of <b>1</b>
1	ACN	66%	40%
2	DMF	38%	16%
3	DMSO	74%	39%
4	NMP	30%	8%
5	DMAc	28%	13%
6	Toluene	0%	0%
7	Dioxane	7%	9%
8	<i>t</i> -BuCN	32%	32%
9	ACN (2 mol% Ir)	63%	43%
10	ACN (1.0 equiv DIPEA)	73%	39%
11	ACN (0.2 M)	70%	51%
12	ACN (0.05 M)	62%	39%

Conversion, yield and ratio were calculated with GC-FID with decane as internal standard.

**Table 2.2. Solvent screening**

With the conditions of entry 5 in hand (Table 2.1), we next focused on screening a wide variety of solvents (Table 2.2). Polar solvents tended to give moderate to good reactivity (Table 2.2, entry 1 to 5) while apolar solvent showed way less or no reactivity (Table 2.2, entry 6 and 7), indicating that the electron transfer event might be favored in the former and inhibited in the latter. Although high conversions were found in DMSO, non-negligible amounts of aliphatic aldehyde (20% by H-NMR) were obtained in the crude mixtures, suggesting that a Kornblum oxidation took place. Among all solvents analyzed, *t*-BuCN without weak *sp*<sup>3</sup> C-H bonds provided the best specificity in terms of chemoselectivity profile, as trace amount of reduced **1-H** was observed, albeit in lower yields (entry 8). This might suggest the reduced product (**1-H**), at least partially, might derive from the weak *sp*<sup>3</sup> C-H bonds present in the solvent via HAT.

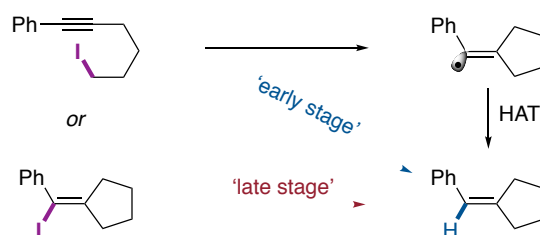
entry	reductant (0.25 equiv)	conversion	yield of <b>1</b>
1	Et <sub>3</sub> N	63%	37%
2	Bu <sub>3</sub> N	71%	48%
3	BnNMe <sub>2</sub>	36%	1%
4	TMEDA	53%	6%
5	EDTA	25%	2%
6	DBU	42%	8%
7	Me <sub>2</sub> S	5%	1%
8	PhNMe <sub>2</sub>	23%	11%
9	<b>B-1</b>	30%	4%
10	<b>B-2</b>	14%	3%
11	<b>B-3</b>	48%	24%
12	<b>B-4</b>	20%	11%

Conversion, yield and ratio were calculated with GC-FID with decane as internal standard.

**Table 2.3. Reductant screening of photoredox ATRC of unactivated alkyl iodide**

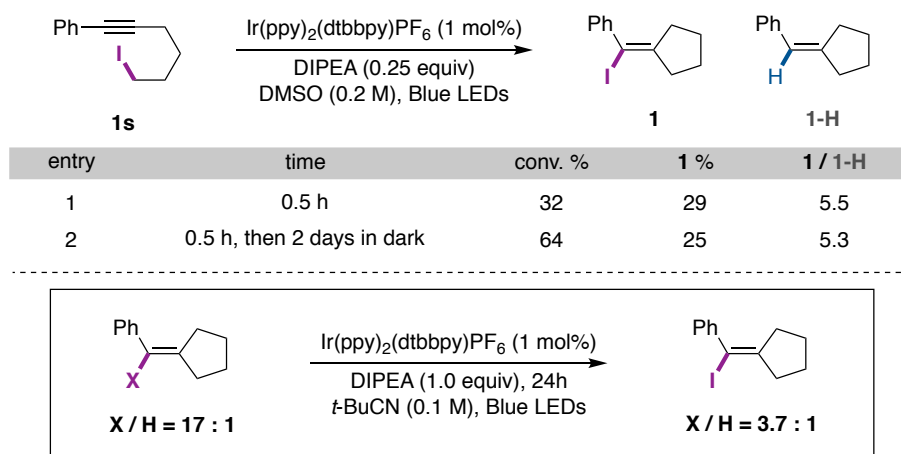
In light of these results, we decided to continue our optimization in DMSO with lower amounts of tertiary amine in order to prevent parasitic HAT reactions. Not surprisingly, amines containing relatively weaker C–H bonds gave rise to more reduced product (Table 2.3, entry 3 to 5) while the utilization of aniline derivatives (Table 2.3, entry 8-12) turned out to be detrimental compared to the corresponding alkyl series (Table 2.3, entry 1 and 3). Interestingly, the employment of bulky and

nucleophile amine DBU showed some reactivity (Table 2.3, entry 6), but with considerable amounts of the corresponding ammonium salt by reaction with **1s**.



**Scheme 2.17. When came out the reduction?**

Taking into consideration the above data, it was unclear whether the reduced product derived from a parasitic side-reaction from the final product under the reaction conditions or whether HAT occurred prior to C–I bond-formation (Scheme 2.17).



**Scheme 2.18. Origin of the reduced product**

Therefore, a series of experiments were designed to find out the pathway from which the reduction event took place. It was found that after 30 min, the reaction of **1s** in DMSO with DIPEA (0.25 equiv) led to a good **1**: **1-H** ratio; interestingly, stirring the reaction for a longer time in the dark gave rise to considerable amounts of aliphatic aldehyde via Kornblum oxidation. Particularly noteworthy was the experiment shown in Scheme 2.18 (bottom), finding out that exposure of the ATRC product (**1**) under *t*-BuCN in DIPEA (1 equiv) resulted in a non-negligible erosion in **1**: **1-H** ratio after 24 h irradiation, thus suggesting that the product is amenable to C–I homolysis followed by HAT.

entry	solvent (0.2 M)	conv. (%) <sup>a</sup>	<b>2</b> (%) <sup>a</sup>	<b>2-H</b> (%) <sup>a</sup>
1	ACN	98	68	25
2	EtCN	53	30	20
3	<i>i</i> -PrCN	47	30	11
<b>4</b>	<b><i>t</i>-BuCN</b>	<b>93</b>	<b>89</b>	<b>0</b>
5	DMF	58	35	13
6	DMSO	100	82	7
7	Acetone	47	33	6
8 <sup>b</sup>	<i>t</i> -BuCN	85	76	1
9 <sup>c</sup>	<i>t</i> -BuCN	45	39	0

<sup>a</sup> determined by GC using decane as internal standard. <sup>b</sup> without freeze-pump-thaw. <sup>c</sup> under air.

**Table 2.4. Solvents screening with 2s**

In light of these results, it was clear that the starting precursor we utilized in our optimization delivered non-negligible amounts of reduced product. Therefore, we decided to slightly modify the starting alkyl iodide with a cyclohexyl-end capped alkyne. As shown in Table 2.4, this seemingly trivial modification resulted in a much more desirable outcome, obtaining significantly lower amounts of reduced product. Specifically, it was found that **2** could be obtained in 68% yield together with 25% of **2-H** in MeCN after half day irradiation (entry 1). As expected, the solvent had a marked influence on both yield and selectivity. For example, while **2-H** was not observed with a protocol based on *t*-BuCN (Table 2.4, entry 4), solvents that can act as HAT donors generated substantial amounts of **2-H** such as MeCN, *i*-PrCN, DMF, DMSO or acetone (Table 2.4, entries 1 to 3 and 5 to 7).<sup>37</sup> In addition, we found that exclusion of oxygen was necessary to obtain high yields of the targeted product (entry 4 vs entries 8-9).

entry	amine (equiv.)	conv. (%) <sup>a</sup>	<b>2</b> (%) <sup>a</sup>	<b>2-H</b> (%) <sup>a</sup>
1	DIPEA (1.0)	93	89	0
2	Et <sub>3</sub> N (1.0)	100	88	2
3	Bu <sub>3</sub> N (1.0)	100	87	0
4	Cy <sub>2</sub> MeN (1.0)	100	82	0
5	PMP (1.0)	100	85	5
6	DIPEA (0.5)	93	86	0
7	DIPEA (0.25)	84	84	0
8	DIPEA (0.13)	69	67	0
9 <sup>b</sup>	DIPEA (0.13)	88	83	0

<sup>a</sup> GC analysis using decane as internal standard. <sup>b</sup> 48.PMP: 1,2,2,6,6-Pentamethyl piperidine

**Table 2.5. Amines screening with 2s**

Encouraged by these results, we next set up to explore the influence of the amine when using **2s** as starting precursor (Table 2.5). Although the nature of the amine did not have a significant influence on reactivity and selectivity (Table 2.5, entries 1 to 5), it is worth noting that *catalytic* amounts of DIPEA delivered **2s** in a remarkable 83% yield, but at a considerably lower rate (Table 2.5, entry 9). This result indicated that a canonical photoredox cycle might not come into play, as a typical reductive quenching requires stoichiometric amounts of the quencher.

entry	photocatalyst	emission	$E$ (M/M <sup>-</sup> )	light source	conv. (%) <sup>a</sup>	<b>2</b> (%) <sup>a</sup>
1	Ir(ppy) <sub>2</sub> (dtbbpy)PF <sub>6</sub>	581 nm	-1.51 V	Blue LEDs	93	89
2	Ru(bpy) <sub>3</sub> (PF <sub>6</sub> ) <sub>2</sub>	615 nm	-1.33 V	Blue LEDs	56	53
3	Ir(ppy) <sub>3</sub>	494 nm	-2.19 V	Blue LEDs	63	58
4	Ir(dFCF <sub>3</sub> ppy) <sub>2</sub> (dtbbpy)PF <sub>6</sub>	470 nm	-1.37 V	Blue LEDs	91	83
5	Ru(bpz) <sub>3</sub> (PF <sub>6</sub> ) <sub>2</sub>	591 nm	-0.80 V	Blue LEDs	12	8
6	Pt(ppy)(acac)	-	-	CFL (2 x 23 W)	98	86
7	Fluorescein	514 nm	-1.27 V	CFL (2 x 23 W)	78	71
8	Fluorescein	514 nm	-1.27 V	Green LEDs	32	26
9	Fluorescein Sodium	515 nm	-	Green LEDs	77	70

<sup>a</sup> GC analysis using decane as internal standard.

**Table 2.6. Photocatalysts screening**

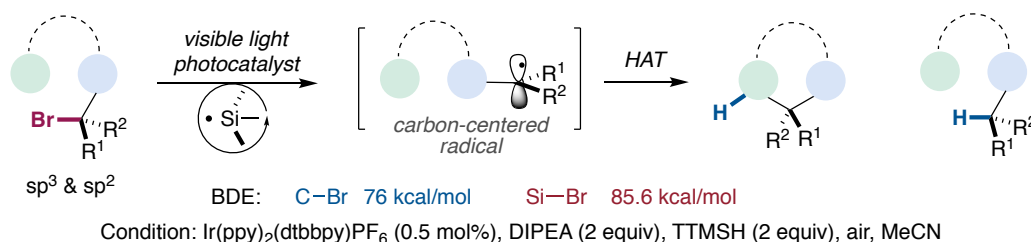
Putting everything into perspective, we questioned whether the efficiency of our photochemical ATRC could be correlated to the redox potential of the Ir photocatalyst employed. Therefore, a systematic screening of photocatalysts was our next goal. The results compiled in Table 2.6 are particularly intriguing if one takes into consideration the remarkable mismatch between the redox potential of **2s** ( $E_{1/2}^{\text{red}} \leq -2.5$  V vs. SCE in MeCN), and the redox potentials of the corresponding photocatalysts. Indeed, we realized that stronger reducing complexes such as *fac*-Ir(ppy)<sub>3</sub> ( $E_{\text{red}} \text{Ir}^{\text{III}}/\text{Ir}^{\text{II}} = -2.19$  V vs SCE in MeCN) resulted in a significant erosion in reaction rate (entry 3), whereas strongly oxidizing Ir(dFCF<sub>3</sub>ppy)<sub>2</sub>(dtbbpy)PF<sub>6</sub> ( $E_{\text{red}} \text{Ir}^{\text{III}}/\text{Ir}^{\text{II}} = -1.37$  V vs SCE in MeCN) delivered otherwise identical yields (83%) (entry 4), thus challenging the perception that a conventional SET photoredox catalytic cycle is operative. Control experiments revealed that the presence of both DIPEA and Ir(III) under visible-light irradiation was absolutely critical for success (Table 2.7).

entry	deviation	conv. (%) <sup>a</sup>	2 (%) <sup>a</sup>	2-H (%) <sup>a</sup>
1	in the dark	-	trace	-
2	no DIPEA	-	≤ 1	-
3	no Ir(III)	-	2	-
4	Ir(III) (0.5 mol%)	78	78	-
5	CFL (2*23 W) instead	87	78	2

<sup>a</sup> determined by GC using decane as internal standard.

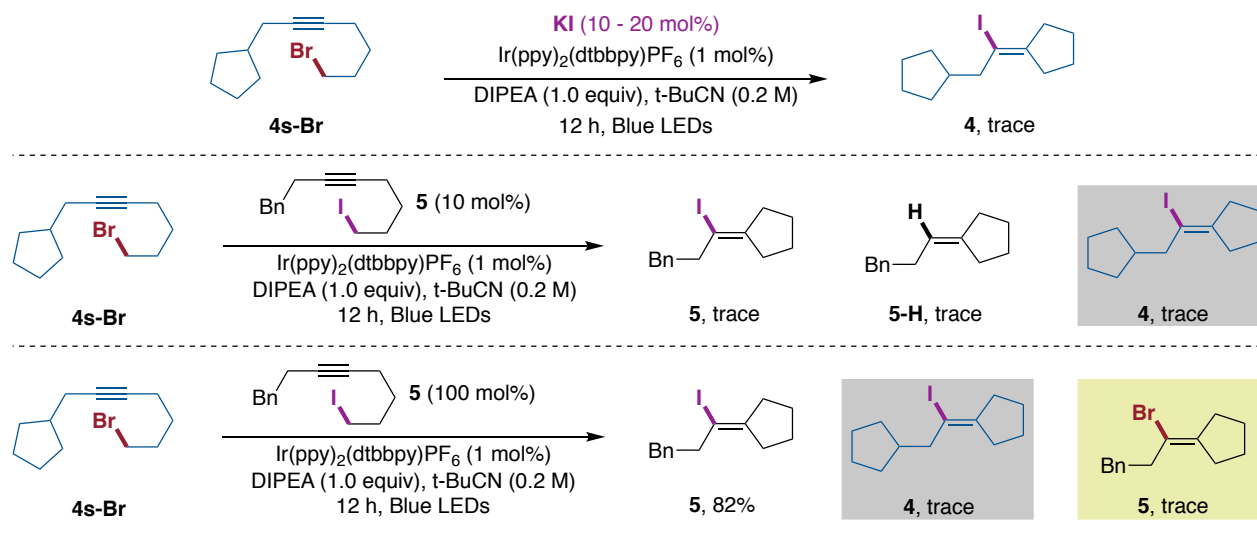
**Table 2.7. Control experiments**

Taking into consideration the results shown above, one might wonder whether an ATRC reaction could be implemented by using alkyl bromides as starting precursors. Unfortunately, however, this turned out not to be the case for a wide number of substrates analyzed with different substitution patterns at the alkyne terminus. Therefore, alternative strategies should be necessary to photochemically cleave inert unactivated alkyl bromides via visible light photoredox technique.



**Scheme 2.19. Visible light photoredox reduction of unactivated bromides**

It is worth noting that in 2016, the Stephenson group described a photodebromination transformation that made use of silyl radicals to abstract bromine atom from even unactivated organic bromides (Scheme 2.19).<sup>36</sup> Obviously, this strategy was not suitable for ATRA type reactions as the corresponding product will react with the corresponding silyl radicals.

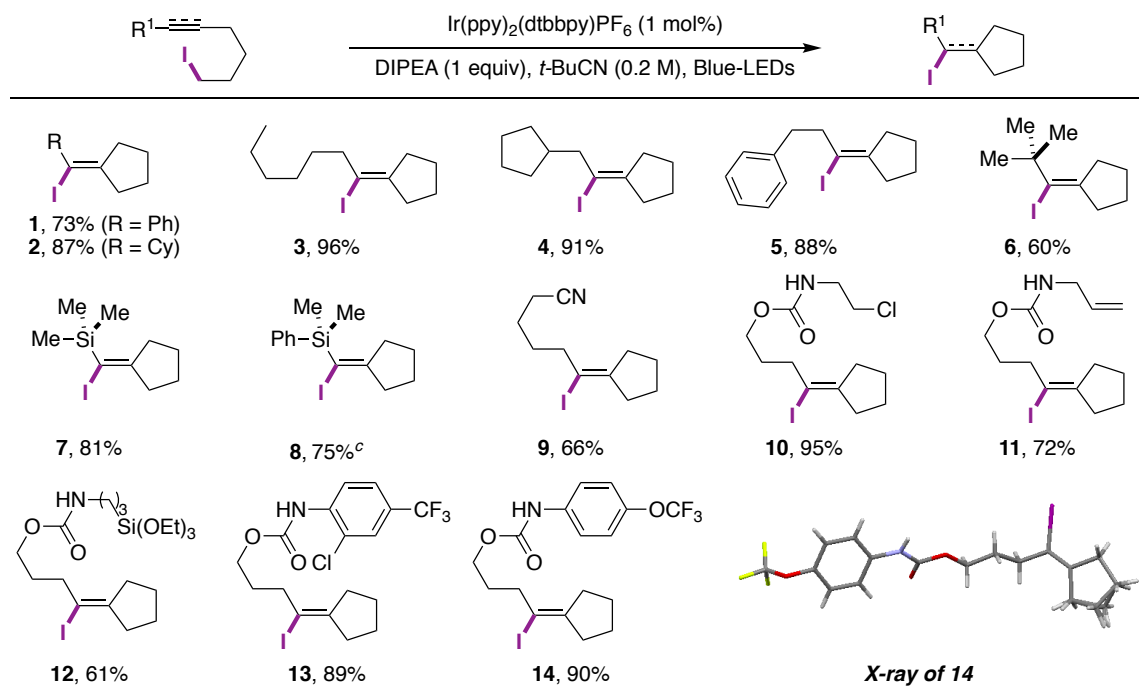


### Scheme 2.20. Interrupted *I*-ATRC by unactivated alkyl bromide

Aiming at providing a solution to this challenge, we questioned whether the addition of KI would trigger the ATRC reaction of an alkyl bromide. However, traces amount of **4** were observed in the crude reaction mixtures (Scheme 2.20, *up*), suggesting that a halide exchange via conventional Finkelstein reaction did not occur, or at least at a decent extent. Intriguingly, traces amount of **4** were found when utilizing catalytic amounts of **5s** in the ATRC reaction of **4s-Br** (Scheme 2.20, *middle*) whereas the utilization of stoichiometric amounts of **5** gave rise to traces of **5** (Scheme 2.20, *bottom*). These results highlight the difficulty for conducting an ATRC reaction with unactivated alkyl bromides in the presence of iodide species, probably due to the ease of C-I bond-homolysis and the high-lying  $\sigma^*$  orbital of the C( $sp^3$ )-Br bond.



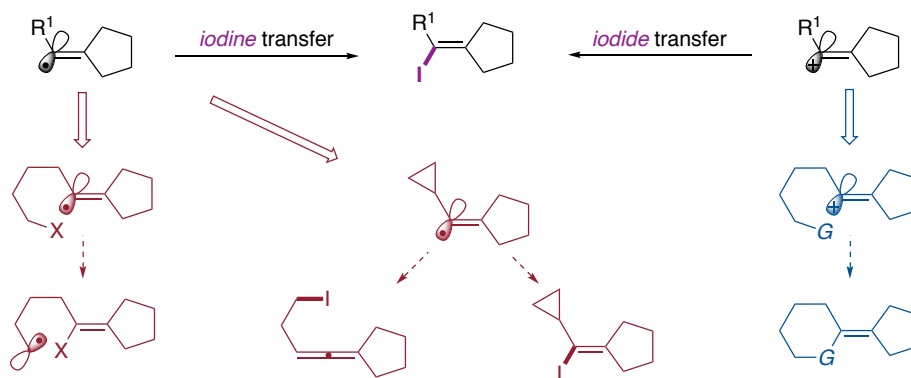
## 2.4.2 Preparative Substrate Scope



<sup>a</sup> As for Table 2.4, entry 1 (12-96 h). <sup>b</sup> Isolated yields, average of at least two runs. <sup>c</sup> **8** (5.80 mmol scale) with **Ir-2** (0.1 mol%).

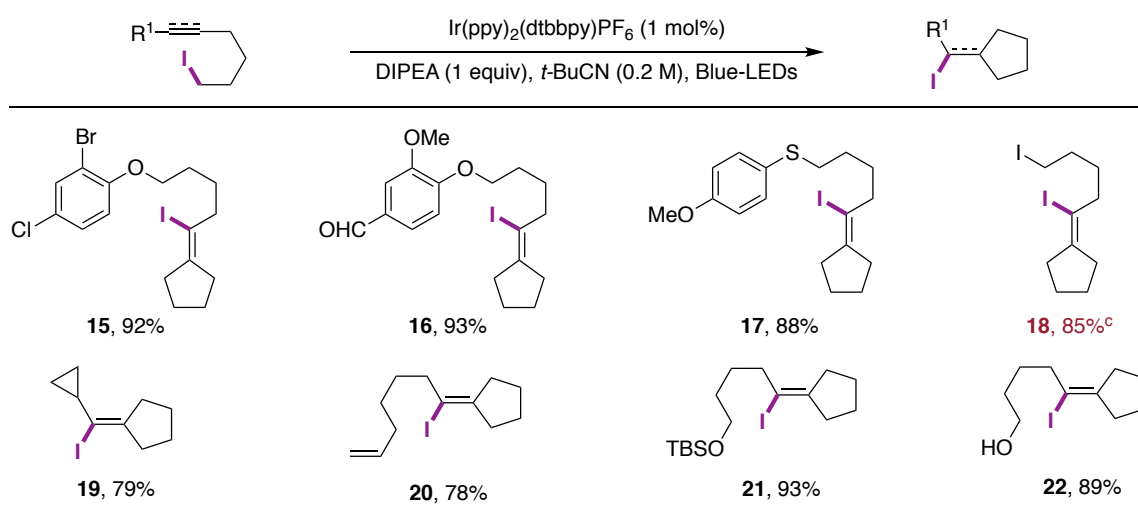
**Table 2.8. Scope of *I*-ATRC with Single Cyclization**

With the optimized conditions in hand for our ATRC reaction of unactivated alkyl iodide (Table 2.4, entry 4), we next focused our attention on exploring the preparative scope of this reaction. As evident from the results compiled in Table 2.8, our visible light photocatalytic ATRC of unactivated alkyl iodides turned out to be highly chemoselective, as alkyl iodides possessing silyl groups (**7**, **8** and **12**), nitriles (**9**), alkenes (**11**), carbamates (**10** to **14**), trifluoromethyl (**13**) or trifluoromethoxyl (**14**) group among others, were accommodated quite well. Importantly, substrates with steric hindrance showed good to excellent reactivity (**6** to **8**). Notably, aryl or alkyl halides do not interfere (**10**, **13**), providing an additional handle via iterative metal-catalyzed cross-coupling techniques. Moreover, the reaction of **8** could be easily scaled up, even at 0.1 mol% loadings of Ir(III) photocatalyst.



**Scheme 2.21. Potential intermediates of the *I*-ATRC**

Next, we decided to synthesize a rather specific starting precursors to study the corresponding iodine transfer event (Scheme 2.21). As shown, substrates possessing weak C–H atoms locating an appropriate location within the side-chain did not result in a parasitic HAT (**15** to **17**). Likewise, the presence of a pending alkyl iodide did not interfere (**18**), with no reduced or bicyclization products being observed in the crude mixtures. In addition, the lack of double cyclization with a pending alcohol (**22**) or an alkene motif (**20**) leaves a reasonable doubt about the involvement of transient vinyl cationic species via an oxidative quenching pathway (Scheme 2.21, *right*).<sup>30,31</sup>



<sup>a</sup> As for Table 2.4, entry 1 (12-96 h). <sup>b</sup> Isolated yields, average of at least two independent runs. <sup>c</sup> impure with SM.

**Table 2.9. Potential substrates for double cyclizations or ring opening of *I*-ATRC**

Interestingly, the utilization of an alkyne end-capped with a cyclopropane did not trigger ring-opening (Table 2.9, **19**). While one might argue that this challenges the perception that vinyl radicals intervene, one should take into consideration the differences between the ring-opening of a carbon or a vinyl radical adjacent to a cyclopropyl unit. Unlike the fast ring-opening of the former, the latter

requires a flip of 90°, a feature that is likely beyond reach with the substrates employed in our ATRC process.<sup>38</sup>

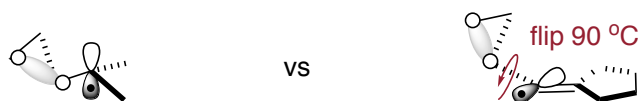
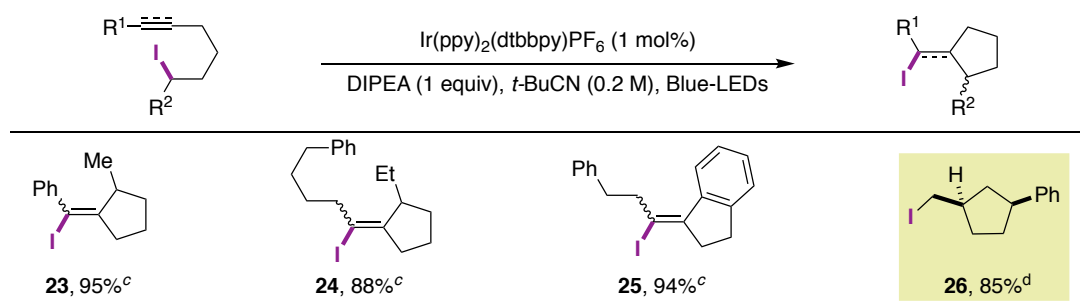


**Figure 2.3. Ring opening of cyclopropane**

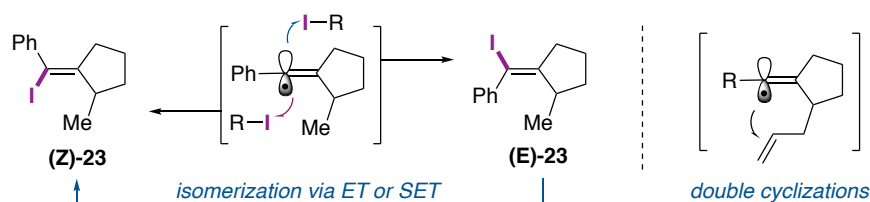
As expected, the reaction of secondary alkyl iodides posed no problems (Table 2.10), although statistical *E/Z* mixtures were obtained for **23** to **25**.<sup>39</sup> As shown for **25**, the fused cyclopentane rings were equally effective. Although we demonstrated the viability for performing a photochemical ATRC with unactivated alkyl iodides (**1** to **25**), it was unclear whether the reaction could be extended to unactivated alkyl iodides bearing alkenes on the side-chain. This perception was reinforced by the notion that the product could be amenable for parasitic *sp*<sup>3</sup> C–I homolysis, leading to undesired HAT processes.



<sup>a</sup> As for Table 2.4, entry 1 (12-96 h). <sup>b</sup> Isolated yields, average of at least two runs. <sup>c</sup> *E/Z* = 1:1. <sup>d</sup> dr = 10:1.

**Table 2.10. Challenging substrate for *I*-ATRC**

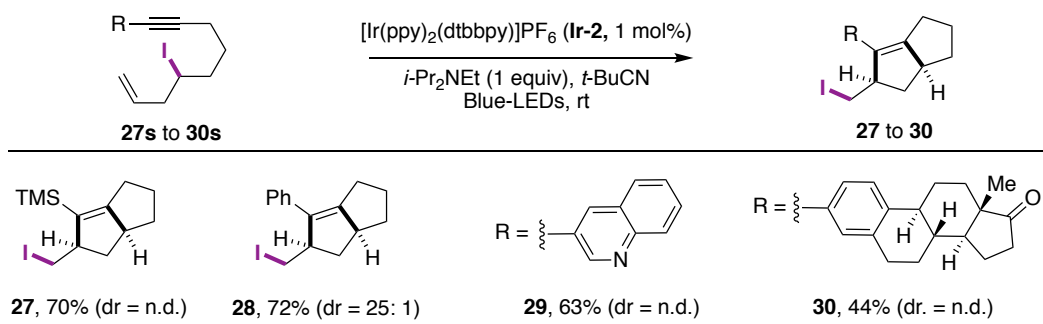
Surprisingly, we found that **26s** possessing a pending alkene reacted equally well to give **26** in 85% yield with an excellent dr, invariably favoring the *cis*-isomer (Table 2.10) These results are particularly noteworthy taking into consideration the low diastereoselectivities found with “radical-type” cyclizations.



**Scheme 2.22. Assessing the *E/Z* problem**

The significant erosion in selectivity obtained for **23** to **25** is consistent with a rapid interconversion of *Z* and *E*-isomers via either SET or ET, ending up in a flat *sp*<sup>2</sup>-type radical or triplet biradical state

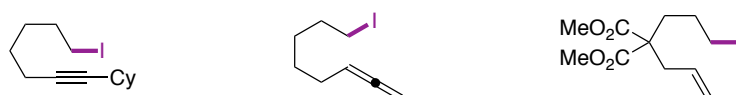
of the tetrasubstituted styrene that can trigger the halide abstraction with equal ease to lead to **E-23** or **Z-23**. In light of these results, we hypothesized that the use of a secondary alkyl iodide bearing an allyl group could allow us to obtain bicyclic skeletons via atom transfer radical double-cyclizations in excellent diastereoselectivities.<sup>23</sup> As shown in Table 2.11, this turned out to be the case and **27** to **30** were obtained in good yields with high levels of diastereoselectivities under the reaction conditions. To the best of our knowledge, these results represent the first atom transfer double radical cyclization performed using photocatalysis under visible light irradiation.<sup>40</sup>



<sup>a</sup> As for Table 2.4, entry 1 (12-96 h). <sup>b</sup> Isolated yields, average of at least two independent runs.

**Table 2.11. Scope of ATRC with double cyclizations**

Although the results shown in Tables 2.8-2.11 illustrate the prospective impact of visible light-mediated *redox-neutral* ATRC reactions with unactivated alkyl iodides, our efforts to extend this concept to the synthesis of six-membered rings failed, even with substrates possessing tethers at an appropriate location on the side-chain that might facilitate the cyclization via Thorpe-Ingold effect (Scheme 2.23).



**Scheme 2.23. Failed substrate to access six membered ring**

## 2.5. Mechanistic Considerations

### 2.5.1. Determination of redox potentials by cyclic voltammetry.

In view of these results, we turned our attention to study the mechanism of our photochemical ATRC reaction. To such end, a cyclic voltammetry study was carried out to investigate the feasibility of the electron transfer between the Ir photocatalyst and the unactivated alkyl iodide **2s** in *t*-BuCN. Photocatalyst [Ir(ppy)<sub>2</sub>(dtbbpy)]PF<sub>6</sub> (**Ir-2**) displayed quasi-reversible redox behavior (Table 2.5,  $E_{1/2}^{\text{red}} = -1.42$  V), whereas **2s** showed an irreversible reduction below -2.5 V (Table 2.5) under the

same conditions. This seemingly trivial experiment reinforced the notion that a direct electron transfer between the reduced Ir(II) complex and compound **2s** is unlikely under the reaction conditions because of the high mismatch in redox potential of the starting material and photocatalyst (1.08V).

	$E_{1/2}$ (vs SCE)	$E_p$ (vs SCE)	Electrolyte
Ferrocene	0.4 V	-	0.1 M Bu <sub>4</sub> NPF <sub>6</sub> (MeCN)
	0.51 V	-	0.1 M Bu <sub>4</sub> NPF <sub>6</sub> ( <i>t</i> BuCN)
	-	-	0.1 M Bu <sub>4</sub> NPF <sub>6</sub> (DMF)
[Ir(ppy) <sub>2</sub> (dtbbpy)]PF <sub>6</sub>	-1.48 V	-	0.1 M Bu <sub>4</sub> NPF <sub>6</sub> (MeCN)
	-1.42 V	-	0.1 M Bu <sub>4</sub> NPF <sub>6</sub> ( <i>t</i> BuCN)
	-1.39 V	-	0.1 M Bu <sub>4</sub> NPF <sub>6</sub> (DMF)
<b>2s</b>	-	≤ -2.5 V	0.1 M Bu <sub>4</sub> NPF <sub>6</sub> (MeCN)
	-	≤ -2.5V	0.1 M Bu <sub>4</sub> NPF <sub>6</sub> ( <i>t</i> BuCN)
	-	-	0.1 M Bu <sub>4</sub> NPF <sub>6</sub> (DMF)

The redox potentials (vs SCE) were determined by cyclic voltammetry using 5.0 mM solutions of **2s** and **Ir-2** in a 0.1 M solution of NBu<sub>4</sub>PF<sub>6</sub> with a glassy carbon disk electrode at a scan rate of 0.1 V/s. The counter-electrode was a platinum disk. Solutions were purged with argon for 30 min prior to the measurement to displace oxygen.

**Table 2.5. Electrochemical data for **2s** and Ir-2**

### 2.5.2. Mechanistic Considerations: ON/OFF experiment.

“ON-OFF” experiments are routinely performed in photochemical transformations to unravel whether the reaction proceeds in the absence of light irradiation or not. However, the interpretation of these results can often be controversial, particularly if excimers or chain-propagation scenarios come into play. As shown in Figure 2.4, we found no conversion during the dark period. While this necessarily invokes that constant irradiation is required, it does not allow us to rule out whether radical-chain mechanisms might be operative.

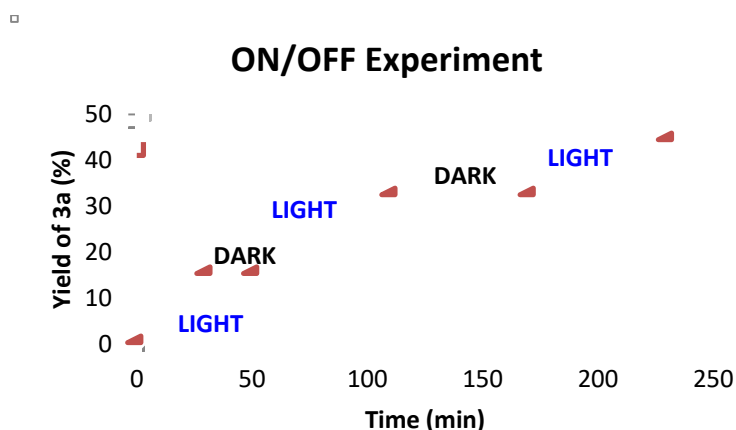


**Figure 2.4. ON/OFF experiment**

### 2.5.3. Mechanistic Considerations: Luminescence Quenching Experiments.

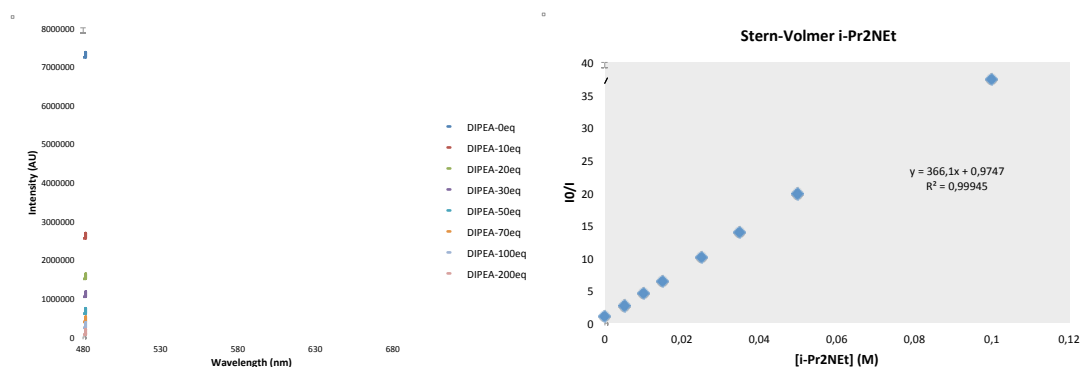


Figure 2.5. Quenching Ir-2\* with DIPEA

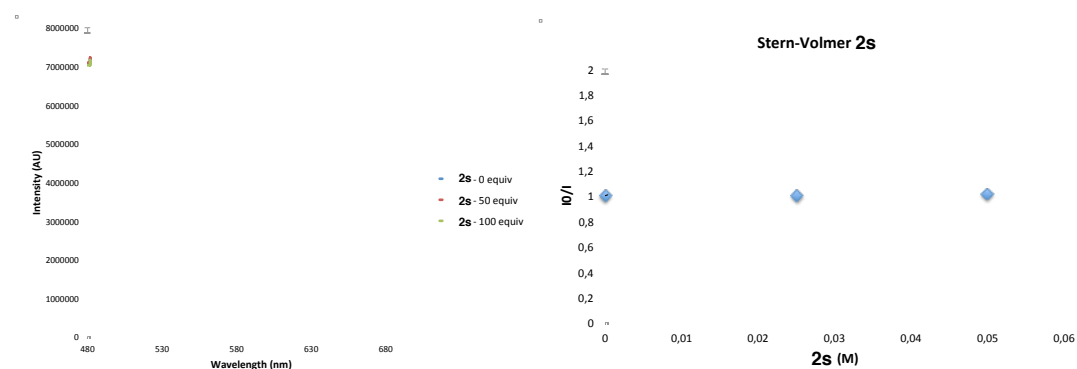


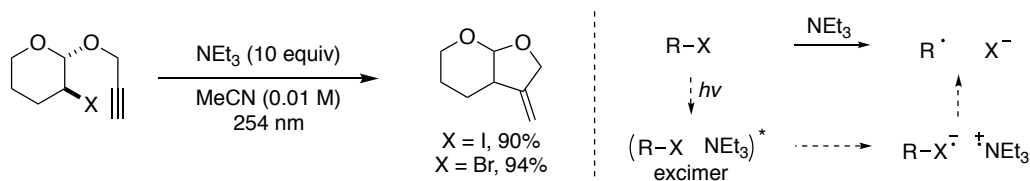
Figure 2.6. Quenching Ir-2\* with 2s

In order to study the interaction of **Ir-2** and the reaction components, Stern-Volmer quenching experiments were performed. As shown in Figures 2.5 and 2.6, luminescence quenching of **Ir-2** was observed when DIPEA was added; as expected for the considerable mismatch in redox-potentials, no quenching occurred with starting material **2s**. Even though the quenching studies indicated a reductive quenching pathway, the large energy mismatch between redox potentials of **Ir-2** ( $E_{red} \text{Ir}^{\text{III}}/\text{Ir}^{\text{II}}$  vs  $E_{red} (\mathbf{2s}) = \sim 1 \text{ V}$ ) suggested that a conventional photocatalytic redox cycle might not be operative. In line with this notion, we measured the quantum yield of the standard reaction with a fluorimeter and our Blue LED strips. The measured quantum yield lied in the range of 2.2 to 2.3. Although this value falls into the category of a radical-chain propagation, this data could not explain that the standard reaction gave 83% yield with *catalytic amounts* of DIPEA (Table 2.5, entry 9), pointing towards the existence of alternate light-consuming events.

It has long been recognized that absorption of high energy UV light by the carbon-halogen chromophore results in homolytic cleavage of the C-X bond. Alkyl iodides afford mixtures of radical- and, in particular, ion-derived photoproducts in solution. However, in the presence of amine, the selectivity can be altered. Irradiation of alkyl halides in the presence of tertiary amines is a

synthetically useful method for generating radical-derived products that avoids the troublesome purification problems associated with the conventional method of using trialkyltin hydrides to generate radicals from alkyl halide precursors.

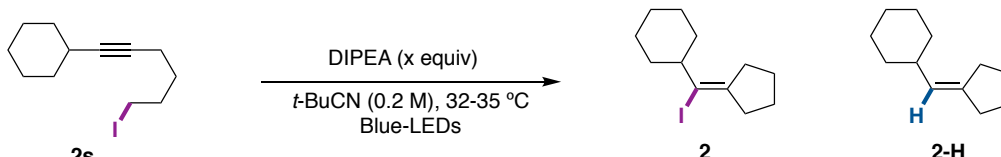
#### 2.5.4. Mechanistic Considerations: Excimer Formation



#### Scheme 2.24. Cossy's Tertiary Amine Promoted Reductive Photocyclization

In 1994, Cossy reported a rather intriguing photochemical reaction that promoted the reductive photocyclization of unactivated alkyl halides without using toxic reagents by using NEt<sub>3</sub> and high energy UV-irradiation (Scheme 2.7). In view of the high yields obtained, the reaction was proposed to operate via the formation of an excimer between the alkyl halide and the tertiary amine, which subsequently would form an alkyl radical via single electron transfer. Such open-shell species could then be trapped in an intramolecular fashion with the pending alkyne followed by HAT from the amino radical cation to deliver the photocyclized product. The importance of these observations can hardly be underestimated, as it suggests that mechanisms other than SET or ET might be operative in photochemical events with rather unreactive bonds. This is particularly illustrative within the context of our ATRC reaction. Indeed, it is worth noting that we observed non-negligible amounts of **2** when **Ir-2** was omitted at longer reaction times (Table 2.12, entry 1), suggesting that excimers might intervene in our photochemical ATRC reaction as well. Unlike Cossy's protocol, however, the observation of **2** in the absence of **Ir-2** under visible light irradiation suggests that the formation of excimers should by no means be limited to high-intensity UV-irradiation.

In light with our expectations, such photochemical reaction could be correlated by the intensity of the visible light irradiation (Table 2.12, entry 2). As shown in entries 3-4, lower yields were obtained at lower temperatures, suggesting that the temperature plays an important role on accelerating the electron transfer from the electron-rich amine to the corresponding alkyl iodide. After further experimentation, it was found that the stoichiometry of the tertiary amine and the solvent played an important role en route to either **2** or **2-H**. Specifically, the best results were accomplished in DMSO with 1 equivalent of the amine, thus predominantly leading to **2** (entry 5); interestingly, a selectivity switch en route to **2-H** was observed under otherwise similar reaction conditions but using 10 equivalents of DIPEA instead (entry 6).



Entry	Light source	DIPEA	Irradiation time	2 (%) <sup>b</sup>	2-H (%) <sup>b</sup>
1	Blue LED (0.364 mW/cm <sup>2</sup> )	1 equiv	60 h	12	0
2	Blue LED (4.21 mW/cm <sup>2</sup> )	1 equiv	60 h	44	0
3	Blue LED (4.21 mW/cm <sup>2</sup> ) <sup>b</sup>	1 equiv	48 h	16	0
4	Blue LED (4.21 mW/cm <sup>2</sup> ) <sup>b,c</sup>	1 equiv	48 h	25	0
5	Blue LED (4.21 mW/cm <sup>2</sup> ) <sup>d</sup>	1 equiv	48 h	70	10
6	Blue LED (4.21 mW/cm <sup>2</sup> ) <sup>d</sup>	10 equiv	84 h	15	70

<sup>a</sup> Isolated yields. <sup>b</sup> 25 °C. <sup>c</sup> In the presence of 1 eq of thioxanthone. <sup>d</sup> DMSO as solvent.

**Table 2.12. Assessing Visible Light Photocatalyst-free ATRC**

### 2.5.5. Mechanistic Considerations: Catalytic Cycle and Discussions.

The large energy mismatch between the redox potentials of **Ir-2** ( $E_{red} [\text{Ir}^{\text{III}}/\text{Ir}^{\text{II}}]$  vs  $E_{red} [\mathbf{2s}] = \sim 1 \text{ V}$ ) suggested that a conventional photocatalytic redox cycle might not be operative.<sup>16</sup> In principle, a number of different pathways can be considered for our visible light-mediated atom transfer radical cyclization of unactivated alkyl iodides, although some of them can be ruled out on the basis of our experimental information.

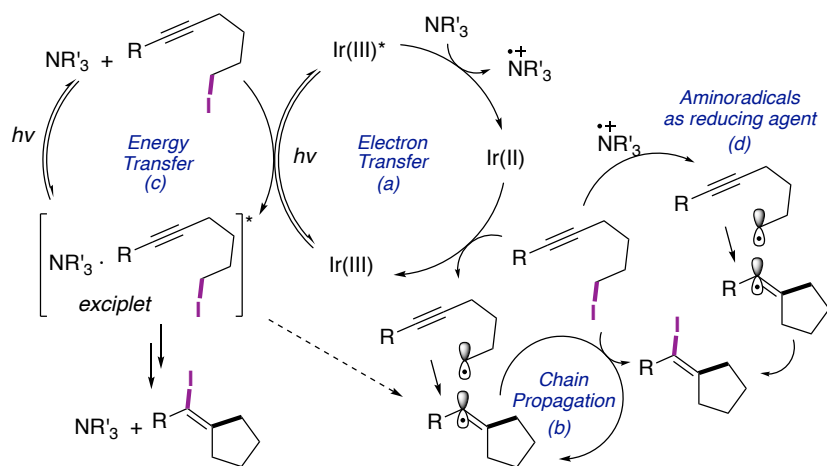


**Figure 2.5. Possible catalytic cycle**

The behavior of the tertiary amine as a quenching agent for the triplet state of the photocatalyst **Ir-2** pointed towards a reductive quenching scenario for the targeted photocatalytic transformation. However, the absence of double cyclization products with substrates **20s** and **22s** (Table 2.9), and the fact that substoichiometric amounts of amine can efficiently promote the reaction (Table 2.5, entry 9) rules out the formation of cationic vinyl intermediates. Therefore, we started considering the possibility of a radical-chain propagation photoinitiated by **Ir-2** (Figure 2.5, pathways *a* and *b*), an



assumption that correlates well with the measurement of the quantum yield of the reaction (2.2-2.4). The formation of the alkyl radical can be explained by the formation of an exciplex under blue light irradiation, which could potentially trigger the chain-propagation event to yield **2**. Although an in-depth mechanistic proposal requires further investigations, we speculate that the formation of an exciplex might be accelerated due to energy transfer from the triplet excited state of **Ir-2** (pathway c) to the substrate, indirectly ruling out the possibility of a canonical SET from the iridium photocatalyst to the starting precursor. However, we cannot exclude the possibility of chain-processes initiated from in situ generated  $\alpha$ -amino radicals generated by deprotonation of the corresponding amine radical cation (pathway d).

## 2.6. Visible Light Photoredox ATRC: The Conclusion

In summary, we have described the development of an unconventional photocatalytic *redox-neutral* ATRC of *unactivated* alkyl iodides under visible light irradiation. The salient features of this transformation are the mild conditions, broad scope and exquisite chemoselectivity, thus enabling the preparation of highly versatile building blocks susceptible to further functionalization. Preliminary mechanistic experiments leave some doubt about a canonical photoredox cycle and suggests the intermediacy of exciplex under visible light irradiation in the presence of tertiary amines.

## 2.7. Bibliography

1. Kamigaito, Ando, M. T., Sawamoto, M. Metal-Catalyzed Living Radical Polymerization. *Chem. Rev.* **2001**, *101*, 3689.
2. Courant, T.; Masson, G. Recent Progress In Visible-Light Photoredox-Catalyzed Intermolecular 1,2-Difunctionalization Of Double Bonds Via An Atra-Type Mechanism. *J. Org. Chem.*, **2016**, *81*, 6945.
3. Wade, L.G. Organic Chemistry. Ed 5. Prentice Hall: **2003**. 314.
4. (a) M. S. Kharasch, And Frank R. Mayo. The Peroxide Effect In The Addition Of Reagents To Unsaturated Compounds. I. The Addition Of Hydrogen Bromide To Allyl Bromide. *J. Am. Chem. Soc.*, 1933, *55*, 2468; (b) Kharasch, M. S., Skell, P. S., Fischer, P. Reaction Of Atom And Free Radical In Solution. Xii. The Addition Of Bromo Esters To Olefins. *J. Am. Chem. Soc.* **1948**, *70*, 1055; (c) Kharasch, M. S., Jensen, E. V., Urry, W. H. Addition Of Carbon Tetrachloride And Chloroform To Olefins. *Science* **1945**, *102*, 128.
5. Curran, D. P., Chen, M.-H., Spletzer, E., Seong, C. M., Chang, C.-T. Atom-Transfer Addition And Annulation Reactions Of Iodomalonates. *J. Am. Chem. Soc.* **1989**, *111*, 8872.
6. Curran, D. P., Bosch, E., Kaplan, J., Newcomb, M. Rate Constants For Halogen Atom Transfer From Representative  $\alpha$ -Halo Carbonyl Compounds To Primary Alkyl Radicals. *J. Org. Chem.* **1989**, *54*, 1826.
7. Curran, D. P., Chang, C.-T. Atom Transfer Cyclization Reactions Of  $\alpha$ -Iodo Ester, Ktones, And Malonates: Examples Of Selective 5-Exo, 6-Endo, And 7-Endo Ring Closures. *J. Org. Chem.* **1989**, *54*, 3140.
8. Curran, D. P., Seong, C. M. Atom-Transfer Addition, Annulation, And Macrocyclization Reactions Of Iodomalononitriles. *J. Am. Chem. Soc.* **1990**, *112*, 9401.
9. Curran, D. P., Tamine, J. Effect Of Temperature On Atom Transfer Cyclization Reactions Of Allylic  $\alpha$ -Iodo Ester And Amides. *J. Org. Chem.* **1991**, *56*, 2746.
10. Curran, D. P., Kim, D. Iodine Atom Transfer Addition Reactions With Alkynes. Part 1: Alkyl Iodides. *Tetrahedron* **1991**, *47*, 6171.
11. Curran, D. P., Kim, D., Ziegler, C. Iodine Atom Transfer Addition Reaction With Alkynes. Part 2;  $\alpha$ -Iodocarbonyls. *Tetrahedron* **1991**, *47*, 6189.
12. Yorimitsu, H., Nakamura, T., Shinokubo, H., Oshima, K. Triethylborane-Mediated Atom Transfer Radical Cyclization Reaction In Water. *J. Org. Chem.* **1998**, *63*, 8604.
13. Yorimitsu, H., Nakamura, T., Shinokubo, H., Oshima, K., Omoto, K., Fujimoto, H. Powerful Solvent Effect Of Water In Radical Reaction: Triethylborane Induced Atom-Transfer Radical Cyclization In Water. *J. Am. Chem. Soc.* **2000**, *122*, 11041.
14. Yorimitsu, H., Shinokubo, H., Matsubara, S., Oshima, K., Omoto, K., Fujimoto, H. Triethylborane-Induced Bromine Atom-Transfer Radical Addition In Aqueous Media: Study Of The Solvent Effect On Radical Addition Reactions. *J. Org. Chem.* **2001**, *66*, 7776.
15. Weidner, K., Giroult, A., Panchaud, P., Renaud, P. Efficient Carboazidation Of Alkenes Using A Radical Desfonylative Azide Transfer Process. *J. Am. Chem. Soc.* **2010**, *132*, 17511.
16. Renaud, P., Ollivier, C., Panchaud, P. Radical Carboazidation Of Alkenes: An Efficient Tool For Preparation Of Pyrrolidinone Derivatives. *Angew. Chem. Int. Ed.* **2002**, *41*, 3460.
17. Panchaud, P., Ollivier, C., Renaud, P., Zigmantas, S. Radical Carboazidation: Expedient Assembly Of The Core Structure Of Various Alkaloid Families. *J. Org. Chem.* **2004**, *69*, 2755.
18. Liu, H., Qiao, Z., Jiang, X. Palladium-Catalyzed Atom Transfer Radical Cyclization Of Unactivated Alkyl Iodide. *Org. Biomol. Chem.* **2012**, *10*, 7274.
19. Bergeot, O., Corsi, C., Quiclet-Sire, B., Zard, S. Z. Radical Instability In Aid Of Efficiency: A Powerful Route To Highly Functional Mida Boronates. *J. Am. Chem. Soc.* **2015**, *137*, 6762.
20. Yang, Z.-Y., Burton, D. J. A New Approach To  $\alpha$ ,  $\alpha$ -Difluoro-Functionalized Esters. *J. Org. Chem.* **1991**, *56*, 5125.
21. Metzger, J. O., Mahler, R. Radical Addition Of Activated Haloalkanes To Alkenes Initiated By Electron Transfer From Copper In Solvent-Free Systems. *Angew. Chem., Int. Ed.* **1995**, *34*, 902.
22. Forti, L., Ghelfi, F., Libertini, E., Pagnoni, U. M., Soragni, E. Halogen Atom Transfer Radical Addition Of  $\alpha$ -Polychroester To Olefins Promoted By Fe<sup>0</sup> Fillings. *Tetrahedron* **1997**, *53*, 17761.
23. Monks, B. M., Cook, S. P. Palladium-Catalyzed Intramolecular Iodine-Transfer Reaction In The Presence Of  $\beta$ -Hydrogen Atoms. *Angew. Chem. Int. Ed.* **2013**, *52*, 14214.
24. Quebatte, L., Scopelliti, R., Severin, K. Combinatorial Catalysis With Bimetallic Complexes: Robust And Efficient Catalysts For Atom Transfer Radical Addition. *Angew. Chem., Int. Ed.* **2004**, *43*, 1520.
25. (a) Lübbers, T., Schäfer, H. J. Iodo-Atom-Transfer Cyclization Of  $\Delta^{6,7}$ -Unsaturated 2-Iodo Esters With Chromium(II) Acetate. *Synlett* **1991**, 861; (b) Gilbert, B. C., Kalz, W., Lindsay, C. I., Mcgrail, P. T., Parsons, A. F., Whittaker, D. T. E. Initiation Of Radical Cyclisation Reaction Using Dimanganese Decarbonyl. A Flexible Approach To Preparing 5-Membered Rings. *J. Chem. Soc., Perkin Trans. 1*, **2000**, 1187.
26. Cao, L., Li, C.  $P\text{-Meoc}_6\text{H}_4\text{N}_2^+\text{BF}_4^-/\text{TiCl}_3$ : A Novel Initiator For Halogen Atom Transfer Radical Reaction In Aqueous Media. *Tetrahedron Lett.* **2008**, *49*, 7380.
27. (a) Liu, H., Li, C., Qiu, D., Tong, X. Palladium-Catalyzed Cycloisomerizations Of (Z)-1-Iodo-1,6-Dienes: Iodine Atom Transfer And Mechanistic Insight To Alkyl Iodide Reductive Elimination. *J. Am. Chem. Soc.* **2011**, *133*, 6187; (b) Newman S. G., Lautens, M. Palladium-Catalyzed Carboiodination Of Alkenes: Carbon-Carbon Bond Formation With Retention Of Reactive Functionality. *J. Am. Chem. Soc.* **2011**, *133*, 1778; (c) Liu, H., Qiao Z., Jiang, X. Palladium-Catalyzed Atom Transfer Radical Cyclization Of Unactivated Alkyl Iodide. *Org. Biomol. Chem.*, **2012**, *10*, 7274; (d) Dennis P. Curran, D. P., Eichenberger, E., Collis, M., Roepel, M. G., Thomat, G. Group Transfer Addition Reactions Of Methyl(Phenylseleno)Malononitrile To Alkenes. *J. Am. Chem. Soc.* **1994**, *116*, 4279.
28. Selected Reviews: (a) Fabry, D. C.; Rueping, M. *Acc. Chem. Res.* **2016**, *49*, 1969; (b) Hopkinson, M. N.; Tlahuext-Aca, A.; Glorius, F. *Acc. Chem. Res.* **2016**, *49*, 2261; (c) Skubi, K. L.; Blum, T. R.; Yoon, T. P. *Chem. Rev.* **2016**, *116*, 10035; (d) Kärkäs, M. D.;

- Porco, J. A.; Stephenson, C. R. J. *Chem. Rev.*, **2016**, *116*, 9683; (e) Hopkinson, M. N., Sahoo, B., Li, J., Glorius, F. *Chem. Eur. J.* **2014**, *20*, 3874; (f) Prier, C. K.; Rankic, D. A.; Macmillan, D. W. C. *Chem. Rev.* **2013**, *113*, 5322.
29. Selected Reviews: (a) Studer, A.; Curran, D. P. *Angew. Chem. Int. Ed.* **2016**, *55*, 58. (b) Focsaneanu, K.-S.; Scaiano, J. C. *Helv. Chim. Acta* **2006**, *89*, 2473. (c) Fischer, H. *Chem. Rev.* **2001**, *101*, 3581.
30. (a) Nguyen, J. D., Tucker, J. W., Konieczynska, M. D., Stephenson, C. R. J. Intermolecular Atom Transfer Radical Addition To Olefins Mediated By Oxidative Quenching Of Photoredox Catalysts. *J. Am. Chem. Soc.* **2011**, *133*, 4160; (b) Wallentin, C., Nguyen, J. D., Finkbeiner, P., Stephenson, C. R. J. Visible Light-Mediated Atom Transfer Radical Addition Via Oxidative Reductive Quenching Of Photocatalysts. *J. Am. Chem. Soc.* **2012**, *134*, 8875.
31. (a) Sun, J., Li, P., Guo, L., Yu, F., He, Y.-P., Chu, L. Catalytic, Metal-Free Sulfonylcyanation Of Alkenes Via Visible Light Organophotoredox Catalysis *Chem. Commun.*, **2018**, *54*, 3162; (b) Arceo, E., Montroni, E., Melchiorre, P. Photo-Organocatalysis Of Atom-Transfer Radical Additions To Alkenes. *Angew. Chem. Int. Ed.* **2014**, *53*, 12064; (c) Arceo, E.; Montroni, E.; Melchiorre, P. Photo-Organocatalysis Of Atom-Transfer Radical Additions To Alkenes. *Angew. Chem. Int. Ed.* **2014**, *53*, 12064.
32. Gu, X.; Li, X.; Qu, Y.; Yang, Q.; Li, P.; Yao, Y. Intermolecular Visible - Light Photoredox Atom - Transfer Radical [3+2] - Cyclization Of 2 - (Iodomethyl)Cyclopropane - 1,1 - Dicarboxylate With Alkenes And Alkynes *Chem. Eur. J.* **2013**, *19*, 11878.
33. (a) Nguyen, J. D.; D'amato, E. M.; Narayanam, J. M. R.; Stephenson, C. R. J. Engaging Unactivated Alkyl, Alkenyl And Aryl Iodides In Visible-Light-Mediated Free Radical Reactions. *Nat. Chem.* **2012**, *4*, 854; (b) Kim, H.; Lee, C. Visible-Light-Induced Photocatalytic Reductive Transformations Of Organohalides *Angew. Chem. Int. Ed.* **2012**, *51*, 12303.
34. (a) Liu, Y. Cornella, J. Martin, R. Ni-Catalyzed Carboxylation Of Unactivated Primary Alkyl Bromides And Sulfonates With Co<sub>2</sub>. *J. Am. Chem. Soc.* **2014**, *136*, 11212; (b) Wang, X., Liu, Y., Martin, R. Ni-Catalyzed Divergent Cyclization/Carboxylation Of Unactivated Primary And Secondary Alkyl Halides With Co<sub>2</sub>. *J. Am. Chem. Soc.* **2015**, *137*, 6476; (c) M. Börjesson, T. Moragas, R. Martin. Ni-Catalyzed Carboxylation Of Unactivated Alkyl Chlorides With Co<sub>2</sub>. *J. Am. Chem. Soc.* **2016**, *138*, 7504; (d) Serrano, E., Martin, R. Nickel-Catalyzed Reductive Amidation Of Unactivated Alkyl Bromides. *Angew. Chem. Int. Ed.* **2016**, 11207.
35. Devery Iii, J. J., Nguyen, J. D., Dai, C., Stephenson, C. R. J. Light-Mediated Reductive Debromination Of Unactivated Alkyl And Aryl Bromides. *Acc. Catal.*, **2016**, *6*, Pp 5962.
36. For C-H Bond Dissociation Energies Of Different Organic Molecules: (a) Blanksby, S. J.; Ellison, G. B. Bond Dissociation Energies Of Organic Molecules *Acc. Chem. Res.* **2003**, *36*, 255. For Hat Processes Using Mecn As Solvent: (b) Delaive, P. J.; Foreman, T. K.; Giannotti, C.; Whitten, D. G. Photoinduced Electron Transfer Reactions Of Transition-Metal Complexes With Amines. Mechanistic Studies Of Alternate Pathways To Back Electron Transfer. *J. Am. Chem. Soc.* **1980**, *102*, 5627.
37. (a) Crandall, J. K.; Tindell, G. L. Manmade, A. Homoallenyl Radicals. *Tetrahedron Lett.* **1982**, *23*, 3769; (b) Back, T. G.; Muralidharan, R. Free-Radical Selenosulfonation Of Vinylcyclopropanes, A Cyclopropylidene, And Cyclopropylacetylene. Relative Rates Of Chain-Transfer, Ring-Opening, And Inversion In Radical Intermediates. *J. Org. Chem.* **1989**, *54*, 121; (c) Bogen, S.; Gulea, M.; Fensterbank, L.; Malacria, M. 5-Endo-Trig Radical Cyclizations Of Bromomethyldimethylsilyl Diisopropylpropargylic Ethers. A Highly Diastereoselective Access To Functionalized Cyclopentanes. *J. Org. Chem.* **1999**, *64*, 4920; (d) Mainetti, E.; Fensterbank, L.; Malacria, M. New Elements In The Reactivity Of A-Cyclopropyl Vinyl Radicals. *Synlett* **2002**, 923. (e) Milnes, K. K.; Gottschling, S. E.; Baines, K. M. Determination Of The Rate Constant For Ring Opening Of An A-Cyclopropylvinyl Radical. *Org. Biomol. Chem.*, **2004**, *2*, 3530; (f) Gottschling, S. E.; Milnes, K. K.; Jennings, M. C.; Baines, K. M. Addition Of A Cyclopropyl Alkyne To Tetramesityldisilene: Evidence For A Biradical Intermediate And Formation Of A Stable 1,2-Disilacyclohepta-3,4-Diene. *Organometallics*, **2005**, *24*, 3811.
38. Isomerization Of Olefins Has Been Previously Reported Under Visible-Light Irradiation: Singh, K.; Staig, S.; Weaver, J. D. Facile Synthesis Of Z-Alkenes Via Uphill Catalysis. *J. Am. Chem. Soc.*, **2014**, *136*, 5275.
39. For A Related Photocatalytic Non-Redox Neutral Reductive Atom Transfer Double Radical Cyclization, See: Tucker, J. W.; Nguyen, J. D.; Narayanam, J. M. R.; Krabbe, S. W.; Stephenson, C. R. J. Tin-Free Radical Cyclization Reactions Initiated By Visible Light Photoredox Catalysis. *Chem. Commun.*, **2010**, *46*, 4985.
40. (a) Kropp, P. J. *Photobehavior Of Alkyl Halides*. Crc Handbook Of Organic Photochemistry And Photobiology, **2004**; (b) Lautenberger, W. J.; Jones, E. N.; Miller, J. G. Reaction Of Amines With Halo Alkanes. I. Photochemical Reaction Of Butylamine With Carbon Tetrachloride. *J. Am. Chem. Soc.* **1968**, *90*, 1110.
41. (a) Cossy, J.; Ranaivosata, J.-L.; Bellosta, V. Formation Of Radicals By Irradiation Of Alkyl Halides In The Presence Of Triethylamine. *Tetrahedron Lett.* **1994**, *35*, 8161. (b) Cossy, J.; Bellosta, V.; Ranaivosata, J.-L.; Gille, B. Formation Of Radicals By Irradiation Of Alkyl Halides In The Presence Of Triethylamine. Application To The Synthesis Of (±)-Bisabolangelone. *Tetrahedron* **2001**, *57*, 5173.
42. Takahide Fukuyama, Yuki Fujita, Muhammad Abid Rashid, And Ilhyong Ryu. Flow Update For A Cossy Photocyclization. *Org. Lett.*, **2016**, *18*, 5444.
43. Kropp, P. J.; Adkins, R. L. Photochemistry Of Alkyl Halides. 12. Bromides Vs. Iodides. *J. Am. Chem. Soc.* **1991**, *113*, 2709.
44. Böhm, A.; Bach, T. Radical Reactions Induced By Visible Light In Dichloromethane Solutions Of Hünig's Base: Synthetic Applications And Mechanistic Observations. *Chem. Eur. J.* **2016**, *22*, 15921.
45. Bahamonde, A.; Melchiorre, P. Mechanism Of The Stereoselective A-Alkylation Of Aldehydes Driven By The Photochemical Activity Of Enamines. *J. Am. Chem. Soc.* **2016**, *138*, 8019.
46. Cismesia, M. A.; Yoon, T. P. Characterizing Chain Processes In Visible Light Photoredox Catalysis. *Chem. Sci.*, **2015**, *6*, 5426.

## 2.8. Experimental Section

### 2.8.1. General Considerations

**Reagents:** Unless otherwise noted, all reactions were carried out in Schlenk tubes with screw cap using standard Schlenk techniques for the manipulation of solvents and reagents. Ir(ppy)<sub>2</sub>(dtbbpy)PF<sub>6</sub> (**Ir-2**) was prepared following the reported literature method.<sup>1</sup> **6s**,<sup>2</sup> **7s**,<sup>3</sup> **1s**<sup>4</sup> and **29s**<sup>5</sup> were all prepared following the reported literature protocols. *t*-BuCN was purchased from Alfa Aesar and used as received. All other reagents were purchased from commercial sources and used as received.

**Analytical Methods:** <sup>1</sup>H NMR, <sup>13</sup>C NMR and <sup>19</sup>F NMR spectra and melting points (where applicable) are included for all new compounds. <sup>1</sup>H NMR, <sup>13</sup>C NMR and <sup>19</sup>F NMR spectra were recorded on a Bruker 300 MHz, a Bruker 400 MHz or a Bruker 500 MHz at 20 °C. All <sup>1</sup>H NMR spectra are reported in parts per million (ppm) downfield of TMS and were measured relative to the signals for CHCl<sub>3</sub> (7.26 ppm). All <sup>13</sup>C NMR spectra were reported in ppm relative to residual CHCl<sub>3</sub> (77.16 ppm) and were obtained with <sup>1</sup>H decoupling. Coupling constants, *J*, are reported in hertz (Hz). In the case of diastereisomeric mixtures, a crude NMR was recorded to determine the ratio. Melting points were measured using open glass capillaries in a Büchi B540 apparatus. Infrared spectra were recorded on a Bruker Tensor 27. Mass spectra were recorded on a Waters LCT Premier spectrometer. Gas chromatographic analyses were performed on HewlettPackard 6890 gas chromatography instrument with a FID detector using 25m x 0.20 mm capillary column with cross-linked methyl siloxane as the stationary phase. Flash chromatography was performed with EM Science silica gel 60 (230- 400 mesh) and using KMnO<sub>4</sub> TLC stain. All electrochemical experiments were performed on a PAR 263A EG&G potentiostat or on an IJ-Cambria HI-660 potentiostat, using a three-electrode cell. Glassy carbon (S = 0.07 cm<sup>2</sup>) as working electrode, platinum mesh as counter electrode, and MSE or SSCE as reference electrode unless otherwise indicated. *E*<sub>1/2</sub> values reported in this work were estimated from Cyclic Voltammetry (CV) experiments as the average of the oxidative and reductive peak potentials. Fluorescence measurements were carried out on a Fluorolog Horiba Jobin Yvon spectrofluorimeter equipped with photomultiplier detector, double monochromator and Xenon light source. UV-Vis measurements were carried out on a Shimadzu UV-1700PC spectrophotometer equipped with a photomultiplier detector, double beam optics and D2 and W light sources. Lifetime measurements were carried out on a Edinburgh Instruments LifeSpec-II based on the time-correlated single photon counting (TCSPC) technique, equipped with a PMT detector, double subtractive monochromator and picosecond pulsed diode lasers source. The yields reported in Table 2 and Scheme 2 refer to isolated yields and represent an average of at least two independent runs. The procedures described in this section are representative. Thus, the yields may differ slightly from those given in the tables of the manuscript.

### 2.8.2. Luminescence Quenching Experiments

Samples for the quenching experiments were prepared in a 2 mL glass cuvette with a septum screw cap. Different amounts of quenchers were added to a solution of the photocatalyst **Ir-2** in *t*-BuCN (5.0 x 10<sup>-5</sup> M). Samples were irradiated at 470 nm and emission was measured at 560 nm.

Luminescence quenching experiments were carried out using the Stern–Volmer relationship:

$$I/I_0 = 1 + k_q\tau_0[\text{quencher}]$$

**I**<sub>0</sub> stands for the luminescence intensity of the photocatalyst (**Ir-2**) and **I** represents the intensity of luminescence in the presence of the quencher.  $\tau_0$  is the lifetime of **Ir-2**, determined to be 661.04±0.75 ns (5.0 x 10<sup>-5</sup> M in *t*-BuCN) using a

time-correlated single photon counting (TCSPC) technique.

Quenching with *i*-Pr<sub>2</sub>NEt:  $k_q = 5.58 \times 10^8 \text{ M}^{-1} \text{ s}^{-1}$ .

Quenching with **2s**: No quenching was observed.

### 2.8.3. Quantum Yield Determination

The determination of the quantum yield of the reaction was carried out using two light sources: (a) a spectrophotometer and (b) using blue LED strip (photoreactor). All manipulations and preparation of samples were carried out in a dark lab with red irradiation. The measurement of the photon flux of both light sources was determined by standard ferrioxalate actinometry following already reported procedures.

Spectrophotometer (Irradiation at 468 nm, slit 3 nm).

Photon flux (average of 3 measurements) =  $5.86 \times 10^{-9} \text{ einstein s}^{-1}$

Blue LED strip photoreactor (Irradiation at 450 nm) (QY of ferrioxalate at 450 nm estimated to be 0.95).

Photon flux (average of 3 measurements) =  $1.56 \times 10^{-8} \text{ einstein s}^{-1}$

#### 2.8.3.1. Quantum Yield Determination Using a Spectrophotometer

In a dark lab, a cuvette was charged with Ir(ppy)<sub>2</sub>(dtbbpy)PF<sub>6</sub> (**Ir-2**, 1 mol%, 3.6 mg), **2s** (0.4 mmol, 1 equiv, 116.0 mg), *i*-Pr<sub>2</sub>NEt (0.4 mmol, 1 equiv, 70 μL), decane (0.4 mmol, 1 equiv, 78 μL) and *t*-BuCN (2.0 mL, 0.2 M). The cuvette was then closed with a septum screw cap and degassed for 30 min. The sample was irradiated at 468 nm (slit 3 nm) for 1800 s (30 min). An aliquot was filtered through a plug of silica and celite and analyzed by GC with FID detector. **2-p-1** was detected in 6% yield.

Under these conditions, the fraction of light absorbed by **Ir-2** was  $f = 0.974$ .

$$\Phi = \frac{\text{mol of } \mathbf{2}}{\text{flux} \cdot t \cdot f}$$

$$\Phi = \frac{2.4 \times 10^{-5} \text{ mol}}{5.86 \times 10^{-9} \text{ einstein s}^{-1} \cdot 1800 \text{ s} \cdot 0.974} = 2.34$$

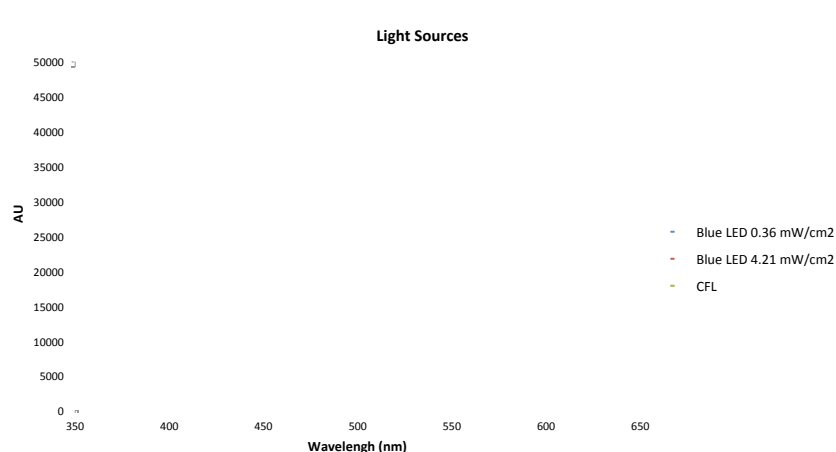
#### 2.8.3.2. Quantum Yield Determination Using the blue LED Photoreactor

A 12.0 mL screw-cap Schlenk tube containing a stirring bar was charged with Ir(ppy)<sub>2</sub>(dtbbpy)PF<sub>6</sub> (**Ir-2**, 1 mol%, 3.6 mg). The tube was then evacuated and back-filled with argon. **2s** (0.4 mmol, 1 equiv, 116 mg) was added with a microsyringe followed by addition of decane (0.4 mmol, 1 equiv, 78 μL), *t*-BuCN (2.0 mL, 0.2 M) and *i*-Pr<sub>2</sub>NEt (0.4 mmol, 1 equiv, 70 μL) under a positive Ar flow. Then three freeze-pump-thaw cycles were conducted in liquid nitrogen. The sample was irradiated with the blue LED photoreactor (FlexLed Inspire. 20 LEDs, 1.7 W, 0.364 mW/cm<sup>2</sup>) for 1800 s (30 min). An aliquot was filtered through a plug of silica and celite and analyzed by GC with FID detector. **2** was detected in 15% yield. Under these conditions, the fraction of light absorbed by **Ir-2** was  $f = 0.974$ .

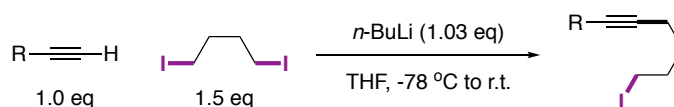
$$\Phi = \frac{\text{mol of } \mathbf{2}}{\text{flux} \cdot t \cdot f}$$

$$\Phi = \frac{6.0 \times 10^{-5} \text{ mol}}{1.56 \times 10^{-8} \text{ einstein s}^{-1} \cdot 1800 \text{ s} \cdot 0.974} = 2.19$$

## 2.8.4. Emission Spectra of Different Light Sources.

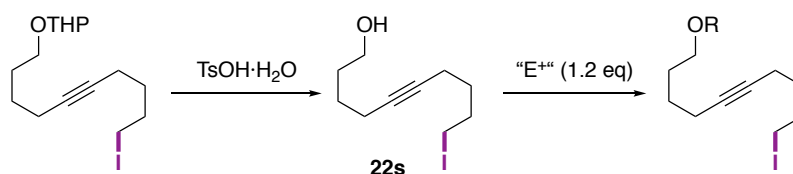


## 2.8.5. Synthesis of Starting Materials



### General reaction conditions A:<sup>4</sup>

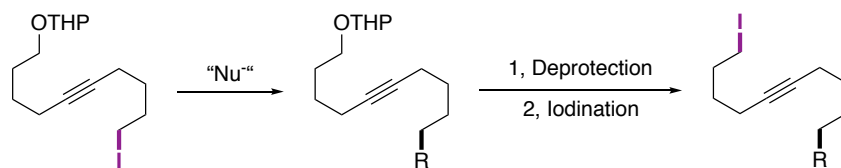
To a stirred solution of the terminal alkyne (1.0 eq) in dry THF (0.3 M) under Ar at  $-78^\circ C$ , *n*-BuLi (2.5 M, 1.03 eq) was slowly added by syringe. The reaction mixture was stirred for 30 min and then warmed up to room temperature. Then, 1,4-diiodobutane (1.5 eq) was added and the mixture was refluxed until total consumption of the alkyne. The reaction was then cooled down to room temperature, diluted with diethyl ether, washed with water (2x), sodium thiosulfate (aq. 10%) and brine (2x). The organic layer was dried over anhydrous  $MgSO_4$ , filtered, and concentrated under vacuum. The residue was purified by silica gel flash chromatography to deliver the corresponding alkyl iodide.



### General reaction conditions B:

**Step 1.** To a stirred solution of  $TsOH \cdot H_2O$  (0.1 eq) in MeOH (0.1 M) at room temperature, the THP protected alcohol was added (1.0 eq). The reaction was allowed to stir overnight at room temperature. Then the solvent was removed under vacuum and the crude diluted with EtOAc, washed with a saturated solution of  $NaHCO_3$  (2x) and brine (2x). The organic layer was dried over anhydrous  $MgSO_4$ , filtered and concentrated under *vacuum*. The residue was purified by silica gel flash chromatography to afford the unprotected alcohol **22s**.

**Step 2.**<sup>7</sup> To a stirred solution of alcohol **22s** (1.0 equiv) in anhydrous DCM (0.1 M) at  $0^\circ C$ ,  $NEt_3$  (3 equiv) and corresponding electrophile (1.2 equiv) were consecutively added and the reaction was stirred overnight at room temperature. The mixture was then concentrated and the residue purified by silica gel column chromatography to afford the corresponding starting material.

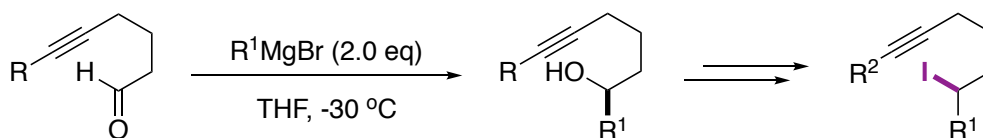


General reaction conditions C:

**Step 1.** The corresponding nucleophile (1.0 equiv) and  $K_2CO_3$  (1.3 equiv) were added to a solution of the protected alcohol (1.0 equiv) in DMF (0.1 M) at room temperature. The mixture was allowed to stir overnight at room temperature. After completion, the reaction was diluted with  $Et_2O$  and the mixture washed with water (2x) and brine (2x). The organic layer was separated, dried over  $MgSO_4$  anhydrous and the solvent evaporated. The crude product was used in the next step without further purification.

**Step 2.** The crude compound from step 1 was added to a stirred solution of  $TsOH \cdot H_2O$  (0.1 eq) in MeOH (0.1 M) at room temperature. The reaction was allowed to stir overnight at room temperature. Then the solvent was removed under vacuum and the crude diluted with EtOAc, washed with a saturated solution of  $NaHCO_3$  (2x) and brine (2x). The organic layer was dried over anhydrous  $MgSO_4$ , filtered and concentrated under *vacuum*. The residue was purified by silica gel flash chromatography to afford the corresponding unprotected alcohol.

**Step 3.** To a solution of triphenylphosphine (1.3 equiv) in anhydrous DCM (0.5 M) was added imidazole (1.3 equiv) at room temperature. Then,  $I_2$  (1.3 equiv) was added in portions over 5 minutes, followed by additional 10 min of stirring in the dark. A solution of the alcohol from the previous step (1.0 equiv) in DCM was added dropwise and the mixture was stirred overnight. After completion, the mixture was diluted with  $Et_2O$  and filtered through a short pad of silica. The filtrate was then concentrated and the residue purified by silica gel flash chromatography to give the corresponding starting material.



General reaction conditions D:<sup>5</sup>

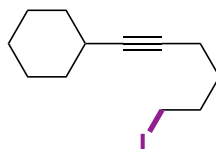
**Step 1.** The corresponding aldehyde (1.0 eq) was dissolved in THF (0.1 M) and the corresponding Grignard reagent  $R^1MgBr$  (2.0 eq) was added slowly at  $-30\text{ }^\circ\text{C}$ . After completion, the reaction was allowed to warm up at room temperature and stirred for 3 h. Then, the mixture was carefully quenched at  $0\text{ }^\circ\text{C}$  upon addition of  $NH_4Cl$  (aq. 10%), and then extracted with EtOAc (3x). The organic phase was washed with water (1x), brine (2x), filtered and concentrated. The residue was utilized in the next step without further purification.

**Step 2 ( $R \neq H$ ).** To a solution of triphenylphosphine (1.3 equiv) in anhydrous DCM (0.5 M) was added imidazole (1.3 equiv) at room temperature. Then,  $I_2$  (1.3 equiv) was added in portions over 5 minutes, followed by additional 10 min of stirring in the dark. After that, a solution of the alcohol obtained in the previous step (1.0 equiv) in DCM was added dropwise and the mixture stirred overnight. After completion, the mixture was diluted with  $Et_2O$  and filtered through a short pad of silica. The filtrate was then concentrated and the residue purified by silica gel flash chromatography to give the corresponding starting material.

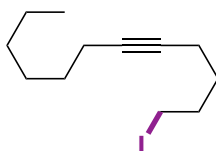
**Step 2 ( $R = H$ ).** To a suspension of  $Pd(PPh_3)_2Cl_2$  (5 mol%) in anhydrous DMF (0.33M), the corresponding terminal alkyne (1.2 equiv), aryl (pseudo)halide (1.0 equiv) and  $NEt_3$  (2.0 equiv) were added. The mixture was stirred at room temperature for 5 minutes. After that,  $CuI$  (5 mol%) was added and the mixture was heated to  $80\text{ }^\circ\text{C}$  for 24 h. Then, the reaction was cooled down to room temperature, quenched with  $H_2O$  and extracted with  $Et_2O$  (3x). The combined organic

phases were washed with H<sub>2</sub>O (2x), brine (2x), dried over MgSO<sub>4</sub>, filtered and concentrated. The residue was purified by silica gel flash chromatography giving rise to the cross-coupled product.

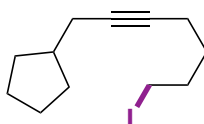
**Step 3 (R = H).** To a solution of triphenylphosphine (1.3 equiv) in anhydrous DCM (0.5 M) was added imidazole (1.3 equiv) at room temperature. Then, I<sub>2</sub> (1.3 equiv) was added in portions over 5 minutes, followed by additional 10 min of stirring in the dark. After that, a solution of the secondary alcohol obtained in the previous step (1.0 equiv) in DCM was added dropwise and the mixture stirred overnight. After completion, the mixture was diluted with Et<sub>2</sub>O and filtered through a short pad of silica. The filtrate was then concentrated and the residue purified by silica gel flash chromatography to give the corresponding starting material.



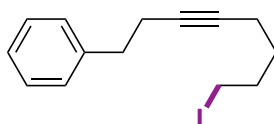
**(6-Iodohex-1-yn-1-yl)cyclohexane (2s):** Following reaction conditions A. 80% yield. Colorless oil. <sup>1</sup>H NMR (300 MHz, CDCl<sub>3</sub>): δ 3.21 (t, *J* = 7.2 Hz, 2H), 2.31 (b, 1H), 2.19 (dt, *J* = 6.9, 2.1 Hz, 2H), 1.93 (quint, *J* = 7.2 Hz, 2H), 1.78-1.24 (m, 12H) ppm. <sup>13</sup>C NMR (75 MHz, CDCl<sub>3</sub>): 85.5, 79.0, 33.2, 32.6, 29.8, 29.2, 26.0, 25.0, 17.8, 6.6 ppm. IR (neat, cm<sup>-1</sup>): 2925, 2851, 1447, 1286, 1211, 1164, 888. HRMS *calcd.* for (C<sub>12</sub>H<sub>20</sub>I) [M+H]<sup>+</sup>: 291.0604, *found* 291.0603.



**1-Iodododec-5-yne (3s):** Following reaction conditions A. 46% yield. Colorless oil. <sup>1</sup>H NMR (300 MHz, CDCl<sub>3</sub>): δ 3.21 (t, *J* = 6.9 Hz, 2H), 2.22-2.10 (m, 4H), 1.93 (quint, *J* = 6.9 Hz, 2H), 1.63-1.54 (m, 2H), 1.52-1.26 (m, 8H), 0.89 (t, *J* = 7.2 Hz, 3H) ppm. <sup>13</sup>C NMR (75 MHz, CDCl<sub>3</sub>): 81.2, 79.2, 32.6, 31.5, 29.9, 29.2, 28.7, 22.7, 18.9, 17.9, 14.2, 6.5 ppm. IR (neat, cm<sup>-1</sup>): 2927, 2856, 1455, 1331, 1287, 1211, 1165. HRMS *calcd.* for (C<sub>13</sub>H<sub>26</sub>I) [M+CH<sub>3</sub>OH+H]<sup>+</sup>: 325.1023, *found* 325.1020.

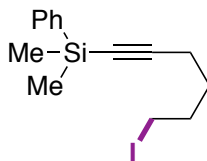


**(7-Iodohept-2-yn-1-yl)cyclopentane (4s):** Following reaction conditions A. 56% yield. Colorless oil. <sup>1</sup>H NMR (300 MHz, CDCl<sub>3</sub>): δ 3.21 (t, *J* = 6.9 Hz, 2H), 2.22-2.12 (m, 4H), 2.07-1.89 (m, 3H), 1.78-1.73 (m, 2H), 1.63-1.52 (m, 6H), 1.31-1.19 (m, 2H) ppm. <sup>13</sup>C NMR (75 MHz, CDCl<sub>3</sub>): 80.6, 79.3, 39.5, 32.6, 32.1, 29.9, 25.4, 24.7, 17.9, 6.6 ppm. IR (neat, cm<sup>-1</sup>): 2943, 2862, 1450, 1429, 1328, 1286, 1211. HRMS *calcd.* for (C<sub>12</sub>H<sub>20</sub>I) [M+H]<sup>+</sup>: 291.0604, *found* 291.0601.

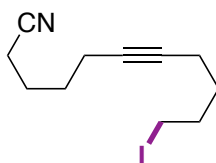


**(8-Iodooct-3-yn-1-yl)benzene (5s):** Following reaction conditions A. 85% yield. Pale yellow oil. <sup>1</sup>H NMR (300 MHz, CDCl<sub>3</sub>): δ 7.33-7.20 (m, 5H), 3.23-3.14 (m, 2H), 2.86-2.76 (m, 2H), 2.50-2.44 (m, 2H), 2.23-2.16 (m, 2H), 1.95-1.82 (m, 2H), 1.64-1.53 (m, 2H) ppm. <sup>13</sup>C NMR (75 MHz, CDCl<sub>3</sub>): 141.0, 128.5, 128.4, 126.3, 80.3, 80.1, 35.6, 32.5, 29.7, 21.0, 17.8, 6.6 ppm. IR (neat, cm<sup>-1</sup>): 3061, 3026, 2928, 2859, 2212, 1453, 1339. HRMS *calcd.* for (C<sub>14</sub>H<sub>18</sub>I) [M+H]<sup>+</sup>: 313.0448, *found* 313.0446.

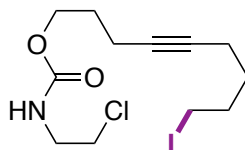




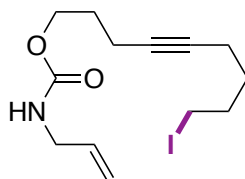
**(6-Iodohex-1-yn-1-yl)dimethyl(phenyl)silane (8s):** Following reaction conditions A. 75% yield. Colorless oil.  $^1\text{H}$  NMR (300 MHz,  $\text{CDCl}_3$ ):  $\delta$  7.66-7.63 (m, 2H), 7.41-7.37 (m, 3H), 3.23 (t,  $J = 6.9$  Hz, 2H), 2.33 (t,  $J = 7.0$  Hz, 2H), 1.98 (quint,  $J = 7.0$  Hz, 2H), 1.68 (quint,  $J = 7.1$  Hz, 2H), 0.41 (s, 6 H) ppm.  $^{13}\text{C}$  NMR (75 MHz,  $\text{CDCl}_3$ ): 137.6, 133.7, 129.4, 128.0, 108.4, 83.4, 32.5, 29.3, 19.1, 6.3, 0.5 ppm. IR (neat,  $\text{cm}^{-1}$ ): 3068, 3048, 2957, 2173, 1427, 1248, 1114. HRMS *calcd.* for  $(\text{C}_{14}\text{H}_{20}\text{ISi})$   $[\text{M}+\text{H}]^+$ : 343.0374, *found* 343.0371.



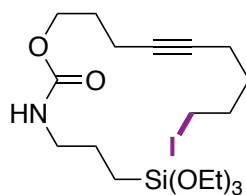
**11-Iodoundec-6-ynenitrile (9s):** Following reaction conditions C, but using KCN (3.0 equiv) as nucleophile in DMSO (0.25 M) in step 1. 75% yield. Colorless oil.  $^1\text{H}$  NMR (300 MHz,  $\text{CDCl}_3$ ):  $\delta$  3.21 (t,  $J = 6.9$  Hz, 2H), 2.38 (t,  $J = 7.2$  Hz, 2H), 2.25-2.15 (m, 4 H), 1.97-1.87 (m, 2H), 1.83-1.74 (m, 2H), 1.68-1.54 (m, 4H) ppm.  $^{13}\text{C}$  NMR (75 MHz,  $\text{CDCl}_3$ ): 119.7, 80.5, 79.5, 32.6, 29.8, 27.8, 24.6, 18.1, 17.8, 16.9, 6.4 ppm. IR (neat,  $\text{cm}^{-1}$ ): 2935, 2866, 2246, 2211, 1672, 1426, 1212. HRMS *calcd.* for  $(\text{C}_{11}\text{H}_{17}\text{IN})$   $[\text{M}+\text{H}]^+$ : 290.0400, *found* 290.0392.



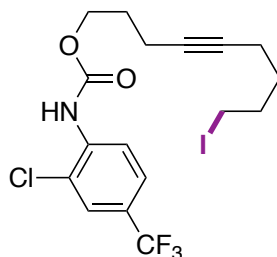
**9-Iodonon-4-yn-1-yl (2-chloroethyl)carbamate (10s):** Following reaction conditions B. 75% yield. White solid. M.P. = 48.0  $^{\circ}\text{C}$ .  $^1\text{H}$  NMR (300 MHz,  $\text{CDCl}_3$ ):  $\delta$  5.14 (b, 1H), 4.14 (t,  $J = 6.3$  Hz, 2H), 3.61-3.47 (m, 4H), 3.19 (t,  $J = 6.9$  Hz, 2H), 2.25-2.14 (m, 4H), 1.93-1.80 (m, 2H), 1.78-1.74 (m, 2H), 1.61-1.52 (m, 2H) ppm.  $^{13}\text{C}$  NMR (75 MHz,  $\text{CDCl}_3$ ): 156.4, 80.1, 79.4, 63.9, 44.2, 42.8, 32.5, 29.7, 28.5, 17.7, 15.5, 6.5 ppm. IR (neat,  $\text{cm}^{-1}$ ): 3344, 2936, 1690, 1539, 1317, 1257, 1152. HRMS *calcd.* for  $(\text{C}_{12}\text{H}_{19}\text{ClINNaO}_2)$   $[\text{M}+\text{Na}]^+$ : 394.0041, *found* 394.0042.



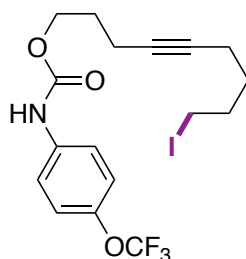
**9-Iodonon-4-yn-1-yl allylcarbamate (11s):** Following reaction conditions B. 83% yield. Brown oil.  $^1\text{H}$  NMR (400 MHz,  $\text{CDCl}_3$ ):  $\delta$  5.87-5.77 (m, 1H), 5.20-5.08 (m, 2H), 4.79 (b, 1H), 4.13 (t,  $J = 6.4$  Hz, 2H), 3.78 (b, 2H), 3.54-3.18 (m, 2H), 2.24-2.13 (m, 4H), 1.94-1.74 (m, 4H), 1.64-1.53 (m, 2H) ppm.  $^{13}\text{C}$  NMR (101 MHz,  $\text{CDCl}_3$ ): 156.5, 134.6, 116.0, 80.09, 80.03, 79.55, 79.52, 68.9, 63.7, 44.7, 43.5, 32.5, 31.6, 29.7, 28.60, 26.2, 18.1, 17.7, 15.1, 6.4 ppm. IR (neat,  $\text{cm}^{-1}$ ): 3337, 2934, 1698, 1518, 1432, 1239, 1144. HRMS *calcd.* for  $(\text{C}_{13}\text{H}_{20}\text{INNaO}_2)$   $[\text{M}+\text{Na}]^+$ : 372.0431, *found* 372.0415.



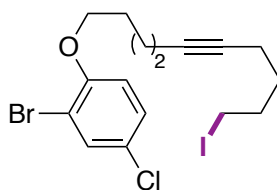
**9-Iodonon-4-yn-1-yl (3-(triethoxysilyl)propyl)carbamate (12s):** Following reaction conditions B. 60% yield. Brown oil.  $^1\text{H NMR}$  (300 MHz,  $\text{CDCl}_3$ ):  $\delta$  4.9 (b, 1H), 4.10 (t,  $J = 6.0$  Hz, 2H), 3.80 (q,  $J = 6.9$  Hz, 6H), 3.21-3.12 (m, 4H), 2.21-2.14 (m, 4H), 1.93-1.54 (m, 8H), 1.21 (t,  $J = 6.9$  Hz, 9H), 0.61 (t,  $J = 8.1$  Hz, 2H) ppm.  $^{13}\text{C NMR}$  (75 MHz,  $\text{CDCl}_3$ ): 156.6, 79.9, 79.6, 63.5, 58.5, 43.4, 32.5, 29.7, 28.6, 23.4, 18.4, 17.8, 15.5, 7.7, 6.4 ppm. IR (neat,  $\text{cm}^{-1}$ ): 3346, 2972, 2927, 1702, 1525, 1240, 1073. HRMS *calcd.* for  $(\text{C}_{19}\text{H}_{36}\text{INNaO}_5\text{Si})$   $[\text{M}+\text{Na}]^+$ : 536.1300, *found* 536.1300.



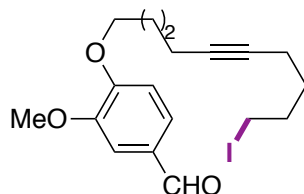
**9-Iodonon-4-yn-1-yl (2-chloro-4-(trifluoromethyl)phenyl)carbamate (13s):** Following reaction conditions B. 78% yield. Yellow oil.  $^1\text{H NMR}$  (300 MHz,  $\text{CDCl}_3$ ):  $\delta$  8.52 (b, 1H), 7.44 (d,  $J = 8.1$  Hz, 1H), 7.24-7.20 (m, 2H), 4.30 (t,  $J = 6.3$  Hz, 2H), 3.18 (t,  $J = 6.9$  Hz, 2H), 2.32-2.26 (m, 2H), 2.20-2.14 (m, 2H), 1.96-1.83 (m, 4H), 1.62-1.53 (m, 2H) ppm.  $^{13}\text{C NMR}$  (75 MHz,  $\text{CDCl}_3$ ): 152.9, 135.5, 130.3 (q,  $J_{\text{C-F}} = 32.7$  Hz), 129.6, 125.1, 123.6 (q,  $J_{\text{C-F}} = 270.8$  Hz), 120.1 (q,  $J_{\text{C-F}} = 3.8$  Hz), 116.6 (q,  $J_{\text{C-F}} = 3.8$  Hz), 80.4, 79.1, 64.8, 32.6, 29.7, 28.2, 17.8, 15.5, 6.4 ppm.  $^{19}\text{F NMR}$  (376 MHz,  $\text{CDCl}_3$ ): -62.883 ppm. IR (neat,  $\text{cm}^{-1}$ ): 3422, 2939, 1739, 1591, 1527, 1434, 1330. HRMS *calcd.* for  $(\text{C}_{17}\text{H}_{18}\text{ClF}_3\text{INNaO}_2)$   $[\text{M}+\text{Na}]^+$ : 509.9915, *found* 509.9903.



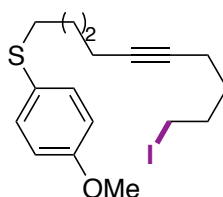
**9-Iodonon-4-yn-1-yl (4-(trifluoromethoxy)phenyl)carbamates (14s):** Following reaction conditions B. 89% yield. White solid. M.P. = 50.3  $^{\circ}\text{C}$ .  $^1\text{H NMR}$  (300 MHz,  $\text{CDCl}_3$ ):  $\delta$  7.40 (d,  $J = 9.0$  Hz, 2H), 7.15 (d,  $J = 9.0$  Hz, 2H), 6.73 (b, 1H), 4.26 (t,  $J = 6.3$  Hz, 2H), 3.20 (t,  $J = 6.9$  Hz, 2H), 2.31-2.25 (m, 2H), 2.21-2.16 (m, 2H), 1.97-1.80 (m, 4H), 1.63-1.53 (m, 2H) ppm.  $^{13}\text{C NMR}$  (75 MHz,  $\text{CDCl}_3$ ): 153.5, 144.8, 136.7, 122.0, 120.6 (q,  $J_{\text{C-F}} = 255.1$  Hz), 119.8, 80.4, 79.3, 64.3, 32.6, 29.7, 28.4, 17.8, 15.5, 6.5 ppm.  $^{19}\text{F NMR}$  (376 MHz,  $\text{CDCl}_3$ ): -58.304 ppm. IR (neat,  $\text{cm}^{-1}$ ): 3330, 2935, 2859, 1702, 1604, 1528, 1153. HRMS *calcd.* for  $(\text{C}_{17}\text{H}_{19}\text{F}_3\text{INNaO}_3)$   $[\text{M}+\text{Na}]^+$ : 492.0254, *found* 492.0257.



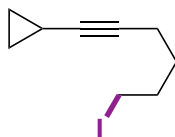
**2-Bromo-4-chloro-1-((10-iododec-5-yn-1-yl)oxy)benzene (15s):** Following reaction conditions C. 43% yield. Brown oil.  $^1\text{H NMR}$  (300 MHz,  $\text{CDCl}_3$ ):  $\delta$  7.52 (d,  $J = 2.7$  Hz, 1H), 7.21 (dd,  $J = 8.7, 2.7$  Hz, 1H), 6.80 (d,  $J = 8.7$  Hz, 1H), 4.02 (t,  $J = 6.3$  Hz, 2H), 3.21 (t,  $J = 6.9$  Hz, 2H), 2.28-2.15 (m, 4H), 1.98-1.88 (m, 4H), 1.75-1.66 (m, 2H), 1.63-1.54 (m, 2H) ppm.  $^{13}\text{C NMR}$  (75 MHz,  $\text{CDCl}_3$ ): 154.4, 132.9, 128.3, 126.0, 113.8, 112.9, 80.5, 79.9, 69.1, 32.7, 29.8, 28.3, 25.6, 18.6, 17.9, 6.5 ppm. IR (neat,  $\text{cm}^{-1}$ ): 2937, 2212, 1672, 1479, 1465, 1262, 1046. HRMS *calcd.* for ( $\text{C}_{16}\text{H}_{19}\text{OClBrI}$ ): 467.9353, *found* 467.9347.



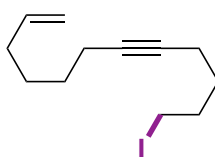
**4-((10-Iododec-5-yn-1-yl)oxy)-3-methoxybenzaldehyde (16s):** Following reaction conditions C. 30% yield. Pale yellow solid. M.P. = 54.7 °C.  $^1\text{H NMR}$  (300 MHz,  $\text{CDCl}_3$ ):  $\delta$  9.85 (s, 1H), 7.45-7.40 (m, 2H), 6.97 (d,  $J = 8.1$  Hz, 1H), 4.13 (t,  $J = 6.6$  Hz, 2H), 3.93 (s, 3H), 3.20 (t,  $J = 6.9$  Hz, 2H), 2.28-2.15 (m, 4H), 2.02-1.87 (m, 4H), 1.73-1.53 (m, 4H) ppm.  $^{13}\text{C NMR}$  (75 MHz,  $\text{CDCl}_3$ ): 191.0, 154.2, 150.0, 130.1, 126.9, 111.5, 109.4, 80.3, 80.0, 68.7, 56.2, 32.6, 29.8, 28.2, 25.5, 18.6, 17.8, 6.5 ppm. IR (neat,  $\text{cm}^{-1}$ ): 3071, 2942, 2925, 1670, 1583, 1508, 1259. HRMS *calcd.* for ( $\text{C}_{18}\text{H}_{23}\text{I}\text{NaO}_3$ ) [ $\text{M}+\text{Na}$ ] $^+$ : 437.0584, *found* 437.0589.



**(10-Iododec-5-yn-1-yl)(4-methoxyphenyl)sulfane (17s):** Following reaction conditions C. 50% yield. Colorless oil.  $^1\text{H NMR}$  (300 MHz,  $\text{CDCl}_3$ ):  $\delta$  7.34 (d,  $J = 8.7$  Hz, 2H), 6.84 (d,  $J = 8.7$  Hz, 2H), 3.79 (s, 3H), 3.19 (t,  $J = 6.9$  Hz, 2H), 2.83 (t,  $J = 6.9$  Hz, 2H), 2.16-2.14 (m, 4H), 1.95-1.86 (m, 2H), 1.73-1.51 (m, 6H) ppm.  $^{13}\text{C NMR}$  (75 MHz,  $\text{CDCl}_3$ ): 158.9, 133.2, 126.7, 114.6, 80.4, 79.8, 55.5, 35.5, 32.6, 29.8, 28.5, 28.0, 18.4, 17.8, 6.5 ppm. IR (neat,  $\text{cm}^{-1}$ ): 2999, 2934, 1591, 1492, 1439, 1240, 1030. HRMS *calcd.* for ( $\text{C}_{17}\text{H}_{24}\text{IOS}$ ) [ $\text{M}+\text{H}$ ] $^+$ : 403.0587, *found* 403.0593.

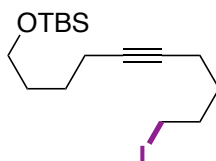


**(6-Iodohept-1-en-1-yl)cyclopropane (19s):** Following reaction conditions A. 67% yield. Colorless oil.  $^1\text{H NMR}$  (300 MHz,  $\text{CDCl}_3$ ):  $\delta$  3.20 (t,  $J = 6.0$  Hz, 2H), 2.16 (dt,  $J = 6.0, 2.1$  Hz, 2H), 1.91 (quint,  $J = 7.2$  Hz, 2H), 1.57 (quint,  $J = 7.2$  Hz, 2H), 1.24-1.14 (m, 1H), 0.74-0.65 (m, 2H), 0.65-0.57 (m, 2H) ppm.  $^{13}\text{C NMR}$  (101 MHz,  $\text{CDCl}_3$ ): 84.1, 74.7, 32.6, 29.8, 17.9, 8.1, 6.5, -0.38 ppm. IR (neat,  $\text{cm}^{-1}$ ): 3009, 2937, 2203, 1700, 1666, 1426, 1168. HRMS *calcd.* for ( $\text{C}_9\text{H}_{14}\text{I}$ ) [ $\text{M}+\text{H}$ ] $^+$ : 249.0135, *found* 249.0131.

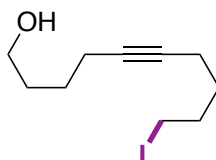


**12-Iodododec-1-en-7-yne (20s):** Following reaction conditions A. 75% yield. Colorless oil.  $^1\text{H NMR}$  (300 Hz):  $\delta$  5.87-

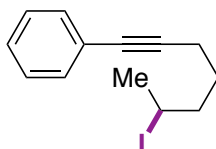
5.74 (m, 1H), 5.04-4.93 (m, 2H), 3.20 (t,  $J = 6.9$  Hz, 2H), 2.21-2.05 (m, 6H), 1.93 (quint,  $J = 7.2$  Hz, 2H), 1.63-1.46 (m, 6H) ppm.  $^{13}\text{C}$  NMR (75 MHz,  $\text{CDCl}_3$ ): 138.8, 114.6, 80.9, 79.4, 33.4, 32.6, 29.8, 28.6, 28.1, 18.7, 17.8, 6.5 ppm. IR (neat,  $\text{cm}^{-1}$ ): 3075, 2931, 2857, 1640, 1432, 1332, 1211. HRMS *calcd.* for  $(\text{C}_{12}\text{H}_{20}\text{I})$   $[\text{M}]^+$ : 291.0604, *found* 291.0596.



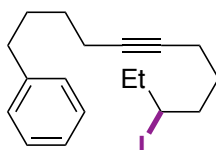
**tert-Butyl((10-iododec-5-yn-1-yl)oxy)dimethylsilane (21s):** Following reaction conditions B. 79% yield. Colorless oil.  $^1\text{H}$  NMR (300 MHz,  $\text{CDCl}_3$ ):  $\delta$  3.62 (t,  $J = 6.0$  Hz, 2H), 3.21 (t,  $J = 6.9$  Hz, 2H), 2.21-2.14 (m, 4H), 1.98-1.89 (m, 2H), 1.63-1.52 (m, 6H), 0.89 (s, 9H), 0.05 (s, 6H) ppm.  $^{13}\text{C}$  NMR (75 MHz,  $\text{CDCl}_3$ ): 80.9, 79.5, 62.9, 32.6, 32.1, 29.9, 26.1, 25.6, 18.7, 18.5, 17.9, 6.5, -5.1 ppm. IR (neat,  $\text{cm}^{-1}$ ): 2929, 2856, 1471, 1253, 1102, 834, 774. HRMS *calcd.* for  $(\text{C}_{16}\text{H}_{32}\text{IOSi})$   $[\text{M}+\text{H}]^+$ : 395.1262, *found* 395.1252.



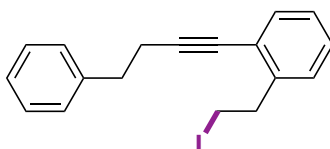
**10-Iododec-5-yn-1-ol (22s):** Following reaction conditions B. 90% yield. Colorless oil.  $^1\text{H}$  NMR (300 MHz,  $\text{CDCl}_3$ ):  $\delta$  3.67 (t,  $J = 4.2$  Hz, 2H), 3.20 (t,  $J = 6.9$  Hz, 2H), 2.21-2.16 (m, 4H), 1.93 (quint,  $J = 7.2$  Hz, 2H), 1.71-1.53 (m, 6H), 1.38 (br, 1H) ppm.  $^{13}\text{C}$  NMR (75 MHz,  $\text{CDCl}_3$ ): 80.6, 79.6, 62.4, 32.5, 31.8, 29.7, 25.3, 18.5, 17.7, 6.5 ppm. IR (neat,  $\text{cm}^{-1}$ ): 3341, 2935, 2862, 1431, 1286, 1211, 1165, 1056. HRMS *calcd.* for  $(\text{C}_{10}\text{H}_{18}\text{OI})$   $[\text{M}+\text{H}]^+$ : 281.0397, *found* 281.0394.



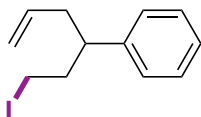
**(6-Iodohept-1-yn-1-yl)benzene (23s):** Following reaction conditions D. 65% yield. Colorless oil.  $^1\text{H}$  NMR (300 MHz,  $\text{CDCl}_3$ ):  $\delta$  7.42-7.38 (m, 2H), 7.31-7.26 (m, 3H), 4.30-4.19 (m, 1H), 2.46 (t,  $J = 6.9$  Hz, 2H), 2.03-1.64 (m, 7H) ppm.  $^{13}\text{C}$  NMR (75 MHz,  $\text{CDCl}_3$ ): 131.6, 128.3, 127.7, 123.9, 89.4, 81.3, 41.9, 29.6, 29.1, 28.9, 18.7 ppm. IR (neat,  $\text{cm}^{-1}$ ): 2943, 1702, 1489, 1442, 1137, 754, 690. HRMS *calcd.* for  $(\text{C}_{13}\text{H}_{15})$   $[\text{M}-\text{I}]^+$ : 171.1168, *found* 171.1174.



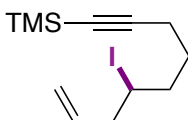
**(10-Iodododec-5-yn-1-yl)benzene (24s):** Following reaction conditions D. 70% yield. Colorless oil.  $^1\text{H}$  NMR (300 MHz,  $\text{CDCl}_3$ ):  $\delta$  7.30-7.25 (m, 2H), 7.19-7.15 (m, 3H), 4.13-4.04 (m, 1H), 2.62 (t,  $J = 7.5$  Hz, 2H), 2.20-2.15 (m, 4H), 2.00-1.47 (m, 10H), 1.01 (t,  $J = 7.2$  Hz, 3H) ppm.  $^{13}\text{C}$  NMR (75 MHz,  $\text{CDCl}_3$ ): 142.5, 128.5, 128.4, 125.8, 80.7, 79.7, 41.6, 39.3, 35.5, 33.9, 30.7, 29.0, 28.7, 18.7, 18.1, 14.2 ppm. IR (neat,  $\text{cm}^{-1}$ ): 3025, 2933, 2858, 1495, 1453, 1332, 1298. HRMS *calcd.* for  $(\text{C}_{18}\text{H}_{26}\text{I})$   $[\text{M}+\text{H}]^+$ : 369.1074, *found* 369.1074.



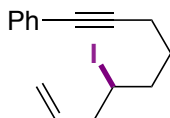
**(6-Iodonon-8-en-1-yn-1-yl)trimethylsilane (25s):** Compound **25s** was prepared following a reported procedure.<sup>2</sup> 78% yield. Colorless oil. <sup>1</sup>H NMR (300 MHz, CDCl<sub>3</sub>):  $\delta$  7.37-7.13 (m, 9H), 3.34-3.20 (m, 4H), 2.96 (t,  $J = 7.5$  Hz, 2H), 2.76 (t,  $J = 7.5$  Hz, 2H) ppm. <sup>13</sup>C NMR (75 MHz, CDCl<sub>3</sub>): 142.5, 140.6, 132.5, 129.0, 128.6, 128.5, 128.0, 126.9, 126.5, 123.2, 93.9, 79.3, 39.3, 35.2, 21.7, 4.8 ppm. IR (neat, cm<sup>-1</sup>): 3061, 3025, 2926, 2221, 1483, 1451, 1172. HRMS *calcd.* for (C<sub>18</sub>H<sub>18</sub>I) [M+H]<sup>+</sup>: 361.0448, *found* 361.0449.



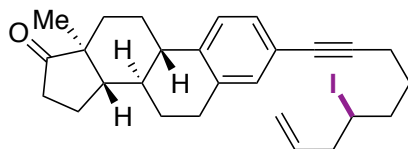
**1-(2-Iodoethyl)-2-(4-phenylbut-1-yn-1-yl)benzene (26s):** Following reaction conditions D. 95% yield. Colorless oil. <sup>1</sup>H NMR (300 MHz, CDCl<sub>3</sub>):  $\delta$  7.33-7.28 (m, 2H), 7.25-7.16 (m, 3H), 5.73-5.59 (m, 1H), 5.02-4.94 (m, 2H), 3.12-3.04 (m, 1H), 2.90-2.74 (m, 2H), 2.41-2.36 (m, 2H), 2.28-2.17 (m, 1H), 2.10-1.98 (m, 1H) ppm. <sup>13</sup>C NMR (75 MHz, CDCl<sub>3</sub>): 143.2, 136.3, 128.7, 127.8, 126.7, 116.6, 46.3, 40.8, 39.6, 5.1 ppm. IR (neat, cm<sup>-1</sup>): 3062, 6026, 2923, 1493, 1453, 1226, 913.



**(6-Iodonon-8-en-1-yn-1-yl)trimethylsilane (27s):** Following reaction conditions D. 83% yield. Colorless oil. <sup>1</sup>H NMR (300 MHz, CDCl<sub>3</sub>):  $\delta$  5.89-5.75 (m, 1H), 5.17-5.10 (m, 2H), 4.16-4.08 (m, 1H), 2.74-2.57 (m, 2H), 2.26 (t,  $J = 6.9$  Hz, 2H), 1.92-1.57 (m, 4H), 0.15 (s, 9H) ppm. <sup>13</sup>C NMR (75 MHz, CDCl<sub>3</sub>): 136.3, 117.8, 106.6, 85.3, 45.0, 38.7, 36.0, 28.4, 19.1, 0.28 ppm. IR (neat, cm<sup>-1</sup>): 3079, 2955, 2924, 2174, 1432, 1248, 838.



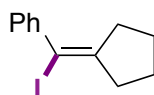
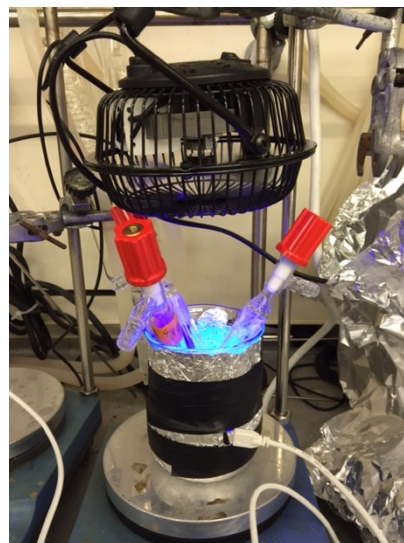
**(1-Iodohex-5-en-3-yl)benzene (28s):** Following reaction conditions D. 75% yield. Pale yellow oil. <sup>1</sup>H NMR (300 MHz, CDCl<sub>3</sub>):  $\delta$  7.42-7.39 (m, 2H), 7.31-7.28 (m, 3H), 5.91-5.78 (m, 1H), 5.19-5.12 (m, 2H), 4.20-4.12 (m, 1H), 2.68 (q,  $J = 6.3$  Hz, 2H), 2.46 (t,  $J = 6.9$  Hz, 2H), 2.00-1.65 (m, 4H) ppm. <sup>13</sup>C NMR (75 MHz, CDCl<sub>3</sub>): 136.3, 131.7, 128.3, 127.8, 123.9, 117.9, 89.4, 81.3, 44.9, 38.9, 36.2, 28.7, 18.7 ppm. IR (neat, cm<sup>-1</sup>): 3077, 2944, 2834, 1489, 961, 754, 690. HRMS *calcd.* for (C<sub>15</sub>H<sub>17</sub>I) [M-I]<sup>+</sup>: 179.1325, *found* 179.1319.



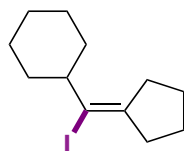
**3-(6-Iodonon-8-en-1-yn-1-yl)-13-methyl-6,7,8,9,11,12,13,14,15,16-decahydro-17H-cyclopenta[a]phenanthren-17-one (30s):** Following reaction conditions D. 35% yield. Yellow solid. M.P. = 75.4 °C. <sup>1</sup>H NMR (300 MHz, CDCl<sub>3</sub>):  $\delta$  7.26-7.14 (m, 3H), 5.90-5.77 (m, 1H), 5.18-5.11 (m, 2H), 4.19-4.11 (m, 1H), 2.90-2.85 (m, 2H), 2.70-2.64 (m, 2H), 2.55-1.39 (m, 19H), 0.91 (s, 3H) ppm. <sup>13</sup>C NMR (75 MHz, CDCl<sub>3</sub>): 220.8, 139.6, 136.5, 136.3, 132.1, 128.9, 125.4, 121.2, 117.8, 88.7, 81.2, 50.6, 48.0, 44.9, 44.5, 38.9, 38.1, 36.2, 35.9, 31.6, 29.2, 28.7, 26.5, 25.7, 21.7, 18.7, 13.9 ppm. IR (neat, cm<sup>-1</sup>): 2930, 2874, 1732, 1495, 1454, 1084, 1006. HRMS *calcd.* for (C<sub>27</sub>H<sub>33</sub>INaO) [M+Na]<sup>+</sup>: 523.1468, *found* 523.1461.

## 2.8.6. Preparative Scope for Iodine Transfer Radical Cyclization

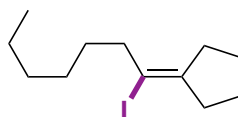
**General Procedure.** A 12.0 mL Schlenk tube with screw cap containing a stirring bar was charged with  $[\text{Ir}(\text{ppy})_2(\text{dtbbpy})]\text{PF}_6$  (**Ir-2**, 1 mol%, 1.8 mg). The tube was then evacuated and back-filled with argon. The corresponding alkyl iodide (0.2 mmol, 1 equiv) was added with a microsyringe followed by addition of *t*-BuCN (1.0 mL, 0.2 M) and *i*-Pr<sub>2</sub>NEt (0.2 mmol, 1 equiv, 35  $\mu\text{L}$ ) under a positive Ar flow. Then three freeze-pump-thaw cycles were conducted in liquid nitrogen. Finally, the reaction was placed in the photoreactor, consisting of a 150 mL beaker surrounded by blue LED strips (FlexLed Inspire. 20 LEDs, 1.7 W, 0.364  $\text{mW}/\text{cm}^2$ ). A mini-fan was necessary on the top to keep internal temperature between 30 and 35°C. The reaction was stirred for 12-96 h, and then the solvent was evaporated under vacuum and the residue purified on silica gel column chromatography.



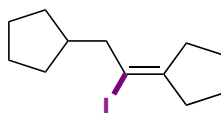
**(Cyclopentylideneiodomethyl)benzene (1).** Following the general procedure, the corresponding vinyl iodide was obtained in 73% yield in 32 h (5% of **1-H** was observed) as colorless oil. <sup>1</sup>H NMR (300 MHz, CDCl<sub>3</sub>):  $\delta$  7.33-7.15 (m, 5H), 2.48-2.43 (m, 2H), 2.32-2.28 (m, 2H), 1.81-1.74 (m, 4H) ppm. <sup>13</sup>C NMR (75 MHz, CDCl<sub>3</sub>): 152.7, 144.2, 128.9, 128.1, 127.4, 89.4, 42.0, 33.8, 28.7, 26.0 ppm. IR (neat,  $\text{cm}^{-1}$ ): 3077, 2953, 2831, 1441, 1305, 1156, 657. HRMS *calcd.* for (C<sub>12</sub>H<sub>14</sub>I) [M+H]<sup>+</sup>: 285.0135, *found* 285.0142.



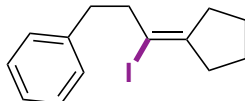
**(Cyclopentylideneiodomethyl)cyclohexane (2).** Following the general procedure, the corresponding vinyl iodide was obtained in 87% yield in 24 h as colorless oil. <sup>1</sup>H NMR (400 MHz, CDCl<sub>3</sub>):  $\delta$  2.37-2.27 (m, 4H), 1.86-1.17 (m, 15H) ppm. <sup>13</sup>C NMR (100 MHz, CDCl<sub>3</sub>): 146.9, 108.1, 45.7, 41.6, 33.6, 32.4, 28.2, 25.9, 25.8, 25.5 ppm. IR (neat,  $\text{cm}^{-1}$ ): 2924, 2851, 1448, 1427, 1230, 1173, 890. HRMS *calcd.* for (C<sub>12</sub>H<sub>20</sub>I) [M+H]<sup>+</sup>: 291.0604, *found* 291.0603.



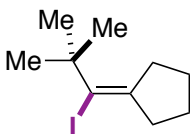
**(1-Iodoheptylidene)cyclopentane (3).** Following the general procedure, the corresponding vinyl iodide was obtained in 96% yield in 24 h as colorless oil. <sup>1</sup>H NMR (300 MHz, CDCl<sub>3</sub>):  $\delta$  2.41 (t, *J* = 7.2 Hz, 2H), 2.34-2.26 (m, 4H), 1.82 (quint, *J* = 6.9 Hz, 2H), 1.66 (quint, *J* = 6.9 Hz, 2H), 1.51-1.45 (m, 2H), 1.35-1.26 (6H), 0.91-0.87 (m, 3H) ppm. <sup>13</sup>C NMR (75 MHz, CDCl<sub>3</sub>): 148.6, 97.5, 41.9, 41.4, 31.9, 31.8, 29.4, 28.4, 28.3, 25.9, 22.8, 14.2 ppm. IR (neat,  $\text{cm}^{-1}$ ): 2954, 2926, 2855, 1452, 1428, 1377, 1305. HRMS *calcd.* for (C<sub>12</sub>H<sub>21</sub>) [M-I]<sup>+</sup>: 165.1638, *found* 165.1637.



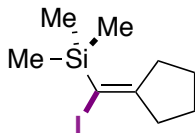
**(2-cyclopentyl-1-iodoethylidene)cyclopentane (4).** Following the general procedure, the corresponding vinyl iodide was obtained in 91% yield in 12 h as colorless oil.  $^1\text{H}$  NMR (300 MHz,  $\text{CDCl}_3$ ):  $\delta$  2.44-2.14 (m, 7H), 1.88-1.54 (m, 10H), 1.22-1.10 (m, 2H) ppm.  $^{13}\text{C}$  NMR (75 MHz,  $\text{CDCl}_3$ ): 148.8, 97.5, 47.4, 41.5, 40.5, 32.4, 31.8, 28.4, 25.8, 25.2 ppm. IR (neat,  $\text{cm}^{-1}$ ): 2974, 2865, 1450, 1427, 1305, 1231, 1174. HRMS *calcd.* for  $(\text{C}_{12}\text{H}_{19})$   $[\text{M}-\text{I}]^+$ : 163.1481, *found* 163.1481.



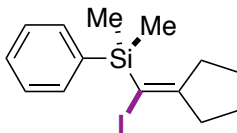
**(3-cyclopentylidene-3-iodopropyl)benzene (5).** Following the general procedure, the corresponding vinyl iodide was obtained in 88% yield in 24 h as colorless oil.  $^1\text{H}$  NMR (400 MHz,  $\text{CDCl}_3$ ):  $\delta$  7.30-7.27 (m, 2H), 7.22-7.17 (m, 3H), 2.81 (t,  $J = 7.2$  Hz, 2H), 2.72 (t,  $J = 7.0$  Hz, 2H), 2.27 (t,  $J = 7.4$  Hz, 2H), 2.04 (t,  $J = 7.2$  Hz, 2H), 1.73-1.58 (m, 4H) ppm.  $^{13}\text{C}$  NMR (100 MHz,  $\text{CDCl}_3$ ): 150.1, 141.1, 128.9, 128.3, 126.1, 95.6, 44.3, 41.4, 35.4, 31.6, 28.3, 25.8 ppm. IR (neat,  $\text{cm}^{-1}$ ): 3061, 3026, 2939, 2864, 1493, 747, 697. HRMS *calcd.* for  $(\text{C}_{14}\text{H}_{17})$   $[\text{M}-\text{I}]^+$ : 185.1325, *found* 185.1322.



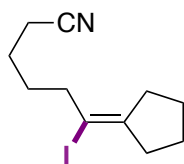
**(1-Iodo-2,2-dimethylpropylidene)cyclopentane (6).** Following the general procedure, the corresponding vinyl iodide was obtained in 60% yield in 48 h as colorless oil.  $^1\text{H}$  NMR (300 MHz,  $\text{CDCl}_3$ ):  $\delta$  2.51 (dt,  $J = 7.2, 1.2$  Hz, 2H), 2.44 (dt,  $J = 7.2, 1.2$  Hz, 2H), 1.85 (quint,  $J = 6.9$  Hz, 2H), 1.56 (quint,  $J = 6.9$  Hz, 2H), 1.31 (s, 9H) ppm.  $^{13}\text{C}$  NMR (75 MHz,  $\text{CDCl}_3$ ): 146.6, 115.7, 48.2, 41.4, 33.0, 32.5, 29.9, 25.4 ppm. IR (neat,  $\text{cm}^{-1}$ ): 2954, 2923, 2864, 1453, 1362, 1220, 764. HRMS *calcd.* for  $(\text{C}_{10}\text{H}_{17})$   $[\text{M}-\text{I}]^+$ : 137.1325, *found* 137.1322.



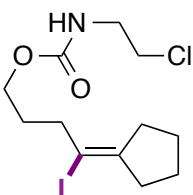
**(Cyclopentylideneiodomethyl)trimethylsilane (7).** Following the general procedure, the corresponding vinyl iodide was obtained in 81% yield in 24 h as colorless oil.  $^1\text{H}$  NMR (300 MHz,  $\text{CDCl}_3$ ):  $\delta$  2.41 (t,  $J = 7.2$  Hz, 2H), 2.34 (t,  $J = 6.9$  Hz, 2H), 1.89 (quint,  $J = 6.9$  Hz, 2H), 1.67 (quint,  $J = 7.2$  Hz, 2H), 0.25 (s, 9H) ppm.  $^{13}\text{C}$  NMR (75 MHz,  $\text{CDCl}_3$ ): 164.4, 100.5, 45.8, 34.7, 29.5, 25.6, 1.1 ppm. IR (neat,  $\text{cm}^{-1}$ ): 2954, 2868, 1595, 1419, 1247, 877, 834. HRMS *calcd.* for  $(\text{C}_9\text{H}_{17}\text{ISi})$ : 280.0144, *found* 280.0155.



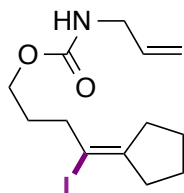
**(Cyclopentylideneiodomethyl)dimethyl(phenyl)silane (8).** Following the general procedure but using **2-s-8** (5.8 mmol), IrXX (0.1 mol%) and *t*-BuCN (0.6 M), the corresponding vinyl iodide was obtained in 84% yield in 24 h as colorless oil.  $^1\text{H}$  NMR (300 MHz,  $\text{CDCl}_3$ ):  $\delta$  7.60-7.56 (m, 2H), 7.40-7.33 (m, 3H), 2.44 (t,  $J = 7.2$  Hz, 2H), 2.08 (t,  $J = 7.2$  Hz, 2H), 1.78 (quint,  $J = 6.6$  Hz, 2H), 1.65 (quint,  $J = 7.2$  Hz, 2H), 0.54 (s, 6H) ppm.  $^{13}\text{C}$  NMR (75 MHz,  $\text{CDCl}_3$ ): 166.7, 138.2, 134.1, 129.3, 128.0, 96.9, 45.9, 35.2, 29.4, 25.6, 0.4 ppm. IR (neat,  $\text{cm}^{-1}$ ): 3067, 3048, 2954, 2867, 1593, 1427, 1247. HRMS *calcd.* for  $(\text{C}_{14}\text{H}_{20}\text{ISi})$   $[\text{M}+\text{H}]^+$ : 343.0374, *found* 343.0374.



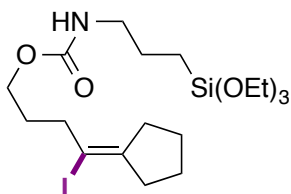
**6-Cyclopentylidene-6-iodohexanenitrile (9).** Following the general procedure, the corresponding vinyl iodide was obtained in 66% yield in 48 h as colorless oil.  $^1\text{H NMR}$  (300 MHz,  $\text{CDCl}_3$ ):  $\delta$  2.47 (br, 2H), 2.38-2.26 (m, 6H), 1.88-1.79 (m, 2H), 1.71-1.64 (m, 6H) ppm.  $^{13}\text{C NMR}$  (75 MHz,  $\text{CDCl}_3$ ): 150.0, 119.7, 95.3, 41.5, 40.8, 32.0, 28.5, 28.4, 25.8, 24.3, 17.3 ppm. IR (neat,  $\text{cm}^{-1}$ ): 2941, 2866, 2246, 1451, 1425, 1305, 1176. HRMS *calcd.* for ( $\text{C}_{11}\text{H}_{16}\text{INNa}$ ) [ $\text{M}+\text{Na}$ ] $^+$ : 312.0220, *found* 312.0215.



**4-Cyclopentylidene-4-iodobutyl (2-chloroethyl)carbamates (10).** Following the general procedure, the corresponding vinyl iodide was obtained in 95% yield in 48 h as colorless oil.  $^1\text{H NMR}$  (300 MHz,  $\text{CDCl}_3$ ):  $\delta$  5.15 (b, 1H), 4.05 (t,  $J$  = 6.3 Hz, 2H), 3.61-3.47 (m, 4H), 2.50 (t,  $J$  = 7.2 Hz, 2H), 2.28 (q,  $J$  = 7.5 Hz, 4H), 1.87-1.76 (m, 4H), 1.70-1.60 (m, 2H) ppm.  $^{13}\text{C NMR}$  (75 MHz,  $\text{CDCl}_3$ ): 156.5, 150.0, 95.1, 63.8, 44.2, 42.8, 41.4, 38.0, 31.7, 28.6, 28.3, 25.8 ppm. IR (neat,  $\text{cm}^{-1}$ ): 3332, 2954, 1695, 1518, 1430, 1244, 1146. HRMS *calcd.* for ( $\text{C}_{12}\text{H}_{19}\text{ClINNaO}_2$ ) [ $\text{M}+\text{Na}$ ] $^+$ : 394.0041, *found* 394.0043.



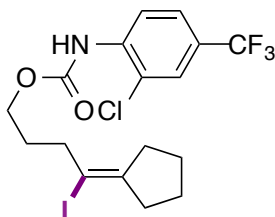
**4-Cyclopentylidene-4-iodobutyl allylcarbamate (11).** Following the general procedure, the corresponding vinyl iodide was obtained in 72% yield in 96 h as brown oil.  $^1\text{H NMR}$  (300 MHz,  $\text{CDCl}_3$ ):  $\delta$  5.90-5.77 (m, 1H), 5.22-5.09 (m, 2H), 4.76 (b, 1H), 4.05 (t,  $J$  = 6.3 Hz, 2H), 3.79 (t,  $J$  = 5.4 Hz, 2H), 2.50 (t,  $J$  = 7.2 Hz, 2H), 2.29 (q,  $J$  = 7.5 Hz, 4H), 1.87-1.77 (m, 4H), 1.70-1.61 (m, 2H) ppm.  $^{13}\text{C NMR}$  (75 MHz,  $\text{CDCl}_3$ ): 156.5, 149.9, 134.7, 116.0, 95.3, 63.6, 43.5, 41.4, 38.1, 31.7, 28.7, 28.3, 25.8 ppm. IR (neat,  $\text{cm}^{-1}$ ): 3339, 2954, 1679, 1520, 1427, 1244, 1060. HRMS *calcd.* for ( $\text{C}_{13}\text{H}_{20}\text{INNaO}_2$ ) [ $\text{M}+\text{Na}$ ] $^+$ : 372.0431, *found* 372.0440.



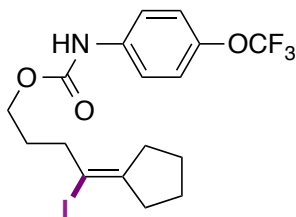
**4-Cyclopentylidene-4-iodobutyl (3-(triethoxysilyl)propyl)carbamates (12).** Following the general procedure, the corresponding vinyl iodide was obtained in 61% yield in 48 h as brown oil.  $^1\text{H NMR}$  (300 MHz,  $\text{CDCl}_3$ ):  $\delta$  4.92 (b, 1H), 4.01 (t,  $J$  = 6.3 Hz, 2H), 3.80 (q,  $J$  = 6.9 Hz, 6H), 3.15 (q,  $J$  = 6.6 Hz, 2H), 2.49 (t,  $J$  = 6.9 Hz, 2H), 2.28 (q,  $J$  = 7.8 Hz, 4H), 1.85-1.75 (m, 4H), 1.69-1.55 (m, 4H), 1.20 (t,  $J$  = 6.9 Hz, 9H), 0.60 (t,  $J$  = 8.1 Hz, 2H) ppm.  $^{13}\text{C NMR}$  (75 MHz,



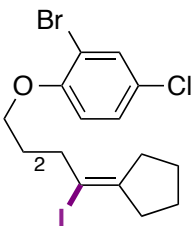
CDCl<sub>3</sub>): 156.7, 149.8, 95.3, 63.3, 58.5, 43.4, 41.3, 38.1, 31.7, 28.7, 28.3, 25.8, 23.4, 18.3, 7.7 ppm. IR (neat, cm<sup>-1</sup>): 3324, 2929, 1689, 1529, 1445, 1248, 1120.



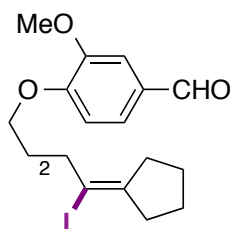
**4-Cyclopentylidene-4-iodobutyl (2-chloro-4-(trifluoromethyl)phenyl)carbamates (13).** Following the general procedure, the corresponding vinyl iodide **3s** was obtained in 89% yield in 48 h as white solid. M.P. = 54.1 °C. <sup>1</sup>H NMR (300 MHz, CDCl<sub>3</sub>): δ 8.53 (b, 1H), 7.47 (d, *J* = 8.1 Hz, 1H), 7.26-7.23 (m, 2H), 4.21 (t, *J* = 6.3 Hz, 2H), 2.57 (t, *J* = 6.9 Hz, 2H), 2.36-2.27 (m, 4H), 1.99-1.90 (m, 2H), 1.87-1.78 (m, 2H), 1.71-1.62 (m, 2H) ppm. <sup>13</sup>C NMR (75 MHz, CDCl<sub>3</sub>): 153.0, 150.3, 135.5, 130.4 (q, *J* (C-F) = 32.8 Hz), 129.6, 125.2, 123.6 (q, *J*<sub>C-F</sub> = 270.8 Hz), 120.3 (q, *J*<sub>C-F</sub> = 3.8 Hz), 116.8 (q, *J*<sub>C-F</sub> = 3.8 Hz), 94.8, 64.7, 41.4, 38.0, 31.8, 28.4, 28.3, 25.8 ppm. <sup>19</sup>F NMR (376 MHz, CDCl<sub>3</sub>): -62.89 ppm. IR (neat, cm<sup>-1</sup>): 3303, 2950, 2846, 1738, 1712, 1588, 1536. HRMS *calcd.* for (C<sub>17</sub>H<sub>18</sub>ClF<sub>3</sub>NNaO<sub>2</sub>) [M+Na]<sup>+</sup>: 509.9915, *found* 509.9919.



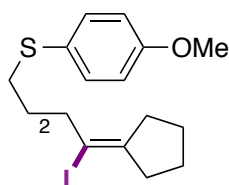
**4-Cyclopentylidene-4-iodobutyl (4-(trifluoromethoxy)phenyl)carbamates (14).** Following the general procedure, the corresponding vinyl iodide was obtained in 90% yield in 48 h as white solid. M.P. = 79.4 °C. <sup>1</sup>H NMR (300 MHz, CDCl<sub>3</sub>): δ 7.41 (d, *J* = 9.0 Hz, 2H), 7.16 (d, *J* = 8.4 Hz, 2H), 6.73 (s, 1H), 4.17 (t, *J* = 6.3 Hz, 2H), 2.55 (t, *J* = 7.2 Hz, 2H), 2.34-2.26 (q, *J* = 7.5 Hz, 4H), 1.95-1.77 (m, 4H), 1.70-1.61 (m, 2H) ppm. <sup>13</sup>C NMR (75 MHz, CDCl<sub>3</sub>): 153.6, 150.2, 144.8, 136.7, 122.0, 120.6 (q, *J*<sub>C-F</sub> = 255.0 Hz), 119.9 (br), 118.9, 94.9, 64.3, 41.4, 38.1, 31.8, 28.6, 28.3, 25.8 ppm. <sup>19</sup>F NMR (376 MHz, CDCl<sub>3</sub>): -58.31 ppm. IR (neat, cm<sup>-1</sup>): 3327, 2958, 2862, 1699, 1541, 1414, 1270. HRMS *calcd.* for (C<sub>17</sub>H<sub>19</sub>F<sub>3</sub>INNaO<sub>3</sub>) [M+Na]<sup>+</sup>: 492.0254, *found* 492.0266.



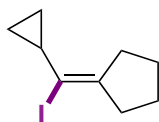
**2-Bromo-4-chloro-1-((5-cyclopentylidene-5-iodopentyl)oxy)benzene (15).** Following the general procedure, the corresponding vinyl iodide was obtained in 92% yield in 48 h as yellow oil. <sup>1</sup>H NMR (300 MHz, CDCl<sub>3</sub>): δ 7.52 (d, *J* = 2.4 Hz, 1H), 7.21 (dd, *J* = 8.7, 2.4 Hz, 1H), 6.79 (d, *J* = 8.7 Hz, 1H), 4.00 (t, *J* = 6.0 Hz, 2H), 2.51 (t, *J* = 6.9 Hz, 2H), 2.35-2.27 (m, 4H), 1.87-1.65 (m, 8H) ppm. <sup>13</sup>C NMR (75 MHz, CDCl<sub>3</sub>): 154.4, 149.4, 132.9, 128.3, 125.9, 113.9, 112.8, 96.5, 69.5, 41.5, 41.3, 31.9, 28.4, 27.9, 25.9, 25.9 ppm. IR (neat, cm<sup>-1</sup>): 2942, 2866, 1585, 1479, 1464, 1284, 1047.



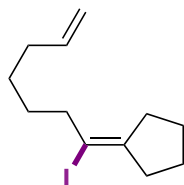
**4-((5-Cyclopentylidene-5-iodopentyl)oxy)-3-methoxybenzaldehyde (16).** Following the general procedure, the corresponding vinyl iodide was obtained in 93% yield in 48 h as slight yellow solid. M.P. = 63.5 °C.  $^1\text{H}$  NMR (300 MHz,  $\text{CDCl}_3$ ):  $\delta$  9.83 (s, 1H), 7.44-7.38 (m, 2H), 6.95 (d,  $J$  = 8.4 Hz, 1H), 4.09 (t,  $J$  = 6.9 Hz, 2H), 3.90 (s, 3H), 2.49 (t,  $J$  = 7.2 Hz, 2H), 2.33-2.24 (m, 4H), 1.91-1.76 (m, 4H), 1.73-1.60 (m, 4H) ppm.  $^{13}\text{C}$  NMR (75 MHz,  $\text{CDCl}_3$ ): 191.0, 154.1, 149.9, 149.5, 130.0, 126.9, 111.5, 109.3, 96.4, 69.1, 56.1, 41.4, 41.2, 31.9, 28.4, 27.7, 25.8 ppm. IR (neat,  $\text{cm}^{-1}$ ): 3078, 2944, 2866, 1677, 1582, 1506, 1465. HRMS *calcd.* for ( $\text{C}_{18}\text{H}_{23}\text{INaO}_3$ ) [ $\text{M}+\text{Na}$ ] $^+$ : 437.0584, *found* 437.0579.



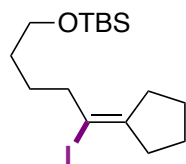
**(5-Cyclopentylidene-5-iodopentyl)(4-methoxyphenyl)sulfane (17).** Following the general procedure, the corresponding vinyl iodide was obtained in 88% yield in 48 h as yellow oil.  $^1\text{H}$  NMR (300 MHz,  $\text{CDCl}_3$ ):  $\delta$  7.37-7.31 (m, 2H), 6.87-6.82 (m, 2H), 3.79 (s, 3H), 2.82 (t,  $J$  = 7.2 Hz, 2H), 2.41 (t,  $J$  = 6.6 Hz, 2H), 2.27 (t,  $J$  = 7.2 Hz, 4H), 1.85-1.76 (m, 2H), 1.70-1.56 (m, 6H) ppm.  $^{13}\text{C}$  NMR (75 MHz,  $\text{CDCl}_3$ ): 158.9, 149.2, 133.4, 114.6, 96.6, 55.5, 41.4, 41.3, 35.9, 31.8, 28.4, 28.4, 28.2, 25.9 ppm. IR (neat,  $\text{cm}^{-1}$ ): 2936, 2862, 2833, 1591, 1492, 1240, 824. HRMS *calcd.* for ( $\text{C}_{17}\text{H}_{24}\text{IOS}$ ) [ $\text{M}+\text{H}$ ] $^+$ : 403.0587, *found* 403.0590.



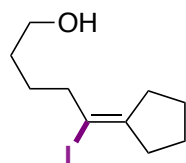
**(Cyclopropylidene)cyclopentane (19).** Following the general procedure, the corresponding vinyl iodide was obtained in 70% yield in 32 h as colorless oil.  $^1\text{H}$  NMR (300 MHz,  $\text{CDCl}_3$ ):  $\delta$  2.45 (t,  $J$  = 7.4 Hz, 2H), 2.30 (t,  $J$  = 7.0 Hz, 2H), 1.85 (quint,  $J$  = 7.2 Hz, 2H), 1.66 (quint,  $J$  = 7.0 Hz, 2H), 1.44-1.35 (m, 1H), 0.76-0.68 (m, 2H), 0.68-0.61 (m, 2H) ppm.  $^{13}\text{C}$  NMR (75 MHz,  $\text{CDCl}_3$ ): 150.1, 100.7, 42.0, 32.9, 28.4, 25.7, 19.9, 9.8 ppm. IR (neat,  $\text{cm}^{-1}$ ): 2956, 2870, 1736, 1373, 1237, 1045, 981. HRMS *calcd.* for ( $\text{C}_9\text{H}_{13}\text{I}$ ) [ $\text{M}$ ] $^+$ : 248.0056, *found* 248.0054.



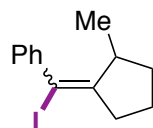
**(1-Iodohept-6-en-1-ylidene)cyclopentane (20).** Following the general procedure, the corresponding vinyl iodide was obtained in 78% yield in 32 h as colorless oil.  $^1\text{H}$  NMR (300 MHz,  $\text{CDCl}_3$ ):  $\delta$  5.88-5.75 (m, 1H), 5.05-4.93 (m, 2H), 2.43 (t,  $J$  = 7.2 Hz, 2H), 2.34-2.26 (m, 4H), 2.11-2.04 (m, 2H), 1.82 (quint,  $J$  = 6.9 Hz, 2H), 1.66 (quint,  $J$  = 6.9 Hz, 2H), 1.57-1.47 (m, 2H), 1.43-1.34 (m, 2H) ppm.  $^{13}\text{C}$  NMR (75 MHz,  $\text{CDCl}_3$ ): 148.8, 138.9, 114.5, 97.1, 41.7, 41.4, 33.8, 31.8, 28.9, 28.4, 27.8, 25.9 ppm. IR (neat,  $\text{cm}^{-1}$ ): 2933, 2859, 1709, 1430, 1373, 1234, 1172. HRMS *calcd.* for ( $\text{C}_{12}\text{H}_{18}\text{I}$ ) [ $\text{M}-\text{H}$ ] $^+$ : 289.0448, *found* 289.0447.



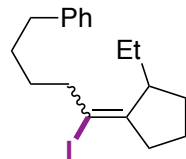
**tert-Butyl((5-cyclopentylidene-5-iodopentyl)oxy)dimethylsilane (21).** Following the general procedure, the corresponding vinyl iodide was obtained in 93% yield in 32 h as colorless oil.  $^1\text{H}$  NMR (300 MHz,  $\text{CDCl}_3$ ):  $\delta$  3.62 (t,  $J$  = 6.0 Hz, 2H), 2.44 (t,  $J$  = 6.9 Hz, 2H), 2.34-2.26 (m, 4H), 1.87-1.77 (m, 2H), 1.71-1.51 (m, 6H), 0.90 (s, 9H), 0.05 (s, 6H) ppm.  $^{13}\text{C}$  NMR (75 MHz,  $\text{CDCl}_3$ ): 148.9, 97.2, 63.2, 41.6, 41.4, 31.8, 31.7, 28.4, 26.1, 25.9, 25.8, 18.5, -5.1 ppm. IR (neat,  $\text{cm}^{-1}$ ): 2934, 2863, 1451, 1428, 1051, 836, 781. HRMS *calcd.* for  $(\text{C}_{10}\text{H}_{16}\text{I})$   $[\text{M}-\text{OTBS}]^+$ : 263.0291, *found* 263.0280.



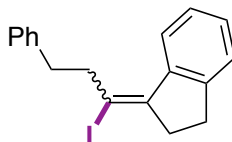
**5-Cyclopentylidene-5-iodopentan-1-ol (22).** Following the general procedure, the corresponding vinyl iodide was obtained in 89% yield in 32 h as colorless oil.  $^1\text{H}$  NMR (300 MHz,  $\text{CDCl}_3$ ):  $\delta$  3.67-3.61 (m, 2H), 2.47-2.43 (m, 2H), 2.34-2.25 (m, 4H), 1.86-1.77 (m, 2H), 1.70-1.52 (m, 7H) ppm.  $^{13}\text{C}$  NMR (75 MHz,  $\text{CDCl}_3$ ): 149.2, 96.8, 62.9, 41.4, 31.9, 31.5, 28.4, 25.9, 25.6 ppm. IR (neat,  $\text{cm}^{-1}$ ): 3497, 2937, 2864, 1438, 1351, 1201, 1159. HRMS *calcd.* for  $(\text{C}_{10}\text{H}_{18}\text{OI})$   $[\text{M}+\text{H}]^+$ : 281.0397, *found* 281.0394.



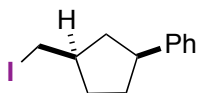
**(Iodo(2-methylcyclopentylidene)methyl)benzene (23).** Following the general procedure, the corresponding vinyl iodide (E/Z mixture = 1.3: 1) was obtained in 95% yield in 72 h as colorless oil.  $^1\text{H}$  NMR (major isomer, 300 MHz,  $\text{CDCl}_3$ ):  $\delta$  7.36-7.20 (m, 5H), 2.93-2.78 (m, 1H), 2.68-2.20 (m, 2H), 2.05-1.54 (m, 4H), 0.75 (d,  $J$  = 6.9 Hz, 3H) ppm.  $^{13}\text{C}$  NMR (major isomer, 75 MHz,  $\text{CDCl}_3$ ): 157.0, 144.6, 128.6, 128.2, 127.5, 90.4, 41.8, 36.8, 33.7, 23.1, 19.5 ppm. IR (neat,  $\text{cm}^{-1}$ ): 3056, 2953, 2865, 1441, 1370, 749, 696. HRMS *calcd.* for  $(\text{C}_{13}\text{H}_{15})$   $[\text{M}-\text{I}]^+$ : 171.1168, *found* 171.1167.



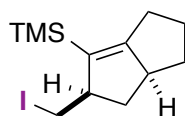
**(5-(2-Ethylcyclopentylidene)-5-iodopentyl)benzene (24).** Following the general procedure, the corresponding vinyl iodide (E/Z mixture = 1: 1) was obtained in 88% yield in 32 h as colorless oil.  $^1\text{H}$  NMR (major isomer, 300 MHz,  $\text{CDCl}_3$ ):  $\delta$  7.33-7.28 (m, 2H), 7.23-7.18 (m, 3H), 2.69-2.21 (m, 7H), 1.87-1.55 (m, 8H), 1.43-1.12 (m, 2H), 0.98-0.89 (m, 3H) ppm.  $^{13}\text{C}$  NMR (major isomer, 75 MHz,  $\text{CDCl}_3$ ): 152.9, 142.64, 128.5, 125.8, 100.1, 52.4, 41.9, 40.9, 36.0, 32.2, 30.4, 30.1, 29.0, 25.5, 22.7, 12.4 ppm. IR (neat,  $\text{cm}^{-1}$ ): 3025, 2929, 2857, 1453, 1160, 744, 697. HRMS *calcd.* for  $(\text{C}_{18}\text{H}_{25})$   $[\text{M}-\text{I}]^+$ : 241.1951, *found* 241.1946.



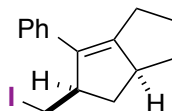
**(Z)-1-(1-Iodo-3-phenylpropylidene)-2,3-dihydro-1H-indene (25).** Following the general procedure, the corresponding vinyl iodide was obtained in 47% yield in 72 h as colorless oil (E/Z mixture = 1:1). Z isomer spectroscopic data:  $^1\text{H NMR}$  (300 MHz,  $\text{CDCl}_3$ ):  $\delta$  7.52 (d,  $J = 7.5$  Hz, 1H), 7.35-7.27 (m, 4H), 7.24-7.13 (m, 4H), 3.35-3.29 (m, 2H), 3.03-2.93 (m, 4H), 2.89-2.84 (m, 2H) ppm.  $^{13}\text{C NMR}$  (75 MHz,  $\text{CDCl}_3$ ): 149.7, 147.1, 140.7, 137.9, 128.6, 128.6, 128.1, 126.6, 126.3, 126.2, 124.0, 100.6, 44.7, 42.9, 35.1, 29.4 ppm. IR (neat,  $\text{cm}^{-1}$ ): 3019, 2921, 2851, 1455, 1376, 749, 699. HRMS *calcd.* for ( $\text{C}_{18}\text{H}_{18}\text{I}$ ) [ $\text{M}+\text{H}$ ] $^+$ : 361.0448, *found* 361.0446.



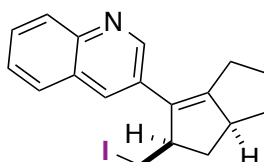
**3-(Iodomethyl)cyclopentylbenzene (26).** Following the general procedure, the corresponding alkyl iodide was obtained in 80% yield in 32 h (cis/trans mixture = 10:1) as colorless oil.  $^1\text{H NMR}$  (300 MHz,  $\text{CDCl}_3$ ):  $\delta$  7.31-7.15 (m, 5H), 3.29-3.25 (m, 2H), 3.18-3.06 (m, 1H), 2.53-2.26 (2H), 2.16-2.08 (m, 1H), 2.05-1.85 (m, 1H), 1.83-1.70 (m, 1H), 1.59-1.48 (m, 1H), 1.43-1.31 (m, 1H) ppm.  $^{13}\text{C NMR}$  (75 MHz,  $\text{CDCl}_3$ ): 145.3, 128.4, 127.0, 126.1, 46.2, 42.7, 42.4, 33.5, 32.6, 14.1 ppm. IR (neat,  $\text{cm}^{-1}$ ): 3025, 2947, 2863, 1492, 1447, 1181, 752, 697. HRMS *calcd.* for ( $\text{C}_{12}\text{H}_{15}\text{I}$ ): 286.0219, *found* 286.0223.



**2-(Iodomethyl)-2,3,3a,4,5,6-hexahydropentalen-1-yl)trimethylsilane (27).** Following the general procedure, the corresponding alkyl iodide (single isomer) was obtained in 70% yield in 72 h as colorless oil.  $^1\text{H NMR}$  (300 MHz,  $\text{CDCl}_3$ ):  $\delta$  3.62 (dd,  $J = 9.0, 3.0$  Hz, 1H), 3.41-3.31 (m, 1H), 3.065 (t,  $J = 9.3$  Hz, 1H), 2.79-2.71 (m, 1H), 2.40-2.33 (m, 1H), 2.21-2.15 (m, 2H), 2.07-1.84 (m, 3H), 1.11-0.97 (m, 2H), 0.13 (s, 9H) ppm.  $^{13}\text{C NMR}$  (75 MHz,  $\text{CDCl}_3$ ): 169.4, 130.4, 59.0, 53.7, 40.5, 31.6, 28.5, 25.8, 17.2, 0.28 ppm. IR (neat,  $\text{cm}^{-1}$ ): 2922, 2852, 1460, 1377, 1249, 839.

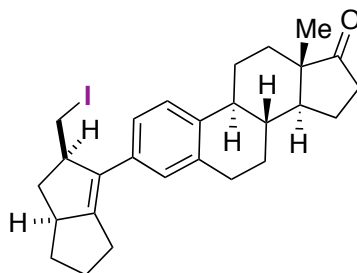


**5-(Iodomethyl)-6-phenyl-1,2,3,3a,4,5-hexahydropentalene (28).** Following the general procedure, the corresponding alkyl iodide was obtained in 72% yield in 60 h as yellow oil (dr = 25:1).  $^1\text{H NMR}$  (400 MHz,  $\text{CDCl}_3$ ):  $\delta$  7.39-7.20 (m, 5H), 3.75-3.66 (m, 1H), 3.53 (dd,  $J = 9.6$  Hz, 3.2 Hz, 1H), 3.13 (dd,  $J = 9.6$  Hz, 8.4 Hz, 1H), 2.97-2.88 (m, 1H), 2.63-2.46 (m, 2H), 2.23-2.11 (m, 2H), 2.04-1.92 (m, 2H), 1.35-1.25 (m, 2H) ppm.  $^{13}\text{C NMR}$  (101 MHz,  $\text{CDCl}_3$ ): 153.5, 137.3, 130.6, 128.5, 127.1, 126.2, 54.4, 51.6, 38.3, 32.2, 28.8, 24.4, 16.5 ppm. IR (neat,  $\text{cm}^{-1}$ ): 3053, 3025, 2953, 2865, 1488, 743, 693. HRMS *calcd.* for ( $\text{C}_{15}\text{H}_{18}\text{I}$ ) [ $\text{M}+\text{H}$ ] $^+$ : 325.0448, *found* 325.0442.



**3-(2-(Iodomethyl)-2,3,3a,4,5,6-hexahydropentalen-1-yl)quinolone (29).** Following the general procedure, the corresponding alkyl iodide was obtained in 63% yield in 96 h as brown oil. The spectroscopic data correspond to those previously reported in the literature.<sup>5</sup>  $^1\text{H NMR}$  (300 MHz,  $\text{CDCl}_3$ ):  $\delta$  8.90 (d,  $J = 2.1$  Hz, 1H), 8.06 (d,  $J = 8.4$  Hz, 1H), 7.93 (d,  $J = 2.1$  Hz, 1H), 7.79-7.76 (m, 1H), 7.69-7.63 (m, 1H), 7.55-7.49 (m, 1H), 3.77-3.66 (m, 1H), 3.47 (dd,  $J = 10.2, 3$  Hz, 1H), 3.19 (dd,  $J = 9.9, 7.5$  Hz, 1H), 3.02-2.93 (m, 1H), 2.67-2.56 (m, 1H), 2.51-2.42 (m, 1H), 2.27-2.12 (m, 2H),

2.05-1.90 (m, 2H), 1.44-1.31 (m, 2H) ppm.  $^{13}\text{C}$  NMR (75 MHz,  $\text{CDCl}_3$ ): 156.5, 150.2, 146.6, 132.7, 130.5, 129.3, 129.0, 128.0, 127.8, 127.6, 126.9, 53.9, 52.0, 37.9, 31.9, 28.7, 24.4, 16.0 ppm.



**3-(2-(iodomethyl)-2,3,3a,4,5,6-hexahydropentalen-1-yl)-13-methyl-6,7,8,9,11,12,13,14,15,16-decahydro-17H-cyclopenta[*a*]phenanthren-17-one (30).** Following the general procedure but using  $\text{Irxx}$  (2 mol%), the corresponding alkyl iodide was obtained in 44% yield in 72 h as yellow oil.  $^1\text{H}$  NMR (300 MHz,  $\text{CDCl}_3$ ):  $\delta$  7.24 (d,  $J = 9.3$  Hz, 1H), 7.08-7.03 (m, 1H), 6.99-6.97 (d,  $J = 4.5$  Hz, 1H), 3.70-3.62 (m, 1H), 3.52 (dt,  $J = 9.6, 2.4$  Hz, 1H), 3.07 (dt, 9.0, 2.4 Hz, 1H), 2.92-2.85 (m, 3H), 2.56-1.91 (m, 14H), 1.68-1.44 (m, 7H), 0.92 (s, 3H) ppm.  $^{13}\text{C}$  NMR (75 MHz,  $\text{CDCl}_3$ ): 221.0, 153.03, 152.99, 137.78, 137.75, 136.49, 136.46, 134.79, 134.77, 130.33, 130.31, 127.54, 127.41, 125.4, 124.70, 124.59, 54.5, 51.5, 50.6, 48.1, 44.5, 44.5, 38.4, 38.2, 36.0, 32.1, 31.7, 29.6, 28.7, 26.7, 25.7, 24.4, 21.7, 14.0 ppm. IR (neat,  $\text{cm}^{-1}$ ): 2924, 2854, 1736, 1453, 1374, 1260, 1084. (MALDI) HRMS *calcd.* for  $(\text{C}_{27}\text{H}_{33}\text{IO})$   $[\text{M}]^+$ : 500.1570, *found* 500.1549.

### 2.8.7. X-Ray Crystallographic Data for 14

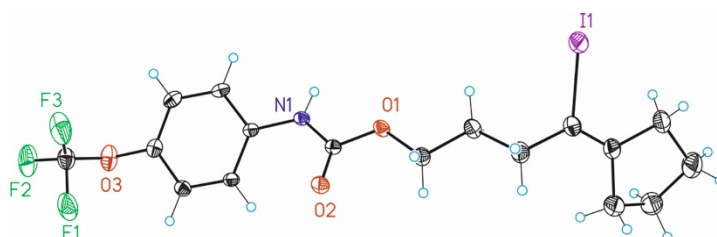


Table 1. Crystal data and structure refinement for 14.

Identification code	yshen03-431a	
Empirical formula	$\text{C}_{17}\text{H}_{19}\text{F}_3\text{I}\text{N}\text{O}_3$	
Formula weight	469.23	
Temperature	100(2) K	
Wavelength	0.71073 $\approx$	
Crystal system	Monoclinic	
Space group	$\text{C}2/c$	
Unit cell dimensions	$a = 47.1143(6) \approx$	$a = 90^\circ$ .
	$b = 4.86847(8) \approx$	$b = 97.7446(11)^\circ$ .
	$c = 16.0241(2) \approx$	$g = 90^\circ$ .
Volume	$3642.00(9) \approx^3$	
Z	8	
Density (calculated)	$1.712 \text{ Mg/m}^3$	

Absorption coefficient	1.803 mm <sup>-1</sup>
F(000)	1856
Crystal size	0.25 x 0.20 x 0.15 mm <sup>3</sup>
Theta range for data collection	2.566 to 34.164°.
Index ranges	-74 ≤ h ≤ 74, -7 ≤ k ≤ 7, -25 ≤ l ≤ 24
Reflections collected	55197
Independent reflections	7329 [R(int) = 0.0289]
Completeness to theta = 34.164°	97.299995%
Absorption correction	Multi-scan
Max. and min. transmission	0.840 and 0.646
Refinement method	Full-matrix least-squares on F <sup>2</sup>
Data / restraints / parameters	7329 / 3 / 262
Goodness-of-fit on F <sup>2</sup>	1.033
Final R indices [I > 2σ(I)]	R1 = 0.0328, wR2 = 0.0949
R indices (all data)	R1 = 0.0363, wR2 = 0.0972
Largest diff. peak and hole	2.049 and -1.418 e. Å <sup>-3</sup>

Table 2. Bond lengths [Å] and angles [°] for **14**.

---

Bond lengths----

C1-C13	1.326(2)
C1-C2	1.507(2)
C1-I1	2.1234(17)
C2-C3	1.529(2)
C3-C4	1.509(2)
C4-O1	1.4502(19)
C5-O2	1.2209(16)
C5-O1	1.3430(17)
C5-N1	1.3560(18)
C6-C7	1.3970(19)
C6-C11	1.3978(19)
C6-N1	1.4118(19)
C7-C8	1.387(2)
C8-C9	1.385(2)
C9-C10	1.389(2)
C9-O3	1.411(2)
C10-C11	1.389(2)
C12-F1'	1.252(4)
C12-F2	1.268(8)

C12-F3	1.285(3)
C12-F2'	1.321(8)
C12-O3	1.325(2)
C12-F3'	1.374(4)
C12-F1	1.396(4)
C13-C14	1.518(3)
C13-C17	1.519(3)
C14-C15	1.538(3)
C15-C16'	1.450(6)
C15-C16	1.484(5)
C16-C17	1.501(5)
C16'-C17	1.599(4)

Angles-----

C13-C1-C2	127.27(16)
C13-C1-I1	118.64(13)
C2-C1-I1	114.09(12)
C1-C2-C3	112.80(14)
C4-C3-C2	111.39(13)
O1-C4-C3	106.40(12)
O2-C5-O1	123.94(13)
O2-C5-N1	126.11(13)
O1-C5-N1	109.93(11)
C7-C6-C11	119.63(13)
C7-C6-N1	123.00(12)
C11-C6-N1	117.28(12)
C8-C7-C6	120.01(13)
C9-C8-C7	119.42(13)
C8-C9-C10	121.67(14)
C8-C9-O3	118.93(15)
C10-C9-O3	119.18(14)
C11-C10-C9	118.62(13)
C10-C11-C6	120.64(13)
F2-C12-F3	114.1(5)
F1'-C12-F2'	110.0(6)
F1'-C12-O3	121.4(2)
F2-C12-O3	112.6(5)
F3-C12-O3	119.3(2)
F2'-C12-O3	110.0(5)
F1'-C12-F3'	106.3(4)

F2'-C12-F3'	103.1(4)
O3-C12-F3'	104.2(2)
F2-C12-F1	104.8(5)
F3-C12-F1	100.9(4)
O3-C12-F1	102.4(2)
C1-C13-C14	126.45( 17)
C1-C13-C17	125.08(17)
C14-C13-C17	108.47(16)
C13-C14-C15	104.43(17)
C16'-C15-C14	108.2(3)
C16-C15-C14	104.4(2)
C15-C16-C17	105.9(3)
C15-C16'-C17	102.7(3)
C16-C17-C13	102.6(2)
C13-C17-C16'	102.8(2)
C5-N1-C6	125.36(11)
C5-O1-C4	115.50(11)
C12-O3-C9	118.07(13)

-----

Table 3. Torsion angles [ $^{\circ}$ ] for **14**.

C13-C1-C2-C3	-115.7(2)
I1-C1-C2-C3	64.30(17)
C1-C2-C3-C4	178.08(14)
C2-C3-C4-O1	175.28(13)
C11-C6-C7-C8	1.1(2)
N1-C6-C7-C8	-175.41(13)
C6-C7-C8-C9	-0.5(2)
C7-C8-C9-C10	-0.3(2)
C7-C8-C9-O3	174.26(13)
C8-C9-C10-C11	0.4(2)
O3-C9-C10-C11	-174.14(13)
C9-C10-C11-C6	0.2(2)
C7-C6-C11-C10	-0.9(2)
N1-C6-C11-C10	175.72(13)
C2-C1-C13-C14	178.19(18)
I1-C1-C13-C14	-1.8(3)
C2-C1-C13-C17	-2.0(3)
I1-C1-C13-C17	178.02(16)



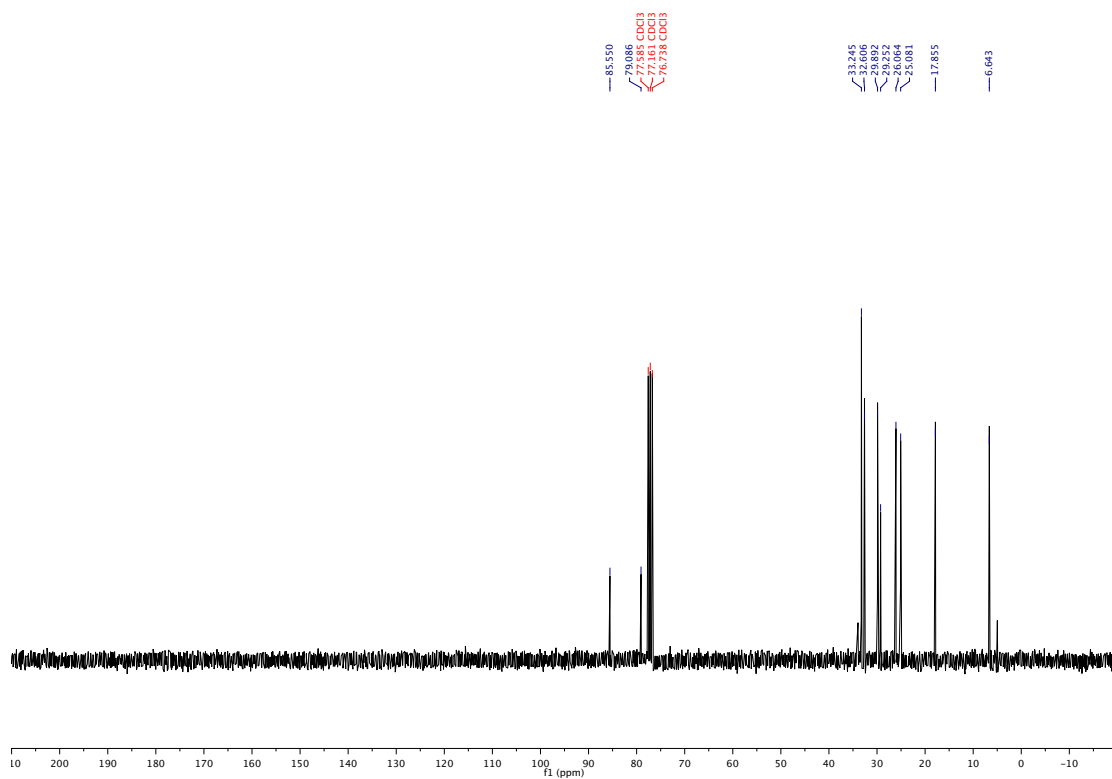
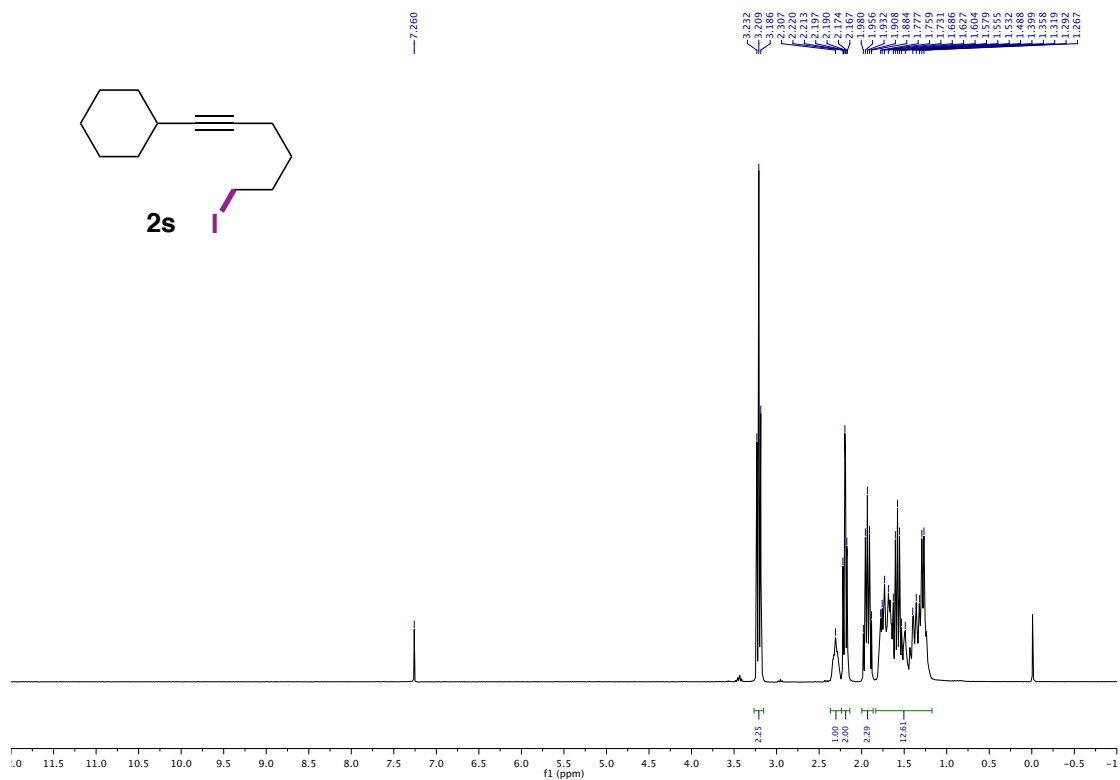
C1-C13-C14-C15	179.0(2)
C17-C13-C14-C15	-0.8(2)
C13-C14-C15-C16'	-22.8(3)
C13-C14-C15-C16	22.9(3)
C16'-C15-C16-C17	64.2(4)
C14-C15-C16-C17	-37.3(4)
C16-C15-C16'-C17	-56.4(3)
C14-C15-C16'-C17	35.6(4)
C15-C16-C17-C13	36.1(4)
C15-C16-C17-C16'	-59.0(4)
C1-C13-C17-C16	159.0(3)
C14-C13-C17-C16	-21.1(3)
C1-C13-C17-C16'	-158.6(3)
C14-C13-C17-C16'	21.3(3)
C15-C16'-C17-C16	59.9(4)
C15-C16'-C17-C13	-34.7(3)
O2-C5-N1-C6	-8.5(2)
O1-C5-N1-C6	172.60(12)
C7-C6-N1-C5	-25.7(2)
C11-C6-N1-C5	157.75(13)
O2-C5-O1-C4	1.7(2)
N1-C5-O1-C4	-179.35(11)
C3-C4-O1-C5	-179.60(12)
F1'-C12-O3-C9	-41.9(5)
F2-C12-O3-C9	170.6(4)
F3-C12-O3-C9	32.8(4)
F2'-C12-O3-C9	-172.3(4)
F3'-C12-O3-C9	77.8(3)
F1-C12-O3-C9	-77.5(3)
C8-C9-O3-C12	91.1(2)
C10-C9-O3-C12	-94.3(2)

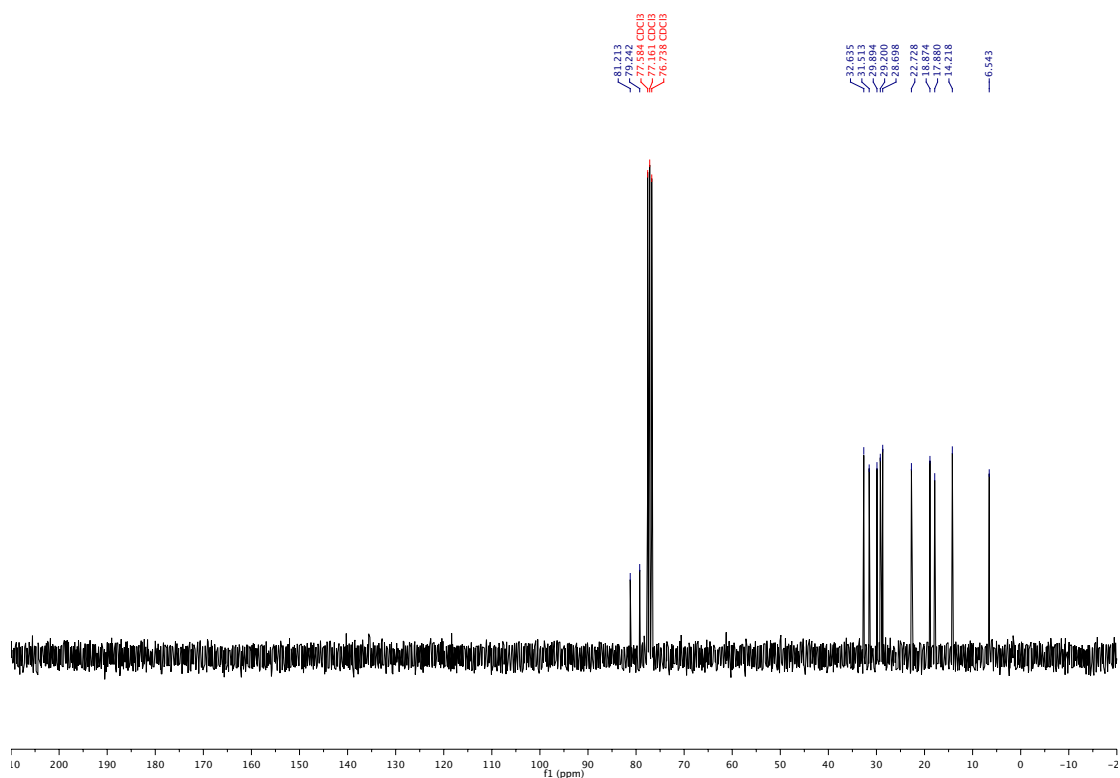
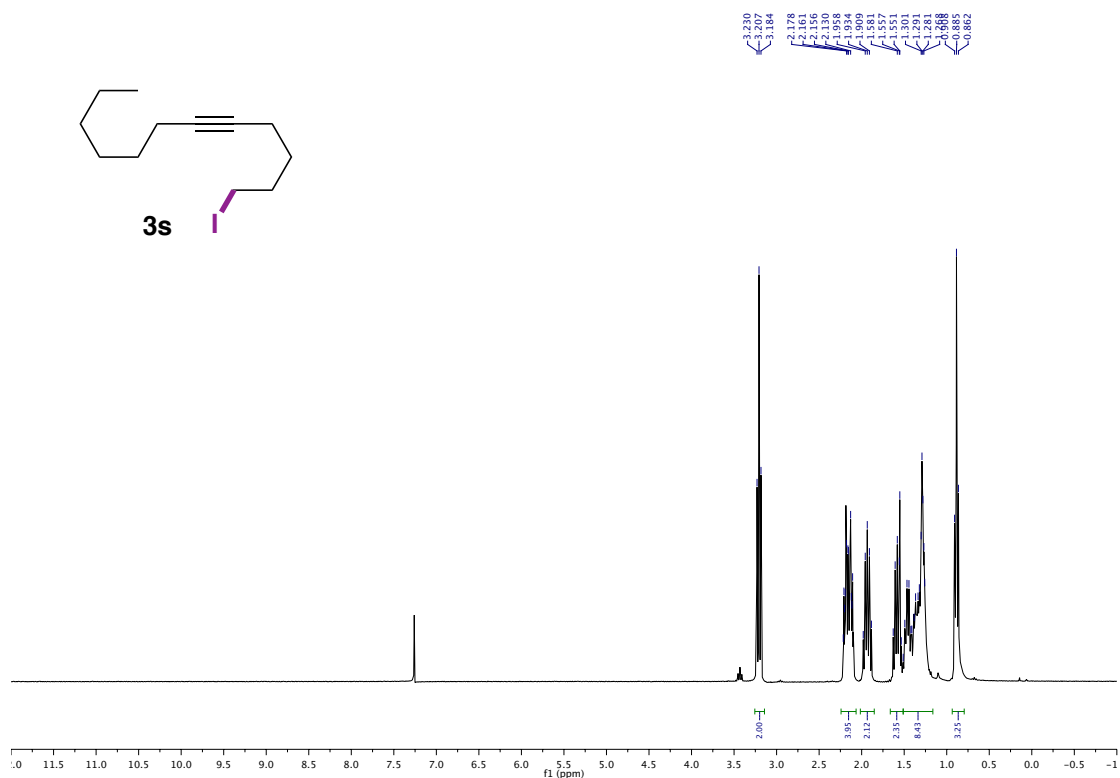
---

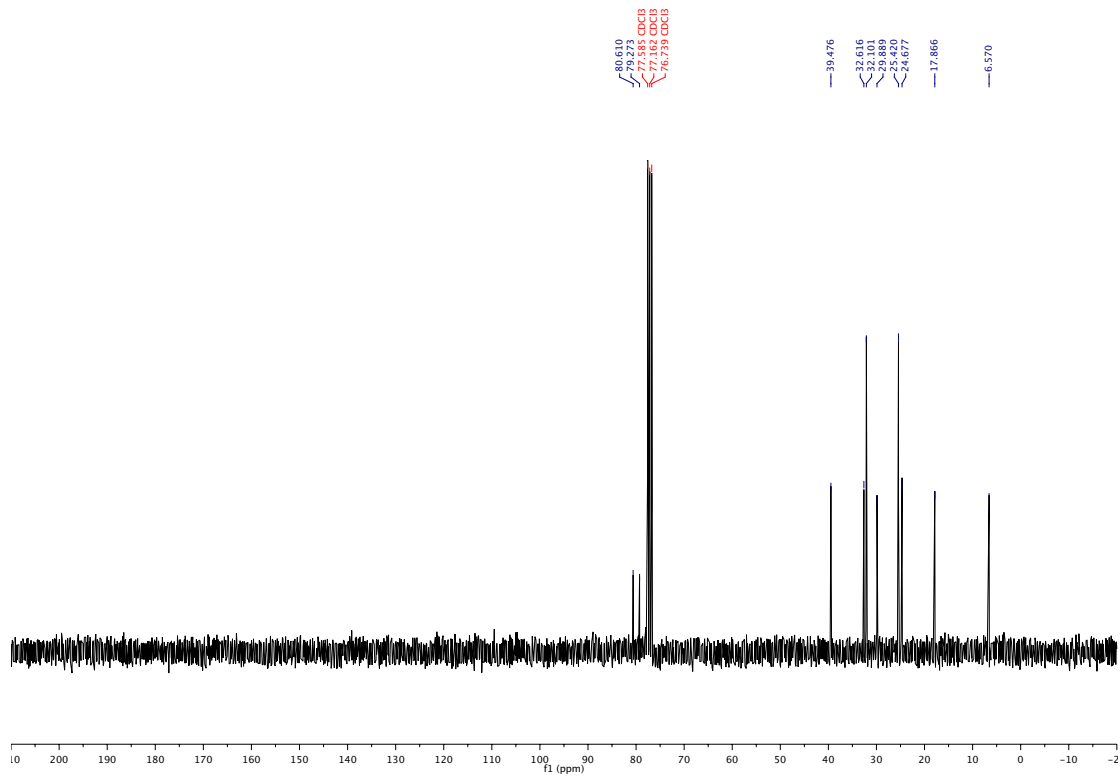
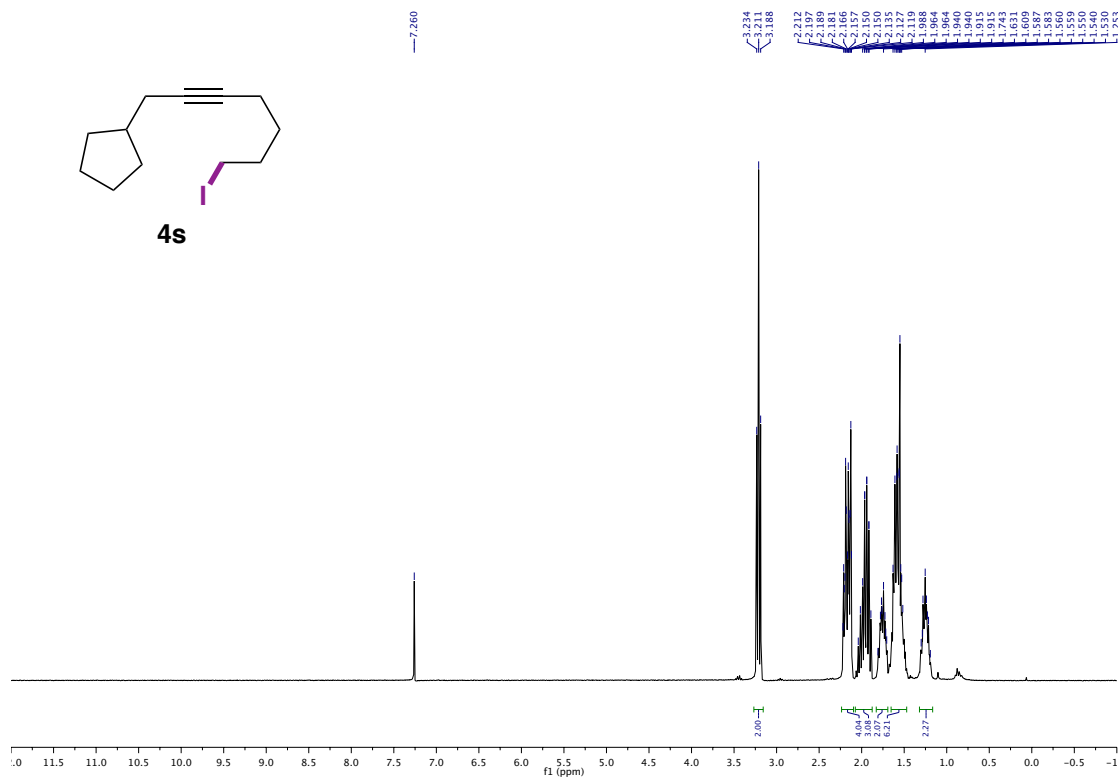
## 2.8.8. Bibliography of Known Compounds

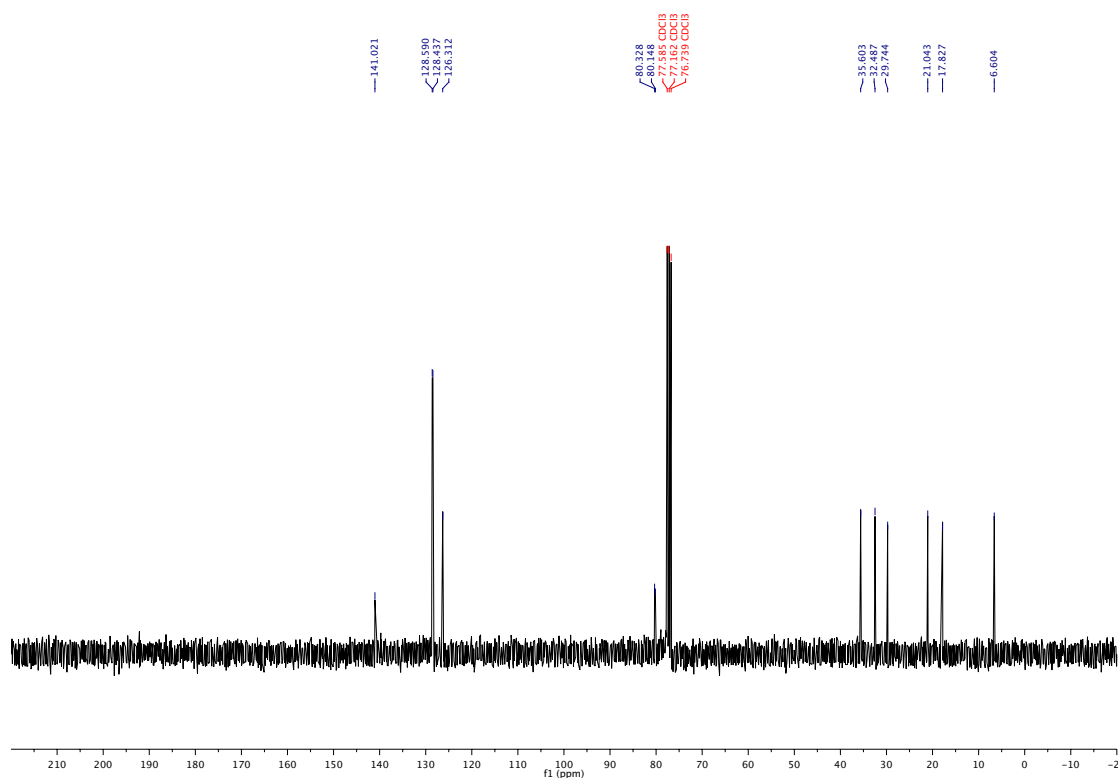
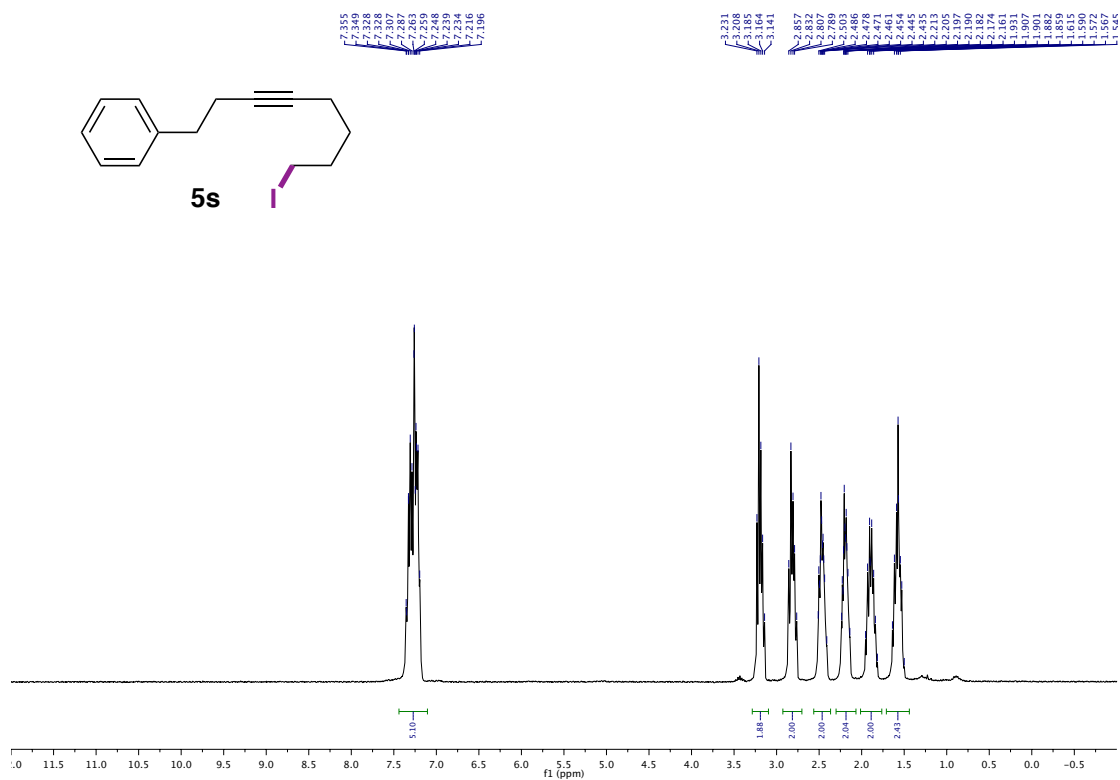
1. Tordera, D., Delgado, M., Ortí, E.; Bolink, H. J.; Frey, J., Nazeeruddin M. K., Baranoff, E. *Chem. Mater.* **2012**, *24*, 1896-1903.
2. Monks, B. M.; Cook, S. P. *J. Am. Chem. Soc.* **2012**, *134*, 15297-15300.
3. Hodgson, D. M.; Labande, A. H.; Pierard, F. Y. T. M.; Castro, M. Á. E. *J. Org. Chem.* **2003**, *68*, 6153-6159.
4. Lu, B., Li, C., Zhang, L. *J. Am. Chem. Soc.* **2010**, *132*, 14070-14072.
5. Monks, B. M., Cook, S. P. *Angew. Chem. Int. Ed.* **2013**, *52*, 14214-14218.
6. Prier, C. K., Rankic, D. A.; MacMillan D. W. C. *Chem. Rev.* **2013**, *113*, 5322-5363.
7. Choi, G. J., Knowles, R. R. *J. Am. Chem. Soc.* **2015**, *137*, 9226-9229.
8. Hatchard, C. G., Parker, C. A. *Proc. Roy. Soc. (London)* **1956**, *A235*, 518-536.
9. Kuhn, H. J.; Braslavsky, S. E.; Schmidt, R. *Pure Appl. Chem.* **2004**, *76*, 2105-2146.
10. Mnalti, M. and co-workers. *Chemical Actinometry. Handbook of Photochemistry*, 3<sup>rd</sup> ed.; Taylor & Francis Group. **2006**, 601-616.
11. Cismesia, M. A.; Yoon, T. P. *Chem. Sci.*, **2015**, *6*, 5426-5434.
12. Kropp, P. J., *Photobehavior of Alkyl Halides. CRC Handbook of organic photochemistry and photobiology*, 2nd ed.; **2004**, *1*, 1-32.
13. (a) Kropp, P. J., Adkins, R. L. *J. Am. Chem. Soc.* **1991**, *113*, 2709-2717. (b) Kropp, P. J., Poindexter, G.S., Pienta, N. J., Hamilton, D. C. *J. Am. Chem. Soc.* **1976**, *98*, 8135-8144.
14. Lautenberger, W. J., Jones, E. N., Miller, J. G. *J. Am. Chem. Soc.* **1968**, *90*, 1110-1115.
15. Biaselle, C. J.; Miller, J. G. *J. Am. Chem. Soc.* **1974**, *96*, 3813-3816.
16. (a) Ismaili, H., Pitre, S. P., Scaiano, J. C. *Catal. Sci. Technol.* **2013**, *3*, 935-937. (b) Lanterna, A. E., Elhage, A., Scaiano, J. C. *Catal. Sci. Technol.* **2015**, *5*, 4336-4340.

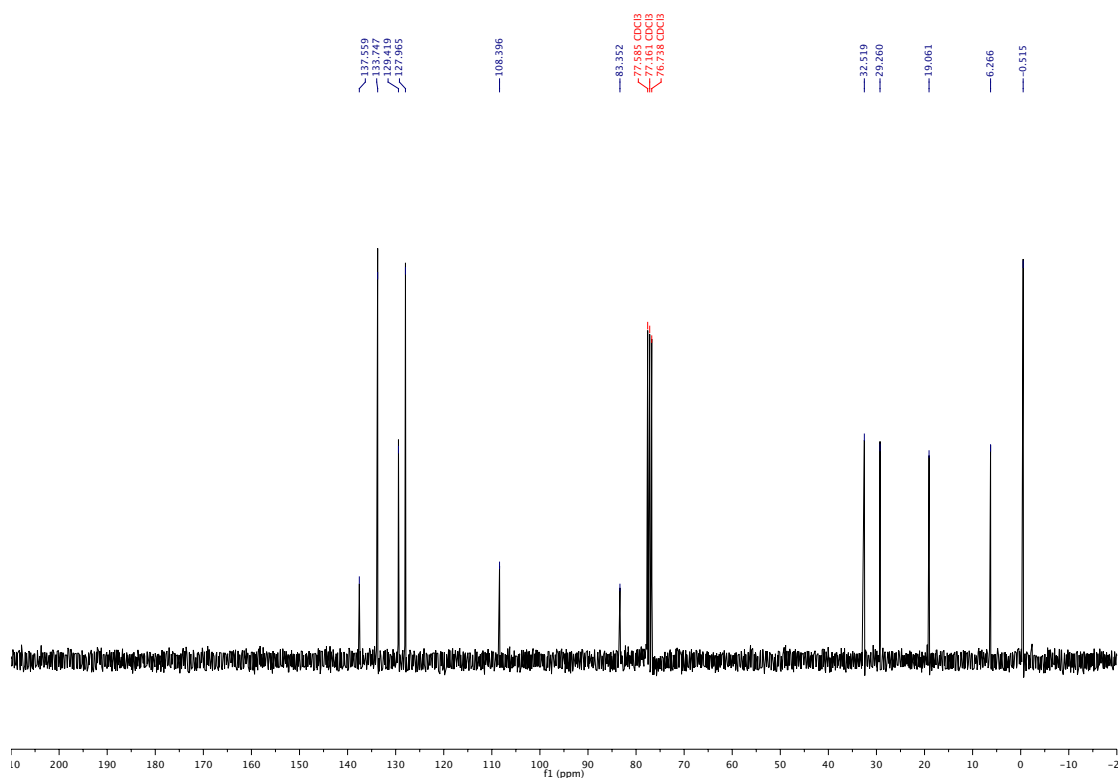
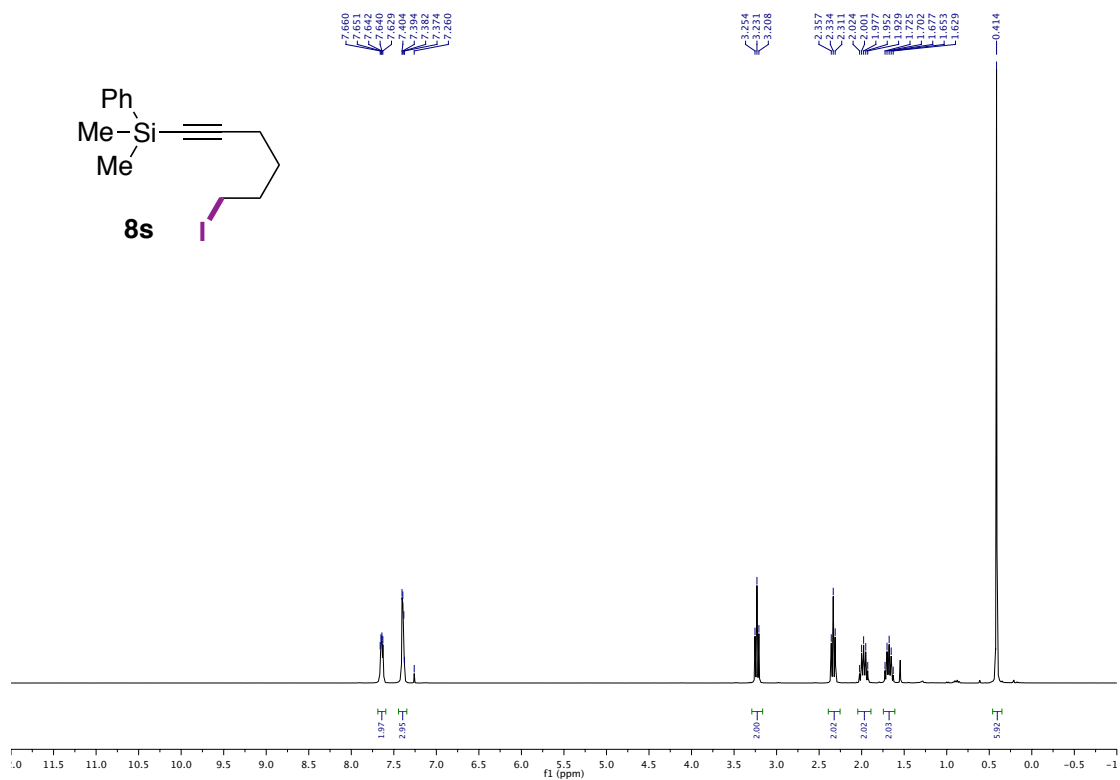
## 2.8.9. $^1\text{H}$ and $^{13}\text{C}$ NMR Spectra

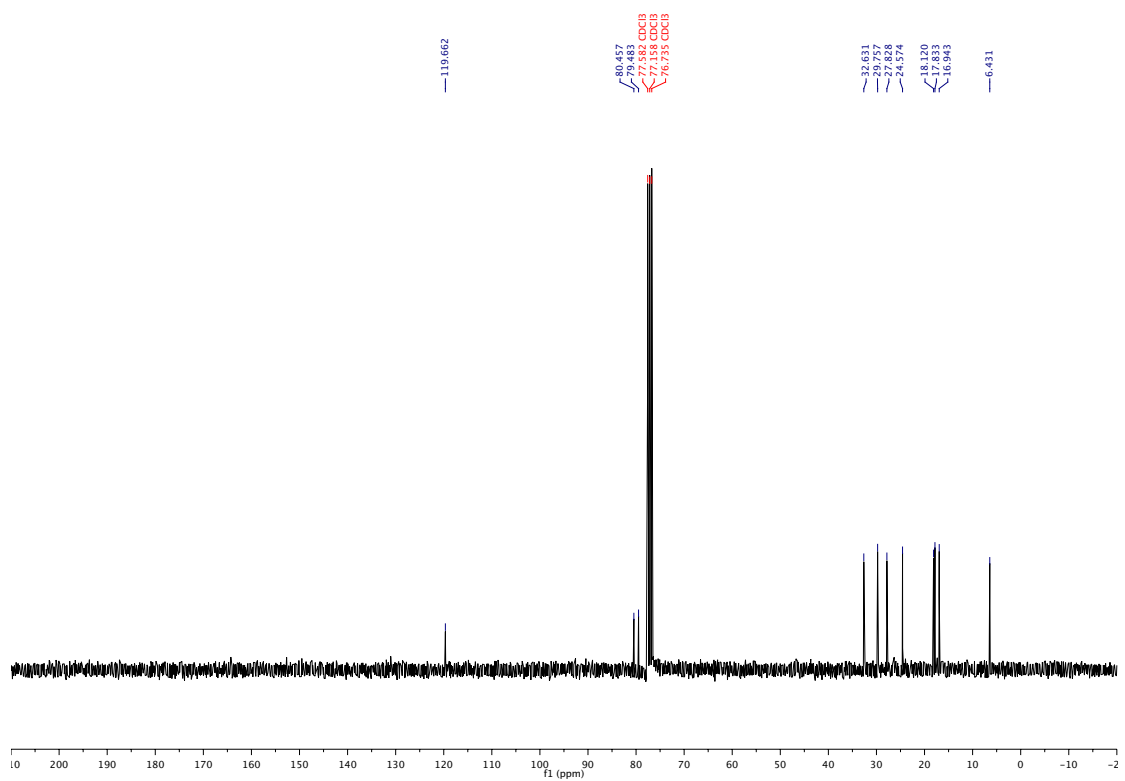
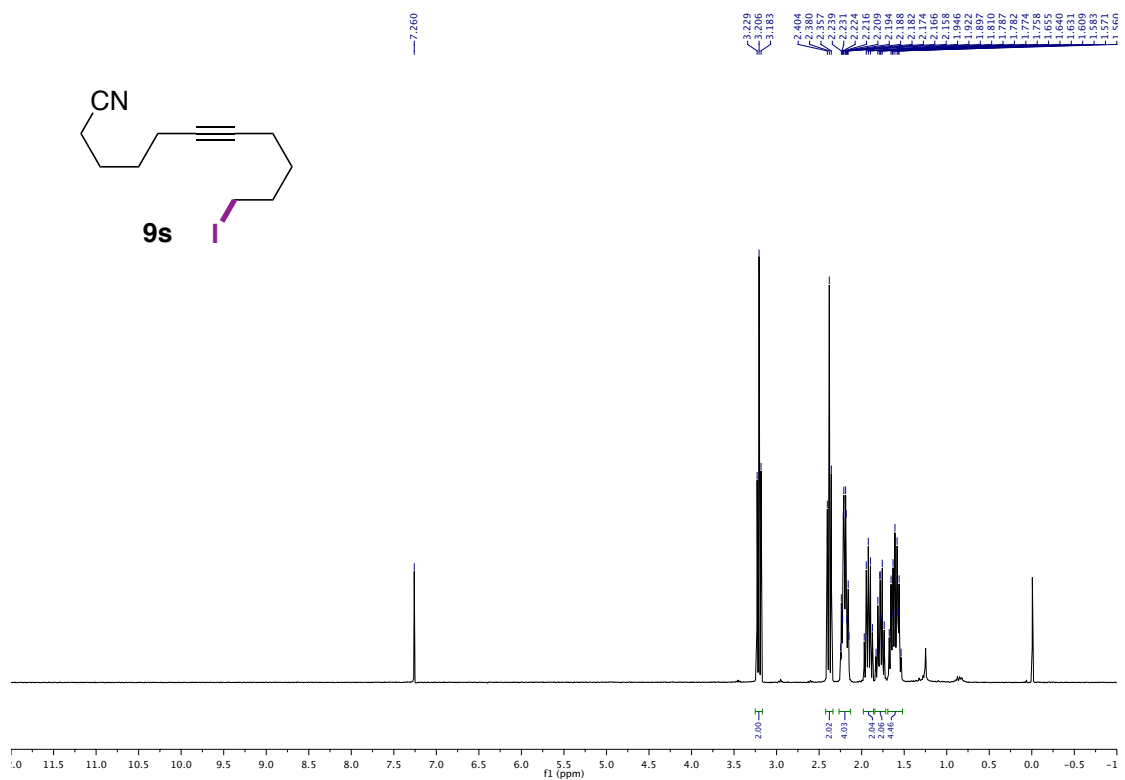




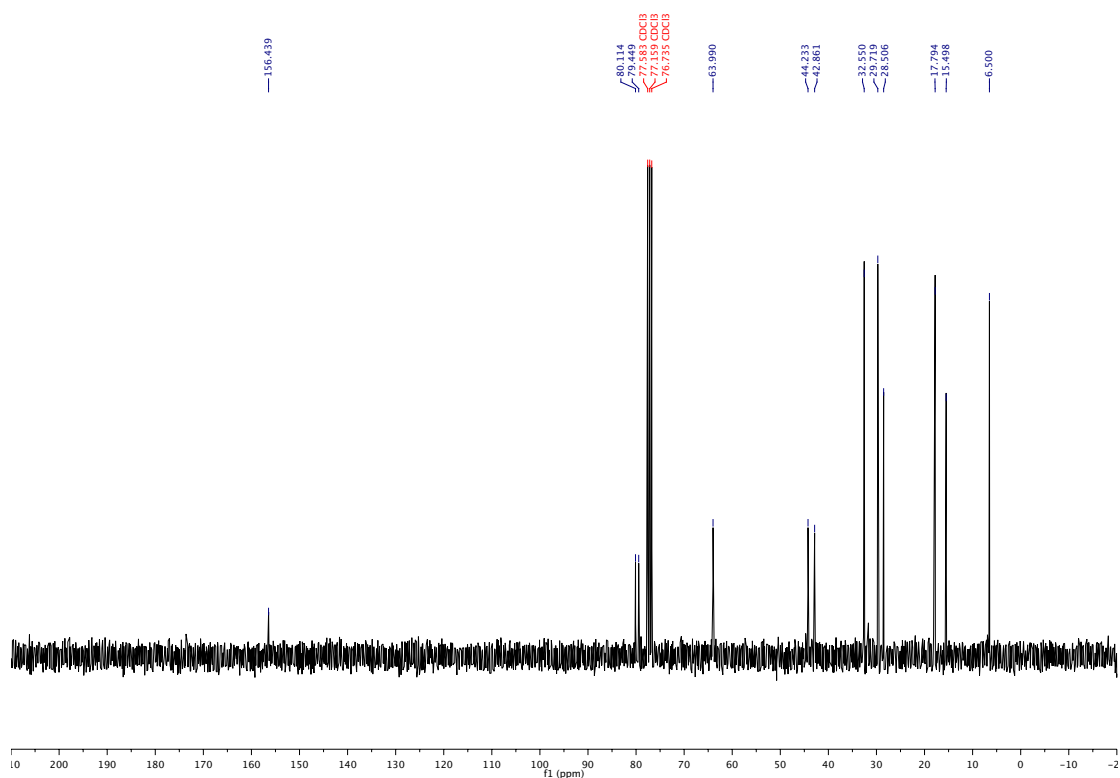
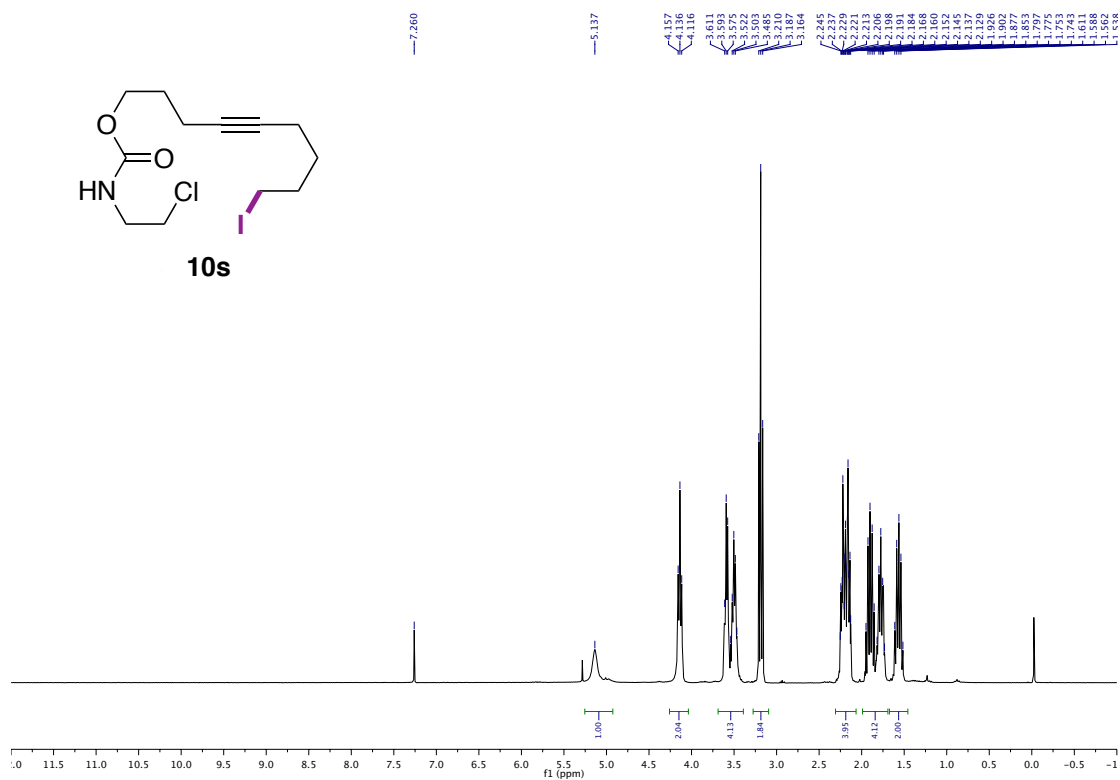


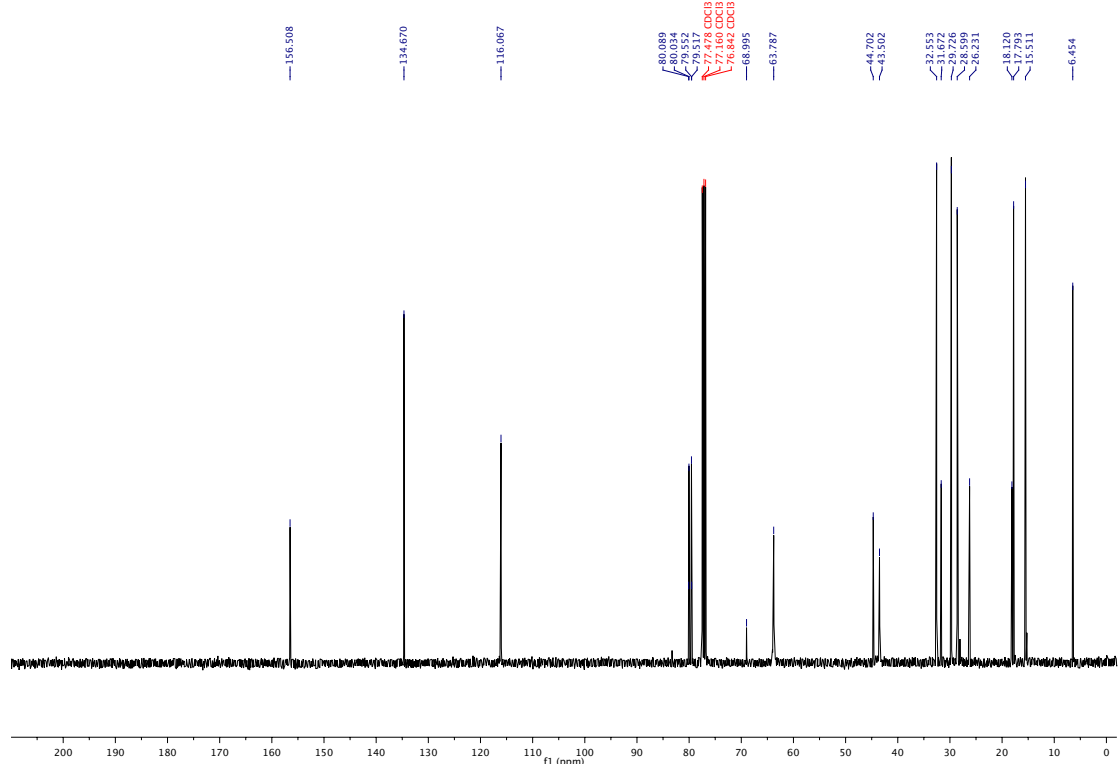
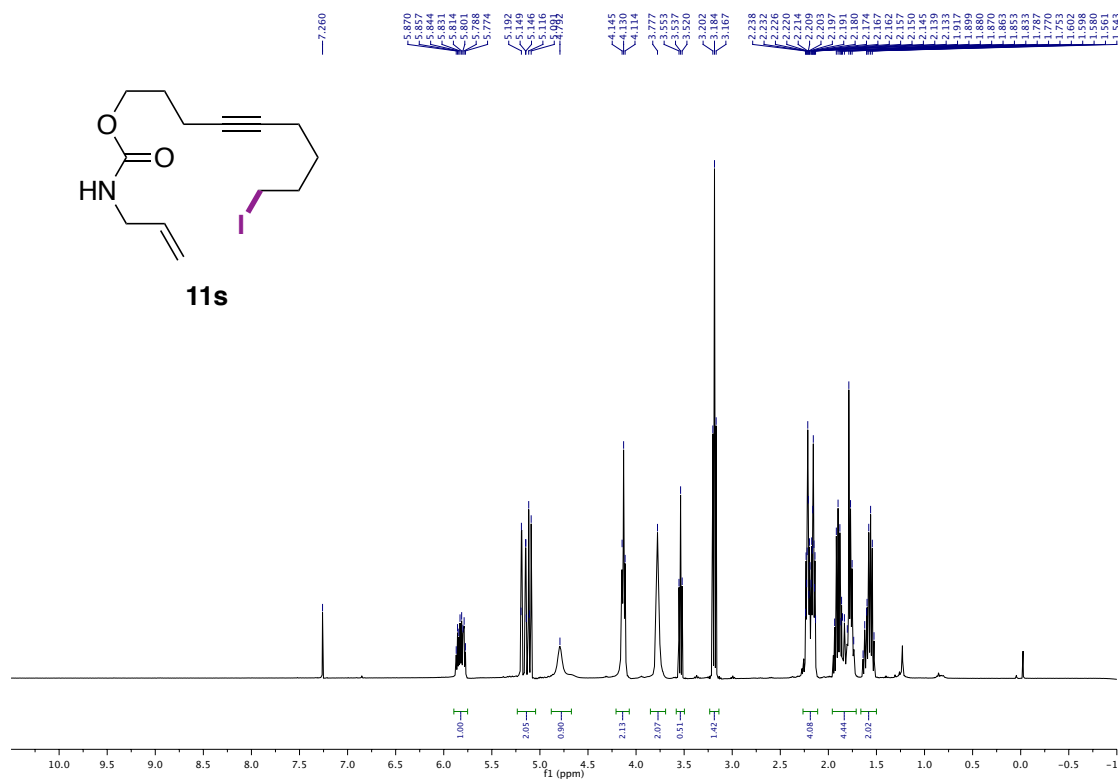


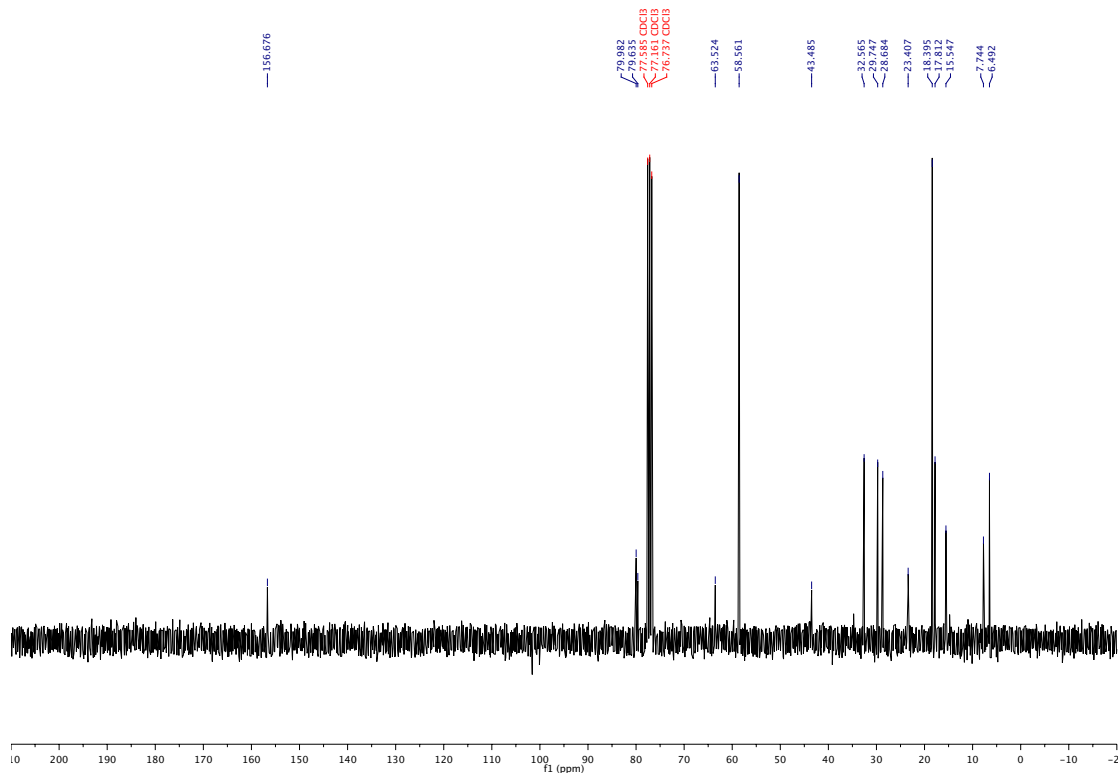
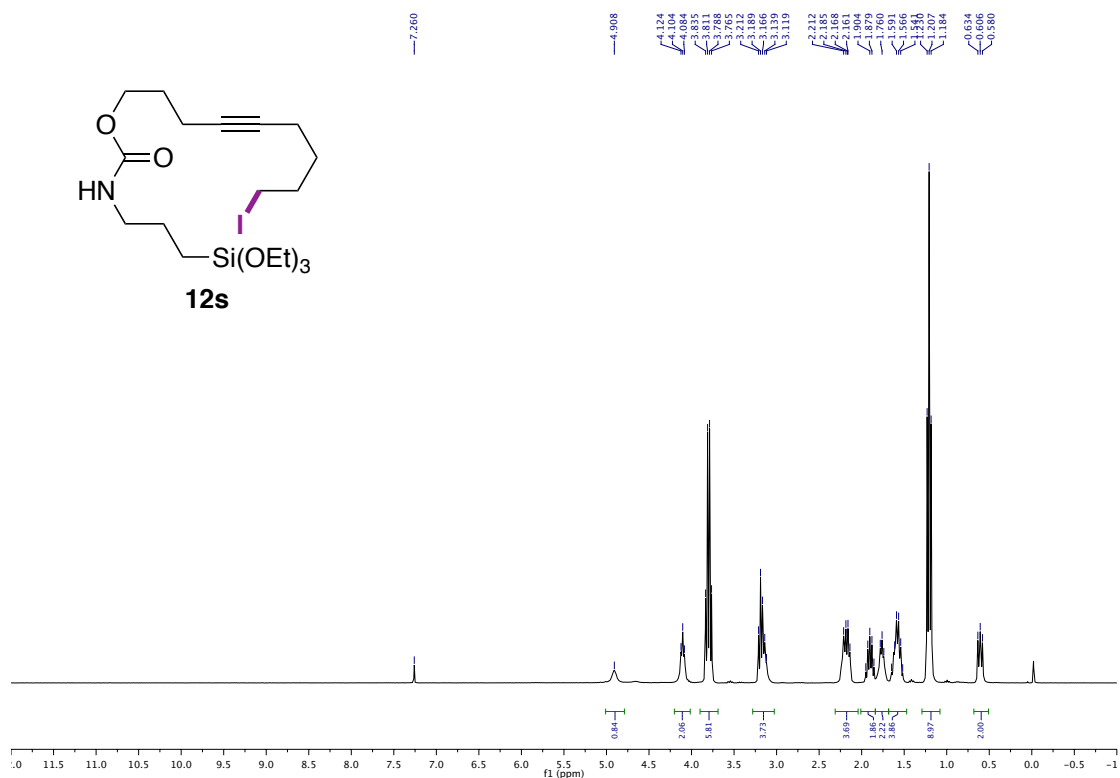


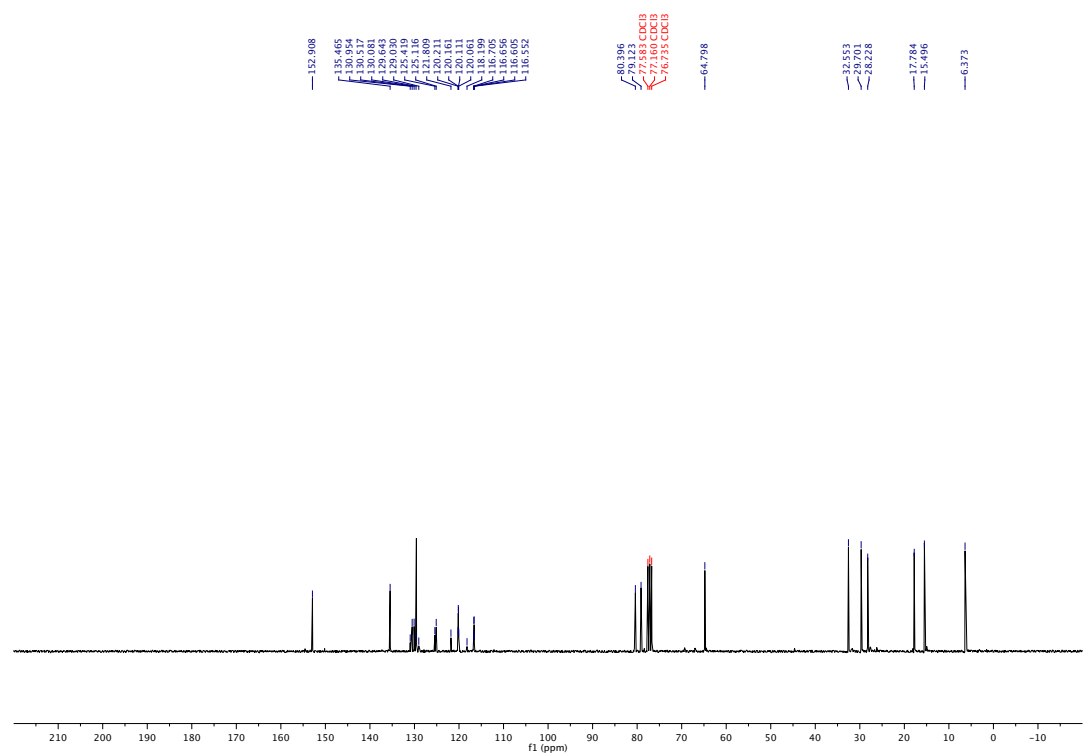
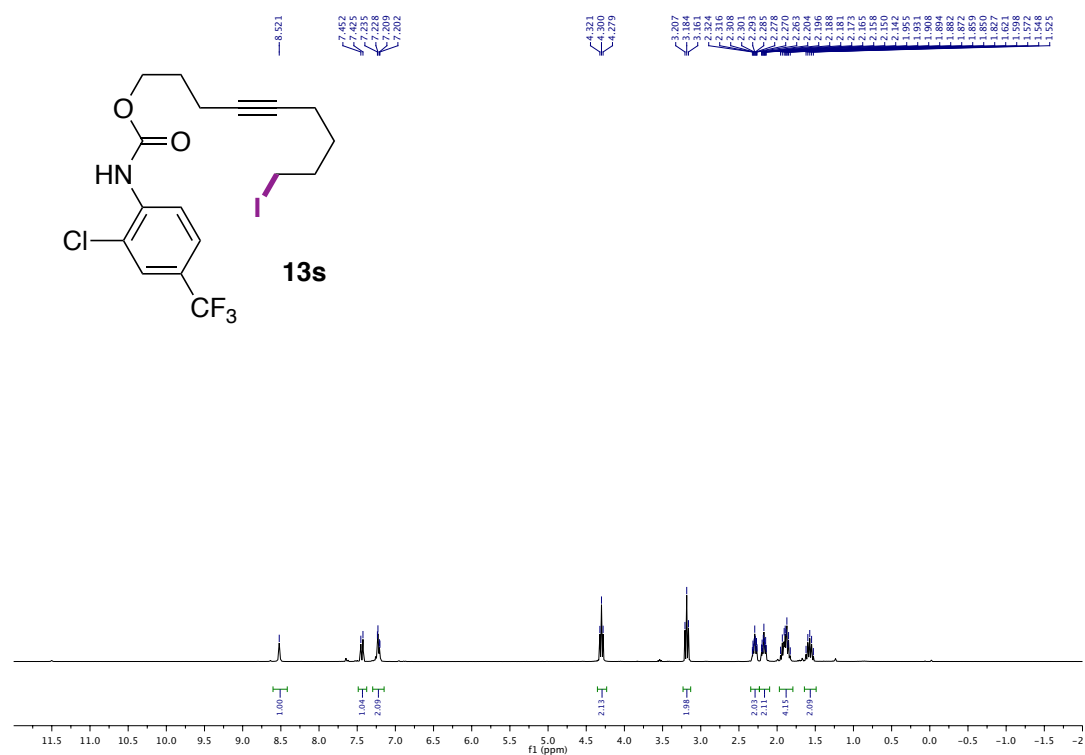


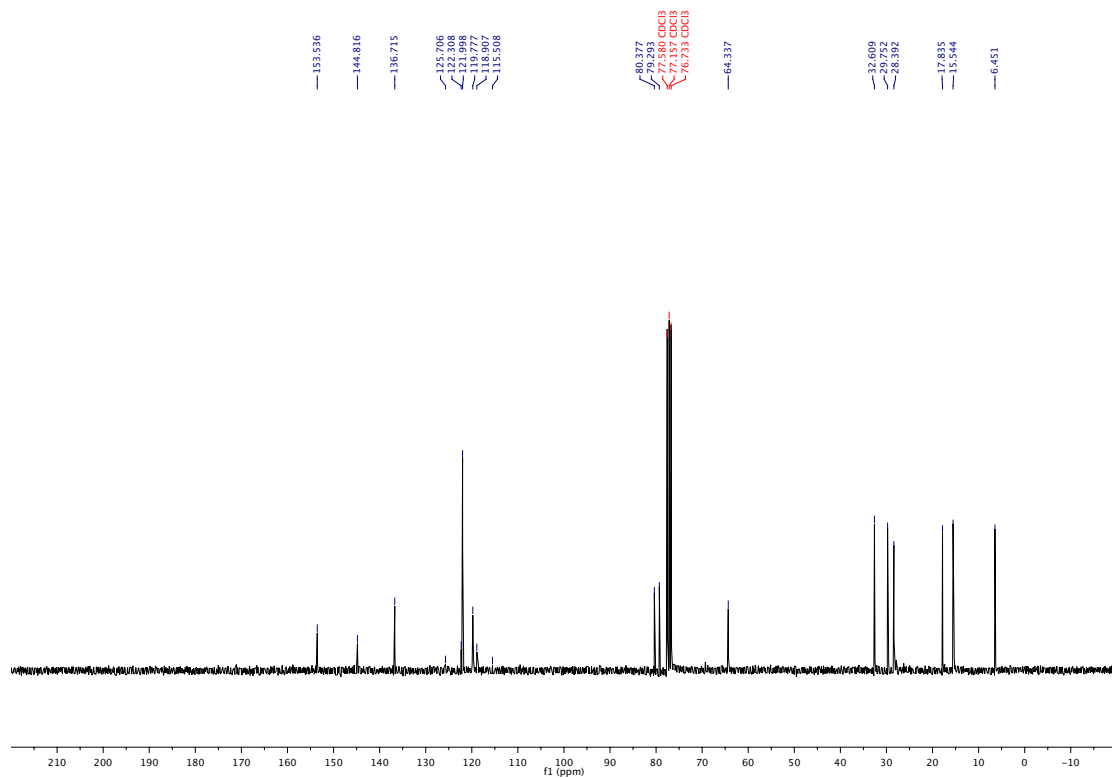
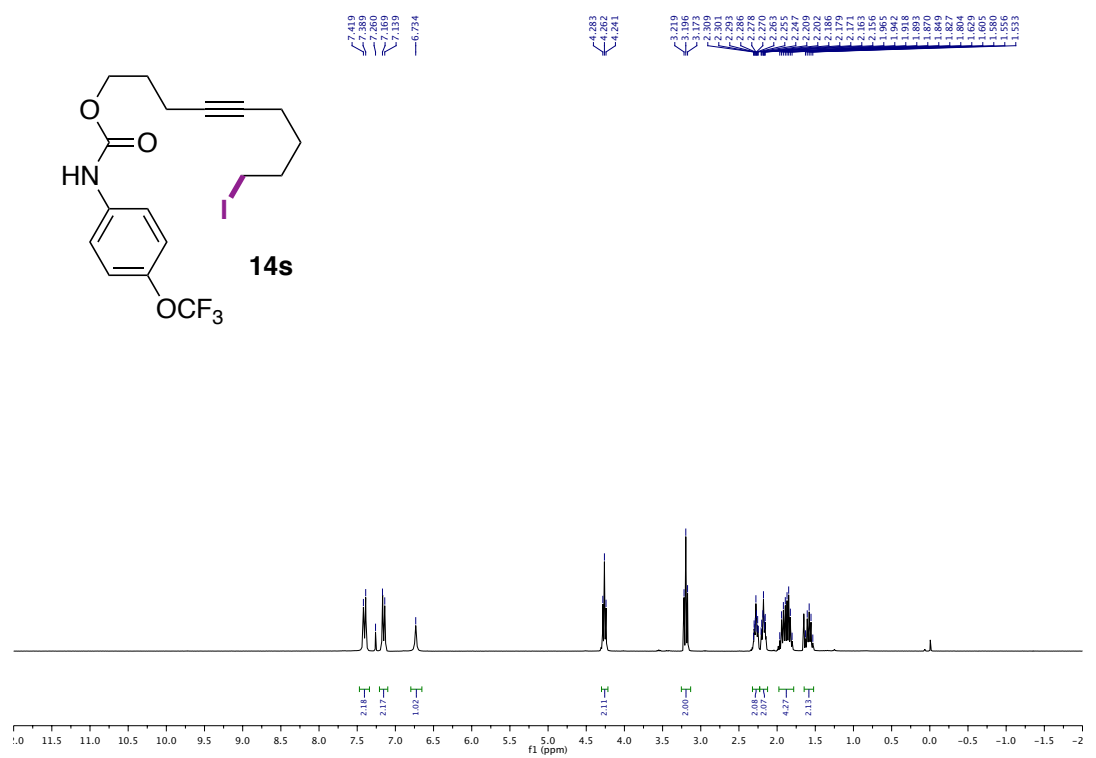


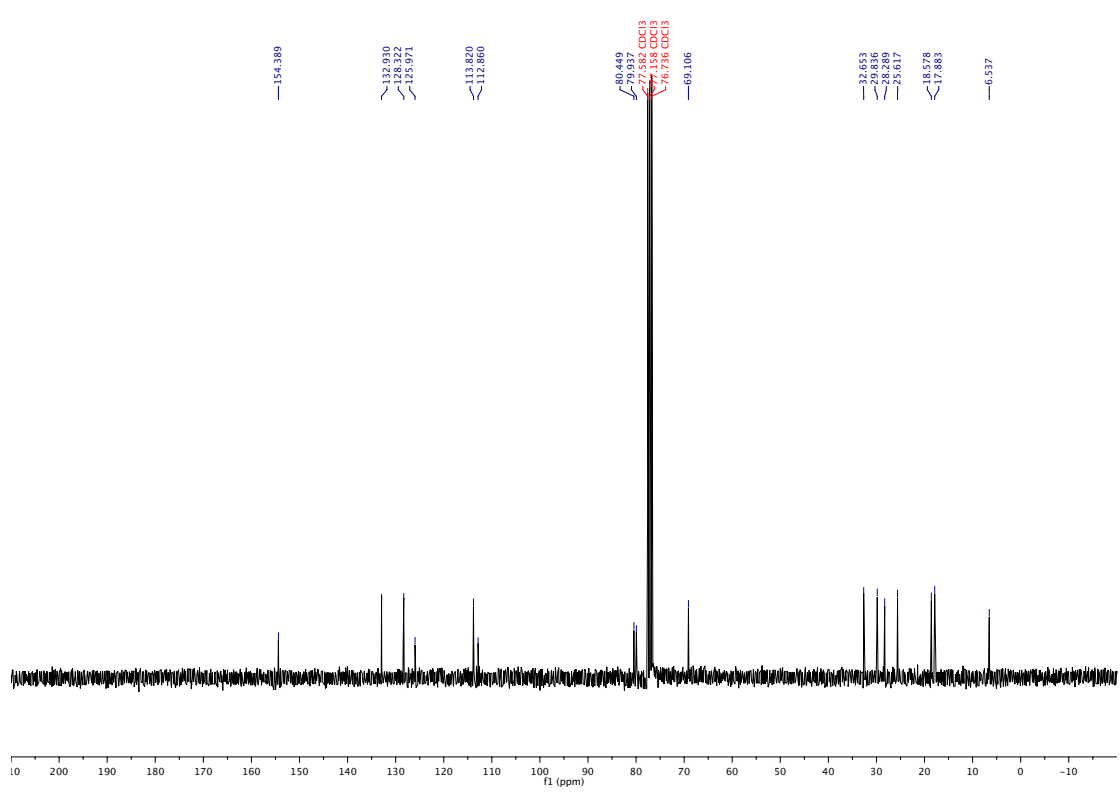
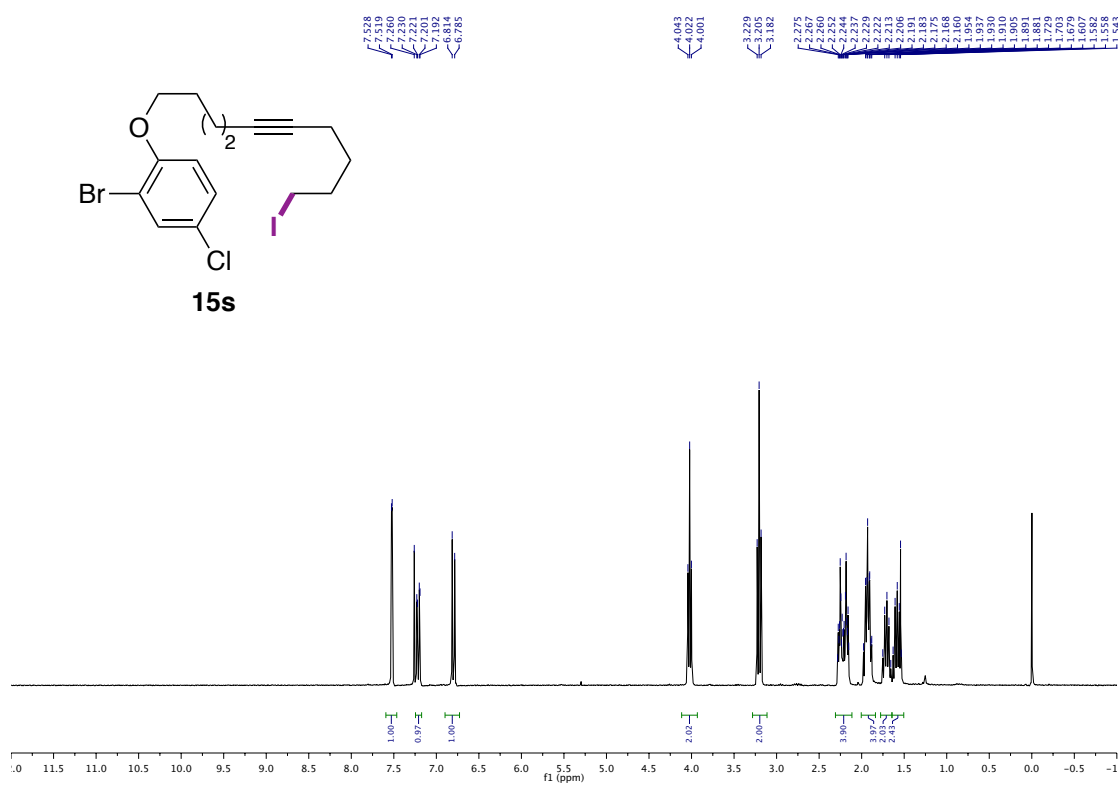


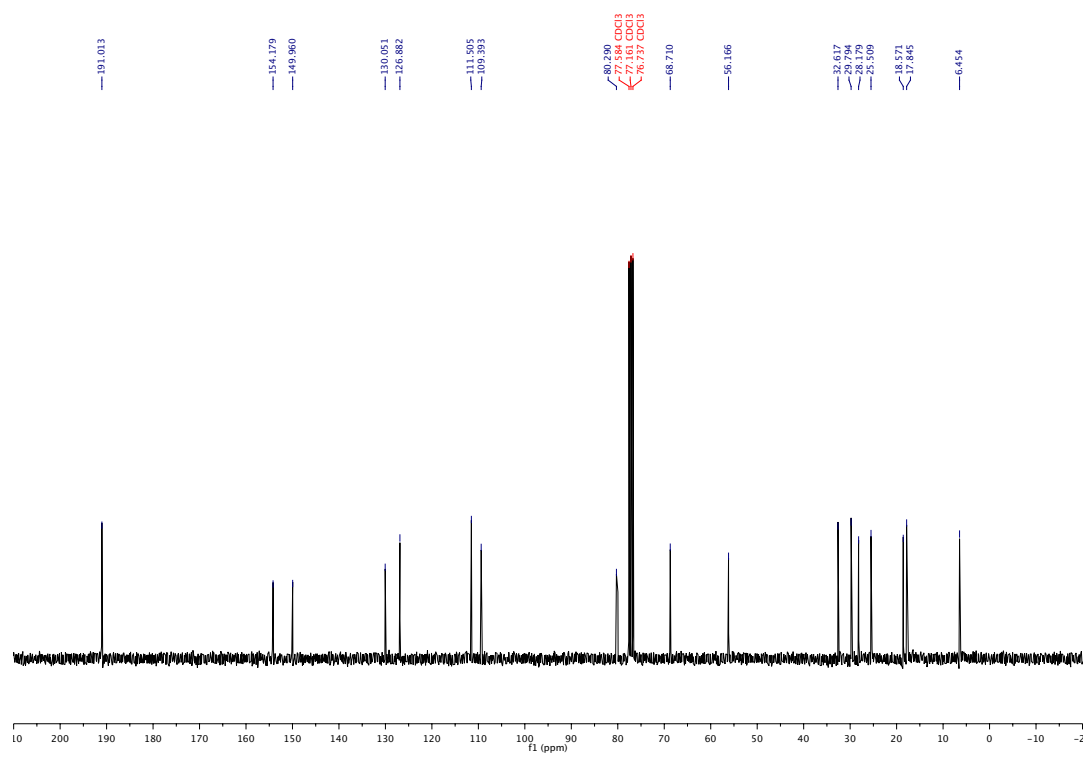
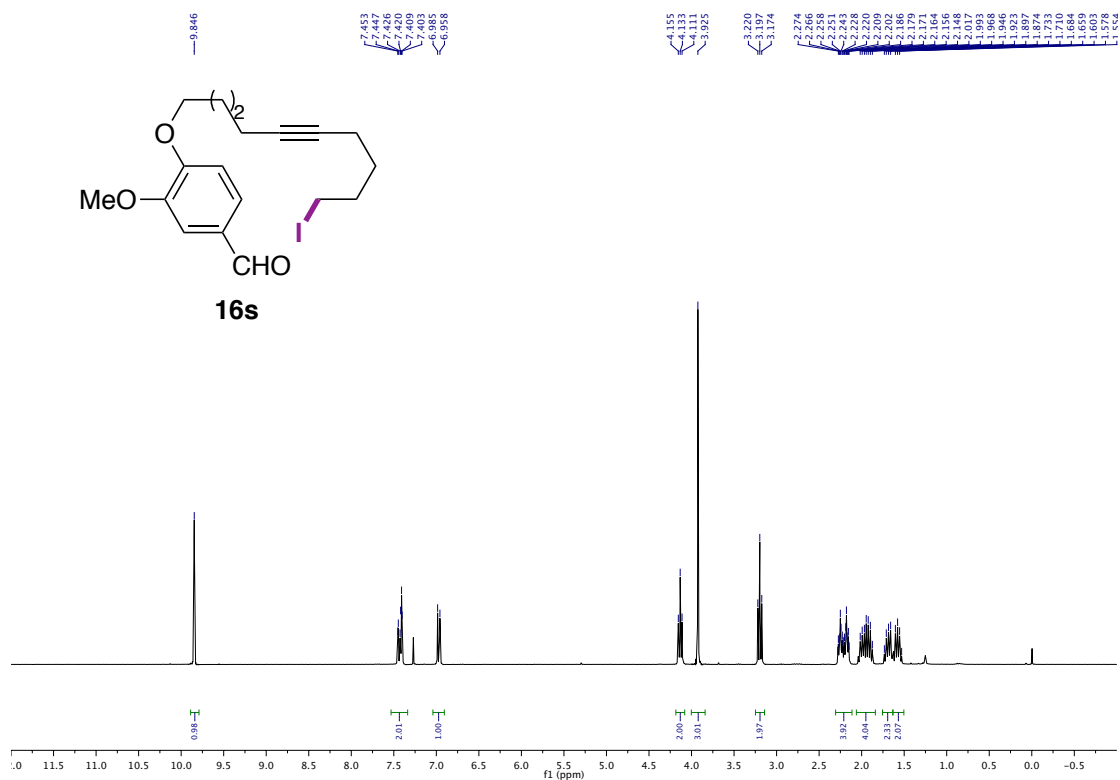


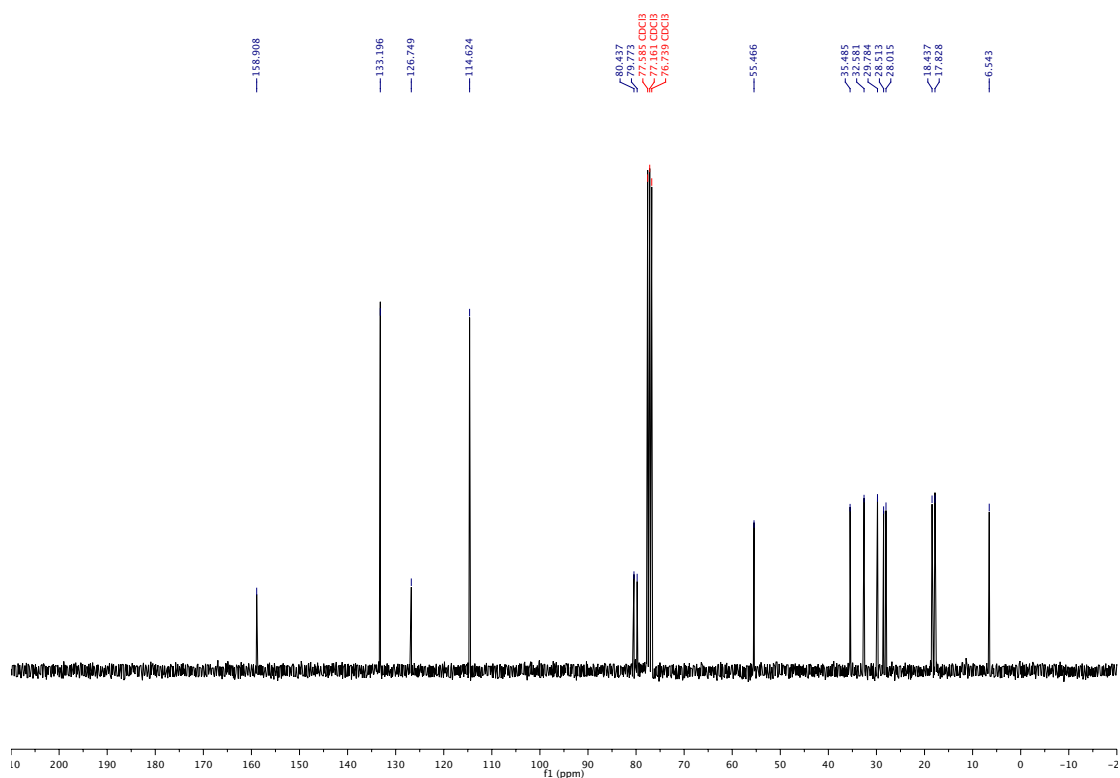
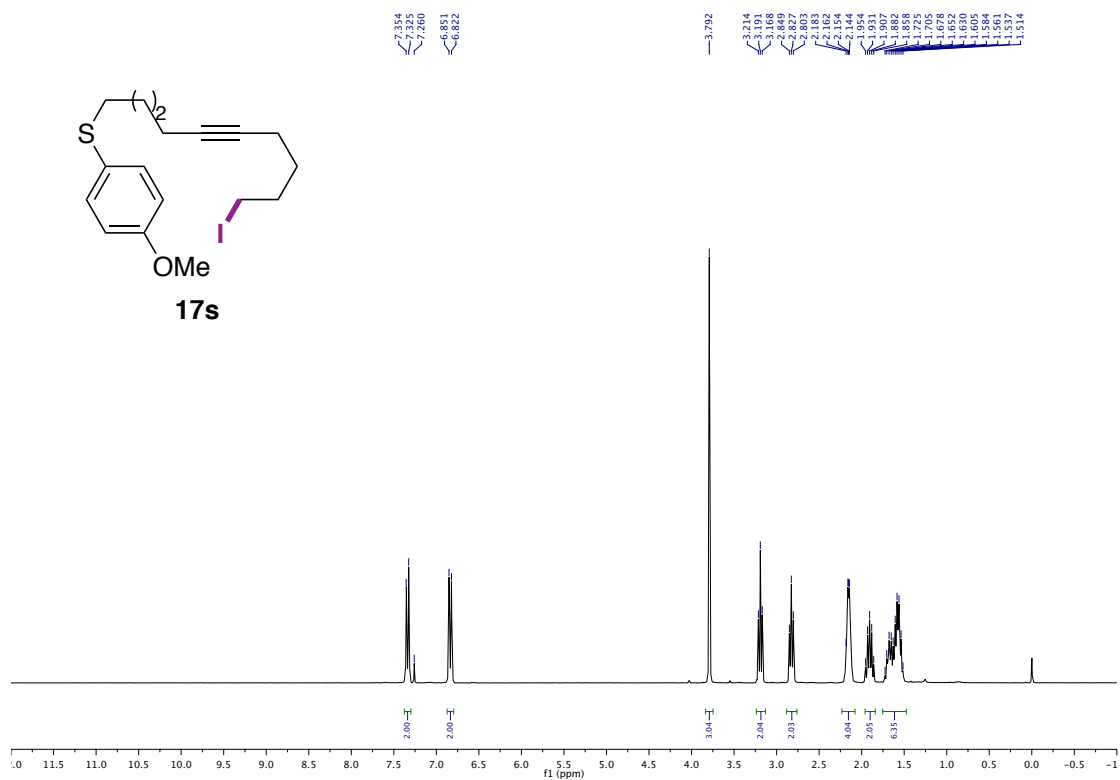




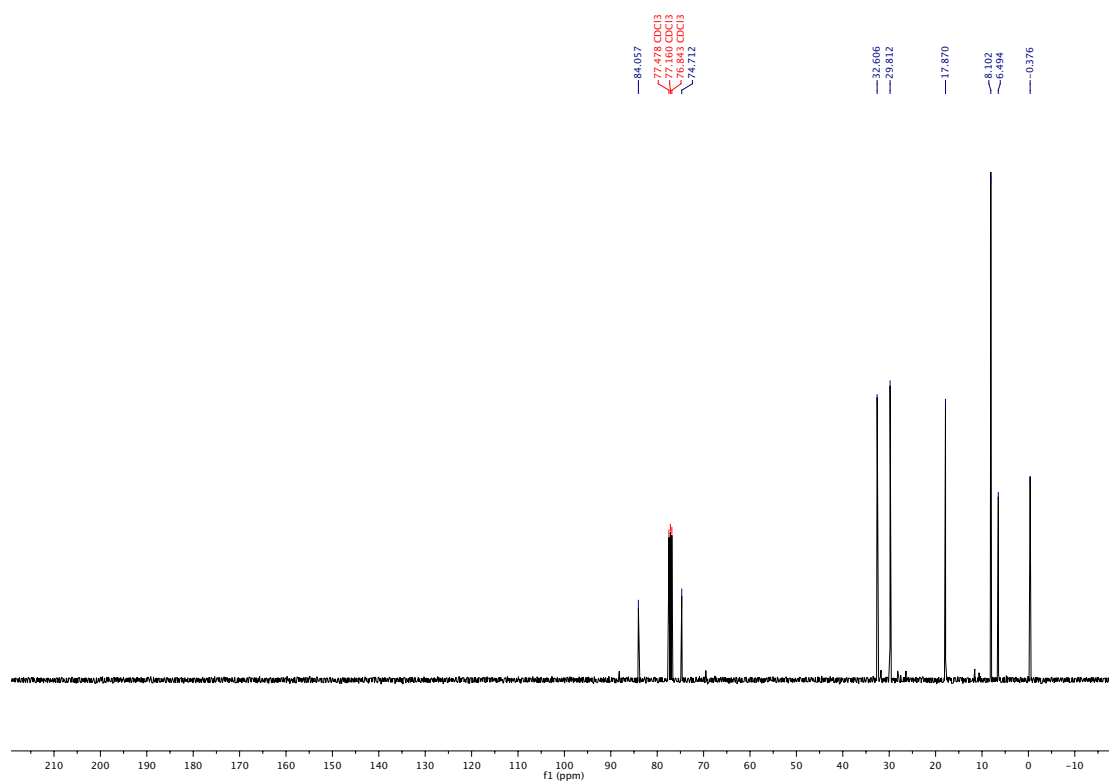
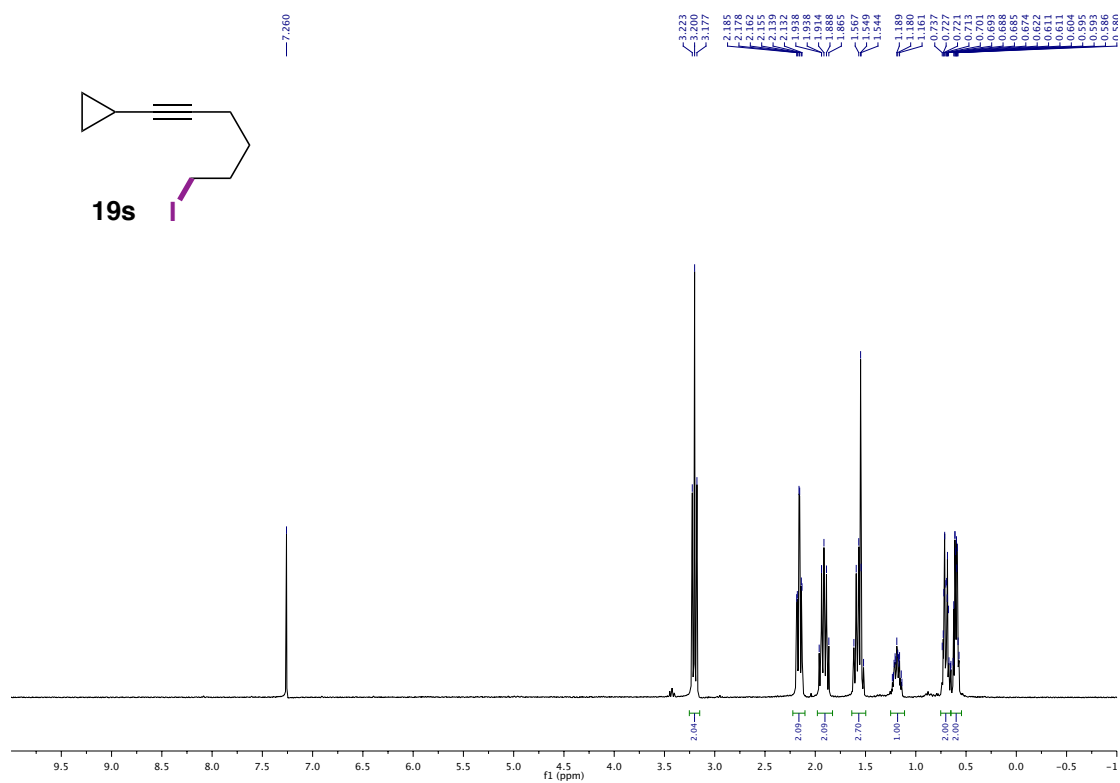


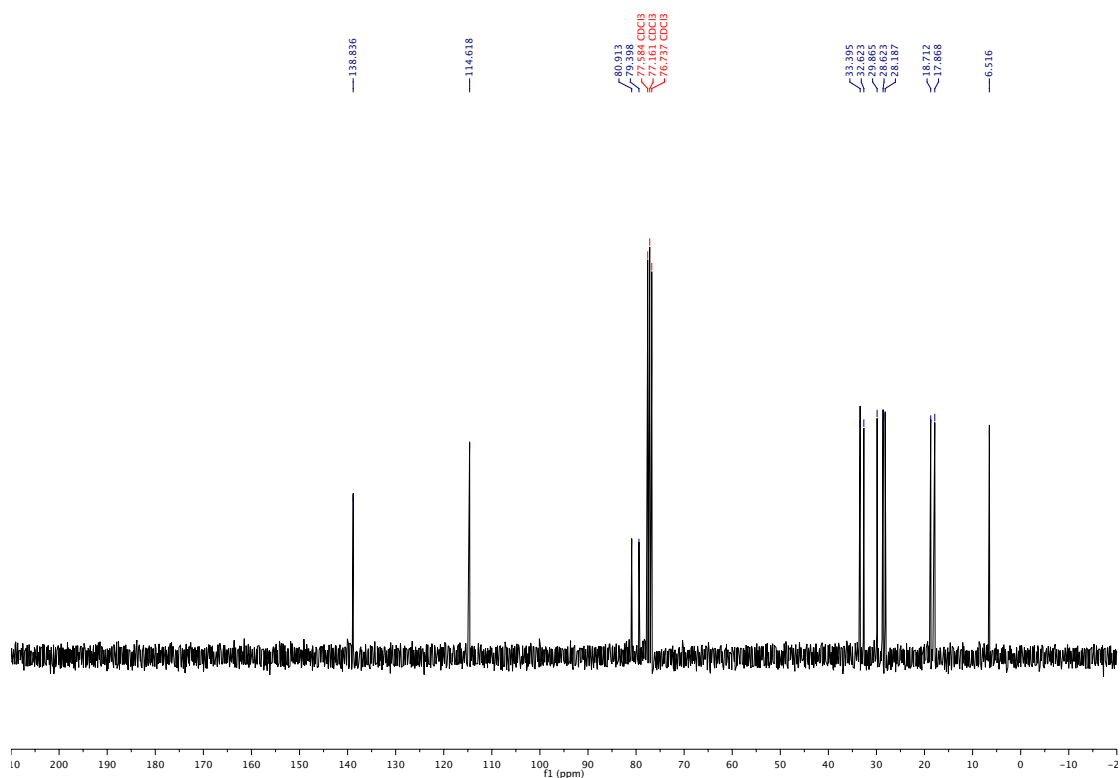
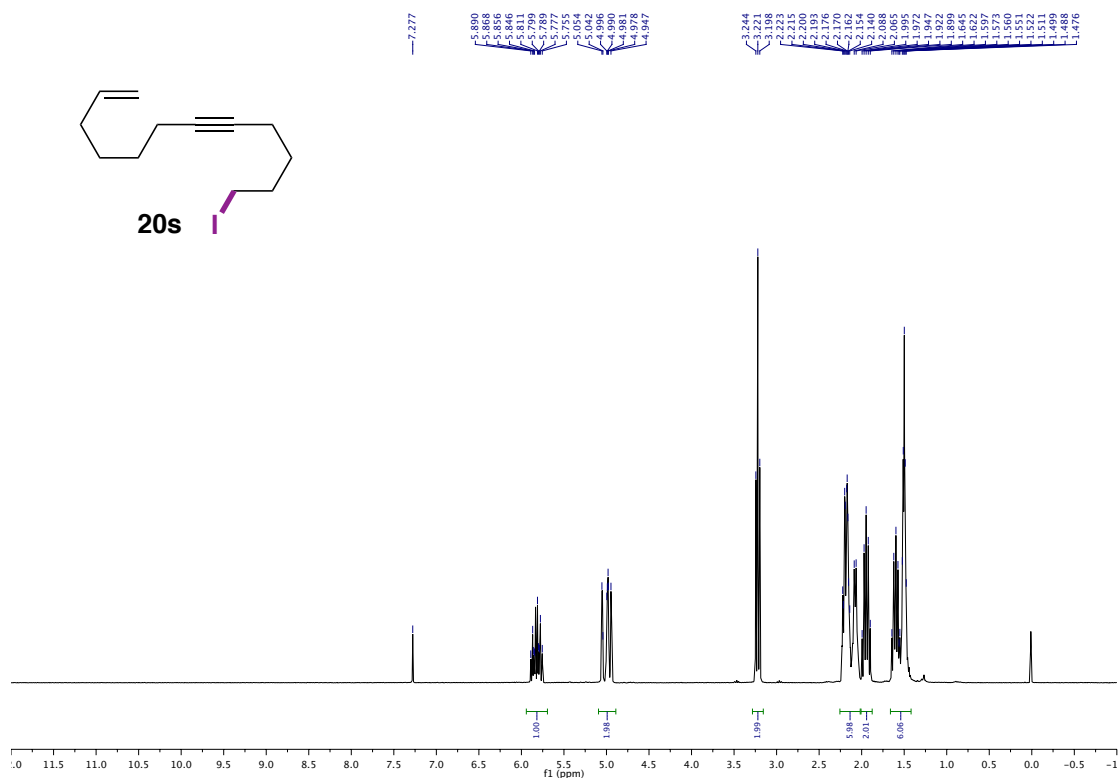


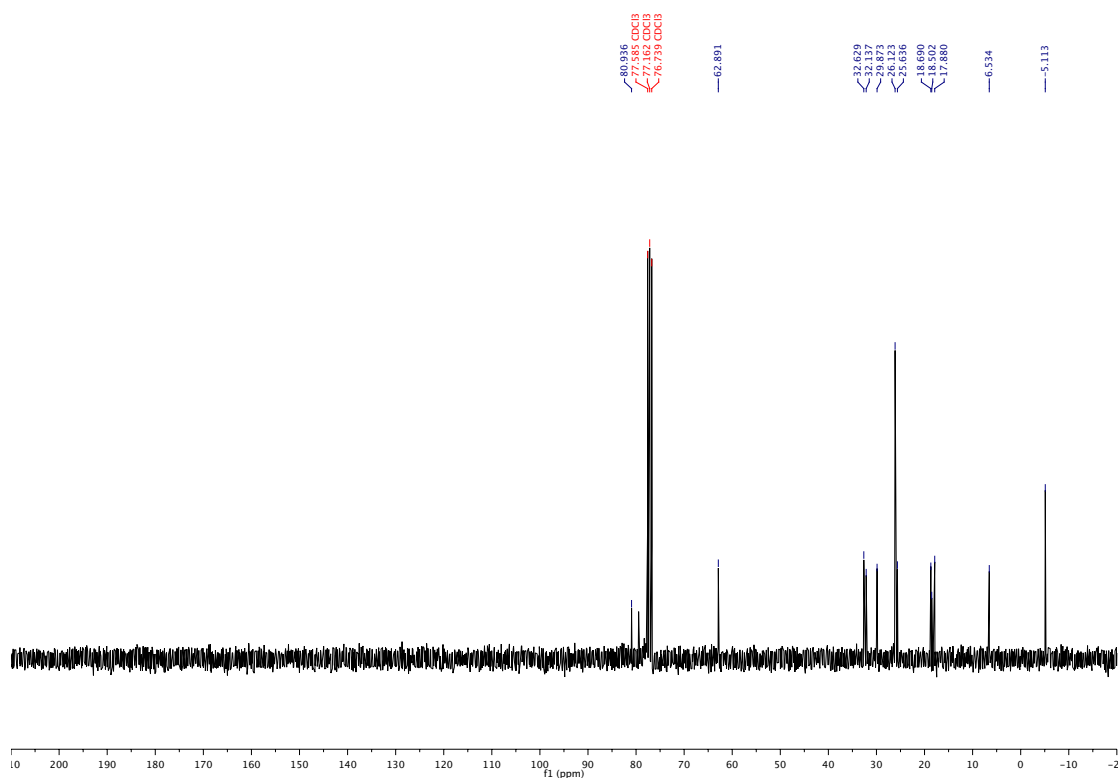
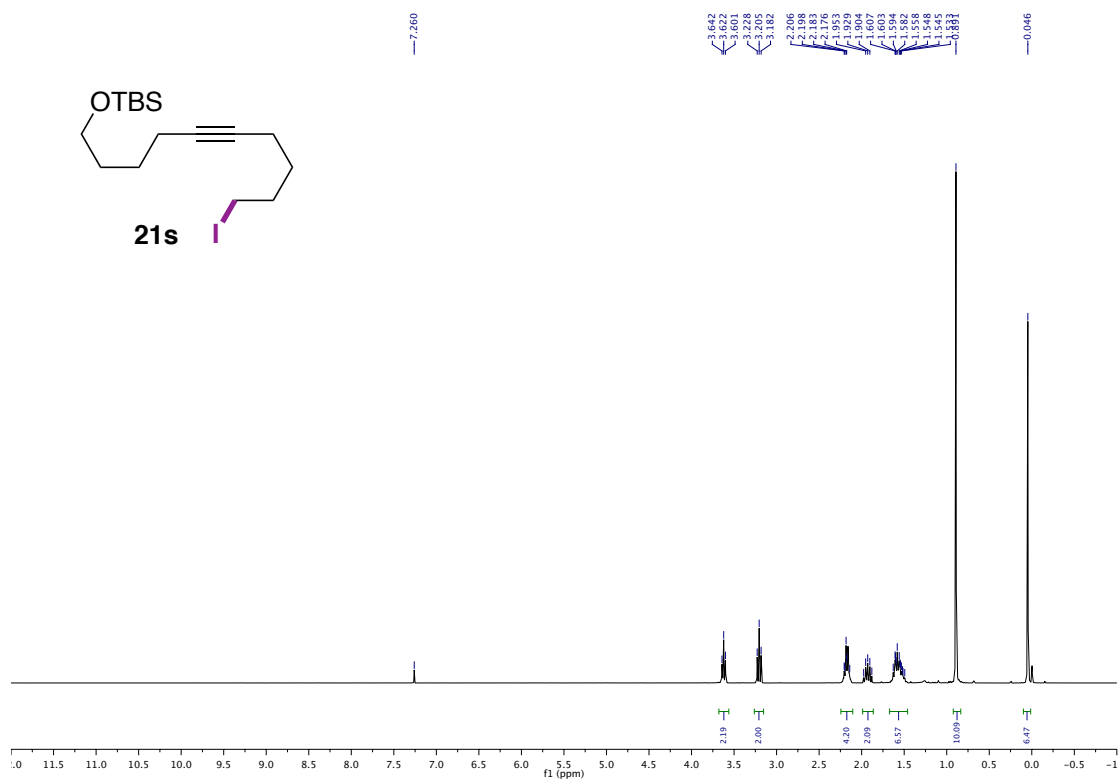


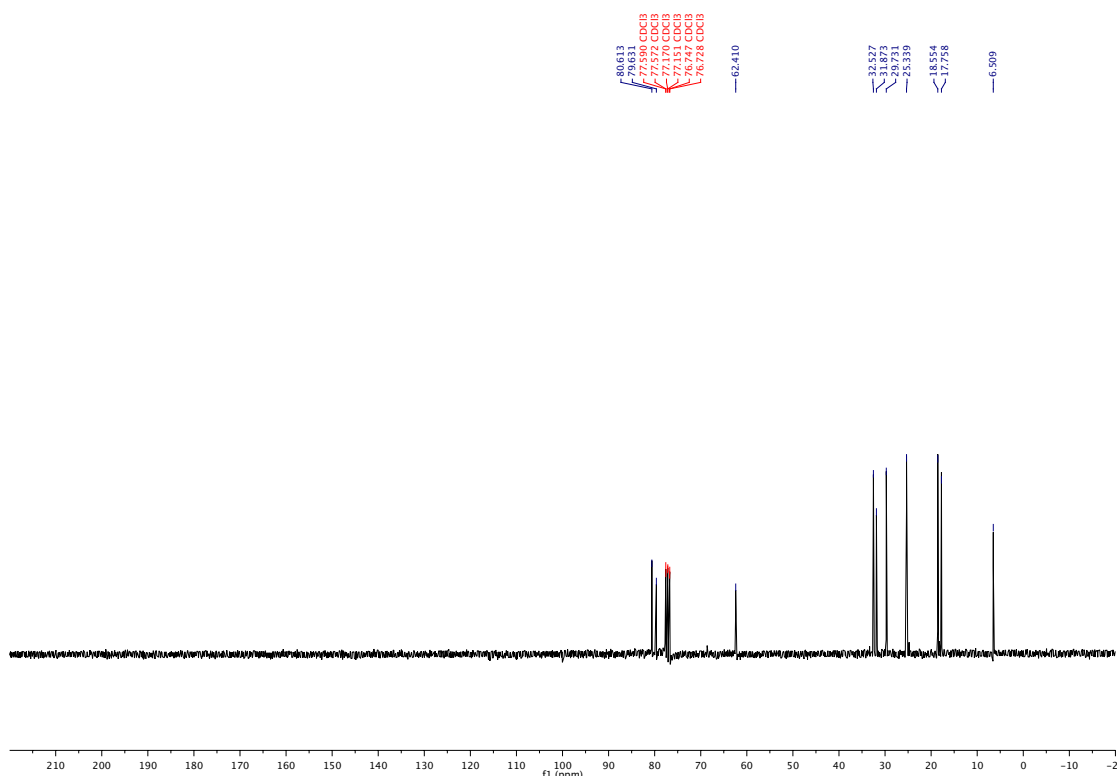
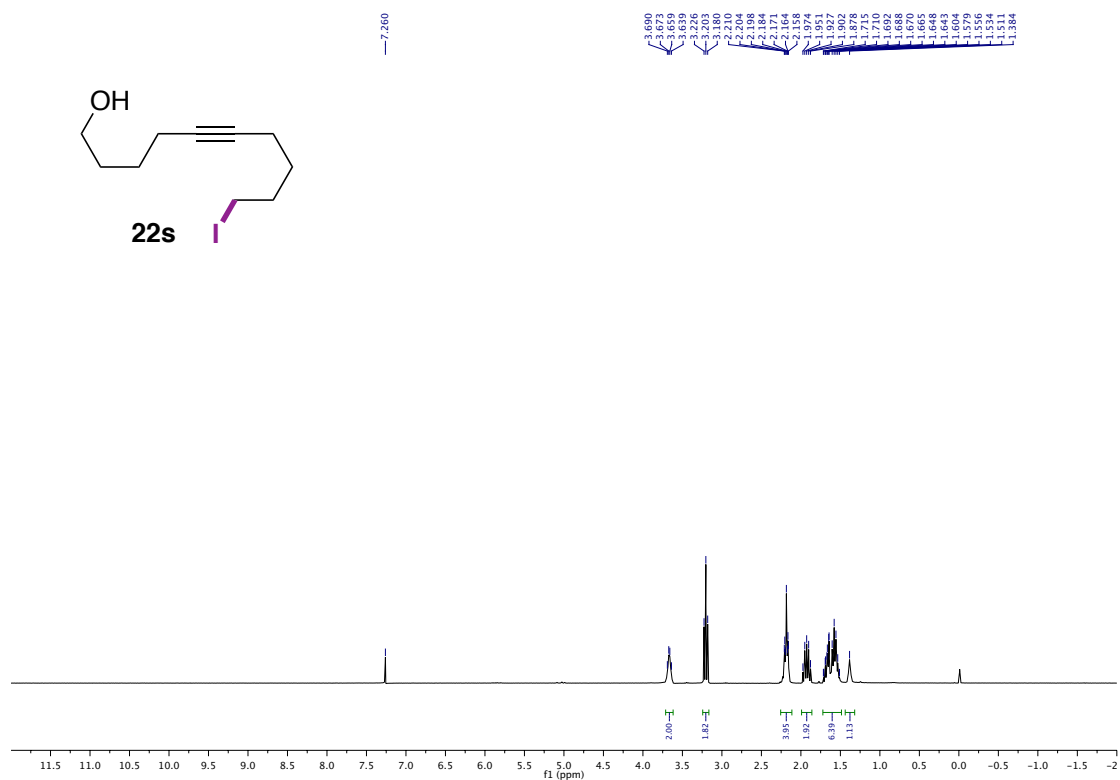


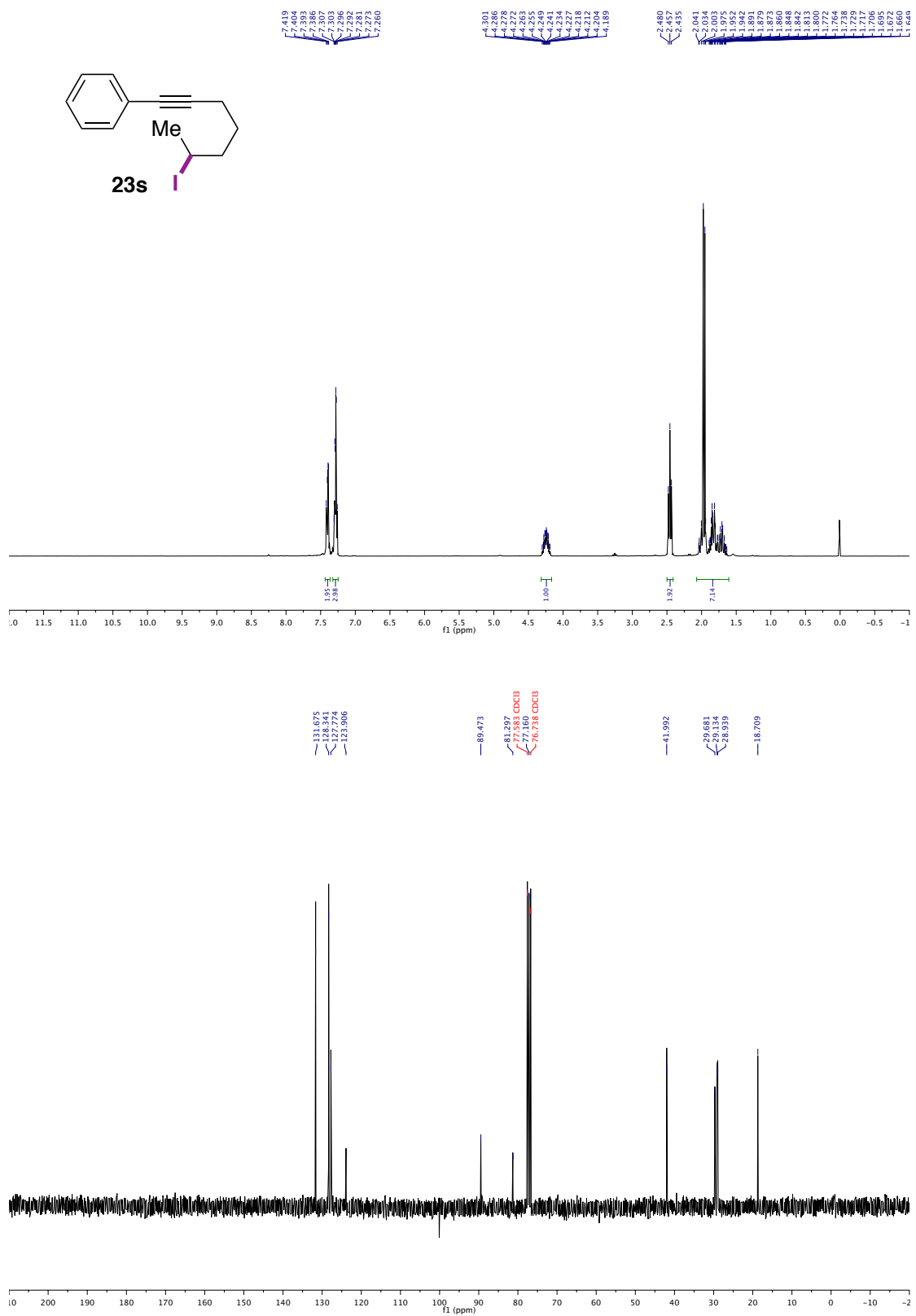


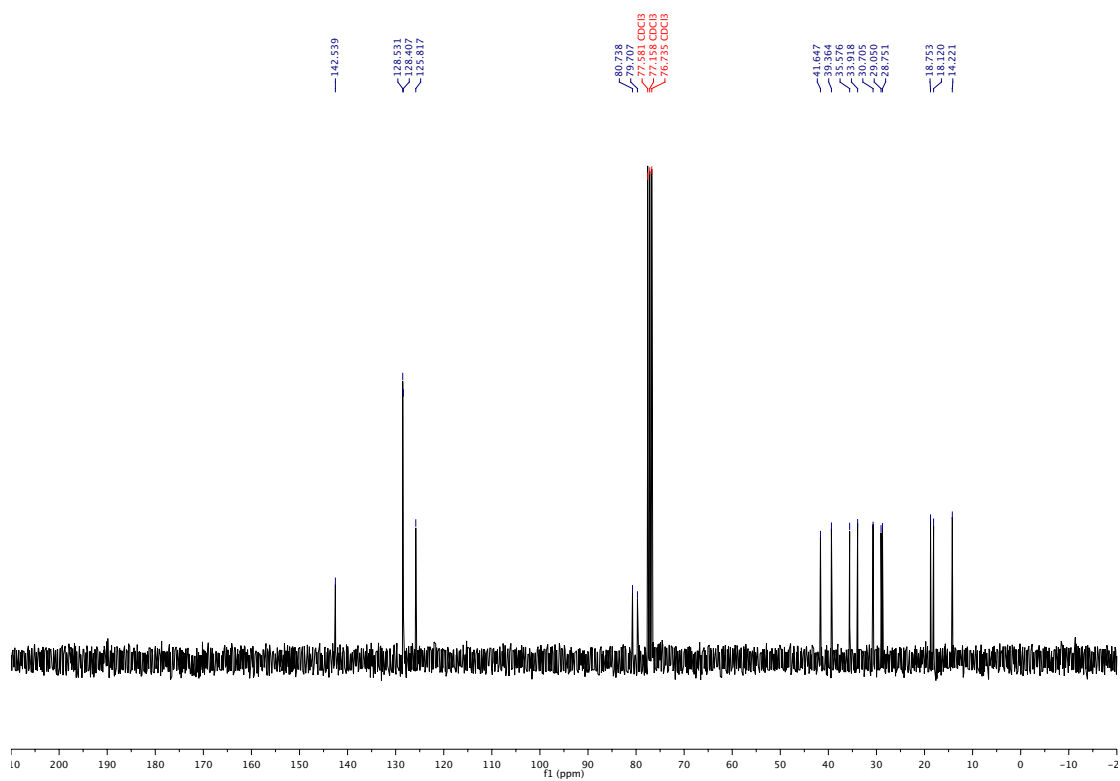
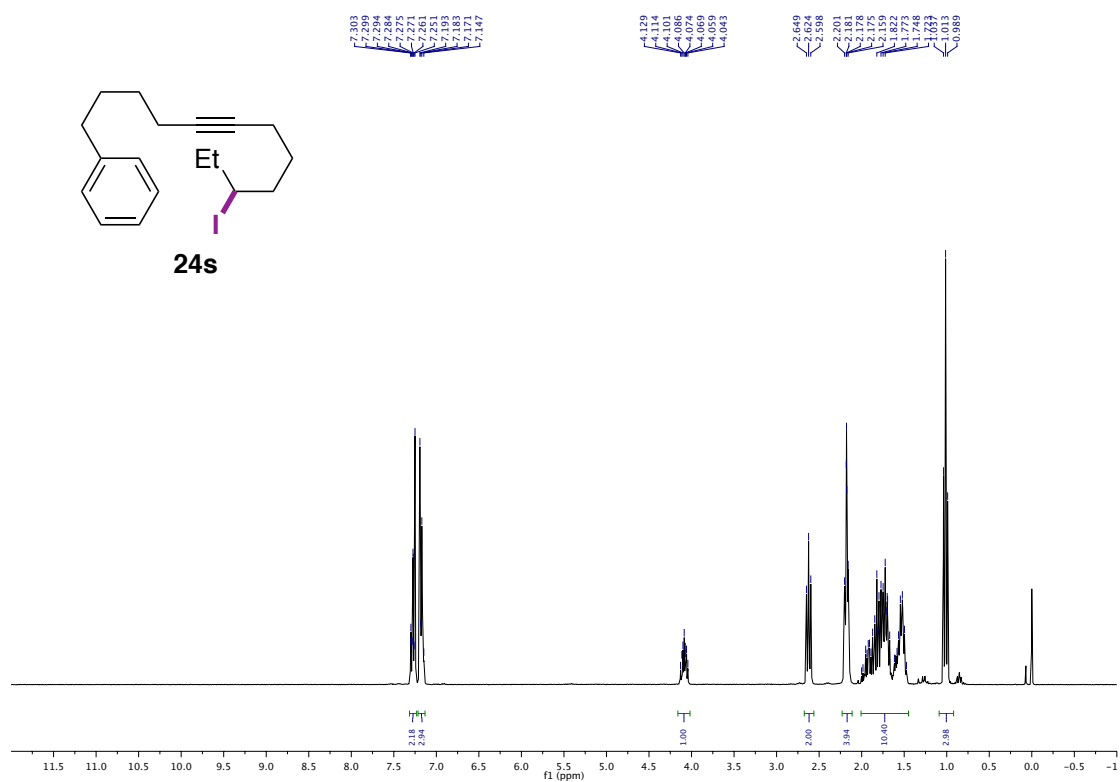


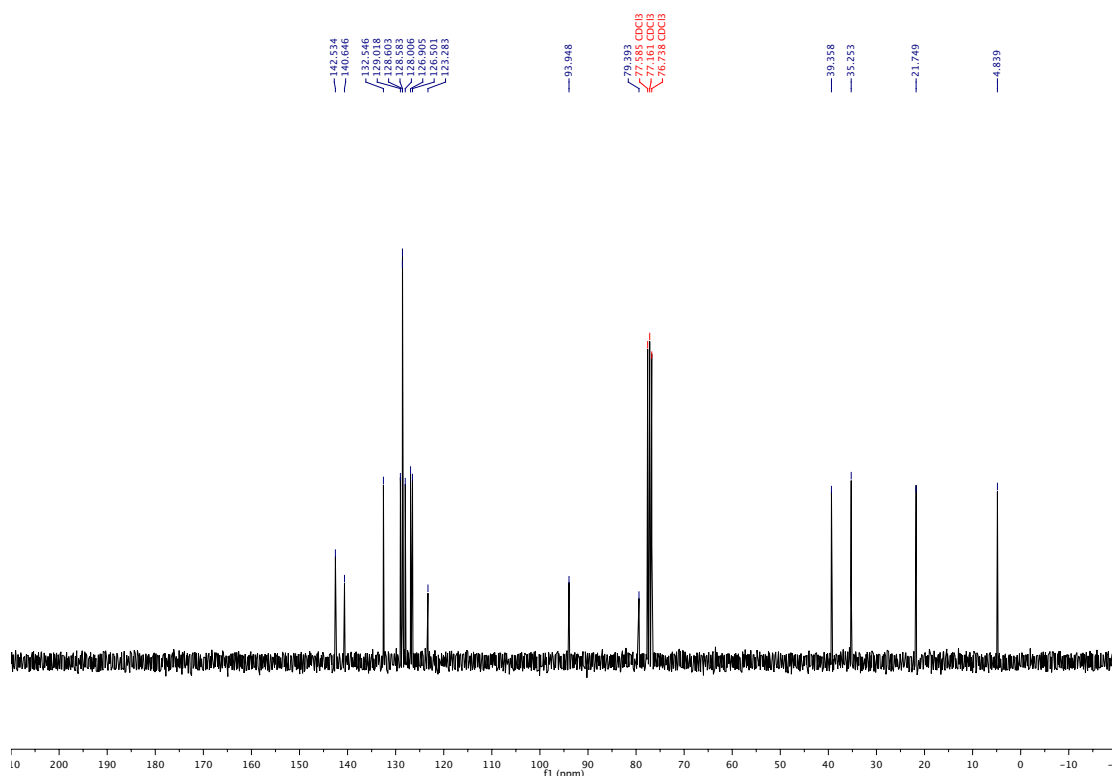
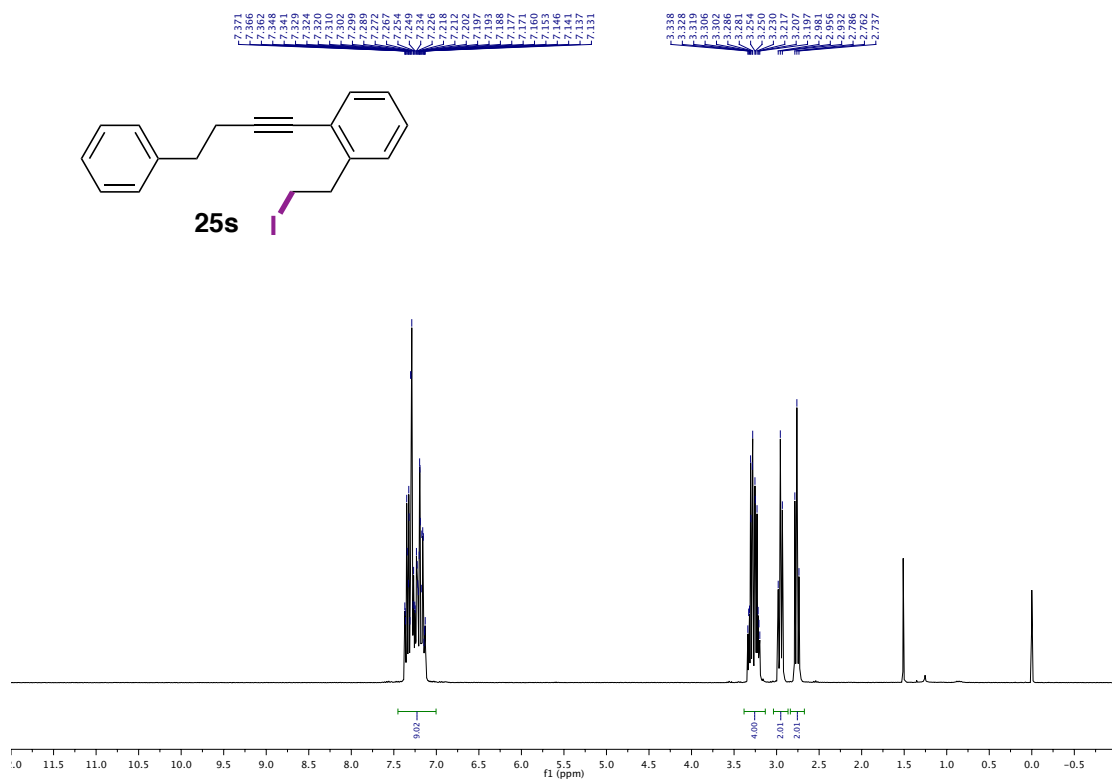


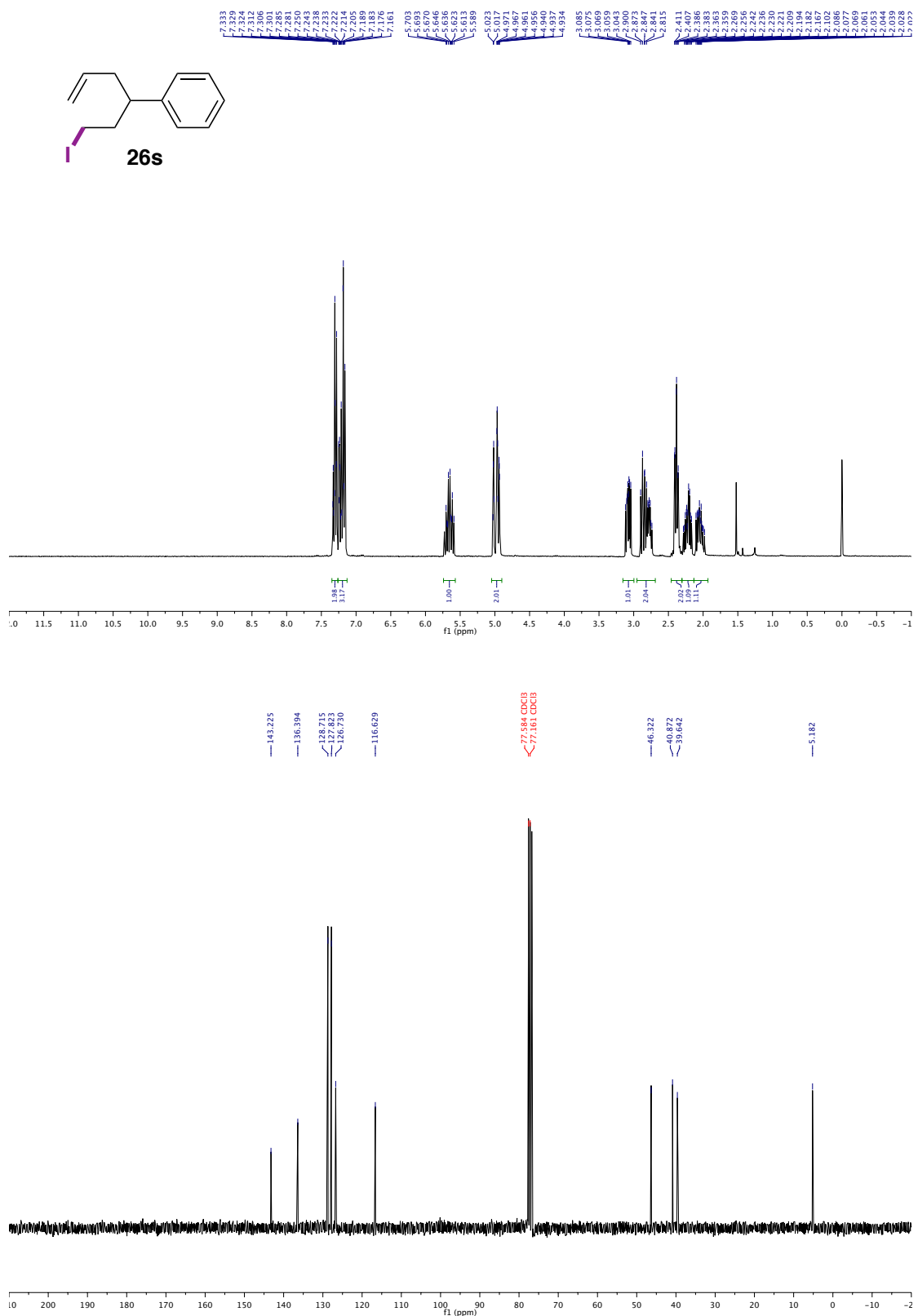




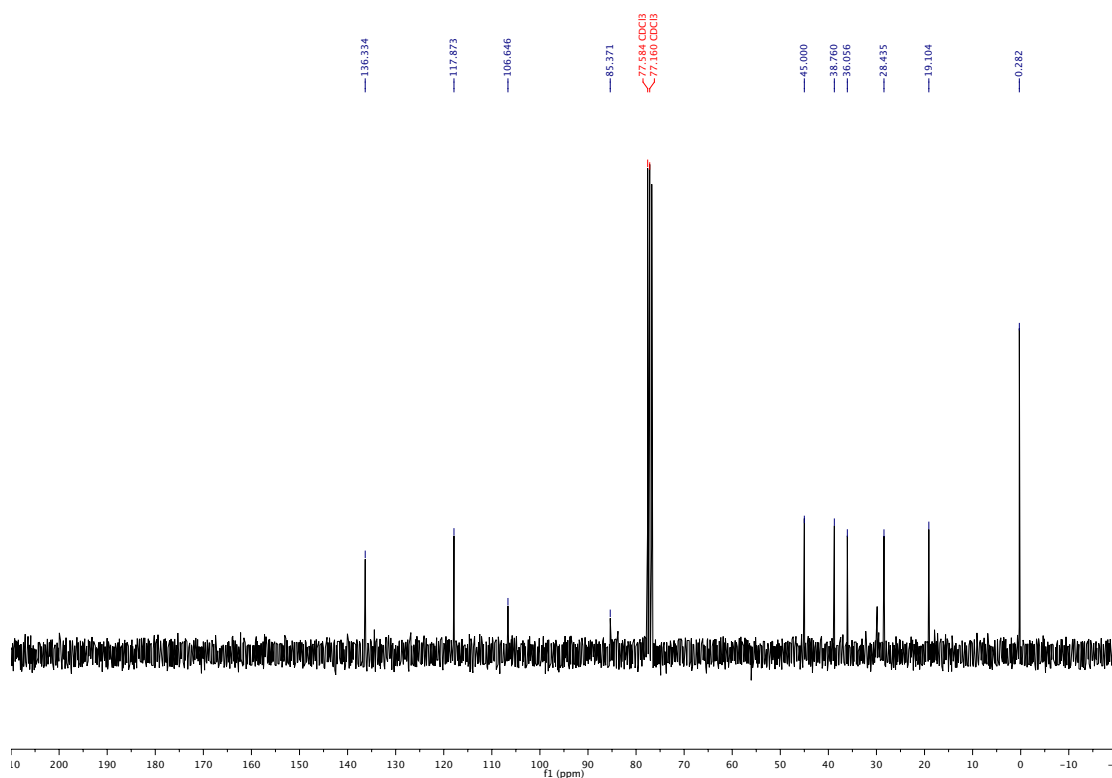
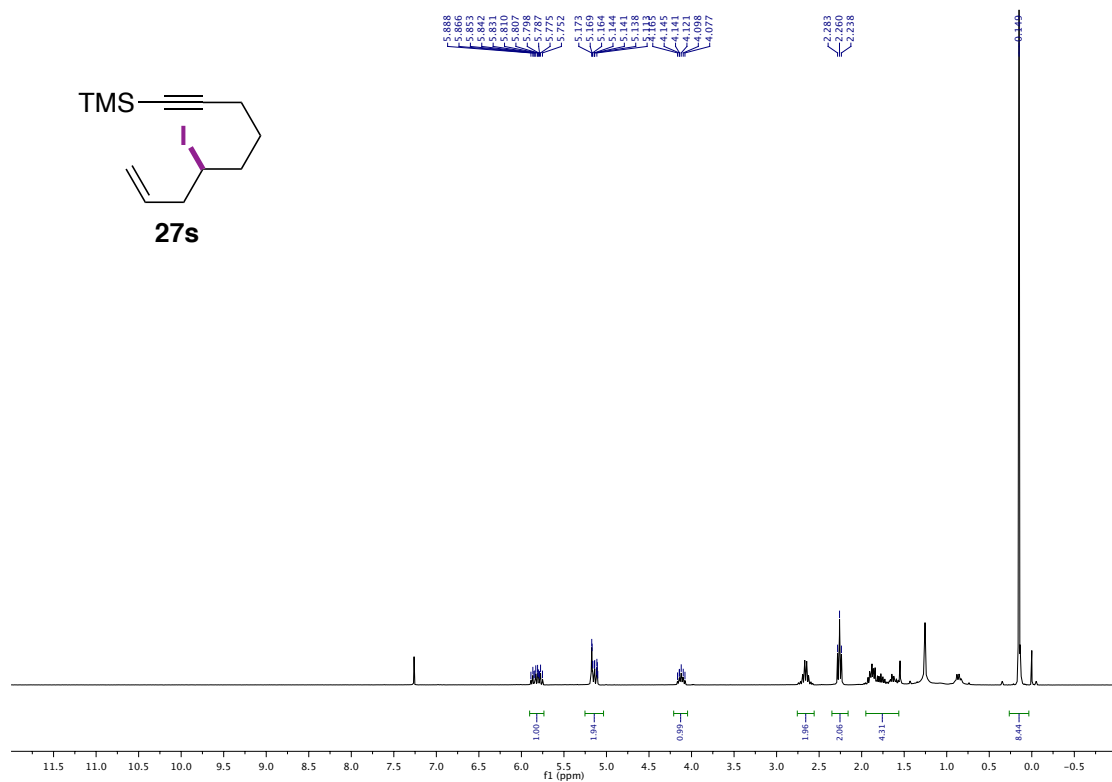


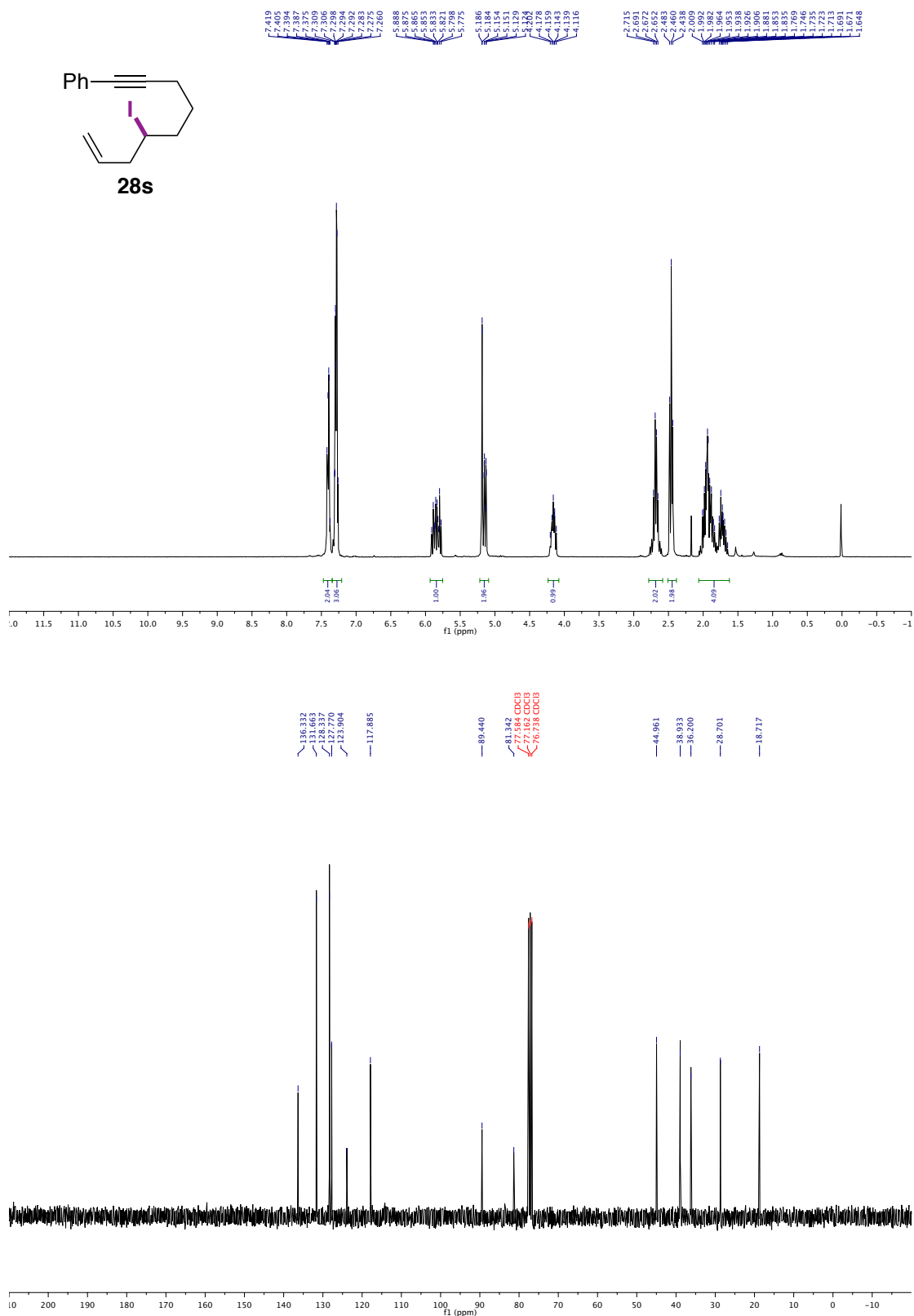


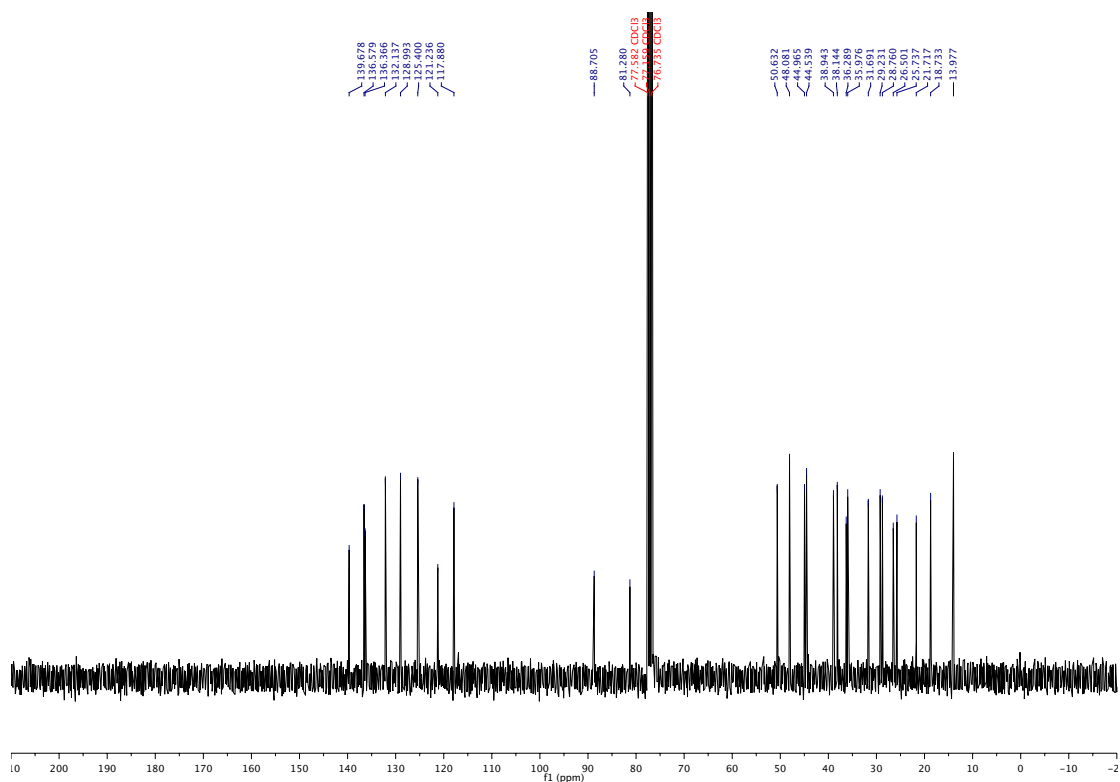
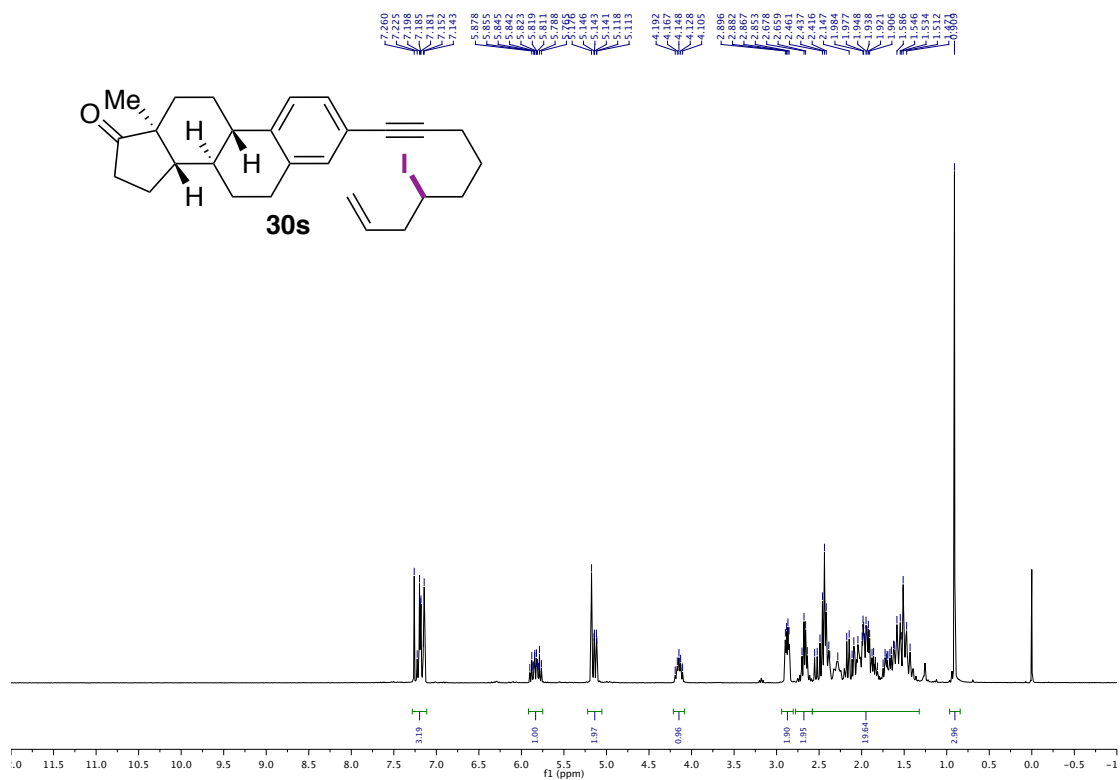


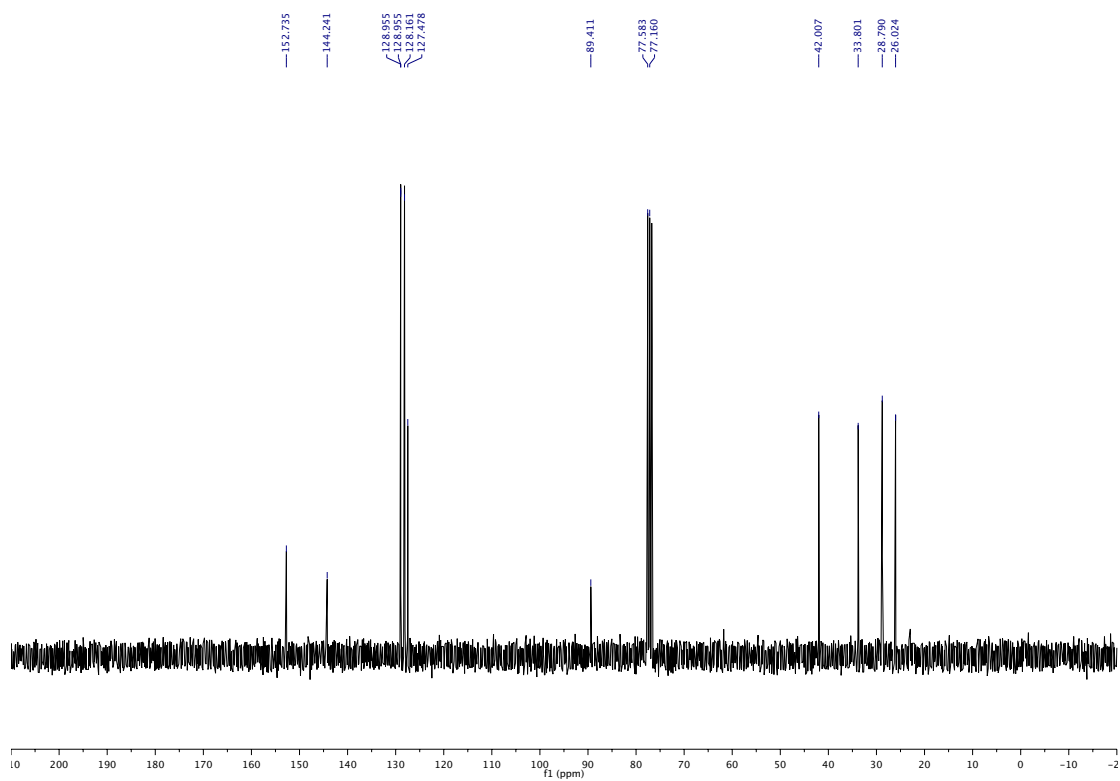
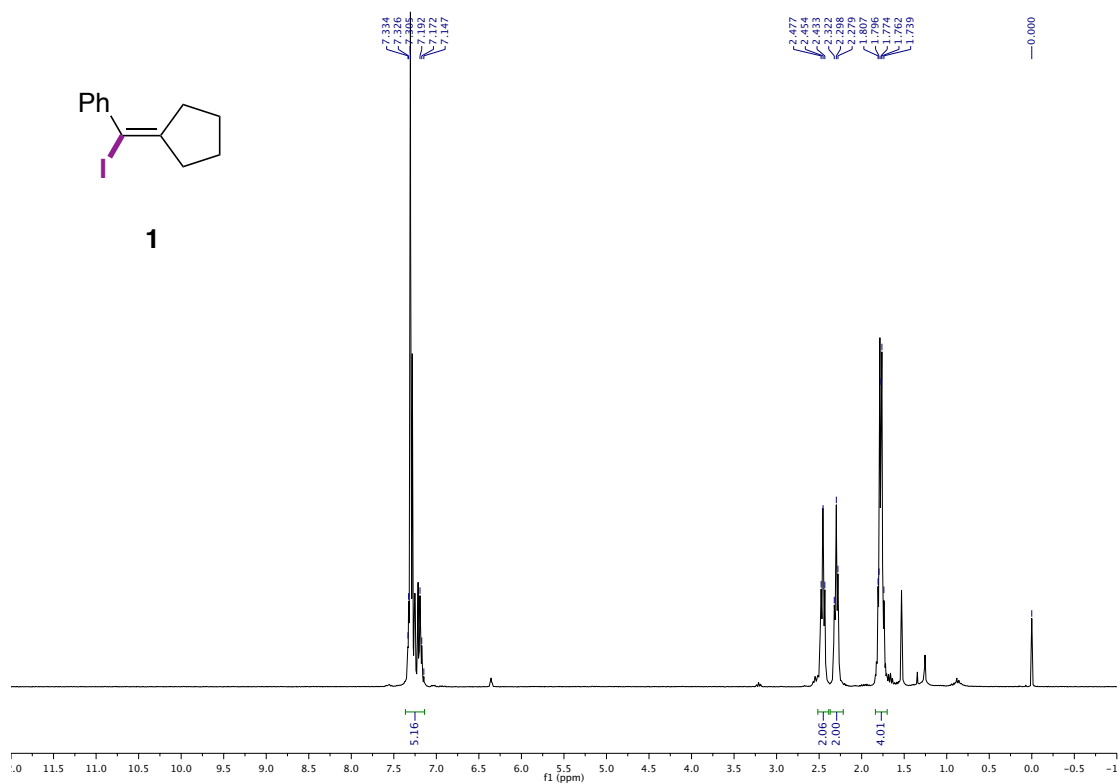


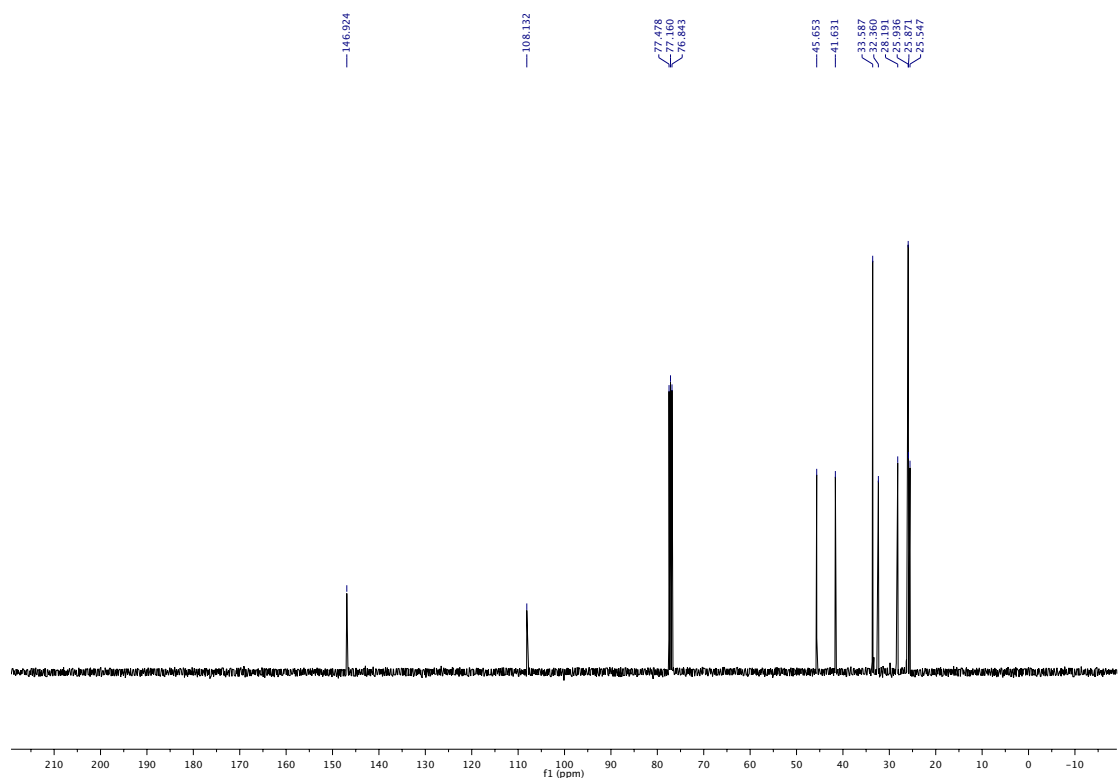
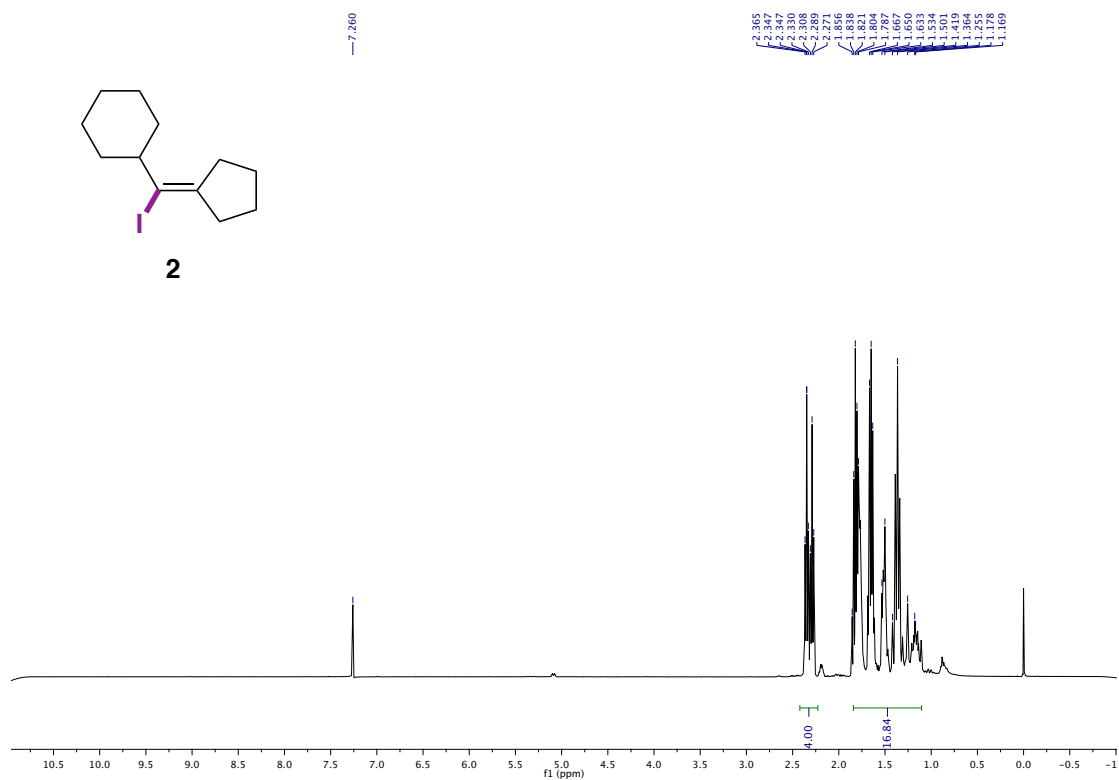


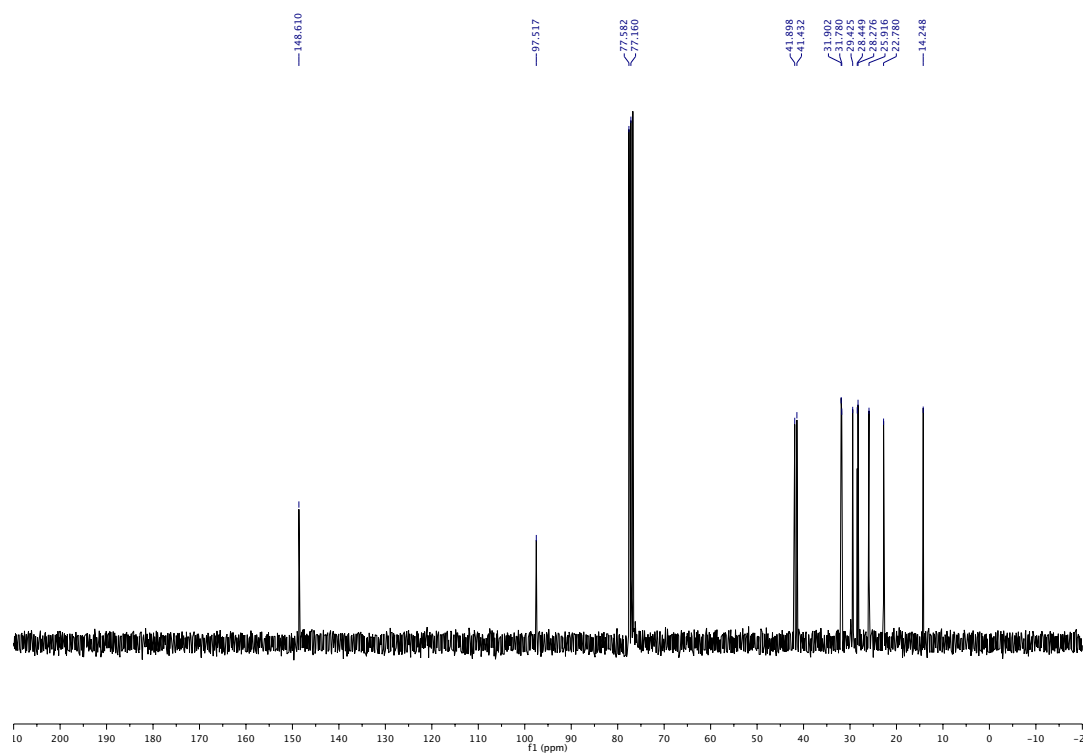
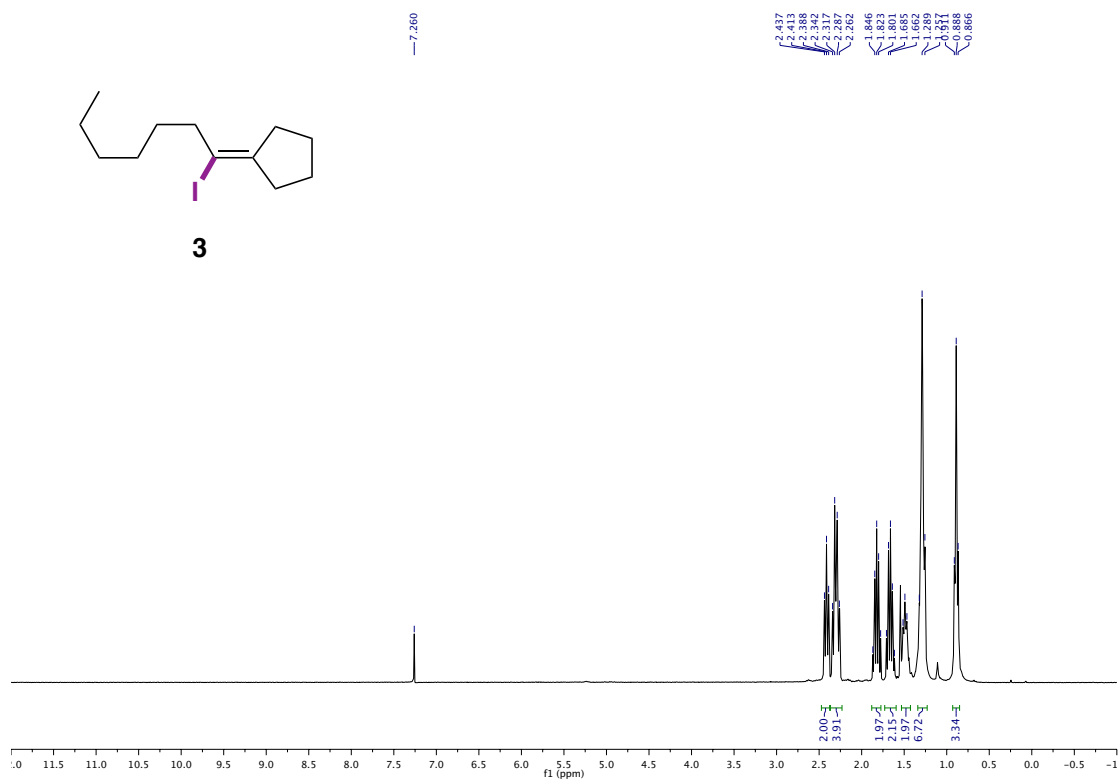


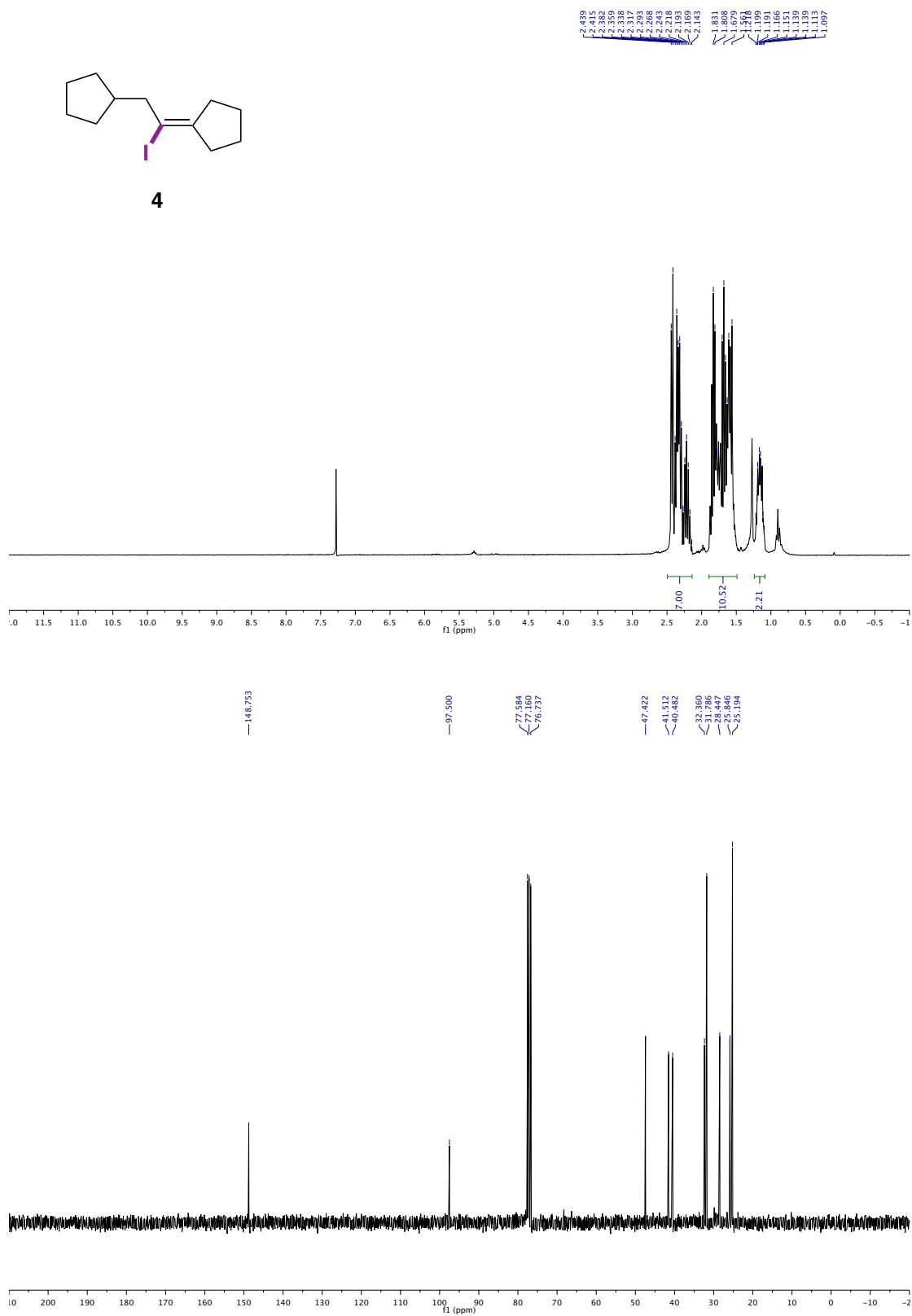


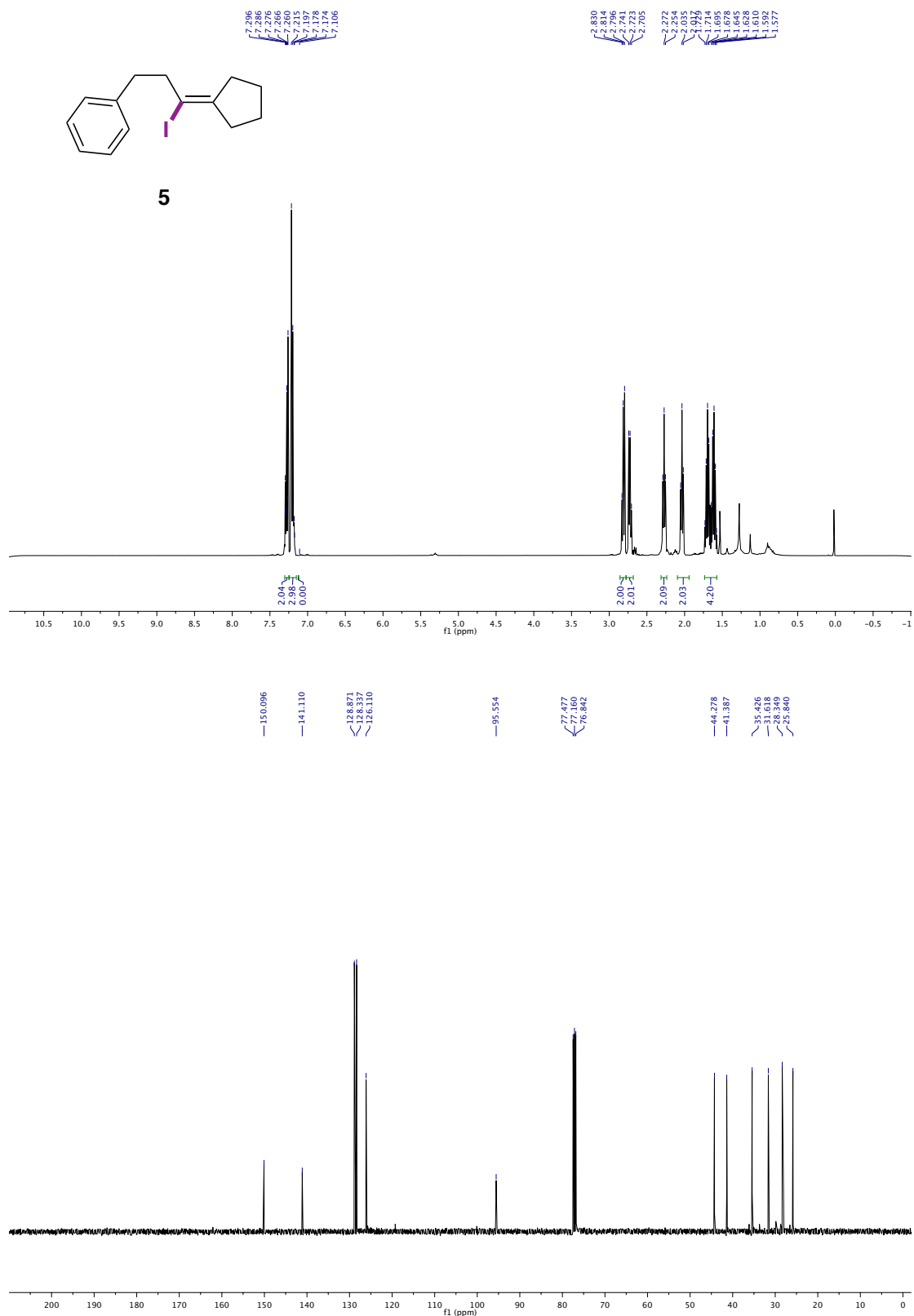




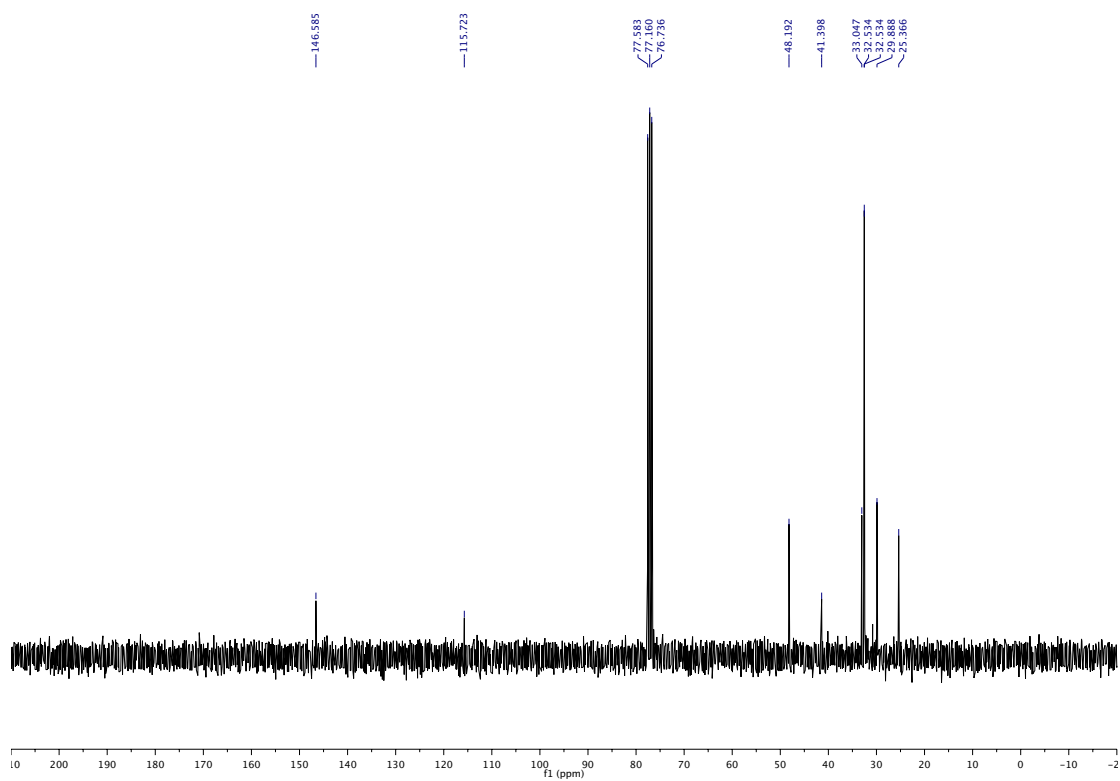
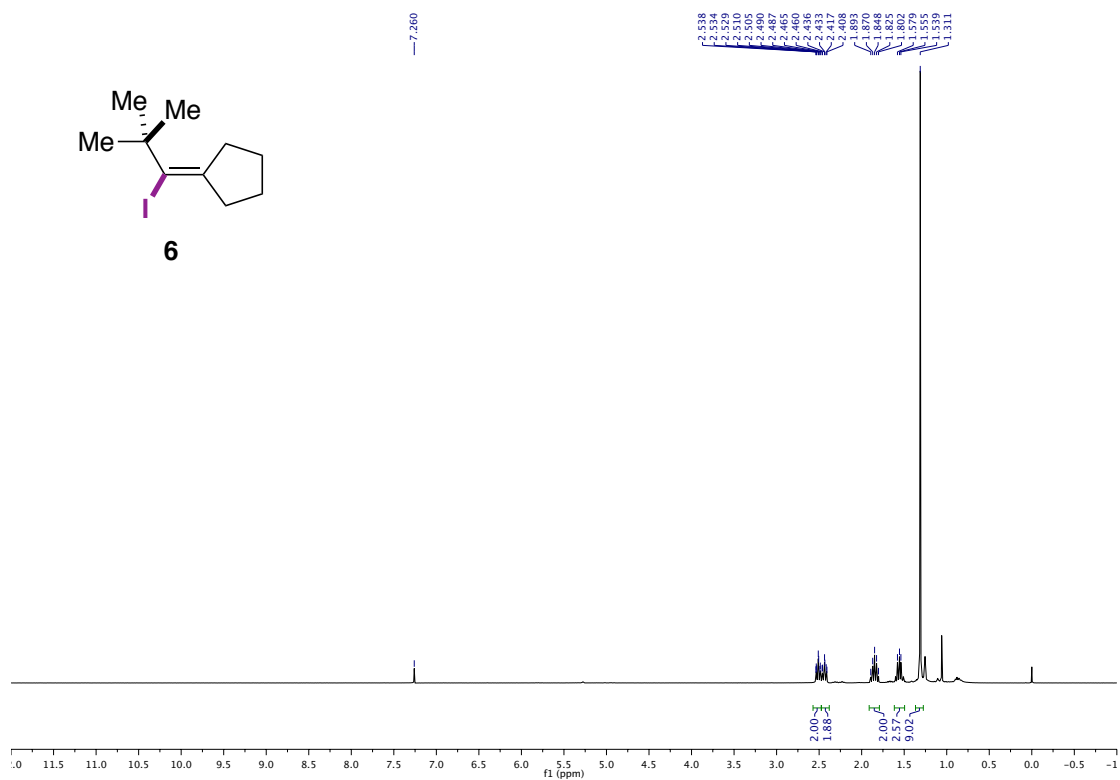


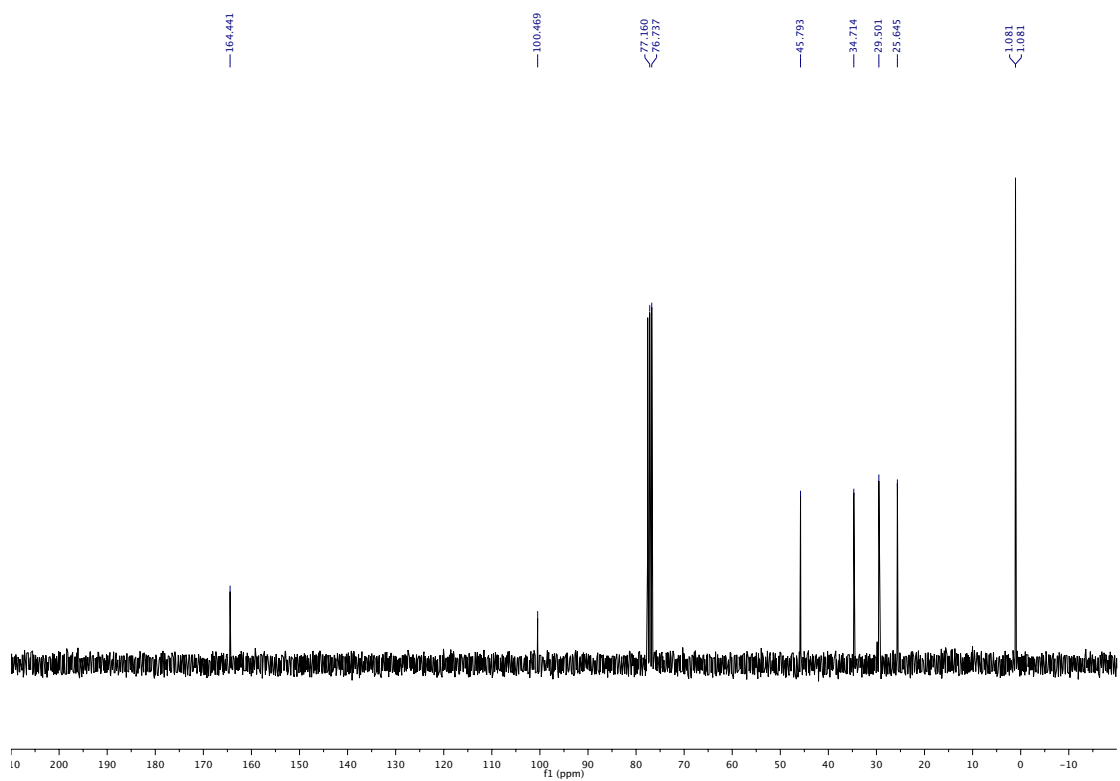
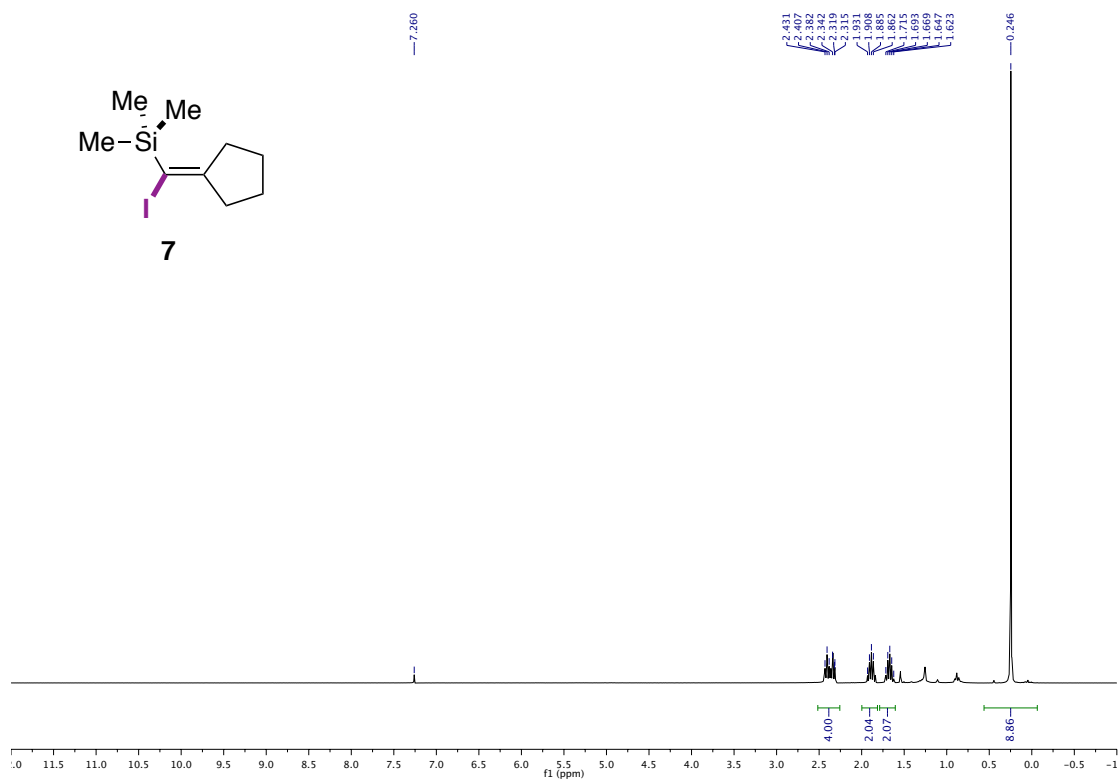


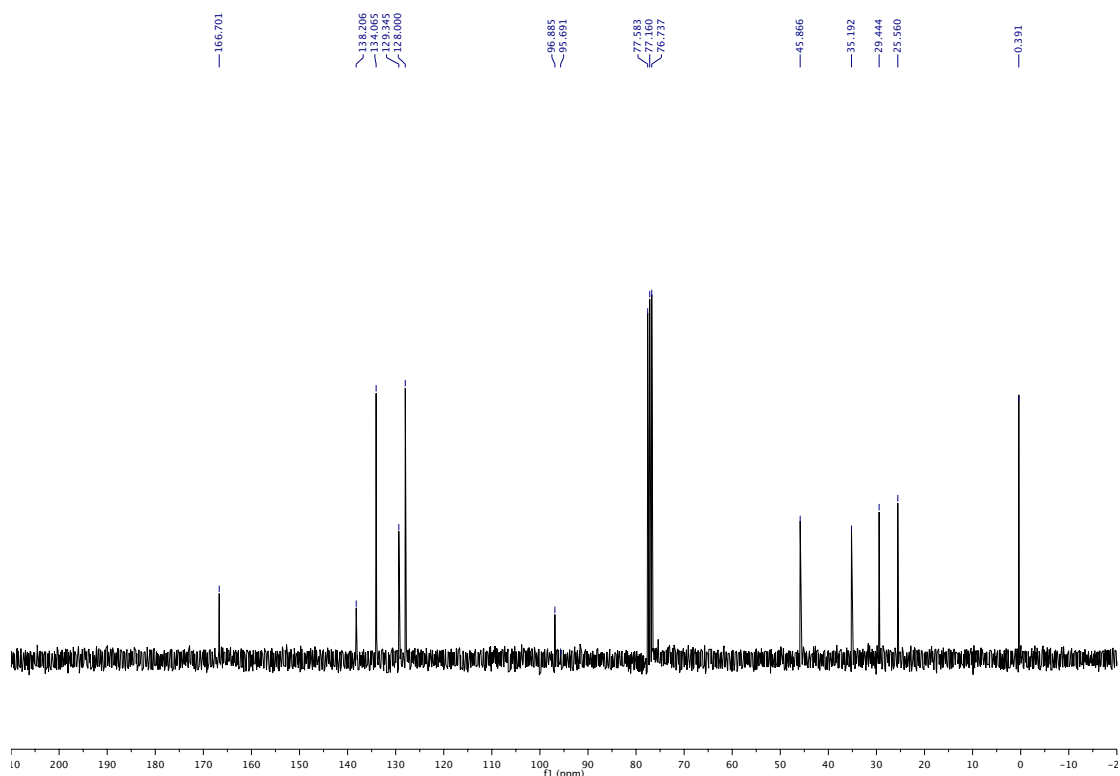
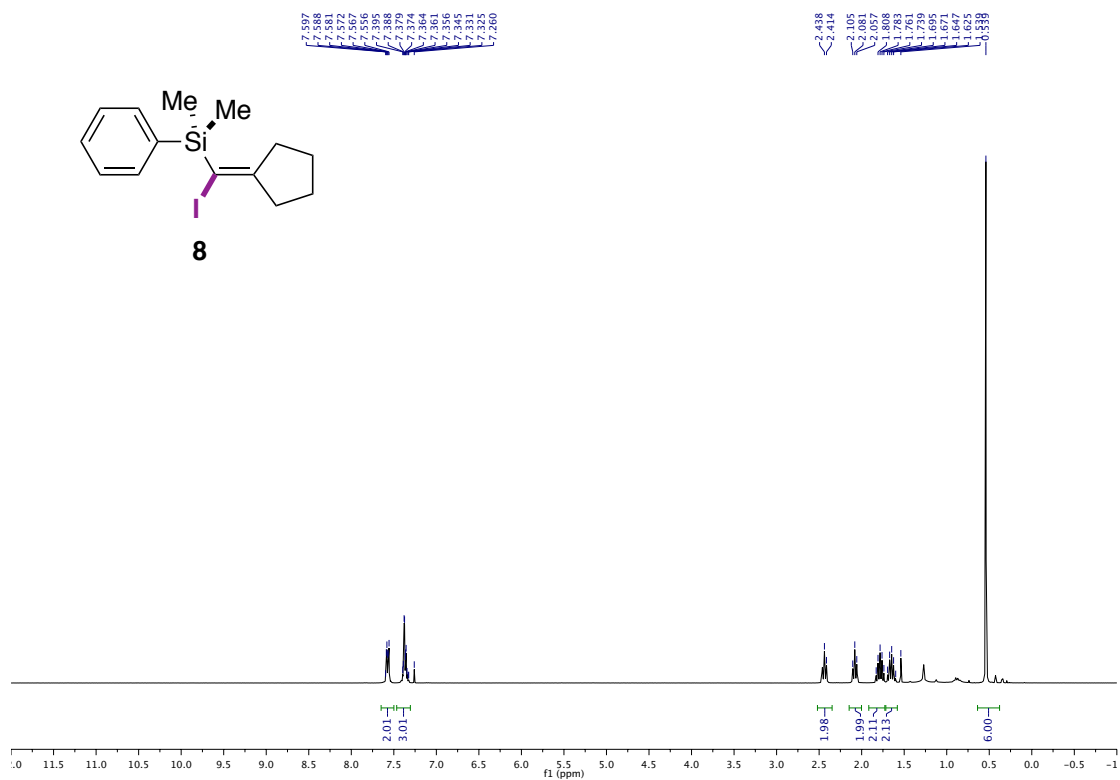


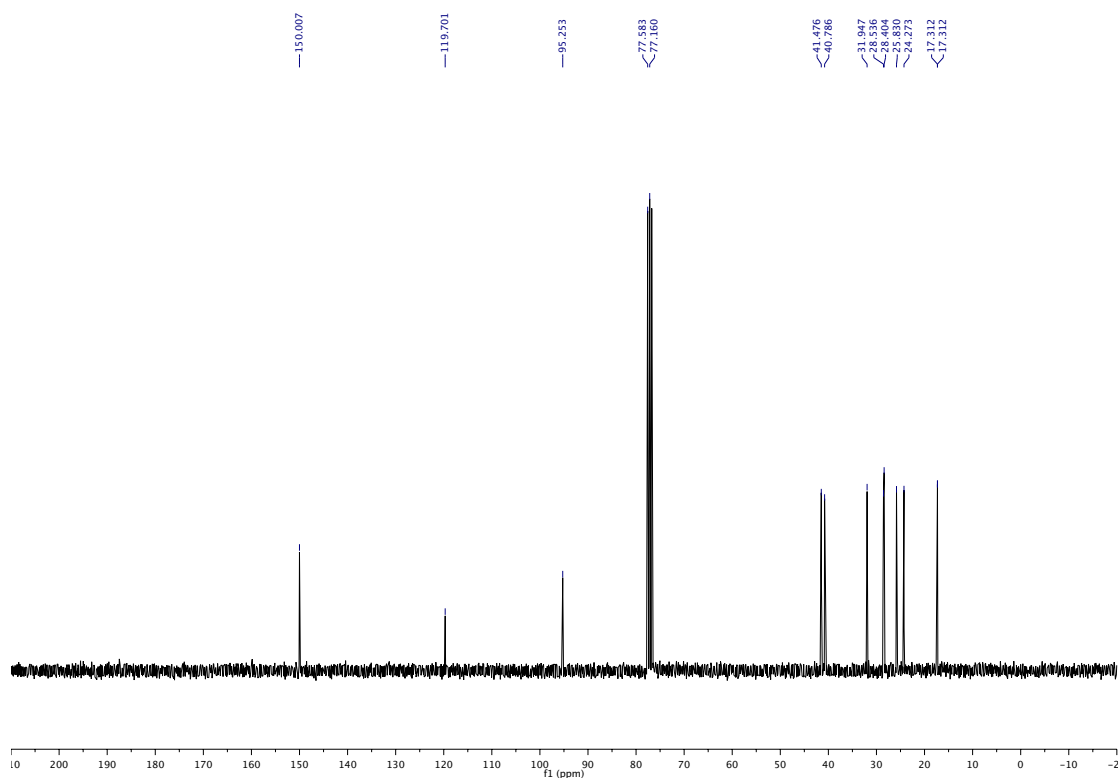
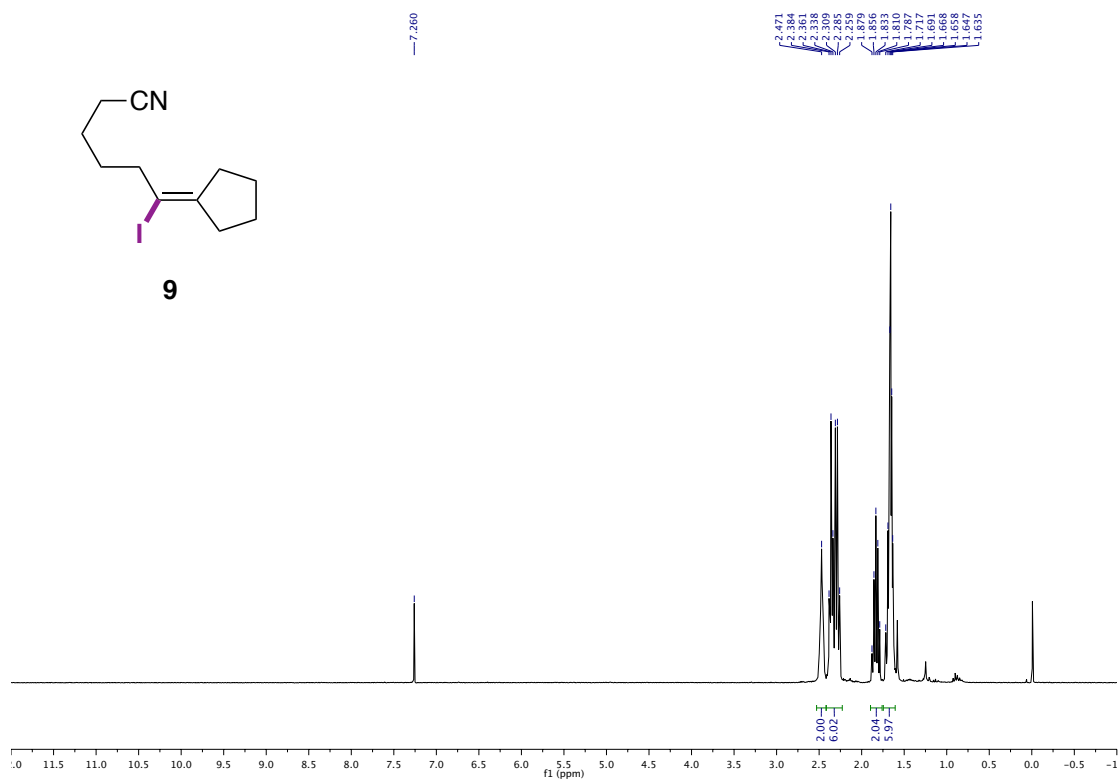


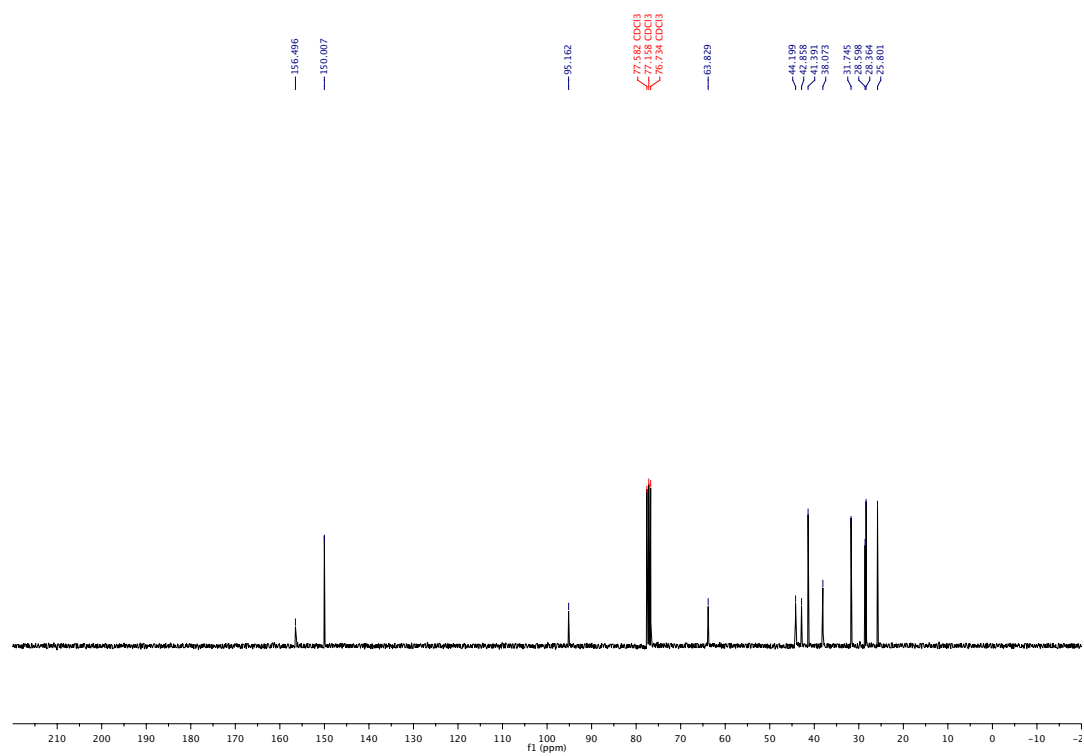
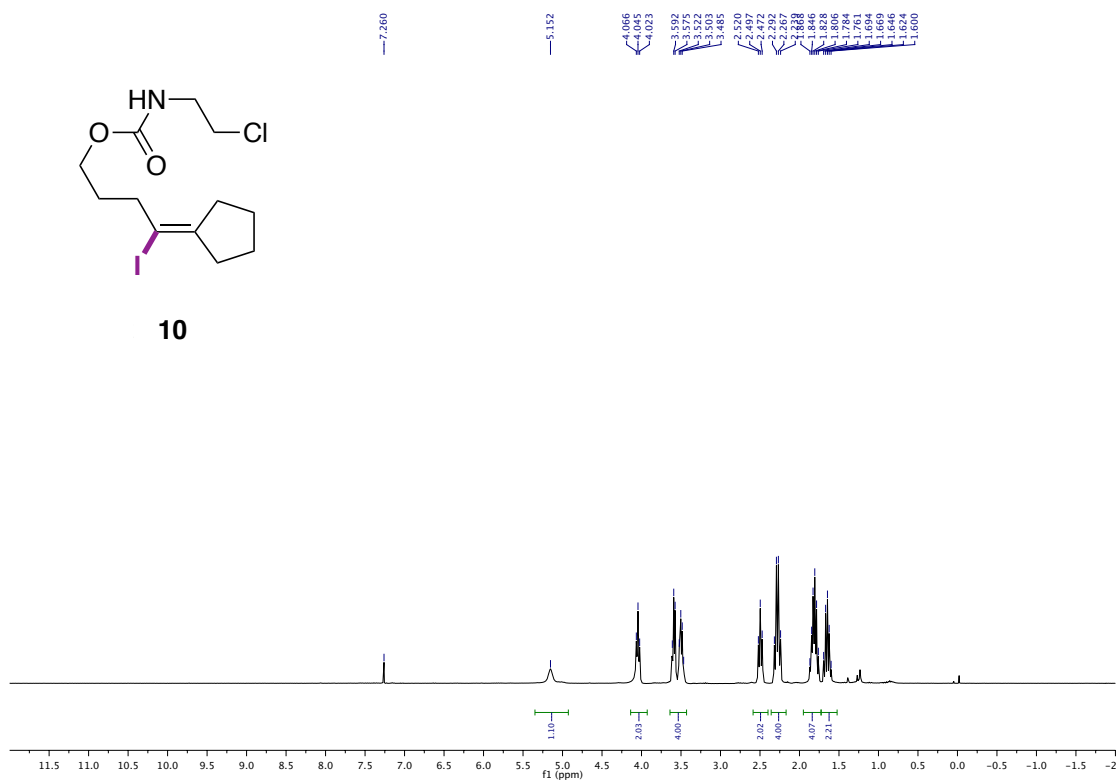


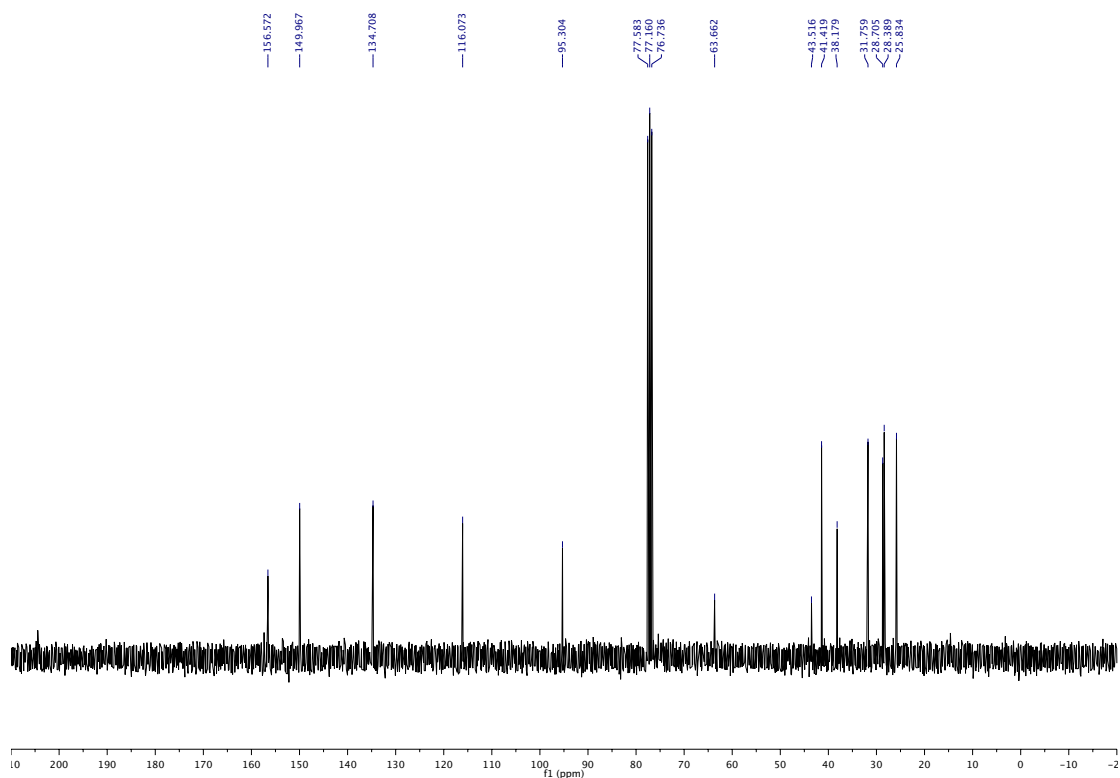
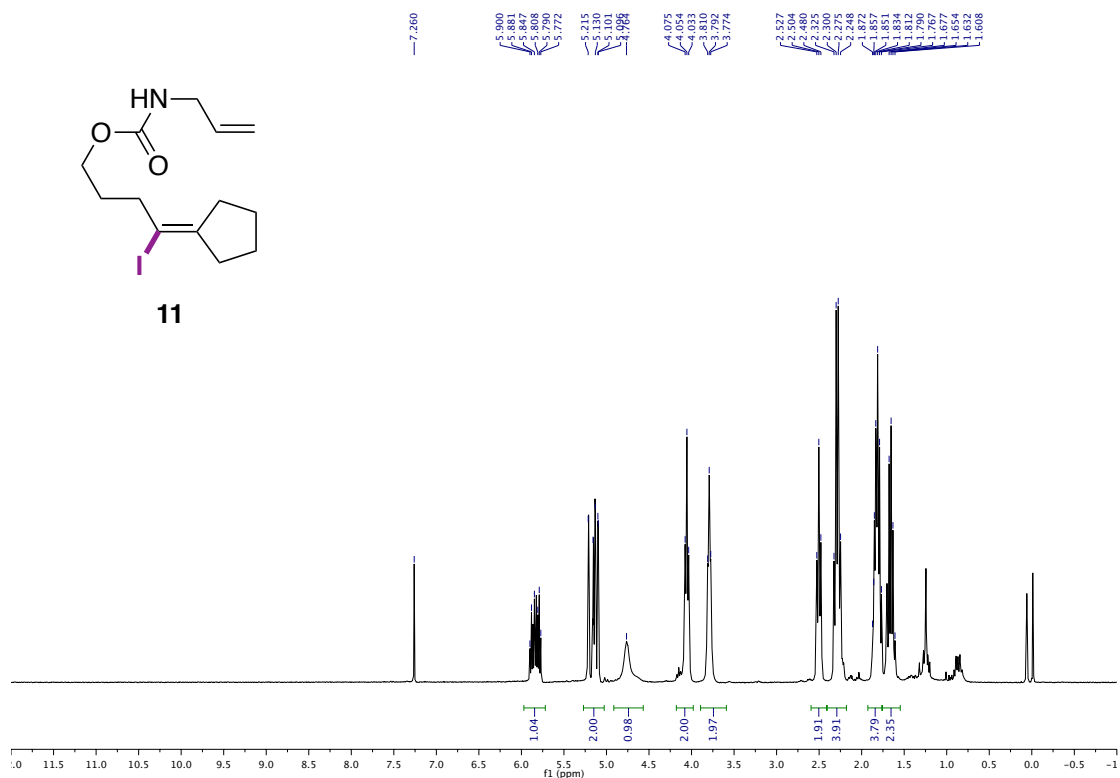


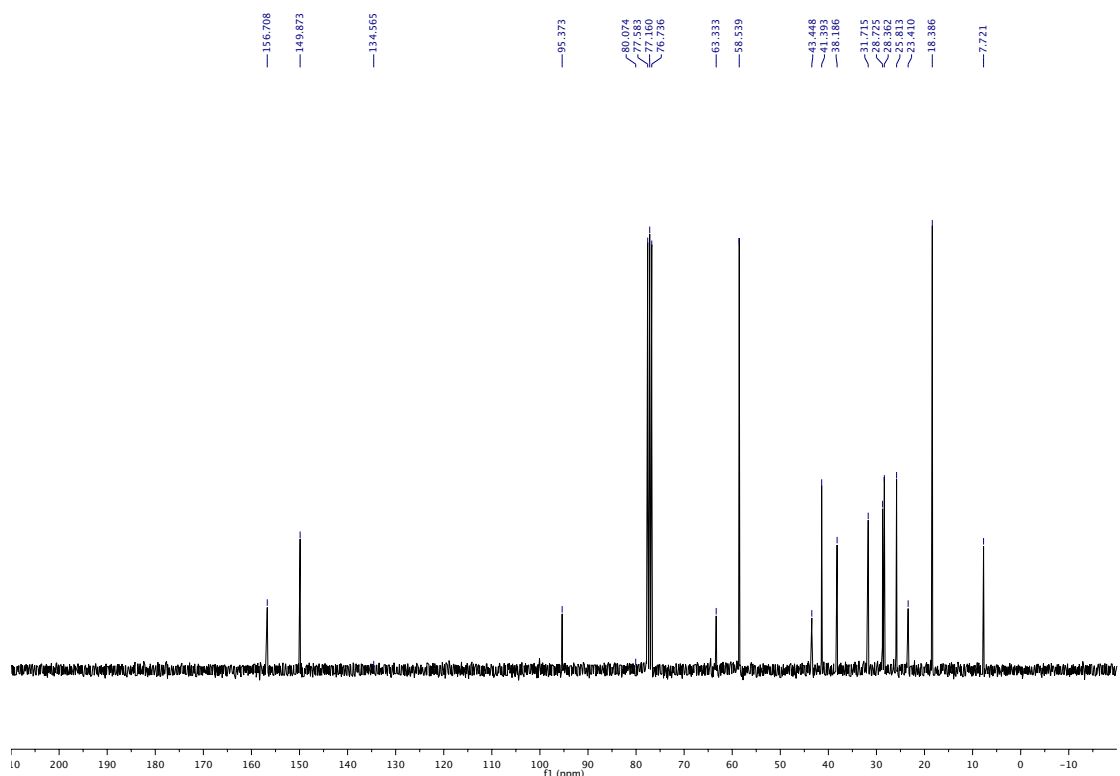
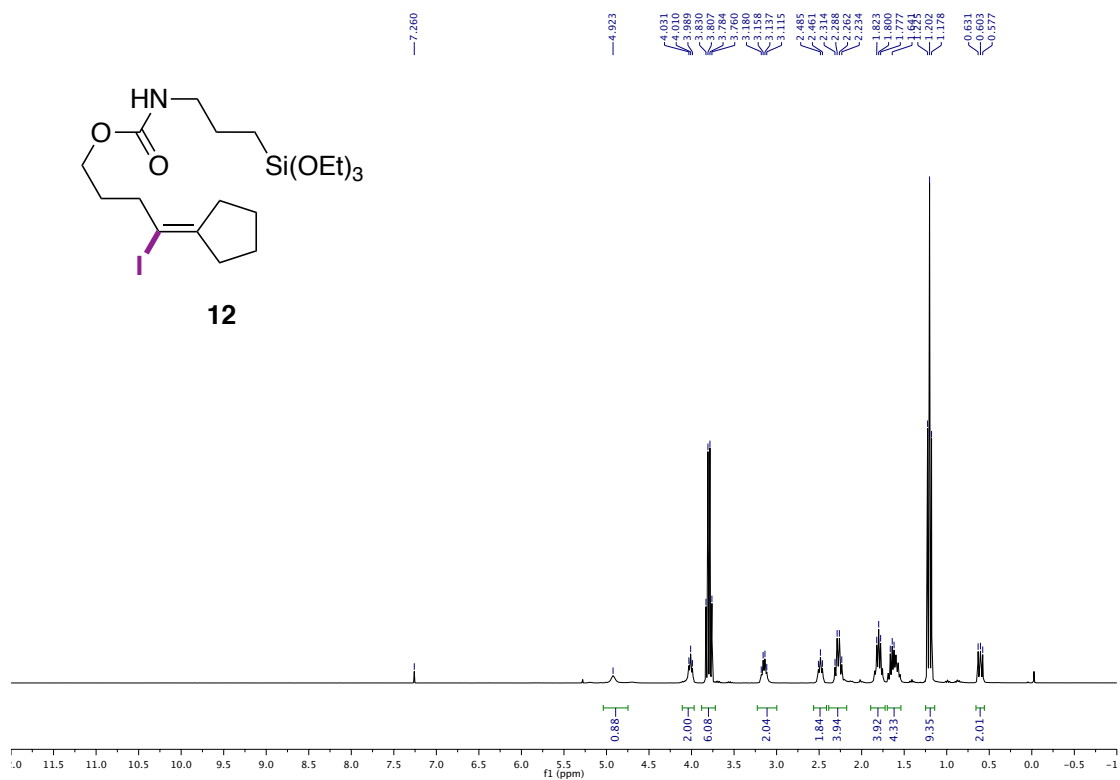


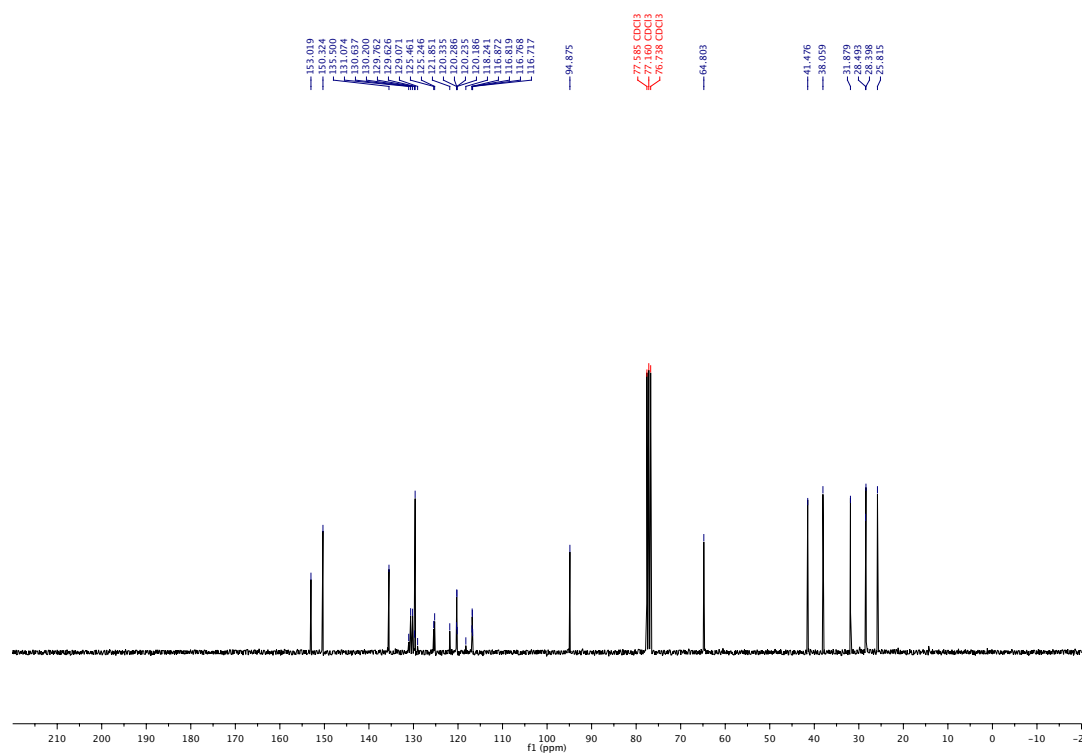
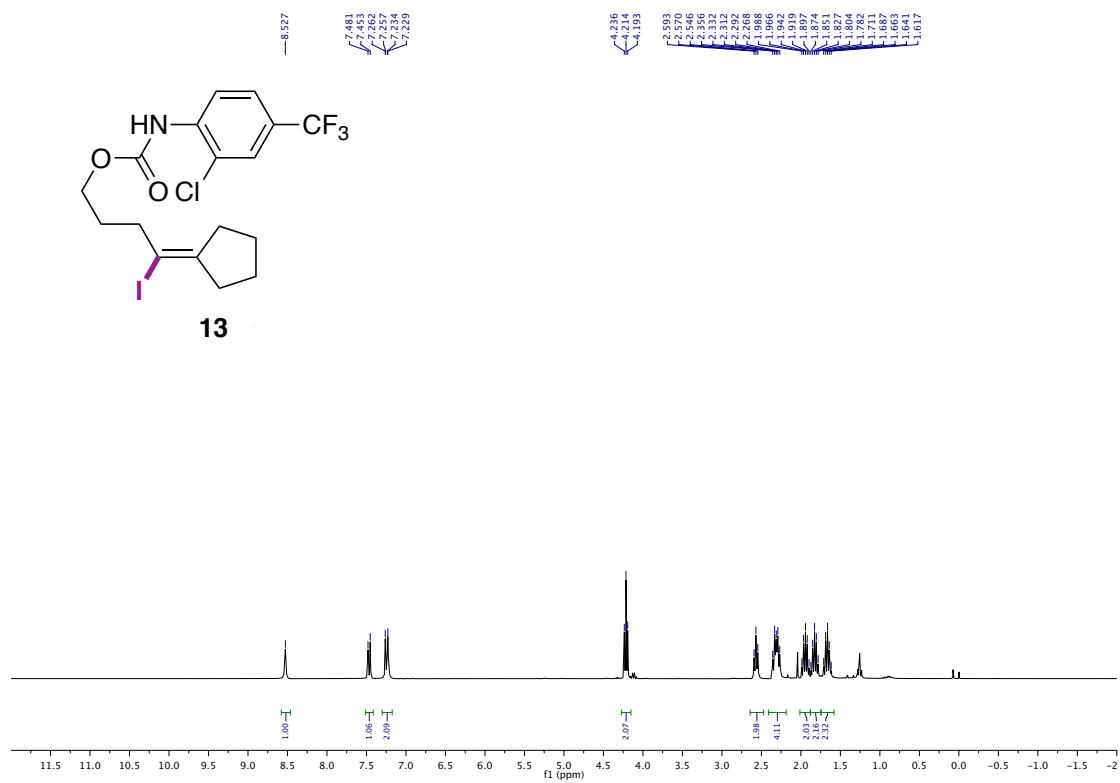




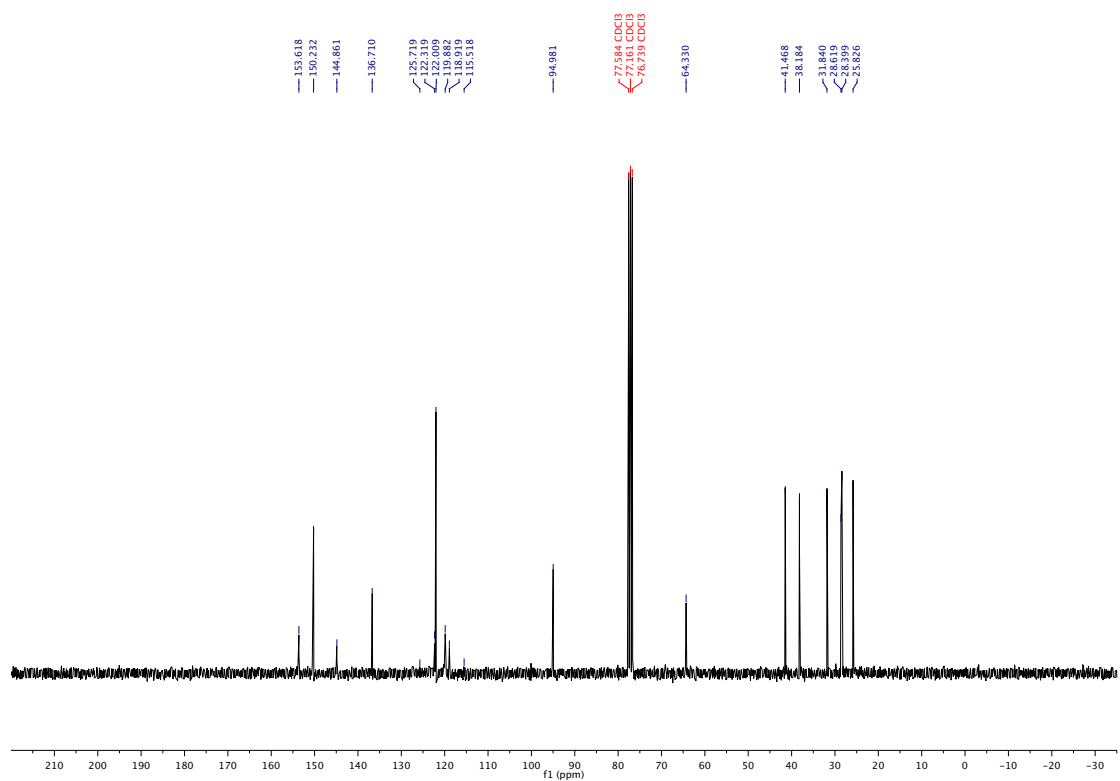
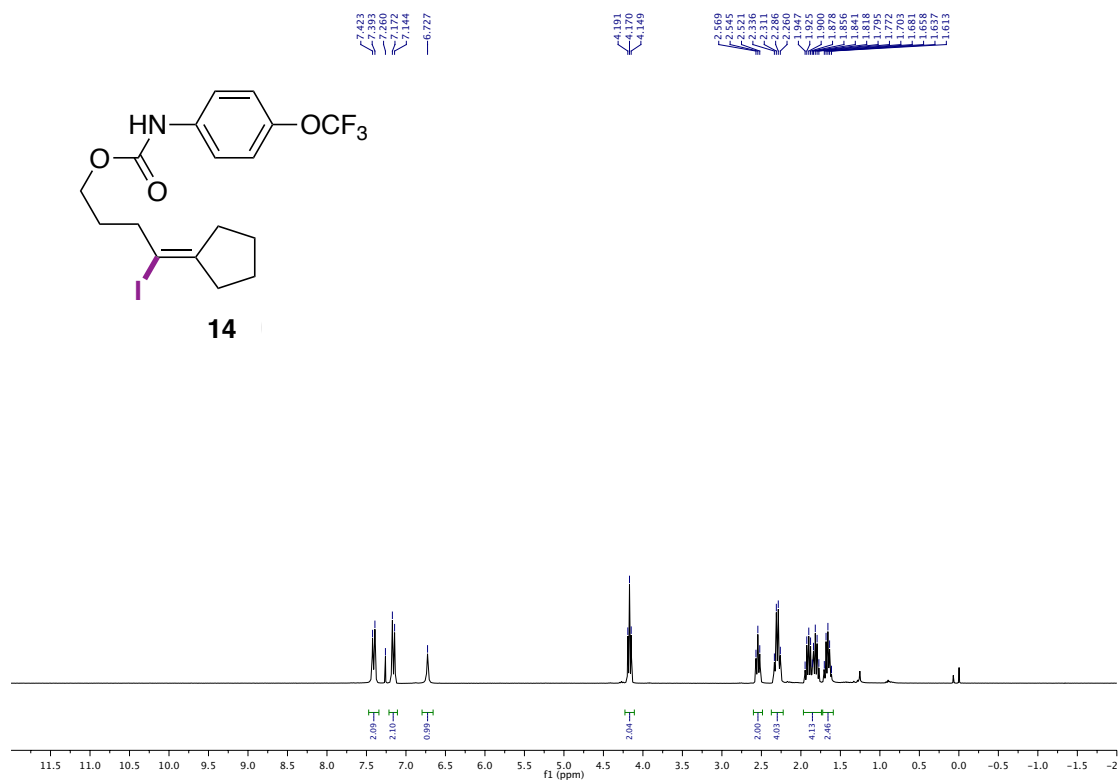


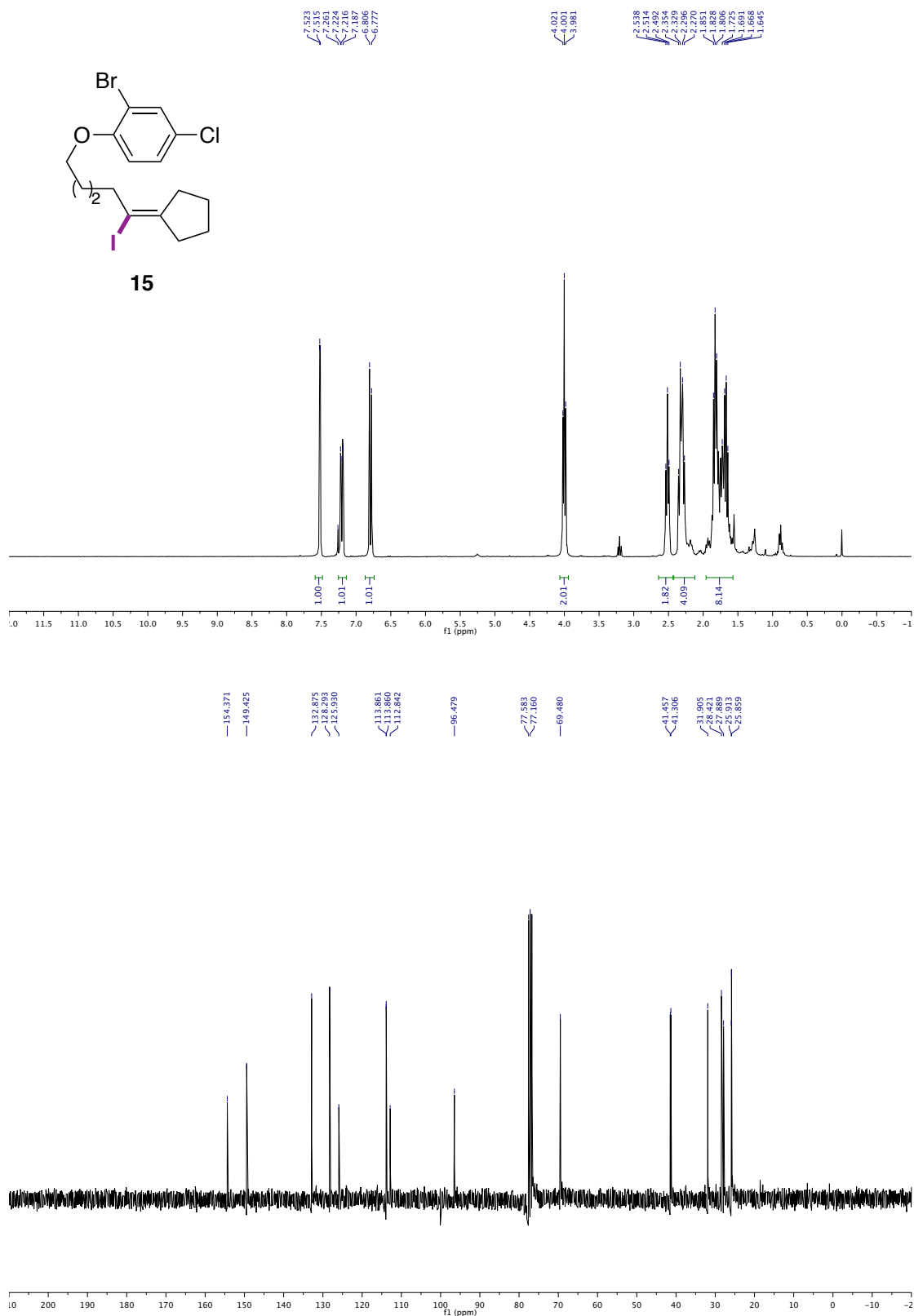


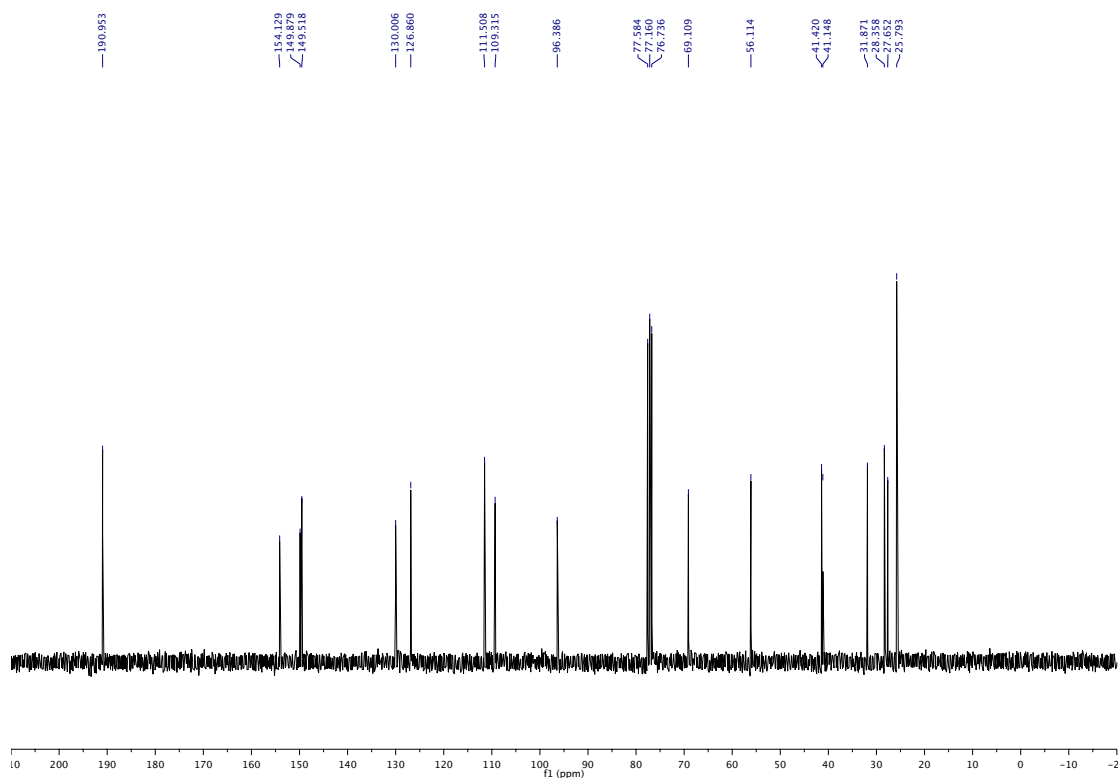
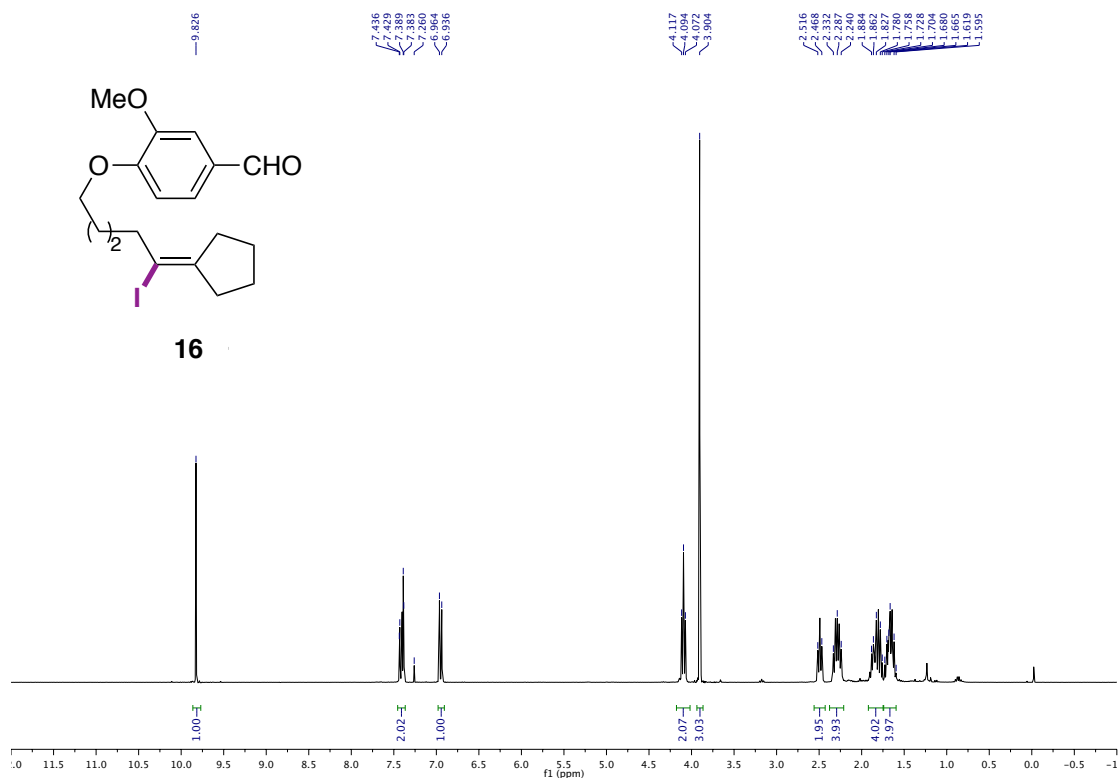


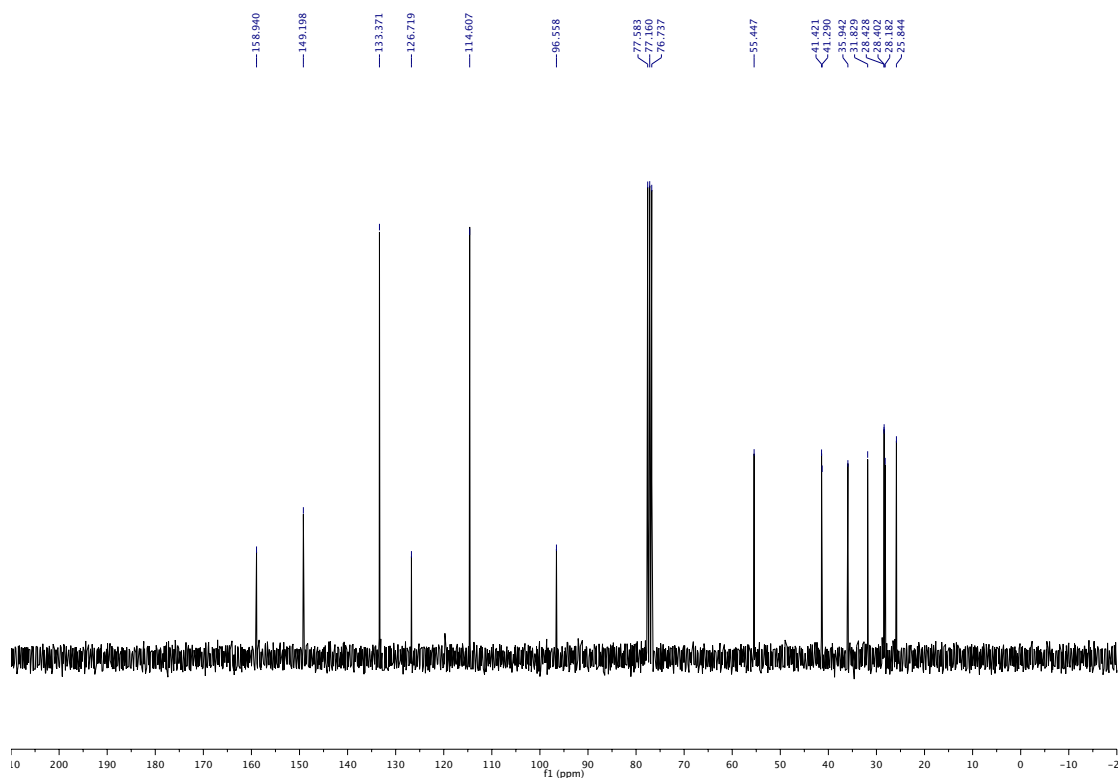
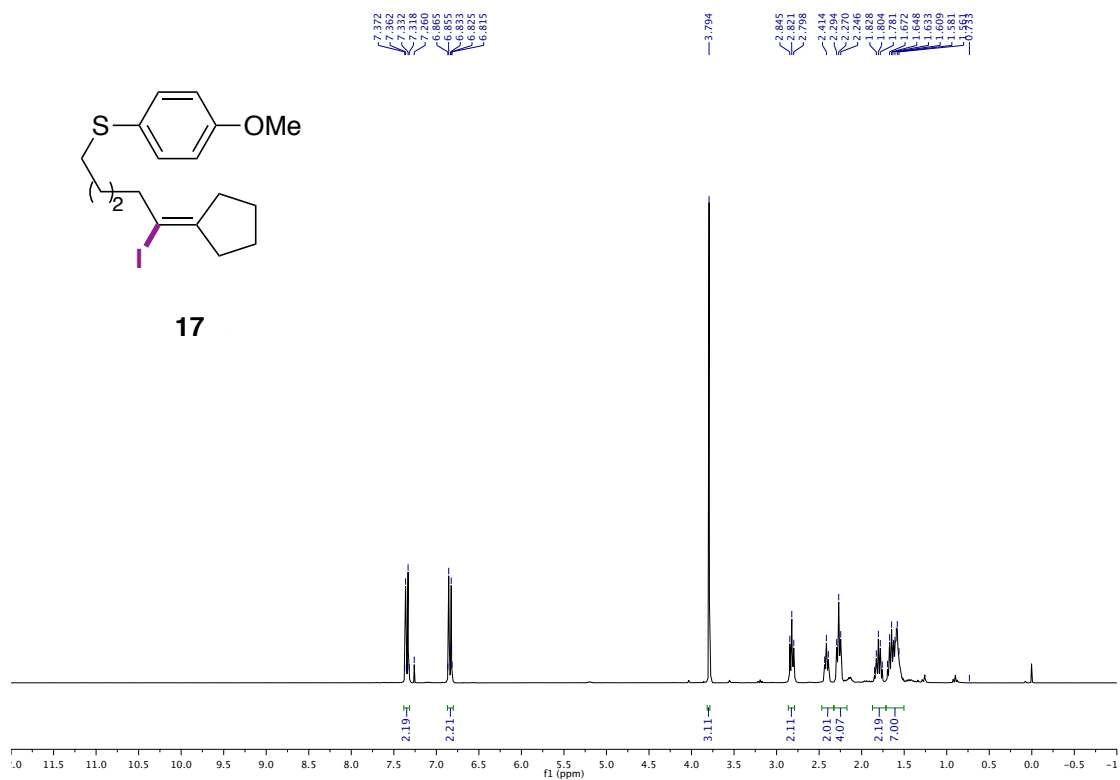


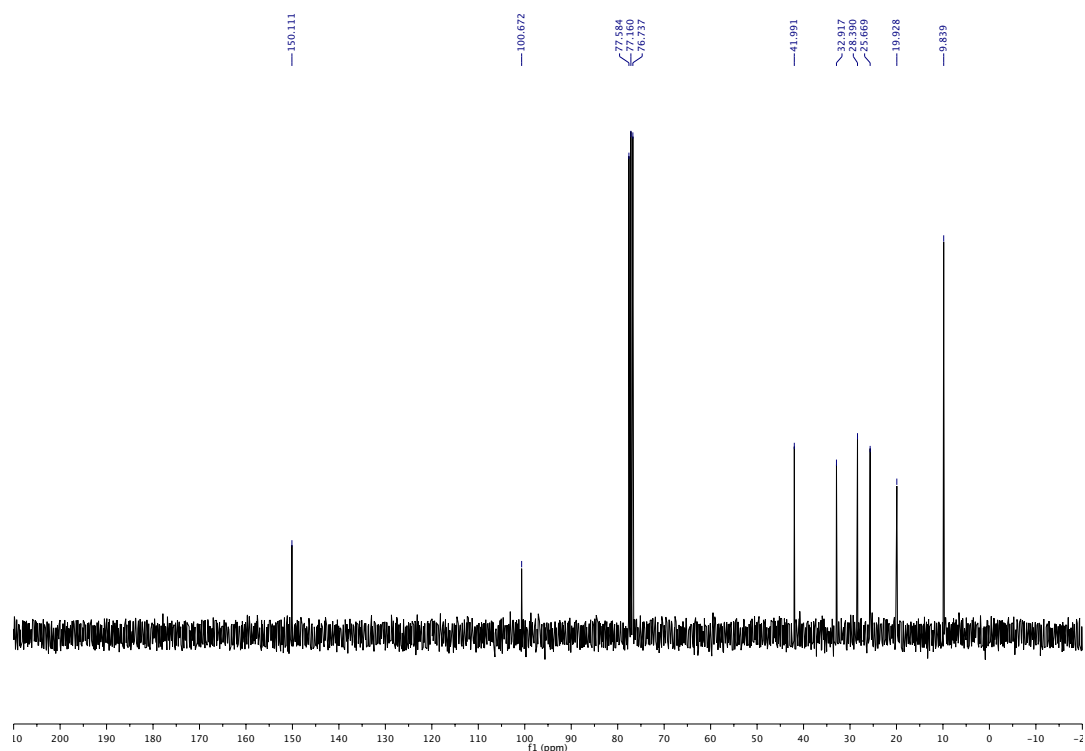
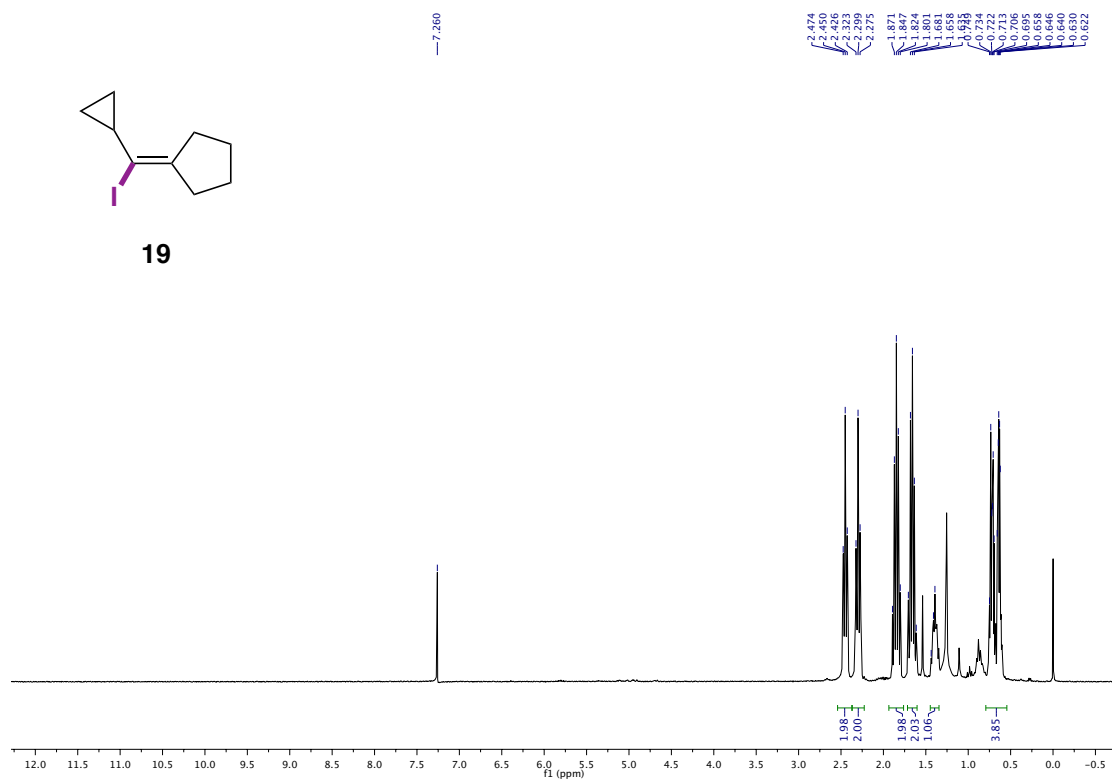


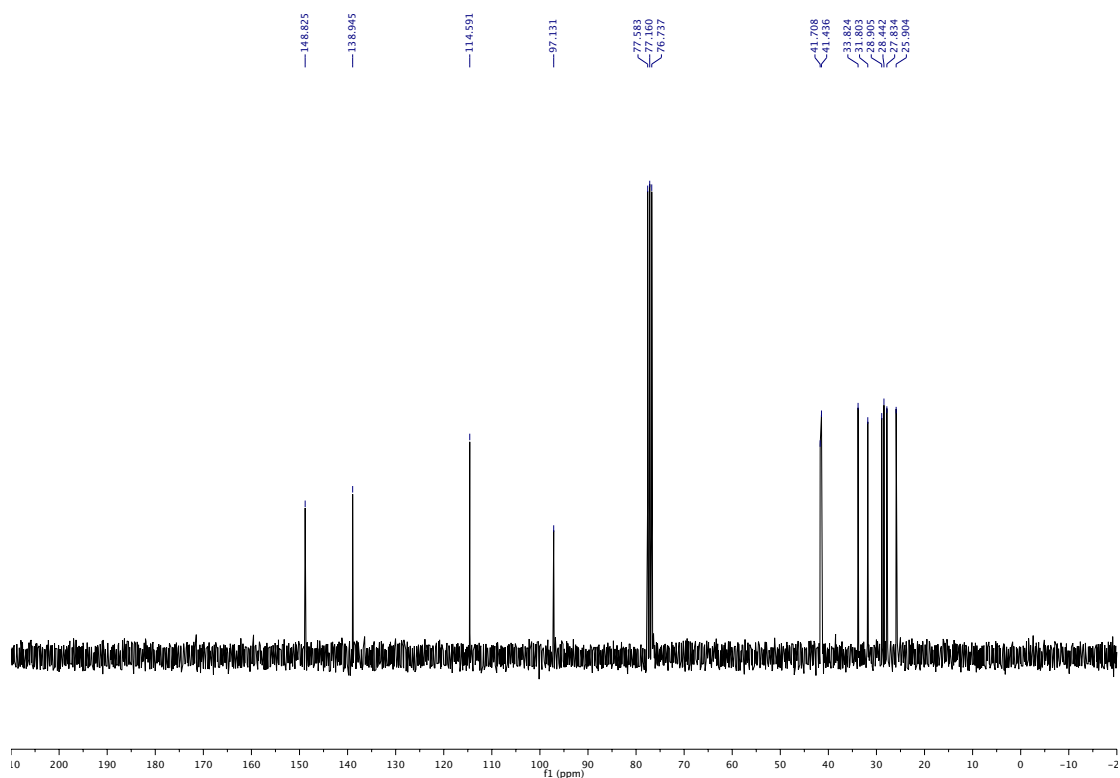
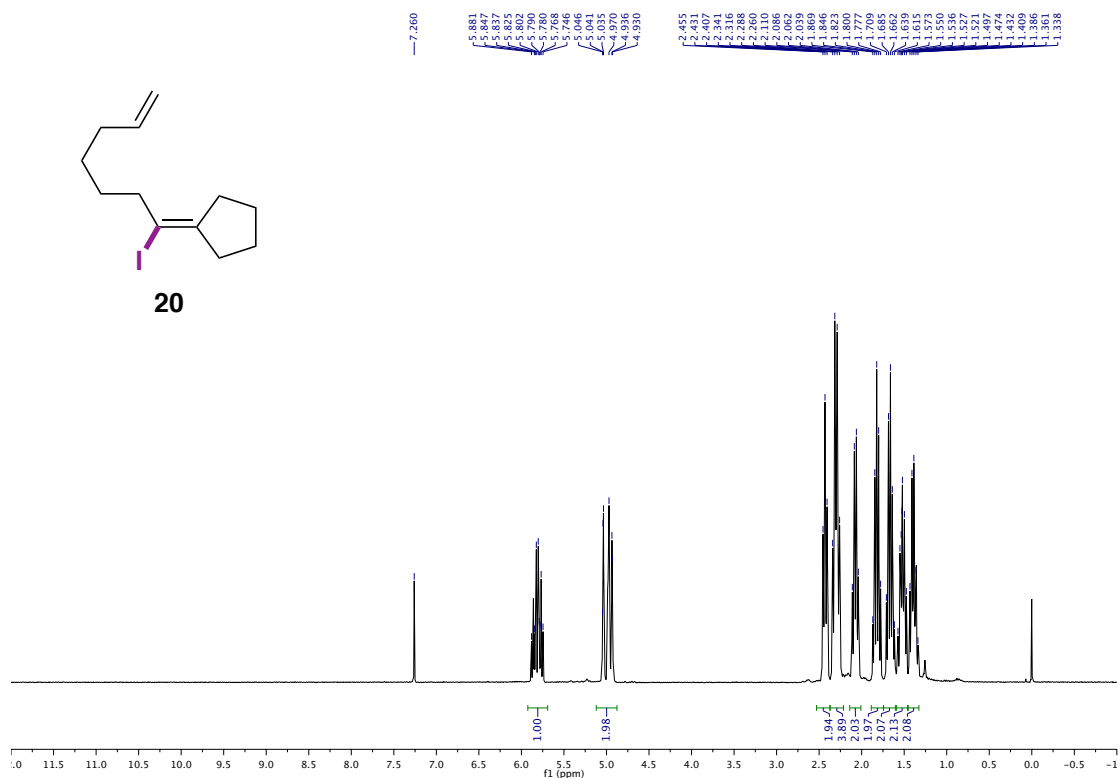


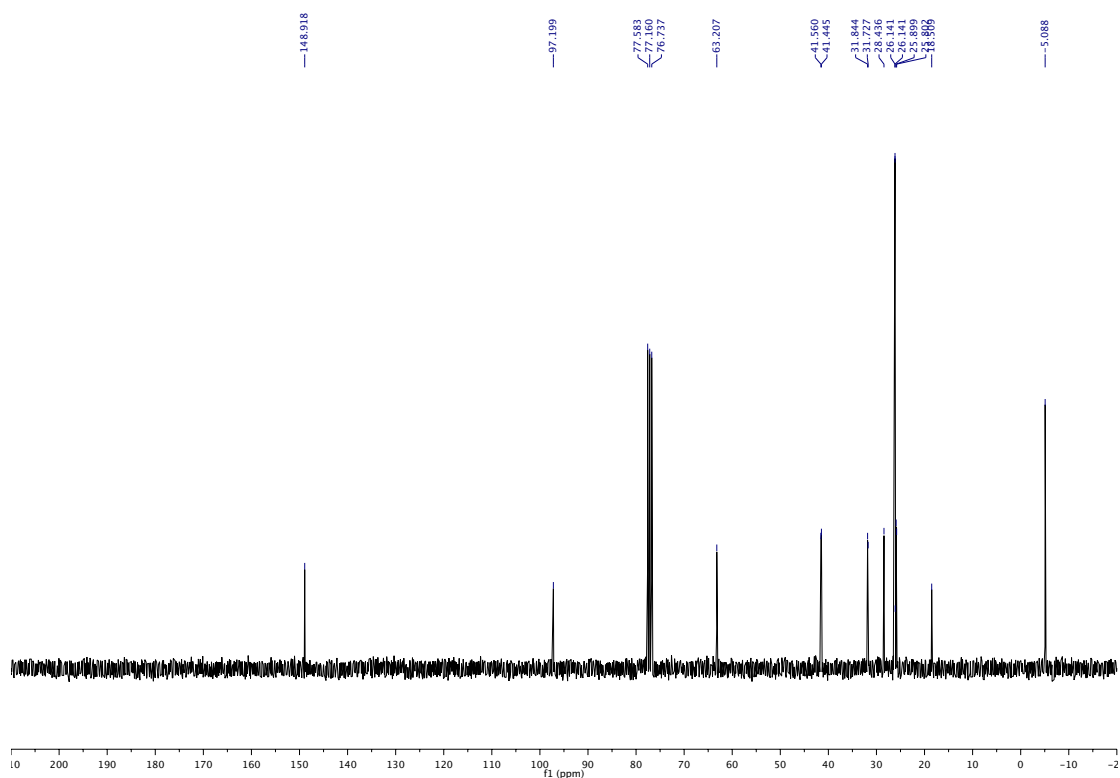
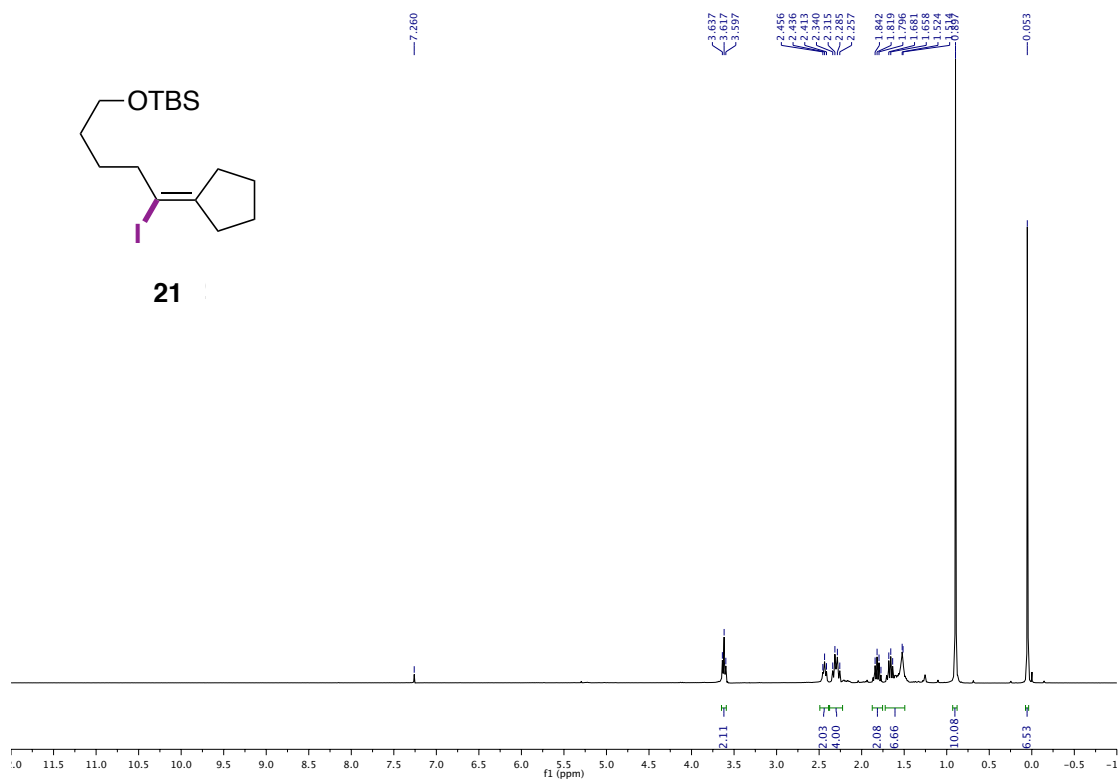


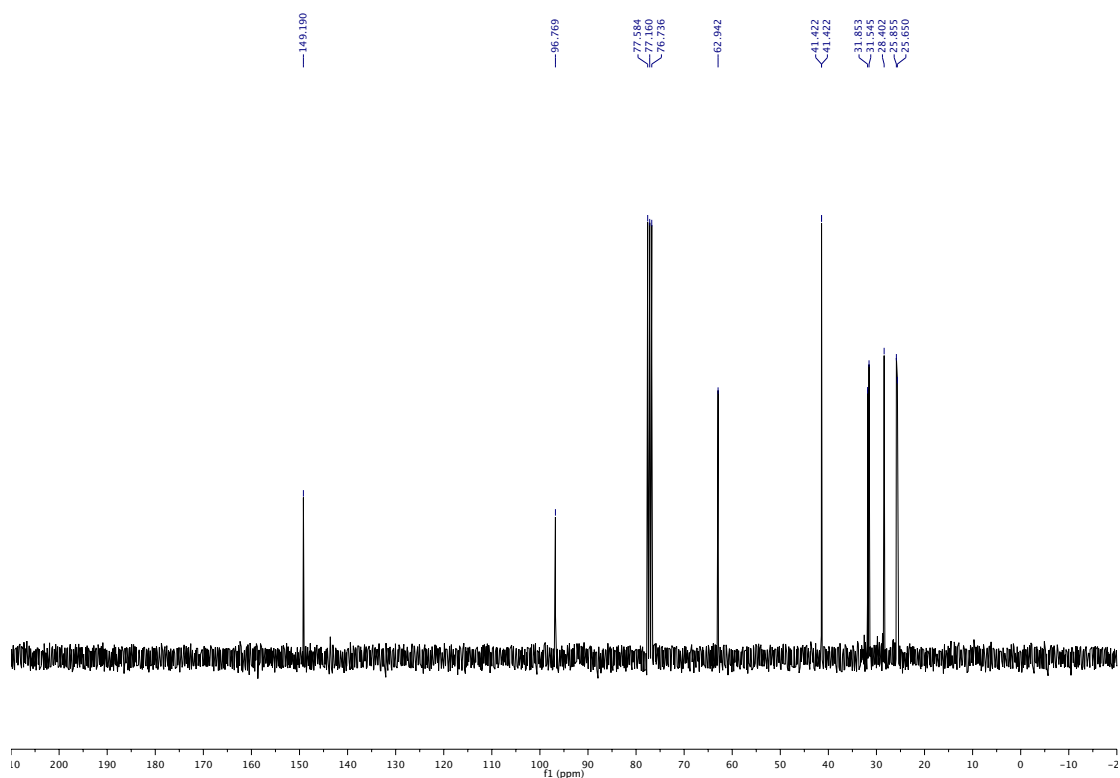
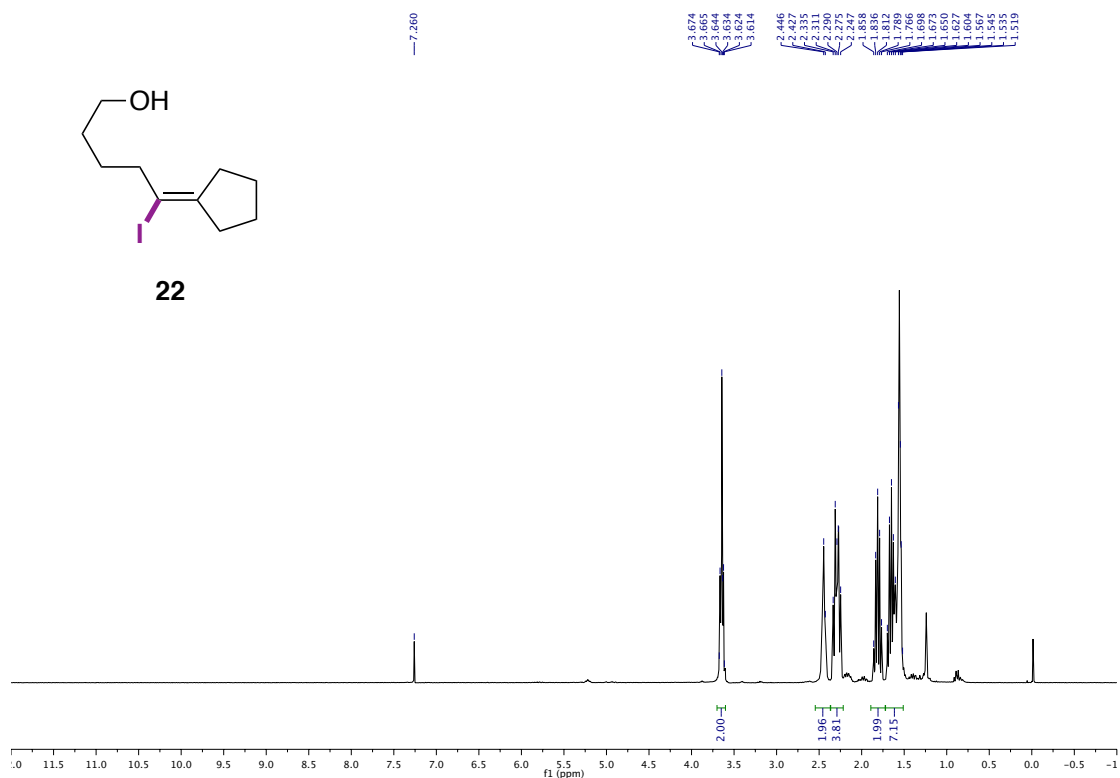




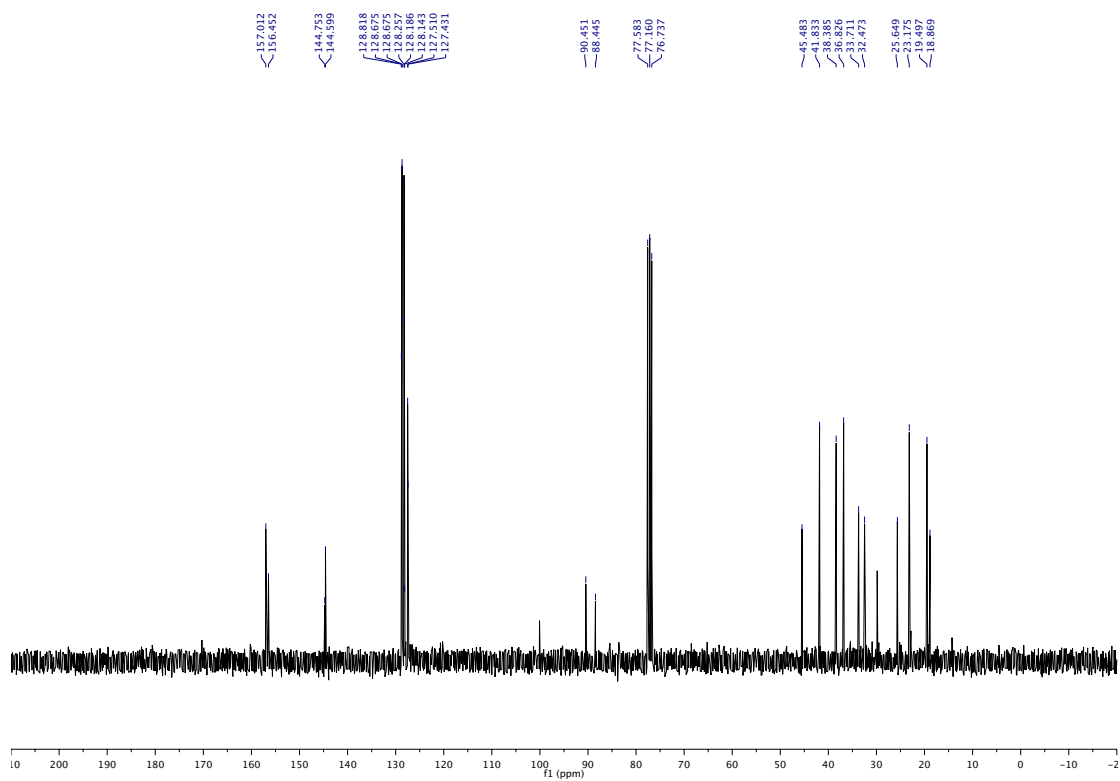
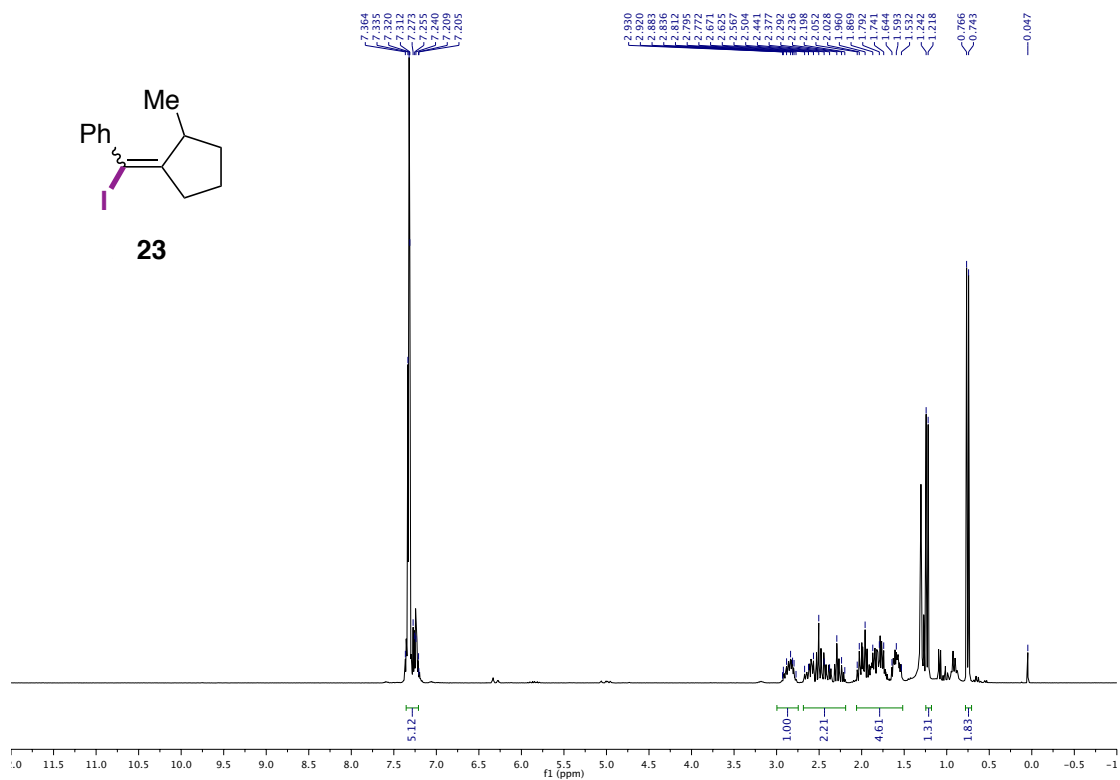


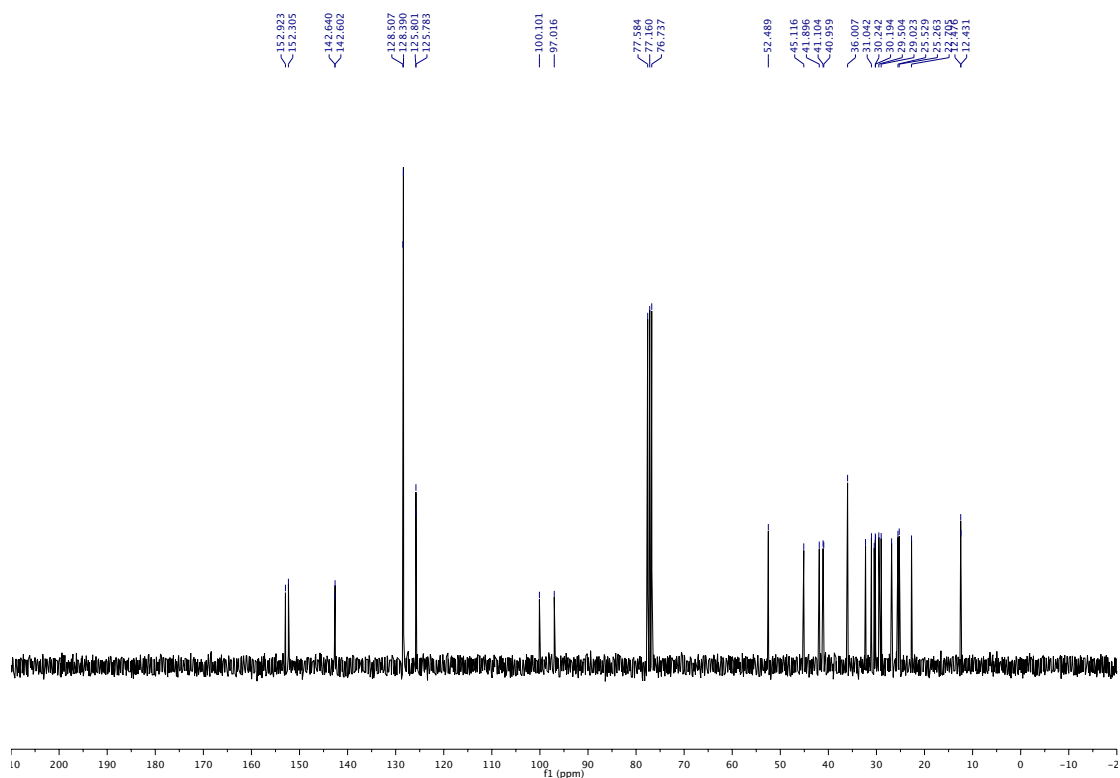
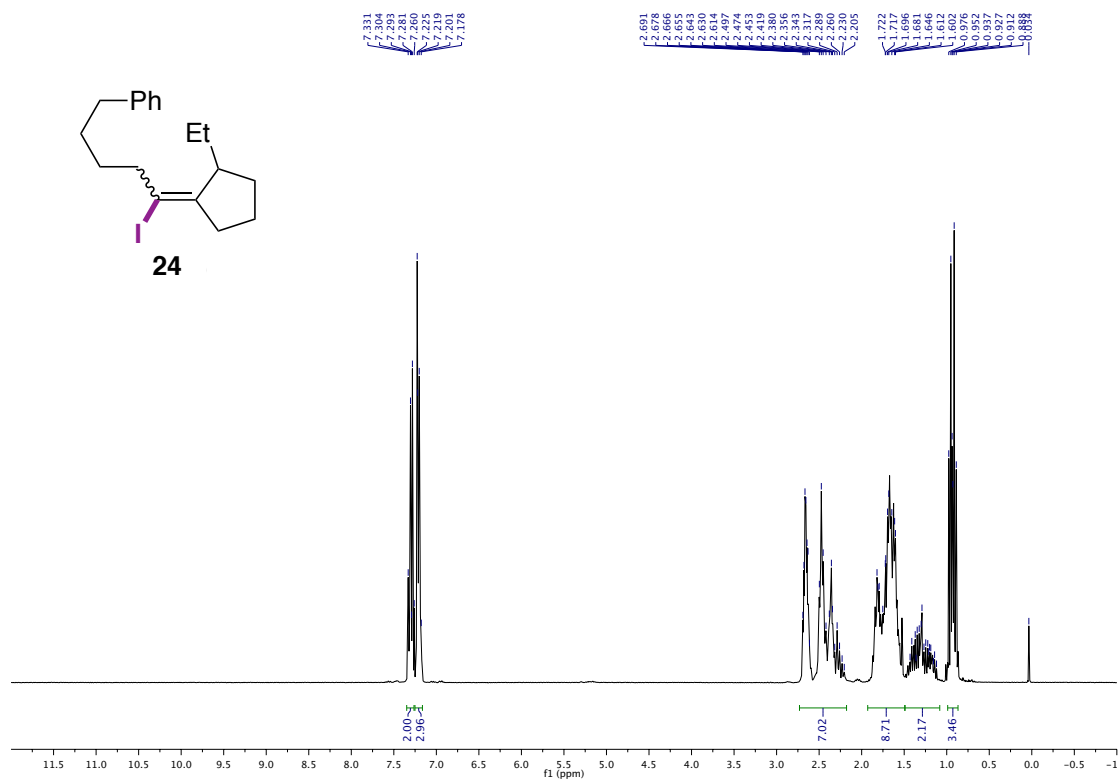


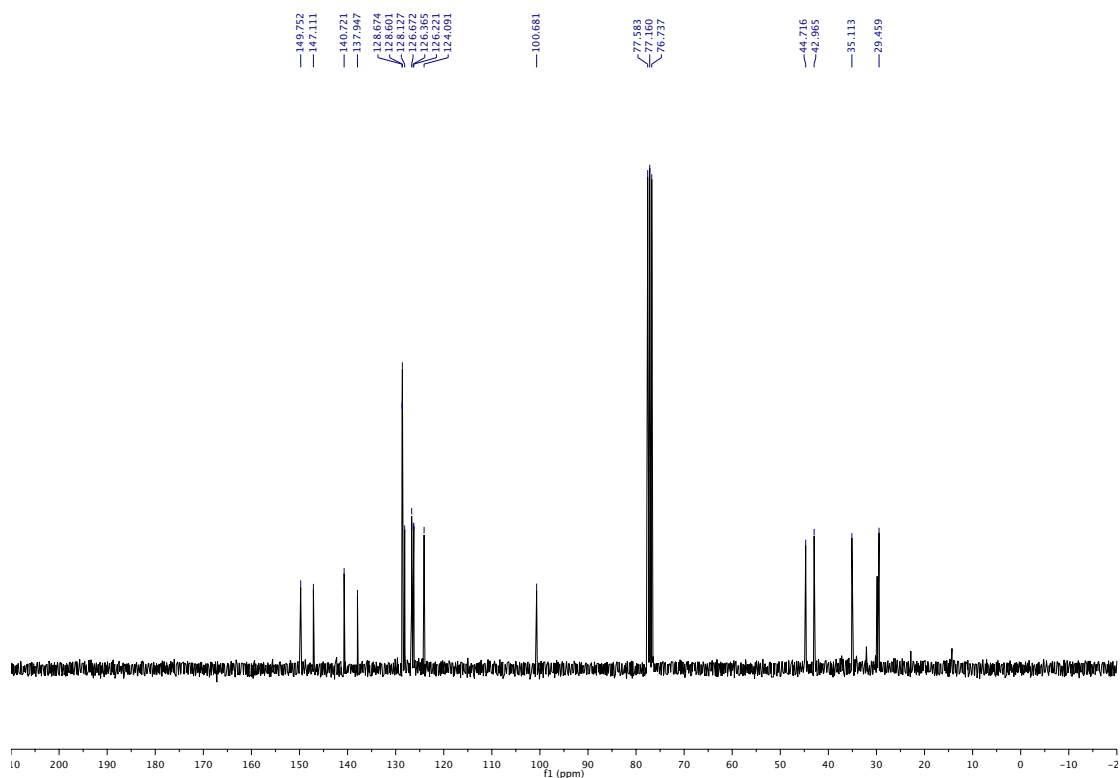
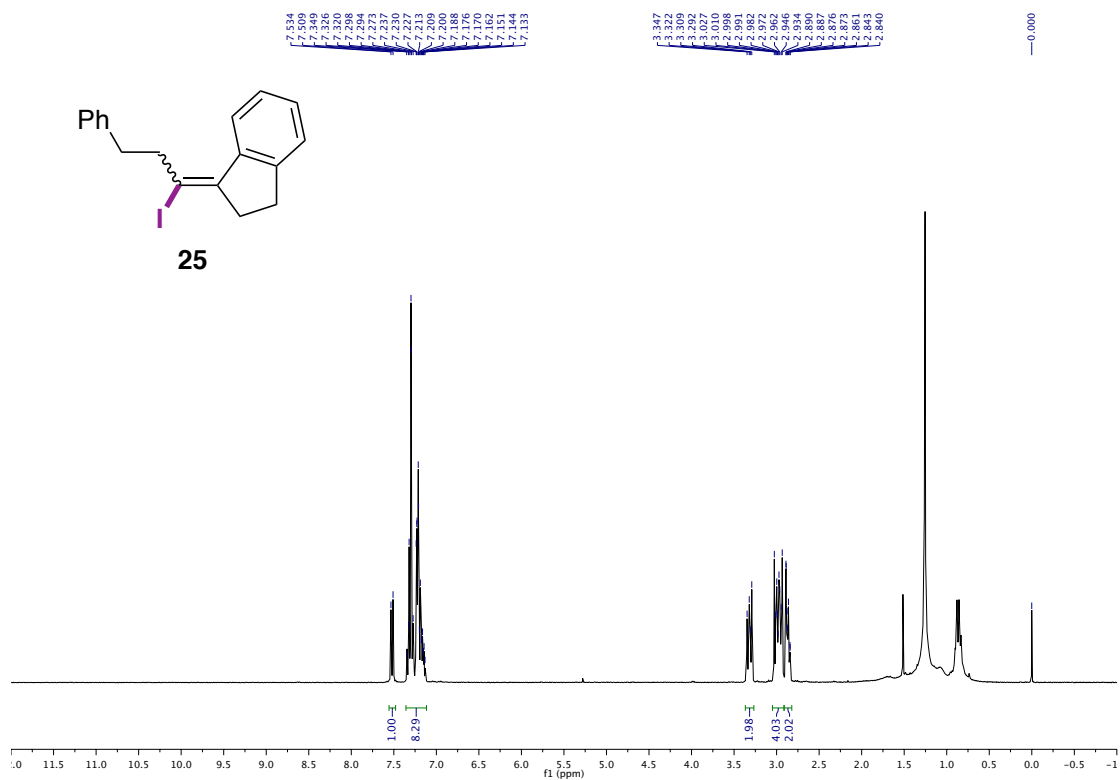


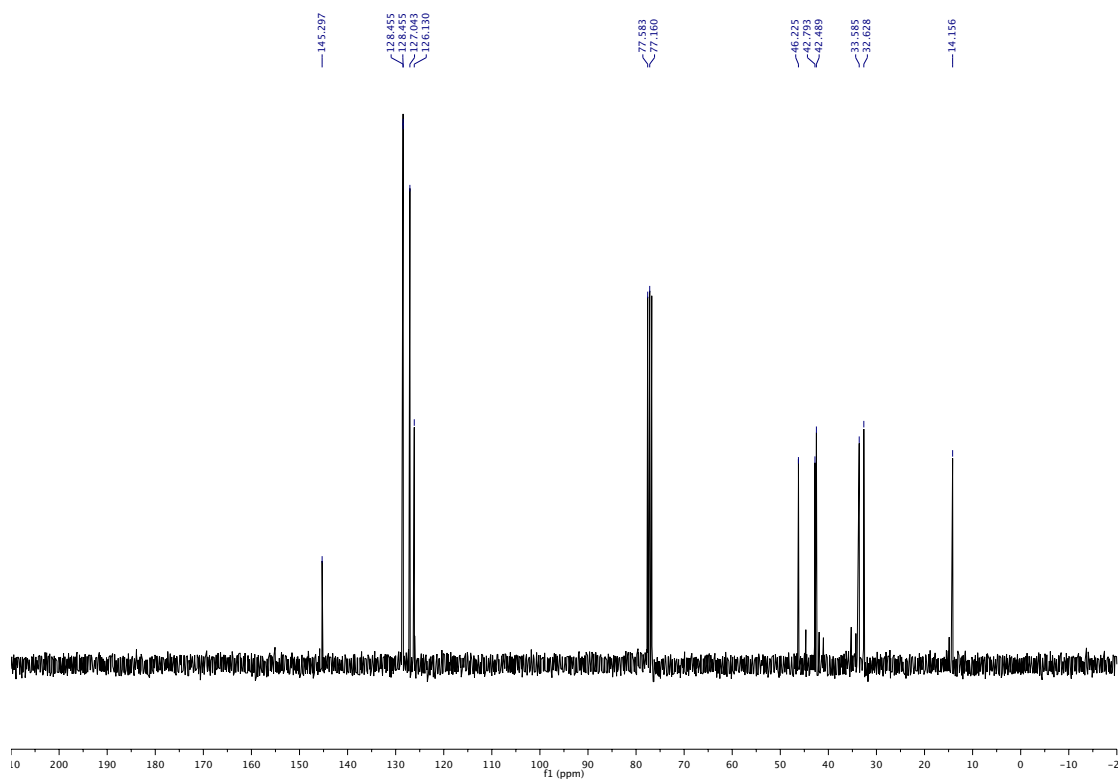
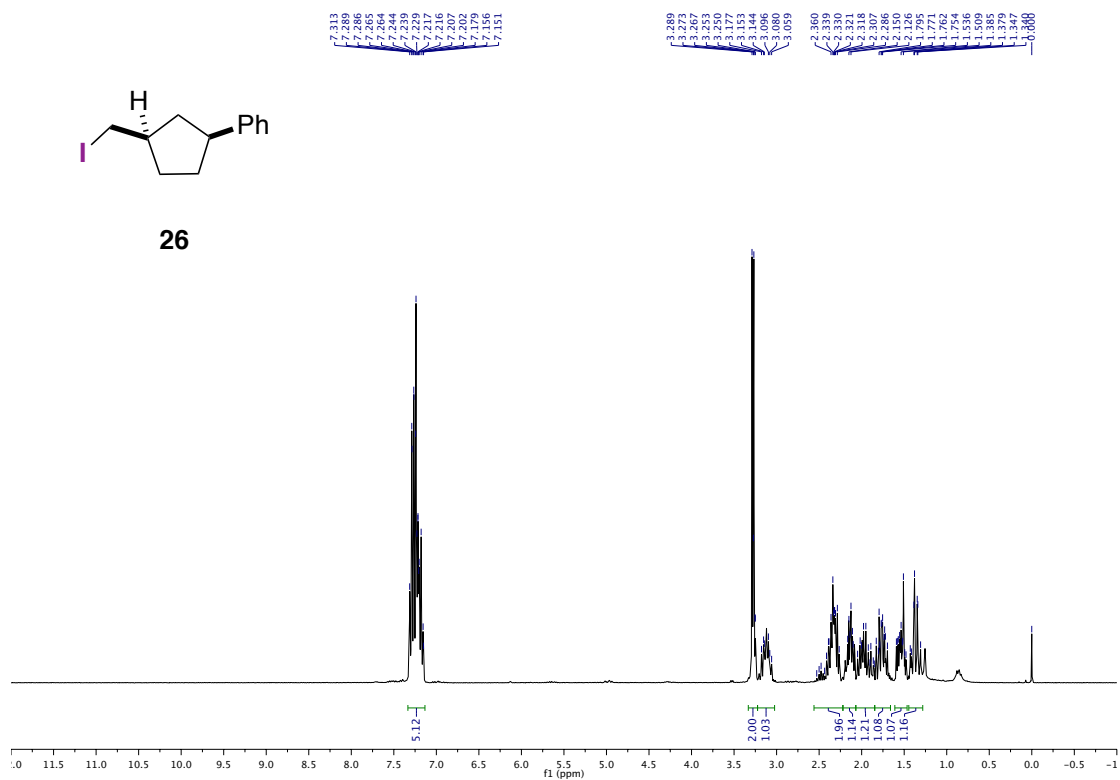


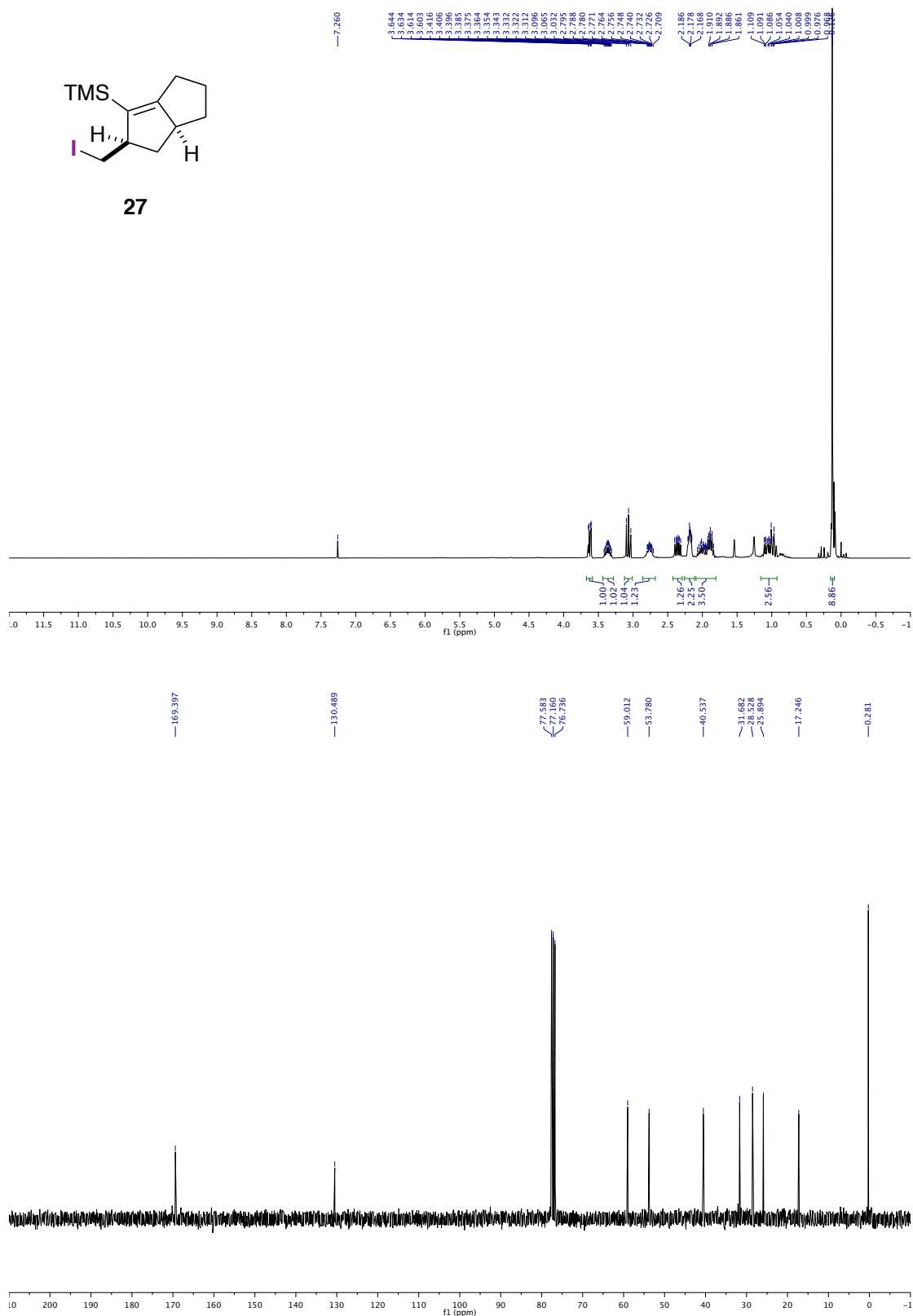


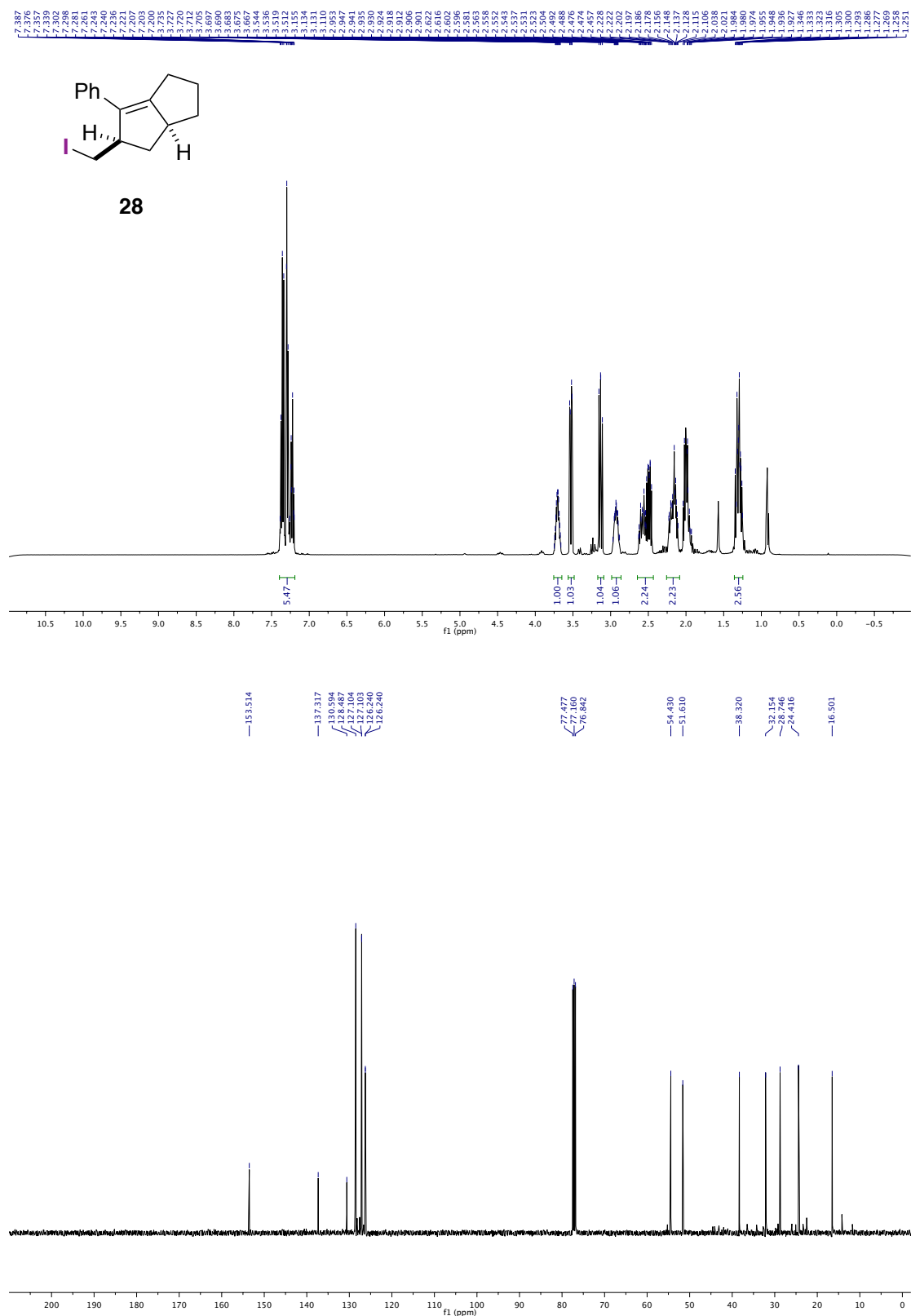


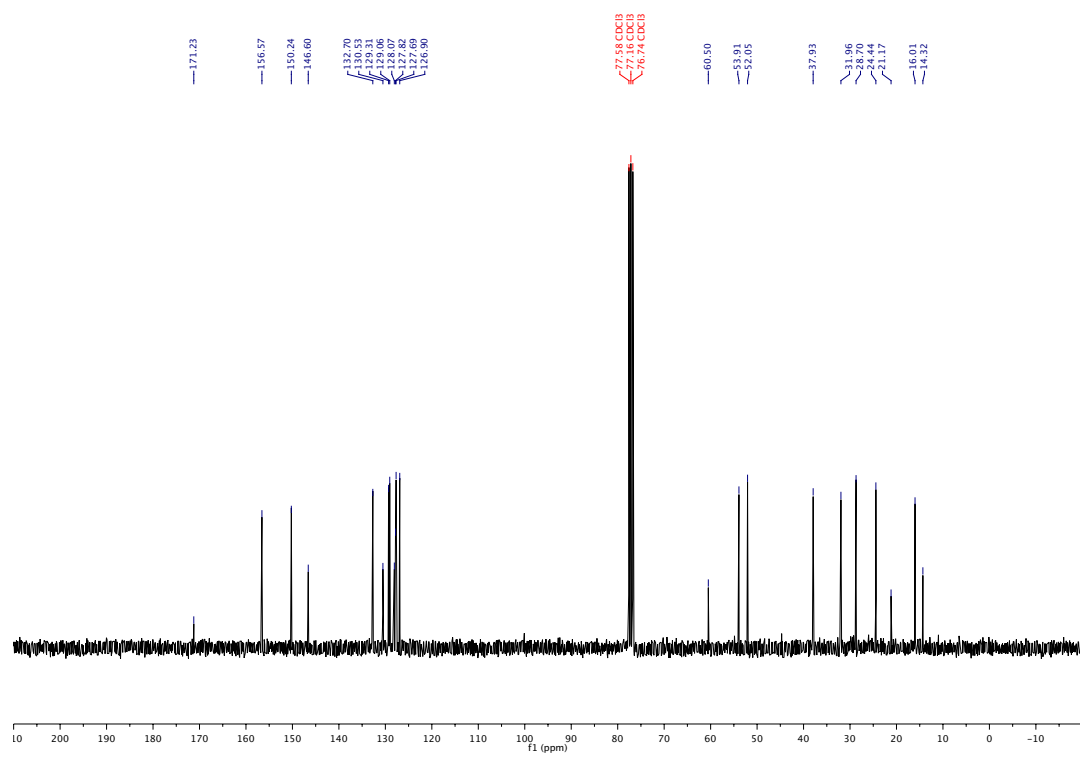
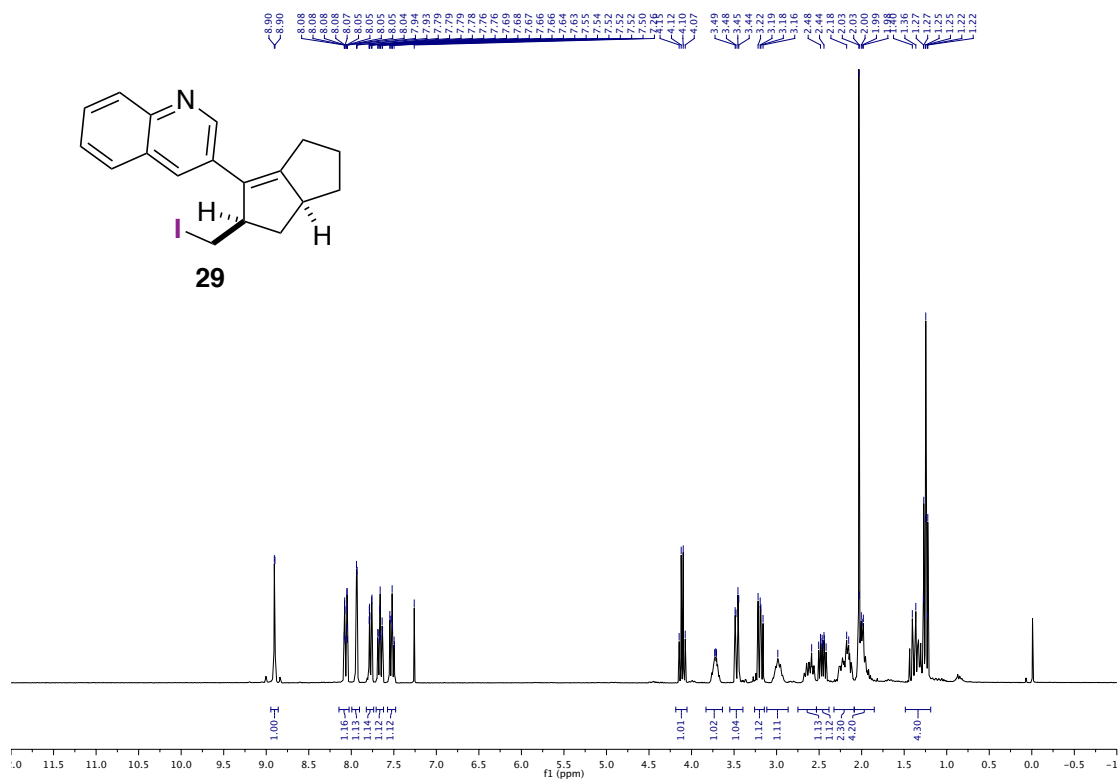


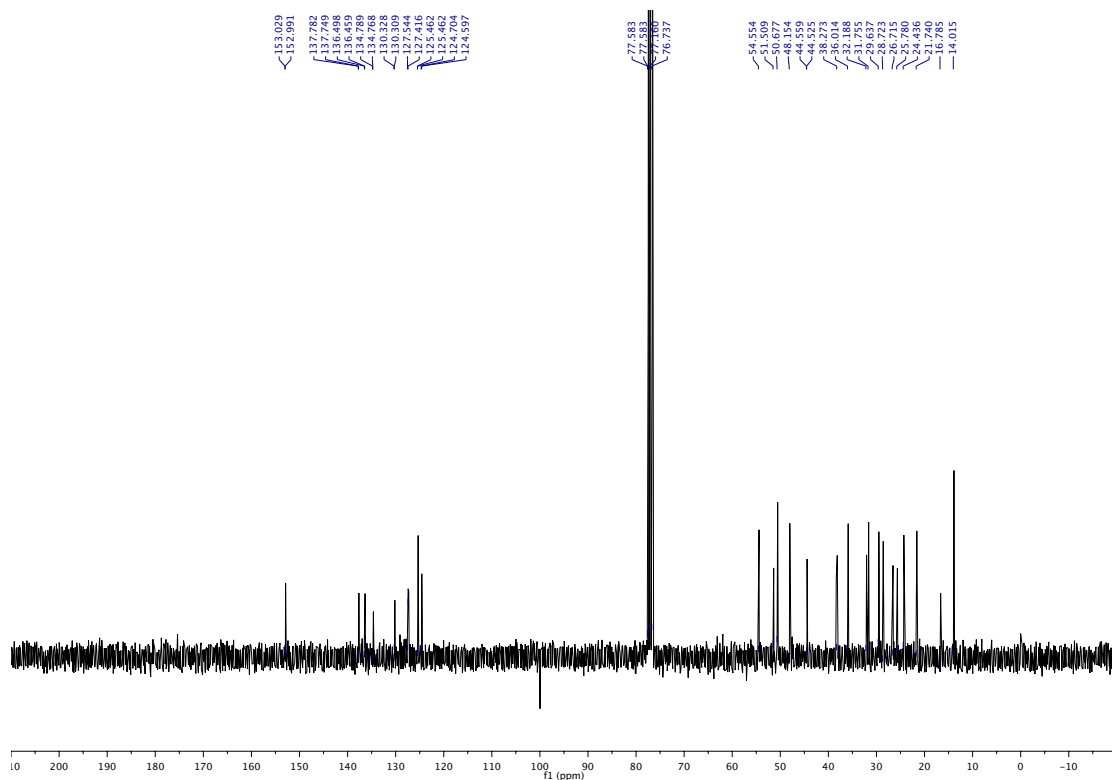
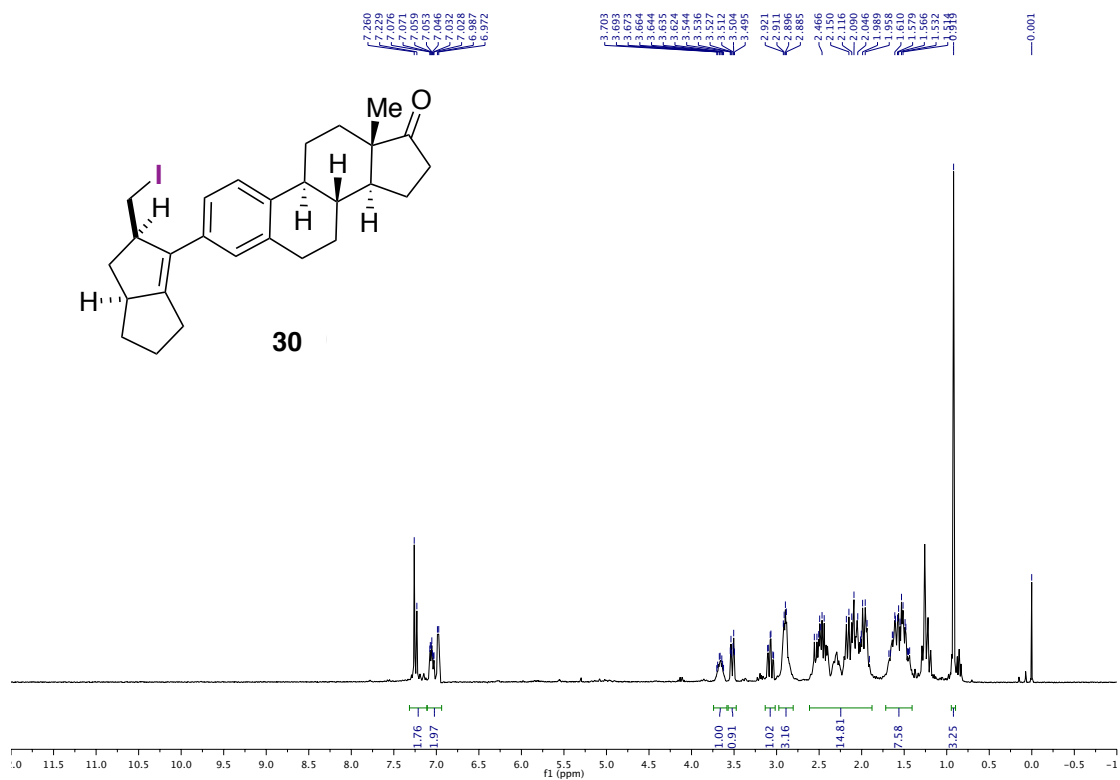














## **Chapter 3.**

### **Catalytic Intermolecular Dicarbofunctionalization of Styrenes with CO<sub>2</sub> and Radical Precursors**

### 3.1. Introduction: CO<sub>2</sub> Fixation *en route* to Phenyl Acetic Acid

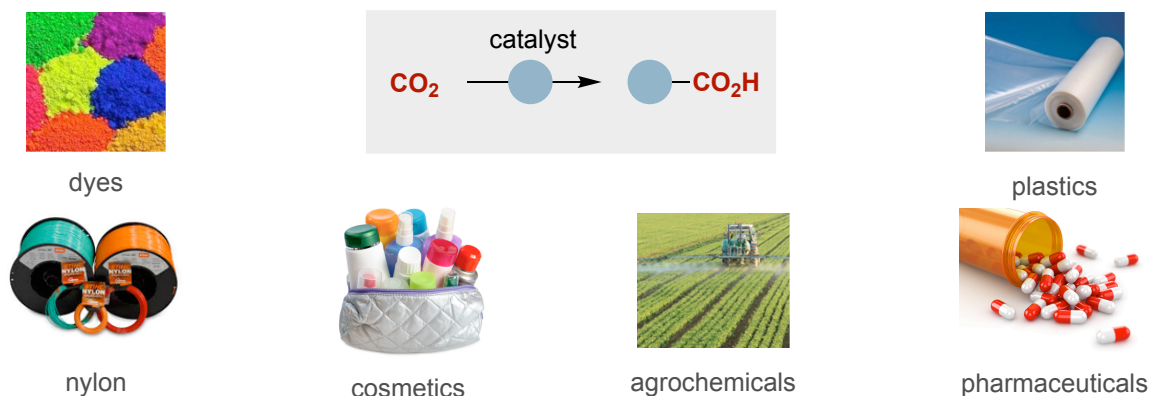
#### 3.1.1. The Global Crisis: Carbon Dioxide Concerning

As a consequence of our ever-increasing industrial activity, the carbon cycle on Earth has been seriously disrupted and the concentration of CO<sub>2</sub> has reached the “point of no return”, causing considerable concern from a both environmental and societal standpoint.<sup>1</sup> A myriad of solutions has been proposed and are currently explored, either at the research or technological stages. CO<sub>2</sub> Capture and storage technologies have the potential to mitigate meaningful volumes of CO<sub>2</sub> and a few demonstration plants are slowly emerging.<sup>1</sup> It is foreseeable, however, that this technology will suffer from the lack of added-value able to compensate the energetic and economic cost of CO<sub>2</sub> capture and deposition and the monitoring of the storage sites. The 30 Gt-CO<sub>2</sub> emitted annually primarily derive from the mineralization of carbon fossil resources, i.e. hydrocarbons, coal and gas.<sup>1</sup> Unfortunately, utilization of these feedstocks in the fuel sector represents 80% of the world energy portfolio and their transformation in the chemical industry accounts for the production of 95% of organic chemical commodities. In this context, CO<sub>2</sub> transformation to fuels and chemicals is a desirable alternative to CO<sub>2</sub> storage for cutting the emissions of this greenhouse gas. Although one might argue that CO<sub>2</sub> conversion into valuable chemicals will unlikely reduce its concentration in the atmosphere, it is worth noting that CO<sub>2</sub> is an abundant, inexpensive, clean and renewable C1 feedstock, thus providing an added value that might compensating the potential costs of its capture and recyclability. Yet, the transformation of CO<sub>2</sub> faces three challenges:

- First, the thermodynamic stability of CO<sub>2</sub> imposes an input of energy to convert CO<sub>2</sub> into other chemicals.
- The second challenge is kinetic in nature: catalysts are required to ensure that the activation barriers remain as low as possible along the chemical transformation pathways so that the overall carbon balance for CO<sub>2</sub> utilization is not hampered by thermal loading needed to overcome high energy transition states.
- CO<sub>2</sub> is not particularly soluble in the classical organic solvents that organic chemists employ for classical synthetic transformations.

While the vast majority of catalytic CO<sub>2</sub> fixation techniques are based on reduction techniques (e.g. methanol, methane, formic acid, formaldehyde),<sup>1c</sup> C-O bond-forming reactions (cyclic carbonates & polycarbonates or C-N bond-forming reactions (synthesis of Urea via Bosch-Meiser process),<sup>1d</sup> the ability to convert CO<sub>2</sub> into fine chemicals by means of catalytic C-C bond-forming reactions still remains largely underexplored. Among various scenarios, particularly attractive would be the ability

of converting CO<sub>2</sub> into carboxylic acids, valuable compounds of utmost relevance in industrial endeavors on the manufacture of cosmetics, soaps, detergents, rubbers, dyes, animal feed, plastics, agrochemicals or pharmaceuticals among others (Scheme 3.1).<sup>1f</sup>

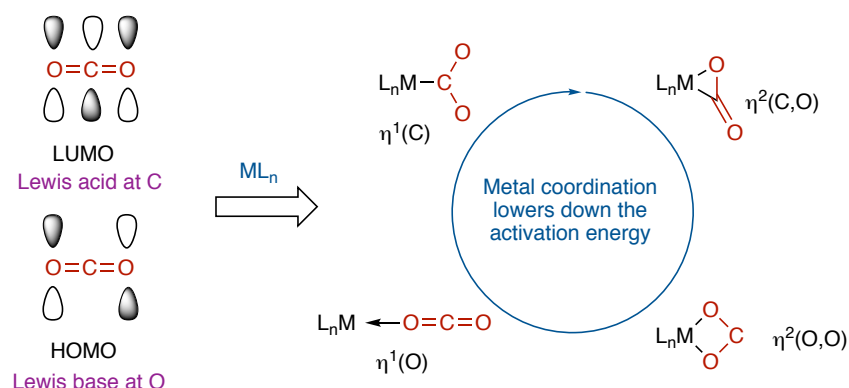


**Scheme 3.1. Daily application of carboxylic acids**

### 3.1.2. Catalytic CO<sub>2</sub> Fixation of Organic Matter en route to Carboxylic Acids

Although making carboxylic acids from CO<sub>2</sub> might constitute an ideal scenario in catalytic endeavors, CO<sub>2</sub> is a triatomic molecule with two dipoles opposite to each other, making the molecule of CO<sub>2</sub> non-polar with a remarkable thermodynamic and kinetic stability.<sup>1g</sup> Not surprisingly, the vast majority of carboxylation reactions are conducted with stoichiometric amounts of highly nucleophilic organometallic reagents capable of overcome the high barriers required for effecting CO<sub>2</sub> activation such as organolithiums, Grignard reagents or organozinc derivatives.<sup>2</sup> However, special precautions need to be taken into consideration when dealing with the utilization of air-sensitive organometallic reagents while the chemoselectivity of these processes is at serious risk, particularly when applying these technologies within the context of late-stage functionalization in the presence of multiple number of sensitive functional groups, thus reinforcing the need for designing catalytic carboxylation techniques in the absence of organometallic reagents. However, this is certainly not a chimera, as the molecule of CO<sub>2</sub> is ambiphilic in nature, possessing Lewis basicity at oxygen and Lewis acidity at carbon as a consequence of having two adjacent electronegative oxygen atoms. Additionally, CO<sub>2</sub> possesses two set of orthogonal  $\pi$ -orbitals that might interact with the d-orbitals of the transition metal. Indeed, multiple binding modes of mononuclear complexes to CO<sub>2</sub> are viable (Scheme 3.1).<sup>1g</sup> The first reported transition metal complex with CO<sub>2</sub> was the Aresta complex (Cy<sub>3</sub>P)<sub>2</sub>Ni(CO<sub>2</sub>), which was characterized as  $\eta^2(\text{C},\text{O})$  coordination mode, with the two corresponding C–O bonds being slightly more elongated (1.17 and 1.22 Å) than free CO<sub>2</sub> (1.16 Å).<sup>3</sup> Regardless of the activation modes of CO<sub>2</sub>

to transition metal complexes, such binding effectively deviates CO<sub>2</sub> from linearity, lowering down the activation energy of CO<sub>2</sub> and facilitating its subsequent functionalization.



**Scheme 3.1. Binding patterns of CO<sub>2</sub> with transition metal**

The conversion of CO<sub>2</sub> into carboxylic acids can formally occur via three different pathways (Figure 3.1): (a) coordination of the transition metal center to CO<sub>2</sub> followed by reaction with the organic substrate; (b) interaction of the organic substrate to the transition metal center prior to CO<sub>2</sub> binding; (c) dual coordination of the substrate and CO<sub>2</sub> to the transition metal center. As judged by the wealth of recent literature data,<sup>4</sup> the catalytic carboxylation reactions with CO<sub>2</sub> have entered a new era of exponential growth, evolving into a mature discipline that allows for streamlining the synthesis of carboxylic acids.

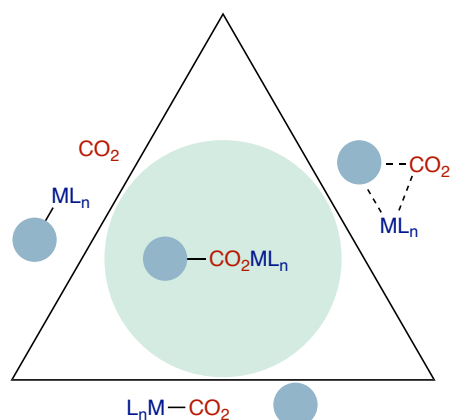
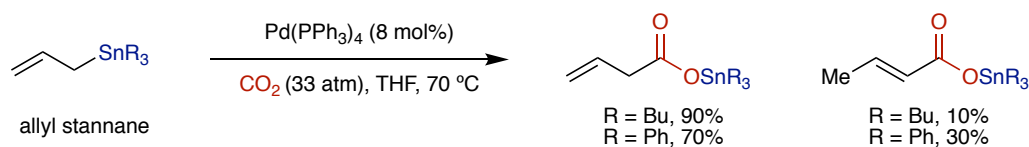


**Figure 3.1. The possible pathway of catalytic carboxylation**

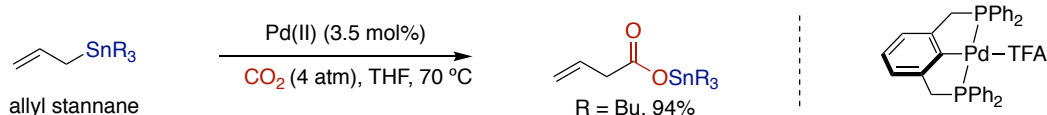
In 1997, Nicholas and co-workers reported the first metal-catalyzed carboxylation of organometallic compounds with CO<sub>2</sub>.<sup>5a</sup> Specifically, it was discovered that the exposure of allyl stannanes and Pd(PPh<sub>3</sub>)<sub>4</sub> to high pressure of CO<sub>2</sub> at 70 °C in THF gave rise to the corresponding allyltin esters (Scheme 5, *top*). Intriguingly, small amount of isomerization to the corresponding  $\alpha,\beta$ -unsaturated ester was observed. Although one might argue that the isomerization might occur from either the

starting allyl stannane or the final allyltin ester, control experiments in the absence of CO<sub>2</sub> revealed otherwise, suggesting that isomerization occurred during the course of the reaction. Although the protocol required high pressures of CO<sub>2</sub>, this discovery paved the way for designing catalytic CO<sub>2</sub> fixation with mild organometallic reagents.



**Scheme 3.2. The first Pd(0)-catalyzed carboxylation reaction with CO<sub>2</sub>**

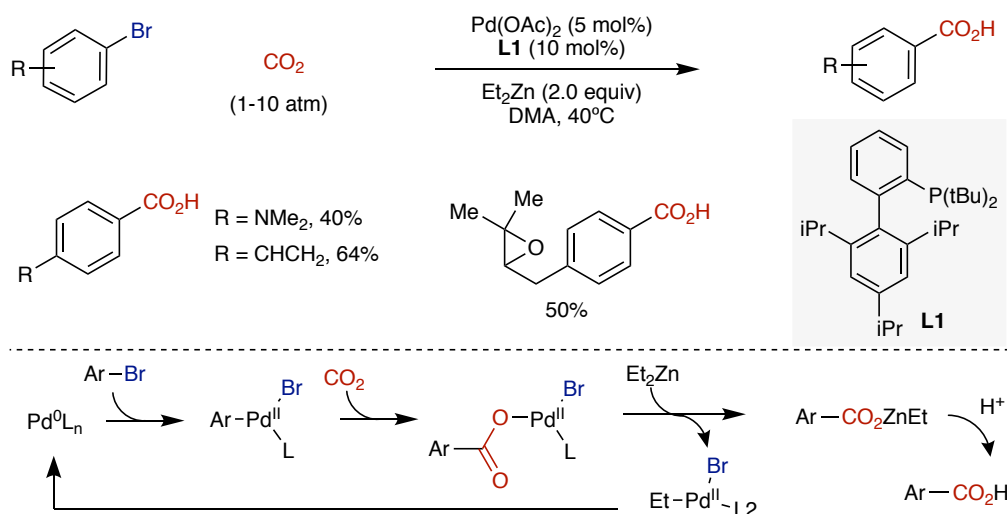
Few years later, it was found that the isomerization could be prevented by using a Pd(II) complex with a pincer ligand (Scheme 3.3).<sup>5b</sup> As the field developed, other organometallic reagents, such as organoboron,<sup>5c,5d,5e</sup> organozinc<sup>5f,5g,5h</sup> or organoaluminum reagents<sup>5i,5j,5k</sup> could all be utilized for preparing the corresponding carboxylic acids.



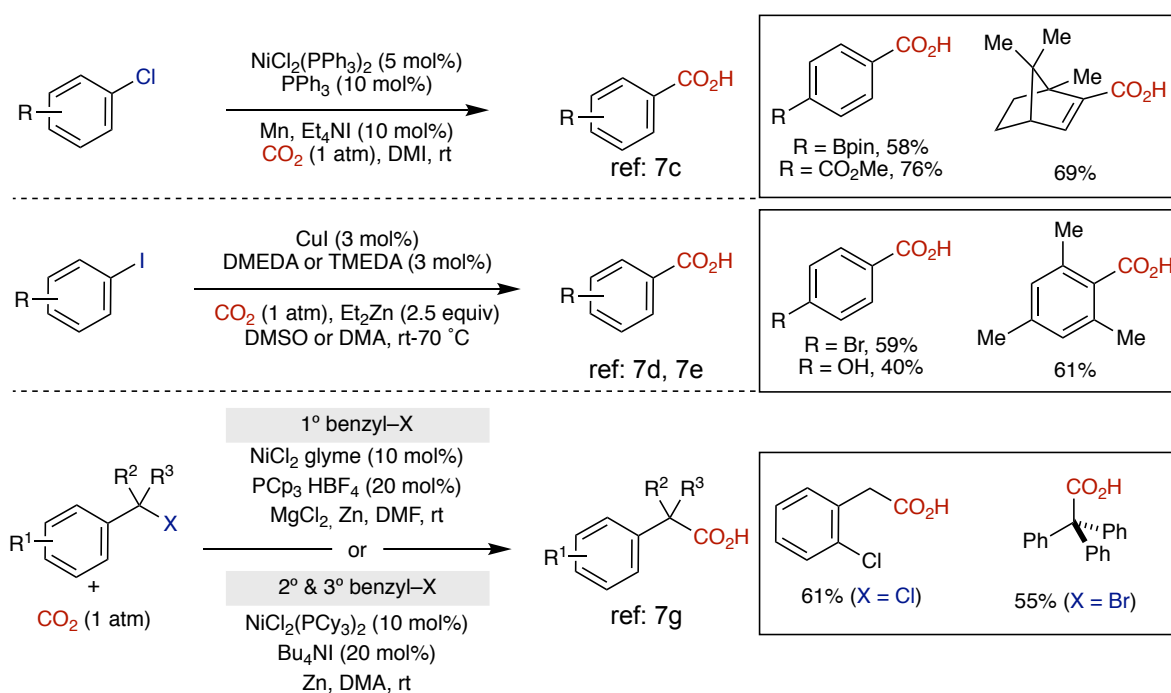
**Scheme 3.3. Pincer Pd(II) complexes in the catalytic carboxylation of allyl stannanes**

Despite the vast literature reported in catalytic carboxylation of organometallic species, these techniques necessarily required stoichiometric amounts of organometallic reagents. Driven by the observation that organometallic reagents are commonly prepared from the corresponding organic halides,<sup>6</sup> chemists were challenged to design catalytic carboxylation reactions with simple organic halides as coupling counterparts. However, this transformation is counterintuitive, as classical cross-coupling reactions are based on the combination of a nucleophile and electrophile, whereas the carboxylation of organic halides would necessarily invoke the coupling of two different electrophilic entities. In 1994, Osakada and Yamamoto reported a seminal paper what demonstrated that the oxidative addition complex PhNiBr(bpy) reacted with atmospheric CO<sub>2</sub> to deliver the corresponding benzoic acid in moderate yield.<sup>7a</sup> This seemingly innocent experiment suggested the viability of designing a catalytic carboxylation technology if a reductant would be employed to turnover the catalytically competent metal species. Intriguingly, however, this possibility remained dormant for nearly 15 years, when our group described the first catalytic carboxylation of aryl bromides with CO<sub>2</sub> (1-10 atm) (Scheme 3.4).<sup>7b</sup> Key for success was the employment of a bulky and electron-rich phosphine (*t*BuXPhos) ligand to avoid deleterious side reactions, such as Negishi-type coupling and reduction of starting materials via  $\beta$ -hydride elimination. Although this technology represented a

proof of concept for designing catalytic carboxylation reactions of organic halides, pyrophoric reducing agents ( $\text{Et}_2\text{Zn}$ ) were required for the reaction to occur.



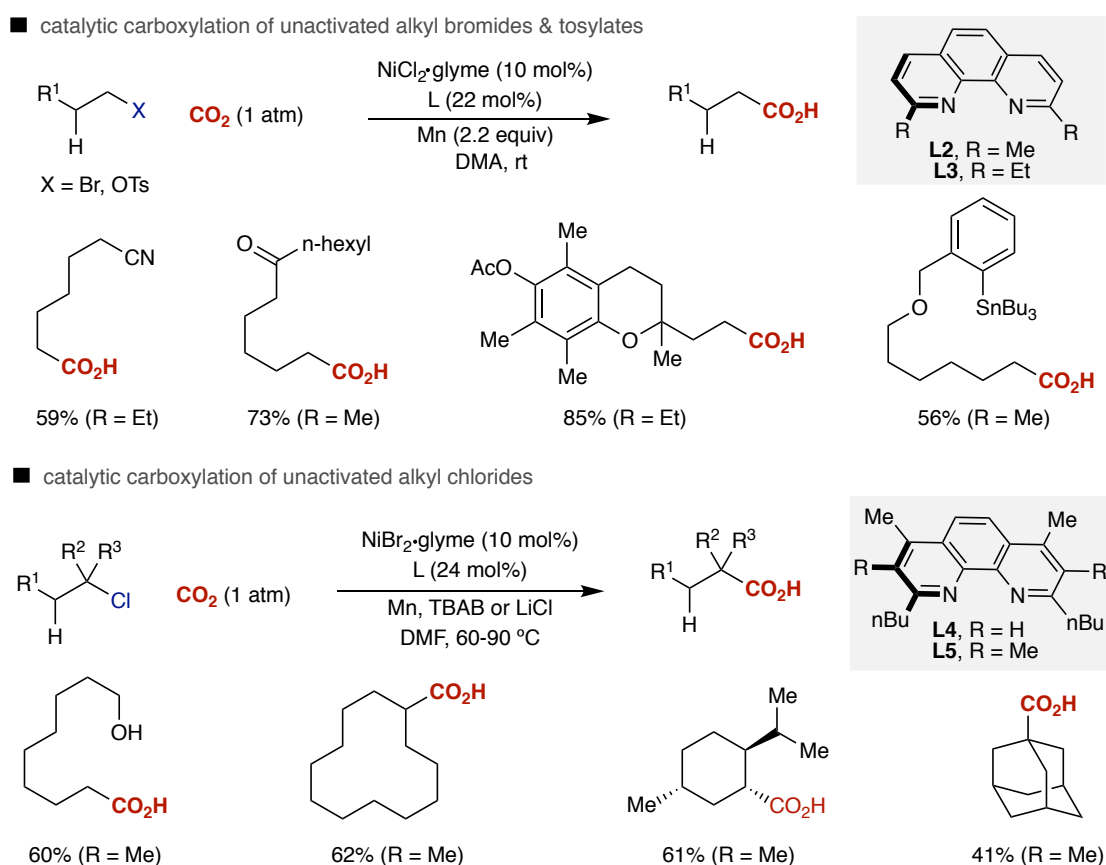
**Scheme 3.4. The first Pd-catalyzed carboxylation of aryl bromides**



**Scheme 3.5. Ni-catalyzed carboxylation of aryl and alkenyl chlorides**

In 2012, Tsuji and co-workers extended the scope of catalytic carboxylations of organic halides to the more challenging and readily available aryl and vinyl chlorides at atmospheric pressure of  $\text{CO}_2$  (Scheme 3.5).<sup>7c</sup> It was shown that the combination of air-stable metallic reductant (Mn) and ammonium salts ( $\text{Et}_4\text{I}$ ) were critical to success. Subsequently, Daugulis described the viability for using Cu catalysts for the carboxylation of aryl iodides using  $\text{Et}_2\text{Zn}$  as reducing agent.<sup>7d,7e</sup> Our group managed to extend the scope of these reactions beyond the use of aryl halides, including the

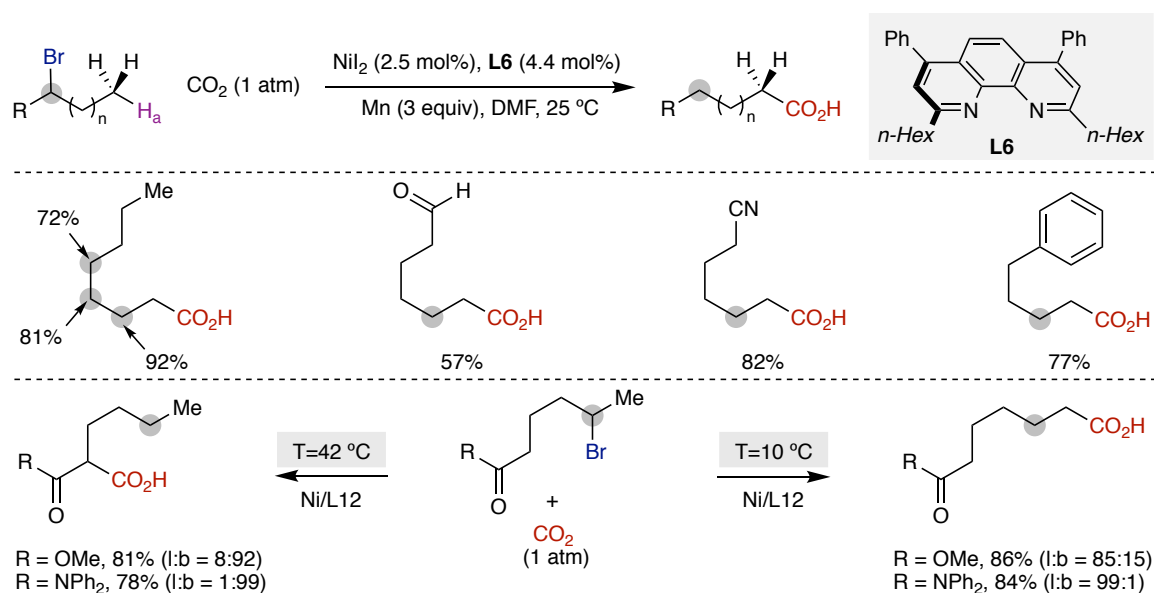
carboxylation of phenol electrophiles,<sup>7f</sup> primary, secondary or tertiary benzyl halides,<sup>7g</sup> benzyl C–O electrophiles,<sup>7f</sup> benzyl amines<sup>7h</sup> or allyl C–O electrophiles.<sup>7i,7j</sup> The latter is particularly noteworthy, as it was found that the ligand, rather than the substrate, dictated the regioselectivity profile, obtaining either branched or linear carboxylic acids depending on the geometry of the ligand employed. Although these methodologies demonstrated the viability of conducting catalytic carboxylation reactions, it is worth noting that these reactions required the utilization of substrates that easily underwent oxidative addition.



**Scheme 3.6. Ni-catalyzed carboxylation of unactivated alkyl electrophiles**

Aimed at improving the generality of catalytic carboxylation reactions, our research group described two protocols for the carboxylation of primary, secondary or tertiary unactivated alkyl bromides, tosylates or even the less-reactive alkyl chlorides (Scheme 3.6).<sup>7k,7l</sup> This extension was particularly important taking into consideration the myriad of pharmaceuticals or molecules that display important biological properties that possess a carboxylic acid within the alkyl side-chain. Additionally, the successful realization of this goal was a remarkable step-forward, indicating that the putative oxidative addition species could be trapped by unreactive CO<sub>2</sub> while avoiding parasitic β-hydride elimination, homodimerization or reduction events via competitive HAT processes. Particularly

intriguing was the role exerted by the ligand backbone. Specifically, it was found that the inclusion of substituents adjacent to the nitrogen-containing ligand, particularly phenanthroline backbones, was critical for success. Although tentative, this feature probably is due to the ability of generating Ni(I) intermediates that react more efficiently with CO<sub>2</sub> than the corresponding Ni(II) congeners.<sup>7k</sup> Under these reaction conditions, a wide variety of substrates possessing a wide variety of functional groups could perfectly be tolerated, serving as a testament to the broad applicability of catalytic carboxylation reactions in the alkyl series.

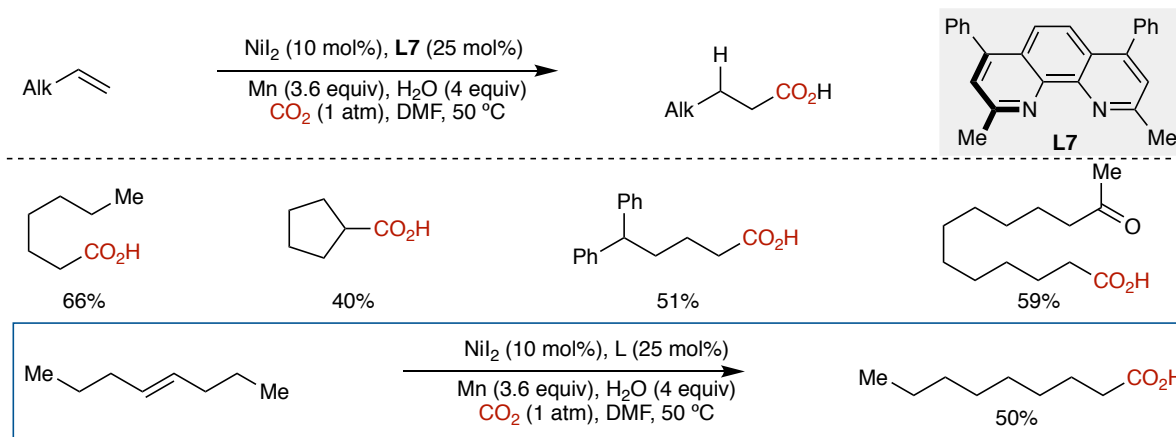


### Scheme 3.7. Ni-catalyzed remote carboxylation

Although  $\beta$ -hydride elimination has long been the goal in organometallic chemistry when dealing with the cross-coupling of unactivated alkyl halides,<sup>7m</sup> our research group envisioned that parasitic  $\beta$ -hydride elimination could be turned into a strategic advantage. Specifically, in 2017 we designed a Ni-catalyzed remote carboxylation of bromoalkenes that occurred at remote unfunctionalized  $sp^3$  C–H reaction sites by means of chain-walking reactions (Scheme 3.7).<sup>7n</sup> Once again, the nature of the ligand was critical for success, with large substituents adjacent to the nitrogen atom as well as electron-withdrawing motifs at 4,7-position on a phenanthroline backbone providing the best results while facilitating an iterative sequence of  $\beta$ -hydride elimination/migratory insertion sequences throughout the alkyl side-chain, thus enabling the implementation of a chain-walking process.<sup>7o</sup> While the role of such *ortho*-substituents was believed to accelerate  $\beta$ -hydride elimination by accelerating halide dissociation at the metal center, the inclusion of electron-withdrawing units made the metal center more electrophilic, thus resulting in a strong binding with the in situ generated olefin. As the site-selectivity was controlled by the chain-walking motion, it was found that even simple



alkanes or mixtures of olefins can be used as substrates, enabling the carboxylation of these chemical feedstocks in a two-step, one-pot fashion, via the intermediacy of an inconsequential mixtures of alkyl halides by unselective halogenation of the starting precursors.

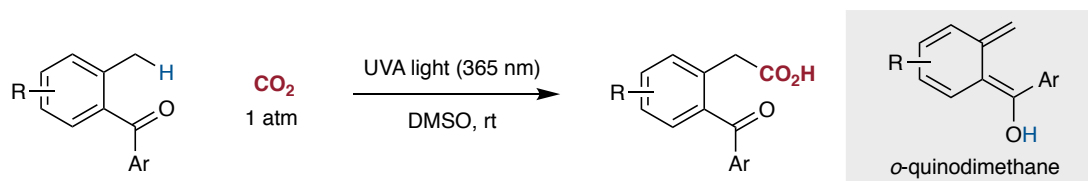


**Scheme 3.8. carboxylation of olefin with H<sub>2</sub>O and CO<sub>2</sub>**

Aimed at improving the practicality of catalytic carboxylation reactions, our group demonstrated that the corresponding alkyl halides can be replaced by simple and abundant olefin partners (Scheme 3.8).<sup>7p</sup> Particularly intriguing was the observation that simple water is capable of triggering the carboxylation of styrenes or even  $\alpha$ -olefins with equal ease, delivering the corresponding phenyl acetic acids or alkyl carboxylic acids, respectively.<sup>7p</sup> The successful realization of this principle was noteworthy if one takes into consideration that stoichiometric amounts of highly reactive organometallic species, in some instances manganese pyrophoric, were required for effecting the carboxylation of either styrenes or unactivated alkenes.<sup>7q,7r,7s</sup> Particularly interesting was the ability to find a chain-walking scenario when using internal, unactivated olefins. Although chain-walking reactions invariably resulted in linear carboxylic acids, the site-selectivity of the process could be switched by employing alkynes instead, resulting in the corresponding  $\alpha$ -branched acids instead. This was explained by the intermediacy of nickelalactones resulting from an oxidative cycloaddition of Ni(0)L<sub>n</sub>, CO<sub>2</sub> and the corresponding alkyne.<sup>7p</sup>

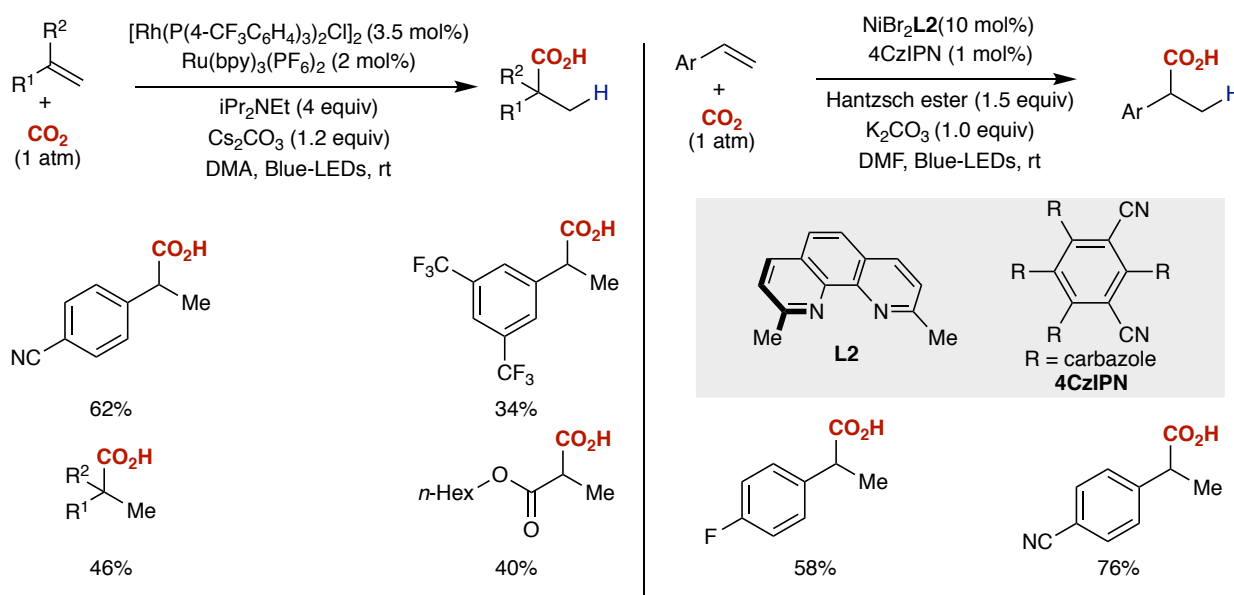
Putting everything into perspective the ability to extend the catalytic carboxylation of alkyl halides to the utilization of simple olefins was particularly noteworthy, constituting a step-forward for the development of more practical reactions. Still, however, it is fair to notice that the catalytic carboxylation of both organic halides and alkenes remains confined to *single C–C bond formations*, necessarily requiring the utilization of stoichiometric metal reductants. Additionally, specialized ancillary ligands are required in the former, reinforcing the need for a change in strategy.

### 3.1.3. Photochemical Carboxylation with CO<sub>2</sub>



**Scheme 3.9. Photochemical benzylic C-H carboxylation**

In 2015, Murakami and co-workers reported a system for the preparation of phenylacetic acids from *ortho*-methyl benzophenones under UVA light (or even sun light) irradiation under CO<sub>2</sub> atmospheres. The transformation formally consists of a benzylic C–H carboxylation without the need for stoichiometric amounts of metal reductants (Scheme 3.9).<sup>8a</sup> The reaction proceeded via the intermediacy of an *o*-quinodimethane and subsequent [4+2] cycloaddition with CO<sub>2</sub> as dienophile, an observation that was supported by DFT calculations.

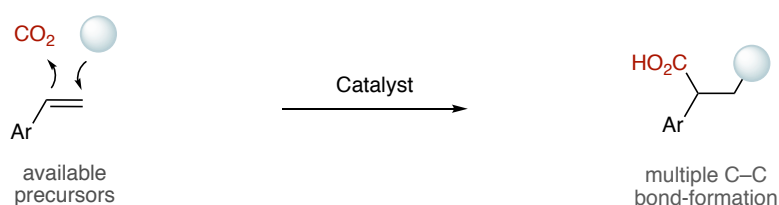


**Scheme 3.10. Photochemical hydrocarboxylation of styrenes**

Taking into consideration that the role of metallic reductants in catalytic carboxylation reactions is to trigger single-electron transfer processes, one might argue that the implementation of photoredox catalysis within the carboxylation arena could represent an important step-forward for improving the practicality and generality of these processes. Driven by these observations, Iwasawa and co-workers described the merger of transition metal catalysis and photocatalysis for the hydrocarboxylation of styrenes in the presence of a tertiary amine and Rh(I) species.<sup>8b</sup> Such a combination likely generates Rh(III) hydride species, which subsequently might react with styrene and CO<sub>2</sub> to deliver the corresponding phenyl acetic acids (Scheme 3.10, *left*). Later on, König disclosed a related system

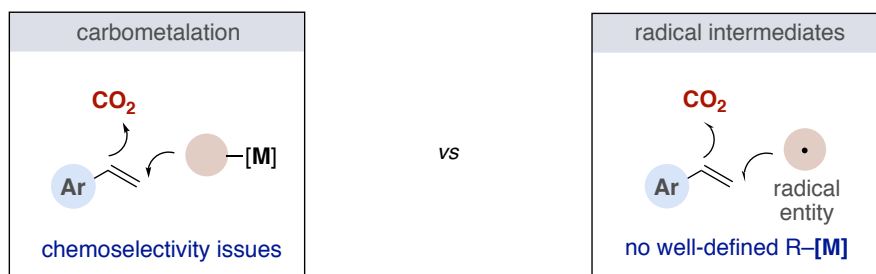
using Hantzsch ester and organic photocatalysts as electron and hydride sources by using Ni catalysis and *ortho*-substituted phenanthroline ligands, giving rise to the corresponding phenyl acetic acids (Scheme 3.10, *right*).<sup>8c</sup> Recently, the group of Da-Gang Yu and Jamison have extended these notions beyond the hydrocarboxylation of olefins.<sup>9</sup> Still, however, these technologies remain predominantly confined to *single* C–C bond-forming reactions, thus suggesting that the ability to trigger *multiple* C–C bond-forming reactions across an olefin with concomitant formation of the targeted carboxylic acid would be highly appreciated.

### 3.2. General Aim of the Project



**Scheme 3.11. General design of carbocarboxylation of styrenes**

Taking a close look at the known literature data on carboxylation reactions of  $\pi$ -components, we wondered whether we could design a site-selective principle for the redox-neutral catalytic dicarbofunctionalization of olefins with CO<sub>2</sub> and an appropriate carbon nucleophile (Scheme 3.11).



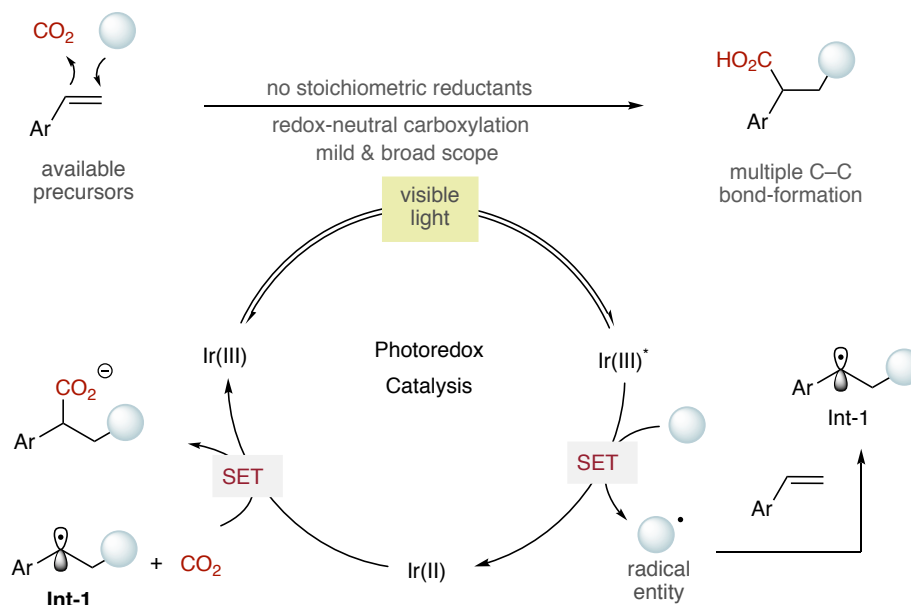
**Scheme 3.12. Dicarbofunctionalization of olefins with CO<sub>2</sub>**

Aimed at providing a rationale for such reaction, we envisioned that two different approaches could be designed for such purposes: (a) a carbometalation of an organometallic reagent across an olefin followed by CO<sub>2</sub> insertion (Scheme 3.12, *left pathway*) or (b) initial addition of a radical precursor across an olefin followed by CO<sub>2</sub> insertion (Scheme 3.12, *right pathway*). However, chemoselectivity issues might arise in the former, as the corresponding organometallic reagent might react with CO<sub>2</sub> prior addition across the olefin. Additionally, such a route might not tolerate a wide range of functional groups. Alternatively, the radical route offers the advantage of reacting preferentially with the corresponding alkene prior to CO<sub>2</sub> insertion in the absence of organometallic reagents. That being set, we wondered whether we could establish a design principle for accomplishing the goal of

triggering a redox neutral dicarbofunctionalization of olefins with in situ generated radical intermediates.

### 3.3. Dicarbofunctionalization of Styrenes with CO<sub>2</sub> and Radical Precursors

#### 3.3.1. Mechanistic Rationale



**Scheme 3.13. Mechanistic rationale of dicarbofunctionalization of styrenes with CO<sub>2</sub>**

A priori, a radical entity will add across a styrene with high regioselectivity profile, ending up in a corresponding benzyl radical. Upon subsequent CO<sub>2</sub> insertion, we expected to generate the corresponding carboxyl radical. While amenable for CO<sub>2</sub> extrusion, we hypothesized that we could reduce this intermediate to the corresponding carboxylate, thus preventing decarboxylative pathways. To such end, and taking into consideration that two SET would be necessary to generate the carbon radical and the subsequent carboxylate anion, we wondered whether a photoredox platform could be designed for tackling the challenge of promoting a dicarbofunctionalization of olefins with CO<sub>2</sub> (Scheme 3.13). If successful, such a scenario might unravel a multifaceted challenge, not only providing the synergistic merger of visible light photoredox catalysis and CO<sub>2</sub> with  $\pi$ -systems,<sup>10,11</sup> but also offering an unrecognized opportunity in catalytic carboxylations to enable multiple, intermolecular C–C bond-formations.<sup>12,13</sup> Indeed, such a technology might offer a complementary approach in classical catalytic carboxylation reactions, as no sophisticated ligand backbones or stoichiometric metal reductants would be required.

### 3.3.2. Optimization of the Reaction Conditions

Entry	Ir(III)	$E_{1/2}[\text{Ir(III)}^*/\text{Ir(II)}]^b$	$E_{1/2}[\text{Ir(III)}/\text{Ir(II)}]^b$	<b>1</b> (%) <sup>a</sup>
1	<b>Ir-2</b>	+0.84 V	-1.34 V (-1.54)	90 (86) <sup>c</sup>
2	<b>Ir-3</b>	+1.39 V	-1.21 V (-1.37)	50
3	<b>Ir-4</b>	+1.50 V	-1.11 V (-1.37)	29
4	<b>Ir-5</b>	+1.17 V	-1.31 V (-1.72)	57
5	<b>Ir-6</b>	+1.34 V	-1.23 V	54
6	<b>Ir-7</b>	+1.29 V	-1.20 V	58
7	<b>Ir-8</b>	+1.39 V	-1.06 V	44
8	<b>Ir-9</b>	+1.27 V	-1.24 V	65

Reaction Conditions: **1s** (0.20 mmol), CF<sub>3</sub>SO<sub>2</sub>Na (0.24 mmol), CO<sub>2</sub> (1 bar), DMF (0.10 M) at rt for 15 h. <sup>a</sup> NMR yields using PhCF<sub>3</sub> as internal standard. <sup>b</sup> vs SCE in DMF (in MeCN). <sup>c</sup> Isolated yield.

**Ir-2**

**Ir-3** (R<sup>1</sup> = CF<sub>3</sub>, R<sup>2</sup> = *t*-Bu)

**Ir-6** (R<sup>1</sup> = CF<sub>3</sub>, R<sup>2</sup> = OMe)

**Ir-4** (R<sup>1</sup> = CF<sub>3</sub>, R<sup>2</sup> = H)

**Ir-7** (R<sup>1</sup> = F, R<sup>2</sup> = *t*-Bu)

**Ir-5** (R<sup>1</sup> = H, R<sup>2</sup> = OMe)

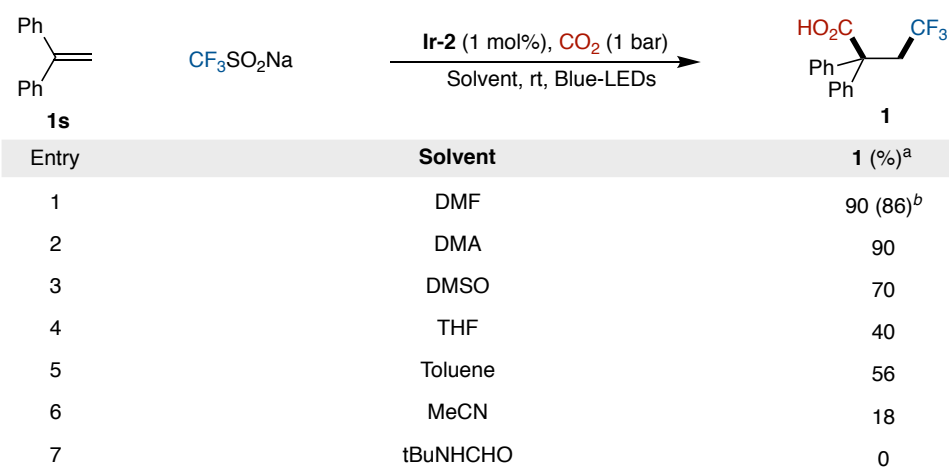
**Ir-8** (R<sup>3</sup> = R<sup>4</sup> = H)

**Ir-9** (R<sup>3</sup> = CF<sub>3</sub>, R<sup>4</sup> = Ph)

**Table 3.1. Photocatalysts screening**

Prompted by the importance of perfluorinated alkyl groups in drug discovery, our investigations started by studying the catalytic redox-neutral trifluoromethylcarboxylation reaction of **1s** with Langlois reagent (CF<sub>3</sub>SO<sub>2</sub>Na) and CO<sub>2</sub> (1 bar) under blue light-emitting diodes (LEDs) irradiation at room temperature (Table 3.1).<sup>15,16</sup> We initially chose DMF as solvent based on the successful carboxylation reactions reported by our group in which this solvent was critical to promote the targeted CO<sub>2</sub> fixation. As anticipated, the nature of the photocatalyst markedly influenced the reaction outcome, with **Ir-2** ( $E_{\text{red}}[\text{Ir}^{\text{III}}/\text{Ir}^{\text{II}}] = -1.34$  V vs SCE in DMF, -1.51 V in MeCN) providing the best results (entry 1).<sup>17</sup> Intriguingly, the use of otherwise related photocatalysts **Ir-3** to **Ir-9** with less reducing ability all resulted in significant lower yields of **1** (entry 2-8). Although speculative, these findings might be interpreted on the basis of a more efficient SET from the reduced photocatalyst **Ir-2**<sup>18</sup> to the corresponding 1,1-diphenyl 3,3,3-trifluoropropane benzyl radical that results from the corresponding addition of the radical across the styrene backbone ( $E_{\text{red}} = -1.34$  V vs SCE in MeCN)<sup>19</sup> prior to CO<sub>2</sub> insertion (Scheme 3.4).<sup>20</sup> It is worth noting that the reduction potential in MeCN is

normally lower than in DMF based on the data we have gathered (Table 3.1, entry 1-4), thus indicating that diphenyl substituted styrenes might be replaced by regular styrenes.

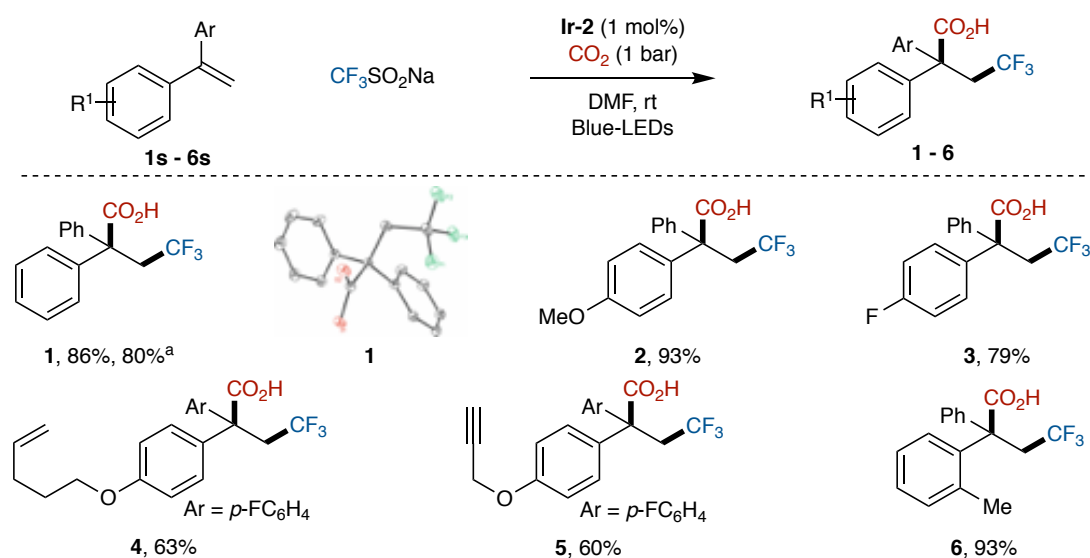


Reaction Conditions: **1s** (0.20 mmol), CF<sub>3</sub>SO<sub>2</sub>Na (0.24 mmol), CO<sub>2</sub> (1 bar), Solvent (0.10 M) at rt for 15 h. <sup>a</sup> NMR yields using PhCF<sub>3</sub> as internal standard. <sup>b</sup> Isolated yield.

**Table 3.2. Solvents screening**

Even though DMF is routinely used in carboxylation reactions,<sup>4</sup> we wondered whether non-amide solvents could also be utilized with equal efficiency. As shown in Table 3.2, this was not the case, and the absence of amide-containing solvents had a deleterious effect on reactivity (entries 4-6). This can be rationalized due to the lower solubility of CO<sub>2</sub> in these solvents and the better solvation of the transient nucleophilic entity in polar aprotic environments. Rigorous control experiments revealed that not even traces of **1** were found in the absence of light or **Ir-2**.

### 3.3.3. Substrate Scope with Langlois Reagent



Conditions as in Table 3.1 (entry 1). Isolated yields, average of at least two independent runs. <sup>a</sup> 1.0 mmol scale (**1s**).

**Table 3.3. Substrate scope with diaryl styrenes and Langlois reagent**

With the optimized conditions in hand (Table 3.1, entry 1), we turned our attention to examine the generality of our trifluoromethylcarboxylation with 1-arylstyrenes and  $\text{CF}_3\text{SO}_2\text{Na}$  (Table 3.3).<sup>21,22</sup> As shown by the results compiled in Table 3.3, diaryl-substituted styrenes offered good to excellent reactivity in the presence of a variety of functional groups. For example, terminal alkyne and alkene could be perfectly accommodated (**5** and **6**), resulting in the corresponding quaternary carbon centers in good yields. This is particularly important given that previous carboxylations aimed at accessing these building blocks typically resulted in low yields or a were particularly substrate-dependent. Importantly, the reaction can be conducted at 1 mmol scale without a significant erosion in yield.

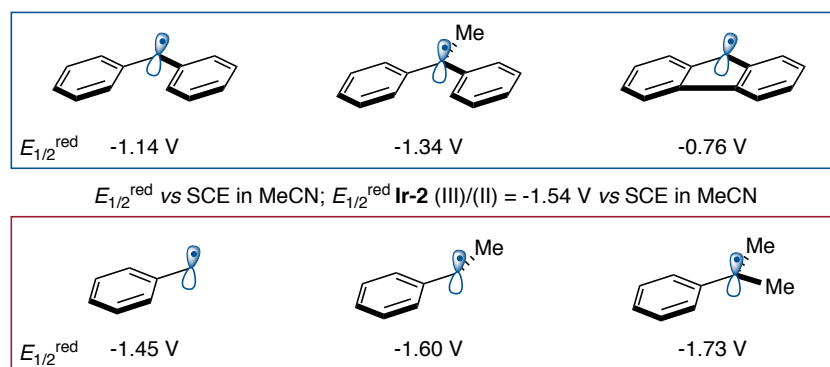
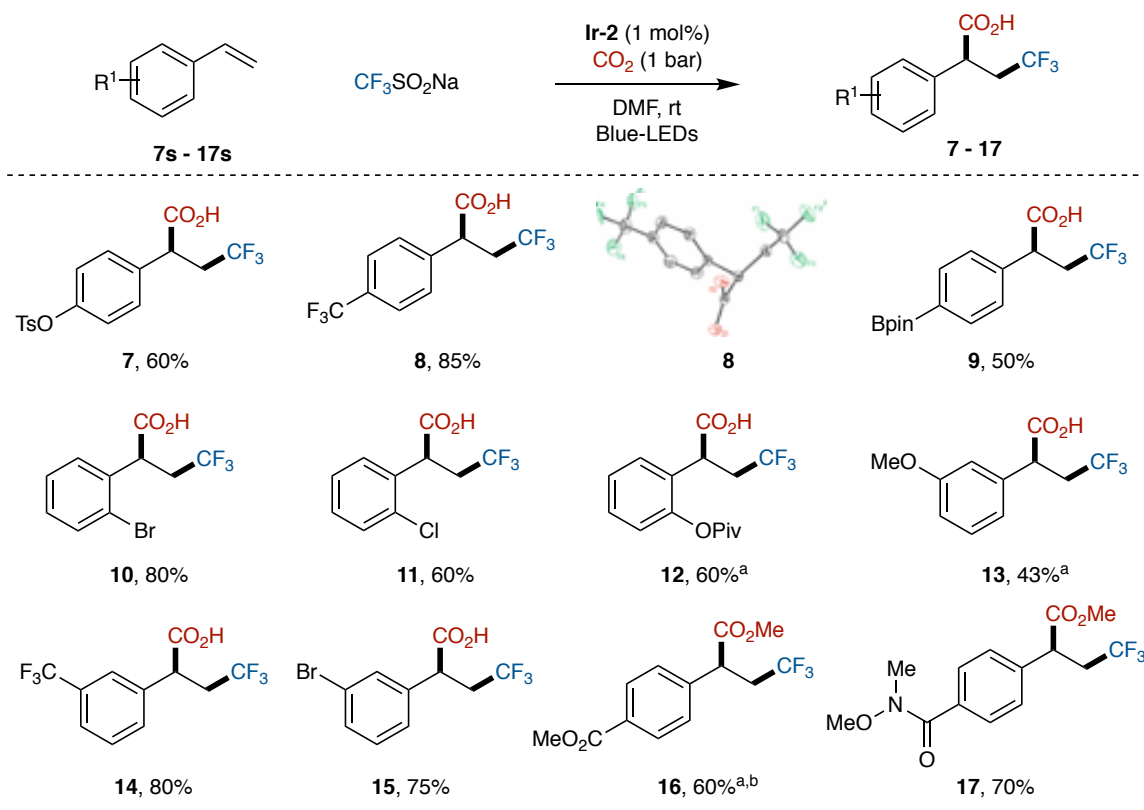


**Figure 3.2. Reduction potential of benzylic radicals**

A close inspection into Table 3.1 indicates that the efficiency of the reaction might indeed be correlated with the reduction potential of the photocatalyst (table 3.1). Therefore, we wondered whether we could extend the scope of our redox-neutral dicarbofunctionalization reaction to regular styrenes. This was certainly challenging as the corresponding redox potential required to trigger a SET to a benzyl radical required a considerable higher potential (Figure 3.2). Under such premise, we found that a host of regular styrenes with different substituents at the arene could be employed for our purposes (Table 3.4). While the use of aryl tosylates (**7**), bromides (**10**), chlorides (**11**), or even aryl pivalates (**12**) as coupling counterparts have become routine in a myriad of metal-catalyzed cross-coupling reactions,<sup>24</sup> including related reductive carboxylation events,<sup>25</sup> we found that the presence of these electrophilic sites did not compete with the efficacy of our trifluoromethylcarboxylation reaction. Similarly, the presence of aryl boronic ester did not interfere, albeit in lower yields (**9**).<sup>26</sup> These observations are particularly noteworthy, providing ample room for further derivatization via either C-B or C-X (X = Br, Cl, OTs or OPiv) bond-cleavage, suggesting the implementation of orthogonal cross-coupling technologies. In view of the results shown in Table 3.4, and taking into consideration the high redox potentials required to reduce a benzyl radical via SET, one might easily argue that these results could also be interpreted on the basis of an attack of

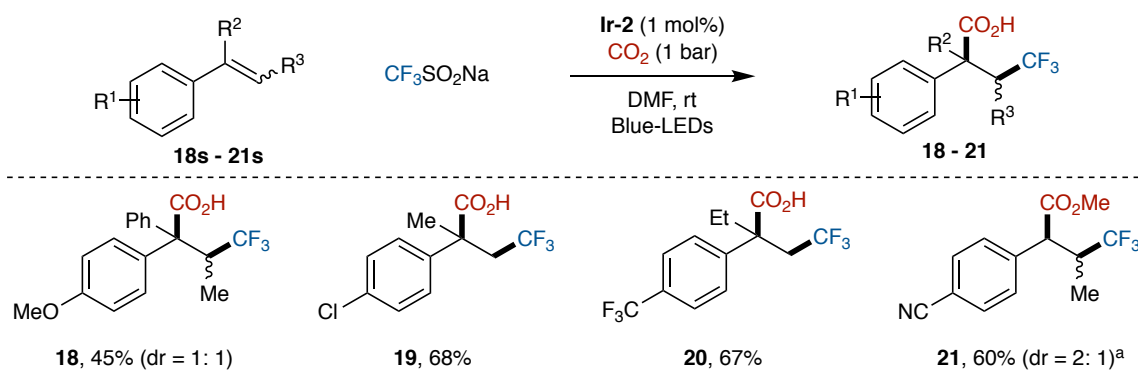
the benzyl radical to CO<sub>2</sub> followed by a downhill SET to the corresponding carboxyl radical intermediate.



Conditions as in Table 3.1 (entry 1). Isolated yields, average of at least two independent runs. <sup>a</sup> Ir-2 (2 mol%),  $\text{CF}_3\text{SO}_2\text{Na}$  (2.0 equiv) in DMF at 5 °C for 15 h. <sup>b</sup> Isolated as ester upon exposure to  $\text{TMSCHN}_2$ .

**Table 3.4. Substrate scope with regular styrenes and Langlois reagent**

Notably, the utilization of 1,2- or 1,1-disubstituted styrenes possessing alkyl substituents posed no problems, and the corresponding phenyl acetic acids could be obtained in good yields (Table 3.5); unfortunately, however, the inclusion of substituents at C2 resulted in statistical diastereomeric mixtures of the targeted carboxylic acids.



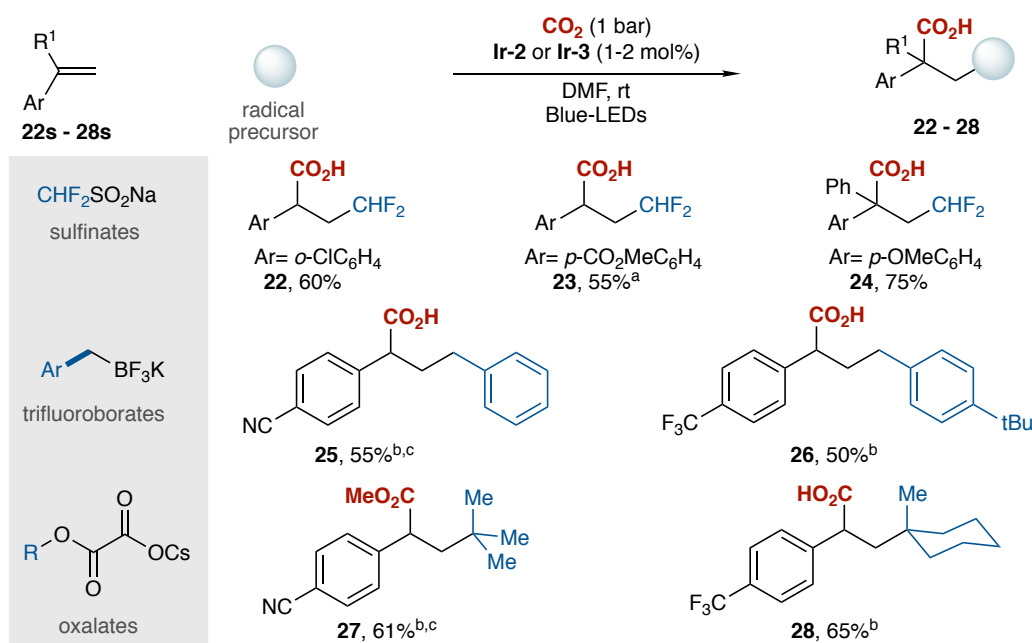
Conditions as in Table 3.1 (entry 1).<sup>a</sup> Isolated as ester upon exposure to  $\text{TMSCHN}_2$ .

**Table 3.5. Substrate scope with alkyl substituted styrenes and Langlois reagent**



### 3.3.4. Substrate Scope with Other Radical Entities

Encouraged by the results using Langlois reagent, we wondered whether our dicarbofunctionalization technique could be extended to other radical entities as well. As shown in Table 3.6, this turned out to be the case. Specifically, we found that difluoromethyl-containing phenyl acetic acids are easily within reach when using  $\text{CHF}_2\text{SO}_2\text{Na}$  under otherwise identical reaction conditions to those shown for  $\text{CF}_3\text{SO}_2\text{Na}$  (**22** to **24**). Subsequently, we turned our attention to study whether non-fluorinated radical analogues could also be used for similar purposes. Indeed, we found that easily accessible benzyl trifluoroborates ( $E_{\text{ox}} = +1.1\text{V}$  vs SCE in MeCN)<sup>28</sup> and *tert*-butyl oxalates ( $E_{\text{ox}} = +1.28\text{V}$  vs SCE in MeCN)<sup>29</sup> could be employed in our dicarbofunctionalization reaction. In this case, however, stronger oxidizing photocatalyst **Ir-3** ( $E_{\text{red}}[\text{Ir}^{\text{III}}/\text{Ir}^{\text{II}}] = +1.21\text{V}$  vs SCE in MeCN) was required, cleanly delivering **25** to **28** in moderate to good yields.<sup>30</sup>



Conditions as in Table 3.1 (entry 1). Isolated yields, average of at least two independent runs.

<sup>a</sup> Ir-2 (2 mol%),  $\text{CHF}_2\text{SO}_2\text{Na}$  (2.0 equiv) at 5 °C. <sup>b</sup> Ir-3 (2 mol%). <sup>c</sup> Quenched with TMSCHN<sub>2</sub>.

**Table 3.6. Substrate scope with other radical entities**

Taken together, the results compiled in table 3.3 to table 3.6 stand as a testament to the prospective potential of redox-neutral catalysis for enabling dicarbofunctionalization reactions of  $\pi$ -components with  $\text{CO}_2$  and radical precursors, representing a different, yet complementary, reactivity mode to existing catalytic carboxylation events that require sophisticated ligands and/or stoichiometric metal reductants. We anticipate that these findings might open up new vistas for effecting otherwise inaccessible coupling processes involving  $\text{CO}_2$  as coupling partner.

Unfortunately, other radical entities such as thiols or amino acids failed to deliver the targeted carboxylic acid, as the potential product of the former might compete with the quenching of Ir(III)\* while the latter might not undergo decarboxylation under CO<sub>2</sub> atmosphere.

### 3.4. Mechanistic Considerations

#### 3.4.1. 'ON/OFF' Experiment

As highlighted previously, "ON-OFF" experiments are routinely performed in photochemical transformations to unravel whether the reaction proceeds in the absence of light irradiation or not. As shown in Figure 3.3, we found no conversion during the dark period. However, this experiment only suggests the absence of background reactions in the dark while constant irradiation was necessary to deliver the targeted products.

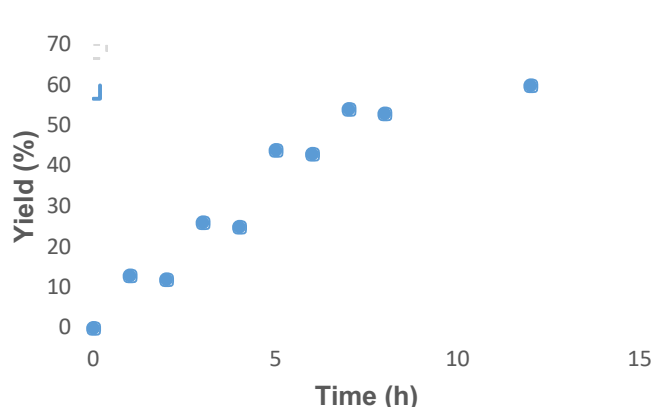


Figure 3.3. 'ON/OFF' experiment

#### 3.4.2. Luminescence Quenching Experiments

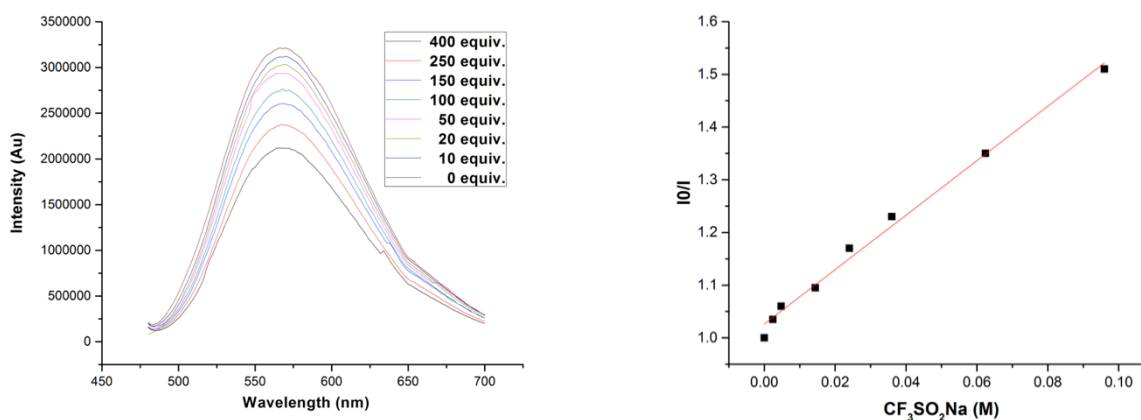


Figure 3.4. Stern Volmer quenching of Ir-2\* with CF<sub>3</sub>SO<sub>2</sub>Na

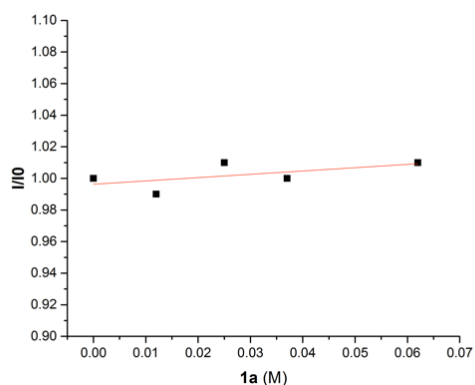


Figure 3.5. Quenching plot of Ir-2\* with 1s

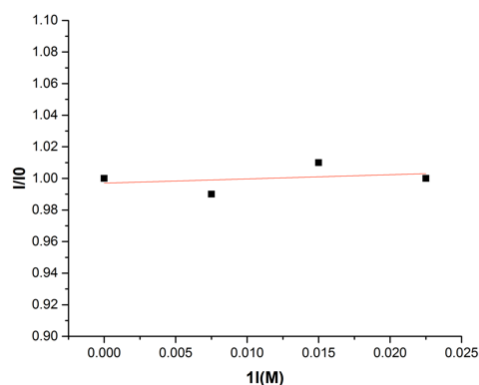
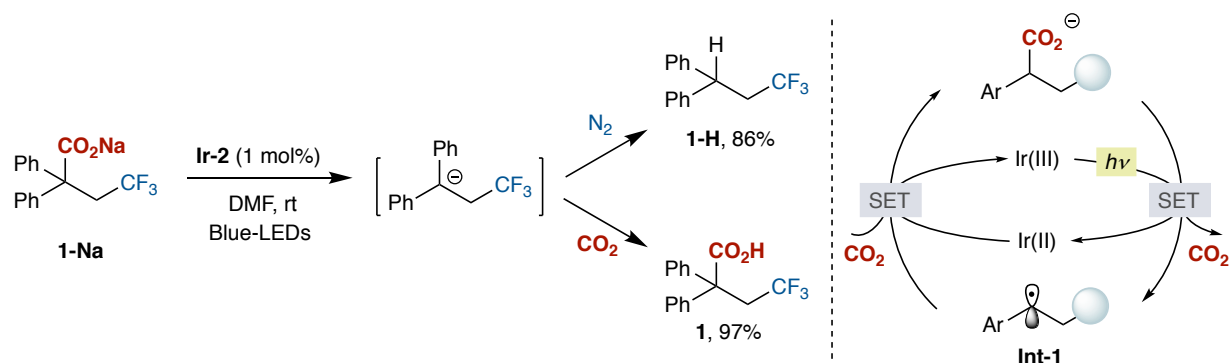


Figure 3.6. Quenching plot of Ir-2\* with 13s

In order to examine our hypothesis in Scheme 3.20, we explored the interaction of **Ir-2** and the reaction components via Stern-Volmer quenching studies. As expected, luminescence quenching of **Ir-2\*** was observed at higher concentrations of  $\text{CF}_3\text{SO}_2\text{Na}$  ( $E_{\text{ox}} = +1.05\text{V}$  vs SCE in MeCN) (Figure 3.4), while negligible quenching occurred with **1s** and **13s** (Figure 3.5 and 3.6). These luminescence quenching studies demonstrated that **Ir-2\*** was quenched by  $\text{CF}_3\text{SO}_2\text{Na}$  ( $E_{\text{ox}} = +1.05\text{V}$  vs SCE in MeCN)<sup>15c</sup> but not by **1s** ( $E_{\text{ox}} = +1.81\text{V}$  vs SCE in MeCN),<sup>17,19a,31</sup> thus suggesting the involvement of a reductive quenching photocatalytic cycle, in which a transient carbon-centered radical generated upon single electron transfer (SET) with the excited state of the photocatalyst, is added across the styrene backbone. A subsequent SET from the reduced photocatalyst to **Int-1** (Scheme 3.20) might give rise to a benzylic carbanion that rapidly reacts with  $\text{CO}_2$ .<sup>32,33</sup>

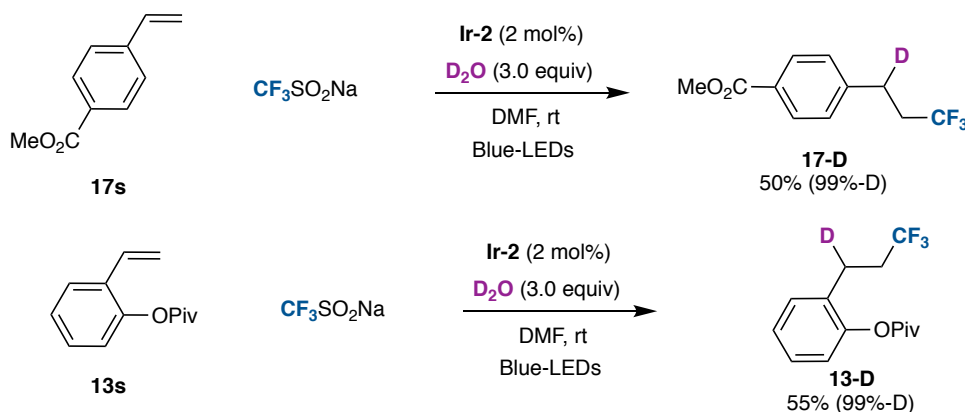
### 3.4.3. The Competitive Off-Cycle via Decarboxylation



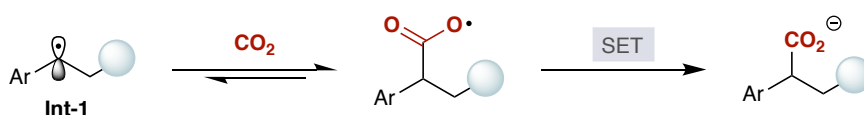
Scheme 3.21. The competitive off-cycle via decarboxylation

During the study of the dicarbofunctionalization reaction, it was found that certain substrate combinations did not lead to full conversion. We hypothesized that this observation could be due to competitive reductive quenching of **Ir-2\*** ( $E_{1/2}^{\text{Ir(III)*}/\text{Ir(II)}} = +0.84\text{V}$ ) by the product. Such a pathway

would result in a competitive decarboxylation reaction that might lead to either reduced product or the corresponding carboxylation, indicating that an off-cycle pathway may undermine the reaction efficiency (Scheme 3.21, *right*). Interestingly, exposure of **1-Na** ( $E_{\text{ox}} = +1.05\text{V vs SCE}$  in MeCN)<sup>34</sup> under our optimized reaction conditions *in the absence* of CO<sub>2</sub> showed significant amounts of decarboxylation while traces amounts of **1-H**, if any, were observed *in the presence* of CO<sub>2</sub> (Scheme 3.21).



Taken together, these results suggested the intermediacy of benzyl anions. Aimed at showing whether these intermediates came into play, we turned our attention to isotope-labelling studies (Scheme 3.22). As shown, **17-D** and **13-D** (99%-D) were exclusively obtained upon exposure of **17s** and **13s** to CF<sub>3</sub>SO<sub>2</sub>Na under visible light irradiation with **Ir-2** and D<sub>2</sub>O in the absence of CO<sub>2</sub>, thus ruling out the involvement of hydrogen atom transfer (HAT) with DMF.



Note, however, that the available data do not allow us to rigorously rule out an alternative mechanistic scenario in which the transient benzyl radical intermediate reacts reversibly with CO<sub>2</sub> followed by SET from the reduced photocatalyst **Ir-2** to the carboxyl radical intermediate, leading the final sodium carboxylate (Scheme 3.23).

### 3.5. Conclusions

In summary, we have demonstrated that visible light photoredox catalysis enables a catalytic photochemical redox-neutral dicarbofunctionalization of styrenes with CO<sub>2</sub> and carbon radical precursors with high regio- and chemo- selectivity profile, thus providing a facile access to substituted

phenyl acetic acids. In addition, our protocol offers a reactivity principle that is complementary to classical non-redox neutral catalytic carboxylations, unlocking previously inaccessible scenarios based on multiple C–C bond-forming events from  $\pi$ -components and in the absence of stoichiometric reductants.

### 3.6. Reference

- (a) von der Assen, N., Voll, P., Peters, M., Bardow, A. Life Cycle Assessment Of CO<sub>2</sub> Capture And Utilization: A Tutorial Review. *Chem. Soc. Rev.* **2014**, *43*, 7982; (b) Markewitz, P., Kuckshinrichs, W., Leitner, W., Linssen, J., Zapp, P., Bongartz, R., Schreiber, A., Müller, T. E. Worldwide Innovations In The Development Of Carbon Capture Technologies And The Utilization Of CO<sub>2</sub>. *Energy Environ. Sci.* **2012**, *5*, 7281; (c) <https://www.CO2.Earth>. (d) Aresta, M. *Carbon Dioxide As Chemical Feedstock*, Wiley-VCH Verlag Gmbh, **2010**; (e) Liu, Q., Wu, L., Jackstell, R., Beller, M. *Nat. Commun.* **2015**, *6*, 5933; (f) <https://www.Gminsights.Com/Industry-Analysis/Carboxylic-Acid-Market>; (g) Aresta, M., Dibenedetto, A., Quaranta, E. Reaction Mechanisms In Carbon Dioxide Conversion Springer-Verlag: Berlin Heidelberg **2016**.
- Hussey, A. S. The Carbonation Of Grigand Reagent. *J. Am. Chem. Soc.* **1951**, *73*, 1364.
- Aresta, M., Nobile, C. F., Albano, V. G., Forni, E., Manassero, M. New Nickel–Carbon Dioxide Complex: Synthesis, Properties, And Crystallographic Characterization Of (Carbon Dioxide)-Bis(Tricyclohexylphosphine)Nickel. *J. Chem. Soc., Chem. Commun.* **1975**, *15*, 636.
- Tortajada, A., Juliá-Hernández, F., Börjesson, M., Moragas, T., Martin, R. Transition Metal-Catalyzed Carboxylation Reactions With Carbon Dioxide. *Angew. Chem. Int. Ed.* **2018**, DOI: 10.1002/anie.201803186.
- (a) Shi, M., Nicholas, K. M. Palladium-Catalyzed Carboxylation Of Allyl Stannanes. *J. Am. Chem. Soc.* **1997**, *119*, 5057; (b) Johansson, R., Wendt, O. F. Insertion Of CO<sub>2</sub> Into A Palladium Allyl Bond And A Pd(II) Catalyzed Carboxylation Of Allyl Stannanes. *Dalton Trans.* **2007**, 488; (c) Ukai, K., Aoki, M., Takaya, J., Iwasawa, N. Rhodium(I)-Catalyzed Carboxylation Of Aryl- And Alkenylboronic Esters With CO<sub>2</sub>. *J. Am. Chem. Soc.* **2006**, *128*, 8706; (d) Takaya, J., Tadami, S., Ukai, K., Iwasawa, N. Copper(I)-Catalyzed Carboxylation Of Aryl- And Alkenylboronic Esters. *Org. Lett.* **2008**, *10*, 2697; (e) Ohishi, T., Nishiura, M., Hou, Z. Carboxylation Of Organoboronic Esters Catalyzed By N-Heterocyclic Carbene Copper(I) Complexes. *Angew. Chem.* **2008**, *127*, 5876; *Angew. Chem., Int. Ed.* **2008**, *47*, 5792; (f) Haas, D., Hammann, J. M., Greiner, R., Knochel, P. Recent Developments In Negishi Cross-Coupling Reactions. *ACS Catal.* **2016**, *6*, 1540; (g) Yeung, C. S., Dong, V. M. Beyond Aresta's Complex: Ni- And Pd-Catalyzed Organozinc Coupling With CO<sub>2</sub>. *J. Am. Chem. Soc.* **2008**, *130*, 7826; (h) Ochiai, H., Jang, M., Hirano, K., Yorimitsu, H., Oshima, K. Nickel-Catalyzed Carboxylation Of Organozinc Reagents With CO<sub>2</sub>. *Org. Lett.* **2008**, *10*, 2681; (i) Uchiyama, M., Naka, H., Matsumoto, Y., Ohwada, T. Region- And Chemoselective Direct Generation Of Functionalized Aromatic Aluminum Compounds Using Aluminum Ate Base. *J. Am. Chem. Soc.* **2004**, *126*, 10526; (j) Ueno, A., Takimoto, M., Wylie, W. N. O., Nishiura, M., Ikariya, T., Hou, Z. Copper-Catalyzed Formal C-H Carboxylation Of Aromatic Compounds With Carbon Dioxide Through Arylaluminum Intermediates. *Chem. Asian J.* **2015**, *10*, 1010; (k) Ueno, A., Takimoto, M., Hou, Z. Synthesis Of 2-Aryloxy Butenoates By Copper-Catalyzed Allylic C-H Carboxylation Of Allyl Aryl Ethers With Carbon Dioxide. *Org. Biomol. Chem.* **2017**, *15*, 2370.
- (a) Seyferth, D. Alkyl And Aryl Derivatives Of The Alkali Metals: Useful Synthetic Reagents As Strong Bases And Potent Nucleophiles. 1. Conversion Of Organic Halides To Organoalkali-Metal Compounds. *Organometallics* **2006**, *25*, 2; (b) Knochel, P., Dohle, W., Gommermann, N., Kneisel, F. F., Kopp, F., Korn, T., Sapountzis, I., Vu, V. A. Highly Functionalized Organomagnesium Reagents Prepared Through Halogen–Metal Exchange. *Angew. Chem., Int. Ed.* **2003**, *42*, 4302.
- (a) Osakada, K., Sato, R., Yamamoto, T., Nickel-Complex-Promoted Carboxylation Of Haloarenes Involving Insertion Of CO<sub>2</sub> Into Ni–C Bonds. *Organometallics* **1994**, *13*, 4645; (b) Correa, A., Martin, R. Palladium-Catalyzed Direct Carboxylation Of Aryl Bromides With Carbon Dioxide. *J. Am. Chem. Soc.* **2009**, *131*, 15974; (c) Fujihara, T., Nogi, K., Xu, T., Terao, J., Tsuji, Y. Nickel-Catalyzed Carboxylation Of Aryl And Vinyl Chlorides Employing Carbon Dioxide. *J. Am. Chem. Soc.* **2012**, *134*, 9106; (d) Ebert, E. G., Juda, W. L., Kosakowski, R. H., Ma, B., Dong, L., Cummings, K. E., Phelps, M. V. B., Mostafa, A. E., Luo, J. Carboxylation And Esterification Of Functionalized Arylcopper Reagents. *J. Org. Chem.* **2005**, *70*, 4314; (e) Tran-Vu, H., Daugulis, O. Copper-Catalyzed Carboxylation Of Aryl Iodides With Carbon Dioxide. *ACS Catal.* **2013**, *3*, 2417; (f) Correa, A., León, T., Martin, R. Ni-Catalyzed Carboxylation Of C(sp<sup>2</sup>)– And C(sp<sup>3</sup>)–O Bonds With CO<sub>2</sub>. *J. Am. Chem. Soc.* **2014**, *136*, 1062; (g) León, T., Correa, A., Martin, R. Ni-Catalyzed Direct Carboxylation Of Benzyl Halides With CO<sub>2</sub>. *J. Am. Chem. Soc.* **2013**, *135*, 1221; (h) Moragas, T., Gaydou, M., Martin, R. Nickel-Catalyzed Carboxylation Of Benzylic C-N Bonds With CO<sub>2</sub>. *Angew. Chem. Int. Ed.* **2016**, *55*, 5053; (i) Moragas, T., Cornella, J., Martin, R. Ligand-Controlled Regioselective Ni-Catalyzed Reductive Carboxylation Of Allyl Esters With CO<sub>2</sub>. *J. Am. Chem. Soc.* **2014**, *136*, 17702; (j) van Gemmeren, M., Börjesson, M., Tortajada, A., Sun, S.-Z., Okura, K., Martin, R. Switchable Site - Selective Catalytic Carboxylation Of Allylic Alcohols With CO<sub>2</sub>. *Angew. Chem., Int. Ed.* **2017**, *56*, 6558; (k) Liu, Y., Cornella, J., Martin, R. Ni-Catalyzed Carboxylation Of Unactivated Primary Alkyl Bromides And Sulfonates With CO<sub>2</sub>. *J. Am. Chem. Soc.* **2014**, *136*, 11212; (l) Börjesson, M., Moragas, T., Martin, R. Ni-Catalyzed Carboxylation Of Unactivated Alkyl Chlorides With CO<sub>2</sub>. *J. Am. Chem. Soc.* **2016**, *138*, 7504; (m) Choi, J., Fu, G. C. Transition Metal-Catalyzed Alkyl-Alkyl Bond Formation: Another Dimension In Cross-Coupling Chemistry. *Science* **2017**, *356*, 152; (n) Juliá-Hernández, F., Moragas, T., Cornella, J., Martin, R. Remote Carboxylation Of Halogenated Aliphatic Hydrocarbons With Carbon Dioxide. *Nature* **2017**, *545*, 84; (o) Sommer, H., Juliá-Hernández, F., Martin, R., Marek, I. Walking Metals For Remote Functionalization. *ACS Cent. Sci.* **2018**, *4*, 153; (p) Gaydou, M., Moragas, T., Juliá-Hernández, F., Martin, R. Site-Selective Catalytic Carboxylation Of Unsaturated Hydrocarbons With CO<sub>2</sub> And Water. *J. Am. Chem. Soc.* **2017**, *139*, 12161; (q) Williams, C. M., Johnson, J. B., Rovis, T. Nickel-Catalyzed Reductive Carboxylation Of Styrenes Using CO<sub>2</sub>. *J. Am. Chem. Soc.* **2008**, *130*, 14936; (r) Shao, P., Wang, S., Chen, C., Xi, C. Cp<sub>2</sub>TiCl<sub>2</sub>-Catalyzed Regioselective Hydrocarboxylation Of Alkenes With CO<sub>2</sub>. *Org. Lett.* **2016**, *18*, 2050; (s) Greenhalgh, M. D., Thomas, S. P. Iron-Catalyzed, Highly Regioselective Synthesis Of *o*-Aryl Carboxylic Acids From Styrene Derivatives And CO<sub>2</sub>. *J. Am. Chem. Soc.* **2012**, *134*, 11900.
- (a) Masuda, Y., Ishida, N., Murakami, M. Light-Driven Carboxylation Of *o*-Alkylphenyl Ketones With CO<sub>2</sub>. *J. Am. Chem. Soc.* **2015**, *137*, 14063; (b) Murata, K., Numasawa, N., Shimomaki, K., Takaya, J., Iwasawa, N. Construction Of A Visible Light-Driven Hydrocarboxylation Cycle Of Alkenes By The Combined Use Of Rh(I) And Photoredox Catalysts. *Chem. Commun.* **2017**, *53*, 3098; (c) Meng, Q.-Y., Wang, S., Huff, G. S., König, B. Ligand-Controlled Regioselective Hydrocarboxylation Of Styrenes With CO<sub>2</sub> By Combining Visible Light And Nickel Catalysis. *J. Am. Chem. Soc.* **2018**, *140*, 3198.

9. (a) Gui, Y.-Y., Hu, N., Chen, X.-W., Liao, L.-L., Ju, T., Ye, J.-H., Zhang, Z., Li, J., Yu, D.-G. Highly Regio- And Enantioselective Copper-Catalyzed Reductive Hydroxymethylation Of Styrenes And 1,3-Dienes With CO<sub>2</sub>. *J. Am. Chem. Soc.* **2017**, *139*, 17011; (b) Seo, H., Liu, A., Jamison, T. F. Direct B-Selective Hydrocarboxylation Of Styrenes With CO<sub>2</sub> Enabled By Continuous Flow Photoredox Catalysis. *J. Am. Chem. Soc.* **2017**, *139*, 13969.
10. For The Recent Use Of Non-Visible Light Irradiation (*UV Light*) And CO<sub>2</sub>: (a) Seo, H., Katcher, M. H., Jamison, T. F., Photoredox Activation Of Carbon Dioxide For Amino Acid Synthesis In Continuous Flow. *Nat. Chem.* **2017**, *9*, 453; (b) Gui, Y.-Y., Zhou, E.-J., Ye, J.-H., Yu, D.-G. Photochemical Carboxylation Of Activated C(*Sp*<sup>3</sup>)-H Bonds With CO<sub>2</sub>. *ChemSuschem* **2017**, *10*, 1337; (c) Masuda, Y., Ishida, N., Murakami, M. Light-Driven Carboxylation Of *O*-Alkylphenyl Ketones With CO<sub>2</sub>. *J. Am. Chem. Soc.* **2015**, *137*, 14063; (d) Ishida, N., Masuda, Y., Uemoto, S., Murakami, M. A Light/Ketone/Copper System For Carboxylation Of Allylic C–H Bonds Of Alkenes With CO<sub>2</sub>. *Chem. Eur. J.* **2016**, *22*, 6524.
11. While This Manuscript Was In Preparation, An Elegant Catalytic Hydrocarboxylation Of Styrenes Mediated By Visible Light Requiring Stoichiometric Amine Reductants And Rh Catalysts Was Described, See Ref 8b.
12. For Multiple C–C Bond-Formations With CO<sub>2</sub> Requiring Organic Halide Counterparts And/Or Stoichiometric Metal Reductants: (a) Wang, X., Liu, Y., Martin, R. Ni-Catalyzed Divergent Cyclization/Carboxylation Of Unactivated Primary And Secondary Alkyl Halides With CO<sub>2</sub>. *J. Am. Chem. Soc.* **2015**, *137*, 6476; (b) Nogi, K., Fujihara, T., Terao, J., Tsuji, Y. Carboxyzincation Employing Carbon Dioxide And Zinc Powder: Cobalt-Catalyzed Multicomponent Coupling Reactions With Alkynes. *J. Am. Chem. Soc.* **2016**, *138*, 5547.
13. For Selected Heterocarbonylation Of Alkenes Not Dealing With Multiple C–C Bond Formations: (a) Zhang, Z., Ju, T., Miao, M., Han, J.-L., Zhang, Y.-H., Zhu, X.-Y., Ye, J.-H., Yu, D.-G., Zhi, Y.-G. Transition-Metal-Free Lactonization Of *sp*<sup>2</sup> C–H Bonds With CO<sub>2</sub>. *Org. Lett.* **2017**, *19*, 396; (b) Zhang, Z., Zhang, L.-L., Yan, S.-S., Wang, L., He, Y.-Q., Ye, J.-H., Li, J., Zhi, Y.-G., Yu, D.-G. Lactamization Of *Sp*<sup>2</sup> C–H Bonds With CO<sub>2</sub>: Transition-Metal-Free And Redox-Neutral. *Angew. Chem. Int. Ed.* **2016**, *55*, 7068; (c) Sasano, K., Takaya, J., Iwasawa, N. Palladium(II)-Catalyzed Direct Carboxylation Of Alkenyl C–H Bonds With CO<sub>2</sub>. *J. Am. Chem. Soc.* **2013**, *135*, 10954.
14. Selected References: (a) Tomashenko, O. A., Grushin, V. V. Aromatic Trifluoromethylation With Metal Complexes. *Chem. Rev.* **2011**, *111*, 4475; (b) Yale, H. L. The Trifluoromethyl Group In Medical Chemistry. *J. Med. Chem.* **1958**, *1*, 121.
15. For Selected Trifluoromethylations Involving Langlois' Reagent: (a) Zhang, C. Application Of Langlois' Reagent In Trifluoromethylation Reactions. *Adv. Synth. Catal.*, **2014**, *356*, 2895; (b) Studer, A. A "Renaissance" In Radical Trifluoromethylation. *Angew. Chem. Int. Ed.* **2012**, *51*, 8950; (c) Wilger, D. J., Gesmundo, N. J., Nicewicz, D. A. Catalytic Hydrotrifluoromethylation Of Styrenes And Unactivated Aliphatic Alkenes *Via* An Organic Photoredox System. *Chem. Sci.* **2013**, *4*, 3160; (d) Zhu, L., Wang, L.-S., Li, B., Fu, B., Zhang, C. P., Li, W. Operationally Simple Hydrotrifluoromethylation Of Alkenes With Sodium Triflinate Enabled By Ir Photoredox Catalysis. *Chem. Commun.* **2016**, *52*, 6371.
16. For A Selection Of Non-Carboxylative Techniques Using CF<sub>3</sub> Radicals In Multiple C–C Bond-Formations With  $\pi$ -Components, See: (a) Wu, L., Wang, F., Wan, X., Wang, D., Chen, P., Liu, G. Asymmetric Cu-Catalyzed Intermolecular Trifluoromethylation Of Styrenes: Enantioselective Arylation Of Benzylic Radicals. *J. Am. Chem. Soc.* **2017**, *139*, 2904; (b) Koike, T., Akita, M. Fine Design Of Photoredox Systems For Catalytic Fluoromethylation Of Carbon–Carbon Multiple Bonds. *Acc. Chem. Res.* **2016**, *49*, 1937; (c) Tomita, R., Koike, T., Akita, M. Photoredox - Catalyzed Stereoselective Conversion Of Alkynes Into Tetrasubstituted Trifluoromethylated Alkenes. *Angew. Chem. Int. Ed.* **2015**, *54*, 12923; (d) Carboni, A., Dagousset, G., Magnier, E., Masson, G. One Pot And Selective Intermolecular Aryl- And Heteroaryl-Trifluoromethylation Of Alkenes By Photoredox Catalysis. *Chem. Commun.* **2014**, *50*, 14197; (e) Kong, W., Casimiro, M., Merino, E., Nevado, C. Copper-Catalyzed One-Pot Trifluoromethylation/Aryl Migration/Desulfonylation And C(*Sp*<sup>2</sup>)-N Bond Formation Of Conjugated Tosyl Amides. *J. Am. Chem. Soc.* **2013**, *135*, 14480.
17. See Supporting Information For Details.
18. Kim, H., Lee, C. Visible-Light-Induced Photocatalytic Reductive Transformations Of Organohalides. *Angew. Chem. Int. Chem.* **2012**, *51*, 12303.
19. (a) Shiraishi, Y., Saito, N., Hirai, T. Visible Light-Induced Highly Selective Transformation Of Olefin To Ketone By 2,4,6-Triphenylpyrylium Cation Encapsulated Within Zeolite Y. *Chem. Commun.* **2006**, 773; (b) Sim, B. A., Griller, D., Wayner, D. D. M. *J. Am. Chem. Soc.* **1989**, *111*, 754; (c) Wayner, D. D. M., McPhee, D. J., Griller, D. Oxidation And Reduction Potentials Of Transient Free Radicals. *J. Am. Chem. Soc.* **1988**, *110*, 132.
20. The Lower Reactivity Of Ir-3 Can Also Be Interpreted On The Basis Of A Non-Productive Energy Transfer Between The Excited State Of Ir-3 (ET = ~63 Kcal/Mol) And 3-S-1 (ET = ~61 Kcal/Mol). See: Ni, T., Caldwell, R. A., Melton, L. A. The Relaxed And Spectroscopic Energies Of Olefin Triplets. *J. Am. Chem. Soc.* **1989**, *111*, 457.
21. The Mass Balance For **1** To **28** Accounts For Unreacted Starting Material, Reduced Product And Traces (If Any) Of Homodimerization.
22. CCDC 1557037 (**1**) And CCDC 1557038 (**8**) Contain The Supplementary Crystallographic Data For This Paper And Can Be Obtained Free Of Charge From The Cambridge Crystallographic Data Centre Via [www.ccdc.cam.ac.uk/Data\\_Request/Cif](http://www.ccdc.cam.ac.uk/Data_Request/Cif).
23. Intriguingly, Competitive Addition Of CF<sub>3</sub> Radical To The  $\alpha$ -Olefin Did Not Compete With The Efficacy Of The Trifluoromethylcarboxylation Event. See: Liu, Z.-Q., Liu, D. Free-Radical Bromotrifluoromethylation Of Olefin *Via* Single-Electron Oxidation Of Naso<sub>2</sub>cf<sub>3</sub> By Nabro<sub>3</sub>. *J. Org. Chem.* **2017**, *82*, 1649.
24. (a) Tasker, S. Z., Standley, E. A., Jamison, T. F. Recent Advances In Homogeneous Nickel Catalysis. *Nature* **2014**, *509*, 299; (b) *Metal-Catalyzed Cross-Coupling Reactions*; F. Diederich, A. Meijere, Eds.; Wiley-VCH: Weinheim, **2004**.
25. For The Catalytic Carboxylation Of Aryl Halides, Sulfonates Or Pivalates: (a) Nogi, K., Fujihara, T., Xu, T., Terao, J., Tsuji, Y. Cobalt- And Nickel-Catalyzed Carboxylation Of Alkenyl And Sterically Hindered Aryl Triflates Utilizing CO<sub>2</sub>. *J. Org. Chem.*, **2015**, *80*, 11618; (b) Ref. 3c; (c) T. Fujihara, K. Nogi, T. Xu, J. Terao, Y. Tsuji, Nickel-Catalyzed Carboxylation Of Aryl And Vinyl Chlorides Employing Carbon Dioxide. *J. Am. Chem. Soc.*, **2012**, *134*, 9106; (d) Correa, A., Martin, R. Palladium-Catalyzed Direct Carboxylation Of Aryl Bromides With Carbon Dioxide. *J. Am. Chem. Soc.* **2009**, *131*, 15974.

26. Competitive Carboxylation At C–B Bond Was Not Observed. The Lower Yield Of **10** Accounts For **10s** Unaltered. For A Review Dealing With The Carboxylation Of Organoboranes: Correa, A., Martin, R. Metal - Catalyzed Carboxylation Of Organometallic Reagents With Carbon Dioxide. *Angew. Chem. Int. Ed.* **2009**, *48*, 6201.
27. For Selected Carbon-Centered Radical Additions (Other Than CF<sub>3</sub>) To Styrenes Without CO<sub>2</sub>: (a) Sumino, S., Uno, M., Fukuyama, T., Ryu, I., Matsuura, M., Yamamoto, A., Kishikawa, Y. Photoredox-Catalyzed Hydrodifluoroalkylation Of Alkenes Using Difluorohaloalkyl Compounds And A Hantzsch Ester. *J. Org. Chem.* **2017**, *82*, 5469; (b) Yang, B., Xu, X.-H., Qing, F.-L. Synthesis Of Difluoroalkylated Arenes By Hydroaryldifluoromethylation Of Alkenes With A,A-Difluoroarylacetic Acids Under Photoredox Catalysis. *Org. Lett.* **2016**, *18*, 5956; (c) G. H Lovett, B. A. Sparling. Decarboxylative Anti-Michael Addition To Olefins Mediated By Photoredox Catalysis. *Org. Lett.*, 2016, *18*, 3494; (d) Mizuta, S., Verhoog, S., Engle, K. M., Khotavivattana, O'Duill, T., M., Wheelhouse, K., Rassias, G., Médebielle, M., Gouverneur, V. Catalytic Hydrotrifluoromethylation Of Unactivated Alkenes. *J. Am. Chem. Soc.* **2013**, *135*, 2505.
28. For Selected References Using Trifluoroborates In Photoredox Catalysis: (a) J. K. Matsui, D. N. Primer, G. A. Molander. Metal-Free C–H Alkylation Of Heteroarenes With Alkyltrifluoroborates: A General Protocol For 1°, 2° And 3° Alkylation. *Chem. Sci.* **2017**, *8*, 3512; (b) Primer, D. N., Karakaya, I., Tellis, J. C., Molander, G. A. Single-Electron Transmetalation: An Enabling Technology For Secondary Alkylboron Cross-Coupling. *J. Am. Chem. Soc.*, **2015**, *137*, 2195; (c) Tellis, J. C., Primer, D. N., Molander, G. A. Single-Electron Transmetalation In Organoboron Cross-Coupling By Photoredox/Nickel Dual Catalysis. *Science*, **2014**, *345*, 433.
29. Selected References Of Oxalates In Photoredox Catalysis: (a) X. Zhang, D. W. C. Macmillan, Alcohols As Latent Coupling Fragments For Metallaphotoredox Catalysis: *Sp*<sup>3</sup>–*Sp*<sup>2</sup> Cross-Coupling Of Oxalates With Aryl Halides. *J. Am. Chem. Soc.* **2016**, *138*, 13862; (b) Nawrat, C. C., Jamison, C. R., Slutskyy, Y., Macmillan, D. W. C., Overman, L. E. Oxalates As Activating Groups For Alcohols In Visible Light Photoredox Catalysis: Formation Of Quaternary Centers By Redox-Neutral Fragment Coupling. *J. Am. Chem. Soc.*, **2015**, *137*, 11270.
30. The Lower Yields Found For **25** To **28** Account For Unreacted Starting Material, Reduced Product And Dimerization.
31. At Present, We Believe That The Reaction Is Likely Driven By The Rapid Addition Of CF<sub>3</sub> Radical Across The Styrene, The Formation Of Two Strong C–C Sigma Bonds And The Stability Of The Final Sodium Carboxylate Salt.
32. Musacchio, A. J., Nguyen, L. Q., Beard, G. H., Knowles, R. R. Catalytic Olefin Hydroamination With Aminium Radical Cations: A Photoredox Method For Direct C–N Bond Formation. *J. Am. Chem. Soc.* **2014**, *136*, 12217.
33. Our Results Suggest That The Addition Of CF<sub>3</sub> Radicals To Styrenes Is Considerably Faster Than Unproductive Reduction To CF<sub>3</sub> Anion By The Reduced Ir(II) Photocatalyst. Notably, Traces Of Benzylic Dimerization Were Observed, Indicating A Lower Concentration Of Benzyl Radicals In Solution Under CO<sub>2</sub> Atmospheres.
34. For Selected Photoredox Transformations Via Decarboxylation Techniques Using Ir Photocatalysts: (a) Johnston, C. P., Smith, R. T., Allmendinger, S., Macmillan, D. W. C. Metallaphotoredox-Catalysed *sp*<sup>3</sup>–*sp*<sup>3</sup>cross-Coupling Of Carboxylic Acids With Alkyl Halides. *Nature* **2016**, *536*, 322; (b) Zuo, Z., Macmillan, D. W. C. Decarboxylative Arylation Of  $\alpha$ -Amino Acids Via Photoredox Catalysis: A One-Step Conversion Of Biomass To Drug Pharmacophore. *J. Am. Chem. Soc.* **2014**, *136*, 5257; (c) Z. Zuo, D. T. Ahneman, L. Chu, J. A. Terrett, A. G. Doyle, D. W. C. Macmillan. Merging Photoredox With Nickel Catalysis: Coupling Of  $\alpha$ -Carboxyl *Sp*<sup>3</sup>-Carbons With Aryl Halides. *Science* **2014**, *345*, 437.



## 3.7. Experimental Section

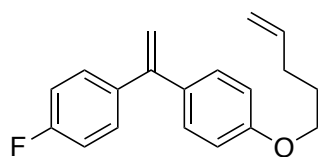
### 3.7.1. General Considerations

**Reagents:** All reactions were conducted in Schlenk tubes. Commercially available materials were used without further purification.  $\text{CF}_3\text{SO}_2\text{Na}$ ,  $\text{CF}_2\text{HSO}_2\text{Na}$ , **1s**, **9s**, **11s**, **12s**, **14s**, **15s**, **16s** and **19s** were purchased from commercial sources and used as received. Anhydrous DMA, DMF, DMSO,  $\text{CH}_3\text{CN}$ , THF and toluene were purchased from Acros Organics. All photo catalysts were prepared following the reported literature methods.<sup>1</sup> Oxalates and benzylic trifluoroborates were prepared following the reported literature method.<sup>2</sup> Styrenes **2s**,<sup>3</sup> **3s**,<sup>3</sup> **6s**,<sup>3</sup> **7s**,<sup>4</sup> **8s**,<sup>5</sup> **10s**,<sup>6</sup> **13s**,<sup>7</sup> **17s**,<sup>8</sup> **18s**,<sup>8</sup> **20s**,<sup>9</sup> and **21s**,<sup>10</sup> were all prepared following reported literature protocols.

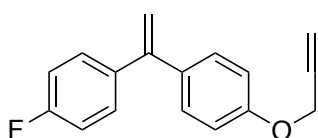
**Analytical Methods:**  $^1\text{H}$  NMR,  $^{13}\text{C}$  NMR and  $^{19}\text{F}$  NMR spectra and melting points (where applicable) are included for all new compounds.  $^1\text{H}$  NMR,  $^{13}\text{C}$  NMR and  $^{19}\text{F}$  NMR spectra were recorded on a Bruker 300 MHz, a Bruker 400 MHz or a Bruker 500 MHz spectrometer at 20 °C. All  $^1\text{H}$  NMR spectra are reported in parts per million (ppm) downfield of TMS and were measured relative to the signals for residual  $\text{CHCl}_3$  (7.26 ppm). All  $^{13}\text{C}$  NMR spectra are reported in ppm relative to residual  $\text{CHCl}_3$  (77.16 ppm) and were obtained with  $^1\text{H}$  decoupling. Coupling constants,  $J$ , are reported in hertz (Hz). Melting points were measured using open glass capillaries in a Büchi B540 apparatus. Infrared spectra were recorded on a Bruker Tensor 27. Mass spectra were recorded on a Waters LCT Premier spectrometer. Flash chromatography was performed with EM Science silica gel 60 (230-400 mesh) using bromocresol, potassium permanganate, or cerium molybdate as TLC stains. All electrochemical experiments were performed on a PAR 263A EG&G potentiostat or on an IJ-Cambria HI-660 potentiostat. A three-electrode cell was used employing a glassy carbon ( $S = 0.07 \text{ cm}^2$ ) working electrode, platinum mesh as the counter electrode, and MSE or SSCE as the reference electrode unless otherwise indicated.  $E_{1/2}$  values reported in this work were estimated from cyclic voltammetry (CV) experiments as the average of the oxidative and reductive peak potentials. Fluorescence measurements were carried out on a Fluorolog Horiba Jobin Yvon spectrofluorimeter equipped with photomultiplier detector, double monochromator and xenon light source. The yields reported in Tables 2-3 refer to isolated yields and represent an average of at least two independent runs. The procedures described in this section are representative. Thus, the yields may differ slightly from those given in the tables of the manuscript

### 3.7.2. Synthesis of Starting Materials

**General procedure for the synthesis of styrenes 4s and 6s:** A round-bottomed flask was charged with the corresponding triphenylphosphonium bromide (0.6 equiv),  $t\text{-BuOK}$  (0.6 equiv) and THF (15 ml) at RT. The mixture was stirred for 1h at this temperature. Then, the corresponding ketone (0.5 equiv) in THF (10 ml) was added dropwise at RT. The solution was then warmed to 60 °C and stirred for further 10 h. The solvent was removed under reduced pressure and the residue was subjected to column chromatography (hexanes) to yield the desired alkene.



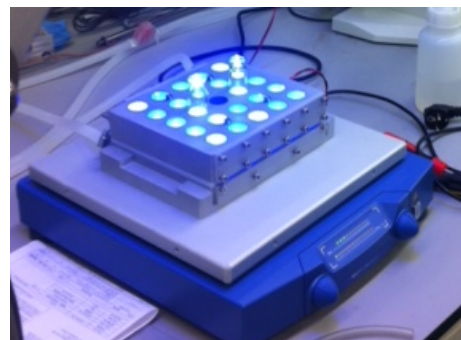
**1-fluoro-4-(1-(4-(pent-4-en-1-yloxy)phenyl)vinyl)benzene (4s):** Following the general procedure, **3-s-4** was obtained as a colorless solid (1.2 g, 85%). Mp 44 °C. <sup>1</sup>H NMR (400 MHz, CDCl<sub>3</sub>): δ 7.34-7.30 (m, 2H), 7.27-7.24 (m, 2H), 7.05-7.0 (m, 2H), 6.89-6.86 (m, 2H), 5.93-5.82 (m, 1H), 5.39-5.31 (m, 2H), 5.12-5.01 (m, 2H), 4.02-3.98 (m, 2H), 2.29-2.24 (m, 2H), 1.95-1.87 (m, 2H) ppm. <sup>13</sup>C NMR (100 MHz, CDCl<sub>3</sub>): δ 162.6 (d, <sup>1</sup>J<sub>C-F</sub> = 245.2 Hz), 159.1, 148.7, 138.0 (d, <sup>4</sup>J<sub>C-F</sub> = 3.2 Hz), 137.9, 133.8, 112.9, 130.0 (d, <sup>3</sup>J<sub>C-F</sub> = 7.9 Hz, 2C), 129.4 (2C), 115.3, 115.1 (d, <sup>2</sup>J<sub>C-F</sub> = 21.2 Hz, 2C), 114.3.1 (2C), 67.3, 30.3, 28.6 ppm. <sup>19</sup>F NMR (376 MHz, CDCl<sub>3</sub>): δ -114.64 to -114.78 (m, 1F) ppm. IR (neat, cm<sup>-1</sup>): 2942, 2871, 1643, 1597, 1503, 1472, 1323, 1242, 1179, 1023, 899, 795.



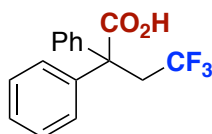
**1-fluoro-4-(1-(4-(prop-2-yn-1-yloxy)phenyl)vinyl)benzene (5s):** Following the general procedure, **3-s-5** was obtained as a colorless solid (1.1 g, 87%). Mp 54 °C. <sup>1</sup>H NMR (400 MHz, CDCl<sub>3</sub>): δ 7.33-7.26 (m, 4H), 7.05-6.95 (m, 2H), 7.0-6.97 (m, 2H), 5.39 (s, 1H), 5.34 (s, 1H), 4.72 (d, <sup>4</sup>J<sub>H-H</sub> = 2.3 Hz, 2H), 2.54 (t, <sup>4</sup>J<sub>H-H</sub> = 2.3 Hz, 1 H) ppm. <sup>13</sup>C NMR (100 MHz, CDCl<sub>3</sub>): δ 162.7 (d, <sup>1</sup>J<sub>C-F</sub> = 245.1 Hz), 148.5, 137.9 (d, <sup>4</sup>J<sub>C-F</sub> = 3.2 Hz, 2C), 134.8, 130.0 (d, <sup>3</sup>J<sub>C-F</sub> = 8.0 Hz, 2C), 129.4 (2C), 115.1 (d, <sup>2</sup>J<sub>C-F</sub> = 21.2 Hz, 2C), 114.7 (2C), 113.3, 78.6, 75.7, 55.8 ppm. <sup>19</sup>F NMR (376 MHz, CDCl<sub>3</sub>): δ -114.78 to -114.85 (m, 1F) ppm. IR (neat, cm<sup>-1</sup>): 3285, 2909, 2137, 1600, 1503, 1377, 1229, 1181, 1019, 897, 840, 785, 732. HRMS calc. for [C<sub>17</sub>H<sub>14</sub>FO + H], 253.1021 found 253.1023.

### 3.7.3. Intermolecular Dicarbofunctionalization of Styrenes with CO<sub>2</sub>

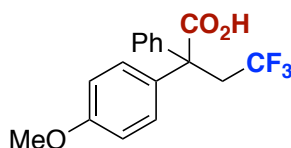
**General procedure for the dicarbofunctionalization of styrenes with CO<sub>2</sub>:** An oven-dried 20 mL Schlenk tube was charged with styrene (0.2-0.3 mmol), photocatalyst (1-2 mol%), and oven-dried 5 glass balls (5 mm diameter). The Schlenk tube was then introduced into a glovebox where it was charged with the appropriate radical precursor [CF<sub>3</sub>SO<sub>2</sub>Na (1.2-2.0 equiv), CF<sub>2</sub>HSO<sub>2</sub>Na (1.2-2.0 equiv), benzylic trifluoroborates (1.2 equiv), or oxalates (1.2 eq)]. The Schlenk tube was then taken out of the glovebox. DMF (2-3 mL) was added under a flow of nitrogen, then three freeze-pump-thaw cycles were conducted in liquid nitrogen. Finally, the Schlenk tube was closed under an atmospheric pressure of CO<sub>2</sub> (1 atm). The reactions were placed in the pre-programmed temperature-controlled blue LED reactor as shown in Figure 1 and the LEDs (36 V, 0.9 A) were turned on at the same time as the orbital shaker plate (250 rpm). After 15-30 h of reaction, the reaction was quenched with HCl (1 mL,



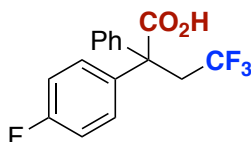
2M) to hydrolyze the resulting carboxylate, then extracted 3 times with EtOAc. The combined organic layers were dried over MgSO<sub>4</sub> and concentrated under reduced pressure. The products were purified by flash chromatography (hexanes/EtOAc 10/1 followed by hexanes/EtOAc 10/4). In the cases where the acid product was unstable, the crude acid was converted after workup to the corresponding methyl ester with TMSCHN<sub>2</sub>. This was followed by column chromatography (hexanes/EtOAc 19/1) to provide the desired ester.



**4,4,4-trifluoro-2,2-diphenylbutanoic acid (1):** Following the general procedure, using Ir photocatalyst **Ir-2** (2.7 mg, 1 mol%), CF<sub>3</sub>SO<sub>2</sub>Na (46.5 mg, 0.36 mmol) and **1s** (54 mg, 0.30 mmol), DMF (3 mL) for 15 h afforded **1** as a white solid in 86% yield (76 mg). Mp 125 °C. <sup>1</sup>H NMR (400 MHz, CDCl<sub>3</sub>): δ 7.37-7.32 (m, 10H), 3.40 (q, <sup>3</sup>J<sub>H-F</sub> = 10.2 Hz, 2H) ppm. <sup>13</sup>C NMR (100 MHz, CDCl<sub>3</sub>): δ 178.6, 140.5 (2C), 129.0 (4C), 128.3 (4C), 127.9 (2C), 125.8 (q, <sup>1</sup>J<sub>C-F</sub> = 275.3 Hz), 56.5, 42.5 (q, <sup>3</sup>J<sub>C-F</sub> = 27.3 Hz) ppm. <sup>19</sup>F NMR (376 MHz, CDCl<sub>3</sub>): δ -58.67 (t, <sup>3</sup>J<sub>F-H</sub> = 10.2 Hz, 3F) ppm. IR (neat, cm<sup>-1</sup>): 3010, 1695, 1496, 1446, 1403, 1367, 1310, 1255, 1209, 1170, 1120, 1034, 991, 933, 833, 782, 758, 689. HRMS calc. for [C<sub>16</sub>H<sub>13</sub>F<sub>3</sub>O<sub>2</sub>-COOH], 249.0892 found 249.0897.

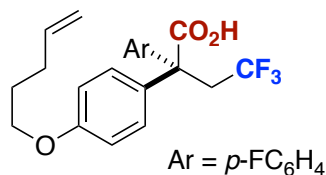


**4,4,4-trifluoro-2-(4-methoxyphenyl)-2-phenylbutanoic acid (2):** Following the general procedure, using Ir photocatalyst **Ir-2** (1.8 mg, 1 mol%), CF<sub>3</sub>SO<sub>2</sub>Na (37.2, 0.24 mmol) and **2s** (42 mg, 0.20 mmol), DMF (2 ml) for 12 h afforded **2** as a white solid in 93% yield (60 mg). Mp: 128°C. <sup>1</sup>H NMR (400 MHz, CDCl<sub>3</sub>): δ 7.34-7.31 (m, 5H), 7.27-7.23 (m, 2H), 6.90-6.86 (m, 2H), 3.81 (s, 3H), 3.40-3.28 (m, 2H) ppm. <sup>13</sup>C NMR (100 MHz, CDCl<sub>3</sub>): δ 178.6, 159.0, 140.7, 132.5, 130.2 (2C), 129.0 (2C), 128.2 (2C), 127.8, 125.8 (q, <sup>1</sup>J<sub>C-F</sub> = 275.6 Hz), 113.6 (2C), 55.9, 55.4, 42.5 (q, <sup>3</sup>J<sub>C-F</sub> = 27.5 Hz) ppm. <sup>19</sup>F NMR (376 MHz, CDCl<sub>3</sub>): δ -58.29 (t, <sup>1</sup>J<sub>F-H</sub> = 10.3 Hz, 3F) ppm. IR (neat, cm<sup>-1</sup>): 2925, 1690, 1611, 1512, 1457, 1436, 1361, 1317, 1251, 1209, 1114, 1026, 949, 827, 800, 774, 739, 717, 691. HRMS calc. for [C<sub>17</sub>H<sub>15</sub>F<sub>3</sub>O<sub>3</sub>-COOH], 279.1005 found 279.1002.

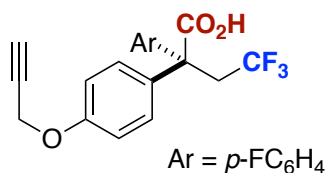


**4,4,4-trifluoro-2-(4-fluorophenyl)-2-phenylbutanoic acid (3):** Following the general procedure, using Ir photocatalyst **Ir-2** (1.8 mg, 1 mol%), CF<sub>3</sub>SO<sub>2</sub>Na (37.2, 0.24 mmol) and **3s** (40 mg, 0.20 mmol), DMF (2 ml) for 15 h afforded **3** as a white solid in 79% yield (50 mg). Mp: 123°C. <sup>1</sup>H NMR (500 MHz, CDCl<sub>3</sub>): δ 7.36-7.32 (m, 7H), 7.04-7.01 (m, 2H), 3.51-3.42 (m, 1H), 3.34-3.25 (m, 1H) ppm. <sup>13</sup>C NMR (125 MHz, CDCl<sub>3</sub>): δ 178.7, 162.1 (d, <sup>1</sup>J<sub>C-F</sub> = 246.4 Hz), 140.5, 136.2 (d, <sup>4</sup>J<sub>C-F</sub> = 3.4 Hz), 131.0 (d, <sup>3</sup>J<sub>C-F</sub> = 8.4 Hz, 2C), 128.7 (2C), 128.5 (2C), 128.2, 125.6 (q, <sup>1</sup>J<sub>C-F</sub> = 276.6 Hz), 115.1 (d, <sup>2</sup>J<sub>C-F</sub> = 21.4 Hz, 2C), 56.0, 42.5 (q, <sup>3</sup>J<sub>C-F</sub> = 27.5 Hz) ppm. <sup>19</sup>F NMR (376 MHz, CDCl<sub>3</sub>): δ -58.75 (t, <sup>3</sup>J<sub>FH</sub> = 10.2 Hz, 3F), -115 to -115.08 (m, 1F) ppm. IR (neat,

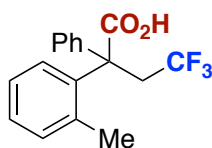
cm<sup>-1</sup>): 2960, 1698, 1605, 1507, 1445, 1409, 1366, 1258, 1234, 1201, 1166, 1126, 1037, 991, 912, 775, 742, 705. HRMS calc. for [C<sub>16</sub>H<sub>12</sub>F<sub>4</sub>O<sub>2</sub>-COOH] 267.0802 found 267.0805.



**4,4,4-trifluoro-2-(4-fluorophenyl)-2-(4-(pent-4-en-1-yloxy)phenyl)butanoic acid (4):** Following the general procedure, using Ir photocatalyst **Ir-2** (1.8 mg, 1 mol%), CF<sub>3</sub>SO<sub>2</sub>Na (37.2, 0.24 mmol) and **4s** (56.4 mg, 0.20 mmol), DMF (3 mL) for 15 h afforded **4** as a clear oil in 62% yield (49 mg). <sup>1</sup>H NMR (400 MHz, CDCl<sub>3</sub>): δ 7.31-7.27 (m, 2H), 7.22-7.20 (m, 2H), 7.01-6.97 (m, 2H), 6.85-6.83 (m, 2H), 5.90-5.80 (m, 1H), 5.1-4.93 (m, 2H), 3.97 (t, <sup>3</sup>J<sub>H-H</sub> = 6.4 Hz, 2H), 3.47-3.36 (m, 1H), 3.24-3.13 (m, 1H), 2.27-2.21 (m, 2H), 1.92-1.85 (m, 2H) ppm. <sup>13</sup>C NMR (100 MHz, CDCl<sub>3</sub>): δ 178.1, 162.1 (d, <sup>1</sup>J<sub>C-F</sub> = 246.2 Hz), 158.7, 137.8, 136.4 (d, <sup>4</sup>J<sub>C-F</sub> = 3.4 Hz), 132.3, 131.0 (d, <sup>3</sup>J<sub>C-F</sub> = 8.6 Hz, 2C), 129.5 (2C), 125.5 (q, <sup>1</sup>J<sub>C-F</sub> = 276.2 Hz), 115.4, 115.1 (d, <sup>2</sup>J<sub>C-F</sub> = 21 Hz, 2C), 114.3 (2C), 67.4, 55.30, 42.6 (q, <sup>2</sup>J<sub>C-F</sub> = 27.4 Hz), 30.2, 28.5 ppm. <sup>19</sup>F NMR (376 MHz, CDCl<sub>3</sub>): δ -58.82 (t, <sup>3</sup>J<sub>F-H</sub> = 10.2 Hz, 3F), -114.61 to -114.68 (m, 1F) ppm. IR (neat, cm<sup>-1</sup>): 2955, 1701, 1606, 1506, 1436, 1364, 1248, 1185, 1118, 1014, 993, 926, 824. HRMS calc. for 351.1369 found 351.1378.

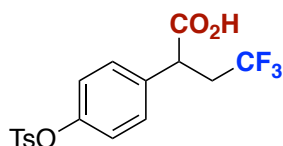


**4,4,4-trifluoro-2-(4-fluorophenyl)-2-(4-(prop-2-yn-1-yloxy)phenyl)butanoic acid (5):** Following the general procedure, using Ir photocatalyst **Ir-2** (1.8 mg, 1 mol%), CF<sub>3</sub>SO<sub>2</sub>Na (37.2 mg, 0.24 mmol) and **5s** (50.4 mg, 0.20 mmol), DMF (3 ml), afforded **5** as a clear oil in 62% yield (45 mg). <sup>1</sup>H NMR (400 MHz, CDCl<sub>3</sub>): δ 7.31-7.24 (m, 4H), 7.02-6.98 (m, 2H), 6.94-6.91 (m, 2H), 4.69 (d, <sup>4</sup>J<sub>H-H</sub> = 2.4 Hz, 2H), 3.46-3.345 (m, 1H), 3.26-3.15 (m, 1H), 2.53 (t, <sup>4</sup>J<sub>H-H</sub> = 2.4 Hz, 1H) ppm. <sup>13</sup>C NMR (100 MHz, CDCl<sub>3</sub>): δ 177.8, 162.1 (d, <sup>1</sup>J<sub>C-F</sub> = 246.2 Hz), 157.2, 136.3 (d, <sup>4</sup>J<sub>C-F</sub> = 3.3 Hz), 133.4, 130.9 (d, <sup>3</sup>J<sub>C-F</sub> = 8.0 Hz, 2C), 129.9 (2C), 125.8 (q, <sup>1</sup>J<sub>C-F</sub> = 276.5 Hz), 115.1 (d, <sup>2</sup>J<sub>C-F</sub> = 21 Hz, 2C), 114.7 (2C), 78.4, 75.9, 55.9, 55.3, 42.6 (q, <sup>2</sup>J<sub>C-F</sub> = 27.2 Hz) ppm. <sup>19</sup>F NMR (376 MHz, CDCl<sub>3</sub>): δ -58.82 (t, <sup>3</sup>J<sub>F-H</sub> = 10.3 Hz, 3F), -114.49 to -114.56 (m, 1F) ppm. IR (neat, cm<sup>-1</sup>): 2956, 1705, 1605, 1506, 1440, 1364, 1259, 1227, 1185, 1121, 1025, 925, 824, 730. HRMS calc. for [C<sub>19</sub>H<sub>14</sub>F<sub>4</sub>O<sub>2</sub>-COOH] 321.0912 found 321.0908.

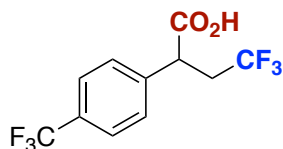


**4,4,4-trifluoro-2-phenyl-2-(o-tolyl)butanoic acid (6):** Following the general procedure, using Ir photocatalyst **Ir-2** (2.7 mg, 1 mol%), CF<sub>3</sub>SO<sub>2</sub>Na (46.5, 0.36 mmol) and **6s** (59 mg, 0.30 mmol), DMF (3 ml) for 12 h, afforded **6** as a white solid in 93% yield (86 mg). Mp: 137°C. <sup>1</sup>H NMR (400 MHz, CDCl<sub>3</sub>): δ 7.44-

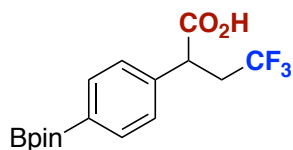
7.41 (m, 3H), 7.35-7.26 (m, 3H), 7.25-7.20 (m, 2H), 7.14-7.12 (m, 1H), 3.56-3.39 (m, 2H), 1.88 (s, 3H) ppm.  $^{13}\text{C}$  NMR (100 MHz,  $\text{CDCl}_3$ ):  $\delta$  178.4, 140.2, 137.7, 137.6, 132.8, 129.7 (2C), 128.5 (2C), 128.4, 128.1, 127.8, 125.8 (q,  $^1J_{\text{C-F}} = 275.2$  Hz), 125.8, 56.5, 40.5 (q,  $^3J_{\text{C-F}} = 27.4$  Hz), 21.54 ppm.  $^{19}\text{F}$  NMR (376 MHz,  $\text{CDCl}_3$ ):  $\delta$  -58.98 (t,  $^3J_{\text{F-H}} = 10.2$  Hz, 3F) ppm. IR (neat,  $\text{cm}^{-1}$ ): 2956, 1691, 1488, 1448, 1368, 1360, 1257, 1209, 1188, 1131, 1098, 1051, 984, 942, 760, 735, 689. HRMS calc. for  $[\text{C}_{17}\text{H}_{15}\text{F}_3\text{O}_2\text{-COOH}]$ , 263.1059 found 263.1053.



**4,4,4-trifluoro-2-(4-(tosyloxy)phenyl)butanoic acid (7):** Following the general procedure, using Ir photocatalyst **Ir-2** (3.6 mg, 2 mol%),  $\text{CF}_3\text{SO}_2\text{Na}$  (74 mg, 0.4 mmol) and **7s** (54.6 mg, 0.20 mmol), DMF (3 ml) at 5 °C for 15 h, afforded **7** as a yellow solid in 60% yield (49 mg). Mp: 103 °C.  $^1\text{H}$  NMR (400 MHz,  $\text{CDCl}_3$ ):  $\delta$  7.68 (d,  $^3J_{\text{H-H}} = 8.3$  Hz, 2H), 7.3 (d,  $^3J_{\text{H-H}} = 8.3$  Hz, 2H), 7.23 (d,  $^3J_{\text{H-H}} = 8.56$  Hz, 2H), 6.97 (d,  $^3J_{\text{H-H}} = 8.56$ , 2H), 3.87 (m, 1H), 3.05-2.94 (m, 1H), 2.49-2.41 (m, 4H) ppm.  $^{13}\text{C}$  NMR (125 MHz,  $\text{CDCl}_3$ ):  $\delta$  176.8, 149.5, 145.7, 135.3, 132.2, 129.9 (2C), 129.1 (2C), 128.5(2C), 125.9 (q,  $^1J_{\text{C-F}} = 275$  Hz), 123.1 (2C), 44.7, 37.0 (q,  $^2J_{\text{C-F}} = 28$  Hz), 21.8 ppm.  $^{19}\text{F}$  NMR (376 MHz,  $\text{CDCl}_3$ ):  $\delta$  -64.82 (t,  $^3J_{\text{H-H}} = 10.3$  Hz, 3F) ppm. IR (neat,  $\text{cm}^{-1}$ ): 1704, 1596, 1501, 1366, 1331, 1285, 1260, 1199, 1173, 1138, 1091, 1016, 969, 948, 867, 810, 770, 703, 660. HRMS calc. for  $[\text{C}_{17}\text{H}_{15}\text{F}_3\text{O}_5\text{S} - \text{H}]$ , 387.0529 found 387.0520.

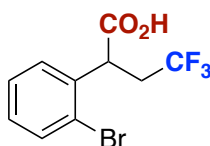


**4,4,4-trifluoro-2-(4-(trifluoromethyl)phenyl)butanoic acid (8):** Following the general procedure, using Ir photocatalyst **Ir-2** (1.8 mg, 1 mol%),  $\text{CF}_3\text{SO}_2\text{Na}$  (37.2 mg, 0.24 mmol), **8s** (34.2 mg, 0.20 mmol) and DMF (2 ml) for 15 h, afforded **8** as a white solid in 85% yield (49 mg). Mp: 100 °C  $^1\text{H}$  NMR (500 MHz,  $\text{CDCl}_3$ ):  $\delta$  7.63 (d,  $^3J_{\text{H-H}} = 8.1$  Hz, 2H), 7.44 (d,  $^3J_{\text{H-H}} = 8.1$  Hz, 2H), 3.99 (dd,  $^3J_{\text{H-H}} = 8.1$  Hz, 5.6 Hz, 1H), 3.14-3.03 (m, 1H), 2.58-2.50 (m, 1H) ppm.  $^{13}\text{C}$  NMR (125 MHz,  $\text{CDCl}_3$ ):  $\delta$  177.4, 140.1, 130.9 (q,  $^2J_{\text{C-F}} = 32.3$  Hz), 128.4 (2C), 126.3 (q,  $^3J_{\text{C-F}} = 3.6$  Hz, 2C), 125.8 (q,  $^1J_{\text{C-F}} = 275.3$  Hz), 123.8 (q,  $^1J_{\text{C-F}} = 275.6$  Hz), 45.3, 36.9 (q,  $^3J_{\text{C-F}} = 28.3$  Hz) ppm.  $^{19}\text{F}$  NMR (376 MHz,  $\text{CDCl}_3$ ):  $\delta$  -62.82 (m, 3F), -65.18 (t,  $^3J_{\text{F-H}} = 10.6$  Hz, 3F) ppm. IR (neat,  $\text{cm}^{-1}$ ): 1696, 1617, 1419, 1393, 1324, 1255, 1120, 1096, 1069, 1016, 928, 834, 810, 743, 715. HRMS calc. for  $[\text{C}_{11}\text{H}_8\text{F}_6\text{O}_2 - \text{H}]$ , 285.0363 found 285.0356.

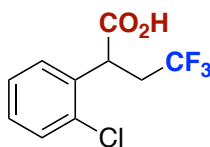


**4,4,4-trifluoro-2-(4-(4,4,5,5-tetramethyl-1,3,2-dioxaborolan-2-yl)phenyl)butanoic acid (9):** Following the general procedure, using Ir photocatalyst **Ir-2** (3.6 mg, 2 mol%),  $\text{CF}_3\text{SO}_2\text{Na}$  (74 mg, 0.24 mmol) and **9s** (46

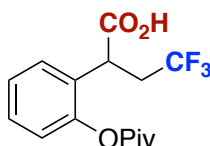
mg, 0.20 mmol), DMF (3 ml) at 5 °C for 10 h afforded **9** as a semi solid in 51% yield (34 mg). <sup>1</sup>H NMR (400 MHz, CDCl<sub>3</sub>): δ 7.79 (d, <sup>3</sup>J<sub>H-H</sub> = 8 Hz, 2H), 7.30 (d, <sup>3</sup>J<sub>H-H</sub> = 8 Hz, 2H), 3.91 (dd, <sup>3</sup>J<sub>H-H</sub> = 5.5 Hz, 8.28 Hz, 1H), 3.15-3.08 (m, 1H), 2.56-2.44 (m, 1H), 1.34 (s, 12H) ppm. <sup>13</sup>C NMR (100 MHz, CDCl<sub>3</sub>): δ 176.4, 139.5, 135.7 (2C), 127.4, 127.2 (2C), 125.7 (q, <sup>1</sup>J<sub>C-F</sub> = 275.1 Hz), 84.7 (2C), 45.4, 36.9 (q, <sup>3</sup>J<sub>C-F</sub> = 28 Hz), 24.9 (4C) ppm. <sup>19</sup>F NMR (376 MHz, CDCl<sub>3</sub>): δ -65.33 (t, 3F, <sup>3</sup>J<sub>C-F</sub> = 10.4 Hz) ppm. IR (neat, cm<sup>-1</sup>): 2978, 1715, 1610, 1516, 1398, 1357, 1258, 1136, 1088, 1020, 961, 856. HRMS calc. for [C<sub>16</sub>H<sub>20</sub>BF<sub>3</sub>O<sub>4</sub> - H], 342.1373 found 342.1370.



**2-(2-bromophenyl)-4,4,4-trifluorobutanoic acid (10):** Following the general procedure, using Ir photocatalyst **Ir-2** (1.8 mg, 1 mol%), CF<sub>3</sub>SO<sub>2</sub>Na (37.2, 0.24 mmol), **10s** (36.2 mg, 0.20 mmol), and DMF (2 ml) for 20 h, afforded **10** as a oil in 80 % yield (48.3 mg). <sup>1</sup>H NMR (300 MHz, CDCl<sub>3</sub>): δ 7.64-7.61 (m, 1H), 7.33-7.32 (m, 2H), 7.22-7.16 (m, 1H), 4.53 (m, 1H), 3.15-2.98 (m, 1H), 2.63-2.46 (m, 1H) ppm. <sup>13</sup>C NMR (100 MHz, CDCl<sub>3</sub>): δ 177.0, 136.1, 133.8, 129.9, 129.0, 128.3, 125.8 (q, <sup>1</sup>J<sub>C-F</sub> = 275 Hz), 124.4, 44.4, 36.4 (q, <sup>2</sup>J<sub>C-F</sub> = 29 Hz) ppm. <sup>19</sup>F NMR (376 MHz, CDCl<sub>3</sub>): δ -65.16 (t, <sup>3</sup>J<sub>F-HH</sub> = 10.3 Hz, 3F) ppm. IR (neat, cm<sup>-1</sup>): 2924, 1711, 1472, 1435, 1375, 1257, 1128, 1098, 1066, 1023, 966, 922, 840, 744, 659. HRMS calc. for [C<sub>10</sub>H<sub>8</sub>BrF<sub>3</sub>O<sub>2</sub> - H], 294.9575 found 294.9587.

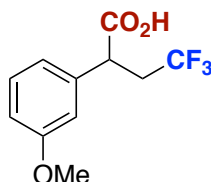


**2-(2-chlorophenyl)-4,4,4-trifluorobutanoic acid (11):** Following the general procedure, using Ir photocatalyst **Ir-2** (2.7 mg, 1 mol%), CF<sub>3</sub>SO<sub>2</sub>Na (46.5, 0.36 mmol) and **11s** (41.2 mg, 0.30 mmol), DMF (3 ml) 18 h, afforded **11** as a oil in 60 % yield (45.3 mg). <sup>1</sup>H NMR (500 MHz, CDCl<sub>3</sub>): δ 7.44-7.42 (m, 1H), 7.34-7.32 (m, 1H), 7.29-7.26 (m, 2H), 4.49 (m, 1H), 3.14-3.03 (m, 1H), 2.61-2.51 (m, 1H) ppm. <sup>13</sup>C NMR (100 MHz, CDCl<sub>3</sub>): δ 177.2, 134.3, 133.7, 130.2, 129.5, 129.1, 127.4, 127.8 (q, <sup>1</sup>J<sub>C-F</sub> = 275.4 Hz), 42.1 (q, <sup>3</sup>J<sub>C-F</sub> = 2.8 Hz), 36.0 (q, <sup>3</sup>J<sub>C-F</sub> = 29 Hz) ppm. <sup>19</sup>F NMR (376 MHz, CDCl<sub>3</sub>): δ -65.32 (t, <sup>2</sup>J<sub>F-H</sub> = 10.2 Hz, 3F) ppm. IR (neat, cm<sup>-1</sup>): 2957, 1712, 1474, 1435, 1378, 1258, 1133, 1102, 1037, 925. HRMS calc. for [C<sub>10</sub>H<sub>8</sub>F<sub>3</sub>O<sub>2</sub> - H], 251.0100 found 251.0092.

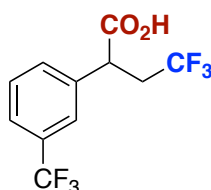


**4,4,4-trifluoro-2-(2-(pivaloyloxy)phenyl)butanoic acid (12):** Following the general procedure, using Ir photocatalyst **Ir-2** (3.6 mg, 2 mol%), CF<sub>3</sub>SO<sub>2</sub>Na (74 mg, 0.24 mmol) and **12s** (40.8 mg, 0.20 mmol), DMF (3 ml) at 5 °C for 20 h, afforded **12** as a clear oil in 60% yield (38 mg). <sup>1</sup>H NMR (500 MHz, CDCl<sub>3</sub>): δ 7.36-7.32 (m, 2H), 7.25-7.22 (m, 1H), 7.05 (m, 1H), 4.09 (dd, <sup>3</sup>J<sub>H-H</sub> = 5.3, 8.25 Hz 1H), 3.11-3.04 (m, 1H), 2.50-2.40 (m, 1H), 1.38 (s, 9H) ppm. <sup>13</sup>C NMR (125 MHz, CDCl<sub>3</sub>): δ 177.1, 176.6, 148.6, 129.4, 128.8, 126.6, 125.9 (q, <sup>1</sup>J<sub>C-</sub>

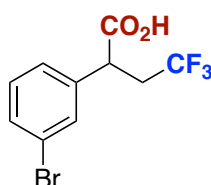
$f = 275.1$  Hz), 123.10, 39.4, 38.7 (q,  $^4J_{C-F} = 2.5$  Hz), 36.4 (q,  $^3J_{C-F} = 29$  Hz), 27.1 (4C) ppm.  $^{19}\text{F}$  NMR (376 MHz,  $\text{CDCl}_3$ ):  $\delta$  -65.66 (t,  $^3J_{F-H} = 10.2$  Hz, 3F) ppm. IR (neat,  $\text{cm}^{-1}$ ): 2974, 1748, 1715, 1480, 1373, 1380, 1259, 1211, 1100, 1027, 965, 941, 894, 839, 753. HRMS calc. for  $[\text{C}_{15}\text{H}_{17}\text{F}_3\text{O}_4 - \text{H}]$ , 317.1018 found 317.1006.



**4,4,4-trifluoro-2-(3-methoxyphenyl)butanoic acid (13):** Following the general procedure, using Ir photocatalyst **Ir-2** (3.6 mg, 2 mol%),  $\text{CF}_3\text{SO}_2\text{Na}$  (74 mg, 0.24 mmol) and **13s** (26.8 mg, 0.20 mmol), DMF (3 ml) at  $5^\circ\text{C}$  for 15 h, afforded **13** as a whit solid in 57 % yield (28 mg). Mp  $112^\circ\text{C}$ .  $^1\text{H}$  NMR (400 MHz,  $\text{CDCl}_3$ ):  $\delta$  7.30-7.26 (m, 1H), 6.91-6.85 (m, 3H), 3.89 (dd,  $^3J_{H-H} = 5.16$  Hz, 8.6 Hz, 1H), 3.81 (s, 3H), 3.15-3.01 (m, 1H), 2.55-2.46 (m, 1H) ppm.  $^{13}\text{C}$  NMR (100 MHz,  $\text{CDCl}_3$ ):  $\delta$  177.7, 160.1, 137.8, 130.3, 125.8 (q,  $^1J_{C-F} = 275.4$  Hz), 120.0, 113.7, 113.7, 55.4, 45.3, 37.1 (q,  $^3J_{C-F} = 28.4$  Hz) ppm.  $^{19}\text{F}$  NMR (376 MHz,  $\text{CDCl}_3$ ):  $\delta$  -65.44 (t,  $^3J_{F-H} = 10.2$  Hz, 3F) ppm. IR (neat,  $\text{cm}^{-1}$ ): 2964, 1714, 1607, 1584, 1487, 1442, 1378, 1254, 1231, 1114, 1087, 1046, 931, 883. HRMS calc. for  $[\text{C}_{11}\text{H}_{11}\text{F}_3\text{O}_3 - \text{H}]$ , 247.0587 found 247.0588.

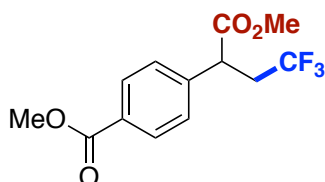


**4,4,4-trifluoro-2-(3-(trifluoromethyl)phenyl)butanoic acid (14):** Following the general procedure, using Ir photocatalyst **Ir-2** (1.8 mg, 1 mol%),  $\text{CF}_3\text{SO}_2\text{Na}$  (46.5, 0.24 mmol), **14s** (34.2 mg, 0.20 mmol) and DMF (2 ml) for 15 h, afforded **14** as a oil in 80% yield (45.7 mg).  $^1\text{H}$  NMR (400 MHz,  $\text{CDCl}_3$ ):  $\delta$  7.62-7.57 (m, 2H), 7.53-7.748 (m, 2H), 4.00 (dd,  $^3J_{H-H} = 8.2$  Hz, 5.8 Hz 1H), 3.17-3.04 (m, 1H), 2.60- 2.48 (m, 1H) ppm.  $^{13}\text{C}$  NMR (100 MHz,  $\text{CDCl}_3$ ):  $\delta$  176.9, 137.2, 131.8 (q,  $^2J_{C-F} = 32.3$  Hz), 131.3, 129.8, 125.7 (q,  $^1J_{C-F} = 275$  Hz), 125.5 (q,  $^3J_{C-F} = 3.7$  Hz), 124.7 (q,  $^3J_{C-F} = 3.7$  Hz), 123.5 (q,  $^1J_{C-F} = 275$  Hz), 45.2 (q,  $^4J_{C-F} = 2.8$  Hz), 36.9 (q,  $^2J_{C-F} = 28.7$  Hz) ppm.  $^{19}\text{F}$  NMR (376 MHz,  $\text{CDCl}_3$ ):  $\delta$  -62.87 (s, 3F), -65.30 (t,  $^3J_{H-F} = 10.6$  Hz, 3F) ppm. IR (neat,  $\text{cm}^{-1}$ ): 1715, 1383, 1326, 1261, 1112, 965, 918, 843, 804, 730, 700. HRMS calc. for  $[\text{C}_{11}\text{H}_8\text{F}_6\text{O}_2 - \text{H}]$ , 285.0356 found 285.0359.

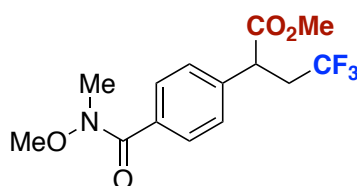


**2-(3-bromophenyl)-4,4,4-trifluorobutanoic acid (15):** Following the general procedure, using Ir photocatalyst **Ir-2** (1.8 mg, 1 mol%),  $\text{CF}_3\text{SO}_2\text{Na}$  (37.2 mg, 0.24 mmol), **15s** (36.4 mg, 0.20 mmol) and DMF (2 ml) for 15 h, afforded **15** as a colorless liquid in 75% yield (45 mg).  $^1\text{H}$  NMR (400 MHz,  $\text{CDCl}_3$ ):  $\delta$  7.53-7.50 (m, 2H), 7.31-7.28 (m, 2H), 3.92 (dd,  $^3J_{H-H} = 8.3$  Hz, 5.6 Hz 1H), 3.17-3.04 (m, 1H), 2.60-2.48 (m, 1H)

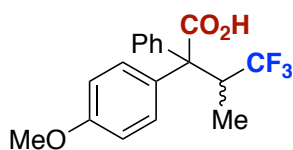
ppm.  $^{13}\text{C}$  NMR (125 MHz,  $\text{CDCl}_3$ ):  $\delta$  177.2, 138.4, 131.7, 130.9, 130.8, 126.5, 125.8 (q,  $^1J_{\text{C-F}} = 275$  Hz), 123.2, 45.0, 36.9 (q,  $^2J_{\text{C-F}} = 29$  Hz) ppm.  $^{19}\text{F}$  NMR (376 MHz,  $\text{CDCl}_3$ ):  $\delta$  -65.31 (t,  $^3J_{\text{F-H}} = 10.1$  Hz, 3F) ppm. IR (neat,  $\text{cm}^{-1}$ ): 1712, 1569, 1473, 1429, 1378, 1328, 1257, 1139, 1111, 997, 966, 903, 840, 784, 757, 693. HRMS calc. for  $[\text{C}_{10}\text{H}_8\text{BrF}_3\text{O}_2 - \text{H}]$ , 294.9580 found 294.9587.



**methyl 4-(4,4,4-trifluoro-1-methoxy-1-oxobutan-2-yl)benzoate (16):** Following the general procedure, using Ir photocatalyst **Ir-2** (3.6 mg, 2 mol%),  $\text{CF}_3\text{SO}_2\text{Na}$  (74 mg, 0.24 mmol) and **16s** (32.4 mg, 0.20 mmol) and DMF (3 ml) at 5 °C for 12 h, followed by the treatment of the crude acid with  $\text{TMSCHN}_2$  afforded **16** (60% yield, 35 mg) as a white solid. Mp 53 °C.  $^1\text{H}$  NMR (400 MHz,  $\text{CDCl}_3$ ):  $\delta$  8.02-7.99 (m, 2H), 7.38-7.35 (m, 2H), 3.95 (dd,  $^3J_{\text{H-H}} = 5.72$  Hz, 8.32 Hz, 1H), 3.95 (s, 3H), 3.67 (s, 3H), 3.17-3.03 (m, 1H), 2.57-2.44 (m, 1H) ppm.  $^{13}\text{C}$  NMR (100 MHz,  $\text{CDCl}_3$ ):  $\delta$  171.8, 166.5, 141.9, 130.3 (2C), 130.1, 127.8, 125.9 (q,  $^1J_{\text{C-F}} = 275.1$  Hz), 52.8, 52.2, 45.3 (q,  $^4J_{\text{C-F}} = 2.8$  Hz), 37.0 (q,  $^3J_{\text{C-F}} = 29$  Hz) ppm.  $^{19}\text{F}$  NMR (376 MHz,  $\text{CDCl}_3$ ):  $\delta$  -65.39 (t,  $^3J_{\text{F-H}} = 10.3$  Hz, 3F) ppm. IR (neat,  $\text{cm}^{-1}$ ): 2952, 1718, 1611, 1435, 1265, 1259, 1207, 1137, 1095, 1060, 1019, 953, 745, 702.



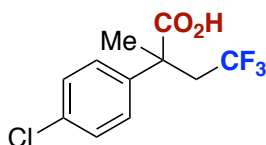
**methyl 4,4,4-trifluoro-2-(4-(methoxy(methyl)carbamoyl)phenyl)butanoate (17):** Following the general procedure, using Ir photocatalyst **Ir-2** (1.8 mg, 1 mol%),  $\text{CF}_3\text{SO}_2\text{Na}$  (37.2, 0.24 mmol) and **17s** (38.2 mg, 0.20 mmol) and DMF (2 ml) for 15 h, followed by the treatment of the crude acid with  $\text{TMSCHN}_2$  afforded **17** (70% yield, 42 mg) as a semi solid.  $^1\text{H}$  NMR (400 MHz,  $\text{CDCl}_3$ ):  $\delta$  7.63-7.60 (m, 2H), 7.30-7.28 (m, 2H), 3.89 (dd,  $^3J_{\text{H-H}} = 5.4$  Hz, 8.68 Hz, 1H), 3.63 (s, 3H), 3.49 (s, 3H), 3.29 (s, 3H), 3.12-2.99 (m, 1H), 2.52-2.39 (m, 1H) ppm.  $^{13}\text{C}$  NMR (100 MHz,  $\text{CDCl}_3$ ):  $\delta$  171.9, 169.1, 139.3, 133.8, 128.9 (2C), 127.3 (2C), 125.9 (q,  $^1J_{\text{C-F}} = 275.4$  Hz), 61.0, 52.6, 45.0 (q,  $^3J_{\text{C-F}} = 2.8$  Hz), 36.9 (q,  $^3J_{\text{C-F}} = 29$  Hz), 33.5 ppm.  $^{19}\text{F}$  NMR (376 MHz,  $\text{CDCl}_3$ ):  $\delta$  -65.47 (t,  $^3J_{\text{H-F}} = 10.2$  Hz, 3F) ppm. IR (neat,  $\text{cm}^{-1}$ ): 2955, 1735, 1645, 1436, 1374, 1259, 1207, 1135, 1098, 1061, 979, 952, 746. HRMS calc. for  $[\text{C}_{14}\text{H}_{16}\text{F}_3\text{NO}_4 + \text{Na}]$ , 342.0924 found 342.0926.



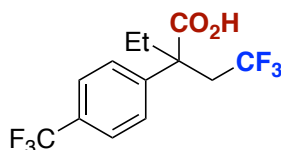
**4,4,4-trifluoro-2-(4-methoxyphenyl)-3-methyl-2-phenylbutanoic acid (18):** Following the general procedure, using Ir photocatalyst **Ir-2** (3.6 mg, 2 mol%),  $\text{CF}_3\text{SO}_2\text{Na}$  (74.4, 0.4 mmol), **18s** (45 mg, 0.20 mmol), and DMF (3 ml) for 30 h, afforded **18** as a mixture of diastereoisomers in 47% yield (30 mg). Mp: 64 °C.  $^1\text{H}$



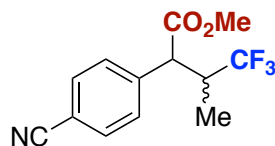
NMR (500 MHz, CDCl<sub>3</sub>):  $\delta$  7.40 – 7.29 (m, 7H), 6.88-6.86 (m, 2H), 4.16-4.10 (m, 1H), 3.82 (s, 3H), 1.20 (d, <sup>3</sup>J<sub>H-H</sub> = 7Hz, 3H) ppm. <sup>13</sup>C NMR (125 MHz, CDCl<sub>3</sub>):  $\delta$  178.8, 159.1, 136.7, 132.4, 131.2 (3C), 127.6 (2C), 127.5 (q, <sup>1</sup>J<sub>C-F</sub> = 279 Hz), 127.2 (2C), 113.6, 60.6, 55.3, 42.5 (q, <sup>2</sup>J<sub>C-F</sub> = 27.2 Hz), 10.17 ppm. <sup>19</sup>F NMR (376 MHz, CDCl<sub>3</sub>):  $\delta$  -64.34 (brs, 3F) ppm. IR (neat, cm<sup>-1</sup>): 1699, 1606, 1509, 1463, 1373, 1250, 1167, 1116, 1091, 1033, 906, 830, 798, 770, 708. HRMS calc. for [C<sub>18</sub>H<sub>17</sub>F<sub>3</sub>O<sub>2</sub>-COOH] 293.1169 found 293.1159.



**2-(4-chlorophenyl)-4,4,4-trifluoro-2-methylbutanoic acid (19):** Following the general procedure, using Ir photocatalyst **Ir-2** (1.8, 1 mol%), CF<sub>3</sub>SO<sub>2</sub>Na (37.2 mg, 0.24 mmol), **19s** (30.4 mg, 0.20 mmol) and DMF (2 ml) for 15 h, afforded **19** as a colorless liquid in 68% yield (36 mg). <sup>1</sup>H NMR (500 MHz, CDCl<sub>3</sub>):  $\delta$  7.36-7.32 (m, 4H), 3.13-3.03 (m, 1H), 2.73-2.64 (m, 1H), 1.76 (s, 3H) ppm. <sup>13</sup>C NMR (125 MHz, CDCl<sub>3</sub>):  $\delta$  180.6, 139.2, 134.1, 127.1 (2C), 127.3 (2C), 125.9 (q, <sup>1</sup>J<sub>C-F</sub> = 276 Hz), 46.8, 42.3 (q, <sup>2</sup>J<sub>C-F</sub> = 27.6 Hz), 21.3 ppm. <sup>19</sup>F NMR (376 MHz, CDCl<sub>3</sub>):  $\delta$  -59.80 (t, <sup>3</sup>J<sub>H-F</sub> = 10.6 Hz, 3F) ppm. IR (neat, cm<sup>-1</sup>): 2895, 1701, 1493, 1431, 1402, 1366, 1259, 1215, 1156, 1111, 1083, 1034, 1011, 909, 845, 821, 754, 724, 695. HRMS calc. for [C<sub>11</sub>H<sub>10</sub>ClF<sub>3</sub>O<sub>2</sub> - H], 265.0245 found 265.0249.

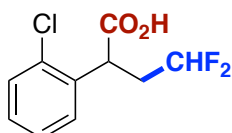


**2-ethyl-4,4,4-trifluoro-2-(4-(trifluoromethyl)phenyl)butanoic acid (20):** Following the general procedure, using Ir photocatalyst **Ir-2** (1.8 mg, 1 mol%), CF<sub>3</sub>SO<sub>2</sub>Na (37.2 mg, 0.24 mmol), **20s** (37.2 mg, 0.20 mmol) and DMF (2 ml) for 15 h, afforded **20** as a white solid in 67% yield (42 mg). Mp: 87 °C. <sup>1</sup>H NMR (500 MHz, CDCl<sub>3</sub>):  $\delta$  7.65 (d, <sup>3</sup>J<sub>H-H</sub> = 8.4 Hz, 2H), 7.46 (d, <sup>3</sup>J<sub>H-H</sub> = 8.4 Hz, 2H), 3.08-3.02 (m, 1H), 2.98 – 2.88 (m, 1H), 2.35- 2.28 (m, 2H), 0.87 (t, <sup>3</sup>J<sub>H-H</sub> = 7.3 Hz, 3H) ppm. <sup>13</sup>C NMR (125 MHz, CDCl<sub>3</sub>):  $\delta$  179.9, 143.7, 130.2 (q, <sup>2</sup>J<sub>C-F</sub> = 32.4 Hz), 126.8 (2C), 126.1 (q, <sup>1</sup>J<sub>C-F</sub> = 276.3 Hz), 125.9 (q, <sup>3</sup>J<sub>C-F</sub> = 3.5 Hz, 2C), 124.0 (q, <sup>1</sup>J<sub>C-F</sub> = 270.3 Hz), 51.7, 37.7 (q, <sup>2</sup>J<sub>C-F</sub> = 27.7 Hz), 26.9, 8.5 ppm. <sup>19</sup>F NMR (376 MHz, CDCl<sub>3</sub>):  $\delta$  -60.16 (t, <sup>3</sup>J<sub>H-F</sub> = 10.6 Hz, 3F), -62.91 (s, 3F) ppm. IR (neat, cm<sup>-1</sup>): 2980, 1699, 1619, 1444, 1404, 1371, 1324, 1252, 1199, 1112, 1057, 1015, 909, 831, 789, 721, 676. HR-MS (EI) *m/z* calcd for [C<sub>13</sub>H<sub>12</sub>O<sub>2</sub>F<sub>6</sub>][M-COOH] 270.0759 found 269.0770.

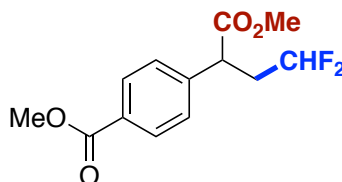


**methyl 2-(4-cyanophenyl)-4,4,4-trifluoro-3-methylbutanoate (21):** Following the general procedure, using Ir photocatalyst **Ir-2** (3.6 mg, 1 mol%), CF<sub>3</sub>SO<sub>2</sub>Na (74, 0.24 mmol), **21s** (26 mg, 0.20 mmol) and DMF (3 ml) for 20 h, followed by the treatment of crude acid with TMSCHN<sub>2</sub> afforded **21** (32 mg, 60% yield) as a clear oil (*dr* 2:1). Major isomer: <sup>1</sup>H NMR (500 MHz, CDCl<sub>3</sub>):  $\delta$  7.65 (d, <sup>3</sup>J<sub>H-H</sub> = 8.3 Hz, 2H), 7.45 (d, <sup>3</sup>J<sub>H-H</sub> = 8.3 Hz,

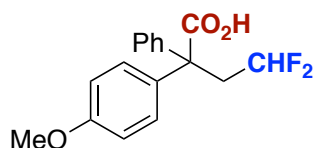
2H), 3.78 (m, 1H), 3.69 (s, 3H), 3.20-3.12 (m, 1H), 0.86 (d,  $^3J_{\text{H-H}} = 7.15$  Hz, 3H) ppm.  $^{13}\text{C}$  NMR (125 MHz,  $\text{CDCl}_3$ ):  $\delta$  171.9, 140.4, 132.7 (2C), 127.4 (q,  $^1J_{\text{C-F}} = 278.4$  Hz) 129.8 (2C), 118.3, 112.4, 52.9, 51.2, 40.5 (q,  $^3J_{\text{C-F}} = 26.2$  Hz, 11.3 ppm. Minor isomer:  $^1\text{H}$  NMR (500 MHz,  $\text{CDCl}_3$ ):  $\delta$  7.62 (d,  $^3J_{\text{H-H}} = 8.3$  Hz, 2H), 7.48 (d,  $^3J_{\text{H-H}} = 8.3$  Hz, 2H), 3.78 (m, 1H), 3.69 (s, 3H), 3.0-2.97 (m, 1H), 1.26 (d,  $^3J_{\text{H-H}} = 6.9$  Hz, 3H) ppm.  $^{13}\text{C}$  NMR (125 MHz,  $\text{CDCl}_3$ ):  $\delta$  171.2, 141.2, 132.5 (2C), 127.4 (q,  $^1J_{\text{C-F}} = 278.7$  Hz) 129.3 (2C), 118.5, 112.2, 52.8, 51.2, 41.8 (q,  $^3J_{\text{C-F}} = 26.4$  Hz), 12.5 ppm. IR (neat,  $\text{cm}^{-1}$ ): 2954, 2229, 1735, 1607, 1505, 1464, 1331, 1258, 1206, 1166, 1123, 1023, 842. HRMS calc. for  $[\text{C}_{13}\text{H}_{12}\text{F}_3\text{NO}_2 + \text{Na}]$ , 294.0717 found 294.0712.



**2-(2-chlorophenyl)-4,4-difluorobutanoic acid (22)**: Following the general procedure, using Ir photocatalyst **Ir-2** (2.7 mg, 1 mol%),  $\text{CF}_2\text{HSO}_2\text{Na}$  (41.4 mg, 0.36 mmol), **22s** (41 mg, 0.30 mmol) and DMF (3 ml) for 15 h, afforded **22** as a colorless liquid in 60% yield (42 mg).  $^1\text{H}$  NMR (400 MHz,  $\text{CDCl}_3$ ):  $\delta$  7.44-7.44 (m, 1H), 7.32-7.28 (m, 3H), 5.85 (tt,  $^1J_{\text{H-F}} = 55.72$  Hz,  $^3J_{\text{H-H}} = 4.80$  Hz, 1H), 4.42 (m, 1H), 2.80-2.66 (m, 1H), 2.38-2.23 (m, 1H) ppm.  $^{13}\text{C}$  NMR (100 MHz,  $\text{CDCl}_3$ ):  $\delta$  177.7, 135.0, 134.0, 130.3, 129.4, 129.2, 127.6, 115.6 (t,  $^1J_{\text{C-F}} = 237.8$  Hz), 42.3 (t,  $^3J_{\text{C-F}} = 6.0$  Hz), 36.4 (t,  $^2J_{\text{C-F}} = 22.9$  Hz) ppm.  $^{19}\text{F}$  NMR (376 MHz,  $\text{CDCl}_3$ ):  $\delta$  -115.26 to -118.31 (m, 2F) ppm. IR (neat,  $\text{cm}^{-1}$ ): 2948, 1705, 1475, 1402, 1259, 1117, 1066, 1033, 912, 748. HRMS calc. for  $[\text{C}_{10}\text{H}_9\text{ClF}_2\text{O}_2 - \text{H}]$ , 233.0188 found 233.0186.

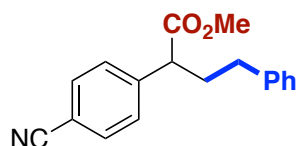


**methyl 4-(4,4-difluoro-1-methoxy-1-oxobutan-2-yl)benzoate (23)**: Following the general procedure, using Ir photocatalyst **Ir-2** (3.6 mg, 2 mol%),  $\text{CF}_2\text{HSO}_2\text{Na}$  (54.8 mg, 0.40 mmol), **23s** (32.4 mg, 0.20 mmol) and DMF (3 ml) for 15 h at 5 °C. followed by the treatment of crude acid with  $\text{TMSCHN}_2$  afforded **23** as a white solid in 55% yield (30 mg). Mp 40 °C.  $^1\text{H}$  NMR (400 MHz,  $\text{CDCl}_3$ ):  $\delta$  8.03-8.0 (m, 2H), 7.38-7.35 (m, 2H), 5.74 (tt,  $^1J_{\text{H-F}} = 55.8$  Hz,  $^3J_{\text{H-H}} = 4.5$  Hz, 1H), 3.94-3.84 (m, 4H), 3.68 (s, 3H), 2.78-2.63 (m, 1H), 2.34-2.19 (m, 1H) ppm.  $^{13}\text{C}$  NMR (100 MHz,  $\text{CDCl}_3$ ):  $\delta$  172.5, 166.7, 142.4, 130.4, 129.9, 127.9, 115.6 (t,  $^1J_{\text{C-F}} = 237.6$  Hz), 52.7, 52.3, 45.3 (t,  $^3J_{\text{C-F}} = 5.9$  Hz), 37.4 (t,  $^2J_{\text{C-F}} = 22.7$  Hz) ppm.  $^{19}\text{F}$  NMR (376 MHz,  $\text{CDCl}_3$ ):  $\delta$  -116.312 to -118.43 (m, 2F). IR (neat,  $\text{cm}^{-1}$ ): 1735, 1718, 1610, 1434, 1365, 1275, 1235, 1215, 1161, 1109, 1075, 1044, 934, 833, 779. HRMS calc. for  $[\text{C}_{13}\text{H}_{14}\text{F}_2\text{O}_4 + \text{H}]$ , 273.0925 found 273.0933.

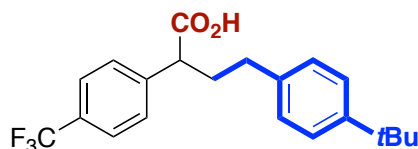


**4,4-difluoro-2-(4-methoxyphenyl)-2-phenylbutanoic acid (24)**: Following the general procedure, using Ir photocatalyst **Ir-2** (1.8 mg, 1 mol%),  $\text{CF}_2\text{HSO}_2\text{Na}$  (27.6, 0.24 mmol), **24s** (42 mg, 0.20 mmol) and DMF (2

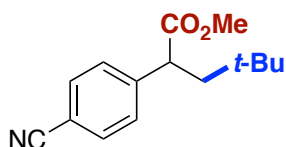
ml) for 15 h, afforded **24** as a colorless liquid in 75% yield (46 mg).  $^1\text{H}$  NMR (400 MHz,  $\text{CDCl}_3$ ):  $\delta$  7.36-7.30 (m, 5H), 7.25-7.23 (m, 2H), 6.88-6.85 (m, 2H), 5.47 (tt,  $^1J_{\text{H-F}} = 55.96$  Hz,  $^3J_{\text{H-H}} 4.64$  Hz, 1H), 3.82 (s, 3H), 3.02-2.93 (m, 2H) ppm.  $^{13}\text{C}$  NMR (100 MHz,  $\text{CDCl}_3$ ):  $\delta$  179.5, 159.0, 141.2, 132.9, 130.0, 128.7, 128.4, 127.7, 116.4 (t,  $^1J_{\text{C-F}} = 237.75$  Hz), 113.8, 56.4 (t,  $^3J_{\text{C-F}} = 5.38$  Hz), 55.3, 42.7 (t,  $^2J_{\text{C-F}} = 22.7$  Hz) ppm.  $^{19}\text{F}$  NMR (376 MHz,  $\text{CDCl}_3$ ):  $\delta$  -113.76 (dt,  $^3J_{\text{H-F}} = 4.1$  Hz,  $^2J_{\text{H-F}} 14.9$  Hz, 2F). IR (neat,  $\text{cm}^{-1}$ ): 2952, 1698, 1607, 1508, 1441, 1398, 1249, 1182, 1115, 1052, 1028, 951, 825.  $[\text{C}_{17}\text{H}_{16}\text{F}_2\text{NaO}_3]$   $[\text{M-COOH}+\text{Na}]$  329.0954 found 329.0960.



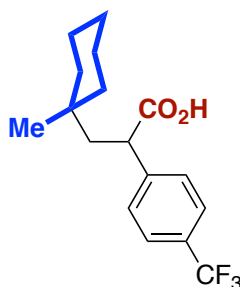
**methyl 2-(4-cyanophenyl)-4-phenylbutanoate (25)**: Following the general procedure, using Ir photocatalyst **Ir-3** (4.4 mg, 2 mol%), potassium benzyltrifluoroborate (47.5 mg, 0.24 mmol) and **25s** (26 mg, 0.20 mmol) and DMF (3 ml) for 20 h, followed by the treatment of crude acid with  $\text{TMSCHN}_2$  afforded desired ester **3-p-25** as a clear oil in 55 % yield (31 mg).  $^1\text{H}$  NMR (400 MHz,  $\text{CDCl}_3$ ):  $\delta$  7.64-7.61 (m, 2H), 7.43-7.40 (m, 2H), 7.31-7.26 (m, 2H), 7.23-7.18 (m, 1H), 7.14-7.12 (m, 2H), 3.67 (s, 3H), 3.62 (t,  $^3J_{\text{H-H}} = 7.64$  Hz 1H), 2.57 (t,  $^3J_{\text{H-H}} = 8.76$  Hz, 2H), 2.49-2.40 (m, 1H), 2.14-2.05 (m, 1H) ppm.  $^{13}\text{C}$  NMR (100 MHz,  $\text{CDCl}_3$ ):  $\delta$  173.2, 144.2, 140.6, 132.5, 129.0, 128.6, 128.5, 126.3, 118.7, 111.4, 52.4, 50.9, 34.8, 33.5 ppm. IR (neat,  $\text{cm}^{-1}$ ): 2950, 2227, 1731, 1605, 1496, 1435, 1214, 1148, 1019, 834, 750, 698. HRMS calc. for  $[\text{C}_{18}\text{H}_{17}\text{NO}_2 + \text{Na}]$ , 302.1158 found 302.1151.



**4-(4-(tert-butyl)phenyl)-2-(4-(trifluoromethyl)phenyl)butanoic acid (26)**: Following the general procedure, using Ir photocatalyst **Ir-3** (4.4 mg, 2 mol%), potassium 4-tert-butyl benzyltrifluoroborate (50.8 mg, 0.24 mmol) and **26s** (26 mg, 0.20 mmol) for 20 h. Purification by column chromatography on silica gel (hexanes/AcOEt 10/1 followed by hexanes/AcOEt 10/4) afforded **26** as a light yellow oil in 50 % yield (37 mg).  $^1\text{H}$  NMR (400 MHz,  $\text{CDCl}_3$ ):  $\delta$  7.60 (d,  $^3J_{\text{H-H}} = 8.12$  Hz, 2H), 7.44 (d,  $^3J_{\text{H-H}} = 8.12$  Hz, 2H), 7.30 (d,  $^3J_{\text{H-H}} = 8.2$  Hz, 2H), 7.07 (d,  $^3J_{\text{H-H}} = 8.2$  Hz, 2H), 3.66 (t,  $^3J_{\text{H-H}} = 7.4$  Hz, 1H), 2.56 (t,  $^3J_{\text{H-H}} = 7.4$  Hz, 2H), 2.49-2.40 (m, 1H), 2.17-2.10 (m, 1H), 1.31 (s, 9H) ppm.  $^{13}\text{C}$  NMR (100 MHz,  $\text{CDCl}_3$ ):  $\delta$  179.0, 149.2, 142.2, 137.6, 130.0 (q,  $^2J_{\text{C-F}} = 32.4$  Hz), 128.7 (2C), 128.1 (2C), 125.8 (q,  $^3J_{\text{C-F}} = 3.5$  Hz, 2C), 125.5 (2C), 124.1 (q,  $^1J_{\text{C-F}} = 270.3$  Hz), 50.6, 34.5, 34.5, 32.8, 31.5 (3C) ppm.  $^{19}\text{F}$  NMR (376 MHz,  $\text{CDCl}_3$ ):  $\delta$  -62.27 (s, 3F) ppm. IR (neat,  $\text{cm}^{-1}$ ): 2956, 1705, 1616, 1506, 1456, 1417, 1322, 1163, 1121, 1067, 1017, 832. HRMS calc. for  $[\text{C}_{21}\text{H}_{23}\text{F}_3\text{O}_2 - \text{H}]$ , 363.1578 found 363.1577.



**methyl 2-(4-cyanophenyl)-4,4-dimethylpentanoate (27):** Following the general procedure, using Ir photocatalyst **Ir-3** (4.4 mg, 2 mol%), tert-butyl cesium oxalate (66.7 mg, 0.24 mmol) and **27s** (26 mg, 0.20 mmol) and DMF (3 ml) for 20 h, followed by the treatment of crude acid with TMSCHN<sub>2</sub> afforded desired ester **27** as a pale-yellow oil in 61 % yield (30 mg). <sup>1</sup>H NMR (500 MHz, CDCl<sub>3</sub>): δ 7.57 (d, <sup>3</sup>J<sub>H-H</sub> = 8.3 Hz, 2H), 7.43 (d, <sup>3</sup>J<sub>H-H</sub> = 8.3 Hz 2H), 3.7 (dd, <sup>3</sup>J<sub>H-H</sub> = 4.05 Hz, 9.0 Hz, 1H), 3.63 (s, 3H), 2.27 (dd, <sup>3</sup>J<sub>H-H</sub> = 14 Hz, 9.0 Hz, 1H), 1.54 (dd, <sup>3</sup>J<sub>H-H</sub> = 4.05 Hz, 14.0 Hz, 1H), 0.88 (s, 9H) ppm. <sup>13</sup>C NMR (125 MHz, CDCl<sub>3</sub>): δ 174.2, 146.1, 132.5 (2C), 128.8 (2C), 118.7, 111.1, 54.4, 48.3, 47.3, 31.1, 29.4 (3C) ppm. IR (neat, cm<sup>-1</sup>): 2955, 2227, 1730, 1604, 1502, 1431, 1365, 1337, 1282, 1208, 1149, 1022, 974, 832, 782. HRMS calc. for [C<sub>15</sub>H<sub>19</sub>NO<sub>2</sub> + Na], 268.1312 found 268.1308.



**3-(1-methylcyclohexyl)-2-(4-(trifluoromethyl)phenyl)propanoic acid (28):** Following the general procedure, using Ir photocatalyst **Ir-3** (4.4 mg, 2 mol%), oxalate (76.3, 0.24 mmol), **28s** (34 mg, 0.20 mmol) and DMF (3 ml) for 20 h, afforded **28** as a light yellow oil in 65 % yield (41 mg). <sup>1</sup>H NMR (500 MHz, CDCl<sub>3</sub>): δ 7.56 (d, <sup>3</sup>J<sub>H-H</sub> = 8.2 Hz, 2H), 7.66 (d, <sup>3</sup>J<sub>H-H</sub> = 8.2 Hz 2H), 3.74 (dd, <sup>3</sup>J<sub>H-H</sub> = 4.3 Hz, 8.3 Hz, 1H), 2.29 (dd, <sup>3</sup>J<sub>H-H</sub> = 8.3 Hz, 14.2 Hz, 1H), 1.64 (dd, <sup>3</sup>J<sub>H-H</sub> = 4.3 Hz, 14.2 Hz, 1H), 1.45-1.17 (m, 10H), 0.87 (s, 3H) ppm. <sup>13</sup>C NMR (125 MHz, CDCl<sub>3</sub>): δ 180.4, 144.5, 129.7 (q, <sup>2</sup>J<sub>C-F</sub> = 32.4 Hz), 128.5 (2C), 125.7 (q, <sup>3</sup>J<sub>C-F</sub> = 3.5 Hz, 2C), 124.3 (q, <sup>1</sup>J<sub>C-F</sub> = 270.3 Hz), 47.1, 45.9, 37.9, 37.8, 33.7, 29.4, 26.3, 24.5, 21.9 ppm. <sup>19</sup>F NMR (376 MHz, CDCl<sub>3</sub>): δ -62.24 (s, 3F) ppm. IR (neat, cm<sup>-1</sup>): 2924, 1704, 1616, 1418, 1321, 1162, 1121, 1067, 1018, 836, 718. HRMS calc. for [C<sub>17</sub>H<sub>21</sub>F<sub>2</sub>O<sub>3</sub> - H], 313.1423 found 313.1421.

### 3.7.4. Fluorescence Quenching Experiments

Fluorescence spectra were collected on Fluorolog Horiba Jobin Yvon spectrofluorimeter. Samples for the quenching experiments were prepared in a 4 mL glass cuvette with a septum screw cap. **Ir-2** was irradiated at 470 nm and the emission intensity at 570 nm was observed. In a typical experiment, the emission spectrum of a 5.0 x 10<sup>-5</sup> M solution of **Ir-2** in DMF was collected.

CF<sub>3</sub>SO<sub>2</sub>Na: A stock solution of CF<sub>3</sub>SO<sub>2</sub>Na (77 mg, 0.5 mmol) in 1 ml of DMF was prepared. Then, different amounts of this stock solution were added to a solution of the photocatalyst **Ir-2** in DMF (5.0 x 10<sup>-5</sup> M). As shown (Figure 3.4), a significant decrease of [Ir(ppy)<sub>2</sub>(dtbbpy)]PF<sub>6</sub> (**Ir-2**) luminescence was observed, suggesting that the mechanism might operate via a canonical photoredox cycle consisting of a reductive quenching with CF<sub>3</sub>SO<sub>2</sub>Na.

Increasing amounts of substrates **1s** ( $E_{\text{ox}} = +1.81\text{V}$  vs SCE in MeCN) and **13s** were added directly to a solution of the photocatalyst **Ir-2** in DMF ( $5.0 \times 10^{-5}\text{M}$ ). In both cases, negligible decrease of **Ir-2**'s luminescence was observed (Figure 3.5 and 3.6).

### 3.7.5. X-Ray Crystallography

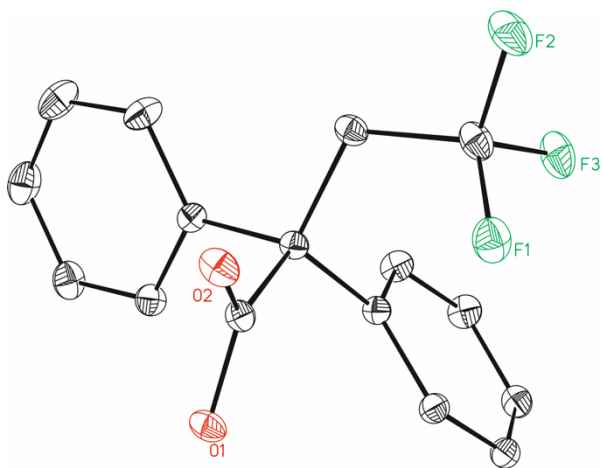


Table 1. Crystal data and structure refinement for **1**

Identification code	II-YVR-3	
Empirical formula	C <sub>16</sub> H <sub>13</sub> F <sub>3</sub> O <sub>2</sub>	
Formula weight	294.26	
Temperature	100(2) K	
Wavelength	0.71073 Å	
Crystal system	Monoclinic	
Space group	P2(1)/n	
Unit cell dimensions	a = 8.46011(9)Å	a = 90°.
	b = 19.1920(2)Å	b = 104.3956(13)°.
	c = 8.76645(13)Å	c = 90°.
Volume	1378.69(3) Å <sup>3</sup>	
Z	4	
Density (calculated)	1.418 Mg/m <sup>3</sup>	
Absorption coefficient	0.119 mm <sup>-1</sup>	
F(000)	608	
Crystal size	0.25 x 0.2 x 0.15 mm <sup>3</sup>	
Theta range for data collection	2.623 to 66.261°.	
Index ranges	-21 ≤ h ≤ 21, -48 ≤ k ≤ 47, -19 ≤ l ≤ 22	
Reflections collected	68168	
Independent reflections	23017 [R(int) = 0.0183]	
Completeness to theta = 66.261°	93.3%	

Absorption correction	Multi-scan
Max. and min. transmission	0.982 and 0.755
Refinement method	Full-matrix least-squares on F <sup>2</sup>
Data / restraints / parameters	23017/ 0/ 192
Goodness-of-fit on F <sup>2</sup>	1.032
Final R indices [I>2sigma(I)]	R1 = 0.0315, wR2 = 0.0998
R indices (all data)	R1 = 0.0418, wR2 = 0.1068
Largest diff. peak and hole	0.600 and -0.332 e.Å <sup>-3</sup>

Table 2. Bond lengths [Å] and angles [°] for **1**.

---

Bond lengths----	
F1-C4	1.3456(3)
C1-C5	1.5328(2)
C1-C2	1.5376(2)
C1-C3	1.5442(2)
C1-C11	1.5491(2)
O1-C2	1.3140(2)
O1-H1	0.786(7)
F2-C4	1.3475(3)
C2-O2	1.2254(2)
F3-C4	1.3469(3)
C3-C4	1.5138(3)
C3-H3A	0.9700
C3-H3AB	0.9700
C5-C10	1.3949(3)
C5-C6	1.4029(2)
C6-C7	1.3902(3)
C6-H6	0.9300
C7-C8	1.3944(4)
C7-H7	0.9300
C8-C9	1.3901(3)
C8-H8	0.9300
C9-C10	1.3982(3)
C9-H9	0.9300
C10-H10	0.9300
C11-C16	1.3946(3)
C11-C12	1.4018(3)

C12-C13	1.3902(3)
C12-H12	0.9300
C13-C14	1.3956(4)
C13-H13	0.9300
C14-C15	1.3858(5)
C14-H14	0.9300
C15-C16	1.3996(4)
C15-H15	0.9300
C16-H16	0.9300

Angles-----

C5-C1-C2	114.924(14)
C5-C1-C3	110.191(14)
C2-C1-C3	108.331(13)
C5-C1-C11	109.528(13)
C2-C1-C11	103.197(13)
C3-C1-C11	110.452(14)
C2-O1-H1	109.5
O2-C2-O1	123.482(15)
O2-C2-C1	121.456(16)
O1-C2-C1	114.891(14)
C4-C3-C1	115.903(16)
C4-C3-H3A	108.3
C1-C3-H3A	108.3
C4-C3-H3AB	108.3
C1-C3-H3AB	108.3
H3A-C3-H3AB	107.4
F1-C4-F3	106.26(2)
F1-C4-F2	106.620(19)
F3-C4-F2	106.076(19)
F1-C4-C3	113.992(17)
F3-C4-C3	113.003(17)
F2-C4-C3	110.375(19)
C10-C5-C6	118.729(16)
C10-C5-C1	123.928(15)
C6-C5-C1	117.228(16)
C7-C6-C5	120.964(19)
C7-C6-H6	119.5

C5-C6-H6	119.5
C6-C7-C8	119.936(19)
C6-C7-H7	120.0
C8-C7-H7	120.0
C9-C8-C7	119.539(18)
C9-C8-H8	120.2
C7-C8-H8	120.2
C8-C9-C10	120.575(19)
C8-C9-H9	119.7
C10-C9-H9	119.7
C5-C10-C9	120.239(17)
C5-C10-H10	119.9
C9-C10-H10	119.9
C16-C11-C12	118.877(19)
C16-C11-C1	122.893(18)
C12-C11-C1	118.207(16)
C13-C12-C11	120.63(2)
C13-C12-H12	119.7
C11-C12-H12	119.7
C12-C13-C14	120.16(3)
C12-C13-H13	119.9
C14-C13-H13	119.9
C15-C14-C13	119.59(2)
C15-C14-H14	120.2
C13-C14-H14	120.2
C14-C15-C16	120.41(3)
C14-C15-H15	119.8
C16-C15-H15	119.8
C11-C16-C15	120.33(2)
C11-C16-H16	119.8
C15-C16-H16	119.8

Table 3. Torsion angles [°] for **1**.

---

C5-C1-C2-O2	140.038(18)
C3-C1-C2-O2	16.33(2)
C11-C1-C2-O2	-100.78(2)
C5-C1-C2-O1	-44.55(2)



C3-C1-C2-O1	-168.256(16)
C11-C1-C2-O1	74.629(18)
C5-C1-C3-C4	-50.187(19)
C2-C1-C3-C4	76.315(18)
C11-C1-C3-C4	-171.336(14)
C1-C3-C4-F1	-41.10(2)
C1-C3-C4-F3	80.36(2)
C1-C3-C4-F2	-161.050(17)
C2-C1-C5-C10	-19.00(2)
C3-C1-C5-C10	103.71(2)
C11-C1-C5-C10	-134.594(18)
C2-C1-C5-C6	164.967(17)
C3-C1-C5-C6	-72.32(2)
C11-C1-C5-C6	49.38(2)
C10-C5-C6-C7	0.34(3)
C1-C5-C6-C7	176.58(2)
C5-C6-C7-C8	0.88(4)
C6-C7-C8-C9	-1.13(4)
C7-C8-C9-C10	0.16(3)
C6-C5-C10-C9	-1.31(3)
C1-C5-C10-C9	-177.281(18)
C8-C9-C10-C5	1.07(3)
C5-C1-C11-C16	-135.15(2)
C2-C1-C11-C16	102.00(2)
C3-C1-C11-C16	-13.61(2)
C5-C1-C11-C12	46.63(2)
C2-C1-C11-C12	-76.216(19)
C3-C1-C11-C12	168.175(16)
C16-C11-C12-C13	0.03(3)
C1-C11-C12-C13	178.32(2)
C11-C12-C13-C14	0.52(4)
C12-C13-C14-C15	-0.51(4)
C13-C14-C15-C16	-0.05(5)
C12-C11-C16-C15	-0.58(4)
C1-C11-C16-C15	-178.79(2)
C14-C15-C16-C11	0.60(5)

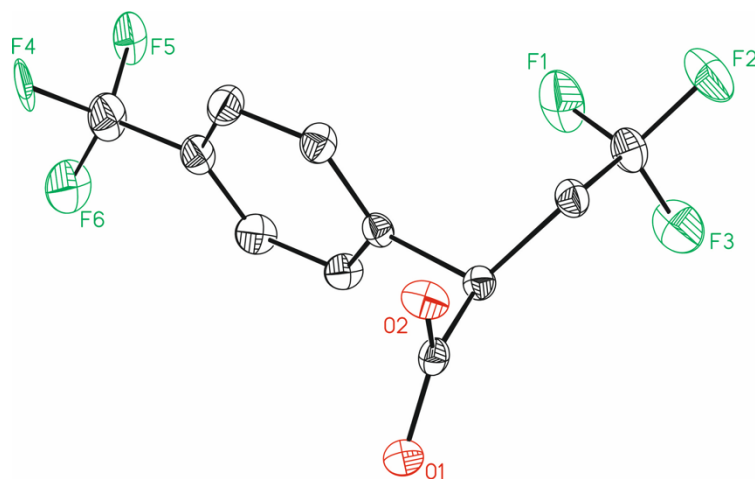


Table 1. Crystal data and structure refinement for **8**

Identification code	mo_II_YVR30_0m	
Empirical formula	C <sub>11</sub> H <sub>8</sub> F <sub>6</sub> O <sub>2</sub>	
Formula weight	286.17	
Temperature	100(2) K	
Wavelength	0.71073 Å	
Crystal system	Triclinic	
Space group	P-1	
Unit cell dimensions	a = 5.4305(3) Å	a = 74.7608(16)°.
	b = 10.0607(6) Å	b = 79.9808(18)°.
	c = 11.3292(7) Å	c = 76.1000(18)°.
Volume	575.64(6) Å <sup>3</sup>	
Z	2	
Density (calculated)	1.651 Mg/m <sup>3</sup>	
Absorption coefficient	0.176 mm <sup>-1</sup>	
F(000)	288	
Crystal size	0.20 x 0.15 x 0.02 mm <sup>3</sup>	
Theta range for data collection	2.143 to 32.511°.	
Index ranges	-5 ≤ h ≤ 8, -13 ≤ k ≤ 15, -16 ≤ l ≤ 17	
Reflections collected	9193	
Independent reflections	3740 [R(int) = 0.0153]	
Completeness to theta = 32.511°	89.700005%	
Absorption correction	Empirical	
Max. and min. transmission	0.996 and 0.945	
Refinement method	Full-matrix least-squares on F <sup>2</sup>	
Data / restraints / parameters	3740 / 180 / 227	

Goodness-of-fit on $F^2$	1.048
Final R indices [ $I > 2\sigma(I)$ ]	$R1 = 0.0519$ , $wR2 = 0.1419$
R indices (all data)	$R1 = 0.0574$ , $wR2 = 0.1473$
Largest diff. peak and hole	0.617 and -0.411 e. $\text{\AA}^{-3}$

Table 2. Bond lengths [ $\text{\AA}$ ] and angles [ $^\circ$ ] for **8**

Bond lengths----	
O1-C10	1.2193(15)
O2-C10	1.3101(15)
F1-C9	1.3368(18)
F2-C9	1.3381(18)
F3-C9	1.3462(18)
F4-C11	1.368(4)
F5-C11	1.332(4)
F6-C11	1.329(4)
F4'-C11	1.251(7)
F5'-C11	1.374(7)
F6'-C11	1.381(5)
F4''-C11	1.373(7)
F5''-C11	1.321(7)
F6''-C11	1.355(7)
C1-C2	1.3879(17)
C1-C6	1.3937(18)
C1-C7	1.5295(16)
C2-C3	1.3950(19)
C3-C4	1.385(2)
C4-C5	1.388(2)
C4-C11	1.4984(19)
C5-C6	1.3915(18)
C7-C10	1.5206(16)
C7-C8	1.5340(17)
C8-C9	1.4987(19)
Angles-----	
C2-C1-C6	119.44(11)
C2-C1-C7	119.37(11)
C6-C1-C7	121.03(11)
C1-C2-C3	120.42(13)

C4-C3-C2	119.70(13)
C3-C4-C5	120.34(12)
C3-C4-C11	120.10(14)
C5-C4-C11	119.56(14)
C4-C5-C6	119.83(13)
C5-C6-C1	120.26(12)
C10-C7-C1	105.48(9)
C10-C7-C8	110.72(10)
C1-C7-C8	115.03(10)
C9-C8-C7	112.92(11)
F1-C9-F2	106.78(13)
F1-C9-F3	106.40(13)
F2-C9-F3	106.29(12)
F1-C9-C8	113.64(12)
F2-C9-C8	111.02(12)
F3-C9-C8	112.25(12)
O1-C10-O2	124.72(11)
O1-C10-C7	120.89(11)
O2-C10-C7	114.34(10)
F6-C11-F5	109.4(3)
F5"-C11-F6"	108.5(7)
F6-C11-F4	103.9(3)
F5-C11-F4	105.3(3)
F5"-C11-F4"	104.3(5)
F6"-C11-F4"	103.0(6)
F4'-C11-F5'	109.8(6)
F4'-C11-F6'	111.9(5)
F5'-C11-F6'	101.1(4)
F4'-C11-C4	116.2(5)
F5"-C11-C4	117.7(5)
F6-C11-C4	113.8(3)
F5-C11-C4	112.2(2)
F6"-C11-C4	111.5(7)
F4-C11-C4	111.6(3)
F4"-C11-C4	110.6(6)
F5'-C11-C4	107.0(5)
F6'-C11-C4	109.7(3)

Table 3. Torsion angles [°] for **8**

---

C6-C1-C2-C3	-1.1(2)
C7-C1-C2-C3	174.41(12)
C1-C2-C3-C4	0.3(2)
C2-C3-C4-C5	1.0(2)
C2-C3-C4-C11	-179.78(13)
C3-C4-C5-C6	-1.5(2)
C11-C4-C5-C6	179.23(13)
C4-C5-C6-C1	0.8(2)
C2-C1-C6-C5	0.5(2)
C7-C1-C6-C5	-174.88(12)
C2-C1-C7-C10	-104.24(13)
C6-C1-C7-C10	71.19(14)
C2-C1-C7-C8	133.45(12)
C6-C1-C7-C8	-51.12(15)
C10-C7-C8-C9	167.59(11)
C1-C7-C8-C9	-72.97(14)
C7-C8-C9-F1	58.89(16)
C7-C8-C9-F2	179.28(11)
C7-C8-C9-F3	-61.91(15)
C1-C7-C10-O1	88.26(13)
C8-C7-C10-O1	-146.70(11)
C1-C7-C10-O2	-89.33(12)
C8-C7-C10-O2	35.70(14)
C3-C4-C11-F4'	120.1(5)
C5-C4-C11-F4'	-60.7(5)
C3-C4-C11-F5''	-72.5(5)
C5-C4-C11-F5''	106.8(5)
C3-C4-C11-F6	27.6(3)
C5-C4-C11-F6	-153.1(3)
C3-C4-C11-F5	-97.3(3)
C5-C4-C11-F5	82.0(3)
C3-C4-C11-F6''	161.2(4)
C5-C4-C11-F6''	-19.6(5)
C3-C4-C11-F4	144.8(3)
C5-C4-C11-F4	-35.9(3)
C3-C4-C11-F4''	47.2(5)

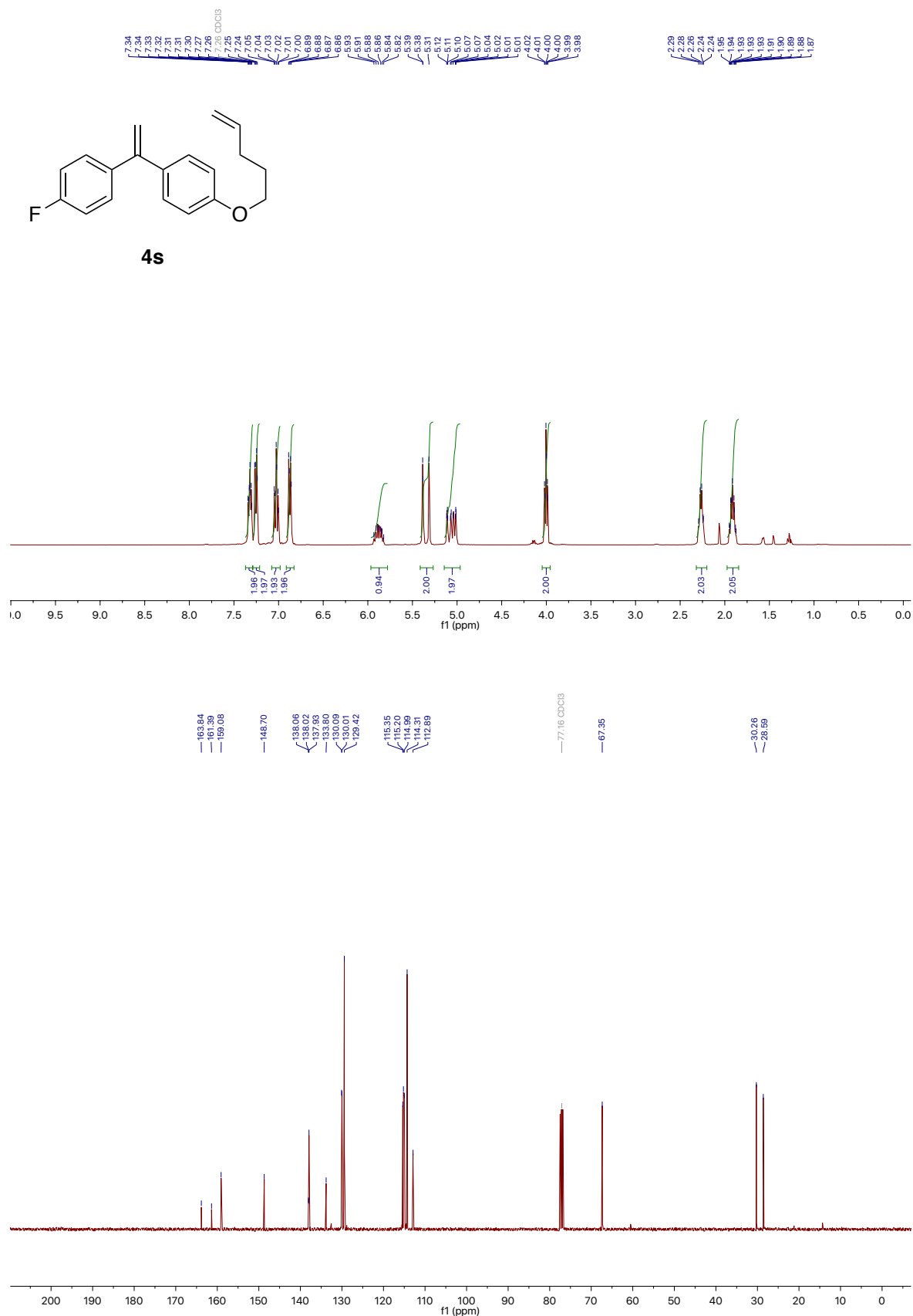
C5-C4-C11-F4''	-133.5(4)
C3-C4-C11-F5'	-116.9(4)
C5-C4-C11-F5'	62.4(4)
C3-C4-C11-F6'	-8.0(4)
C5-C4-C11-F6'	171.2(4)

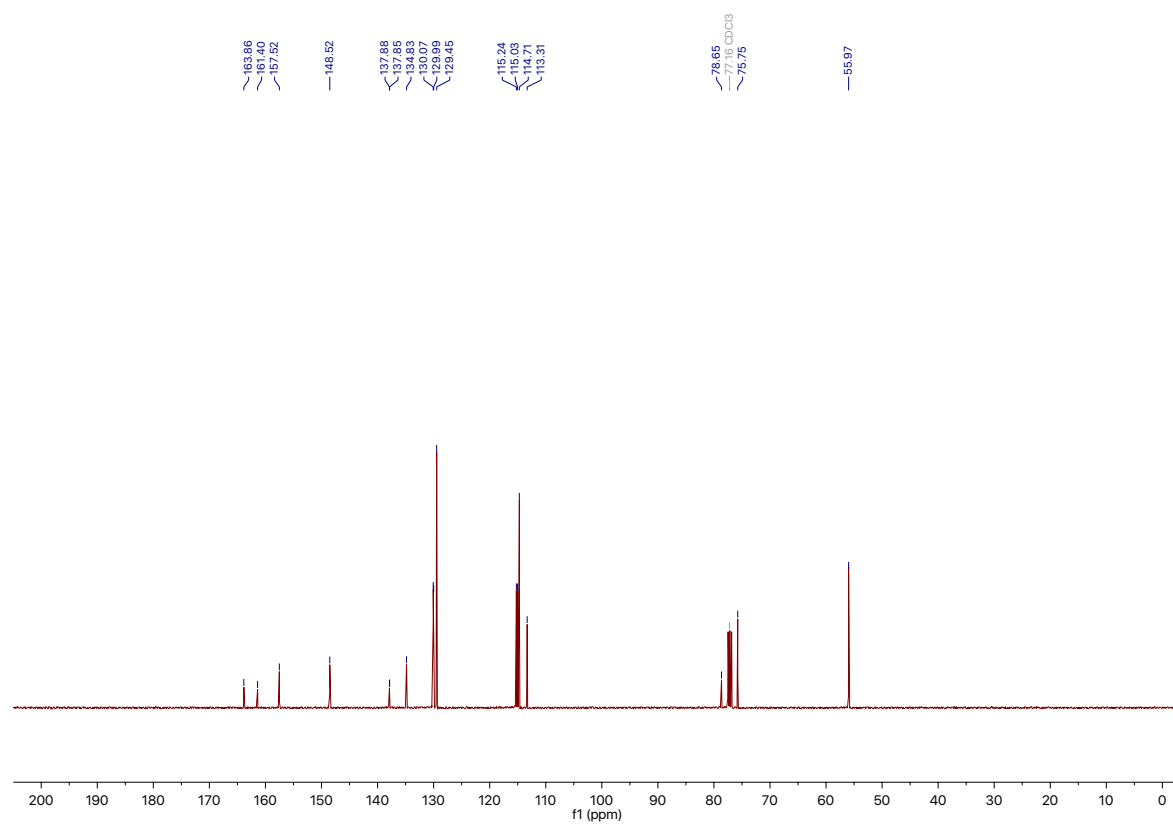
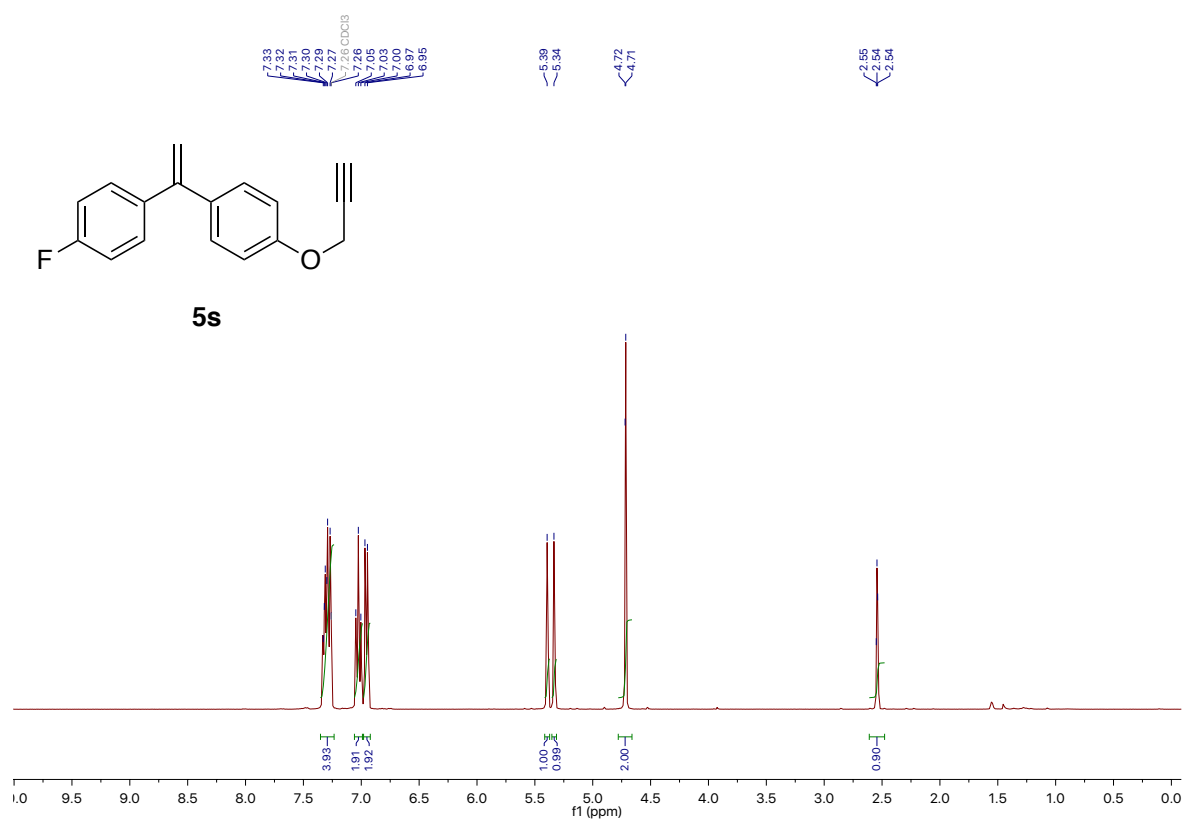
---

### 3.7.6. References of Known Compounds

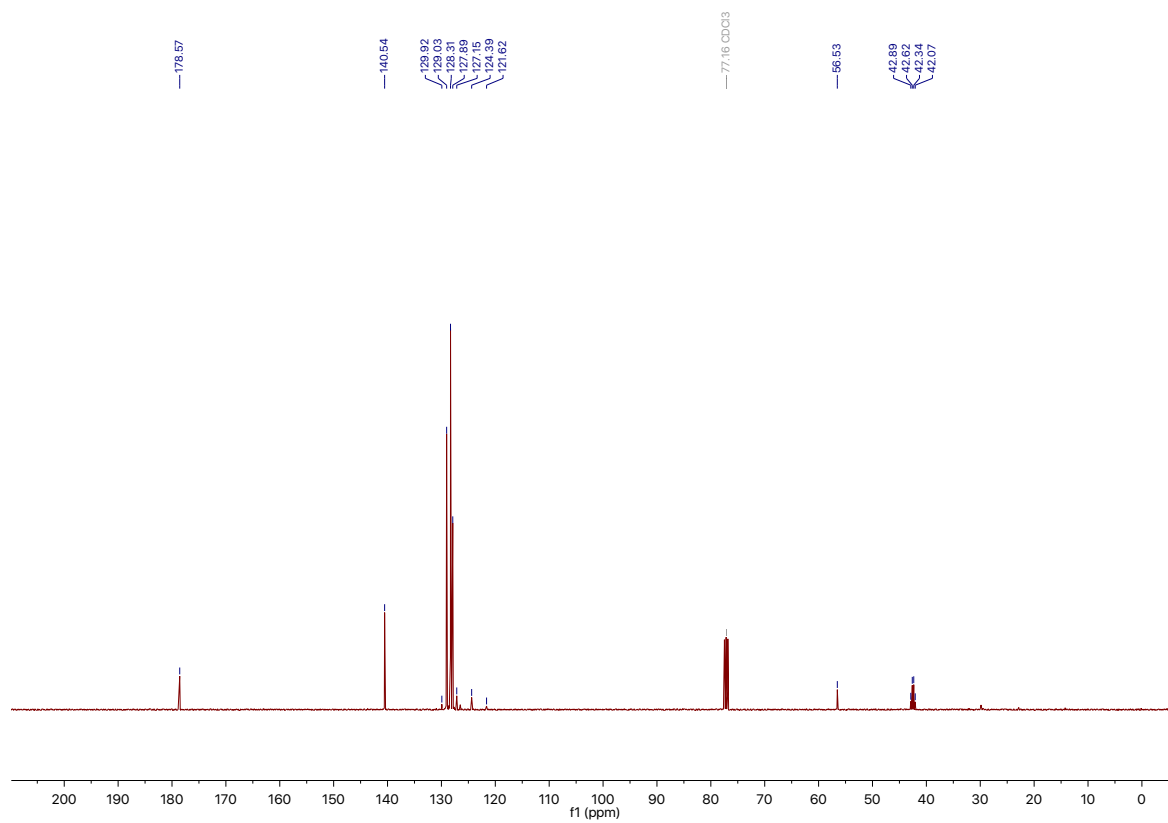
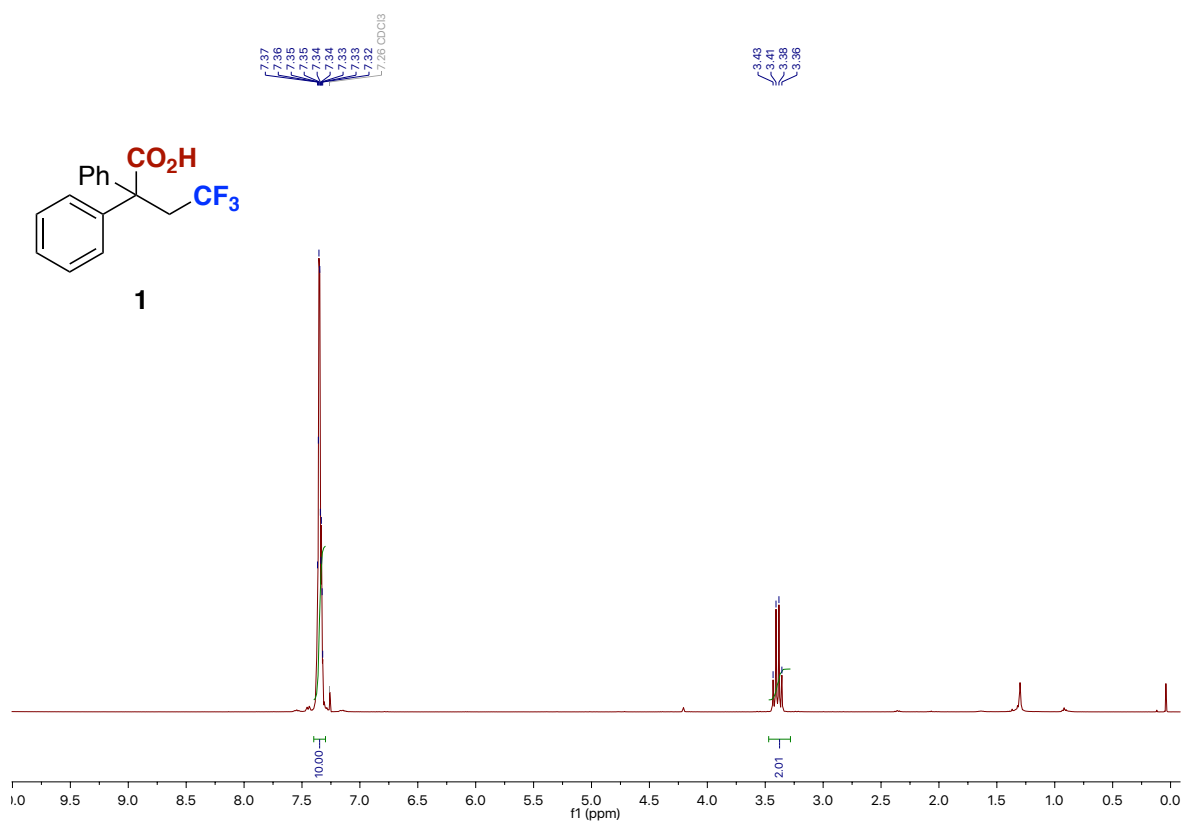
1. (a) Tordera, D.; Delgado, M.; Ortí, E.; Bolink, H. J.; Frey, J.; Nazeeruddin M. K.; Baranoff, E. *Chem. Mater.* **2012**, *24*, 1896. (b) Tordera, D.; Delgado, M.; Ortí, E.; Bolink, H. J.; Frey, J.; Nazeeruddin, M. K.; Baranoff, E. *Chem. Mater.* **2012**, *24*, 1896. (c) Monos, T.M.; Sun, A. C.; McAtee, R. C.; Devery, III, J. J.; Stephenson, C. R. J. *J. Org. Chem.* **2016**, *81*, 6988. (d) Skofka, L.; Filapek, M.; Zur, L.; Małecki, J. G.; Pisarski, W.; Olejnik, M.; Danikiewicz, W.; Krompiec, S. *J. Phys. Chem. C* **2016**, *120*, 7284–7294. (e) Singh, A.; Teegardin, K.; Kelly, M.; Prasad, K. S.; Krishnan, S.; Weaver, D. *J. Organomet. Chem.* **2015**, *776*, 51
2. (a) Tellis, J. C.; Primer, D. N.; Molander, G. A. *Science*, **2014**, *345*, 433. (b) Nawrat, C. C.; Jamison, C. R.; Slutskyy, Y.; MacMillan, D. W. C.; Overman, L. E. *J. Am. Chem. Soc.*, **2015**, *137*, 11270;
3. Stein, T. V.; Perz, M.; Dobrovetsky, R.; Winkelhaus, D.; Caputo, C. B.; Douglas, W. S. *Angew. Chem, Int. Ed.* **2015**, *54*, 10178.
4. Zhao, X.; Wu, G.; Yan, Chong.; Lu, K.; Li, H.; Zhang, Y.; Wang, J. *Org. Lett.* **2010**, *12*, 5580.
5. Min, G. K.; Bjerglund, K.; Kramer, S.; Gøgsig, T. M.; Lindhardt, A. T.; Skrydstrup, T.; *Chem. Eur. J.* **2013**, *19*, 17603.
6. Conner, M. L.; Brown, M. K. *J. Org. Chem.* **2016**, *81*, 8050.
7. (a) Han, Y.-P. et al *Org. Lett.* **2016**, *18*, 3866. (b) Mayer, M. et al *ChemCatChem.* **2011**, *3*, 1567.
8. Schedler, M.; Wurz, N. E.; Daniliuc, C. G.; Glorius, F. *Organic Letters*, **2014**, *16*, 3134. (b) Kawashima, S.; Aikawa, K.; Mikami, K. *Eur. J. Org. Chem.* **2016**, *19*, 3166.
9. Hanazawa, T. et al. *PCT Int. Appl.* **2006**, 2006097817
10. A. Falk, A.-L. Göderz, H.-G. Schmalz. *Angew. Chem. Int. Ed.* **2013**, *52*, 1576.

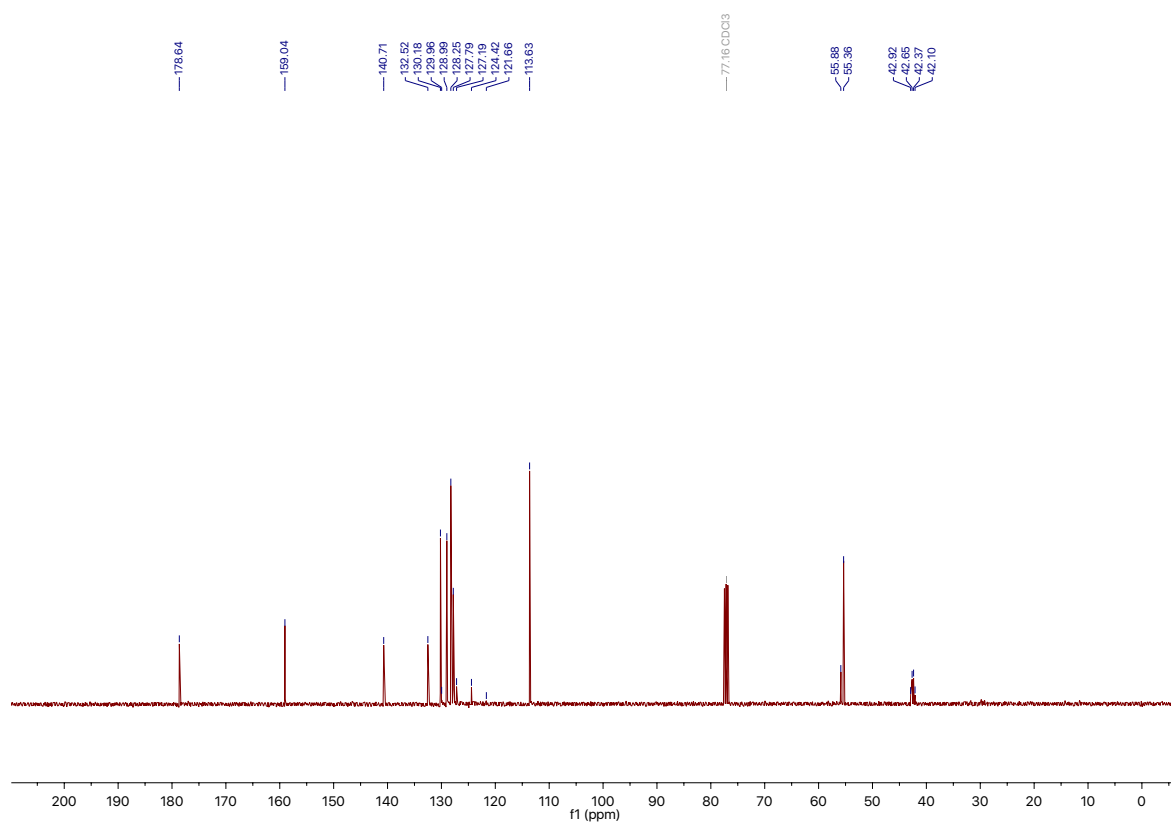
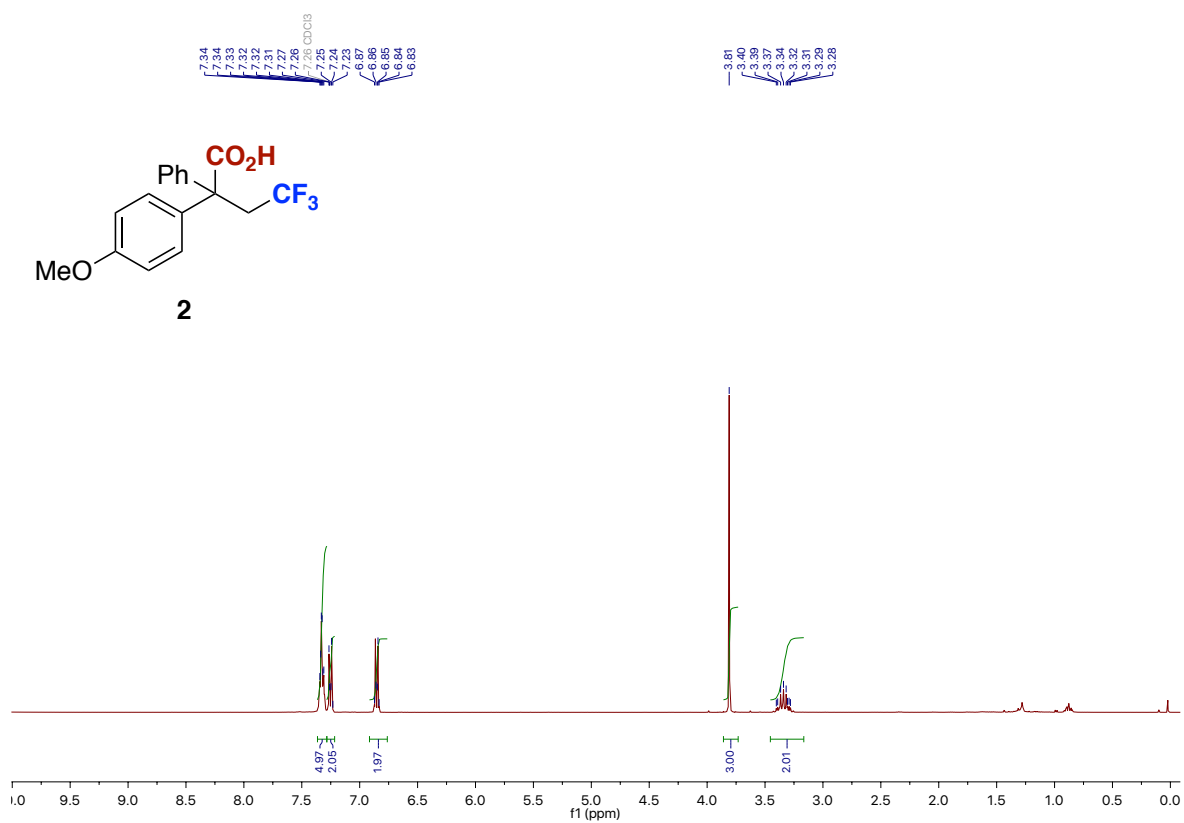
### 3.7.7. $^1\text{H}$ and $^{13}\text{C}$ Spectra

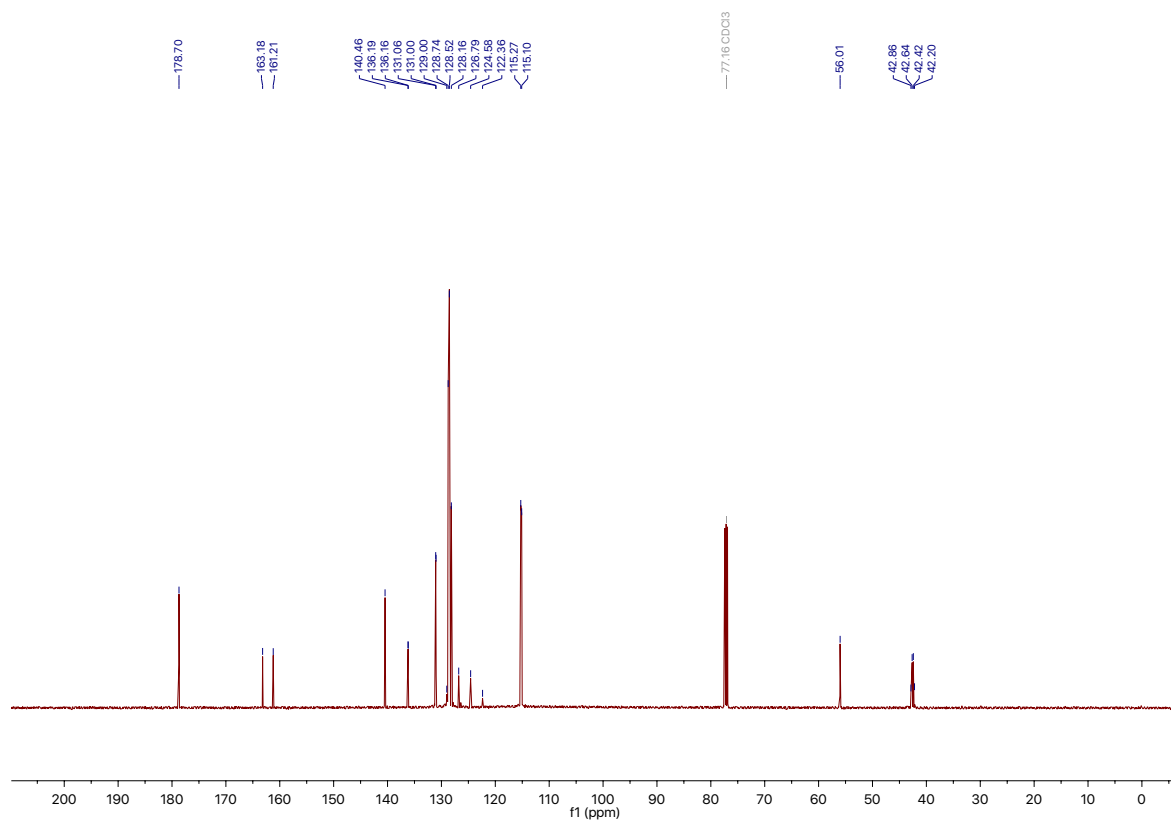
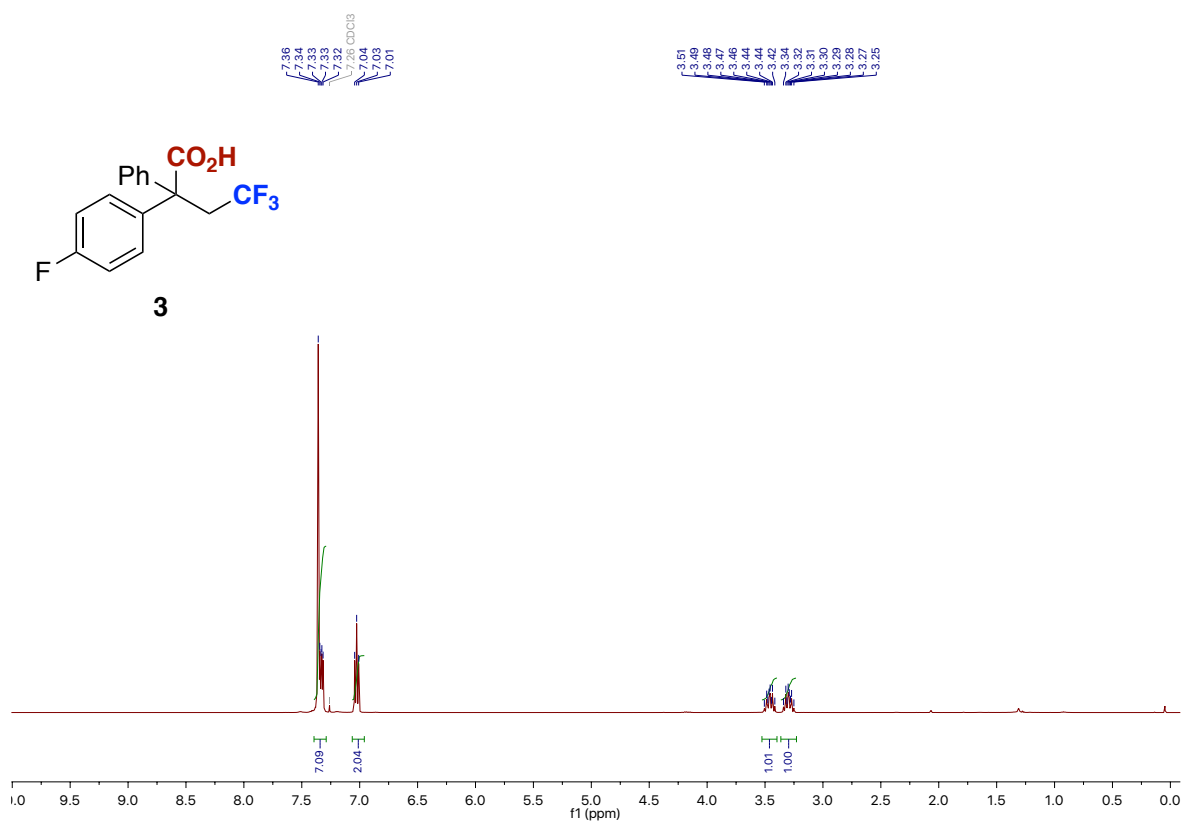


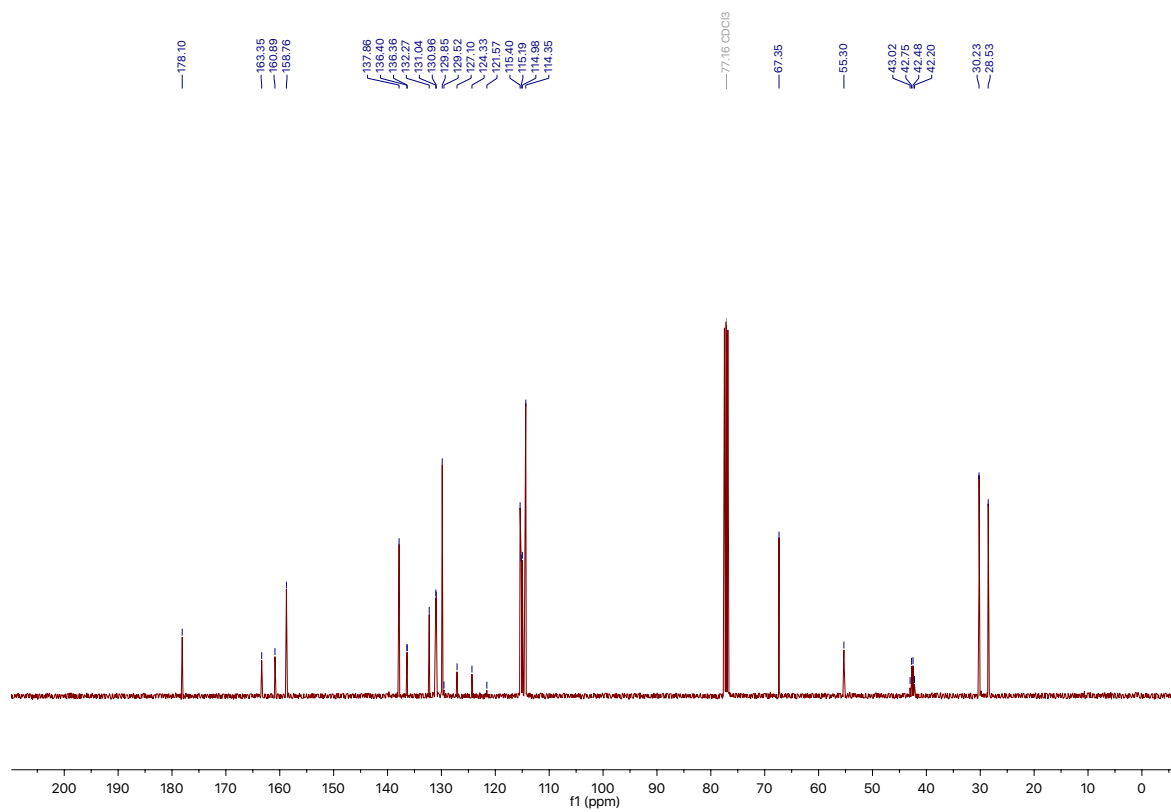
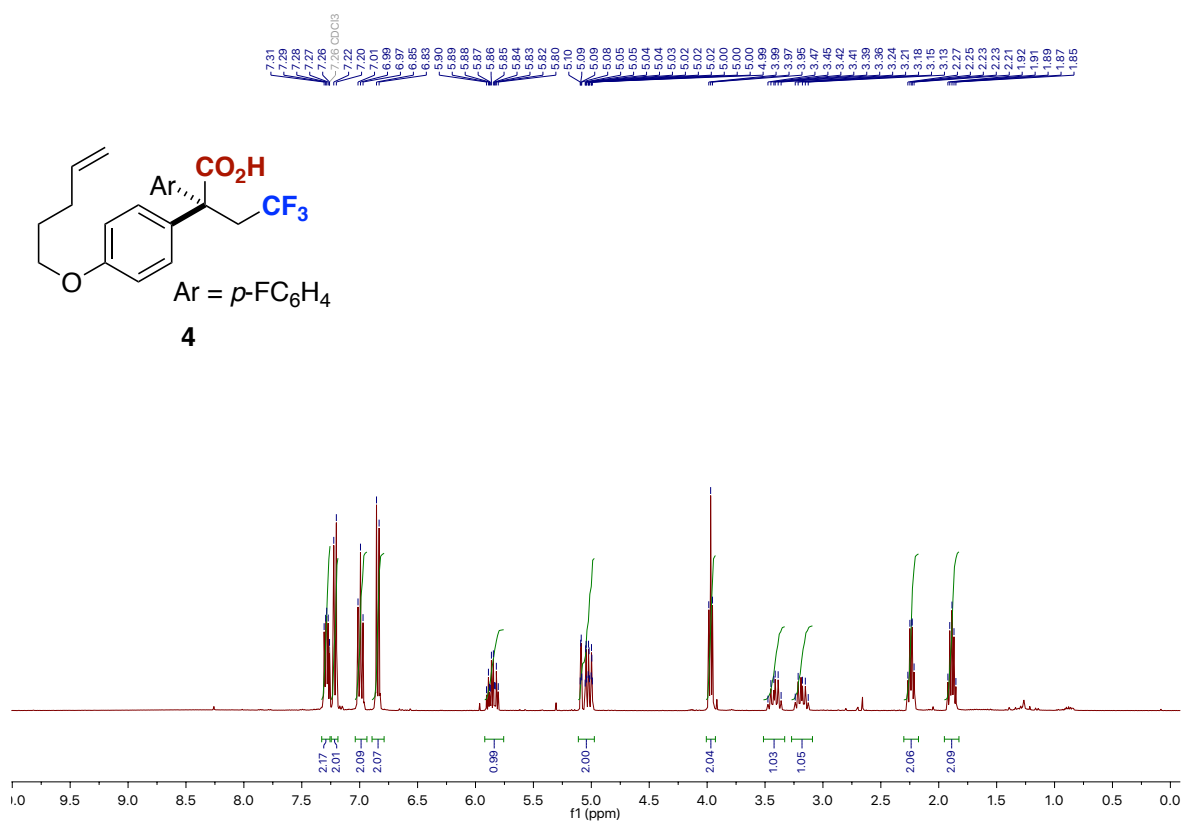


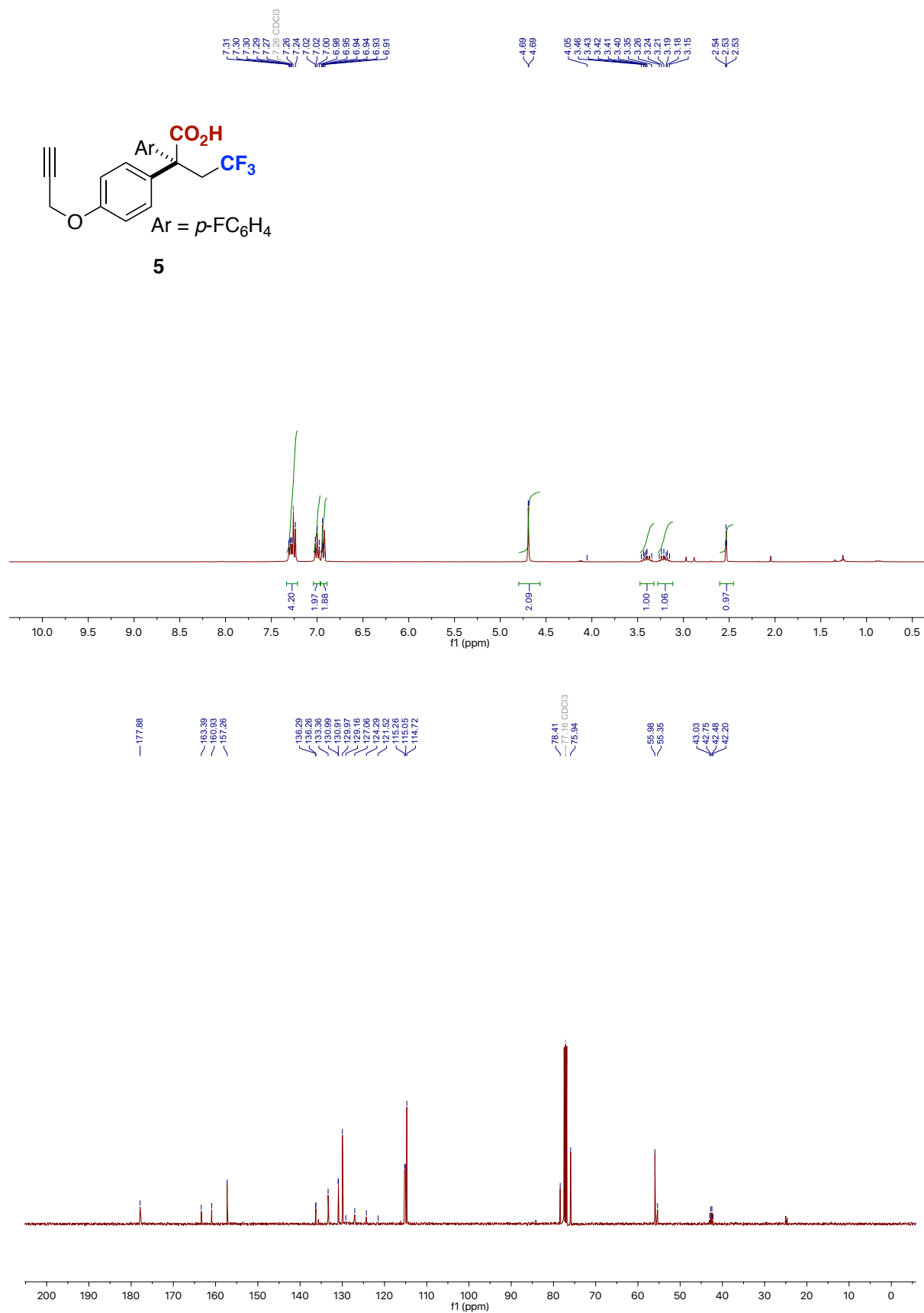


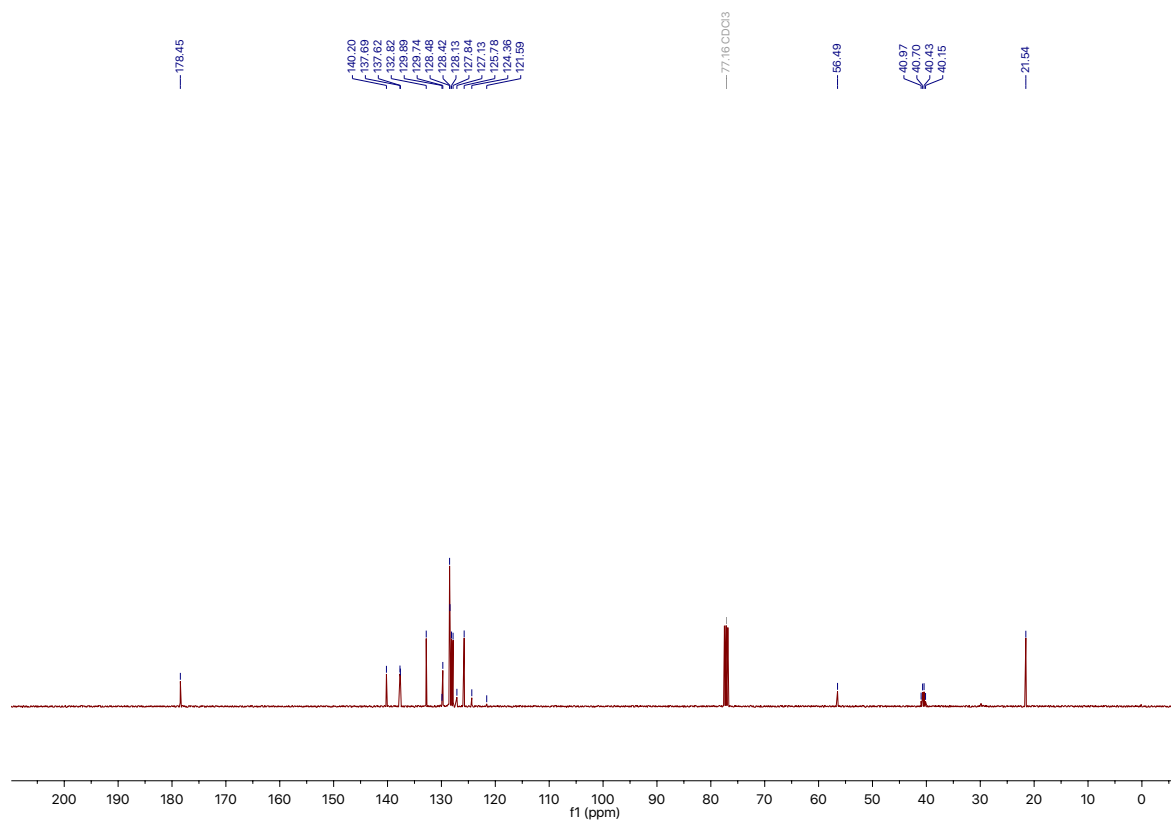
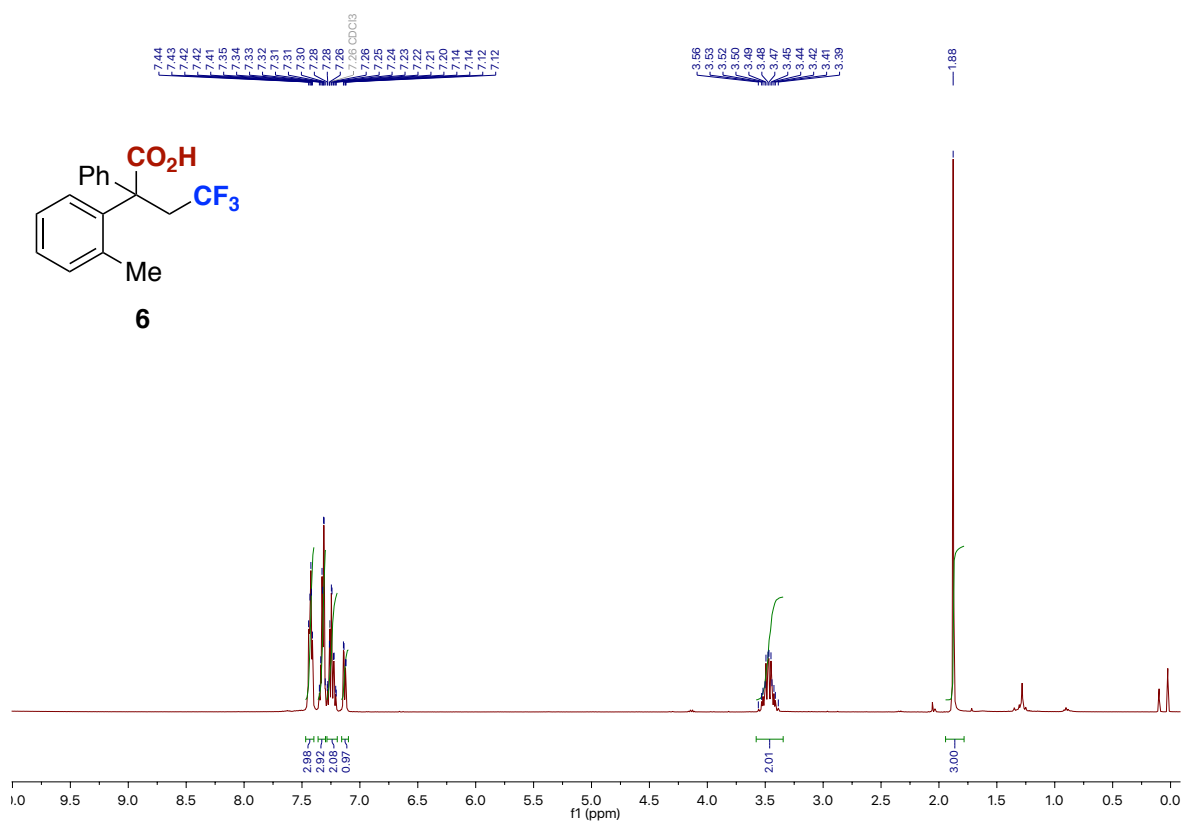


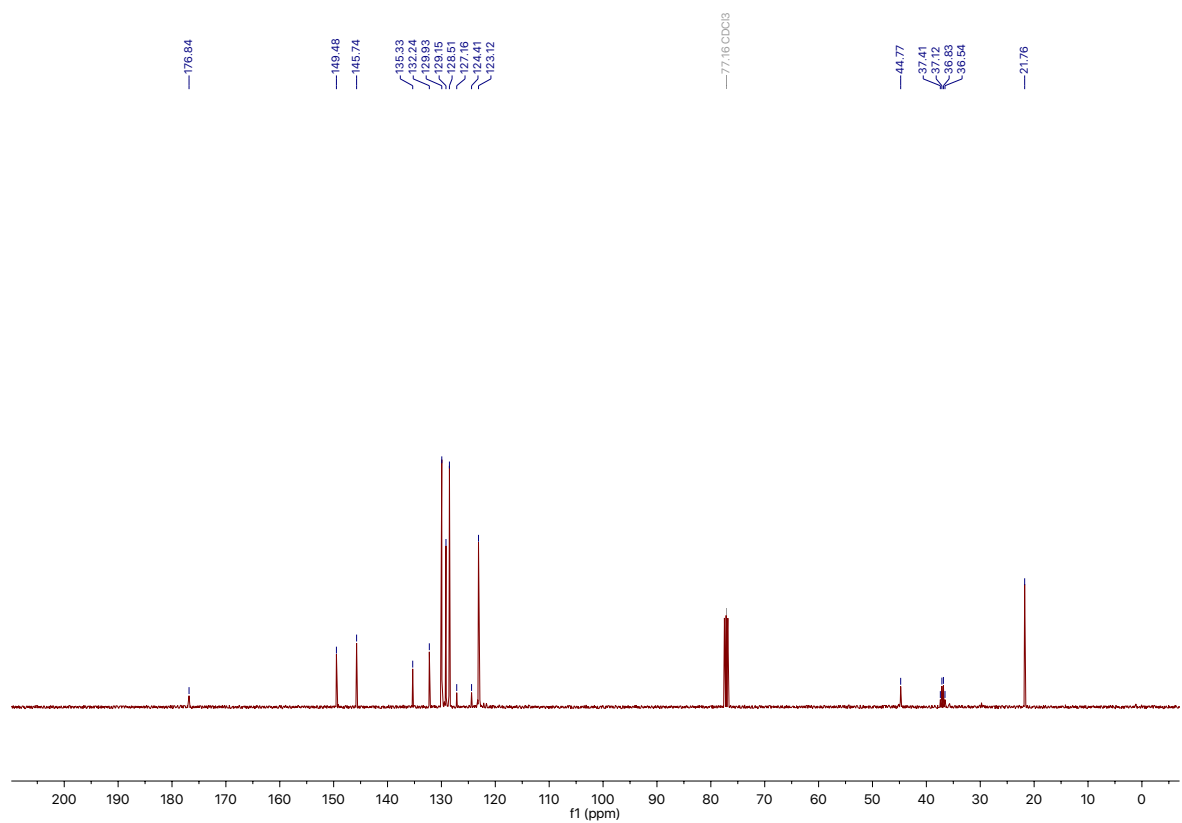
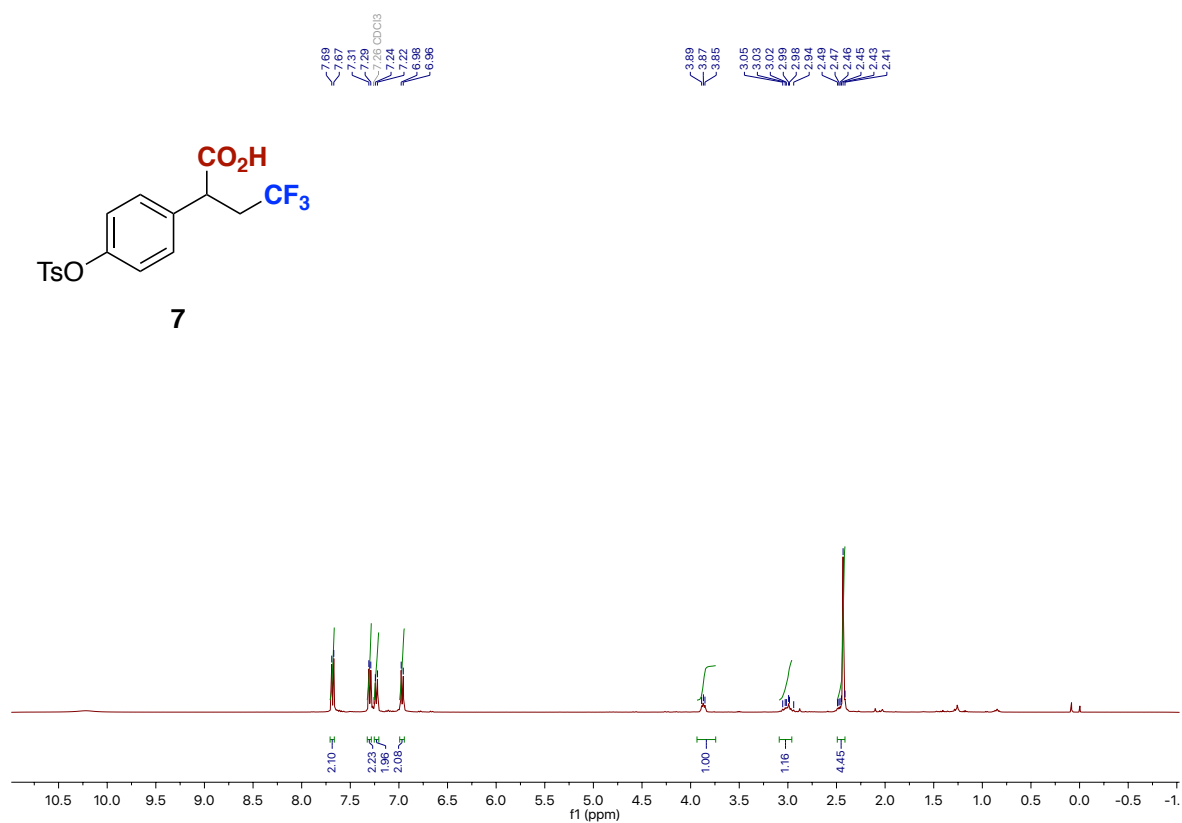


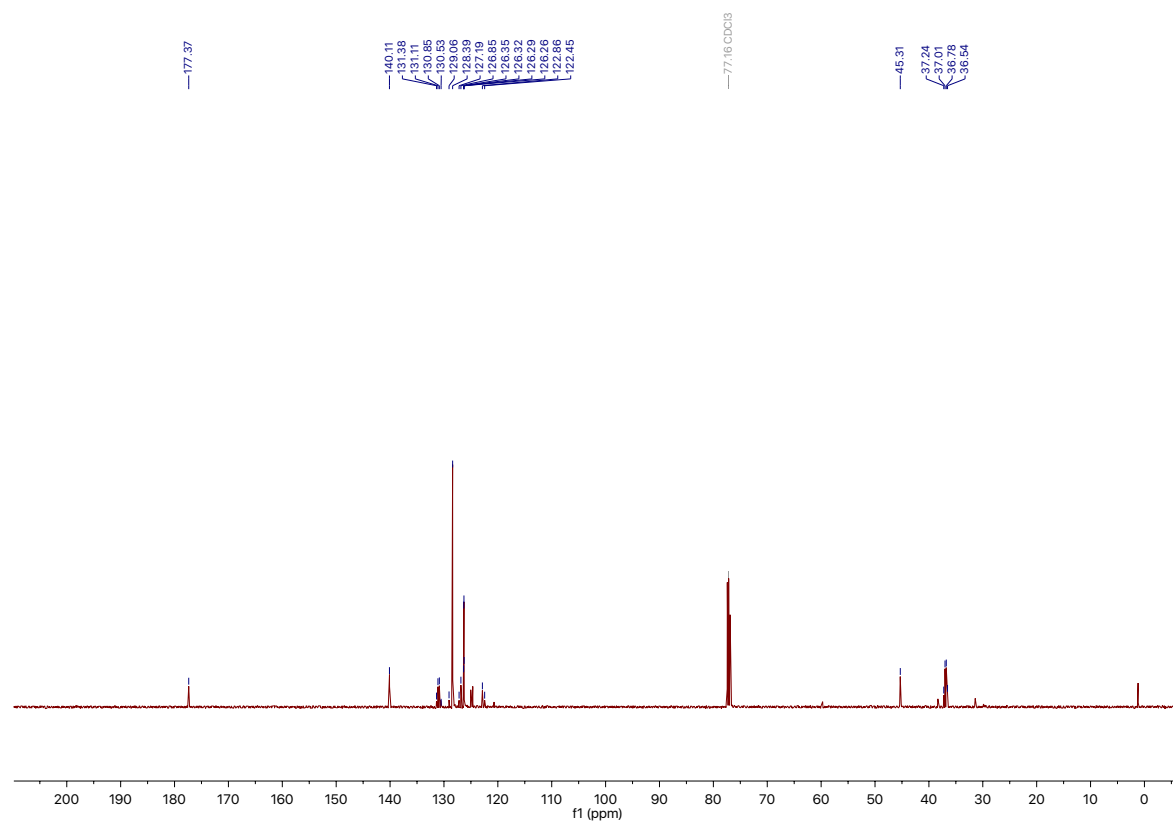
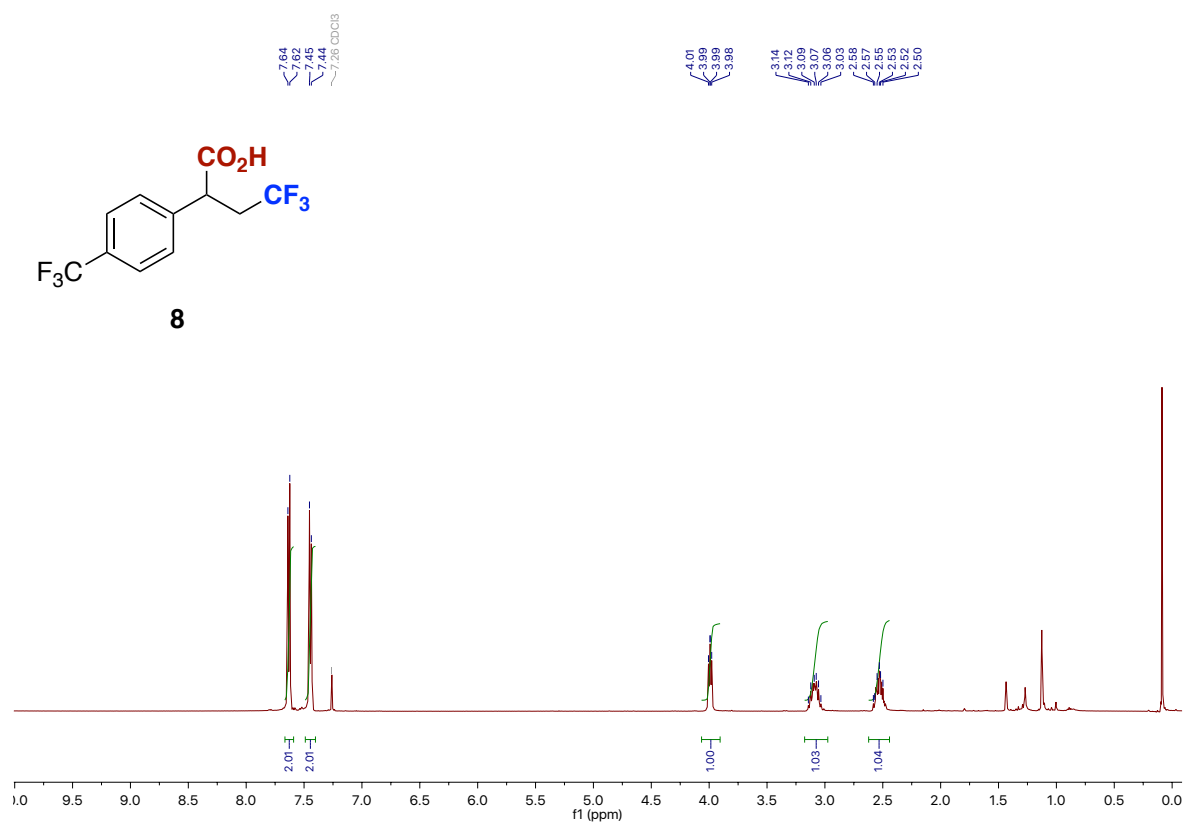




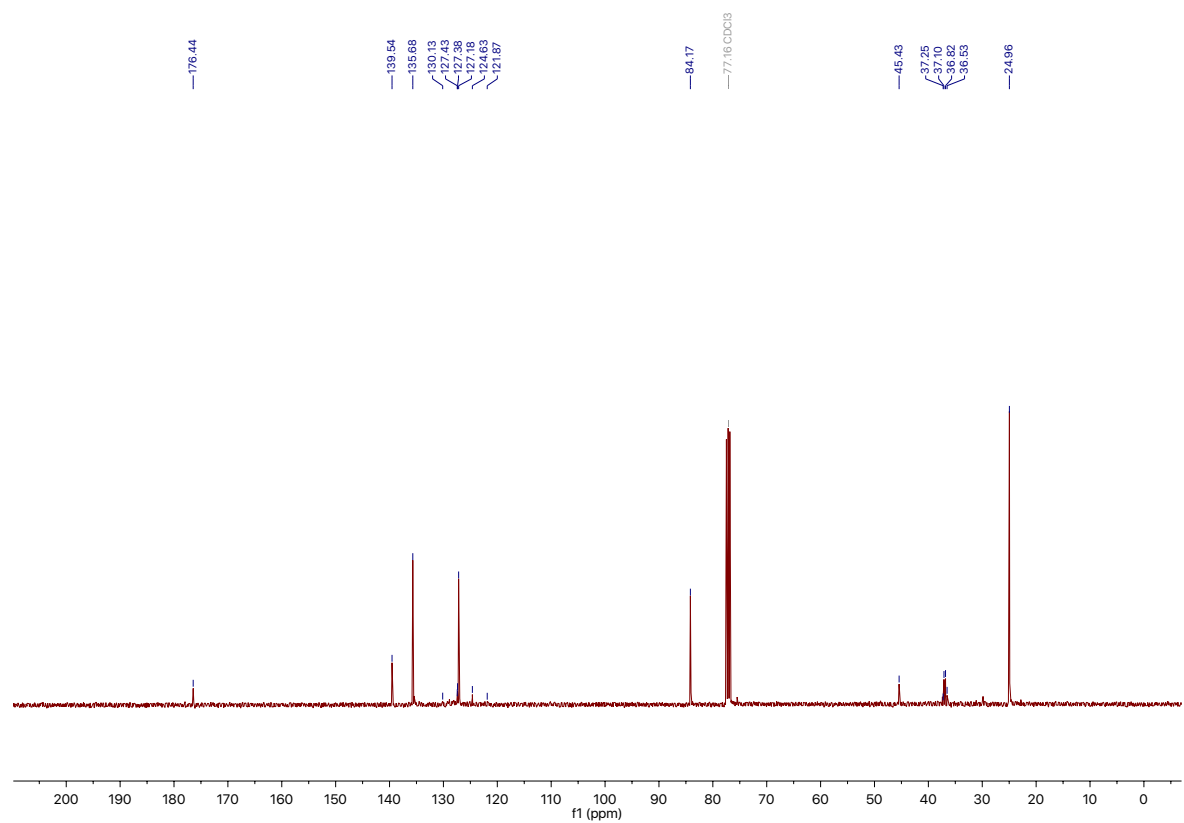
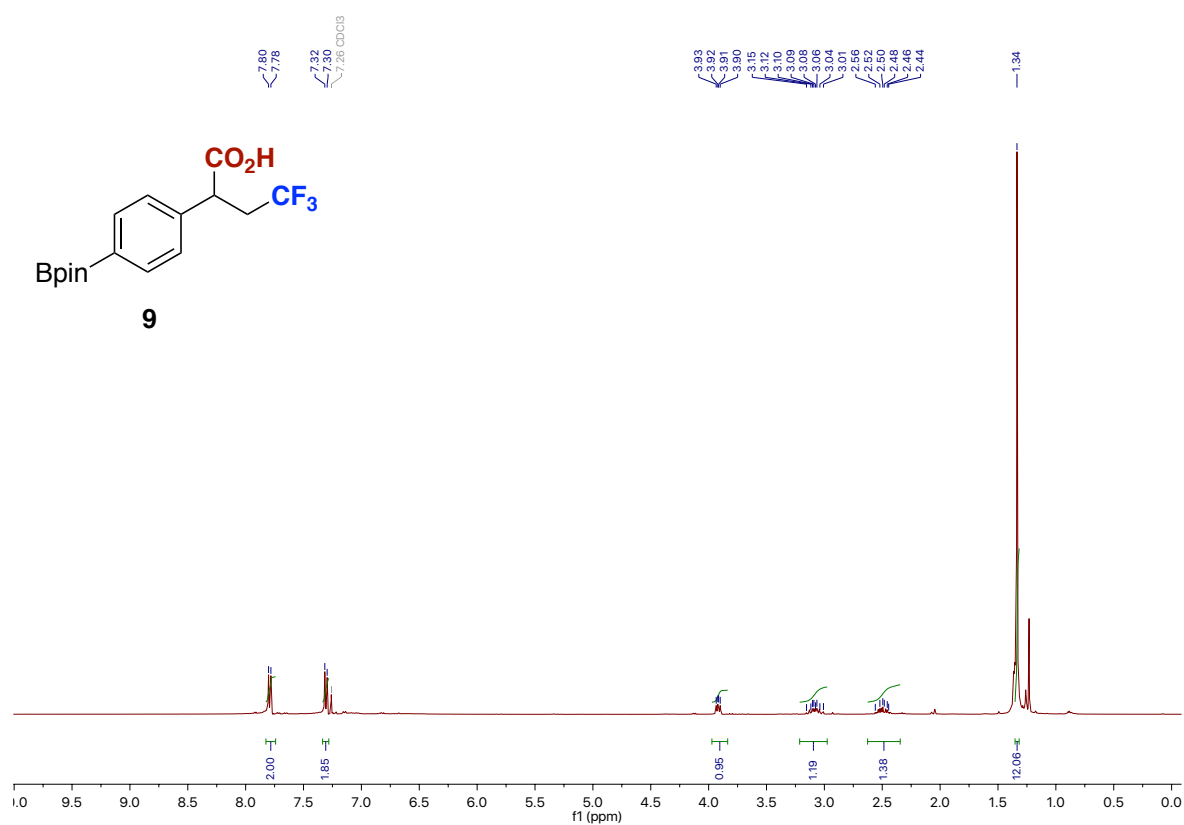


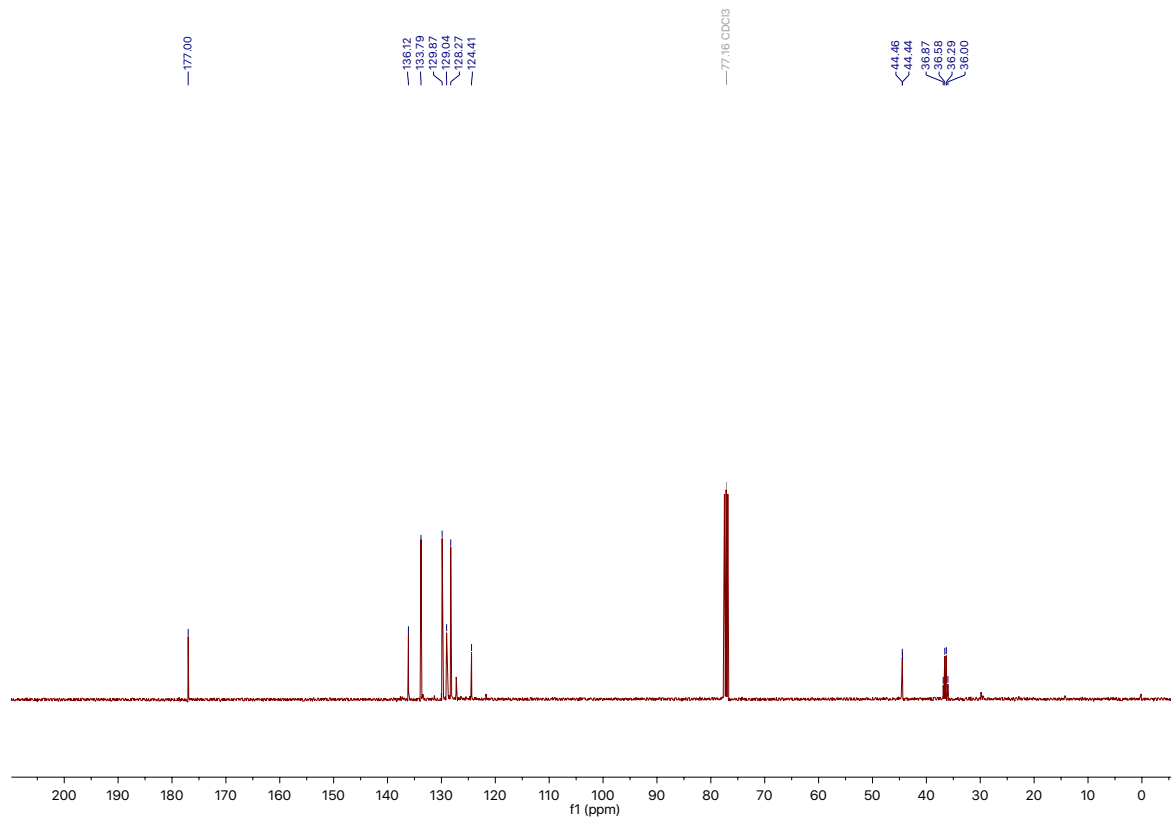
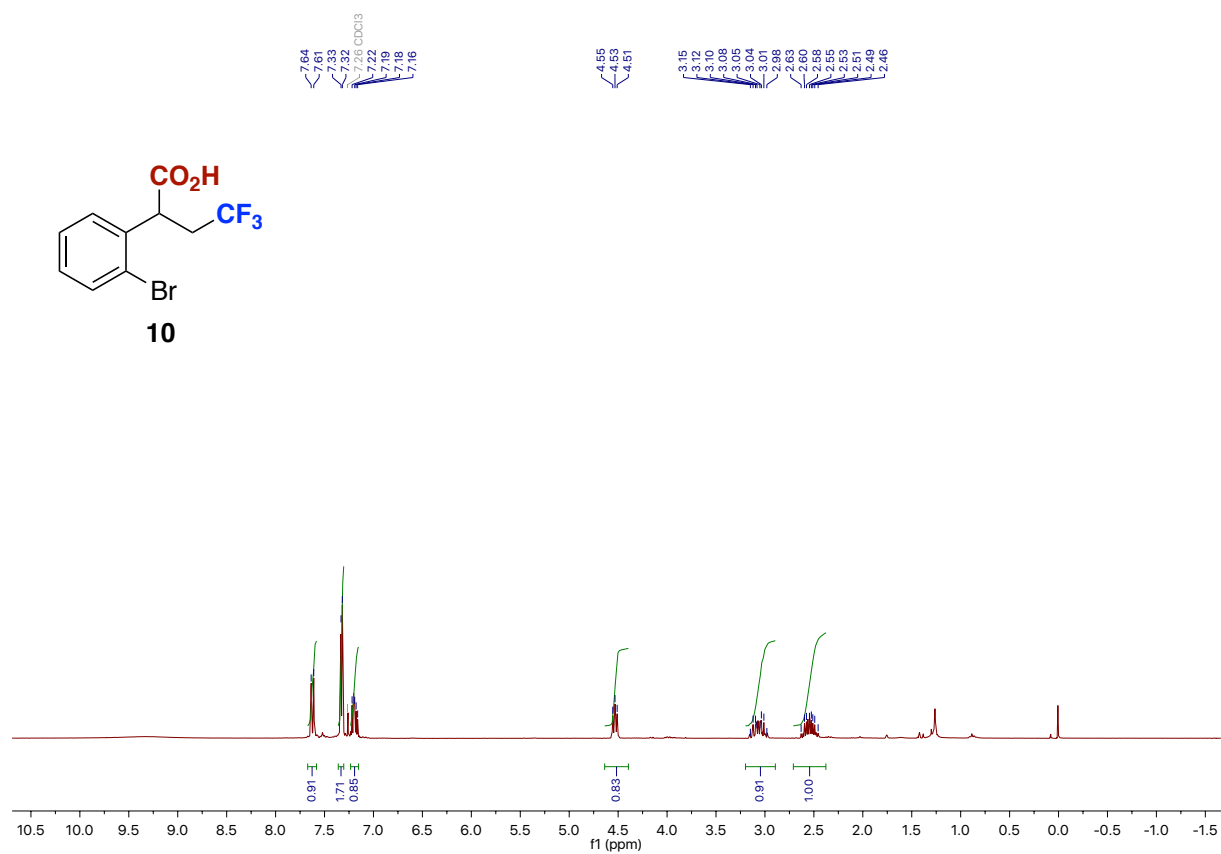


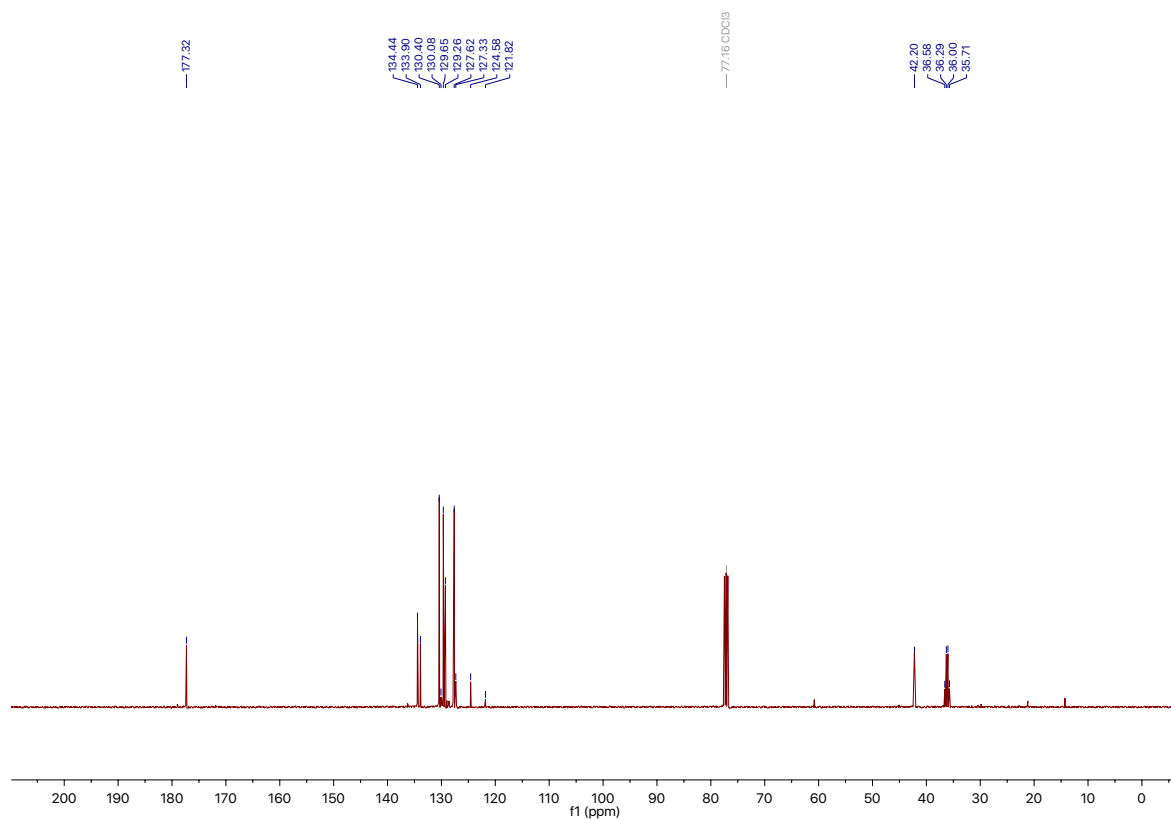
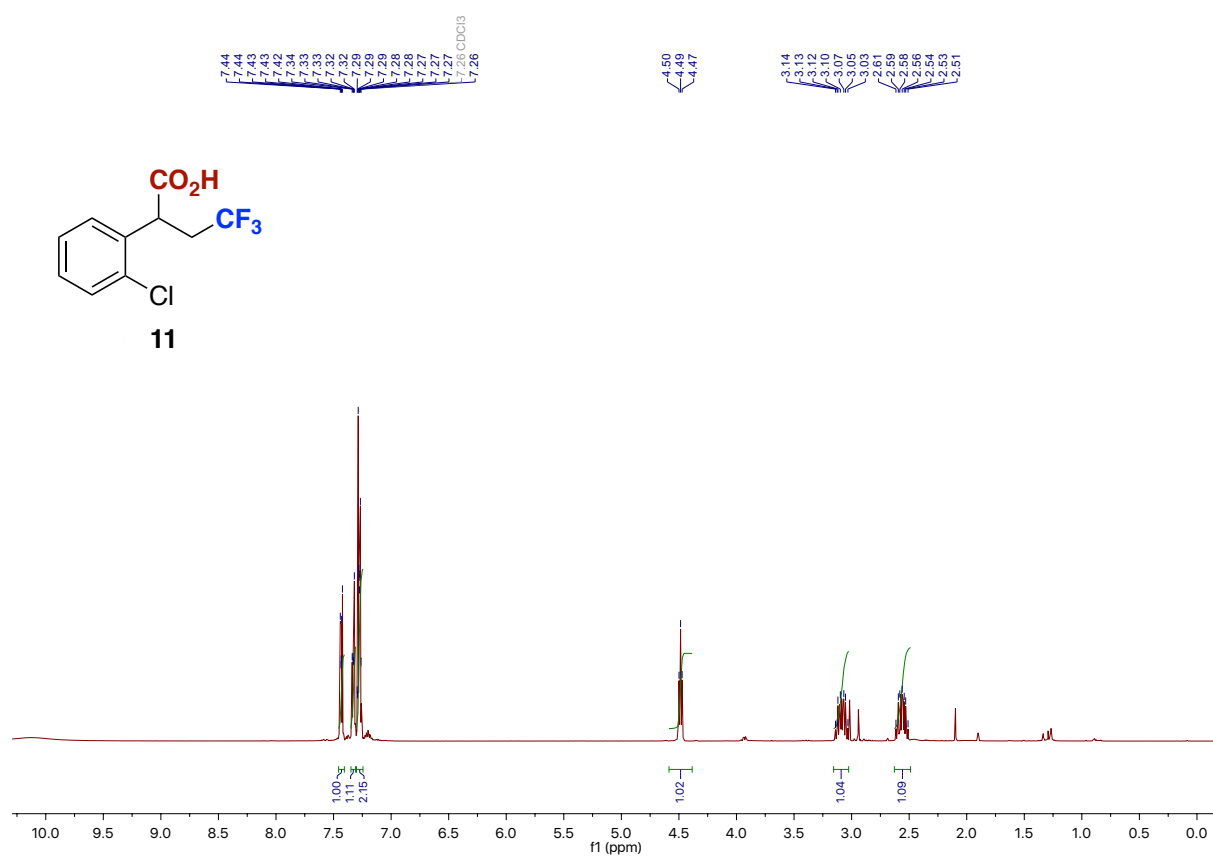


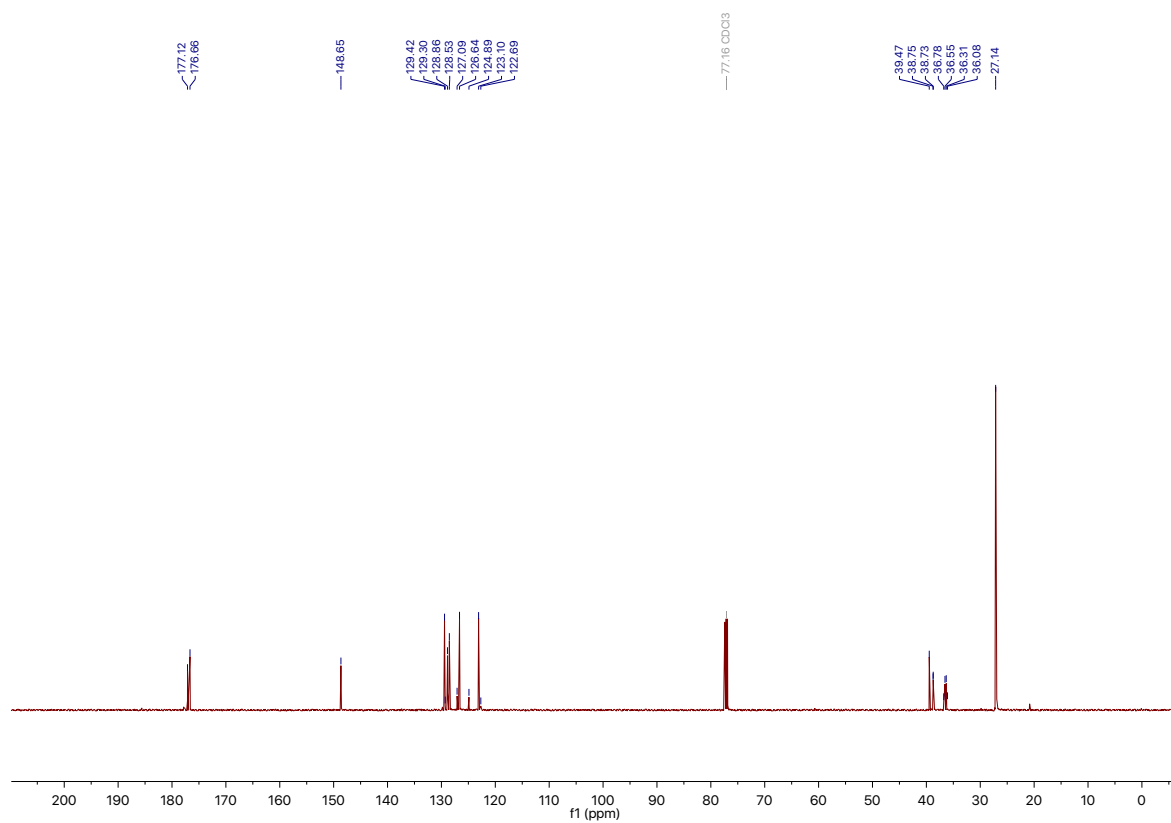
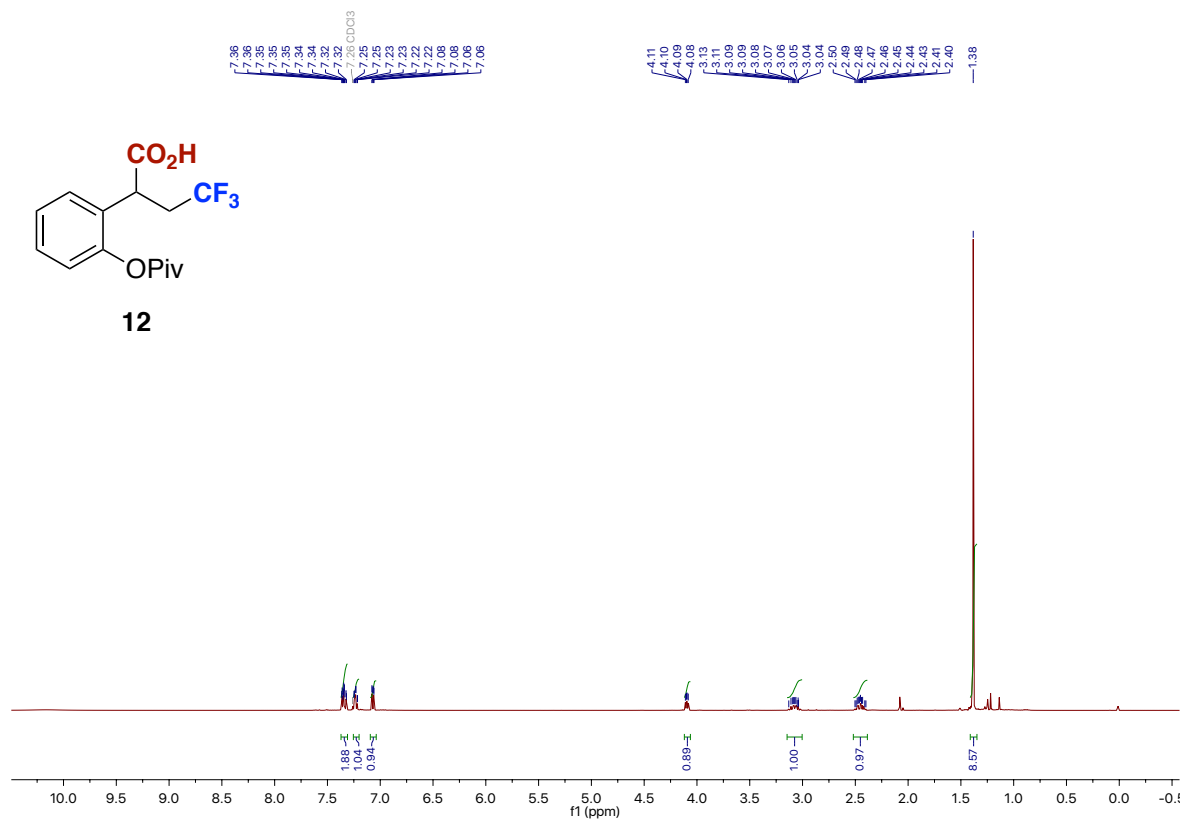


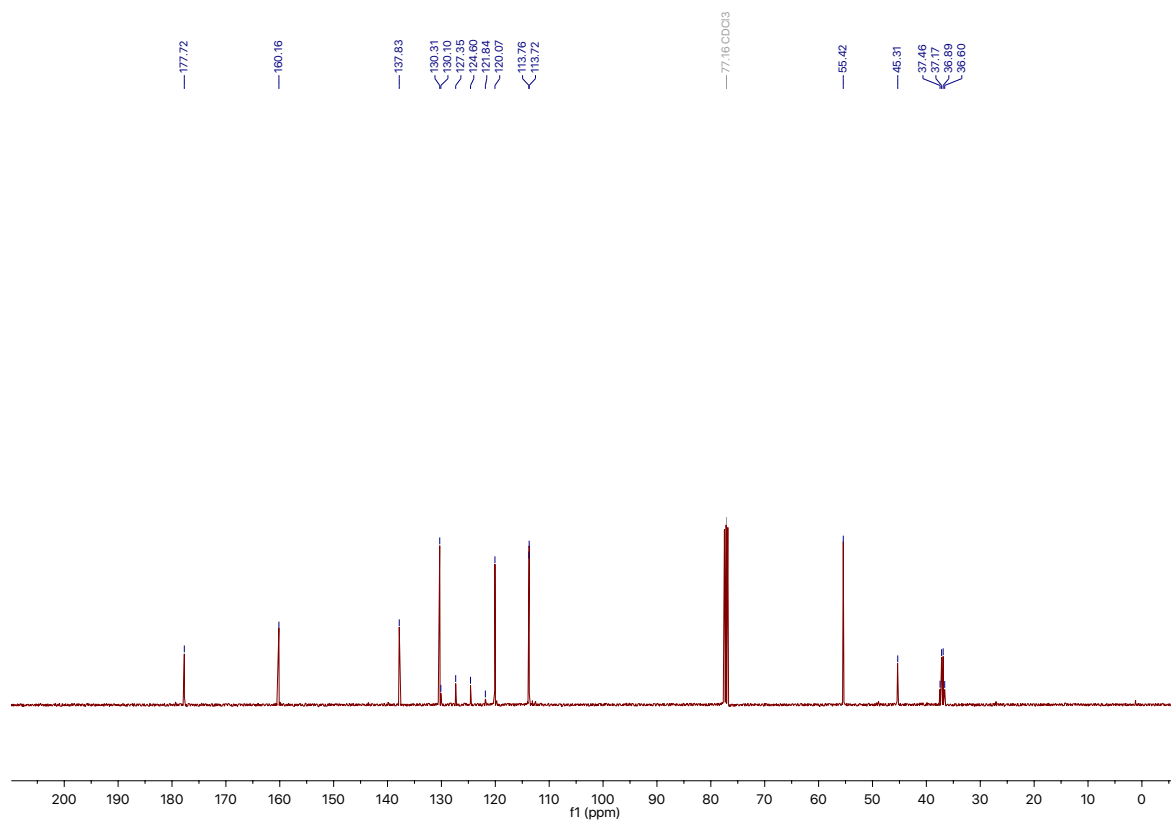
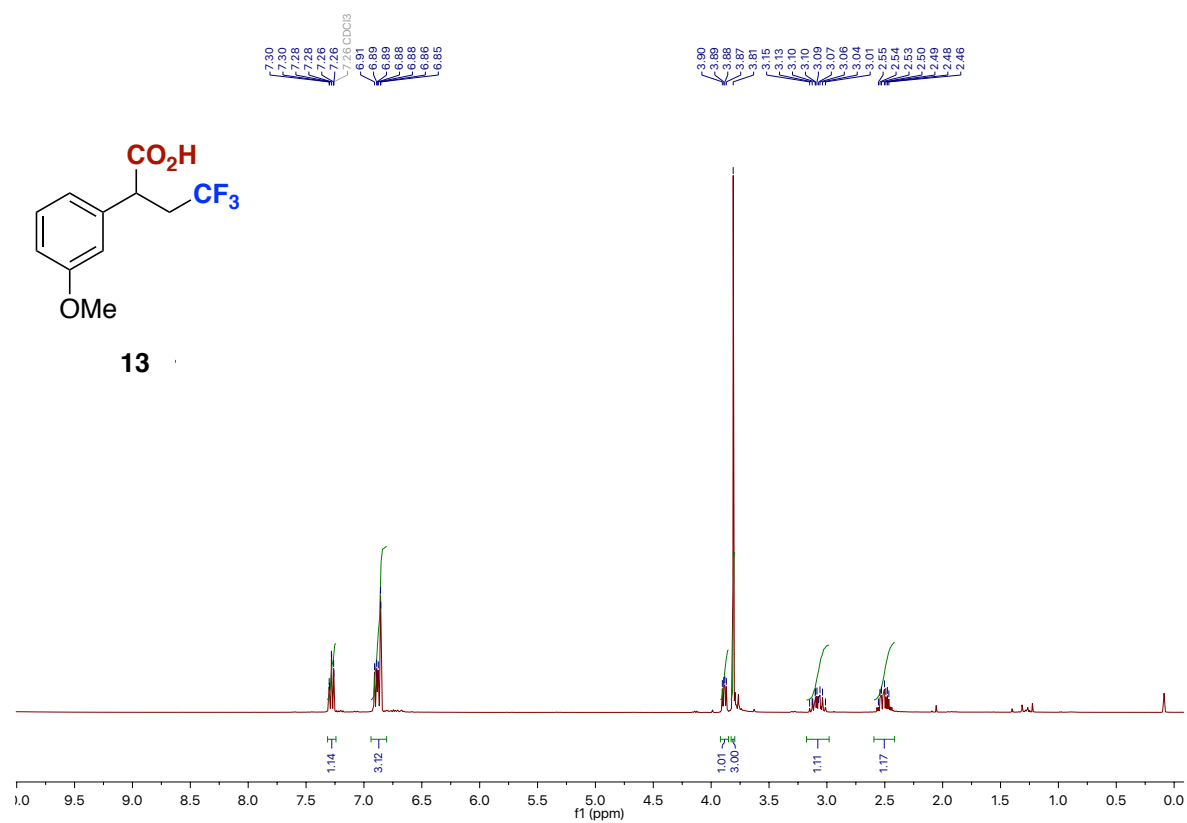


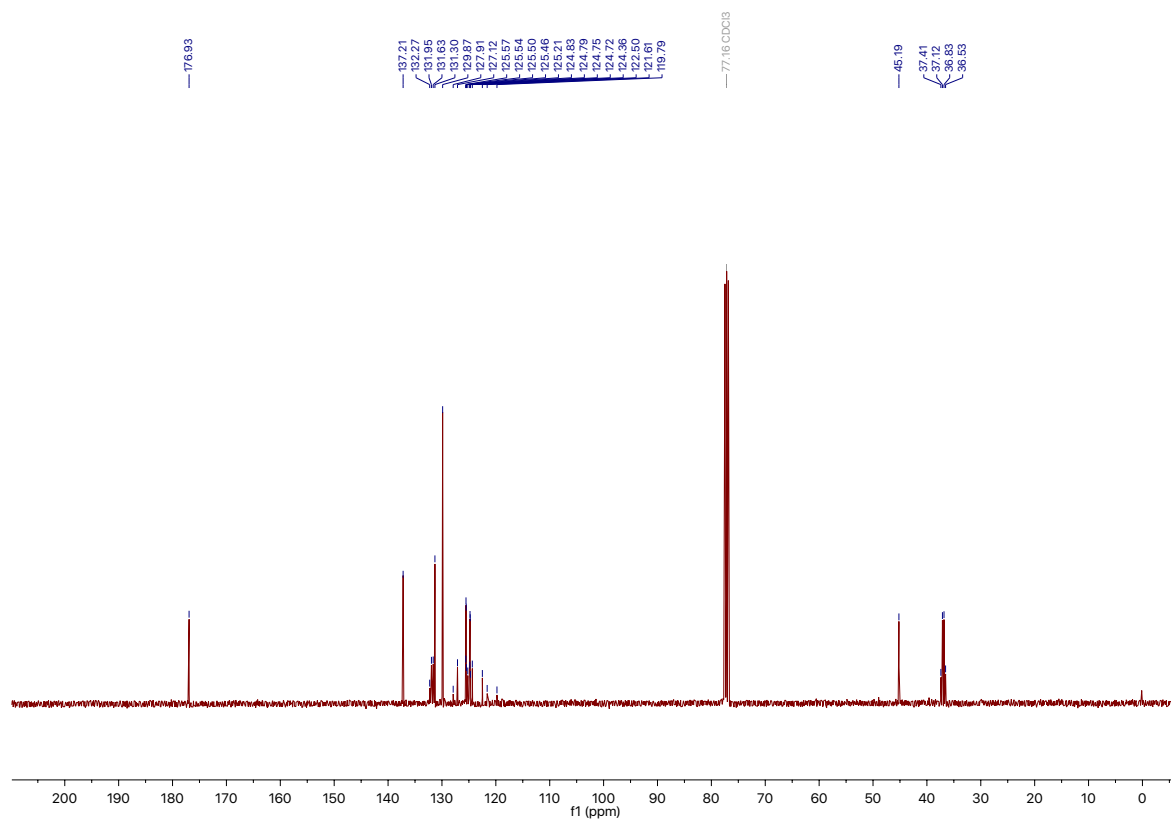
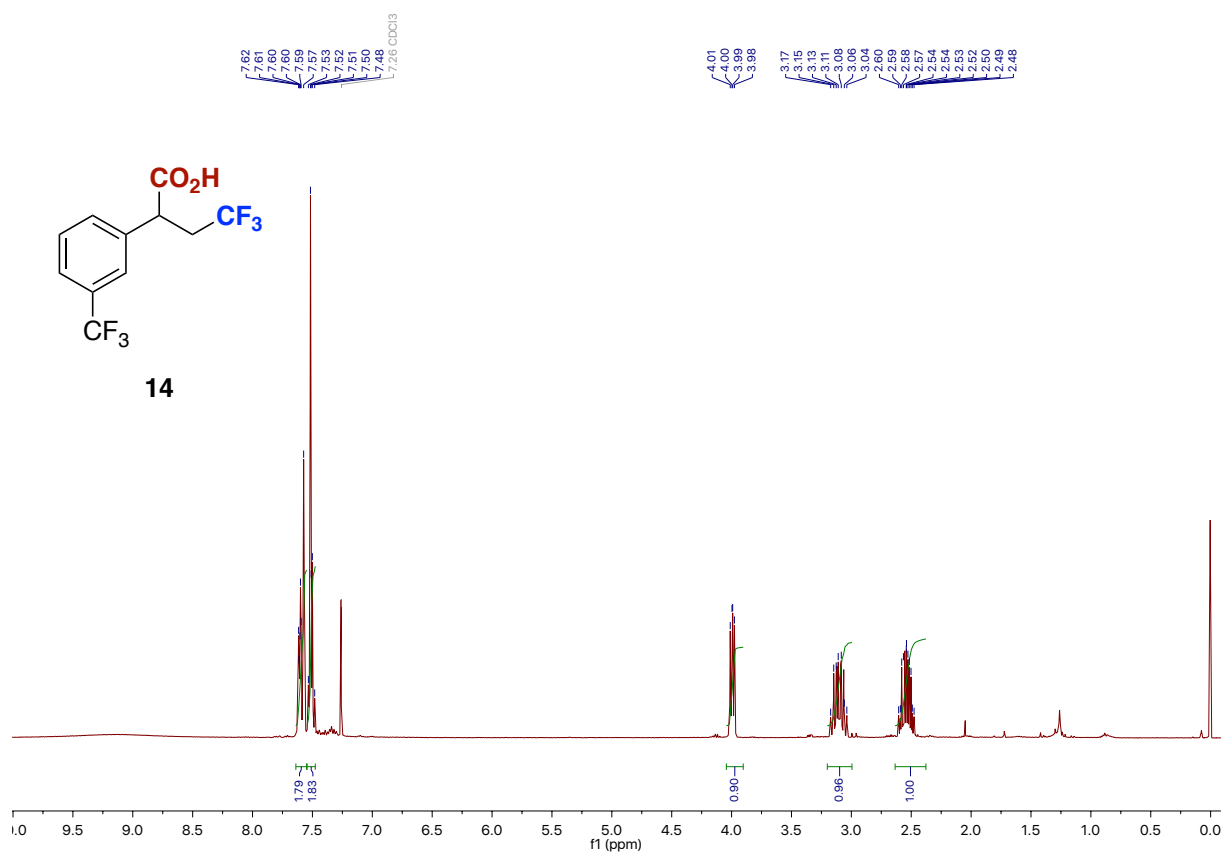


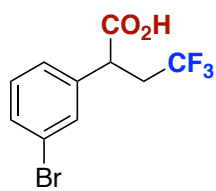




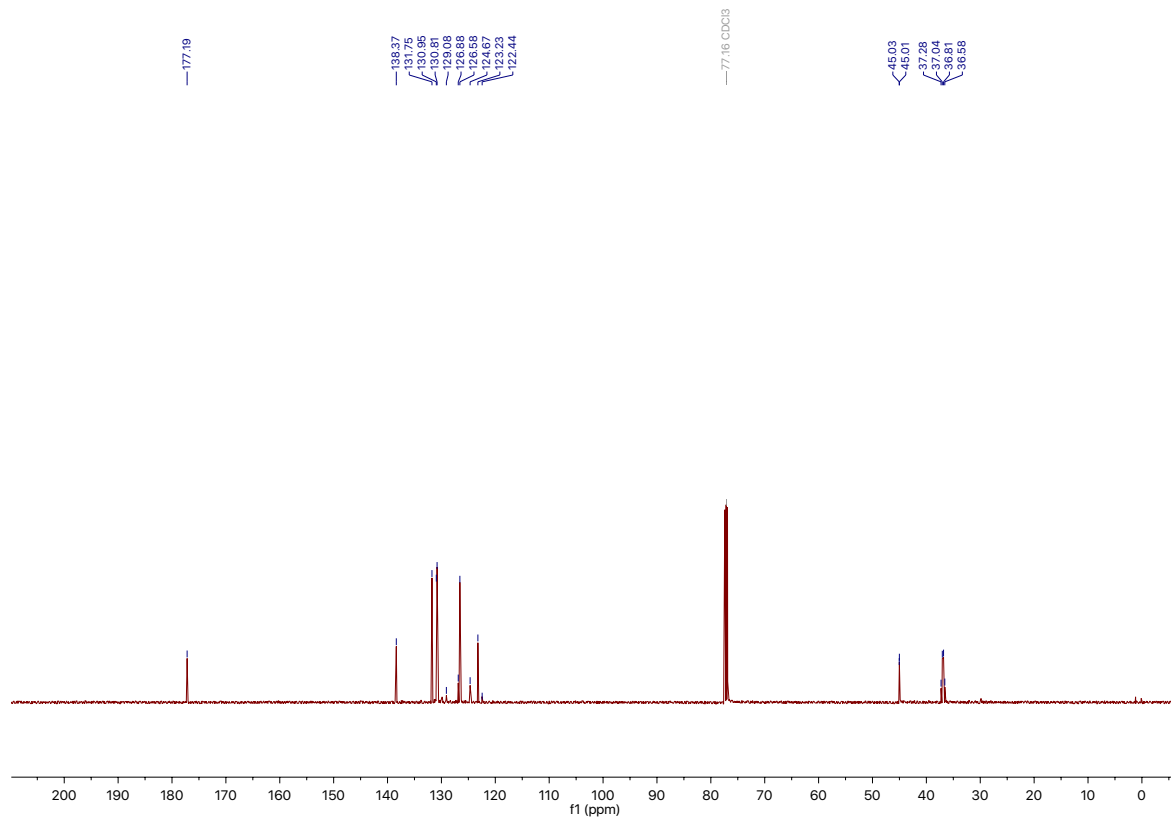
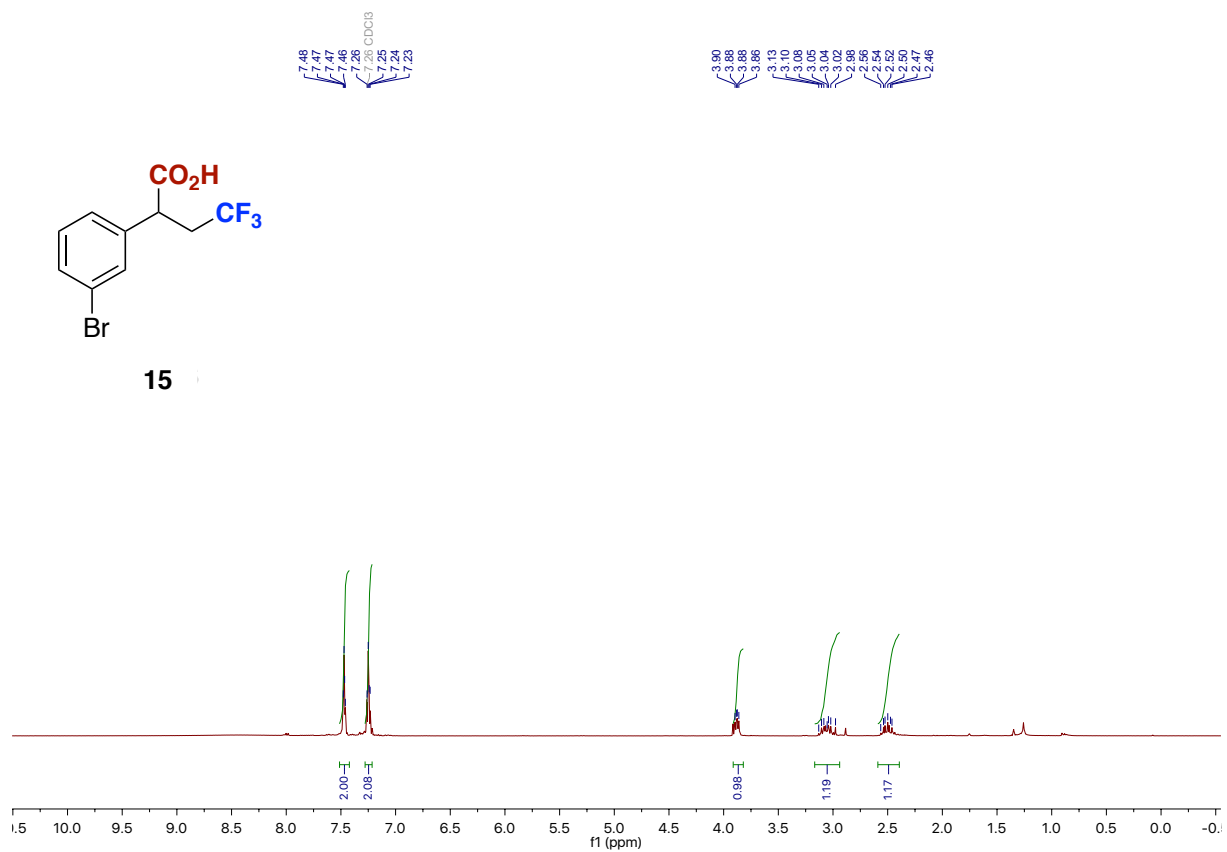


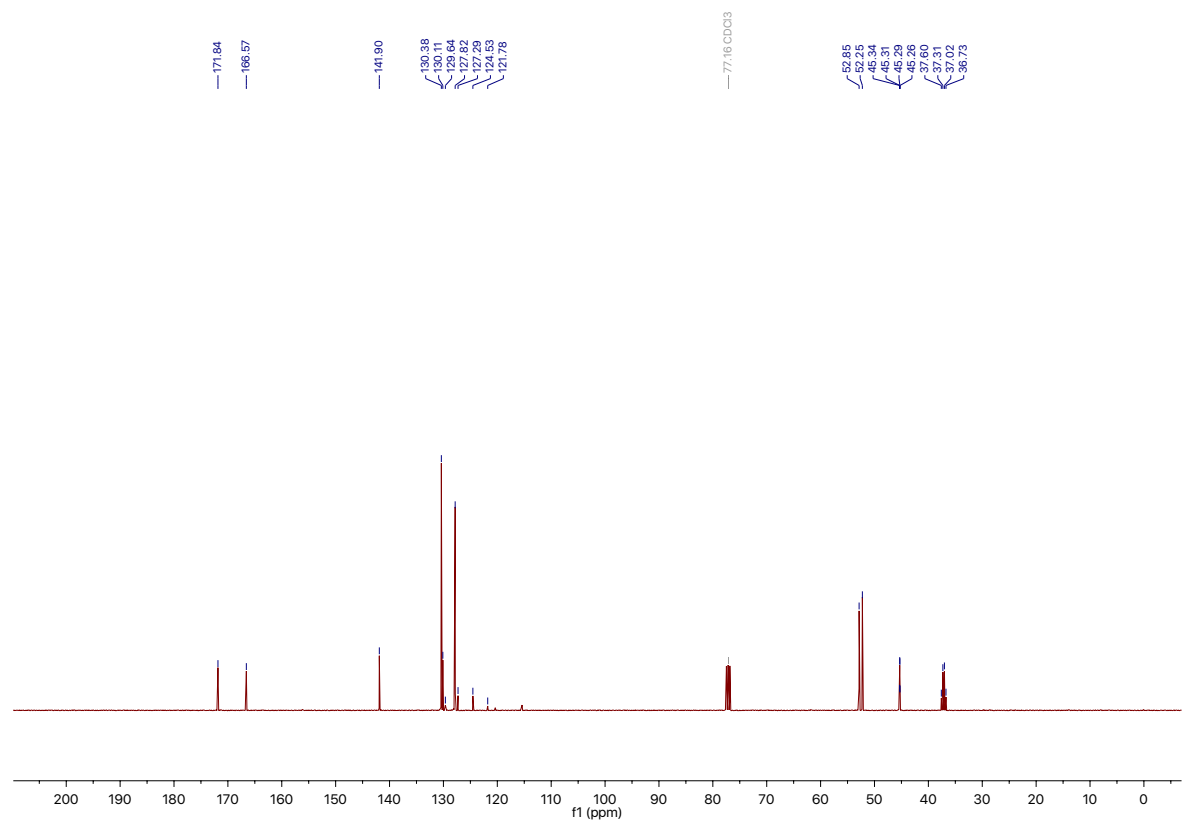
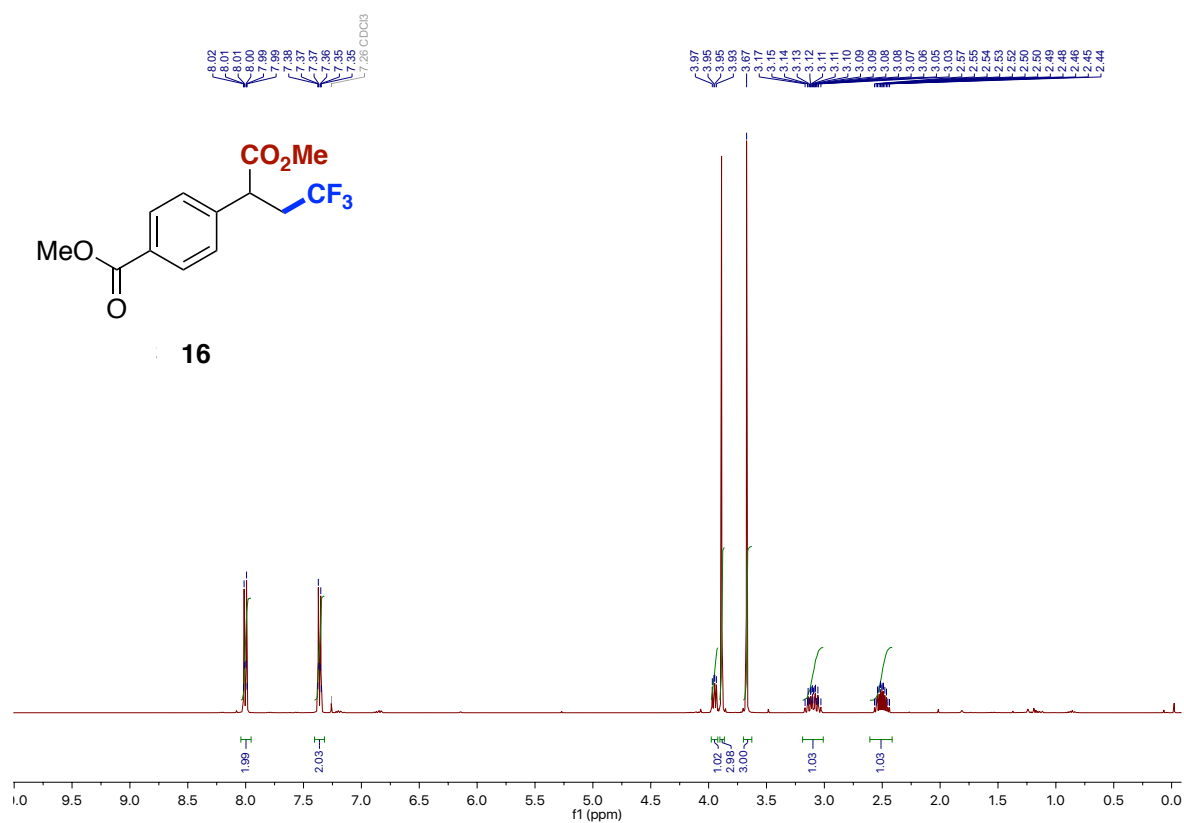




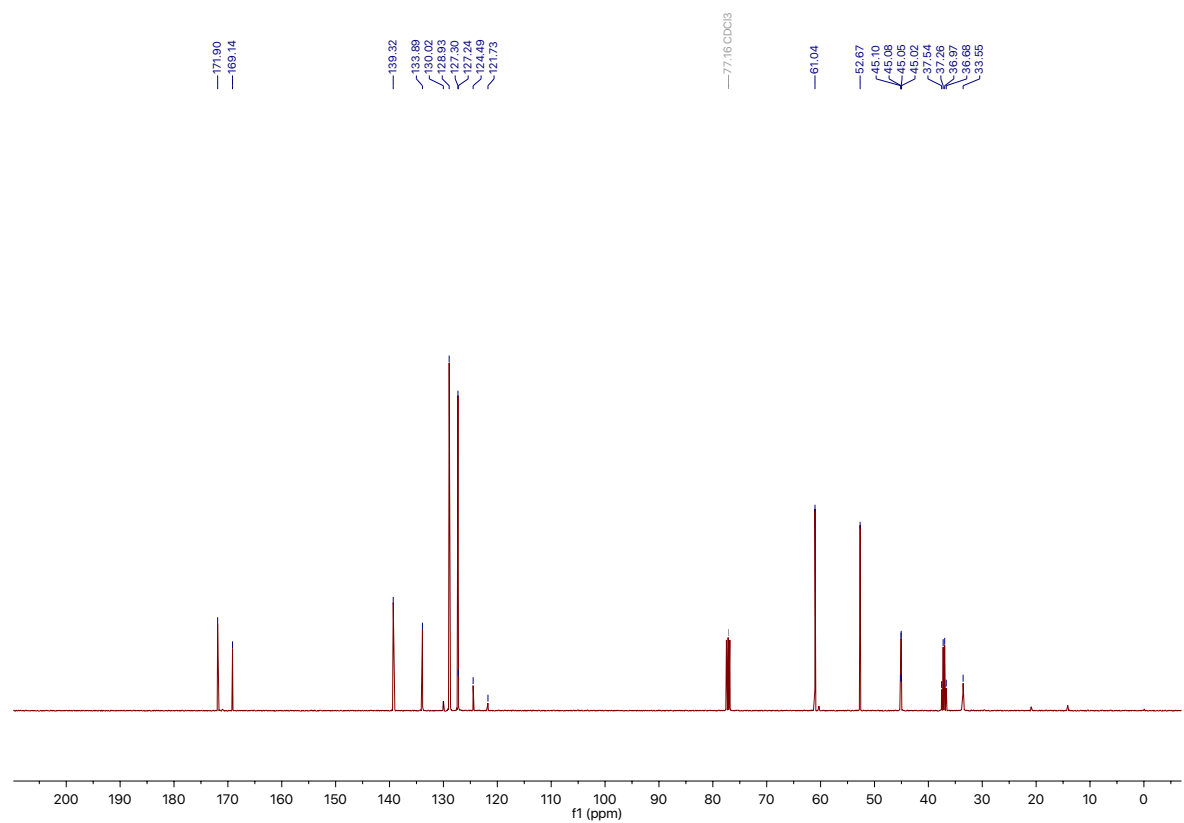
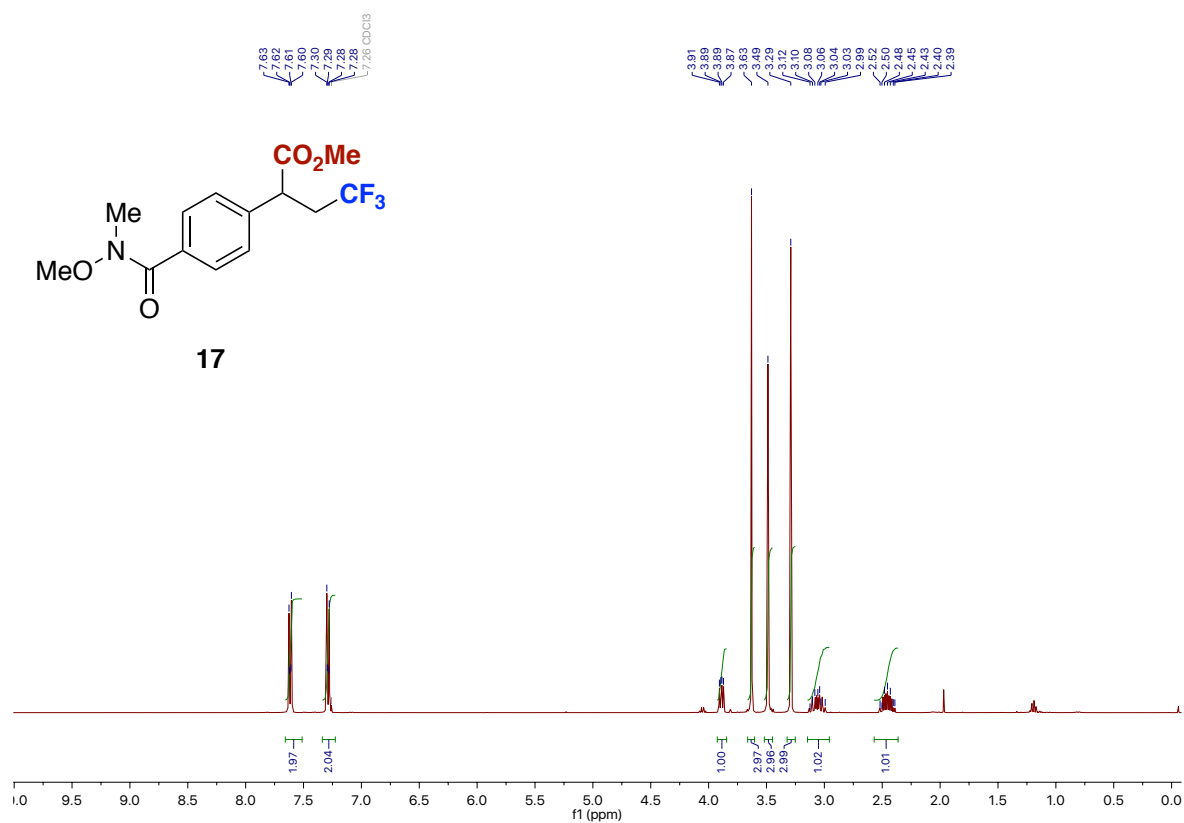


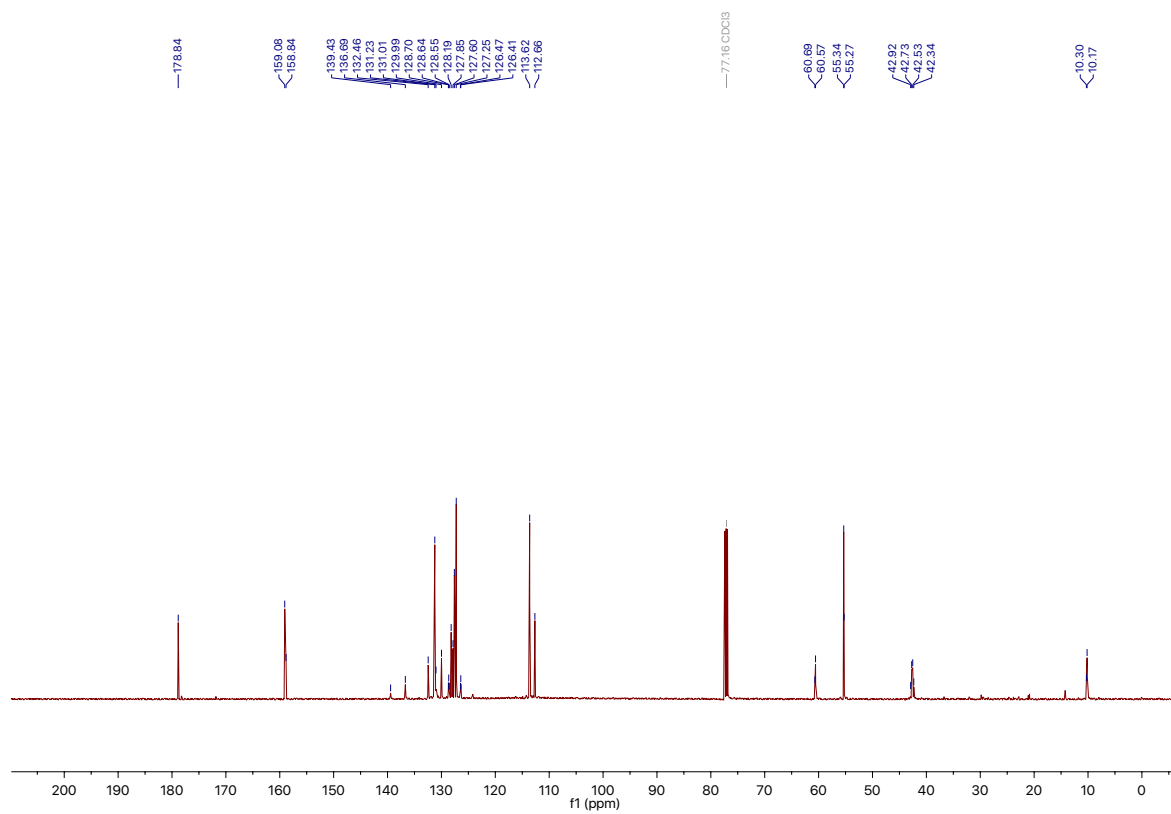
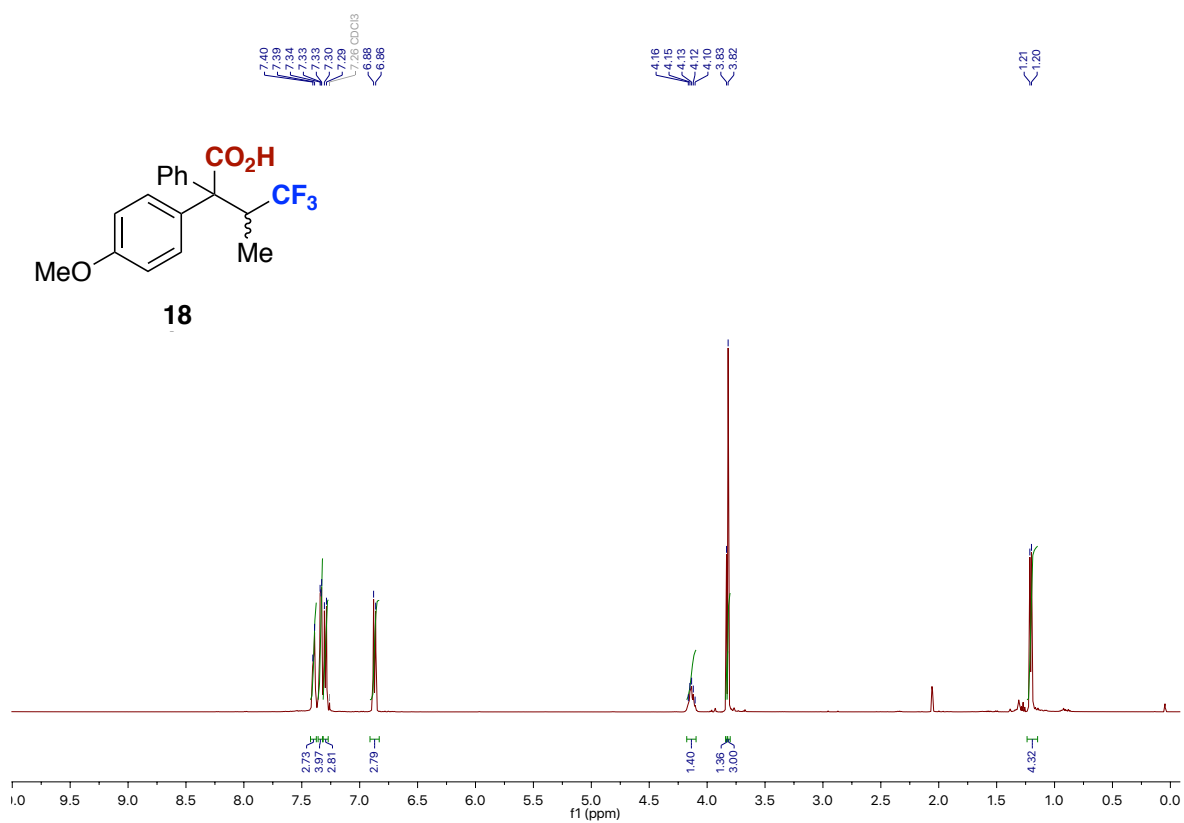
15

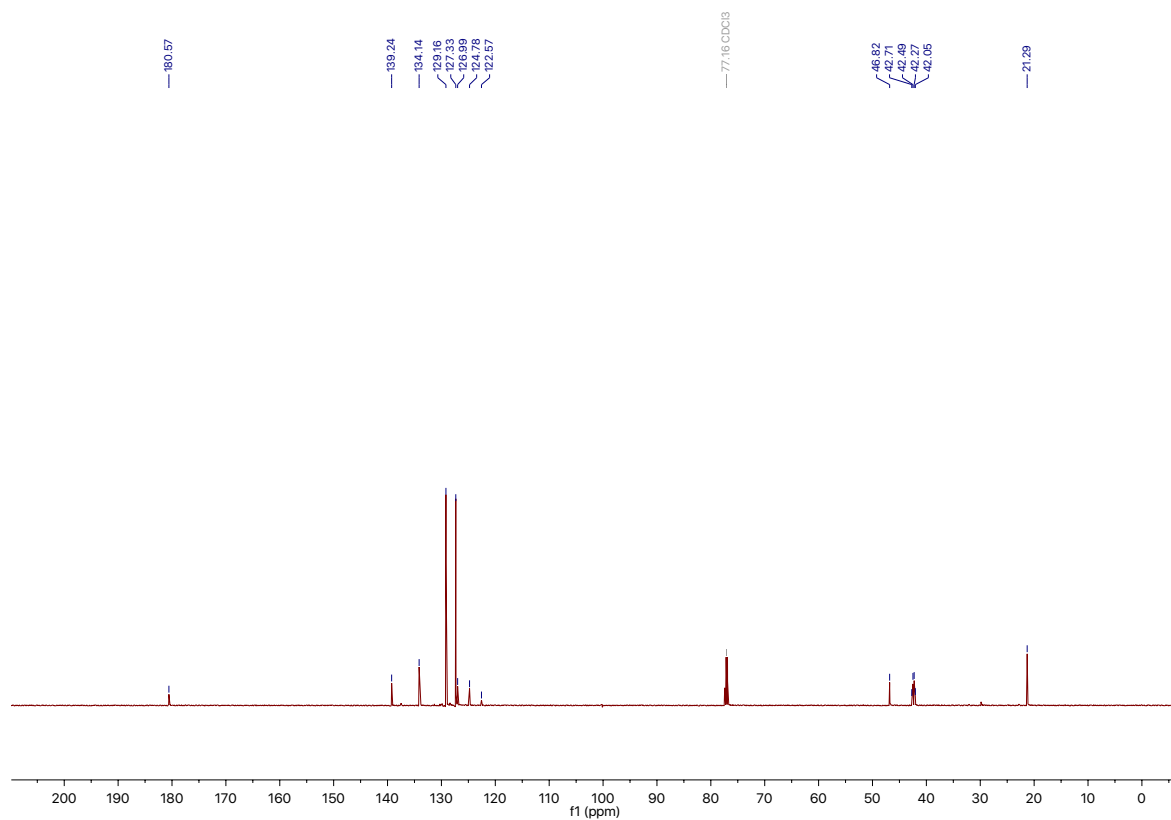
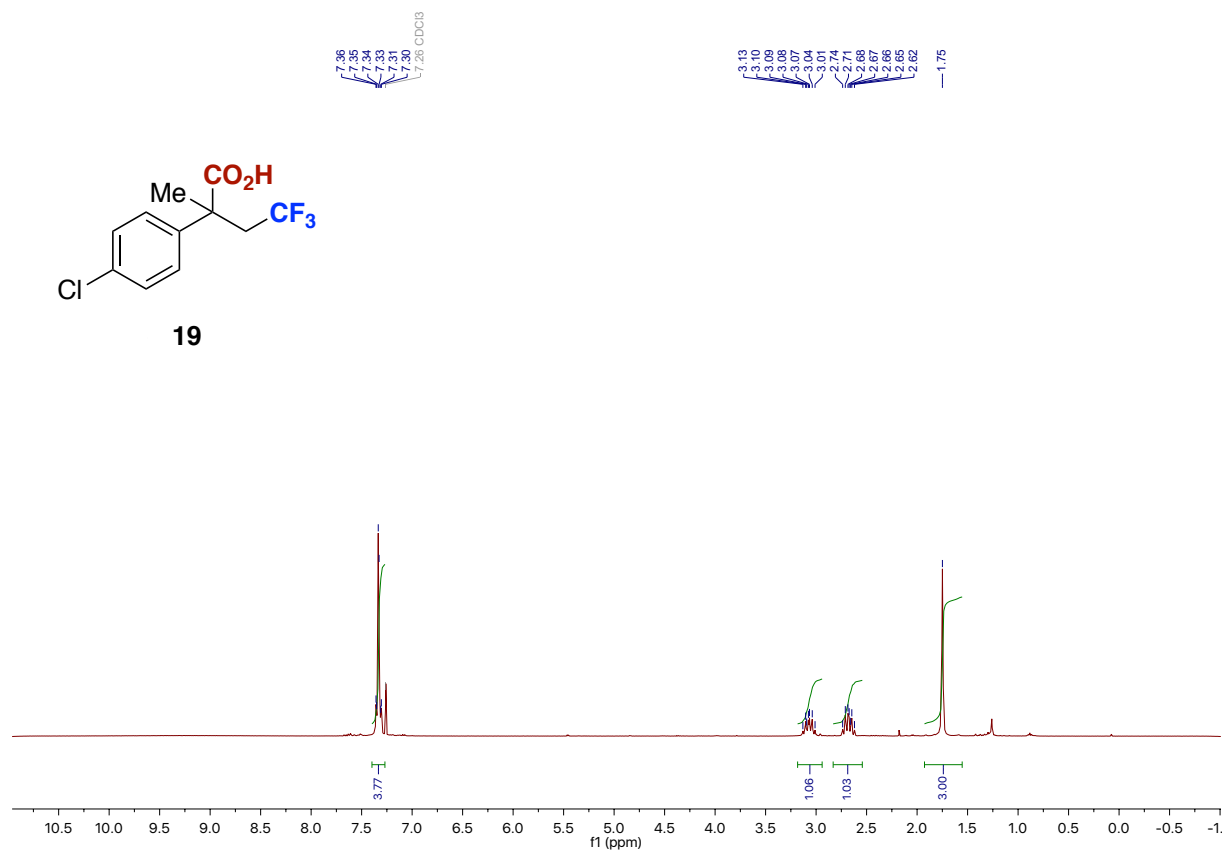
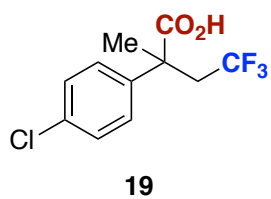


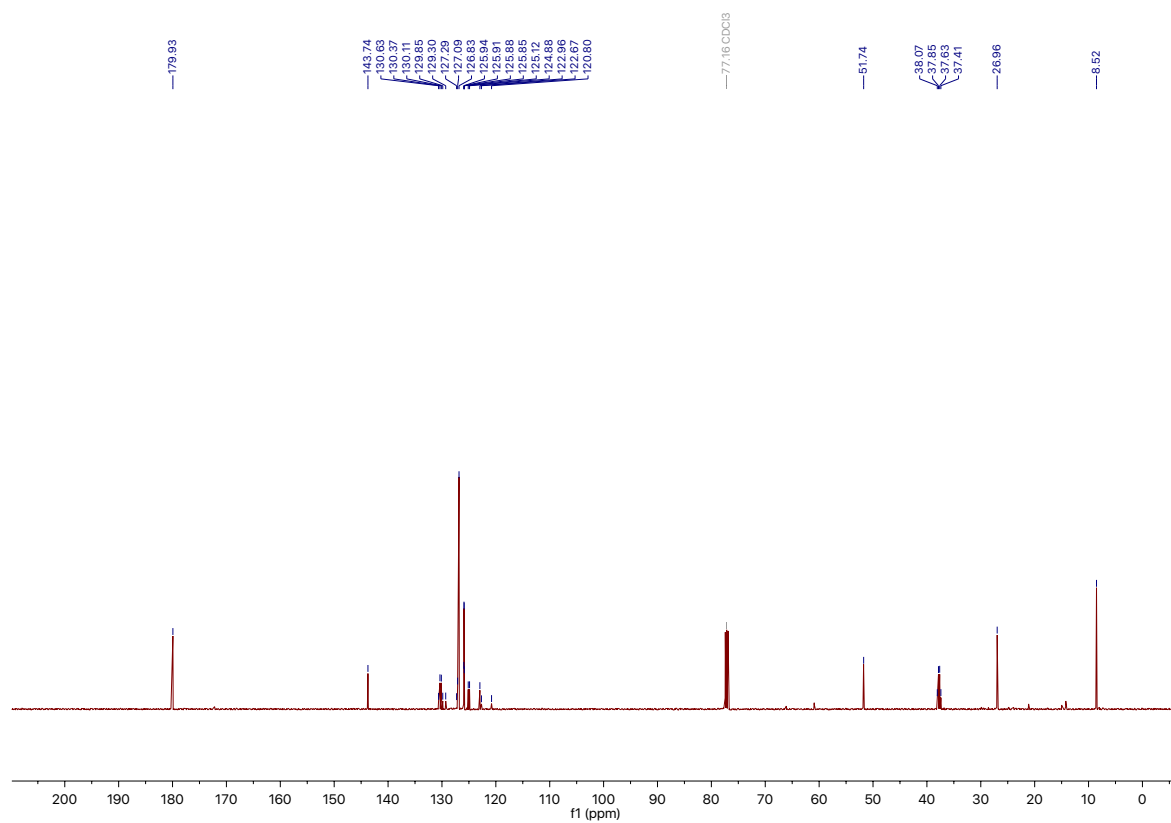
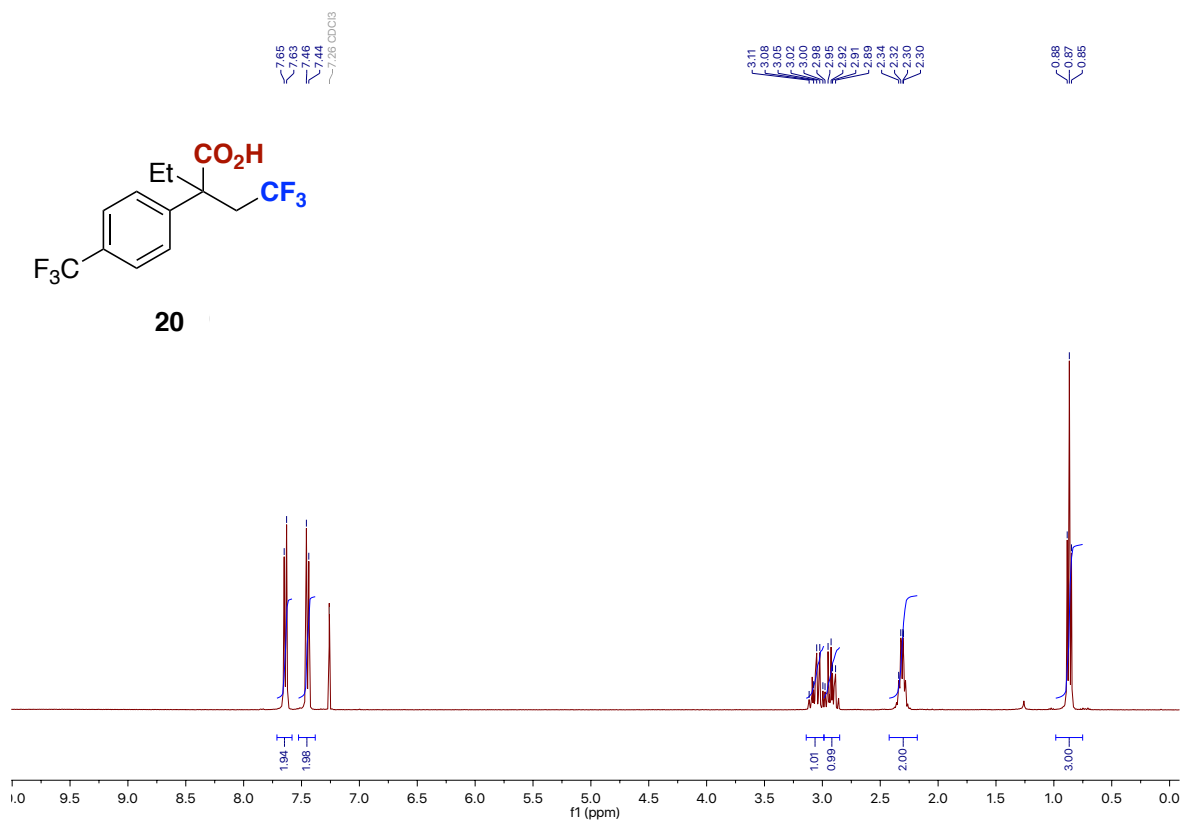




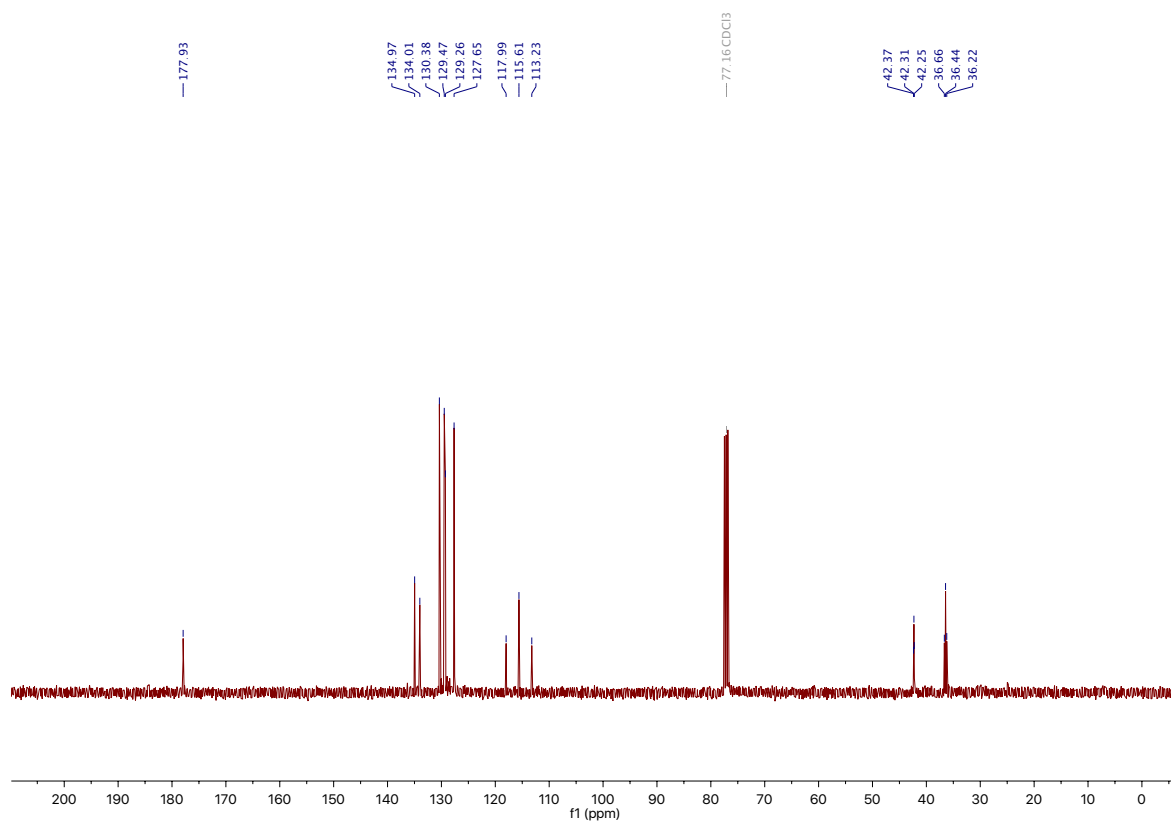
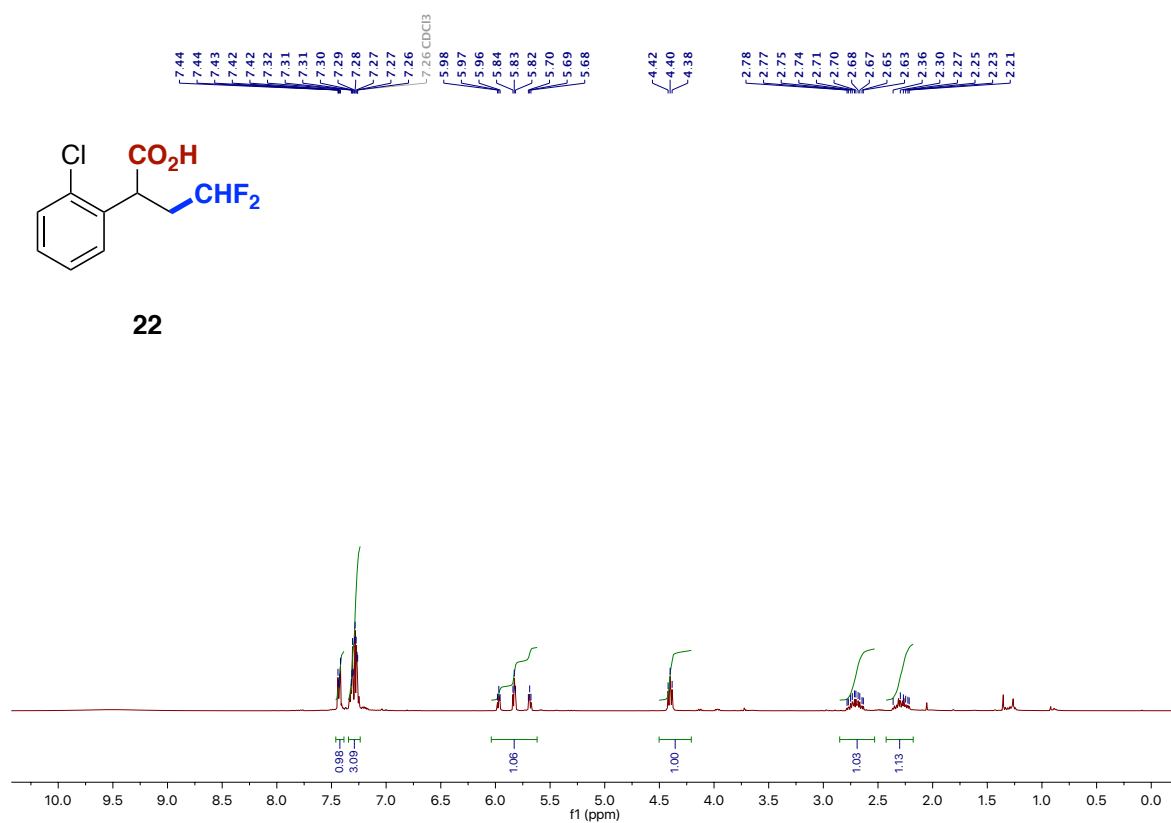


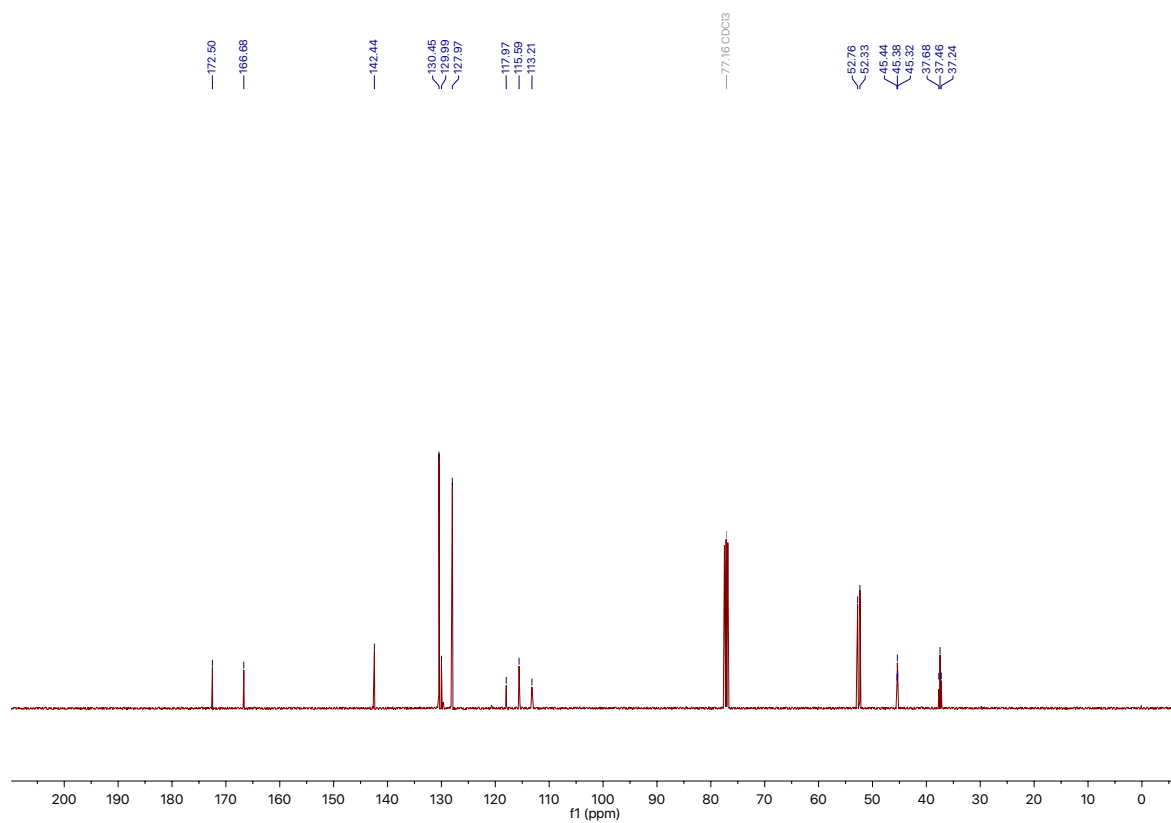
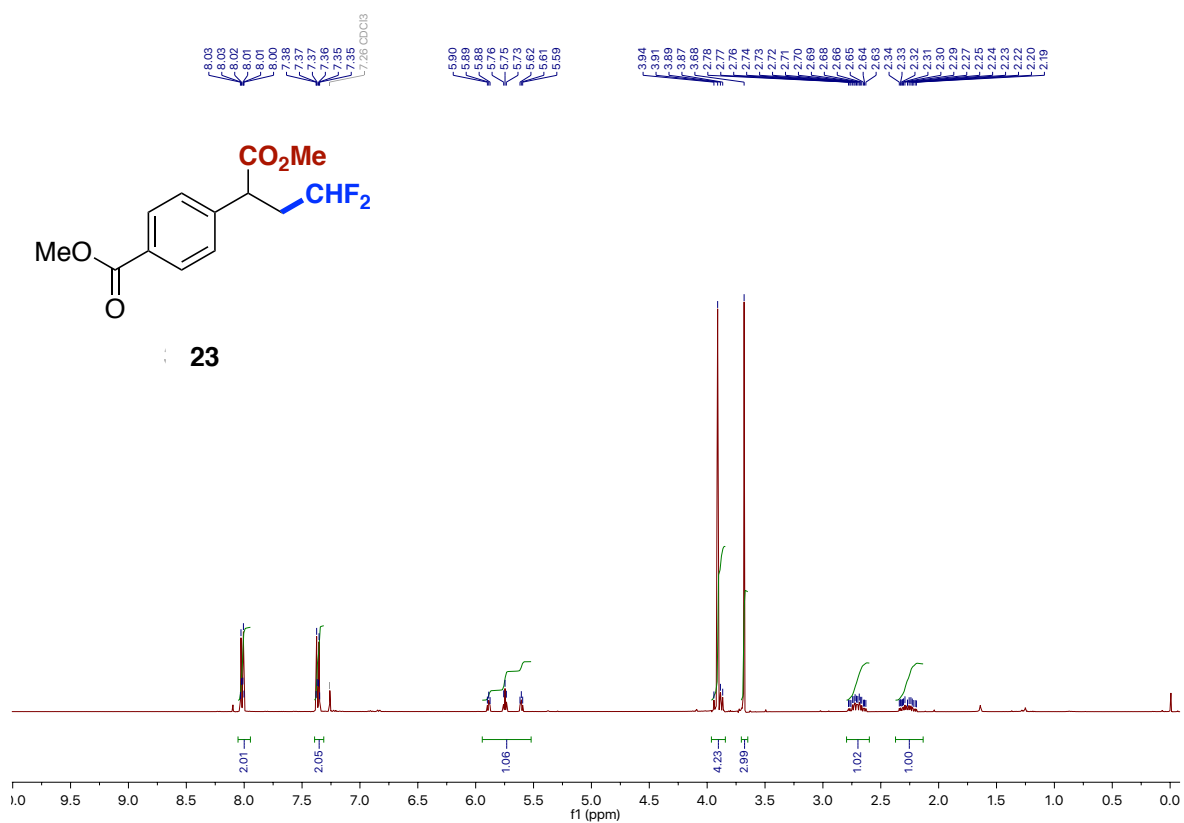


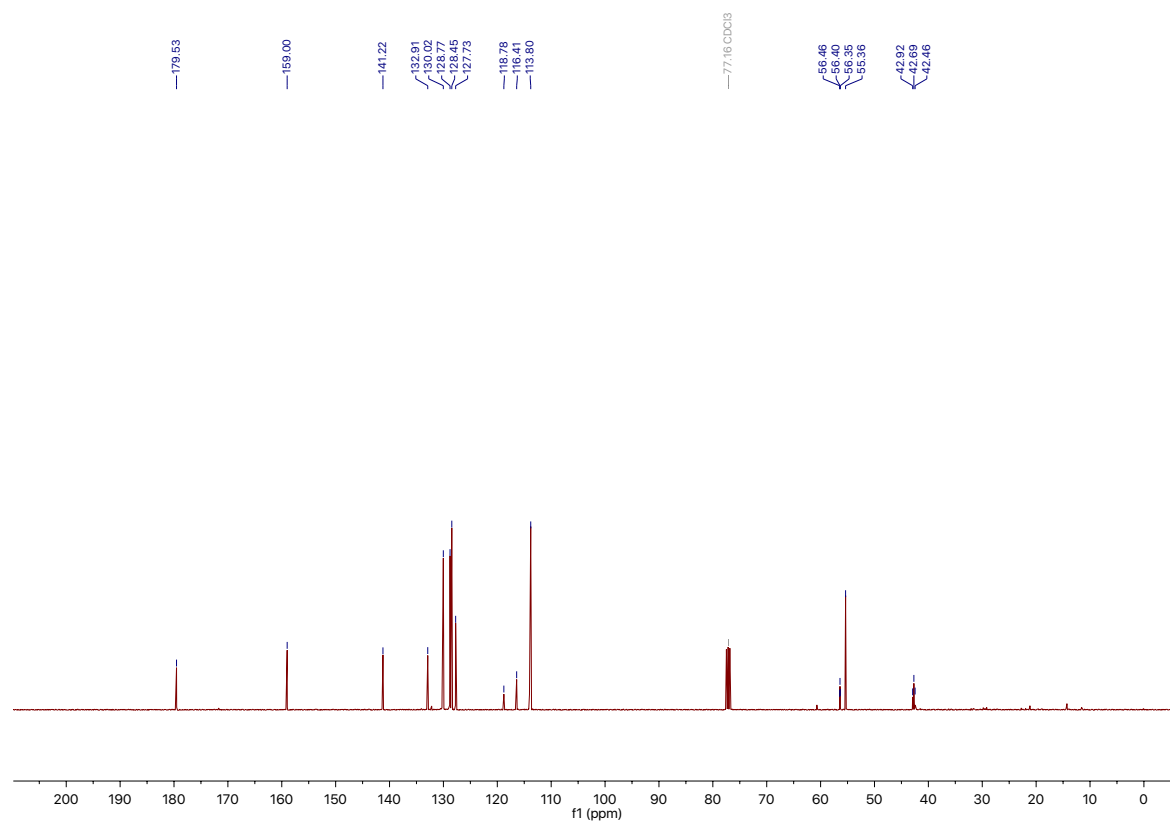
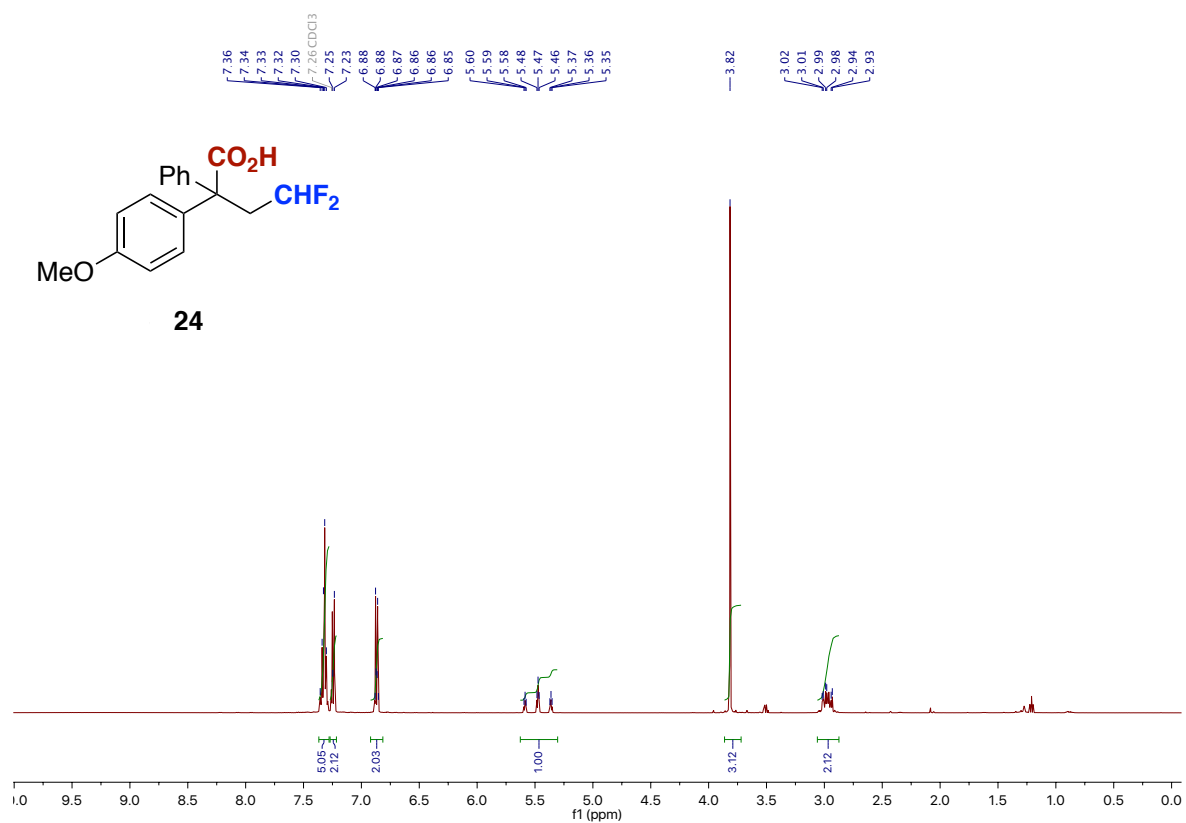




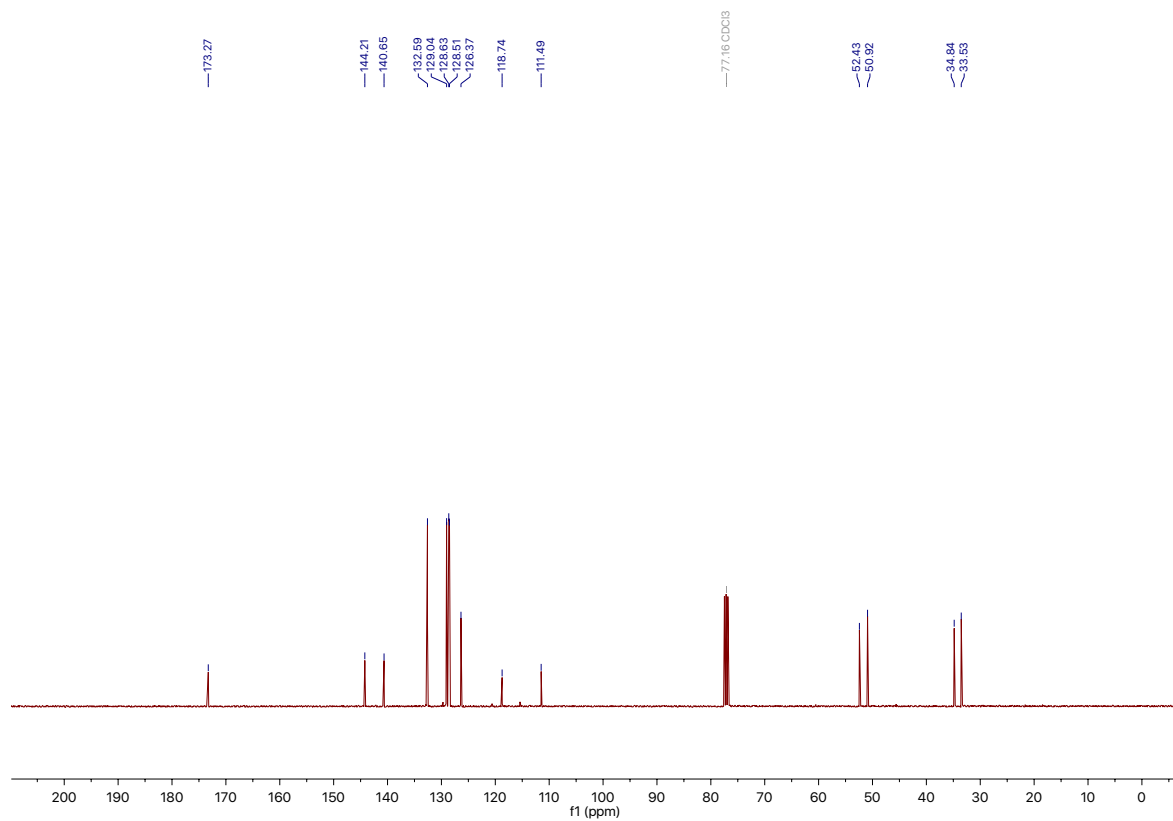
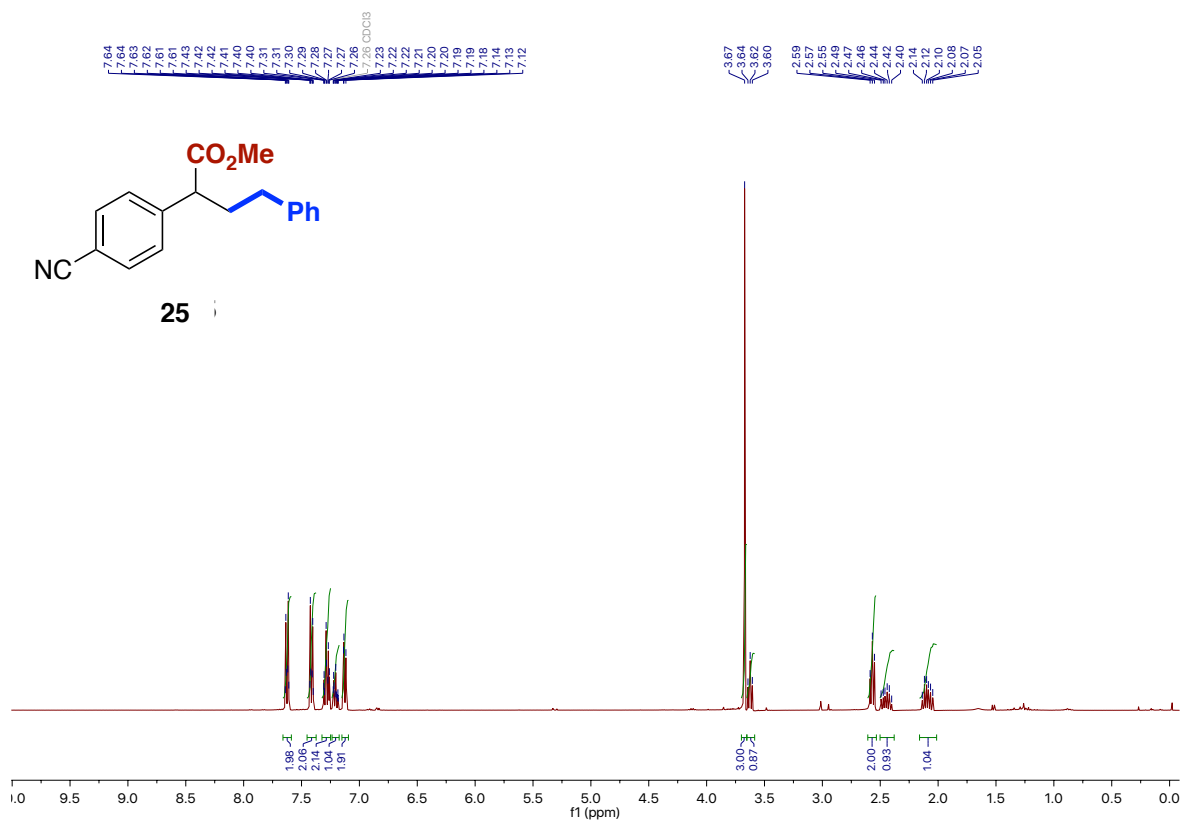


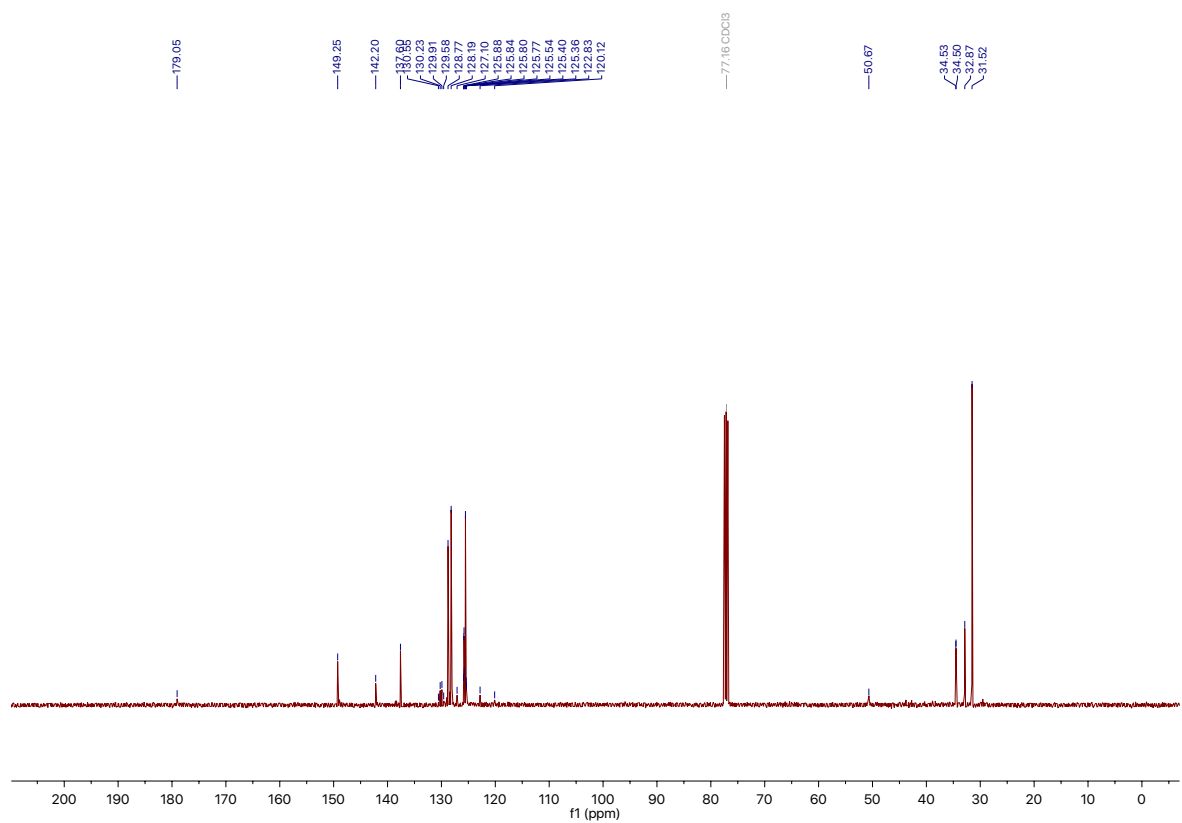
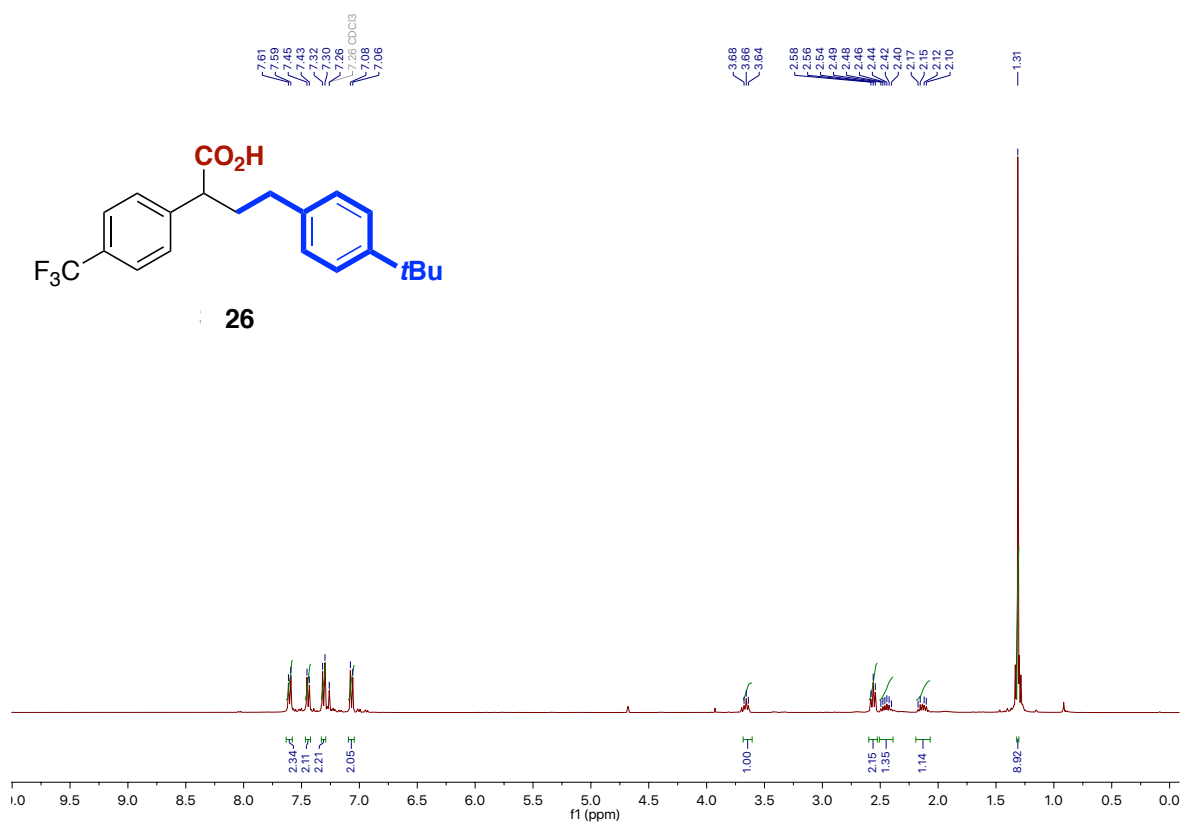


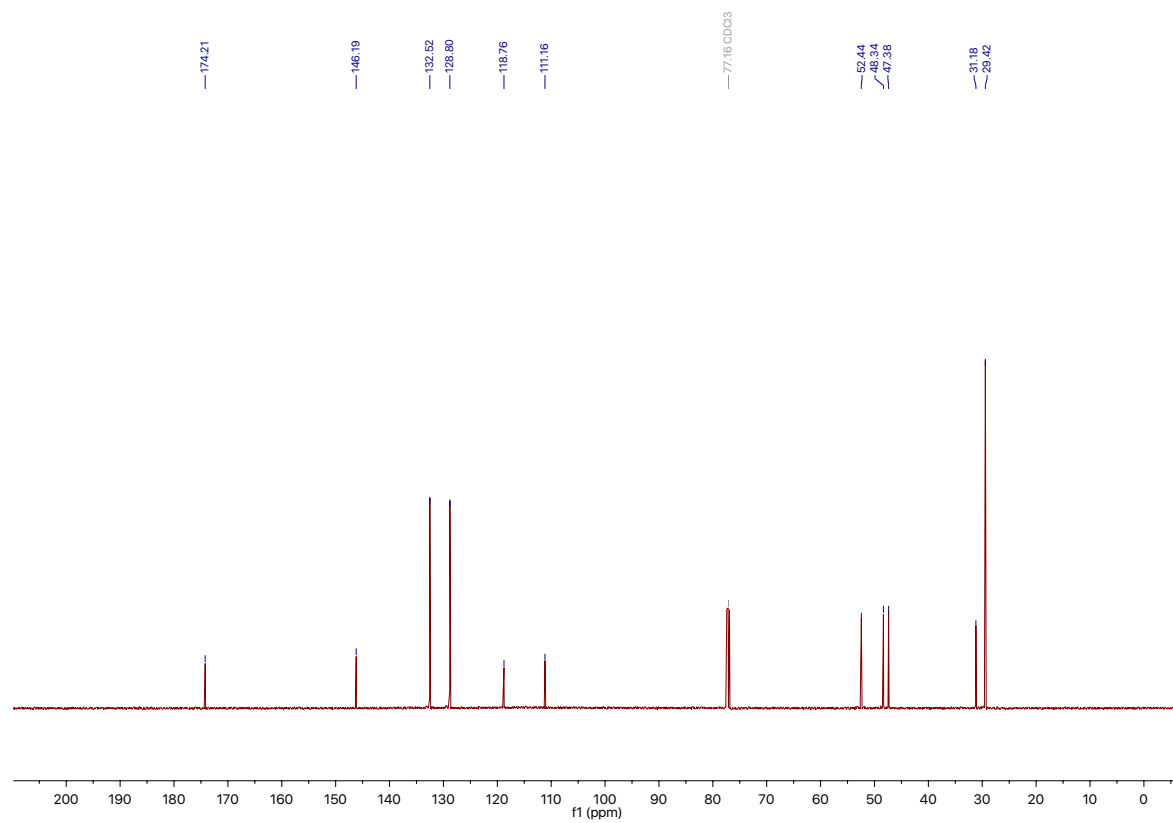
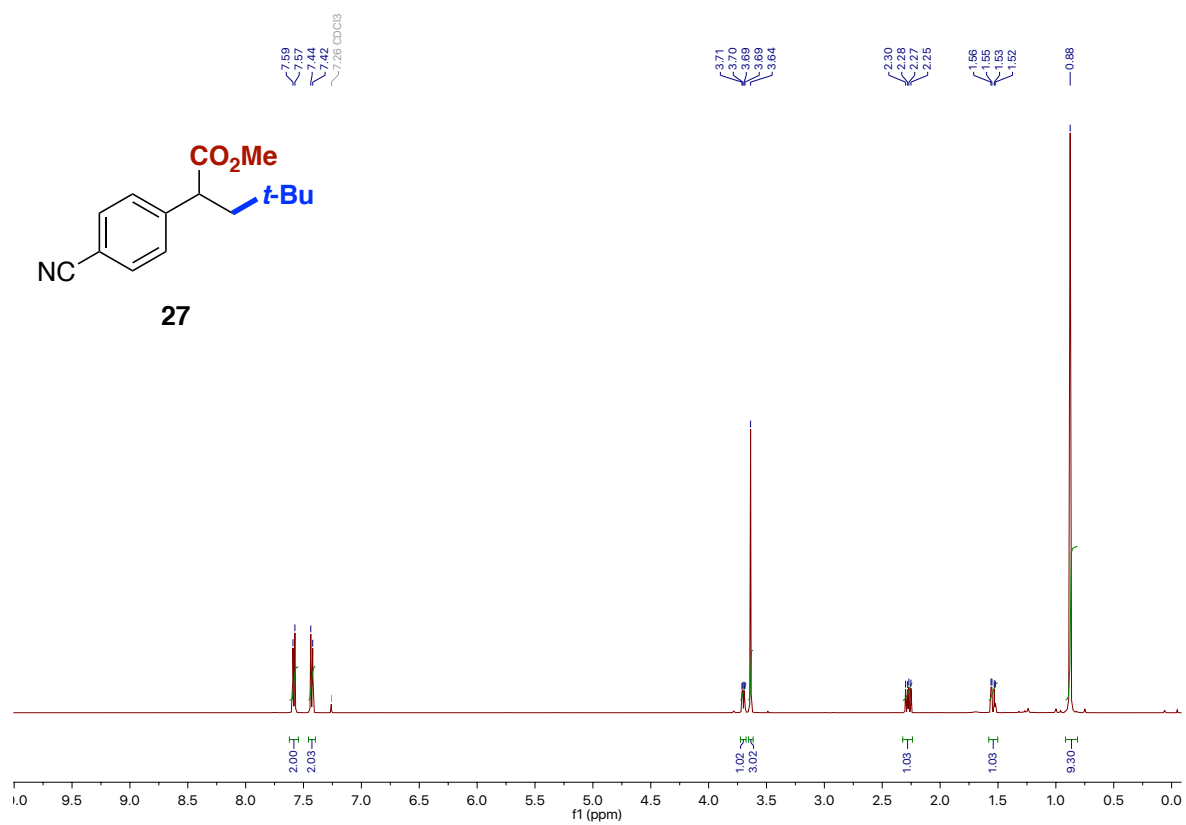


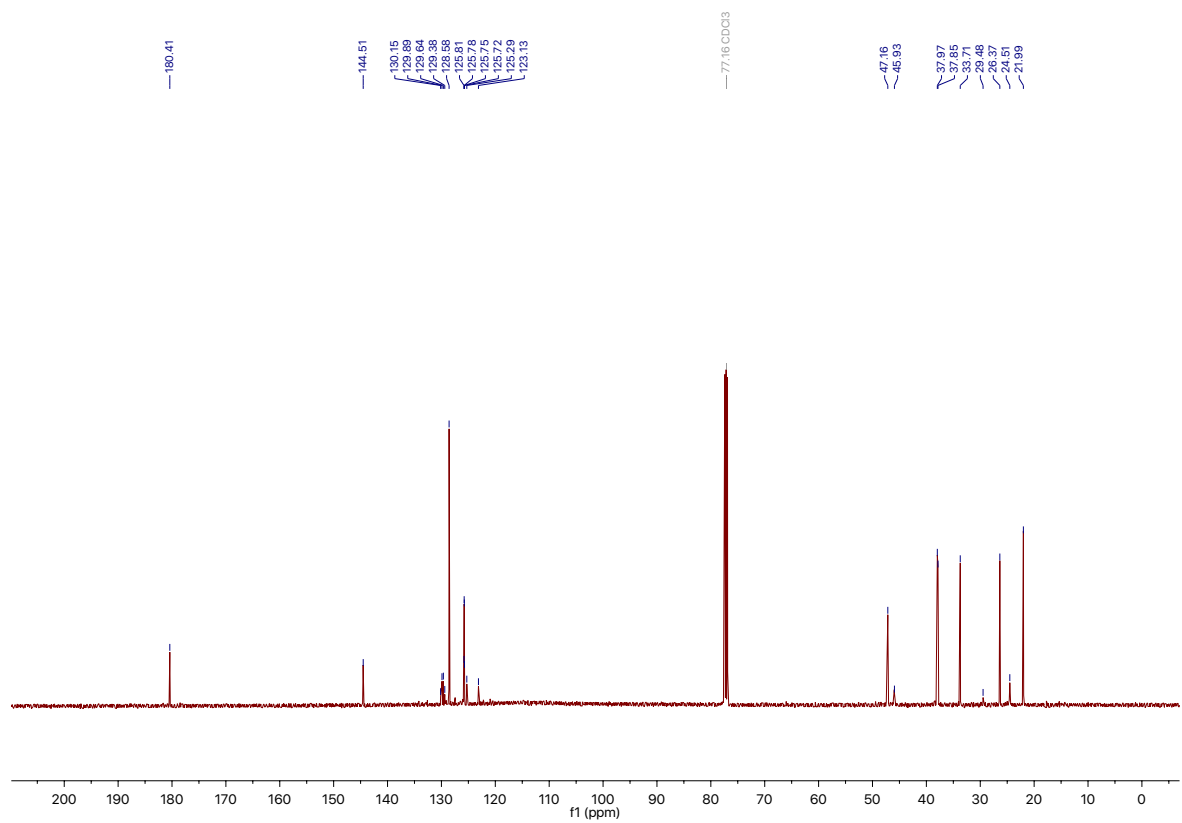
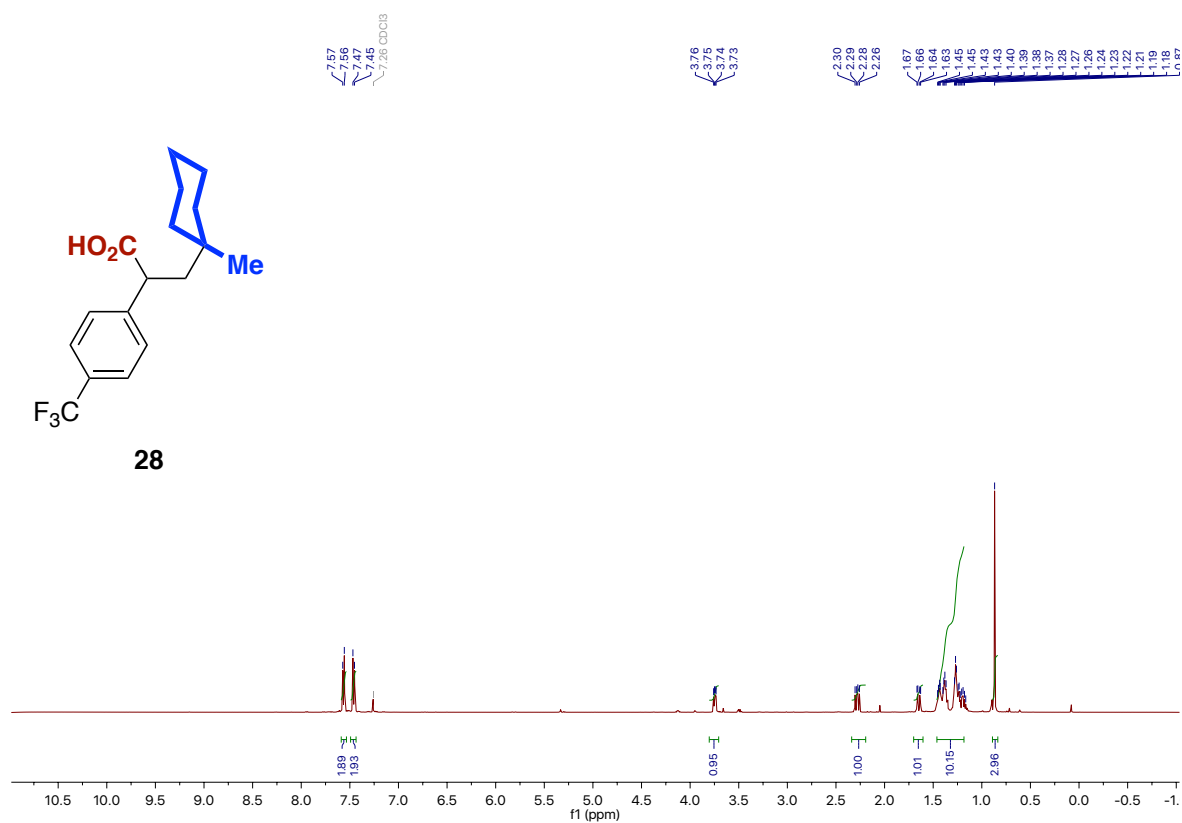


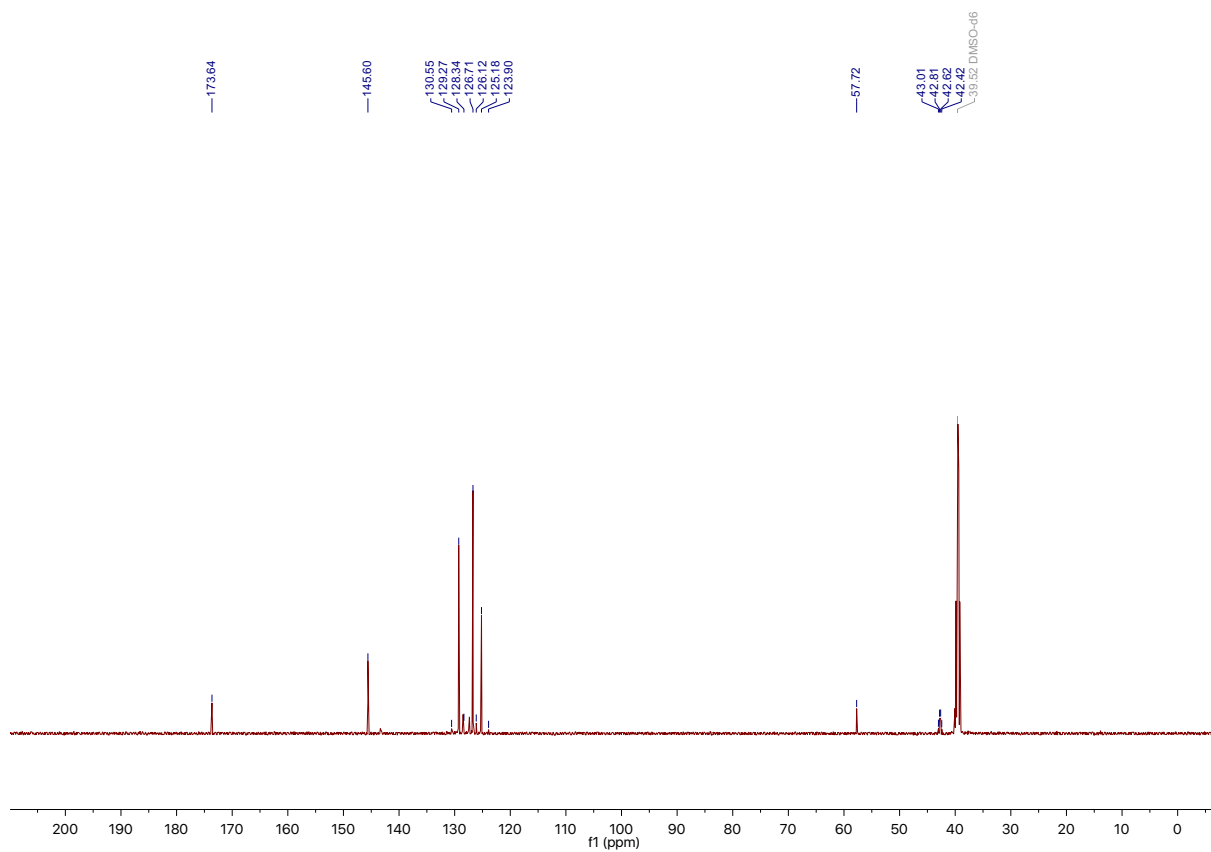
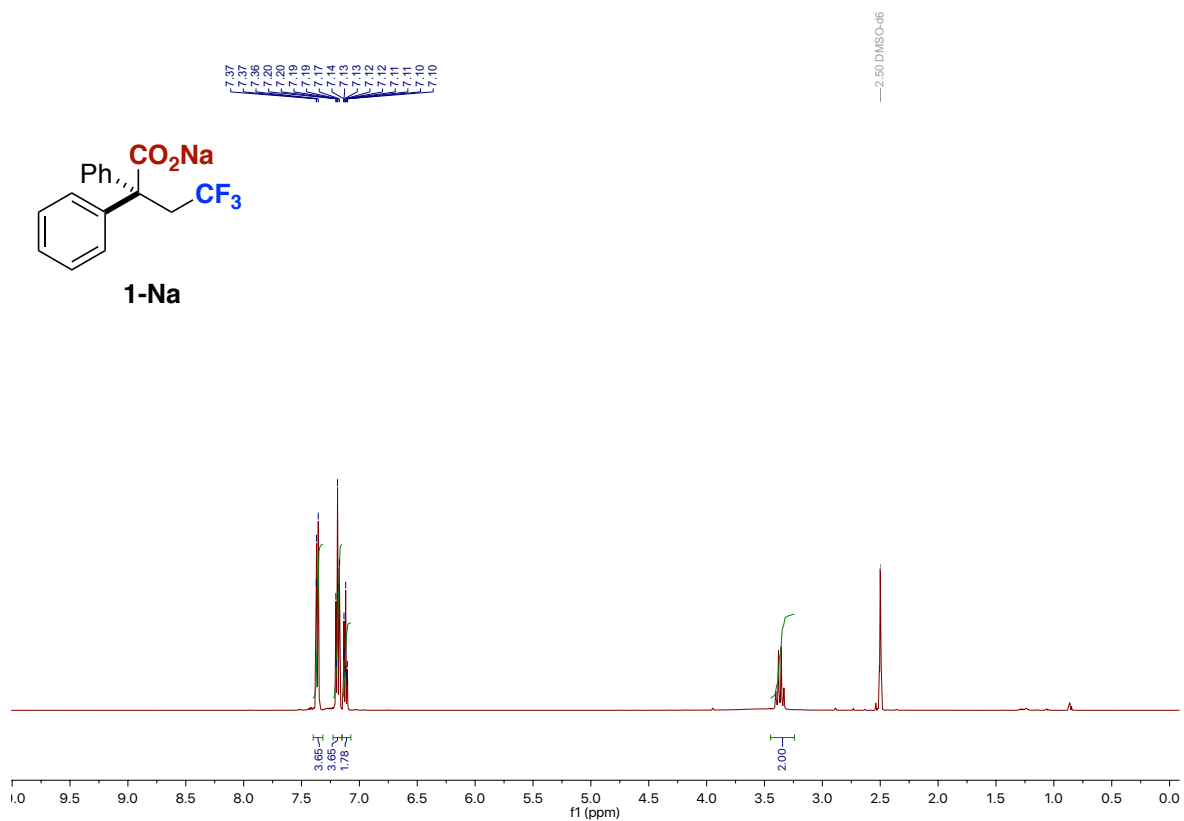


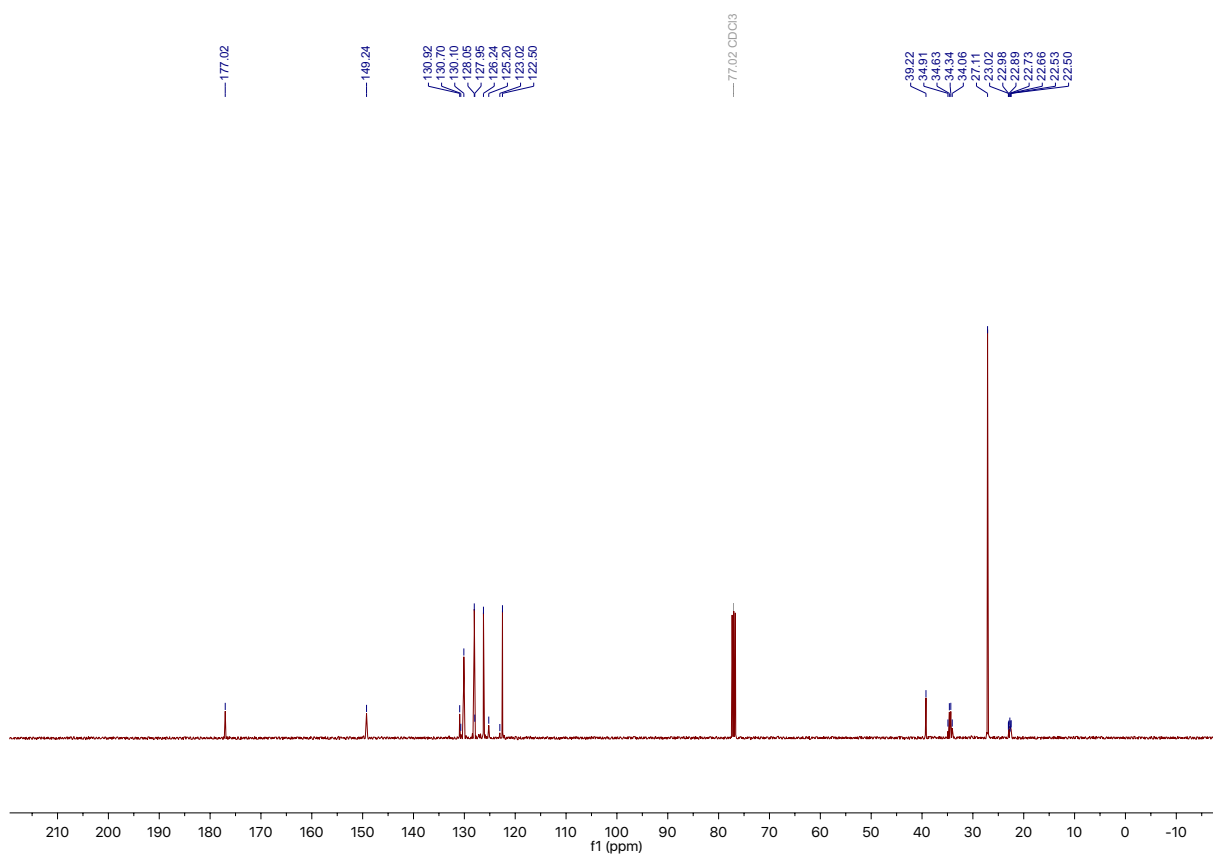
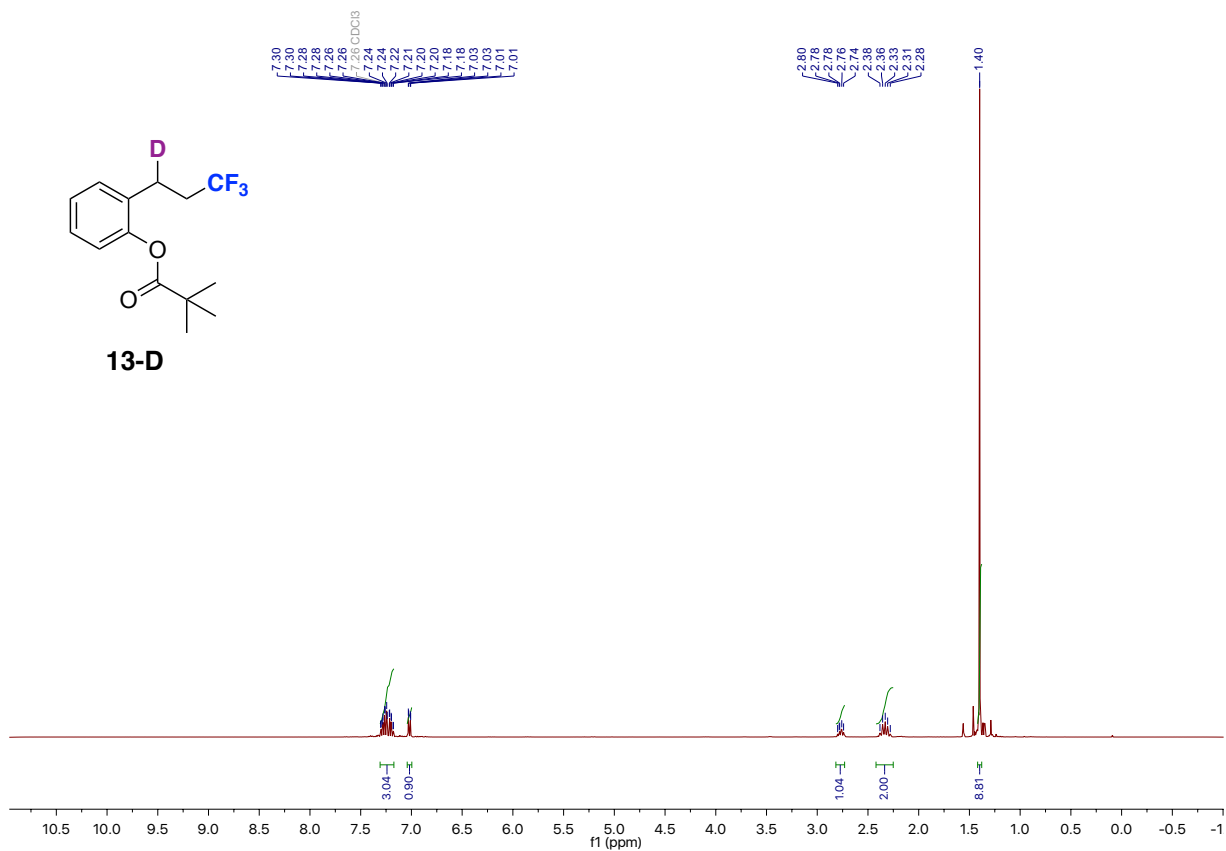


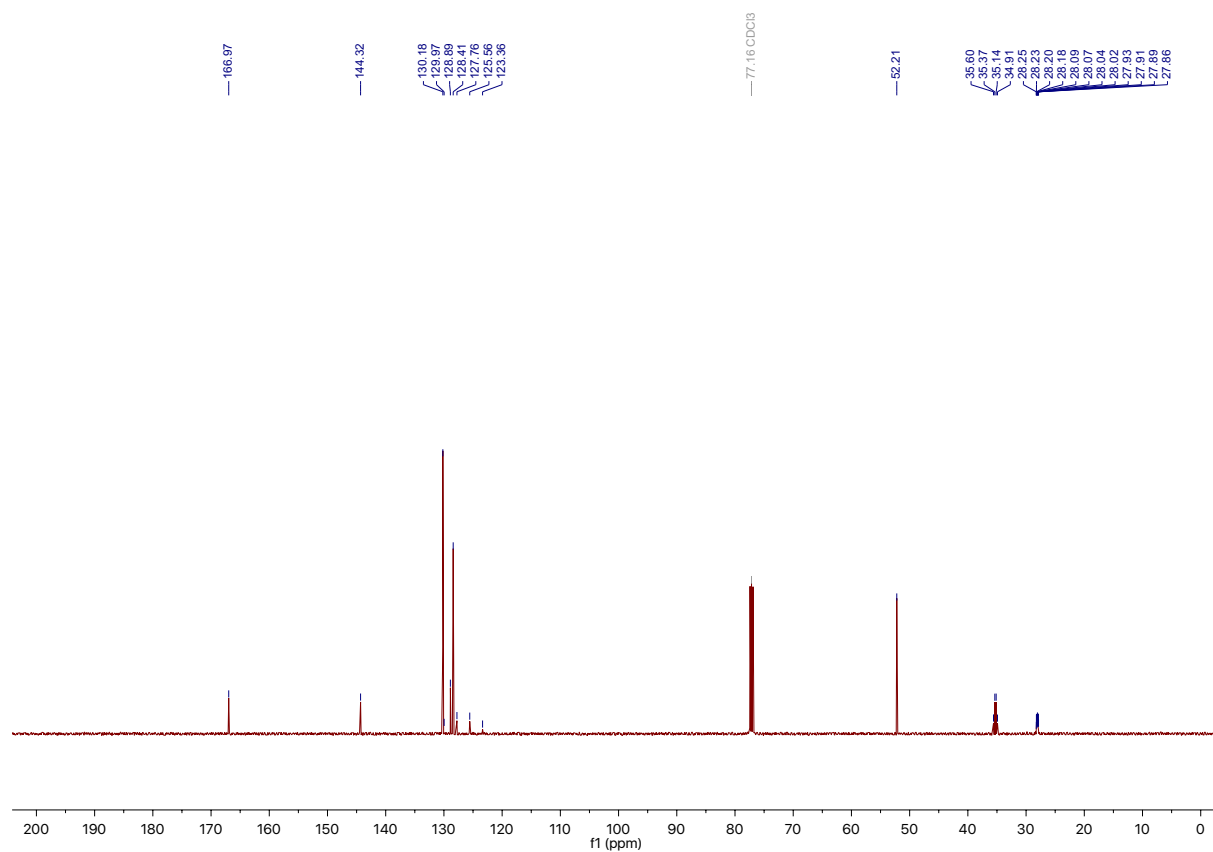
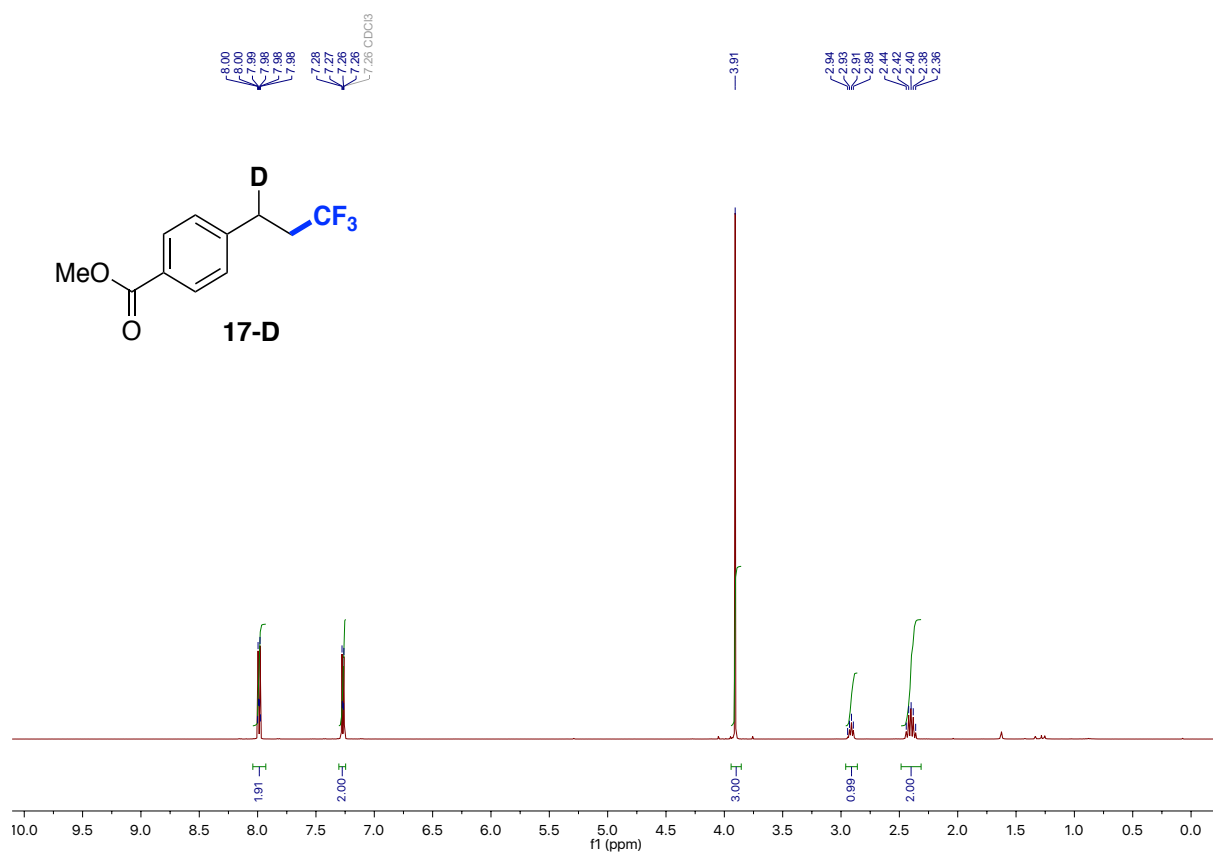












## **Chapter 4.**

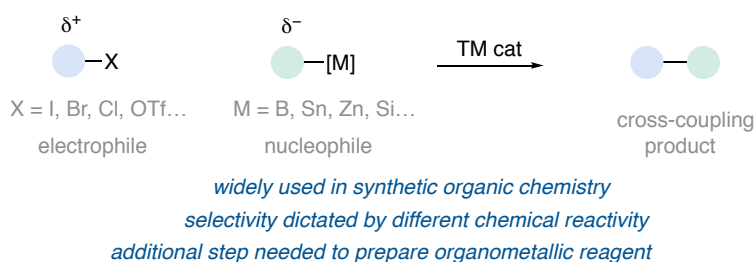
### ***sp*<sup>3</sup> C-H Arylation and Alkylation Enabled by the Synergy of Triplet Excited Ketones and Nickel Catalysts**



## 4.1. The Merger of Nickel Catalysis and Photoredox

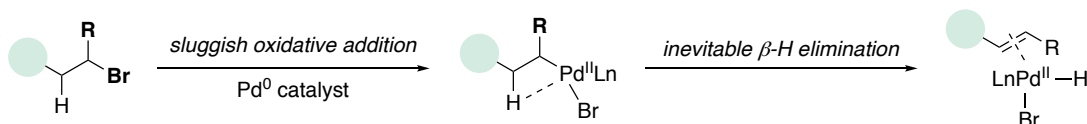
### 4.1.1. Fundamental Aspects of Ni Catalysis in Cross-Coupling Reactions

Over the last decades, transition metal-catalyzed cross-coupling reactions have provided new dogmas in retrosynthetic analysis for building up molecular complexity from readily available precursors.<sup>1</sup> Indeed, these transformations have changed the practice of C–C bond-forming reactions and their wide applicability have contributed to the full adoption of these techniques in both academic and pharmaceutical laboratories (Scheme 4.1).<sup>1</sup>



#### Scheme 4.1. Traditional paradigm for cross coupling reactions

Not surprisingly, the impact of these methodologies was finally awarded with the Nobel Prize in Chemistry (2010) by acknowledging the seminal contributions from Heck, Suzuki and Negishi within the area of Pd-catalyzed cross coupling reactions.<sup>1</sup> As judged by the wealth of literature data, a considerable effort has been made to expand the repertoire of the coupling partners that can be utilized in these endeavors.<sup>1</sup>



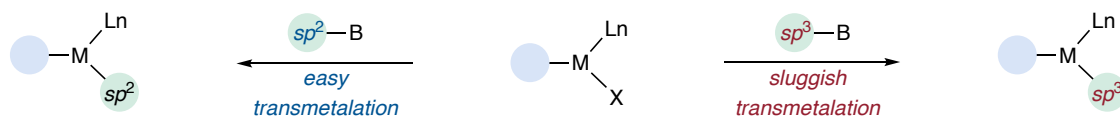
#### Scheme 4.2. Oxidative addition problem of Pd(0) to alkyl electrophile

While the Pd-catalyzed cross-coupling reactions of aryl or vinyl halides have become routine, extensions to *unactivated*  $sp^3$  fragments still remains challenging. This is largely due their reluctance to oxidative addition and the propensity of the in situ generated alkyl metal species to parasitic  $\beta$ -hydride elimination (Scheme 4.2). Although the subtle modulation of the electronic properties of the ligands might offer a solution to these challenges when employing Pd catalysts, the recent years have witnessed the implementation of Ni-catalyzed cross-coupling reactions of unactivated alkyl halides,<sup>2</sup> offering new alternate pathways that are typically beyond reach with Pd catalysts. The interpretation behind the superior reactivity of Ni vs Pd can be explained by the weak agostic interaction observed for alkyl-Ni(II) complexes when compared with the corresponding alkyl-Pd(II) congeners. This is

due to the fact that the main contribution for the agostic interaction with electropositive metals is the  $\sigma$ -donation of the proximal C-H bond to the metal center; when using Ni(II) complexes, the vacant  $d$  orbital is way high in energy than the corresponding Pd(II) analogue, making a rather poor orbital overlap that causes an elongation in the agostic interaction.<sup>2-5</sup> Additionally, it is worth noting that Ni is way more electropositive than Pd; therefore, oxidative addition, that is nothing else than the loss of electron density at the metal center, is way more facile for Ni than for Pd, an aspect that has been turned into a strategic advantage when tackling the functionalization of rather strong C-O or C-F bonds.<sup>2-5</sup> Moreover, the C-Ni bond is considerable weaker than the corresponding C-Pd, an observation that can hardly be underestimated taking into consideration that weak organometallic bonds provide the fundamental basis for uphill transformations or for generating open-shell intermediates via SET processes. The latter is particularly relevant, as multiple catalytic regimes are known in Ni-catalyzed reactions (Ni(0)/Ni(II), Ni(I)/Ni(II) or Ni(I)/Ni(III)) whereas classical polar Pd(0)/Pd(II) mechanisms dominate the cross-coupling arena.<sup>2-5</sup> Taken together, the available data argues against Ni being a mere cheap substitute of Pd in the  $d^{10}$  series, offering complementary new reactivity for forging C-C and C-heteroatom bonds.

#### 4.1.2. The Macroscopic Revolution of Ni Catalysis

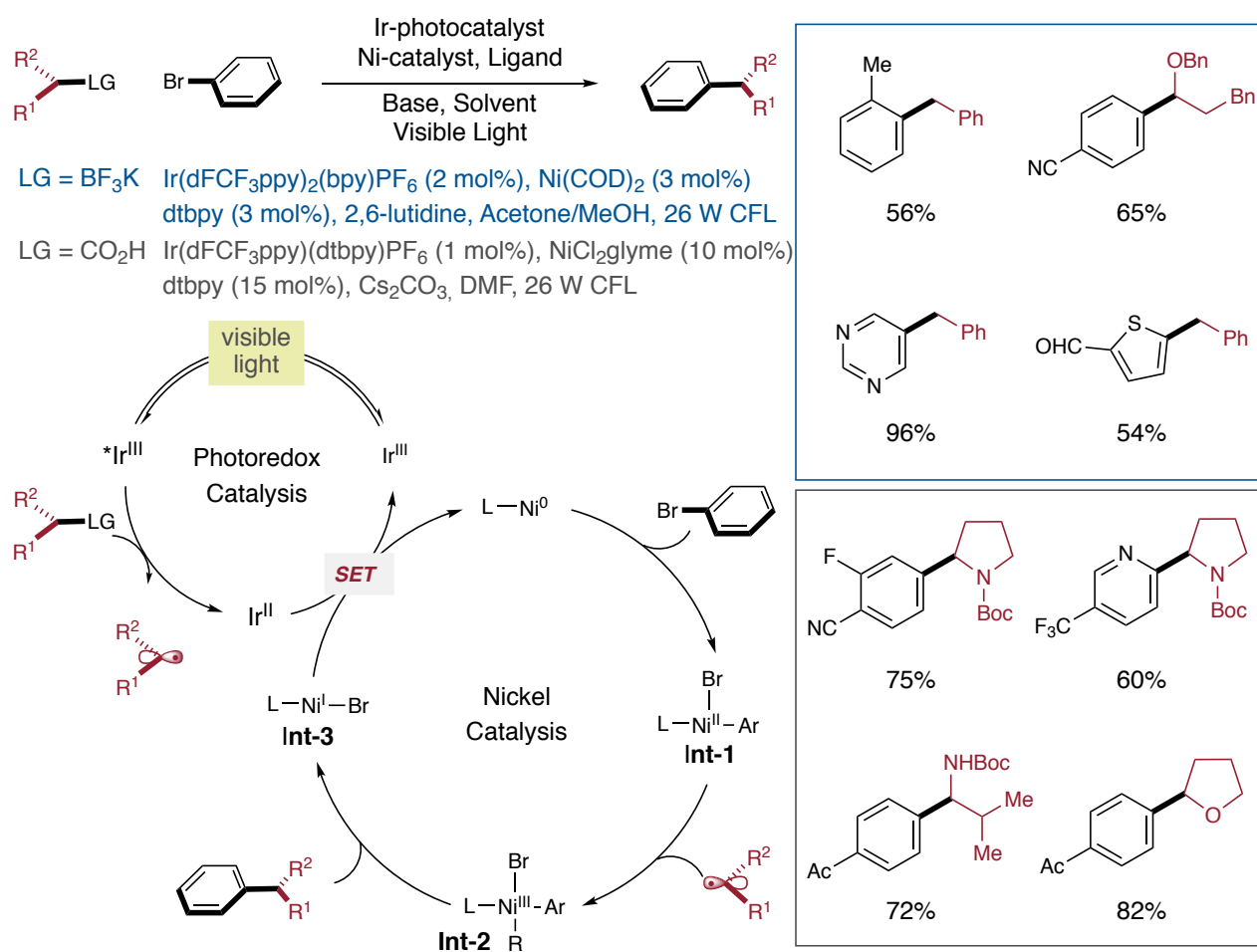
Beyond any reasonable doubt, the impact of the Suzuki-Miyaura reaction on academic and industrial research has been immense.<sup>6</sup> Over the past two decades, it has become arguably one of the most efficient methods for the construction of C-C bonds. The key advantages of the Suzuki-Miyaura coupling over other methods are the mild conditions under which it is conducted, the high chemoselectivity profile, the stability of boronic acids and the ease of handling, thus making this reaction an indispensable tool in medicinal chemistry as well as in the large-scale synthesis of pharmaceuticals and fine chemicals.<sup>7</sup>



**Scheme 4.3. The challenge posed by coupling C( $sp^3$ )-boron species**

Despite the advances realized, the cross-coupling of  $sp^3$  C-boron reagents still remain largely problematic due to sluggish transmetalation, resulting in detrimental side reactions (Scheme 4.3, *right*).<sup>8</sup> To date, strategies aimed at accelerating the rate of transmetalation of C( $sp^3$ ) organoboronic reagents have found limited success. In most cases, excess base and high temperatures are employed, limiting the substrate generality and applicability.<sup>9,10</sup>

Driven by the ability of nickel to promote SET processes and radical-capture scenarios, Molander came up with a catalytic technology that merges the ability of Ir photocatalysts for generating transient radical intermediates with nickel catalysts, thus becoming a powerful platform for the cross-coupling of alkyl potassium trifluoroborate salts with aryl halides (Scheme 4.4).<sup>11,12a</sup> Such single-electron transmetalation event occurred under exceptionally mild conditions, constituting a powerful, yet practical, alternative to the classical two-electron transmetalation that require the use of strong bases and, in some instances, harsh reaction conditions.



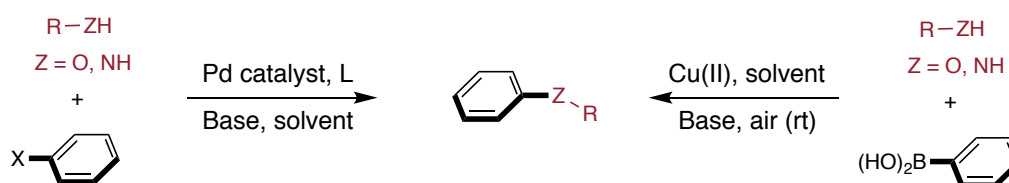
**Scheme 4.4. Nickel metallaphotoredox catalyzed arylation reactions**

The mechanistic hypothesis for this dual protocol is shown in Scheme 4.4 (LG = BF<sub>3</sub>K, *bottom left*). Upon excitation of Ir(III) photocatalyst by visible light, the highly oxidizing species Ir(III)\* ( $E_{1/2}^{\text{Ir(III)*}} = 1.32 \text{ V vs SCE in MeCN}$ ) can facilitate single-electron oxidation of an alkyl trifluoroborate ( $E_{1/2} = 1.1 \text{ V vs SCE in MeCN}$ ) to yield the corresponding nucleophilic carbon-centered radical. Concurrently, a Ni(0) complex can undergo facile oxidative addition with an aryl bromide to give a Ni(II)-aryl complex (**Int-1**), which can subsequently be trapped by the corresponding electron-rich alkyl radical. The resulting high-valent Ni(III) intermediate (**Int-2**) is prone to reductive elimination, setting the

basis for forging the desired  $C(sp^3)-C(sp^2)$  bond. The two cycles are finally intertwined by a SET between the reduced Ir(II) ( $E_{1/2}^{Ir(III)/Ir(II)} = -1.37$  V vs SCE in MeCN) and Ni(I) species **Int-3** ( $E_{1/2}^{Ni(I)/Ni(0)} \approx -1.10$  V vs SCE in MeCN).

Independently, MacMillan and Doyle reported an otherwise similar mechanistic rationale for the coupling of readily available  $\alpha$ -amino acids with aryl halides, representing an alternative to the coupling of conventional organometallic reagents.<sup>12b</sup> Overall, these two technologies represented major changes in both scientific strategy and research knowledge, allowing to expand the toolbox of cross-coupling reactions by using readily available coupling partners while providing a new rationale for the coupling of  $C(sp^3)-C(sp^2)$  fragments via single electron transmetalation under exceptionally mild conditions when compared to conventional cross-coupling technologies that typically operate via two-electron processes. These seminal contributions helped to establish the merger of photoredox catalysis and nickel catalysis as a fertile ground in catalysis.<sup>13</sup>

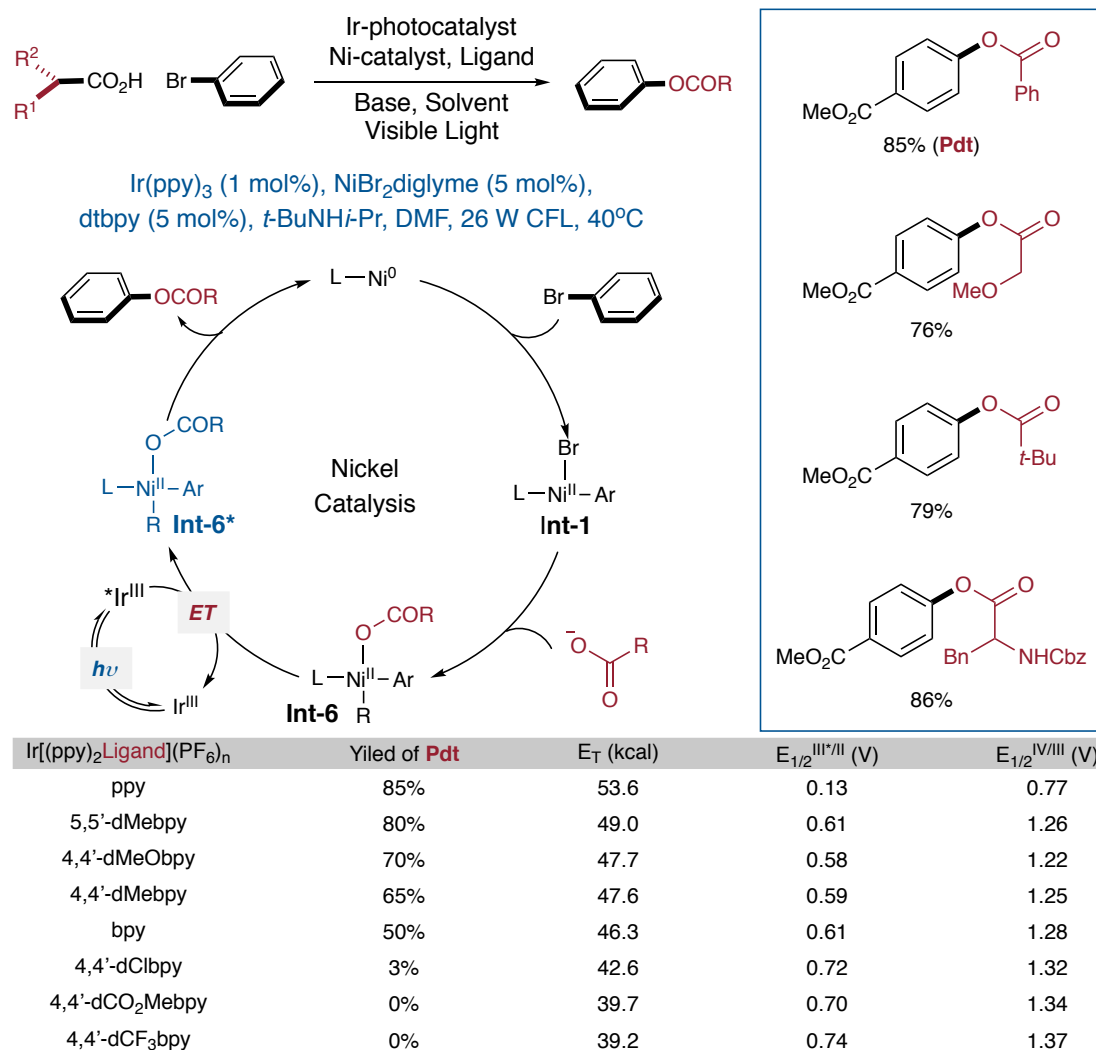
Although forging C–C bonds have become routine, C–heteroatom bond-formation could a priori be within reach within the area of Ni/photoredox catalysis, either by single electron transfer (SET) or triplet energy transfer (ET).<sup>13</sup> While Buchwald-Hartwig or Chan-Evans-Lam reactions have become the methods of choice for forging C–O or C–N bonds,<sup>14</sup> the former typically require sophisticated ligands and Pd catalysts under basic conditions whereas the latter typically require stoichiometric amounts of both Cu catalysts and organometallic reagents (Scheme 4.5).



**Scheme 4.5. Buchwald-Hartwig& Chan-Evans-Lam reactions**

Recently, MacMillan has described a photochemical C–O bond-forming scenario, thus enabling a previously challenging reductive elimination process at a Ni(II) center **Int-4** ( $E_p = 0.83$  V vs SCE in MeCN), but using a Ni(III) center instead (Scheme 4.6, **Int-5**) via SET by the Ir(III)\* photocatalyst ( $E_{1/2}^{Ir(III)*} = 1.21$  V vs SCE in MeCN).<sup>15a</sup> Surprisingly, even H<sub>2</sub>O can be used to synthesize phenol from bromobenzene under exceptionally mild conditions. Low amounts of product were found in the absence of quinuclidine, an observation that could be explained by its role as an electron shuttle to facilitate the turnover of the two propagating cycles. In addition to the C–O cross couplings, C–N bond forming protocol was reported with similar strategy by the same group in collaboration with





Scheme 4.7. Esterification of aryl bromide enabled by photosensitized Ni-catalysis

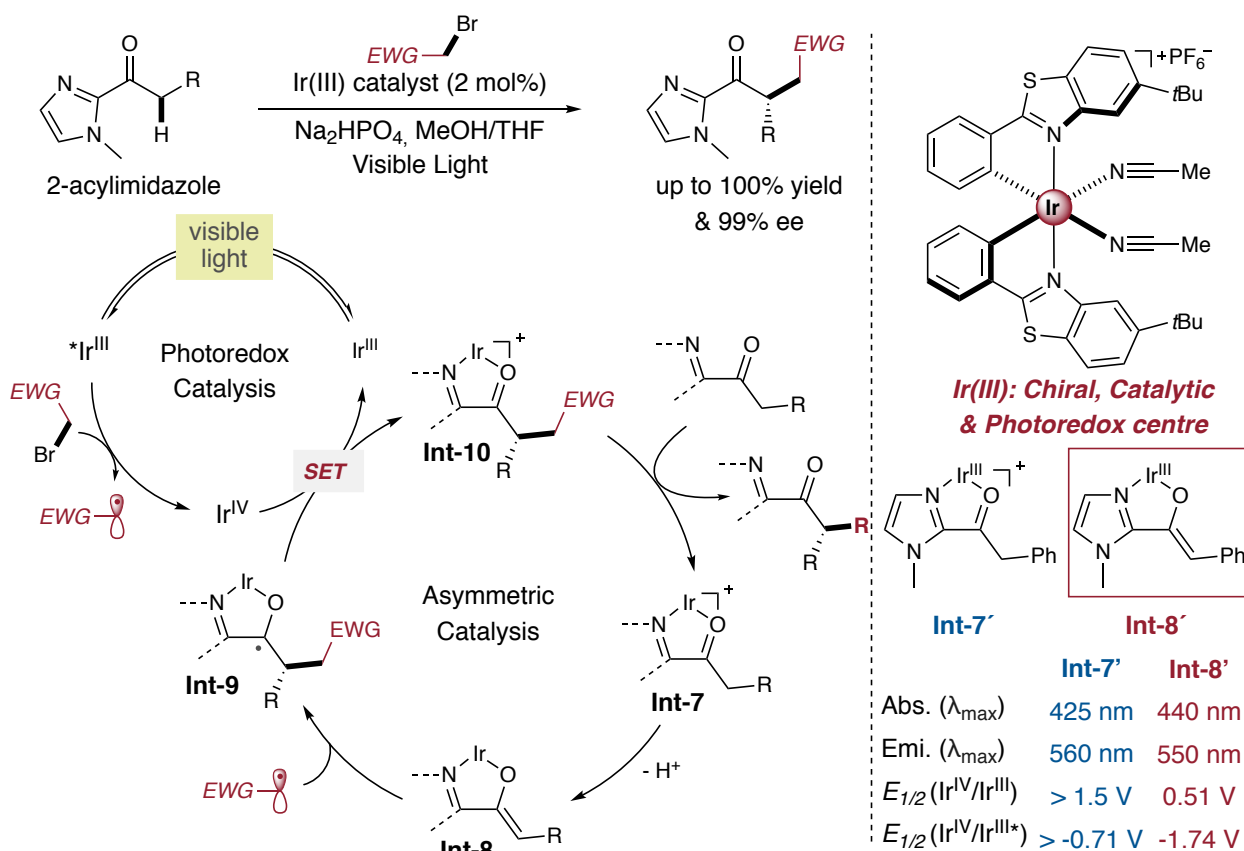
## 4.2. Multifunctional Visible Light Photocatalysts

As judged by the recent literature data on photoredox catalysts, the role of the photosensitizer remains largely confined to single electron transfer (SET) or energy transfer (ET) processes.<sup>13</sup> However, the discovery of multifunctional photocatalysts that might expand the boundaries of commonly-employed metal-based polypyridyl sensitizers or organic dyes beyond SET or ET while offering new strategies for functionalizing complex molecules still remains a relatively underdeveloped area of expertise.

### 4.2.1. Chiral-at-metal Complex as Multifunctional Photocatalyst

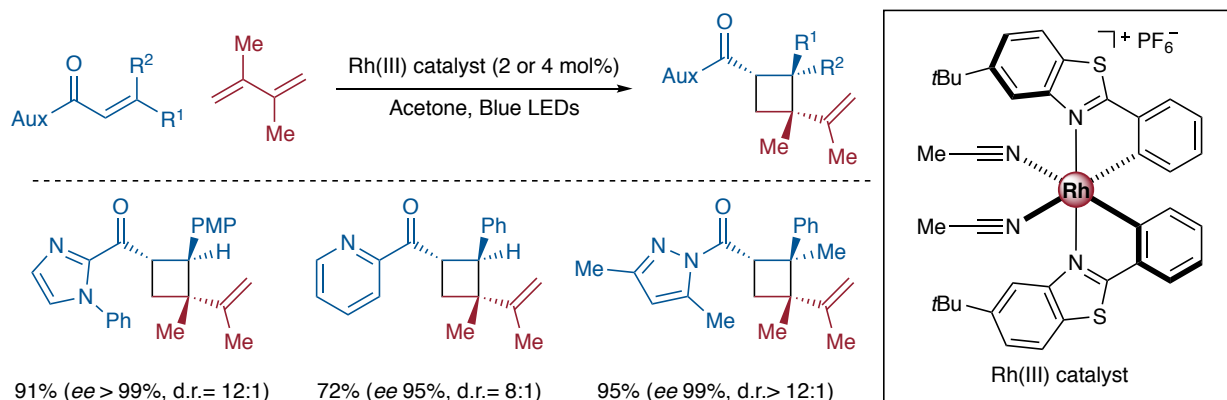
Prompted by the successful implementation of iridium or ruthenium complexes as photosensitizers in numerous transformations,<sup>17</sup> and the unique role exerted by chiral transition metals for promoting an array of enantioselective reactions, Meggers proposed that these two features could be combined

with the design of a single asymmetric photoredox catalysts.<sup>18</sup> As shown in Scheme 4.8, Meggers disclosed a novel asymmetric platform for the  $\alpha$ -functionalization of carbonyl compounds based on a “one-component” Ir photocatalyst with central chirality. The authors hypothesized that ligand exchange of the 2-acylimidazole with the Ir center generated **Int-7**. Subsequently, facile deprotonation generated a chiral, electron-neutral nucleophilic Ir(III) enolate complex (**Int-8**) that could react with a photochemically generated electrophilic radical by an oxidative quenching scenario. The identity of **Int-8** is particularly important, facilitating the asymmetric induction while constituting a more reactive chiral photosensitizer. Oxidation of the corresponding ketyl radical **Int-9** by Ir(IV) via SET leads to **Int-10** that releases the product upon exchange with the starting precursor, thus setting the basis for turnover the catalytically competent species. Undoubtedly, this pioneering work served as a blueprint for designing other catalytic asymmetric photoredox reactions, providing new avenues for the synthesis of highly complex chiral molecules.<sup>19-23</sup>



**Scheme 4.8. Asymmetric photochemical alkylation enabled by chiral-at-metal complex**

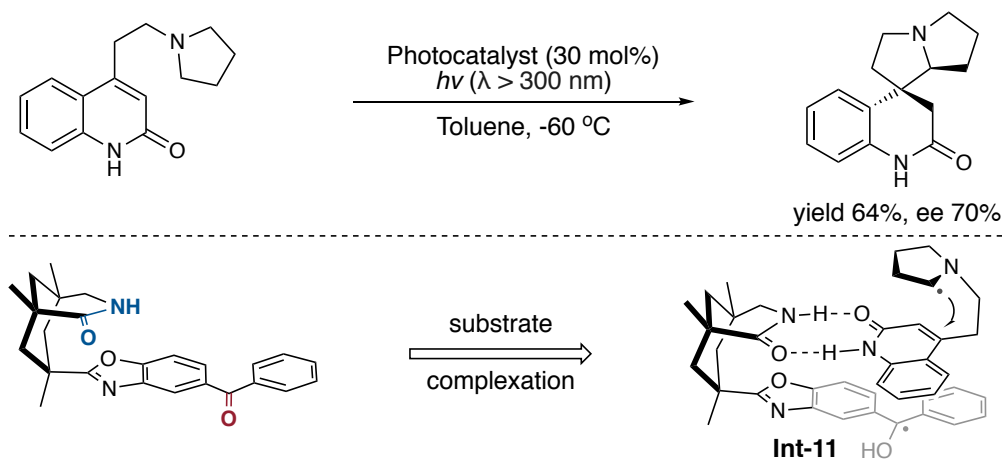
In 2017, Meggers and coworkers explored the possibility to further extend the ability of this chiral-at-metal photoredox catalyst to trigger an enantioselective intermolecular [2+2] cycloaddition reactions via ET (Scheme 4.9). Excellent enantiomeric excesses and diastereoselectivities were found for a wide variety of dienes and cyclobutanes with a wide range of auxiliaries (Aux).



**Scheme 4.9. Asymmetric [2+2] cycloaddition enabled by chiral-at-metal complex**

#### 4.2.2. Diaryl Ketone with Hydrogen Bonding as Multifunctional Photocatalyst

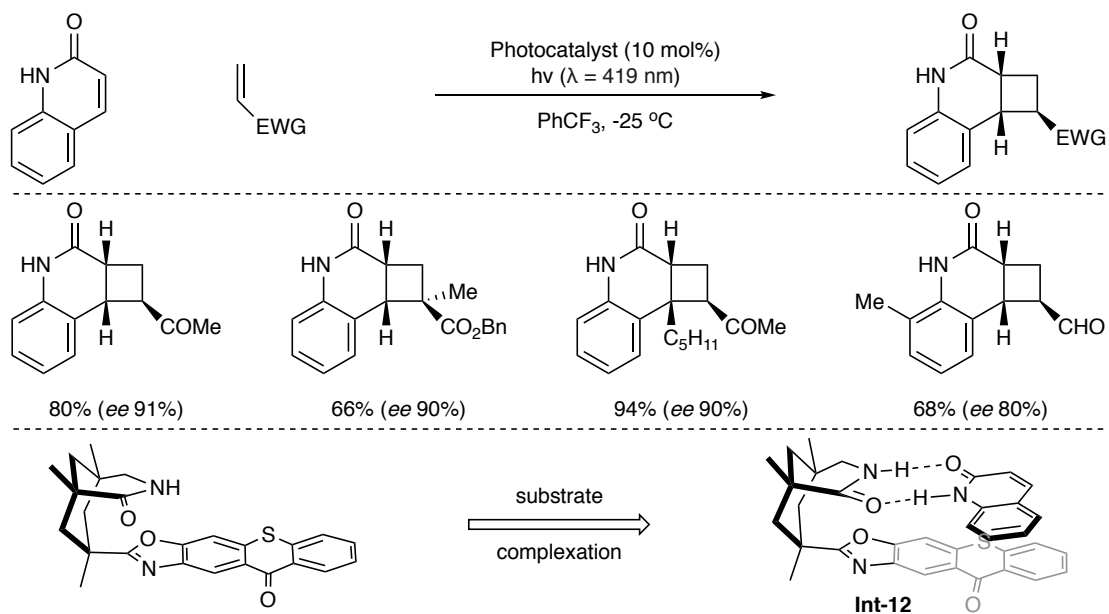
While the work of Meggers constituted a significant step-forward in the field of asymmetric photoredox catalysis, a general solution for interfacing visible-light-induced photochemistry and asymmetric catalysis with non-noble metal reagents with functions expanded beyond SET or ET would be highly appreciated. Aimed at providing a solution to this challenge, Bach and co-workers reported a novel bifunctional diaryl ketone photocatalyst which was able to promote an asymmetric intramolecular 1,4-radical addition (Scheme 4.10).<sup>24a</sup> The catalyst contains a benzophenone unit which could induce SET upon irradiation,<sup>25,26</sup> while the presence of a rigid chiral-bicyclic secondary amide backbone was capable of providing hydrogen bonding interactions (**Int-11**), ultimately ended up in a highly asymmetric event for the formation of a chiral spiro-cyclic structure. Unfortunately, however, the transformation was restricted to the use of a rather specific substrate, UV irradiation, and high catalyst loadings. While undoubtedly a significant step-forward, these limitations might require modifying the template to improve practicality and flexibility.



**Scheme 4.10. Asymmetric photochemical addition enabled by hydrogen bonding interaction**

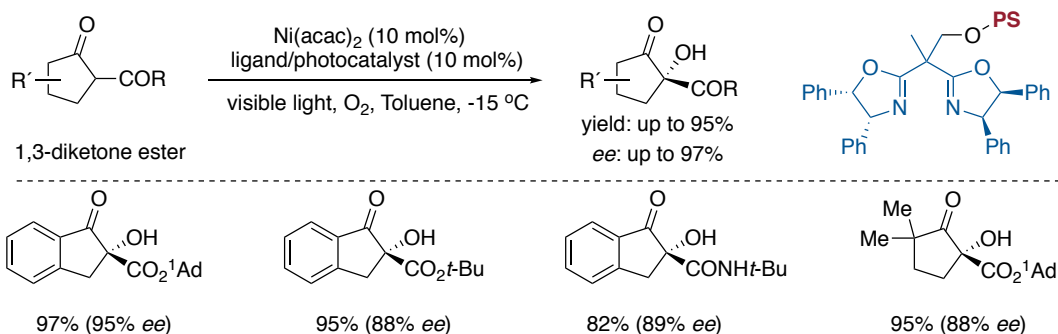


In 2016, Bach and coworkers took advantage of this unique template to develop an enantioselective intermolecular [2+2] cycloaddition.<sup>24b</sup> In this case, the thioxanthone unit served as an efficient triplet energy transfer catalyst under visible light irradiation (**Int-12**), resulting in four-membered rings with high enantioselective induction and chemoselectivity (Scheme 4.11).



**Scheme 4.11. Asymmetric [2+2] cycloaddition enabled by a chiral template**

#### 4.2.3. Photoactive Diaryl Ketones Possessing Chiral Ligands



**Scheme 4.12. Asymmetric photochemical hydroxylation with O<sub>2</sub>**

Driven by the observation that chiral bisoxazolines (BOXs) are privileged ligands in asymmetric catalysis<sup>27,28</sup> and that diarylketones (e.g., xanthone, thioxanthone, and 9-fluorenone) can activate many functional groups under UV or visible-light irradiation,<sup>26,29</sup> Xiao and co-workers designed a new family of visible-light-responsive ligands by decorating chiral BOX ligands with a thioxanthone motif (Scheme 4.12).<sup>30</sup> Complexation of these new ligands in situ with metal catalyst precursor [Ni(acac)<sub>2</sub>] resulted in a broad spectrum of chiral bifunctional photocatalysts (Scheme 4.13, **Int-13**).



triplet state (Figure 4.2), which then quickly decays to a  $n-\pi^*$  triplet with lower energy.<sup>32,35</sup> In the absence of potential  $T_n(\pi, \pi^*)$ , the ISC rates from  $n-\pi^*$  singlets to triplets are slow in aliphatic ketones.

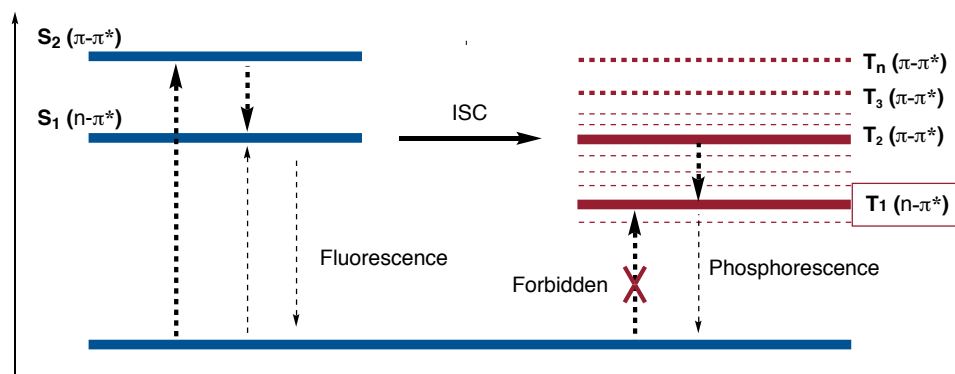
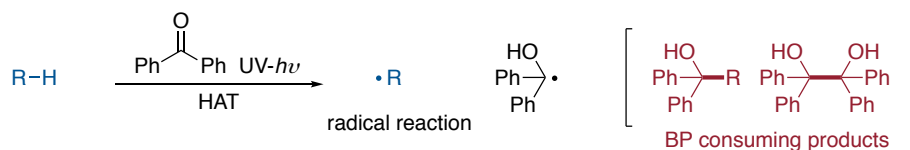


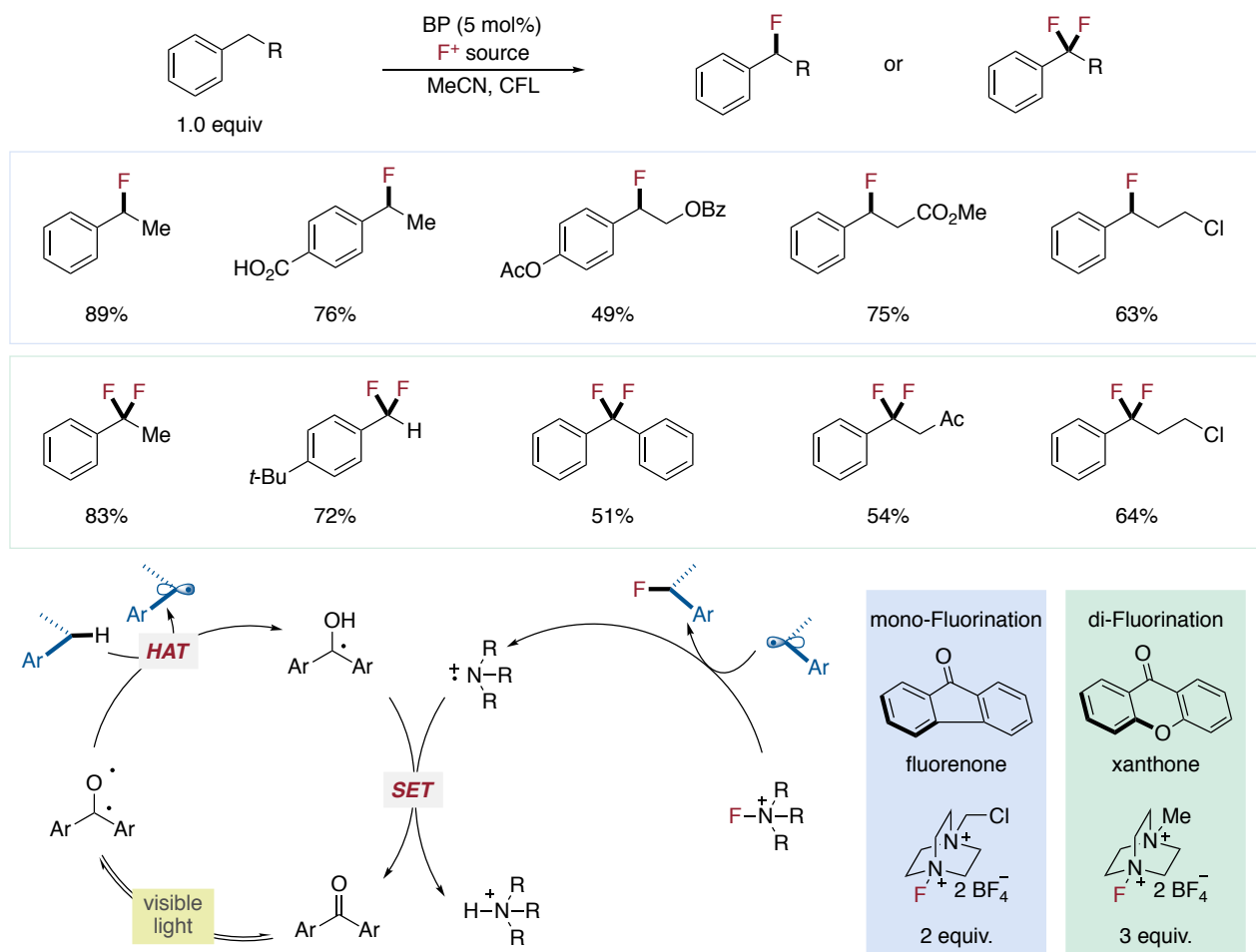
**Figure 4.2. Jablonski diagram of the benzophenone excited state**

From a synthetic standpoint, the triplet excited state of benzophenones holds considerable potential to provide opportunities to build up molecular complexity. The “biradical-type” triplet excited state can then relax in many different ways, leading to photosensitization, [2+2] cycloaddition, radical addition, and most importantly, hydrogen atom abstraction (HAT).<sup>31,34,36</sup>



**Scheme 4.14. The challenge of using BP as visible light photocatalyst**

The utilization of triplet benzophenones to facilitate synthetically useful C-H functionalization under visible light irradiation might not be as straightforward as initially anticipated (Scheme 4.14). Indeed, high-energy UV irradiation is typically required when using benzophenone as photosensitizers.<sup>31,35</sup> This might be potentially problematic as a wide range of functional groups absorb in the UV region, which could lead to deleterious side reactions. In addition, stoichiometric amounts of diaryl ketones are frequently employed due to self-dimerization pathways and radical recombination after HAT from the corresponding C-H precursor.<sup>31,35</sup> However, there are ample precedents that show that subtle differences on both the electronic and steric effects of the substituents on the arene might have a positive effect on the photochemical behavior of benzophenones by changing the properties of the triplet excited state while shifting the maximum ( $n,\pi^*$ ) absorption to longer wavelengths.<sup>37,38</sup>



**Scheme 4.15. Diaryl ketones catalyzed radical fluorinations of benzylic C-H bonds**

The utilization of diaryl ketones in visible light photoredox catalysis was first described by Chen (Scheme 4.15)<sup>55</sup> in which catalytic amounts of fluorenone and xanthone promoted the radical mono- and difluorination of benzylic C–H bonds under visible light irradiation. In this case, the ketone served as triplet HAT catalyst with high turnover efficiency. By changing the benzophenone catalyst and fluorinating reagents, a rather elusive difluorination could be affected, even by using C–H precursors as limiting reagents. This seminal work suggested that a judicious choice of the benzophenone catalyst might lead to a more prolific utilization of simple diarylketones as photocatalysts for visible light-mediated transformations.

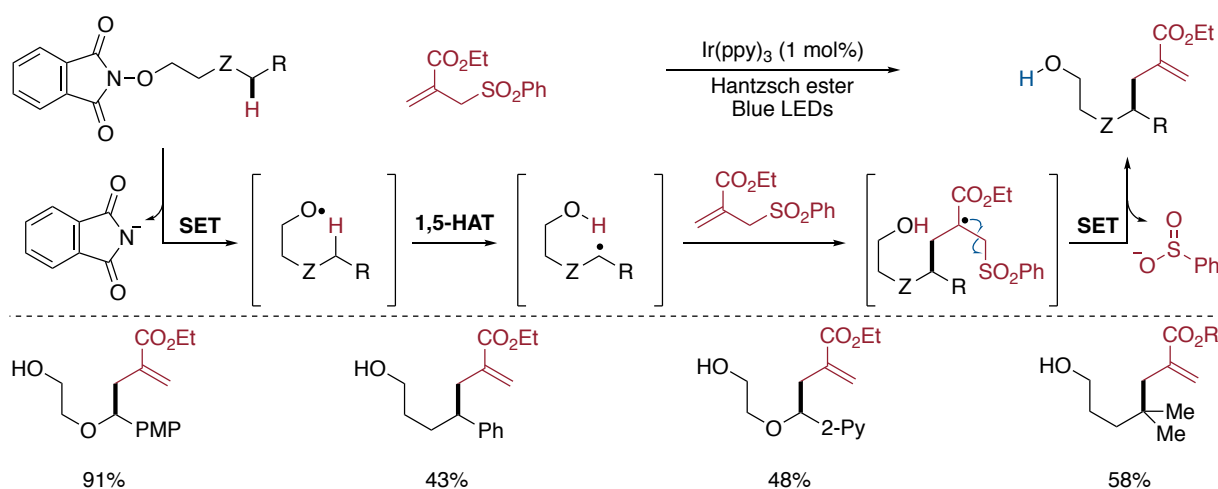
#### 4.4. *sp*<sup>3</sup> C-H Functionalization via HAT Enabled by Photoredox Catalysis

In recent years, *sp*<sup>3</sup> C–H functionalization has provided new synthetic alternatives to conventional cross-coupling reactions for forging saturated C–C bonds by using native *sp*<sup>3</sup> C–H bonds as functional handles in lieu of prefunctionalized organic halides or well-defined organometallic reagents.<sup>41,42</sup> While the functions of photoredox catalysts rely primarily on SET or ET processes, the recent years

have witnessed the design of photochemical  $sp^3$  C–H functionalizations via 1,5-HAT processes, thus enabling atom- and step-economical transformations under mild conditions and visible light irradiation.<sup>39a</sup>

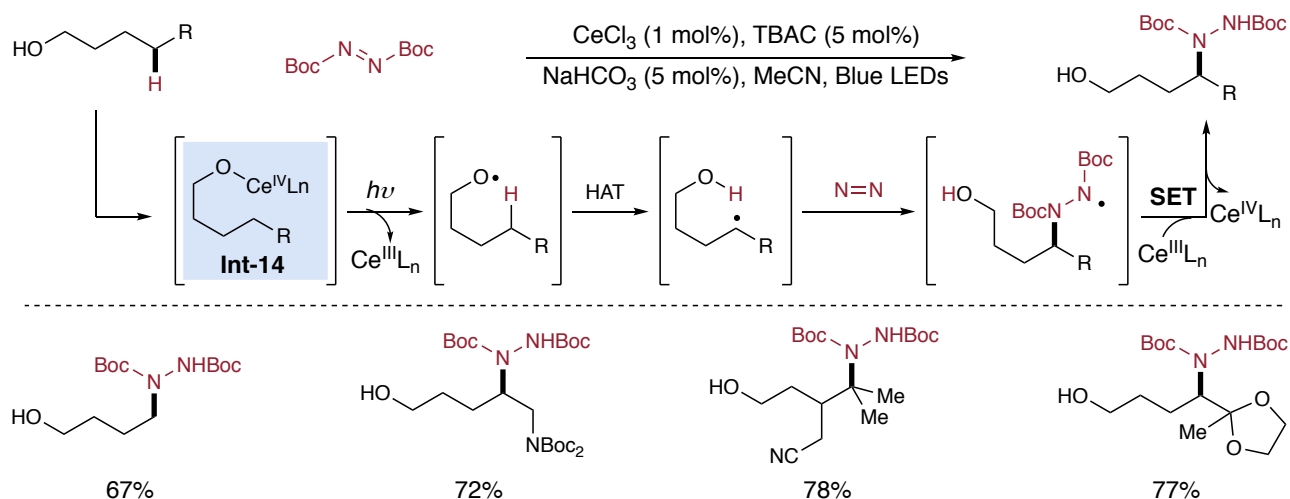
#### 4.4.1. Photoredox generated Alkoxy Radical enabled Remote C-H Functionalization

The propensity of alkoxy radicals to abstract hydrogen atoms from simple hydrocarbons (BDE of O–H bonds: 110 kcal/mol) has attracted considerable attention.<sup>39a</sup> Unfortunately, however, the *in situ* generation of such highly reactive entities under mild conditions and their application within the area of C–H functionalization still remains particularly challenging.



#### Scheme 4.16. Remote C-C bond-formation via C-H Functionalization of aliphatic alcohols

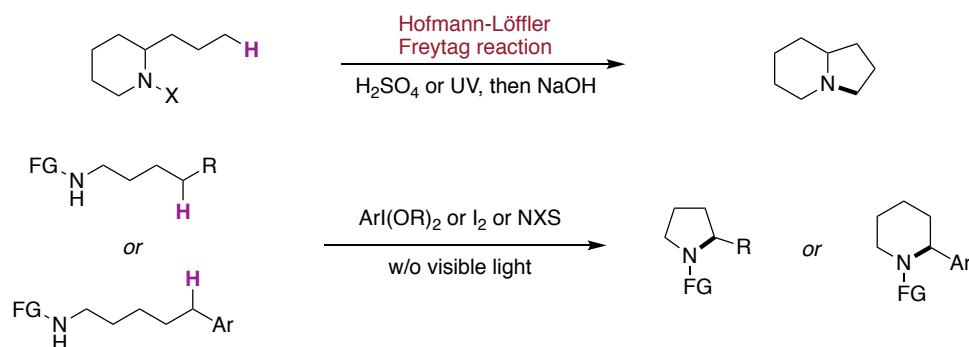
In 2015, the Chen group reported a strategy for the remote allylation of simple aliphatic alcohols. It was found that a phthalimide unit was required to activate the corresponding aliphatic alcohol under visible light irradiation.<sup>39b</sup> Specifically, the phthalimide backbone ( $E_{1/2} = -1.35$  V vs SCE in MeCN) was prone to accept a single electron from a reduced Ir(II) photocatalyst ( $E_{1/2}^{\text{Ir(II)/Ir(III)}} = -2.20$  V vs SCE in MeCN) to trigger the N–O bond homolysis (Scheme 4.16), thus generating a highly reactive alkoxy radical under mild conditions. Subsequently, a 1,5-HAT process might take place via a six-membered chair transition state, generating a nucleophilic carbon center radical. In the presence of electron-deficient olefins, a fast C–C bond forming reaction took place, resulting in a formal remote functionalization of aliphatic alcohols. Although this protocol provided an indirect technique to activated remote positions of aliphatic alcohols, preactivation of the hydroxyl group was required, thus lowering down the practicality and prospective impact of this methodology.



**Scheme 4.17. Remote photoredox C-H Amination of aliphatic alcohols**

The direct generation of alkoxy radicals via photoredox catalysis for an intermolecular amination under mild conditions was first reported by Zuo and co-workers (Scheme 4.17).<sup>39c</sup> Mechanistic studies revealed that *in situ* generated Ce(IV)-alkoxides (**Int-14**) might be photoexcited under blue LEDs irradiation.<sup>39d</sup> Subsequently, a metal to ligand charge transfer (MLCT) might take place, thus generating alkoxy radical species that could enable 1,5-HAT followed by C–N bond-forming reaction. Under these reaction conditions, a wide range of primary alcohols could be aminated at a remote *sp*<sup>3</sup> C–H bond. Strikingly, even a primary *sp*<sup>3</sup> C–H bond can be functionalized. The synthetic application of the corresponding light sensitive Ce(IV)-OR complexes has recently been exploited within the context of intermolecular HAT processes with light saturated hydrocarbons.<sup>39e</sup>

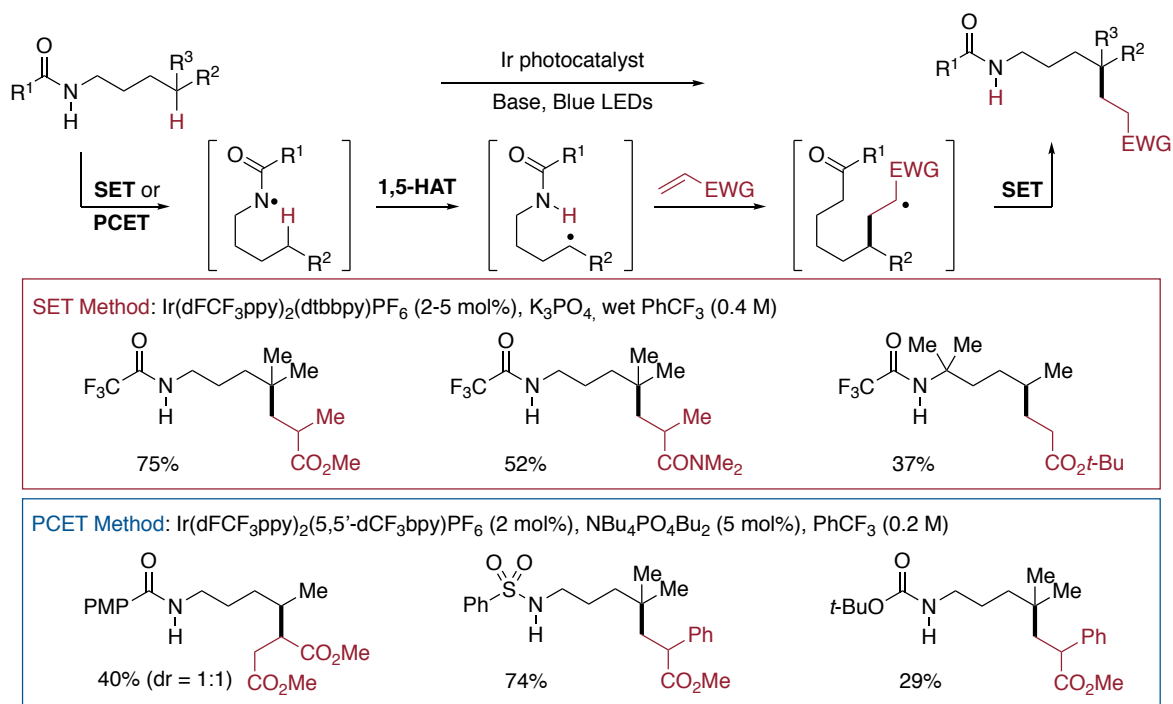
#### 4.4.2. Photoredox generated Amidyl Radical enabled Remote C-H Functionalization



**Scheme 4.18. Hofmann-Löffler-Freytag reactions**

Nitrogen-centered radicals are well-known entities that might trigger hydrogen atom from hydrocarbons (BDE of the N–H bond:95-107 kcal/mol). Particularly useful is the Hofmann-Löffler-Freytag reaction that enables an intramolecular amination en route to pyrrolidines and piperidines. The reaction was initiated by photoactivation of a N–halide bond under strong acidic conditions and

UV irradiation (Scheme 4.18). Subsequently, Suarez, Muniz and others have expanded the utility of this reaction by using hypervalent iodine reagents or molecular iodine to generate *N*-centered radicals.<sup>39a</sup> It is worth noting, however, that the utilization of *N*-centered radicals for triggering intermolecular C–C bond-forming reactions still remains a challenging scenario in photochemical endeavors.



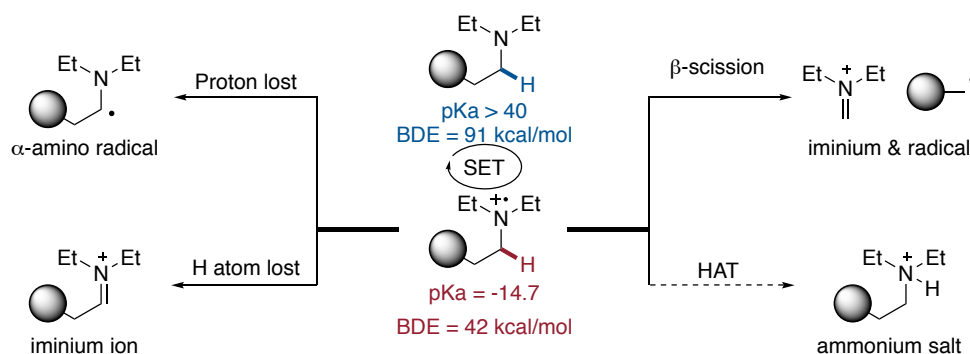
#### Scheme 4.19. Photoredox catalyzed 1,5-HAT alkylation of protected aliphatic amine

In 2016, Rovis and co-workers reported a remote regioselective *sp*<sup>3</sup> C–H alkylation of protected aliphatic amines via photoredox catalysis.<sup>40a</sup> A wide range of remote tertiary *sp*<sup>3</sup> C–H bonds could be alkylated whereas the functionalization of secondary *sp*<sup>3</sup> C–H bonds proved to be considerably more challenging (Scheme 4.19, *middle*). The reaction was proposed to proceed via initial SET oxidation of the deprotonated amide ( $E_{ox} = 0.77$  V vs SCE,  $pK_a = 12.6$ ) to an amidyl radical with photoexcited Ir(III)\* catalyst ( $E_{1/2}^{Ir(III)^*/Ir(II)} = 1.21$  V vs SCE) in a reductive quenching manifold. Subsequently, the electrophilic nitrogen-centered radical underwent a fast 1,5-HAT at a remote *sp*<sup>3</sup> C–H position giving rise a nucleophilic tertiary carbon-centered radical (BDE of Amide N–H bond: 97–110 kcal/mol; BDE of unactivated tertiary C–H bond: 95 kcal/mol). In the presence of  $\alpha,\beta$ -unsaturated compounds bearing electron withdrawing groups (EWG), a rapid 1,4-addition was effected, yielding an electrophilic radical that could be subsequently reduced by Ir(II) ( $E_{1/2}^{Ir(III)/Ir(II)} = -1.37$  V vs SCE) prior to a final protonation event. The success of this transformation was attributed by the presence of an appropriate electron-withdrawing group attached to the amine terminus, thus lowering down the  $pK_a$

of the N–H bond while facilitating the initial SET oxidation event. Independently from Rovis work, Knowles and co-workers found a similar remote  $sp^3$  C–H alkylation event (Scheme 4.19, *up*) following an otherwise identical mechanistic rationale.<sup>40b</sup> Unlike the previous deprotonation strategy that led to a SET oxidation, however, the corresponding nitrogen-centered intermediate was generated by proton-coupled electron transfer (PCET) that enabled the homolysis of the strong N–H bond (BDE of Amide N–H: 97–110 kcal/mol; BDE of unactivated tertiary C–H: 95 kcal/mol). Using this technology, a broad range of aliphatic amines bearing numerous protecting groups delivered the targeted  $sp^3$  C–H alkylation in the presence of  $\alpha,\beta$ -unsaturated compounds as electron acceptors (Scheme 4.19, *bottom*).

#### 4.4.4. Photoredox, HAT and Ni-Catalyzed $sp^3$ C–H Arylation

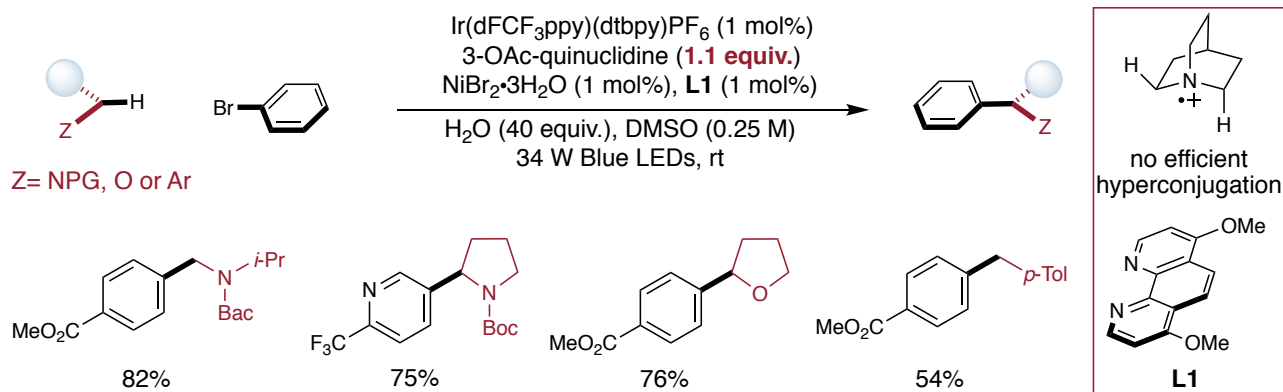
Although Rovis and Knowles tacitly demonstrated the ability to trigger  $sp^3$  C–H functionalization via *intramolecular* HAT from in situ generated amidyl radicals,<sup>40</sup> it was unclear whether it would be possible to establish a visible light photochemical rationale by which HAT could be conducted in an *intermolecular* fashion for forging C–C bonds via  $sp^3$  C–H functionalization. Indeed, this is certainly not impossible as a number of organic molecules are known to effect HAT processes. Among these, simple tertiary amine radical cations are known to abstract hydrogen atoms to form stable ammonium salts (BDE of ammonium N–H: 100 kcal/mol). However, this process is typically accompanied by parasitic side-reactions such as the formation of an  $\alpha$ -amino radical or iminium ion that derive from the remarkable acidity of the proximal  $\alpha$  C–H bond (Scheme 4.20).<sup>43</sup>



**Scheme 4.20. The fate of amine radical cation**

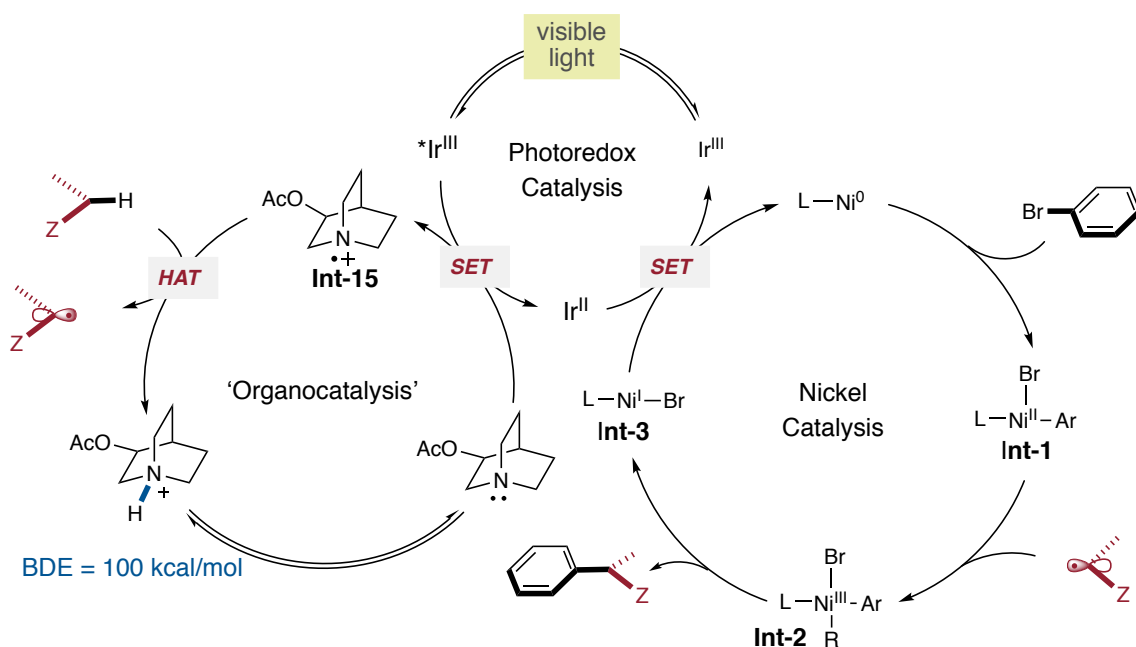
This phenomenon is attributed to hyperconjugation of the adjacent  $sp^3$  C–H bond into the proximal singly occupied  $p$ -orbital of the nitrogen atom. If a substituent is located at the  $\beta$  position of an amine radical cation, a C–C bond cleavage could also be observed whereas the absence of  $\alpha$ -C–H or hyperconjugation may enable efficient HAT by the amine radical cation.<sup>43</sup>





### Scheme 4.21. Photoredox, HAT and Ni-catalyzed $sp^3$ C-H arylation

Driven by such a rationale, MacMillan and co-workers anticipated that tertiary amine radical cations lacking an effective hyperconjugation into the proximal  $p$ -orbital of the nitrogen atom would be critical for effecting an *intermolecular*  $sp^3$  C–H arylation of simple alkane feedstocks by the merger of photoredox and nickel catalysis.<sup>44</sup> Specifically, it was found that 1 equivalent of a rigid bicyclic tertiary amine (3-OAc-quinuclidine) could be used as both base and HAT reagent (Scheme 4.21, **Int-15**) when combined with nickel catalysts supported by nitrogen-containing ligands. Under these conditions, a wide variety of aryl halides could be coupled with native  $sp^3$  C–H bonds, even in stoichiometric amounts (2-5 equivalents).

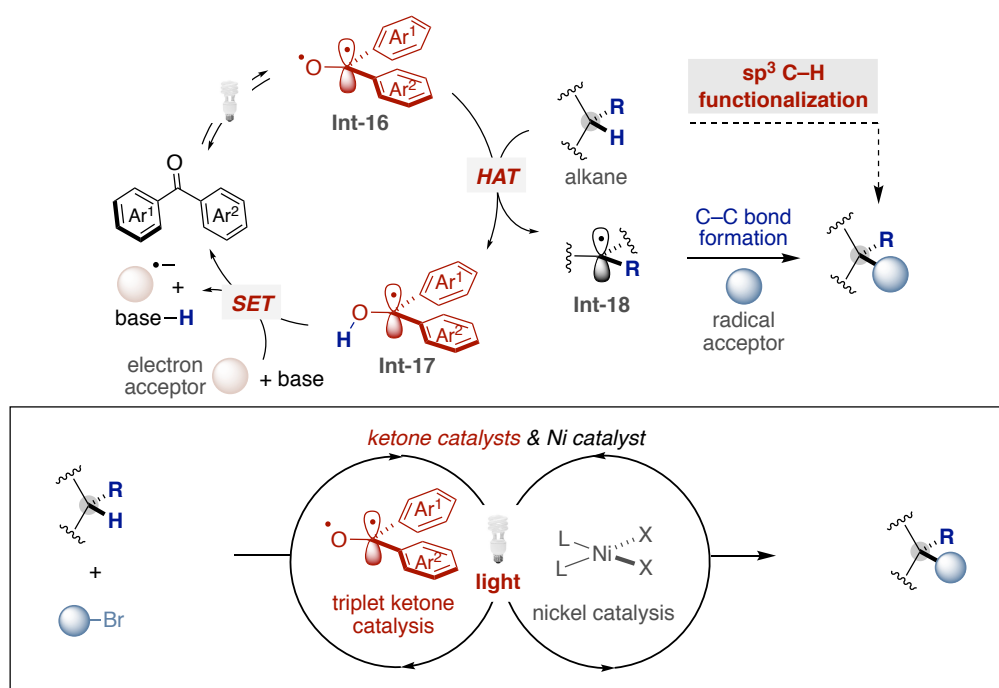


### Scheme 4.22. Mechanistic Rationale of the Triple Catalysis

The mechanism of the reaction was proposed to proceed via a triplet cascade initiated by SET oxidation of the quinuclidine derivative triggered by Ir(III)\*. A thermodynamic downhill HAT

process then takes place with an appropriate alkane C–H bond, that ultimately recombine with a Ni(II) oxidative addition complex (Scheme 4.22). Reductive elimination followed by a final SET delivers the targeted product while recovering back both Ni(0)L<sub>n</sub> and Ir(III) photocatalyst. It is worth noting, however, that the reaction required the utilization of stoichiometric amounts of a non-particularly cheap quinuclidine derivative, reinforcing the need for a more applicable *sp*<sup>3</sup> C–H functionalization technique via *intermolecular* HAT processes.

#### 4.5. General Aim of the Project



**Scheme 4.23. Triplet ketone catalyzed *sp*<sup>3</sup> C–H functionalization**

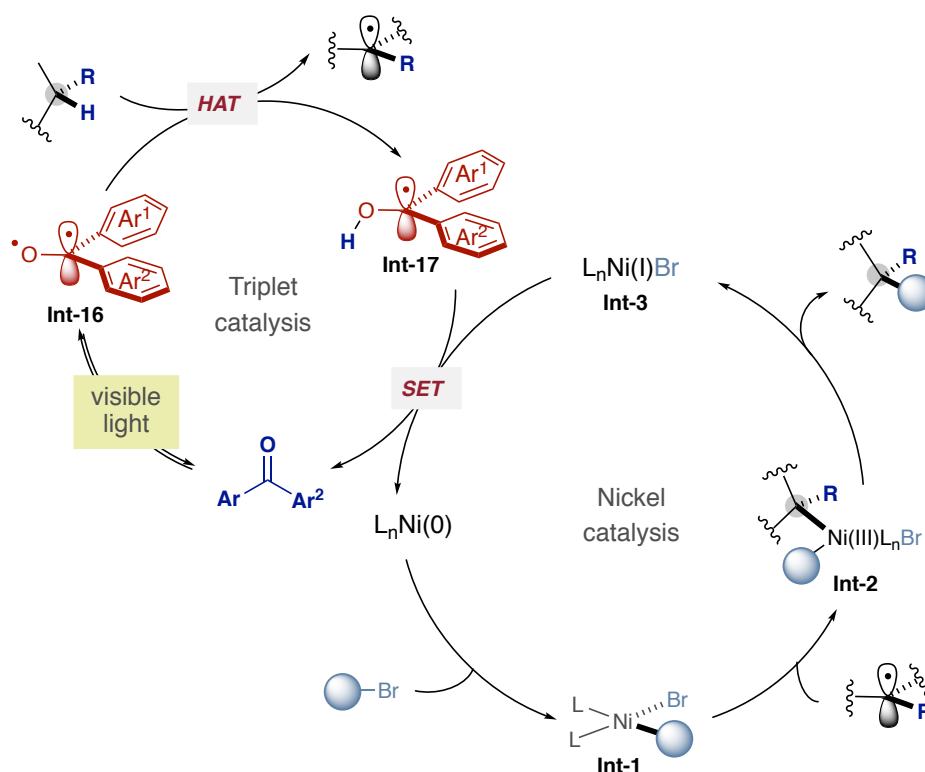
At the outset of our investigations, the ability to forge C–C bonds by means of visible light photochemical *sp*<sup>3</sup> C–H functionalizations initiated by HAT was dominated by the use of noble, yet precious, Ir(III) photocatalysts, whose functions remained confined to either SET or ET.<sup>40,44</sup> Therefore, we anticipated that the utility of cheap, and easily accessible photocatalysts that enable both hydrogen atom transfer (HAT) for functionalizing *sp*<sup>3</sup> C–H bonds and SET to recover the propagating catalytic species would be particularly attractive. Undoubtedly, the high cost and limited supply of iridium in the earth’s crust reinforces the need for mechanistically-distinct C–C bond-forming techniques from simple alkane C–H feedstocks that circumvent the need for noble metals while exhibiting complementary scope with improved practicality, flexibility and generality.

## 4.6. Metallatriplet Catalysis: The Synergy of Triplet Ketones and Nickel Catalysts

Among various conceivable scenarios, we focused our attention on the inherent ability of triplet excited ketones to trigger a HAT process, thus generating a persistent ketyl radical and a transient nucleophilic radical via  $sp^3$  C–H functionalization.<sup>31,35</sup> While the former is inherently predisposed to SET with appropriate electron acceptors, the latter is prone to C–C bond formation in the presence of radical acceptors (Scheme 4.23, *up*). Taking this into consideration, we wondered whether simple nickel catalysts could serve as both electron donor for the transient nucleophilic radical and electron acceptor for the persistent ketyl radical, thus resulting in a general platform for the functionalization of  $sp^3$  C–H bonds by the merger of cheap triplet excited ketones and nickel catalysts.

Prompted by the seminal studies of Chow, Murakami and Chen on the photoreduction of Ni(acac)<sub>2</sub> by triplet benzophenones<sup>46,47</sup>, the propensity of ketyl radicals to undergo SET processes<sup>48</sup> and the possibility to photoexcite benzophenones under visible light irradiation,<sup>55</sup> we anticipated that the approach delineated in Scheme 4.23 could be realized under appropriate reaction conditions. If successful, we recognized that this platform would provide new reactivity within the field of triplet ketone catalysis while at the same time complementing existing *inner-sphere* directed  $sp^3$  C–H functionalization techniques<sup>49</sup> and recent *outer-sphere* HAT-metallaphotoredox processes<sup>50-52</sup> based on Ir polypyridyl sensitizers.<sup>58</sup> Unlike Ir photocatalysts that are used as either SET or ET catalysts,<sup>53,54</sup> however, the utilization of simple and easily-accessible diaryl ketones as photocatalysts offers the added value of activating  $sp^3$  C–H bonds<sup>55</sup> via HAT processes, thus expanding the boundaries of metallaphotoredox processes.<sup>56</sup>

#### 4.6.1. Metallatriplet Catalysis: Mechanistic Hypothesis



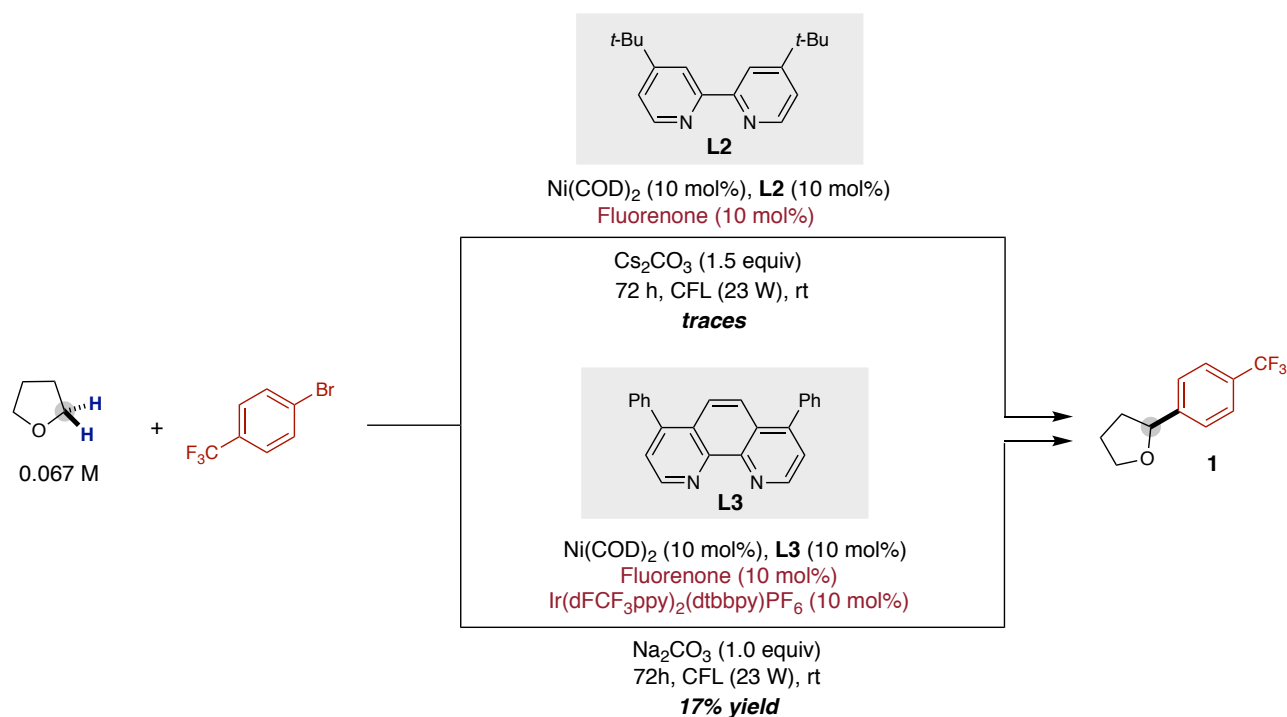
**Scheme 4.24. Metallatriplet Catalysis: Mechanistic hypothesis**

A detailed description of our proposed mechanistic cycle for the direct  $sp^3$  C-H cross coupling by organic triplet catalysis and nickel catalysis is outlined in Scheme 4.24. Our in situ generated active Ni(0) species would undergo oxidative addition into the aryl bromide electrophile, forming the electrophilic Ni(II)-aryl intermediate **Int-1**. This Ni(II) species would rapidly intercept radical from HAT by triplet excited state **Int-16** ( $\tau$  [ $Ph_2CO$ ] = 6.5  $\mu s$ )<sup>59</sup> to generate a Ni(III)-aryl-alkyl complex **Int-2**, which upon reductive elimination would forge the desired C-C bond and Ni(I) complex **Int-3**. We anticipated that the corresponding benzophenone catalyst and Ni(0) species could be regenerated by a final SET between the persistent ketyl radical **Int-17** ( $E_{1/2}^{red}$  ( $Ph_2CO$ ) = -2.20 V vs Ag/AgNO<sub>3</sub> in MeCN)<sup>61</sup> and Ni(I) complex **Int-3** ( $E_{red}$  [ $Ni^I/Ni^0$ ]  $\approx$  -1.13V vs Ag/AgNO<sub>3</sub> in DMF)<sup>62</sup> under basic conditions.<sup>60</sup> If not as expected, a photoredox catalyst should be able to transfer the single electron from **Int-17** to **Int-3** to regenerate all the catalytic species.

#### 4.6.2. Metallatriplet Catalysis: Optimization of the Reaction Conditions

At the outset of our investigations, the  $sp^3$  C-H arylation of alkanes could only be effected by the merger of Ir photoredox catalysis and Ni catalysis using expensive quinuclidine as stoichiometric HAT mediators.<sup>50</sup> As part of our ongoing investigations in Ni catalysis,<sup>45</sup> we wondered whether we

could design an alternative scenario by replacing noble Ir catalysts and expensive, stoichiometric HAT mediators, thus offering new reactivity within the field of photoredox catalysis.



**Scheme 4.25. Initial results**

We started our investigations by studying the  $sp^3$  C–H arylation of 4-bromotrifluoromethyl benzene using  $\text{Ni}(\text{COD})_2$ , nitrogen-containing ligands and fluorenone with or without Ir photocatalyst under CFL irradiation. While trace amounts of the targeted arylation event could be observed without Ir(III) photocatalyst (Scheme 4.25, *top*), the inclusion of the latter with bathophenanthroline as the ligand resulted in 17% yield of product together with non-negligible amounts of homocoupling, indirectly pointing at a difficult turnover of the Ni catalyst with fluorenone via SET. Although the results without Ir photocatalyst were initially discouraging, we decided to explore this pathway in detail, as we were convinced about the potential of diarylketones as both HAT and SET photocatalysts.

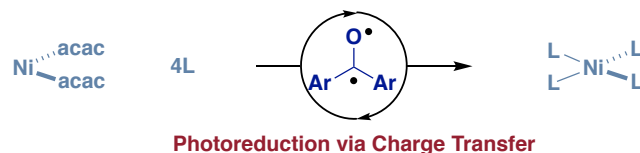


**Figure 4.3. Photoreduction of  $\text{Ni}(\text{acac})_2$  with diaryl ketones**

Driven by the known photochemical behaviour of metal 1,3-diketonates reported in the early 1960's, Chow and Scaiano described the photoreduction of  $\text{Ni}(\text{acac})_2$  by triplet excited benzophenones in the presence of C–H donor solvents such as MeOH, toluene or THF under UV irradiation (Figure

4.3).<sup>46,47</sup> Systematic investigations revealed that such photoreduction likely occurred via a mechanism consisting of a charge transfer processes.

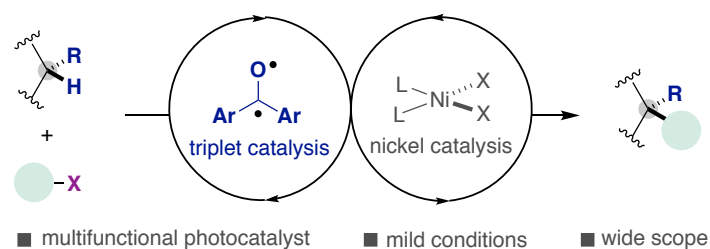
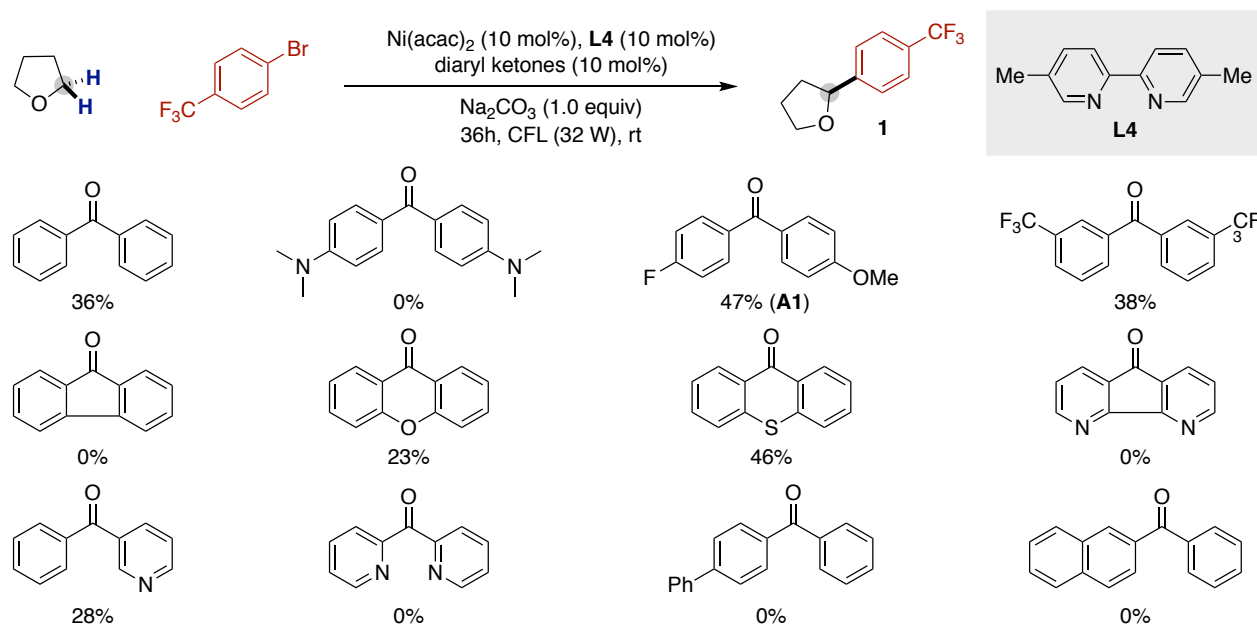


**Figure 4.4. Metallatriplet catalysis for forging C–C bonds via  $sp^3$  C–H functionalization**

With Chow and Scaiano's seminal work in mind,<sup>46,47,55</sup> we wondered whether we could identify a diaryl ketone that might be acting as CT, HAT and/or SET photocatalyst in combination with Ni(acac)<sub>2</sub> in order to functionalize  $sp^3$  C–H bonds in hydrocarbon feedstocks (Figure 4.4).

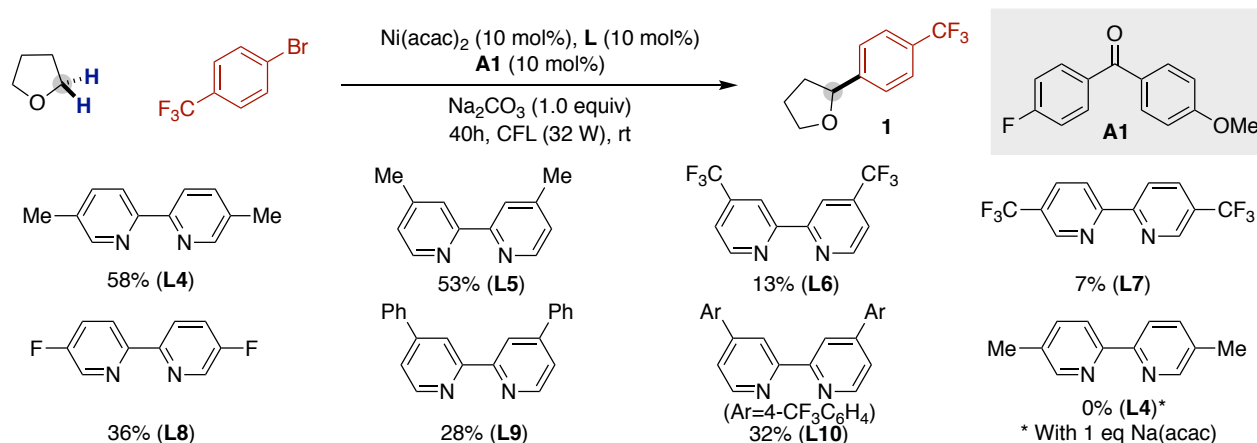


<sup>a</sup> Reaction conditions: aryl bromide (0.30 mmol), Ni(acac)<sub>2</sub> (10 mol%), 5,5'-dimethyl-2,2'-bipyridine (**L4**, 10 mol%), **A** (10 mol%), Na<sub>2</sub>CO<sub>3</sub> (0.30 mmol), THF (0.075M), CFL (32W) at rt for 36 h. <sup>b</sup> GC yields using decane as internal standard.

**Table 4.2. Screening of Diaryl Ketone Photocatalysts**

We started our explorative work on the metallaphotoredox catalysis by studying the  $sp^3$  C–H arylation of 4-trifluoromethyl bromobenzene with tetrahydrofuran as both the C–H precursor and solvent under household compact fluorescent lamp (CFL) irradiation for 36 h (Table 4.2). As expected, the reactions worked better with Ni(acac)<sub>2</sub> as precatalyst and no homocoupling of aryl bromide can be observed with **L4** as the ligand. Among all commercially available diaryl ketone tested, we quickly identified push-pull ketone **A1** as the best photocatalyst compare to those shown

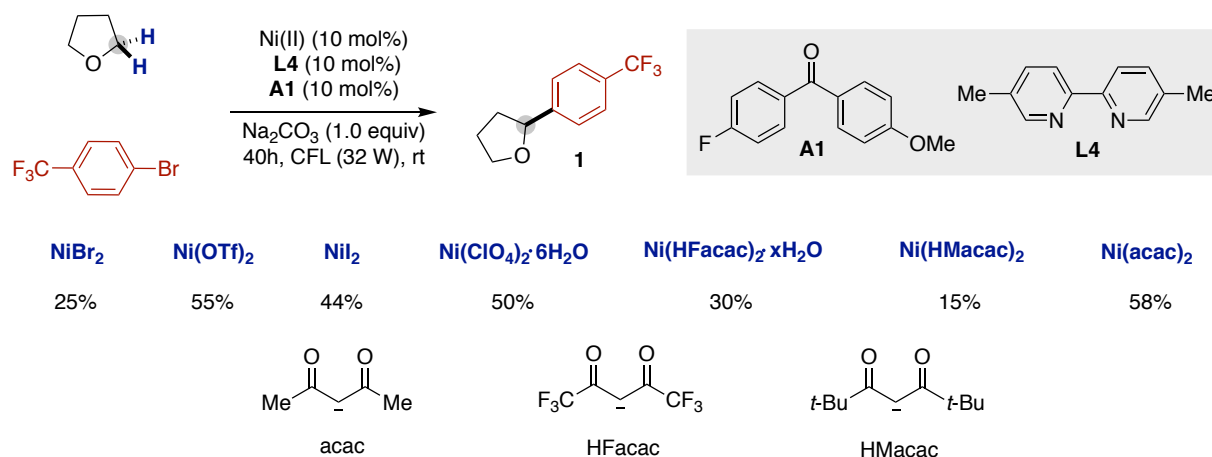
in Table 4.2. Interestingly, the utilization of diaryl ketones possessing extended  $\pi$ -systems resulted in no conversion to products, probably due to the fact that the excited ( $\pi, \pi^*$ ) transition in these compounds was unable to trigger HAT or the photoreduction of Ni(acac)<sub>2</sub>.



<sup>a</sup> Reaction conditions: aryl bromide (0.30 mmol), Ni(acac)<sub>2</sub> (10 mol%), L (10 mol%), **A1** (10 mol%), Na<sub>2</sub>CO<sub>3</sub> (0.30 mmol) THF (0.075M), CFL (32W) at rt for 36 h. <sup>b</sup> GC yields using decane as internal standard.

**Table 4.3. Screening of Ligands**

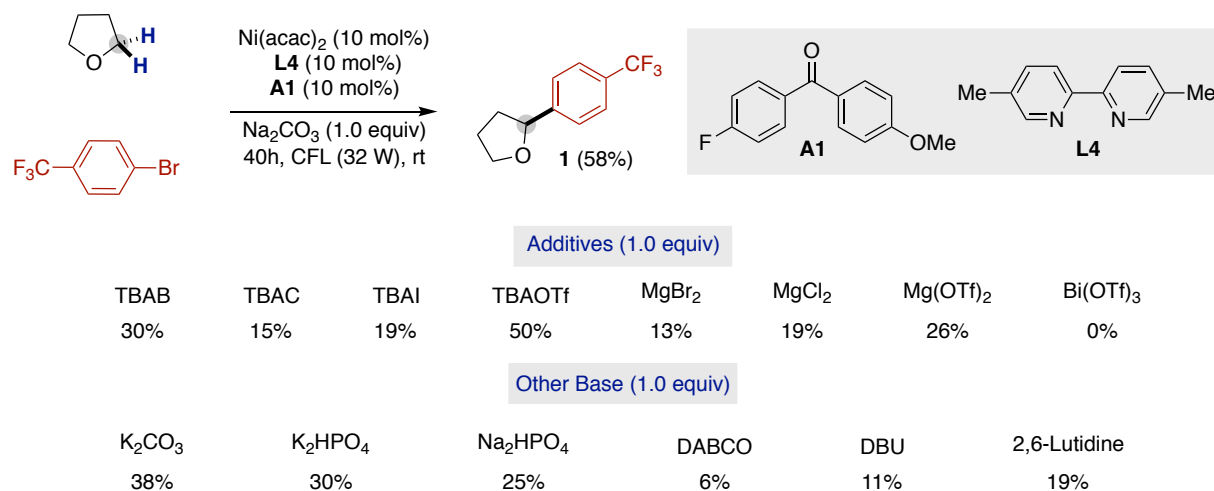
Taking **A1** as photocatalyst, we then turned our attention to study in detail the electronic and steric environments at the ligand backbone. As shown in table 4.3, the utilization of electron poor bipyridine ligands (**L6** to **L10**) resulted in low conversion to products whereas the location of the dimethyl substituents had a negligible impact on both reactivity and selectivity (**L4** and **L5**). Intriguingly, the inclusion of 1 equivalent of acac anion shut down the reactivity.



<sup>a</sup> Reaction conditions: aryl bromide (0.30 mmol), Ni(II)<sub>2</sub> (10 mol%), L4 (10 mol%), **A1** (10 mol%), Na<sub>2</sub>CO<sub>3</sub> (0.30 mmol) THF (0.075M), CFL (32W) at rt for 40 h. <sup>b</sup> GC yields using decane as internal standard.

**Table 4.4. Screening of Ni precatalysts**

Next, we turned our attention on exploring the effect of the Ni(II) precatalyst utilized (Table 4.4). Among all Ni precatalysts utilized, it was found that Ni(OTf)<sub>2</sub> was slightly less efficient than Ni(acac)<sub>2</sub> while other Ni(II) sources were considerably less effective. While one might have expected an influence on the nature of the acac-type ligands, the employment of HFacac or HMacac led to lower yields of the targeted C–H arylation event.

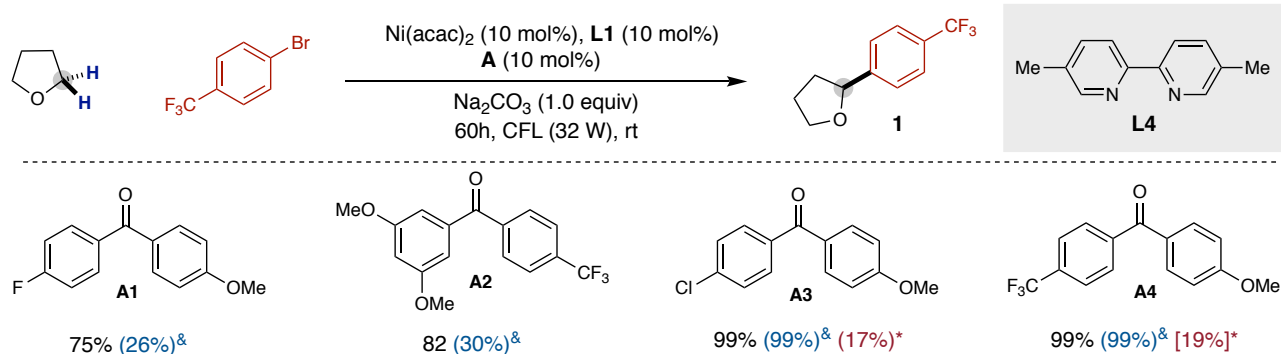


<sup>a</sup> Reaction conditions: aryl bromide (0.30 mmol), Ni(acac)<sub>2</sub> (10 mol%), **L4** (10 mol%), **A1** (10 mol%), Base (0.30 mmol) THF (0.075M), CFL (32W) at rt for 40 h. <sup>b</sup> GC yields using decane as internal standard.

**Table 4.5. Additives and bases screenings**

We hypothesized that the generation of cationic oxidative addition complexes might potentially accelerate the *sp*<sup>3</sup> C–H arylation event. To such end, we decided to study the influence of non-coordinating ions or Lewis acids, as these compounds are known halide scavengers. However, these additives turned out to be detrimental for the reaction to occur, particularly Lewis acids. This is probably due to the coordination of the Lewis acid to the ketone, hampering its triplet excited reactivity. Sodium carbonate was found to be critical for success, as other commonly employed inorganic or organic bases were considerably less effective. The lack of reactivity of organic bases such as DBU or 2,6-lutidine is tentatively ascribed to the formation of insoluble byproducts inside the wall of reaction vials, thus decreasing the penetration of visible light.

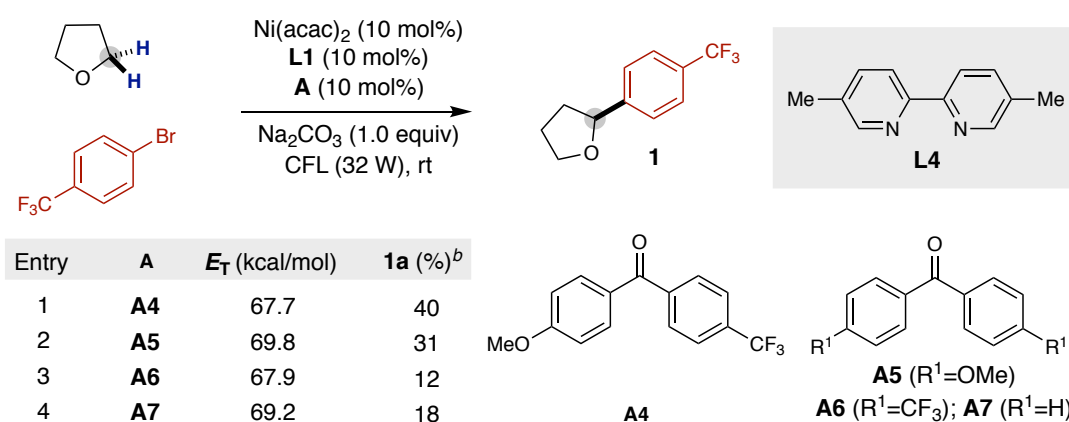




<sup>a</sup> Reaction conditions: aryl bromide (0.30 mmol), Ni(acac)<sub>2</sub> (10 mol%), **L1** (10 mol%), **A** (10 mol%), Na<sub>2</sub>CO<sub>3</sub> (0.30 mmol), CFL (32W) THF (0.075M) at rt for 36 h. <sup>b</sup> GC yields using decane as internal standard. & 96h, 5 mol% of Ni/L/A \* 96h, 1 mol% of Ni/L/A.

**Table 4.6. Push-pull diaryl ketones screening**

In light of these results, we then focused our attention on modifying the diaryl ketone backbone. We anticipated that the electronic properties of the aryl substituents of the diaryl ketone might influence its reactivity<sup>37,38</sup> by (1) enhancing and shifting the (n,π\*) absorption into the visible light region, (2) tuning the rate of decay of the triplet excited state **Int-16** (Scheme 4.24), and/or (3) stabilizing the ketyl radical **Int-17** that results from the HAT process (Scheme 4.24);<sup>63</sup> the latter is particularly important, as this putative intermediate is critical for turnover of the triplet ketone catalyst and nickel catalyst upon a final SET (Scheme 4.24). In line with this notion, three additional diaryl ketones were synthesized with push-pull substituents. Replacing the F atom in **A1** with *meta*-di-MeO groups (**A2**) slightly improved the efficiency. Surprisingly, changing the F in **A1** to Cl (**A3**) or CF<sub>3</sub> (**A4**) significantly enhanced the reactivity as quantitative yield could be obtained after 60h irradiation while **A1** only give rise to 75% yield. By decreasing the catalysts loadings, we could identify **A4** as the most promising triplet ketone photocatalyst.



<sup>a</sup> Reaction conditions: aryl bromide (0.30 mmol), Ni(acac)<sub>2</sub> (10 mol%), 5,5'-dimethyl-2,2'-bipyridine (**L1**, 10 mol%), **A** (10 mol%), Na<sub>2</sub>CO<sub>3</sub> (0.30 mmol), THF (0.075M), CFL (32W) at rt for 18 h. <sup>b</sup> GC yields using decane as internal standard.

**Table 4.7. Electronic Effects on the Diaryl Ketone**

Having identified the positive role of the *p*-methoxy and *p*-trifluoromethyl groups, we then decided to study in detail the electronic effects on the reaction outcome. It was quickly apparent that electron-poor or neutral ketones (**A6** or **A7**) resulted in a markedly lower reactivity compared with electron-rich or ‘push-pull’ ketones (**A4** or **A5**). These seemingly innocent results can be correlated with the excitation of the corresponding diaryl ketones. The singlet excited state is more likely an ionic intermediate while the triplet state is a biradical derived from the singlet state via ISC. It is then expected that the singlet state is difficult to achieve for **A6** bearing electron-poor substituent whereas it can be easily reached with electron-rich substituents (**A5**). The neutral benzophenone **A7** lies between **A4** and **A5**. Therefore, it is tempting to speculate that bench-stable **A4** ( $E_{1/2}^{\text{red}} = -2.05 \text{ V vs Ag/AgNO}_3 \text{ in MeCN}$ )<sup>61</sup> possesses an appropriate electron balance for reaching both the singlet and triplet excited state. A close look at the triplet energy of **A4-A7** argued against a mechanism consisting of an energy transfer.

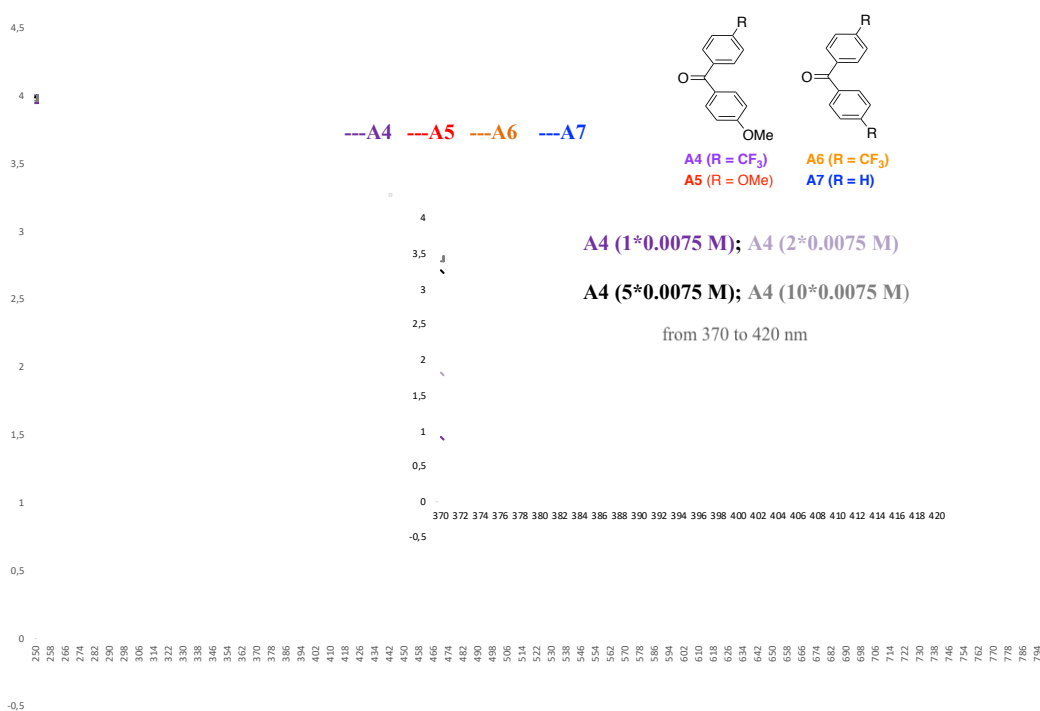
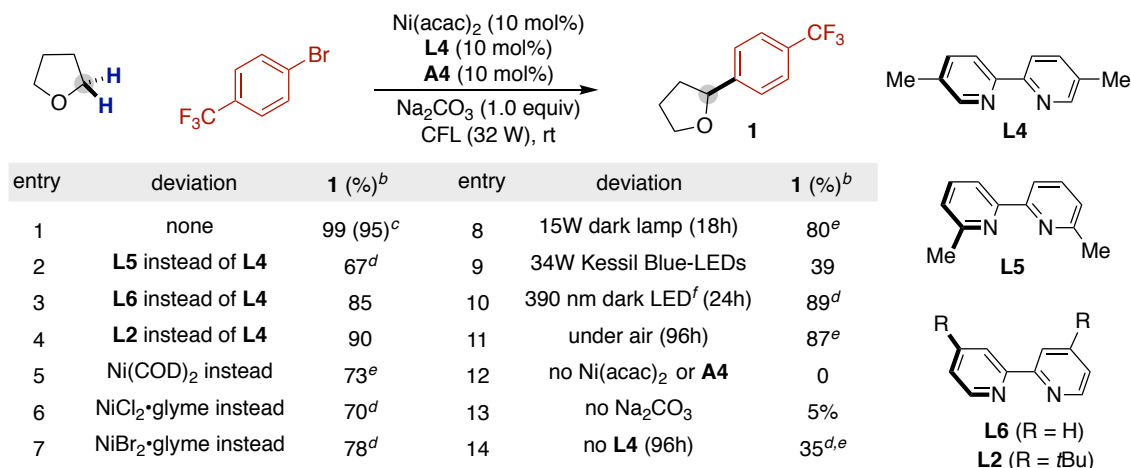


**Figure 4.5.** Uv-vis of A1-A4 (0.0075 M in THF) (Y-axis: absorbance; X-axis: wavelength)

Although **A4-A7** have similar absorption spectra (Figure 4.5), we found that **A4** possesses the ( $n,\pi^*$ ) absorption maximum at longer wavelengths. Thus, the higher yields of **1** obtained with **A4** can also be interpreted on the basis of a higher molar absorption coefficient in the visible light region and the stability of the corresponding ketyl radicals with  $\text{CF}_3$ -substituted aryl rings.<sup>63,31</sup>



<sup>a</sup> Reaction conditions: As Table 4.2, 60 h. <sup>b</sup> GC yields with dodecane as internal standard. <sup>c</sup> Isolated yield, average of two runs. <sup>d</sup> Mass balance accounts for reduced ArBr. <sup>e</sup> Mass balance accounts for homocoupling of ArBr. <sup>f</sup> 47 mW/cm<sup>2</sup>.

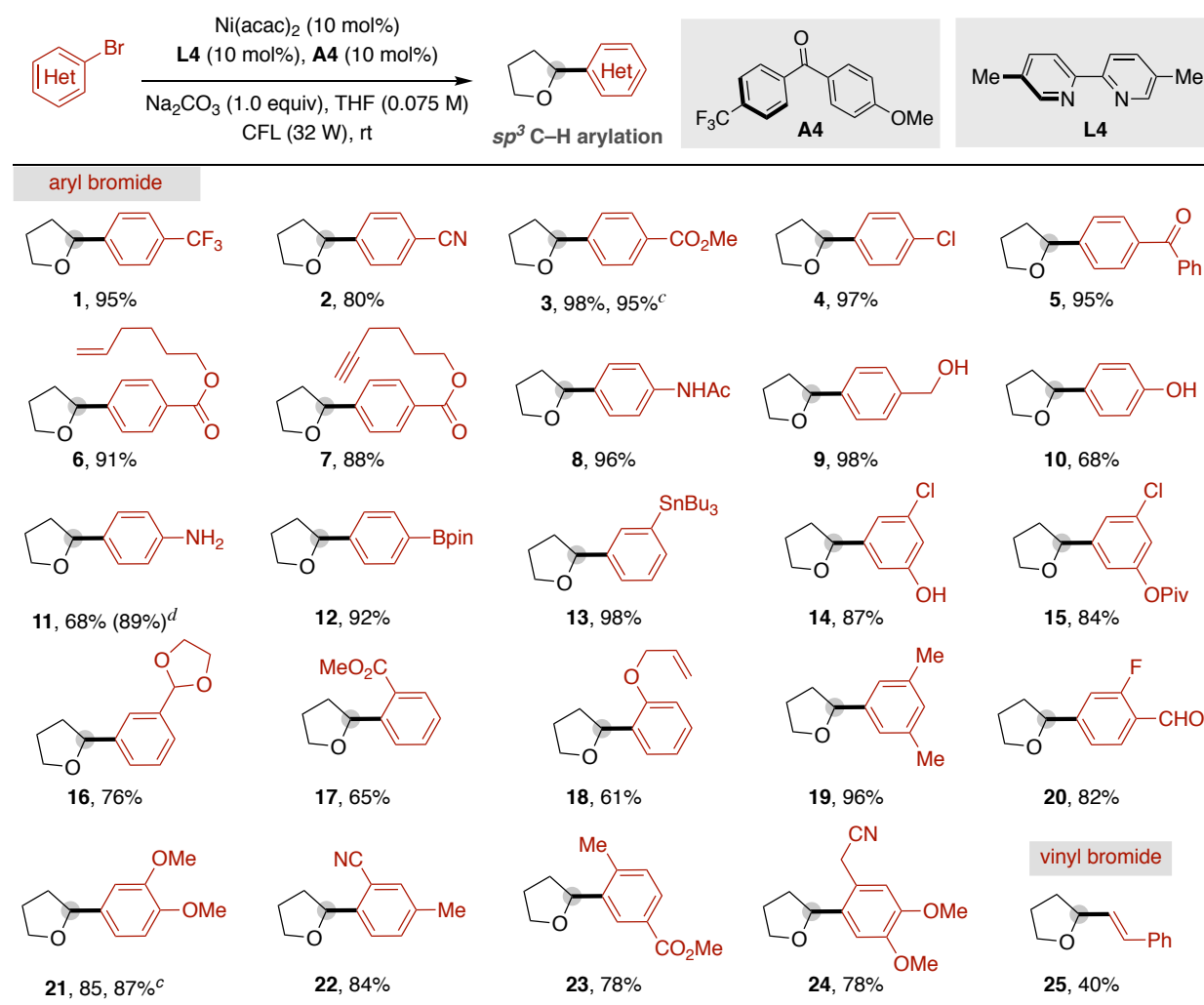
**Table 4.8. Optimization of the reaction conditions**

With the best ketone catalyst in hand, we revisited the role of other reaction parameters (Table 4.8).<sup>91</sup> As expected, the nature of the ligand did not show a dramatic influence in reactivity except **L5** with methyl groups adjacent to the nitrogen atom that led to considerable amounts of reduced product, likely due to the increased steric hindrance of the ligand backbone (Table 4.8, entry 1 to 4). As shown in entries 5-7, Ni(COD)<sub>2</sub> and Ni(II) salts other than Ni(acac)<sub>2</sub> could also be employed as precatalysts, albeit in lower yields due to competitive homocoupling or reduction of the aryl bromide.

Next, we turned our attention to examine the influence of light source. Driven by the observation that CFL normally contains traces UV and the reaction was accelerated with lower selectivity under UV irradiation (Table 4.8, entry 8 and 10), one might argue that the observed reactivity might come from the UV traces in CFL. The homocoupling or reduced product might come from the direct excitation of Ni intermediate or the fast photoreduction of Ni(acac)<sub>2</sub>. However, the desired product was selectively observed under 34 W Kessil Blue LEDs, albeit in lower yield (Table 4.8, entry 9). These results suggest that reactivity and selectivity of the standard reaction could not be just attributed to residual UV in our CFL. Importantly, an 87% yield of product was obtained under air (Table 4.8, entry 11), which is an advantage from a practical standpoint and complements existing photocatalytic reactions with iridium polypyridyl catalysts that often require exclusion of oxygen.<sup>92</sup> The longer reaction time under air (Table 4.8, entry 11) indicates that our system might consume oxygen with THF, **A4** and base under irradiation. Although control experiments revealed the unique role exerted by all our reaction parameters, 35% yield of desired product could still be obtained without **L4**, albeit with considerable amounts of homocoupling and reduced product. This result indicated that the additional supporting ligand may affect the selectivity profile of this process.

### 4.6.3. Metallatriplet Catalysis: Scope of $sp^3$ C-H Arylation

With the optimized reaction conditions in hand, we turned our attention to studying the generality of our  $sp^3$  C-H arylation. As evident from the results compiled in Tables 4.9 to 4.11, a wide variety of aryl bromides bearing either electron-rich or electron-poor substituents underwent the targeted  $sp^3$  C-H arylation in good to excellent yields under CFL irradiation.



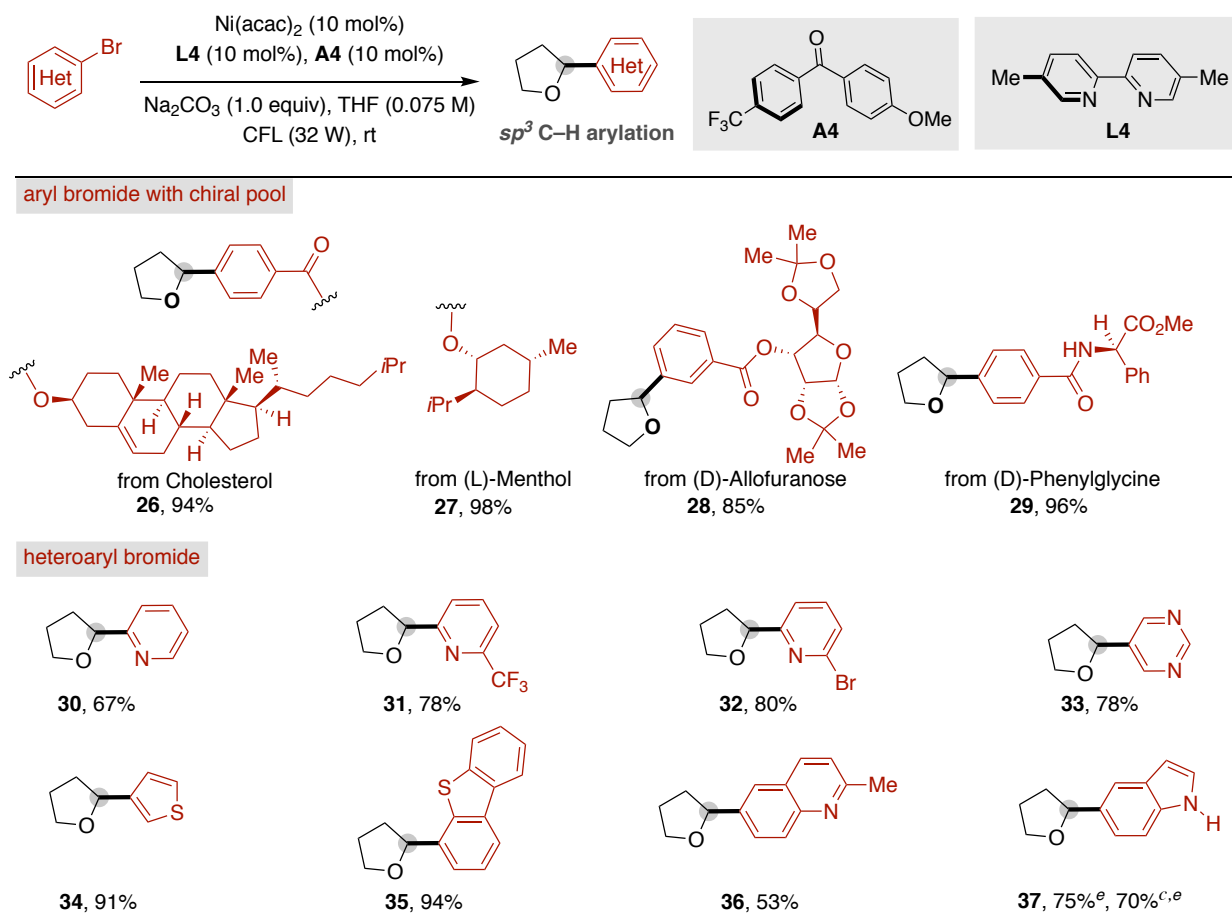
<sup>a</sup> Reaction conditions: as Table 4.3 (entry 1), ArBr (0.3 mol). <sup>b</sup> Isolated yields, average of at least two independent runs. <sup>c</sup> 10 mmol scale.

<sup>d</sup> 4-Br-C<sub>6</sub>H<sub>4</sub>N(TMS)<sub>2</sub> (0.30 mmol) was used as masked aniline. <sup>e</sup> 20 mol% of **A4**.

**Table 4.9. Scope of aryl bromides**

Notably, our C-H arylation of THF displayed an excellent chemoselectivity profile, with ketones (**5**), primary alcohols (**9**), amides (**8**, **29**), nitriles (**2**, **22**, **24**), esters (**3**, **6**, **7**, **17**, **26 to 29**), terminal alkynes (**7**), terminal alkenes (**6**, **18**), acetals (**16**) and aldehydes (**20**) being tolerated. It was worth noting that free anilines (**11**) and phenols (**10**, **14**) did not affect the function of ketone and Ni. As for product **5**, we observed a considerable faster rate, an argument that goes in line with the ability of

both the starting precursor and the final product to act as photocatalysts as well. In general, however, electron-deficient aryl bromides worked better than the electron rich ones. As for other cross-coupling reactions, *ortho*-substituted aryl bromides showed slower reaction rates (**17**, **18**, **22** to **24**). Notably, no cyclized product was observed with substrate **18**, suggesting that the oxidative addition pathway did not trigger a 5-*exo*-trig type cyclization with the pending alkene. Importantly, base sensitive aryl boronates (**12**) and organostannanes (**13**) or electrophilic sites that are prone to Ni-catalyzed cross-coupling reactions such as aryl chlorides (**4**, **14**, **15**) and aryl pivalates (**15**) were all well-accommodated, thus offering an additional site for further functionalization.<sup>67</sup> As shown for **25**, the photochemical *sp*<sup>3</sup> C–H arylation could smoothly be extended to vinyl bromides, albeit with lower yields; notably, *trans*-*cis* isomerization was observed in the product. Importantly, the reaction could easily be carried out at 10 mmol scale without obvious erosion in yield (**3** and **21**).



<sup>a</sup> Reaction conditions: as Table 4.3 (entry 1), ArBr (0.3 mol). <sup>b</sup> Isolated yields, average of at least two independent runs  
<sup>c</sup> 10 mmol scale. <sup>e</sup> 20 mol% of A4.

**Table 4.10. Scope of (hetero)aryl bromides with chiral pool.**

As expected, substrates derived from the chiral pool, such as cholesterol (**26**), (L)-menthol (**27**), (D)-allofuranose (**28**) and (D)-phenylglycine (**29**) could also be accommodated (Table 4.10). More

importantly, our protocol tolerated the coupling of a wide-variety of nitrogen-containing heterocycles. Indeed, electron neutral or poor pyridines (**30 to 32**), pyrimidines (**33**) and quinolines (**36**) could all be employed as starting precursors. The low yields found for **30** and **32** are tentatively attributed to volatility or to a slower reaction rate for **33** and **34**. It was worth noting that electron rich heterocycles, such as thiophenes and free indole (**34**, **35** and **37**) – typically giving low yields with classical metallaphotoredox reactions based on iridium polypyridyl complexes due to competitive SET processes<sup>13</sup> – did not pose problems, thus showcasing the complementarity of our photochemical technique with Ir(III) photoredox processes.

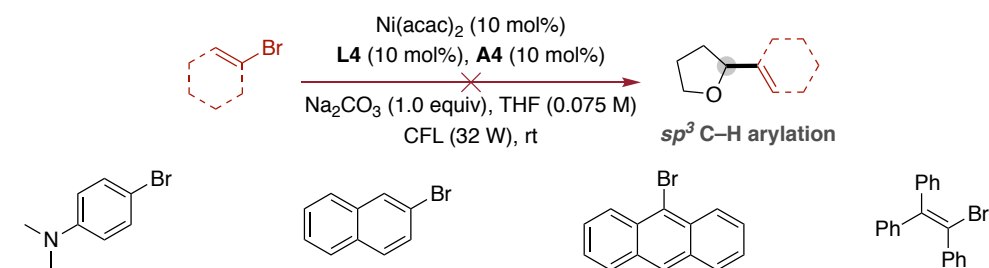
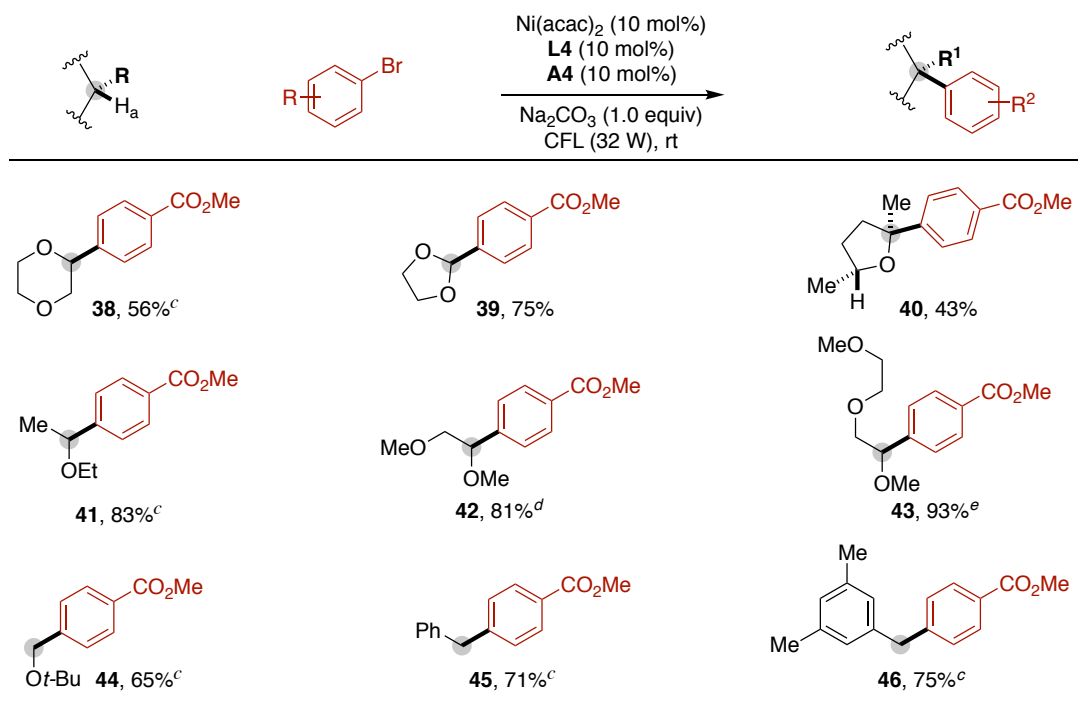


**Table 4.11. Selected failed substrates**

Even though the compiled data in table 4.9 and 4.10 showed great generality of our protocols, there was still some challenging substrates we could not couple under our conditions. As shown in table 4.11, the presence of dimethyl amino groups did not afford any product due to the competitive SET from the electron rich amine with triplet state of **A4**; as for the low efficiency of the other products listed in Table 4.11, the low efficiency is probably explained by the high conjugation that might quench the triplet excited state and prevent the reaction from occurring.

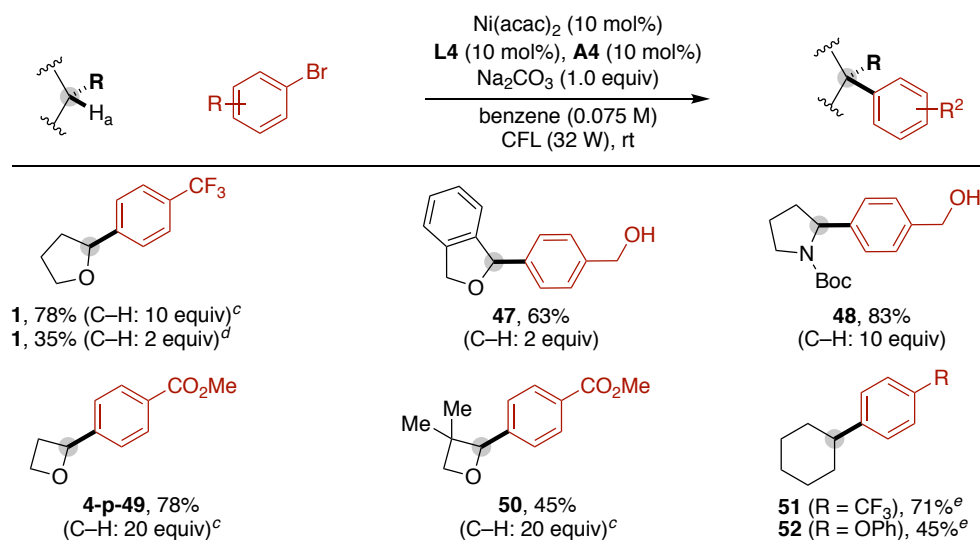


<sup>a</sup> Reaction conditions: as Table 4.3 (entry 1). <sup>b</sup> Isolated yields, average of at least two independent runs.

<sup>c</sup> Using  $\text{NaHCO}_3$  (1.0 equiv). <sup>d</sup> 1.8:1 regioisomeric ratio. <sup>e</sup> 2:2:1 regioisomeric ratio.

**Table 4.12. Scope of alkane  $sp^3$  C–H precursors**

With the results of table 4.9 and table 4.10 in hand, we wondered whether our photochemical arylation could be extended to  $sp^3$  C–H precursors other than tetrahydrofuran.<sup>68</sup> We were pleased to find that a variety of cyclic ethers (**38** to **40**) and acyclic ether analogues (**41** to **44**) could be employed with equal ease (Table 4.12). Particularly attractive was the ability to couple 1,3-dioxolane (**39**) which might provide a complementary approach to introduce the formyl group into arenes after routine acid workup.<sup>58d,69</sup> Particular noteworthy was the observation that **40** was obtained as a single diastereoisomer containing a tetrasubstituted carbon center; to the best of our knowledge, this example constitutes the first nickel-catalyzed cross-coupling reaction that occurs via functionalization of a sterically-encumbered tertiary  $sp^3$  C–H bond possessing an  $\alpha$ -heteroatom.<sup>70</sup> Another interesting example is **44**, as the *t*-Bu group can easily be deprotected under acid conditions to deliver the corresponding benzyl alcohols. As shown for **45** and **46**,<sup>97</sup> our protocol was not limited to ether motifs and the targeted  $sp^3$  C–H arylation could also be conducted with less reactive methyl-substituted benzene backbones, furnishing the corresponding diarylmethanes in good yields. However, the developed conditions were not appropriate for ethyl benzene or anisole; in the former, considerable amounts of styrene were found in the crude mixtures, while the latter as solvent may quench the triplet state of **A1**.

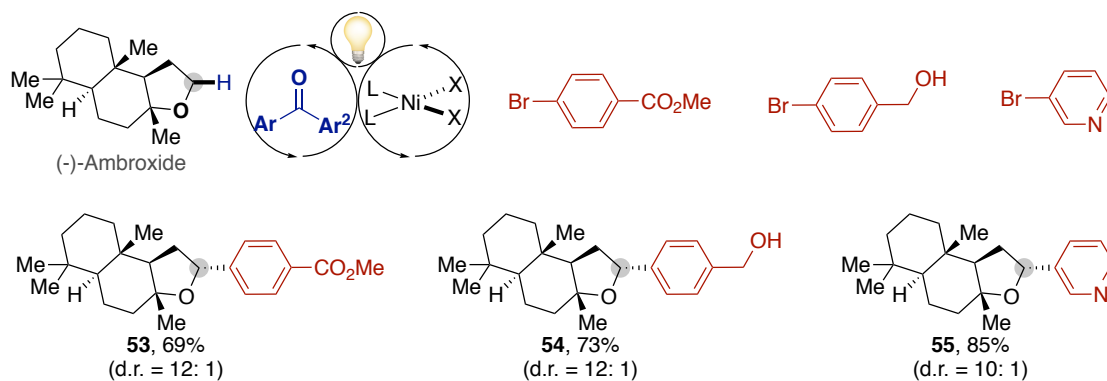


<sup>a</sup> Reaction conditions: as Table 4.3 (entry 1), in benzene as solvent (0.075 M). <sup>b</sup> Isolated yields, average of at two independent runs. <sup>c</sup> NaHCO<sub>3</sub> (1 equiv). <sup>d</sup> **A4** (50 %) was used. <sup>e</sup> Cyclohexane:benzene (1:1, 0.05 M).

**Table 4.13. *sp*<sup>3</sup> C–H arylation in benzene as solvent**

Aiming at examining the practicality of our system, we decided to explore whether we could employ the C–H precursor in stoichiometric amounts. We were pleased to find that excellent yield (78%) of **1** could be observed with 10 equiv of THF in benzene as solvent and NaHCO<sub>3</sub> as base. Further decreasing the loading of THF (2 equiv) while increasing **A4** (50 mol%) delivered moderate yield (35%) with considerable amount of reduced product probably deriving from the  $\alpha$ -hydrogen of THF. Fortunately, the good reactivity and selectivity obtained with phthalane (2 equiv) holds promise for designing future photochemical *sp*<sup>3</sup> C–H functionalizations with improved practicality, flexibility and generality. Other challenging C–H precursors with small rings (**49** and **50**) or steric hindrance (**50**) afforded the targeted products in moderate to good yields. Notably, N-Boc pyrrolidine was an excellent substrate for our transformation as high yield was obtained in this case (**48**, 83%). Although the results compiled in previous tables showed the diversity for a wide number of substrates possessing weak C–H bonds, it was unclear whether such technique could be extended to unactivated, yet particularly strong, *sp*<sup>3</sup> C–H bonds. Gratifyingly, we found that the *sp*<sup>3</sup> C–H arylation of cyclohexane is within reach (**51**, **52**), constituting a step-forward for the functionalization of particularly unactivated *sp*<sup>3</sup> C–H bonds which cannot proceed with quinuclidine as HAT mediator.<sup>71</sup>

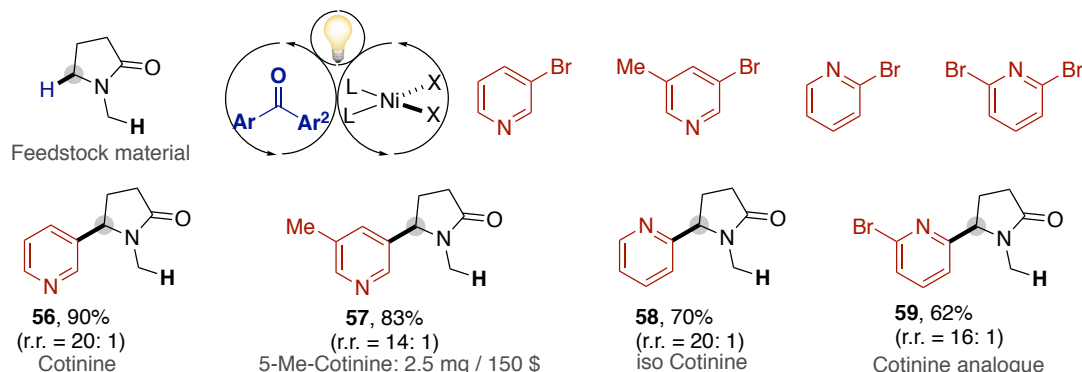




As Table 4.13, with benzene as solvent (0.06M) and C–H precursor (10 equiv)

**Figure 4.6. Late-stage diversification of (-)-ambroxide**

Prompted by the generality of our photochemical  $sp^3$  C–H arylation, we anticipated that we might be able to streamline the synthesis of complex molecules via late-stage functionalization.<sup>72</sup> To this end, we found that (–)-ambroxide, a naturally occurring terpenoid responsible for the odor of ambergris, underwent the targeted late-stage  $sp^3$  C–H functionalization with a different set of (hetero)aryl bromides in benzene as solvent, giving rise to **53** to **55** in high yields and excellent diastereoselectivities (Figure 4.6).

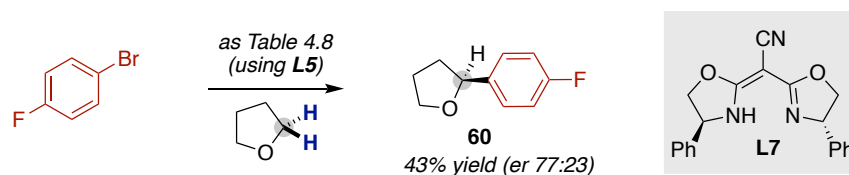


As Table 4.3, with benzene as solvent (0.06M) and C–H precursor (10 equiv).

**Figure 4.7. Site-selectivity and natural product synthesis**

We were also pleased to find that the  $sp^3$  C–H arylation of NMP (*N*-methylpyrrolidone) with 3-bromopyridine rapidly afforded cotinine (**56**), an alkaloid found in tobacco and currently being studied as a treatment for depression, PTSD, schizophrenia, Alzheimer’s disease and Parkinson’s disease,<sup>73</sup> in high yields and with excellent site-selectivity (Figure 4.7). Likewise, a variety of valuable, yet difficult to access with traditional methods, cotinine analogues such as **57** (60 \$/mg)<sup>74</sup> to **59** could also be accessed under otherwise identical reaction conditions from cheap starting precursors, even at 10 mmol scale without an apparent erosion in yield and site-selectivity (**57**). Strikingly, there is no general method to access cotinine and its aryl derivatives in Scifinder, further

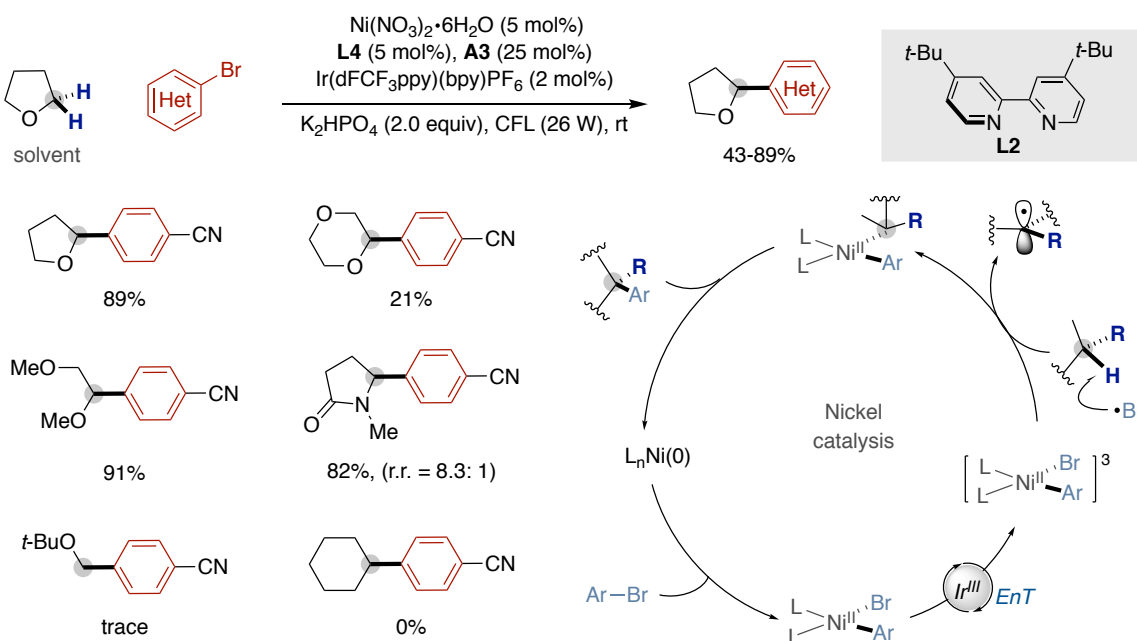
demonstrating the potential of our system in functionalizing cheap C-H precursors and quickly generating molecular complexity.



**Scheme 4.26. Enantioselective  $sp^3$  C-H arylation**

Encouraged by our results, we wondered whether the merger of triplet excited ketones and nickel catalysis might enable the development of an asymmetric  $sp^3$  C-H arylation if appropriate chiral ligands were employed. Gratifyingly, we found that **60** could be accessed in moderate enantioselectivities and yields when a Ni/L7 catalyst was used (Scheme 4.26).<sup>75</sup> Although preliminary, this result constitutes the first example of an enantioselective C-C bond-forming reaction of native  $sp^3$  C-H bonds within the metallaphotoredox arena. These results are currently being followed up by other members of the group and will be reported in due course.

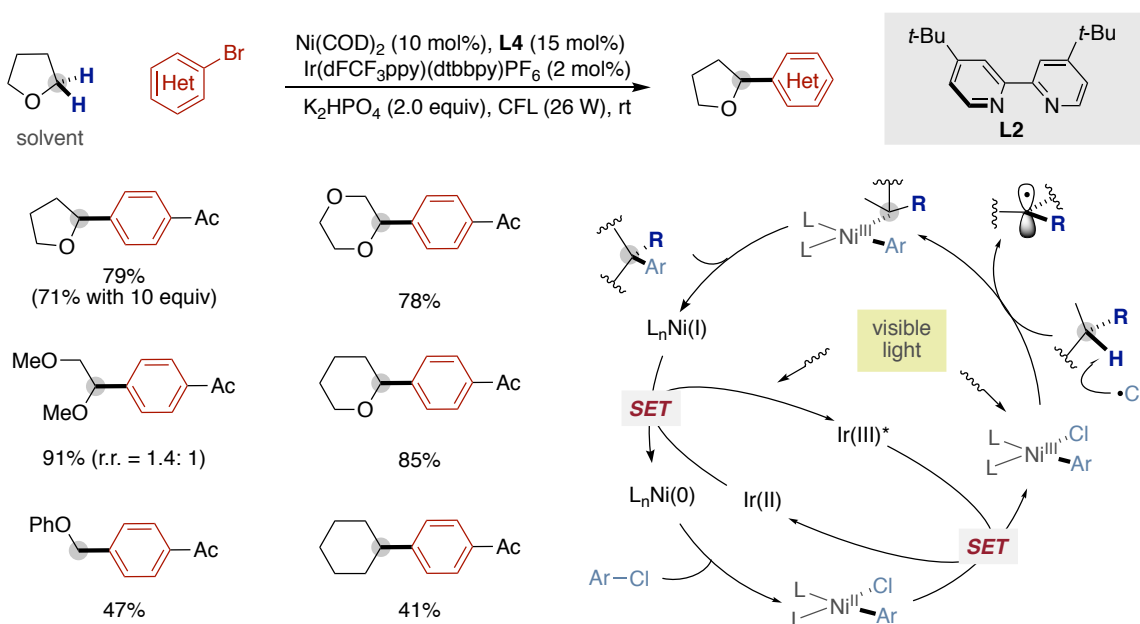
It is worth noting that, during the course of our investigations, Molander and Doyle concurrently reported a rather similar  $sp^3$  arylation event of C-H precursors (as solvents) via energy transfer or SET/HAT process, in both cases using Ir(III) photocatalysts.<sup>51,52a</sup>



**Scheme 4.27. Molander's  $sp^3$  C-H arylation via energy transfer**

In Molander's work,<sup>51</sup> the authors confirmed an energy transfer pathway by which the photosensitized ArNi(II)Br oxidative addition complex releases Br-radical (BDE of H-Br:

88kcal/mol) that was capable of selectively abstracting weak C–H bonds in the presence of **A5**. This was illustrated by the fact that DME gave a single regioisomer in good yields while no reaction occurred with *t*-BuOMe and cyclohexane (BDE C–H bond: 99 kcal/mol) (Scheme 4.27, *bottom left*). Control experiments in the absence of **A5** afforded 76% yield of the desired product, but Ir(III) photocatalyst was required for the reaction to occur.



**Scheme 4.28. Doyle's  $sp^3$  C–H arylation via SET/HAT process**

In Doyle's case,<sup>52a</sup> the authors proposed a single electron oxidation of  $ArNi(II)Cl$  to  $ArNi(III)Cl$  intermediate, which was subsequently photosensitized under visible light irradiation to release highly reactive Cl-radical (BDE of H–Cl: 105kcal/mol) that was responsible for the HAT process (Scheme 4.28). As a consequence, arylation of DME gave rise to mixture of regioisomers while PhOMe and cyclohexane (BDE C–H bond: 99 kcal/mol) could be utilized as C–H precursors. Very recently, Doyle group solved the problem of using the C–H precursor as solvent by conducting a  $sp^3$  C–H acylation in which the functionalized position was deactivated by a proximal electron withdrawing group, thus allowing to use 2–5 equiv of the corresponding C–H precursor.<sup>52b</sup> While the work of Molander<sup>51</sup> and Doyle<sup>52a</sup> was certainly devastating for our purposes, we decided to continue our investigations on the utilization of diaryl ketones as both HAT/SET catalysts in the absence of noble Ir photocatalysts. In particular, we decided to show the possibility of conducting a  $sp^3$  C–H alkylation event, as the work of Molander and Doyle did not show such possibility with Ir photocatalysts.<sup>51,52a</sup>

#### 4.6.4. Metallatriplet Catalysis: $sp^3$ C-H Alkylation

After firmly establishing the ability of triplet excited ketones to trigger a  $sp^3$  C-H arylation, we turned our attention to study the possibility of effecting a  $sp^3$  C-H alkylation with the corresponding unactivated alkyl bromides. If successful, we recognized that such a reaction would provide an opportunity to couple two  $sp^3$  carbon fragments from readily accessible precursors and catalysts in a redox neutral manifold.<sup>76</sup> However, the lower propensity of alkyl halides for oxidative addition, and the proclivity to undergo  $\beta$ -hydride elimination reactions, reduction or parasitic homodimerization were important challenges to be overcome (Figure 4.8).<sup>77</sup>

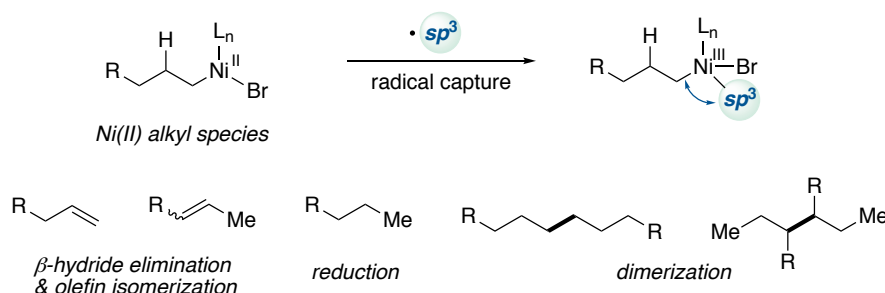


**Figure 4.8. Potential byproducts of Ni-alkyl species**

We started our investigations on the  $sp^3$  C-H alkylation of 4-phenyl-1-bromobutane (Table 4.14). As shown, low yields were obtained due to competitive  $\beta$ -hydride elimination and benzylic dimerization. Interestingly, more electron-rich **L2** gave consistently better yields compared to **L4** whereas quantitative dimerization was obtained with **L5** as the ligand, thus showing the subtleties of our protocol when slightly modifying the electronic and steric parameters at the ligand backbone.

entry	Ligand	conversion (%)	<b>65</b> (%) <sup>a</sup>
1	<b>L4</b>	54 <sup>b</sup>	27
2	<b>L5</b>	100 <sup>c</sup>	0
3	<b>L2</b>	86 <sup>b</sup>	56
4	<b>L8</b>	38 <sup>b</sup>	15

**L4**

**L5**

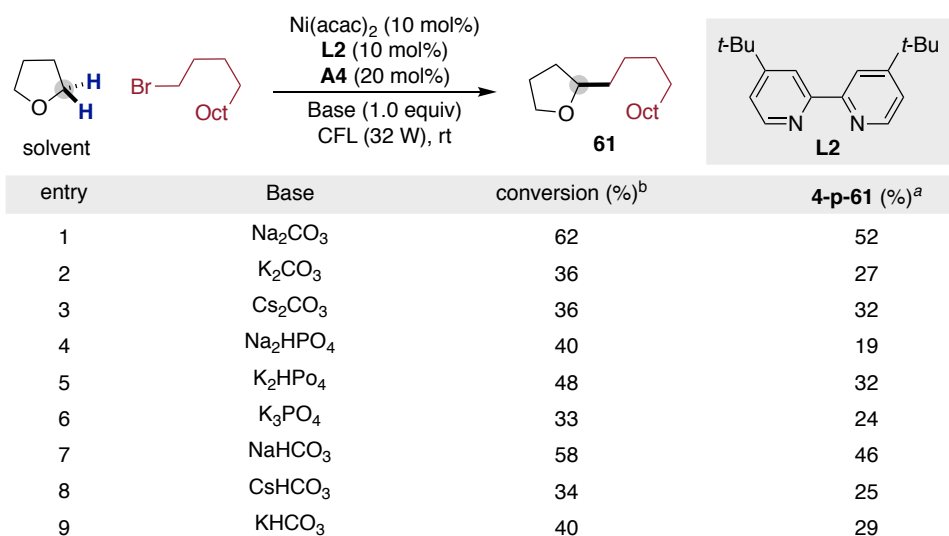
**L2**

**L8**

Reaction conditions: alkyl bromide (0.3 mmol), THF (0.075 M), 72h. <sup>a</sup> GC yields with decane as internal standard.

<sup>b</sup> Mass balance accounts for olefin isomers. <sup>c</sup> Mass balance accounts for dimerization of benzylic position.

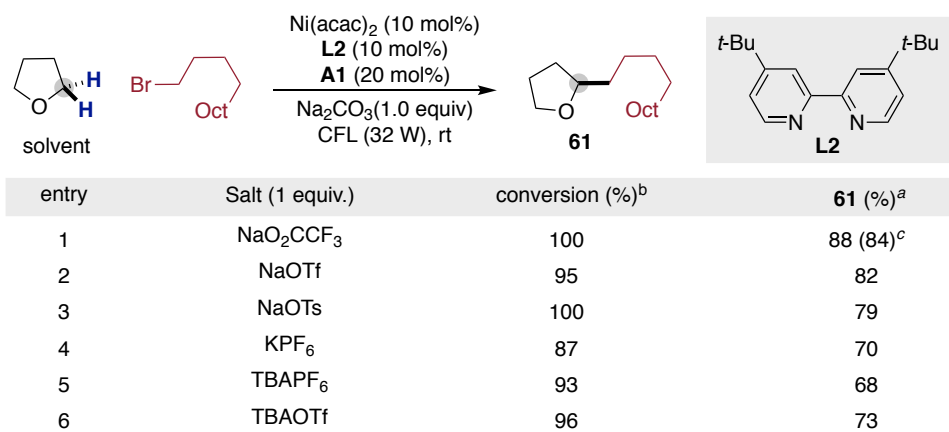
**Table 4.14. Preliminary trials of  $sp^3$  C-H alkylation**



Reaction conditions: alkyl bromide (0.3 mmol), THF (0.075 M), 56h. <sup>a</sup> GC yields with decane as internal standard. <sup>b</sup> Mass balance accounts for olefin, reduction and dimerization

**Table 4.15. Base screening for the *sp*<sup>3</sup> C-H alkylation event**

Encouraged by these preliminary results, we carried out further optimization using Ni(acac)<sub>2</sub>/L2 (10 mol%) and A4 (20 mol%) to improve both reactivity and selectivity. Indeed, chemoselectivity was increased with higher A4 loading. Still, however, some amount of olefin, reduction and dimerization were still observed in the crude mixtures. Among all inorganic bases utilized, Na<sub>2</sub>CO<sub>3</sub> turned out to be the best one regarding both reactivity and selectivity.

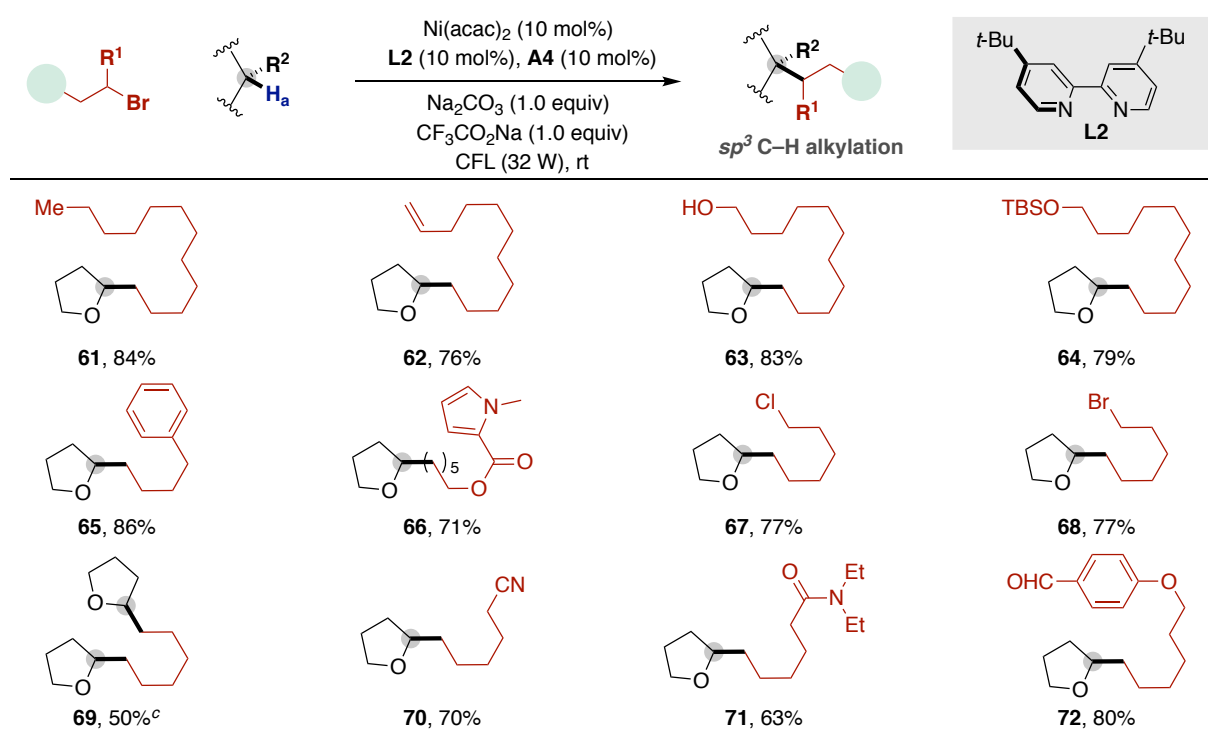


Reaction conditions: alkyl bromide (0.3 mmol), THF (0.075 M), 72h. <sup>a</sup> GC yields with decane as internal standard. <sup>b</sup> Mass balance accounts for olefin and dimerization. <sup>c</sup> isolated yield.

**Table 4.16. Additive screening of *sp*<sup>3</sup> C-H alkylation**

In light of these results, it was evident that dimerization, reduction and β-hydride elimination were difficult to control, preventing the formation of the final *sp*<sup>3</sup> C–H alkylation in high yields. We hypothesized that these drawbacks could be partially alleviated by the *in situ* generation of a cationic oxidative addition complex. If so, a rapid radical recombination would be effected, thus preventing

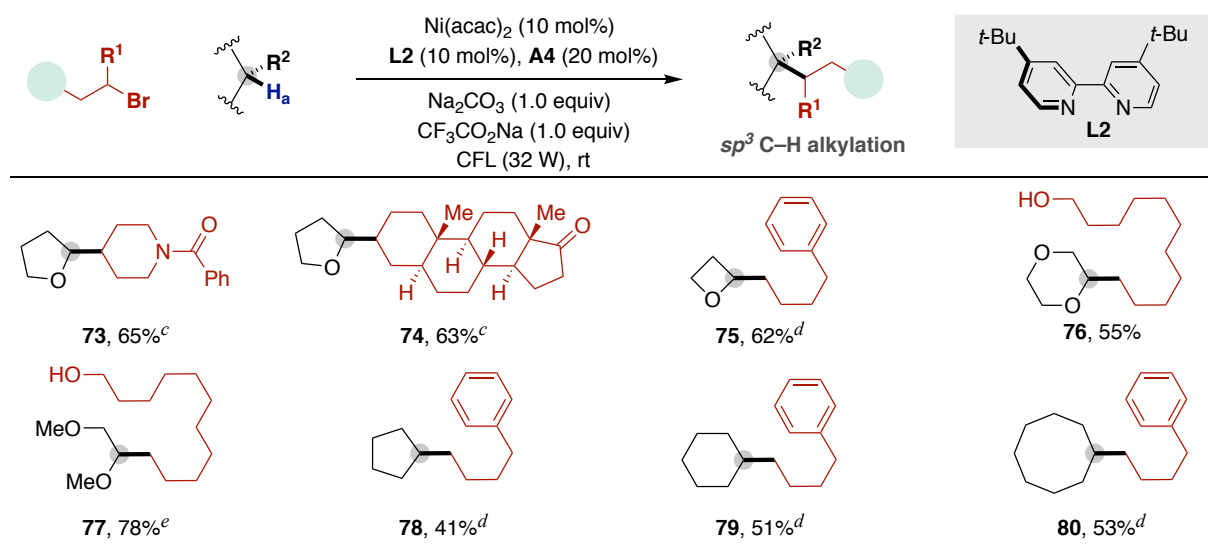
the formation of parasitic  $\beta$ -hydride elimination, reduction or homodimerization pathways.<sup>77</sup> To such end, we turned our attention to study the addition of non-coordinated anions as cation scavengers. Gratifyingly, we obtained 84% isolated yield when  $\text{NaO}_2\text{CCF}_3$  (1 equiv) was used as additive (Table 4.16, entry 1), and without detectable dimerization. Notably, the utilization of  $\text{NaOTf}$  or  $\text{NaOTs}$  were slightly less reactive, thus showing the non-negligible influence of the corresponding anion (Table 4.16, entry 2 and 3). Likewise, the counteraction had a non-negligible influence on yield, as  $\text{NaOTf}$  showed superior reactivity than  $\text{TBAOTf}$  (Table 4.16, entry 2 and 6). Control experiments confirmed the absence of a Finkelstein-type anion exchange; therefore, the improvement observed cannot merely be attributed to the *in situ* formation of the corresponding  $\text{R-O}_2\text{CCF}_3$ .



<sup>a</sup> Reaction conditions: alkyl bromide (0.30 mmol),  $\text{Ni}(\text{acac})_2$  (10 mol%), **L2** (10 mol%), **A4** (20 mol%), C-H precursor (0.075 M),  $\text{Na}_2\text{CO}_3$  (1.0 equiv),  $\text{CF}_3\text{CO}_2\text{Na}$  (1 equiv), CFL (32W), 25 °C. <sup>b</sup> Isolated yields, average of at least two independent runs. <sup>c</sup> 120 h.

**Table 4.17. Scope of  $sp^3$  C-H alkylation with unactivated primary alkyl bromide**

Under the optimized reaction conditions of Table 4.16 (entry 1), a wide variety of unactivated alkyl bromides possessing alkenes (**62**), free alcohols (**63**), silyl ethers (**64**), esters (**66**), N-containing heterocycles (**66**), nitriles (**70**), amides (**71**, **73**) or aldehydes (**72**) were all accommodated. As shown for **67**, the presence of alkyl chlorides did not interfere with productive  $sp^3$  C–Br bond-cleavage (**67**), whereas exhaustive or selective  $sp^3$  C–H alkylation could be accomplished when 1,6-dibromohexane was employed as substrate (**68**, **69**).

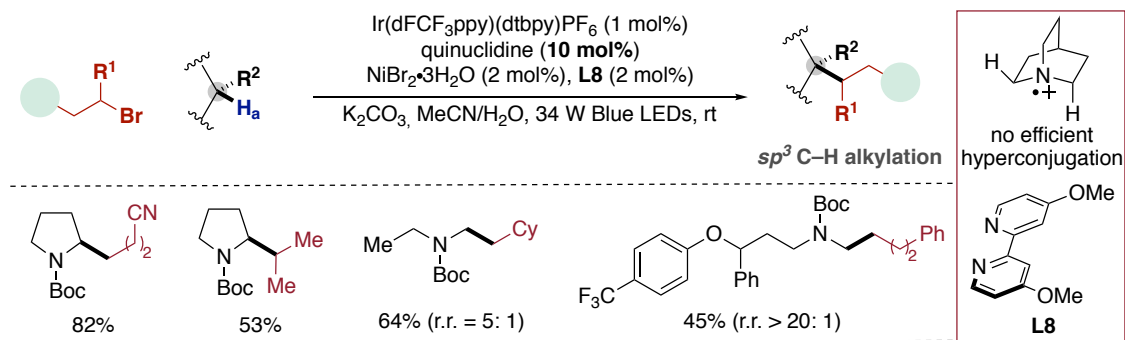


<sup>a</sup> Reaction conditions: alkyl bromide (0.30 mmol),  $\text{Ni(acac)}_2$  (10 mol%),  $\text{L2}$  (10 mol%),  $\text{A4}$  (20 mol%), C–H precursor (0.075 M),  $\text{Na}_2\text{CO}_3$  (1.0 equiv),  $\text{CF}_3\text{CO}_2\text{Na}$  (1 equiv), CFL (32W), 25 °C. <sup>b</sup> Isolated yields, average of at least two independent runs.

<sup>c</sup> Without  $\text{CF}_3\text{CO}_2\text{Na}$ . <sup>d</sup> Benzene as cosolvent (1:1, 0.05 M),  $\text{A5}$  (50 mol%). <sup>e</sup>  $\text{NaHCO}_3$  (1.0 equiv)

**Table 4.18. Scope of secondary alkyl bromides and other C–H precursors**

Although we anticipated that a C–C bond reductive elimination between two fragments derived from secondary  $sp^3$  C–H bonds would be even more problematic, we found that our protocol could tolerate the coupling of challenging secondary alkyl bromides (**73**, **74**). Unfortunately, our protocol did not allow the coupling of tertiary and acyclic secondary alkyl bromides; in the former, no reaction took place whereas significant  $\beta$ -hydride elimination was observed in the latter. Unlike the  $sp^3$  C–H arylation event, the corresponding  $sp^3$  C–H alkylation could not be extended to a wide number of C–H precursors. After considerable screening of a variety of C–H precursors, we found that three additional ethereal motifs could be used to deliver the targeted  $sp^3$  C–H alkylation event (**75** to **77**). Particularly noteworthy was the unprecedented C( $sp^3$ )-C( $sp^3$ ) bond-formation at unactivated  $sp^3$  C–H bonds possessing particularly high BDE (**78** to **80**). These results suggest that our Ni/**A1** regime might complement existing metallaphotoredox scenarios based on the utilization of Ir polypyridyl photocatalysts for the functionalization of  $sp^3$  C–H via HAT processes.<sup>13b</sup> It is worth noting that when our manuscript was in revision, MacMillan reported a  $sp^3$  C–H alkylation based on quinuclidine and Ir(III) photocatalyst (Scheme 4.29).<sup>76</sup> As for their previous  $sp^3$  C–H arylation event,<sup>50</sup> however, no tentative explanation of the observed selectivity was given for their Ni/photoredox/HAT work.



**Scheme 4.29. Photoredox, HAT and Ni-catalyzed *sp*<sup>3</sup> C-H alkylation**

#### 4.6.5. Metallatriplet Catalysis: Mechanistic studies

Although our data suggested that the merger of triplet excited ketone catalysts and nickel catalysts exploited an unrecognized opportunity in the C–H functionalization arena, it was unclear whether the promiscuous photoreactivity of triplet excited ketones (SET, HAT, ET) would allow us to understand how the C–H bond cleavage operates at the molecular level. In order to unravel the mode of action by which **A1** enables *sp*<sup>3</sup> C–H arylation, several mechanistic experiments were carried out. Although control experiments corroborated the efficient photoreduction of Ni(acac)<sub>2</sub> by **A1** under CFL irradiation (see experimental section for details), various scenarios might be conceivable for the results highlighted above.

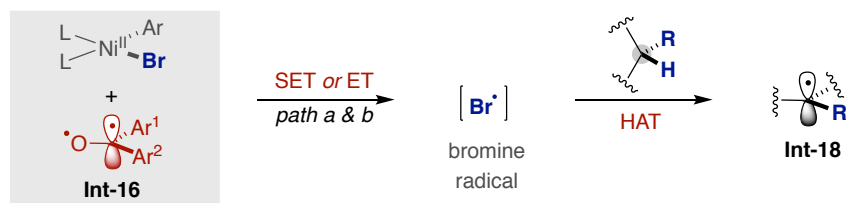
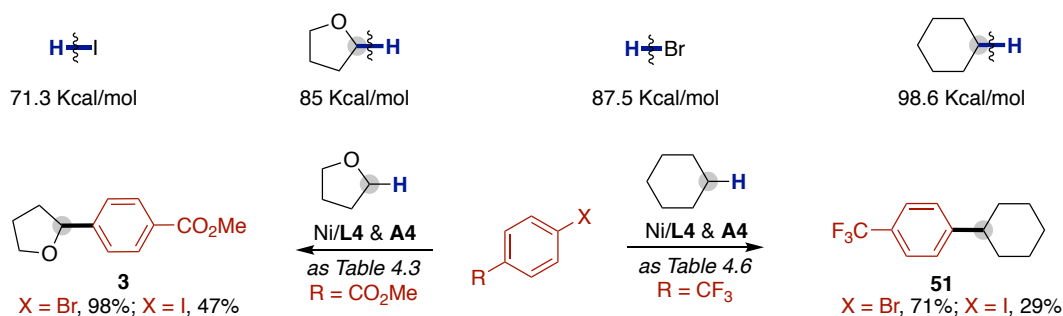


**Figure 4.9. Br radical involved HAT process via SET or ET**

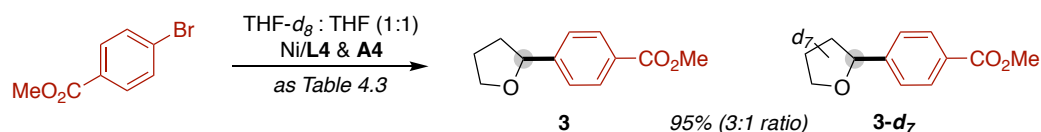
In view of Molander and Doyle's work, we could not rule out the possibility that the oxidative addition complex ArNi(II)X could either be sensitized via ET or oxidized via SET to generate halide radical (Figure 4.9).<sup>51</sup> Although this was certainly reasonable, we believed that this pathway made only a minor contribution to productive *sp*<sup>3</sup> C–H arylation, if any.





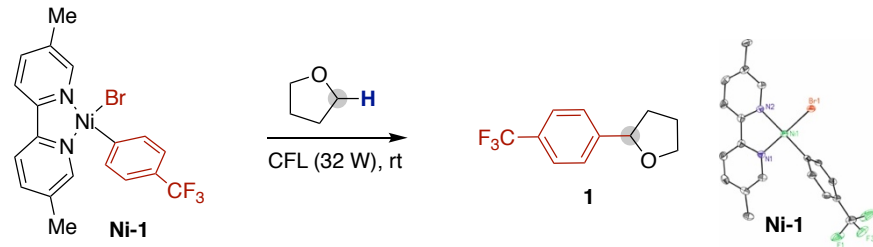
**Scheme 4.30. The BDE mismatch experiments**

Taking into consideration the mismatch of bond-dissociation energies (BDE)<sup>78</sup> of H–Br (87 Kcal/mol) and the C–H bond of cyclohexane (98 Kcal/mol), one might argue that the  $sp^3$  C–H arylation of the latter with bromoarenes should not take place (Scheme 4.30). However, the successful arylation of cyclohexane (**51** and **52**, Table 4.13) and alkylation of cycloalkanes (**78** to **80**; Table 4.18) indicated otherwise. In addition, the lack of Ni–X homolysis gained credence when considering the non-negligible reactivity obtained when promoting the  $sp^3$  C–H arylation of tetrahydrofuran (C–H: 85 Kcal/mol) and cyclohexane (C–H: 98 Kcal/mol) with iodoarenes<sup>79</sup> (H–I: 71 Kcal/mol) en route to **3** and **51**. However, care must be taken when generalizing this, as the oxidative addition of aryl iodide to Ni(0)L<sub>n</sub> might follow a SET-type pathway, leading to an aryl radical that can escape the solvent cage and act as a HAT mediator. If that's the case, a maximum 50% yield should be observed for iodoarenes, together with non-negligible amount of reduced arenes. However, a close inspection into the crude mixtures of our arylation of iodoarenes revealed that only trace amount of the corresponding reduced arene were observed, thus leaving a reasonable doubt on whether this pathway is being populated.



**Scheme 4.31. Deuterium labelling experiments**

Notably, deuterium labelling studies showed an exothermic radical  $sp^3$  C–H abstraction, providing additional evidence that might rule out a Br radical pathway (Scheme 4.31).<sup>80</sup> This interpretation is based on the BDE of H–Br (87.5 Kcal/mol) and  $\alpha$ -H of THF (85 Kcal/mol), suggesting that a thermoneutral HAT process should occur via Br radical, an observation that was confirmed by Molander and coworkers with the same deuterium labelling experiment.



entry	photocatalyst	$E_{1/2}^{(M^+/M^{\cdot-})}$	Em $\lambda$ (nm)	light source	<b>1</b> (%) <sup>a</sup>
1	<b>A4</b>	-	425	CFL (32 W)	71%
2	-	-	-	CFL (32 W)	0 <sup>b</sup>
3	-	-	-	UVB (365 nm)	0 <sup>b</sup>
4	Ru(bpz) <sub>3</sub> (PF <sub>6</sub> ) <sub>2</sub>	1.45 V	591	CFL (32 W)	0 <sup>b</sup>
5	9-MesAcr(ClO <sub>4</sub> )	2.05 V	590	CFL (32 W)	0 <sup>b</sup>

<sup>a</sup> in presence of 1 equiv. of 1-Br-4-CO<sub>2</sub>Me-C<sub>6</sub>H<sub>4</sub>. <sup>b</sup> dimerization of aryl partner.

**Table 4.19. Stoichiometric experiments with Ni-1**

While we could certainly rule out the intermediacy of bromine radicals on the  $sp^3$  C–H arylation of cyclohexane, it was still ambiguous whether the Br-radical was involved or not in the functionalization of THF. To shed light into this observation, we prepared the putative oxidative addition complex **Ni-1** upon exposure of 4-bromotrifluoromethyl benzene to Ni(COD)<sub>2</sub> and **L4**. As shown in Table 4.19, stoichiometric experiments revealed that **Ni-1** gave rise to the targeted product in THF with **A4** (entry 1), while dimerization of the aryl motif was observed without **A4** (entry 2). Importantly, direct irradiation of a solution of **Ni-1** in THF resulted in dimerization (entry 3) whereas not even traces of product were detected when employing strongly oxidizing photocatalysts that would be perfectly capable of oxidize the corresponding oxidative addition complex **Ni-1**. Putting all the pieces together (Scheme 4.30, 4.31 and Table 4.19), we strongly believe that a scenario based on bromine radicals is highly unlikely.

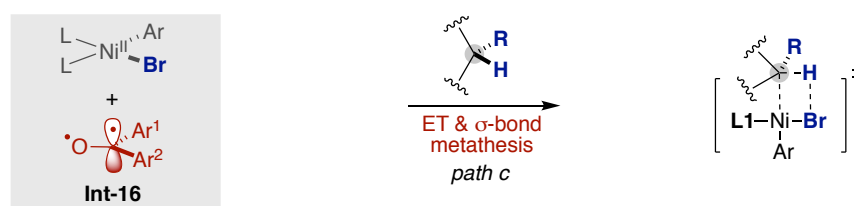
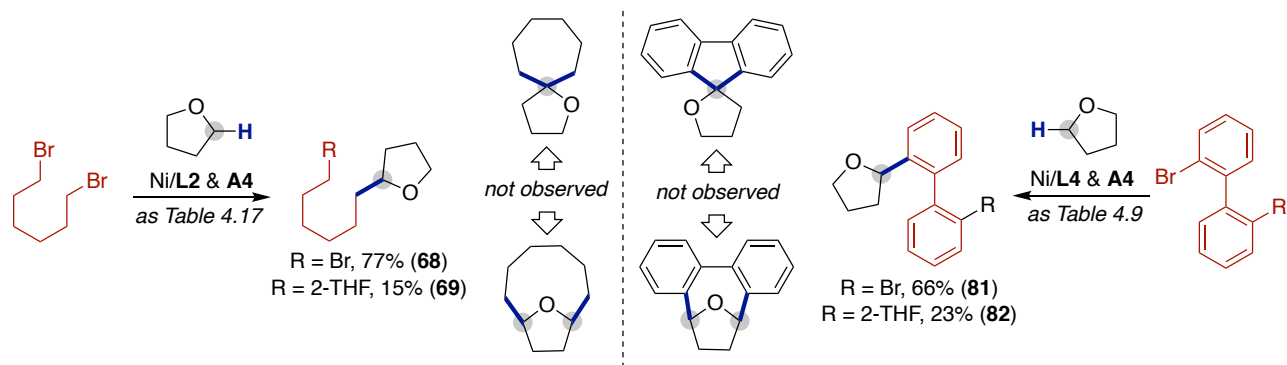


**Figure 4.10. Involvement of sigma bond metathesis**

Next, we turned our attention to explore the viability of a triplet-triplet ET followed by  $\sigma$ -bond metathesis (Figure 4.10, *pathway c*). If such a pathway intervenes, non-negligible amounts of  $sp^3$  C–H arylation were anticipated when **Ni-1** was exposed in the absence of **A4** under irradiation by a dark lamp ( $\lambda_{\text{max}} = 365 \text{ nm}$ ) (Table 4.19, entry 3).<sup>82</sup> However, not even traces of **1** were observed.



**Scheme 4.32. Accessing  $\sigma$ -bond metathesis via bromides selection**

Further support for the lack of  $\sigma$ -bond metathesis came from the reactivity of the dibromo derivatives shown in Scheme 4.32. Although the absence of double cyclization cannot be taken as a definitive proof, pathways other than  $\sigma$ -bond metathesis seemed to be the most plausible avenue for explaining our  $sp^3$  C–H arylation event.<sup>83</sup>

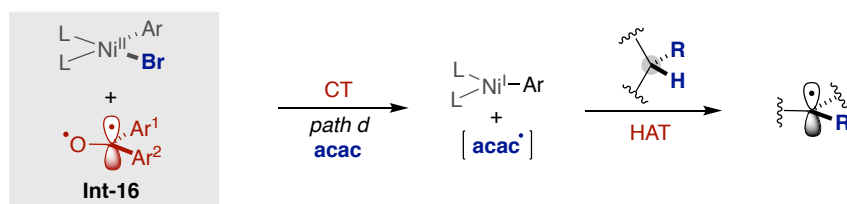
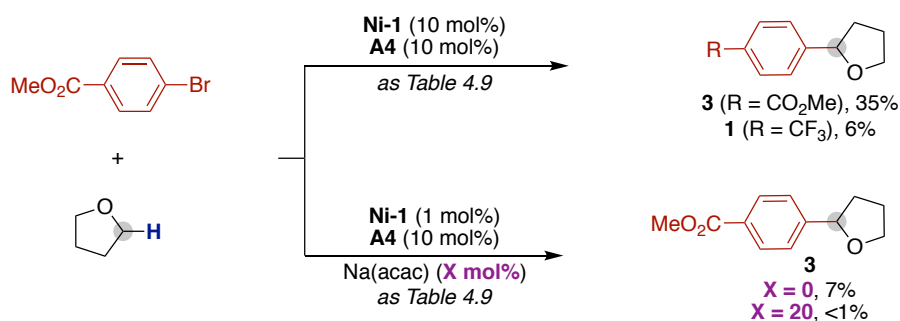


**Figure 4.11. Involvement of acac radical via charge transfer**

Since the photoreduction of  $\text{Ni}(\text{acac})_2$  via charge-transfer (CT) had a direct correlation with the generation of acac-radical species, another possibility that could explain our results would be the ability to trigger a charge-transfer (CT) from  $\text{A4}^*$  to in situ generated  $\text{ArNi}(\text{II})\text{acac}$ . Such a pathway would result in acac radical that could trigger a HAT process with the corresponding C–H precursor (Figure 4.11, *path d*).<sup>46</sup>



**Scheme 4.33. Catalytic competence of Ni-1**

In line with our expectations, **Ni-1** turned out to be an active precatalyst in the absence of acac anion, furnishing **3** in 35% yield together with 6% of **1** derived from **Ni-1** (Scheme 4.33, *up right*). The

marked decrease in reactivity of **Ni-1** compared to the *in situ* protocol can tentatively be attributed to (a) the stunning absorption of **Ni-1** in the visible light region which may affect the absorption of **A4**, and/or (b) the absence of the acac anion which contributed to product formation (Figure 4.11, *pathway d*).<sup>46</sup> The former possibility was assessed by performing the reaction with 1 mol% of **Ni-1**. Although reduced yields were detected, an improved turnover number (TON) was observed, suggesting either an unproductive quenching of **A4\*** by **Ni-1** or that the high concentration of deep colored **Ni-1** affected the absorption of **A4** (Scheme 4.33, *bottom right*). The latter was evaluated by adding additional Na(acac) to the reaction. Surprisingly, significant inhibition was observed in the presence of Na(acac) (Scheme 4.33, *bottom right*). As a consequence, the presence of acac in our catalytic protocol does not have an influence on product formation, suggesting that acac may merely facilitate the initial photoreduction of Ni(acac)<sub>2</sub> to deliver the catalytically competent nickel intermediates. In line with this, it is worth noting that no significant deleterious effect was observed when replacing Ni(acac)<sub>2</sub> with other Ni(II) precatalysts or Ni(COD)<sub>2</sub> (Table 4.8, entry 5-7). Taken together, all the experiments in Scheme 4.33 left a reasonable doubt about the operation of *pathway d* (Figure 4.11) based on a CT event.

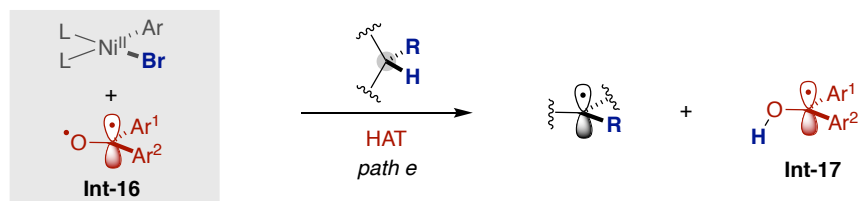


**Figure 4.12. HAT/SET via triplet diaryl ketone**

Although our empirical observations should not be taken as definitive proof that other pathways do not occur,<sup>84</sup> the available data favored out mechanistic rational where a HAT process from the triplet excited state of **A4** (Figure 4.12, *pathway e*) was followed by SET to recover the propagating **A4** and low-valent Ni(0)L species (Scheme 4.24). In general, photocatalysts have the highest molar absorption coefficient in the visible light region. In our reaction, however, the low absorption of **A4** in either THF or benzene was exacerbated by the high absorption of **Ni-1** in the ( $n,\pi^*$ ) excitation region, thus making particularly difficult to unambiguously determine the most basic quenching features of **A4** and **Ni-1**. Additionally, the propensity of **Ni-1** to decomposition in highly diluted conditions prevented the implementation of Stern-Volmer quenching studies or flash photolysis.<sup>85</sup>

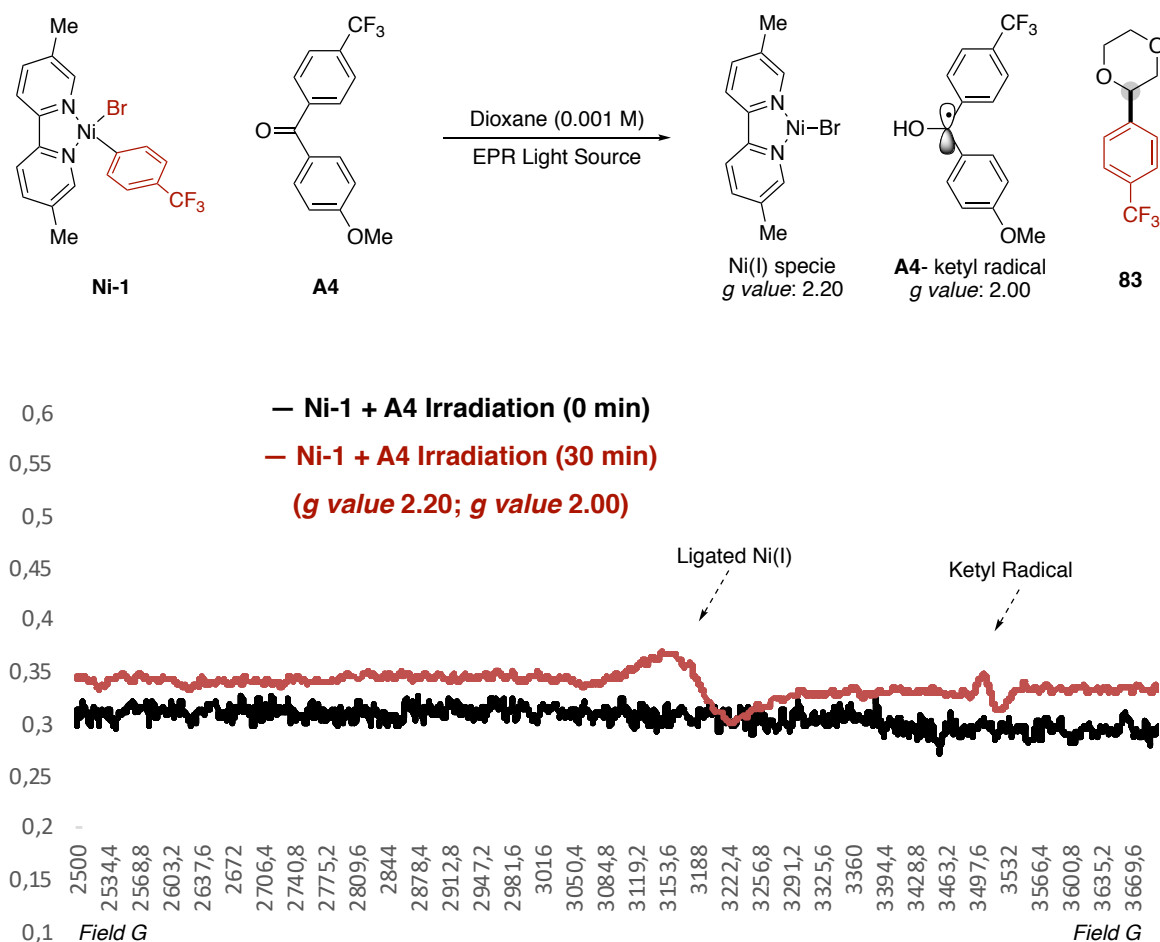


**Figure 4.13. EPR experiment of stoichiometric Ni with A4 under irradiation (X-axis Magnetic Field / G; Y-axis Intensity)**

In order to provide indirect evidence to confirm the productive mode of action of **A4**, we decided to monitor a stoichiometric reaction of **Ni-1** and **A4** in dioxane by EPR spectroscopy with constant irradiation (>300 nm) (Figure 4.13). A direct comparison with the known *g*-values of related species<sup>46b</sup> indicated the formation of Ni(I) intermediates and the corresponding ketyl radical together with the desired *sp*<sup>3</sup> C–H arylation of dioxane (**83**). Taken together, all the data acquired is consistent with triplet excited ketone **A4** acting as HAT & SET catalysts.

#### 4.7. Conclusion

In conclusion, we have developed a catalytic platform for the functionalization of native *sp*<sup>3</sup> C–H bonds by using the merger of cheap nickel salts with simple, modular diaryl ketone photocatalysts. Although preliminary, the method showed promising results in the context of late-stage functionalization of naturally-occurring molecules and asymmetric *sp*<sup>3</sup> C–H arylation event. Our metallatriplet catalytic scenario might represent a powerful alternative to existing photochemical

metallaphotoredox reactions based on commonly employed noble metal-based photocatalysts. Mechanistic experiments suggest an unprecedented activation mode in which photoexcited ketones serve as both HAT and SET catalysts in the context of Ni-catalysis. We expect that the broader consequences of this concept will foster systematic investigations into a more prolific use of simple ketones as photocatalysts for streamlining synthetic sequences that rapidly build-up molecular complexity from simple chemical feedstocks. It is worth noting, however, that our method required high quantities of C–H precursor, thus significantly lowering down the potential of this protocol. Although beyond the scope of this PhD thesis, our research group is currently studying the possibility of further engineering the ketone catalyst for meeting this goal.

## 4.8. Bibliography

1. de Meigere, A. & Diederich, F. (eds) *Metal-Catalyzed Cross-Coupling Reactions* 2nd edn (Wiley, 2004).
2. Tasker, S. Z., Standley, E. A., Jamison, T. F. Recent Advances in Homogeneous Nickel Catalysis. *Nature* **2014**, *509*, 299.
3. *Modern Organonickel Chemistry*. (ed. Tamaru, Y.) (Wiley-VCH Verlag GmbH & Co. KGaA, 2005).
4. (a) Ananikov, V. P. Nickel: The 'Spirited Horse' of Transition Metal Catalysis. *ACS Catal.* **2015**, *5*, 1964;
5. Clementi, E.; Raimond, D. L.; Reinhardt, W. P. Atomic Screening Constants from SCF Functions. II. Atoms with 37 to 86 Electrons. *J. Chem. Phys.* **1967**, *47*, 1300.
6. Miyaura, N., Suzuki, A. Palladium-catalyzed cross-coupling reactions of organoboron compounds. *Chem. Rev.*, **1995**, *95*, 2457.
7. Han, F.-S. Transition-metal-catalyzed Suzuki–Miyaura cross-coupling reactions: a remarkable advance from palladium to nickel catalysts. *Chem. Soc. Rev.*, **2013**, *42*, 5270.
8. Saito, B., Fu, G. C. Alkyl-alkyl Suzuki cross-couplings of unactivated secondary alkyl halides at room temperature. *J. Am. Chem. Soc.*, **2007**, *129*, 9602.
9. (a) Imao, D., Glasspoole, B. W., Laberge, V. S., Crudden, C. M. Cross coupling reactions of chiral secondary organoboronic esters with retention of configuration. *J. Am. Chem. Soc.* **2009**, *131*, 5024; (b) Zou, G., Reddy, Y. K., Falck, J. R. Ag(I) promoted Suzuki–Miyaura cross-couplings of *n*-alkylboronic acids. *Tetrahedron Lett.* **2001**, *42*, 7213; (c) Deng, J. Z., Paone, D. V., Ginnetti, A. T., Kurihara, H., Dreher, S. D., Weissman, S. A., Stauffer, S. R., Burgey, C. S. Copper-facilitated Suzuki reactions: Application to 2-heterocyclic boronates. *Org. Lett.* **2009**, *11*, 345.
10. Aufiero, M., Proutiere, F., Schoenebeck, F. Redox reactions in palladium catalysis: On the accelerating and/or inhibiting effects of copper and silver salt additives in cross-coupling chemistry involving electron-rich phosphine ligands. *Angew. Chem. Int. Ed.* **2012**, *51*, 7226.
11. (a) Yasu, Y., Koike, T., Akita, M. Visible light-induced selective generation of radicals from organotrifluoroborates by photoredox catalysis. *Adv. Synth. Catal.* **2012**, *354*, 3414; (b) Miyazawa, K., Yasu, Y., Koike, T., Akita, M. Visible-light-induced hydroalkoxymethylation of electron-deficient alkenes by photoredox catalysis. *Chem. Commun.* **2013**, *49*, 7249.
12. (a) Tellis, J. C., Primer, D. N., Molander, G. A. Single-electron transmetalation in organoboron cross-coupling by photoredox/nickel dual catalysis. *Science* **2014**, *345*, 433. (b) Zuo, Z., Ahneman, D. T., Chu, L., Terrett, J. A., MacMillan, D. W. C. Merging photoredox with nickel catalysis: coupling of  $\alpha$ -carboxyl  $sp^3$ -carbons with aryl halides. *Science* **2014**, *345*, 437.
13. (a) Prier, C. K., Rankic, D. A., MacMillan, D. W. C. Visible light photoredox catalysis with transition metal complexes: applications in organic synthesis. *Chem. Rev.* **2013**, *113*, 5322; (b) Twilton, J.; Le, C.; Zhang, P.; Shaw, M. H.; Evans, R. W.; MacMillan, D. W. C. The Merger of Transition Metal and Photocatalysis. *Nat. Rev. Chem.* **2017**, *1*, 0052.
14. (a) Chan, D., Monaco, K., Wang, R., Winter, M. New N- and O-Arylations with Phenylboronic acids and Cupric Acetate. *Tetrahedron Lett.* **1998**, *39*, 2933; (b) Evans, D., Katz, J., West, T. Synthesis of Diaryl Ethers through the Copper-Promoted Arylation of Phenols with Arylboronic Acids. An Expedient Synthesis of Thyroxine. *Tetrahedron Lett.* **1998**, *39*, 2937; (c) Lam, P., Bonne, D., Vincent, G., Clark, C. Copper-promoted/catalyzed C-N and C-O Bond Cross-coupling with Vinylboronic Acid and Its Utilities. *Tetrahedron Lett.*, **2003**, *44*, 4927. (d) Chan, D., Monaco, K., Li, R., Bonne, D., Clark, C., Lam, P. Copper Promoted C-N and C-O Bond Cross-coupling with Phenyl and Pyridylboronates. *Tetrahedron Lett.*, **2003**, *44*, 3863; (e) Muci, A. R., Buchwald, S. L. Practical Palladium Catalysts for C-N and C-O Bond Formation. *Topics in Curr. Chem.*, **2002**, *219*, 131; (f) Hartwig, J. F. Approaches to catalyst discovery. New carbon-heteroatom and carbon-carbon bond formation. *Pure Appl. Chem.*, **1999**, *71*, 1416.
15. (a) Terrett, J. A., Cuthbertson, J. D., Shurtleff, V. W., MacMillan, D. W. C. Metallaphotoredox C–O Coupling of Alcohols with Aryl Halides. *Nature* **2015**, *524*, 330; (B) Corcoran, E. B., Pirnot, M. T., Lin, S., Dreher, S. D., DiRocco, D. A., Davies, I. W., Buchwald, S. L., MacMillan, D. W. C. Aryl Amination Using Ligand-Free Ni(II) Salts and Photoredox Catalysis. *Science* **2016**, *353*, 279.
16. E. R. Welin, C. C. Le, D. M. Arias-Rotondo, J. K. McCusker, D. W. C. MacMillan. Photosensitized, Energy Transfer-Mediated Organometallic Catalysis Through Electronically Excited Nickel(II). *Science* **2017**, *355*, 380.
17. Walsh, P. J., Kozlowski, M. C. Fundamentals of Asymmetric Catalysis (University Science Books, **2009**).
18. Huo, H.; Shen, X.; Wang, C.; Zhang, L.; Röse, P.; Chen, L.-A.; Harms, K.; Marsch, M.; Hilt, G.; Meggers, E. Asymmetric Photoredox Transition-Metal Catalysis Activated by Visible Light. *Nature* **2014**, *515*, 100.
19. Ma, J., Rosales, A. R., Huang, X., Harms, K., Riedel, R., Wiest, O., Meggers, E. Visible-Light-Activated Asymmetric  $\beta$ -C–H Functionalization of Acceptor-Substituted Ketones with 1,2-Dicarbonyl Compounds. *J. Am. Chem. Soc.*, **2017**, *139*, 17245.
20. Chen, S., Huang, X., Meggers, E., Houk, K. N. Origins of Enantioselectivity in Asymmetric Radical Additions to Octahedral Chiral-at-Rhodium Enolates: A Computational Study. *J. Am. Chem. Soc.*, **2017**, *139*, 17902.
21. Huang, X., Quinn, T. R., Harms, K., Webster, R. D., Zhang, L., Wiest, O., Meggers, E. Direct Visible-Light-Excited Asymmetric Lewis Acid Catalysis of Intermolecular [2+2] Photocycloadditions. *J. Am. Chem. Soc.*, **2017**, *139*, 9120.
22. (a) Tutkowski, B., Meggers, E., Wiest, O. Understanding Rate Acceleration and Stereoinduction of an Asymmetric Giese Reaction Mediated by a Chiral Rhodium Catalyst. *J. Am. Chem. Soc.*, **2017**, *139*, 8062; (b) Huang, X., Webster, R. D., Harms, K., Meggers, E. Asymmetric Catalysis with Organic Azides and Diazo Compounds Initiated by Photoinduced Electron Transfer. *J. Am. Chem. Soc.*, **2016**, *138*, 12636.
23. Huang, X., Quinn, T. R., Harms, K., Webster, R. D., Zhang, L., Wiest, O., Meggers, E. Direct Visible-Light-Excited Asymmetric Lewis Acid Catalysis of Intermolecular [2+2] Photocycloadditions. *J. Am. Chem. Soc.*, **2017**, *139*, 9120.
24. (a) Bauer, A.; Westkämper, F.; Grimme, S.; Bach, T. Catalytic Enantioselective Reactions Driven by Photoinduced Electron Transfer. *Nature* **2005**, *436*, 1139. (b) Tröster, A., Alonso, R., Bauer, A., Bach, T. Enantioselective Intermolecular [2+2] Photocycloaddition Reactions of 2(1H)-Quinolones Induced by Visible Light Irradiation. *J. Am. Chem. Soc.*, **2016**, *138*, 7808.
25. Jeon, Y. T., Lee, C.-P. & Mariano, P. S. Radical cyclization reactions of  $\alpha$ -silyl amine  $\alpha,\beta$ -unsaturated ketone and ester systems promoted by single electron transfer photosensitization. *J. Am. Chem. Soc.* **1991**, *113*, 8847.

26. Bertrand, S.; Hoffmann, N.; Pete, J.-P. Highly efficient and stereoselective radical addition of tertiary amines to electron-deficient alkenes-Application to the enantioselective synthesis of necine bases. *Eur. J. Org. Chem.*, **2000**, 2227.
27. Yoon, T. P.; Jacobsen, E. N. Privileged Chiral Catalysts. *Science* **2003**, *299*, 1691
28. Desimoni, G.; Faita, G.; Jørgensen, K. A. C<sub>2</sub>-Symmetric Chiral Bis(oxazoline) Ligands in Asymmetric Catalysis. *Chem. Rev.* **2011**, *111*, 284.
29. Xia, J. B.; Zhu, C.; Chen, C. Visible Light-Promoted Metal-Free C–H Activation: Diarylketone-Catalyzed Selective Benzylic Mono- and Difluorination. *J. Am. Chem. Soc.* **2013**, *135*, 17494.
30. Ding, W.; Lu, L.-Q.; Zhou, Q.-Q.; Wei, Y.; Chen, J.-R.; Xiao, W.-J. Bifunctional Photocatalysts for Enantioselective Aerobic Oxidation of  $\beta$ -Ketoesters. *J. Am. Chem. Soc.* **2017**, *139*, 63
31. Turro, N. J.; Ramamurthy, V.; Scaiano, J. C. *Modern Molecular Photochemistry of Organic Molecules*; University Science Books: Sausalito, California, **2010**.
32. Pérez-Prieto, P.; Galian, R. E.; Miranda, M. A. Diaryl Ketones as Photoactivators. *Mini-Reviews in Organic Chemistry*, **2006**, *3*, 117.
33. (a) Mostafa A. El-Sayed, M. A. Triplet state. Its radiative and nonradiative properties. *Acc. Chem. Res.*, **1968**, *1*, 8. (b) Lower, S. K. and M. A. El-Sayed, M. A. The Triplet State and Molecular Electronic Processes in Organic Molecules. *Chem. Rev.*, **1966**, *66*, 199; (c) Aloïse, S.; Ruckebusch, C.; Blanchet, L.; Réhault, J.; Buntinx, G.; Huvenne, J. -P. The Benzophenone S<sub>1</sub>(n, $\pi^*$ ) $\rightarrow$ T<sub>1</sub>(n, $\pi^*$ ) States Intersystem Crossing Reinvestigated by Ultrafast Absorption Spectroscopy and Multivariate Curve Resolution. *J. Phys. Chem. A* **2008**, *112*, 224.
34. (a) Dormán, G.; Nakamura, H.; Pulsipher, A.; Prestwich, G. D. The Life of Pi Star: Exploring the Exciting and Forbidden Worlds of the Benzophenone Phosphore. *Chem. Rev.* **2016**, *116*, 15284. (b) Ghazipura, M.; McGowan, R.; Arslan, A.; Hossain, T. Exposure to Benzophenone-3 and Reproductive Toxicity: A Systematic Review of Human and Animal Studies. *Reprod. Toxicol.* **2017**, *73*, 175. (c) Dumont, E.; Wibowo, M.; Roca-Sanjuán, D.; Garavelli, M.; Assfeld, X.; Monari, A. Resolving the Benzophenone DNA-Photosensitization Mechanism at QW/MM Level. *J. Phys. Chem. Lett.* **2015**, *6*, 576.
35. Zhao, J.; Wu, W.; Sun, J.; Guo, S. Triplet Photosensitizers: from Molecular Design to Applications. *Chem. Soc. Rev.* **2013**, *42*, 5323.
36. Selected reference: (a) Bertrand, S.; Glapski, C.; Hoffmann, N.; Pete, J.-P. Highly Efficient Photochemical Addition of Tertiary Amines to Electron Deficient Alkenes. Diastereoselective Addition to (5R)-5-Menthyloxy-2[5H]-furanone. *Tetrahedron Lett.* **1999**, *40*, 3169. (b) Manfrotto, C.; Mella, M.; Freccero, M.; Fagnoni, M.; Albini, A. Photochemical Synthesis of 4-Oxobutanol Acetals and of 2-Hydroxycyclobutanone Ketals. *J. Org. Chem.* **1999**, *64*, 5024. (c) Bertrand, S.; Hoffmann, N.; Pete, J.-P. Highly Efficient and Stereoselective Radical addition of Tertiary Amines to Electron Deficient Alkenes – Application to the Enantioselective Synthesis of Necine Bases. *Eur. J. Org. Chem.* **2000**, 2227. (d) Kamijo, S.; Hoshikawa, T.; Inoue, M. Photochemically Induced Radical Transformation of C(sp<sup>3</sup>)-H Bonds to C(sp<sup>3</sup>)-CN Bonds. *Org. Lett.* **2011**, *13*, 5928. (e) Hoshikawa, T.; Inoue, M. Photochemically Induced Radical Alkynylation of C(sp<sup>3</sup>)-H Bonds. *Org. Biomol. Chem.* **2013**, *11*, 164. (f) Tröster, A.; Alonso, R.; Bauer, A.; Bach, T. Enantioselective Intermolecular [2+2] Photocycloaddition Reactions of 2(1H)-Quinolones Induced by Visible Light Irradiation. *J. Am. Chem. Soc.* **2016**, *138*, 7808. (g) Tripathi, C. B.; Ohtani, T.; Corbett, M. T.; Ooi, T. Photoredox Ketone Catalysis for Direct C-H Imidation and Acyloxylation of Arenes. *Chem. Sci.* **2017**, *8*, 5622. (h) Kavarnos, G. J.; Turro, N. J. Photosensitization by reversible electron transfer: theories, experimental evidence, and examples. *Chem. Rev.* **1986**, *86*, 401. (i) Schaefer, C. G.; Peters, K. S. Picosecond dynamics of the photoreduction of benzophenone by trimethylamine. *J. Am. Chem. Soc.* **1980**, *102*, 7566.
37. Selected reference: (a) Ortica, F.; Romani, A.; Favaro, G. Light-induced hydrogen abstraction from isobutanol by thienyl phenyl dithienyl, and thienyl pyridyl ketones. *J. Phys. Chem. A*, **1999**, *103*, 1335. (b) Bhasikuttan, A. C.; Singh, A. K.; Palit, D. K.; Sapre, A. V.; Mittal, J. P. Laser flash photolysis studies on the monohydroxy derivatives of benzophenone. *J. Phys. Chem. A*, **1998**, *102*, 3470. (c) Wagner, P. J.; Kemppainen, A. E.; Schott, H. N. Effects of Ring Substituents on the Type II Photoreactions of Phenyl Ketones. How Interactions Between Nearby Excited Triplets Affect Chemical Reactivity. *J. Am. Chem. Soc.* **1973**, *95*, 5604.
38. (a) Castro, G. T.; Blanco, S. E.; Giordano, O. S. UV Spectral Properties of Benzophenone. Influence of Solvents and Substituents. *Molecules* **2000**, *5*, 424. (b) Vachev, V. D.; Frederick, J. H. The (n, $\pi^*$ ) Absorption Spectrum of Benzophenone. A New Model for The Excited State Dynamics. *Chem. Phys. Lett.* **1996**, *249*, 476.
39. (a) Stateman, L.M.; Nakafuku, K. M.; Nagib, D. A. Remote C–H Functionalization via Selective Hydrogen Atom Transfer. *Synthesis*, **2018**, *50*, 1569; (b) Zhang, J., Li, Y., Zhang, F., Hu, C., Chen, Y. Generation of Alkoxy Radicals by Photoredox Catalysis Enables Selective C(sp<sup>3</sup>)-H Functionalization under Mild Reaction Conditions. *Angew. Chem. Int. Ed.* **2016**, *55*, 1872; (c) Hu, A., Guo, J.-J., Pan, H., Tang, H., Gao, Z., Zuo, Z.  $\delta$ -Selective Functionalization of Alkanols Enabled by Visible-Light-Induced Ligand-to-Metal Charge Transfer. *J. Am. Chem. Soc.* **2018**, *140*, 1612; (d) Friedrich, J.; Schneider, D.; Bock, L.; Maichle-Mossmer, C.; Anwender, R. Cerium(IV) Neopentoxide Complexes. *Inorg. Chem.* **2017**, *56*, 8114; (e) Hu, A., Guo, J.-J., Pan, H., Zuo, Z. Selective functionalization of methane, ethane, and higher alkanes by cerium photocatalysis *Science* **2018**, *361*, 668; (f) (g)
40. (a) Chu, J. C. K.; Rovis, T. Amide-directed photoredox-catalysed C–C bond formation at unactivated sp<sup>3</sup> C–H bonds *Nature*, **2016**, *539*, 272; (b) Choi, G. J.; Zhu, Q.; Miller, D. C.; Gu, C. J.; Knowles, R. R. Catalytic alkylation of remote C–H bonds enabled by proton-coupled electron transfer. *Nature*, **2016**, *539*, 268
41. Newhouse, T.; Baran, P. S. If C–H bonds could talk: selective C–H bond oxidation. *Angew. Chem. Int. Ed.* **2011**, *50*, 3362.
42. White, M. C. Adding aliphatic C–H bond oxidations to synthesis. *Science* **335**, 807-809 (2012).
43. Beatty, J. W.; Stephenson, C. R. J. Amine Functionalization via Oxidative Photoredox Catalysis: Methodology Development and Complex Molecule Synthesis. *Acc. Chem. Res.* **2015**, *48*, 1474.
44. M. H. Shaw, V. W. Shurtleff, J. A. Terrett, D. W. C. MacMillan, Native functionality in triple catalytic cross-coupling: sp<sup>3</sup> C–H bonds as latent nucleophiles. *J. Science* **2016**, *352*, 1304.
45. For selected recent reference: (a) Tortajada, A.; Ninokata, R.; Martin, R. Ni-catalyzed Site-Selective Decarboxylation of 1,3-Dienes with CO<sub>2</sub>. *J. Am. Chem. Soc.* **2018**, *140*, 2050. (b) Yatham, V. R.; Shen, Y.; Martin, R. Catalytic Intermolecular



- Dicarbofunctionalization of Styrenes with CO<sub>2</sub> and Radical Precursors. *Angew. Chem. Int. Ed.* **2017**, *56*, 10915. (c) Shen, Y.; Cornella, J.; Juliá-Hernández, F.; Martín, R. Visible-Light-Promoted Atom Transfer Radical Cyclization of Unactivated Alkyl Iodides. *ACS Catal.*, **2017**, *7*, 409. (d) Juliá-Hernández, F.; Moragas, T.; Cornella, J.; Martín, R. Remote Carboxylation of Halogenated Aliphatic Hydrocarbons with Carbon Dioxide. *Nature* **2017**, *545*, 84.
46. Chow, Y. L.; Buono-Core, G. E. Photoreduction of Bis(acetylacetonato)nickel(II) by Triplet State Ketones. *J. Chem. Soc., Chem. Commun.*, **1985**, 592.
47. Chow, Y. L.; Buono-Core, G. E.; Lee, C. W. B.; Scaiano, J. C. Sensitized Photoreduction of Bis(acetylacetonato)nickel (II) by Triplet State Aromatic Ketones. *J. Am. Chem. Soc.* **1986**, *108*, 7620.
48. Masuda, Y.; Ishida, N.; Murakami, M. Aryl Ketones as Single-Electron Transfer Photoredox Catalysts in Nickel-Catalyzed Homocoupling of Aryl Halides. *Eur. J. Org. Chem.*, **2016**, *35*, 5822.
49. (a) Lyons, T. W.; Sanford, M. S. Palladium-Catalyzed Ligand-Directed C-H Functionalization Reactions. *Chem. Rev.* **2010**, *110*, 1147. (b) Wencel-Delord, J.; Dröge, T.; Liu, F.; Glorius, F.; Towards Mild Metal-Catalyzed C-H Bond Activation. *Chem. Soc. Rev.* **2011**, *40*, 4740. (c) Davies, H. M. L.; Morton, D. Recent Advances in C-H Functionalization. *J. Org. Chem.*, **2016**, *81*, 343. (d) He, J.; Wasa, M.; Chan, K. S. L.; Shao, Q.; Yu, J.-Q. Palladium-Catalyzed Transformations of Alkyl C-H Bonds. *Chem. Rev.* **2017**, *117*, 8754.
50. Shaw, M. H.; Shurtleff, V. W.; Terrett, J. A.; Cuthbertson, J. D.; MacMillan, D. W. C. Native Functionality in Triple Catalytic Cross-Coupling: sp<sup>3</sup> C-H Bonds as Latent Nucleophiles. *Science* **2016**, *352*, 1304.
51. Heitz, D. R.; Tellis, J. C.; Molander, G. A. Photochemical Nickel-Catalyzed C-H Arylation: Synthetic Scope and Mechanistic Investigations. *J. Am. Chem. Soc.* **2016**, *138*, 12715.
52. (a) Shields, B. J.; Doyle, A. G. Direct C(sp<sup>3</sup>)-H Cross Coupling Enabled by Catalytic Generation of Chlorine Radicals. *J. Am. Chem. Soc.* **2016**, *138*, 12719; (b) Ackerman, L. K. G.; Alvarado, J. I. M.; Doyle, A. G. Direct C-C Bond Formation from Alkanes Using Ni-Photoredox Catalysis. *J. Am. Chem. Soc.*, DOI: 10.1021/jacs.8b09191.
53. For selected reviews in visible light photoredox catalysis: (a) Fabry, D. C.; Rueping, M. Merging Visible Light Photoredox Catalysis with Metal Catalyzed C-H Activations: On the Role of Oxygen and Superoxide Ions as Oxidants. *Acc. Chem. Res.* **2016**, *49*, 1969. (b) Hopkinson, M. N.; Tlahuext-Aca, A.; Glorius, F. Merging Visible Light Photoredox and Gold Catalysis. *Acc. Chem. Res.* **2016**, *49*, 2261. (c) Kärkäs, M. D.; Porco, J. A.; Stephenson, C. R. J. photochemical Approaches to Complex Chemotypes: Applications in Natural Product -synthesis. *Chem. Rev.*, **2016**, *116*, 9683. (d) Prier, C. K.; Rankic, D. A.; MacMillan, D. W. C. Visible Light Photoredox Catalysis with Transition Metal Complexes: Applications in Organic Synthesis. *Chem. Rev.* **2013**, *113*, 5322.
54. For the use of bifunctional photocatalysts, see: Ding, W.; Lu, L.-Q.; Zhou, Q.-Q.; Wei, Y.; Chen, J.-R.; Xiao, W.-J. Bifunctional Photocatalysts for Enantioselective Aerobic Oxidation of β-Ketoesters. *J. Am. Chem. Soc.* **2017**, *139*, 63. (b) Huo, H.; Shen, X.; Wang, C.; Zhang, L.; Röse, P.; Chen, L.-A.; Harms, K.; Marsch, M.; Hilt, G.; Meggers, E. Asymmetric Photoredox Transition-Metal Catalysis Activated by Visible Light. *Nature* **2014**, *515*, 100.
55. For ketone-catalyzed sp<sup>3</sup> C-H functionalization using visible light sources: (a) Xia, J.-B.; Zhu, C.; Chen, C. Visible Light-Promoted Metal-Free C-H Activation: Diarylketone-Catalyzed Selective Benzylic Mono- and Difluorination. *J. Am. Chem. Soc.* **2013**, *135*, 17494. (b) Xia, J.-B.; Zhu, C.; Chen, C. Visible Light-Promoted Metal-Free sp<sup>3</sup>-C-H Fluorination. *Chem. Commun.*, **2014**, *50*, 11701. (c) Paul, S.; Guin, J. Radical C(sp<sup>3</sup>)-H Alkenylation, Alkynylation and Allylation of Ethers and Amides Enabled by Photocatalysis. *Green Chem.* **2017**, *19*, 2530.
56. For reviews on dual catalysis in photochemical events: (a) Twilton, J.; Le, C.; Zhang, P.; Shaw, M. H.; Evans, R. W.; MacMillan, D. W. C. The Merger of Transition Metal and Photocatalysis. *Nat. Rev. Chem.* **2017**, *1*, 0052. (b) Levin, M. D.; Kim, S.; Toste, F. D. Photoredox Catalysis Unlocks Single-Electron Elementary Steps in Transition Metal Catalyzed Cross-Coupling. *ACS Cent. Sci.* **2016**, *2*, 293. (c) Hopkinson, M. N.; Sahoo, B.; Li, J.-L.; Glorius, F. Dual Catalysis Sees the Light: Combining Photoredox with Organo-, Acids, and Transition-Metal Catalysis. *Chem. Eur. J.* **2014**, *20*, 3874. (d) Skubi, K. L.; Blum, T. R.; Yoon, T. P. dual catalysis strategies in photochemical synthesis. *Chem. Rev.* **2016**, *116*, 10035. (e) Marzo, L.; Pagore, S. K.; Reiser, O.; König, B. Visible-Light Photocatalysis: Does It Make A Difference in Organic Synthesis? *Angew. Chem. Int. Ed.* **2018**, *57*, 2.
57. For recent reviews on organic photocatalysts, see: (a) Romero, N. A.; Nicewicz, D. A. Organic Photoredox Catalysis. *Chem. Rev.*, **2016**, *116*, 10075. (b) Majek, M.; von Wangelin, A. J. Mechanistic Perspectives on Organic Photoredox Catalysis for Aromatic Substitutions. *Acc. Chem. Res.*, **2016**, *49*, 2316. (c) Chen, C. The Past, Present, and Future of the Yang Reaction. *Org. Biomol. Chem.* **2016**, *14*, 8641. (d) Ravelli, Fagnoni, M.; Albini, A. Photoorganocatalysis. What for? *Chem. Soc. Rev.*, **2013**, *42*, 97. (e) Fagnoni, M.; Dondi, D.; Ravelli, D.; Albini, A. Photocatalysis for the Formation of the C-C Bond. *Chem. Rev.* **2007**, *107*, 2725.
58. For non-noble metal-based photocatalysts in arylation reactions initiated by SET: (a) Luo, J.; Zhang, J. Donor-Acceptor Fluorophores for Visible-Light-Promoted Organic Synthesis: Photoredox/Ni Dual Catalytic C(sp<sup>3</sup>)-C(sp<sup>2</sup>) Cross-Coupling. *ACS Catal.*, **2016**, *6*, 873. (b) McTiernan, C. D.; Leblanc, X.; Scaiano, J. C. Heterogeneous Titinia-Photoredox/Nickel Dual Catalysis: Decarboxylative Cross-Coupling of Carboxylic Acids with Aryl Iodides. *ACS Catal.*, **2017**, *7*, 2171. (c) Matsui, J. K.; Molander, G. A. Direct α-Arylation/Heteroarylation of 2-Trifluoroboratochromanones via Photoredox/Nickel Dual Catalysis. *Org. Lett.* **2017**, *19*, 436. (d) Huang, H.; Li, X.; Yu, C.; Zhang, Y.; Mariano, P. S.; Wang, W. Visible-Light-Promoted Nickel- and Organic-Dye-Co-Catalyzed Formylation Reaction of Aryl Halides and Triflates and Vinyl bromides with Diethoxyacetic Acid as A Formyl Equivalent. *Angew. Chem. Int. Ed.* **2017**, *56*, 1500.
59. Clark, W. D. K.; Litt, A. D.; Steel, C. Triplet Lifetimes of Benzophenone, Acetophenone, and Triphenylene in Hydrocarbons. *J. Am. Chem. Soc.* **1969**, *91*, 5413.
60. For acidity of ketyl radicals: (a) Kalinowski, M. K.; Grabowski, Z. R.; Pakula, B. Reactivity of Ketyl Free Radicals. Part 1.-Acid Dissociation of Aromatic Ketyls and Pinacols. *Trans. Faraday. Soc.*, **1966**, *62*, 918. (b) Lund, T.; Wayner, D. D. M. Jonsson, M.; Larsen, A.; Daasbjerg, K. Oxidation Potentials of α-Hydroxyl Radicals in Acetonitrile Obtained by Photomodulated Voltammetry. *J. Am. Chem. Soc.* **2001**, *123*, 12590. (b) Tang, X.; Studer, A. Alkene 1,2-Difunctionalization by Radical Alkenyl Migration. *Angew. Chem. Int. Ed.* **2018**, *57*, 814.

61. Leigh, W. J.; Arnold, D. R.; Humphreys, R. W. R.; Wong, P. C. Merostabilization in Radical Ions, Triplets, and Biradicals. 4. Substituent Effects on the Half-Wave Reduction Potentials and  $n, \pi^*$  Triplet Energies of Aromatic Ketones. *Can. J. Chem.* **1980**, *58*, 2537.
62. For  $E_{\text{red}}[\text{Ni}^{\text{I}}/\text{Ni}^{\text{0}}]$  vs  $\text{Ag}/\text{AgNO}_3$ , see: (a) Börjesson, M.; Moragas, T.; Martin, R. Ni-Catalyzed Carboxylation of Unactivated Alkyl Chlorides with  $\text{CO}_2$ . *J. Am. Chem. Soc.* **2016**, *138*, 7504. For  $E_{\text{red}}[\text{Ni}^{\text{I}}/\text{Ni}^{\text{0}}]$  vs SCE, see: (b) Klein, A.; Kaiser, A.; Sarkar, B.; Wanner, M.; Fiedler, J. The Electrochemical Behaviour of Organonickel Complexes: Mono-, Di- and Trivalent Nickel. *Eur. J. Inorg. Chem.* **2007**, 965. (c) Cannes, C.; Labbé, E.; Durandetti, M.; Devaud, M.; Nédélec, J. Y. Nickel-Catalyzed Electrochemical Homo coupling of Alkenyl Halides: Rates and Mechanisms. *J. Electroanal. Chem.* **1996**, *412*, 85.
63. Selected reference: (a) Demeter, A.; Horváth, K.; Böör, K.; Molnár, L.; Soós, T.; Lendvay, G. Substituent effect on the photoreduction kinetics of benzophenone. *J. Phys. Chem. A*, **2013**, *117*, 10196; (b) Jacques, P.; Lougnot, D. J.; Fouassier, J. P.; Scaiano, J. C. Location Effects upon the Kinetic Behavior of Benzophenone in Micellar Solution. *Chem. Phys. Lett.* **1986**, *127*, 469. (c) refs 50, 70 and 86.
64. See for example: (a) Zhang, X.; Wang, C.-J.; Liu, L.-H.; Jiang, Y.-B. *J. Phys. Chem. B*, **2002**, *106*, 12432. (b) Wagner, P. J.; Truman, R. J.; Scaiano, J. C. *J. Am. Chem. Soc.* **1985**, *107*, 7093. (c) Wintgens, V.; Valat, P.; Kossanyi, J.; Demeter, A.; Biczók, L.; Bérces, T. *J. Photochem. Photobiol. A*, **1996**, *93*, 109.
65. For a non-photocatalytic C–H arylation of THF requiring stoichiometric amounts of di-*tert*-butyl peroxide: Liu, D.; Liu, C.; Li, H.; Lei, A. Direct Functionalization of Tetrahydrofuran and 1,4-Dioxane: Nickel-Catalyzed Oxidative  $\text{C}(\text{sp}^3)\text{-H}$  Arylation. *Angew. Chem. Int. Ed.* **2013**, *52*, 4453.
66. For a discussion on the intriguing role of oxygen in Ir photoredox/nickel catalysis: Oderinde, M. S.; Varela-Alvarez, A.; Aquila, B.; Robbins, D. W. Effects of Molecular Oxygen, Solvent, and Light on Iridium-Photoredox/Nickel Dual-Catalyzed Cross-Coupling Reactions. *J. Org. Chem.* **2015**, *80*, 7642.
67. (a) Tasker, S. Z.; Standley, E. A.; Jamison, T. F. Recent Advances in Homogeneous Nickel Catalysis. *Nature* **2014**, *509*, 299-309. (b) Diederich, F.; Meijere, A., Eds. *Metal-Catalyzed Cross-Coupling Reactions*; Wiley-VCH: Weinheim, **2004**.
68. Barry, J. T.; Berg, D. J.; Tyler, D. R. Radical Cage Effects; Comparison of Solvent Bulk Viscosity and Microviscosity in Predicting the Recombination Efficiencies of Radical Cage Pairs. *J. Am. Chem. Soc.* **2016**, *138*, 9389.
69. Nielsen, M. K.; Shields, B. J.; Liu, J.; Williams, M. J.; Zacuto, M. J.; Doyle, A. G. Mild, Redox-Neutral Formylation of Aryl Chlorides via Photocatalytic Generation of Chlorine radicals. *Angew. Chem. Int. Ed.* **2017**, *56*, 7191.
70. For an elegant formation of quaternary centers by Ir photoredox initiated by SET from stoichiometric organotrifluoroborates: Primer, D. N.; Molander, G. A. Enabling the Cross-Coupling of Tertiary Organoboron Nucleophiles through Radical-mediated Alkyl Transfer. *J. Am. Chem. Soc.* **2017**, *139*, 9847.
71. For photoreduction of benzophenone in toluene and cyclohexane, see: Walling, C.; Gibian, M. J. Hydrogen Abstraction Reactions by the Triplet States of ketones. *J. Am. Chem. Soc.* **1965**, *87*, 3361.
72. Cernak, T.; Dykstra, K. D.; Tyagarajan, S.; Vachal, P.; Krska, S. W. The Medicinal Chemist's Toolbox for Late Stage Functionalization of drug-like molecules. *Chem. Soc. Rev.* **2016**, *45*, 546.
73. Echeverria, V.; Zeitlin, R. Cotinine: A Potential New Therapeutic Agent against Alzheimer's Disease. *CNS Neuroscience & Therapeutics* **2012**, *18*, 517.
74. According to eBioChem, USBiological, GENTAUR or Toronto Research Chemicals, **57** costs approximately 60\$/mg. The utilization of our protocol, however, allows for preparing **57** at 10 mmol scale from cheap and simple precursors.
75. Modest results were found when using commonly employed Pyrox, Box or Phox-type ligands. For a recent enantioselective Ni/photoredox decarboxylative arylation, see: Zuo, Z.; Cong, H.; Choi, L. J.; Fu, G. C.; MacMillan, D. W. C. Enantioselective Decarboxylative Arylation of  $\alpha$ -Amino Acids via the Merger of Photoredox and Nickel Catalysis. *J. Am. Chem. Soc.* **2016**, *138*, 1832.
76. For a recent technique based on Ir-polypyridyl complexes: (a) Le, C.; Liang, Y.; Evans, R. W.; Li, X. & MacMillan, D. W. C. Selective  $\text{sp}^3$  C–H Alkylation via Polarity-Match-Based Cross-Coupling. *Nature* **2017**, *547*, 79-83. (b) For a single example of an alkylation event in moderate yields, see ref. 69.
77. Choi, J.; Fu, G. C. Transition Metal-Catalyzed Alkyl-Alkyl Bond Formation: Another Dimension in Cross-Coupling Chemistry. *Science* **2017**, *356*, 152.
78. Xue, X.-S.; Ji, P.; Zhou, B.; Cheng, J.-P. The Essential Role of Bond Energetics in C-H Activation/Functionalization. *Chem. Rev.* **2017**, *117*, 8622.
79. (a) ref. 78. (b) Tsou, T. T.; Kochi, J. K. Mechanism of Oxidative Addition. Reaction of Nickel(0) Complexes with Aromatic Halides. *J. Am. Chem. Soc.* **1979**, *101*, 6319. (c) Funes-Ardoiz, I.; Nelson, D. J.; Maseras, F. Halide Abstraction Competes with Oxidative Addition in the Reactions of Aryl Halides with  $[\text{Ni}(\text{PMe}_n\text{Ph}_{(3-n)})_4]$ . *Chem. Eur. J.* **2017**, *23*, 16728.
80. (a) Deneš, F.; Pichowicz, M.; Povie, G.; Renaud, P. Thiyl Radicals in Organic Synthesis. *Chem. Rev.* **2014**, *114*, 2587. (b) Simmons, E. M.; Hartwig, J. F. On the Interpretation of Deuterium Kinetic Isotope Effects in C-H Bond Functionalizations by Transition-Metal Complexes. *Angew. Chem. Int. Ed.* **2012**, *51*, 3066.
81. For the generation of halogen radical from high valent Ni complex, see: Mondal, P.; Pirovano, P.; Das, A.; Farquhar, E. R.; McDonald, A. R. Hydrogen Atom Transfer by A High-Valent Nickel Chloride Complex. *J. Am. Chem. Soc.* **2018**, *140*, 1834.
82. These results are in sharp contrast to a recent arylation of toluene under UV irradiation, see: Ishida, N.; Masuda, Y.; Ishikawa, N.; Murakami, M. Cooperative of A Nickel-Bipyridine Complex with Light for Benzylic C-H Arylation of Toluene Derivatives. *Asian. J. Org. Chem.* **2017**, *6*, 669.
83. Although the site-selectivity observed for **42** or **43** favoring secondary vs primary  $\text{sp}^3$  C–H sites may argue against a  $\sigma$ -bond metathesis regime, we cannot rigorously rule out this pathway due to the reversibility of high valent Ni–C bonds. For a computational study, see: Gutierrez, O.; Tellis, J. C.; Primer, D. N.; Molander, G. A. Nickel-Catalyzed Cross-Coupling of Photoredox-Generated Radicals: Uncovering a General Manifold for Stereoconvergence in Nickel-Catalyzed Cross-Couplings. *J. Am. Chem. Soc.* **2015**, *137*, 4896.

84. For a fundamental study of photochemical properties of bipyridine ligated Ni(II) complex, see: Shields, B. J.; Kudisch, B.; Scholes, G. D.; Doyle, A. G. Long-Lived Charge-Transfer States of Ni(II) Aryl Halide Complexes Facilitate Bimolecular Photoinduced Electron Transfer. *J. Am. Chem. Soc.* **2018**, *140*, 3035.
85. It is worth considering the quenching rate of triplet benzophenone by Ni(acac)<sub>2</sub> ( $2.9 \times 10^9 M^{-1} sec^{-1}$  in MeOH) and *n*Pr<sub>2</sub>O ( $9.2 \times 10^6 M^{-1} sec^{-1}$  in benzene). See: (a) Guttenplan, J.; Cohen, S. G. Triplet Energies, Reduction Potential, and Ionization potentials in Carbonyl-Donor Partial Charge-Transfer Interactions. *J. Am. Chem. Soc.* **1972**, *94*, 4040. (b) ref. 10b. Although tentative, these quenching rates might be responsible for the observed efficiency of our Ni/A1 regime.

## 4.9. Experimental Section

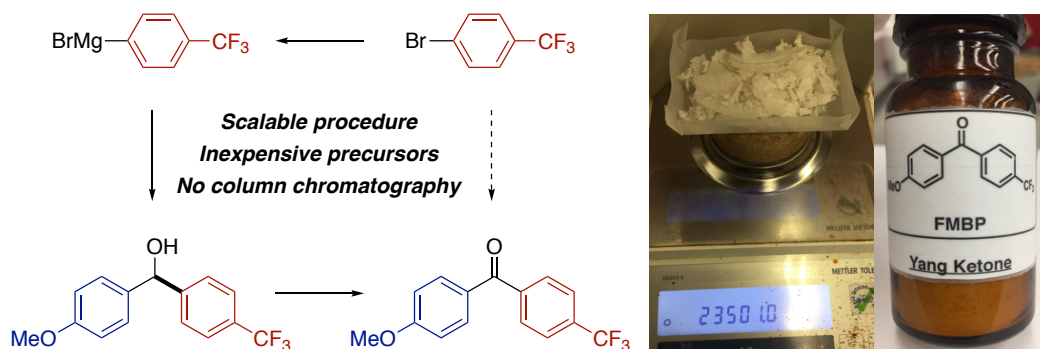
### 4.9.1 General considerations

**Reagents:** All of the reactions were carried out in Schlenk tubes. Commercially available aryl, alkyl halides and C–H precursors were used without further purification. Ni(acac)<sub>2</sub> (95% purity) was purchased from Strem and Na<sub>2</sub>CO<sub>3</sub>, 4,4'-Di-tert-butyl-2,2'-dipyridyl (**L2**), 5,5'-Dimethyl-2,2'-dipyridyl (**L4**) were purchased from Aldrich. Anhydrous Benzene, Tetrahydrofuran (THF) and other C-H precursors were purchased from Aldrich, Acros, TCI or Alfa Aesar, and used as received.

**Analytical Methods.** <sup>1</sup>H NMR, <sup>13</sup>C NMR and <sup>19</sup>F NMR spectra are included for all compounds. <sup>1</sup>H NMR, <sup>13</sup>C NMR and <sup>19</sup>F NMR spectra were recorded on a Bruker 300 MHz, a Bruker 400 MHz or a Bruker 500 MHz at 20 °C. All <sup>1</sup>H NMR spectra are reported in parts per million (ppm) downfield of TMS and were measured relative to the signals for CHCl<sub>3</sub> (7.26 ppm). All <sup>13</sup>C NMR spectra were reported in ppm relative to residual CHCl<sub>3</sub> (77.16 ppm) and were obtained with <sup>1</sup>H decoupling. Coupling constants, *J*, are reported in hertz (Hz). In case of diastereisomeric or regioisomeric mixtures, the corresponding ratio was measured by NMR of the crude product. Melting points were measured using open glass capillaries in a Büchi B540 apparatus. Infrared spectra were recorded on a Bruker Tensor 27. Mass spectra were recorded on a Waters LCT Premier spectrometer. Specific optical rotation measurements were carried out on a Jasco P-1030 model polarimeter equipped with a PMT detector using the Sodium line at 589 nm. Gas chromatographic analyses were performed on HewlettPackard 6890 gas chromatography instrument with a FID detector using 25m x 0.20 mm capillary column with cross-linked methyl siloxane as the stationary phase. Flash chromatography was performed with EM Science silica gel 60 (230-400 mesh) and using KMnO<sub>4</sub> TLC stain. UV-Vis measurements were carried out on a Shimadzu UV-1700PC spectrophotometer equipped with a photomultiplier detector, double beam optics and D2 and W light sources. EPR signals were recorded with EMX Micro EPR spectrometer. The yields reported in Tables 1-4 correspond to isolated yields and represent an average of at least two independent runs. The procedures described in this section are representative. Thus, the yields may differ slightly from those given in the tables of the manuscript.

### 4.9.2. Synthesis of Triplet Catalyst A1 and Starting Materials

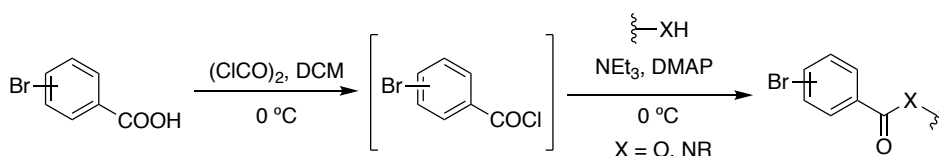
#### 4.9.2.1 Scalable Synthesis of the Diary Ketone Catalyst



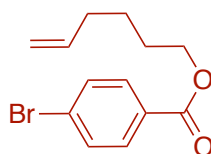
An oven-dried 500 mL flask containing a stirring bar was charged with Mg (150 mmol, 1.5 eq, 3.65 g). The flask was then evacuated and back-filled with argon (this sequence was repeated three times). Then, 4-bromobenzotrifluoride (100 mmol, 1.0 eq, 14.0 mL) was added dropwise followed by addition of THF (200 mL, 2.0 M) under an argon flow (if the reaction was not initiated, small amount of I<sub>2</sub> and gentle heating was necessary), and the reaction was stirred for additional

3h. This solution was added dropwise to a flask containing a solution of 4-methoxybenzaldehyde (100 mmol, 12.2 mL) in THF (100 mL) in a dry-ice/acetone under an argon flow. The reaction was allowed to warm up to room temperature and stirred for 4h, at which time the reaction was carefully quenched with  $\text{NH}_4\text{Cl}$  (sat.) until a clear solution was observed. Then, the aqueous phase was abstracted with ethyl acetate and the combining organic phase was washed with brine, dried over anhydrous  $\text{MgSO}_4$  and the solvent was evaporated. The crude product was directly diluted with DCM (100 mL) and then slowly added to a mixture of pyridinium chlorochromate (200 mmol, 2.0 eq, 43.1 g) and silica gel (35.0 g) in DCM (100 mL). After the addition, the reaction was monitored by TLC. Once completion was observed, the reaction mixture was filtered through a short pad of silica gel several times until a clear light-yellow solution was obtained. The organic solvent was then evaporated under vacuum, and the crude reaction mixture was directly recrystallized in  $\text{CH}_2\text{Cl}_2$ /hexanes to provide the title compound as a white, crystalline solid (83.9 mmol, 23.5 g, 84% yield).  $^1\text{H}$  NMR (400 MHz,  $\text{CDCl}_3$ )  $\delta$  7.85-7.80 (m, 4H), 7.74 (d,  $J = 8.0$  Hz, 2H), 7.00-6.96 (m, 2H), 3.90 (s, 3H) ppm.  $^{13}\text{C}$  NMR (101 MHz,  $\text{CDCl}_3$ )  $\delta$  194.40, 163.88, 141.68, 133.41 (q,  $J_{\text{C-F}} = 32.7$  Hz), 132.77, 129.93, 129.52, (q,  $J_{\text{C-F}} = 3.8$  Hz), 123.88 (q,  $J_{\text{C-F}} = 273.6$  Hz), 113.97, 55.71 ppm.  $^{19}\text{F}$  NMR (376 MHz,  $\text{CDCl}_3$ )  $\delta$  -63.05 ppm.<sup>1</sup>

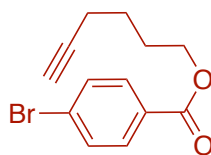
#### 4.9.2.2. Synthesis of the starting materials



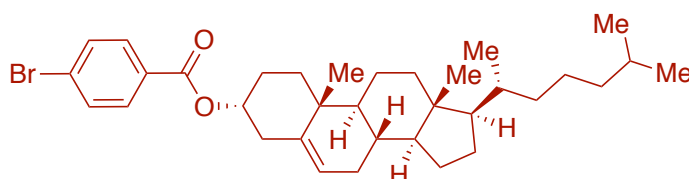
**General conditions:** To a stirred solution of bromobenzoic acid (7 mmol, 1.0 eq) in DCM (0.35 M, 20 mL) and DMF (0.1 mL) under argon was added oxalyl chloride (9.1 mmol, 1.3 eq) by syringe. The reaction mixture was stirred for 1 h at 0 °C and then warmed up to room temperature. After 3 h, a clear light-yellow solution was obtained and all of the volatiles were removed under vacuum. The residue was then dissolved in DCM (10 mL) and added to a mixture of an alcohol or amine nucleophile (5 mmol, 1.0 eq), DMAP (0.5 mmol, 0.1 eq) and  $\text{Et}_3\text{N}$  (10 mmol, 2.0 eq) in DCM (10 mL). The reaction was allowed to stirred overnight at room temperature. Then, the mixture was quenched upon addition of  $\text{NH}_4\text{Cl}$  (aq. 10%), and extracted with DCM (3x). The organic phase was washed with brine, concentrated and purified by silica gel flash chromatography to give the corresponding substituted aryl bromide.



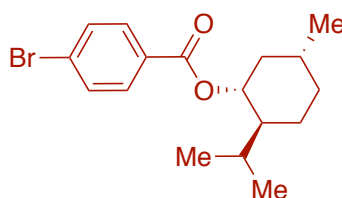
**hex-5-yn-1-yl 4-bromobenzoate (6s):** Following the general conditions, 4-bromobenzoic acid and hex-5-en-1-ol were used. The title compound was obtained in 93% as colorless oil.  $^1\text{H}$  NMR (300 MHz,  $\text{CDCl}_3$ )  $\delta$  7.89 (d,  $J = 8.4$  Hz, 2H), 7.57 (d,  $J = 8.4$  Hz, 2H), 5.88-5.74 (m, 1H), 5.06-4.96 (m, 2H), 4.34-4.29 (t,  $J = 6.3$  Hz, 2H), 2.15-2.09 (m, 2H), 1.80-1.73 (m, 2H), 1.59-1.49 (m, 2H) ppm.  $^{13}\text{C}$  NMR (75 MHz,  $\text{CDCl}_3$ )  $\delta$  166.01, 138.37, 131.79, 131.20, 129.47, 128.04, 115.07, 65.29, 33.42, 28.24, 25.40 ppm. IR (neat,  $\text{cm}^{-1}$ ): 3010, 2968, 2951, 1715, 1615, 1484, 1266, 1173, 946. HRMS *calcd.* for  $(\text{C}_{13}\text{H}_{16}\text{BrO}_2)$   $[\text{M}+\text{H}]^+$ : 283.0155, *found* 283.0149.



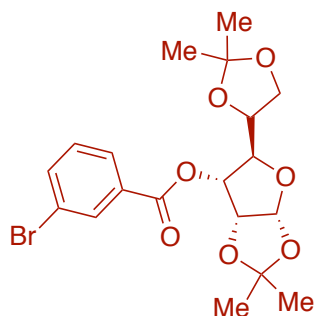
**hex-5-yn-1-yl 4-bromobenzoate (7s):** Following the general conditions, 4-bromobenzoic acid and hex-5-yn-1-ol were used. The title compound was obtained in 95% as colorless oil.  $^1\text{H}$  NMR (300 MHz,  $\text{CDCl}_3$ )  $\delta$  7.91-7.87 (m, 2H), 7.59-7.54 (m, 2H), 4.33 (t,  $J = 6.6$  Hz, 2H), 3.27 (dt,  $J = 6.9, 2.4$  Hz, 2H), 1.97 (t,  $J = 2.4$  Hz, 1H), 1.94-1.85 (m, 2H), 1.73-1.63 (m, 2H) ppm.  $^{13}\text{C}$  NMR (75 MHz,  $\text{CDCl}_3$ )  $\delta$  165.95, 131.80, 131.20, 129.33, 128.11, 83.89, 68.98, 64.84, 27.82, 25.13, 18.23 ppm. IR (neat,  $\text{cm}^{-1}$ ): 3301, 2952, 1715, 1590, 1483, 1398, 1266, 1173. HRMS *calcd.* for ( $\text{C}_{13}\text{H}_{14}\text{BrO}_2$ )  $[\text{M}+\text{H}]^+$ : 281.0172, *found* 281.0167.



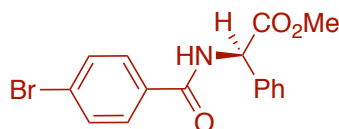
**(3*S*,8*S*,9*S*,10*R*,13*R*,14*S*,17*R*)-10,13-dimethyl-17-((*R*)-6-methylheptan-2-yl)-2,3,4,7,8,9,10,11,12,13,14,15,16,17-tetradecahydro-1*H*-cyclopenta[*a*]phenanthren-3-yl 4-bromobenzoate (26s):** Following the general conditions, 4-bromobenzoic acid and Cholesterol were used. The title compound was obtained in 90% as white solid. Mp 187-188 °C.  $^1\text{H}$  NMR (300 MHz,  $\text{CDCl}_3$ )  $\delta$  7.90 (d,  $J = 8.4$  Hz, 2H), 7.57 (d,  $J = 8.4$  Hz, 2H), 5.42 (d,  $J = 4.2$  Hz, 1H), 4.90-4.79 (m, 1H), 4.45 (d,  $J = 7.8$  Hz, 2H), 2.04-1.75 (m, 6H), 1.66-0.96 (m, 23H), 0.93-0.86 (m, 9H), 0.69 (s, 3H) ppm.  $^{13}\text{C}$  NMR (75 MHz,  $\text{CDCl}_3$ )  $\delta$  165.40, 139.65, 131.73, 131.24, 129.88, 127.93, 123.06, 75.09, 56.84, 56.29, 50.19, 42.47, 39.88, 39.67, 38.32, 37.15, 36.79, 36.34, 35.95, 32.08, 32.02, 28.39, 28.17, 28.00, 24.45, 23.99, 22.98, 22.72, 21.20, 19.52, 18.88, 12.02 ppm.  $[\alpha]_{\text{D}}^{26} = -2.9$  ( $c = 0.0950$ ,  $\text{CH}_2\text{Cl}_2$ ). IR (neat,  $\text{cm}^{-1}$ ): 2940, 2903, 2867, 2848, 1705, 1588, 1271, 1103. HRMS *calcd.* for ( $\text{C}_{34}\text{H}_{50}\text{BrO}_2$ )  $[\text{M}+\text{H}]^+$ : 569.2989, *found* 569.2974.



**(1*R*,2*S*,5*R*)-2-isopropyl-5-methylcyclohexyl 4-bromobenzoate (27s):** Following the general conditions, 4-bromobenzoic acid and (1*R*,2*S*,5*R*)-(-)-Menthol were used. The title compound was obtained in 92% as colorless oil.  $^1\text{H}$  NMR (300 MHz,  $\text{CDCl}_3$ )  $\delta$  7.92-7.88 (m, 2H), 7.59-7.55 (m, 2H), 4.92 (dt,  $J = 10.8, 4.5$  Hz, 1H), 2.14-2.07 (m, 1H), 1.97-1.86 (m, 1H), 1.77-1.67 (m, 2H), 1.62-1.474 (m, 2H), 1.19-1.03 (m, 2H), 0.94-0.90 (m, 7H), 0.78 (d,  $J = 6.9$  Hz, 3H) ppm.  $^{13}\text{C}$  NMR (75 MHz,  $\text{CDCl}_3$ )  $\delta$  165.49, 131.75, 131.23, 129.88, 127.91, 75.35, 47.38, 41.06, 34.42, 31.58, 26.69, 23.79, 22.17, 20.88, 16.67 ppm.  $[\alpha]_{\text{D}}^{26} = -76.1$  ( $c = 0.1000$ ,  $\text{CH}_2\text{Cl}_2$ ). IR (neat,  $\text{cm}^{-1}$ ): 2954, 2869, 1714, 1589, 1265, 1172, 1101, 1012. HRMS *calcd.* for ( $\text{C}_{17}\text{H}_{22}\text{BrO}_2$ )  $[\text{M}+\text{H}]^+$ : 337.0798, *found* 337.0792.



**(3aR,5R,6R,6aR)-5-((R)-2,2-dimethyl-1,3-dioxolan-4-yl)-2,2-dimethyltetrahydrofuro[2,3-d][1,3]dioxol-6-yl 3-bromobenzoate (28s)**: Following the general conditions, 3-bromobenzoic acid and 1,2:5,6-Bis-O-(1-methylethylidene)- $\alpha$ -D-Glucufuranose were used. The title compound was obtained in 90% as colorless oil.  $^1\text{H}$  NMR (300 MHz,  $\text{CDCl}_3$ )  $\delta$  8.17 (t,  $J = 1.5$  Hz, 1H), 7.98 (dt,  $J = 7.8, 1.5$  Hz, 1H), 7.71 (ddd,  $J = 7.8, 2.1, 1.2$  Hz, 1H), 7.34 (t,  $J = 7.8$  Hz, 1H), 5.88 (d, 1H), 5.07-5.02 (m, 1H), 4.97-4.94 (m, 1H), 4.53-4.28 (m, 2H), 4.14-4.09 (m, 1H), 3.98-3.94 (m, 1H), 1.55 (s, 3H), 1.41 (s, 3H), 1.33 (s, 6H) ppm.  $^{13}\text{C}$  NMR (75 MHz,  $\text{CDCl}_3$ )  $\delta$  164.47, 136.40, 132.94, 131.51, 130.16, 128.49, 122.66, 113.41, 110.16, 104.41, 77.93, 77.90, 75.43, 73.93, 66.11, 26.86, 26.82, 26.53, 25.10 ppm.  $[\alpha]_{\text{D}}^{26} = +111.7$  ( $c = 0.0850$ ,  $\text{CH}_2\text{Cl}_2$ ). IR (neat,  $\text{cm}^{-1}$ ): 2986, 1726, 1571, 1372, 1253, 1214, 1066, 1015. HRMS *calcd.* for  $(\text{C}_{19}\text{H}_{23}\text{BrNaO}_7)$   $[\text{M}+\text{Na}]^+$ : 465.0519, *found* 465.0518.



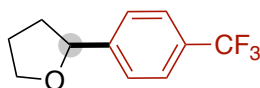
**methyl (R)-2-(4-bromobenzamido)-2-phenylacetate (29s)**: Following the general conditions, 4-bromobenzoic acid and (*R*)-(-)-2-Phenylglycine methyl ester hydrochloride (with 3.0 eq of  $\text{Et}_3\text{N}$ ) were used. The title compound was obtained in 85% as white solid. Mp 136-137  $^\circ\text{C}$ .  $^1\text{H}$  NMR (300 MHz,  $\text{CDCl}_3$ )  $\delta$  7.69-7.66 (m, 2H), 7.58-7.53 (m, 2H), 7.44-7.33 (m, 5H), 7.18 (d,  $J = 6.6$  Hz, 1H), 5.75 (d,  $J = 6.9$  Hz, 1H), 3.76 (s, 3H) ppm.  $^{13}\text{C}$  NMR (75 MHz,  $\text{CDCl}_3$ )  $\delta$  171.54, 165.73, 136.44, 132.52, 131.95, 129.19, 128.90, 128.83, 127.46, 126.75, 56.98, 53.11 ppm.  $[\alpha]_{\text{D}}^{26} = -48.2$  ( $c = 0.0900$ ,  $\text{CH}_2\text{Cl}_2$ ). IR (neat,  $\text{cm}^{-1}$ ): 3322, 1736, 1639, 1590, 1530, 1482, 1183, 1066. HRMS *calcd.* for  $(\text{C}_{16}\text{H}_{14}\text{BrNNaO}_3)$   $[\text{M}+\text{Na}]^+$ : 370.0049, *found* 370.0048.

### 4.9.3. Preparative scope for metallatriplet catalysis

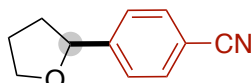
#### 4.9.3.1. $sp^3$ C-H arylations

**General Procedure A**: An oven-dried 12.0 mL Schlenk tube containing a stirring bar was charged with **A4** (10 mol%, 8.4 mg, 0.03 mmol), **L4** (10 mol%, 5.6 mg, 0.03 mmol), aryl bromide (0.30 mmol, if solid). The schlenk tube was transferred to a nitrogen-filled glove-box where the  $\text{Ni}(\text{acac})_2$  (10 mol%, 7.7 mg, 0.03 mmol),  $\text{Na}_2\text{CO}_3$  (1.0 eq, 32.0 mg, 0.30 mmol), aryl bromide (0.30 mmol, if liquid) and anhydrous THF (0.075 M, 4mL) were added. Then, the reaction mixture was stirred for 1 minute and taken out of the glovebox. The Schlenk tube was placed approximately ~3 cm away from a 32 W CFL and it was rigorously stirred for 24-96 h. After completion of the reaction, the crude material concentrated under reduced pressure. The desired product was directly purified by flash column chromatography in silica gel with pentane/EtOAc.

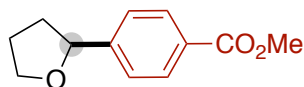
*Note*: In few cases where the final crude was contaminated with **A4**, it could be easily removed by simple treatment with  $\text{NaBH}_4$  in MeOH at rt.



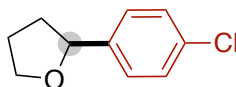
**2-(4-(trifluoromethyl)phenyl)tetrahydrofuran (1).** Following the general procedure A, using 1-bromo-4-(trifluoromethyl)benzene (67.5 mg, 0.3 mmol), the title compound was obtained in 95% yield (61.6 mg) after 60 h as colorless oil. <sup>1</sup>H NMR (300 MHz, CDCl<sub>3</sub>) δ 7.59 (d, *J* = 8.5 Hz, 2H), 7.45 (d, *J* = 8.5 Hz, 2H), 4.94 (t, *J* = 7.5 Hz, 1H), 4.10 (dt, *J* = 8.0, 7.0 Hz, 1H), 3.96 (dt, *J* = 8.0, 7.0 Hz, 1H), 2.39-2.33 (m, 1H), 2.03-1.98 (m, 2H), 1.80-1.73 (m, 1H) ppm. <sup>13</sup>C NMR (126 MHz, CDCl<sub>3</sub>) δ 147.93, 129.38 (q, *J*<sub>C-F</sub> = 32.3 Hz), 125.88, 125.31 (q, *J*<sub>C-F</sub> = 3.8 Hz), 124.40 (q, *J*<sub>C-F</sub> = 272.3 Hz), 80.07, 68.93, 34.80, 26.02 ppm. <sup>19</sup>F NMR (376 MHz, CDCl<sub>3</sub>): -62.56 ppm. The observed spectral data are in good agreement with the ones reported in literature<sup>2</sup>.



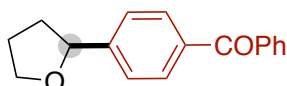
**4-(tetrahydrofuran-2-yl)benzotrile (2).** Following the general procedure A, using 4-bromobenzotrile (54.6 mg, 0.3 mmol), the title compound was obtained in 80% yield (41.6 mg) after 60 h as colorless oil. <sup>1</sup>H NMR (300 MHz, CDCl<sub>3</sub>) δ 7.60 (d, *J* = 8.4 Hz, 2H), 7.42 (d, *J* = 8.1 Hz, 2H), 4.92 (t, *J* = 7.2 Hz, 1H), 4.12-4.05 (m, 1H), 3.98-3.91 (m, 1H), 2.42-2.31 (m, 1H), 2.05-1.95 (m, 2H), 1.78-1.67 (m, 1H) ppm. <sup>13</sup>C NMR (75 MHz, CDCl<sub>3</sub>) δ 149.34, 132.25, 126.25, 119.06, 110.87, 79.90, 69.04, 34.79, 26.01 ppm. The observed spectral data are in good agreement with the ones reported in literature<sup>2</sup>.



**methyl 4-(tetrahydrofuran-2-yl)benzoate (3).** Following the general procedure A, using methyl 4-bromobenzoate (64.5 mg, 0.3 mmol), the title compound was obtained in 96% yield (59.4 mg) after 60 h as colorless oil. <sup>1</sup>H NMR (300 MHz, CDCl<sub>3</sub>) δ 7.99 (d, *J* = 8.4 Hz, 2H), 7.38 (d, *J* = 8.4 Hz, 2H), 4.93 (t, *J* = 7.2 Hz, 1H), 4.13-4.06 (m, 1H), 3.98-3.93 (m, 1H), 3.90 (s, 3H), 2.40-2.29 (m, 1H), 2.04-1.94 (m, 2H), 1.81-1.69 (m, 1H) ppm. <sup>13</sup>C NMR (75 MHz, CDCl<sub>3</sub>) δ 167.07, 149.04, 129.74, 129.00, 125.51, 80.26, 68.93, 52.10, 34.79, 26.05 ppm. The observed spectral data are in good agreement with the ones reported in literature<sup>2</sup>.



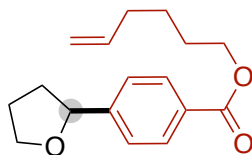
**2-(4-chlorophenyl)tetrahydrofuran (4).** Following the general procedure A, using 1-bromo-4-chlorobenzene (57.4 mg, 0.3 mmol), the title compound was obtained in 96% yield (52.6 mg) after 60 h as colorless oil. <sup>1</sup>H NMR (300 MHz, CDCl<sub>3</sub>) δ 7.23-7.16 (m, 4H), 4.77 (t, *J* = 7.2 Hz, 1H), 4.04-3.96 (m, 1H), 3.88-3.81 (m, 1H), 2.28-2.18 (m, 1H), 1.96-1.87 (m, 2H), 1.72-1.60 (m, 1H) ppm. <sup>13</sup>C NMR (75 MHz, CDCl<sub>3</sub>) δ 142.15, 132.82, 128.50, 127.10, 80.10, 68.82, 34.79, 26.08 ppm. The observed spectral data are in good agreement with the ones reported in literature<sup>2</sup>.



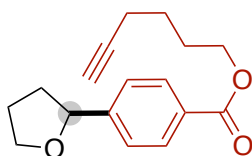
**Phenyl(4-(tetrahydrofuran-2-yl)phenyl)methanone (5).** Following the general procedure A, using (4-bromophenyl)(phenyl)methanone (78.3 mg, 0.3 mmol), the title compound was obtained in 95% yield (71.9 mg) after 36 h as colorless oil. <sup>1</sup>H NMR (300 MHz, CDCl<sub>3</sub>) δ 7.80-7.76 (m, 4H), 7.60-7.54 (m, 1H), 7.48-7.42 (m, 4H), 4.96 (t, *J* = 7.2 Hz, 1H), 4.15-4.08 (m, 1H), 4.0-3.92 (m, 1H), 2.43-2.32 (m, 1H), 2.06-1.97 (m, 2H), 1.86-1.74 (m, 1H) ppm. <sup>13</sup>C



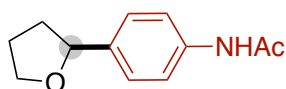
NMR (75 MHz, CDCl<sub>3</sub>)  $\delta$  196.48, 148.59, 137.83, 136.45, 132.37, 130.32, 130.06, 128.31, 125.45, 80.27, 68.95, 34.77, 26.08 ppm. The observed spectral data are in good agreement with the ones reported in literature<sup>3</sup>.



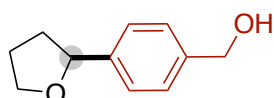
**hex-5-en-1-yl 4-(tetrahydrofuran-2-yl)benzoate (6)**: Following the general procedure A, the title compound was obtained in 91% yield after 60 h as colorless oil. <sup>1</sup>H NMR (300 MHz, CDCl<sub>3</sub>)  $\delta$  8.00 (d, *J* = 8.1 Hz, 2H), 7.39 (d, *J* = 8.1 Hz, 2H), 5.88-5.74 (m, 1H), 5.06-4.91 (m, 3H), 4.31 (t, *J* = 6.6 Hz, 2H), 4.13-4.06 (m, 1H), 3.98-3.91 (m, 1H), 2.40-2.30 (m, 1H), 2.16-2.09 (m, 2H), 2.04-1.95 (m, 2H), 1.82-1.72 (m, 3H), 1.59-1.49 (m, 2H) ppm. <sup>13</sup>C NMR (75 MHz, CDCl<sub>3</sub>)  $\delta$  166.62, 148.97, 138.43, 129.70, 129.31, 125.47, 114.94, 80.27, 68.93, 64.88, 34.81, 33.41, 28.27, 26.04, 25.40 ppm. IR (neat, cm<sup>-1</sup>): 3005, 2951, 1715, 1612, 1487, 1238, 957, 911. HRMS *calcd.* for (C<sub>17</sub>H<sub>22</sub>NaO<sub>3</sub>) [M+Na]<sup>+</sup>: 297.1461, *found* 297.1462.



**hex-5-yn-1-yl 4-(tetrahydrofuran-2-yl)benzoate (7)**. Following the general procedure A, using hex-5-yn-1-yl 4-bromobenzoate (84.3 mg, 0.3 mmol), the title compound was obtained in 89% yield (72.7 mg) after 60 h as colorless oil. <sup>1</sup>H NMR (300 MHz, CDCl<sub>3</sub>)  $\delta$  7.99 (d, *J* = 8.1 Hz, 2H), 7.38 (d, *J* = 8.1 Hz, 2H), 4.93 (t, *J* = 7.2 Hz, 1H), 4.32 (t, *J* = 6.6 Hz, 2H), 4.12-4.05 (m, 1H), 3.97-3.90 (m, 1H), 2.39-2.23 (m, 3H), 2.03-1.63 (m, 8H) ppm. <sup>13</sup>C NMR (75 MHz, CDCl<sub>3</sub>)  $\delta$  166.54, 149.03, 129.70, 129.17, 125.47, 83.94, 80.23, 68.91, 68.87, 64.41, 34.79, 27.86, 26.02, 25.13, 18.20 ppm. IR (neat, cm<sup>-1</sup>): 3303, 2952, 1713, 1269, 1115, 1057, 1018, 910. HRMS *calcd.* for (C<sub>17</sub>H<sub>20</sub>NaO<sub>3</sub>) [M+Na]<sup>+</sup>: 295.1305, *found* 295.1301.

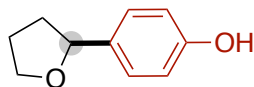


**N-(4-(tetrahydrofuran-2-yl)phenyl)acetamide (8)**. Following the general procedure A, using *N*-(4-bromophenyl)acetamide (64.2 mg, 0.3 mmol), the title compound was obtained in 94% yield (57.8 mg) after 72 h as colorless oil. <sup>1</sup>H NMR (300 MHz, CDCl<sub>3</sub>)  $\delta$  8.09 (br, 1H), 7.42 (d, *J* = 8.4 Hz, 2H), 7.22 (d, *J* = 8.4 Hz, 2H), 4.82 (t, *J* = 7.2 Hz, 1H), 4.10-4.03 (m, 1H), 3.93-3.86 (m, 1H), 2.32-2.21 (m, 1H), 2.08 (s, 3H), 2.05-1.93 (m, 2H), 1.81-1.69 (m, 1H) ppm. <sup>13</sup>C NMR (75 MHz, CDCl<sub>3</sub>)  $\delta$  168.93, 139.13, 137.18, 126.29, 120.13, 80.50, 68.66, 34.59, 26.06, 24.37 ppm. IR (neat, cm<sup>-1</sup>): 3305, 2975, 2871, 1665, 1602, 1515, 1410, 1370. HRMS *calcd.* for (C<sub>12</sub>H<sub>15</sub>NNaO<sub>2</sub>) [M+Na]<sup>+</sup>: 228.0995, *found* 228.0991.

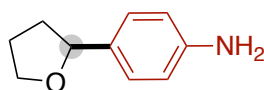


**(4-(tetrahydrofuran-2-yl)phenyl)methanol (9)**. Following the general procedure A, using (4-bromophenyl)methanol (56.1 mg, 0.3 mmol), the title compound was obtained in 99% yield (52.9 mg) after 72 h as colorless oil. <sup>1</sup>H NMR (300 MHz, CDCl<sub>3</sub>):  $\delta$  7.20 (s, 4H), 4.78 (t, *J* = 7.2 Hz, 1H), 4.52 (s, 2H), 4.03-3.96 (m, 1H), 3.87-3.79 (m, 1H), 2.39 (br, 1H), 2.71-2.17 (m, 1H), 1.96-1.86 (m, 2H), 1.75-1.63 (m, 1H) ppm. <sup>13</sup>C NMR (75 MHz, CDCl<sub>3</sub>)  $\delta$  142.70, 140.01, 127.02,

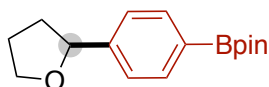
125.83, 80.58, 68.70, 64.97, 34.69, 26.05 ppm. IR (neat,  $\text{cm}^{-1}$ ): 3376, 2927, 2869, 1513, 1459, 1420, 1327, 1048. HRMS *calcd.* for  $(\text{C}_{11}\text{H}_{14}\text{NaO}_2)$   $[\text{M}+\text{Na}]^+$ : 201.0885, *found* 201.0886.



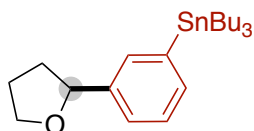
**4-(tetrahydrofuran-2-yl)phenol (10).** Following the general procedure A, using 4-bromophenol (51.9 mg, 0.3 mmol), the title compound was obtained in 68% yield (33.5 mg) after 72 h as colorless oil.  $^1\text{H}$  NMR (300 MHz,  $\text{CDCl}_3$ )  $\delta$  7.18-7.13 (m, 2H), 6.72-6.67 (m, 2H), 6.43 (br, 1H), 4.84 (t,  $J = 7.2$  Hz, 1H), 4.13-4.06 (m, 1H), 3.93 (dt,  $J = 7.8, 6.3$  Hz, 1H), 2.32-2.22 (m, 1H), 2.08-1.97 (m, 2H), 1.88-1.76 (m, 1H) ppm.  $^{13}\text{C}$  NMR (75 MHz,  $\text{CDCl}_3$ )  $\delta$  155.46, 134.33, 127.41, 115.40, 80.96, 68.57, 34.40, 26.17 ppm. The observed spectral data are in good agreement with the ones reported in literature<sup>4</sup>.



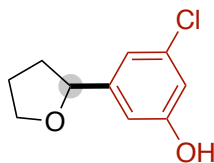
**4-(tetrahydrofuran-2-yl)aniline (11).** Following the general procedure A, using 4-bromoaniline (51.6 mg, 0.3 mmol) or *N*-(4-bromophenyl)-1,1,1-trimethyl-*N*-(trimethylsilyl)silanamine (94.9 mg, 0.3 mmol), the title compound was obtained in 68% or 89% yield (33.7 mg or 44.1 mg) after 72 h as light brown oil.  $^1\text{H}$  NMR (300 MHz,  $\text{CDCl}_3$ )  $\delta$  7.15-7.11 (m, 2H), 6.67-6.63 (m, 2H), 4.77 (t,  $J = 7.2$  Hz, 1H), 4.10 (m, 1H), 3.89 (dt,  $J = 7.8, 6.3$  Hz, 1H), 3.61 (br, 2H), 2.29-2.19 (m, 1H), 2.05-1.90 (m, 2H), 1.85-1.73 (m, 1H) ppm.  $^{13}\text{C}$  NMR (75 MHz,  $\text{CDCl}_3$ )  $\delta$  145.70, 133.14, 127.09, 115.08, 80.82, 68.45, 34.38, 26.20 ppm. IR (neat,  $\text{cm}^{-1}$ ): 3437, 3349, 2970, 2866, 1614, 1515, 1281, 1046. HRMS *calcd.* for  $(\text{C}_{10}\text{H}_{14}\text{NO})$   $[\text{M}+\text{H}]^+$ : 164.1070, *found* 164.1073.



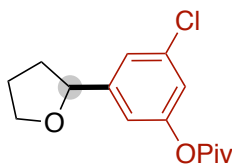
**4,4,5,5-tetramethyl-2-(4-(tetrahydrofuran-2-yl)phenyl)-1,3,2-dioxaborolane (12).** Following the general procedure A, using 2-(4-bromophenyl)-4,4,5,5-tetramethyl-1,3,2-dioxaborolane (84.9 mg, 0.3 mmol), the title compound was obtained in 93% yield (41.1 mg) after 72 h as colorless oil.  $^1\text{H}$  NMR (300 MHz,  $\text{CDCl}_3$ )  $\delta$  7.78 (d,  $J = 7.8$  Hz, 2H), 7.34 (d,  $J = 7.8$  Hz, 2H), 4.92 (t,  $J = 6.9$  Hz, 1H), 4.13-4.06 (m, 1H), 3.98-3.90 (m, 1H), 2.38-2.27 (m, 1H), 2.04-1.94 (m, 2H), 1.84-1.72 (m, 1H), 1.34 (s, 12 H) ppm.  $^{13}\text{C}$  NMR (75 MHz,  $\text{CDCl}_3$ )  $\delta$  146.98, 134.95, 124.95, 83.84, 80.71, 68.86, 34.84, 26.08, 24.99 ppm. IR (neat,  $\text{cm}^{-1}$ ): 2976, 2929, 2868, 1613, 1398, 1358, 1142, 1062. HRMS *calcd.* for  $(\text{C}_{16}\text{H}_{24}\text{O}_3^{10}\text{B})$   $[\text{M}+\text{H}]^+$ : 274.1849, *found* 274.1850.



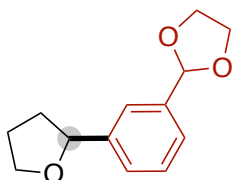
**tributyl(3-(tetrahydrofuran-2-yl)phenyl)stannane (13).** Following the general procedure A, using (3-bromophenyl)tributylstannane (113.8 mg, 0.3 mmol), the title compound was obtained in 73% yield (95.7 mg) after 72 h as colorless oil.  $^1\text{H}$  NMR (300 MHz,  $\text{CDCl}_3$ )  $\delta$  7.43 (s, 1H), 7.38-7.26 (m, 3H), 4.90 (t,  $J = 7.2$  Hz, 1H), 4.15-4.08 (m, 1H), 3.99-3.92 (m, 1H), 2.39-2.29 (m, 1H), 2.08-1.98 (m, 2H), 1.90-1.79 (m, 1H), 1.59-1.51 (m, 6H), 1.41-1.29 (m, 6H), 1.10-1.05 (m, 6H), 0.91 (t,  $J = 7.2$  Hz, 9H) ppm.  $^{13}\text{C}$  NMR (75 MHz,  $\text{CDCl}_3$ )  $\delta$  142.64, 142.00, 135.44, 133.87, 127.90, 125.46, 81.01, 68.77, 34.71, 29.23, 27.51, 26.19, 13.81, 9.70 ppm. IR (neat,  $\text{cm}^{-1}$ ): 2955, 2923, 2852, 1462, 1376, 1061, 960, 781. HRMS *calcd.* for  $(\text{C}_{22}\text{H}_{38}\text{NaO}^{116}\text{Sn})$   $[\text{M}+\text{Na}]^+$ : 457.1832, *found* 457.1833.



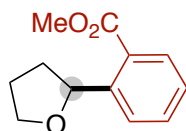
**3-chloro-5-(tetrahydrofuran-2-yl)phenol (14).** Following the general procedure A, using 3-bromo-5-chlorophenol (62.2 mg, 0.3 mmol), the title compound was obtained in 84% yield (50.1 mg) after 72 h as colorless oil.  $^1\text{H NMR}$  (300 MHz,  $\text{CDCl}_3$ )  $\delta$  6.94 (br, 1H), 6.82 (br, 1H), 6.67-6.64 (m, 2H) 4.83 (t,  $J = 7.2$  Hz, 1H), 4.11-4.03 (m, 1H), 4.00-3.93 (m, 1H), 2.35-2.24 (m, 1H), 2.04-1.95 (m, 2H), 1.83-1.76 (m, 1H) ppm.  $^{13}\text{C NMR}$  (75 MHz,  $\text{CDCl}_3$ )  $\delta$  156.98, 146.16, 134.92, 117.87, 114.99, 111.22, 80.25, 69.01, 34.56, 25.92 ppm. IR (neat,  $\text{cm}^{-1}$ ): 3253, 2953, 2875, 1598, 1581, 1444, 1280, 1045. HRMS *calcd.* for ( $\text{C}_{10}\text{H}_{10}\text{ClO}_2$ ) [ $\text{M}-\text{H}$ ] $^-$ : 197.0375, *found* 197.0372.



**3-chloro-5-(tetrahydrofuran-2-yl)phenyl pivalate (15).** Following the general procedure A, using 3-bromo-5-chlorophenyl pivalate (87.5 mg, 0.3 mmol), the title compound was obtained in 89% yield (75.5 mg) after 72 h as colorless oil.  $^1\text{H NMR}$  (300 MHz,  $\text{CDCl}_3$ )  $\delta$  7.18 (s, 1H), 6.99-6.94 (m, 1H), 6.93 (s, 1H), 4.87 (t,  $J = 7.2$  Hz, 1H), 4.11-4.04 (m, 1H), 3.96-3.89 (m, 1H), 2.39-2.28 (m, 1H), 2.03-1.94 (m, 2H), 1.83-1.72 (m, 1H), 1.34 (s, 9H) ppm.  $^{13}\text{C NMR}$  (75 MHz,  $\text{CDCl}_3$ )  $\delta$  176.78, 151.67, 146.99, 134.56, 123.07, 120.77, 117.18, 79.68, 68.97, 39.25, 34.71, 27.22, 25.98 ppm. IR (neat,  $\text{cm}^{-1}$ ): 2974, 2873, 1752, 1583, 1438, 1253, 1102, 1066. HRMS *calcd.* for ( $\text{C}_{15}\text{H}_{19}\text{ClNaO}_3$ ) [ $\text{M}+\text{Na}$ ] $^+$ : 305.0915, *found* 305.0912.

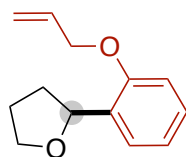


**2-(3-(tetrahydrofuran-2-yl)phenyl)-1,3-dioxolane (16).** Following the general procedure A, using 2-(3-bromophenyl)-1,3-dioxolane (68.7 mg, 0.3 mmol), the title compound was obtained in 74% yield (48.9 mg) after 72 h as colorless oil.  $^1\text{H NMR}$  (300 MHz,  $\text{CDCl}_3$ )  $\delta$  7.45 (s, 1H), 7.38-7.26 (m, 3H), 5.81 (s, 1H), 4.91 (t,  $J = 7.2$  Hz, 1H), 4.15-4.00 (m, 5H), 3.97-3.89 (m, 1H), 2.38-2.27 (m, 1H), 2.04-1.95 (m, 2H), 1.86-1.74 (m, 1H) ppm.  $^{13}\text{C NMR}$  (75 MHz,  $\text{CDCl}_3$ )  $\delta$  143.88, 137.99, 128.47, 126.53, 125.29, 123.75, 103.85, 80.59, 68.78, 65.40, 65.37, 34.74, 26.10 ppm. IR (neat,  $\text{cm}^{-1}$ ): 2950, 2875, 1696, 1285, 1201, 1065, 799, 755. HRMS *calcd.* for ( $\text{C}_{13}\text{H}_{17}\text{O}_3$ ) [ $\text{M}+\text{H}$ ] $^+$ : 221.1172, *found* 221.1169.

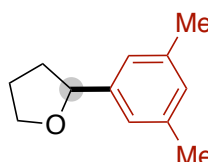


**methyl 2-(tetrahydrofuran-2-yl)benzoate (17).** Following the general procedure A, using methyl 2-bromobenzoate (64.5 mg, 0.3 mmol), the title compound was obtained in 65% yield (40.2 mg) after 72 h as colorless oil.  $^1\text{H NMR}$  (300 MHz,  $\text{CDCl}_3$ )  $\delta$  7.89 (dd,  $J = 7.8, 1.2$  Hz, 1H), 7.69 (dt,  $J = 7.8, 0.6$  Hz, 1H), 7.51 (dt,  $J = 7.5, 1.2$  Hz, 1H), 7.29 (dt,  $J = 7.8, 1.2$  Hz, 1H), 5.61 (d,  $J = 6.9$  Hz, 1H), 4.15 (dt,  $J = 8.1, 5.7$  Hz, 1H), 3.99-3.91 (m, 1H), 3.88 (s, 3H), 2.62-2.50 (m, 1H), 2.03-1.87 (m, 2H), 1.71-1.60 (m, 1H) ppm.  $^{13}\text{C NMR}$  (75 MHz,  $\text{CDCl}_3$ )  $\delta$  167.73, 146.54, 132.46, 130.44, 127.66,

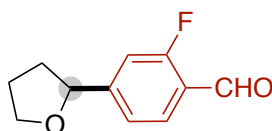
126.68, 125.90, 78.34, 69.13, 52.11, 34.92, 26.01 ppm. The observed spectral data are in good agreement with the ones reported in literature<sup>5</sup>.



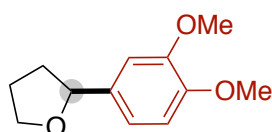
**2-(2-(allyloxy)phenyl)tetrahydrofuran (18).** Following the general procedure A, using 1-(allyloxy)-2-bromobenzene (63.9 mg, 0.3 mmol), the title compound was obtained in 61% yield (37.3 mg) after 72 h as colorless oil. <sup>1</sup>H NMR (300 MHz, CDCl<sub>3</sub>) δ 7.44 (dd, *J* = 7.5, 1.5 Hz, 1H), 7.20 (dt, *J* = 7.8, 1.8 Hz, 1H), 6.96 (dt, *J* = 7.5, 0.9 Hz, 1H), 6.84 (d, *J* = 8.4 Hz, 1H), 6.12-6.00 (m, 1H), 5.41 (dq, *J* = 17.1, 1.5 Hz, 1H), 5.27 (dq, *J* = 10.5, 1.5 Hz, 1H), 5.23 (t, *J* = 6.9 Hz, 1H), 4.58-4.54 (m, 2H), 4.12 (dt, *J* = 8.1, 6.3 Hz, 1H), 3.97-3.89 (m, 1H), 2.47-2.38 (m, 1H), 2.01-1.92 (m, 2H), 1.78-1.67 (m, 1H) ppm. <sup>13</sup>C NMR (75 MHz, CDCl<sub>3</sub>) δ 155.17, 133.58, 132.79, 127.76, 125.75, 120.75, 117.08, 111.40, 76.12, 68.77, 68.68, 33.39, 26.04 ppm. IR (neat, cm<sup>-1</sup>): 2977, 2868, 1601, 1487, 1451, 1236, 1059, 997. HRMS *calcd.* for (C<sub>13</sub>H<sub>16</sub>NaO<sub>2</sub>) [M+Na]<sup>+</sup>: 227.1043, *found* 227.1039.



**2-(3,5-dimethylphenyl)tetrahydrofuran (19).** Following the general procedure A, using 1-bromo-3,5-dimethylbenzene (55.5 mg, 0.3 mmol), the title compound was obtained in 98% yield (51.8 mg) after 72 h as colorless oil. <sup>1</sup>H NMR (300 MHz, CDCl<sub>3</sub>) δ 6.98 (s, 2H), 6.91 (s, 1H), 4.80 (t, *J* = 7.2 Hz, 1H), 4.15-4.08 (m, 1H), 3.94 (dt, *J* = 7.8, 6.3 Hz, 1H), 2.37-2.26 (m, 7H), 2.08-1.95 (m, 2H), 1.88-1.76 (m, 1H) ppm. <sup>13</sup>C NMR (75 MHz, CDCl<sub>3</sub>) δ 143.40, 137.90, 128.86, 123.52, 80.84, 68.71, 34.61, 26.17, 21.44 ppm. IR (neat, cm<sup>-1</sup>): 2970, 2918, 2864, 1606, 1459, 1065, 1014, 844. HRMS *calcd.* for (C<sub>12</sub>H<sub>16</sub>NaO) [M+Na]<sup>+</sup>: 199.1093, *found* 199.1086.

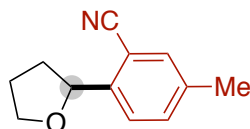


**2-fluoro-4-(tetrahydrofuran-2-yl)benzaldehyde (20).** Following the general procedure A, using 4-bromo-2-fluorobenzaldehyde (60.9 mg, 0.3 mmol), the title compound was obtained in 82% yield (47.8 mg) after 60 h as colorless oil. <sup>1</sup>H NMR (400 MHz, CDCl<sub>3</sub>) δ 10.31 (s, 1H), 7.83-7.79 (m, 1H), 7.20-7.15 (m, 2H), 4.93 (t, *J* = 7.2 Hz, 1H), 4.12-4.06 (m, 1H), 3.99-3.93 (m, 1H), 2.42-2.34 (m, 1H), 2.04-1.96 (m, 2H), 1.79-1.71 (m, 1H) ppm. <sup>13</sup>C NMR (101 MHz, CDCl<sub>3</sub>) δ 187.04 (d, *J*<sub>C-F</sub> = 6.36 Hz), 165.00 (d, *J*<sub>C-F</sub> = 259.6 Hz), 154.13 (d, *J*<sub>C-F</sub> = 8.18 Hz), 128.83 (d, *J*<sub>C-F</sub> = 2.22 Hz), 123.03 (d, *J*<sub>C-F</sub> = 8.38 Hz), 121.73 (d, *J*<sub>C-F</sub> = 3.23 Hz), 113.37 (d, *J*<sub>C-F</sub> = 21.72 Hz), 79.68 (d, *J*<sub>C-F</sub> = 1.62 Hz), 69.14, 34.74, 26.01 ppm. <sup>19</sup>F NMR (376 MHz, CDCl<sub>3</sub>) δ -121.50 ppm. IR (neat, cm<sup>-1</sup>): 2954, 2871, 1692, 1620, 1575, 1422, 1259, 1196. HRMS *calcd.* for (C<sub>11</sub>H<sub>12</sub>FO<sub>2</sub>) [M+H]<sup>+</sup>: 195.0816, *found* 195.0814.

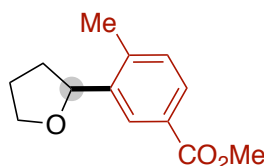


**2-(3,4-dimethoxyphenyl)tetrahydrofuran (21).** Following the general procedure A, using 4-bromo-1,2-dimethoxybenzene (65.1 mg, 0.3 mmol), the title compound was obtained in 85% yield (53.1 mg) after 72 h as yellow

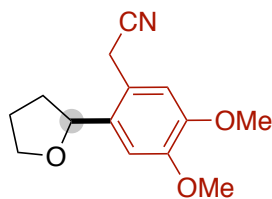
oil.  $^1\text{H}$  NMR (300 MHz,  $\text{CDCl}_3$ )  $\delta$  6.90-6.80 (m, 3H), 4.82 (t,  $J = 7.2$  Hz, 1H), 4.12-4.05 (m, 1H), 3.94-3.86 (m, 7H), 2.33-2.23 (m, 1H), 2.06-1.95 (m, 2H), 1.85-1.73 (m, 1H) ppm.  $^{13}\text{C}$  NMR (75 MHz,  $\text{CDCl}_3$ )  $\delta$  149.04, 148.26, 135.93, 118.01, 111.05, 109.04, 80.68, 68.61, 56.04, 55.94, 34.57, 26.13 ppm. The observed spectral data are in good agreement with the ones reported in literature<sup>6</sup>.



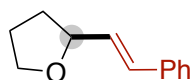
**5-methyl-2-(tetrahydrofuran-2-yl)benzonitrile (22).** Following the general procedure A, using 2-bromo-5-methylbenzonitrile (58.8 mg, 0.3 mmol), the title compound was obtained in 83% yield (46.6 mg) after 72 h as colorless oil.  $^1\text{H}$  NMR (300 MHz,  $\text{CDCl}_3$ )  $\delta$  7.47-7.35 (m, 3H), 5.14 (t,  $J = 7.2$  Hz, 1H), 4.19-4.12 (m, 1H), 4.00-3.93 (m, 1H), 2.55-2.45 (m, 1H), 2.35 (s, 3H), 2.08-1.99 (m, 2H), 1.79-1.67 (m, 1H) ppm.  $^{13}\text{C}$  NMR (75 MHz,  $\text{CDCl}_3$ )  $\delta$  144.94, 137.61, 133.88, 133.27, 126.06, 117.92, 109.68, 78.83, 69.23, 34.60, 26.30, 20.81 ppm. IR (neat,  $\text{cm}^{-1}$ ): 2977, 2950, 2872, 2224, 1496, 1457, 1062, 830. HRMS *calcd.* for  $(\text{C}_{12}\text{H}_{13}\text{NNaO})$   $[\text{M}+\text{Na}]^+$ : 210.0889, *found* 210.0890.



**methyl 4-methyl-3-(tetrahydrofuran-2-yl)benzoate (23).** Following the general procedure A, using methyl 3-bromo-4-methylbenzoate (68.7 mg, 0.3 mmol), the title compound was obtained in 76% yield (50.2 mg) after 72 h as colorless oil.  $^1\text{H}$  NMR (300 MHz,  $\text{CDCl}_3$ )  $\delta$  8.10 (d,  $J = 1.8$  Hz, 1H), 7.80 (dd,  $J = 7.8, 1.8$  Hz, 1H), 7.17 (d,  $J = 7.8$  Hz, 1H), 5.04 (t,  $J = 7.2$  Hz, 1H), 4.21-4.14 (m, 1H), 3.96-3.88 (m, 1H), 3.88 (s, 3H), 2.41-2.30 (m, 1H), 2.33 (s, 3H), 2.05-1.96 (m, 2H), 1.71-1.59 (m, 1H) ppm.  $^{13}\text{C}$  NMR (75 MHz,  $\text{CDCl}_3$ )  $\delta$  167.34, 142.22, 139.90, 130.36, 128.11, 128.09, 126.00, 77.66, 68.75, 51.96, 33.17, 26.09, 19.52 ppm. IR (neat,  $\text{cm}^{-1}$ ): 2950, 2869, 1715, 1612, 1435, 1289, 1255, 1212. HRMS *calcd.* for  $(\text{C}_{13}\text{H}_{17}\text{O}_3)$   $[\text{M}+\text{H}]^+$ : 221.1172, *found* 221.1177.

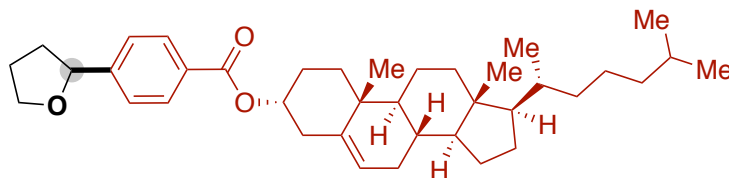


**2-(4,5-dimethoxy-2-(tetrahydrofuran-2-yl)phenyl)acetonitrile (24).** Following the general procedure A, using 2-(2-bromo-4,5-dimethoxyphenyl)acetonitrile (76.8 mg, 0.3 mmol), the title compound was obtained in 80% yield (59.3 mg) after 72 h as colorless oil.  $^1\text{H}$  NMR (300 MHz,  $\text{CDCl}_3$ )  $\delta$  6.96 (s, 1H), 6.84 (s, 1H), 4.87 (dd,  $J = 8.1, 6.3$  Hz, 1H), 4.15-4.07 (m, 1H), 3.93-3.86 (m, 1H), 3.87 (s, 6H), 3.72 (d,  $J = 0.9$  Hz, 2H), 2.40-2.29 (m, 1H), 2.10-1.99 (m, 2H), 1.79-1.67 (m, 1H) ppm.  $^{13}\text{C}$  NMR (75 MHz,  $\text{CDCl}_3$ )  $\delta$  148.88, 148.34, 133.09, 118.98, 118.27, 112.36, 109.50, 77.88, 68.55, 56.12, 56.05, 33.46, 26.09, 20.72 ppm. IR (neat,  $\text{cm}^{-1}$ ): 2939, 2857, 2220, 1609, 1515, 1463, 1269, 1094. HRMS *calcd.* for  $(\text{C}_{14}\text{H}_{17}\text{NNaO}_3)$   $[\text{M}+\text{Na}]^+$ : 270.1101, *found* 270.1109.

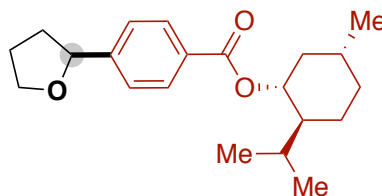


**(E)-2-styryltetrahydrofuran (25).** Following the general procedure A, using (E)-(2-bromovinyl)benzene (54.9 mg, 0.3 mmol), the title compound was obtained in 39% yield (20.4 mg) after 60 h as colorless oil.  $^1\text{H}$  NMR (300 MHz,  $\text{CDCl}_3$ )

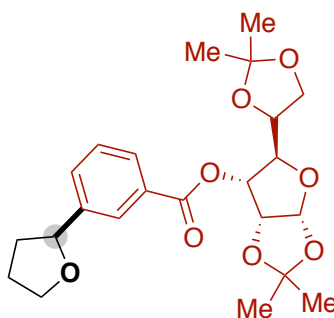
$\delta$  7.40-7.22 (m, 5H), 6.59 (d,  $J$  = 15.9 Hz, 1H), 6.21 (dd,  $J$  = 15.9, 6.6 Hz, 1H), 4.48 (q,  $J$  = 6.6 Hz, 1H), 4.01-3.94 (m, 1H), 3.88-3.81 (m, 1H), 2.19-2.08 (m, 1H), 2.03-1.90 (m, 2H), 1.78-1.66 (m, 1H) ppm.  $^{13}\text{C}$  NMR (75 MHz,  $\text{CDCl}_3$ ) ppm.  $^{13}\text{C}$  NMR (75 MHz,  $\text{CDCl}_3$ )  $\delta$  137.00, 130.67, 130.58, 128.64, 127.62, 126.60, 79.81, 68.32, 32.54, 26.06 ppm. The observed spectral data are in good agreement with the ones reported in literature<sup>7</sup>.



**(3*S*,8*S*,9*S*,10*R*,13*R*,14*S*,17*R*)-10,13-dimethyl-17-((*R*)-6-methylheptan-2-yl)-2,3,4,7,8,9,10,11,12,13,14,15,16,17-tetradecahydro-1*H*-cyclopenta[*a*]phenanthren-3-yl 4-(tetrahydrofuran-2-yl)benzoate (26)**. Following the general procedure A, using **s26** (170.9 mg, 0.3 mmol), the title compound was obtained in 94% yield (158.1 mg) after 60 h as colorless oil (inseparable mixture of diastereoisomers).  $^1\text{H}$  NMR (300 MHz,  $\text{CDCl}_3$ )  $\delta$  8.00 (d,  $J$  = 8.4 Hz, 2H), 7.38 (d,  $J$  = 8.4 Hz, 2H), 5.41 (d,  $J$  = 3.9 Hz, 1H), 4.94 (t,  $J$  = 7.2 Hz, 1H), 4.89-4.80 (m, 1H), 4.14-4.06 (m, 1H), 3.98-3.91 (m, 1H), 2.46 (d,  $J$  = 7.8 Hz, 2H), 2.40-2.30 (m, 1H), 2.041-0.86 (m, 41H), 0.69 (s, 3H) ppm.  $^{13}\text{C}$  NMR (75 MHz,  $\text{CDCl}_3$ )  $\delta$  165.95, 148.83, 139.77, 129.72, 125.40, 122.83, 80.29, 74.56, 68.92, 56.80, 56.26, 50.16, 42.43, 39.86, 39.64, 38.35, 37.16, 36.76, 36.31, 35.92, 34.85, 32.05, 31.99, 28.36, 28.13, 28.01, 26.05, 24.41, 23.97, 22.95, 22.69, 21.17, 19.50, 18.85, 11.98 ppm. IR (neat,  $\text{cm}^{-1}$ ): 2941, 2888, 2866, 1712, 1466, 1271, 1109, 1065. HRMS *calcd.* for ( $\text{C}_{38}\text{H}_{56}\text{NaO}_3$ ) [ $\text{M}+\text{Na}$ ] $^+$ : 583.4120, *found* 583.4122.

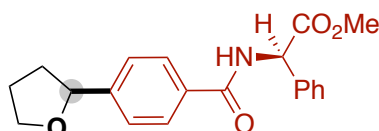


**(1*R*,2*S*,5*R*)-2-isopropyl-5-methylcyclohexyl 4-(tetrahydrofuran-2-yl)benzoate (27)**. Following the general procedure A, using **s27** (101.8 mg, 0.3 mmol), the title compound was obtained in 96% yield (95.1 mg) after 60 h as colorless oil (inseparable mixture of diastereoisomers).  $^1\text{H}$  NMR (300 MHz,  $\text{CDCl}_3$ )  $\delta$  8.00 (d,  $J$  = 8.4 Hz, 2H), 7.39 (d,  $J$  = 8.1 Hz, 2H), 4.96-4.88 (m, 2H), 4.13-4.06 (m, 1H), 3.98-3.91 (m, 1H), 2.40-2.30 (m, 1H), 2.13-1.93 (m, 4H), 1.81-1.70 (m, 3H), 1.58-1.51 (m, 2H), 1.15-1.03 (m, 2H), 0.97-0.86 (m, 7H), 0.78 (d,  $J$  = 6.9 Hz, 3H) ppm.  $^{13}\text{C}$  NMR (75 MHz,  $\text{CDCl}_3$ )  $\delta$  166.08, 148.86, 129.73, 125.45, 125.42, 80.28, 74.80, 68.93, 47.38, 41.09, 34.84, 34.44, 31.55, 26.62, 26.05, 23.78, 22.16, 20.87, 16.65 ppm. IR (neat,  $\text{cm}^{-1}$ ): 2953, 2868, 1709, 1611, 1456, 1369, 1267, 1109. HRMS *calcd.* for ( $\text{C}_{21}\text{H}_{30}\text{NaO}_3$ ) [ $\text{M}+\text{Na}$ ] $^+$ : 353.2087, *found* 353.2085.

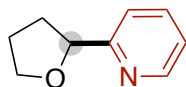


**(3*aR*,5*R*,6*R*,6*aR*)-5-((*R*)-2,2-dimethyl-1,3-dioxolan-4-yl)-2,2-dimethyltetrahydrofuro[2,3-*d*][1,3]dioxol-6-yl 3-(tetrahydrofuran-2-yl)benzoate (28)**. Following the general procedure A, using **s28** (132.9 mg, 0.3 mmol), the title

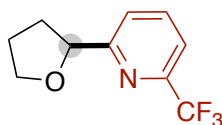
compound was obtained in 86% yield (112.1 mg) after 60 h as colorless oil, and as a mixture of rotamers.  $^1\text{H}$  NMR (300 MHz,  $\text{CDCl}_3$ )  $\delta$  7.99 (br, 1H), 7.92 (d,  $J = 7.8$  Hz, 1H), 7.57-7.53 (m, 1H), 7.40 (t,  $J = 7.8$  Hz, 1H), 5.87 (d,  $J = 3.6$  Hz, 1H), 5.06-5.02 (m, 1H), 4.97-4.89 (m, 2H), 4.36-4.30 (m, 2H), 4.12-4.05 (m, 2H), 3.99-3.89 (m, 2H), 2.39-2.33 (m, 1H), 2.04-1.95 (m, 2H), 1.82-1.73 (m, 1H), 1.52 (s, 3H), 1.39 (s, 3H), 1.31 (s, 3H), 1.30 (s, 3H) ppm.  $^{13}\text{C}$  NMR (75 MHz,  $\text{CDCl}_3$ )  $\delta$  165.72, 144.24, 130.67, 130.64, 129.49, 129.48, 128.61, 128.53, 127.20, 127.14, 113.20, 110.03, 104.41, 104.38, 80.16, 77.94, 77.89, 75.36, 75.33, 73.38, 68.84, 65.84, 34.78, 34.74, 26.86, 26.84, 26.75, 26.46, 26.43, 26.04, 25.12 ppm. IR (neat,  $\text{cm}^{-1}$ ): 2984, 2936, 2877, 1721, 1455, 1372, 1260, 1199. HRMS *calcd.* for  $(\text{C}_{23}\text{H}_{30}\text{NaO}_8)$   $[\text{M}+\text{Na}]^+$ : 457.1833, *found* 457.1843.



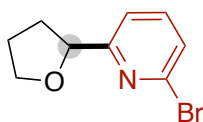
**methyl (*R*)-2-phenyl-2-(4-(tetrahydrofuran-2-yl)benzamido)acetate (29).** Following the general procedure A, using methyl **s29** (104.5 mg, 0.3 mmol), the title compound was obtained in 98% yield (99.7 mg) after 60 h as colorless oil (inseparable mixture of diastereoisomers).  $^1\text{H}$  NMR (300 MHz,  $\text{CDCl}_3$ )  $\delta$  7.77 (d,  $J = 8.4$  Hz, 2H), 7.44-7.24 (m, 8H), 5.77 (d,  $J = 6.9$  Hz, 1H), 4.90 (t,  $J = 7.2$  Hz, 1H), 4.10-4.03 (m, 1H), 3.95-3.88 (m, 1H), 3.73 (s, 3H), 2.37-2.27 (m, 1H), 2.02-1.92 (m, 2H), 1.78-1.66 (m, 1H) ppm.  $^{13}\text{C}$  NMR (75 MHz,  $\text{CDCl}_3$ )  $\delta$  171.52, 166.43, 147.84, 136.59, 132.31, 128.99, 128.57, 127.38, 127.27, 125.62, 80.08, 68.80, 56.83, 52.87, 34.74, 25.93 ppm. IR (neat,  $\text{cm}^{-1}$ ): 3314, 2953, 2875, 1742, 1643, 1526, 1494, 1270. HRMS *calcd.* for  $(\text{C}_{20}\text{H}_{21}\text{NNaO}_4)$   $[\text{M}+\text{Na}]^+$ : 362.1363, *found* 362.1363.



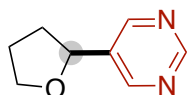
**2-(tetrahydrofuran-2-yl)pyridine (30).** Following the general procedure A, using 2-bromopyridine (47.4 mg, 0.3 mmol), the title compound was obtained in 67% yield (29.9 mg) after 72 h as colorless oil.  $^1\text{H}$  NMR (300 MHz,  $\text{CDCl}_3$ )  $\delta$  8.56-8.53 (m, 1H), 7.66 (dt,  $J = 1.8, 7.8$  Hz, 1H), 7.43 (d,  $J = 7.8$  Hz, 1H), 7.17-7.12 (m, 1H), 5.01 (t,  $J = 6.6$  Hz, 1H), 4.14-4.07 (m, 1H), 4.01-3.94 (m, 1H), 2.49-2.34 (m, 1H), 2.05-1.92 (m, 3H) ppm.  $^{13}\text{C}$  NMR (75 MHz,  $\text{CDCl}_3$ )  $\delta$  163.02, 148.95, 136.90, 122.20, 119.99, 81.32, 69.19, 33.22, 25.90 ppm. The observed spectral data are in good agreement with the ones reported in literature<sup>8</sup>.



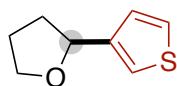
**2-(tetrahydrofuran-2-yl)-6-(trifluoromethyl)pyridine (31).** Following the general procedure A, using 2-bromo-6-(trifluoromethyl)pyridine (67.8 mg, 0.3 mmol), the title compound was obtained in 78% yield (50.8 mg) after 60 h as colorless oil.  $^1\text{H}$  NMR (400 MHz,  $\text{CDCl}_3$ )  $\delta$  7.83 (t,  $J = 8.0$  Hz, 1H), 7.66 (d,  $J = 8.0$  Hz, 1H), 7.53 (d,  $J = 8.0$  Hz, 1H), 5.08 (dd,  $J = 7.2, 5.6$  Hz, 1H), 4.12-4.07 (m, 1H), 4.01-3.96 (m, 1H), 2.50-2.41 (m, 1H), 2.05-1.89 (m, 3H) ppm.  $^{13}\text{C}$  NMR (101 MHz,  $\text{CDCl}_3$ )  $\delta$  167.4 (q,  $J_{\text{C-F}} = 1.3$  Hz), 146.1 (q,  $J_{\text{C-F}} = 4.1$  Hz), 133.8 (q,  $J_{\text{C-F}} = 3.5$  Hz), 125.2 (q,  $J_{\text{C-F}} = 32.9$  Hz), 123.8 (q,  $J_{\text{C-F}} = 273.1$  Hz), 119.6, 81.1, 69.4, 33.2, 25.8 ppm.  $^{13}\text{C}$  NMR (101 MHz,  $\text{CDCl}_3$ ): 164.44, 147.53 (q,  $J_{\text{C-F}} = 34.5$  Hz), 137.93, 122.68, 121.67 (q,  $J_{\text{C-F}} = 275.1$  Hz), 118.71 (q,  $J_{\text{C-F}} = 2.8$  Hz), 81.04, 69.32, 33.20, 25.77 ppm.  $^{19}\text{F}$  NMR (376 MHz,  $\text{CDCl}_3$ ): -68.1 ppm. IR (neat,  $\text{cm}^{-1}$ ): 2983, 2883, 1598, 1463, 1347, 1183, 1134, 1114. HRMS *calcd.* for  $(\text{C}_{10}\text{H}_{11}\text{F}_3\text{NO})$   $[\text{M}+\text{H}]^+$ : 218.0787, *found* 218.0785.



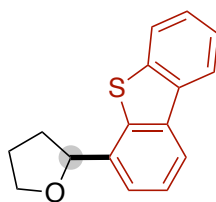
**2-bromo-6-(tetrahydrofuran-2-yl)pyridine (32).** Following the general procedure A, using 2,6-dibromopyridine (71.1 mg, 0.3 mmol), the title compound was obtained in 83% yield (56.7 mg) after 60 h as colorless oil.  $^1\text{H NMR}$  (300 MHz,  $\text{CDCl}_3$ )  $\delta$  7.51 (t,  $J = 7.5$  Hz, 1H), 7.40 (d,  $J = 7.5$  Hz, 1H), 7.31 (d,  $J = 7.5$  Hz, 1H), 5.00-4.96 (m, 1H), 4.10-4.04 (m, 1H), 3.98-3.91 (m, 1H), 2.47-2.34 (m, 1H), 2.02-1.85 (m, 3H) ppm.  $^{13}\text{C NMR}$  (75 MHz,  $\text{CDCl}_3$ )  $\delta$  165.15, 141.42, 139.00, 126.35, 118.55, 80.77, 69.28, 33.24, 25.69 ppm. IR (neat,  $\text{cm}^{-1}$ ): 2977, 2950, 2874, 1580, 1534, 1434, 1323, 1156. HRMS *calcd.* for ( $\text{C}_9\text{H}_{11}\text{BrNO}$ )  $[\text{M}+\text{H}]^+$ : 228.0019, *found* 228.0012.



**5-(tetrahydrofuran-2-yl)pyrimidine (33).** Following the general procedure A, using 5-bromopyrimidine (47.7 mg, 0.3 mmol), the title compound was obtained in 77% yield (34.7 mg) after 72 h as colorless oil.  $^1\text{H NMR}$  (300 MHz,  $\text{CDCl}_3$ )  $\delta$  9.11 (s, 1H), 8.69 (s, 2H), 4.90 (t,  $J = 7.2$  Hz, 1H), 4.12-4.05 (m, 1H), 3.98-3.91 (m, 1H), 2.46-2.35 (m, 1H), 2.09-1.99 (m, 2H), 1.86-1.74 (m, 1H) ppm.  $^{13}\text{C NMR}$  (75 MHz,  $\text{CDCl}_3$ )  $\delta$  157.84, 154.75, 136.55, 76.59, 69.01, 34.38, 26.05 ppm. IR (neat,  $\text{cm}^{-1}$ ): 2974, 2873, 1564, 1436, 1409, 1165, 1062, 910. HRMS *calcd.* for ( $\text{C}_8\text{H}_{11}\text{N}_2\text{O}$ )  $[\text{M}+\text{H}]^+$ : 151.0866, *found* 151.0870.

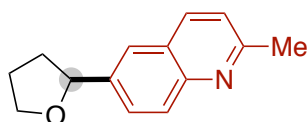


**2-(thiophen-3-yl)tetrahydrofuran (34).** Following the general procedure A, using 3-bromothiophene (48.9 mg, 0.3 mmol), the title compound was obtained in 91% yield (42.1 mg) after 60 h as colorless oil.  $^1\text{H NMR}$  (300 MHz,  $\text{CDCl}_3$ )  $\delta$  7.29 (dd,  $J = 5.1, 3.0$  Hz, 1H), 7.18-7.17 (m, 1H), 7.04 (dd,  $J = 5.1, 0.9$  Hz, 1H), 4.95 (t,  $J = 6.9$  Hz, 1H), 4.08-4.00 (m, 1H), 3.92-3.85 (m, 1H), 2.33-2.22 (m, 1H), 2.06-1.82 (m, 3H) ppm.  $^{13}\text{C NMR}$  (75 MHz,  $\text{CDCl}_3$ )  $\delta$  144.62, 126.04, 125.96, 120.59, 77.29, 68.34, 33.52, 26.03 ppm. IR (neat,  $\text{cm}^{-1}$ ): 3103, 2957, 2926, 2872, 1717, 1673, 1412, 1262. HRMS *calcd.* for ( $\text{C}_8\text{H}_{10}\text{NaOS}$ )  $[\text{M}+\text{Na}]^+$ : 177.0345, *found* 177.0349.

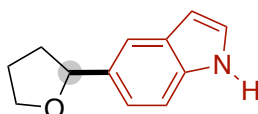


**2-(dibenzo[*b,d*]thiophen-4-yl)tetrahydrofuran (35).** Following the general procedure A, using 4-bromodibenzo[*b,d*]thiophene (78.9 mg, 0.3 mmol), the title compound was obtained in 93% yield (68.4 mg) after 60 h as colorless oil.  $^1\text{H NMR}$  (300 MHz,  $\text{CDCl}_3$ )  $\delta$  8.21-8.15 (m, 2H), 7.86-7.80 (m, 2H), 7.48-7.41 (m, 3H), 5.08 (t,  $J = 7.2$  Hz, 1H), 4.24-4.16 (m, 1H), 4.05-3.98 (m, 1H), 2.48-2.37 (m, 1H), 2.13-2.01 (m, 2H), 1.95-1.84 (m, 1H) ppm.  $^{13}\text{C NMR}$  (75 MHz,  $\text{CDCl}_3$ )  $\delta$  140.14, 139.94, 138.29, 135.72, 135.65, 126.78, 124.79, 124.42, 122.97, 122.76, 121.80, 118.66, 80.89, 68.92, 35.16, 26.23 ppm. IR (neat,  $\text{cm}^{-1}$ ): 2971, 2944, 2865, 1469, 1430, 1309, 1229, 1060. HRMS *calcd.* for ( $\text{C}_{16}\text{H}_{14}\text{NaOS}$ )  $[\text{M}+\text{Na}]^+$ : 277.0658, *found* 277.0664.

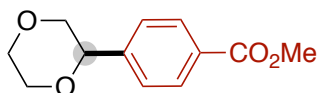




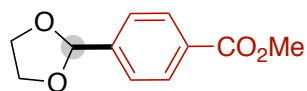
**2-methyl-6-(tetrahydrofuran-2-yl)quinolone (36):** Following the general procedure A, using 6-bromo-2-methylquinoline (66.6 mg, 0.3 mmol), the title compound was obtained in 54% yield (34.6 mg) after 72 h as yellow oil.  $^1\text{H}$  NMR (300 MHz,  $\text{CDCl}_3$ )  $\delta$  8.01 (t,  $J = 7.2$  Hz, 2H), 7.73 (s, 1H), 7.62 (dd,  $J = 8.7, 1.8$  Hz, 1H), 7.26 (d,  $J = 8.4$  Hz, 1H), 5.05 (t,  $J = 7.2$  Hz, 1H), 4.20-4.12 (m, 1H), 4.03-3.95 (m, 1H), 2.73 (s, 3H), 2.45-2.34 (m, 1H), 2.05-2.00 (m, 2H), 1.92-1.80 (m, 1H) ppm.  $^{13}\text{C}$  NMR (75 MHz,  $\text{CDCl}_3$ )  $\delta$  158.75, 147.30, 141.05, 136.44, 128.66, 127.81, 126.37, 123.70, 122.30, 80.54, 68.99, 34.75, 26.19, 25.28 ppm. IR (neat,  $\text{cm}^{-1}$ ): 2950, 2870, 1717, 1682, 1601, 1498, 1388, 1057. HRMS *calcd.* for  $(\text{C}_{14}\text{H}_{16}\text{NO})$   $[\text{M}+\text{H}]^+$ : 214.1226, *found* 214.1231.



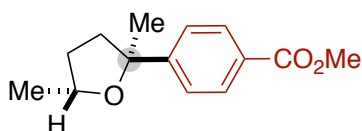
**5-(tetrahydrofuran-2-yl)-1H-indole (37):** Following the general procedure A, using 5-bromo-1H-indole (58.8 mg, 0.3 mmol), the title compound was obtained in 75% yield (42.1 mg) after 72 h as yellow oil.  $^1\text{H}$  NMR (300 MHz,  $\text{CDCl}_3$ )  $\delta$  8.24 (br, 1H), 7.64 (s, 1H), 7.33 (d,  $J = 8.4$  Hz, 1H), 7.21-7.15 (m, 2H), 6.53-6.51 (m, 1H), 5.01 (t,  $J = 7.2$  Hz, 1H), 4.20-4.13 (m, 1H), 4.01-3.94 (m, 1H), 2.40-2.30 (m, 1H), 2.12-2.00 (m, 2H), 1.97-1.85 (m, 1H) ppm.  $^{13}\text{C}$  NMR (75 MHz,  $\text{CDCl}_3$ )  $\delta$  135.37, 134.66, 127.86, 124.64, 120.36, 117.97, 111.09, 102.67, 81.67, 68.66, 34.99, 26.30 ppm. IR (neat,  $\text{cm}^{-1}$ ): 3408, 3284, 2971, 2869, 1720, 1583, 1322, 1042. HRMS *calcd.* for  $(\text{C}_{12}\text{H}_{13}\text{NNaO})$   $[\text{M}+\text{Na}]^+$ : 210.0889, *found* 210.0892.



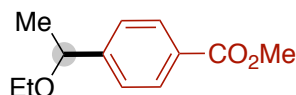
**methyl 4-(1,4-dioxan-2-yl)benzoate (38):** Following the general procedure A, using methyl 4-bromobenzoate (64.5 mg, 0.3 mmol), 1,4-dioxane (4.0 mL) and  $\text{NaHCO}_3$  (1.0 eq, 25.2 mg, 0.3 mmol), the title compound was obtained in 58% yield (38.6 mg) after 72 h as colorless oil.  $^1\text{H}$  NMR (300 MHz,  $\text{CDCl}_3$ )  $\delta$  8.01 (d,  $J = 8.1$  Hz, 2H), 7.41 (d,  $J = 8.1$  Hz, 2H), 4.67 (dd,  $J = 10.2, 2.7$  Hz, 1H), 3.98-3.65 (m, 8H), 3.41 (dd,  $J = 11.4, 10.2$  Hz, 1H) ppm.  $^{13}\text{C}$  NMR (75 MHz,  $\text{CDCl}_3$ )  $\delta$  166.89, 143.38, 129.90, 129.84, 126.18, 77.56, 72.37, 67.10, 66.46, 52.23 ppm. The observed spectral data are in good agreement with the ones reported in literature<sup>9</sup>.



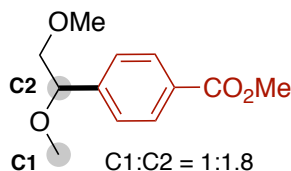
**(4-(1,3-dioxolan-2-yl)phenyl)methanol (39):** Following the general procedure A, using methyl 4-bromobenzoate (64.5 mg, 0.3 mmol), 1,3-dioxolane (3.0 mL), benzene (3.0 mL), **A1** (50 mol%, 42.0 mg, 0.15 mmol),  $\text{Ni}(\text{acac})_2$  (20 mol%, 15.4 mg, 0.06 mmol), and **L1** (20 mol%, 11.2 mg, 0.06 mmol), the title compound was obtained in 75% yield (46.8 mg) after 72 h as colorless oil.  $^1\text{H}$  NMR (300 MHz,  $\text{CDCl}_3$ )  $\delta$  8.07-8.03 (m, 2H), 7.56-7.53 (m, 2H), 5.85 (s, 1H), 4.15-4.00 (m, 4H), 3.91 (s, 3H) ppm.  $^{13}\text{C}$  NMR (75 MHz,  $\text{CDCl}_3$ )  $\delta$  166.87, 142.88, 130.91, 129.78, 126.55, 103.12, 65.49, 52.28 ppm. The observed spectral data are in good agreement with the ones reported in literature<sup>10</sup>.



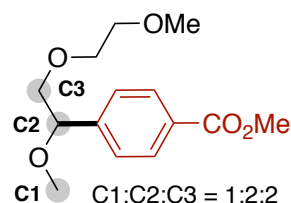
**methyl 4-(2,5-dimethyltetrahydrofuran-2-yl)benzoate (40).** Following the general procedure A, using methyl 4-bromobenzoate (64.5 mg, 0.3 mmol), 2,5-dimethyltetrahydrofuran (2.0 mL), benzene (4.0 mL) and  $\text{NaHCO}_3$  (1.0 eq, 25.2 mg, 0.3 mmol), the title compound was obtained in 43% yield (30.2 mg) after 96 h as colorless oil.  $^1\text{H}$  NMR (300 MHz,  $\text{CDCl}_3$ )  $\delta$  8.00-7.96 (m, 2H), 7.48-7.44 (m, 2H), 4.17-4.07 (m, 1H), 3.90 (s, 3H), 2.25-2.09 (m, 2H), 1.97-1.86 (m, 1H), 1.67-1.58 (m, 1H), 1.53 (s, 3H), 1.33 (d,  $J = 7.5$  Hz, 3H) ppm.  $^{13}\text{C}$  NMR (75 MHz,  $\text{CDCl}_3$ )  $\delta$  167.22, 154.30, 129.71, 128.38, 124.84, 84.56, 75.33, 52.15, 39.71, 33.47, 31.05, 21.99 ppm. IR (neat,  $\text{cm}^{-1}$ ): 2970, 2928, 1723, 1611, 1436, 1277, 1179, 1111. HRMS *calcd.* for  $(\text{C}_{14}\text{H}_{19}\text{O}_3)$   $[\text{M}+\text{H}]^+$ : 235.1329, *found* 235.1329.



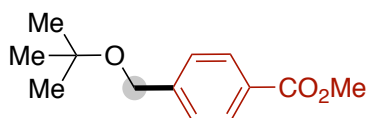
**methyl 4-(1-ethoxyethyl)benzoate (41).** Following the general procedure A, using methyl 4-bromobenzoate (64.5 mg, 0.3 mmol), diethyl ether (4.0 mL) and  $\text{NaHCO}_3$  (1.0 eq, 25.2 mg, 0.3 mmol), the title compound was obtained in 83% yield (51.8 mg) after 96 h as colorless oil.  $^1\text{H}$  NMR (300 MHz,  $\text{CDCl}_3$ )  $\delta$  8.00 (d,  $J = 8.1$  Hz, 2H), 7.37 (d,  $J = 8.1$  Hz, 2H), 4.44 (q,  $J = 6.6$  Hz, 1H), 3.90 (s, 3H), 3.40-3.30 (m, 1H), 1.42 (d,  $J = 6.6$  Hz, 3H), 1.18 (t,  $J = 6.9$  Hz, 3H) ppm.  $^{13}\text{C}$  NMR (75 MHz,  $\text{CDCl}_3$ )  $\delta$  167.06, 149.77, 129.91, 129.30, 126.09, 77.49, 64.31, 52.14, 24.19, 15.48 ppm. IR (neat,  $\text{cm}^{-1}$ ): 2975, 2953, 2869, 1720, 1611, 1435, 1273, 1096. HRMS *calcd.* for  $(\text{C}_{12}\text{H}_{17})$   $[\text{M}+\text{H}]^+$ : 209.1172, *found* 209.1167.



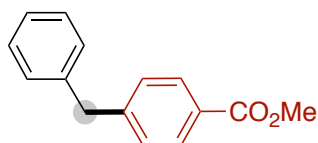
**arylated 1,2-dimethoxyethane (42).** Following the general procedure A, methyl 4-bromobenzoate (64.5 mg, 0.3 mmol), 1,2-dimethoxyethane (4.0 mL) were used, the product was obtained in 81% yield (54.5 mg) in a mixture (C1:C2 = 1:1.8) after 96 h as a colorless oil. [C1]:  $^1\text{H}$  NMR (300 MHz,  $\text{CDCl}_3$ )  $\delta$  7.99 (d,  $J = 8.4$  Hz, 2H), 7.40 (d,  $J = 8.4$  Hz, 2H), 4.61 (s, 2H), 3.89 (s, 3H), 3.64-3.56 (m, 4H), 3.38 (s, 3H) ppm. [C2]: 8.02 (d,  $J = 8.4$  Hz, 2H), 7.39 (d,  $J = 8.4$  Hz, 2H), 4.42 (d,  $J = 7.8$ , 3.6 Hz, 1H), 3.56 (dd,  $J = 10.5$ , 7.8 Hz, 1H), 3.41 (dd,  $J = 10.5$ , 3.6 Hz, 1H), 3.36 (s, 3H), 3.28 (s, 3H) ppm.  $^{13}\text{C}$  NMR (75 MHz,  $\text{CDCl}_3$ )  $\delta$  167.01, 166.89, 144.30, 143.64, 129.98, 129.86, 129.76, 129.42, 127.31, 127.02, 82.70, 72.76, 72.02, 69.82, 59.37, 59.16, 57.31, 52.18, 52.13. ppm. IR (neat,  $\text{cm}^{-1}$ ): 2930, 2886, 2826, 1719, 1612, 1435, 1275, 1098. HRMS *calcd.* for  $(\text{C}_{12}\text{H}_{16}\text{NaO}_4)$   $[\text{M}+\text{Na}]^+$ : 247.0941, *found* 247.0944.



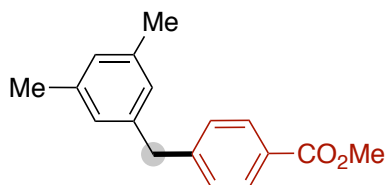
**arylated diethylene glycol dimethyl ether (43).** Following the general procedure A, methyl 4-bromobenzoate (64.5 mg, 0.3 mmol), diethylene glycol dimethyl ether (4.0 mL) were used, the product was obtained in 94% yield (75.6 mg) in a mixture (C1:C2:C3 = 1:2:2) after 96 h as colorless oil.  $^1\text{H}$  NMR (300 MHz,  $\text{CDCl}_3$ )  $\delta$  8.01-7.96 (m, 10H), 7.42-7.36 (m, 10H), 4.59(s, 2H), 4.55 (dd,  $J = 7.2$ , 4.3 Hz, 2H), 4.45 (dd,  $J = 7.6$ , 3.8 Hz, 2H), 3.88 (s, 15H), 3.66-3.48 (m, 32H), 3.35(s, 3H), 3.33-3.33(m, 12H), 3.31 (s, 6H), 3.27 (s, 6H) ppm.  $^{13}\text{C}$  NMR (75 MHz,  $\text{CDCl}_3$ )  $\delta$  166.97, 166.88, 144.85, 144.48, 143.73, 129.86, 129.79, 129.77, 129.71, 127.24, 127.00, 126.97, 82.86, 81.39, 76.86, 75.71, 72.66, 72.01, 71.97, 71.95, 70.94, 70.70, 70.67, 69.92, 68.70, 59.32, 59.07, 59.01, 57.27, 52.13, 52.09 ppm. IR (neat,  $\text{cm}^{-1}$ ): 2860, 2878, 1719, 1612, 1436, 1275, 1098, 1019. HRMS *calcd.* for  $(\text{C}_{14}\text{H}_{20}\text{NaO}_5)$   $[\text{M}+\text{Na}]^+$ : 291.1203, *found* 291.1212.



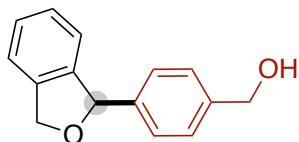
**methyl 4-(*tert*-butoxymethyl)benzoate (44).** Following the general procedure A, using methyl 4-bromobenzoate (64.5 mg, 0.3 mmol), *tert*-butyl methyl ether (4.0 mL) and NaHCO<sub>3</sub> (1.0 eq, 25.2 mg, 0.3 mmol), the title compound was obtained in 65% yield (43.3 mg) after 96 h as colorless oil. <sup>1</sup>H NMR (300 MHz, CDCl<sub>3</sub>) δ 8.00 (d, *J* = 8.1 Hz, 2H), 7.41 (d, *J* = 8.1 Hz, 2H), 4.50 (s, 2H), 3.90 (s, 3H), 1.30 (s, 9H) ppm. <sup>13</sup>C NMR (75 MHz, CDCl<sub>3</sub>) δ 167.23, 145.52, 129.74, 129.00, 127.06, 73.88, 63.75, 52.15, 27.78 ppm. IR (neat, cm<sup>-1</sup>): 2974, 1720, 1435, 1274, 1190, 1107, 1081, 1019. HRMS *calcd.* for (C<sub>13</sub>H<sub>19</sub>O<sub>3</sub>) [M+H]<sup>+</sup>: 223.1329, *found* 223.1322.



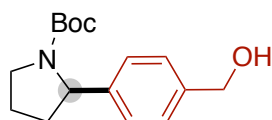
**methyl 4-benzylbenzoate (45).** Following the general procedure A, using methyl 4-bromobenzoate (64.5 mg, 0.3 mmol), toluene (4.0 mL) and NaHCO<sub>3</sub> (1.0 eq, 25.2 mg, 0.3 mmol), the title compound was obtained in 71% yield (48.2 mg) after 96 h as colorless oil. <sup>1</sup>H NMR (300 MHz, CDCl<sub>3</sub>) δ 7.96 (d, *J* = 8.4 Hz, 2H), 7.33-7.17 (m, 7H), 4.04 (s, 2H), 3.90 (s, 3H) ppm. <sup>13</sup>C NMR (75 MHz, CDCl<sub>3</sub>) δ 167.19, 146.65, 140.25, 129.96, 129.08, 128.74, 128.23, 126.51, 52.14, 42.06 ppm. The observed spectral data are in good agreement with the ones reported in literature<sup>11</sup>.



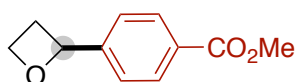
**methyl 4-(3,5-dimethylbenzyl)benzoate (46).** Following the general procedure A, using methyl 4-bromobenzoate (64.5 mg, 0.3 mmol), mesitylene (4.0 mL) and NaHCO<sub>3</sub> (1.0 eq, 25.2 mg, 0.3 mmol), the title compound was obtained in 60% yield (45.7 mg) after 96 h as colorless oil. <sup>1</sup>H NMR (300 MHz, CDCl<sub>3</sub>) δ 7.96 (d, *J* = 8.4 Hz, 2H), 7.26 (d, *J* = 8.4 Hz, 2H), 3.95 (s, 2H), 3.90 (s, 3H), 2.28 (s, 6H) ppm. <sup>13</sup>C NMR (75 MHz, CDCl<sub>3</sub>) δ 167.26, 146.93, 140.14, 138.25, 129.92, 129.08, 128.14, 126.91, 52.14, 41.95, 21.40 ppm. IR (neat, cm<sup>-1</sup>): 3015, 2950, 2918, 1718, 1601, 1434, 1275, 1104. HRMS *calcd.* for (C<sub>17</sub>H<sub>19</sub>O<sub>2</sub>) [M+H]<sup>+</sup>: 255.1380, *found* 255.1374.



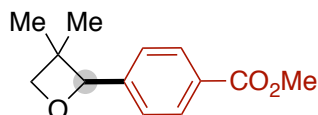
**(4-(1,3-dihydroisobenzofuran-1-yl)phenyl)methanol (47).** Following the general procedure A, using (4-bromophenyl)methanol (56.1 mg, 0.3 mmol), phthalan (2.0 eq, 72.1 mg, 0.6 mmol), benzene (4.0 mL), and **L2** (10 mol%, 5.6 mg), the title compound was obtained in 63% yield (42.7 mg) after 96 h as colorless oil. <sup>1</sup>H NMR (300 MHz, CDCl<sub>3</sub>) δ 7.36-7.20 (m, 7H), 7.02 (d, *J* = 7.5 Hz, 1H), 6.17 (s, 1H), 5.34 (dd, *J* = 12.0, 2.4 Hz, 1H), 5.21 (dd, *J* = 12.0, 1.8 Hz, 1H), 4.66 (s, 2H), 1.91 (br, 1H) ppm. <sup>13</sup>C NMR (75 MHz, CDCl<sub>3</sub>) δ 142.00, 141.70, 140.91, 139.15, 127.78, 127.64, 127.32, 122.36, 121.06, 86.09, 73.38, 65.16 ppm. IR (neat, cm<sup>-1</sup>): 3375, 2921, 2855, 1460, 1420, 1357, 1029, 1013. HRMS *calcd.* for (C<sub>15</sub>H<sub>13</sub>O<sub>2</sub>) [M-H]<sup>+</sup>: 225.0910, *found* 226.0907.



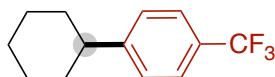
**tert-butyl 2-(4-(hydroxymethyl)phenyl)pyrrolidine-1-carboxylate (48).** Following the general procedure A, using (4-bromophenyl)methanol (56.1 mg, 0.3 mmol), *N*-Boc-pyrrolidine (10 eq, 513.7 mg, 3.0 mmol), benzene (4.0 mL) and **A4** (20 mol%, 16.8 mg, 0.06 mmol), the title compound was obtained as rotamers in 83% yield (69.0 mg) after 72 h as a pale oil.  $^1\text{H}$  NMR (300 MHz,  $\text{CDCl}_3$ ):  $\delta$  7.27 (d,  $J = 7.8$  Hz, 2H), 7.13 (d,  $J = 7.8$  Hz, 2H), 4.92 and 4.76 (2 brs, 1H, rotamer), 4.63 (s, 2H), 3.75-3.52 (m, 2H), 2.51-2.29 (m, 2H), 1.97-1.74 (m, 3H), 1.43 (s, 3H), 1.17 (s, 6H) ppm.  $^{13}\text{C}$  NMR (75 MHz,  $\text{CDCl}_3$ )  $\delta$  154.72 (154.60), 144.45 (143.61), 139.38, (127.24) 126.92, 125.67, (82.90) 79.37, 65.04, 61.14 (60.59), (47.41) 47.12, 36.03 (34.93), (28.58) 28.27, (23.53) 23.16 ppm. IR (neat,  $\text{cm}^{-1}$ ): 3433, 2974, 2929, 2874, 1693, 1672, 1395, 1366. HRMS *calcd.* for ( $\text{C}_{16}\text{H}_{23}\text{NNaO}_3$ ) [ $\text{M}+\text{Na}$ ] $^+$ : 300.1570, *found* 300.1561.



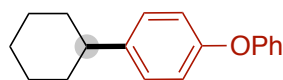
**methyl 4-(oxetan-2-yl)benzoate (49).** Following the general procedure A, using methyl 4-bromobenzoate (64.5 mg, 0.3 mmol), oxetane (20 eq, 348.5 mg, 6.0 mmol), benzene (4.0 mL), **A1** (20 mol%, 16.8 mg, 0.06 mmol) and  $\text{NaHCO}_3$  (1.0 eq, 25.2 mg, 0.3 mmol), the title compound was obtained in 78% yield (44.9 mg) after 96 h as colorless oil.  $^1\text{H}$  NMR (300 MHz,  $\text{CDCl}_3$ )  $\delta$  8.05 (d,  $J = 8.1$  Hz, 2H), 7.48 (d,  $J = 8.1$  Hz, 2H), 5.85 (t,  $J = 7.5$  Hz, 1H), 4.84 (dt,  $J = 7.8, 6.0$  Hz, 1H), 4.67 (dt,  $J = 9.0, 6.0$  Hz, 1H), 3.91 (s, 3H), 3.12-3.01 (m, 1H), 2.67-2.55 (m, 1H) ppm.  $^{13}\text{C}$  NMR (75 MHz,  $\text{CDCl}_3$ )  $\delta$  167.00, 148.83, 129.98, 129.57, 124.99, 82.34, 68.54, 52.21, 30.73 ppm. The observed spectral data are in good agreement with the ones reported in literature<sup>12</sup>.



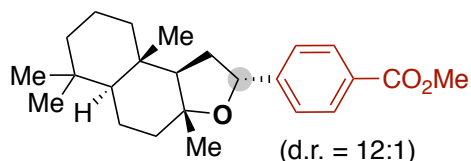
**methyl 4-(3,3-dimethyloxetan-2-yl)benzoate (50).** Following the general procedure A, using methyl 4-bromobenzoate (64.5 mg, 0.3 mmol), 3,3-dimethyloxetane (20 eq, 516.8 mg, 6.0 mmol), benzene (4.0 mL), **A4** (20 mol%, 16.8 mg, 0.06 mmol) and  $\text{NaHCO}_3$  (1.0 eq, 25.2 mg, 0.3 mmol), the title compound was obtained in 45% yield (29.7 mg) after 96 h as colorless oil.  $^1\text{H}$  NMR (300 MHz,  $\text{CDCl}_3$ )  $\delta$  8.04 (d,  $J = 8.1$  Hz, 2H), 7.35 (d,  $J = 8.1$  Hz, 2H), 5.54 (s, 1H), 5.54 (d,  $J = 5.4$  Hz, 1H), 4.26 (d,  $J = 5.4$  Hz, 1H), 3.91 (s, 3H), 1.42 (s, 3H), 0.77 (s, 3H) ppm.  $^{13}\text{C}$  NMR (75 MHz,  $\text{CDCl}_3$ )  $\delta$  167.15, 145.61, 129.64, 129.27, 125.09, 91.34, 81.49, 77.58, 77.16, 52.20, 40.83, 27.05, 22.58 ppm. IR (neat,  $\text{cm}^{-1}$ ): 2955, 2869, 1719, 1611, 1435, 1273, 1173, 1101. HRMS *calcd.* for ( $\text{C}_{13}\text{H}_{16}\text{NaO}_3$ ) [ $\text{M}+\text{Na}$ ] $^+$ : 243.0992, *found* 243.0992.



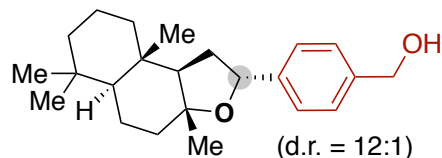
**1-cyclohexyl-4-(trifluoromethyl)benzene (51).** Following the general procedure A, using 1-bromo-4-(trifluoromethyl)benzene (67.5 mg, 0.3 mmol), cyclohexane (3.0 mL), benzene (3.0 mL), **A4** (20 mol%, 42.0 mg, 0.06 mmol)  $\text{Ni}(\text{acac})_2$  (10 mol%, 7.7 mg, 0.03 mmol) and **L1** (10 mol%, 5.6 mg, 0.03 mmol), the title compound was obtained in 71% yield (48.6 mg) after 96 h as colorless oil.  $^1\text{H}$  NMR (300 MHz,  $\text{CDCl}_3$ )  $\delta$  7.56 (d,  $J = 8.1$  Hz, 2H), 7.32 (d,  $J = 8.1$  Hz, 2H), 2.65-2.48 (m, 1H), 1.91-1.76 (m, 5H), 1.51-1.23 (m, 5H) ppm.  $^{13}\text{C}$  NMR (75 MHz,  $\text{CDCl}_3$ )  $\delta$  152.17, 128.24 (q,  $J_{\text{C-F}} = 32.0$  Hz), 127.29, 125.35 (q,  $J_{\text{C-F}} = 3.8$  Hz), 124.58 (q,  $J_{\text{C-F}} = 269.9$  Hz), 44.67, 34.37, 26.89, 26.18 ppm.  $^{19}\text{F}$  NMR (376 MHz,  $\text{CDCl}_3$ )  $\delta$  -62.37 ppm. The observed spectral data are in good agreement with the ones reported in literature<sup>13</sup>.



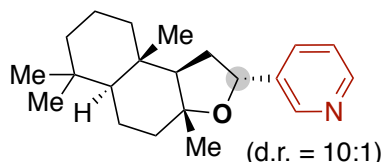
**1-cyclohexyl-4-phenoxybenzene (52).** Following the general procedure A, using 1-bromo-4-phenoxybenzene (74.7 mg, 0.3 mmol), cyclohexane (3.0 mL), benzene (3.0 mL) and **A4** (20 mol%, 16.8 mg, 0.06 mmol), the title compound was obtained in 45% yield (34.1 mg) after 96 h as colorless oil.  $^1\text{H NMR}$  (300 MHz,  $\text{CDCl}_3$ )  $\delta$  7.35-7.30 (m, 2H), 7.20-7.16 (m, 2H), 7.11-6.93 (m, 5H), 2.56-2.45 (m, 1H), 1.90-1.74 (m, 5H), 1.44-1.20 (m, 5H) ppm.  $^{13}\text{C NMR}$  (75 MHz,  $\text{CDCl}_3$ )  $\delta$  157.80, 155.10, 143.30, 129.77, 128.06, 122.99, 118.98, 118.69, 44.02, 34.79, 27.06, 26.29 ppm. IR (neat,  $\text{cm}^{-1}$ ): 2972, 2850, 1590, 1488, 1222, 1190, 1167, 861. HRMS *calcd.* for ( $\text{C}_{18}\text{H}_{21}\text{O}$ ) [ $\text{M}+\text{H}$ ] $^+$ : 253.1587, *found* 253.1586.



**methyl 4-((2R,3aR,5aS,9aS,9bR)-3a,6,6,9a-tetramethyldodecahydronaphtho[2,1-b]furan-2-yl)benzoate (53).** Following the general procedure A, using (-)-ambroxide (709.2 mg, 3.0 mmol), methyl 4-bromobenzoate (64.5 mg, 0.3 mmol), benzene (5.0 mL) and  $\text{NaHCO}_3$  (25.2 mg, 0.3 mmol), the title compound was obtained in 69% yield (76.7 mg, dr = 12: 1) after 96 h as colorless oil.  $^1\text{H NMR}$  (300 MHz,  $\text{CDCl}_3$ )  $\delta$  7.98 (d,  $J = 8.4$  Hz, 2H), 7.39 (d,  $J = 8.4$  Hz, 2H), 5.17-5.13 (m, 1H), 3.90 (s, 3H), 2.37-2.23 (m, 1H), 2.09-2.03 (m, 1H), 1.85-0.83 (m, 24 H) ppm.  $^{13}\text{C NMR}$  (75 MHz,  $\text{CDCl}_3$ )  $\delta$  167.20, 150.71, 129.71, 128.78, 125.70, 82.23, 76.89, 58.74, 57.40, 52.12, 42.49, 39.96, 36.35, 33.67, 33.23, 32.39, 21.81, 21.25, 20.75, 18.44, 15.18 ppm. IR (neat,  $\text{cm}^{-1}$ ): 2925, 2868, 1721, 1611, 1436, 1379, 1274, 1111. HRMS *calcd.* for ( $\text{C}_{24}\text{H}_{34}\text{NaO}_3$ ) [ $\text{M}+\text{Na}$ ] $^+$ : 393.2400, *found* 393.2404.

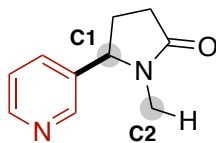


**4-((2R,3aR,5aS,9aS,9bR)-3a,6,6,9a-tetramethyldodecahydronaphtho[2,1-b]furan-2-yl)phenylmethanol (54).** Following the general procedure A, using [(-)-ambroxide (709.2 mg, 3.0 mmol), (4-bromophenyl)methanol (51.1 mg, 0.3 mmol), benzene (5.0 mL) and **A4** (20 mol%, 16.8 mg, 0.06 mmol), the title compound was obtained in 73% yield (75.0 mg, d.r. = 12: 1) after 96 h as colorless oil.  $^1\text{H NMR}$  (300 MHz,  $\text{CDCl}_3$ )  $\delta$  7.35-7.26 (m, 4H), 5.12-5.08 (m, 1H), 4.62 (s, 2H), 2.32-2.19 (m, 1H), 2.08-2.03 (m, 2H), 1.84-0.84 (m, 25H) ppm.  $^{13}\text{C NMR}$  (75 MHz,  $\text{CDCl}_3$ )  $\delta$  144.69, 139.63, 127.04, 125.99, 81.97, 77.09, 65.20, 58.90, 57.42, 42.52, 39.99, 39.97, 36.33, 33.68, 33.22, 32.29, 21.76, 21.25, 20.75, 18.46, 15.16. IR (neat,  $\text{cm}^{-1}$ ): 3406, 2995, 2867, 1459, 1378, 1122, 1078, 1004. HRMS *calcd.* for ( $\text{C}_{23}\text{H}_{34}\text{NaO}_2$ ) [ $\text{M}+\text{Na}$ ] $^+$ : 365.2451, *found* 365.2454.



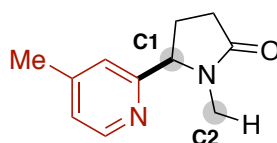
**3-((2R,3aR,5aS,9aS,9bR)-3a,6,6,9a-tetramethyldodecahydronaphtho[2,1-b]furan-2-yl)pyridine (55).** Following the general procedure A, using [(-)-ambroxide (709.2 mg, 3.0 mmol), 3-bromopyridine (47.4 mg, 0.3 mmol), benzene (5.0 mL) and **A4** (20 mol%, 16.8 mg, 0.06 mmol), the title compound was obtained in 85% yield (79.9 mg, d.r. = 10: 1) after 96 h as colorless oil.  $^1\text{H NMR}$  (300 MHz,  $\text{CDCl}_3$ )  $\delta$  8.57-8.46 (m, 2H), 7.72-7.64 (m, 1H), 7.26-7.22 (m, 1H), 5.15-5.04

(m, 1H), 2.37-2.24 (m, 1H), 2.08-2.02 (m, 1H), 1.85-0.83 (m, 24H) ppm.  $^{13}\text{C}$  NMR (75 MHz,  $\text{CDCl}_3$ )  $\delta$  148.38, 147.85, 140.58, 133.58, 123.37, 82.29, 75.19, 58.95, 57.44, 42.49, 39.98, 39.93, 36.37, 33.68, 33.23, 32.18, 21.75, 21.24, 20.74, 18.44, 15.17 ppm. IR (neat,  $\text{cm}^{-1}$ ): 2995, 2850, 2667, 1459, 1378, 1217, 1123, 1005. HRMS *calcd.* for  $(\text{C}_{21}\text{H}_{32}\text{NO})$   $[\text{M}+\text{H}]^+$ : 314.2478, *found* 314.2475.



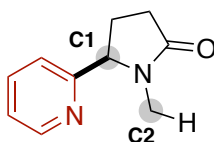
C1:C2 = 20:1

**1-methyl-5-(pyridine-3-yl)pyrrolidin-2-one ( $\pm$ )-Cotinine (56).** Following the general procedure A, using *N*-methyl-2-pyrrolidone (297.4 mg, 3.0 mmol), 3-bromopyridine (47.4 mg, 0.3 mmol), benzene (5.0 mL) and **A4** (20 mol%, 16.8 mg, 0.06 mmol). The reaction mixture was directly purified by flash column chromatography in silica gel with EtOAc/MeOH to give the title compound in 90% yield (47.6 mg, C1:C2 = 20: 1) after 72 h as colorless oil.  $^1\text{H}$  NMR (300 MHz,  $\text{CDCl}_3$ )  $\delta$  8.60 (dd,  $J = 4.8, 1.5$  Hz, 1H), 8.51 (d,  $J = 2.1$  Hz, 1H), 7.54 (dt,  $J = 7.8, 2.1$  Hz, 1H), 7.37-7.33 (m, 1H), 4.58 (t,  $J = 6.6$  Hz, 1H), 2.68 (s, 3H), 2.60-2.48 (m, 3H), 1.96-1.84 (m, 1H) ppm.  $^{13}\text{C}$  NMR (75 MHz,  $\text{CDCl}_3$ )  $\delta$  175.35, 149.73, 148.45, 136.55, 133.73, 124.01, 62.16, 29.96, 28.25 ppm. IR (neat,  $\text{cm}^{-1}$ ): 2955, 2932, 1674, 1578, 1460, 1422, 1396, 1269. HRMS *calcd.* for  $(\text{C}_{10}\text{H}_{13}\text{N}_2\text{O})$   $[\text{M}+\text{H}]^+$ : 177.1022, *found* 177.1023.



C1:C2 = 16:1

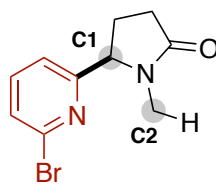
**1-methyl-5-(4-methylpyridine-2-yl)pyrrolidin-2-one (57).** Following the general procedure A, using *N*-methyl-2-pyrrolidone (297.4 mg, 3.0 mmol), 2-bromo-4-methylpyridine (51.6 mg, 0.3 mmol), benzene (5.0 mL) and **A4** (20 mol%, 16.8 mg, 0.06 mmol). The reaction mixture was directly purified by flash column chromatography in silica gel with EtOAc/MeOH to give the title compound in 78% yield (44.5 mg, C1:C2 = 16: 1) after 72 h as pale yellow oil.  $^1\text{H}$  NMR (400 MHz,  $\text{CD}_3\text{OD}$ )  $\delta$  8.38 (s, 1H), 8.29 (s, 1H), 4.72 (t,  $J = 6.4$  Hz, 1H), 2.65 (s, 3H), 2.61-2.47 (m, 3H), 2.40 (s, 3H), 1.96-1.89 (m, 1H) ppm.  $^{13}\text{C}$  NMR (75 MHz, MeOD)  $\delta$  178.13, 150.42, 146.09, 138.31, 136.74, 136.14, 63.53, 30.98, 28.92, 28.55, 18.31 ppm. IR (neat,  $\text{cm}^{-1}$ ): 2960, 2924, 1671, 1582, 1450, 1397, 1272, 1116. HRMS *calcd.* for  $(\text{C}_{11}\text{H}_{15}\text{N}_2\text{O})$   $[\text{M}+\text{H}]^+$ : 191.1179, *found* 191.1175.



C1:C2 = 20:1

**1-methyl-5-(pyridine-2-yl)pyrrolidin-2-one (58).** Following the general procedure A, using *N*-methyl-2-pyrrolidone (297.4 mg, 3.0 mmol), 2-bromopyridine (47.4 mg, 0.3 mmol), benzene (5.0 mL) and **A4** (20 mol%, 16.8 mg, 0.06 mmol). The reaction mixture was directly purified by flash column chromatography in silica gel with EtOAc/MeOH to give the title compound in 70% yield (37.0 mg, C1:C2 = 20: 1) after 72 h as colorless oil.  $^1\text{H}$  NMR (300 MHz,  $\text{CDCl}_3$ )  $\delta$  8.56 (dt,  $J = 4.8, 0.9$  Hz, 1H), 7.68 (dt,  $J = 7.8, 1.8$  Hz, 1H), 7.20 (dd,  $J = 5.1, 7.5$  Hz, 1H), 7.12 (d,  $J = 7.8$  Hz, 1H), 4.64-4.60 (m, 1H), 2.68 (s, 3H), 2.56-2.37 (m, 3H), 1.99-1.93 (m, 1H) ppm.  $^{13}\text{C}$  NMR (75 MHz,  $\text{CDCl}_3$ )  $\delta$  175.83, 160.40, 150.09,

137.16, 122.94, 120.52, 65.81, 29.92, 28.47, 26.52 ppm. IR (neat,  $\text{cm}^{-1}$ ): 2938, 2925, 1666, 1592, 1437, 1396, 1262, 1115. HRMS *calcd.* for  $(\text{C}_{10}\text{H}_{13}\text{N}_2\text{O})$   $[\text{M}+\text{H}]^+$ : 177.1022, *found* 177.1027.



C1:C2 = 14:1

**5-(6-bromopyridin-2-yl)-1-methylpyrrolidin-2-one (59).** Following the general procedure A, using *N*-methyl-2-pyrrolidone (297.4 mg, 3.0 mmol), 2,6-dibromopyridine (71.1 mg, 0.3 mmol), benzene (5.0 mL) and **A4** (20 mol%, 16.8 mg, 0.06 mmol). The reaction mixture was directly purified by flash column chromatography in silica gel with EtOAc/MeOH to give the title compound in 62% yield (47.4 mg, C1:C2 = 14: 1) after 72 h as colorless oil.  $^1\text{H}$  NMR (300 MHz,  $\text{CD}_3\text{OD}$ )  $\delta$  7.57 (t,  $J = 7.5$  Hz, 1H), (d,  $J = 8.1$  Hz, 1H), (d,  $J = 7.5$  Hz, 1H), 4.65-4.61 (m, 1H), 2.74 (s, 3H), 2.60-2.36 (m, 3H), 2.07-1.93 (m, 1H) ppm.  $^{13}\text{C}$  NMR (75 MHz,  $\text{CDCl}_3$ )  $\delta$  175.84, 162.30, 142.59, 139.53, 127.48, 119.05, 65.41, 29.72, 28.67, 26.61. IR (neat,  $\text{cm}^{-1}$ ): 2950, 2923, 1678, 1556, 1433, 1395, 1277, 1119. HRMS *calcd.* for  $(\text{C}_{10}\text{H}_{11}\text{BrN}_2\text{NaO})$   $[\text{M}+\text{Na}]^+$ : 276.9947, *found* 276.9948.

#### 4.9.3.2. Scalable Synthesis of **3**, **21**, **37** and **57**

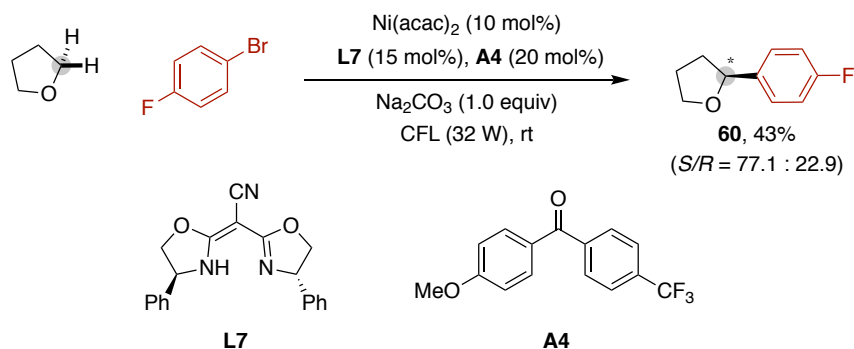
**Gram scale reaction of **3**, **21** and **37**:** An oven-dried 150 mL Schlenk tube containing a stirring bar was charged with **A4** (10 mol%, 280 mg, 1 mmol), **L4** (10 mol%, 186 mg, 1 mmol), aryl bromide (20 mol% of **A4** was used when employing 5-bromo-1*H*-indole). The schlenk tube was transferred to a nitrogen-filled glove-box where the Ni(acac)<sub>2</sub> (10 mol%, 256 mg, 1 mmol), Na<sub>2</sub>CO<sub>3</sub> (1.06 g, 10 mmol) and anhydrous THF (0.075 M, 133mL) were added. Then, the tube was stirred for 1 minute and taken out of the glovebox. The reaction tube was placed approximately ~3 cm away in the middle of two 32 W CFL and it was rigorously stirred for 168-200 h. After completion of the reaction, the crude material concentrated under reduced pressure. The product was directly purified by flash column chromatography in silica gel with pentane/EtOAc to yield corresponding product **3** (95%, 1.9 g), **21** (87%, 1.8 g) and **37** (70%, 1.3 g) and 80-90% of **A4** could be recovered.

**Gram scale reaction of **57**.** An oven-dried 150 mL Schlenk tube containing a stirring bar was charged with **A4** (20 mol%, 560 mg, 2 mmol), **L4** (10 mol%, 186 mg, 1 mmol). The schlenk tube was transferred to a nitrogen-filled glove-box where the Ni(acac)<sub>2</sub> (10 mol%, 256 mg, 1 mmol), Na<sub>2</sub>CO<sub>3</sub> (1.06 g, 10 mmol), anhydrous Benzene (0.075 M, 133mL) 3-Bromo-5-methylpyridine (1.72 g, 10 mmol) and *N*-methyl-2-pyrrolidone (9.91 g, 100 mmol) were added. Then, the reaction tube was stirred for 1 minute and taken out of the glovebox. The tube was placed approximately ~3 cm away in the middle of two 32 W CFL and it was rigorously stirred for 200 h. After completion of the reaction, the crude material was under reduced pressure. The product was directly purified by flash column chromatography in silica gel with EtOAc /MeOH to give **57** in 83% yield (1.6 g) and 91% of **A4** is recovered.



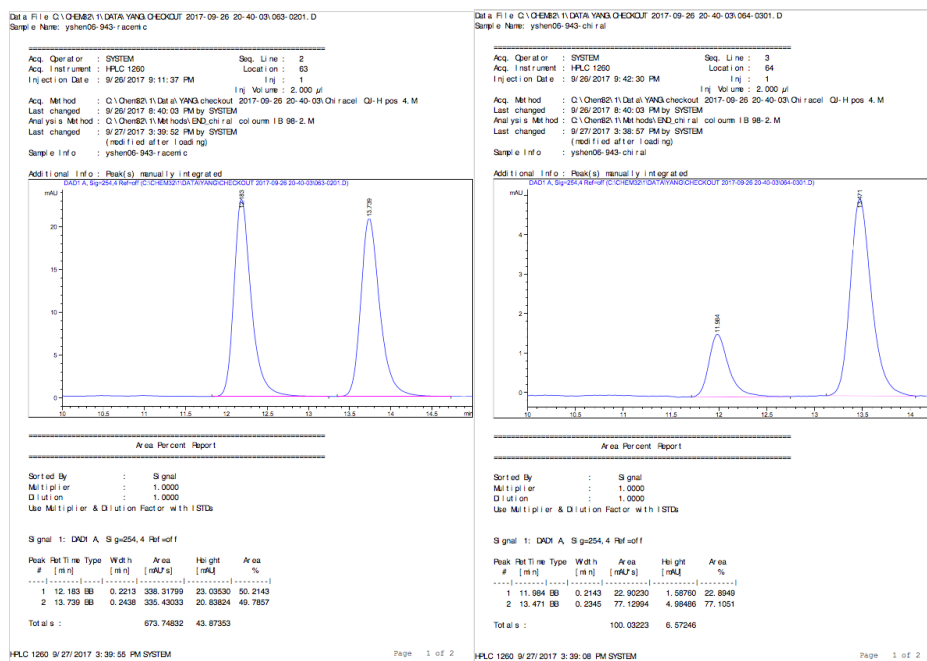
(Left) Gram scale reaction of 3-Bromo-5-methylpyridine and *N*-methyl-2-pyrrolidone (NMP) at  $t = 0$  h. (Middle) Gram scale reaction of 3-Bromo-5-methylpyridine and *N*-methyl-2-pyrrolidone (NMP) at  $t = 200$  h. (Right) Purified by silica gel chromatography, 1.6 g desired product **57** (2.5 mg-\$150) and recovered ketone catalyst.

#### 4.9.3.3. Enantioselective $sp^3$ C-H Arylation



Following the general procedure A, using 1-bromo-4-fluorobenzene (52.5 mg, 0.3 mmol), **L7** (15%, 14.9 mg, 0.045 mmol), and **A4** (20 mol%, 16.8 mg, 0.06 mmol), the chiral compound was obtained in 43% yield (21.4 mg) with 54% *ee* after 60 h as colorless oil.  $^1\text{H}$  NMR (400 MHz,  $\text{CDCl}_3$ )  $\delta$  7.31-7.27 (m, 2H), 7.03-6.98 (m, 2H), 4.85 (t,  $J = 7.2$  Hz, 1H), 4.11-4.06 (m, 1H), 3.92 (q,  $J = 7.2$  Hz, 1H), 2.35-2.27 (m, 1H), 2.04-1.97 (m, 1H), 1.81-1.72 (m, 1H) ppm.  $^{13}\text{C}$  NMR (101 MHz,  $\text{CDCl}_3$ )  $\delta$  162.15 (d,  $J_{\text{C-F}} = 245.5$  Hz), 139.21 (d,  $J_{\text{C-F}} = 2.93$  Hz), 127.39 (d,  $J_{\text{C-F}} = 7.98$  Hz), 115.20 (d,  $J_{\text{C-F}} = 21.4$  Hz), 80.26, 68.77, 34.82, 26.15 ppm.  $^{19}\text{F}$  NMR (376 MHz,  $\text{CDCl}_3$ )  $\delta$  -116.04 ppm.

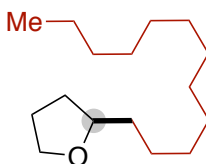




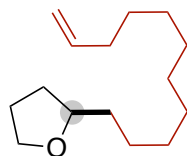
The enantiomeric ratio of **60** was determined by chiral HPLC analysis using Daicel Chiralcel OJ-H column. Conditions: nHexane: isopropanol = 80:20, flow rate 0.5 mL/min,  $\lambda = 254$  nm. For racemic sample  $t_1 = 12.2$  min,  $t_2 = 13.7$  min; chiral sample  $t_1$  (minor) = 12.0 min,  $t_2 = 13.5$  min (major). The absolute configuration of major isomer was assigned as (*S*) based based on reported data in literature.<sup>14</sup>

#### 4.9.3.4. *sp*<sup>3</sup> C-H alkylations

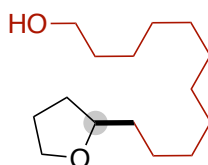
**General Procedure B:** An oven-dried 12.0 mL Schlenk tube containing a stirring bar was charged with **A4** (10 mol%, 8.4 mg, 0.03 mmol), **L2** (10 mol%, 8.1 mg, 0.03 mmol), alkyl bromide (0.30 mmol, if solid), CF<sub>3</sub>CO<sub>2</sub>Na (1.0 eq, 40.8 mg, 0.3 mmol). The schlenk tube was transferred to a nitrogen-filled glove-box where the Ni(acac)<sub>2</sub> (10 mol%, 7.7 mg, 0.03 mmol), Na<sub>2</sub>CO<sub>3</sub> (1.0 eq, 32.0 mg, 0.30 mmol), alkyl bromide (0.30 mmol, if liquid) and anhydrous THF (0.075 M, 4mL) were added. Then, the mixture was stirred for 1 minute and taken out of the glovebox. The Schlenk tube was placed approximately ~3 cm away in the middle of two 32 W CFL and it was rigorously stirred for 36-96 h. After completion of the reaction, the crude material concentrated under reduced pressure. The desired product was directly purified by flash column chromatography in silica gel with pentane/EtOAc.



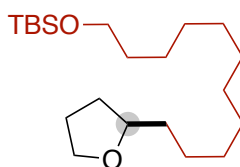
**2-dodecyltetrahydrofuran (61).** Following the general procedure B, using 1-bromododecane (74.8 mg, 0.3 mmol), the title compound was obtained in 84% yield (60.5 mg) after 72 h as colorless oil. <sup>1</sup>H NMR (300 MHz, CDCl<sub>3</sub>)  $\delta$  3.89-3.62 (m, 3H), 2.02-1.76 (m, 3H), 1.55-1.50 (m, 1H), 1.46-1.38 (m, 3H), 1.30-1.14 (m, 19H), 0.87 (t,  $J = 6.4$  Hz, 3H) ppm. <sup>13</sup>C NMR (75 MHz, CDCl<sub>3</sub>)  $\delta$  79.61, 67.72, 35.90, 32.06, 31.52, 29.91, 29.82, 29.79, 29.77, 29.75, 29.50, 26.56, 25.86, 22.83, 14.24 ppm. IR (neat, cm<sup>-1</sup>): 2955, 2935, 2852, 1464, 1378, 1182, 1070, 919. HRMS *calcd.* for (C<sub>16</sub>H<sub>33</sub>O) [M+H]<sup>+</sup>: 241.2526, *found* 241.2526.



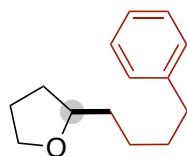
**2-(undec-10-en-1-yl)tetrahydrofuran (62).** Following the general procedure B, using 11-bromoundec-1-ene (69.9 mg, 0.3 mmol), the title compound was obtained in 74% yield (49.8 mg) after 72 h as colorless oil.  $^1\text{H}$  NMR (300 MHz,  $\text{CDCl}_3$ )  $\delta$  5.87-5.73 (m, 1H), 5.01-4.88 (m, 2H), 3.88-3.65 (m, 3H), 2.06-1.78 (m, 6H), 1.64-1.26 (m, 16H) ppm.  $^{13}\text{C}$  NMR (75 MHz,  $\text{CDCl}_3$ )  $\delta$  139.35, 114.20, 79.59, 67.71, 35.89, 33.95, 31.52, 29.88, 29.73, 29.67, 29.62, 29.27, 29.07, 26.54, 25.85, 3.80, 1.42 ppm. IR (neat,  $\text{cm}^{-1}$ ): 2953, 2923, 2853, 1641, 1461, 1069, 1020, 909. HRMS *calcd.* for  $(\text{C}_{15}\text{H}_{29}\text{O})$   $[\text{M}+\text{H}]^+$ : 225.2213, *found* 225.2219.



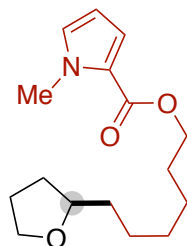
**11-(tetrahydrofuran-2-yl)undecan-1-ol (63).** Following the general procedure B, using 11-bromoundecan-1-ol (75.4 mg, 0.3 mmol), the title compound was obtained in 83% yield (60.3 mg) after 72 h as colorless oil.  $^1\text{H}$  NMR (300 MHz,  $\text{CDCl}_3$ )  $\delta$  3.87-3.63 (m, 3H), 3.59 (t,  $J = 6.6$  Hz, 2H), 2.02-1.78 (m, 4H), 1.56-1.23 (m, 20H) ppm.  $^{13}\text{C}$  NMR (75 MHz,  $\text{CDCl}_3$ )  $\delta$  79.59, 67.66, 63.02, 35.81, 32.88, 31.45, 29.82, 29.68, 29.64, 29.52, 26.47, 25.84, 25.79 ppm. IR (neat,  $\text{cm}^{-1}$ ): 3372, 2922, 2852, 1462, 1350, 1057, 964, 722. HRMS *calcd.* for  $(\text{C}_{15}\text{H}_{30}\text{NaO}_2)$   $[\text{M}+\text{Na}]^+$ : 265.2138, *found* 265.2143.



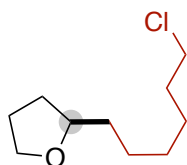
**tert-butyl dimethyl((11-(tetrahydrofuran-2-yl)undecyl)oxy)silane (64):** Following the general procedure B, using ((11-bromoundecyl)oxy)(tert-butyl)dimethylsilane (109.6 mg, 0.3 mmol), the title compound was obtained in 77% yield (82.3 mg) after 72 h as colorless oil.  $^1\text{H}$  NMR (300 MHz,  $\text{CDCl}_3$ )  $\delta$  3.89-3.64 (m, 3H), 3.58 (t,  $J = 6.6$  Hz, 2H), 2.01-1.71 (m, 3H), 1.52-1.36 (m, 21H) ppm.  $^{13}\text{C}$  NMR (75 MHz,  $\text{CDCl}_3$ )  $\delta$  79.59, 67.70, 63.45, 35.89, 33.03, 31.52, 29.90, 29.76, 29.72, 29.58, 26.55, 26.11, 25.94, 25.85, 18.50, -5.13 ppm. IR (neat,  $\text{cm}^{-1}$ ): 2925, 2854, 1463, 1361, 1253, 1098, 1006, 834. HRMS *calcd.* for  $(\text{C}_{21}\text{H}_{44}\text{NaO}_2\text{Si})$   $[\text{M}+\text{Na}]^+$ : 379.3003, *found* 379.3004.



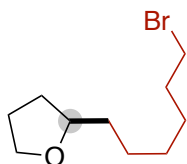
**2-(4-phenylbutyl)tetrahydrofuran (65).** Following the general procedure B, using (4-bromobutyl)benzene (63.9 mg, 0.3 mmol), the title compound was obtained in 85% yield (52.1 mg) after 72 h as colorless oil.  $^1\text{H}$  NMR (300 MHz,  $\text{CDCl}_3$ ):  $\delta$  7.48-7.41 (m, 2H), 7.37-7.30 (m, 3H), 4.08-4.78 (m, 3H), 2.83-2.76 (m, 2H), 2.19-1.97 (m, 3H), 1.88-1.74 (m, 3H), 1.69-1.50 (m, 4H).  $^{13}\text{C}$  NMR (75 MHz,  $\text{CDCl}_3$ )  $\delta$  142.80, 128.50, 128.35, 125.71, 79.44, 67.73, 36.07, 35.72, 31.77, 31.52, 26.26, 25.84 ppm. The observed spectral data are in good agreement with the ones reported in literature.<sup>15</sup>



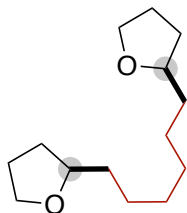
**6-(tetrahydrofuran-2-yl)hexyl 1-methyl-1H-pyrrole-2-carboxylate (66).** Following the general procedure B, using 6-bromohexyl 1-methyl-1H-pyrrole-2-carboxylate (86.5 mg, 0.3 mmol), the title compound was obtained in 74% yield (62.0 mg) after 72 h as colorless oil.  $^1\text{H}$  NMR (300 MHz,  $\text{CDCl}_3$ )  $\delta$  6.93 (dd,  $J = 3.9, 1.7$  Hz, 1H), 6.76 (t,  $J = 2.0$  Hz, 1H), 6.09 (dd,  $J = 3.8, 2.6$  Hz, 1H), 4.20 (t,  $J = 6.6$  Hz, 2H), 3.91 (s, 3H), 3.90-3.62 (m, 3H), 2.02-1.77 (m, 3H), 1.77-1.66 (m, 2H), 1.49-1.24 (m, 9H) ppm.  $^{13}\text{C}$  NMR (75 MHz,  $\text{CDCl}_3$ )  $\delta$  161.54, 129.44, 122.83, 117.77, 107.86, 79.48, 67.72, 63.99, 36.92, 35.76, 31.51, 29.50, 28.89, 26.43, 26.17, 25.84 ppm. IR (neat,  $\text{cm}^{-1}$ ): 2930, 2856, 1699, 1531, 1466, 1413, 1243, 1107. HRMS *calcd.* for  $(\text{C}_{16}\text{H}_{25}\text{NNaO}_3)$   $[\text{M}+\text{Na}]^+$ : 302.1729, *found* 302.1734.



**2-(6-chlorohexyl)tetrahydrofuran (67).** Following the general procedure B, using 1-bromo-6-chlorohexane (59.9 mg, 0.3 mmol), the title compound was obtained in 77% yield (44.0 mg) after 72 h as colorless oil.  $^1\text{H}$  NMR (300 MHz,  $\text{CDCl}_3$ )  $\delta$  3.89-3.65 (m, 3H), 3.52 (t,  $J = 6.7$  Hz, 2H), 2.02-1.69 (m, 5H), 1.58-1.3 (m, 9H) ppm.  $^{13}\text{C}$  NMR (75 MHz,  $\text{CDCl}_3$ )  $\delta$  79.45, 67.75, 45.25, 35.74, 32.68, 31.53, 29.09, 26.96, 26.36, 25.84 ppm. IR (neat,  $\text{cm}^{-1}$ ): 2930, 2857, 1461, 1309, 1063, 919, 727, 652. HRMS *calcd.* for  $(\text{C}_{10}\text{H}_{20}\text{ClO})$   $[\text{M}+\text{H}]^+$ : 191.1197, *found* 191.1196.

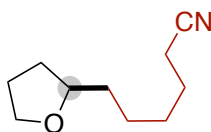


**2-(6-bromohexyl)tetrahydrofuran (68).** Following the general procedure B, using 1,6-dibromohexane (73.2 mg, 0.3 mmol), the title compound was obtained in 70% yield (49.4 mg) after 72 h as colorless oil.  $^1\text{H}$  NMR (300 MHz,  $\text{CDCl}_3$ )  $\delta$  3.09-3.65 (m, 3H), 3.40 (t,  $J = 6.8$  Hz, 2H), 2.02-1.79 (m, 5H), 1.54-1.28 (m, 9H) ppm.  $^{13}\text{C}$  NMR (75 MHz,  $\text{CDCl}_3$ )  $\delta$  79.45, 67.76, 35.75, 34.11, 32.87, 31.54, 28.98, 28.26, 26.35, 25.85. IR (neat,  $\text{cm}^{-1}$ ): 2929, 2856, 1460, 1325, 1258, 1172, 1131, 1065. HRMS *calcd.* for  $(\text{C}_{10}\text{H}_{20}\text{BrO})$   $[\text{M}+\text{H}]^+$ : 235.0692, *found* 235.0688.

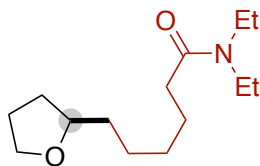


**1,6-bis(tetrahydrofuran-2-yl)hexane (69).** Following the general procedure B, using 1,6-dibromohexane (73.2 mg, 0.3 mmol), the title compound was obtained in 49% yield (33.2 mg) after 240 h as colorless oil.  $^1\text{H}$  NMR (300 MHz,  $\text{CDCl}_3$ )  $\delta$  3.88-3.64 (m, 6H), 2.01-1.76 (m, 6H), 1.58-1.28 (m, 14H) ppm.  $^{13}\text{C}$  NMR (75 MHz,  $\text{CDCl}_3$ )  $\delta$  79.56, 67.71, 35.84,

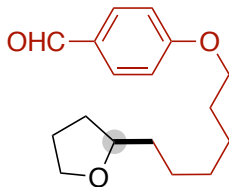
31.50, 29.82, 26.46, 25.84 ppm. IR (neat,  $\text{cm}^{-1}$ ): 2948, 2929, 2857, 1461, 1326, 1065, 907, 728. HRMS *calcd.* for ( $\text{C}_{14}\text{H}_{27}\text{O}_2$ ) [ $\text{M}+\text{H}$ ] $^+$ : 227.2006, *found* 227.1996.



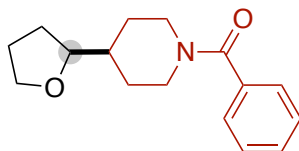
**6-(tetrahydrofuran-2-yl)hexanenitrile (70).** Following the general procedure B, using 6-bromohexanenitrile (52.8 mg, 0.3 mmol), the title compound was obtained in 70% yield (35.1 mg) after 72 h as colorless oil.  $^1\text{H}$  NMR (300 MHz,  $\text{CDCl}_3$ ):  $\delta$  3.89-3.63 (m, 3H), 2.33 (t,  $J = 7.1$  Hz, 2H), 2.04-1.79 (m, 3H), 1.72-1.60 (m, 2H), 1.59-1.31 (m, 7H) ppm.  $^{13}\text{C}$  NMR (75 MHz,  $\text{CDCl}_3$ )  $\delta$  119.93, 79.19, 67.77, 35.48, 31.53, 28.83, 25.81, 25.74, 25.47, 17.19 ppm. IR (neat,  $\text{cm}^{-1}$ ): 2934, 2860, 2230, 1461, 1420, 1171, 1110, 1055. HRMS *calcd.* for ( $\text{C}_{10}\text{H}_{18}\text{NO}$ ) [ $\text{M}+\text{H}$ ] $^+$ : 168.1383, *found* 168.1382.



**N,N-diethyl-6-(tetrahydrofuran-2-yl)hexanamide (71).** Following the general procedure B, using 6-bromo-N,N-diethylhexanamide (70.1 mg, 0.3 mmol), the title compound was obtained in 60% yield (43.4 mg) after 72 h as colorless oil.  $^1\text{H}$  NMR (300 MHz,  $\text{CDCl}_3$ )  $\delta$  3.86-3.62 (m, 3H), 3.38-3.22 (m, 4H), 2.30-2.21 (m, 2H), 1.97-1.78 (m, 3H), 1.65-1.49 (m, 3H), 1.46-1.29 (m, 6H), 1.16-1.03 (m, 6H) ppm.  $^{13}\text{C}$  NMR (75 MHz,  $\text{CDCl}_3$ )  $\delta$  172.29, 79.42, 67.67, 42.02, 40.08, 35.69, 33.15, 31.47, 29.68, 26.34, 25.79, 25.52, 14.48, 13.20 ppm. IR (neat,  $\text{cm}^{-1}$ ): 2968, 2930, 2857, 1637, 1460, 1427, 1379, 1269. HRMS *calcd.* for ( $\text{C}_{14}\text{H}_{28}\text{NO}_2$ ) [ $\text{M}+\text{H}$ ] $^+$ : 242.2115, *found* 242.2119.

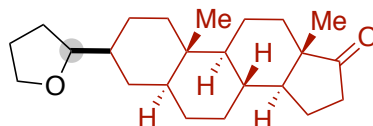


**4-((6-(tetrahydrofuran-2-yl)hexyl)oxy)benzaldehyde (72).** Following the general procedure B, using 4-((6-bromohexyl)oxy)benzaldehyde (85.6 mg, 0.3 mmol), the title compound was obtained in 83% yield (68.8 mg) after 72 h as colorless oil.  $^1\text{H}$  NMR (300 MHz,  $\text{CDCl}_3$ )  $\delta$  9.86 (s, 1H), 7.81 (d,  $J = 8.8$  Hz, 2H), 6.97 (d,  $J = 8.7$  Hz, 2H), 4.02 (t,  $J = 6.5$  Hz, 2H), 3.89-3.63 (m, 3H), 2.02-1.75 (m, 5H), 1.59-1.26 (m, 9H) ppm.  $^{13}\text{C}$  NMR (75 MHz,  $\text{CDCl}_3$ )  $\delta$  190.91, 164.35, 132.08, 129.85, 114.85, 79.44, 68.46, 67.73, 35.75, 31.52, 29.50, 29.08, 26.41, 26.03, 25.83 ppm. IR (neat,  $\text{cm}^{-1}$ ): 2930, 2856, 1688, 1598, 1577, 1509, 1253, 1157. HRMS *calcd.* for ( $\text{C}_{17}\text{H}_{25}\text{O}_3$ ) [ $\text{M}+\text{H}$ ] $^+$ : 277.1798, *found* 277.1801.

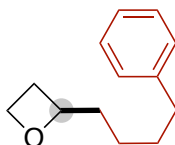


**phenyl(4-(tetrahydrofuran-2-yl)piperidin-1-yl)methanone (73).** Following the general procedure B, using (4-bromopiperidin-1-yl)(phenyl)methanone (80.4 mg, 0.3 mmol), without  $\text{CF}_3\text{CO}_2\text{Na}$ , the title compound was obtained in 68% yield (52.9 mg) after 72 h as colorless oil.  $^1\text{H}$  NMR (300 MHz,  $\text{CDCl}_3$ )  $\delta$  7.30 (s, 5H), 4.74 (br, 1H), 3.85-3.67 (m, 3H), 3.55 (br, 1H), 2.94 (br, 1H), 2.74 (br, 1H), 1.90-1.24 (m, 9H) ppm.  $^{13}\text{C}$  NMR (75 MHz,  $\text{CDCl}_3$ )  $\delta$  170.37, 136.46,

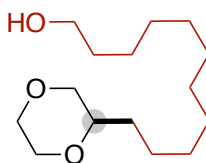
129.51, 128.49, 126.91, 82.79, 67.94, 47.81 (br), 42.25 (br), 41.65, 29.06 (br), 25.89 ppm. IR (neat,  $\text{cm}^{-1}$ ): 2942, 2856, 1625, 1577, 1431, 1284, 1243, 1063. HRMS *calcd.* for  $(\text{C}_{16}\text{H}_{22}\text{NO}_2)$   $[\text{M}+\text{H}]^+$ : 260.1645, *found* 260.1652.



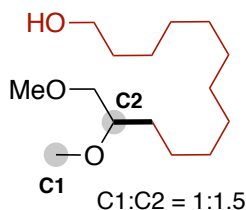
**(5S,8R,9S,10S,13S,14S)-10,13-dimethyl-3-(tetrahydrofuran-2-yl)hexadecahydro-17H-cyclopenta[a]phenanthren-17-one (74).** Following the general procedure B, using (3R,5S,8R,9S,10S,13S,14S)-3-bromo-10,13-dimethylhexadecahydro-17H cyclopenta[a]phenanthren-17-one (106.0 mg, 0.3 mmol), without  $\text{CF}_3\text{CO}_2\text{Na}$ , the title compound was obtained in 63% yield (65.1 mg) after 72 h as colorless oil (inseparable mixture of diastereoisomers).  $^1\text{H}$  NMR (300 MHz,  $\text{CDCl}_3$ )  $\delta$  3.86-3.78 (m, 1H), 3.74-3.67 (m, 1H), 3.53-3.46 (m, 1H), 2.11-1.63 (m, 10H), 1.55-1.15 (m, 12H), 1.11-0.78 (m, 10H) ppm. Signal of major isomer  $^{13}\text{C}$  NMR (75 MHz,  $\text{CDCl}_3$ )  $\delta$  221.51, 83.95, 67.74, 54.68, 51.52, 47.83, 46.32, 43.23, 38.06, 36.22, 35.87, 35.11, 31.60, 31.36, 30.97, 29.13, 28.73, 25.84, 25.31, 21.77, 20.26, 13.83, 12.29 ppm. IR (neat,  $\text{cm}^{-1}$ ): 2917, 2853, 1738, 1449, 1376, 1256, 1064, 732. HRMS *calcd.* for  $(\text{C}_{23}\text{H}_{36}\text{NaO}_2)$   $[\text{M}+\text{Na}]^+$ : 367.2608, *found* 367.2603.



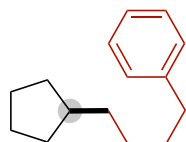
**2-(4-phenylbutyl)oxetane (75).** Following the general procedure B, using (4-bromobutyl)benzene (63.9 mg, 0.3 mmol), oxetane (3.0 mL), benzene (3.0 mL), the title compound was obtained in 60% yield (34.2 mg) after 72 h as colorless oil.  $^1\text{H}$  NMR (300 MHz,  $\text{CDCl}_3$ )  $\delta$  7.29-7.25 (m, 2H), 7.19-7.14 (m, 3H), 4.81 (quint,  $J = 6.9$  Hz, 1H), 4.65 (dt,  $J = 6.0, 8.1$  Hz, 1H), 4.49 (dt,  $J = 6.0, 9.0$  Hz, 1H), 2.69-2.58 (m, 3H), 2.36-2.25 (m, 1H), 1.90-1.78 (m, 1H), 1.71-1.60 (m, 3H), 1.44-1.28 (m, 2H) ppm.  $^{13}\text{C}$  NMR (75 MHz,  $\text{CDCl}_3$ )  $\delta$  142.64, 128.51, 128.38, 125.78, 82.81, 68.20, 38.00, 36.05, 31.49, 27.80, 23.91 ppm. IR (neat,  $\text{cm}^{-1}$ ): 2929, 2877, 2857, 1496, 1453, 1226, 970, 909. HRMS *calcd.* for  $(\text{C}_{13}\text{H}_{19}\text{O})$   $[\text{M}+\text{H}]^+$ : 191.1436, *found* 191.1437.



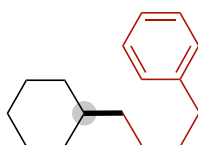
**11-(1,4-dioxan-2-yl)undecan-1-ol (76).** Following the general procedure B, using 11-bromoundecan-1-ol (73.4 mg, 0.3 mmol), 1,4-dioxane (4.0 mL) and  $\text{NaHCO}_3$  (1.0 eq, 25.2 mg, 0.3 mmol), the title compound was obtained in 56% yield (43.4 mg) after 96 h as colorless oil.  $^1\text{H}$  NMR (300 MHz,  $\text{CDCl}_3$ )  $\delta$  3.79-3.46 (m, 8H), 3.25 (dd,  $J = 11.4, 10.0$  Hz, 1H), 1.59-1.50 (m, 2H), 1.43-1.25 (m, 19H) ppm.  $^{13}\text{C}$  NMR (75 MHz,  $\text{CDCl}_3$ )  $\delta$  75.64, 71.57, 67.00, 66.69, 63.19, 32.93, 31.84, 29.76, 29.70, 29.65, 29.59, 29.54, 25.86, 25.20 ppm. IR (neat,  $\text{cm}^{-1}$ ): 3303, 2963, 2914, 2847, 1464, 1367, 1132, 1117. HRMS *calcd.* for  $(\text{C}_{15}\text{H}_{30}\text{NaO}_3)$   $[\text{M}+\text{Na}]^+$ : 281.2087, *found* 281.2086.



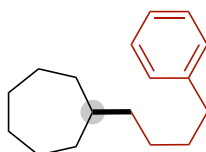
**alkylated 1,2-dimethoxyethane (77).** Following the general procedure B, using 11-bromoundecan-1-ol (73.4 mg, 0.3 mmol), 1,2-dimethoxyethane (4.0 mL) and  $\text{NaHCO}_3$  (1.0 eq, 25.2 mg, 0.3 mmol), the product was obtained in 78% yield (60.9 mg) after 96 h in a mixture (C1:C2 = 1: 1.5) as colorless oil.  $^1\text{H}$  NMR (300 MHz,  $\text{CDCl}_3$ )  $\delta$  3.61 (t,  $J = 4.8$  Hz, 3H), 3.57-3.50 (m, 2H), 3.44 (t,  $J = 6.9$  Hz, 1H), 3.39-3.35 (m, 10H), 3.32-3.26 (m, 1H), 1.57-1.45 (m, 8H), 1.32-1.26 (m, 25H) ppm.  $^{13}\text{C}$  NMR (101 MHz,  $\text{CDCl}_3$ )  $\delta$  80.24, 74.91, 72.11, 71.75, 70.07, 63.13, 59.30, 59.18, 57.48, 32.92, 31.31, 29.90, 29.70, 29.67, 29.58, 29.54, 26.18, 25.86, 25.50 ppm. IR (neat,  $\text{cm}^{-1}$ ): 3415, 2923, 2853, 1462, 1358, 1196, 1017, 722. HRMS calcd. for  $(\text{C}_{15}\text{H}_{32}\text{NaO}_3)$   $[\text{M}+\text{Na}]^+$ : 283.2244, found 283.2248.



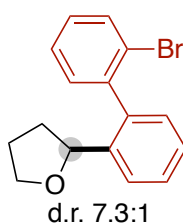
**(4-cyclopentylbutyl)benzene (78).** Following the general procedure B, using (4-bromobutyl)benzene (63.9 mg, 0.3 mmol), cyclopentane (3.0 mL), benzene (3.0 mL), the title compound was obtained in 40% yield (24.3 mg) after 120 h as colorless oil.  $^1\text{H}$  NMR (500 MHz,  $\text{CDCl}_3$ )  $\delta$  7.31-7.28 (m, 2H), 7.20-7.17 (m, 3H), 2.62 (t,  $J = 8.0$  Hz, 2H), 1.79-1.72 (m, 3H), 1.66-1.57 (m, 4H), 1.55-1.47 (m, 2H), 1.39-1.32 (m, 4H), 1.12-1.04 (m, 2H) ppm.  $^{13}\text{C}$  NMR (126 MHz,  $\text{CDCl}_3$ )  $\delta$  143.11, 128.53, 128.35, 125.67, 40.28, 36.21, 36.17, 32.89, 31.96, 28.66, 25.34 ppm. The observed spectral data are in good agreement with the ones reported in literature<sup>16</sup>.



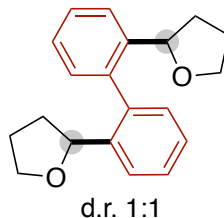
**(4-cyclohexylbutyl)benzene (79).** Following the general procedure B, using (4-bromobutyl)benzene (63.9 mg, 0.3 mmol), cyclohexane (3.0 mL), benzene (3.0 mL), the title compound was obtained in 54% yield (35.1 mg) after 120 h as colorless oil.  $^1\text{H}$  NMR (300 MHz,  $\text{CDCl}_3$ )  $\delta$  7.30-7.23 (m, 2H), 7.18-7.14 (m, 3H), 2.63-2.57 (m, 2H), 1.70-1.51 (m, 7H), 1.39-1.11 (m, 8H), 0.95-0.80 (m, 2H) ppm.  $^{13}\text{C}$  NMR (75 MHz,  $\text{CDCl}_3$ )  $\delta$  143.10, 128.53, 128.35, 125.67, 37.78, 37.53, 36.18, 33.61, 32.00, 26.91, 26.74, 26.61 ppm. The observed spectral data are in good agreement with the ones reported in literature<sup>16</sup>.



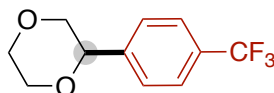
**(4-phenylbutyl)cycloheptane (80).** Following the general procedure B, using (4-bromobutyl)benzene (63.9 mg, 0.3 mmol), cycloheptane (3.0 mL), benzene (3.0 mL), the title compound was obtained in 54% yield (37.3 mg) after 120 h as colorless oil.  $^1\text{H}$  NMR (300 MHz,  $\text{CDCl}_3$ )  $\delta$  7.31-7.26 (m, 2H), 7.21-7.15 (m, 3H), 2.62 (t,  $J = 7.8$  Hz, 2H), 1.72-1.14 (m, 19H) ppm.  $^{13}\text{C}$  NMR (75 MHz,  $\text{CDCl}_3$ )  $\delta$  143.11, 128.53, 128.35, 125.67, 39.37, 38.21, 36.18, 34.81, 32.02, 28.72, 27.29, 26.71 ppm. The observed spectral data are in good agreement with the ones reported in literature<sup>16</sup>.



**2-(2'-bromo-[1,1'-biphenyl]-2-yl)tetrahydrofuran (81)**: Following the general procedure A, using 2,2'-dibromo-1,1'-biphenyl (93.6 mg, 0.3 mmol), the title compound was obtained in 66% yield (60.0 mg) after 72 h as colorless oil.  $^1\text{H}$  NMR (300 MHz,  $\text{CDCl}_3$ )  $\delta$  7.69-7.60 (m, 2H), 7.46-7.21 (m, 5H), 7.14-7.07 (m, 1H), 4.90-4.63 (m, 1H), 4.14-4.03 (m, 1H), 3.89-3.76 (m, 1H), 2.07-1.53 (m, 4H) ppm. Selected signal for  $^{13}\text{C}$  NMR (75 MHz,  $\text{CDCl}_3$ )  $\delta$  142.08, 141.25, 139.01, 132.70, 129.79, 128.44, 125.49, 123.70, 78.48, 77.97, 68.91, 68.80, 34.99, 34.09, 26.50, 26.41 ppm. IR (neat,  $\text{cm}^{-1}$ ): 2977, 2952, 2874, 1580, 1555, 1434, 1401, 1123. HRMS *calcd.* for  $(\text{C}_{16}\text{H}_{15}\text{BrNaO})$   $[\text{M}+\text{Na}]^+$ : 325.0198, *found* 325.0188.



**2,2'-bis(tetrahydrofuran-2-yl)-1,1'-biphenyl (82)**. Following the general procedure A, using 2,2'-dibromo-1,1'-biphenyl (93.6 mg, 0.3 mmol), the title compound was obtained in 23% yield (20.3 mg) after 72 h as colorless oil.  $^1\text{H}$  NMR (300 MHz,  $\text{CDCl}_3$ )  $\delta$  7.62-7.55 (m, 2H), 7.42-7.37 (m, 2H), 7.29-7.23 (m, 2H), 7.16-7.13 (m, 1H), 7.05-7.02 (m, 1H), 4.63 (dd,  $J = 8.4, 6.3$  Hz, 1H), 4.37 (dd,  $J = 8.4, 6.3$  Hz, 1H), 4.14-4.01 (m, 2H), 3.81-3.74 (m, 2H), 2.08-1.53 (m, 8H) ppm.  $^{13}\text{C}$  NMR (75 MHz,  $\text{CDCl}_3$ )  $\delta$  142.39, 141.48, 138.78, 138.73, 130.11, 129.27, 128.11, 128.00, 126.81, 126.36, 125.46, 125.43, 78.46, 78.11, 69.04, 68.72, 35.67, 34.12, 26.68, 26.57 ppm. IR (neat,  $\text{cm}^{-1}$ ): 2973, 2947, 2927, 2868, 1473, 1441, 1216, 1056. HRMS *calcd.* for  $(\text{C}_{20}\text{H}_{22}\text{NaO}_2)$   $[\text{M}+\text{Na}]^+$ : 317.1512, *found* 317.1518.



**methyl 4-(1,4-dioxan-2-yl)benzoate (83)**. Following the same procedure as **38**, using 4-bromobenzotrifluoride (67.5 mg, 0.3 mmol), 1,4-dioxane (4.0 mL) and  $\text{NaHCO}_3$  (1.0 eq, 25.2 mg, 0.3 mmol), the title compound was obtained in 65% yield (45.3 mg) after 72 h as colorless oil.  $^1\text{H}$  NMR (400 MHz,  $\text{CDCl}_3$ )  $\delta$  7.61 (d,  $J = 8.1$  Hz, 2H), 7.47 (d,  $J = 8.5$  Hz, 2H), 4.68 (dd,  $J = 10.1, 2.7$  Hz, 1H), 3.98-3.70 (m, 5H), 3.41 (dd,  $J = 11.7, 10.2$  Hz, 1H).  $^{13}\text{C}$  NMR (101 MHz,  $\text{CDCl}_3$ )  $\delta$  142.39, 130.36 (q,  $J_{\text{C-F}} = 3243$  Hz), 126.59, 125.52 (q,  $J_{\text{C-F}} = 3.8$  Hz), 124.20 (q,  $J_{\text{C-F}} = 273.0$  Hz), 77.35, 72.4, 67.15, 66.49 ppm.  $^{19}\text{F}$  NMR (376 MHz,  $\text{CDCl}_3$ )  $\delta$  -62.70 ppm. IR (neat,  $\text{cm}^{-1}$ ): 2953, 2869, 1717, 1606, 1453, 1385, 1057, 991. HRMS *calcd.* for  $(\text{C}_{20}\text{H}_{22}\text{NaO}_2)$   $[\text{M}+\text{H}]^+$ : 233.0784, *found* 233.0787.

#### 4.9.4. Bibliography of Known Compounds

1. Leigh, W. J., Arnold, D. R., Humphreys, R. W. R. & Wong, P. C. Merostabilization in radical ions, triplets, and biradicals. 4. Substituent effects on the half-wave reduction potentials and  $n, \pi^*$  triplet energies of aromatic ketones. *Can. J. Chem.* **58**, 2537-2549 (1980).
2. Heitz, D. R.; Tellis, J. C.; Molander, G. A. Photochemical nickel-catalyzed C–H arylation: synthetic scope and mechanistic investigations. *J. Am. Chem. Soc.* **2016**, *138*, 12715-12718.
3. Shields, B. J.; Doyle, A. G. Direct C(sp<sup>3</sup>)–H cross coupling enabled by catalytic generation of chlorine radicals. *J. Am. Chem. Soc.* **2016**, *138*, 12719-12722.
4. Protti, S., Dondi, D., Fagnoni, M. & Albini, A., Photochemical Arylation of Alkenols: Role of Intermediates and Synthetic Significance. *Eur. J. Org. Chem.* **2008**, 2240–2247.
5. Ueno, R. & Shirakawa, E. Base-promoted dehydrogenative coupling of benzene derivatives with amides or ethers. *Org. Biomol. Chem.*, **2014**, *12*, 7469-7473.
6. Li, W., Yang, C., Gao, G.-L. & Xia, W. Visible-Light-Induced Cyclization of Electron-Enriched Phenyl Benzyl Sulfides: Synthesis of Tetrahydrofurans and Tetrahydropyrans. *Synlett* **2016**, *27*, 1391-1396.
7. Zhang, F.-Z., Tian, Y., Li, G.-X. & Qu, J. Intramolecular Etherification and Polyene Cyclization of  $\pi$ -Activated Alcohols Promoted by Hot Water. *J. Org. Chem.*, **2015**, *80*, 1107-1115.
8. Fang, L., Chen, L., Yu, J. & Wang, L. Benzoyl Peroxide Promoted Radical *ortho*-Alkylation of Nitrogen Heteroaromatics with Simple Alkanes and Alcohols. *Eur. J. Org. Chem.* **2015**, 1910-1914.
9. Liu, D., Liu, C., Li, H. & Lei, A. Direct functionalization of tetrahydrofuran and 1,4-dioxane: Nickel-catalyzed oxidative C(sp<sup>3</sup>)-H arylation. *Angew. Chem. Int. Ed.* **2013**, *52*, 4453-4456.
10. Yasukawa, N., Asai, S., Kato, M., Monguchi, Y., Sajiki, H. & Sawama, Y. Palladium on Carbon-Catalyzed Chemoselective Oxygen Oxidation of Aromatic Acetals. *Org. Lett.*, **2016**, *18*, 5604-5607.
11. Zhang, X. & MacMillan, D. W. C. Alcohols as Latent Coupling Fragments for Metallaphotoredox Catalysis: sp<sup>3</sup>-sp<sup>2</sup> Cross-Coupling of Oxalates with Aryl Halides. *J. Am. Chem. Soc.* **2016**, *138*, 13862–13865.
12. Shaw, M. H., Shurtleff, V. W., Terrett, J. A., Cuthbertson, J. D. & MacMillan, D. W. C. Native functionality in triple catalytic cross-coupling: sp<sup>3</sup> C-H bonds as latent nucleophiles. *Science* **2016**, *352*, 1304-1308.
13. Liu, D., Li, Y., Qi, X., Liu, C., Lan, Y. & Lei, A. Nickel-catalyzed selective oxidative radical cross-coupling: An effective strategy for inert Csp<sup>3</sup>-H functionalization. *Org. Lett.* **2015**, *17*, 998-1001.
14. Bunrit, A., Dahlstrand, C., Olsson, S. K., Srifa, P., Huang, G., Orthaber, A., Sjöberg, P. J. R., Biswas, S., Himo, F. & Samec J. S. M. Brønsted Acid-Catalyzed Intramolecular Nucleophilic Substitution of the Hydroxyl Group in Stereogenic Alcohols with Chirality Transfer. *J. Am. Chem. Soc.* **2015**, *137*, 4646–4649.
15. Kaiser, S., Smidt, S. P. & Pfaltz, A. Iridium Catalysts with Bicyclic Pyridine-Phosphinite Ligands: Asymmetric Hydrogenation of Olefins and Furan Derivatives *Angew. Chem. Int. Ed.* **2006**, *45*, 5194-5197.
16. Lu, X., Xiao, B., Liu, L. & Fu, Y. Formation of C(sp<sup>3</sup>)–C(sp<sup>3</sup>) Bonds through Nickel-Catalyzed Decarboxylative Olefin Hydroalkylation Reactions. *Chem. Eur. J.* **2016**, *22*, 11161-11164.



#### 4.9.5. X-ray diffraction of Ni-1

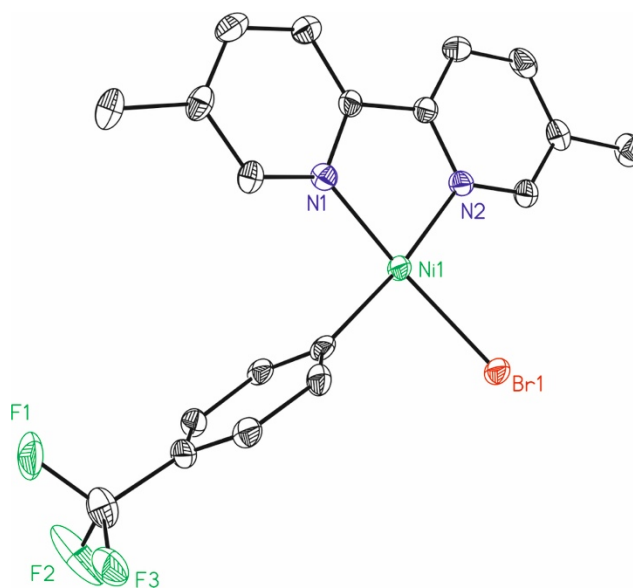


Table 1. Crystal data and structure refinement for **Ni-1**.

Identification code	yshen2018_twin1_hklf5	
Empirical formula	C <sub>22</sub> H <sub>19</sub> Br F <sub>3</sub> N <sub>2</sub> Ni	
Formula weight	507.01	
Temperature	100(2) K	
Wavelength	0.71073 Å	
Crystal system	Triclinic	
Space group	P-1	
Unit cell dimensions	a = 9.3825(6)Å	α = 76.894(4)°.
	b = 10.3799(6)Å	β = 89.918(4)°.
	c = 11.1183(3)Å	γ = 73.255(5)°.
Volume	1007.51(9) Å <sup>3</sup>	
Z	2	
Density (calculated)	1.671 Mg/m <sup>3</sup>	
Absorption coefficient	2.983 mm <sup>-1</sup>	
F(000)	510	
Crystal size	0.02 x 0.01 x 0.005 mm <sup>3</sup>	
Theta range for data collection	1.885 to 28.734°.	
Index ranges	-12 ≤ h ≤ 12, -12 ≤ k ≤ 13, -14 ≤ l ≤ 14	
Reflections collected	9274	
Independent reflections	9274 [R(int) = ?]	
Completeness to theta = 28.734°	90.4%	
Absorption correction	Multi-scan	

Max. and min. transmission	0.985 and 0.758
Refinement method	Full-matrix least-squares on $F^2$
Data / restraints / parameters	9274/ 0/ 265
Goodness-of-fit on $F^2$	0.919
Final R indices [ $I > 2\sigma(I)$ ]	R1 = 0.0455, wR2 = 0.1031
R indices (all data)	R1 = 0.0777, wR2 = 0.1112
Largest diff. peak and hole	1.043 and -0.592 e.Å <sup>-3</sup>

Table 2. Bond lengths [Å] and angles [°] for **Ni-1**.

---

Bond lengths----

Ni1-C13	1.884(4)
Ni1-N1	1.921(3)
Ni1-N2	1.986(3)
Ni1-Br1	2.3066(6)
C1-N1	1.341(5)
C1-C2	1.388(6)
C1-H1	0.9300
C2-C3	1.384(6)
C2-C12	1.511(6)
C3-C4	1.379(6)
C3-H3	0.9300
C4-C5	1.379(6)
C4-H4	0.9300
C5-N1	1.361(5)
C5-C6	1.465(6)
C6-N2	1.350(5)
C6-C7	1.387(6)
C7-C8	1.385(6)
C7-H7	0.9300
C8-C9	1.383(6)
C8-H8	0.9300
C9-C10	1.391(6)
C9-C11	1.504(6)
C10-N2	1.339(5)
C10-H10	0.9300
C11-H11A	0.9600
C11-H11B	0.9600

C11-H11C	0.9600
C12-H12A	0.9600
C12-H12B	0.9600
C12-H12C	0.9600
C13-C14	1.394(6)
C13-C18	1.400(6)
C14-C15	1.384(5)
C14-H14	0.9300
C15-C16	1.387(6)
C15-H15	0.9300
C16-C17	1.388(6)
C16-C19	1.491(6)
C17-C18	1.381(5)
C17-H17	0.9300
C18-H18	0.9300
C19-F3	1.329(5)
C19-F2	1.330(5)
C19-F1	1.348(5)
C1S-C3S#1	1.373(6)
C1S-C2S	1.385(6)
C1S-H1S	0.9300
C2S-C3S	1.387(6)
C2S-H2S	0.9300
C3S-C1S#1	1.373(6)
C3S-H3S	0.9300

Angles-----

C13-Ni1-N1	91.97(15)
C13-Ni1-N2	170.53(15)
N1-Ni1-N2	82.98(14)
C13-Ni1-Br1	88.80(11)
N1-Ni1-Br1	171.75(10)
N2-Ni1-Br1	97.34(10)
N1-C1-C2	124.0(4)
N1-C1-H1	118.0
C2-C1-H1	118.0
C3-C2-C1	117.2(4)
C3-C2-C12	122.9(4)

C1-C2-C12	119.9(4)
C4-C3-C2	119.8(4)
C4-C3-H3	120.1
C2-C3-H3	120.1
C3-C4-C5	119.8(4)
C3-C4-H4	120.1
C5-C4-H4	120.1
N1-C5-C4	121.3(4)
N1-C5-C6	114.6(3)
C4-C5-C6	124.1(4)
N2-C6-C7	121.2(4)
N2-C6-C5	114.2(3)
C7-C6-C5	124.6(4)
C8-C7-C6	119.4(4)
C8-C7-H7	120.3
C6-C7-H7	120.3
C9-C8-C7	120.1(4)
C9-C8-H8	119.9
C7-C8-H8	119.9
C8-C9-C10	117.0(4)
C8-C9-C11	122.1(4)
C10-C9-C11	120.9(4)
N2-C10-C9	123.8(4)
N2-C10-H10	118.1
C9-C10-H10	118.1
C9-C11-H11A	109.5
C9-C11-H11B	109.5
H11A-C11-H11B	109.5
C9-C11-H11C	109.5
H11A-C11-H11C	109.5
H11B-C11-H11C	109.5
C2-C12-H12A	109.5
C2-C12-H12B	109.5
H12A-C12-H12B	109.5
C2-C12-H12C	109.5
H12A-C12-H12C	109.5
H12B-C12-H12C	109.5
C14-C13-C18	117.8(4)

C14-C13-Ni1	117.4(3)
C18-C13-Ni1	124.4(3)
C15-C14-C13	121.4(4)
C15-C14-H14	119.3
C13-C14-H14	119.3
C14-C15-C16	119.8(4)
C14-C15-H15	120.1
C16-C15-H15	120.1
C15-C16-C17	119.7(4)
C15-C16-C19	119.8(4)
C17-C16-C19	120.5(4)
C18-C17-C16	120.1(4)
C18-C17-H17	119.9
C16-C17-H17	119.9
C17-C18-C13	121.1(4)
C17-C18-H18	119.5
C13-C18-H18	119.5
F3-C19-F2	106.7(4)
F3-C19-F1	104.9(3)
F2-C19-F1	105.6(4)
F3-C19-C16	114.1(4)
F2-C19-C16	112.8(4)
F1-C19-C16	112.0(4)
C1-N1-C5	117.9(3)
C1-N1-Ni1	127.2(3)
C5-N1-Ni1	114.7(3)
C10-N2-C6	118.6(3)
C10-N2-Ni1	128.0(3)
C6-N2-Ni1	113.2(3)
C3S-C1S-C2S#1	120.3(4)
C3S-C1S-H1S#1	119.8
C2S-C1S-H1S	119.8
C1S-C2S-C3S	119.9(4)
C1S-C2S-H2S	120.0
C3S-C2S-H2S	120.0
C1S-C3S-C2S#1	119.8(4)
C1S-C3S-H3S#1	120.1
C2S-C3S-H3S	120.1

-----  
Symmetry transformations used to generate equivalent atoms:

#1 -x+1, -y+1, -z+1

Table 3. Torsion angles [°] for **Ni-1**.

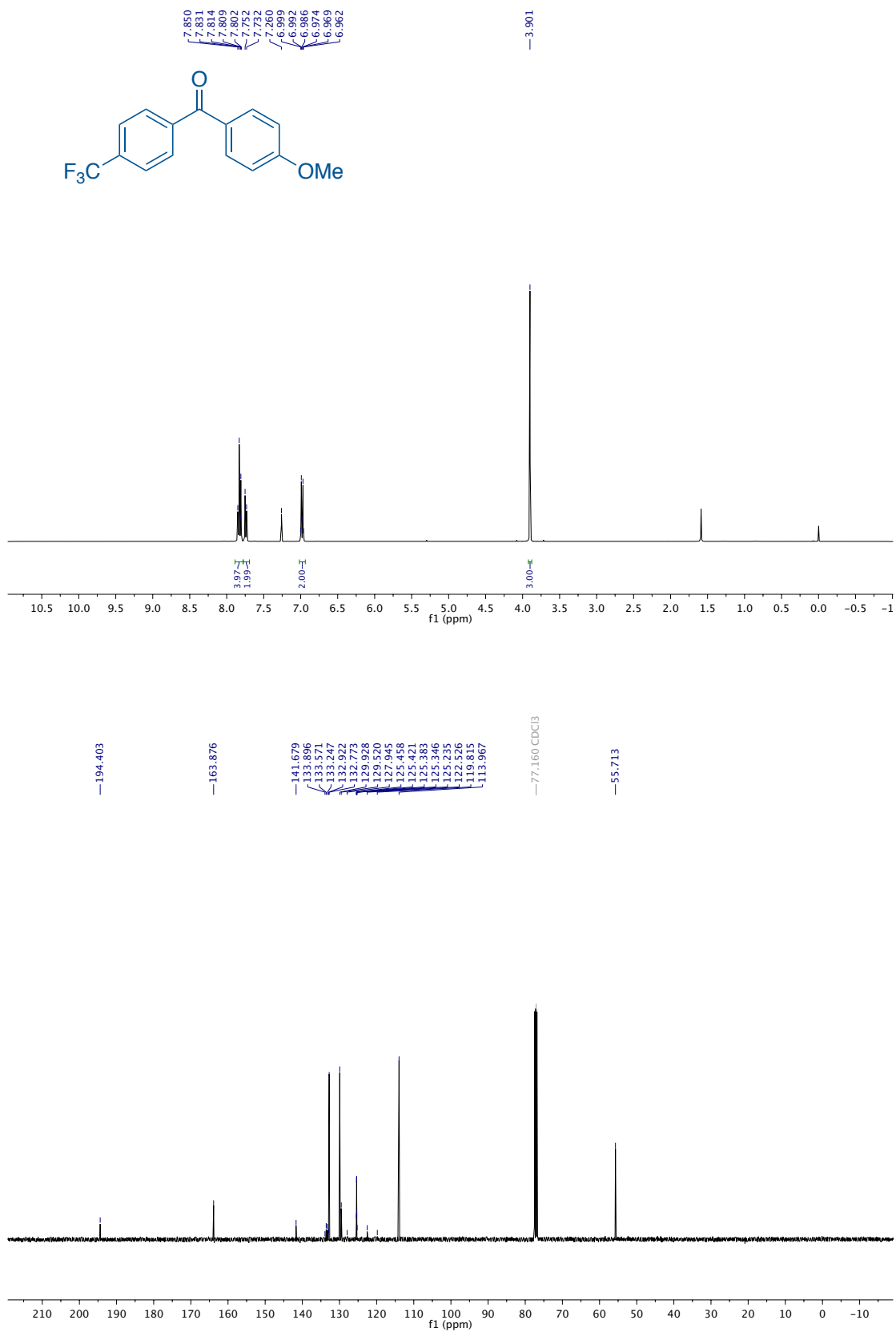
N1-C1-C2-C3	-1.0(6)
N1-C1-C2-C12	177.5(4)
C1-C2-C3-C4	2.2(6)
C12-C2-C3-C4	-176.3(4)
C2-C3-C4-C5	-2.1(6)
C3-C4-C5-N1	0.8(6)
C3-C4-C5-C6	-178.6(4)
N1-C5-C6-N2	-5.6(5)
C4-C5-C6-N2	173.8(4)
N1-C5-C6-C7	174.3(4)
C4-C5-C6-C7	-6.3(6)
N2-C6-C7-C8	-0.4(6)
C5-C6-C7-C8	179.7(4)
C6-C7-C8-C9	0.7(6)
C7-C8-C9-C10	-0.3(6)
C7-C8-C9-C11	-178.3(4)
C8-C9-C10-N2	-0.6(6)
C11-C9-C10-N2	177.4(4)
N1-Ni1-C13-C14	80.8(3)
Br1-Ni1-C13-C14	-107.5(3)
N1-Ni1-C13-C18	-91.7(3)
Br1-Ni1-C13-C18	80.1(3)
C18-C13-C14-C15	1.5(6)
Ni1-C13-C14-C15	-171.5(3)
C13-C14-C15-C16	1.0(6)
C14-C15-C16-C17	-1.8(6)
C14-C15-C16-C19	175.5(4)
C15-C16-C17-C18	0.0(6)
C19-C16-C17-C18	-177.3(4)
C16-C17-C18-C13	2.6(6)
C14-C13-C18-C17	-3.3(6)
Ni1-C13-C18-C17	169.2(3)

C15-C16-C19-F3	156.2(4)
C17-C16-C19-F3	-26.5(6)
C15-C16-C19-F2	34.2(6)
C17-C16-C19-F2	-148.5(4)
C15-C16-C19-F1	-84.8(5)
C17-C16-C19-F1	92.5(5)
C2-C1-N1-C5	-0.3(6)
C2-C1-N1-Ni1	173.9(3)
C4-C5-N1-C1	0.4(5)
C6-C5-N1-C1	179.8(3)
C4-C5-N1-Ni1	-174.5(3)
C6-C5-N1-Ni1	5.0(4)
C9-C10-N2-C6	0.9(6)
C9-C10-N2-Ni1	176.2(3)
C7-C6-N2-C10	-0.4(6)
C5-C6-N2-C10	179.5(3)
C7-C6-N2-Ni1	-176.4(3)
C5-C6-N2-Ni1	3.5(4)
C3S#1-C1S-C2S-C3S	0.7(7)
C1S-C2S-C3S-C1S#1	-0.7(7)

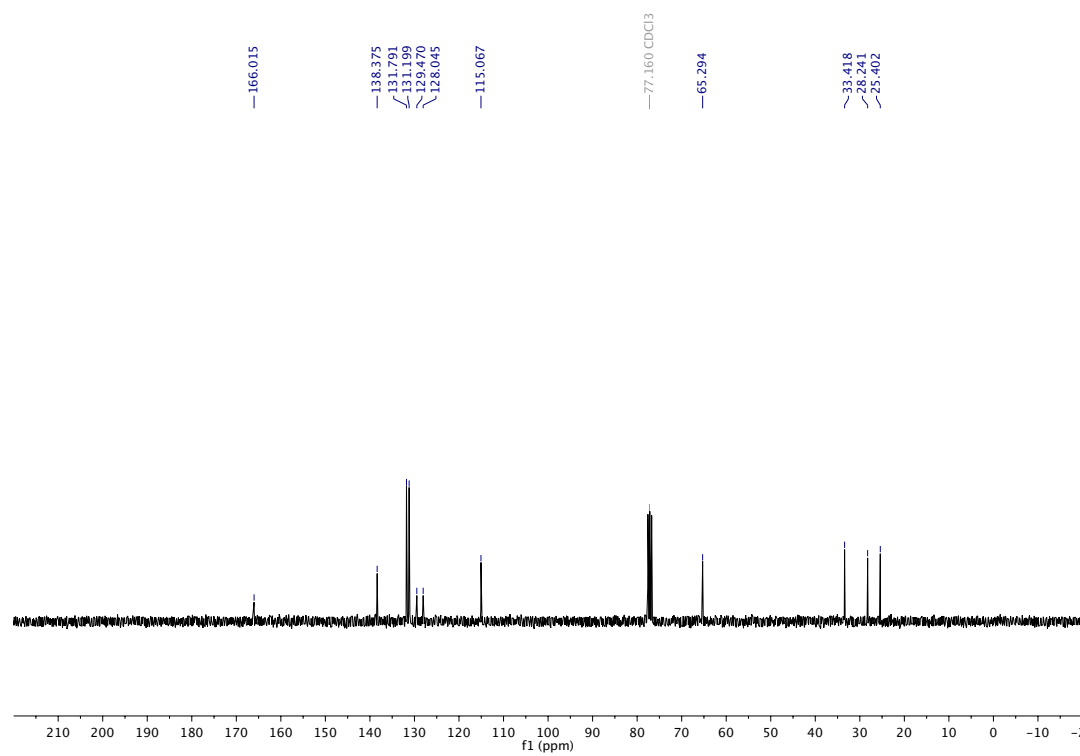
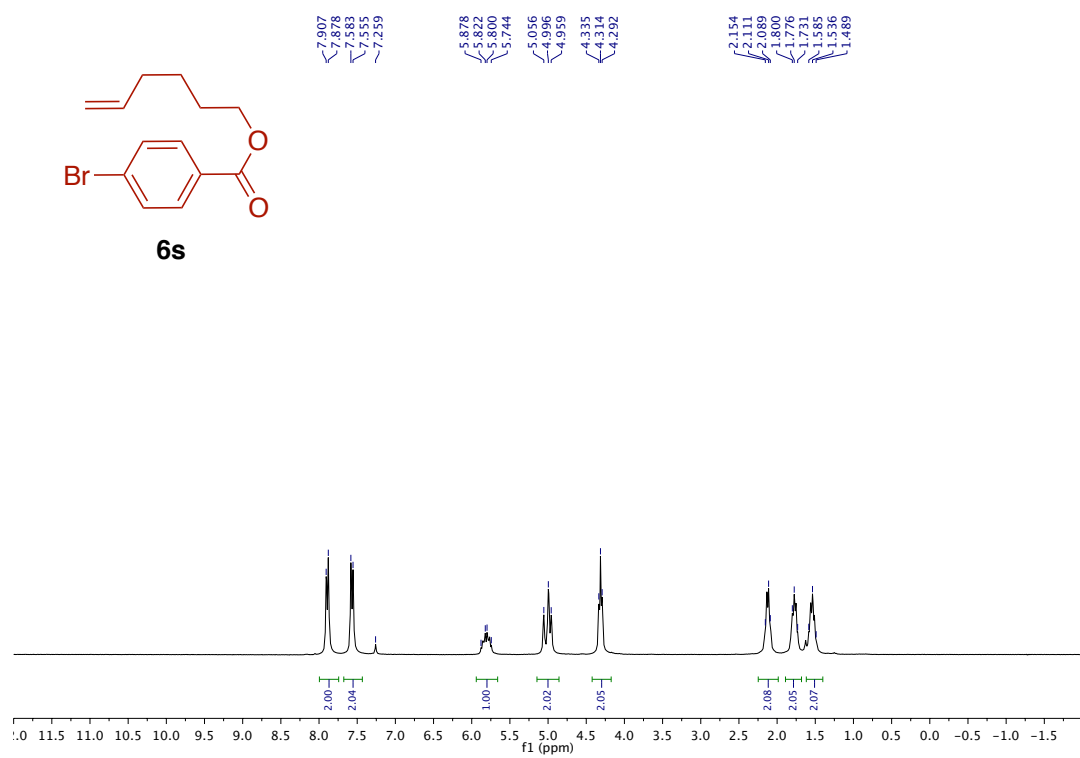
-----  
Symmetry transformations used to generate equivalent atoms:

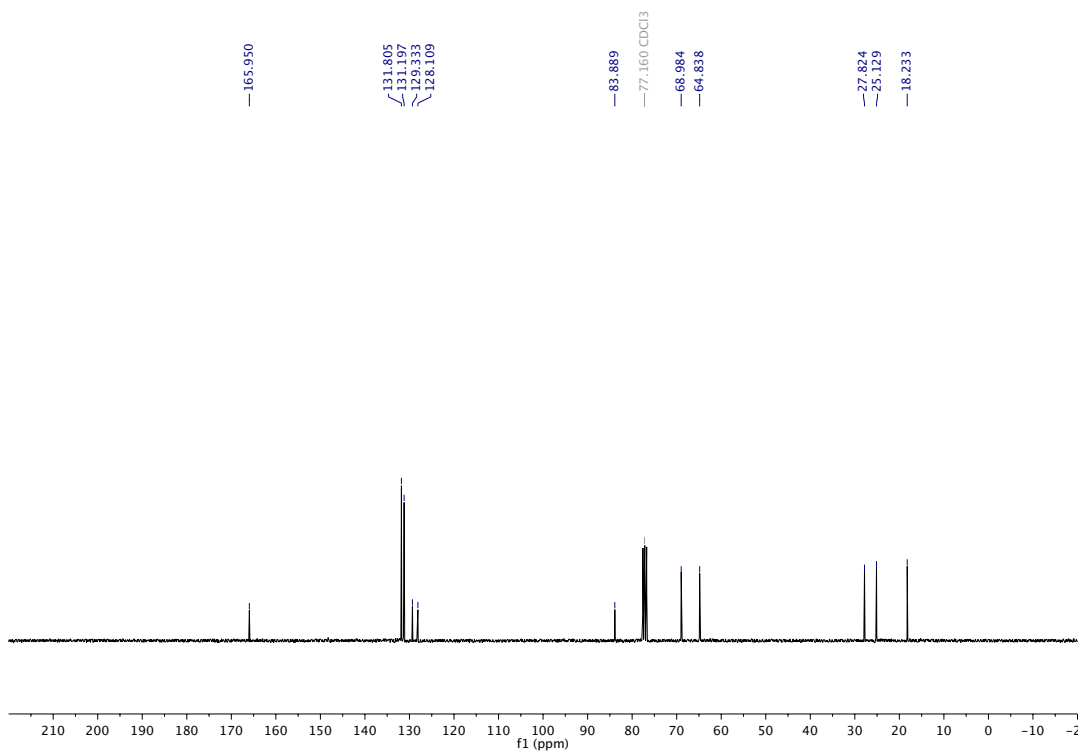
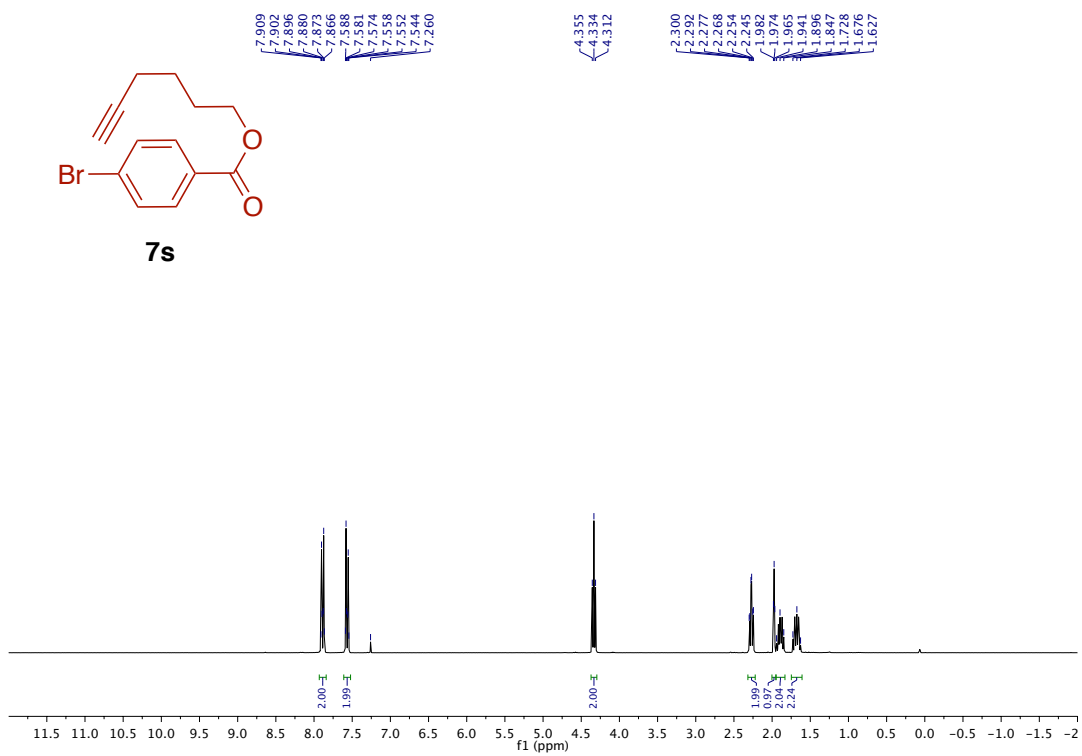
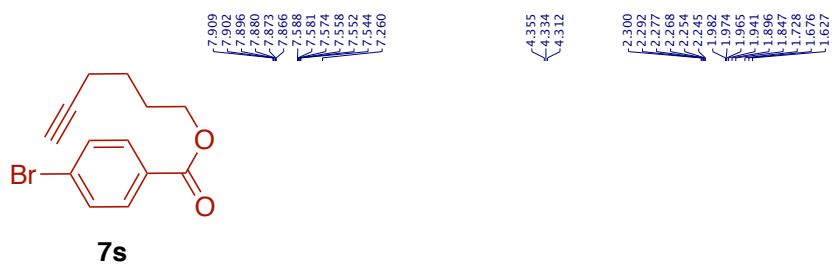
#1 -x+1, -y+1, -z+1

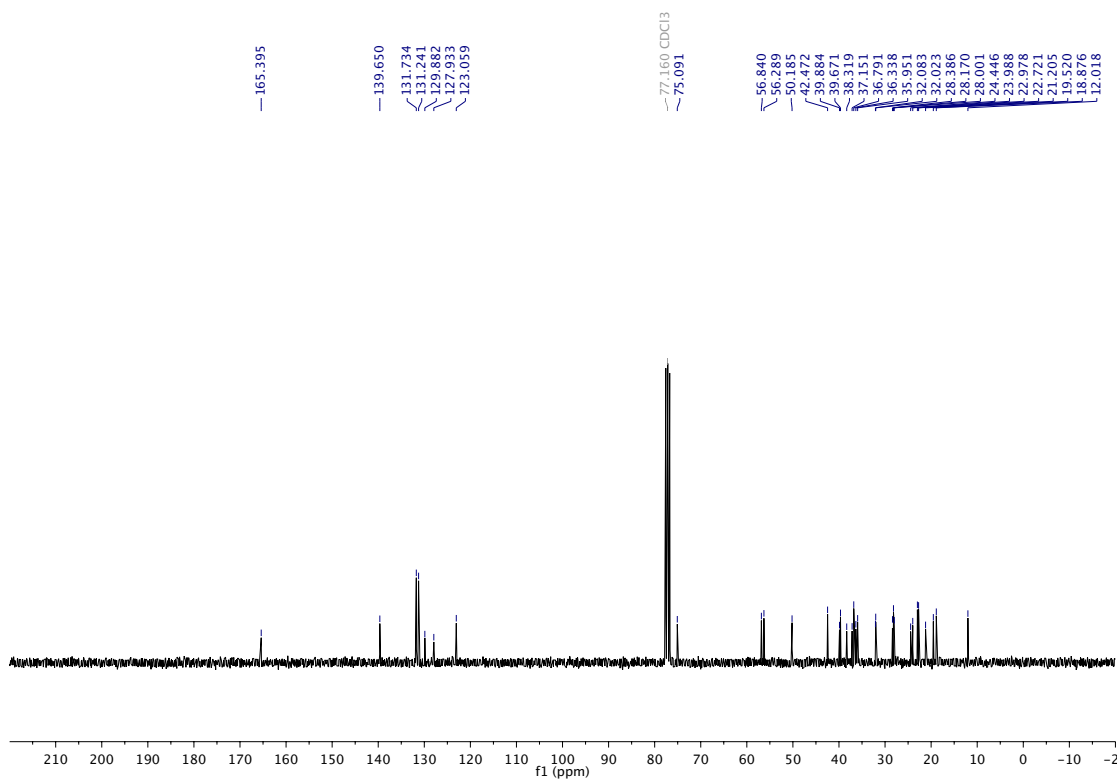
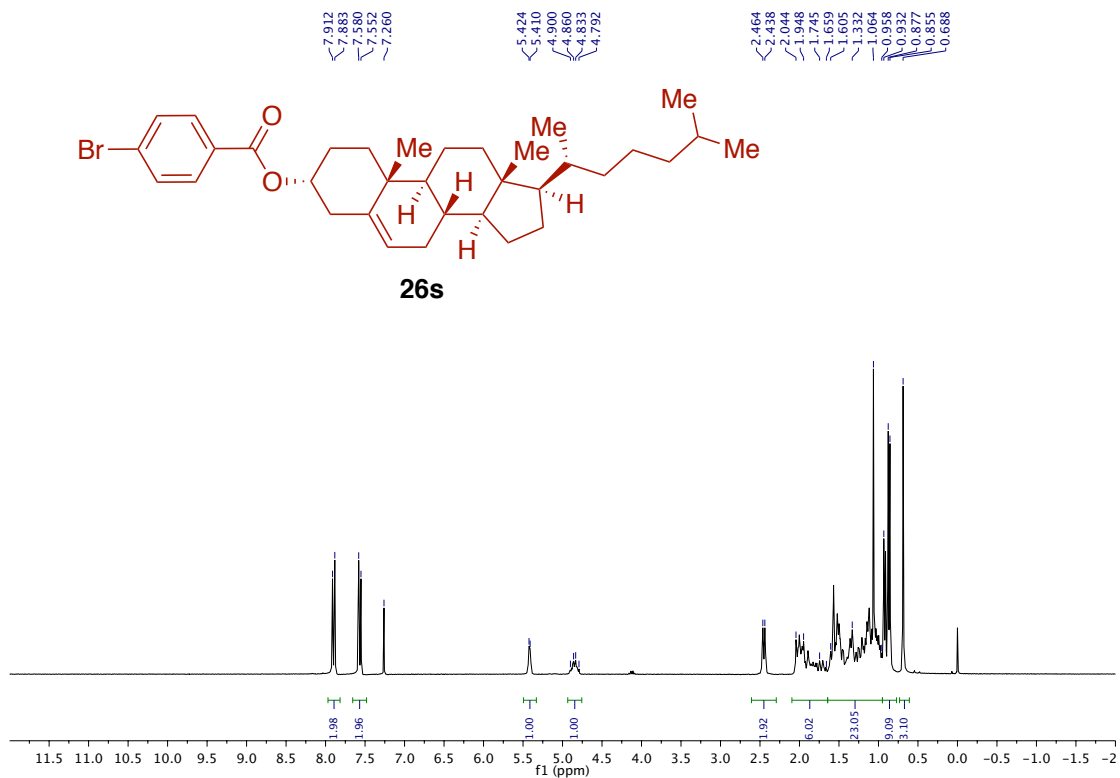
### 4.9.6. $^1\text{H}$ and $^{13}\text{C}$ NMR Spectra

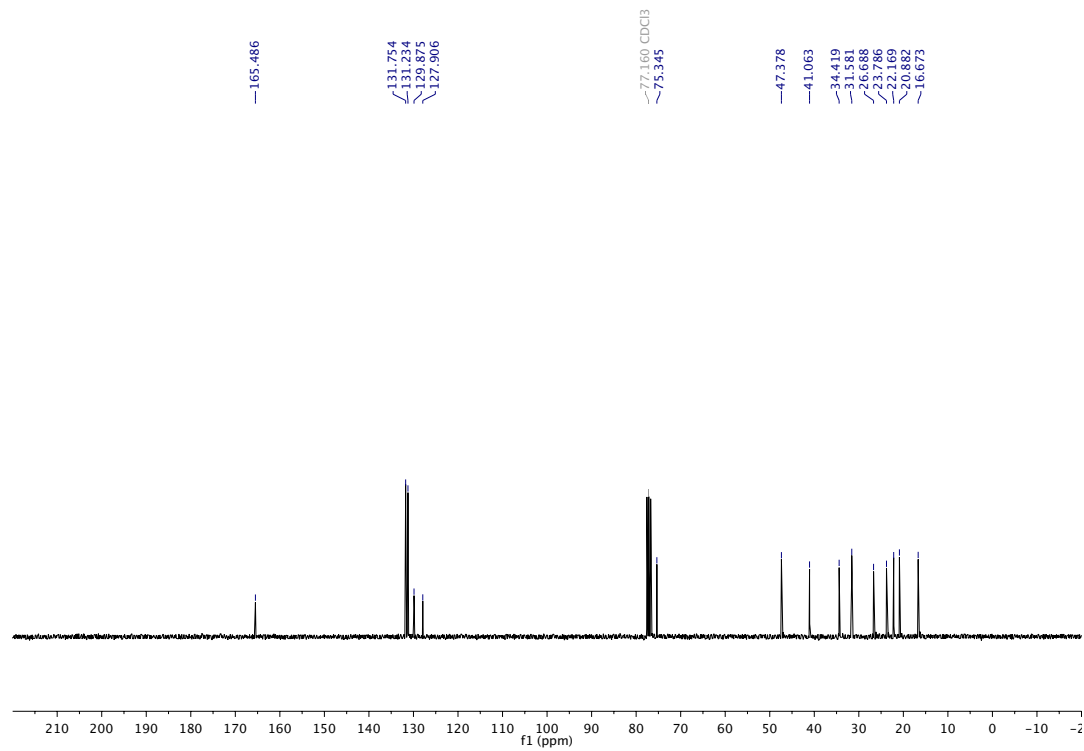
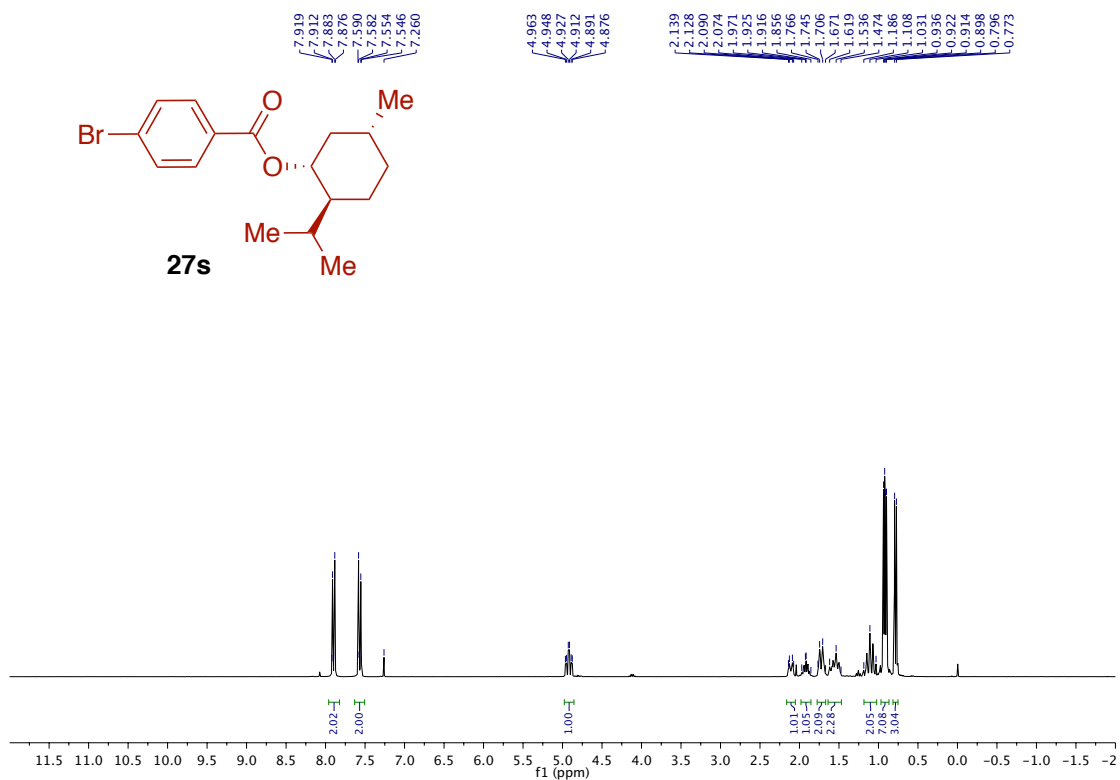


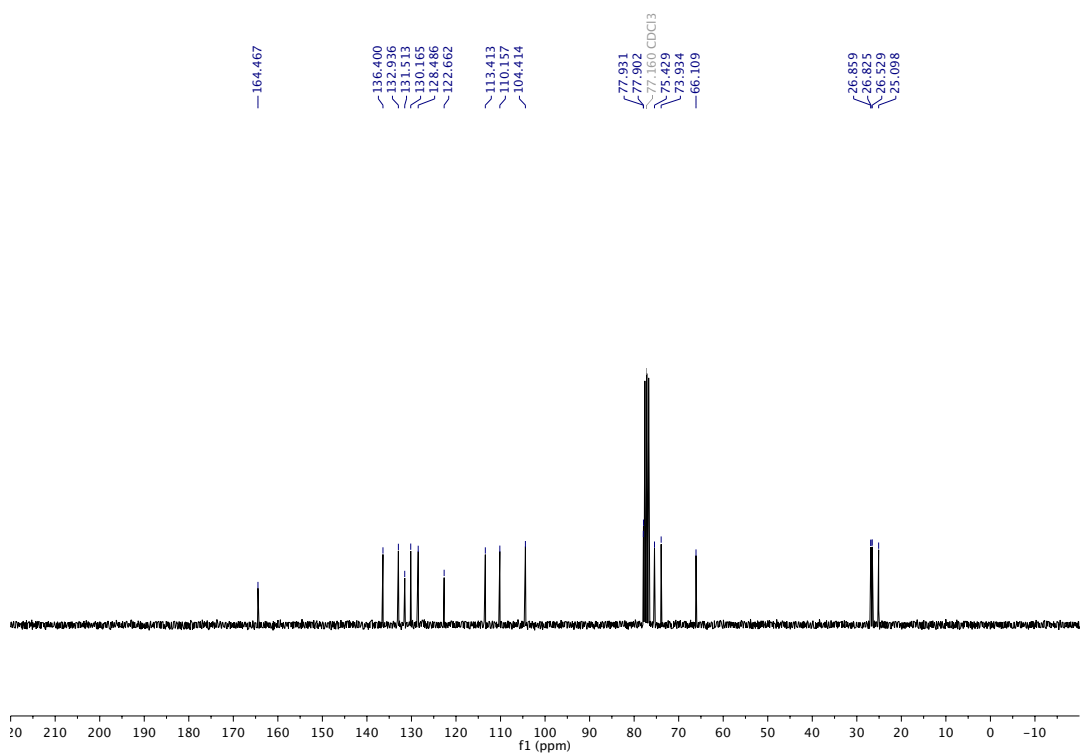
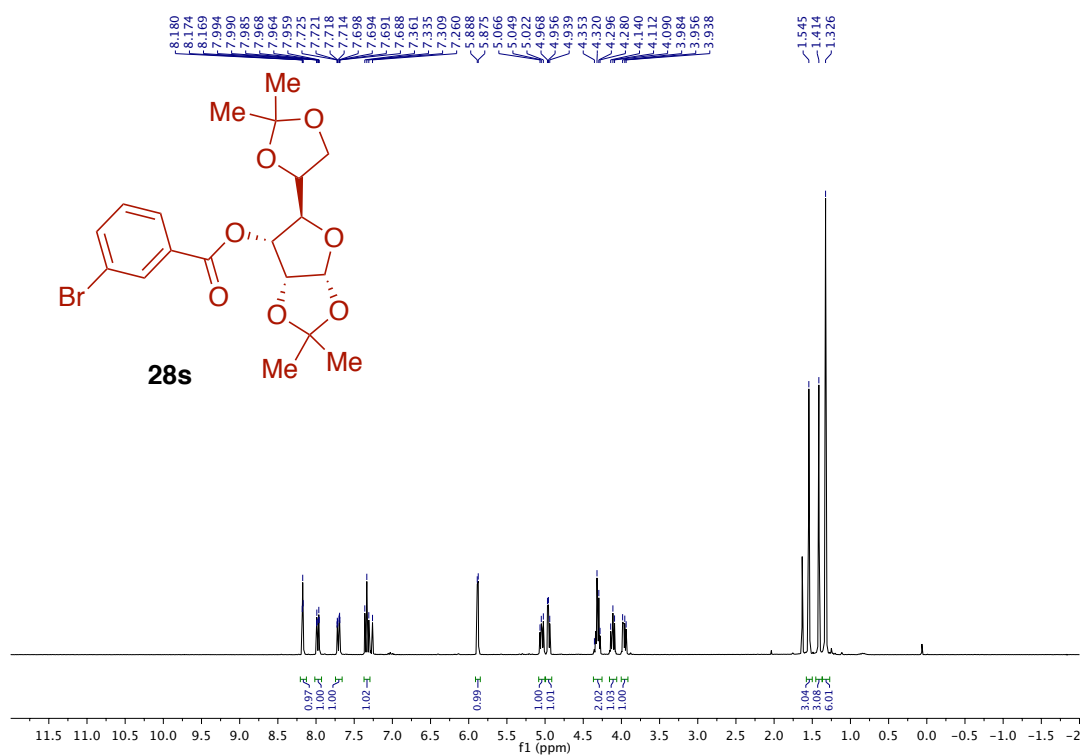


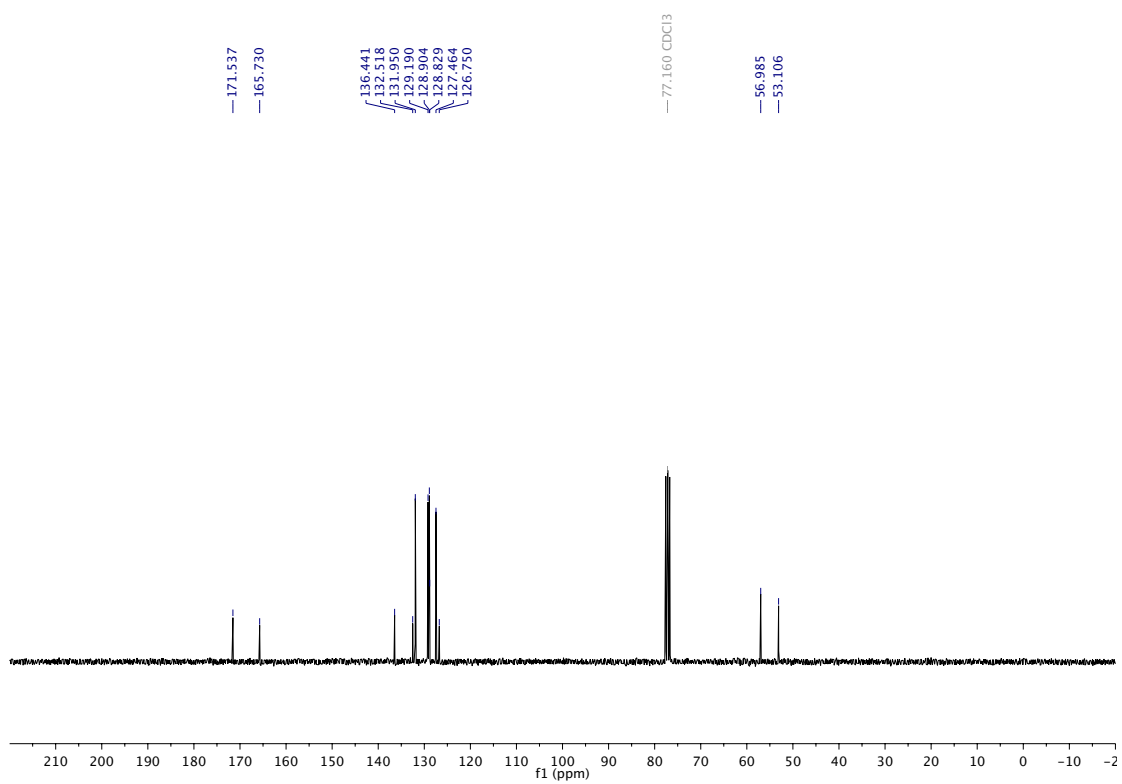
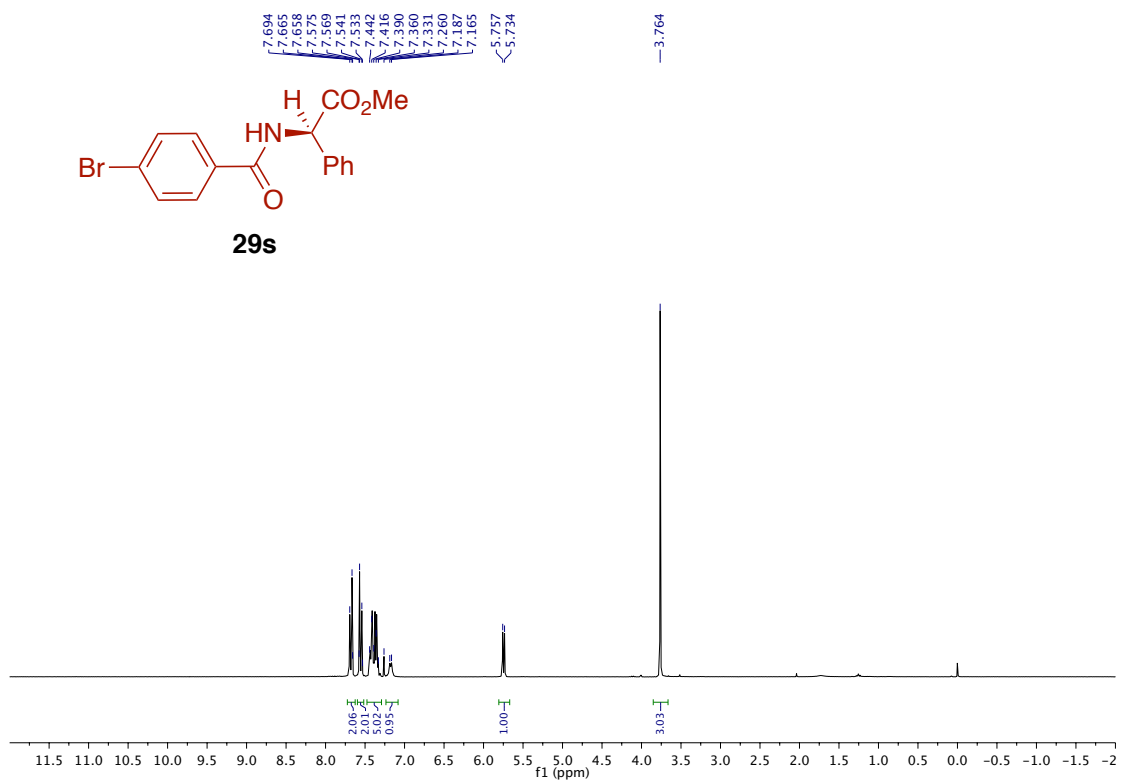




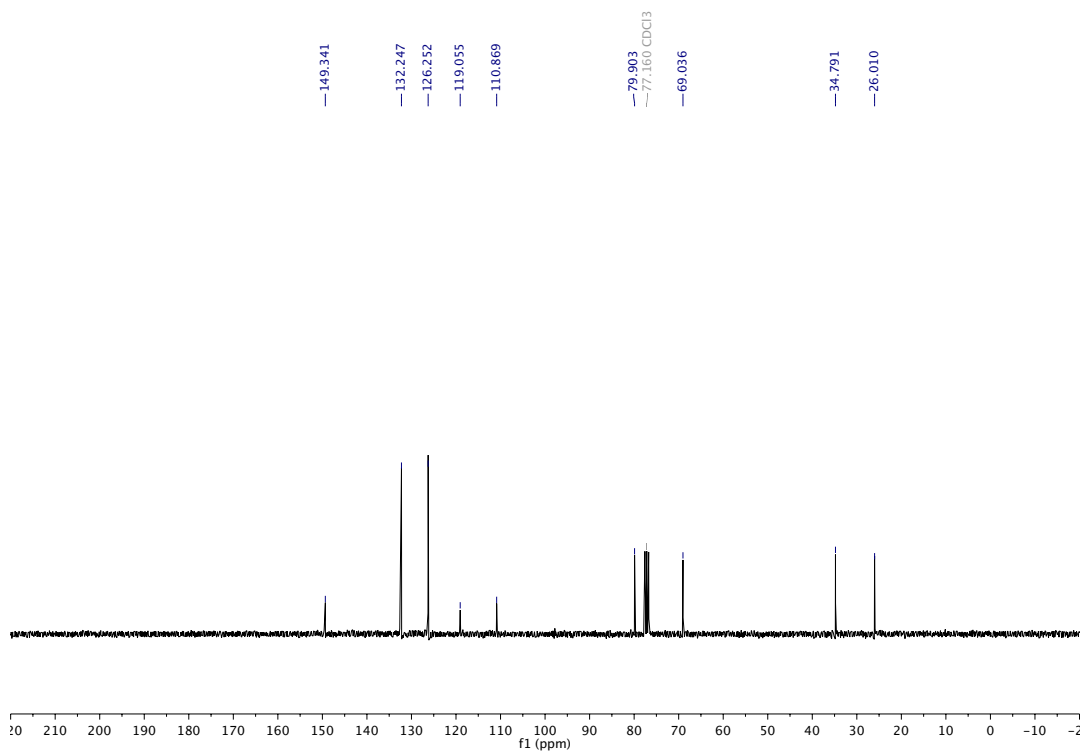
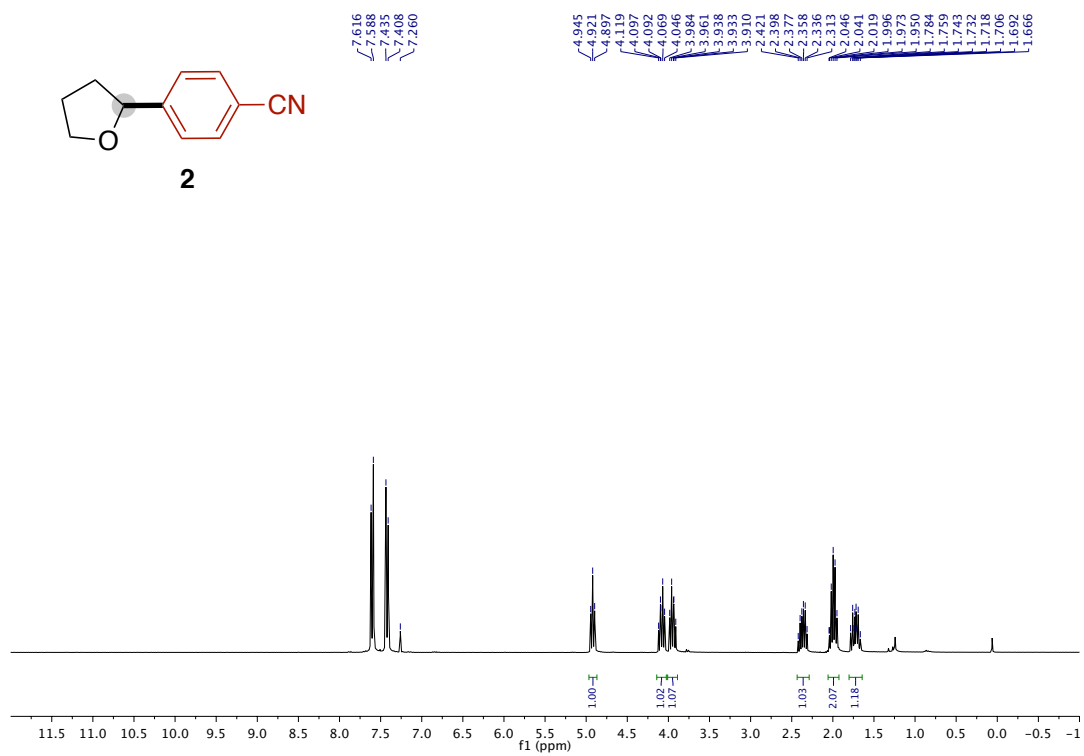




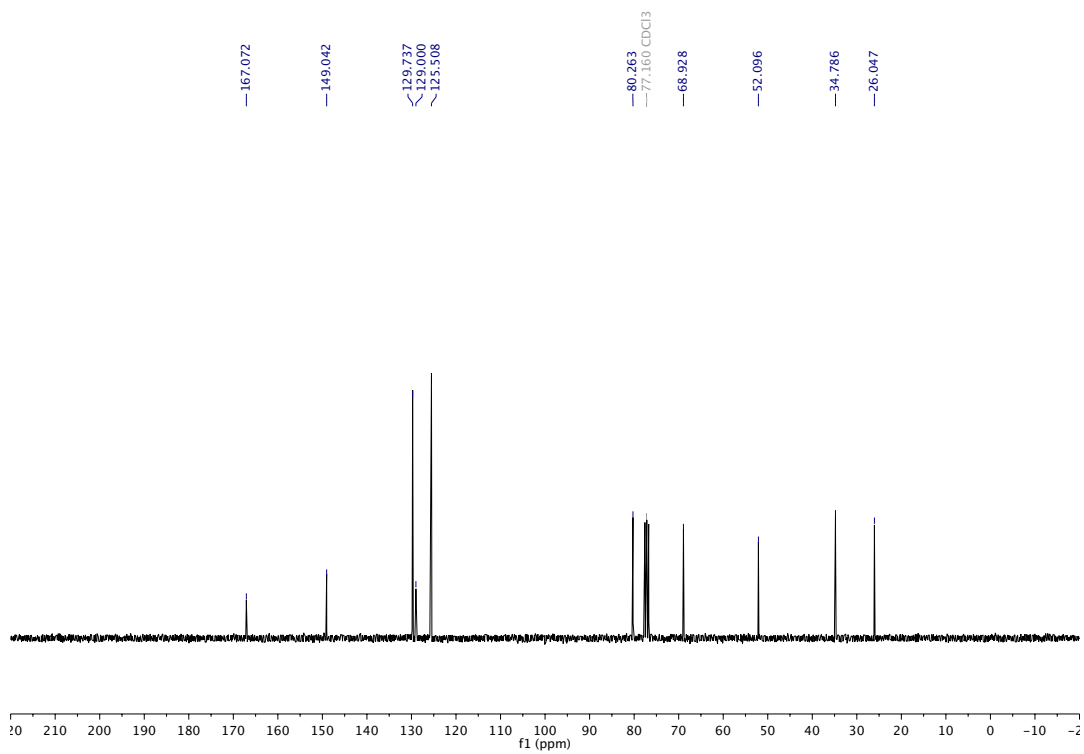
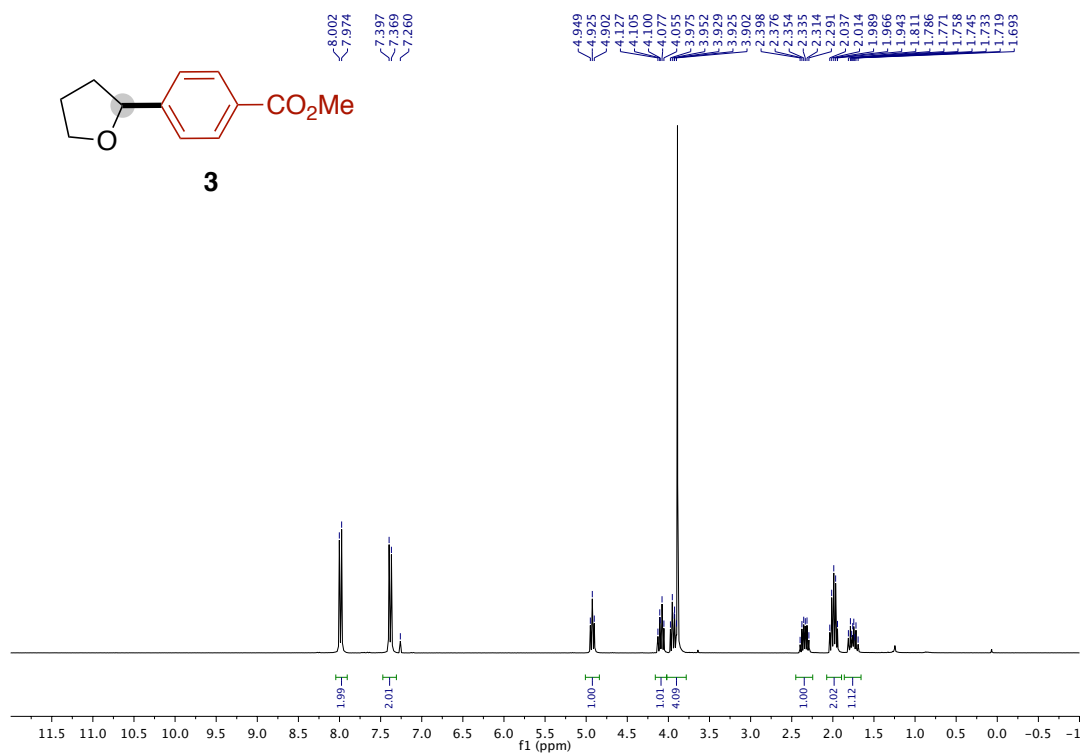


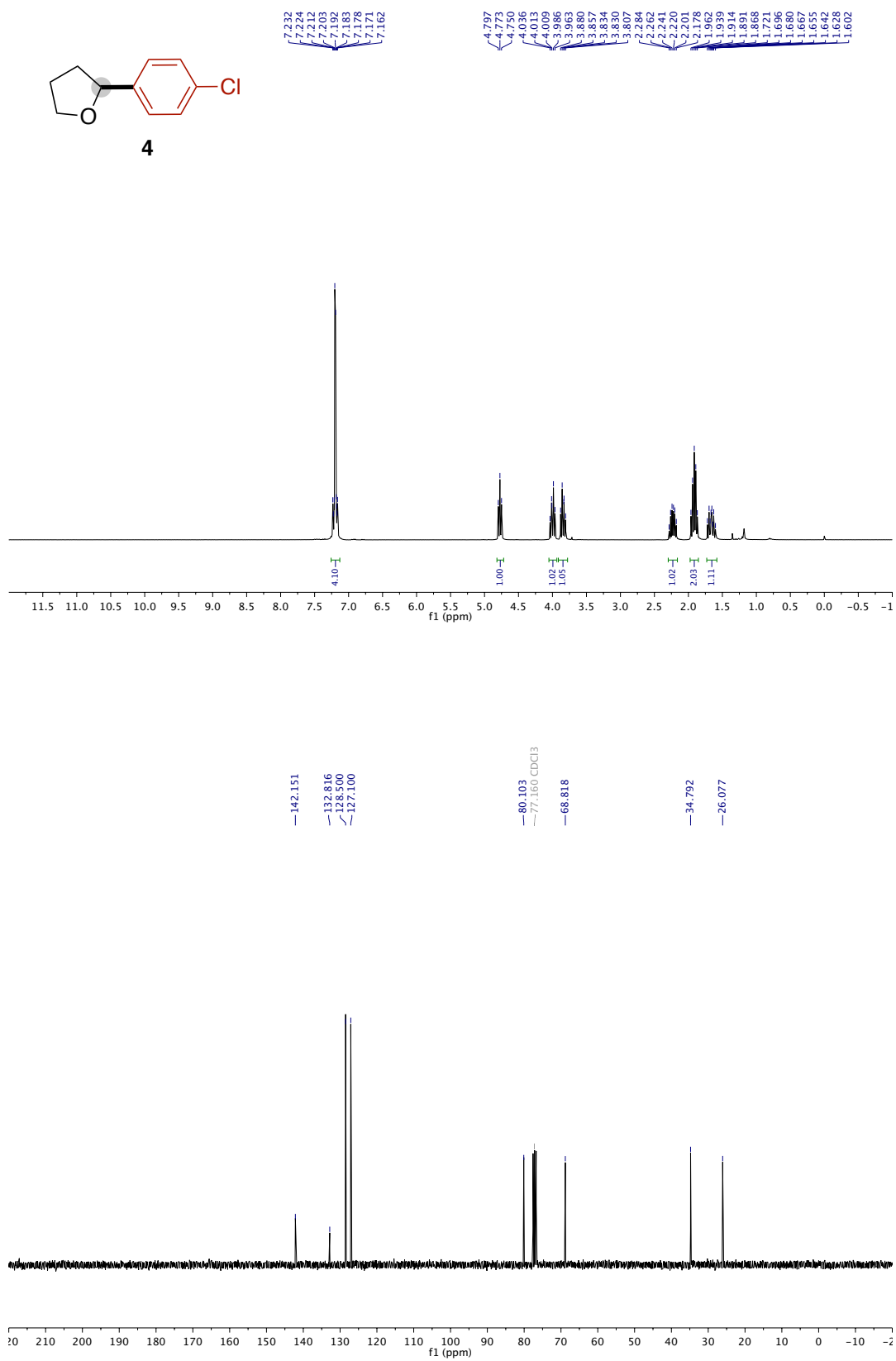


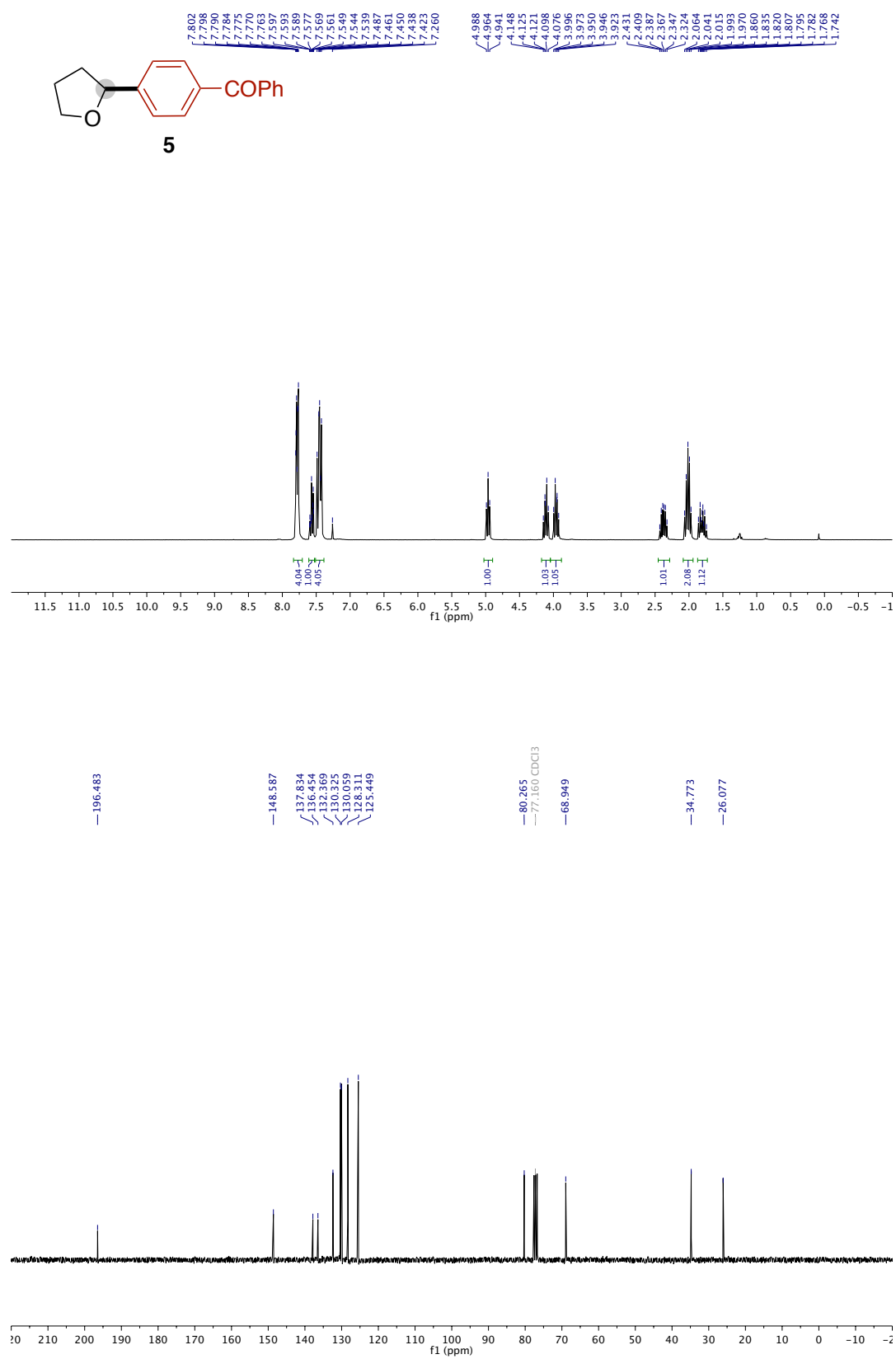


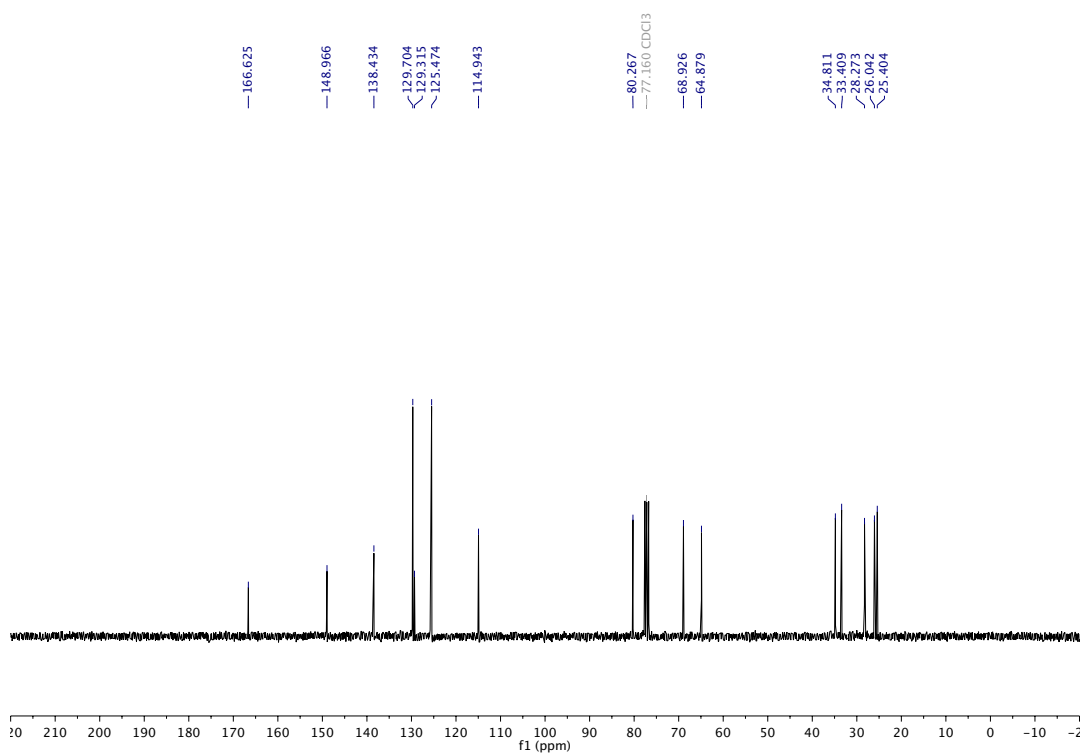
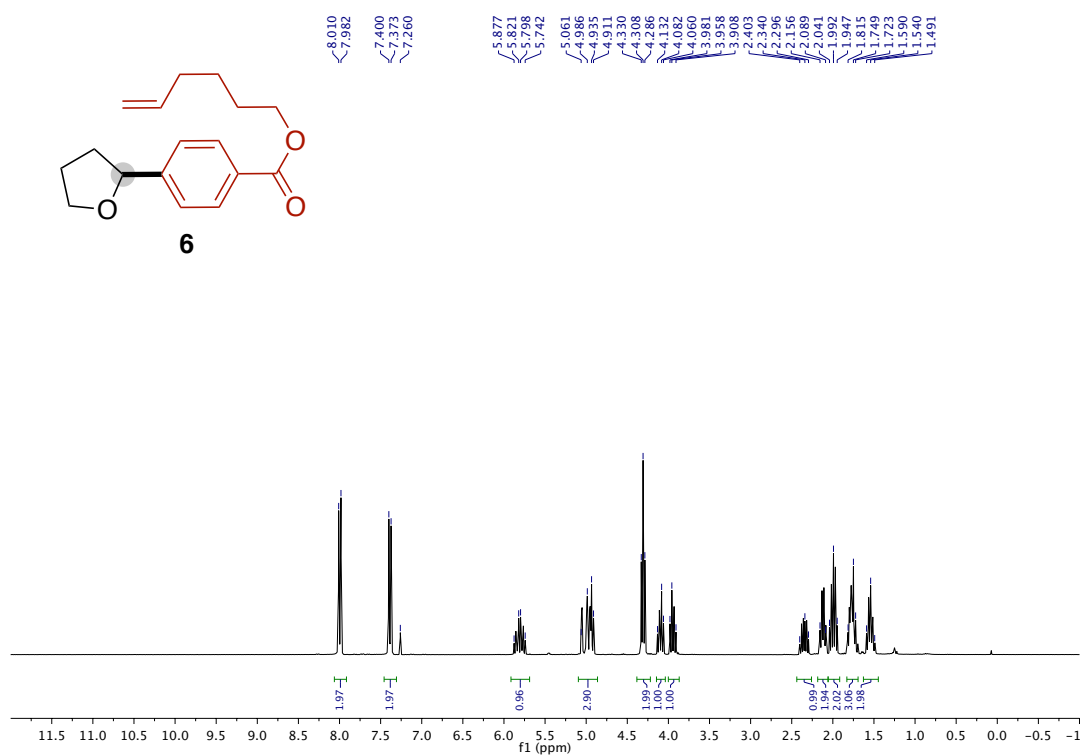


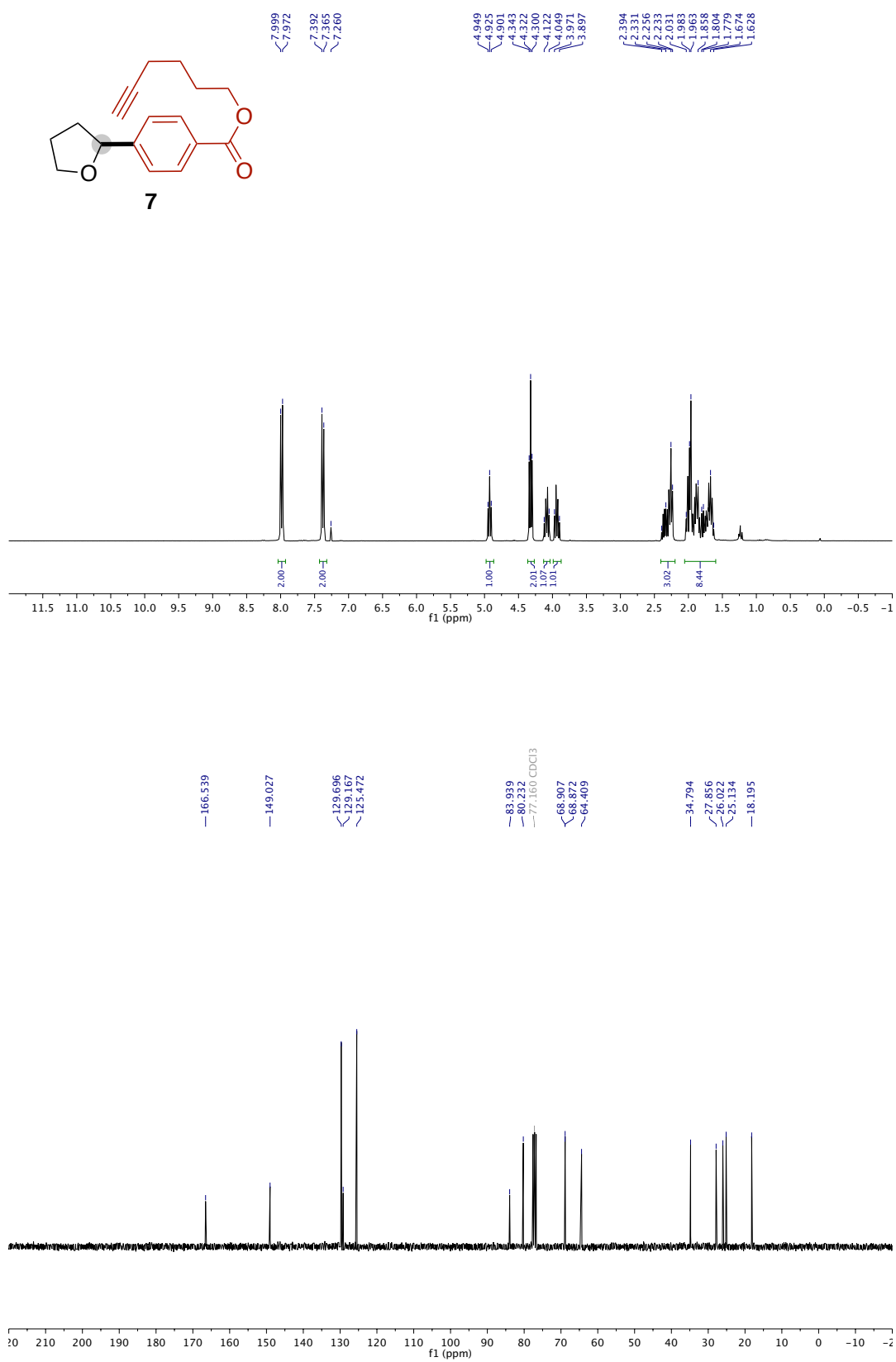


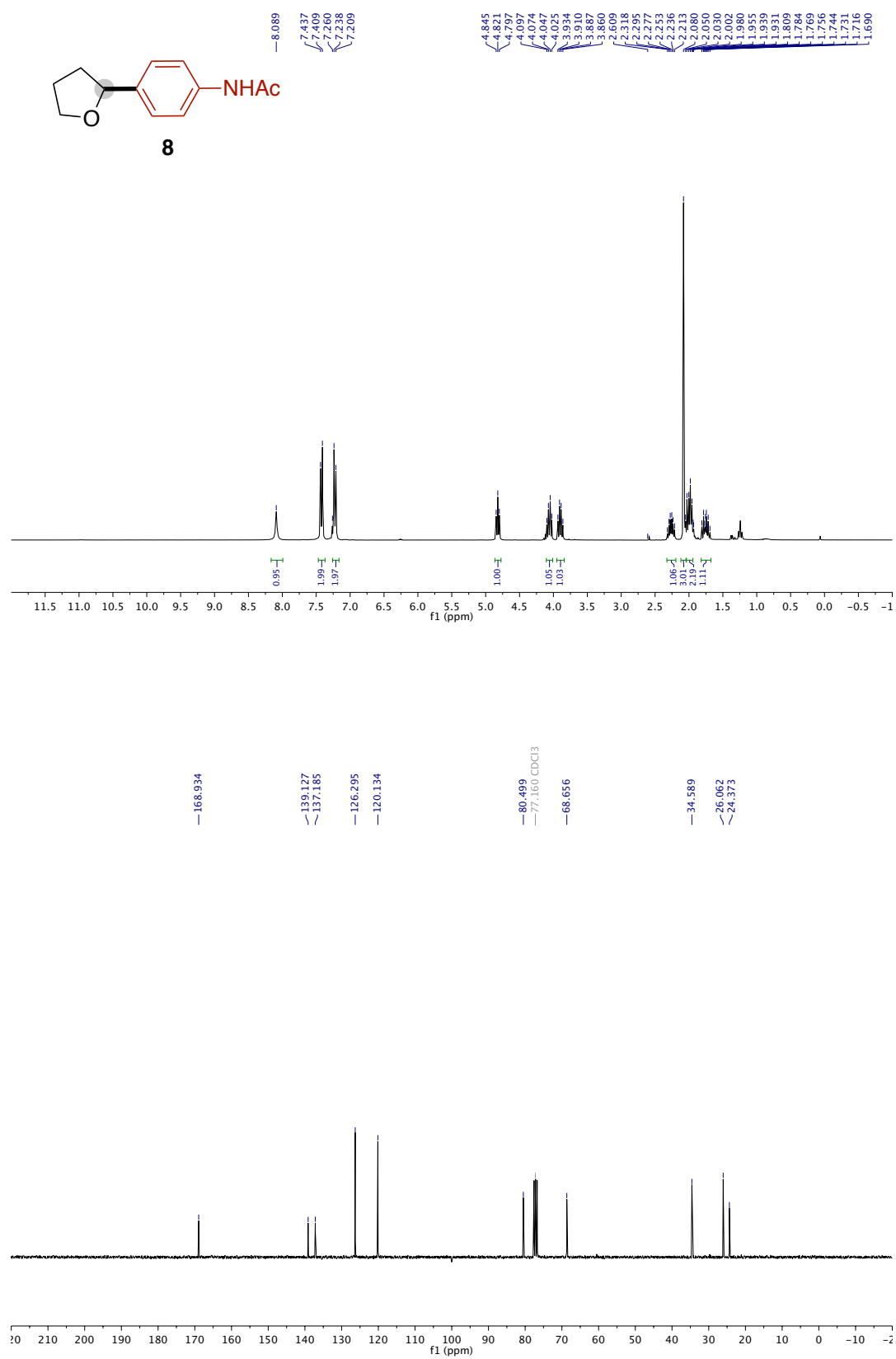


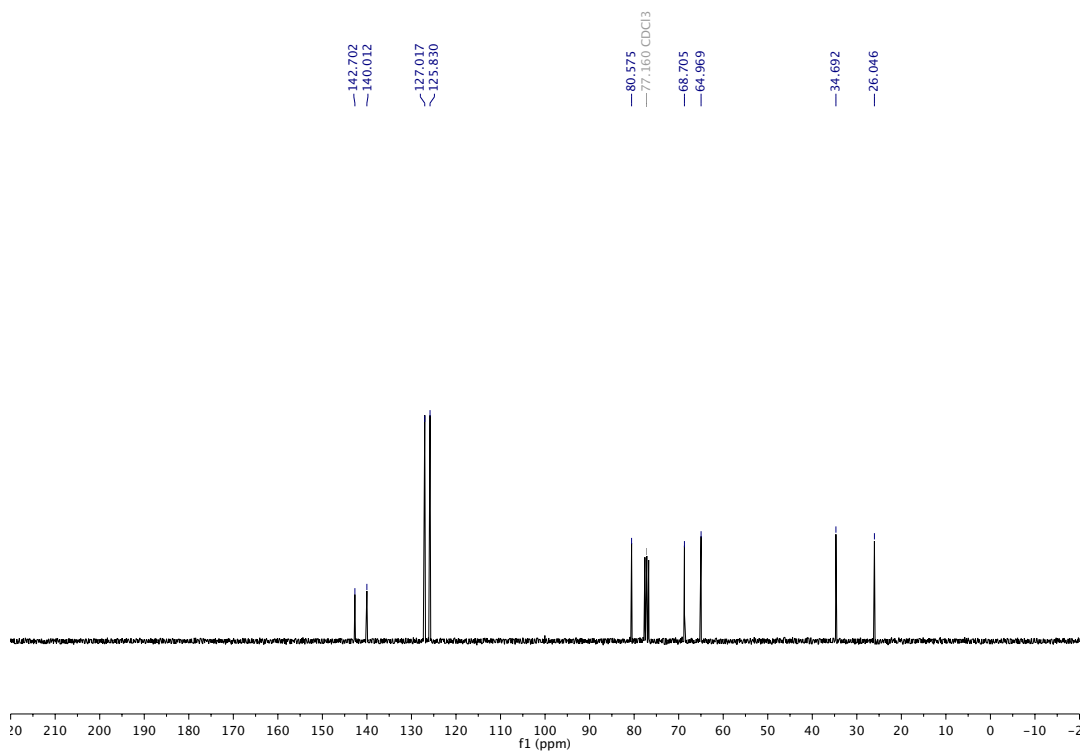
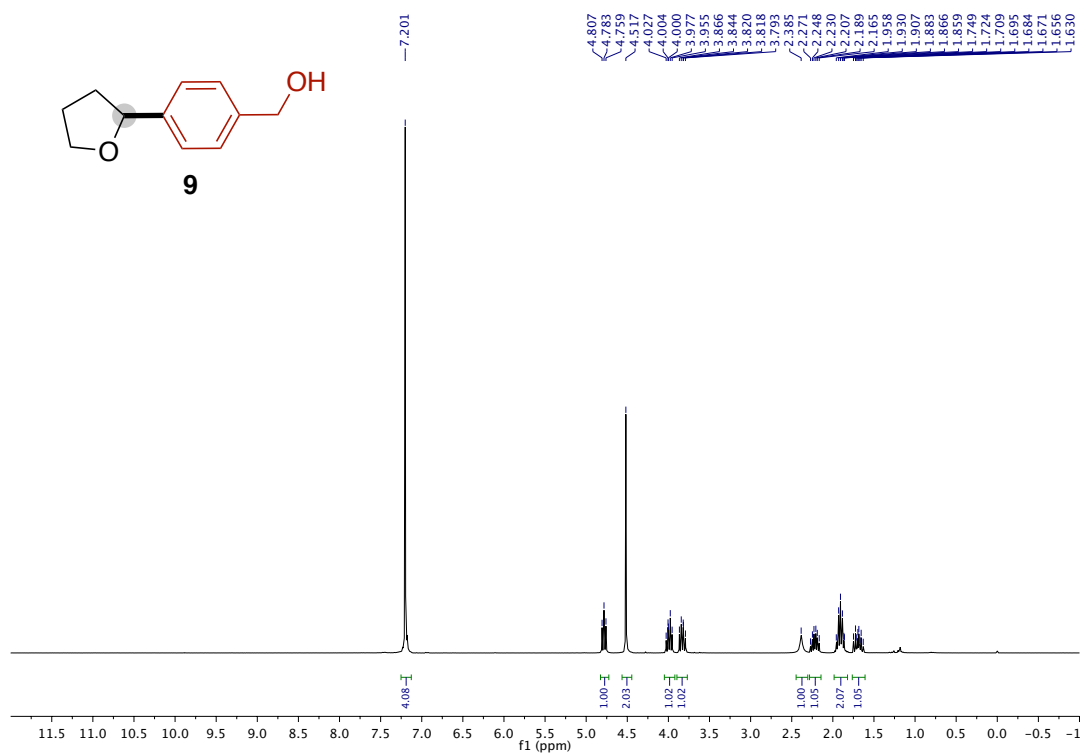


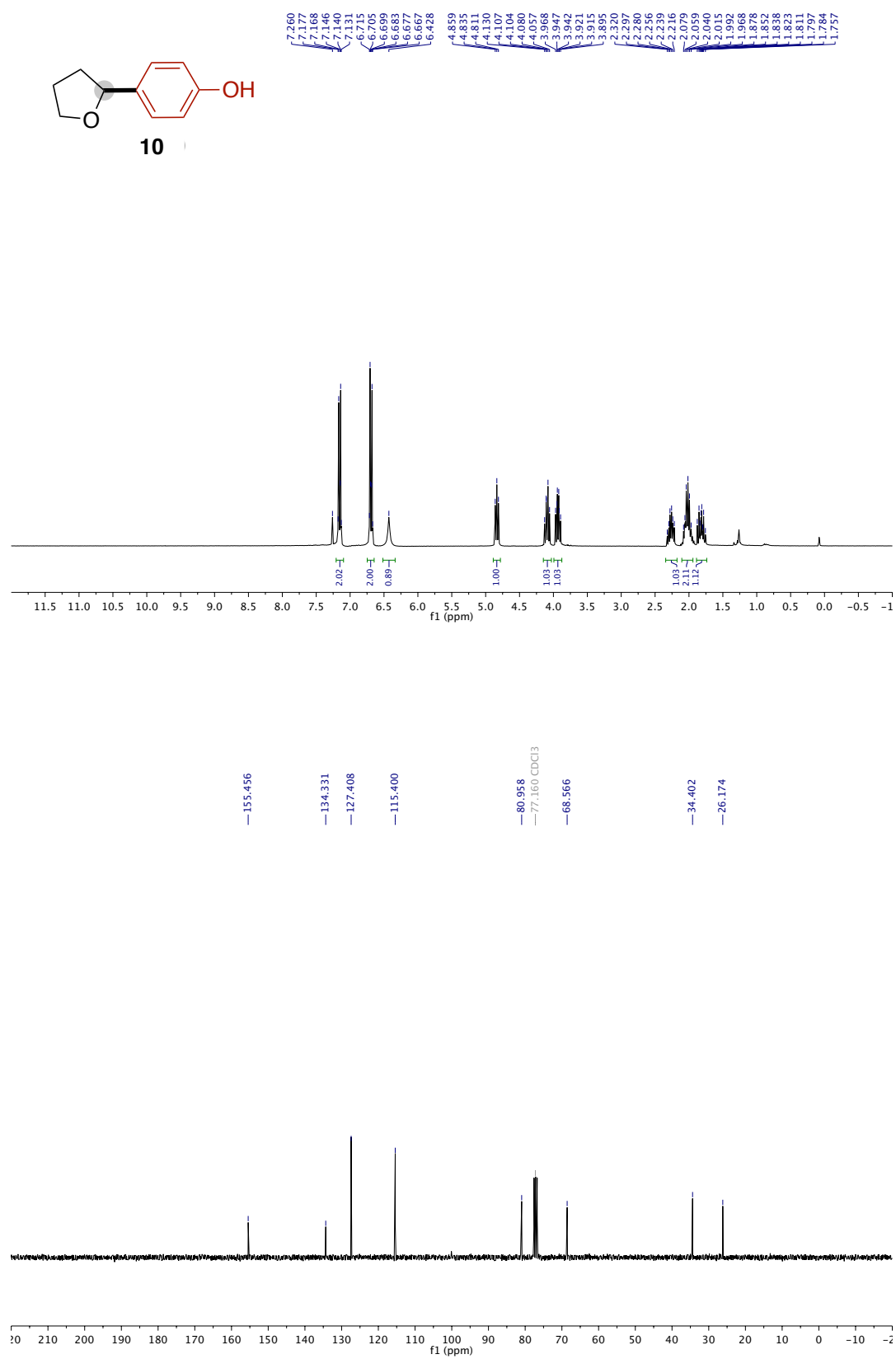




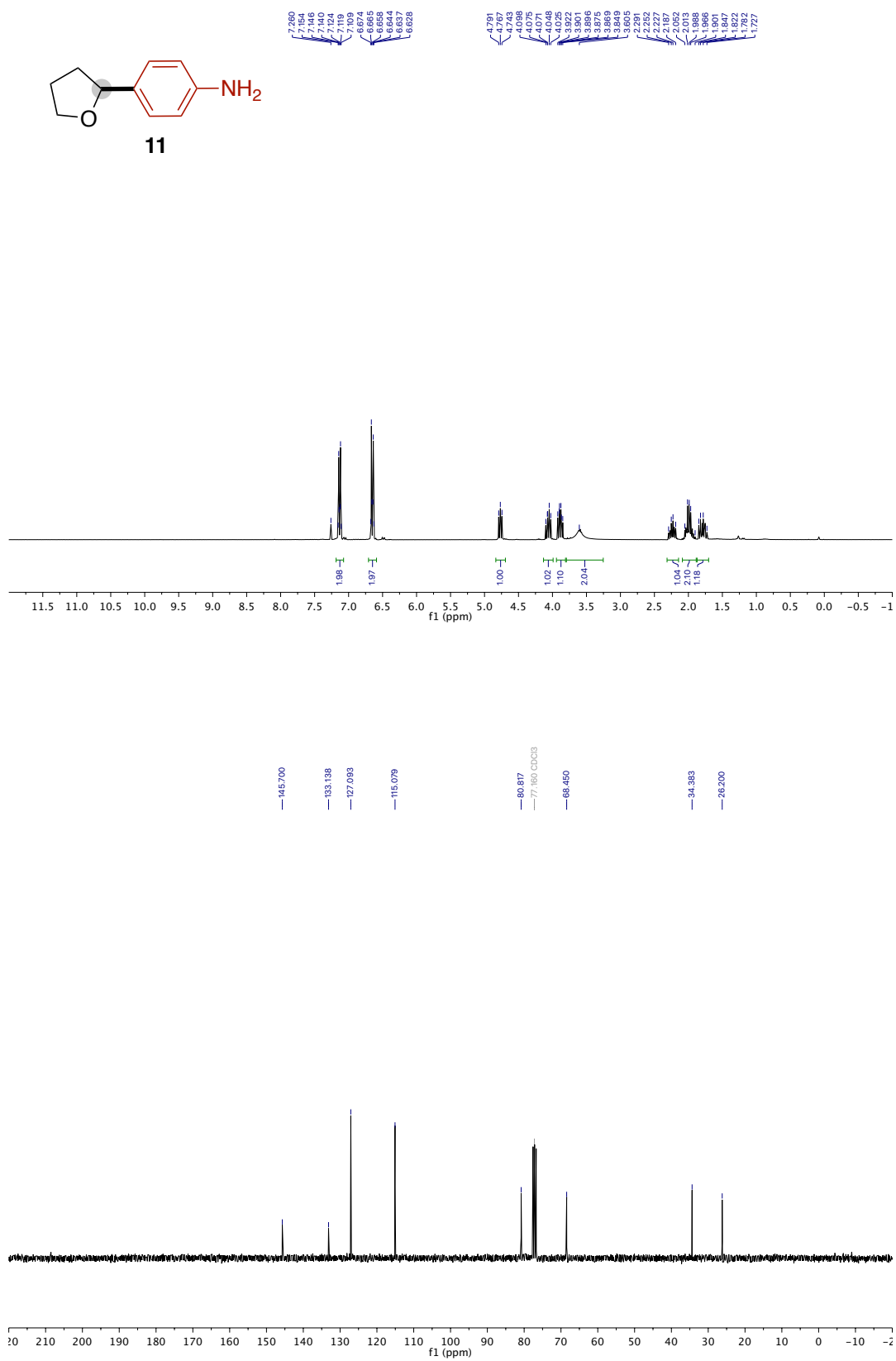


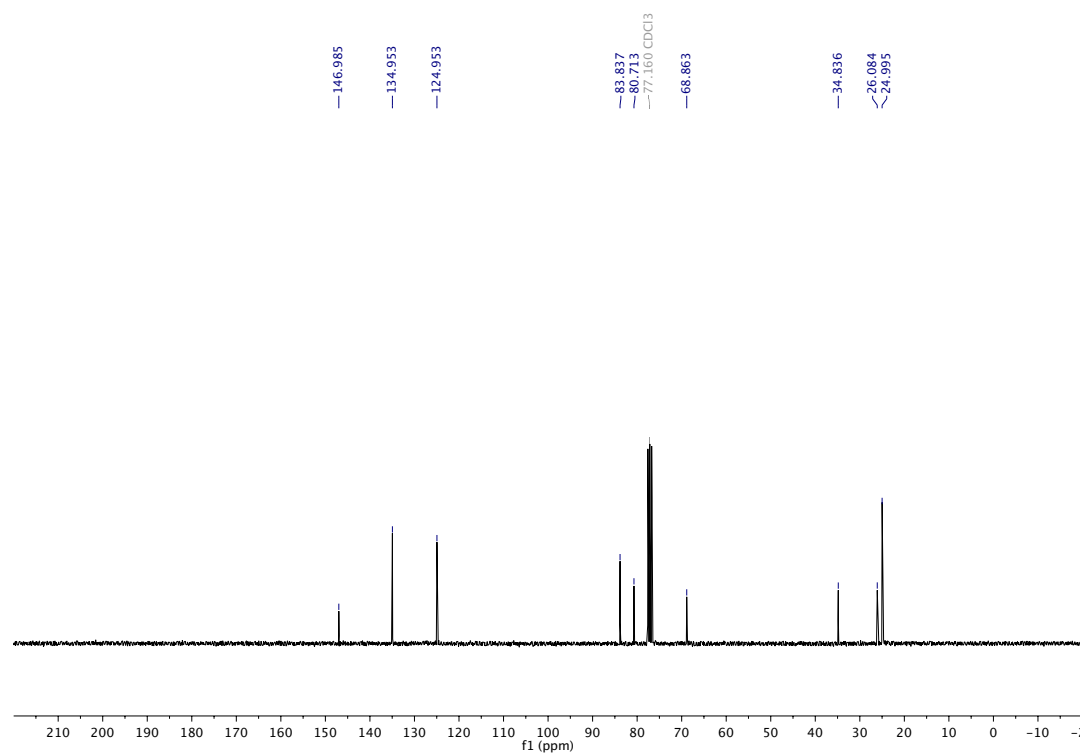
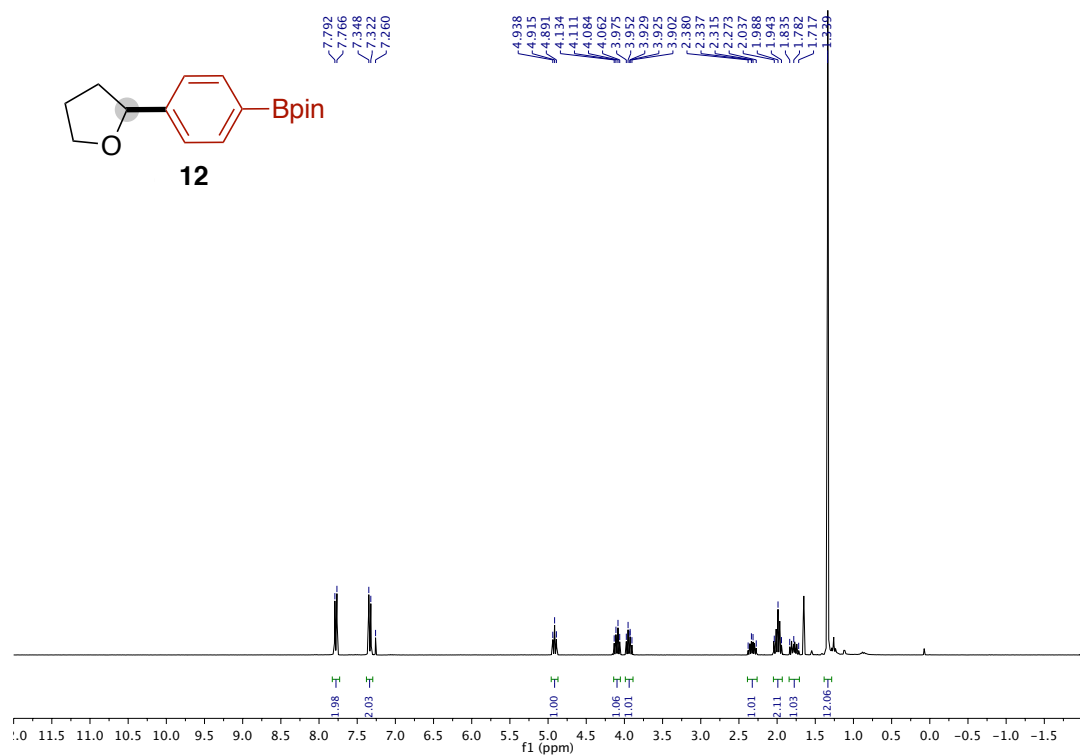


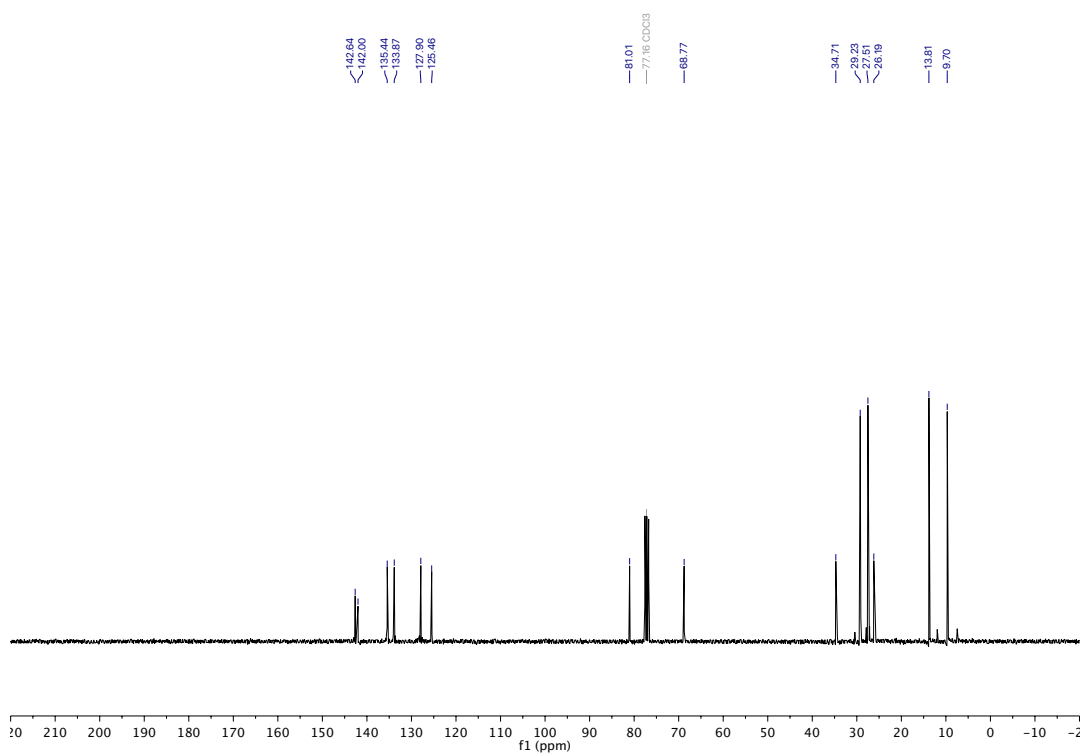
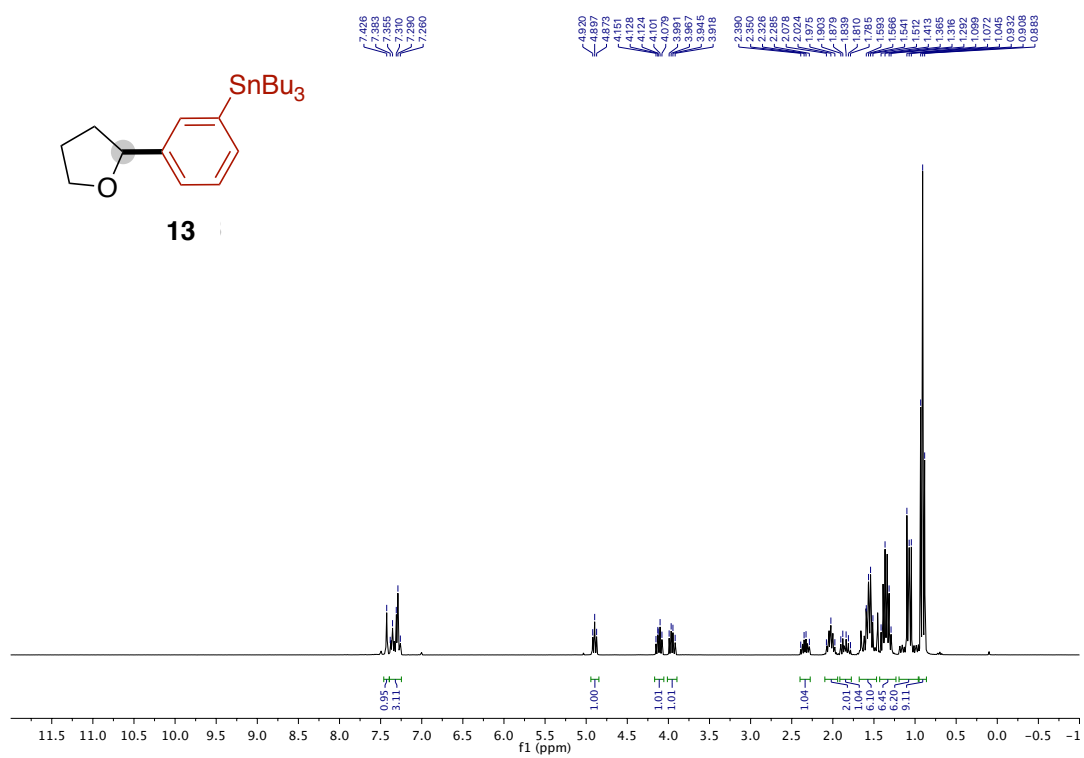


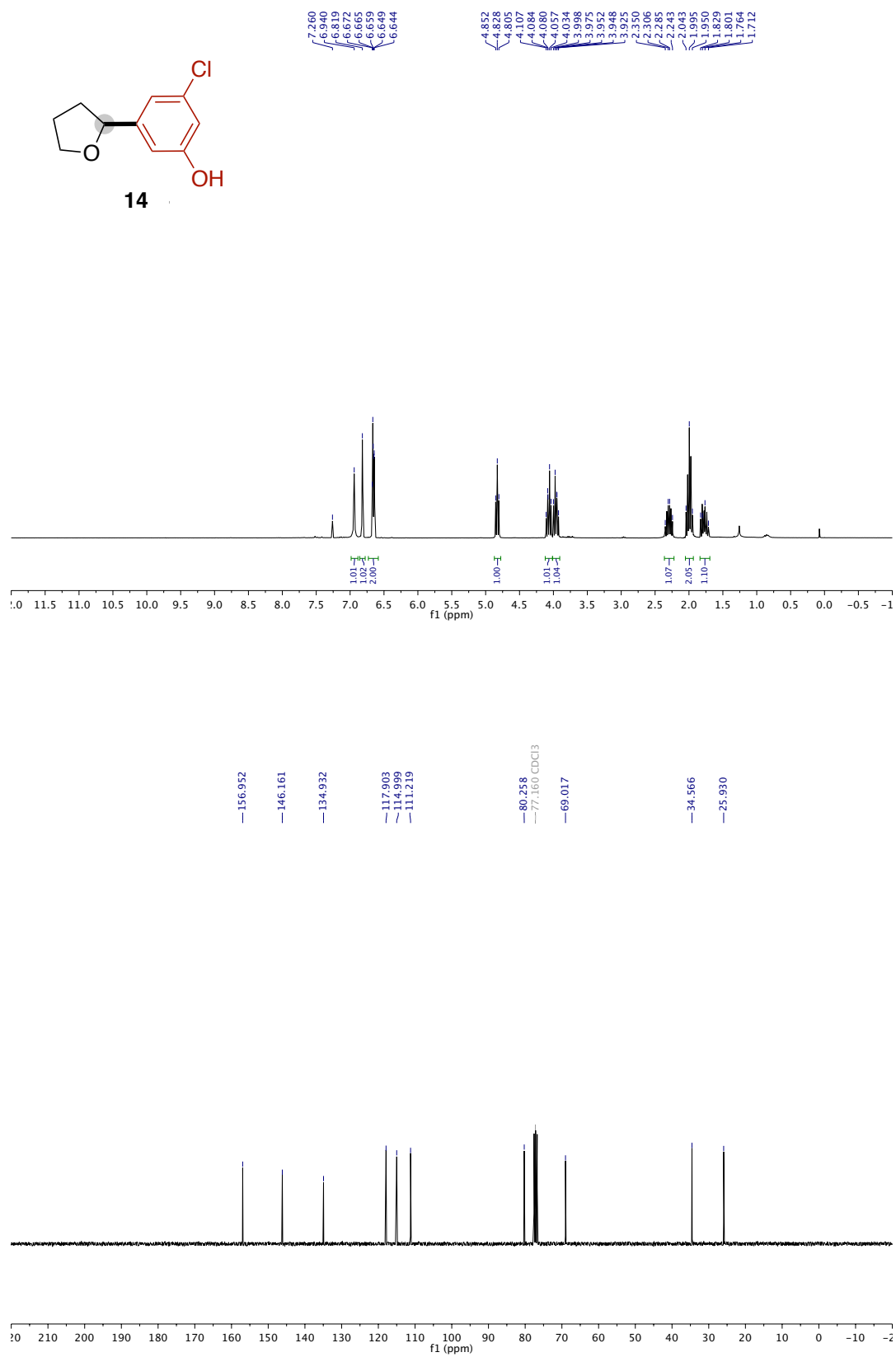


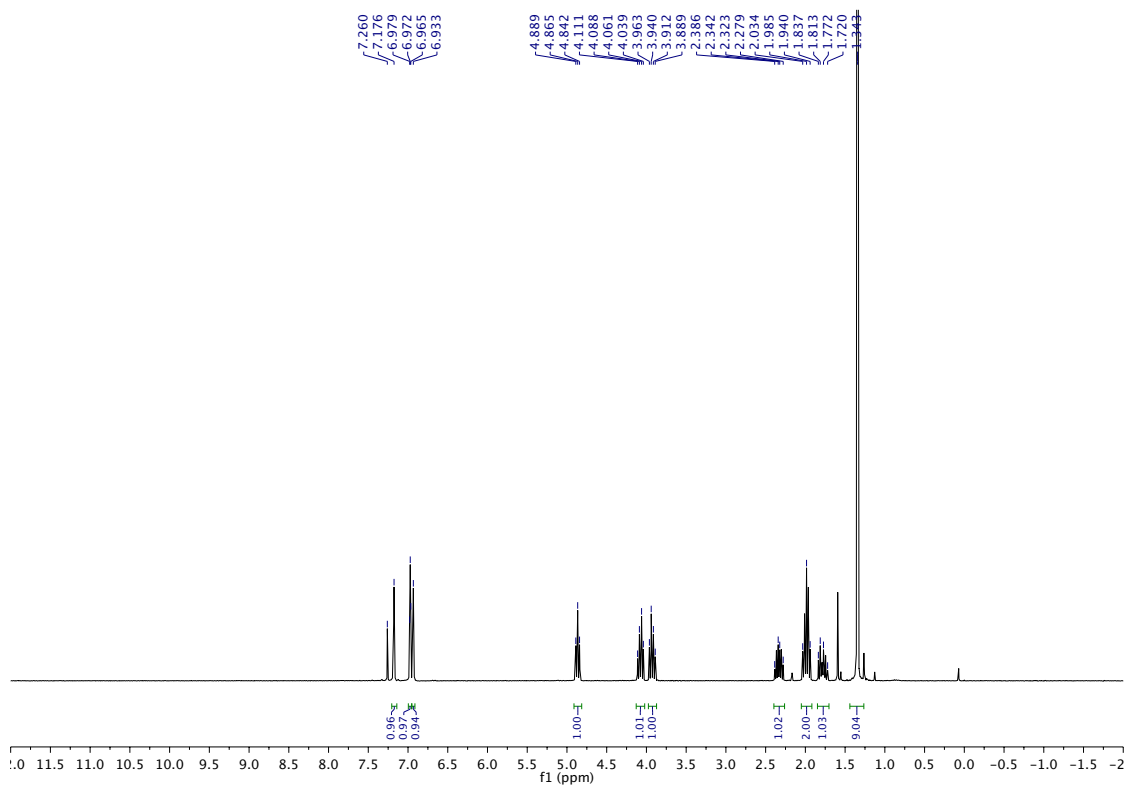
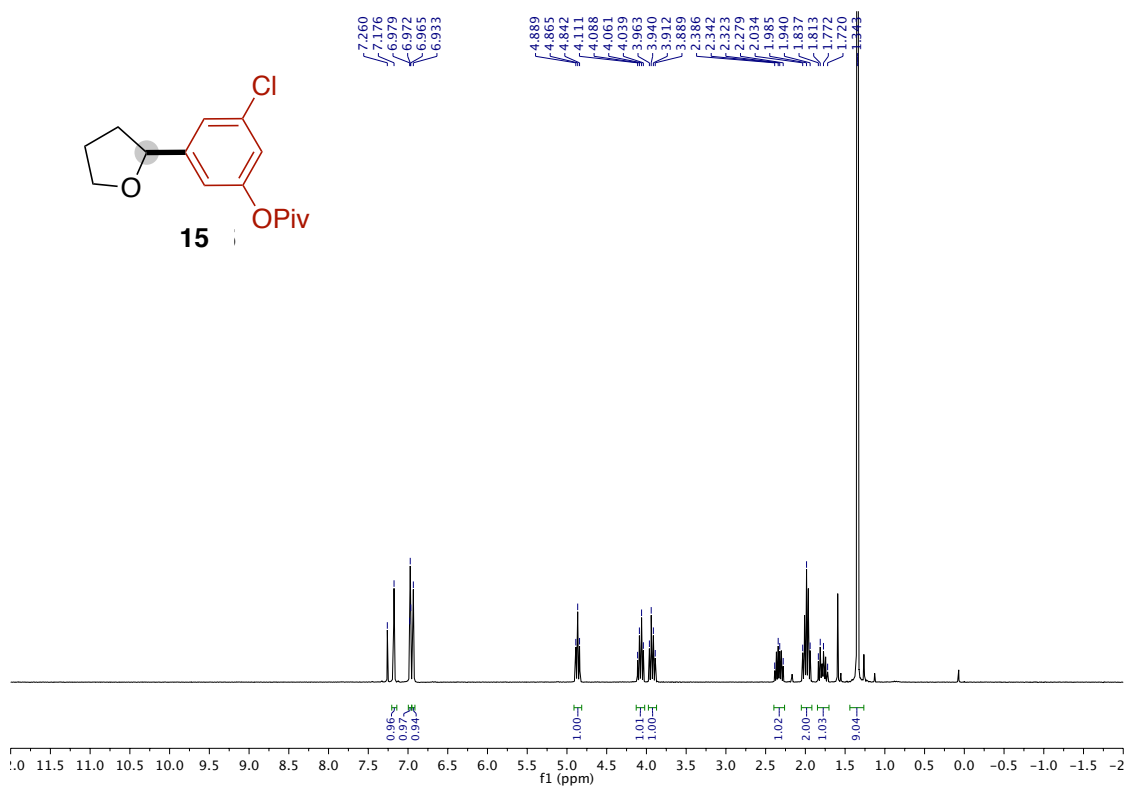


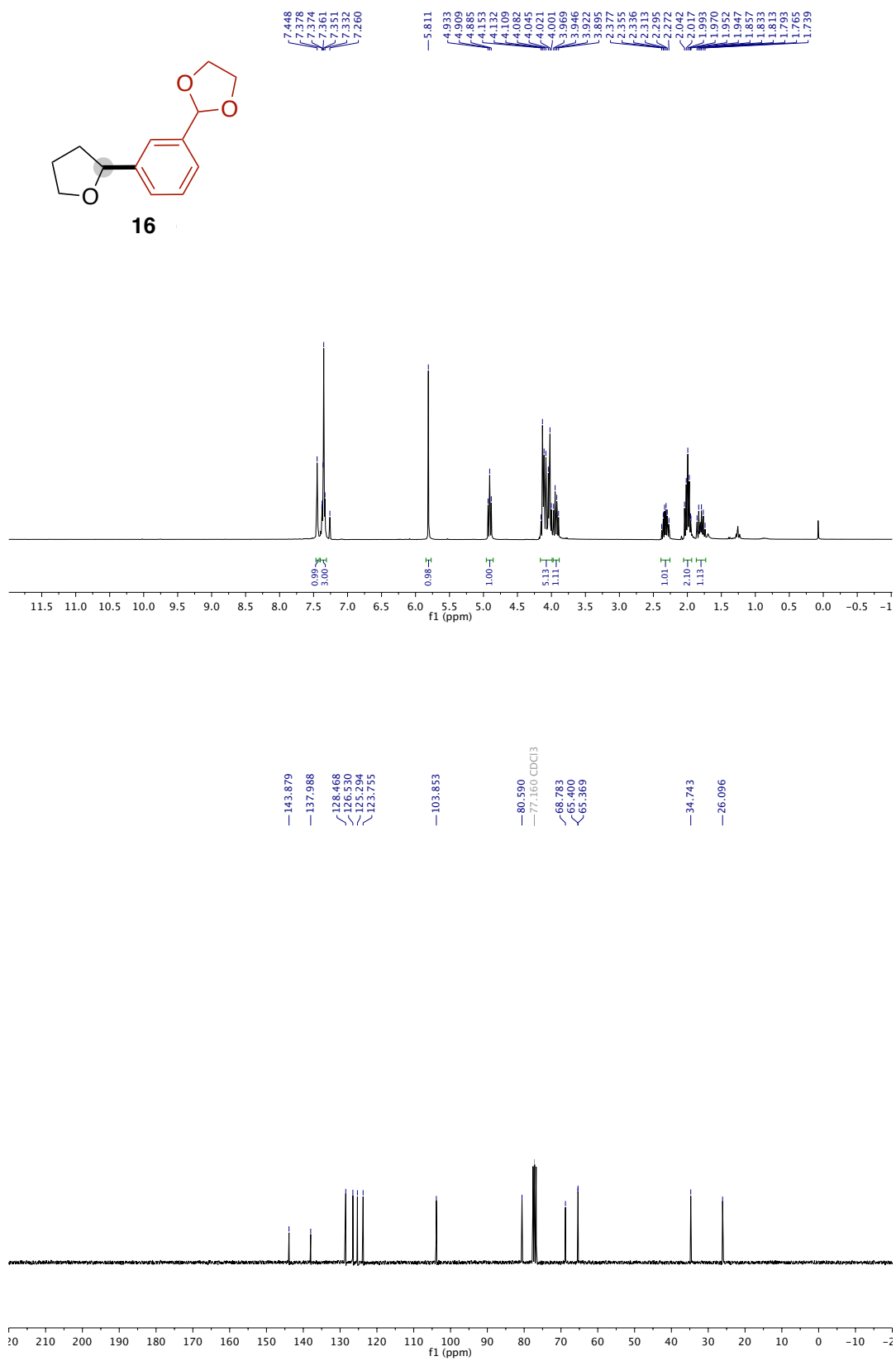


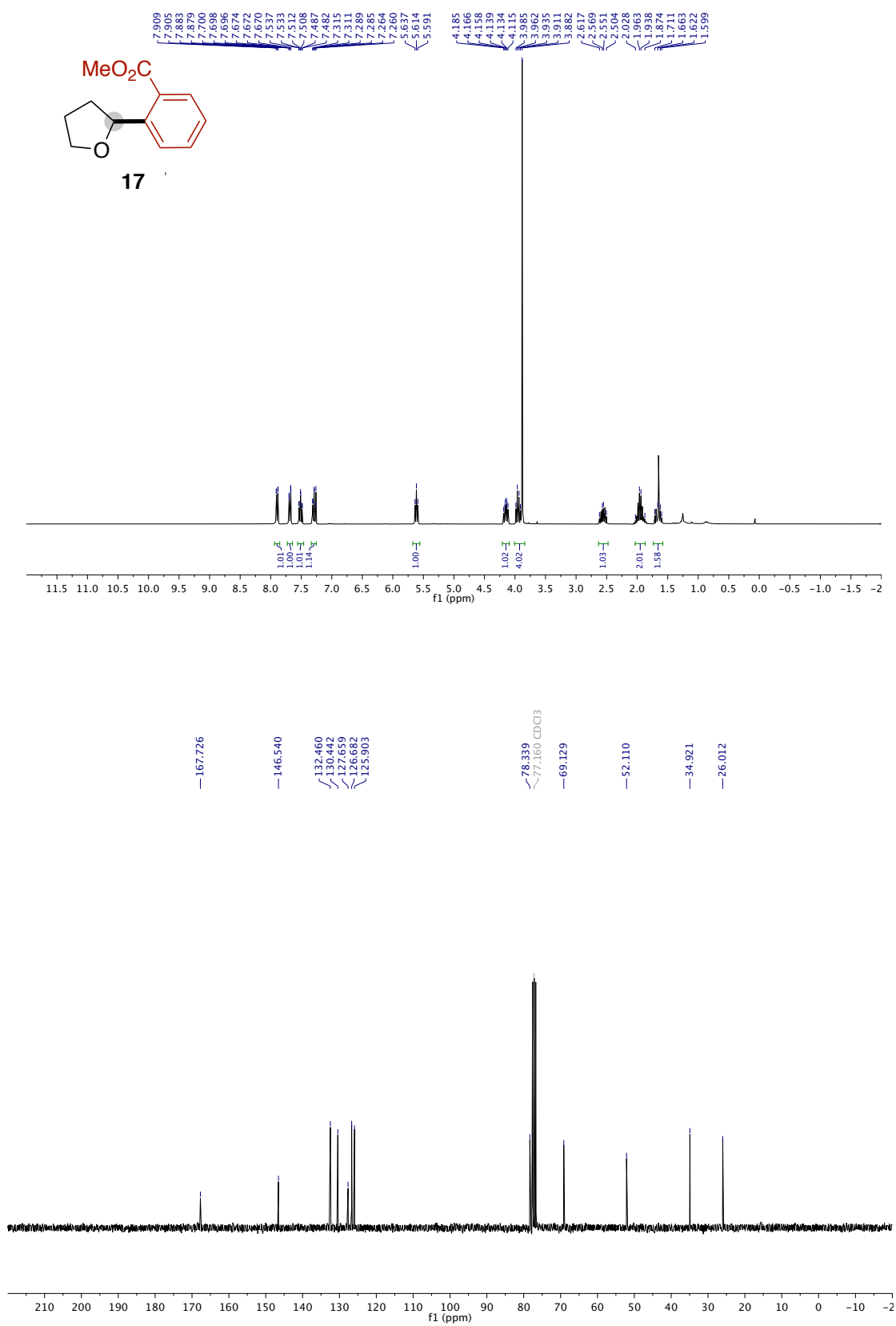


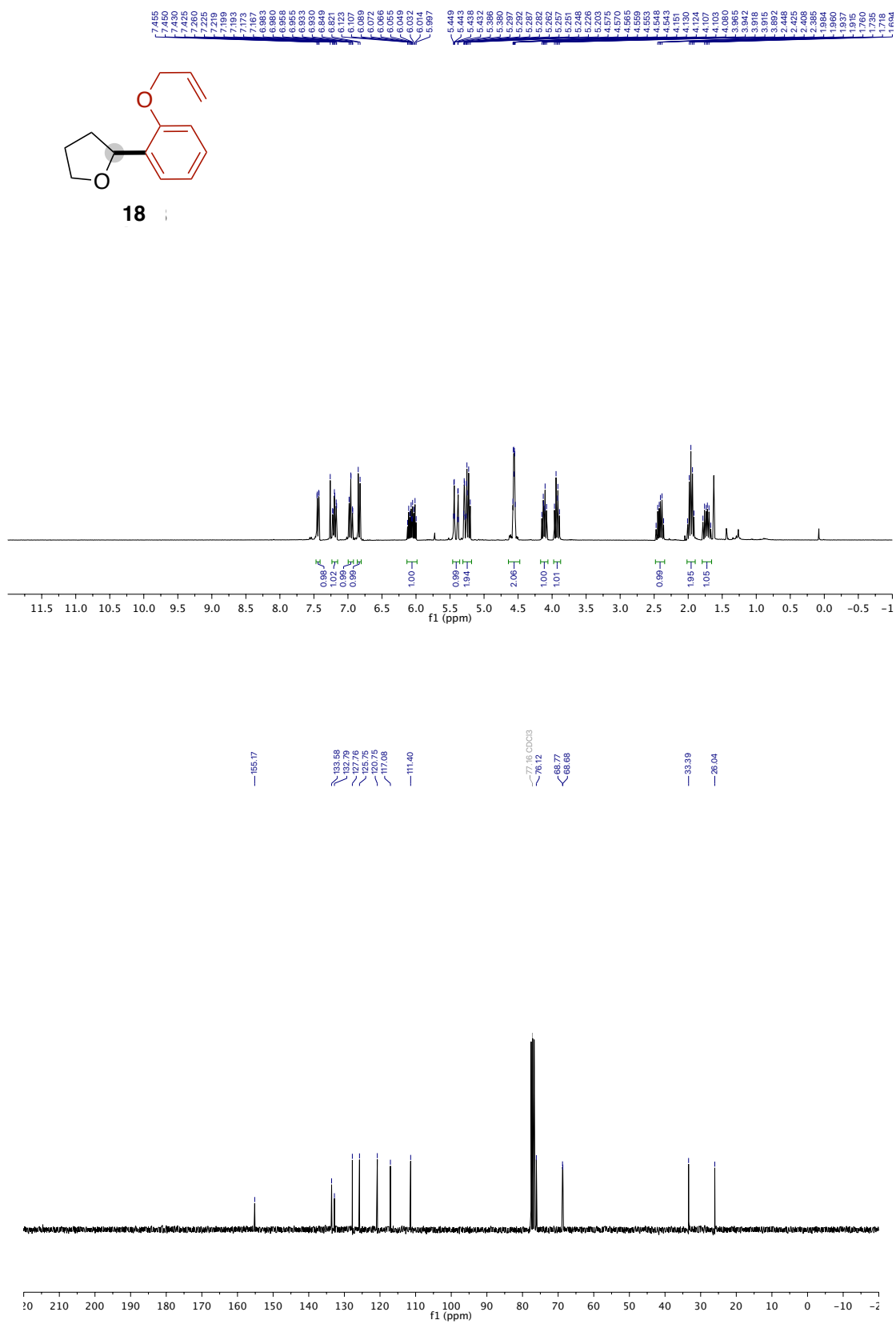




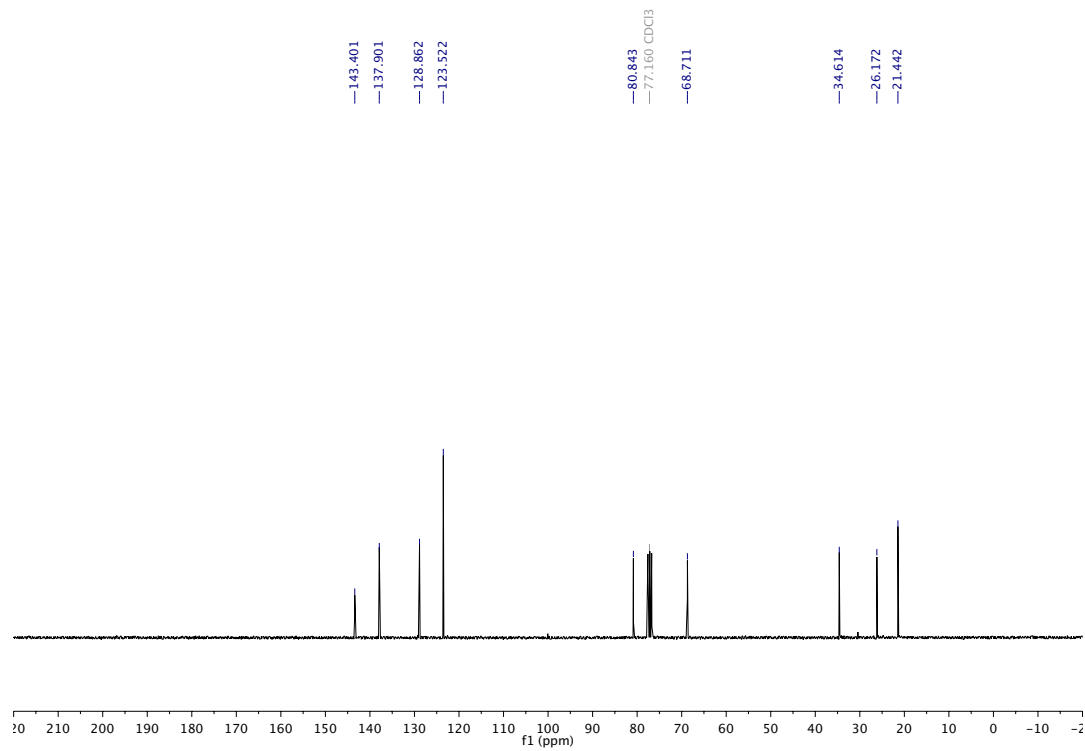
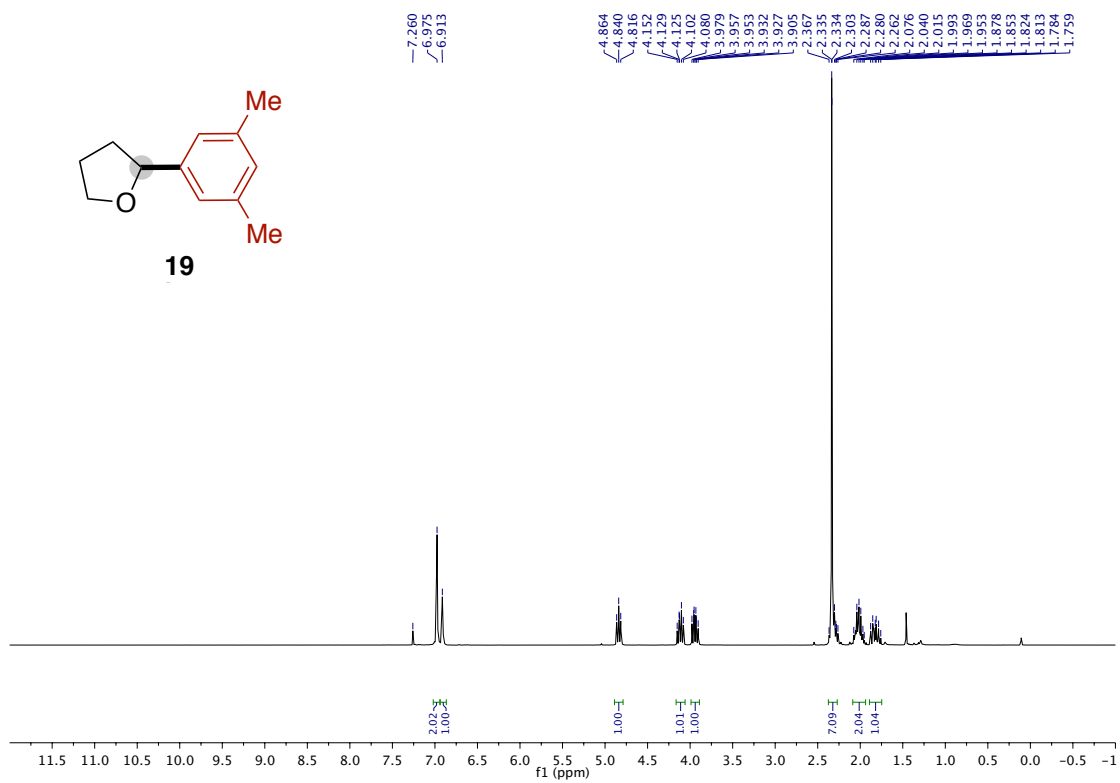


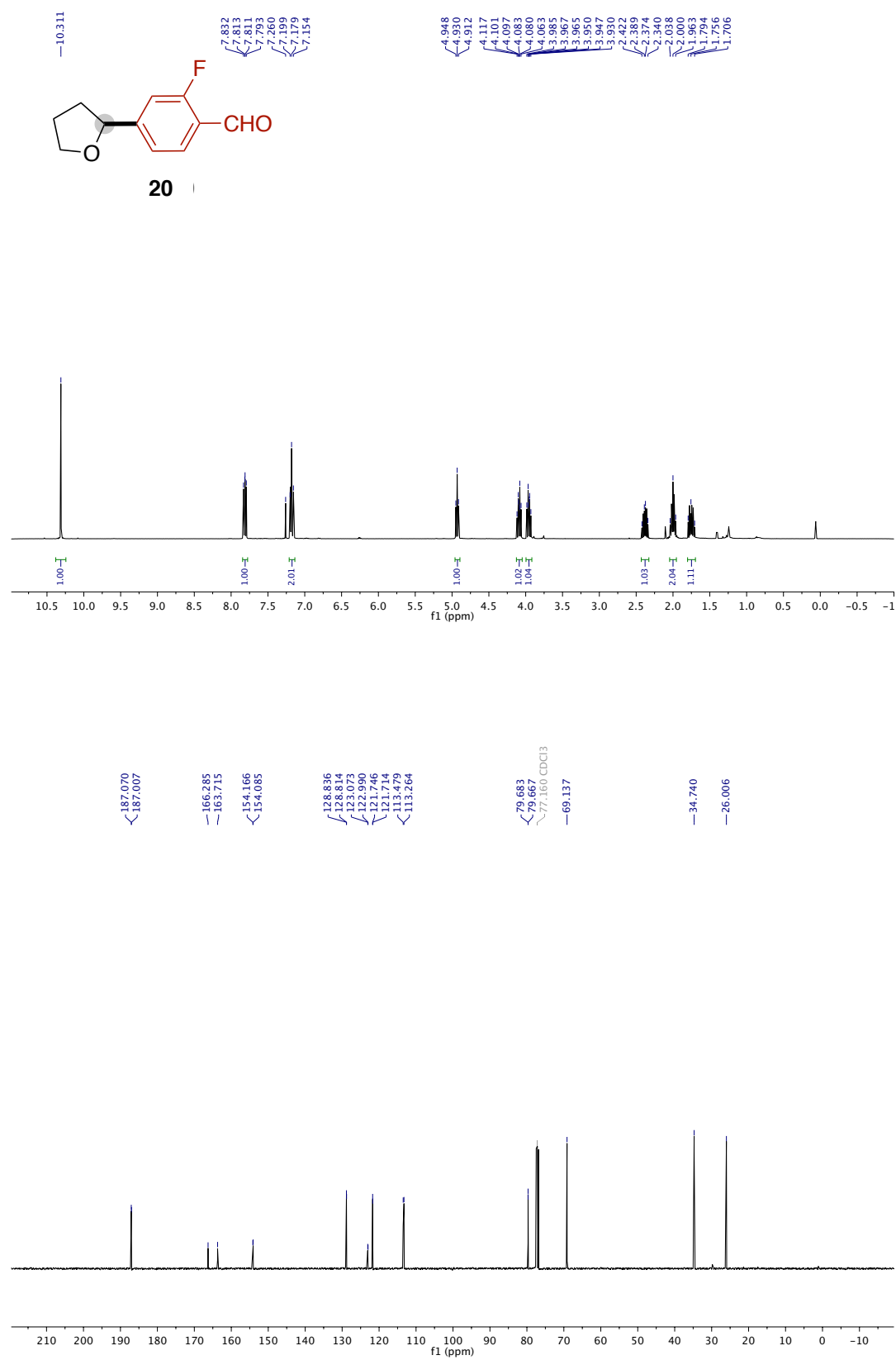


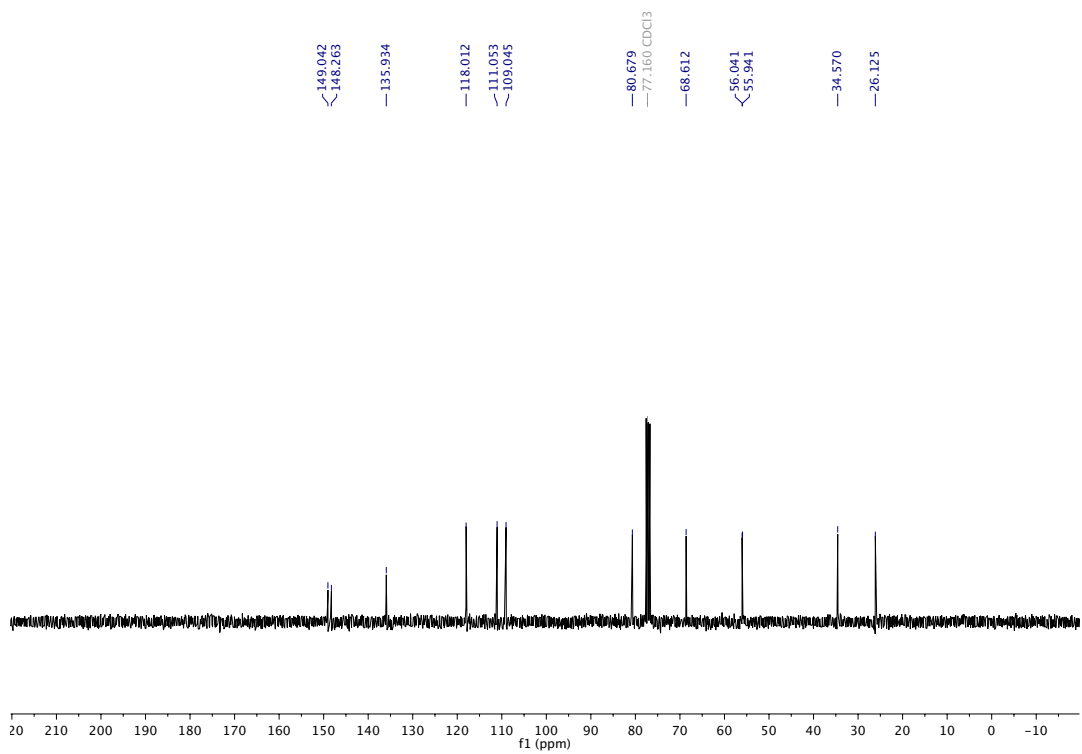
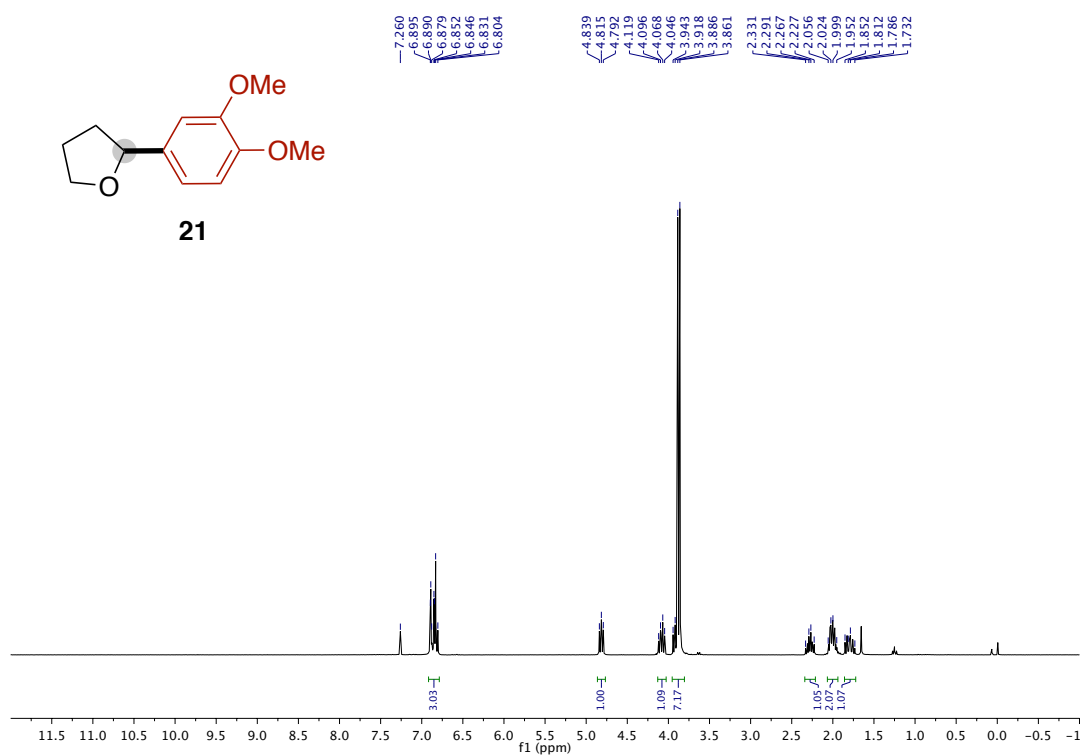


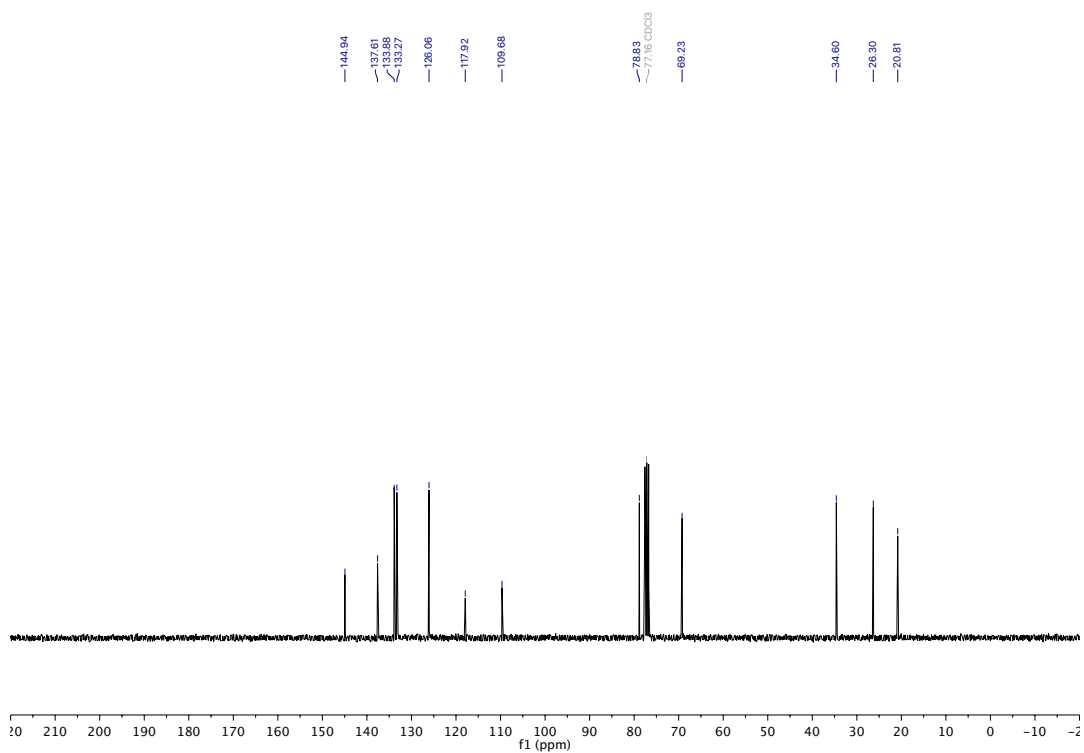
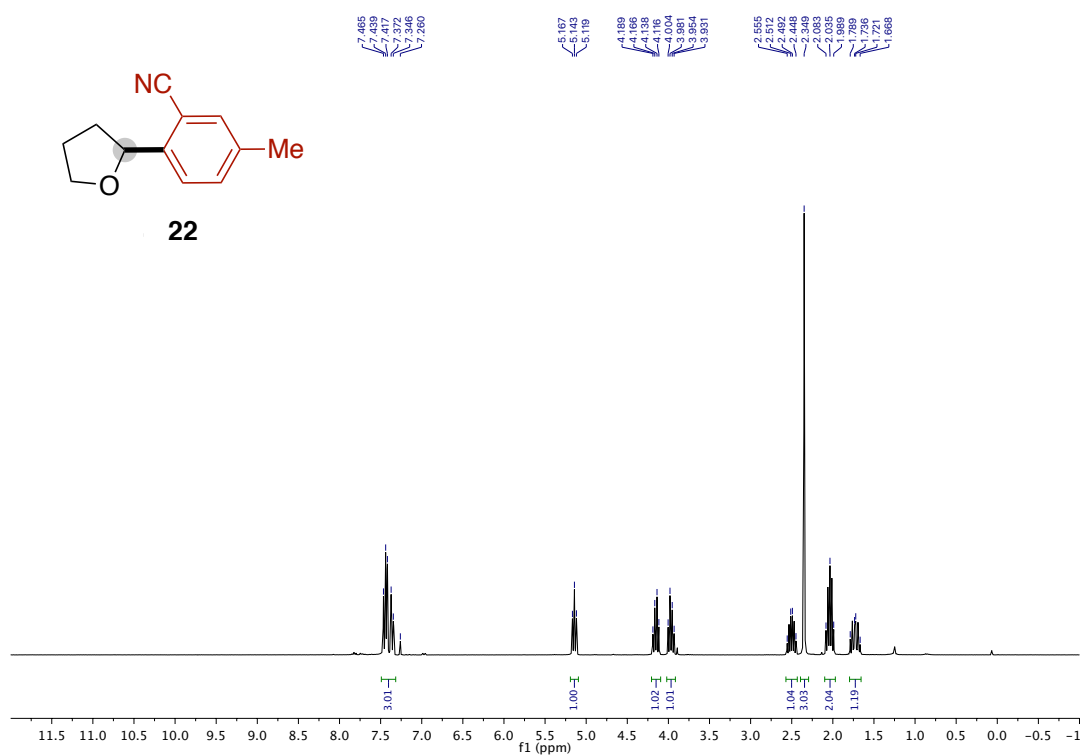


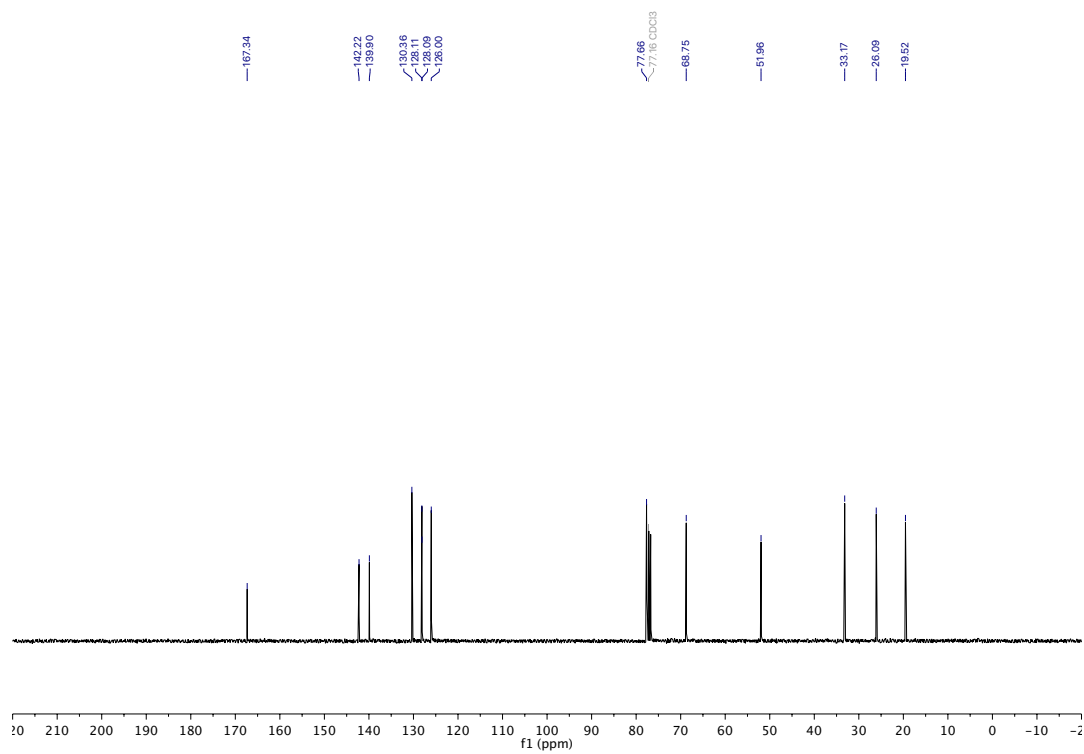
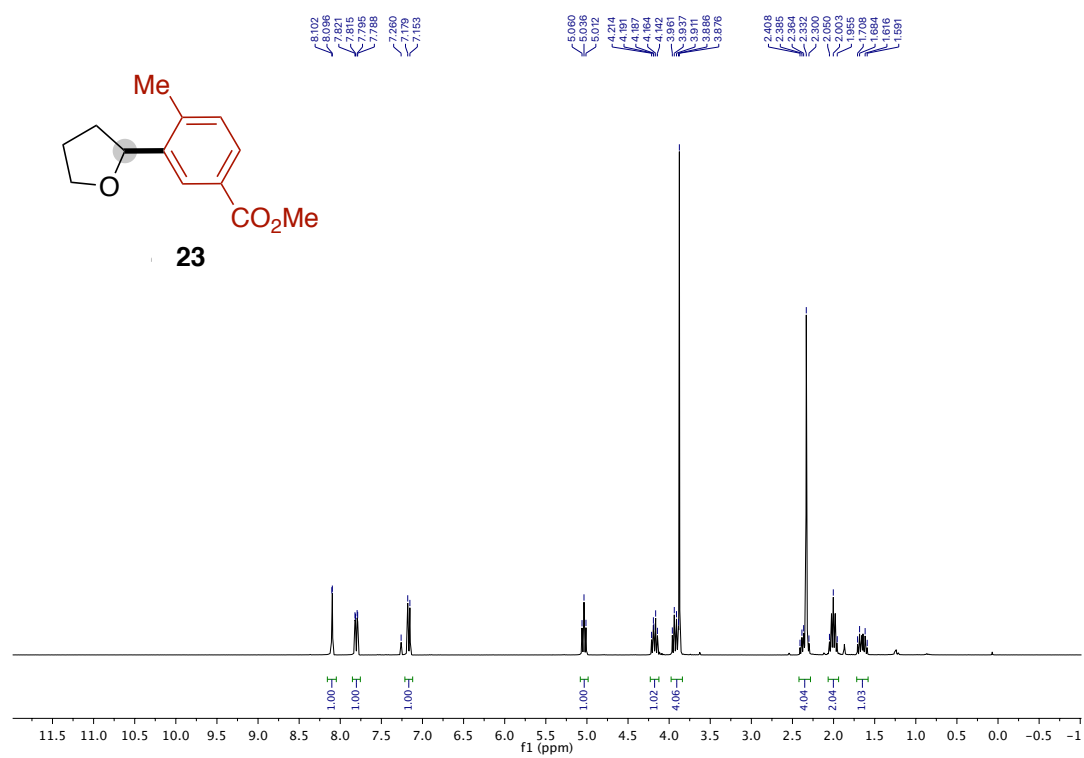


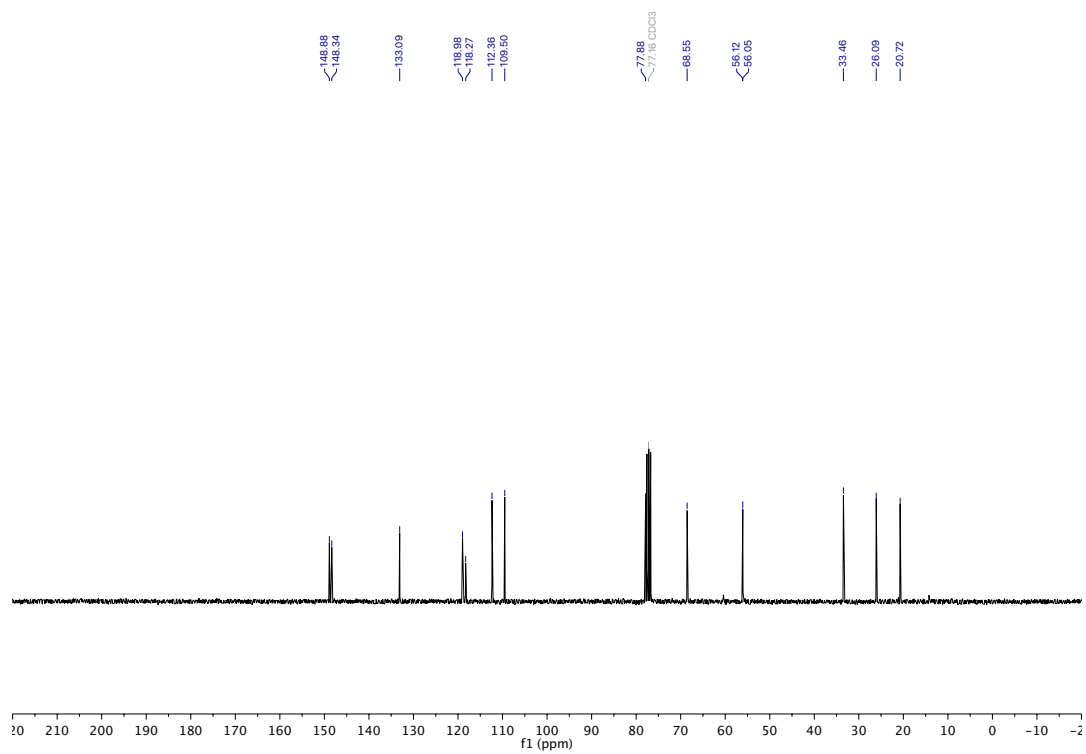
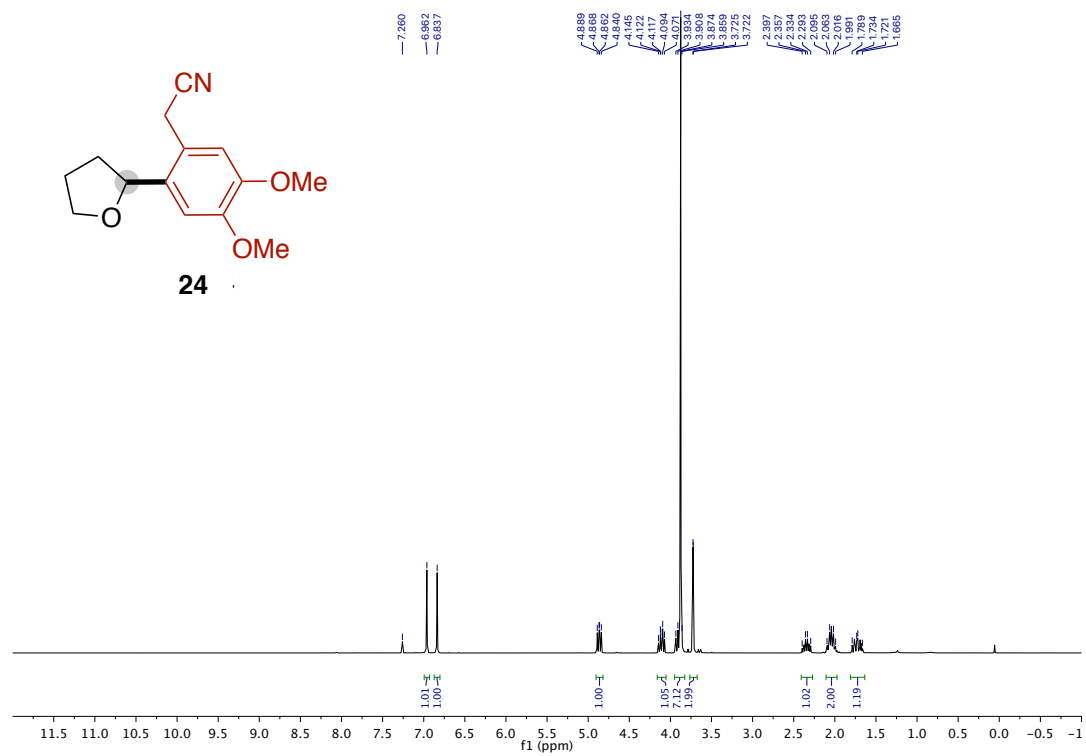


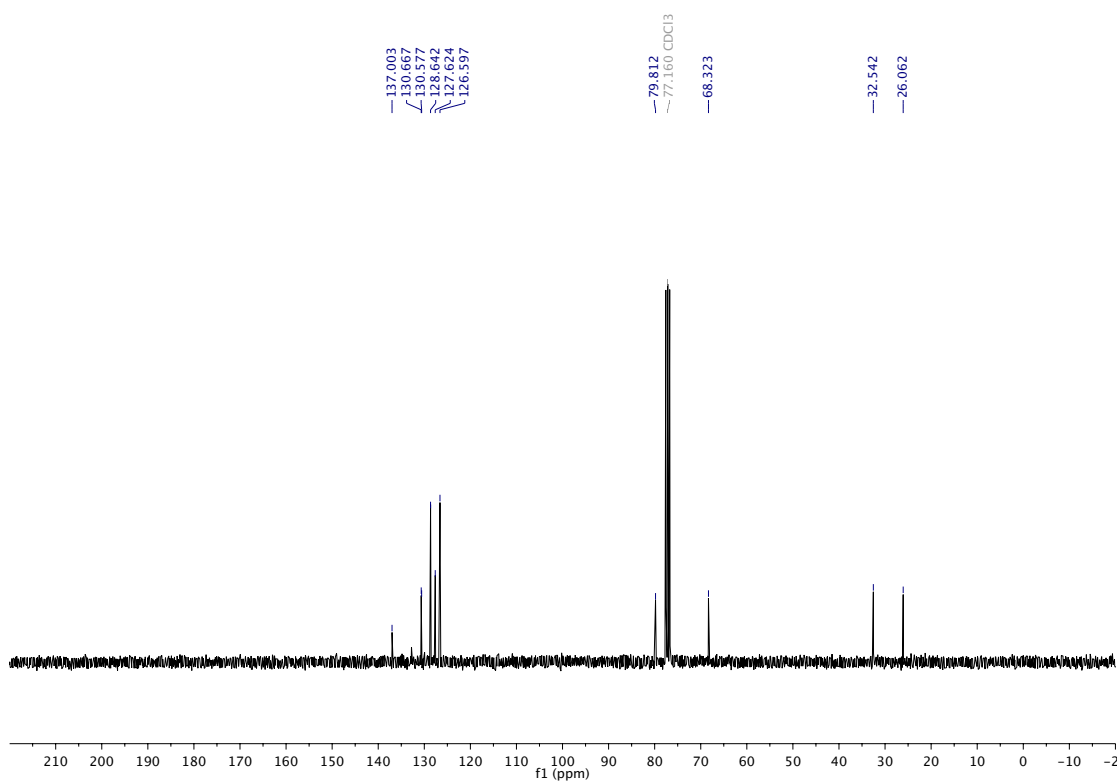
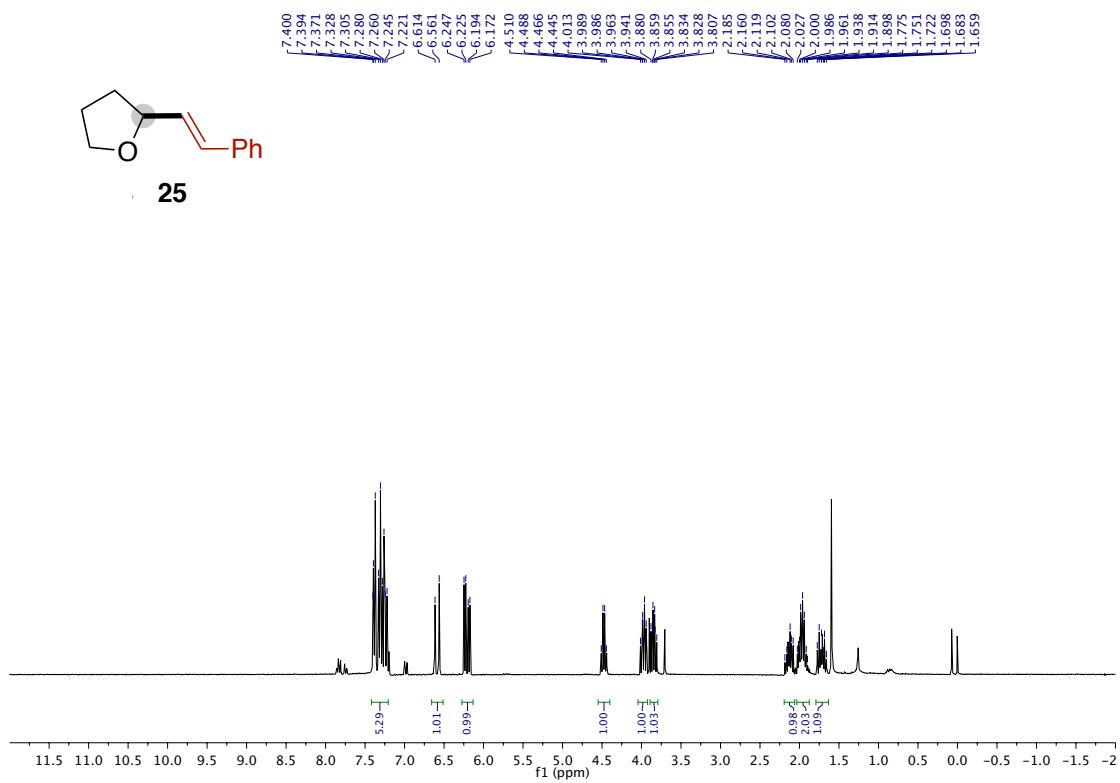


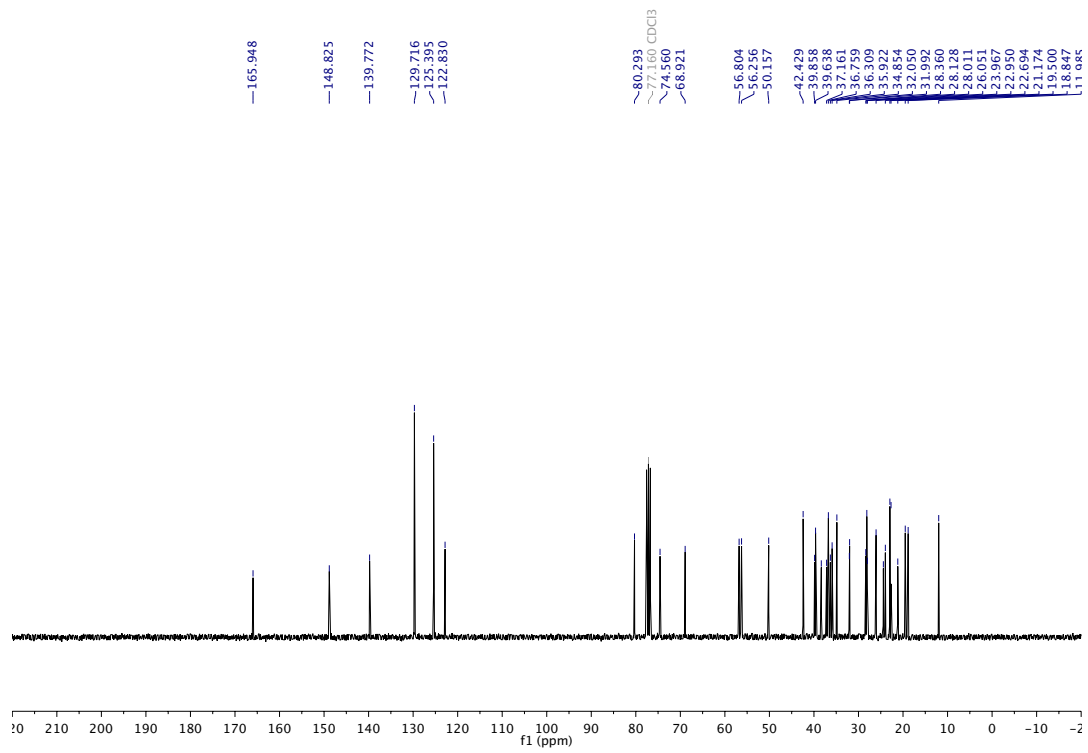
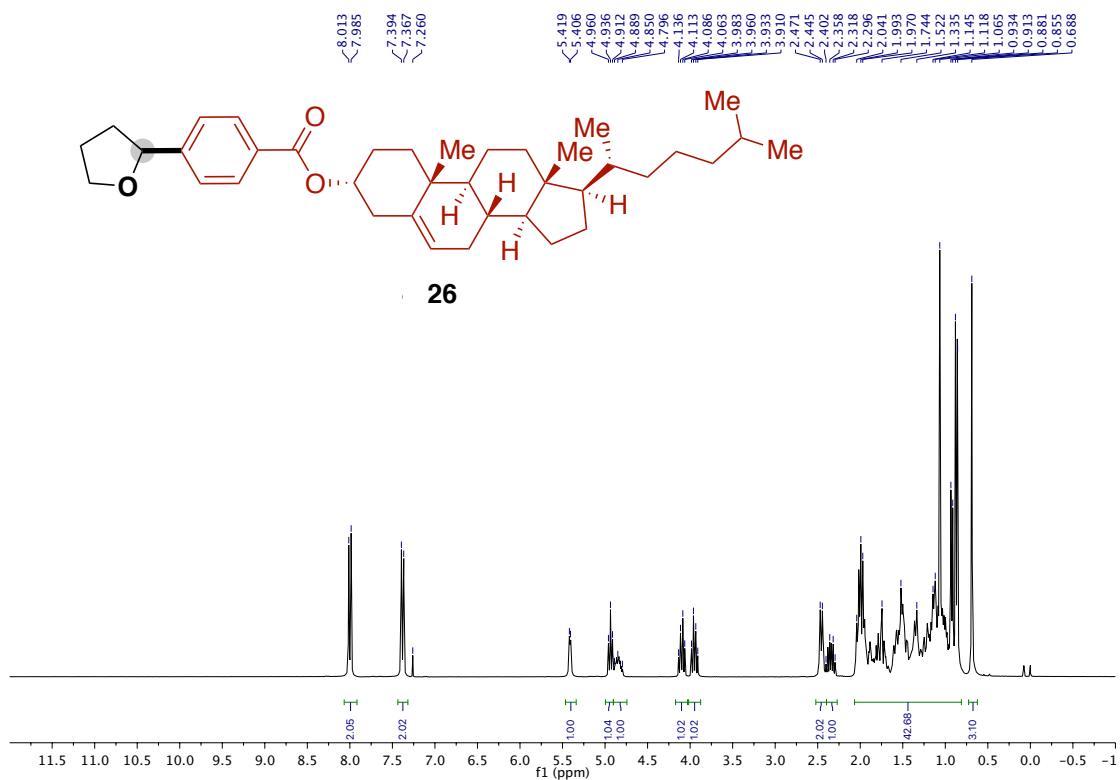




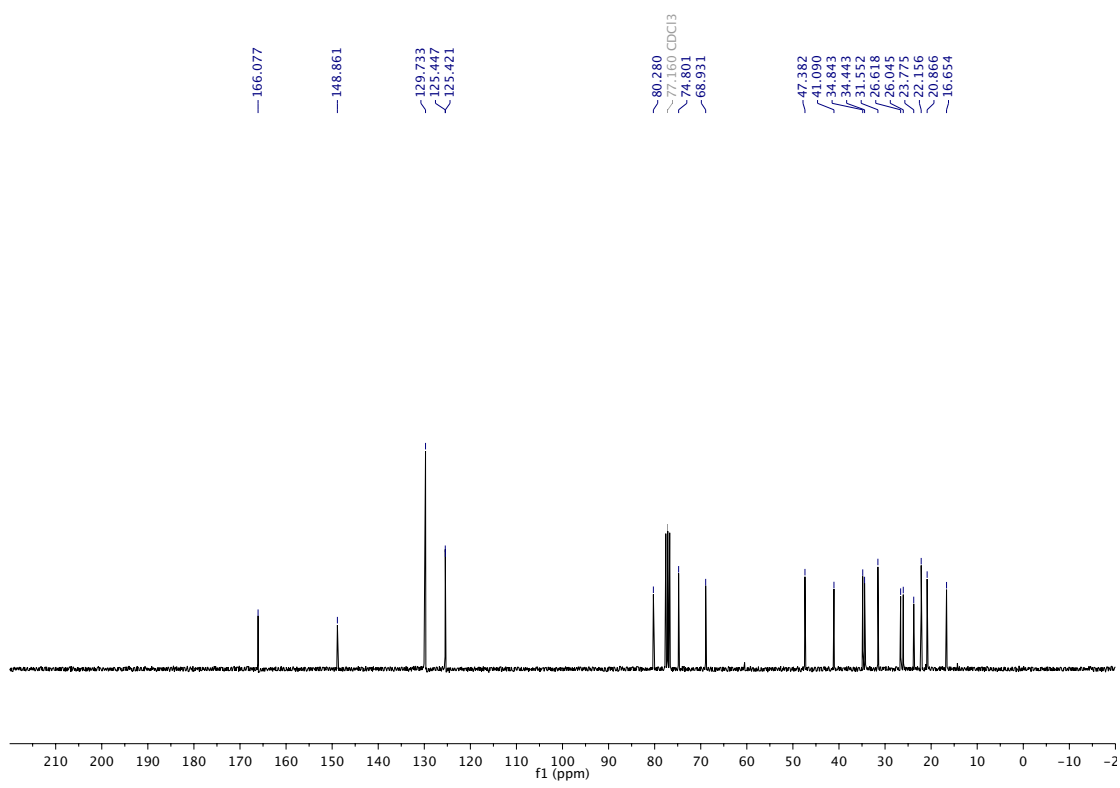
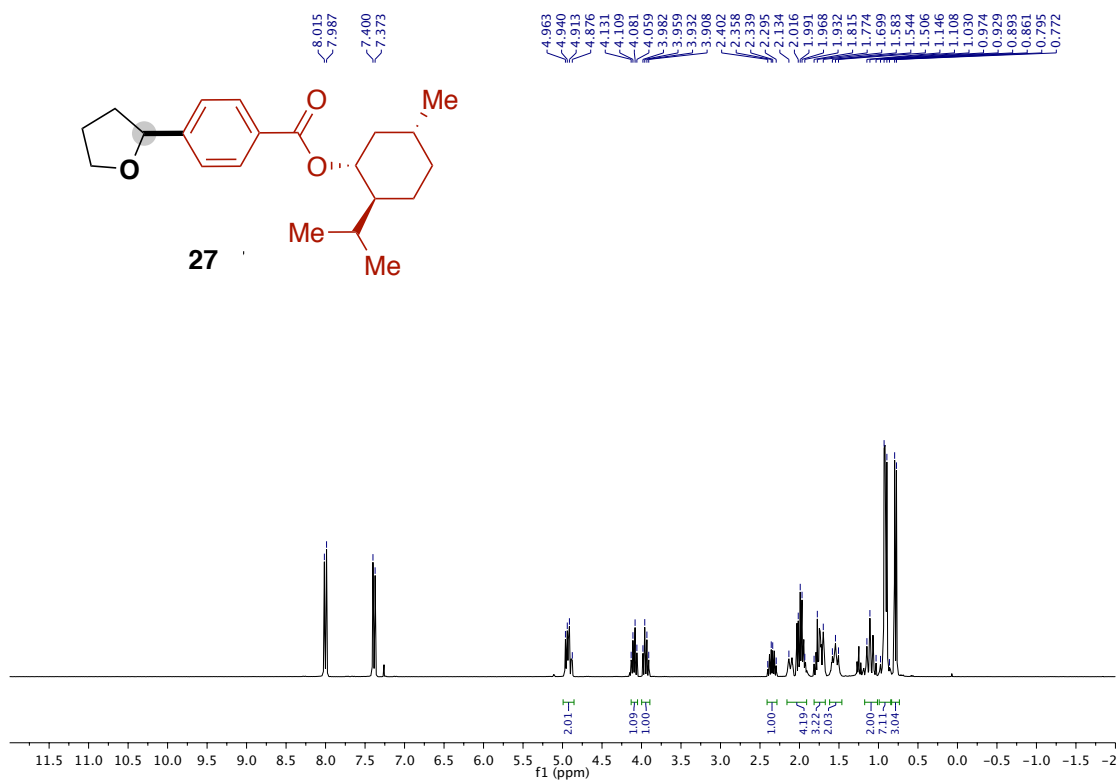


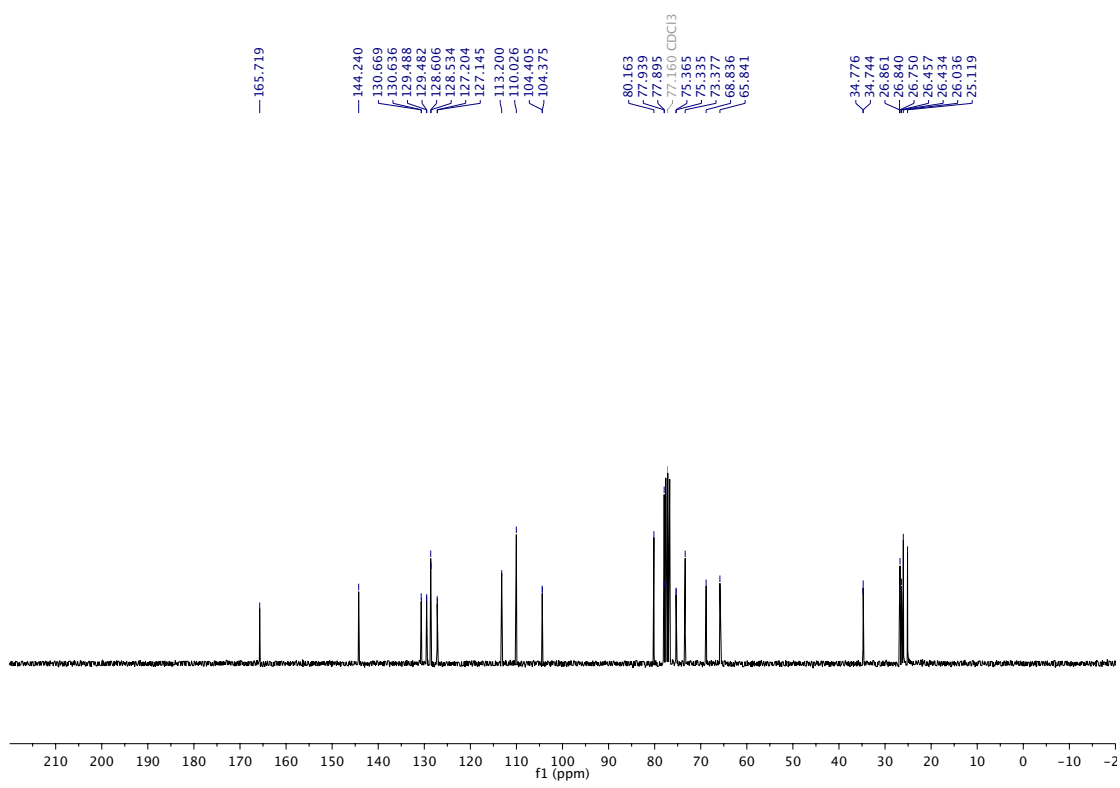
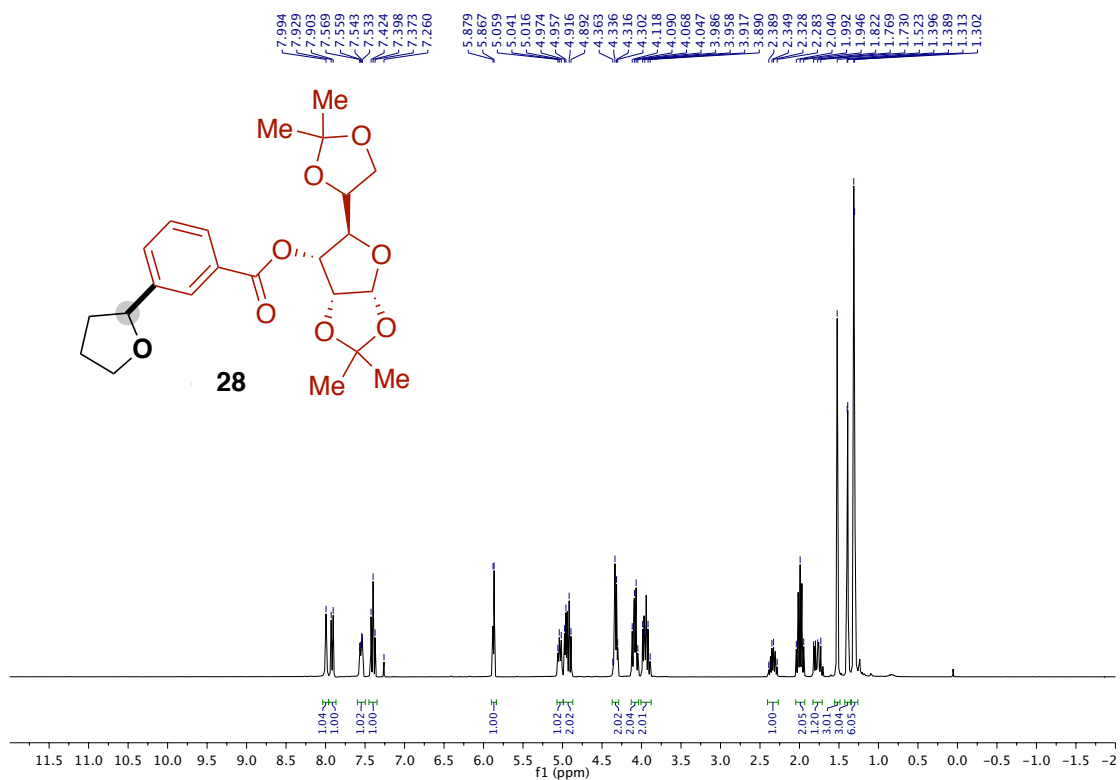


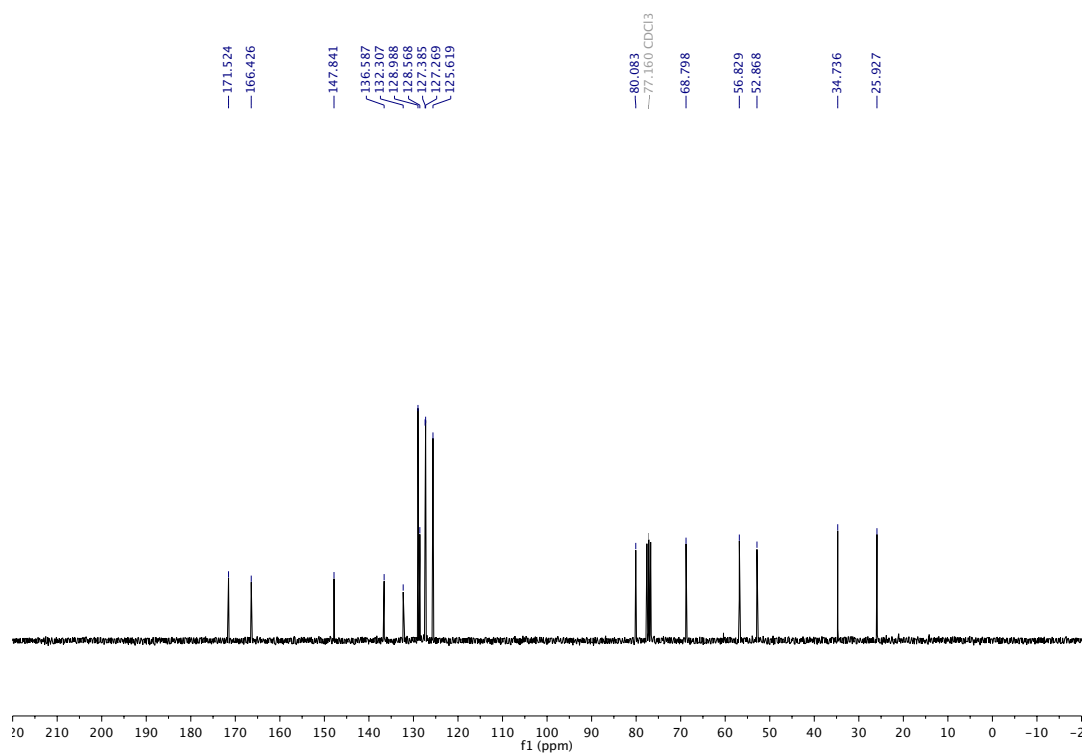
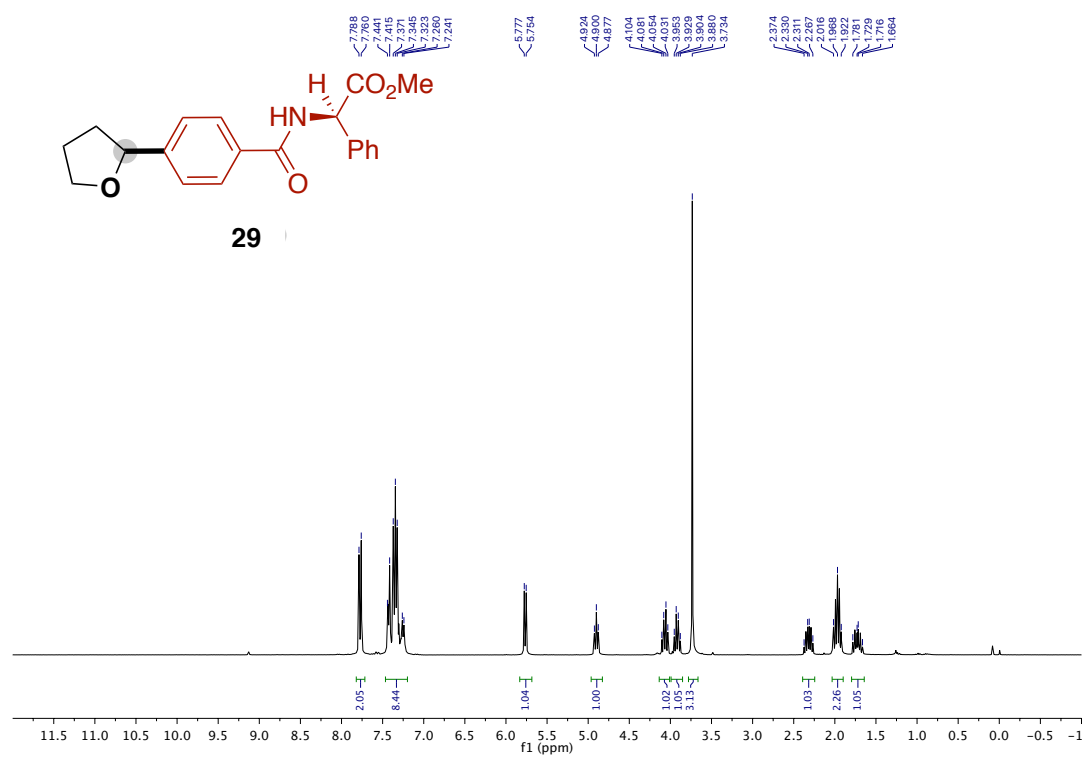


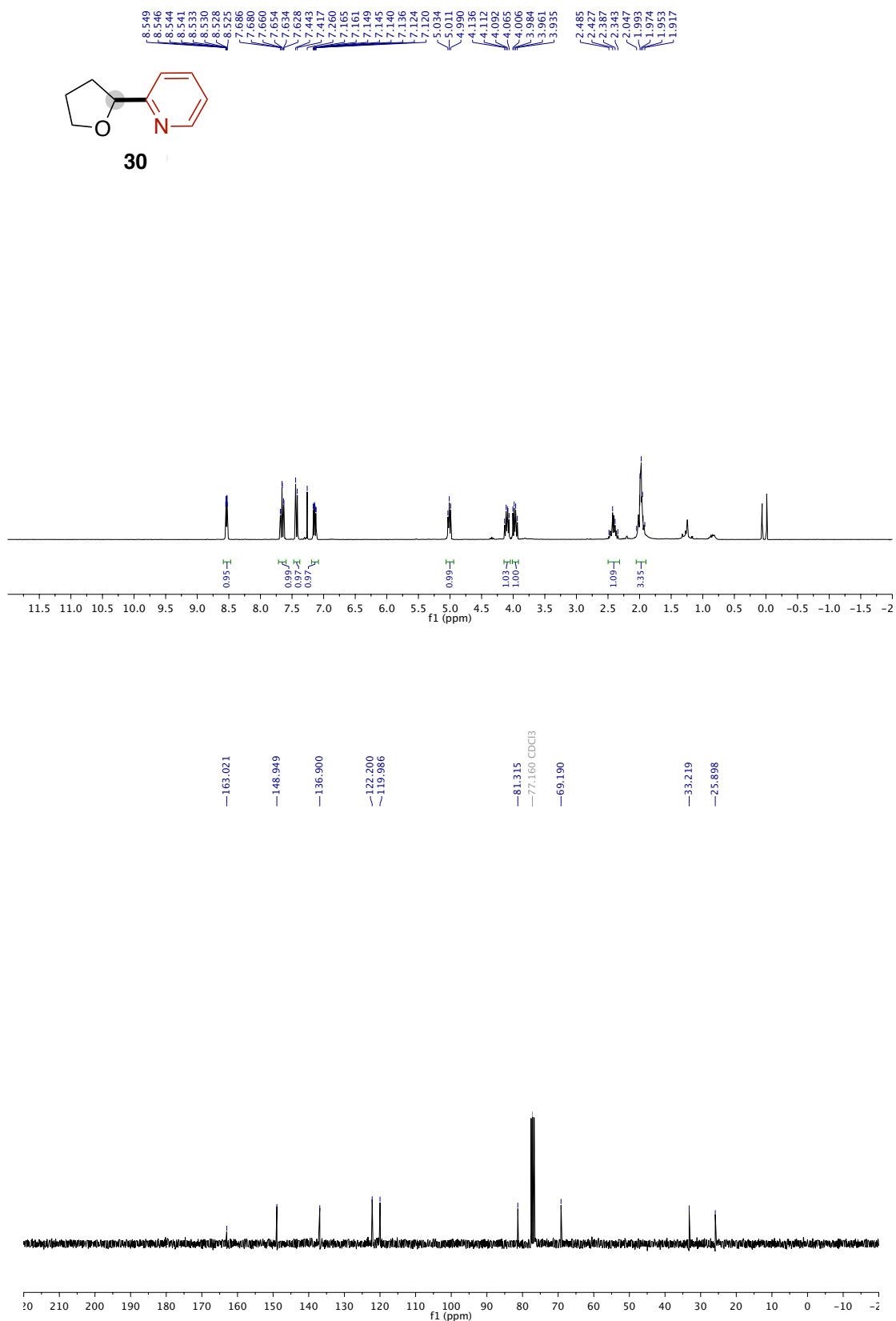


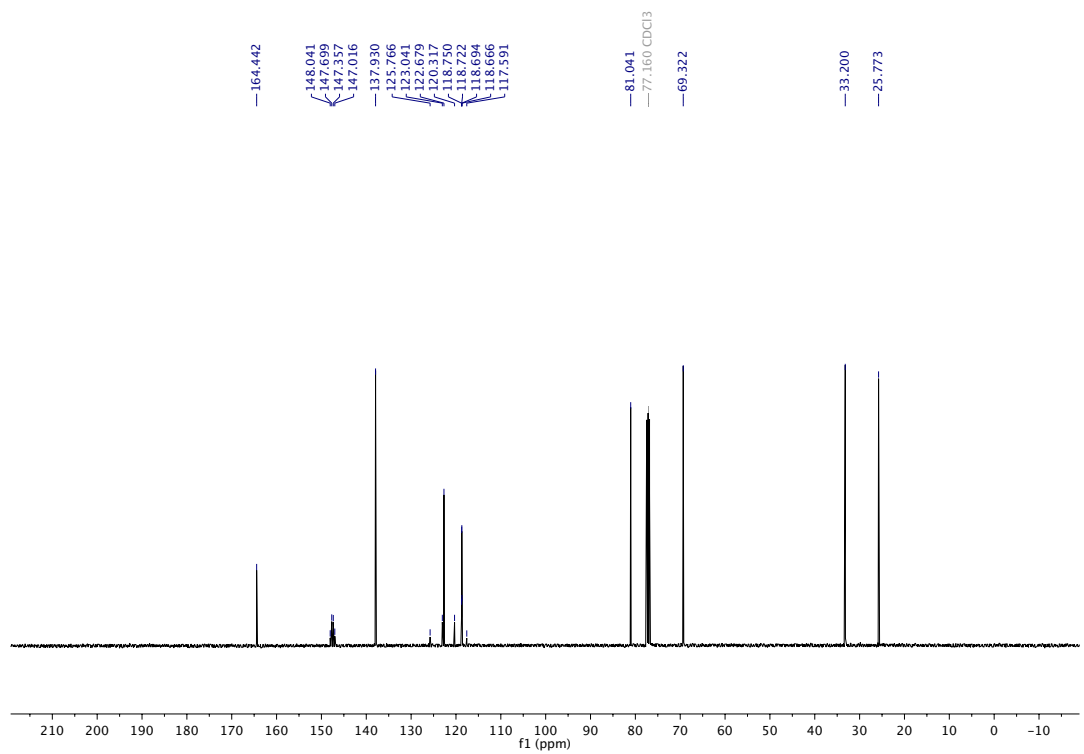
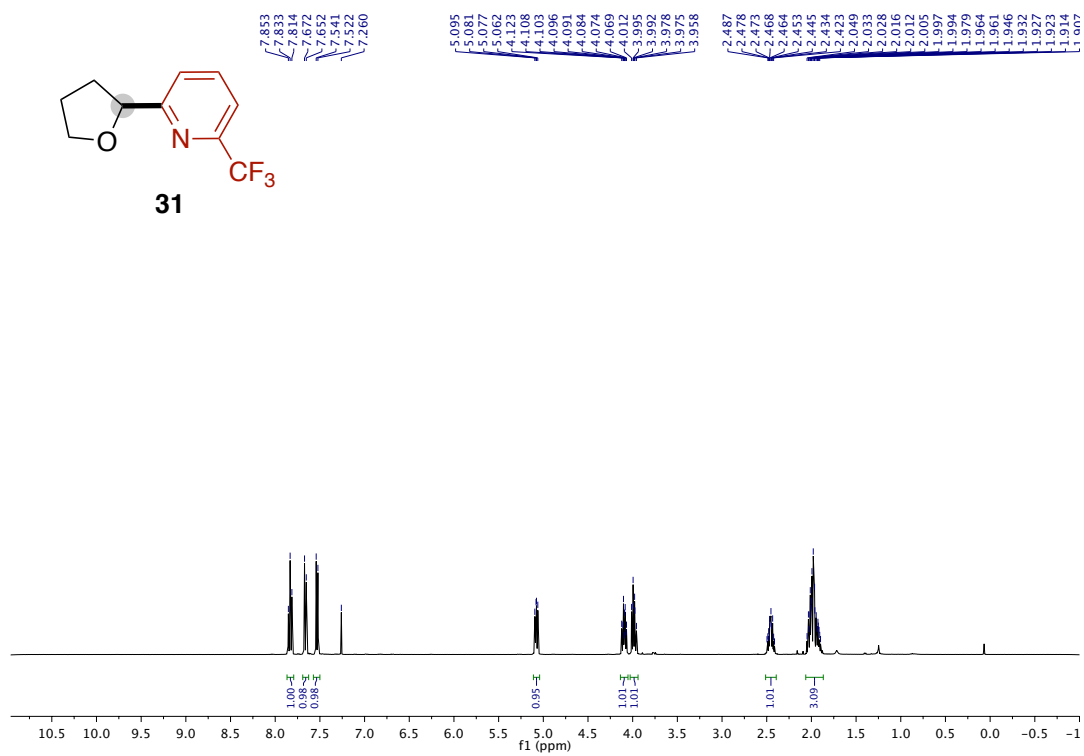


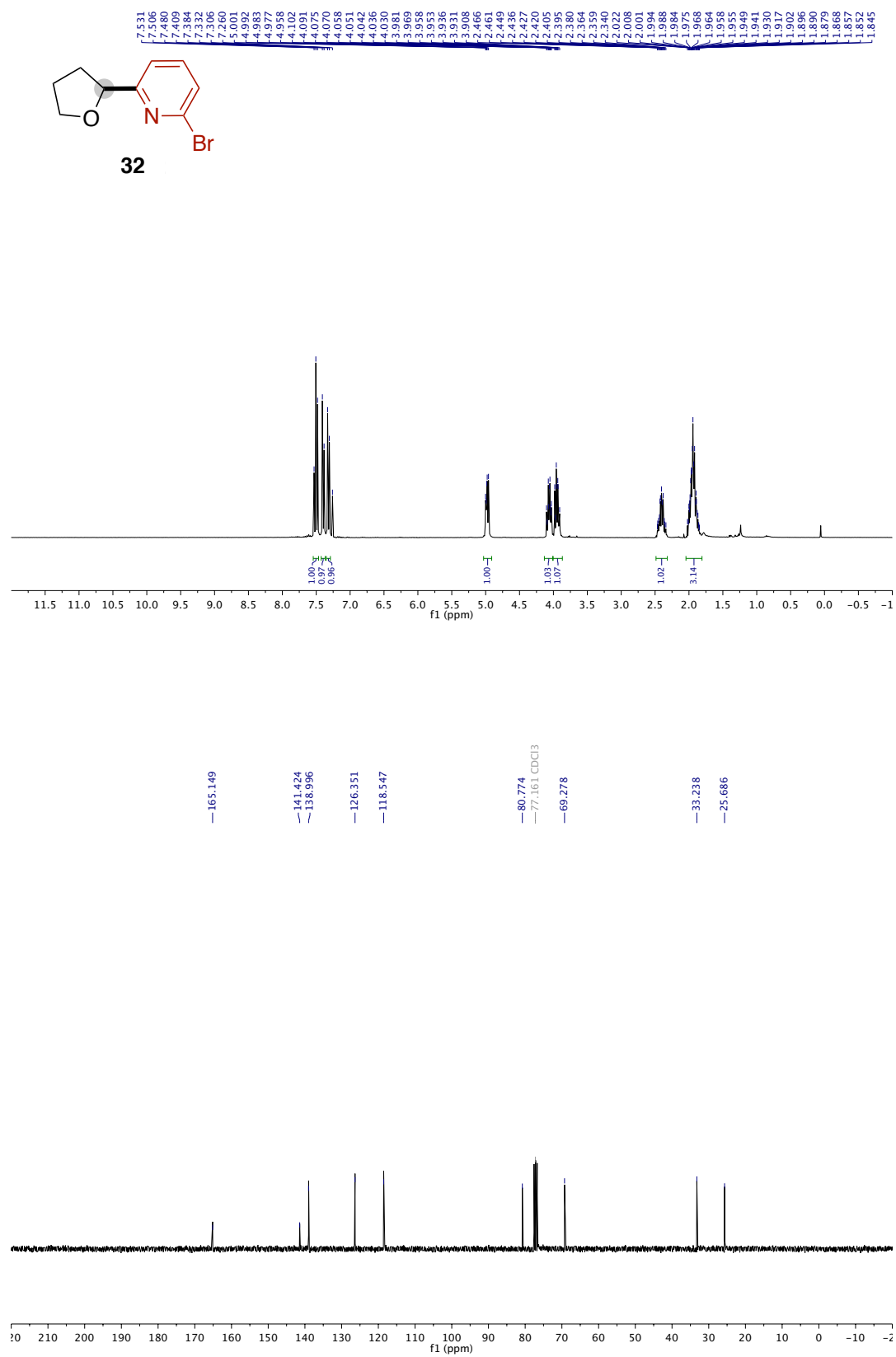


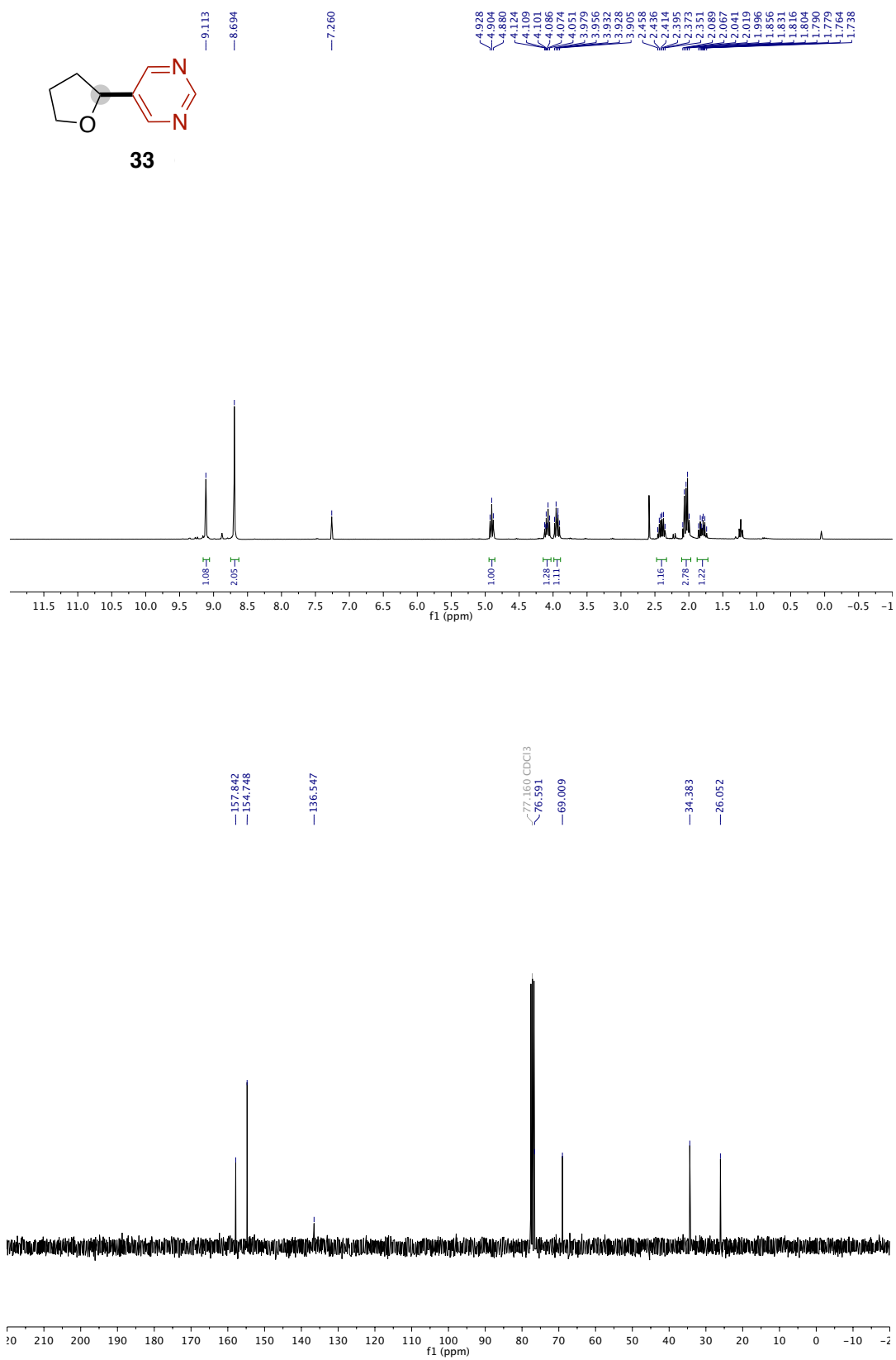


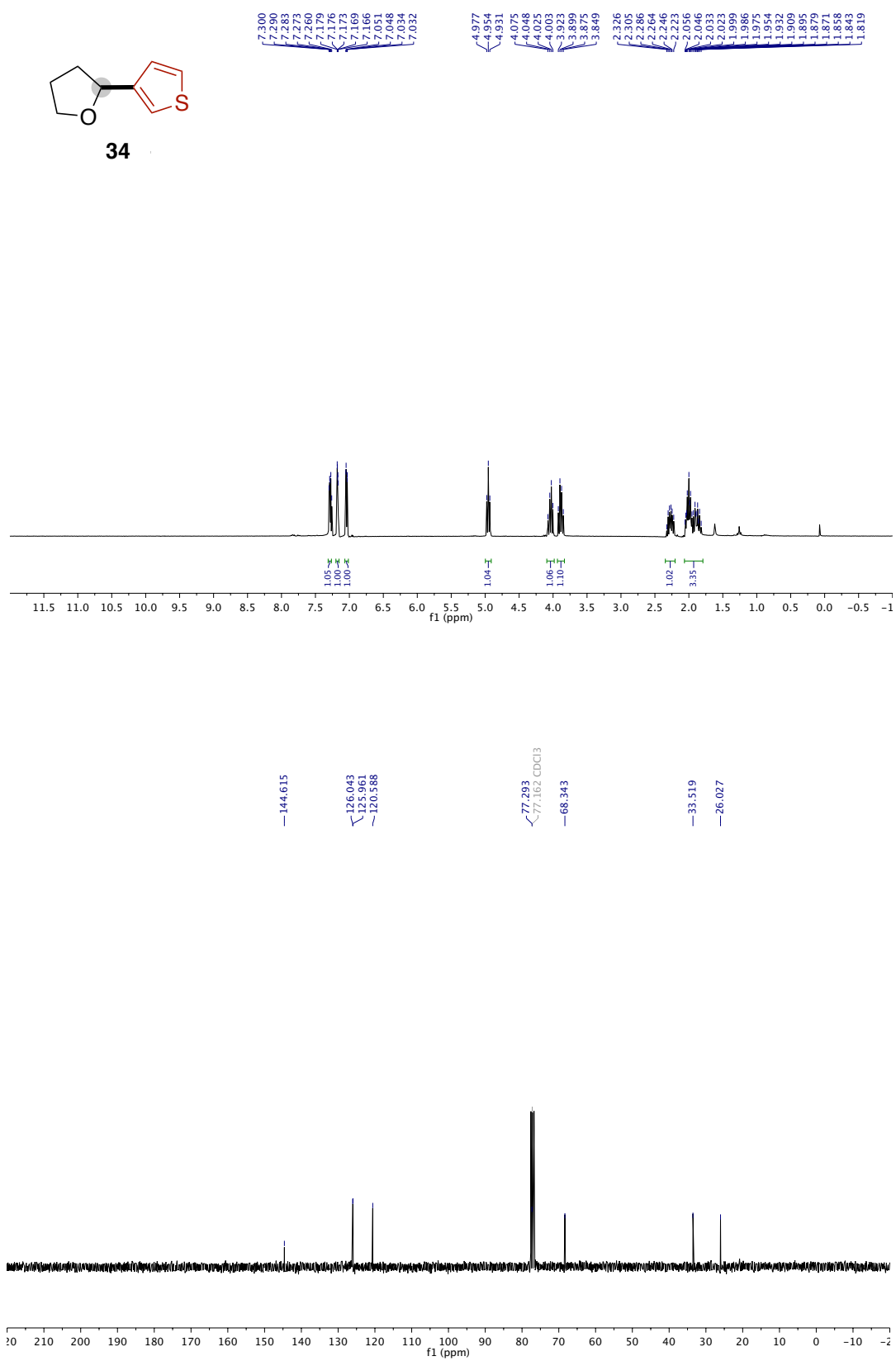




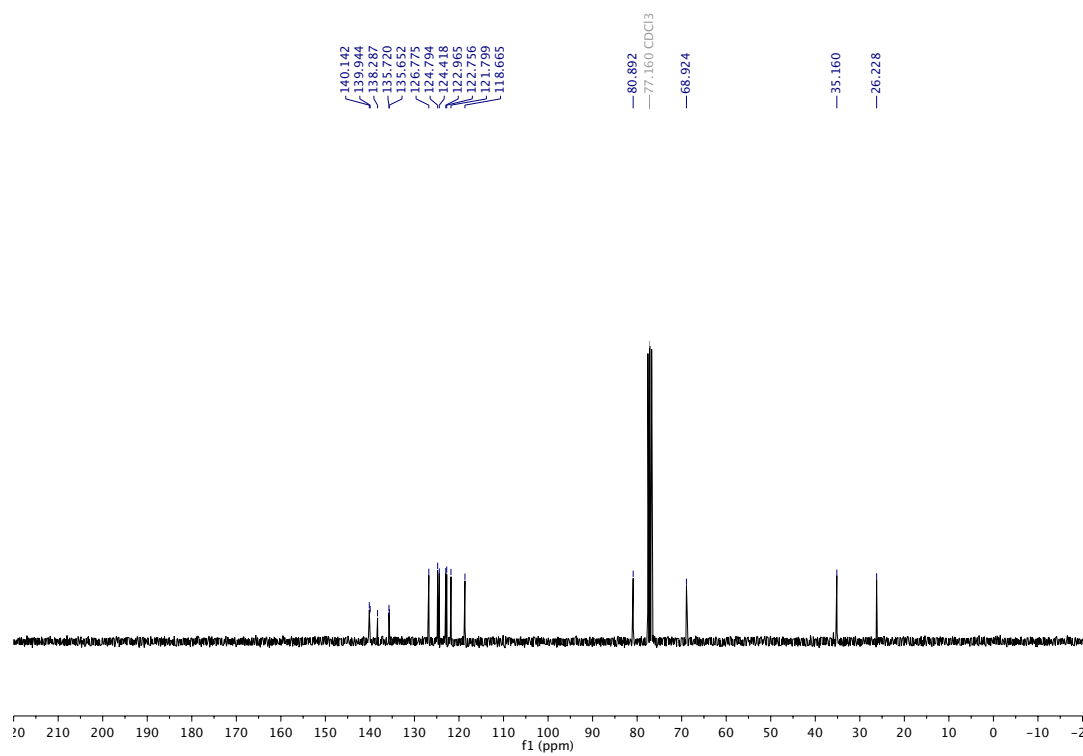
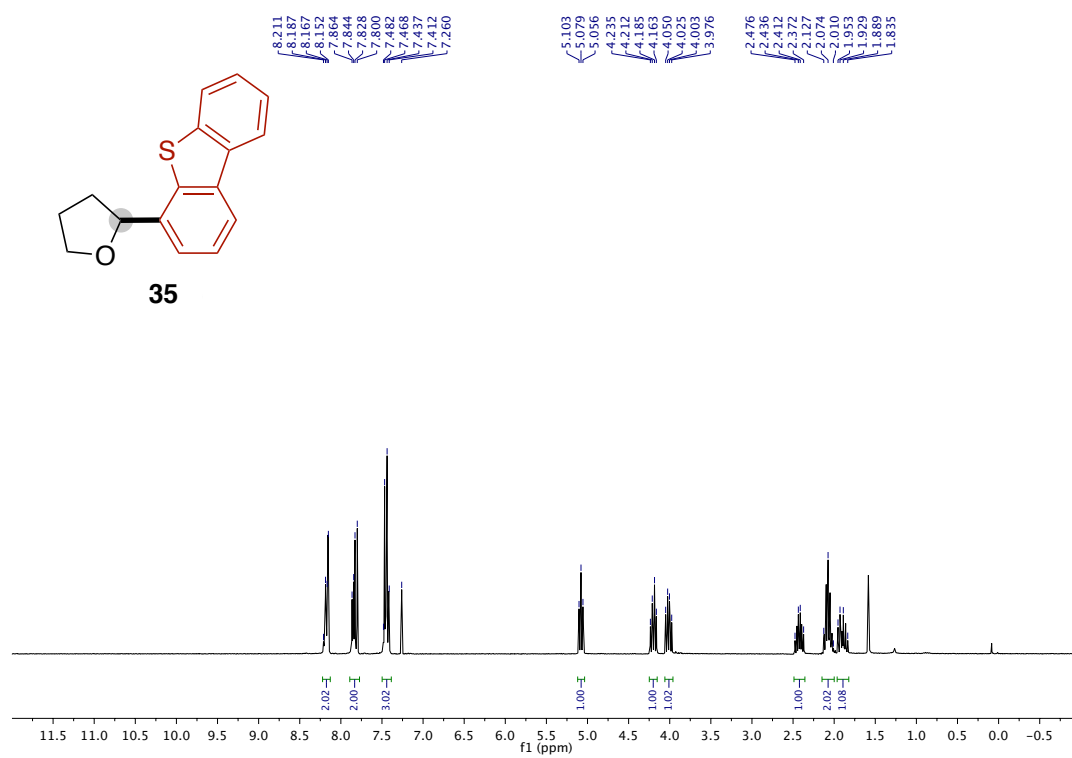


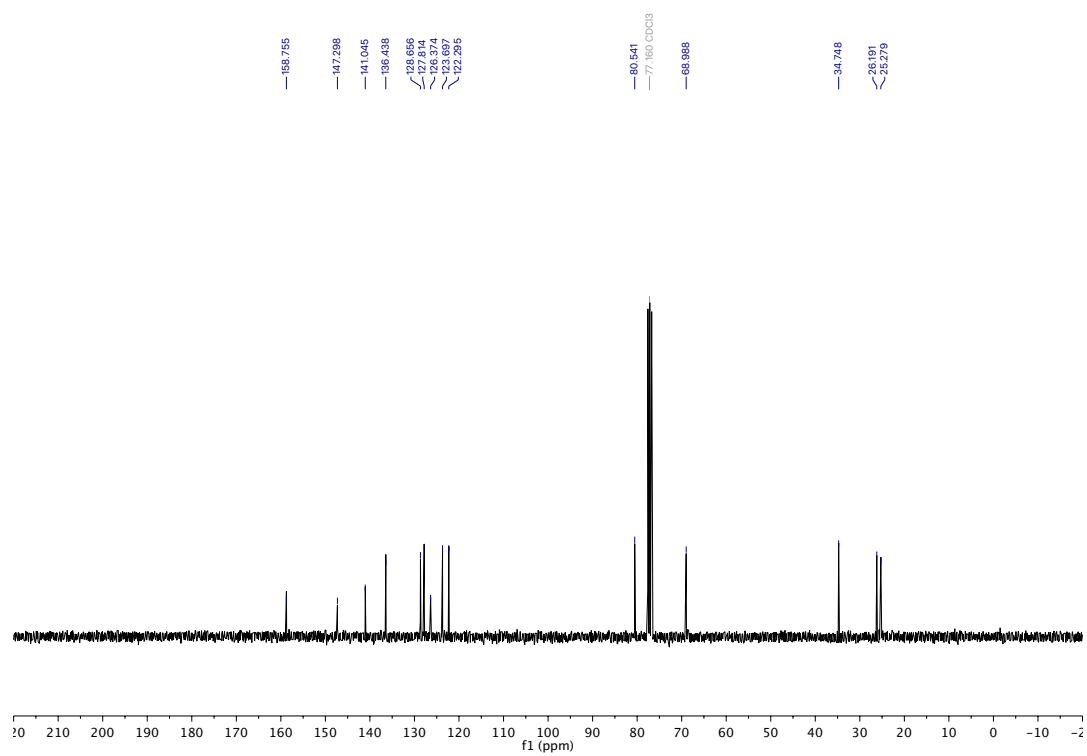
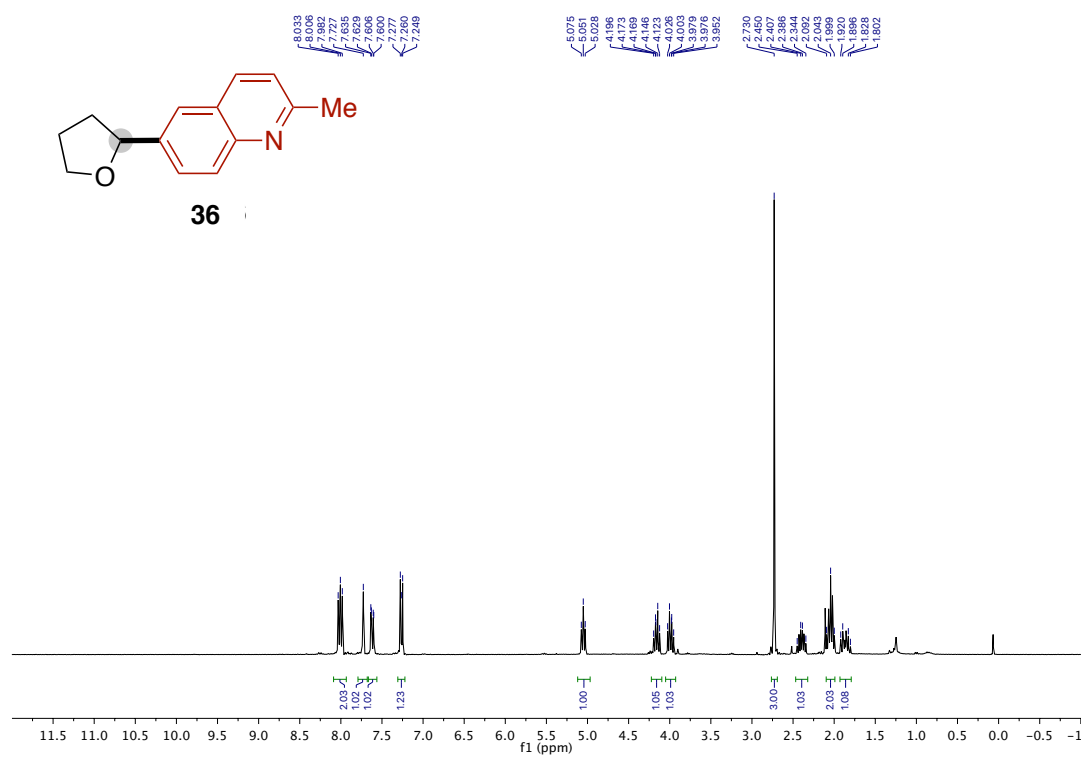


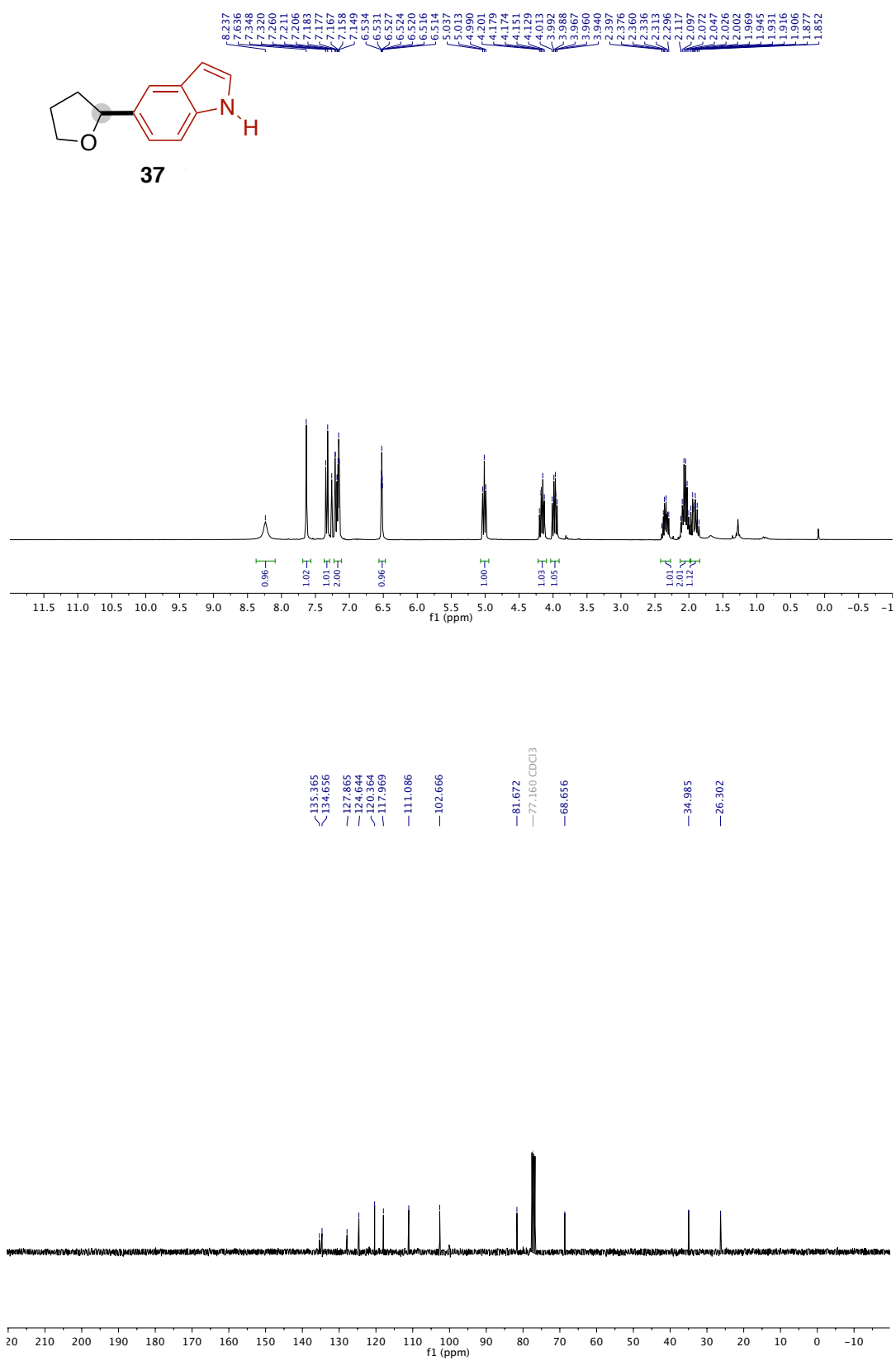


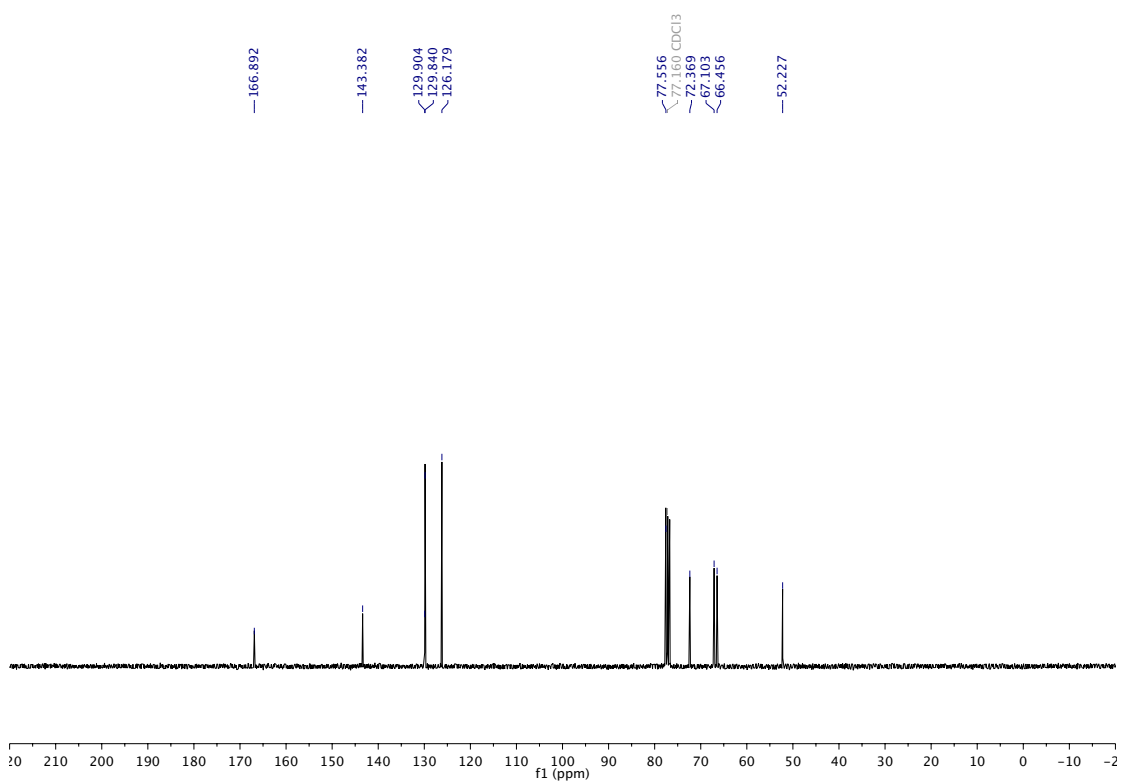
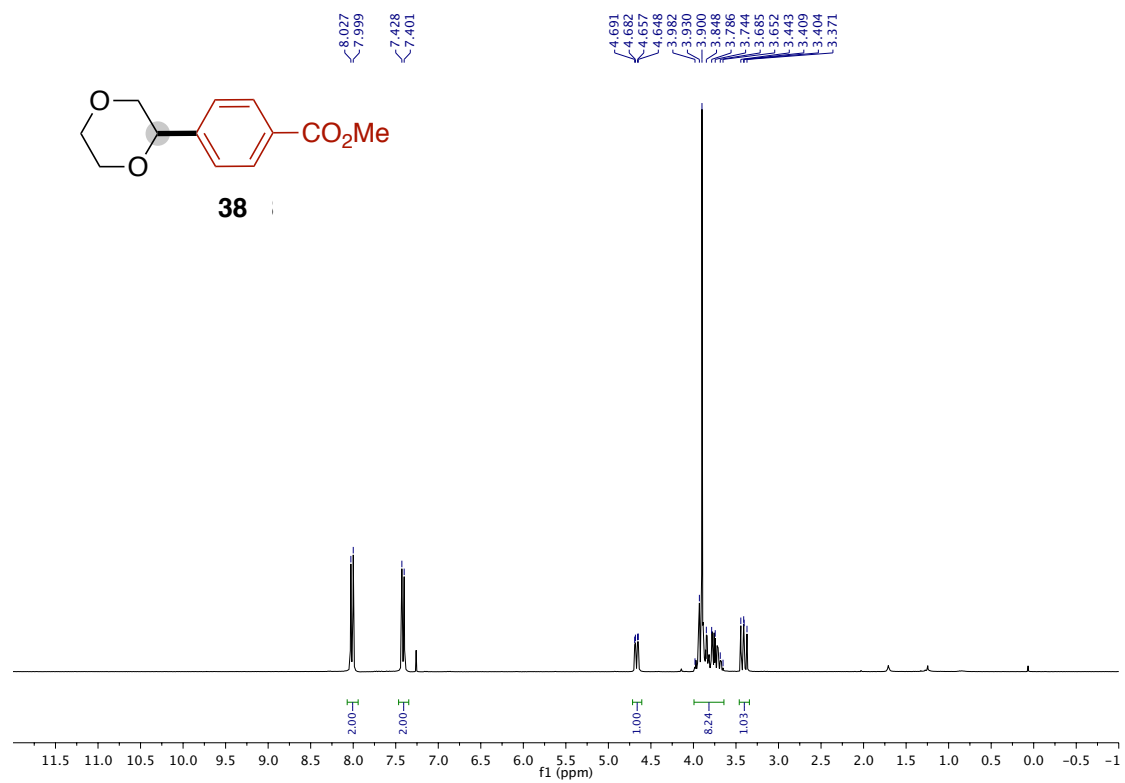


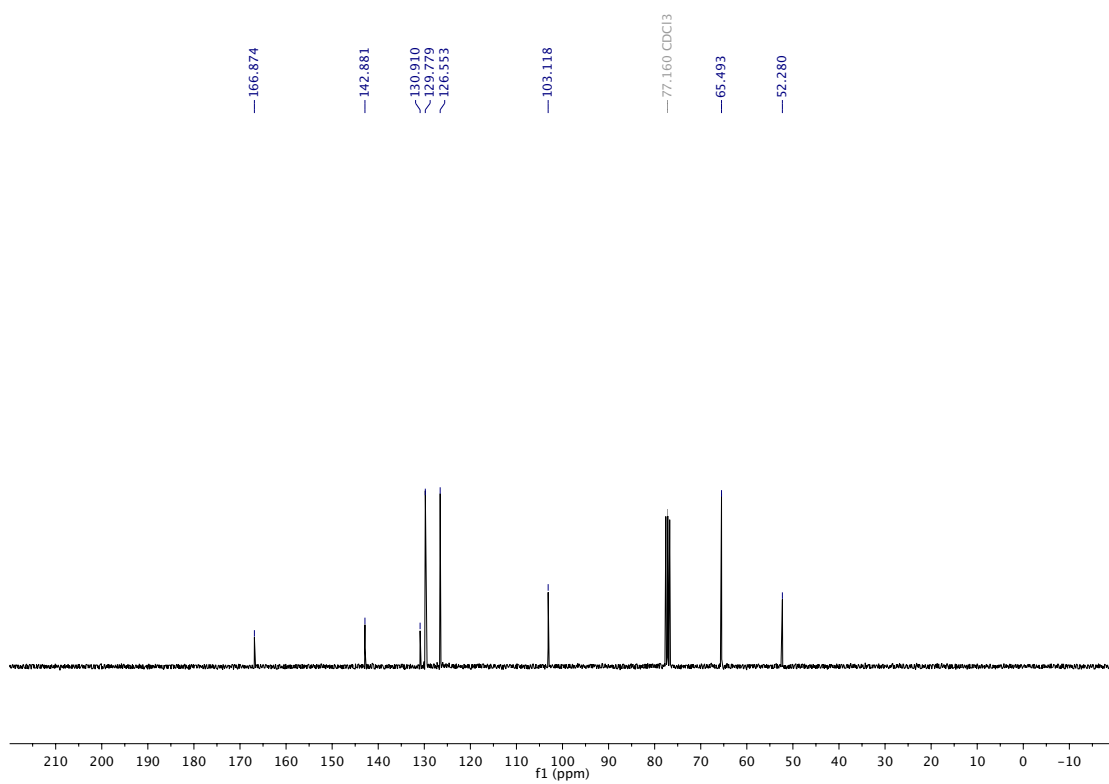
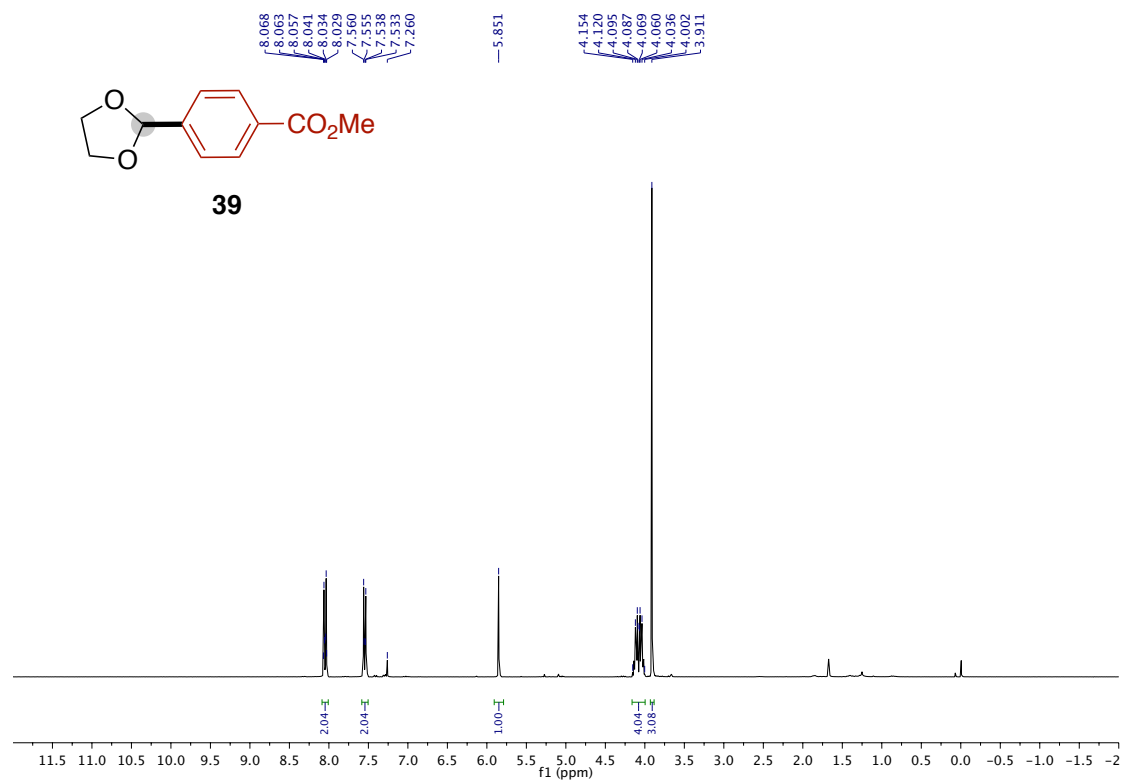


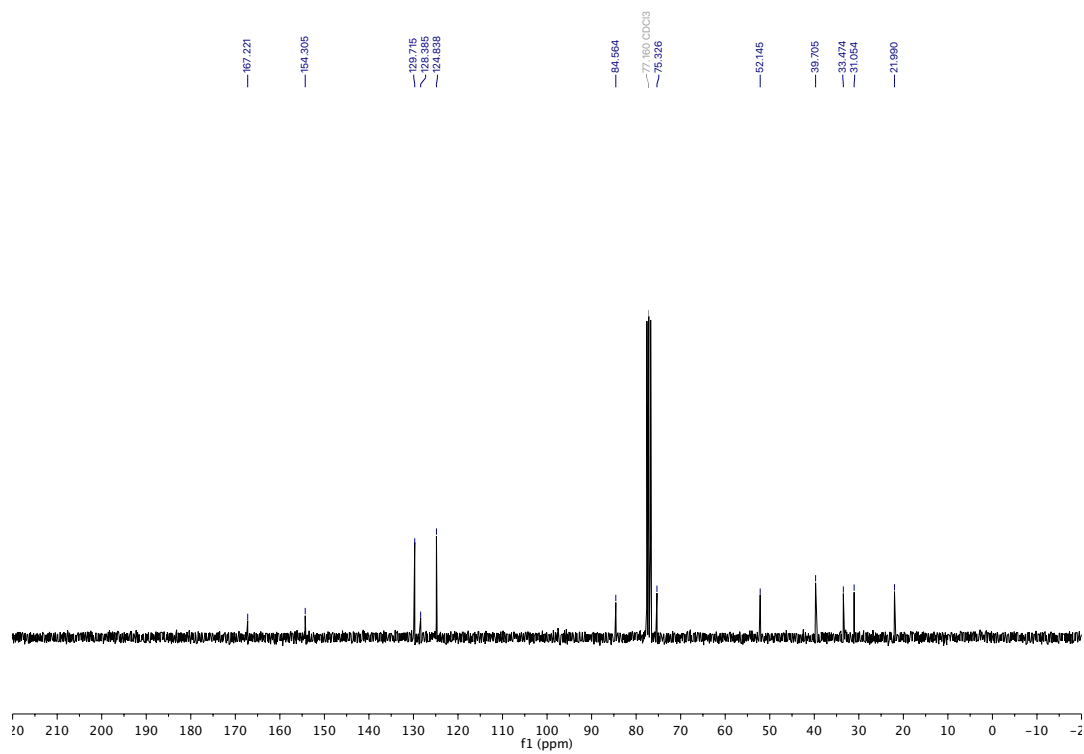
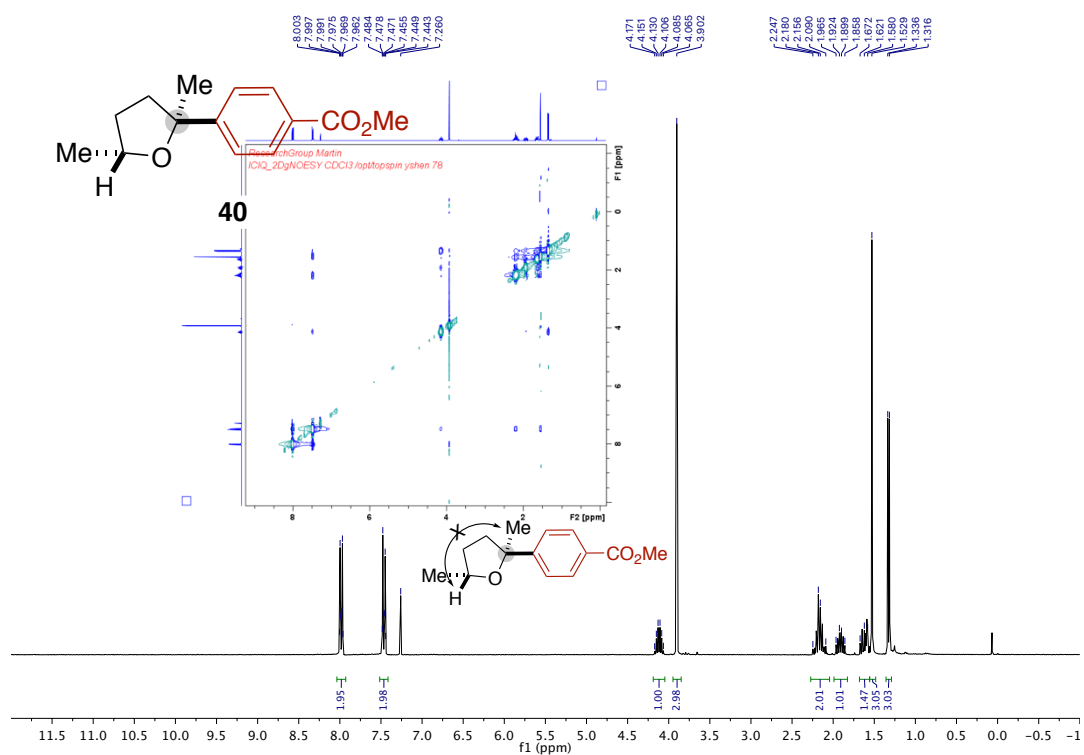


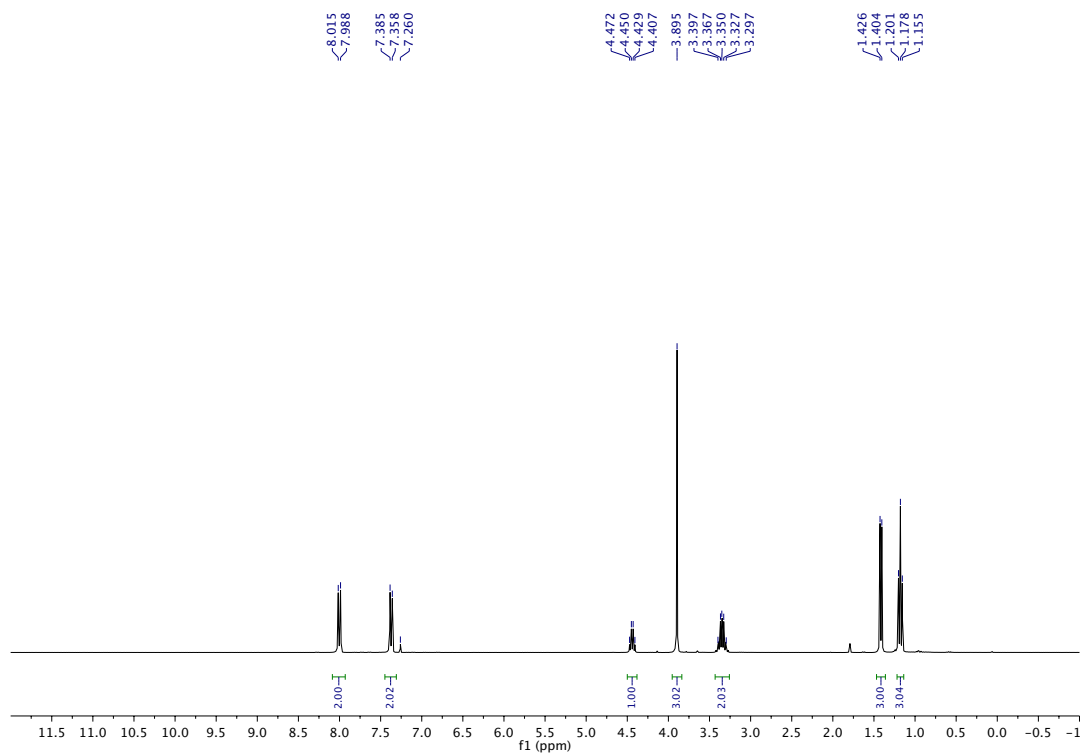
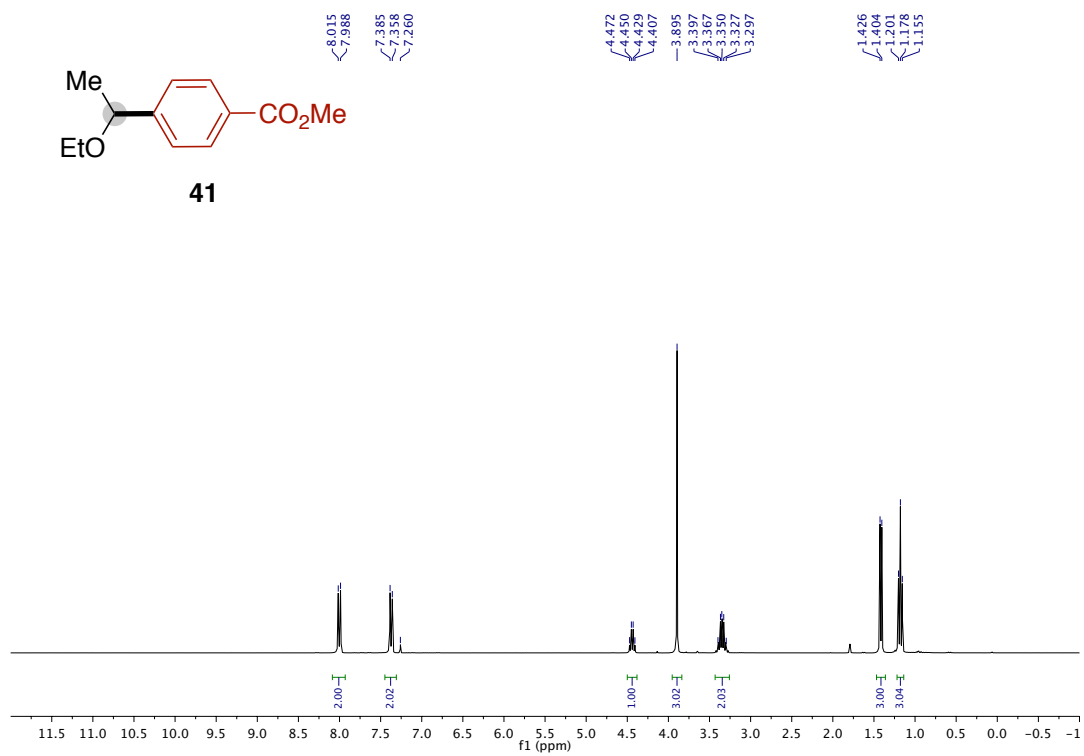
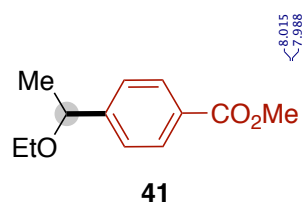


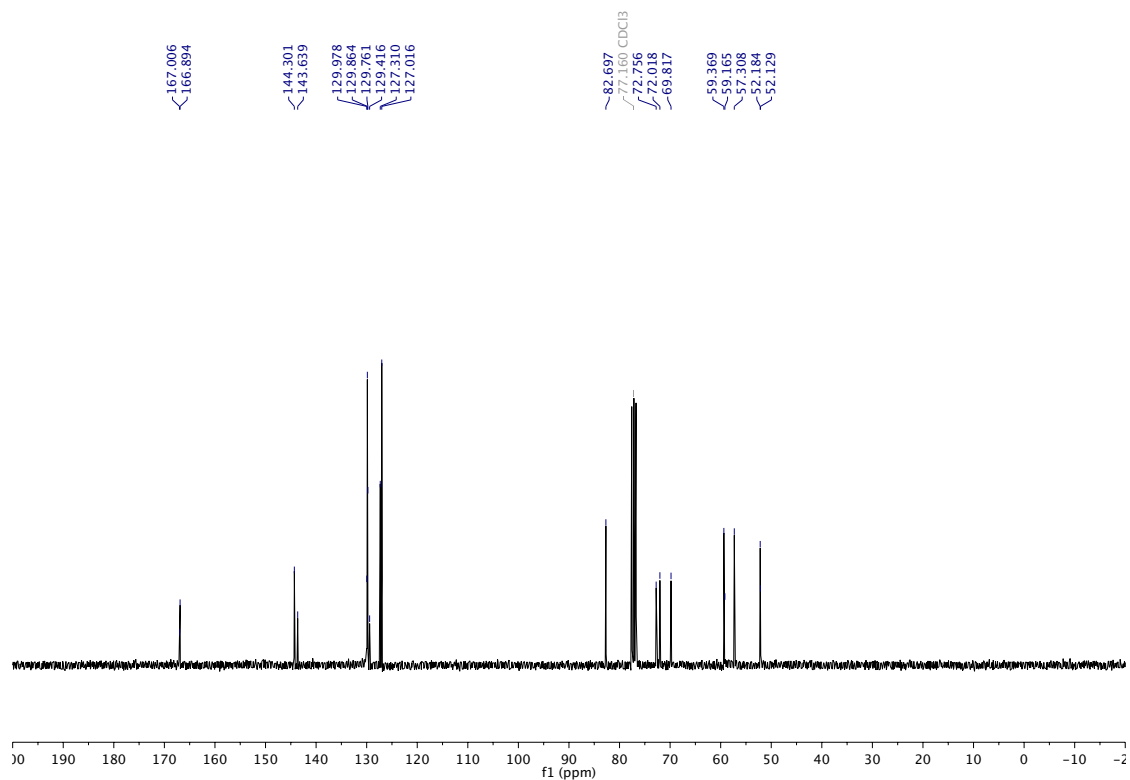
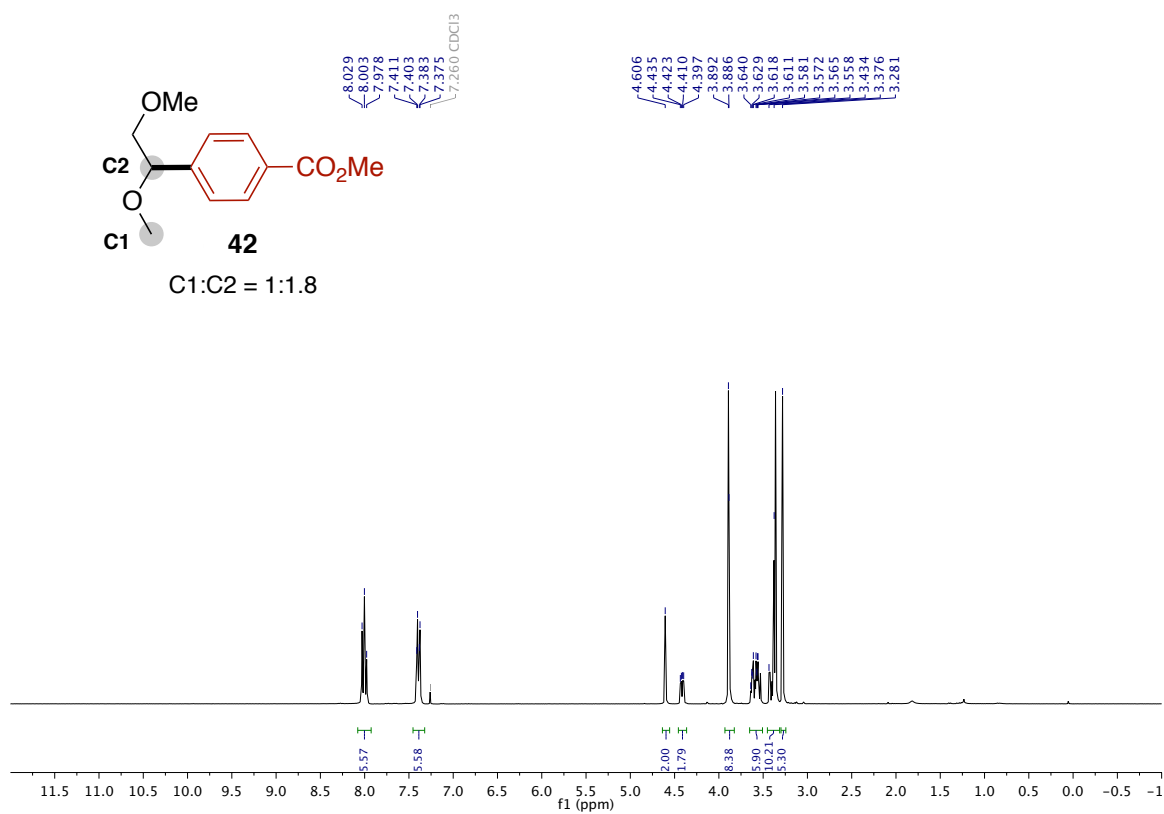




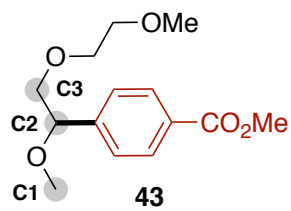




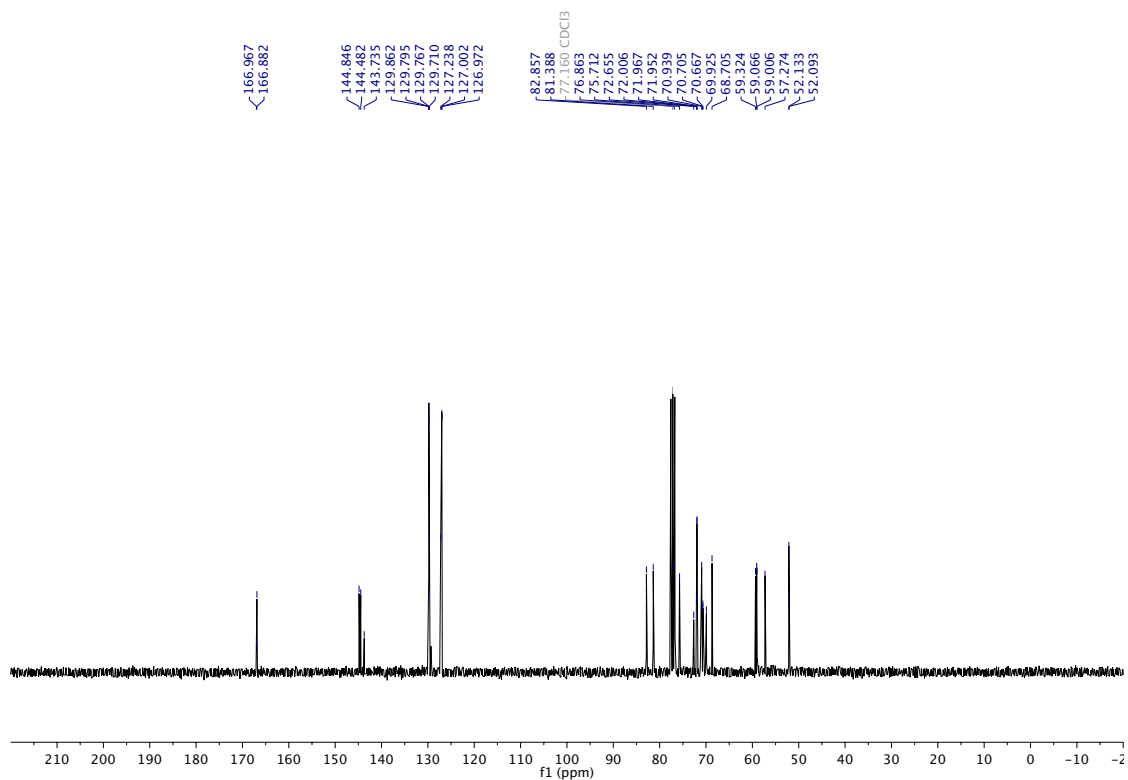
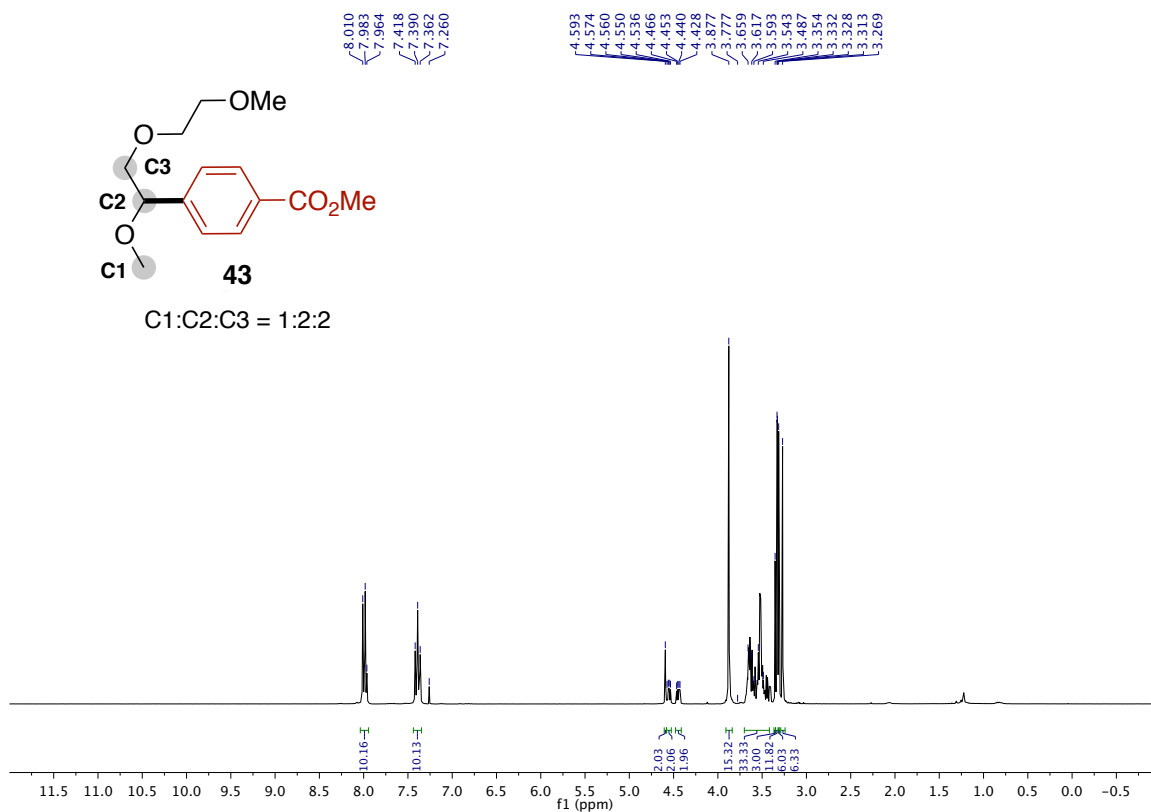


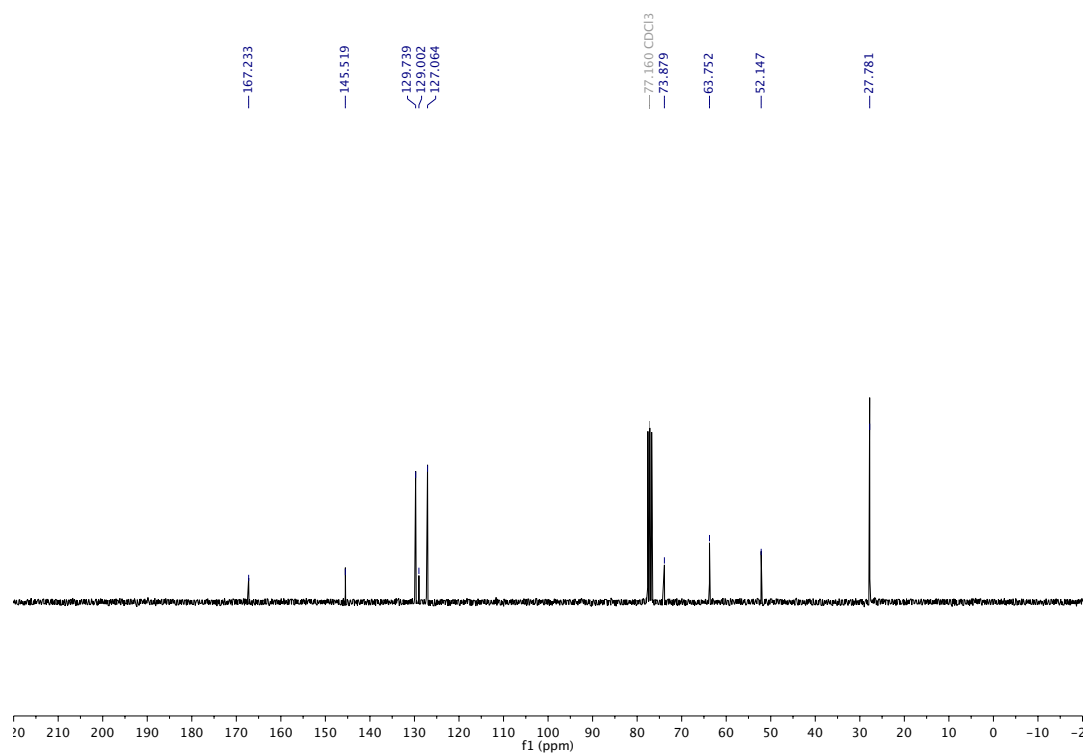
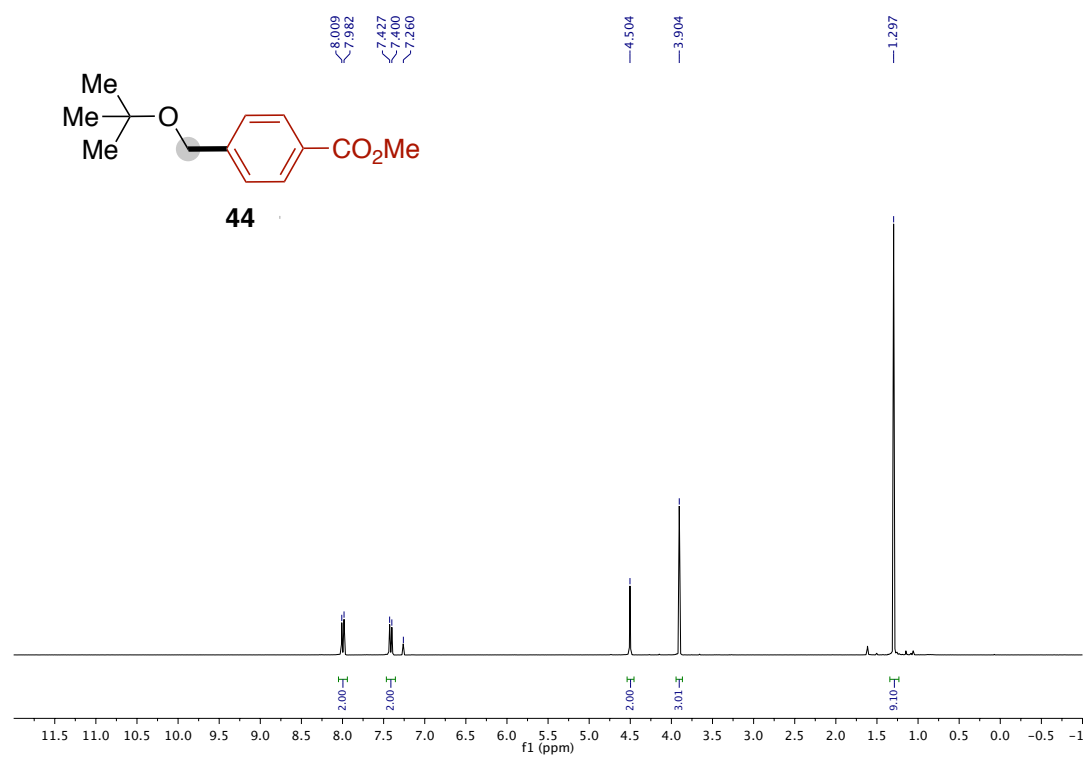


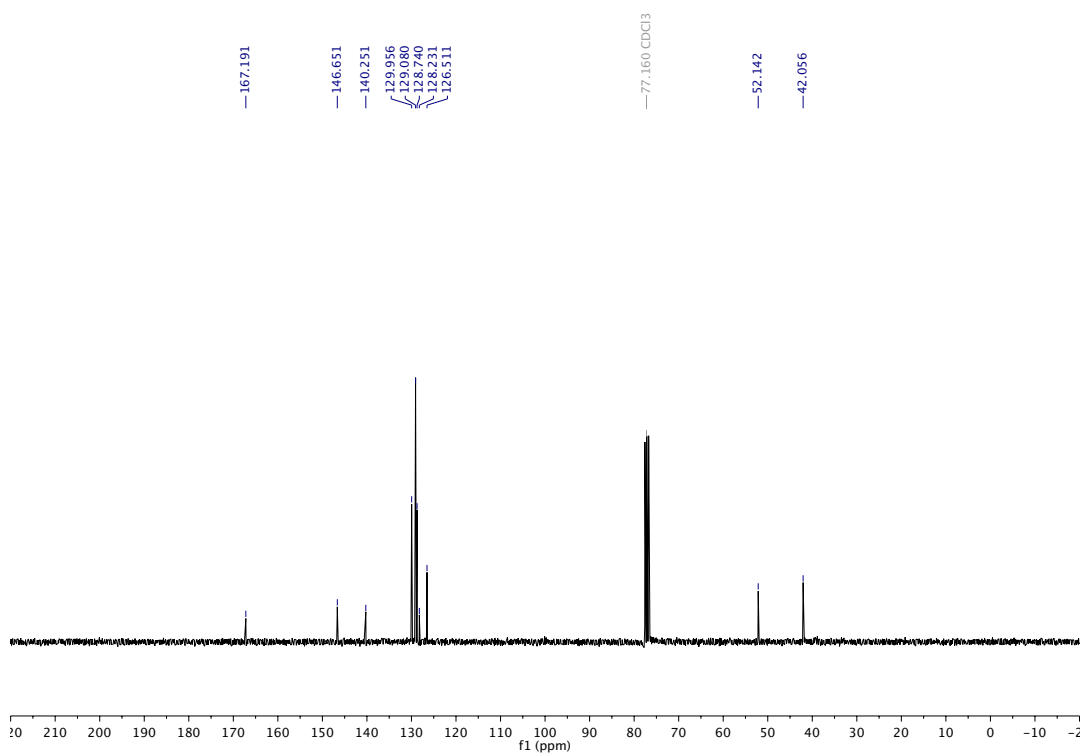
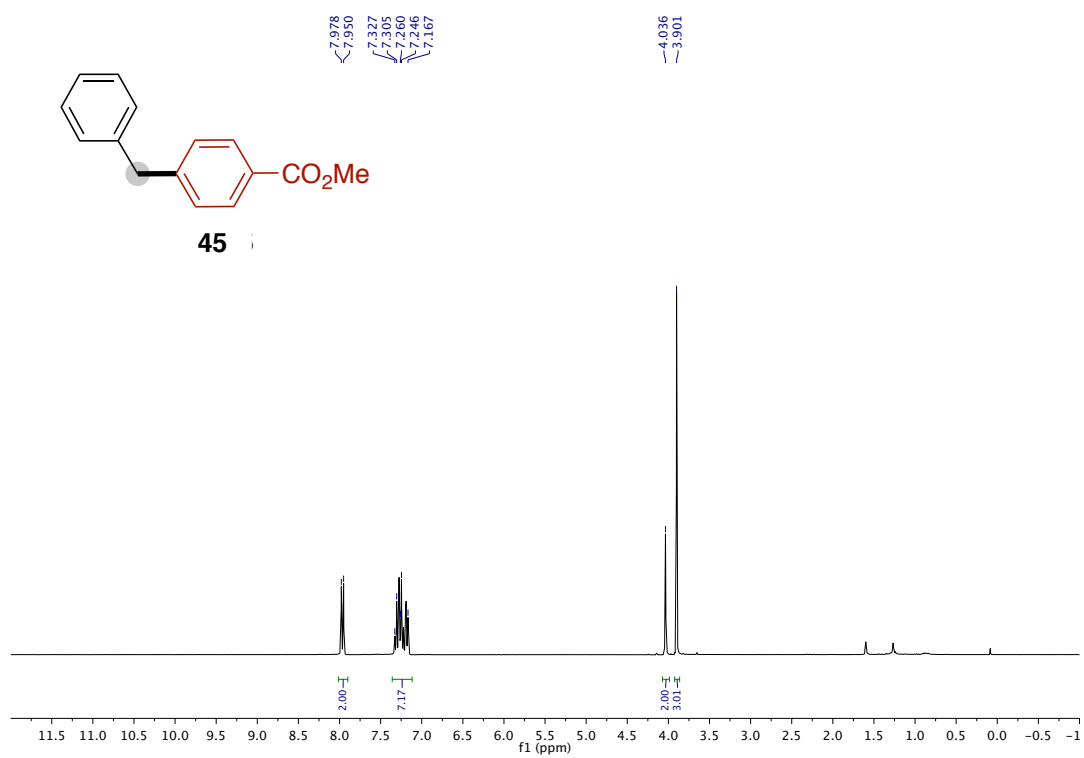


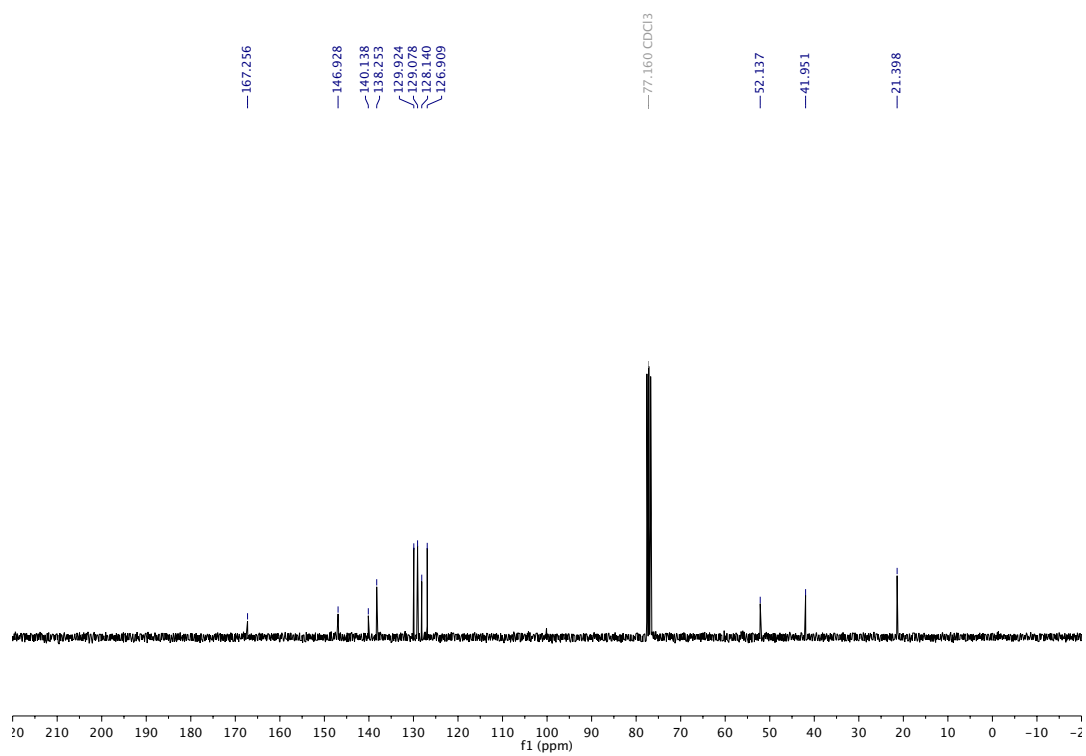
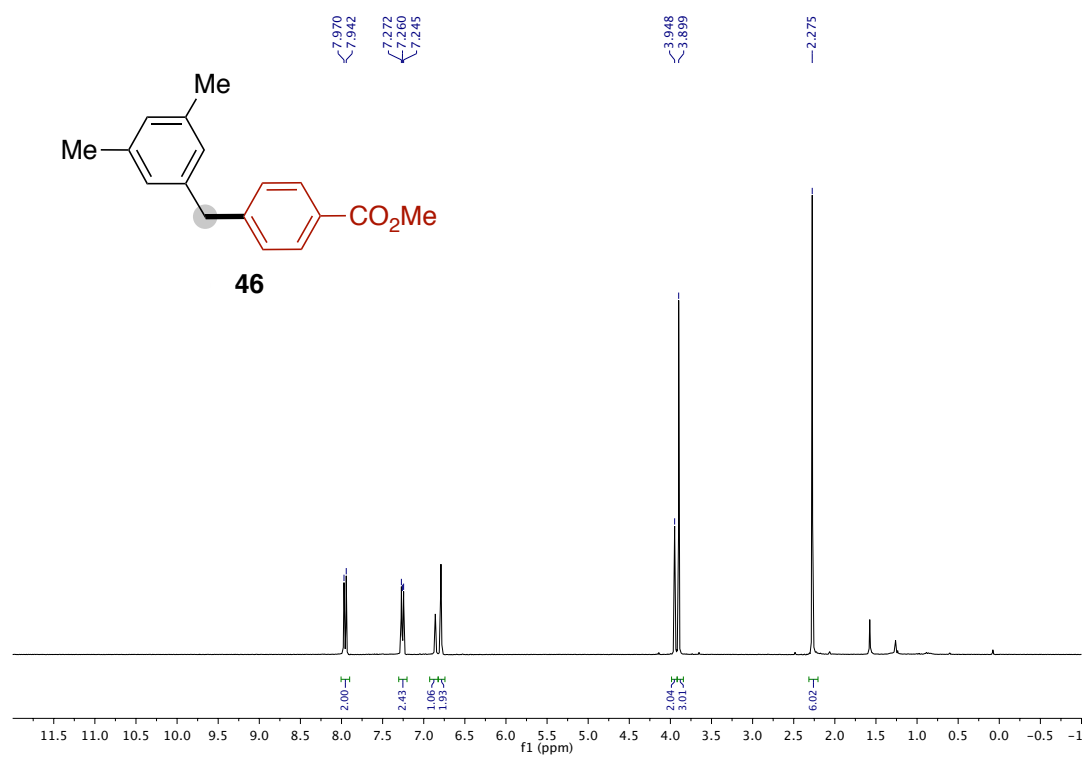


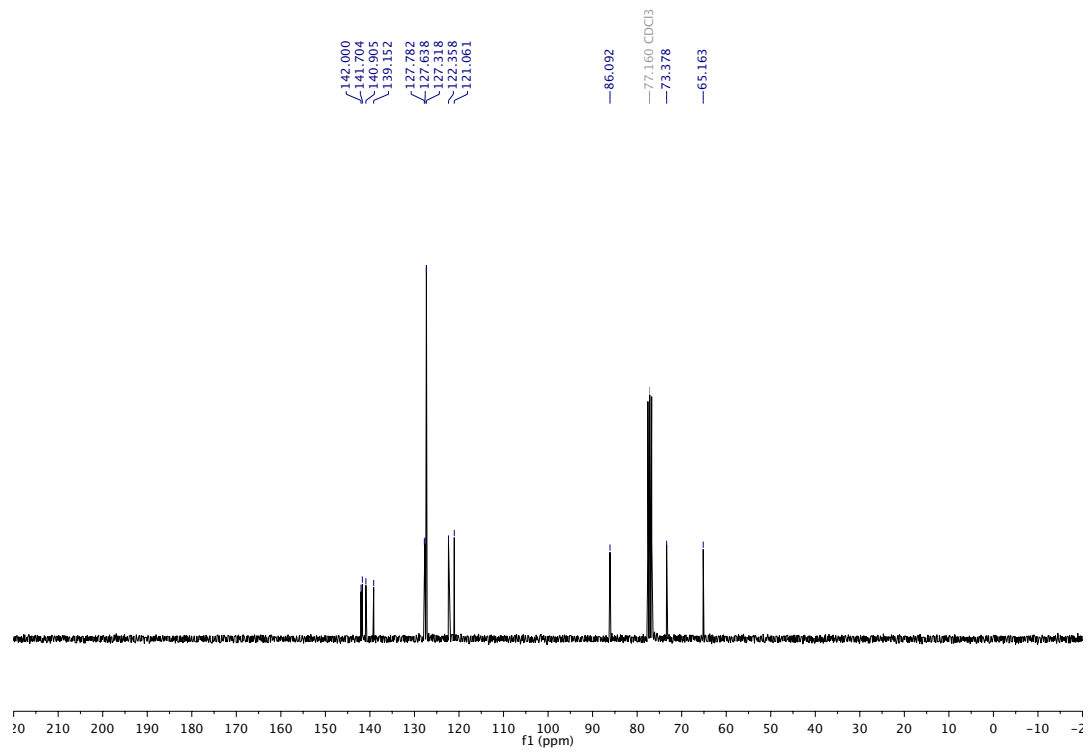
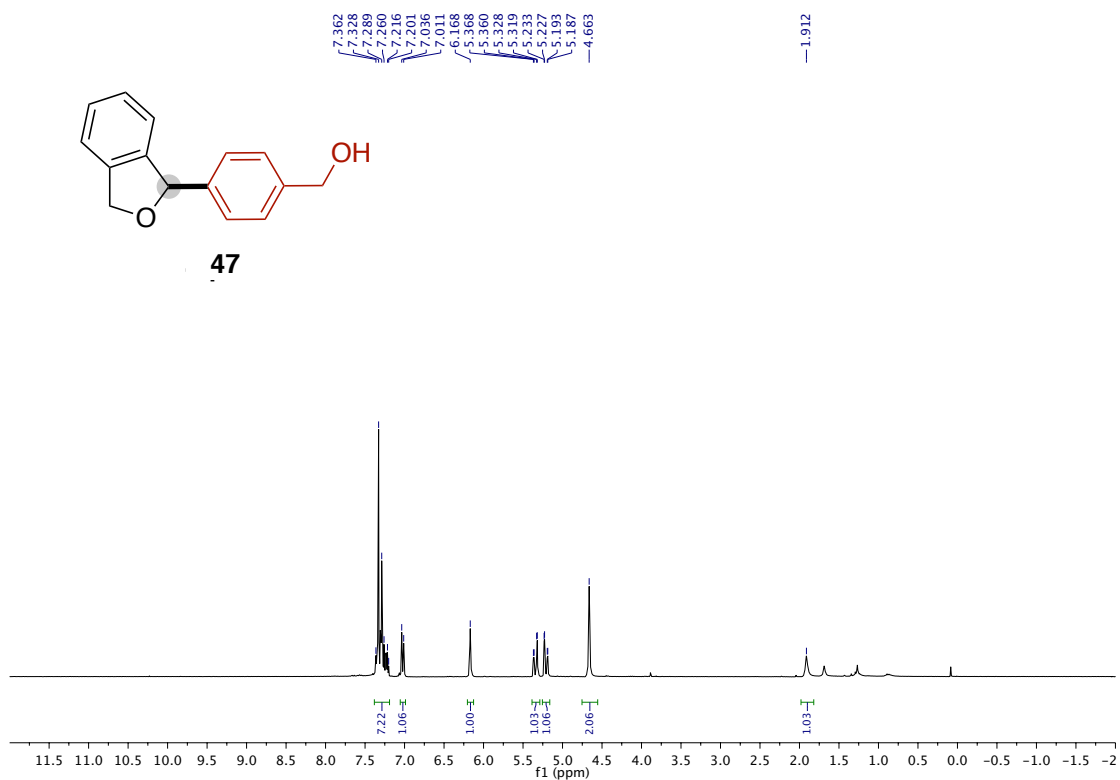
C1:C2:C3 = 1:2:2

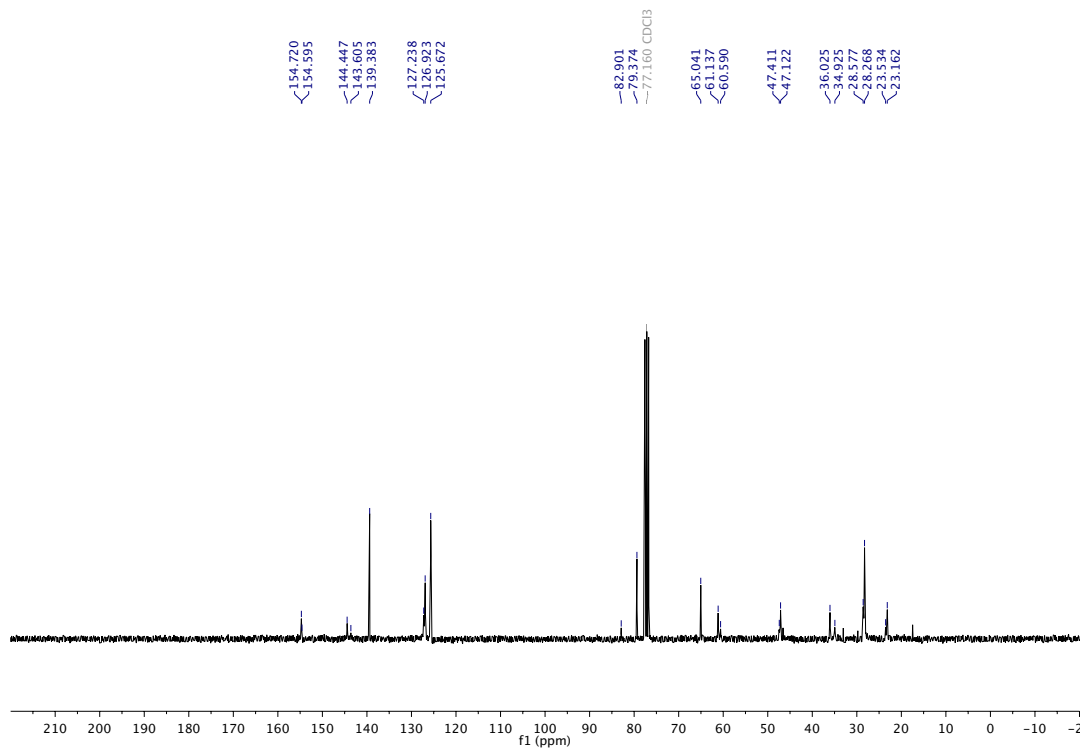
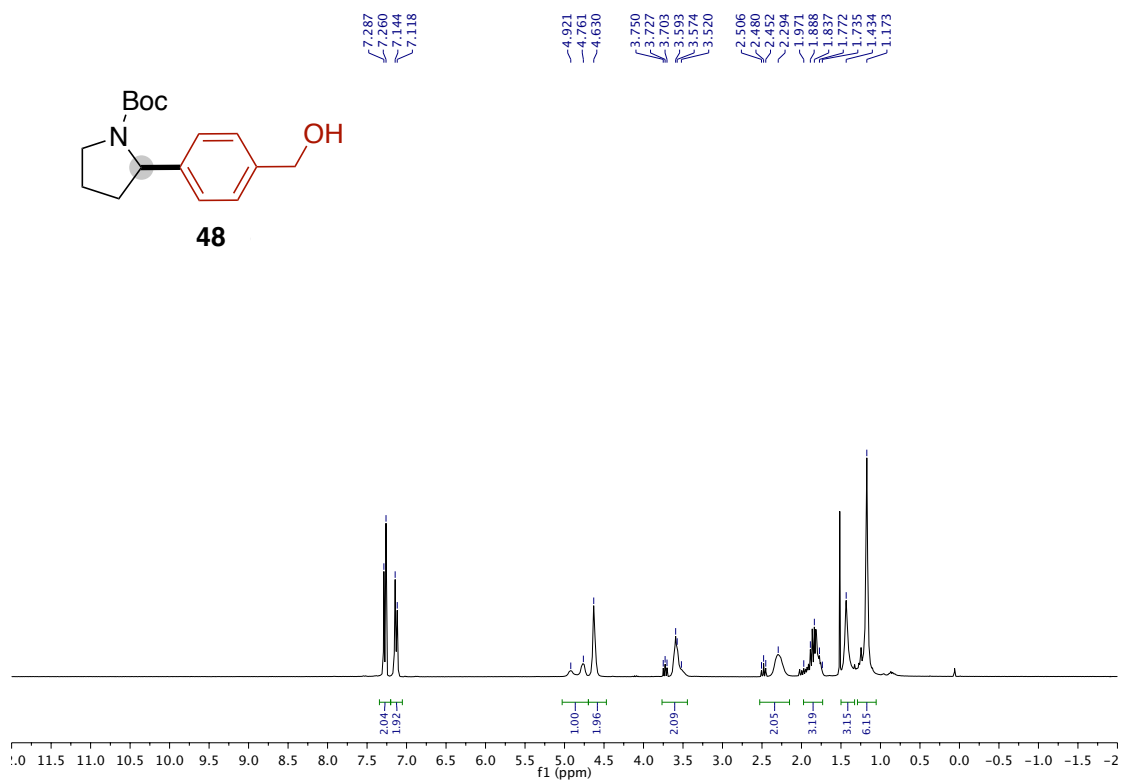


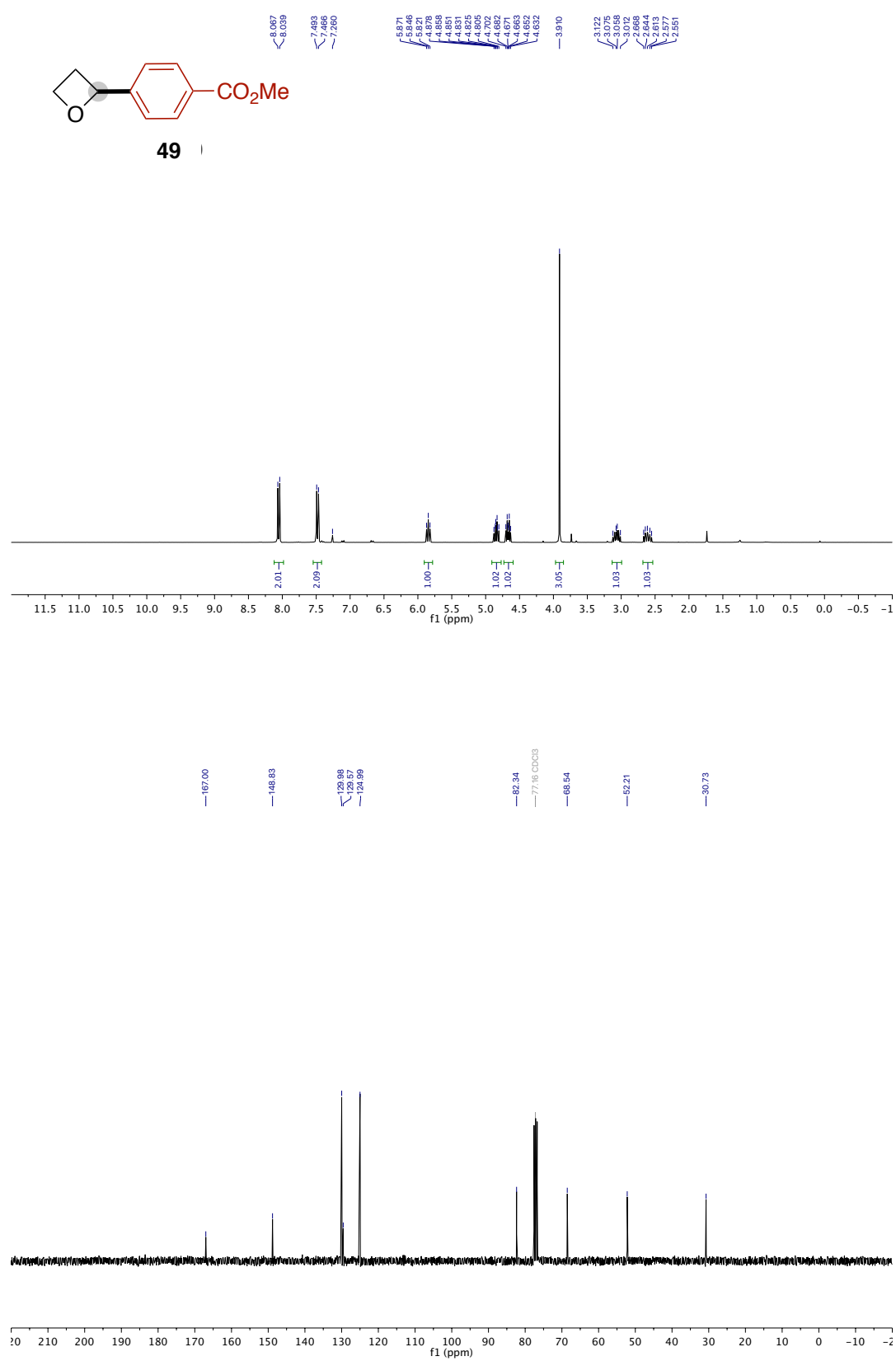


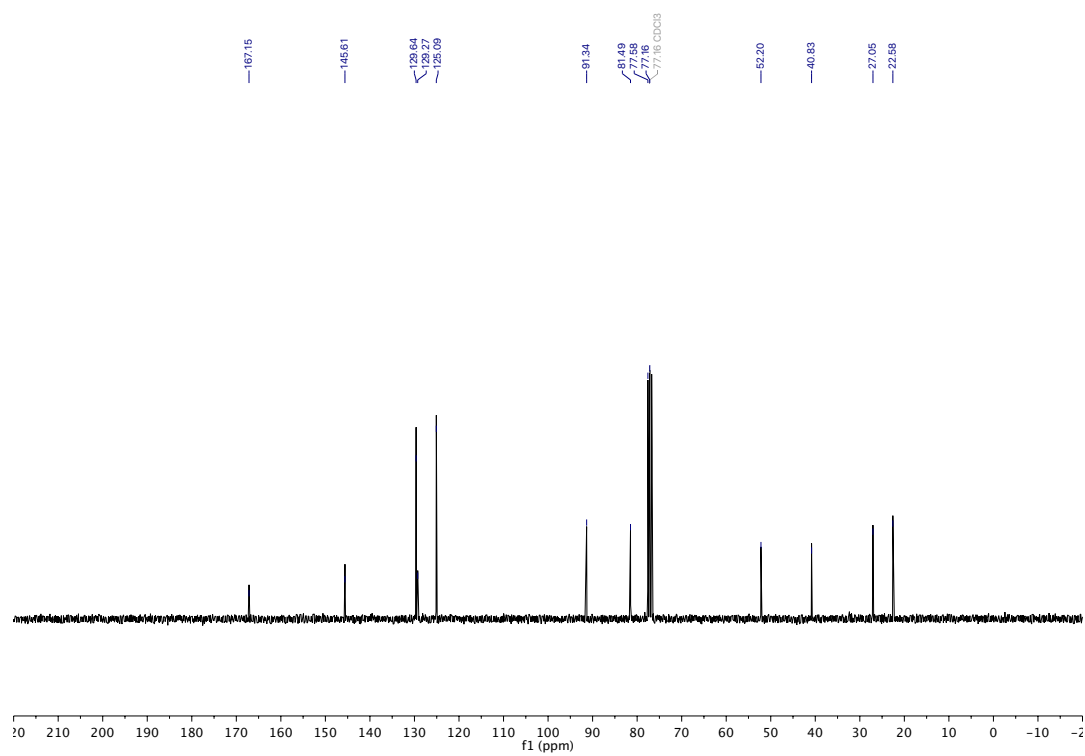
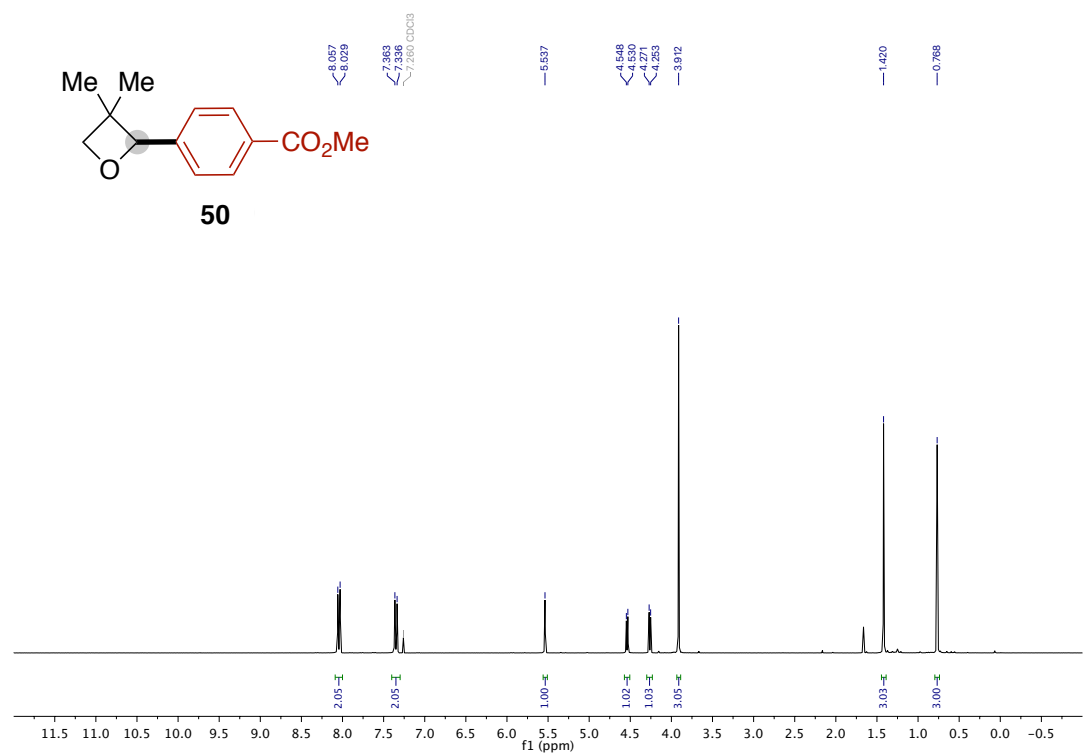




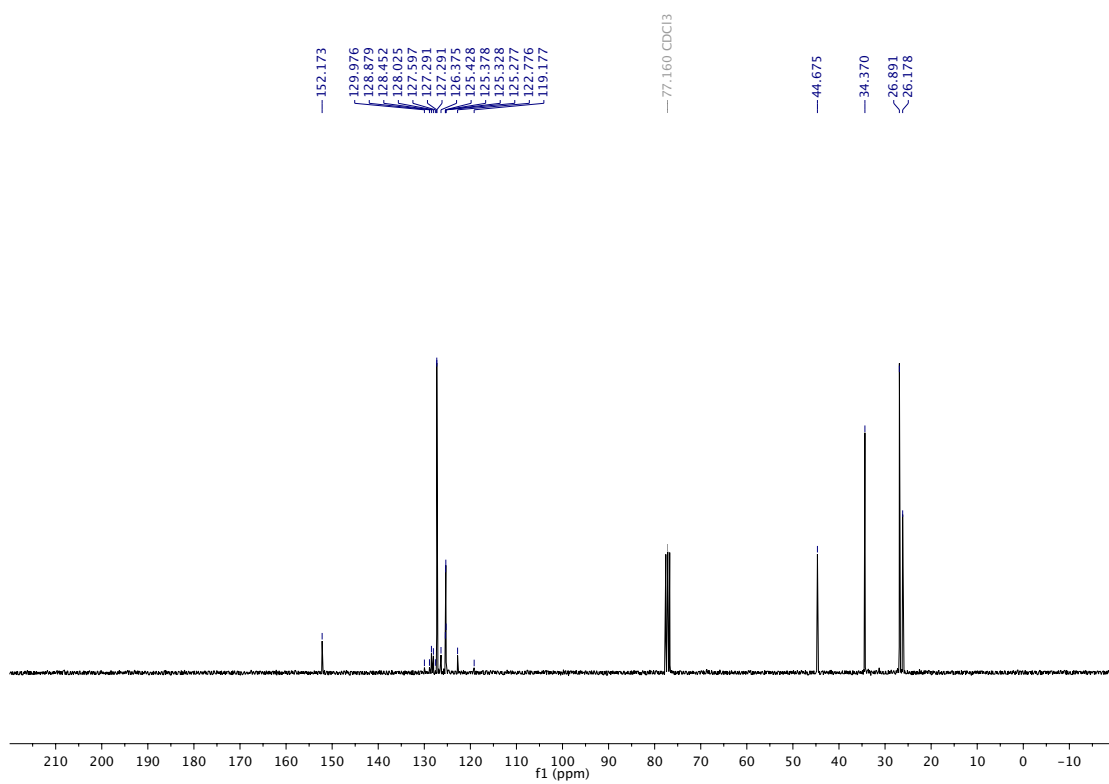
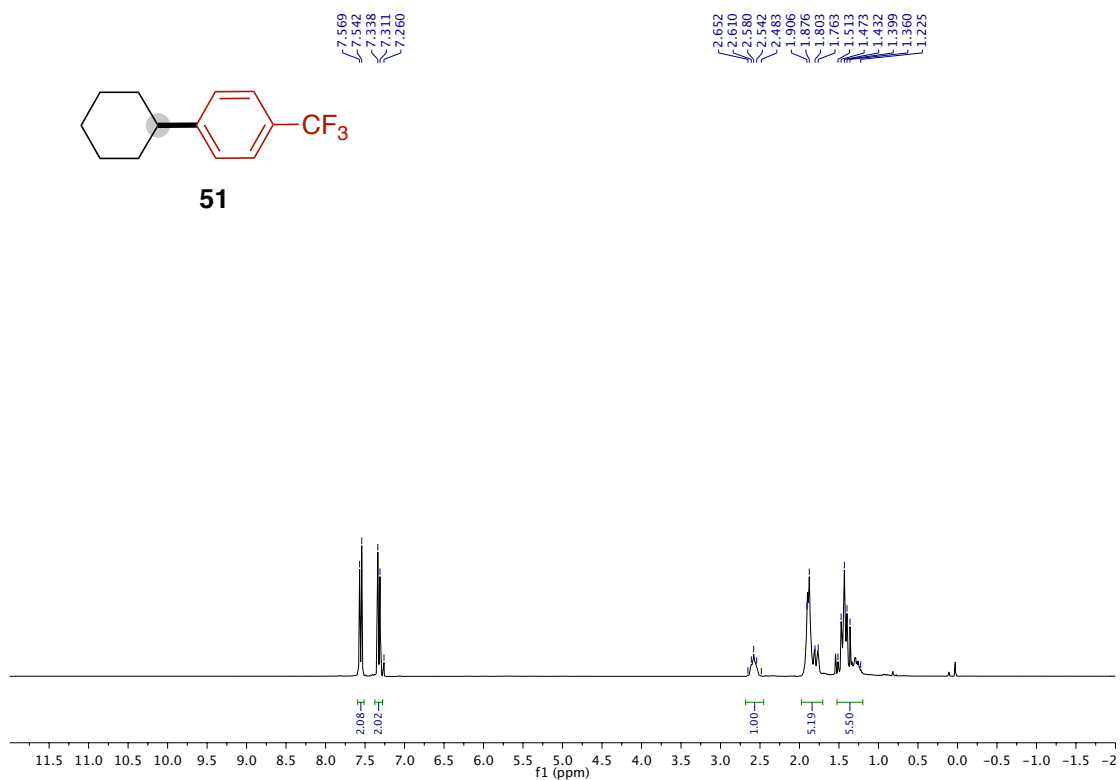


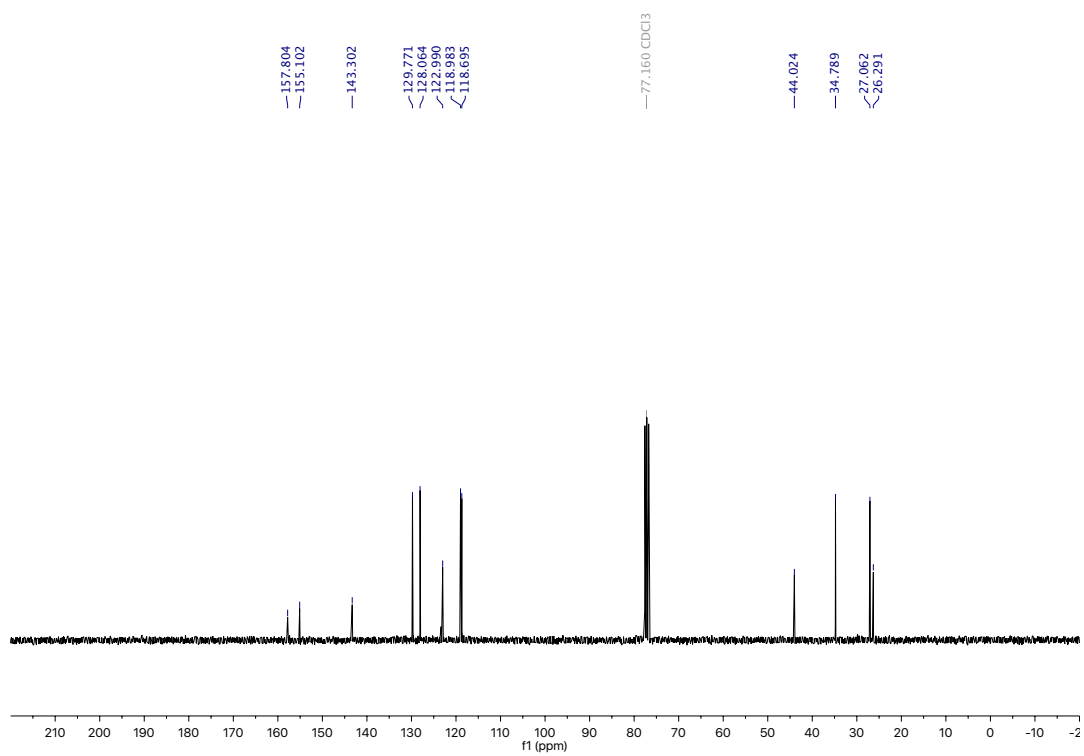
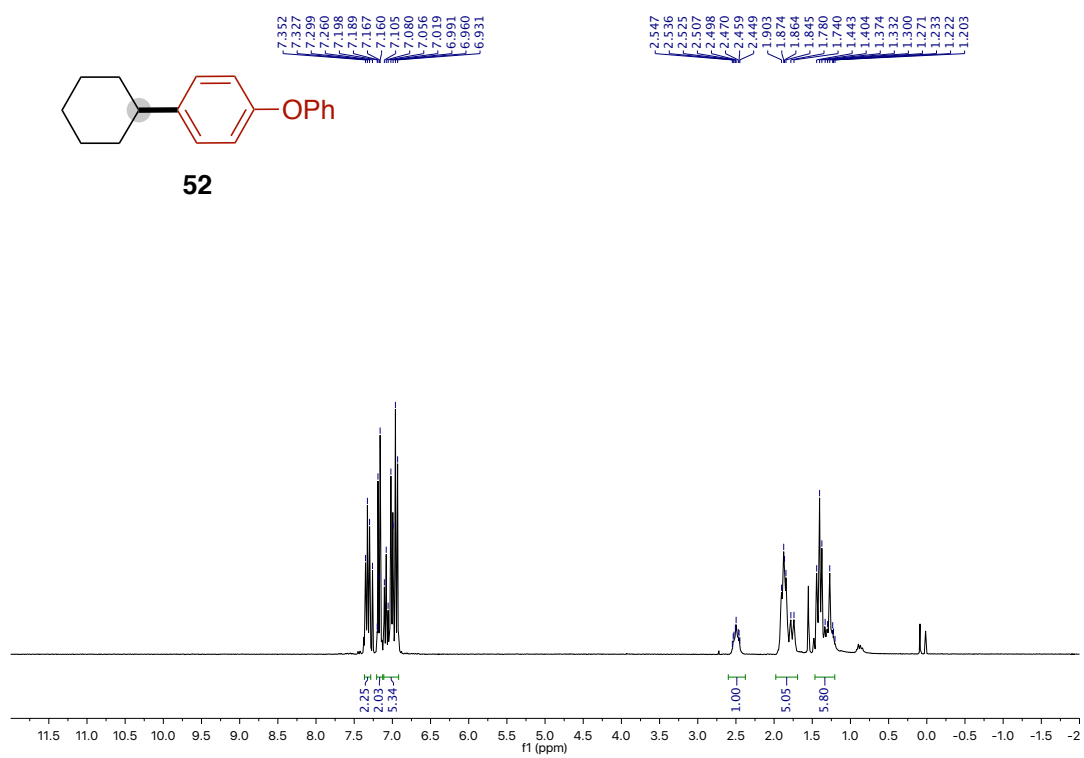


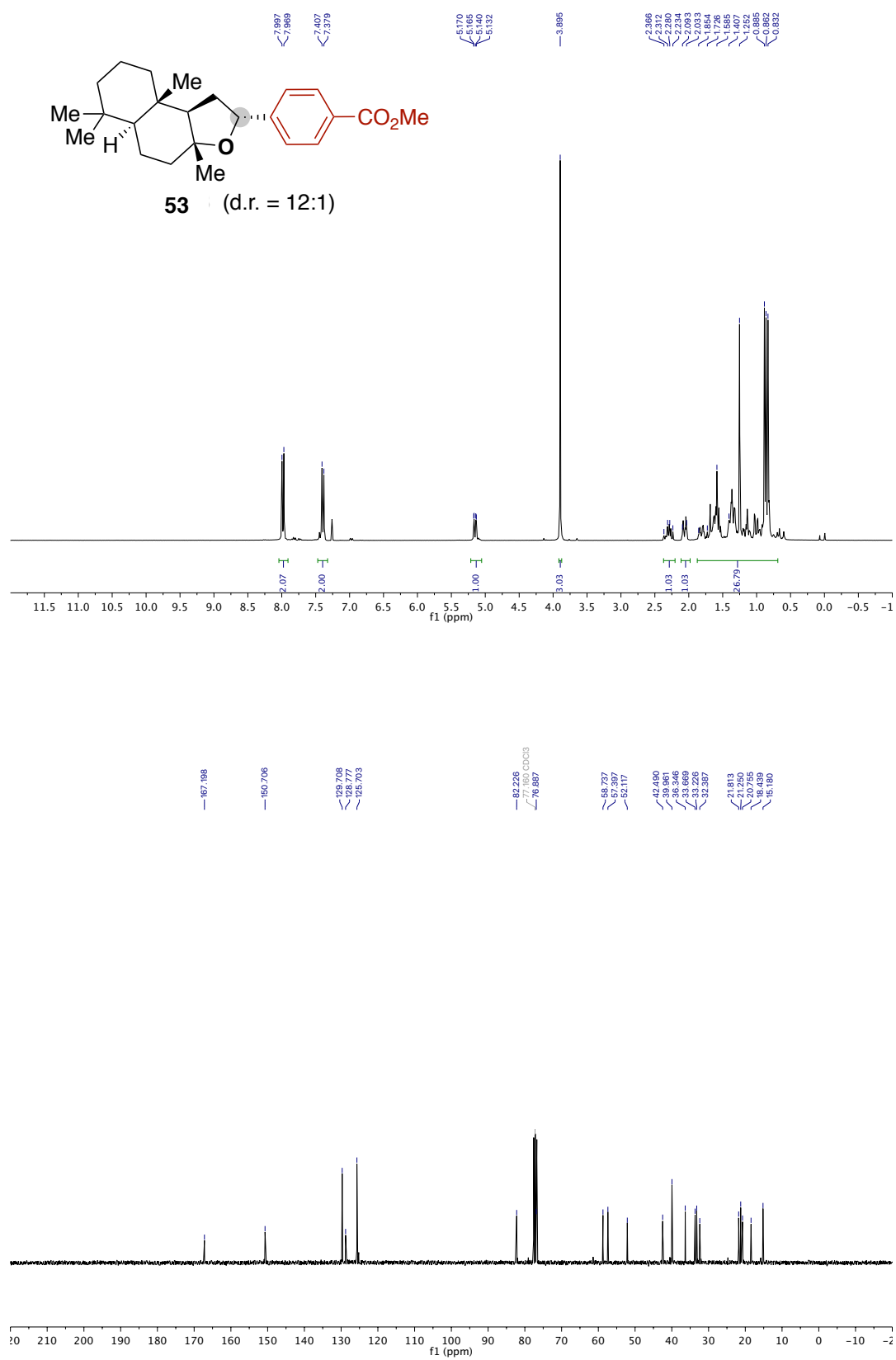


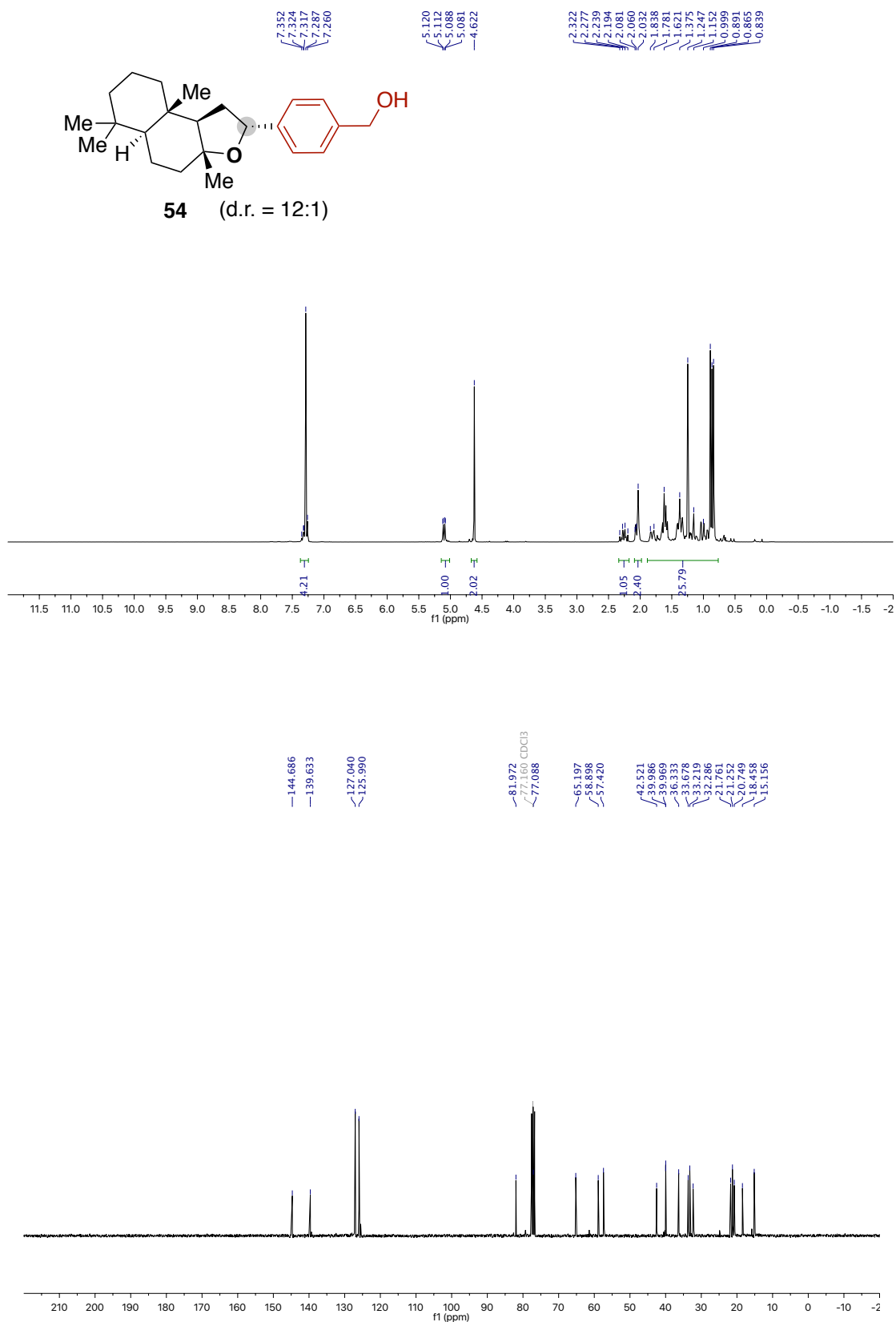


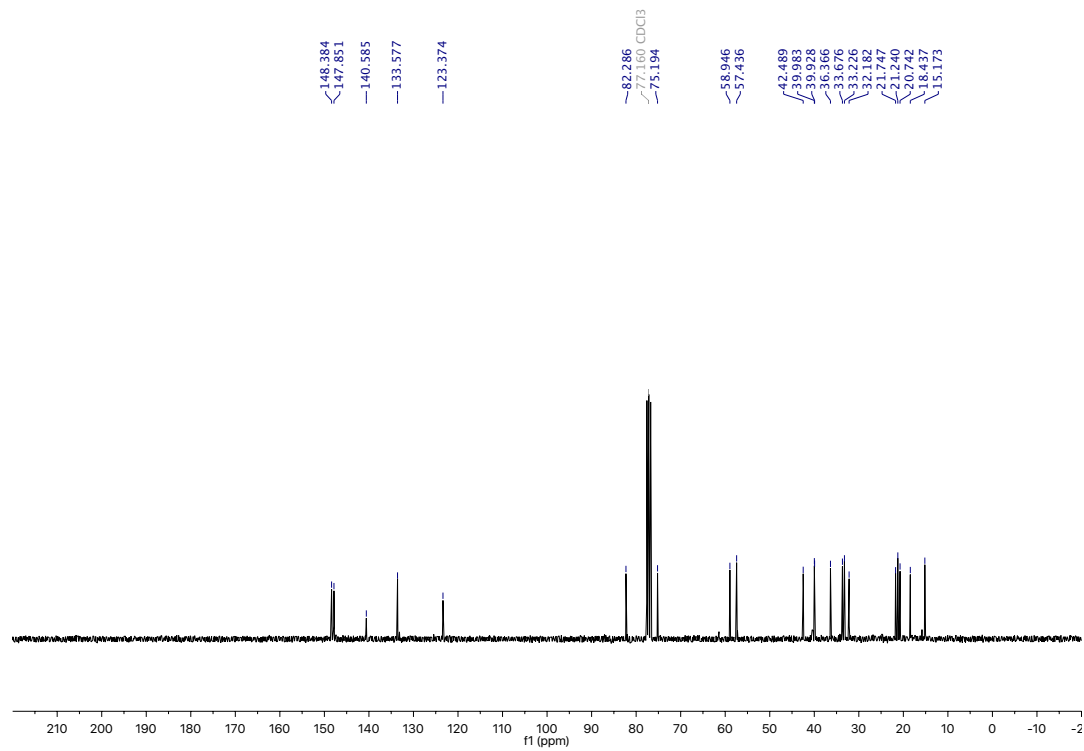
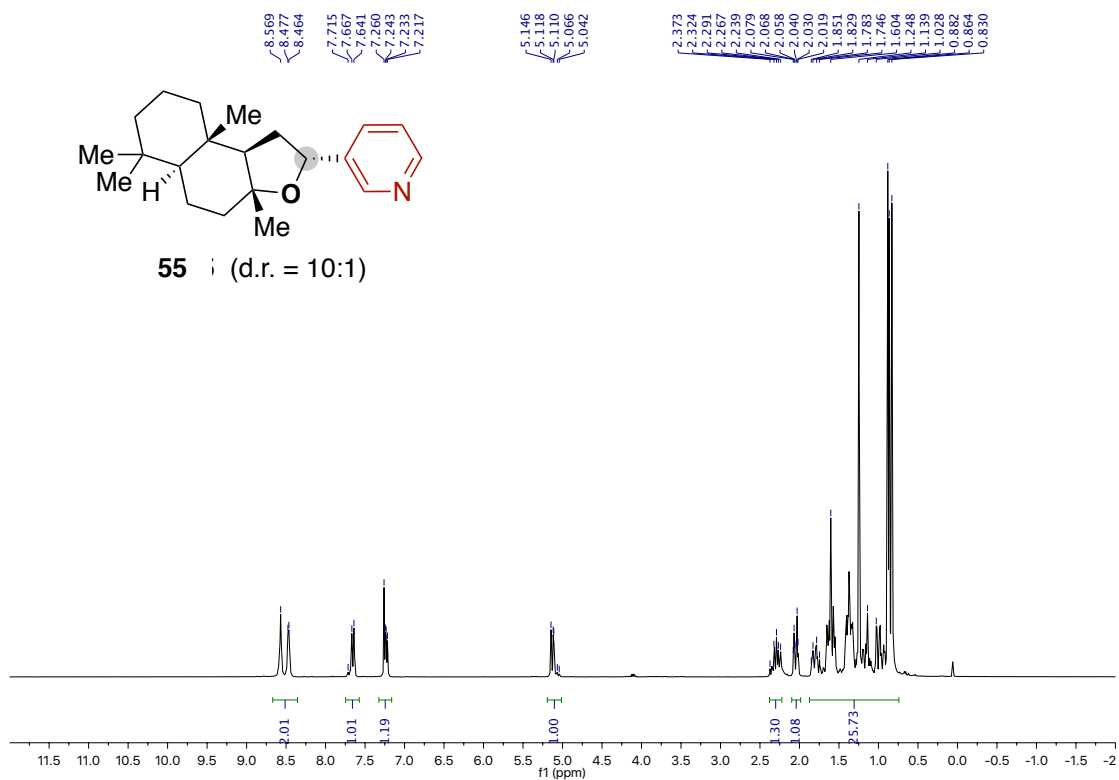


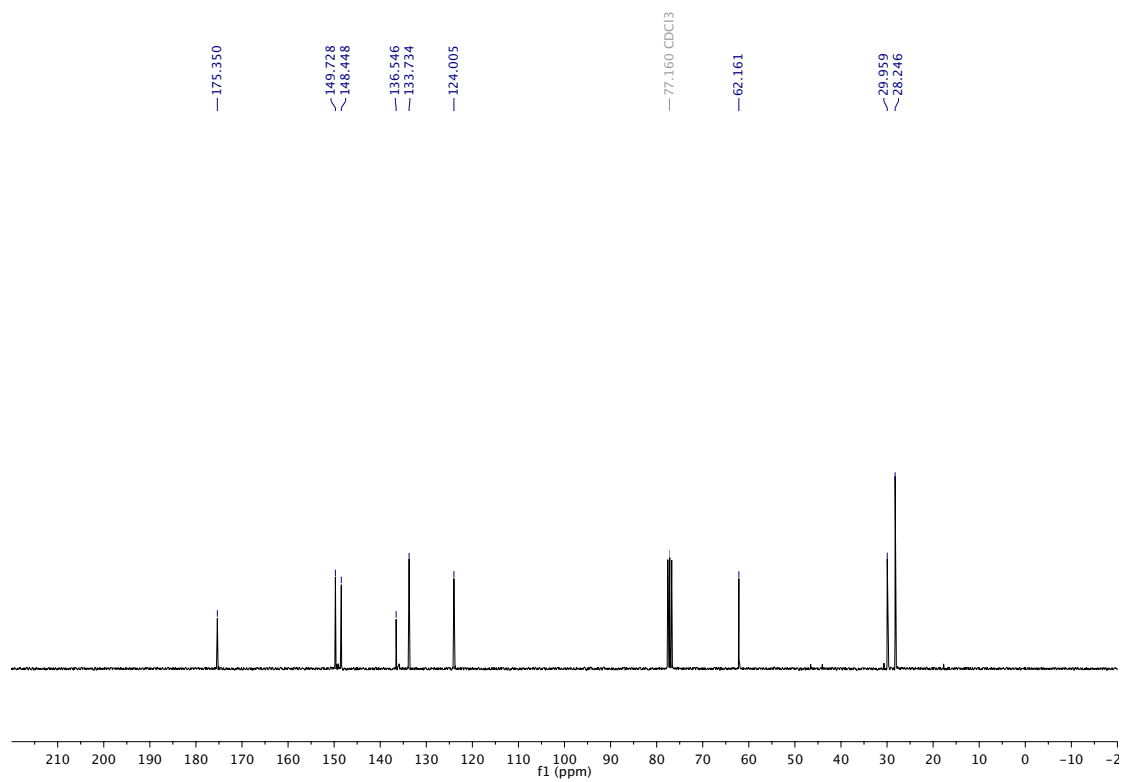
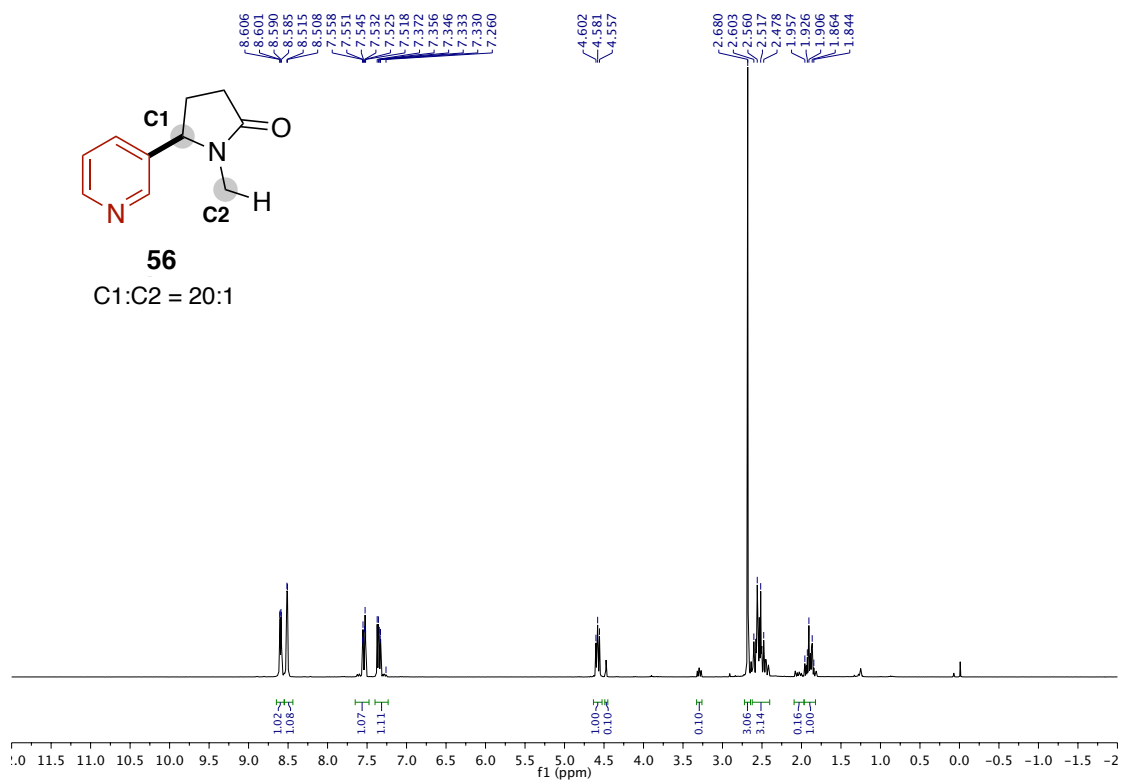


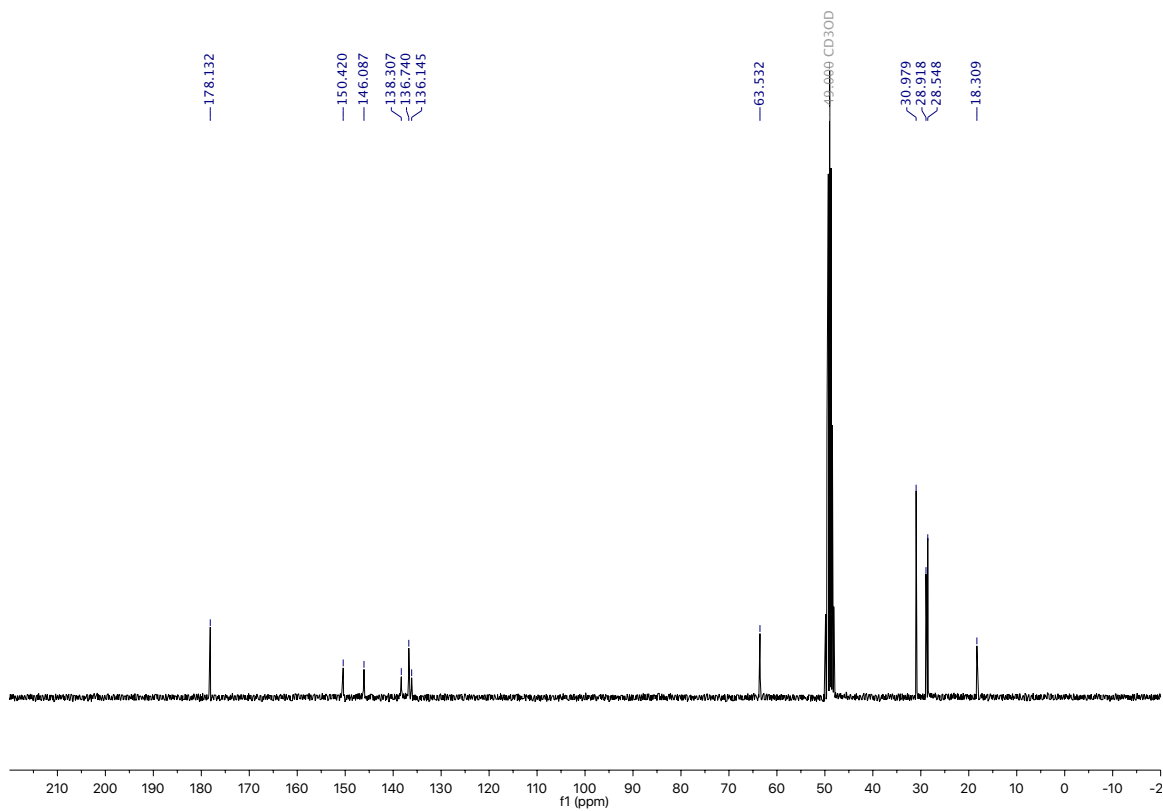
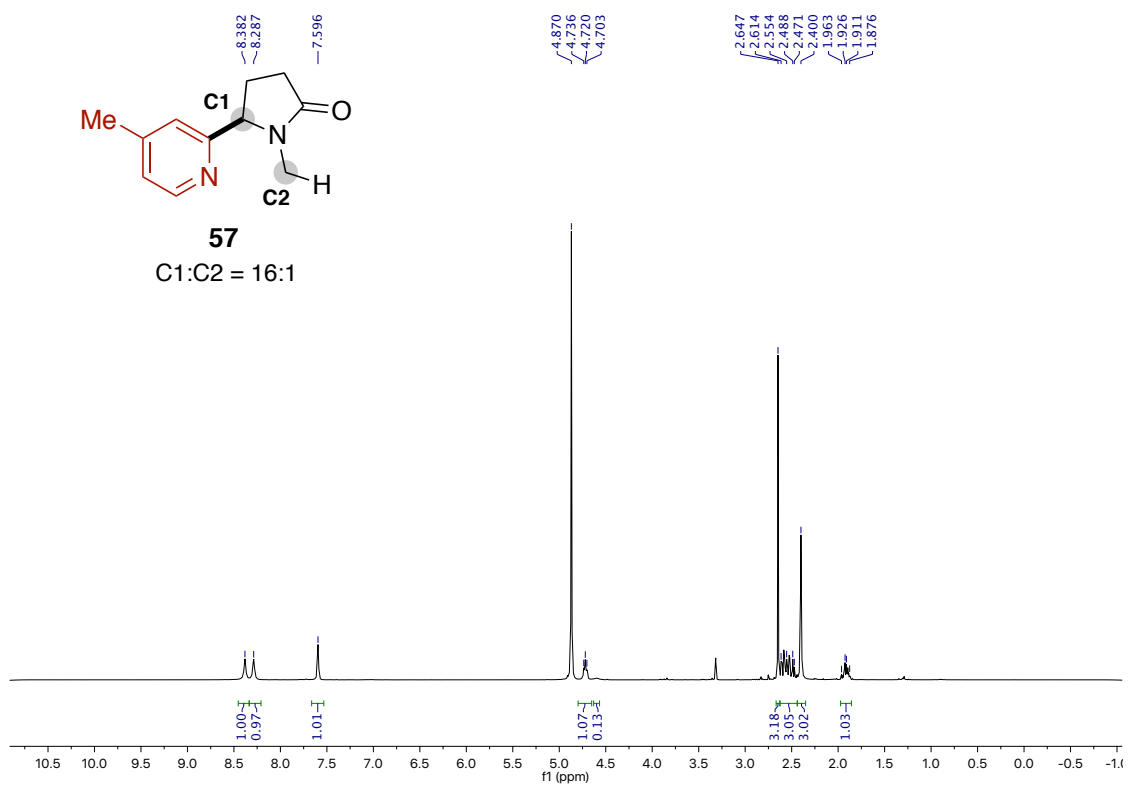


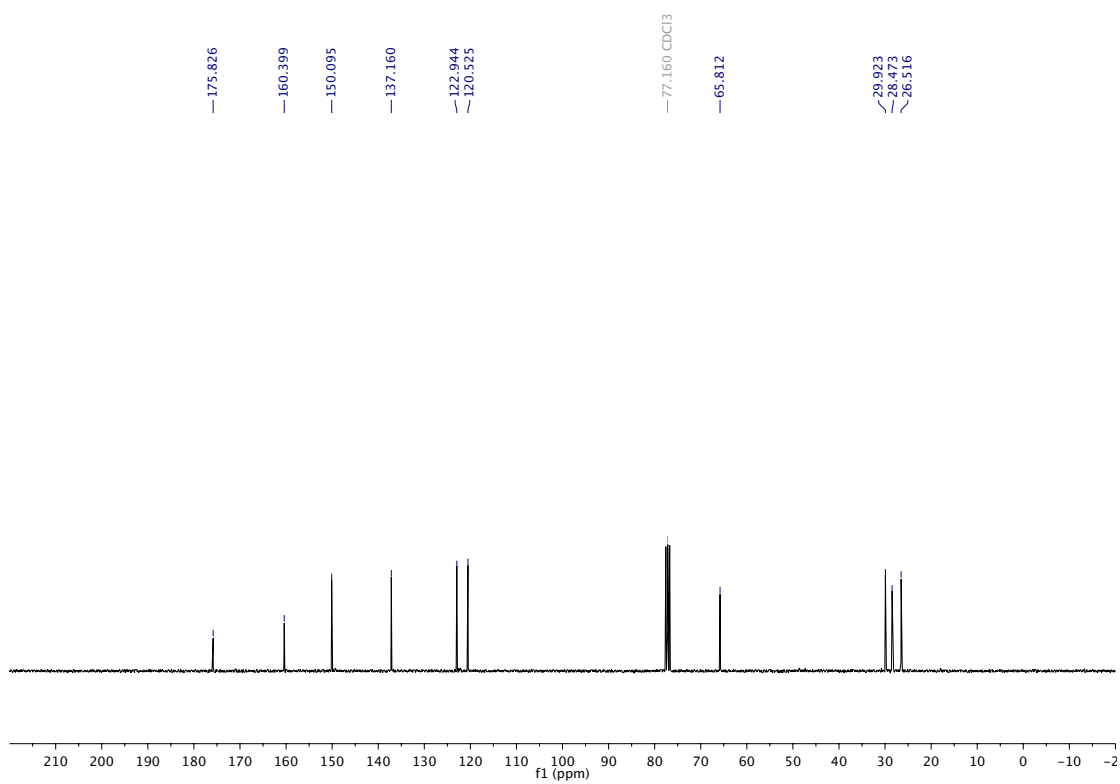
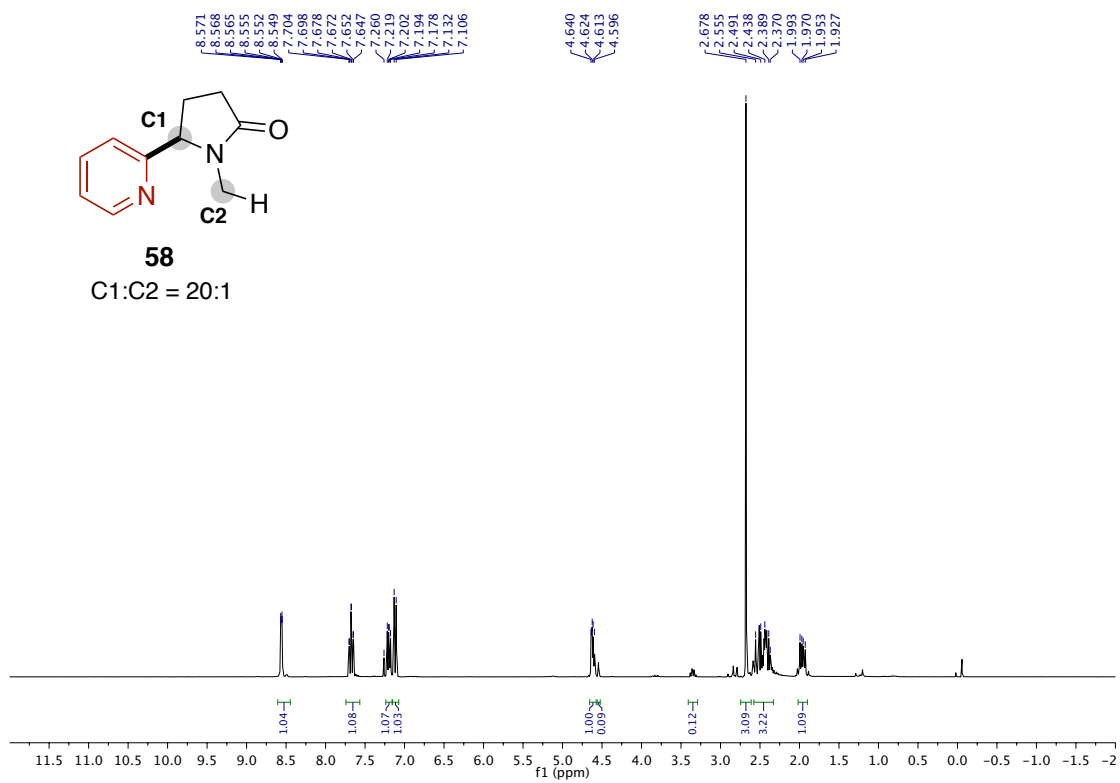




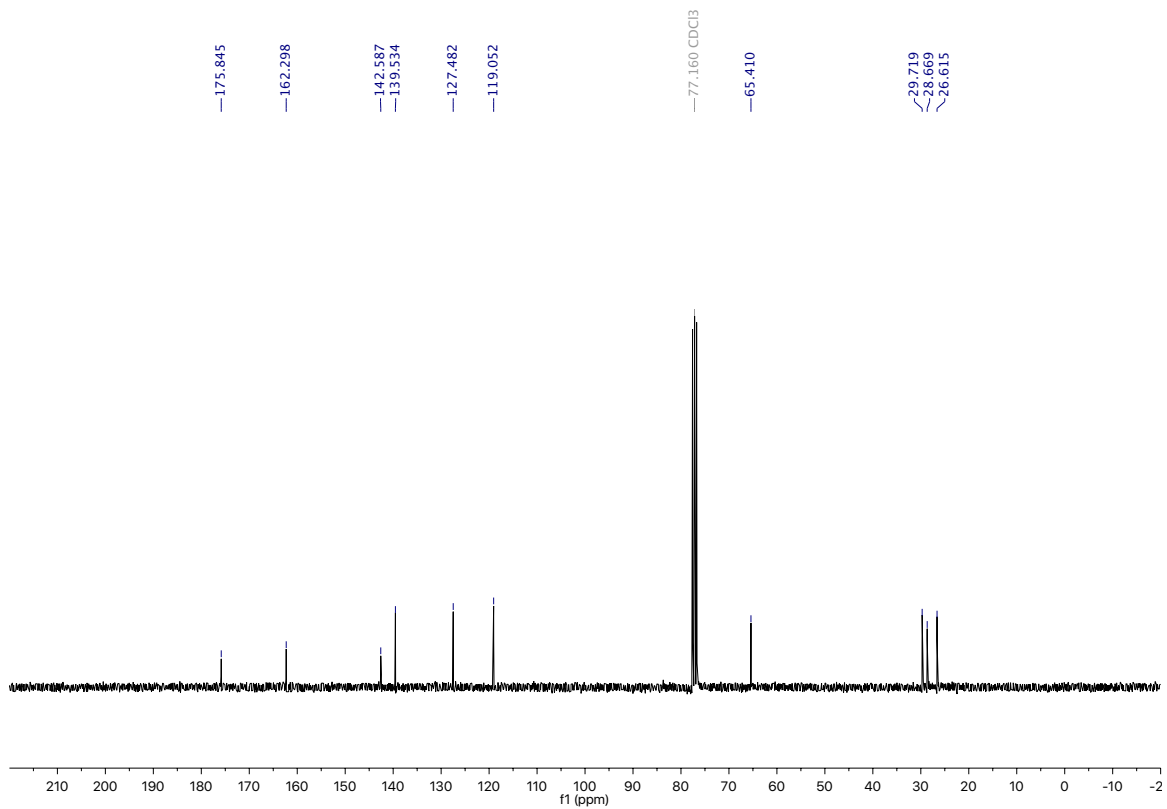
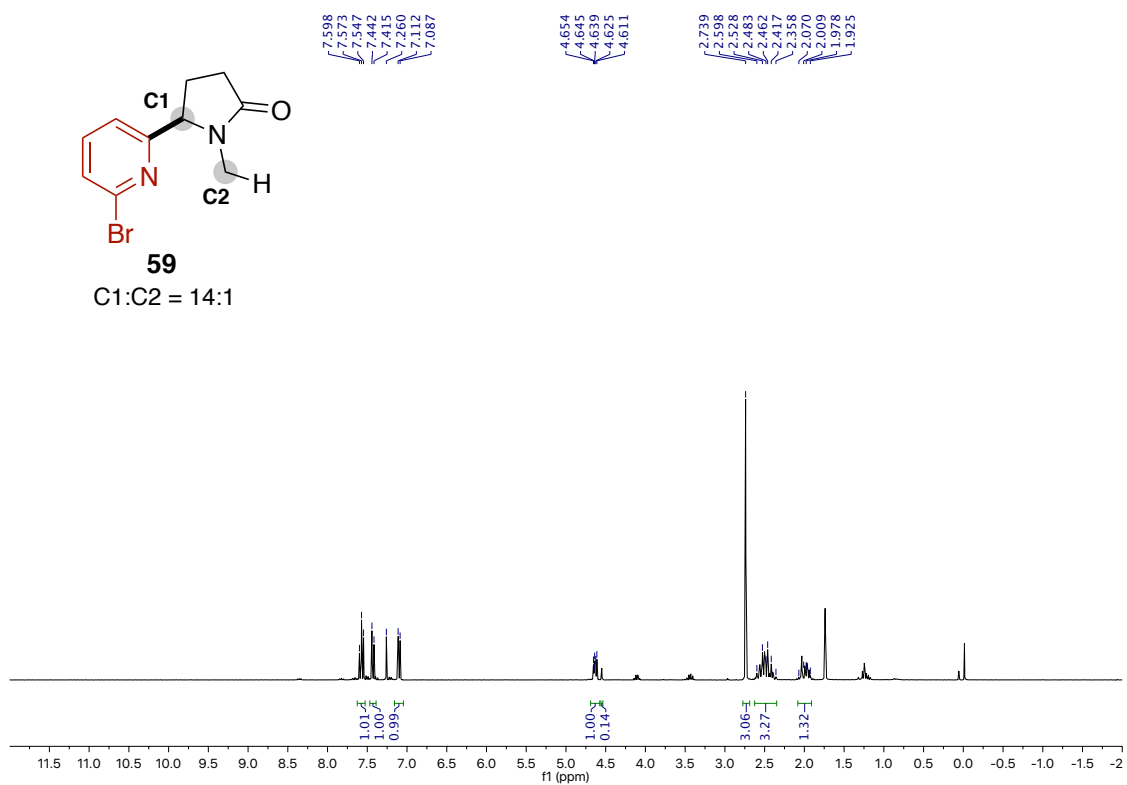
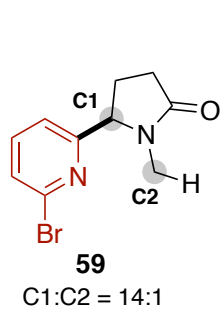


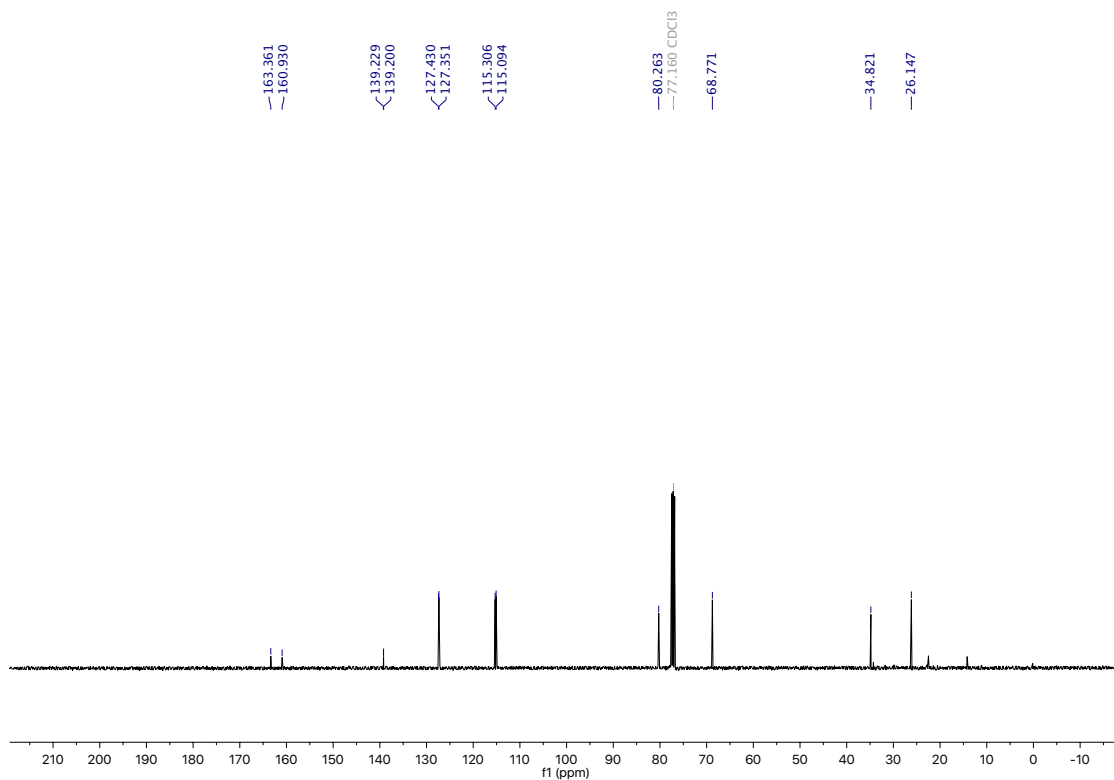
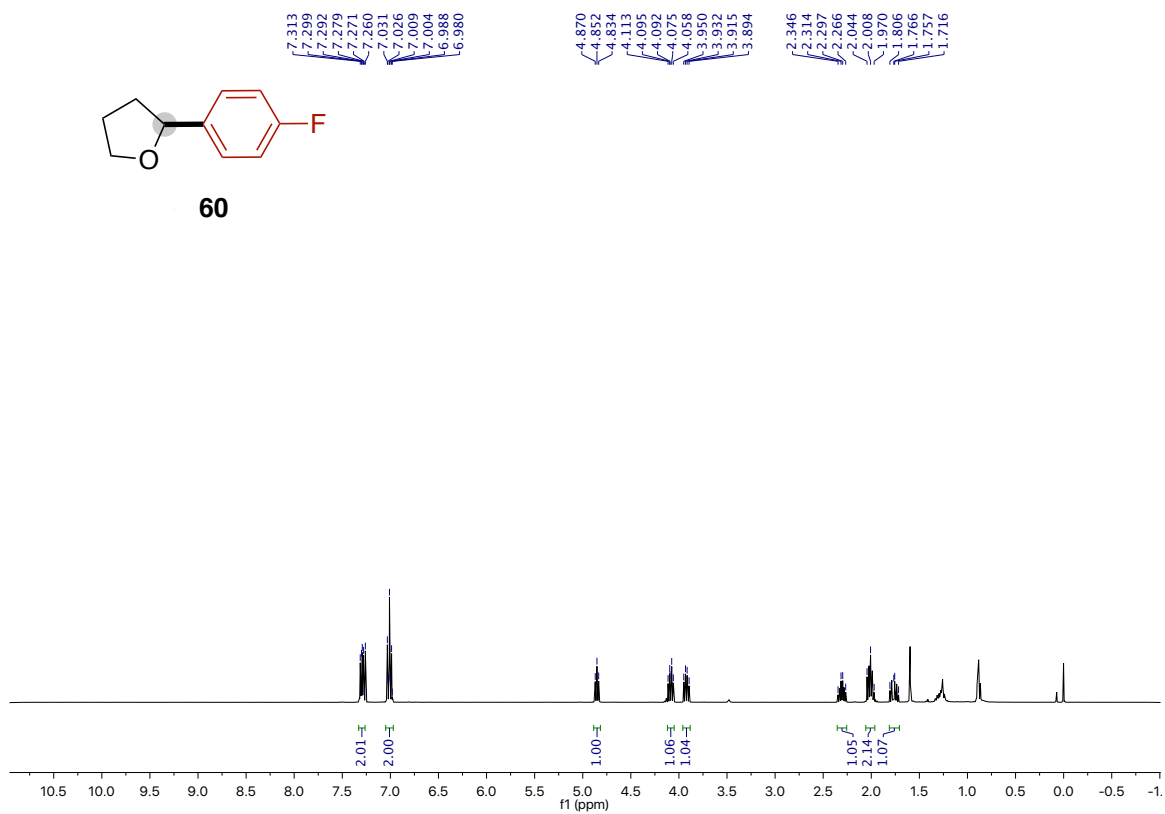


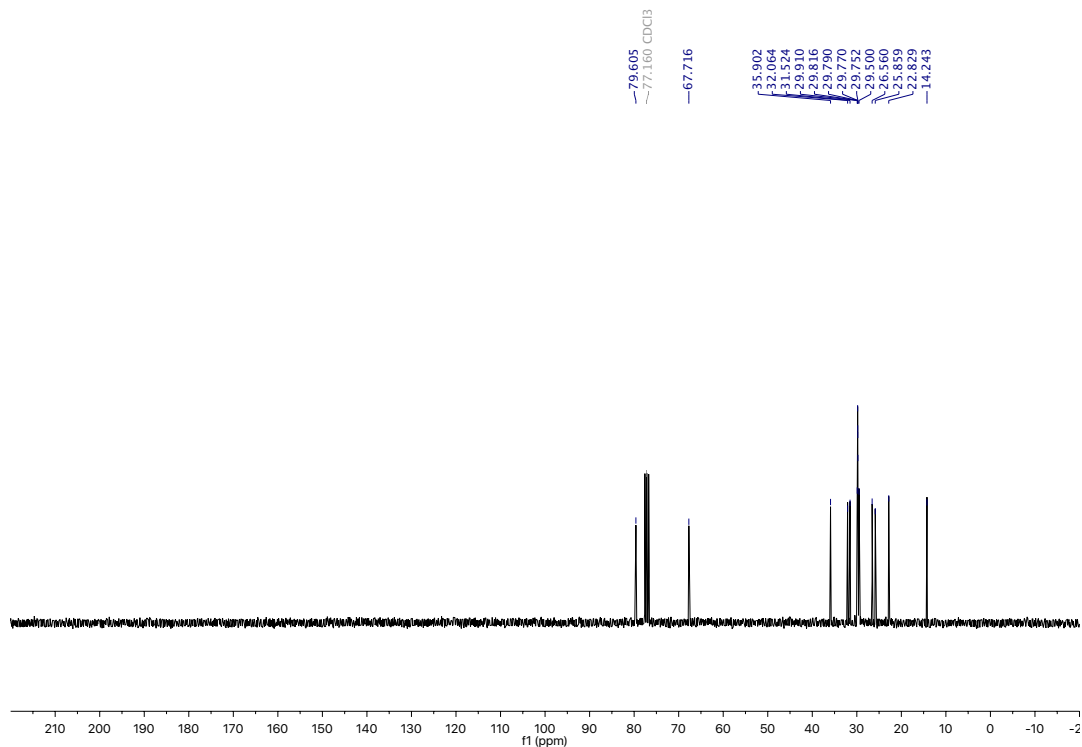
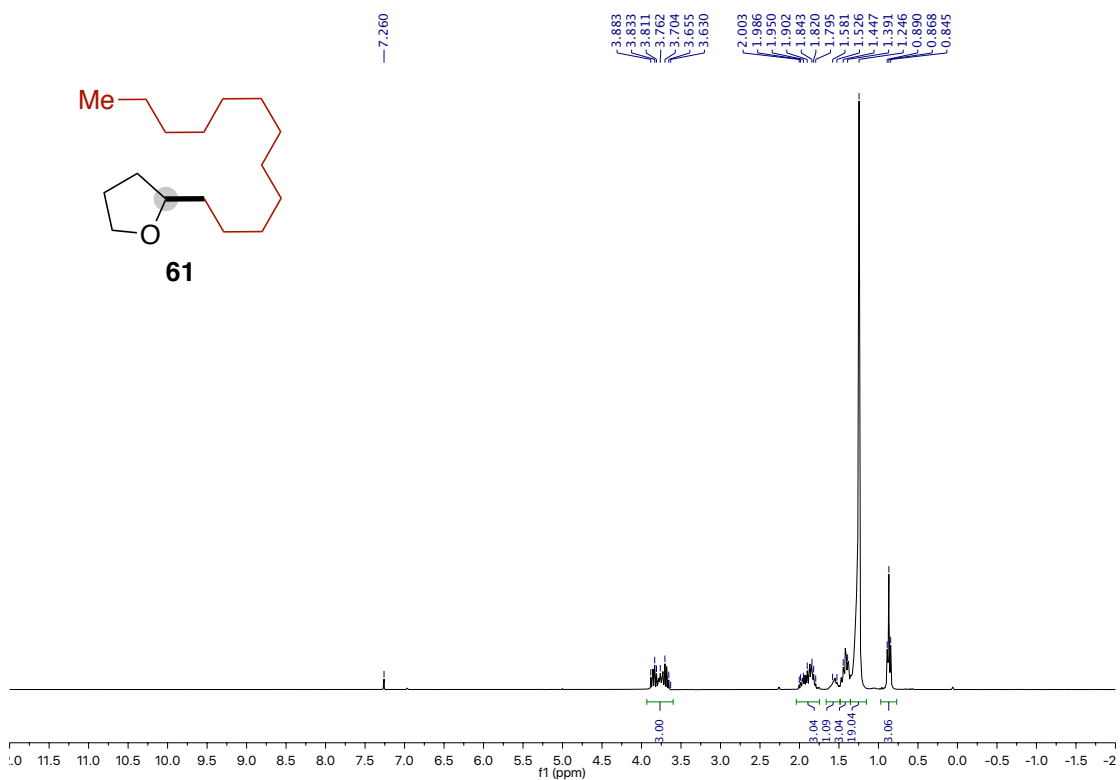


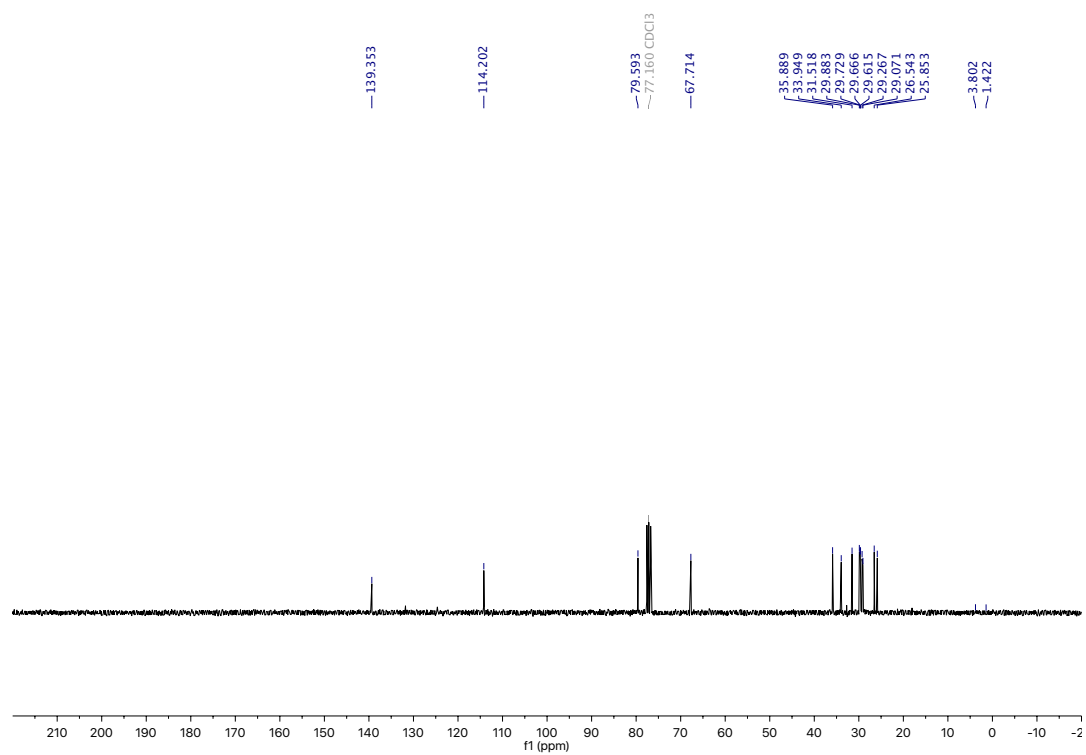
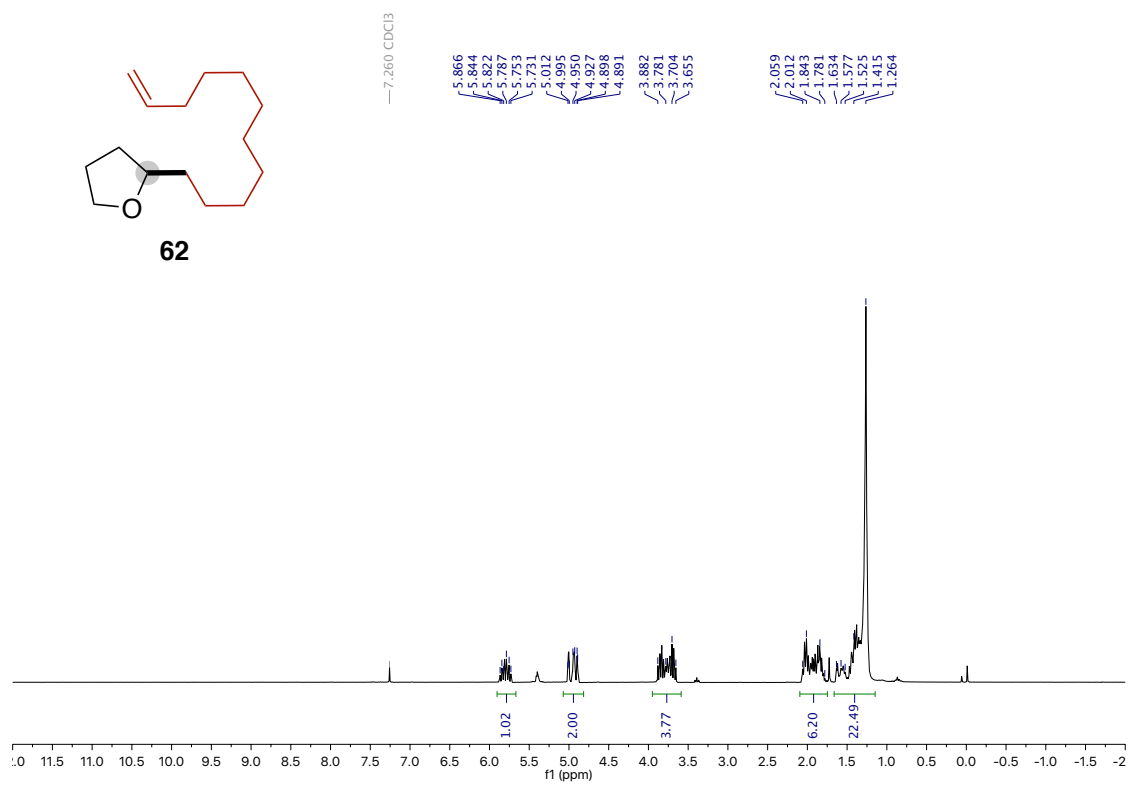


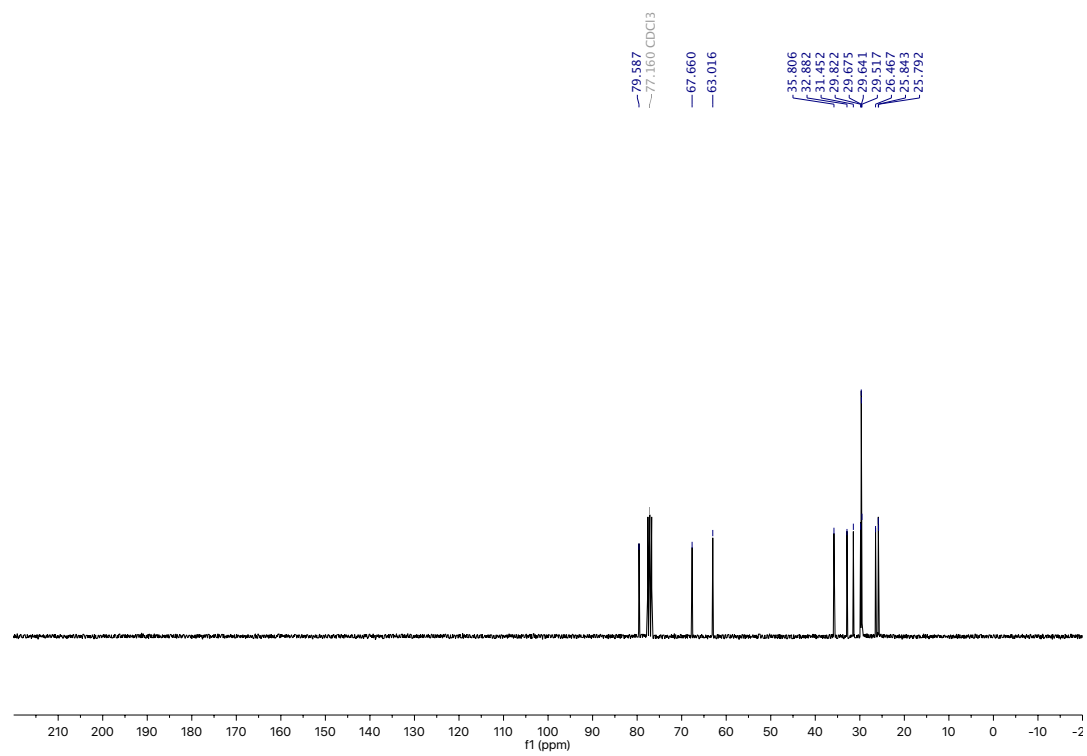
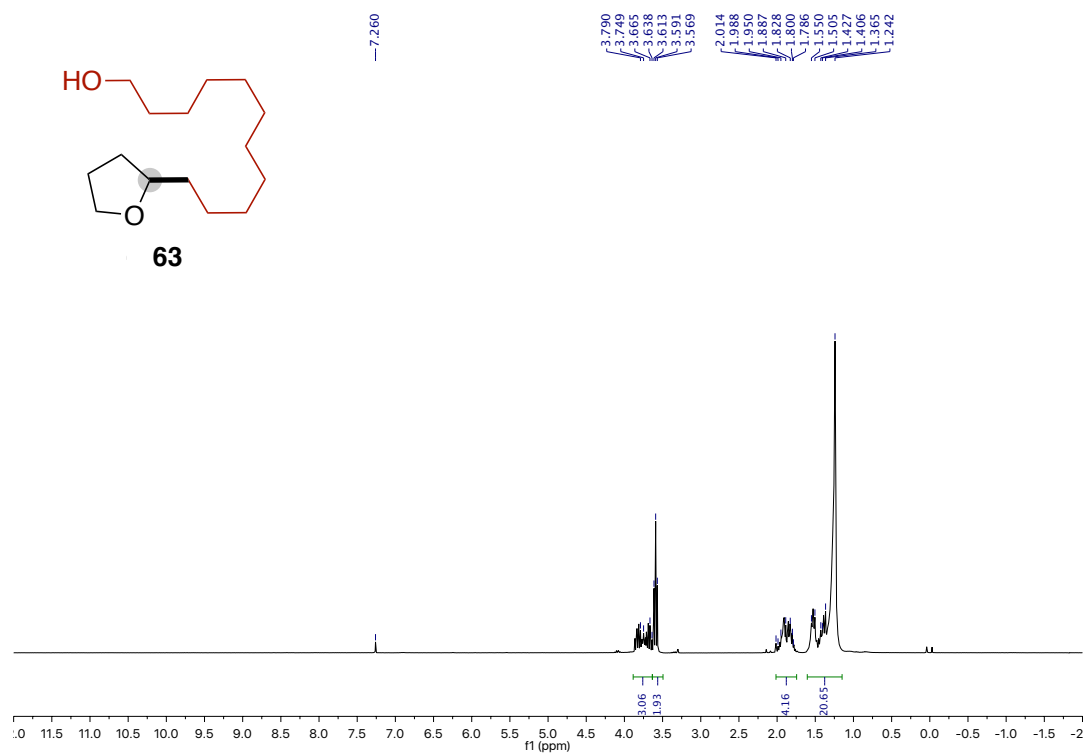


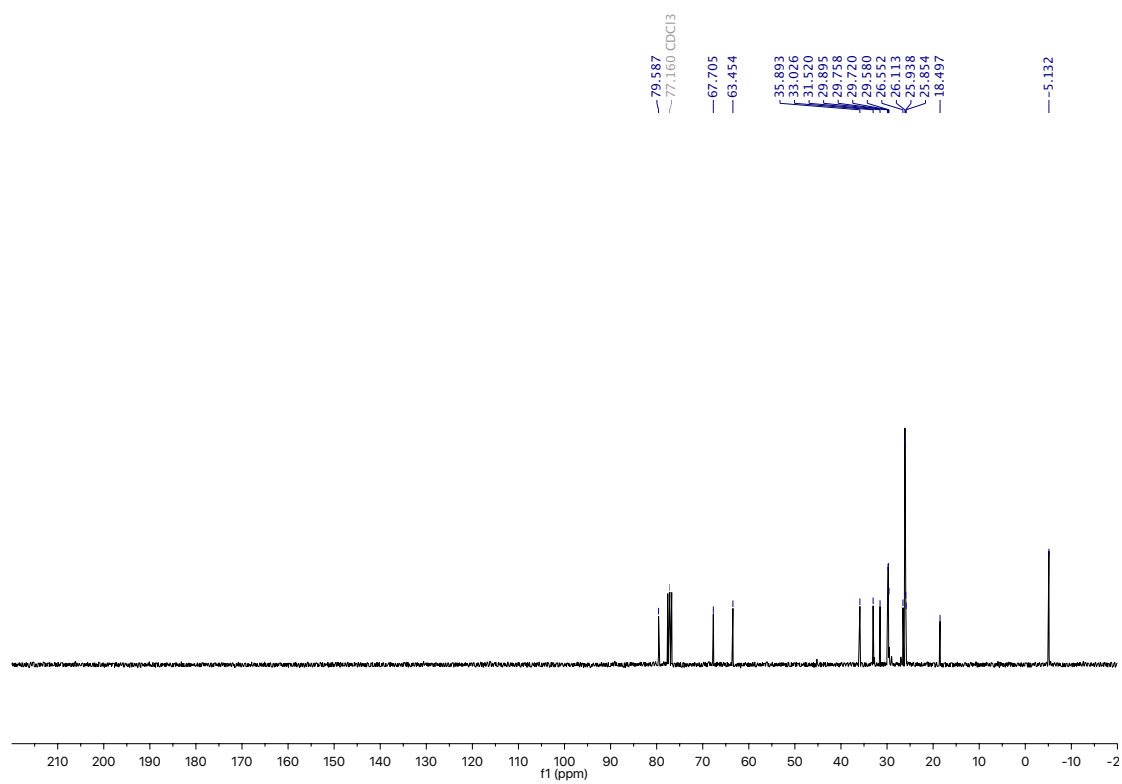
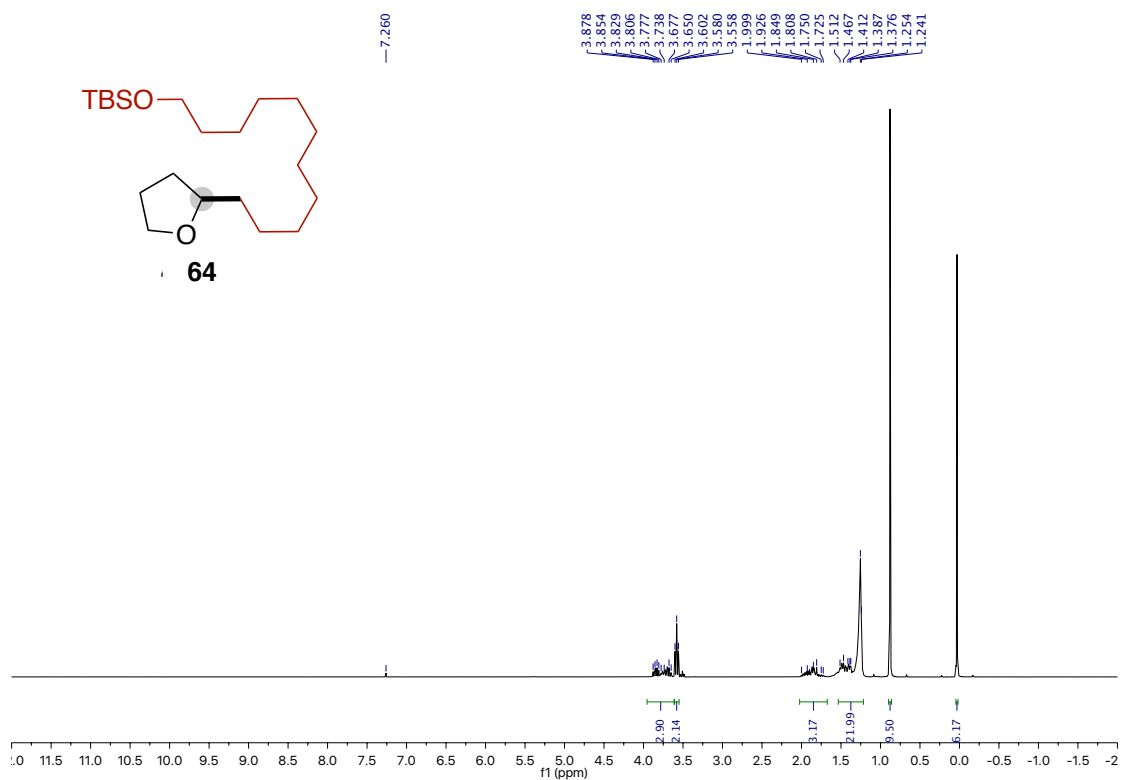


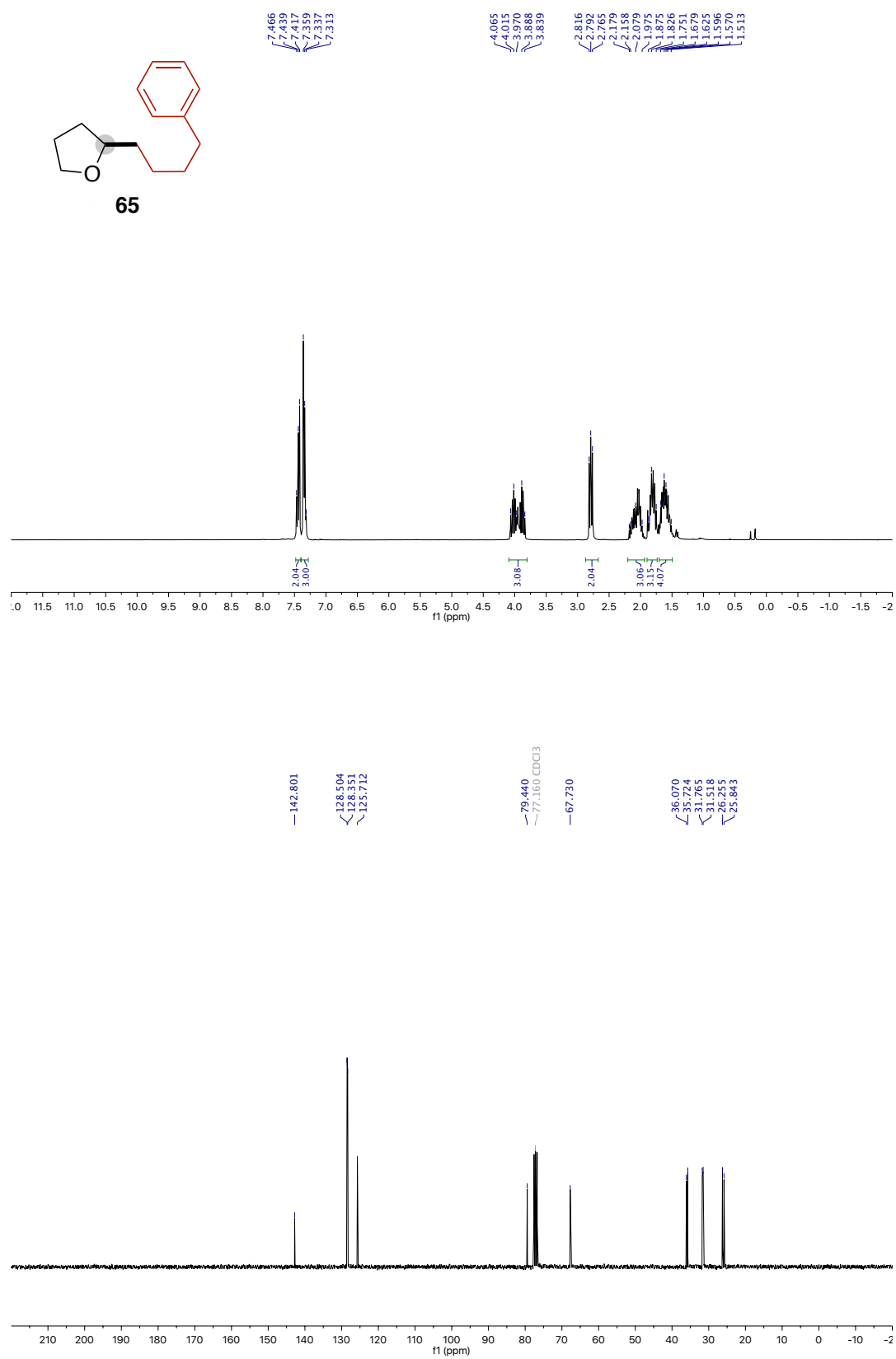


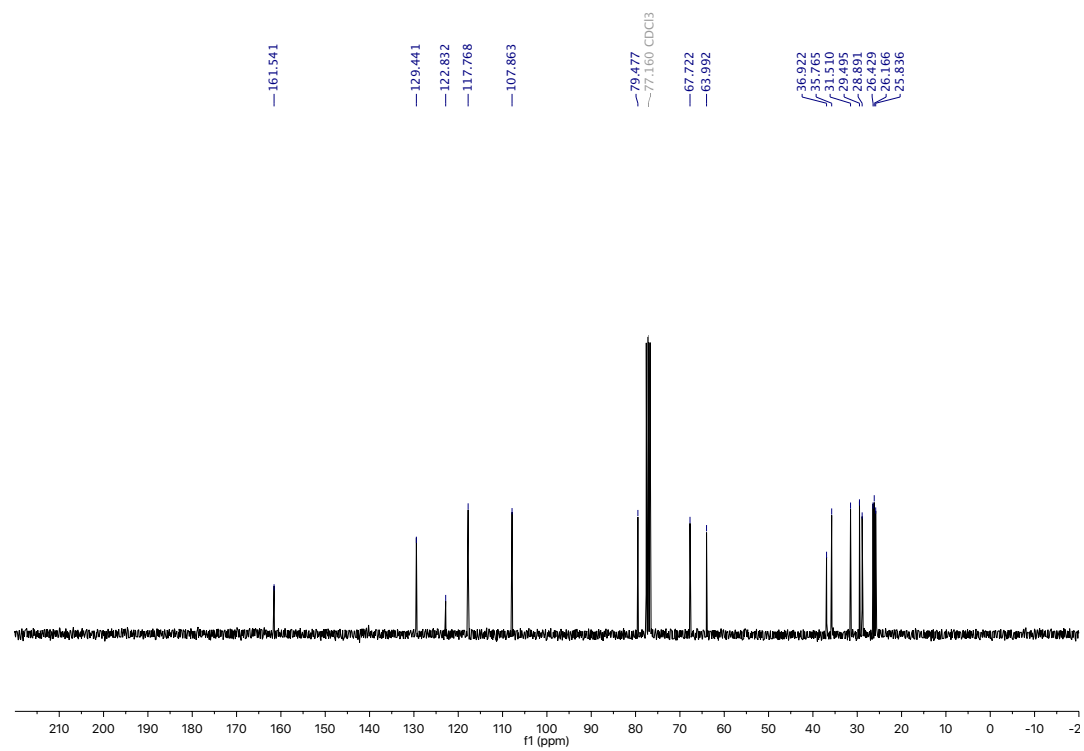
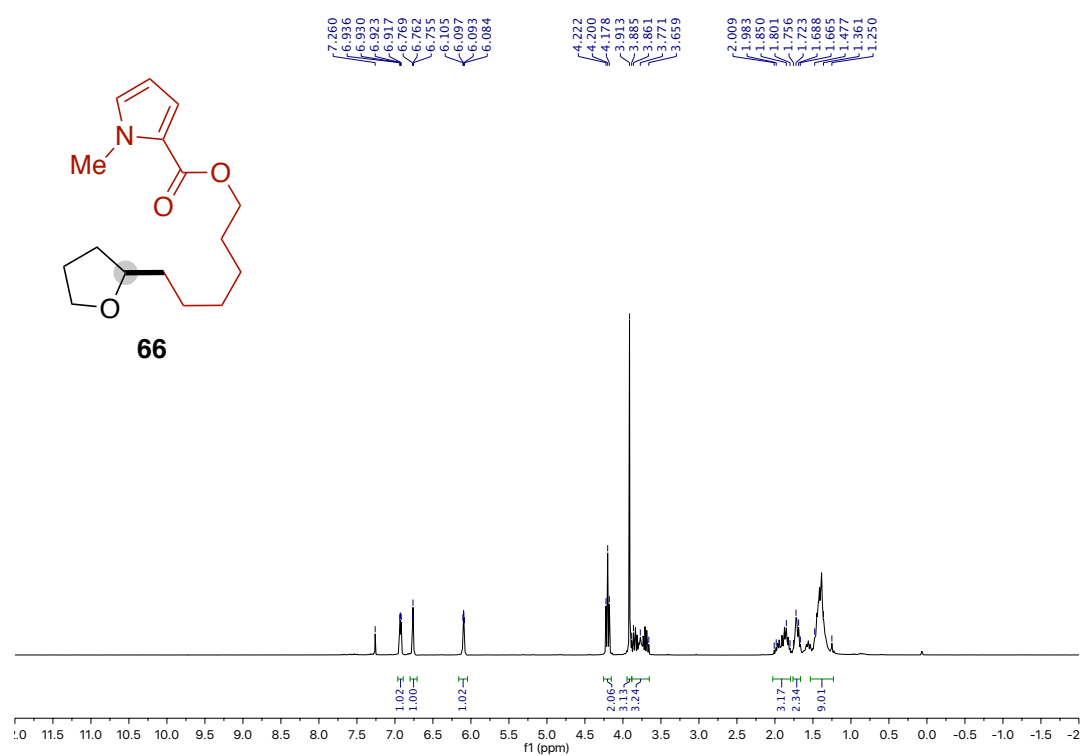




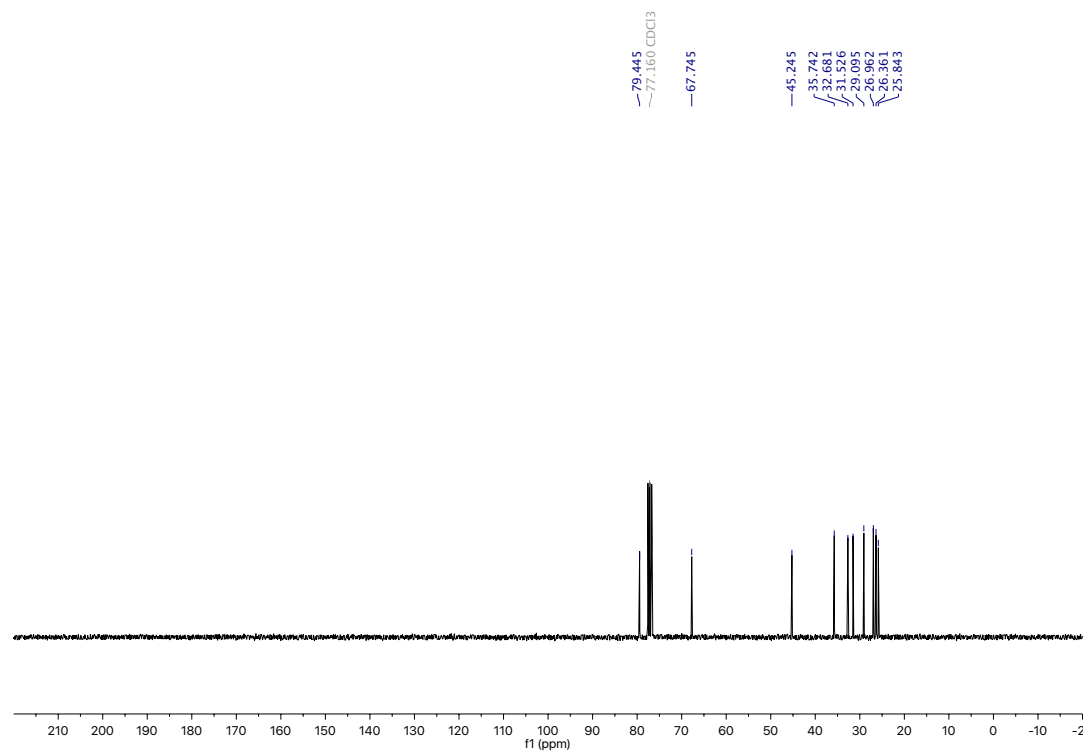
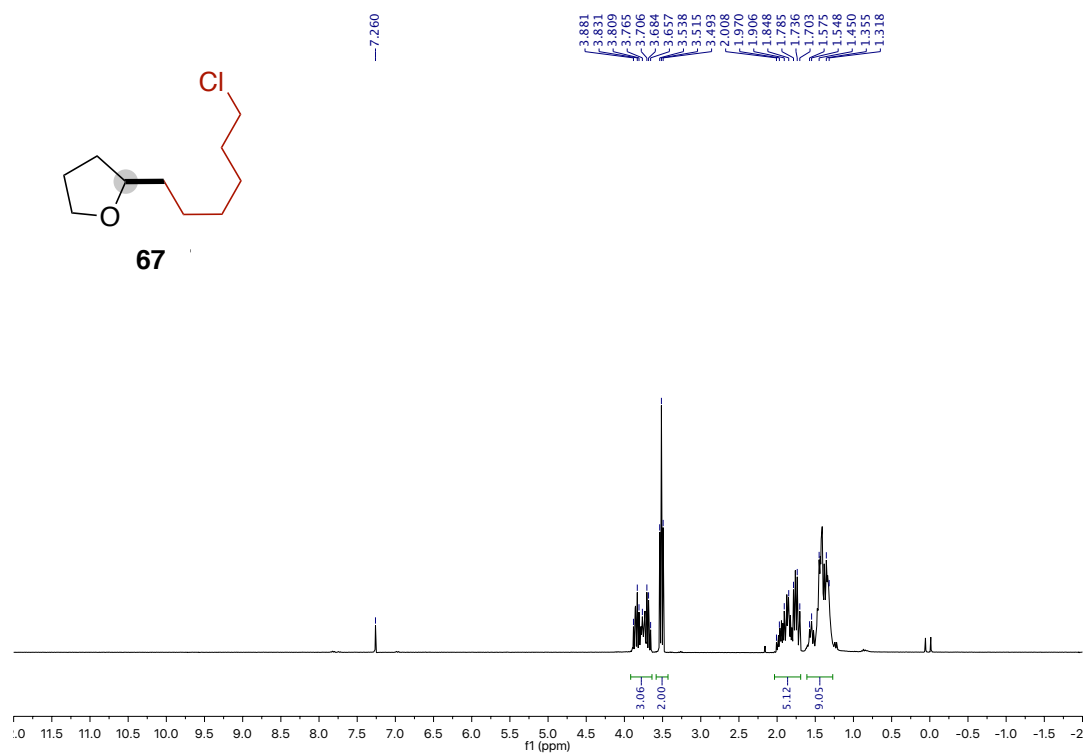


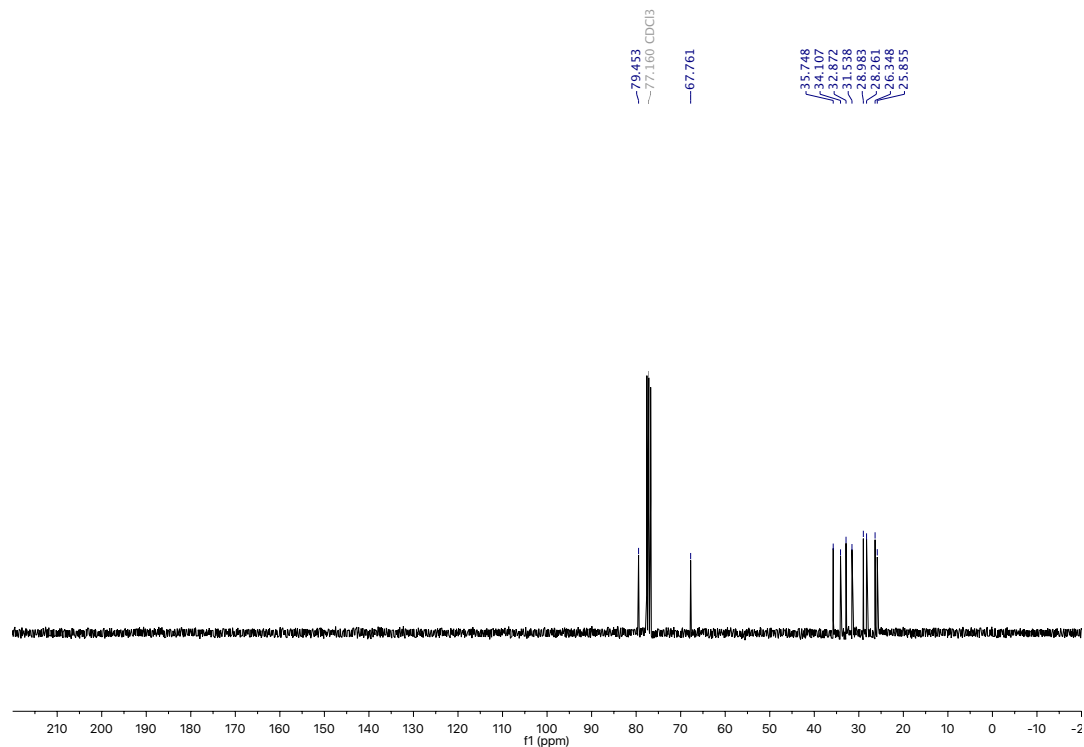
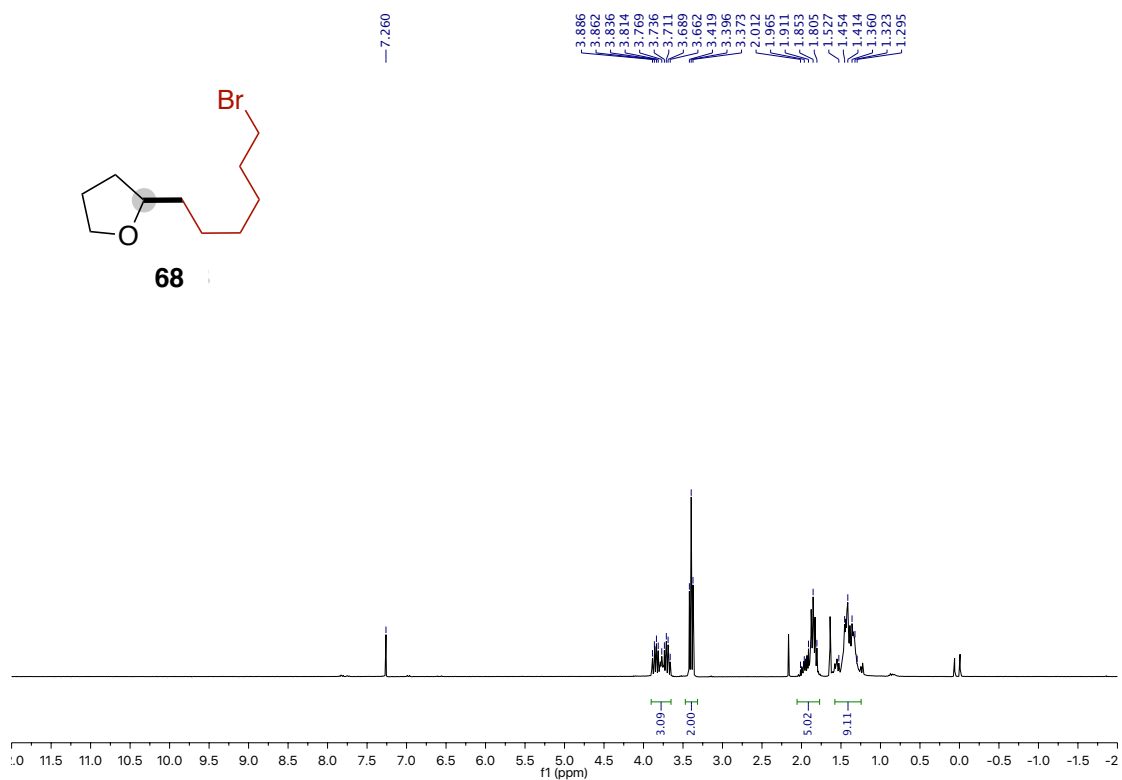


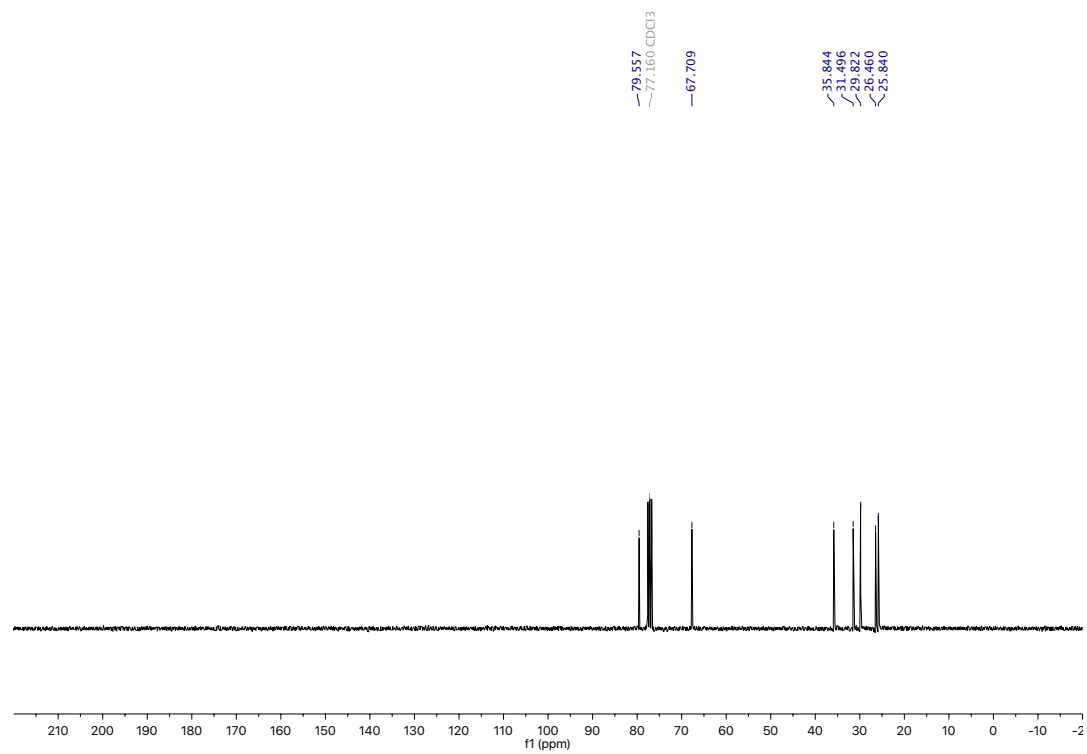
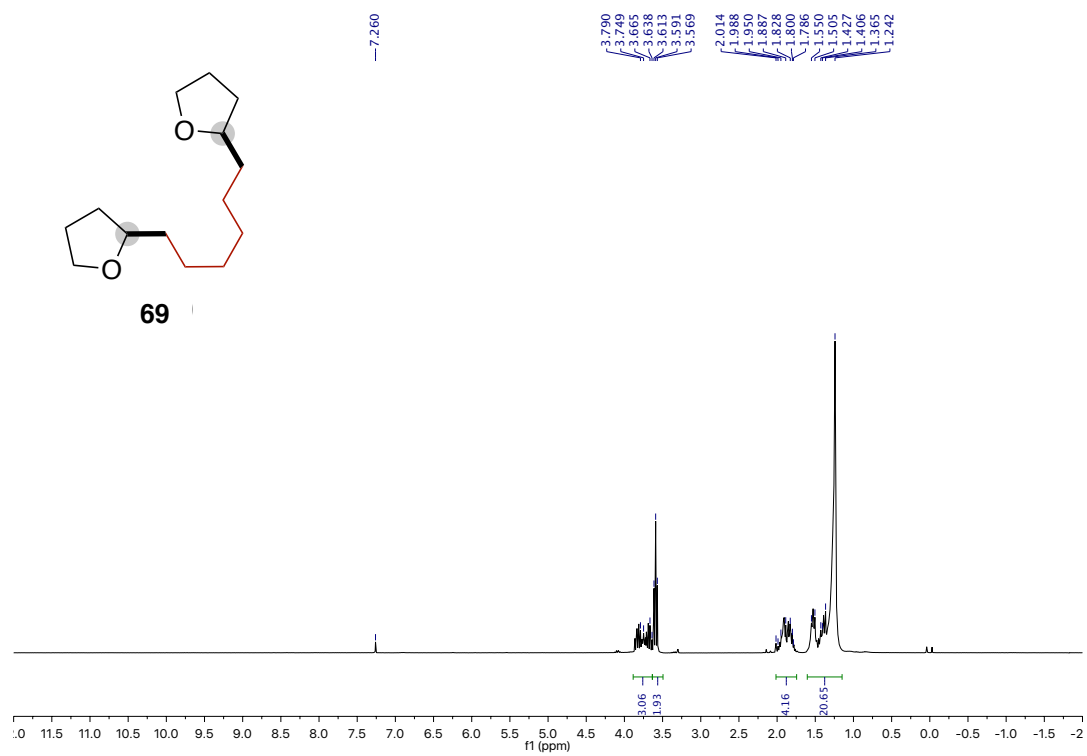


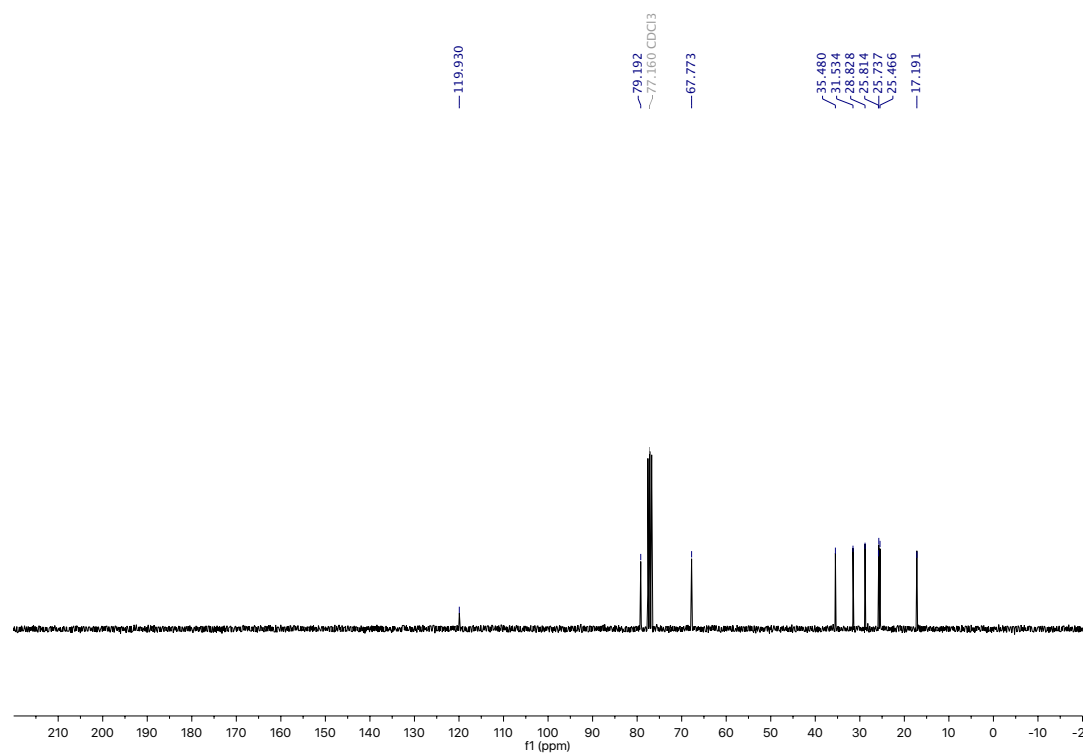
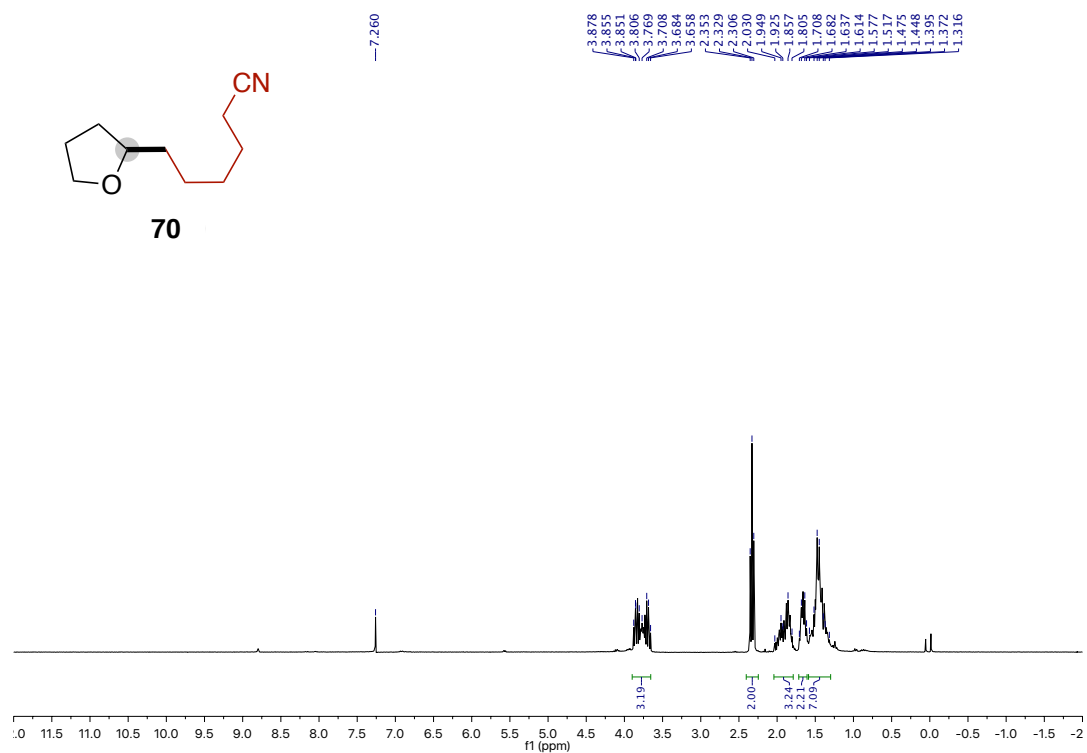


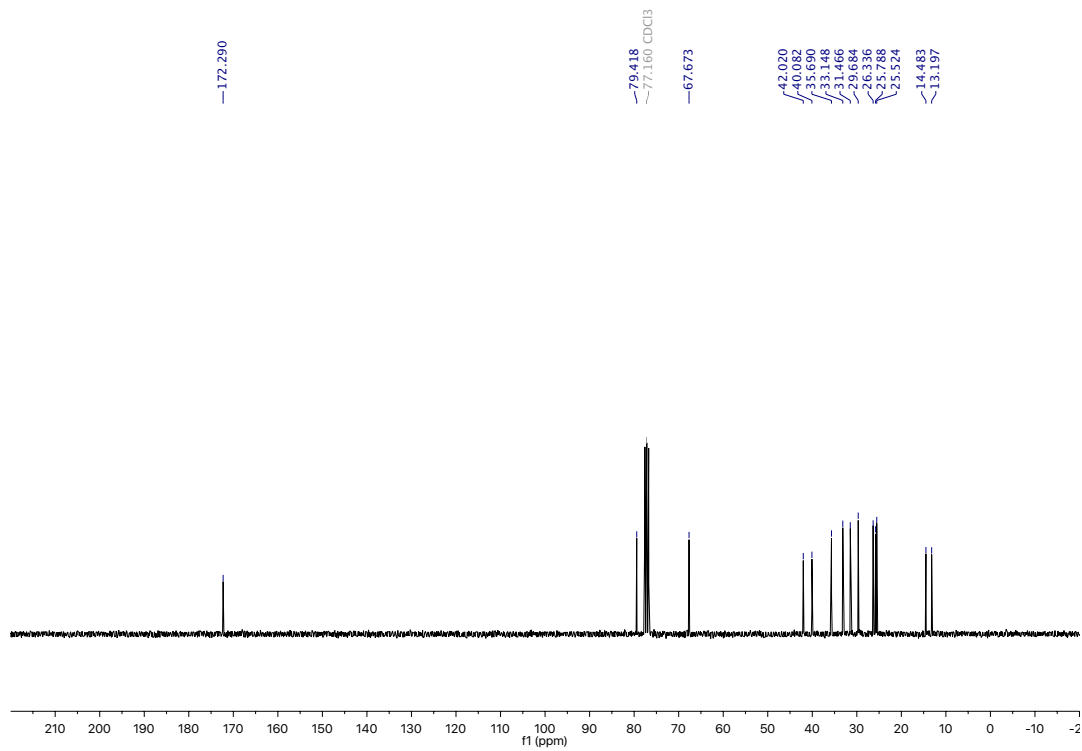
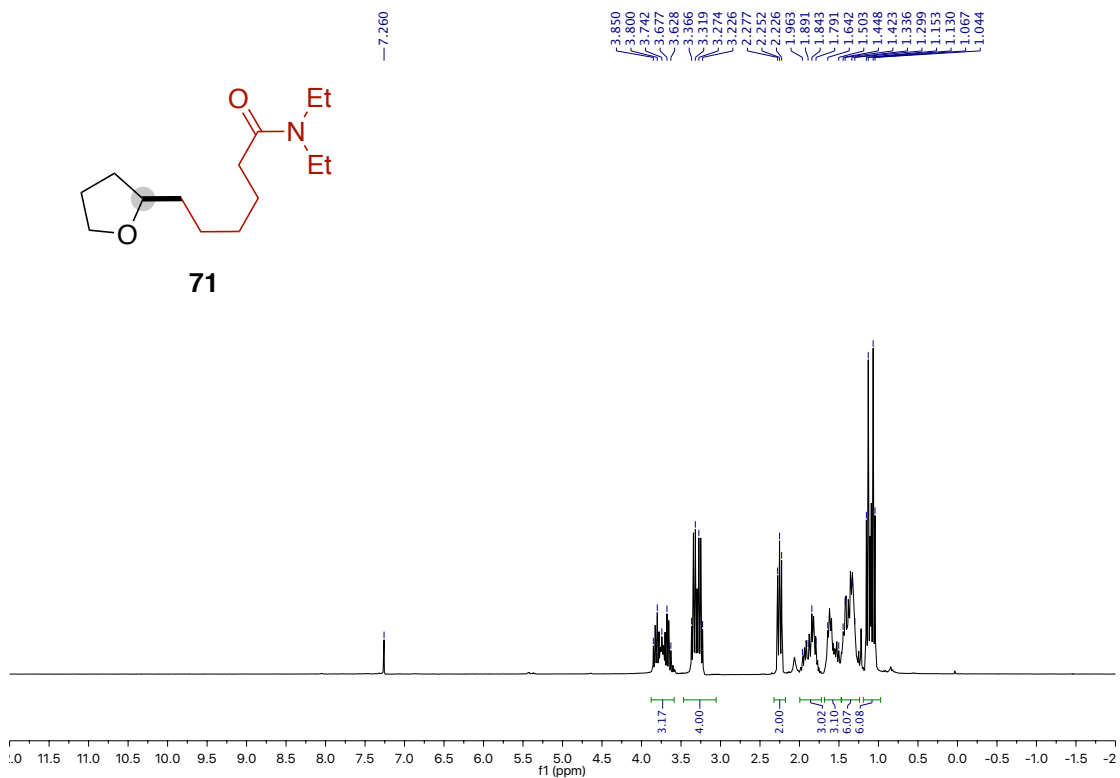


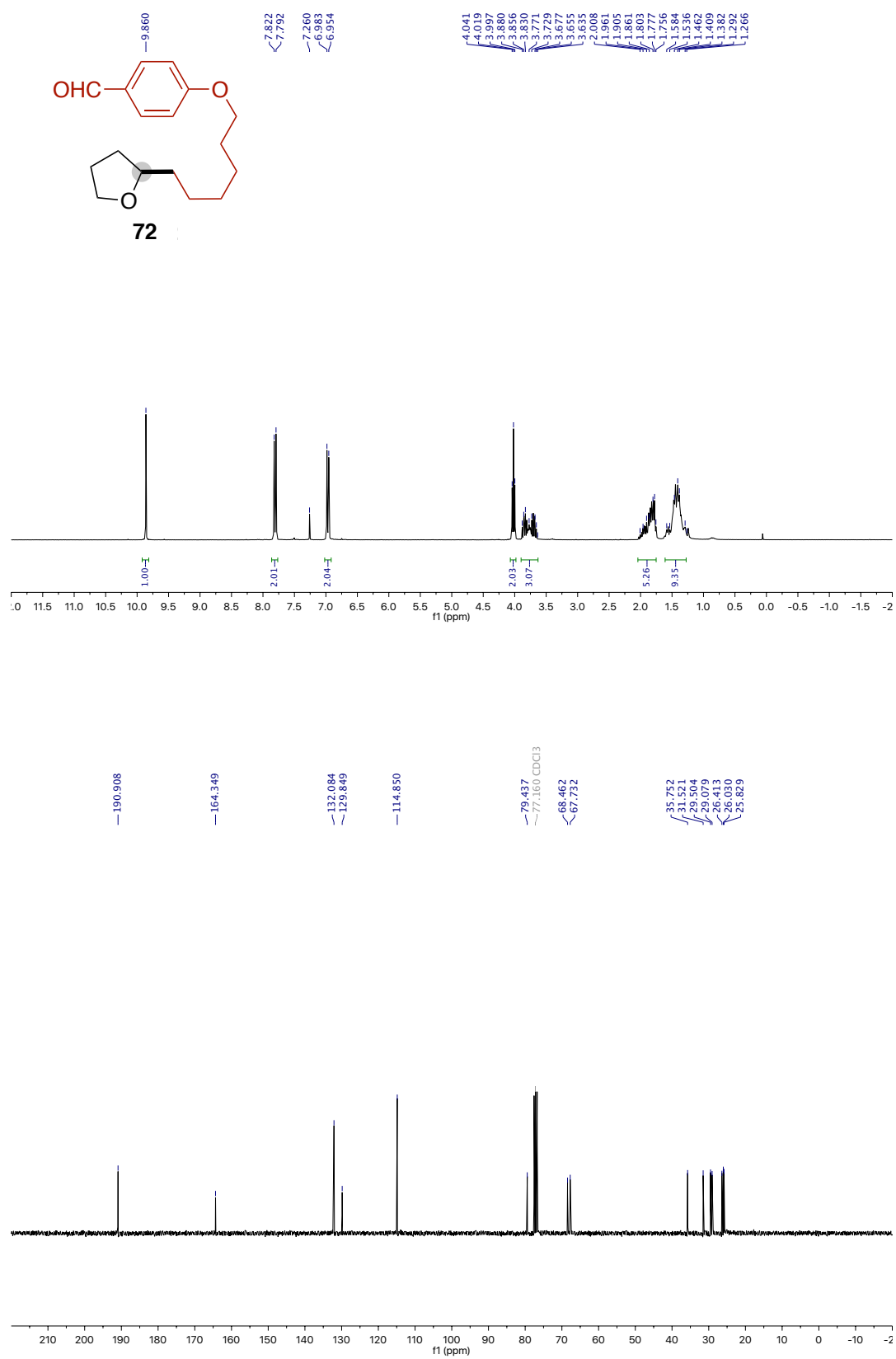


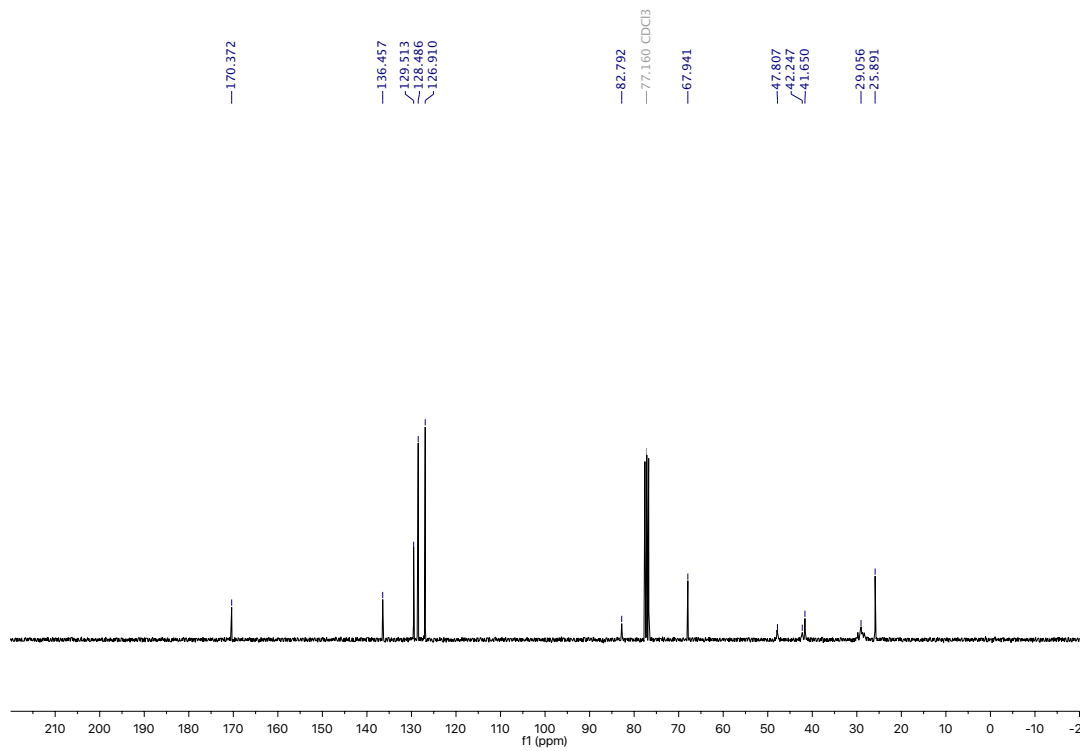
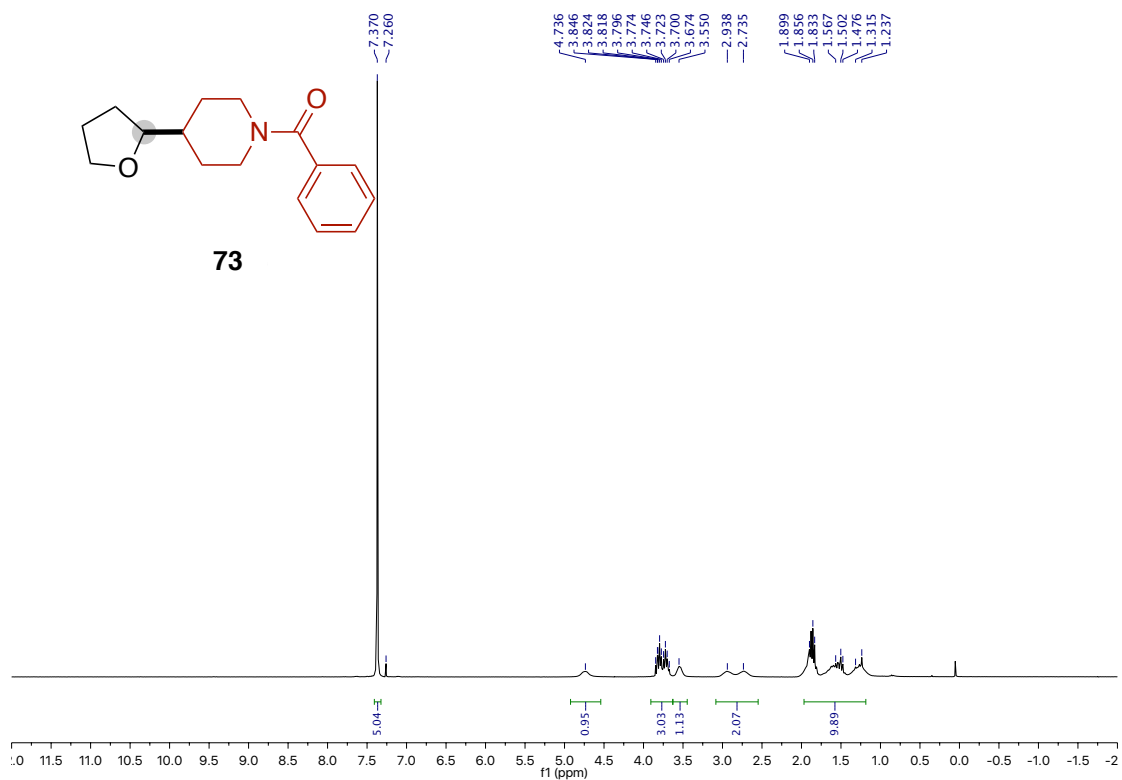


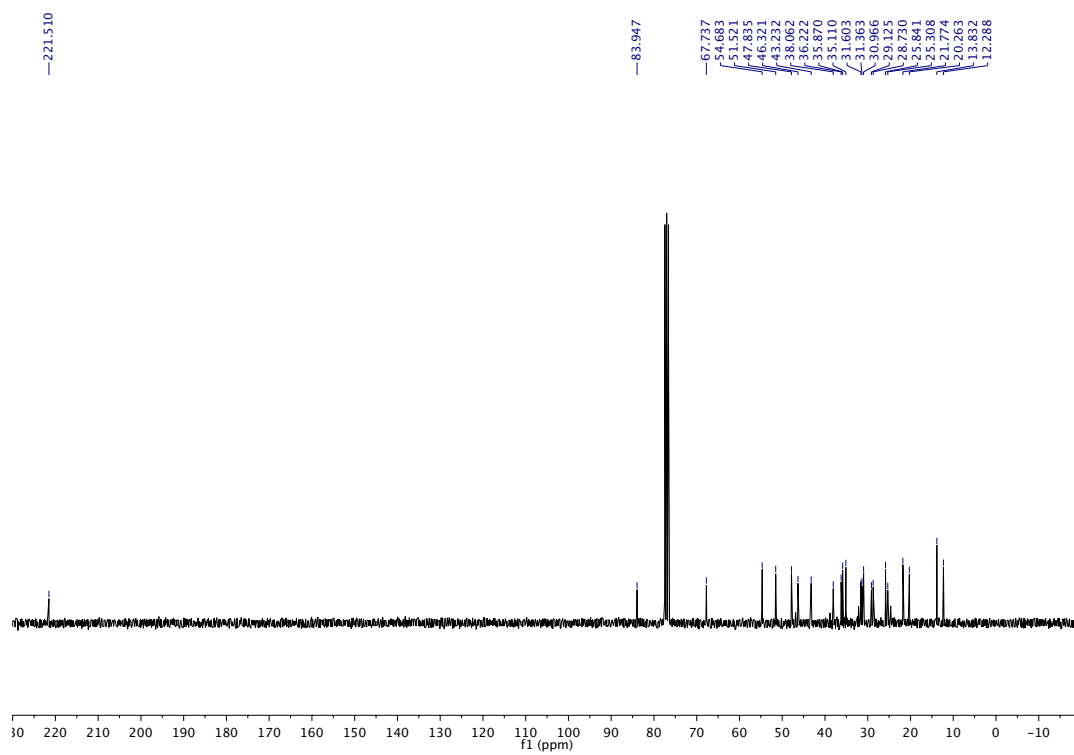
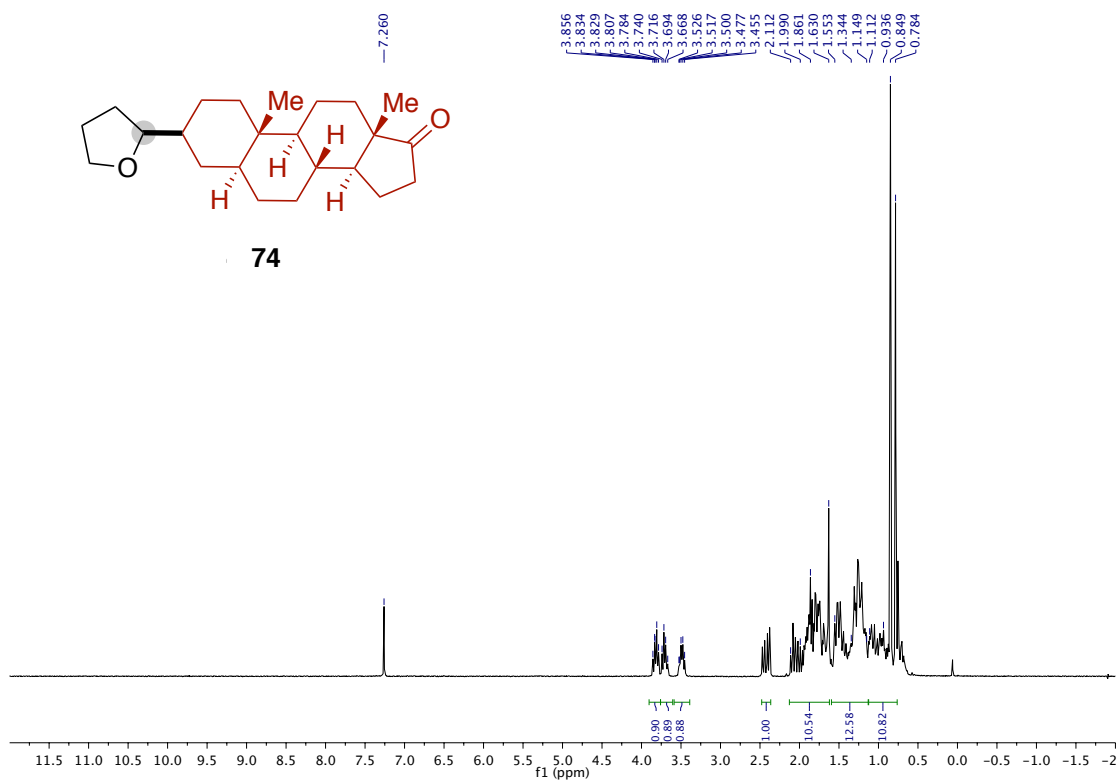






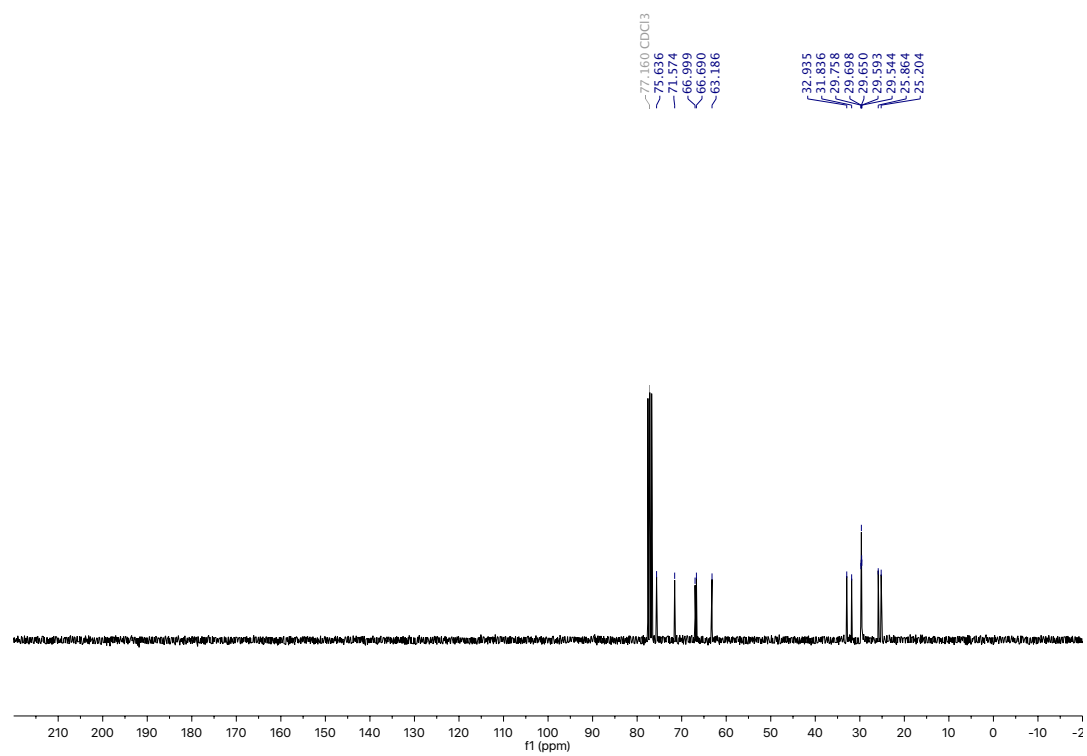
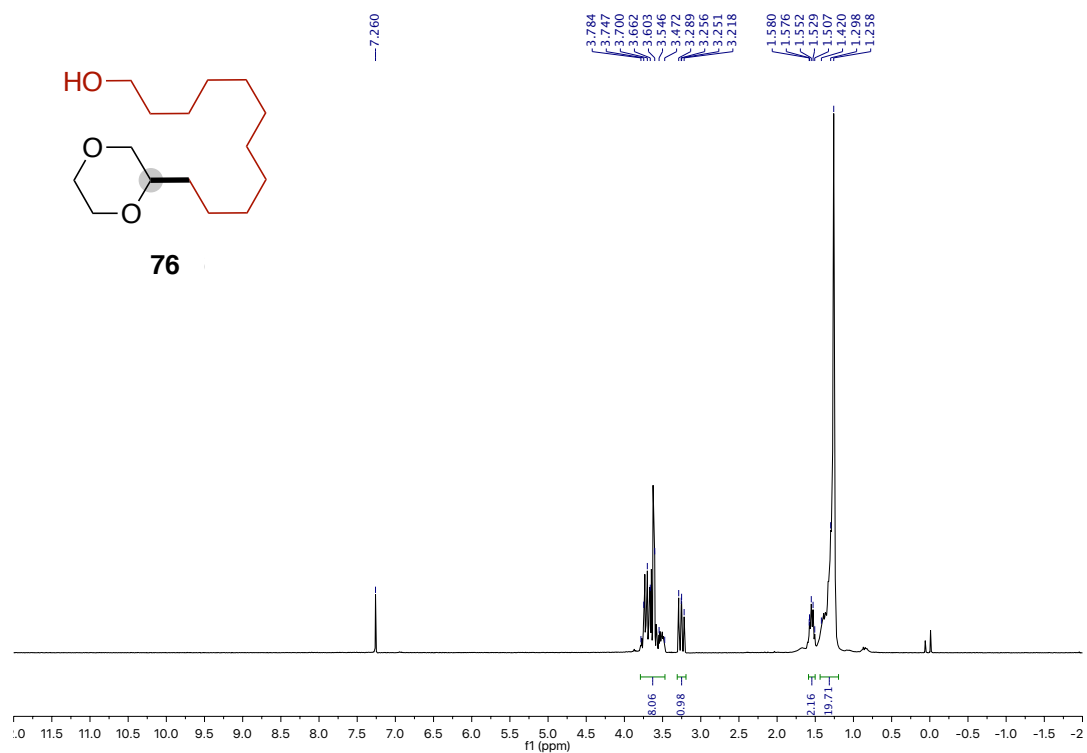


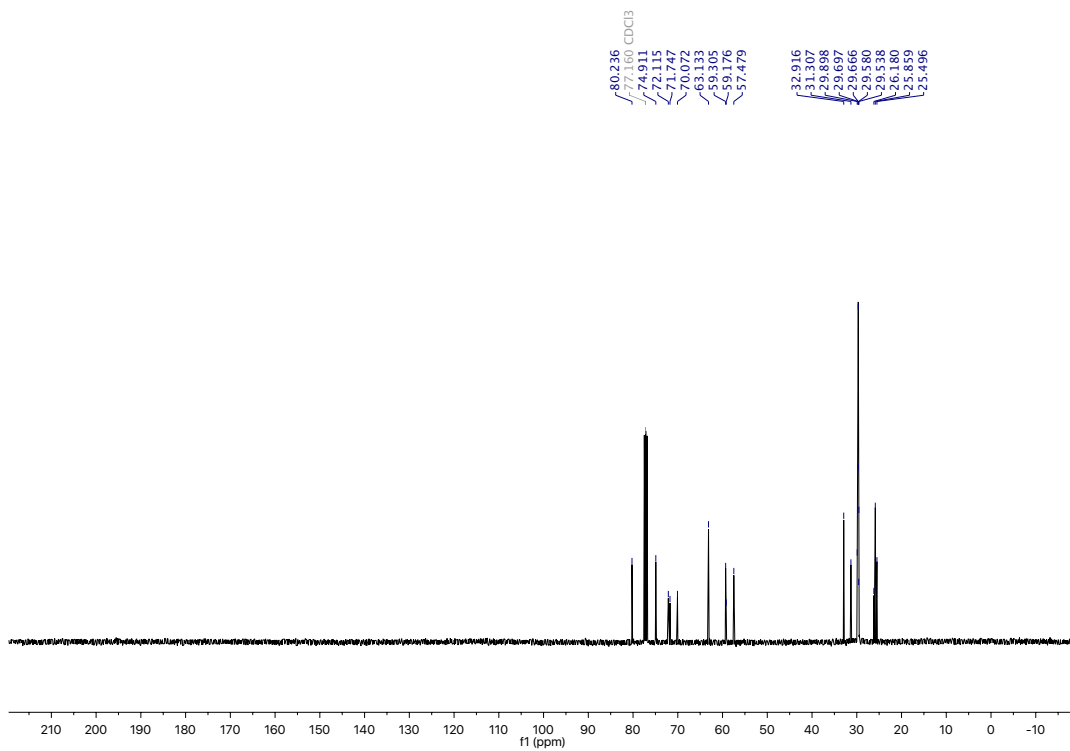
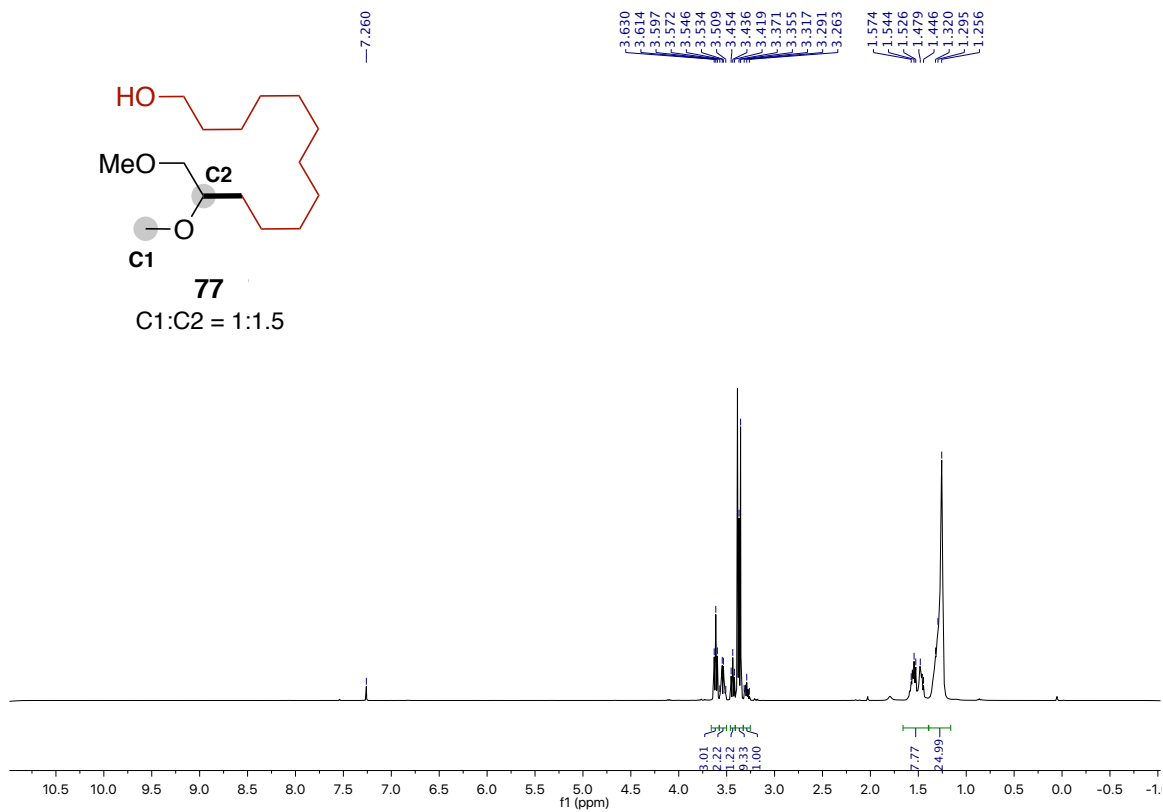
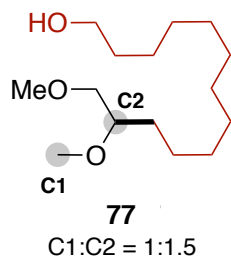


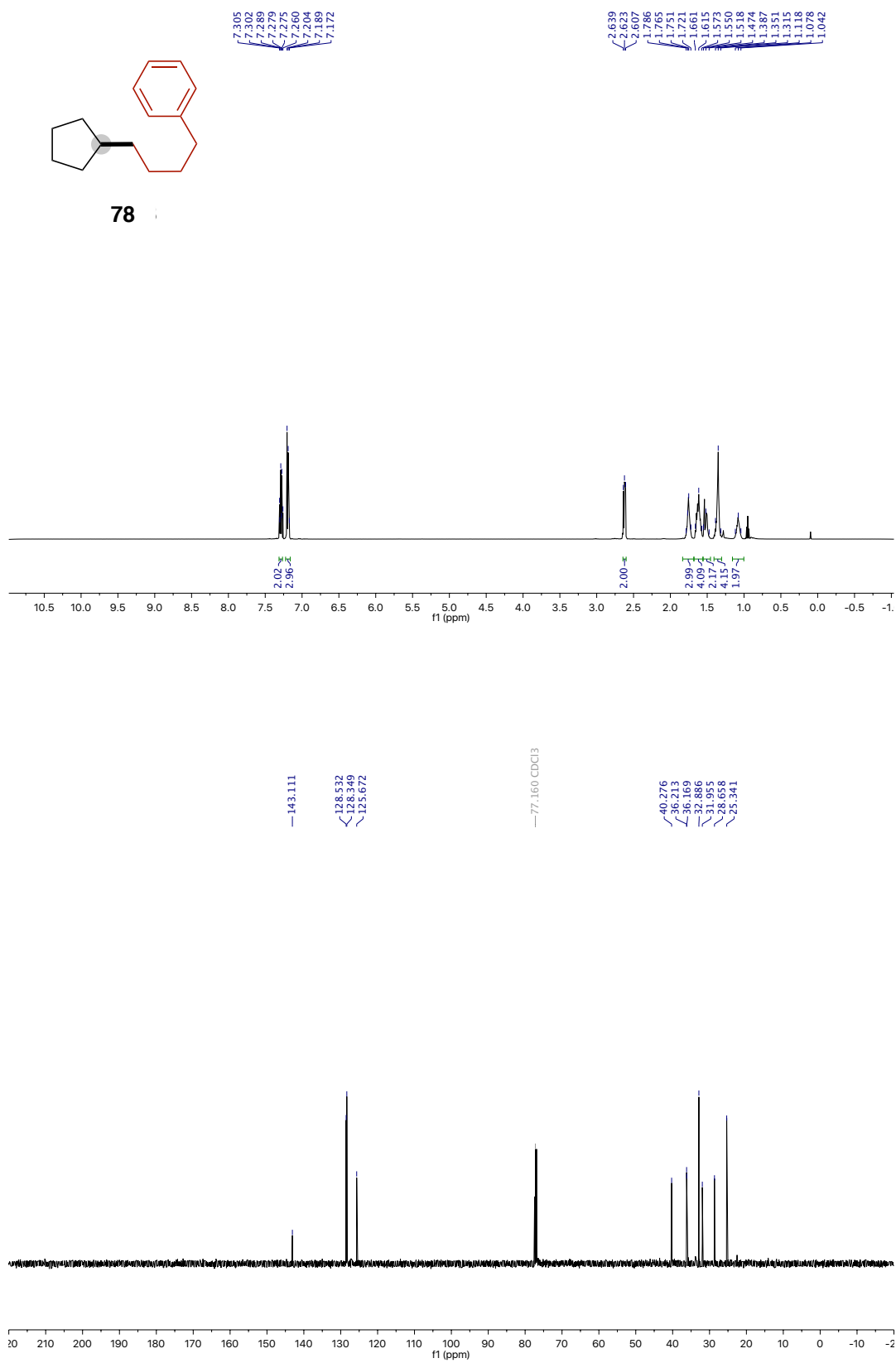


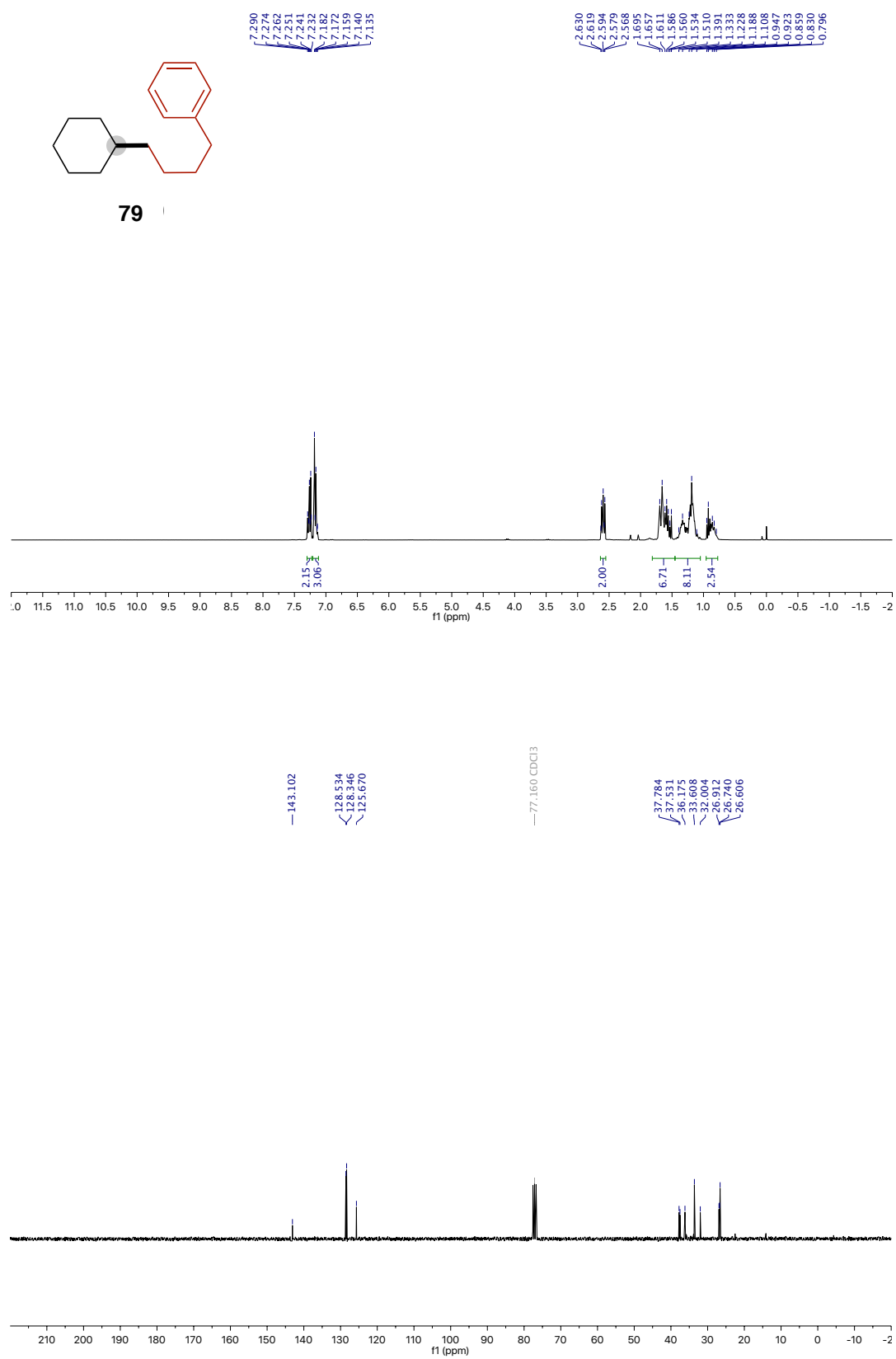


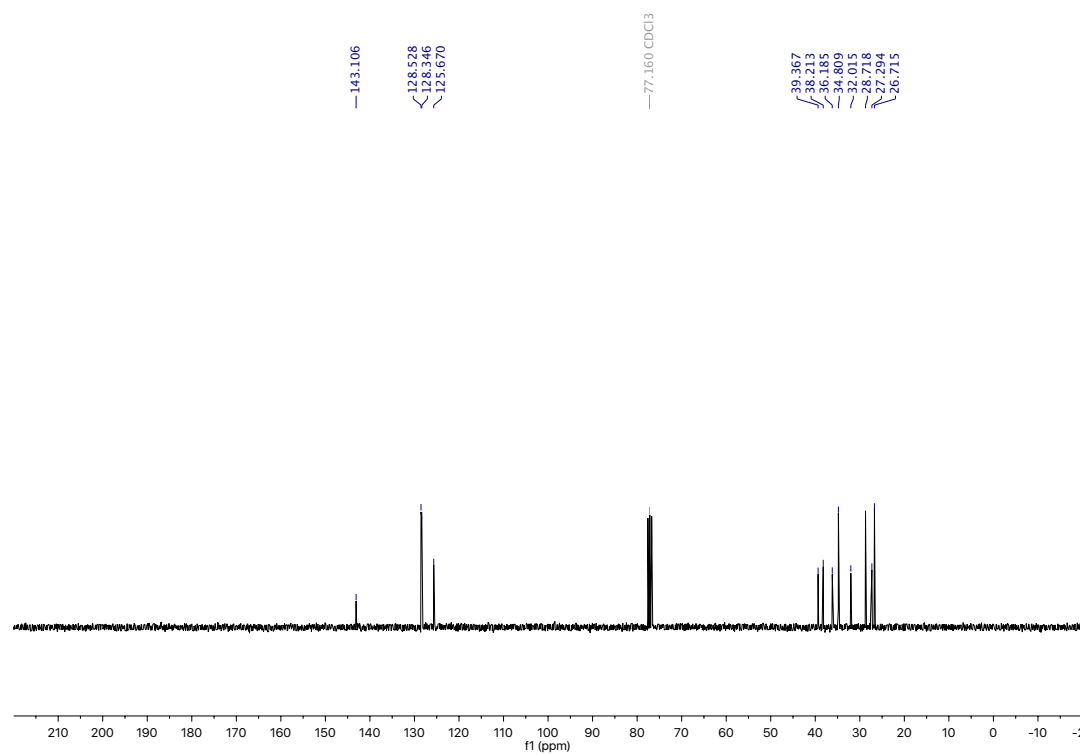
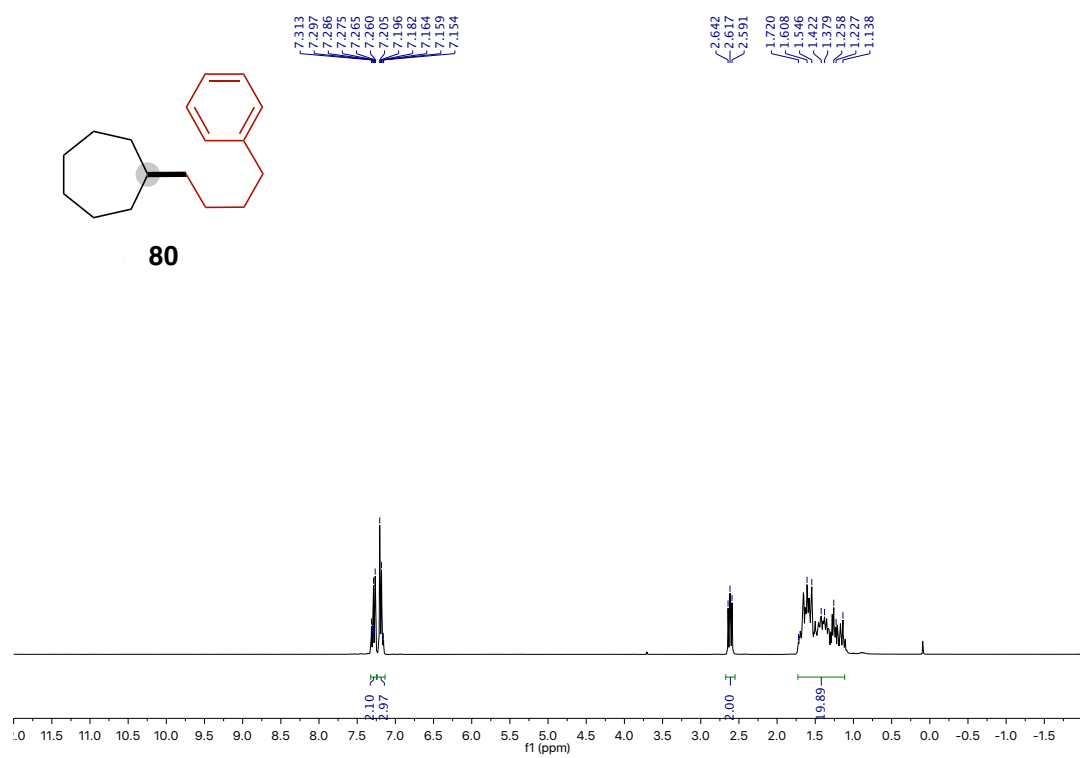


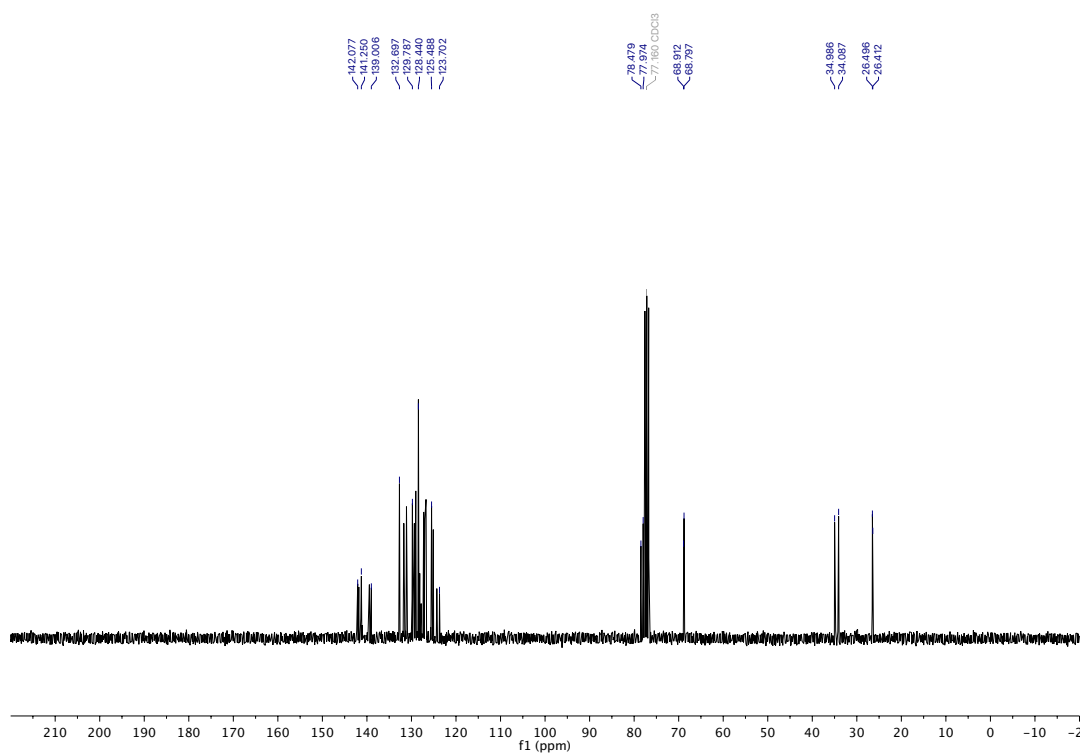
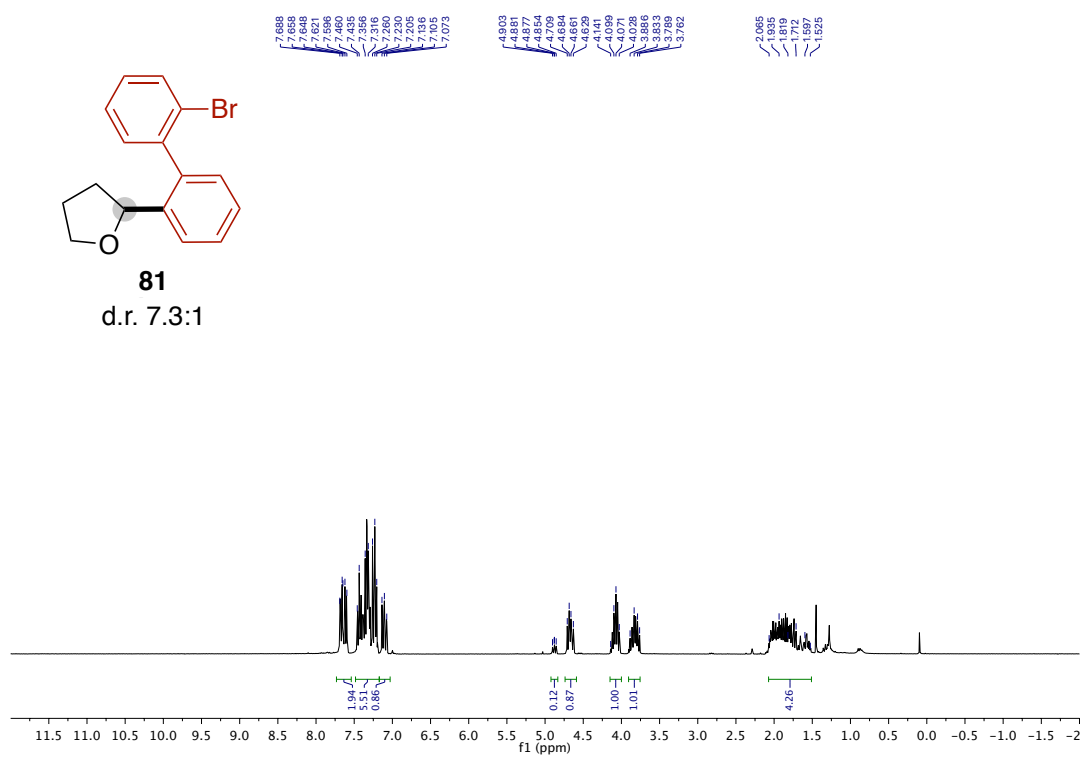


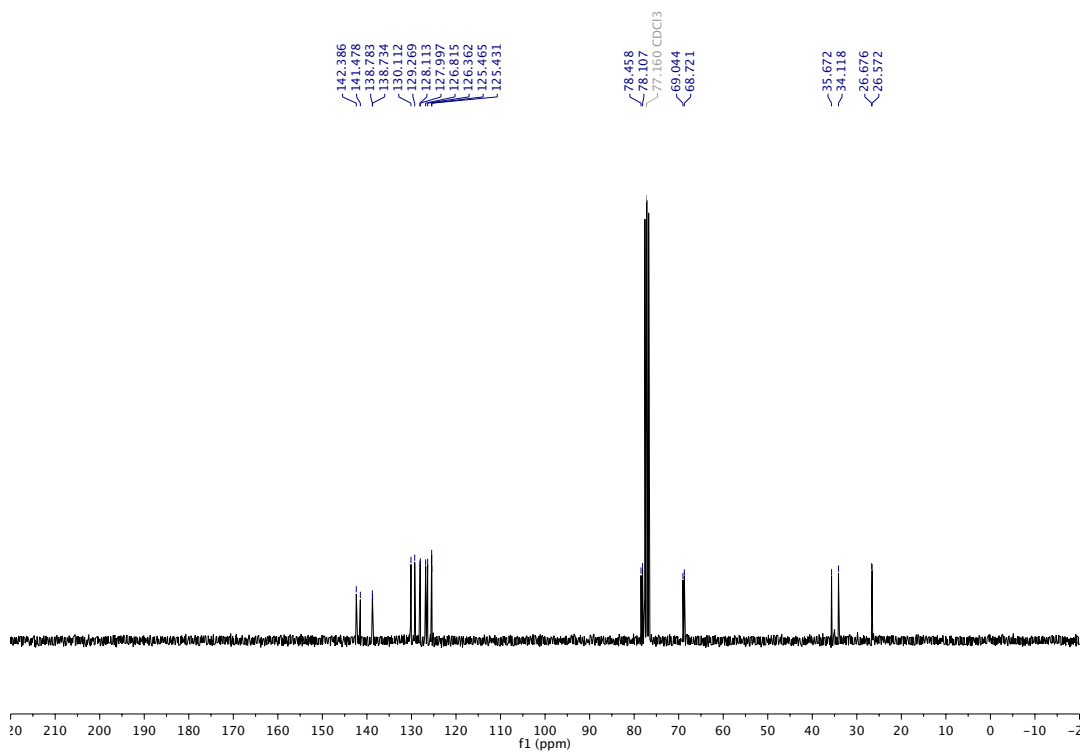
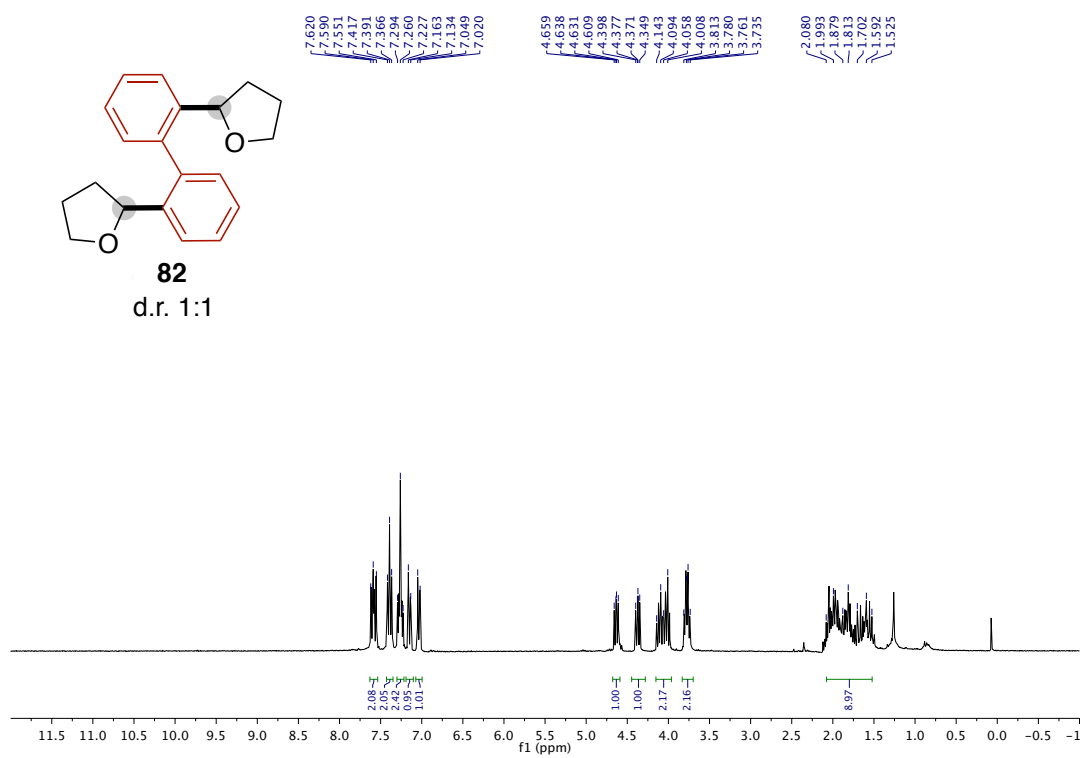




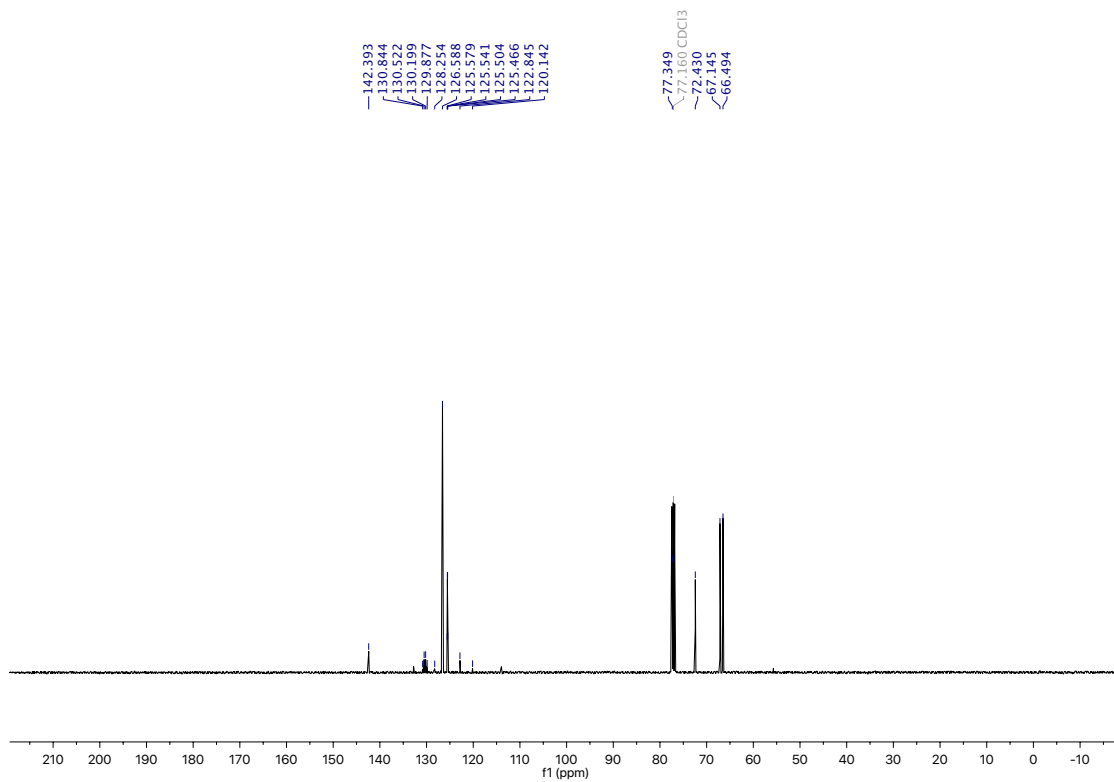
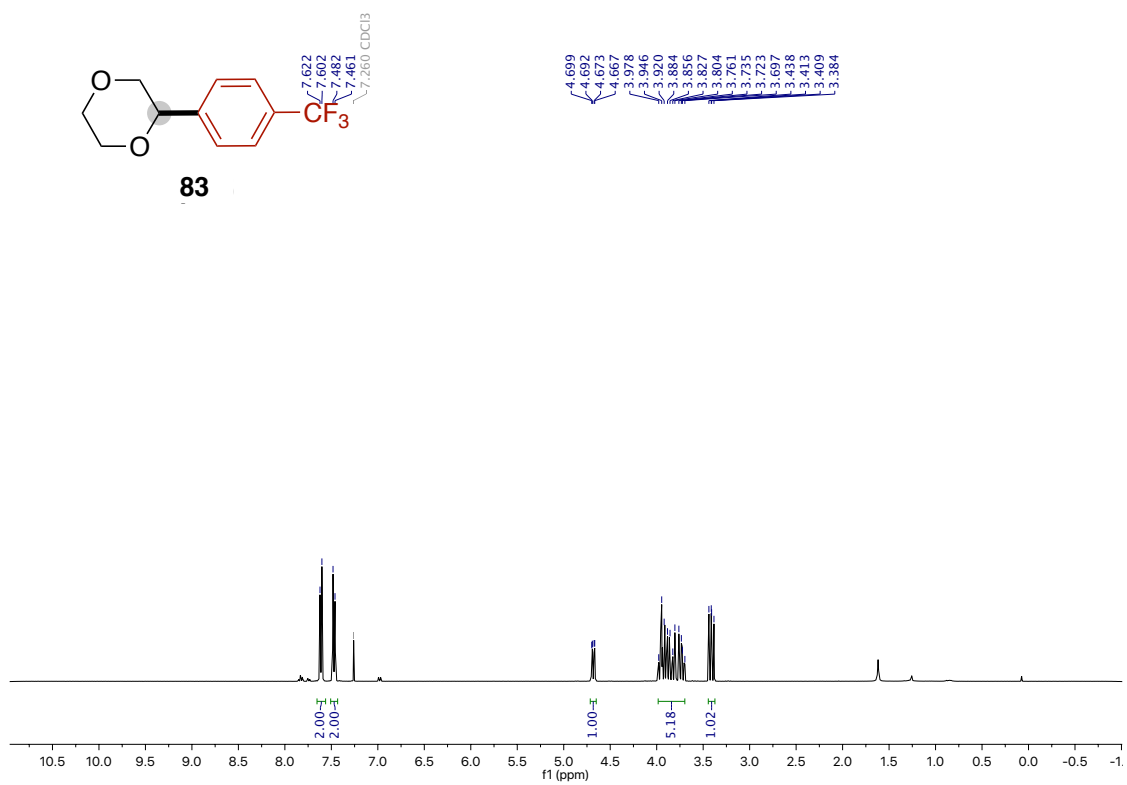


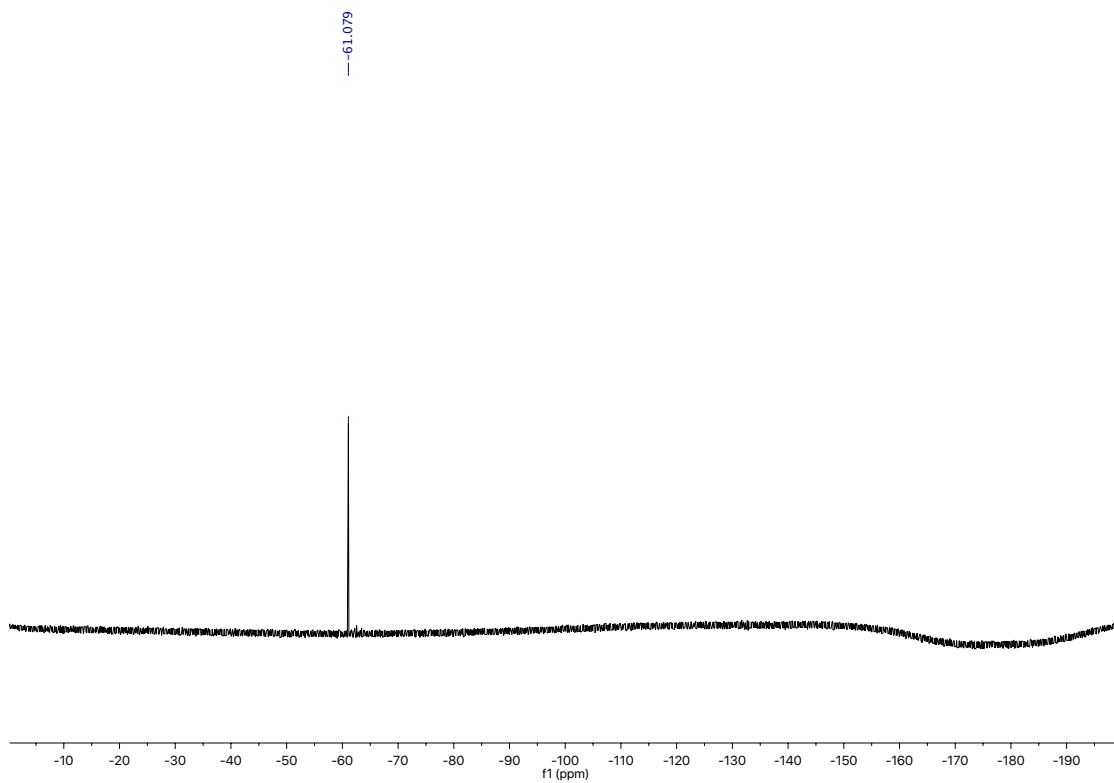
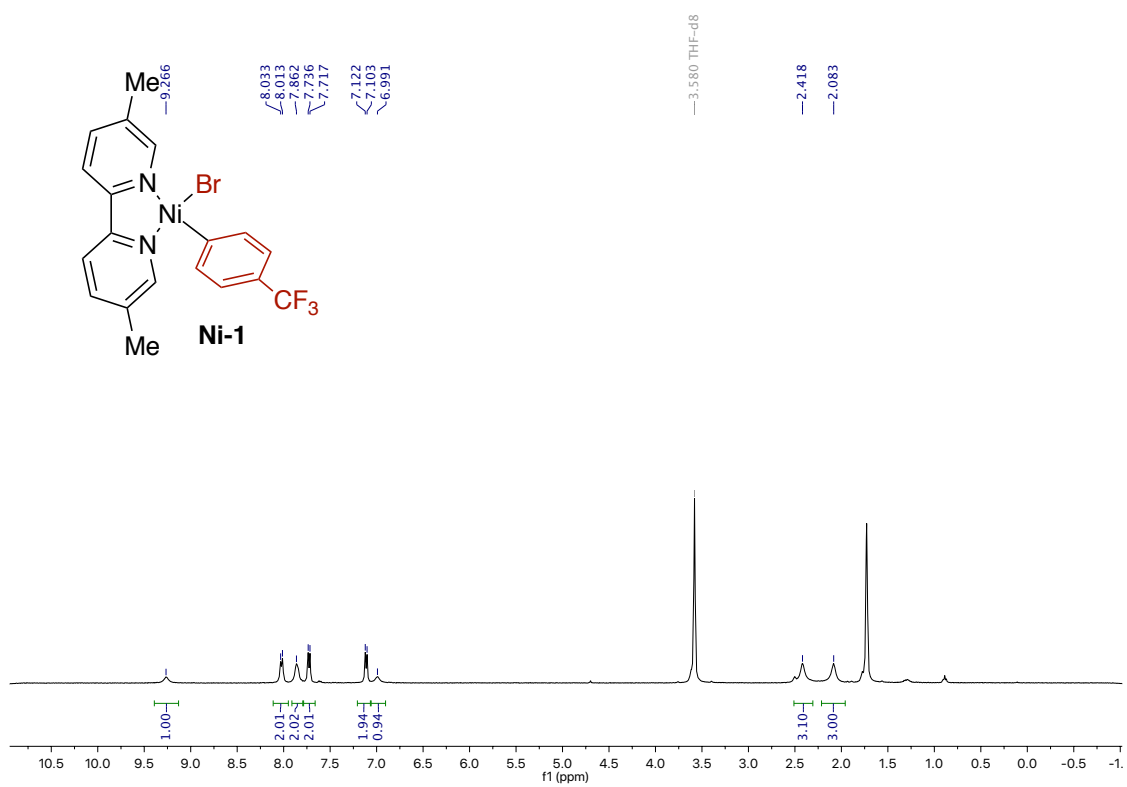












## **Chapter 5.**

### **Conclusions**

The reported methods in this Doctoral Thesis showed the power of photoredox technique to transform inert chemical bonds into added value compounds via novel mechanistic rationale under mild conditions. It would be useful to highlight the challenges we have solved in our initial aim.

#### Chapter 2:

- A mild visible light photoredox promoted intramolecular ATRC of unactivated alkyl iodides has been developed.
- The method featured on the efficient synthesis tetrasubstituted vinyl iodides and double cyclization with excellent diastereoselectivity.
- Preliminary mechanistic studies challenge the perception that a canonical photoredox catalytic cycle is being operative.

#### Chapter 3:

- A mild visible light photoredox catalyzed intramolecular dicarbon functionalization of styrenes has been developed.
- The method featured on multiple bonds formation with fluoro-containing group or quaternary carbon center.
- A complementary way to promote photochemical CO<sub>2</sub> fixation.

#### Chapter 4:

- A visible light promoted novel catalytic mode of nickel and ketone has been developed.
- The method featured on arylation and alkylation of native sp<sup>3</sup> C-H bonds with high chemoselectivity and site-selectivity without economic burden.
- Detailed mechanistic studies and discussions suggest the synergistic relationship of nickel and diaryl ketone.



UNIVERSITAT  
ROVIRA i VIRGILI

